Catalytic Enantioselective Additions of Allyl Moieties to α-Halomethyl Ketones, Trifluoromethyl Substituted NH-Ketimines, and Nitriles:

Author: Diana Catherine Fager

CATALYTIC ENANTIOSELECTIVE ADDITIONS OF ALLYL MOIETIES TO α-HALOMETHYL KETONES, TRIFLUOROMETHYL SUBSTITUTED NH-KETIMINES, AND NITRILES

Diana C. Fager

A dissertation

submitted to the Faculty of

the department of Chemistry

in partial fulfillment

of the requirements for the degree of

Doctor of Philosophy

Boston College
Morrissey College of Arts and Sciences
Graduate School

June 2020

CATALYTIC ENANTIOSELECTIVE ADDITIONS OF ALLYL MOIETIES TO α-HALOMETHYL KETONES, TRIFLUOROMETHYL SUBSTITUTED NH-KETIMINES, AND NITRILES

Diana C. Fager

Advisor: Professor Amir H. Hoveyda, Ph.D.

Homoallylic alcohols and amines are commonly used building blocks for synthesis of biologically active molecules, yet a survey of the methods for their synthesis reveals a plague of limitations. Notably, the use of toxic reagents (Cr-, Mn-, and Sn-containing), precious metal catalysts (Ir- and In-based), non-ambient reaction temperatures (–78 to 140 °C), and extended reaction times (up to 240 hours), limit application on larger scale. The protection/deprotection sequences required to install directing/activating groups for reaction efficiency and enantioselectivity not only add synthetic steps but the conditions required for removal of such entities are not amenable to more complex and sensitive molecules. The development of catalytic enantioselective methods for addition of allyl moieties to readily available substrates including halomethyl ketones, trifluoromethyl-substituted ketimines, and nitriles have been developed. In the first two cases, an aminophenol-based boryl catalyst is utilized for enantioselective additions of allyl moieties through transition states controlled by either electrostatic attraction between a C–X bond and the catalyst's ammonium moiety or minimization of steric and dipolar repulsion. In the latter, multicomponent additions to nitriles have been developed for synthesis of cyclic amines. In all cases, application is demonstrated through synthesis of otherwise difficult-to-access derivatives or biologically active molecules.

Acknowledgments

As I write this, I cannot believe that five years have gone by. Coming straight to graduate school from my undergraduate studies at Stonehill College, I was ready to take on the next challenge. Early on in my first year however, when I was juggling teaching, coursework, and beginning research in the lab, I realized just how challenging this journey was going to be. There have been highs and lows over the last five years, but if given the option, I most certainly would do it all over again. Studying at a highly renowned and collaborative institution under the guidance of Professor Amir H. Hoveyda has been a rewarding experience and has prepared me for my career in the pharmaceutical industry.

I would like to start my thanking Professor Amir H. Hoveyda for his incredible dedication to training young scientists. I am grateful to have been accepted into his group and be given the opportunity to work on the projects described herein. He has taught me so much, not only chemistry, but also how to hold your own and excel in a competitive field. He has both supported me and challenged me, and provided me with countless opportunities to grow and become the scientist I am today. I can only hope that I will live up to his expectations and make equally as important contributions to the scientific community.

I would like to thank Professors Masayuki Wasa and Marc Snapper for serving on my second-year candidacy and thesis committees. I would like to thank all of the professors in the department for their contributions to my success here at Boston College through teaching, lectures, collaboration, and questions. Thank you all for your continued support and investment in advancing my research and scientific skills.

I would like to thank the graduate students and post-doctoral fellows that have mentored me through the years. Dr. KyungA Lee for training me as a first-year graduate student and

collaborating on the haloketone project. Dr. Farid van der Mei for being a constant source of both knowledge and comic relief. Dr. Juan del Pozo for his continued support, mentoring, and friendship. Ryan Morrison for being one of my closest friends and collaborators throughout both college and graduate school. Meagan Hackey for taking on my group responsibilities and collaborating with me on the cyclic amine project. I am thankful for all of the Hoveyda Group members past and present for the stimulating conversations, suggestions for improving chemistries, and their support through the job application and dissertation writing process.

The Chemistry department, and this program as a whole, would not have the incredible reputation it does without the support of all of the Chemistry Department staff. Thank you, Dale, Lynne P., Leah, Ian, Dumazo, Bob, Lori, Steve, Tim, TJ, Jing, Marek, Bo, Lynne O., and Amarjit for all of your assistance.

I would like to thank my incredible family and friends who have encouraged and supported me and my passion for science from a young age. Thank you, Ally and Kathleen, for being the best friends (and bridesmaids) a girl could ask for. Thank you, Julie and Brian, for being the best siblings and friends to go through life with. Thank you to my grandparents, Donald and Patricia, for challenging me to explain my chemistry in layman's terms each time I visit and for often times being more excited about this journey than I have been. Thank you to my soon-to-be husband (thank you, COVID-19) for walking alongside me throughout this experience. And finally, I would like to thank my mother, Dolores, who has taught me how to be a strong-willed, independent, and hard-working young woman with a good head on her shoulders. I would not be who I am or where I am today without her.

Table of Contents

Chapter One

Catalytic Methods for Stereoselective Transformation of Readily Available Organofluorine Compounds to High-Value Products

1.1. Introduction

Contemporary research performed both in academia and industry reveals that the number of fluorine-containing molecules displaying optimal properties is ever-increasing. By analyzing recent trends regarding the structure of these organofluorines, one can see that molecules are becoming progressively more complex and diverse. To explore fully the potential of fluorine-containing molecules in chemical research, the following questions must be addressed: 1) considering that nearly no organofluorine compounds are available in nature, how might we synthesize such entities reliably, efficiently, and selectively? 2) How might organofluorine compounds be accessed stereoselectively and how will their properties compare?

A synthetic strategy that has been extensively explored entails the stereoselective incorporation of one or more fluorine atoms (e.g., fluorination, trifluoromethylation, etc.). This Chapter highlights a different approach, namely, one that centers on utilizing commercially available fluoro-organic compounds for synthesis of more complex fluorine-containing organic molecules in a stereoselective manner.

1.2. Background

The majority of small molecules approved as pharmaceuticals[1] and agrochemicals[2] over the last ten years contain one or more C–F bonds. Paradoxically, among the more than four thousand halogen-containing natural products,[3] less than 40 contain a fluorine atom,[4] despite fluorine being the most abundant halogen in Earth's crust. Three factors contribute to the low incorporation of fluorine in natural products: 1) halogens are incorporated by enzymatic electrophilic halogenation,[5] which is prohibited by the high oxidation potential of the fluoride anion, or by nucleophilic substitutions that are slowed due to the high solvation enthalpy of the fluoride anion; 2) fluoride salts are significantly less soluble in water than chloride and bromide

---

[1] (a) Purser, S.; Moore, P. R.; Swallow, S.; Gouvernour, V. *Chem. Soc. Rev.* **2008**, *37*, 320–330. (b) O'Hagan, D. *J. Fluorine Chem.* **2010**, *131*, 1071–1081. (c) Wang, J.; Sanchez-Rosello, M.; Acena, J. L.; del Pozo, C.; Sorochinsky, A. E.; Fustero, S.; Soloshonok, V. A.; Liu, H. *Chem. Rev.* **2014**, *114*, 2432–2506. (d) Gillis, E. P.; Eastman, K. J.; Hill, M. D.; Donnelly, D. J.; Meanwell, N. A. *J. Med. Chem.* **2015**, *58*, 8315–8359. (e) Zhou, Y.; Wang, J.; Gu, Z.; Wang, S.; Zhu, W.; Aceña, J. L.; Soloshonok,V. A.; Izawa, K.; Liu, H. *Chem. Rev.* **2016**, *116*, 422–518. (f) Mei, H.; Han, J.; Fustero, S.; Medio-Simon, M.; Sedgwick, D. M.; Santi, D.; Ruzziconi, R.; Soloshonok, V. A. *Chem. Eur. J.* **2019**, *25*, 11797–11819.

[2] (a) Fujiwara, T.; O'Hagan, D. *J. Fluorine Chem.* **2014**, *167*, 16–29. (b) Harsanyi, A.; Sandford, G. *Green Chem.* **2015**, *17*, 2081–2086. (c) Pazenok, S.; Leroux, F. R. Chapter 16: Modern Fluorine-Containing Agrochemicals. In *Frontiers in Organofluorine Chemistry;* Ojiwa, I. World Scientific, Stony Brook, NY, 2020; pp 695–722.

[3] (a) Erikson, K. L. *Mar. Nat. Prod*. **1983**, 31–256. (b) Butler, A.; Walker, J. V. *Chem. Rev.* **1993**, *93*, 1937–1944. (c) Franssen, M. C. R. *Catalysis Today* **1995**, *22*, 441–457. (d) Butler, A; *Coord. Chem. Rev.* **1999**, *187*, 17–35. (e) Gribble, G. W.; Naturally Occurring Organohalogen Compounds – A Comprehensive Survey. In *Progress in the Chemistry of Organic Natural Products*; Zechmeister, L. Springer Chemistry, New York, NY, 1996; pp 1–423. (f) Murai, A. Total synthesis of cyclic halo ether compounds from marine origin. In *Studies in Natural Product Synthesis*; Rahman, A.-U., Elsevier, New York, NY, 1997; pp 411–461. (g) Gribble, G. W. *Acc. Chem. Res.* **1998**, *31*, 141–154. (h) Wagner, C.; El Omari, M.; Konig, G. M. *J. Nat. Prod.* **2009**, *72*, 540–553. (i) Gribble, G. W. *Mar. Drugs* **2015**, *13*, 4044–4136. (j) Chung, W.-J.; Vanderwal, C. D. *Angew. Chem., Int. Ed.* **2016**, *55,* 4396–4434.

[4] (a) O'Hagan, D.; Harper, D. B. *J. Fluorine Chem.* **1999**, *100*, 127–133. (b) Deng, H.; O'Hagan, D.; Schaffrath, C. *Nat. Prod. Rep.* **2004**, *21*, 773–874. (c) Harper, D. B.; O'Hagan, D.; Murphy, C. D. *Fluorinated Natural Products: Occurrence and Biosynthesis.* In *Natural Production of Organohalogen Compounds*; Gribble, D. Springer, Berlin, Heidelberg, 2012; pp 141–169. (d) Chan, K. K. J.; O'Hagan, D. Chapter Eleven – The Rare Fluorinated Natural Products and Biotechnological Prospects for Fluorine Enzymology. In *Methods in Enzymology;* Galluzzi, L.; Rudqvist, N.-P., Academic Press, Cambridge, MA, 2012; pp 219–235.

[5] For references regarding enzymatic fluorine incorporation, see: (a) Cobb, S. L.; Deng, H.; McEwan, A. R.; Naismith, J. H.; O'Hagan, D.; Robinson, D. A. *Org. Biomol. Chem.* **2006**, *4*, 1458–1460. (b) Zhu, X.; Robinson, D. A.; McEwan, A. R.; O'Hagan, D. Naismith, J. H. *J. Am. Chem. Soc.* **2007**, *129*, 14597–14604. (c) Rentmeister, A.; Arnold, F. H.; Fasan, R. *Nature Chem. Bio.* **2009**, *5*, 26–28. (d) Iwai, N.; Tsuboki, Y.; Kitazume, M.; Kitazume, T. *J. Fluorine Chem.* **2010**, *131*, 369–372. (f) O'Hagan, D.; Deng, H. *Chem. Rev.* **2015**, *115*, 634–649. (g) Carvalho, M. F.; Oliveira, R. S. *Crit. Rev. Biotechnol.* **2017**, *37*, 880–897. (h) Tong, W.; Huang, Q.; Li, M.; Wang, J.-B. *Bioresour. Bioprocess.* **2019**, *6*, article 46.

salts;[6] and 3) several enzymes have evolved to metabolize organofluorides by C–F bond cleavage.[7] Thus, organic synthesis plays a major role in accessing such molecules, especially considering that fluorine incorporation through bioengineering is still in its infancy.[8]

This introductory Chapter will focus on recently developed, efficient catalytic processes for stereoselective transformation of organofluorine compounds. Small-molecule pharmaceuticals containing fluorine are becoming increasingly complex, a phenomenon referred to as an "escape from the flatland."[9] There are two general approaches to the stereoselective synthesis of complex organofluorides, one based on the incorporation of fluorine into organic molecules, and the other based on transformations of fluorine-containing organic molecules. Numerous strategies have been developed for fluorine incorporation (e.g., fluorination, trifluoromethylation, etc.), and this has been reviewed several times.[10] In this Chapter, catalytic stereoselective transformations wherein readily available organofluorine precursors are transformed into more complex molecules will be highlighted (Scheme 1.1a). This is an area of research that is likely to see considerable attention, as many key questions remain unresolved (Scheme 1.1b).

---

[6] Reynolds, J. G; Relsher, J. D. *J. Chem. Eng. Data* **2017**, *62*, 1743–1748.

[7] For references regarding enzymatic C–F bond cleavage, see: (a) Tiedt, O.; Mergelsberg, M.; Boll, K.; Muller, M.; Adrian, L.; Jehmlich, N.; von Bergen, M.; Boll, M. *mBio* **2016**, *7*, 1–9. (b) Li. Y.; Zhang, R.; Du, L.; Zhang, Q.; Wang, W. *Catal. Sci. Technol.* **2016**, *6*, 73–80. (c) Li, J.; Griffith, W. P.; Davis, I.; Shin, I.; Wang, J.; Li, F.; Wang, Y.; Wherritt, D. J.; Liu, A. *Nat. Chem. Biol*. **2018**, *14*, 853–860. (d) Tong, W.; Huang, Q.; Li, M.; Wang, J.-B. *Bioresources and Bioprocessing* **2019**, *6*, article 46. (e) Wang, Y.; Davis, I.; Shin, I.; Wherritt, D. J.; Griffith, W. P.; Dornevil, K.; Colabroy, K. L.; Liu, A. *ACS Catal.* **2019**, *9*, 4764–4776.

[8] (a) Biava, H.; Budisa, N. *Eng. Life Sci.* **2014**, *14*, 340–35. (b) O'Hagan, D.; Deng, H. *Chem. Rev*. **2015**, *115*, 634–649. (c) Carvalho, M. F.; Oliveira, R. S. *Crit. Rev. Biotechnol*. **2017**, *37*, 880–897.

[9] (a) Leeson, P. D.; Springthorpe, B. *Nat. Rev. Drug. Disc*. **2007**, *6*, 881–890. (b) Lovering, F.; Bikker, J.; Humblet, C. *J. Med. Chem*. **2009**, *52*, 6752–6756. (c) Lovering, F. *Med. Chem. Commun*. **2013**, *4*, 515–519.

[10] (a) Champagne, P. A.; Desroches, J.; Hamel, J.-D.; Vandamme, M.; Paquin, J.-F. *Chem. Rev*. **2015**, *115*, 9073–9174. (b) Zhu, R.-Y.; Tanaka, K.; Li, G.-C.; He, J.; Fu, H.-Y.; Li, S.-H.; Yu, J.-Q. *J. Am. Chem. Soc.* **2015**, *137*, 7067–7070. (c) Xu, Y.-S.; Yang, Y.; Feng, H.-J.; Liu, J.-T.; Hsung, R. P. *Org. Lett*. **2015**, *17*, 572–575. (d) Neumann, C. N; Ritter, T. *Angew. Chem., Int. Ed*. **2015**, *54*, 3216–3221. (e) Yerien, D. E.; Bonesi, S.; Postigo, A. *Org. Biomol. Chem*. **2016**, *14*, 8398–8427. (f) Cheng, Q.; Ritter, T. *Trends in Chem*. **2019**, *1*, 461–470.

Scheme 1.1. Readily Available Organofluorine Compounds and Transformations Involving Them

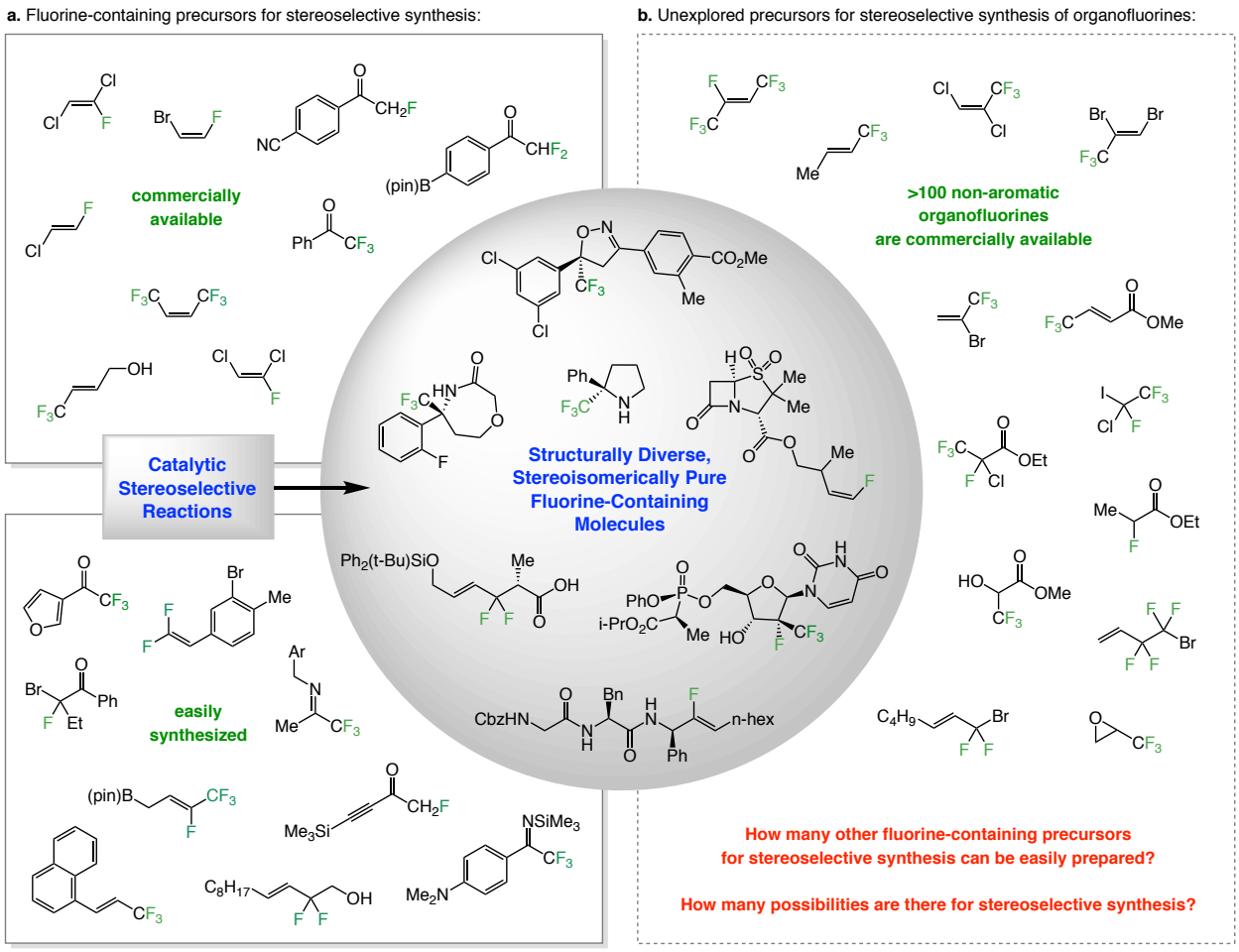

This Chapter is divided into four sections: reactions involving alkenyl fluorides, allylic fluorides, fluorine-containing compounds with carbonyl or imine functional groups, and alkyl fluorides. The term "readily available" refers to a molecule that is either commercially available or synthesized in two steps or fewer from inexpensive and purchasable materials. The examples that will be discussed have been selected primarily based on applicability to medicinally relevant targets. A few others, which are perhaps less synthetically applicable, are mechanistically significant.

1.3. Alkenyl Fluoride Products

Among the array of relevant organofluorine compounds, alkenyl fluorides are noteworthy for their electronic and structural properties, which can mimic those of amides, ketones, and aldehydes.[11] Many fluorine-substituted olefins are readily accessible,[12] inexpensive, and easy-to-handle (Scheme 1.2). Tri- and tetrasubstituted 1,1-difluoroolefins can be synthesized in a single step by the Julia-Kocienski method involving an aldehyde or a ketone and difluoromethyl 2-pyridyl sulfone.[13]

Scheme 1.2. A Method for Synthesis of 1,1-Difluoroalkenes

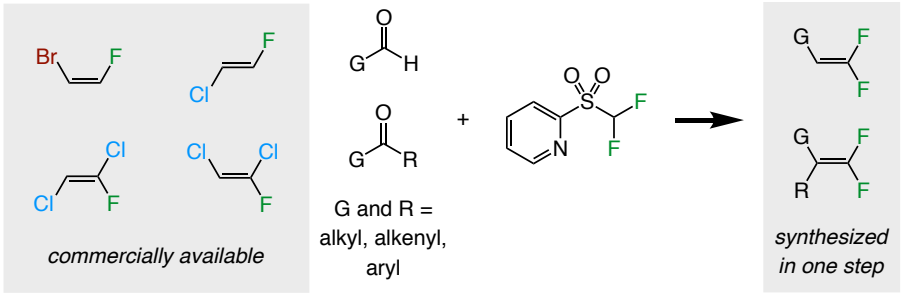

Catalytic stereoselective conversion of the resulting alkenyl fluorides into more complex molecules represents an attractive strategy for synthesis of functionalized and bioactive fluorine-containing molecules. In this regard, stereoselective olefin cross-metathesis, cross-coupling, and their combination will be discussed below.

---

[11] (a) Landelle, G.; Bergeron, M.; Turcotte-Savard, M.-O.; Paquin J.-F. *Chem. Soc. Rev*. **2011**, *40*, 2867–2908. (b) Gillis, E. P.; Eastman, K. J.; Hill, M. D.; Donnelly, D. J.; Meanwell N. A. *J. Med. Chem*. **2015**, *58*, 8315–8359.

[12] Furuya, T.; Ritter T. *Org. Lett*. **2009**, *11*, 2860–2863.

[13] Zhao, Y.; Huang, W.; Zhu, L.; Hu, J. *Org. Lett*. **2010**, *12*, 1444–1447.

1.3.1. Through Catalytic Cross-Metathesis

In 2016, our group disclosed the catalytic stereoselective synthesis of *Z*-[14] and *E*-disubstituted[15] alkenyl fluorides, catalyzed by a molybdenum alkylidene monoaryloxide pyrrolide (MAP) complex (**Mo-1**, Scheme 1.3). A variety of alkenyl fluorides were obtained after four hours, at ambient temperature, and with 1.0-10 mol % **Mo-1**. The feasibility of late-stage fluorine incorporation is one of the more notable aspects of this advance.

Scheme 1.3. Late-Stage Fluorine Incorporation by Stereoretentive Catalytic Cross-Metathesis

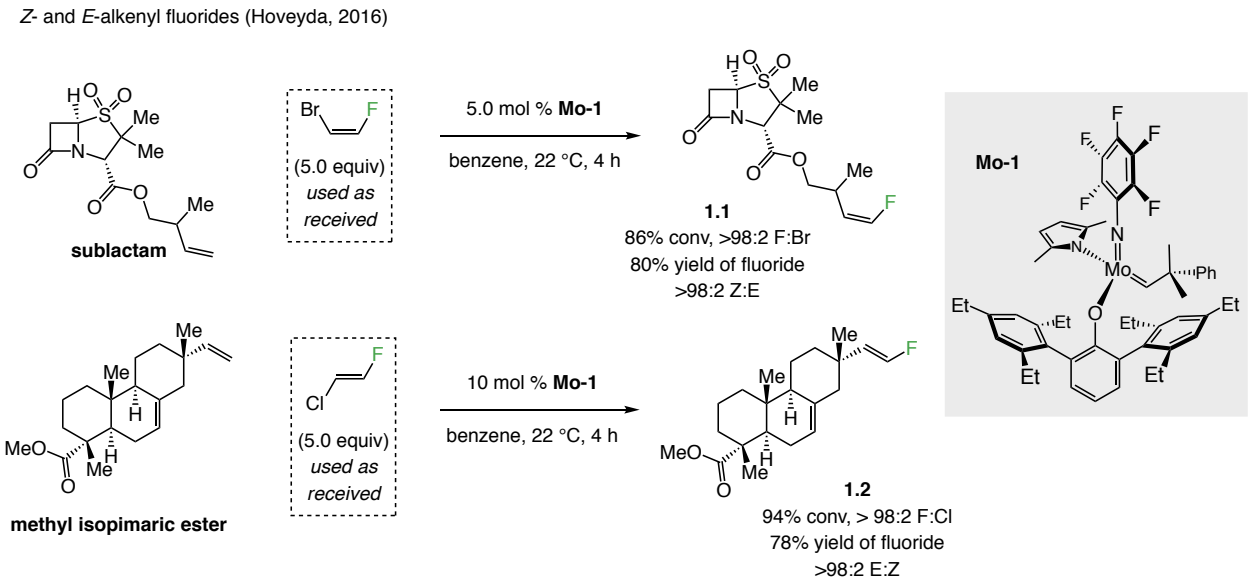

Thus, sulbactam was converted to **1.1** in 80% yield and >98:2 *Z*:*E* ratio, and **1.2** was synthesized from methyl isopimaric ester in 78% yield and >98:2 *E*:*Z* ratio (Scheme 1.3). The reactions are chemoselective (>98:2 F:Br for **1.1** and >98:2 F:Cl for **1.2**), and exceptionally stereoretentive. Reagents were used as received without purification, and **Mo-1** can be purchased.

[14] Koh, M. J.; Nguyen, T. T.; Zhang, H.; Schrock, R. R.; Hoveyda, A. H. *Nature* **2016**, *531*, 459–465.

[15] Nguyen, T. T.; Koh, M. J.; Shen, X.; Romiti, F.; Schrock, R. R.; Hoveyda, A. H. *Science* **2016**, *352*, 569–575.

1.3.2. Through Catalytic Cross-Coupling

To avoid the relatively harsh conditions required for the nickel-catalyzed Suzuki-Miyaura cross-coupling of 1-aryl-2,2-difluoroalkenes and arylboronic acids described by Cao *et al.*,[16] Toste and coworkers developed a redox-neutral Pd-catalyzed strategy.[17] Olefin addition/elimination affords monofluorostilbene products (>98:2 *Z*:*E*) without the need for a base or oxidant.

Scheme 1.4. Synthesis of Alkenyl Fluorides by Catalytic Cross-Coupling

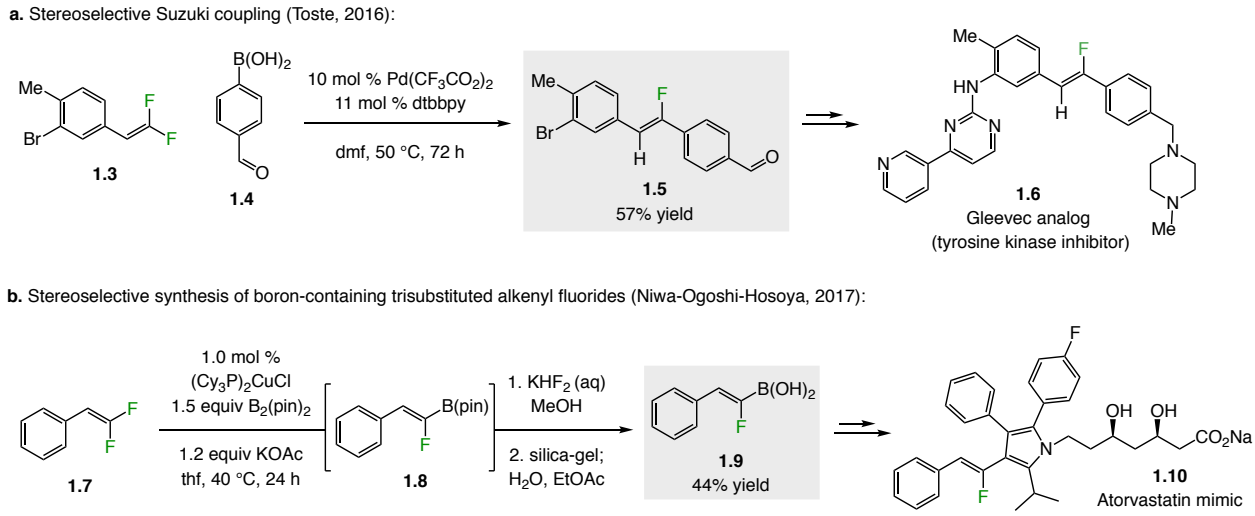

Although relatively high loadings of palladium(II) trifluoroacetate and extended reaction times were needed, a variety of functional groups on either the difluoroalkene or the boronic acid coupling partners proved to be compatible. The synthesis of **1.5** from *gem*-difluoroalkene **1.3** and aldehyde-containing boronic acid **1.4** is illustrative, underscoring the utility of the approach (Scheme 1.4a).

A complementary approach was introduced by Niwa, Ogoshi, and Hosoya, entailing addition of a Cu–B(pin) complex to an olefin followed by Cu–F β-elimination to furnish

[16] Xiong, Y.; Huang, T.; Ji, X.; Wu, J.; Cao, S. *Org. Biomol. Chem*. **2015**, *13,* 7389–7392.

[17] Thornbury, R. T.; Toste, F. D. *Angew. Chem., Int. Ed.* **2016**, *55*, 11629–11632.

monofluoroalkenyl boronic esters, such as **1.9** (Scheme 1.4b).[18] The identity of the organoboron reagent is key, with bis(pinacolato)diboron [$B_2(pin)_2$] being more suitable for electron-deficient substrates, and bis(neopentyl glycolato)diboron [$B_2(nep)_2$] for those that are more electron-rich. Several trisubstituted alkenyl fluorides, which can serve as amide bond mimics, were synthesized stereoselectively, including atorvastatin analog **1.10**. The ease with which 1,1-difluoroalkenes can be accessed is an appealing feature of this method. However, reactions with alkyl-substituted substrates were inefficient.

Sigman, Toste, and coworkers recently reported a phosphine–Pd-catalyzed oxidative Heck reaction of acyclic alkenyl fluorides and arylboronic acids, resulting in formation of F-substituted quaternary carbon stereogenic centers with high enantioselectivity (Scheme 1.5).[19] For example, synthesis of **1.13** began from allylic alcohol **1.12**, a readily available substrate prepared in two steps by catalytic stereoselective hydrofluorination of commercially available alkyne **1.11** followed by ester reduction.[20]

Scheme 1.5. Cross-Coupling and Synthesis of F-Containing Quaternary Stereogenic Centers

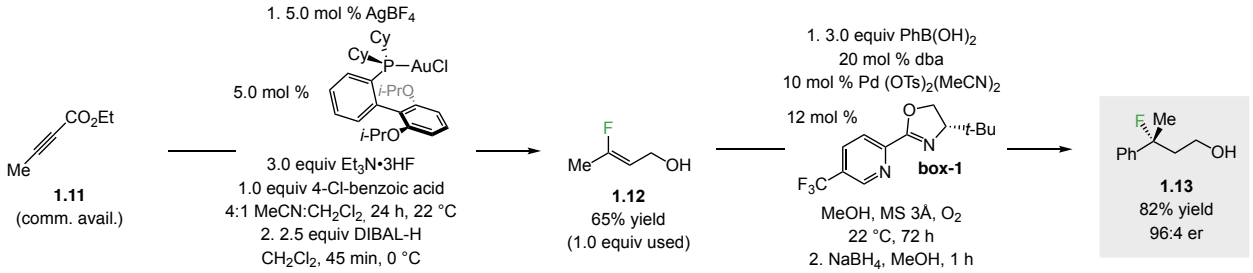

[18] Sakaguchi, H.; Uetake, Y.; Ohashi, M.; Niwa, T.; Ogoshi, S.; Hosoya., T. *J. Am. Chem. Soc.* **2017**, *139*, 12855–12862.

[19] Liu, J.; Yuan, Q.; Toste, F. D.; Sigman, M. S. *Nat. Chem*. **2019**, *11*, 710–715.

[20] O'Connor, T. J.; Toste, F. D. *ACS Catal*. **2018**, *8*, 5947–5951.

1.3.3. Merging Catalytic Cross-Metathesis and Cross-Coupling

In 2017, our group demonstrated that merger of two catalytic processes, cross-coupling and cross-metathesis, can provide access to various trisubstituted alkenes (Scheme 1.6).[21] Cross-metathesis of *Z*- or *E*-1,2-dichloro-1-fluoroethylene with a trisubstituted alkene afforded *Z*- or *E*-1,1-fluoro,chloro-trisubstituted alkenes.

Scheme 1.6. Merging Catalytic Cross-Metathesis and Cross-Coupling

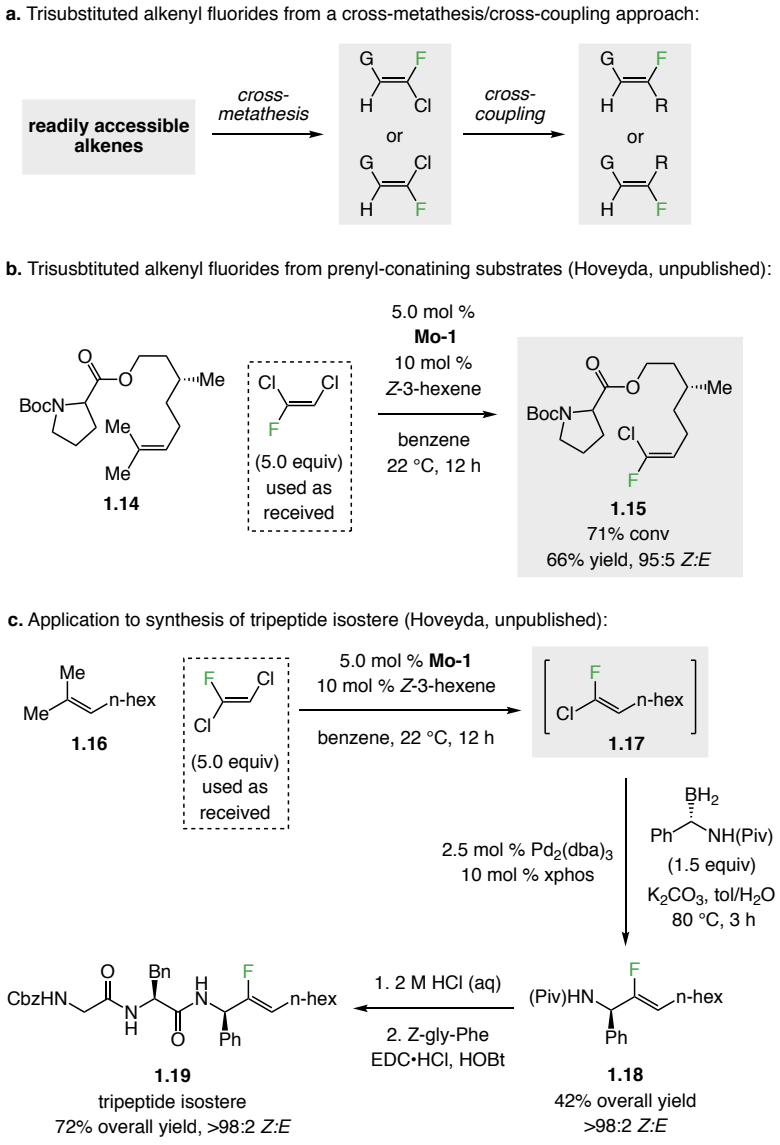

[21] (a) Nguyen, T. T.; Koh, M. J.; Mann, T. J.; Schrock, R. R.; Hoveyda, A. H. *Nature* **2017**, *552*, 347–354. (b) Koh, M. J.; Nguyen, T. T.; Lam, J. K.; Torker, S.; Hyvl, J.; Schrock, R. R.; Hoveyda, A. H. *Nature* **2017**, *542*, 80–85.

These products are particularly interesting because they can be easily transformed into trisubstituted alkenyl fluorides by catalytic cross-coupling (Scheme 1.6a). Cross-coupling reactions can be used to access a variety of trisubstituted alkenyl fluorides with high stereoisomeric purity.[22] Accordingly, *Z*-alkene **1.15** was formed in 95:5 *Z*:*E* ratio from *Z*-1,2-dichloro-1-fluoroethylene (Scheme 1.6b), and **1.18** in >98:2 *E*:*Z* ratio with *E*-1,2-dichloro-1-fluoroethylene (Scheme 1.6c). The versatility of the approach was further highlighted by combining cross-metathesis with cross-coupling for synthesis of *Z*-tripeptide isostere **1.19** in three steps starting from readily available 2-methyl-non-2-ene and *E*-1,2-dichloro-1-fluoroethylene (Scheme 1.6c).

1.4. Processes Involving Allylic Fluorides

Z-Trifluoromethyl-substituted alkenes may be generated from transformations involving commercially available olefin, *Z*-1,1,1,4,4,4-hexafluoro-2-butene (Scheme 1.7a).[23] One of the two (easily separable) products (**1.22**) was then utilized in catalytic enantioselective boryl substitution, affording 1,1-difluoroallyl boronate **1.23** (Scheme 1.7b).[24] This approach was inspired by reaction of α-trifluoromethylstyrene, reported by our group in 2011;[25] the enantioselective variant was disclosed more recently.[26] Catalytic cross-metathesis followed by NHC–Cu- or phosphine–Cu-catalyzed boryl substitution has been used to generate structurally diverse fluorine-containing compounds (e.g., **1.20**, **1.21**, **1.23**, and **1.24**, Scheme 1.7b).

---

[22] Liu, Q.; Mu, Y.; Schrock, R. R.; Hoveyda, A. H. unpublished results.

[23] Koh, M. J.; Nguyen, T. T.; Lam, J. K.; Torker, S.; Hyvl, J.; Schrock, R. R.; Hoveyda, A. H. *Nature* **2017**, *542*, 80–86.

[24] Lee, J. in Expedient Synthesis of Organoboronates through Catalytic Enantioselective Alkene Functionalization, Ph.D, Boston College, 2017.

[25] Corberán, R.; Mszar, N. W.; Hoveyda, A. H. *Angew. Chem., Int. Ed.* **2011**, *50*, 7079–7082.

[26] (a) Hoveyda, A. H.; Zhou, Y.; Shi, Y.; Brown, M. K.; Wu, H.; Torker, S. *Angew. Chem., Int. Ed.* **2020**, DOI: 10.1002/anie.202003755. (b) Paioti, P. H. S.; del Pozo, J.; Mikus, M. S.; Lee, J.; Koh, M. J.; Romiti, F.; Torker, S.; Hoveyda, A. H. *J. Am. Chem. Soc.* **2019**, *141*, 19917–19934.

Scheme 1.7. Catalytic Cross-Metathesis Used to Synthesize Allylic Fluorides

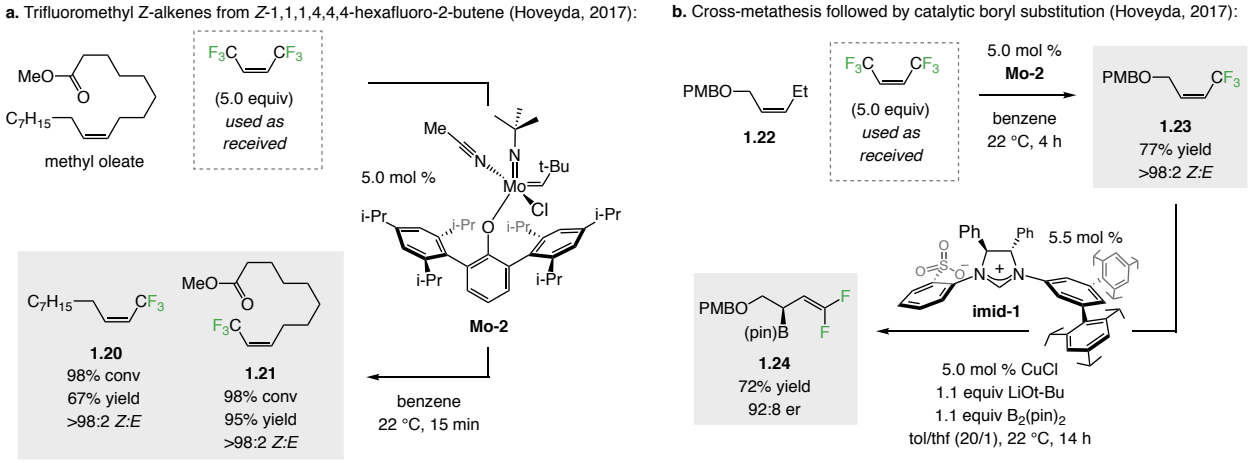

1.4.1. Allylic Fluorides as Electrophiles

The number of stereoselective reactions involving trifluoromethyl- and difluoromethyl-substituted alkenes has considerably increased in the past few years. There are several commercially available trifluoromethyl alkene substrates and many others can be prepared in a single step (Scheme 1.8a) by an ever-growing number of protocols using inexpensive reagents (e.g., Me_3SiCF_3, NaO_2SCF_3, or 2-trifluoromethylacrylic acid).[27]

Preparation of difluoromethyl-substituted alkenes is less well established and the majority of syntheses involve a ketone in combination with hazardous and expensive fluorinating reagents, such as diaminosulfur trifluoride (DAST), under demanding conditions.[28] Only recently have more amenable catalytic (and stereoselective) strategies been introduced.[29] One such example

[27] (a) Morimoto, H.; Tsubogo, T.; Litvinas, N. D.; Hartwig, J. F. *Angew. Chem., Int. Ed*. **2011**, *50*, 3793–3798. (b) Yin, J.; Li, Y.; Zhang, R.; Jin, K.; Duan, C. *Synthesis* **2014**, *46*, 607–612. (c) Kathiravan, S.; Nicholls, I. A. *Org. Lett.* **2015**, *17*, 1874–1877. (d) Omote, M.; Tanaka, M.; Ikeda, A.; Nomura, S.; Tarui, A.; Sato, K.; Ando, A. *Org. Lett.* **2012**, *14*, 2286–2289.

[28] (a) Thozer, M. J.; Herpin, T. F. *Tetrahedron* **1996**, *52*, 8619–8683. (b) Chambers, R. D. in Fluorine in Organic Chemistry, Blackwell Publishing Ltd, Hoboken, NJ; 2004, pp 62-69.

[29] Akiyama, S.; Kubota, K.; Mikus, M. S.; Paioti, P. H. S.; Romiti, F.; Liu, Q.; Zhou, Y.; Hoveyda, A. H.; Ito, H. *Angew. Chem., Int. Ed.* **2019**, *58*, 11998–12003.

entails the use of commercially available 1-bromo-1,1-difluoroethene, which undergoes C–C bond formation followed by catalytic cross-metathesis to deliver *E*-difluoroalkenes (Scheme 1.8b). A second approach involved alkyne–C bond formation with commercially available dibromodifluoromethane and subsequent alkene reduction to afford a *Z*-difluoroalkene (Scheme 1.8b).

Scheme 1.8. Synthesis of Trifluoro- and Difluoromethyl Alkenes

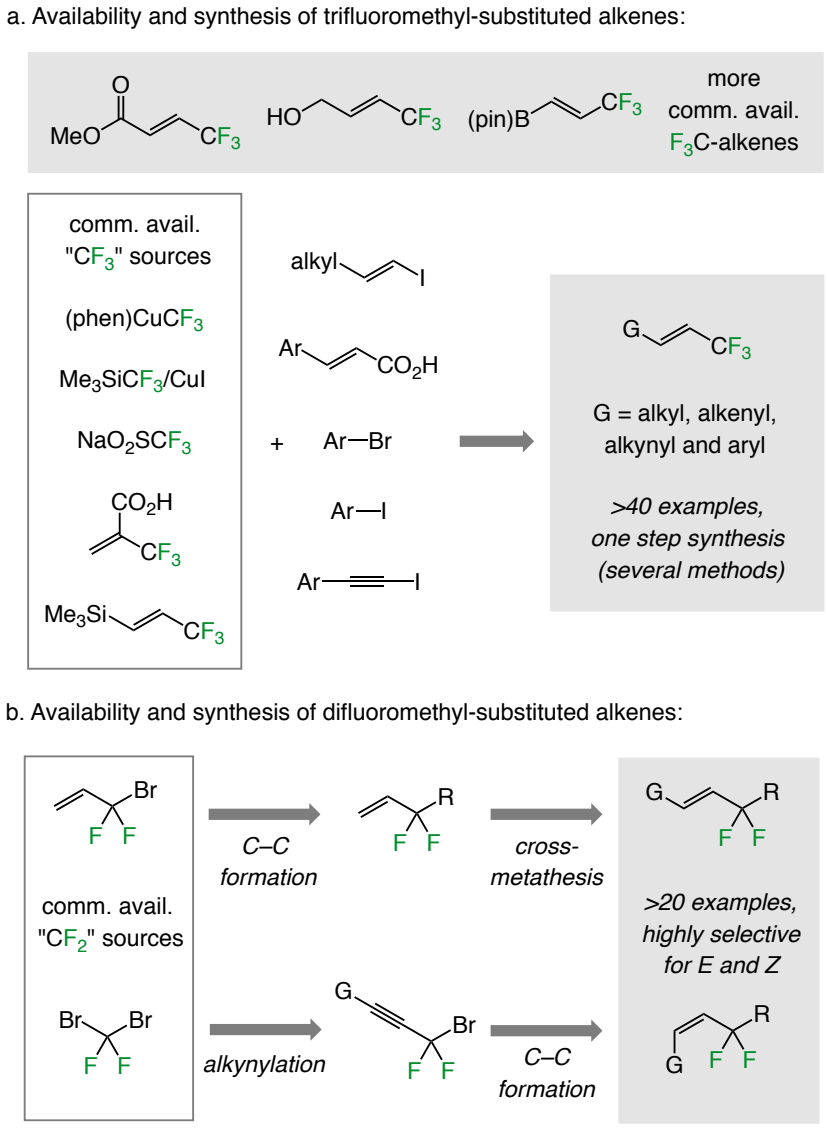

1.4.1.1. In Allylic Substitution Reactions

An early example of catalytic enantioselective allylic substitution with trifluoromethyl alkenes was a phosphine–Rh-catalyzed C–aryl bond forming process, reported by Hayashi *et al.*[30] More recently, Cu-based complexes have been used. Shi[31] published on an alkyl substitution process promoted by NHC–Cu complexes (Scheme 1.9a). Subsequently, Ito[32] and Shi[33] concomitantly disclosed the first examples of boryl substitution reactions (confined to aliphatic substrates) promoted by bisphosphine-Cu–B(pin) complexes (Scheme 1.9b). Our group[27] described a more broadly applicable strategy for boryl as well as silyl substitution reactions (aliphatic and aromatic alkenes may be used), catalyzed by an NHC–Cu complex (Scheme 1.9c-d). Most recently, Miura and Hirano[34] disclosed a method for boryl substitution facilitated by bisphosphine–Cu catalysts (Scheme 1.9e).

The aforementioned approaches have a key feature in common, namely, a Cu–F elimination step, the mechanism of which has been a topic of much debate. In 2019, our group disclosed the results of detailed mechanistic studies, revealing that a Cu–alkyl species is the resting state of the catalytic cycle, and that fluoride elimination, which occurs in an antiperiplanar fashion and is assisted by a hard Lewis acid (Li^+ or Na^+), is the slow step. It was further shown that a Lewis base can accelerate C–F elimination in C–B (vs C–Si) bond forming processes, likely through an activated boronate complex (Scheme 1.9f).[27]

---

[30] Huang, Y.; Hayashi, T. *J. Am. Chem. Soc.* **2016**, *138*, 12340–12343.

[31] Wang, P.; Pu, X.; Zhao, Y.; Wang, P.; Li, Z.; Zhu, C.; Shi, Z. *J. Am. Chem. Soc*. **2018**, *140*, 9061–9065.

[32] Kojima, R.; Akiyama, S.; Ito, H. *Angew. Chem., Int. Ed.* **2018**, *57*, 7196–7199.

[33] Gao, P.; Yuan, C.; Zhao, Y.; Shi, Z. *Chem* **2018**, *4*, 2201–2211.

[34] Kojima, Y.; Takata, T.; Hirano, K.; Miura, M. *Chem. Lett*. **2020**, 637–640.

Scheme 1.9. Catalytic Allylic Substitution Reactions with Allylic Fluorides as Substrates

a. Alkyl substitution with aliphatic and aryl alkenes (Shi, 2018):

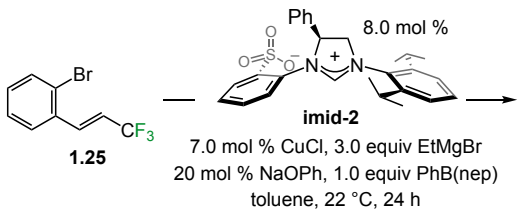

b. Boryl substitution with aliphatic alkenes (Ito, 2018):

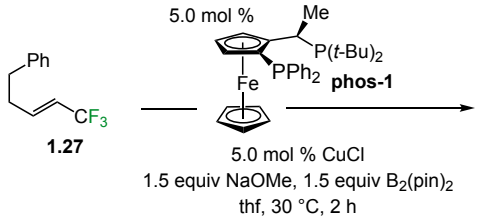

c. Boryl substitution with aliphatic and aryl alkenes (Hoveyda-Torker, 2019)**:**

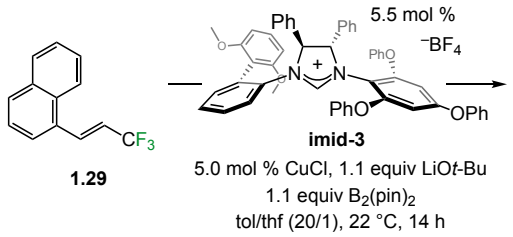

d. Silyl substitution with aliphatic and aryl alkenes (Hoveyda-Torker, 2019)**:**

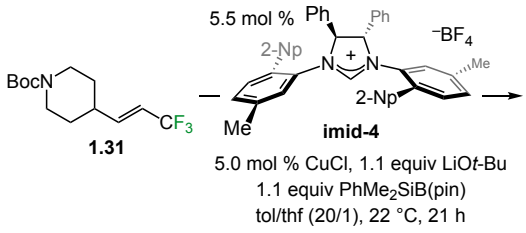

e. Reductive substitution with trisubstituted alkenes (Miura-Hirano, 2020):

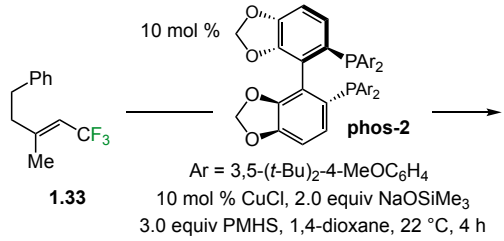

f. Key findings of mechanistic studies (Hoveyda, 2019):

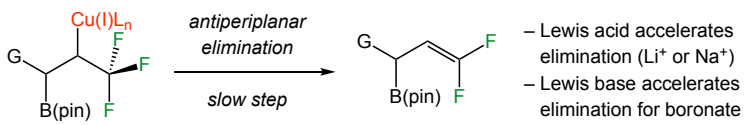

1,1-Difluoroalkenes, such as **1.26**, **1.28**, **1.30**, **1.32**, and **1.34** (Scheme 1.9), are valuable partly because they are amide bond mimics[35] and masked carboxylic acids.[36] Synthesis of these entities by allylic substitution is complementary to the aforementioned Julia-Kocienski reactions (see Scheme 1.2). 1,1-Difluoroallyl boronates can be further transformed with stereospecificity (Scheme 1.10).[27,32] For instance, oxidation of **1.35** followed by esterification generated 1,1-difluoroallyl ester **1.36**, which then underwent stereospecific Ireland-Claisen rearrangement to give difluoro carboxylic acid **1.37** (Scheme 1.10a).[37] *Gem*-difluoromethylene groups are carbonyl mimics; thus, **1.37** is a configurationally stable β-ketoacid surrogate.[38]

Another transformation consists of stereospecific allyl addition to an aldehyde[39] to give difluoromethyl homoallylic alcohol **1.38**, which can undergo a second catalytic boryl substitution, this time catalyzed by a bisphosphine-Cu–B(pin) complex (**1.39**, Scheme 1.10a). The latter process, is based on an approach developed collaboratively by Ito and Hoveyda groups (Scheme 1.10b); such transformations afford trisubstituted alkenyl fluorides (amide mimics) with a (pin)B-substituted allylic carbon stereogenic center. Two additional features merit specific mention: 1) the *E*-difluoroalkene (**1.41**) can be prepared by catalytic stereoselective cross-metathesis. 2) The fluoro-containing allylic boronate **1.44** underwent reaction with an imine to give **1.45**. This is in contrast to 1,1-difluoroallyl boronate **1.35**, which while sufficiently reactive to add to an aldehyde,

---

[35] (a) Bobek, M.; Kavai, I.; De Clercq, E. *J. Med. Chem.* **1987**, *30*, 1494−1497. (b) Leriche, C.; He, X.; Chang, C.-W. T; Liu, H.-W. *J. Am. Chem. Soc.* **2003**, *125*, 6348–6349.

[36] Juncosa, J. I.; Takaya, K.; Le, H. V.; Moschitto, M. J.; Weerawarna, P. M.; Mascarenhas, R.; Liu, D.; Dewey, S. L.; Silverman, R. B. *J. Am. Chem. Soc.* **2018**, *140*, 2151–2164.

[37] (a) Damon, D. B.; Hoover, D. J. *J. Am. Chem. Soc*. **1990**, *112*, 6439−6442. (b) Hirai, G.; Watanabe, M.; Yamaguchi, K.; Miyagi, T.; Sodeoka, M. *J. Am. Chem. Soc*. **2007**, *129*, 15420–15421.

[38] (a) Ellis, B. D.; Milligan, J. C.; White, A. R.; Duong, V.; Altman, P. X.; Mohammed, L. Y.; Crump, M. P; Crosby, J.; Luo, R.; Vanderwal, C. D.; Tsai, S.-C. *J. Am. Chem. Soc*. **2018**, *140*, 4961–4964. (b) Shi, T.; Liu, L.; Tao, W.; Luo, S.; Fan, S.; Wang, X.; Bai, L; Zhao, Y. *ACS Catal.* **2018**, *8*, 4323–4332.

[39] Chen, J. Y.-L.; Aggarwal, V. K. *Angew. Chem., Int. Ed.* **2014**, *53*, 10992–10996.

could not be used for additions to less reactive aldimines. Reaction between **1.35** and imines is yet to be developed, and is a potentially useful method applicable to synthesis of trisubstituted alkenyl fluorides, which are peptidomimetics.[40]

Scheme 1.10. Represenative Applications of Stereochemically Defined Fluoro-Allyl Boronates

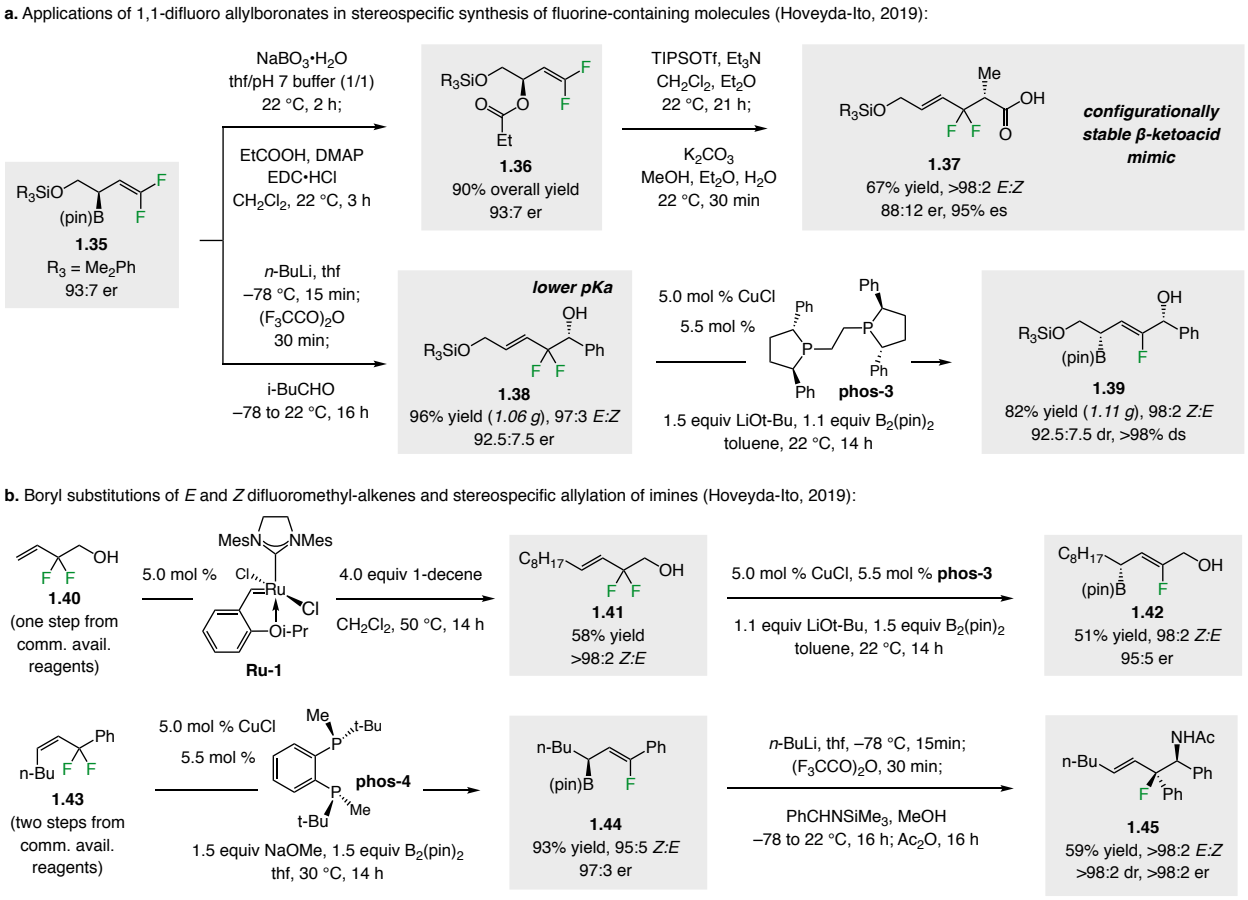

A mechanistically noteworthy aspect of these processes relates to the effect of the metal cation on reactivity (Li>Na>K), implying that the cation interacts with the fluorine to facilitate C–F bond rupture. Similar conclusions were reached by our group in the course of investigating

[40] (a) Drouin, M.; Paquin, J. F. *Beilstein J. Org. Chem*. **2017**, *13*, 2637−2658. (b) Altman, R. A.; Sharma, K. K.; Rajewski, L. G.; Toren, P. C.; Baltezor, M. J.; Pal, M.; Karad, S. N. *ACS Chem. Neurosci*. **2018**, *9*, 1735–1742.

the mechanism of boryl and silyl substitution reactions with trifluoromethyl alkenes (Scheme 1.9f).[27]

1.4.1.2. In Additions of Cu–X Complexes

Trifluoromethyl-substituted alkenes are attractive substrates for methods that allow for synthesis of compounds bearing F_3C-substituted tertiary or quaternary carbon stereogenic centers.[41] In addition processes that are catalyzed by a transition metal-based complex, a key issue is competitive metal–fluoride elimination. Two recent reports involve preferential trapping of Cu–alkyl intermediates in preference to Cu–F β-elimination (Scheme 1.11).

Scheme 1.11. Examples of Cu–B(pin) Additions to F_3C-Substituted Olefins

a. Hydroamination of trifluoromethyl-substituted alkenes (Miura-Hirano, 2019):

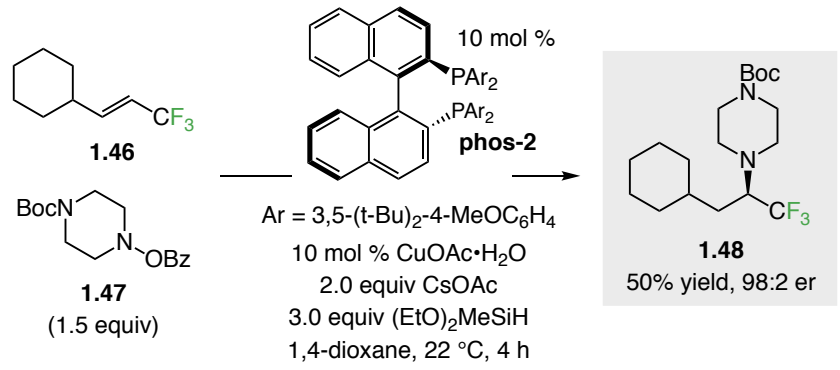

b. Deuteroboration of trifluoromethyl-substituted alkenes (Hoveyda-Torker, 2019):

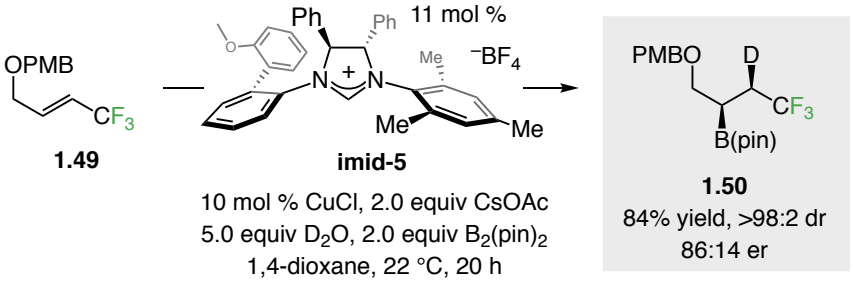

[41] Nie, J.; Guo, H-C.; Cahard, D.; Ma, J.-A. *Chem. Rev.* **2011**, *111*, 455–529.

One example, developed by Miura and Hirano,[42] entails a bisphosphine-Cu–H addition to an alkene, followed by trapping of the resulting Cu–alkyl species with benzoyloxyamine to furnish α-CF_3-amine products (e.g., **1.48**, Scheme 1.11a). Our group introduced an early example of diastereo- and enantioselective Cu–B(pin) addition to an alkene[43] and we have demonstrated recently that deuterolysis of the Cu–C bond with D_2O generated **1.50** diastereoselectively, indicating that Cu–B addition occurs with *syn* stereochemistry (Scheme 1.11b). The stereochemical integrity of the Cu–alkyl intermediate was preserved and the presence of CsOAc was key in curtailing Cu–F β-elimination (owing to the weakly Lewis acidic cesium cation and the weakly Lewis basic acetate anion).[27]

Trifluoromethyl alkenes can be incorporated into Michael acceptors, a strategy utilized by Huang and coworkers in their NHC-catalyzed enantioselective conjugate addition of primary amines to β-trifluoromethyl nitro-olefins (Scheme 1.12); the F_3C-containing nitroolefins were synthesized in one step from trifluoromethyl ketones. The resulting β-nitro,α-CF_3 amines (**1.52**) can be reduced to diamines, which are precursors to different heterocycles (**1.54** or **1.65**).

[42] (a) Takata, T.; Hirano, K.; Miura, M. *Org. Lett.* **2019**, *21*, 4284–4288. (b) Paioti, P. H. S.; del Pozo, J.; Mikus, M. S.; Lee, J.; Koh, M. J.; Romiti, F.; Torker, S.; Hoveyda, A. H. *J. Am. Chem. Soc.* **2019**, *141*, 19917–19934.

[43] Lee, Y.; Hoveyda, A. H. *J. Am. Chem. Soc.* **2009**, *131*, 3160–3161.

Scheme 1.12. Enantioselective Conjugate Additions

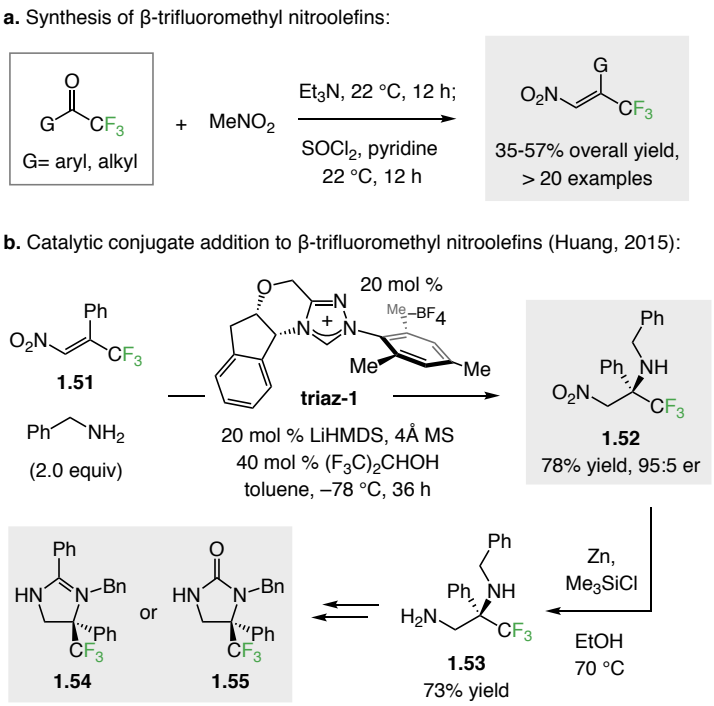

1.4.2. In Reactions with Fluoro-Substituted Allyl Nucleophiles

The presence of an allylic fluorine atom reduces the nucleophilicity of the neighboring alkene.[44] Yet, it is noteworthy that catalytic transformations have been developed where a trifluoromethyl-substituted alkene serves as a nucleophile.

1.4.2.1. Allyl Addition Processes

One strategy to address the diminished nucleophilicity of a trifluoromethyl alkene is to incorporate it within an allyl boronate. Accordingly, and based on the substitutions discussed above (Scheme 1.10), our group has developed a method for *Z*-selective NHC–Cu-catalyzed boryl substitution of 3,3,4,4,4-pentafluoro-1-butene for synthesis of F/CF_3-substituted allyl boronate

[44] Pacheco, M. C.; Purser, S.; Gouverneur, V. *Chem. Rev.* **2008**, *108*, 1943–1981.

1.56 (Scheme 1.13a).[45] The allyl boronate was shown to react with an aldehyde (**1.57**), in the presence of 5.0 mol % of a commercially available aminophenol, to afford homoallylic alcohol **1.58**, bearing a fluorine- and trifluoromethyl-substituted allylic stereogenic center, in high γ:α ratio, as well as diastereo- and enantioselectivity. Further transformations afforded a known intermediate (**1.60**) of a CF_3 analog of the anti-hepatitis C drug sofosbuvir (sold as Sovaldi; Scheme 1.13b).

Scheme 1.13. Catalytic γ-, Diastereo-, and Enantioselective Reactions of Fluoroallyl Boronates

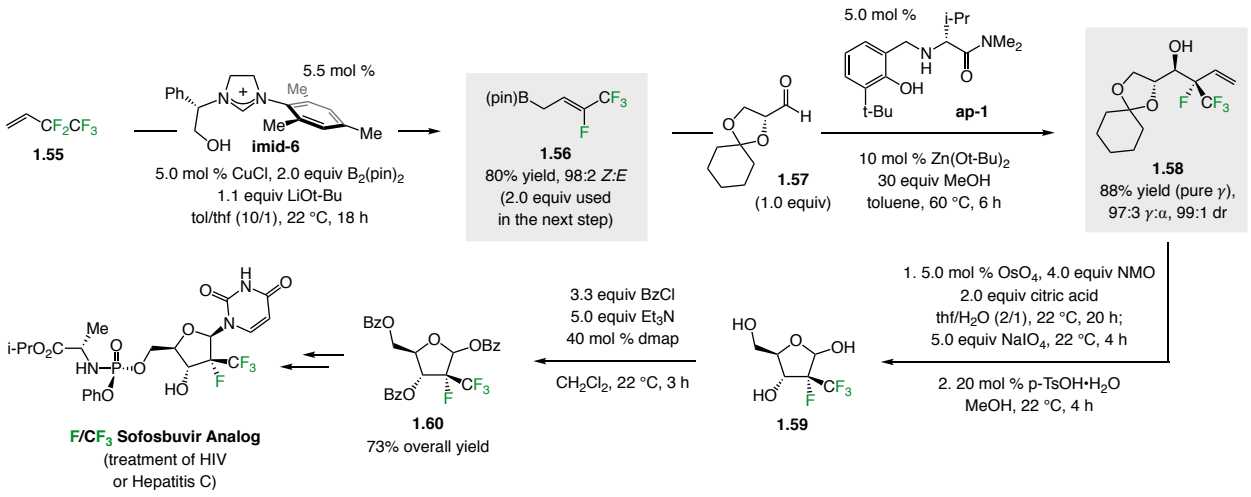

Krische *et al.* have developed a method for diastereo- and enantioselective (*anti*) synthesis of homoallylic alcohols with a F_3C-substituted stereogenic center (Scheme 1.14).[46] The requisite allylic benzoate **1.62** was prepared in two steps from commercially available trifluoromethylacetaldehyde. The reaction is proposed to proceed via a π-allyl Ir(III) intermediate, generated in situ by dehydrogenation of a primary alcohol. The utility of the approach was demonstrated by synthesis of 3-trifluoromethylpiperidine **1.64**, a motif encountered in epidermal

[45] Morrison, R. J.; Romiti, F.; Lee, K.; Lee, J.; Koh, M. J.; Hu, S.; Hoveyda, A. H., manuscript in preparation.
[46] Gao, X.; Zhang, Y. J.; Krische, M. J. *Angew. Chem., Int. Ed.* **2011**, *50*, 4173–4175.

growth factor receptor inhibitors (EGFR). More recently, the same team reported a related strategy that involves F_3C-substituted allenes.[47]

Scheme 1.14. Catalytic *Anti*- and Enantioselective F_3C-Substituted Allyl Additions to Aldehydes

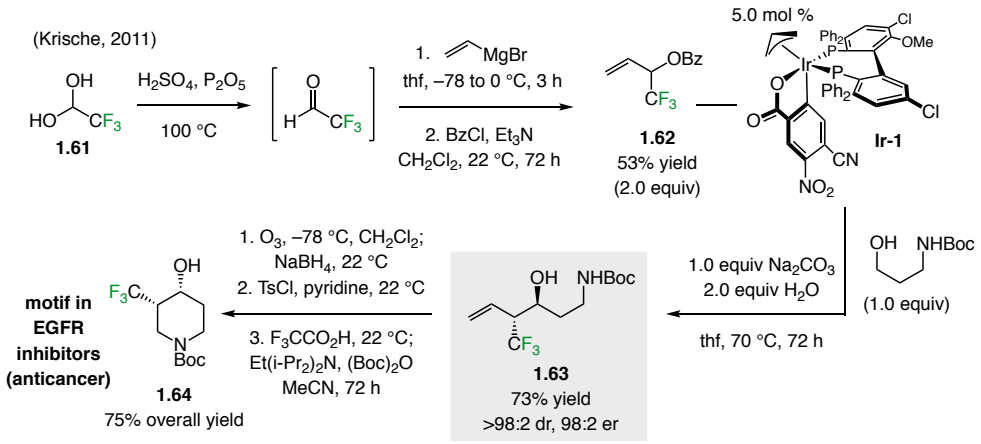

1.4.2.2. Cycloadditions

Inspired by previous reports involving π-allyl–Pd intermediates, Trost has developed a set of catalytic diastereo- and enantioselective cycloaddition reactions, which proceed via a fluorine-containing Pd–TMM (TMM = trimethylenemethane) complex (Scheme 1.15).[48] The starting F_3C-substituted allyl carbonate (**1.66**) was synthesized from a readily available allyl bromide (**1.65**) and Me_3SiCF_3. It was shown that difluoromethyl-substituted allyl carbonates may be used with similar efficiency and selectivity. The applicability of the method was highlighted by stereoselective synthesis of nicotinic acetylcholine receptor (nAChR) agonist **1.68**.

[47] Holmes, M.; Nguyen, K. D.; Schwartz, L. A.; Luong, T.; Krische, M. J. *J. Am. Chem. Soc.* **2017**, *139*, 8114–8117.

[48] Trost, B. M.; Wang, Y.; Hung, C.-I. *Nat. Chem.* **2020**, *12*, 294–301.

Scheme 1.15. Catalytic Cycloadditions Involving F_3C-Substituted TMM Compounds

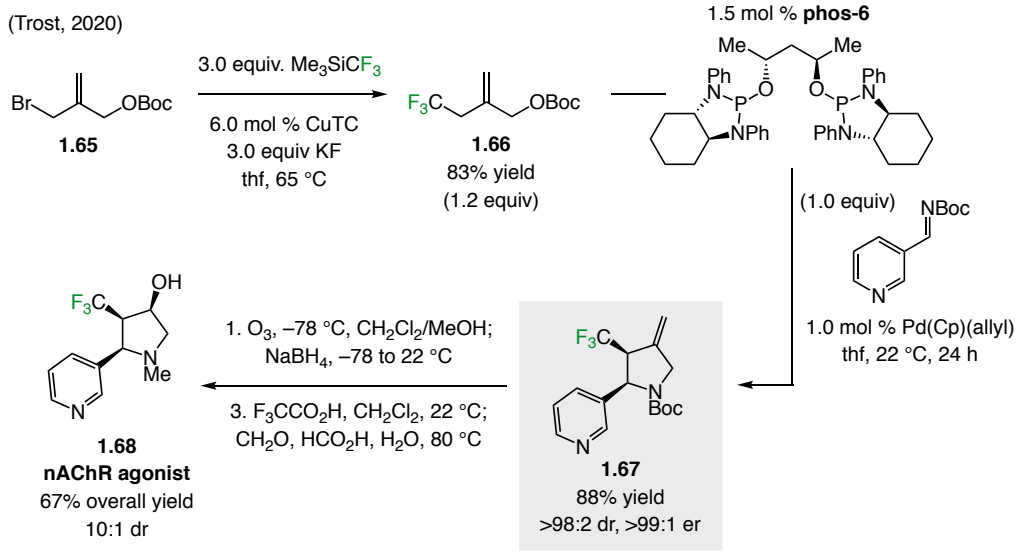

1.5. Processes Involving Fluorine-Containing Ketones and Ketimines

Fluorine-containing compounds that contain a carbonyl or imine functional group have been shown to serve as either electrophiles or nucleophiles. When used as an electrophile, homoallylic, propargylic, or alkynyl alcohols and amines can be synthesized. When playing the role of a nucleophile, a variety of other products can be generated by means of different transformations (e.g., cross-coupling or Mannich-type processes).

1.5.1. Transformations Involving Ketones and Imines as Substrates

Because of the importance of organofluorine compounds in medicine, a significant number of fluorine-containing organic molecules are now commercially offered, and many can be purchased at low cost. These include a range of *o-, m-, p*-substituted fluoromethyl ketones (Scheme 1.16a). Ketones that cannot be purchased can be easily prepared through substitution reactions. For instance, treatment of a fluoro-substituted ethyl ester, an inexpensive source of fluoromethyl groups (Scheme 1.16b), with an organolithium or Grignard reagent (G = alkyl,

alkenyl, alkynyl, aryl) leads to the formation of such ketones.[49] Additionally, Ruppert's reagent, or a derivative, may be used to synthesize fluoro-containing ketones from a corresponding ester or aldehyde and a relatively inexpensive fluoride source (e.g., tetrabutylammonium fluoride (tbaf) or cesium fluoride).[50]

Another popular strategy entails reaction of a silyl enol ether with Selectfluor, an inexpensive and easy to handle reagent, affording a monofluoromethyl ketone product (Scheme 1.16b).[51] Selectfluor can be used in conjunction with an activated ketimine; subsequent hydrolysis then gives the fluoro-substituted ketone (Scheme 1.16b).[52]

Scheme 1.16. Sources of Fluorinated Ketones and Imines

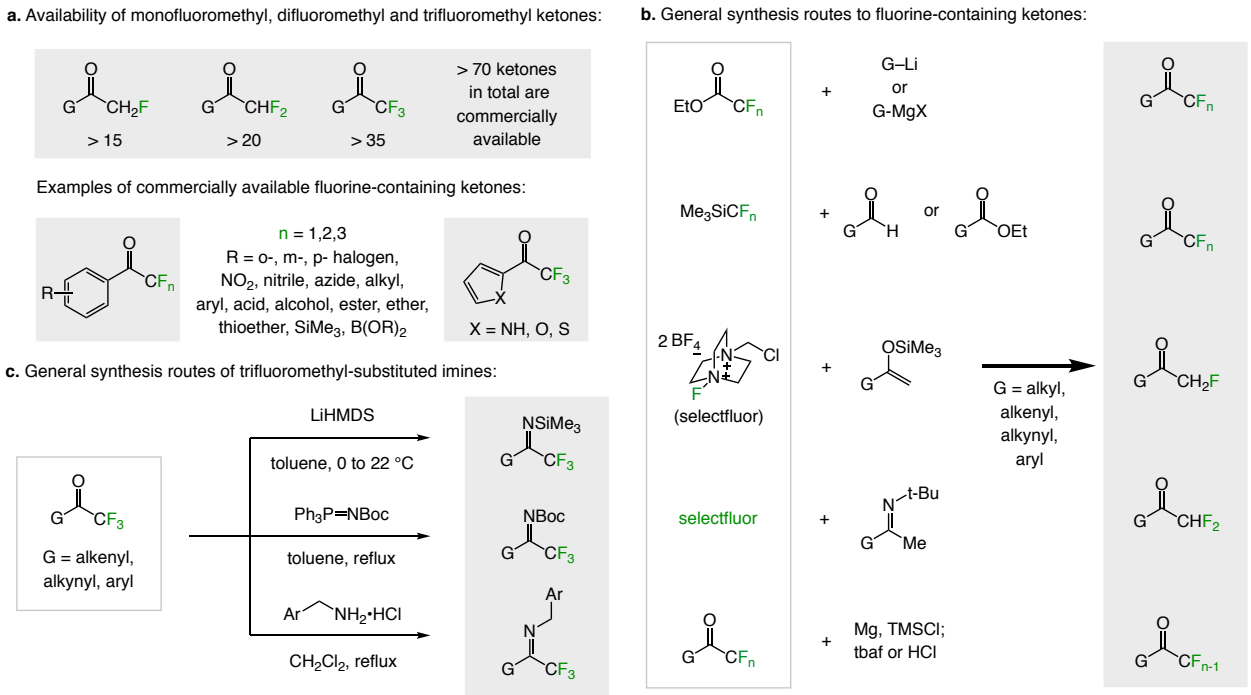

[49] (a) Kitazume, T.; Asai, M.; Lin, J. T.; Yamazaki, T. *J. Fluorine Chem.* **1987**, *35*, 477–488. (b) Chong, J. M.; Mar, E. K. *J. Org. Chem.* **1991**, *56*, 893–896. (c) Matador, E.; de Gracia Retamosa, M.; Jiménez-Sánchez, A.; Monge, D.; Fernández, R.; Lassaletta, J. M. *Eur. J. Org. Chem.* **2019**, *1*, 130–138.

[50] (a) Singh, R. P.; Kirchmeier, R. L.; Shreeve, J. M. *Org. Lett.* **1999**, *1*, 1047–1049. (b) Singh, R. P.; Cao, G.; Kirchmeier, R. L.; Shreeve, J. M. *J. Org. Chem.* **1999**, *64*, 2873–2876. (c) Pravst, I.; Zupan, M.; Stavber, S. *Synthesis* **2005**, *18*, 3140–3146.

[51] Fuglseth, E.; Thvedt, T. H. K.; Møll, M. F.; Hoff, B. H. *Tetrahedron* **2008**, *64*, 7318–7323.

[52] Pravst, I.; Zupan, M.; Stavber, S. *Synthesis* **2005**, *18*, 3140–3146.

Other strategies include oxidation/fluorine incorporation within a commercially available styrene,[53] and nucleophilic substitution involving a commercially available α-bromomethylketone.[54] Removal of one or more fluorine atoms from a readily available trifluoromethyl ketone is another way of accessing a difluoro- or monofluoromethyl derivative.[55]

Trifluoromethyl ketimines can be readily synthesized from ketones, and additions to such electrophiles offer access to the corresponding α-tertiary amines (Scheme 1.16c).[1] There are two reported strategies along these lines, each of which entail the use of either LiHMDS or *n*-BuLi/HMDS (HMDS – hexamethyldisilazide) to afford a *N*-trimethylsilyl ketimine.[56] *N*-Boc imines can be obtained from a commercially available ylide reagent,[57] and *N*-benzyl ketimines can be synthesized from the commercially available benzyl amine salt.[58] Preparation of Fmoc imines from a combination of a trifluoromethyl ketone and Fmoc-NH_2 or trifluoromethyl amine and fluoroenone is yet another option.[59]

1.5.1.1. Additions to Ketones

Because of their relatively high electrophilicity, trifluoromethyl ketones are difficult substrates for development of catalytic enantioselective additions (i.e., fast uncatalyzed side

[53] Yang, Q.; Mao, L.-L.; Yang, B.; Yang, S.-D. *Org. Lett.* **2014**, *16*, 3460–3463.

[54] Moughamir, K.; Atmani, A.; Mestdagh, H.; Rolando, C.; Francesch, C. *Tetrahedron Lett.* **1998**, *39*, 7305–7306.

[55] Prakash, G. K. S.; Hu, J.; Olah, G. A. *J. Fluorine Chem.* **2001**, *112*, 357–362.

[56] (a) Krüger, C.; Rochow, E. G.; Wannagat, U. *Chem. Ber.* **1963**, *96*, 2132–2137. (b) Gosselin, F.; O'Shea, P. D.; Roy, S.; Reamer, R. A.; Chen, C.; Volante, R. P. *Org. Lett.* **2005**, *7*, 355–358. (c) Sukach, V.; Melnykov, S.; Bertho, S.; Diachenko, I.; Retailleau, P.; Vovk, M.; Gillaizeau, I. *Org. Lett.* **2019**, *21*, 2340–2345.

[57] Morisaki, K.; Morimoto, H.; Ohshima, T. *Chem. Commun.* **2017**, *53*, 6319–6322.

[58] Wu, Y.; Deng, L. *J. Am. Chem. Soc.* **2012**, *134*, 14334–14337.

[59] (a) Shen, C.; Wang, R.-Q.; Wei, L.; Wang, Z.-F.; Tao, H.-Y.; Wang, C.-J. *Org. Lett.* **2019**, *21*, 6940–6945. (b) Wang, Y.; Deng, L.-F.; Zhang, X.; Niu, D. *Org. Lett.* **2019**, *21*, 6951–6956.

reactions). Over the last 20 years, there have been several noteworthy advances,[60] but a number of shortcomings persist. Among these are the need for costly precious metals (indium and rhodium) and/or toxic tin-based reagents, low enantioselectivities, and high catalyst loadings.[61] In 2016 and 2017, our group outlined broadly applicable and highly enantioselective strategies for additions of allyl and crotyl moieties to trifluoromethyl ketones. Aminophenol-based boryl catalysts, which contain an ammonium moiety were used. Enantioselectivity is likely the result of electrostatic attraction between the catalyst's ammonium moiety and a C–F bond of the trifluoromethyl unit of the substrate (Scheme 1.17a).[62]

Notably, the aforementioned catalytic method proved to be ineffective for di- and monofluoromethyl ketones, but this shortcoming can be resolved through the use of silyl-containing aminophenols **ap-3** and **ap-4** (Scheme 1.17b).[63] Steric factors are more dominant when the corresponding chiral catalysts are involved, and, as a result, the tertiary homoallylic alcohol products are obtained in high enantioselectivity. To demonstrate applicability, we synthesized a set of fluoro-substituted triazole-containing homoallylic alcohols. Ketones **1.71** and **1.74** were prepared from the corresponding commercially available fluoromethyl ethyl esters and a single-

---

[60] For additions of aryl groups, see: (a) Bai, X.; Zeng, G; Shao, T.; Jiang, Z. *Angew. Chem., Int. Ed.* **2017**, *56*, 3684–3688. (b) Nie, J.; Zhang, G.-W.; Wang, L.; Fu, A.; Zheng, Y.; Ma, J.-A. *Chem. Commun.* **2009**, 2356–2358. For alkenyl and prenyl additions, see: Motoki, R.; Tomita, D.; Kanai, M.; Shibasaki, M. *Tetrahedron Lett.* **2006**, *47*, 8083–8086. For additions of enynes, see: Gan, X.-C.; Zhang, Q.; Jia, X.-S.; Yin, L. *Org. Lett.* **2018**, *20*, 1070–1073.

[61] (a) Loh, T.-P.; Zhou, J.-R.; Li, X.-R. *Tetrahedron Lett.* **1999**, *40*, 9333–9336. (b) Zhang, X.; Chen, D.; Liu, X.; Feng, X. *J. Org. Chem.* **2007**, *72*, 5227–5233. (c) Haddad, T. D.; Hirayama, L. C.; Taynton, P.; Singaram, B. *Tetrahedron Lett.* **2008**, *49*, 508–511. (d) Haddad, T. D.; Hirayama, L. C.; Singaram, B. *J. Org. Chem.* **2010**, *75*, 642–649. (e) Ito, J.; Ubukata, S.; Muraoka, S.; Nishiyama, H. *Chem. Eur. J.* **2016**, *22*, 16801–16804. (f) Nakamura, S.; Hara, Y.; Furukawa, T.; Hirashita, T. *RSC Adv.* **2017**, *7*, 15582–15585.

[62] (a) Lee, K.; Silverio, D. L.; Torker, S.; Haeffner, F.; Robbins, D. W.; van der Mei, F. W.; Hoveyda, A. H. *Nat. Chem.* **2016**, *8*, 768–777. (b) van der Mei, F. W.; Qin, C.; Morrison, R. J.; Hoveyda, A. H. *J. Am. Chem. Soc.* **2017**, *139*, 9053–9065.

[63] Fager, D. C.; Lee, K.; Hoveyda, A. H. *J. Am. Chem. Soc.* **2019**, *141*, 16125–16138.

vessel allyl addition/cycloaddition afforded triazoles **1.73** and **1.75** efficiently and in high enantiomeric purity.

Scheme 1.17. Catalytic Enantioselective Allyl Additions to Fluoromethyl Ketones

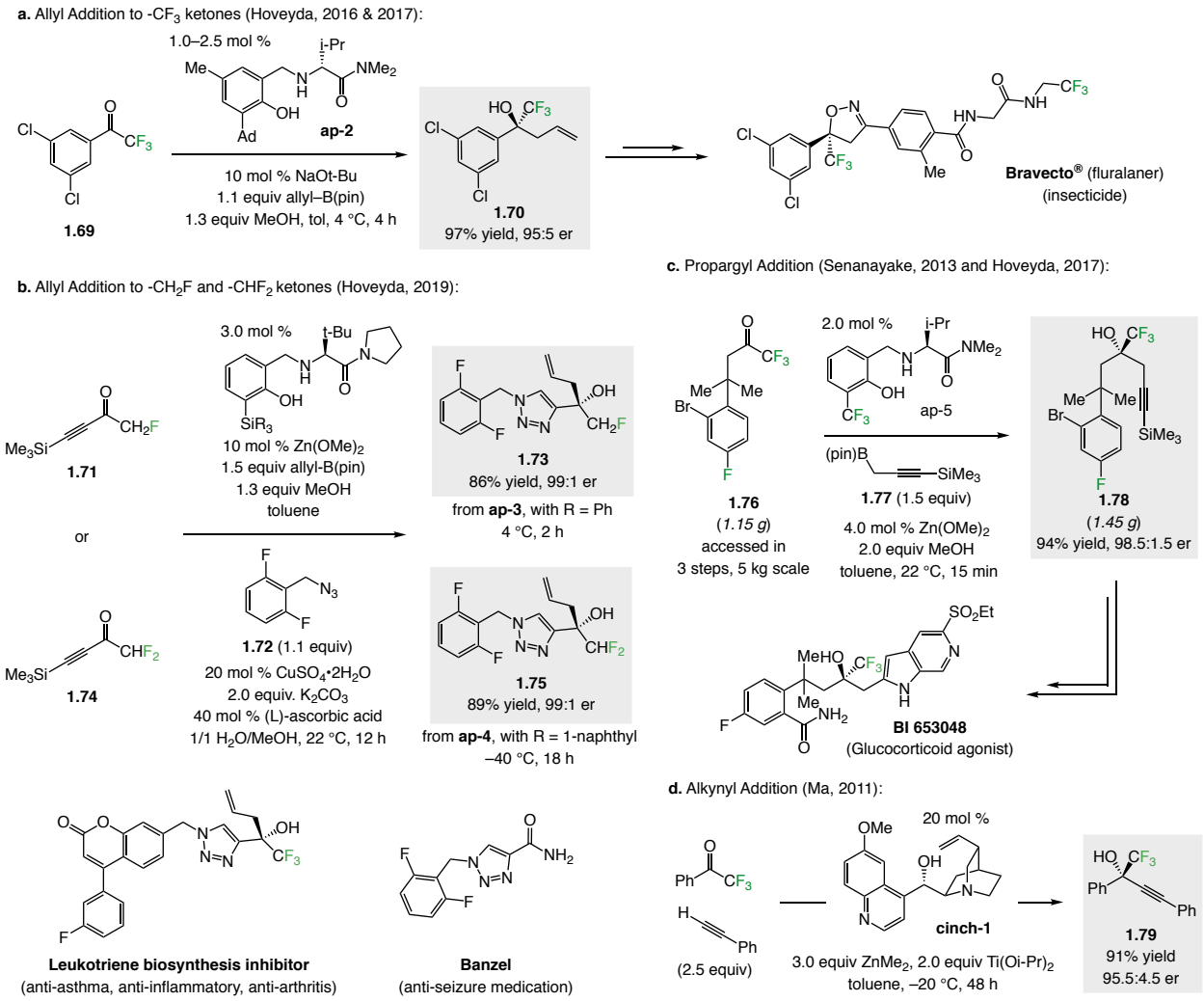

Related catalytic enantioselective propargyl additions can be effected by the use of trimethylsilyl-substituted propargyl–B(pin) **1.77** as the reagent (Scheme 1.17c).[64] The ketone substrate **1.76** has been prepared on kilogram scale from readily available trifluoroacetic

[64] Mszar, N. W.; Mikus, M. S.; Torker, S.; Hoveyda, A. H. *Angew. Chem., Int. Ed.* **2017**, *56*, 8736–8741.

anhydride.[65] As a highlight, **1.78**, the key intermediate for the synthesis of BI 653048, was synthesized enantioselectively through an addition process that was complete in just 15 minutes (94% yield, 1.45 g). It merits note that methods for alkynyl additions[66] have been reported. Notably, in 2011, Ma *et al.* disclosed a method involving a cinchona-alkaloid catalyst (Scheme 1.17d).[67]

1.5.1.2. Additions to NH-Ketimines

There have been important recent advances regarding enantioselective synthesis of trifluoromethyl α-tertiary amines,[68] however, there are shortcomings here as well. Among these are the frequent use of protecting/activating groups, deprotection/oxidation state adjustments limit application in more complex molecules,[69] and costly iridium- and indium-based catalysts prevent

---

[65] Reeves, J. T.; Fandrick, D. R.; Tan, Z.; Song, J. J.; Rodriguez, S.; Qu, B.; Kim, S.; Niemeier, O.; Li, Z.; Byrne, D.; Campbell, S.; Chitroda, A.; DeCroos, P.; Fachinger, T.; Fuchs, V.; Gonnella, N. C.; Grinberg, N.; Haddad, N.; Jäger, B.; Lee, H.; Lorenz, J. C.; Ma, S.; Narayanan, B. A.; Nummy, L. J.; Premasiri, A.; Roschangar, F.; Sarvestani, M.; Shen, S.; Spinelli, E.; Sun, X.; Varsolona, R. J.; Yee, N.; Brenner, M.; Senanayake, C. H. *J. Org. Chem.* **2013***, 78,* 3616–3635.

[66] For additional examples of alkynyl additions, see: (a) O'Hagan, D.; Zaidi, N. A.; Lamont, R. B. *Tetrahedron: Asymm.* **1993**, *4*, 1703–1708. (b) Thompson, A.; Corley, E. G; Huntington, M. F.; Grabowski, E. J. J.; Remenar, J. F.; Collum, D. B. *J. Am. Chem. Soc.* **1998**, *120*, 2028–2038. (c) Motoki, R.; Kanai, M.; Shibasaki, M. *Org. Lett.* **2007**, *9*, 2997–3000. (d) Ito, J.; Ubukata, S.; Muraoka, S.; Nishiyama, H. *Chem. Eur. J.* **2016**, *22*, 16801–16804.

[67] Zhang, G.-W.; Meng, W.; Ma, H.; Nie, J.; Zhang, W.-Q.; Ma, J.-A. *Angew. Chem., Int. Ed.* **2011**, *50*, 3534–3542.

[68] For methods for synthesis of trifluoromethyl α-tertiary amines, see: (a) Lauzon, C.; Charette, A. B. *Org. Lett.* **2006**, *8*, 2743–2745. (b) Fu, P.; Snapper, M. L.; Hoveyda, A. H. *J. Am. Chem. Soc.* **2008**, *130*, 5530–5541. (c) Jiang, B.; Dong, J. J.; Si, Y. G.; Zhao, X. L.; Huang, Z. G.; Xu, M. *Adv. Synth. Catal.* **2008**, *350*, 1360–1366. (d) Sukach, V. A.; Golovach, N. M.; Pirozhenko, V. V.; Rusanov, E. D.; Vovk, M. V. *Tetrahedron: Asymm.* **2008**, *19*, 761–764. (e) Hara, N.; Tamura, R.; Funahashi, Y.; Nakamura, S. *Org. Lett.* **2011**, *13*, 1662–1665. (f) Husmann, R.; Sugiono, E.; Mersmann, S.; Raabe, G.; Rueping, M.; Bolm, C. *Org. Lett.* **2011**, *13*, 1044–1047. (g) Huang, G.; Yang, J.; Zhang, X. *Chem. Commun.* **2011**, *47*, 5587–5589. (h) Liu, Y.-L.; Shi, T.-D.; Zhou, F.; Zhao, X.-L.; Wang, X.; Zhou, J. *Org. Lett.* **2011**, *13*, 3826–3829. (i) Sun, L.-H.; Liang, Z.-Q.; Jia, W.-Q.; Ye, S. *Angew. Chem., Int. Ed.* **2013**, *52*, 5803–5806. (j) Zhang, S.; Li, L.; Hu, Y.; Li, Y.; Yang, Y.; Zha, Z.; Wang, Z. *Org. Lett.* **2015**, *17*, 5036–5039. (k) Chen, P.; Yue, Z.; Zhang, J.; Lv, X.; Wang, L.; Zhang, J. *Angew. Chem., Int. Ed.* **2016**, *55*, 13316–13320. (l) Sawa, M.; Morisaki, K.; Kondo, Y.; Morimoto, H.; Ohshima, T. *Chem Eur. J.* **2017**, *23*, 17022–17028. (m) Chen, P.; Zhang, J. *Org. Lett.* **2017**, *19*, 6550–6553. (n) Trost, B. M.; Hung, C.-I.; Scharf, M. J. *Angew. Chem., Int. Ed.* 2018, *57*, 11408–11412. (o) Yonesaki, R.; Kondo, Y.; Akkad, W.; Sawa, M.; Morisaki, K.; Morimoto, H.; Ohshima, T. *Chem. Eur. J.* **2018**, *24*, 15211–15214. (p) Miyagawa, M.; Yoshia, M.; Kiyota, Y.; Akiyama, T. *Chem. Eur. J.* **2019**, *25*, 5677–5681. (q) Zhu, J.; Huang, L.; Dong, W.; Li, N.; Yu, X.; Deng, W.-P.; Tang, W. *Angew. Chem., Int. Ed.* **2019**, *58*, 1–6.

[69] Chen, P.; Yue, Z.; Zhang, J.; Lv, X.; Wang, L.; Zhang, J. *Angew. Chem., Int. Ed.* **2016**, *55*, 13316–13320.

cost-effective and large-scale synthesis.[70] A recent report from our group overcomes these limitations and describes the addition of commercially available, or easy-to-synthesize, *Z*-substituted organoboron reagents to *N*-trimethylsilyl F_3C-ketimines to afford unprotected H_2N-α-tertiary amines enantioselectively (by way of electrostatic attraction as in Scheme 1.17a).[71] Application to gram-scale synthesis of a BACE-1 inhibitor utilized a single-vessel crotyl addition/acylation sequence to afford **1.82** in 69% yield (1.86 g, Scheme 1.18a). Subsequent ozonolysis/reductive workup and cyclization afforded the key intermediate for the synthesis of BACE-1 inhibitor, in 76% yield (**1.83**, 1.21 g).

Scheme 1.18. Catalytic, Regio-, *Z*-, and Enantioselective Additions to Ketimines

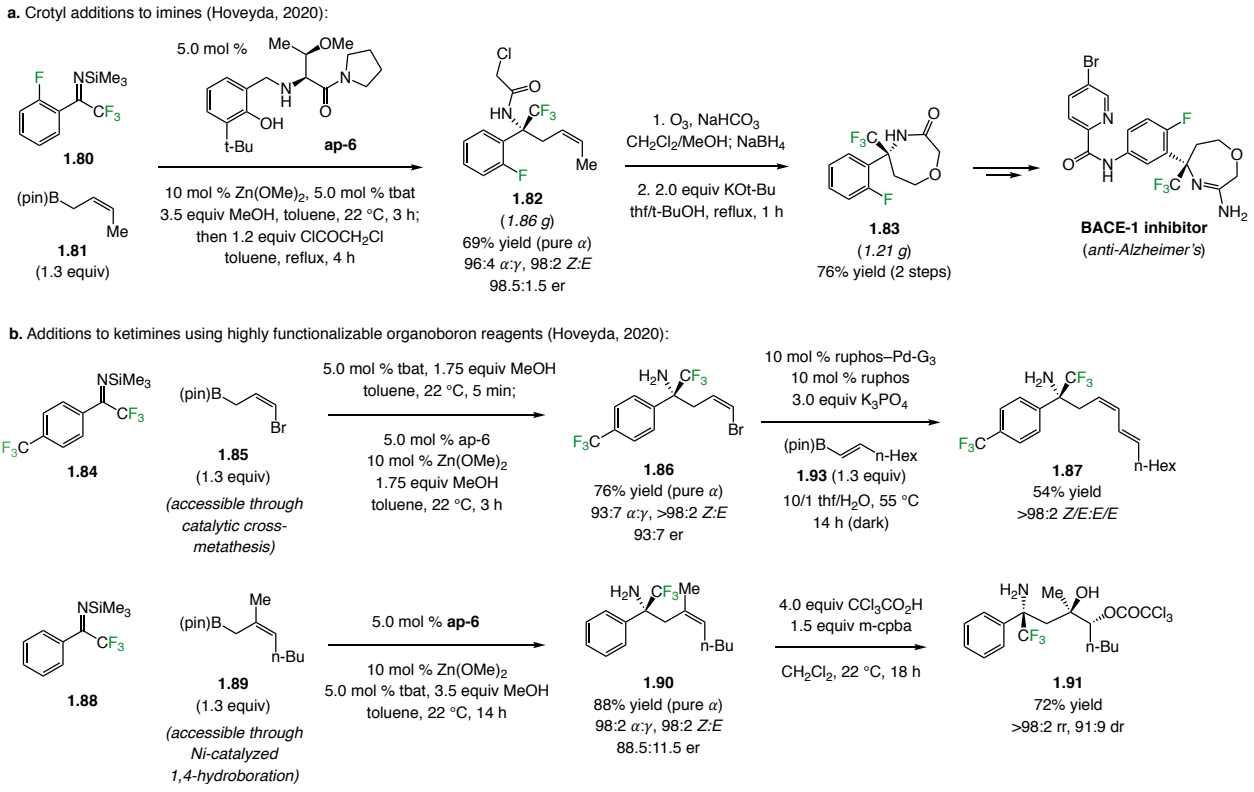

[70] (a) Grellepois, F.; Jamaa, A. B.; Rosa, N. S. *Org. Biomol. Chem.* **2017**, *15*, 9696–9709. (b) Shen, C.; Wang, R.-Q.; Wei, L.; Wang, Z.-F.; Tao, H.-Y.; Wang, C.-J. *Org. Lett.* **2019**, *21*, 6940–6945. (c) Wang, Y.; Deng, L.-F.; Zhang, X.; Niu, D. *Org. Lett.* **2019**, *21*, 6951–6956.

[71] Fager, D. C.; Morrison, R. J.; Hoveyda, A. H. *Angew. Chem., Int. Ed.* **2020**, *59*, 11448–11455.

Additions with other organoboron reagents, accessed by stereoretentive cross-metathesis, afforded **1.86** and **1.90**, which were then subject to cross-coupling (**1.87**, >98:2 *Z/E:E/E)* or diastereoselective epoxidation/ring-opening protocols [**1.91**, >98:2 regioisomeric ratio (rr), 91:9 dr], respectively (Scheme 1.18b).

1.5.2. Cross-Coupling Processes

In 2014, Fu and coworkers disclosed[72] the first example of catalytic enantioselective cross-coupling by employing geminal dihalides as electrophiles. Through a **box-2**–Ni catalyzed Negishi coupling of phenyl zinc chloride and racemic α-bromo-α-fluoroketone **1.94** (obtained in three steps from a ketone), tertiary alkyl fluoride **1.95** was isolated in 73% yield and 99:1 er (Scheme 1.19a). The resulting enantiomerically enriched fluoroketone **1.95** was derivatized by addition of an allyl nucleophile to afford **1.96** diastereo- and enantioselectively (Scheme 1.19b).

Scheme 1.19. Catalytic Enantioselective Cross-Coupling Reactions

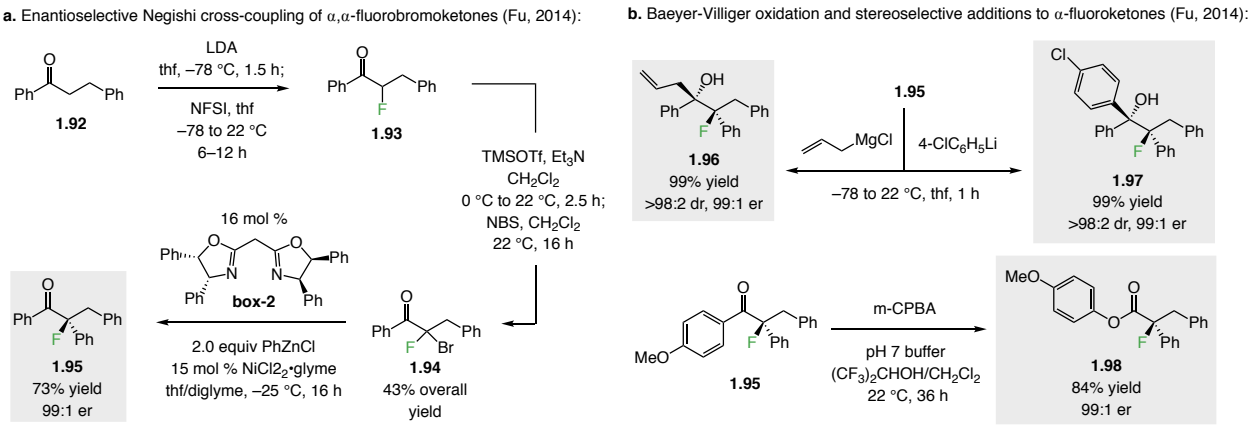

[72] Liang, Y.; Fu G. C. *J. Am. Chem. Soc.* **2014**, *136*, 5520–5524.

Alternatively, by selective migration during a Baeyer-Villiger oxidation, tertiary α-fluoroester **1.98** could be prepared. Use of readily available ketones for the synthesis of α-bromo-α-fluoroketone substrates would simplify accessing a variety of enantiomerically enriched organofluorine targets.

1.5.3. With Carbonyl-Containing Compounds and Imines as Nucleophiles

Fluorine-containing compounds with carbonyl or imine functional groups, some of which are even structurally similar to those shown above, have been utilized in stereoselective transformations as nucleophiles.

1.5.3.1. Aldol and Mannich Reactions

There are several examples of catalytic, diastereo- and enantioselective aldol, Mannich, and related methods which utilize organofluorides derived from readily accessible carboxylic acids.[73] Shibasaki has shown that an α-trifluoromethyl-substituted amide may be used in Mannich-type reactions with an *N*-Boc-imine (Scheme 1.20).[74] Catalyzed by a bisphosphine–Cu complex and Barton's base, amide **1.101** was isolated in 94% yield, >98:2 dr, and 99:1 er. Amide **1.101** was subsequently converted to carboxylic acid **1.102** in two steps.

[73] (a) Gong, Y.; Yu, J.-S.; Hao, Y.-J.; Zhou, Y.; Zhou, J. *Asian J. Org. Chem.* **2019**, *8*, 610–626. (b) Brewitz, L.; Arteaga, F. A.; Yin, L.; Alagiri, K.; Kumagai, N.; Shibasaki, M. *J. Am. Chem. Soc.* **2015**, *137*, 15929–15939.

[74] Yin, L.; Brewitz, L.; Kumagai, N.; Shibasaki, M. *J. Am. Chem. Soc.* **2014**, *136*, 17958–17961.

Scheme 1.20. Mannich Reaction with β-CF_3 Ketone

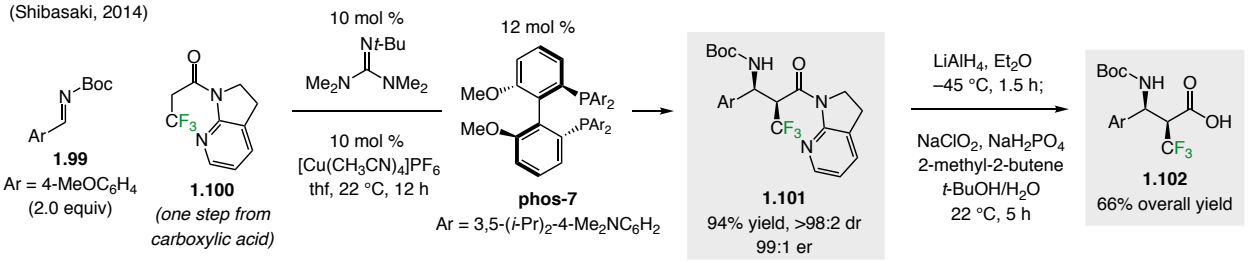

1.5.3.2. Umpolung Strategies for Reactions with Imines

Deng *et al.* have adapted umpolung strategies to the design of catalytic enantioselective transformations that involve trifluoromethyl imines.[75] Specifically, a deprotonated imine is made to react with an α,β-unsaturated aldehyde (Scheme 1.21) to give trifluoromethyl-substituted α-tertiary amines (after reduction; **1.106** or **1.107**).[76] The enantioselective process proceeds through formation of an ion pair consisting of a deprotonated imine and a cinchona alkaloid-based catalyst (**cinch-2**).

Scheme 1.21. Umpolung Strategies for Catalytic Enantioselective Additions to CF_3 Ketimines

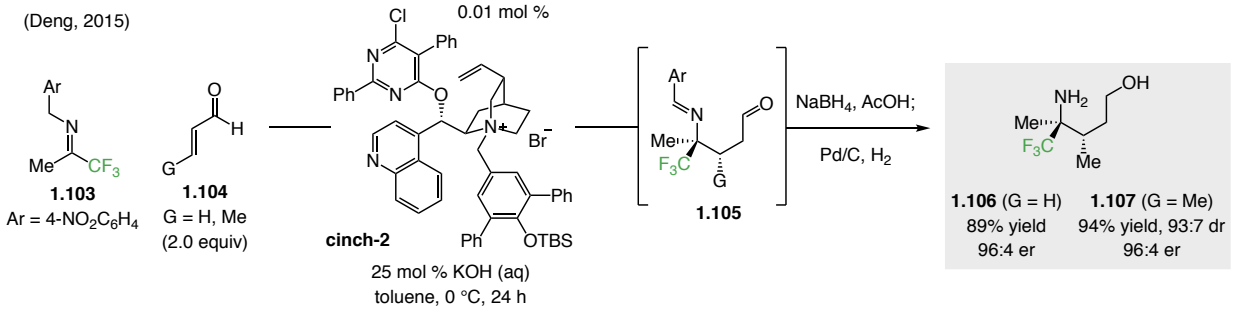

[75] (a) Li, Z.; Hu, B.; Wu, Y.; Fei, C.; Deng, L. *Proc. Natl. Acad. Sci.* **2018**, *115*, 1730–1735. (b) Wang, Y.; Deng, L.-F; Zhang, X.; Niu, D. *Org. Lett.* **2019**, *21*, 6951–6956. (c) Shi, L.-M.; Sun, X.-S.; Shen, C.; Wang, Z.-F.; Tao, H.-Y.; Wang, C.-J. *Org. Lett.* **2019**, *21*, 4842–4848.

[76] Wu, Y.; Hu, L.; Li., Z.; Deng, L. *Nature* **2015**, *523*, 445–450.

1.6. Processes Involving Fluoro-Alkyl Compounds

Catalytic stereoselective reactions involving alkyl fluorides are of considerable value. Although still largely unexplored, this has been achieved to some extent by means of some noteworthy progress outlined by Gandelman *et al.*, in the area of cross-coupling reactions (Scheme 1.22).[77] Reaction between racemic F_3C-substituted alkyl ethers and silanes may be catalyzed by a bisoxazoline–Ni complex to furnish enantiomerically enriched α-trifluoromethyl ethers (and alcohols upon deprotection). Syntheses of **1.108** and **1.109** are illustrative. The fluoro-organic substrates were prepared in three steps from trifluoroacetic anhydride and an alcohol (Scheme 1.22). The same research team had formerly demonstrated a strategy for related Suzuki cross-coupling processes,[77a] however, preparation of geminal fluoro-haloalkane starting materials were inefficient.

Scheme 1.22. Catalytic Enantioselective Reactions Involving Alkyl Fluorides

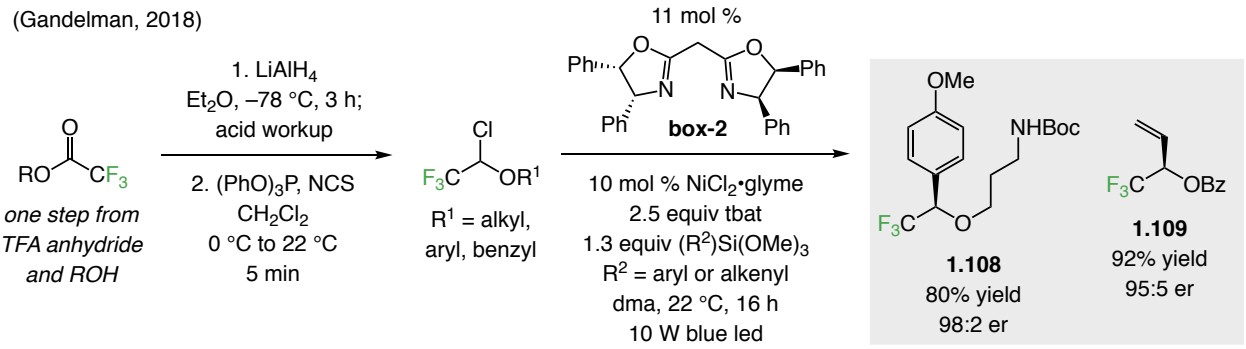

[77] For recent examples, see: (a) Jiang, X.; Sakthivel, S.; Kulbitski, K.; Nisnevich, G.; Gandelman, M. *J. Am. Chem. Soc.* **2014**, *136*, 9548–9551. (b) Jiang, X.; Gandelman M. *J. Am. Chem. Soc.* **2015**, *137*, 2542-2547. (c) Liang, Y.; Fu G. C. *Angew. Chem., Int. Ed.* **2015**, *54*, 9047-9051. (d) Liang, Y.; Fu G. C. *J. Am. Chem. Soc.* **2015**, *137*, 9523-9526. (e) Varenikov, A.; Gandelman M. *Nat. Comm.* 2018, *9*, 3566. (f) Varenokov, A.; Gandelman, M. *J. Am. Chem. Soc.* **2019**, *141*, 10994–10999.

1.7. Conclusion

This Chapter highlights some of the more recently developed and noteworthy methods for stereoselective transformation of readily accessible organofluorine compounds to an assortment of desirable products. This has been achieved through catalytic cross-metathesis, cross-coupling, substitution, and addition reactions. Nonetheless, the advances described above involve but a fraction of the commercially available or easy-to-access fluoro-organic compounds. Significant potential remains untapped.

Chapter Two

A Study of the Nature of Carbon-Halogen Bonds and Their Influence on Enantioselective Additions to α-Halomethylketones

2.1. Introduction and Background

Homoallylic alcohols, and more specifically, those containing α-halomethyl groups (chlorine, bromine, or fluorine), are prevalent in pharmaceuticals,[78] agrochemicals,[79] and natural products[80] (Scheme 2.1), and can serve as precursors to a variety of other desirable entities.[81] Over the last 40 years, there have been significant advances in catalytic enantioselective additions to carbonyl-containing compounds by the use of enantiomerically pure allyl nucleophiles and more recently, related catalytic enantioselective strategies have been introduced.[82] Research in our group has led to the development of a set of chiral aminophenol-based boryl catalysts that have

---

[78] (a) Bedke, D. K.; Vanderwal, C. D. *Nat. Prod. Rep.* **2011**, *28*, 15−25. (b) Nilewski, C.; Carreira, E. M. *Eur. J. Org. Chem.* **2012**, *2012*, 1685−1698. (c) Chung, W.; Vanderwal, C. D. *Angew. Chem., Int. Ed.* **2016**, *55*, 4396−4434. (d) Bringmann, G.; Feineis, D.; Brückner, R.; God, R.; Grote, C.; Wesemann, W. *Eur. J. Pharm. Sci.* **2006**, *28*, 412–422. (e) Krasowski, M. D.; Harrison, N. L. *Br. J. Pharmacol.* **2000**, *129*, 731–743. (f) Verhaeghe, P.; Dumétre, A.; Castera-Ducros, C.; Hutter, S.; Laget, M.; Fersing, C.; Prieri, M.; Yzombard, J.; Sifredi, F.; Rault, S.; Rathelot, P.; Vanelle, P.; Azas, N. *Bioorg. Med. Chem. Lett.* **2011**, *21*, 6003–6006.

[79] (a) Schmidt, W.; Schuzle, T. M.; Brasse, G.; Nagrodzka, E.; Maczka, M.; Zettel, J.; Jones. P. G.; Grunenberg, J.; Hilker, M.; Trauer-Kizilelma, U.; Braun, U.; Schulz, S. *Angew. Chem., Int. Ed.* **2015**, *54,* 7698–7702. (b) Orjala, J.; Gerwick, W. H. *J. Nat. Prod.* **1996**, *59*, 427–430.

[80] (a) Gribble, G., *Mar. Drugs* **2015**, *13*, 4044–4136. (b) Woolard, F. X.; Moore, R. E.; Roller, P. P. *Tetrahedron* **1976**, *32*, 2843–2846. (c) McConnell, O. J.; Fenical, W. *Phytochemistry* **1980***, 19*, 233–247. (d) Orjala, J.; Gerwick, W. H. *J. Nat. Prod.* **1996**, *59*, 427–430.

[81] (a) Yus, M; González-Gómez, J. C.; Foubelo, F. *Chem Rev.* **2011**, *111*, 7774–7854. (b) Huo, H.-X.; Duvall, J. R.; Huang, M.-Y.; Hong, R. *Org. Chem. Front.* **2014**, *1*, 303–320.

[82] Roush, W. R. In *Comprehensive Organic Synthesis*; Trost, B. M.; Fleming, I., Eds.; Pergamon Press: New York, 1991, Vol 2, pp 1–53.

been found to be exceptionally effective for enantioselective addition of different types of allyl boronates to aldimines, ketimines, ketones, and aldehydes.[83]

Scheme 2.1. Representative Bioactive Compounds with a Tri-, Di-, and Monohalomethyl Moiety

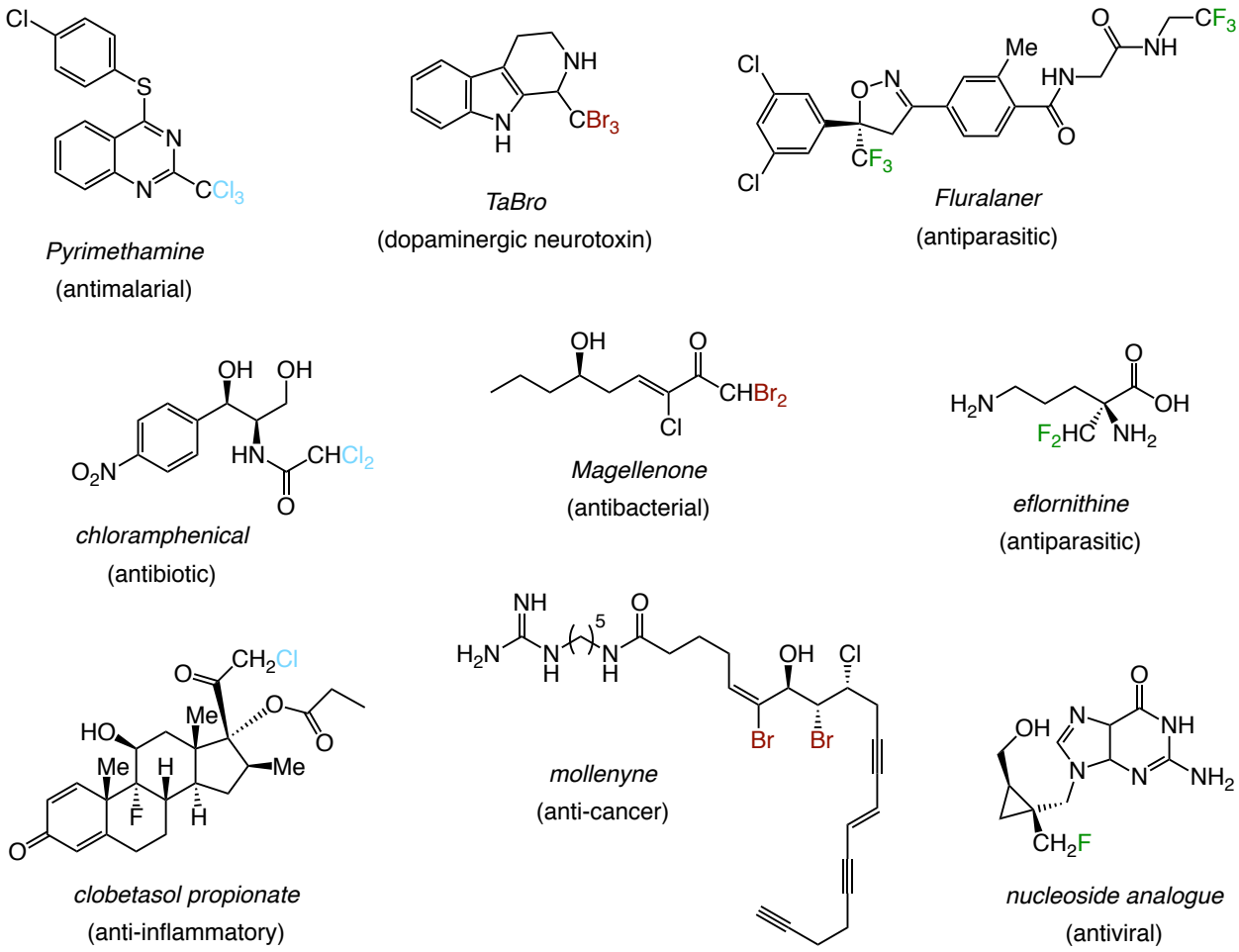

[83] (a) Silverio, D. L.; Torker, S.; Pilyugina, T.; Vieira, E. M.; Snapper, M. L.; Haeffner, F.; Hoveyda, A. H. *Nature* **2013**, *14*, 216–221. (b) Wu, H.; Haeffner, F.; Hoveyda, A. H. *J. Am. Chem. Soc.* **2014**, *136*, 3780–3783. (c) Lee, K.; Silverio, D. L.; Torker, S.; Haeffner, F.; Robbins, D. W.; van der Mei, F. W.; Hoveyda, A. H. *Nat. Chem.* **2016**, *8*, 768–777. (d) Robbins, D. W.; Lee, K.; Silverio, D. L.; Volkov, A.; Torker, S.; Hoveyda, A. H. *Angew. Chem., Int. Ed.* **2016**, *55*, 9610–9614. (e) van der Mei, F. W.; Miyamoto, H.; Silverio, D. L.; Hoveyda, A. H. *Angew. Chem., Int. Ed.* **2016**, *55*, 4701–4706. (f) Mszar, N. W.; Mikus, M. S.; Torker, S.; Haeffner, F.; Hoveyda, A. H. *Angew. Chem., Int. Ed.* **2017**, *56*, 8736–8741. (g) van der Mei, F. W.; Qin, C.; Morrison, R. J.; Hoveyda, A. H. *J. Am. Chem. Soc.* **2017**, *139*, 9053–9065. (h) Morrison, R. J.; Hoveyda, A. H. *Angew. Chem., Int Ed.* **2018**, *57*, 11654–11661. (i) Fager, D. C.; Lee, K.; Hoveyda, A. H. *J. Am. Chem. Soc.* **2018**, *141*, 16125–16138. (j) Morrison, R. J.; van der Mei, F. W.; Hoveyda, A. H. *J. Am. Chem. Soc.* **2020**, *142*, 436–447. (k) Fager, D. C.[†]; Morrison, R. J.[†]; Hoveyda, A. H. *Angew. Chem., Int. Ed.* **2020**, *59*, 11448–11455.

Aminophenols can be synthesized on gram-scale from inexpensive commercially available materials (Scheme 2.2). Their modular structure allows for facile steric and electronic tuning. Recently, a few of these ligands have become commercially available, making the method more readily accessible. Previous studies suggest that upon exposure of the ligand to allyl–B(pin) and methanol, the active chiral allylboron catalyst is generated (Scheme 2.2). These ligands have a low molecular weight and can be recovered during purification and reused. Mechanistic studies indicate that this class of catalysts contain an ammonium ion, providing the possibility of exploiting electrostatic interactions in reaction development.

Scheme 2.2. Aminophenol-Based Boryl Catalysts for Enantioselective Allyl Additions

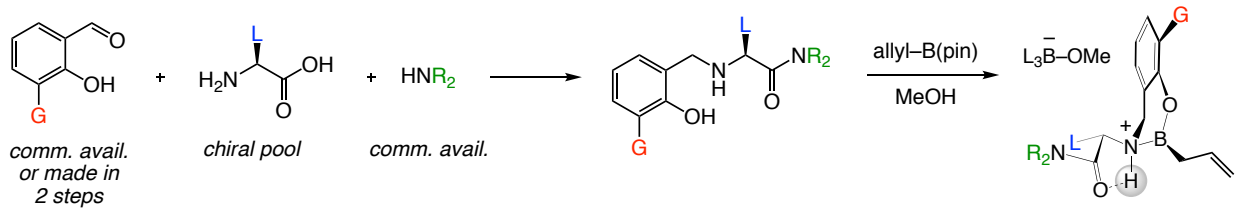

Key Features:

▪ Gram-scale synthesis ▪ Indefinitely air stable ▪ Readily accessible ▪ Low molecular weight
▪ Easily modifiable ▪ Embedded H-bond for organization, increased B Lewis acidity

A plausible mechanistic scenario entails the initial formation of boron-methoxide complex **I** (Scheme 2.3). Coordination of allyl–B(pin) (**II**) and subsequent γ-addition provides allyl boronate complex **III**, releasing just (pin)B–OMe as the byproduct. As will be discussed below, substrate coordination to give **IV** is likely impacted, to various degrees, by electronic and steric factors. A second γ-addition generates the net α-addition product after protonolysis of the O–B bond by methanol. It should be noted that, based on computational and experimental evidence, the lower energy transition is one in which the substrate approaches the catalyst from behind.[83a] Models in which the substrate approaches from the front are higher in energy due to steric repulsion between the substrate and amide backbone of the catalyst.

Scheme 2.3. Plausible Catalytic Cycle for Reactions Promoted by Aminophenol-Boryl Catalysts

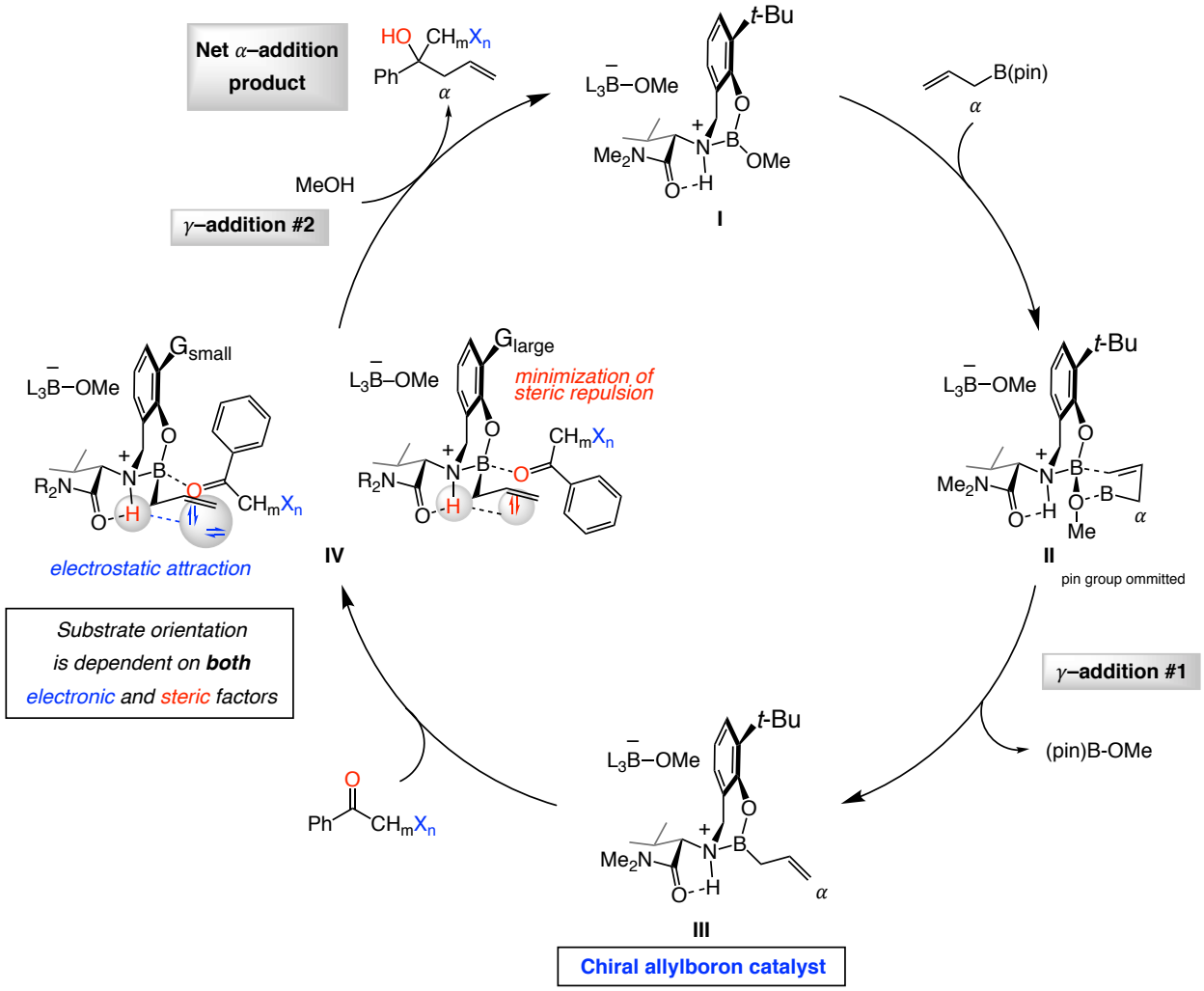

2.1.1. Additions to Methyl Ketones (Steric Control)

In 2016, our group reported an aminophenol-boron catalyzed enantioselective addition to methyl ketones (Scheme 2.4).[84] It was found that reactions involving a more sizeable triphenylsilyl-substituted aminophenol afforded the highest enantioselectivity. This was attributed to steric repulsion when a large substrate moiety was oriented pseudoaxially. Thus, transition state **V** represented the preferred mode of addition (Scheme 2.4).

[84] Robbins, D. W.; Lee, K.; Silverio, D. L.; Volkov, A.; Torker, S.; Hoveyda, A. H. *Angew. Chem., Int. Ed.* **2016**, *55*, 9610–9614.

Scheme 2.4. Catalytic Enantioselective Allyl Addition to Alkyl Ketones

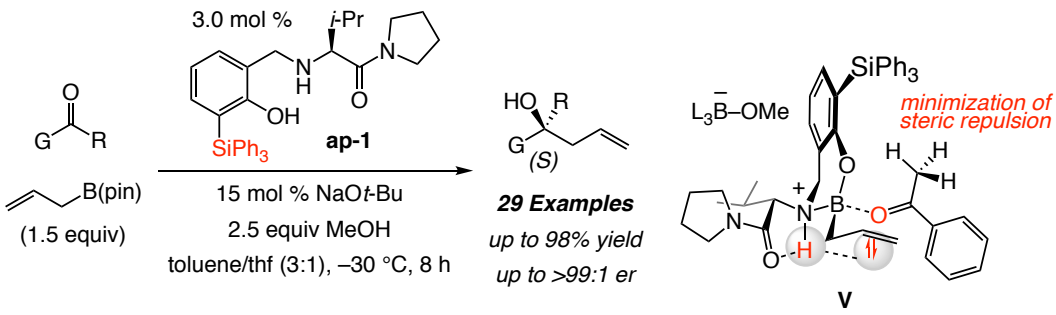

2.2.2. Additions to Trifluoromethyl-Substituted Ketones (Electronic Control)

Soon after, our group reported a catalytic enantioselective method for allyl additions to trifluoromethyl ketones (Scheme 2.5).[85] One of the mechanistically revealing aspects of this study was the finding that the major enantiomer arises from C–C bond formation to the enantiotopic face that is opposite to that when the aforementioned alkyl ketones were used. Based on a series of computational and experimental data, it was proposed that the preferred mode of addition is one wherein electron-electron repulsion between non-bonding electrons of the carbonyl unit and those of a fluorine atom can be ameliorated by the proximity of the catalyst's ammonium moiety (**VI**, Scheme 2.5).

Scheme 2.5. Catalytic Enantioselective Allyl Additions to Trifluoromethyl-Substituted Ketones

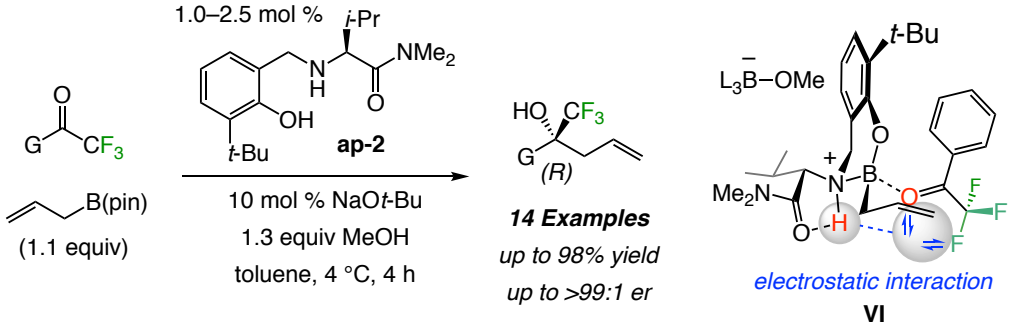

[85] Lee, K.; Silverio, D. L.; Torker, S.; Robbins, D. W.; Haeffner, F.; van der Mei, F. W.; Hoveyda, A. H. *Nat. Chem.* **2016**, *8,* 768–777.

Further studies indicated that these electrostatic interactions are likely not operative for additions to difluoromethyl and monofluoromethyl ketones, and thus enantioselectivity was much lower (see **2.1**, **2.2**, and **2.3**, Scheme 2.6). It was reasoned that this difference is due to the fact that minimization of dipolar repulsion is a dominant factor in the latter systems (**VII-VIII**, Scheme 2.6).

Scheme 2.6. Minimization of Dipolar Repulsion is Key in Additions to Other Halomethyl Ketones

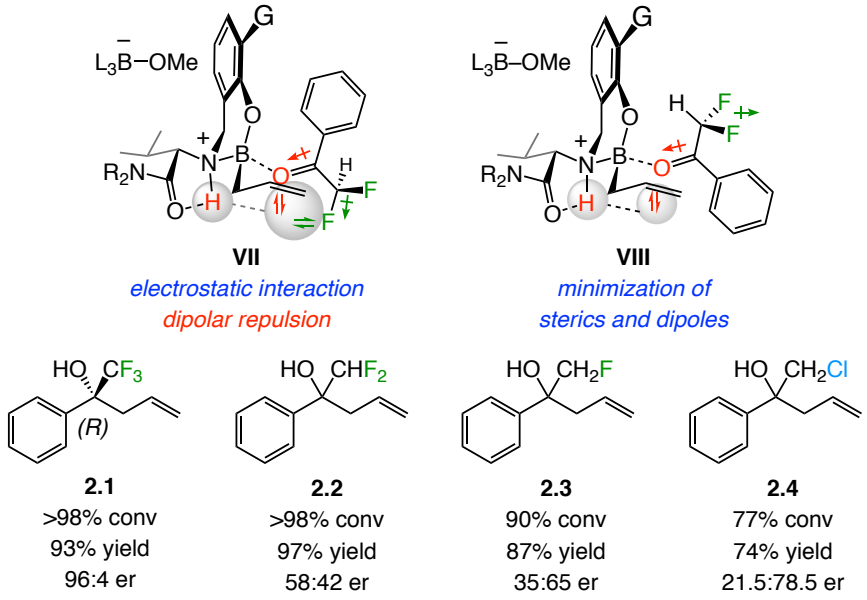

We therefore reasoned that addition to α-chloroacetophenone should afford the tertiary homoallylic alcohol product in even lower enantiomeric ratio because of the greater C–Cl bond dipole moment (C–F = 1.39, C–Cl = 1.47). However, this proved to be hardly the case, as the formation of monochloromethyl-substituted tertiary alcohol **2.4** was more enantioselective than either the difluoro- **2.2** or the monofluoromethyl **2.3** variants (Scheme 2.6). It was thus clear that there is more to the story than it was originally assumed, and that a more sophisticated appreciation of electronic as well as steric differences between different halogen-substituted ketones would likely be required for better understanding of selectivity variations.

2.2.3. Distinguishing Steric and Electronic Factors

There are several approaches to evaluating steric effects. These include Taft's steric parameters, Charton values, and the more recently introduced, Sterimol parameters. By the start of the twentieth century, chemists such as Emil Fisher[86] and Victor Meyer[87] had established that steric hinderance could alter the rate of a reaction. Out of this discovery came the development of A-values,[88] Tolman cone angles,[89] and quantitative structure-activity relationships (QSAR),[90] principles commonly taught in organic chemistry courses. As the years continued on and the study of stereochemistry became a central topic of research, eventually being awarded a Nobel Prize in 1975 shared between Vladimir Prelog and John Cornforth for their work on the stereochemistry of enzyme-catalyzed reactions and organic molecules and transformations, respectively, it became increasingly imperative to find ways to distinguish between steric and electronic factors.

Robert Taft was among the first utilize experimental findings (rates of ester hydrolysis with relatively large carbonyl substituents) to delineate steric and electronic effects.[91] He elucidated, that under acidic conditions, the positive charge is conserved throughout a process, implicating that electronic attributes of substituent R probably have little or no influence on rate and that the size of the nucleophile is likely a more influential factor (Scheme 2.7). Years later, Charton took

---

[86] Fischer, E. *Chem. Ber.* **1894**, *27*, 298.

[87] Walden, P.; Bischoff, C. A.; Band, I.; Bechhold, H. *Nature*, **1894**, *49*, 409–410.

[88] (a) Winstein, S.; Holness, N. J. *J. Am. Chem. Soc.* **1955**, *77*, 5562–5578. (b) Seeman, J. I. *Chem. Rev.* **1983**, *83*, 83–134.

[89] (a) Tolman, C. A. *J. Am. Chem. Soc.* **1970**, *92*, 2956–2965. (b) Tolman, C. A. *Chem. Rev.* **1977**, *77*, 313–348.

[90] Hansch, C. Maloney, P. P.; Fujita, T.; Muir, R. M. *Nature*, **1962**, *194*, 178–190. (b) Hansch, C.; Fujita, T. *J. Am. Chem. Soc.* **1964**, *86*, 1616–1626. (c) Hansch, C. *Acc. Chem. Res.* **1969**, *2*, 232–239. (d) Franke, R.; Jürgen Streich, W. *Mol. Inform.* **1985**, *4*, 51–63. (e) Franke, R.; Schmidt, W. *Acta Biol. Med. Germ.* **1973**, *31*, 273–X. (f) Franke, R. In *Theoretical Drug Design Methods;* Nauta, W. T.; Rekker, R. F. Eds.; Elsevier: New York, 1984, pp 256. (g) Selassie, C. D. In *Burger's Medicinal Chemistry and Drug Discovery;* Abraham, D. J., Ed.; John Wiley & Sons: New York, 2003; Vol 1, pp 1–48.

[91] (a) Taft, R. W., Jr. *J. Am. Chem. Soc.* **1952**, *74*, 2729–2732. (b) Taft, R. W., Jr. *J. Am. Chem. Soc.* **1953**, *75*, 4538–4539.

Taft's initial experiments a step further by correlating reaction rates to van der Waals radii for different carbonyl substituents (R).[92] Charton's method allowed values to be calculated, including cases for which experimental data were not available.

Scheme 2.7. The General Process Used in the Development of Taft Steric Parameters

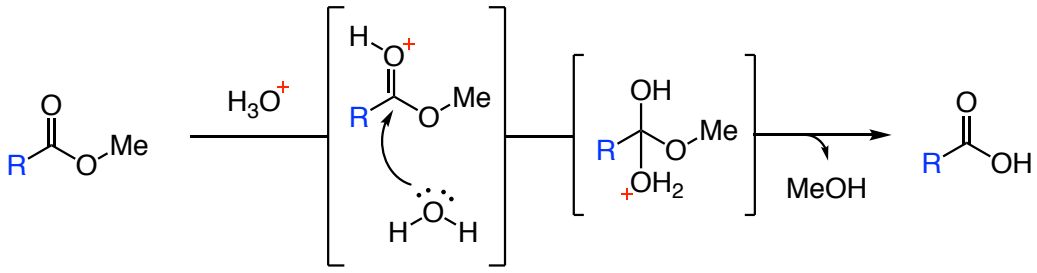

In the 1970s, Verloop and coworkers sought to improve the accuracy with which these parameters were determined and developed a computational program called, Sterimol.[93] These parameters are calculated by considering several different atomic measurements (measured in Å) for a single substituent (R): minimum width (B_1), maximum width (B_5), and length parameter (L) (Scheme 2.8). When Sterimol values are plotted against the observed enantioselectivity for a given transformation, the slope provides an energy/distance ratio describing the amount of repulsive steric interaction.[94] Parenthetically, we have determined that the B_1 value is the most illustrative

[92] (a) Charton, M. J. *J. Am. Chem. Soc.* **1975**, *97*, 1552–1556. (b) Charton, M. J. *J. Am. Chem. Soc.* **1975**, *97*, 3691–3693. (c) Charton, M. J. *J. Am. Chem. Soc.* **1975**, *97*, 3694–3697. (d) Charton, M. J. *J. Org. Chem.* **1976**, *41*, 2217–2220.

[93] (a) Verloop, A. In *Drug Design*; Ariens, E. J., Ed.; Academic Press: New York, 1976; Vol. III, pp 133–187. (b) Verloop, A.; Hoogenstraaten, W.; Tipker, J. In *Drug Design*; Ariens, E. J., Ed.; Academic Press: New York, 1976, Vol. VII, pp 165–207. (c) Verloop, A.; Tipker, J. In *Biological Activity and Chemical Structure*; Keverling-Buisman, J. A., Ed.; Elsevier: Amsterdam, 1977, pp 63. (c) Verloop, A. *Phil. Trans. R. Soc. Lond.* **1981**, *295*, 45–55. (d) Verloop, A. In *IUPAC Pesticide Chemistry*; Miyamoto, J., Ed.; Pergamon: Oxford, 1983; Vol. 1, pp 339. (d) Verloop, A. In *QSAR in Drug Design and Toxicology*; Hadzi, D. B. J.-B., Ed.; Elsevier: Amsterdam, 1987, pp 97.

[94] (a) Harpker, K. C.; Bess, E. N.; Sigman, M. S. *Nat. Chem.* **2012**, *4*, 366–374. (b) Piou, T.; Romanov-Michailidis, F.; Romanova-Michaelides, M.; Jackson, K. E.; Semakul, N.; Taggart, T. D.; Newell, B. S.; Rithner, C. D.; Paton, R. S.; Rovis, T. *J. Am. Chem. Soc.* **2017**, *139*, 1296–1310. (c) Brethome, A. V.; Fletcher, S. P.; Paton, R. S. *ACS Catal.* **2019**, *9*, 2313–2323.

for our system, and only occasionally, does the L parameter become important for substituents with extended side chains.

Scheme 2.8. Different Sterimol Parameters and What They Signify

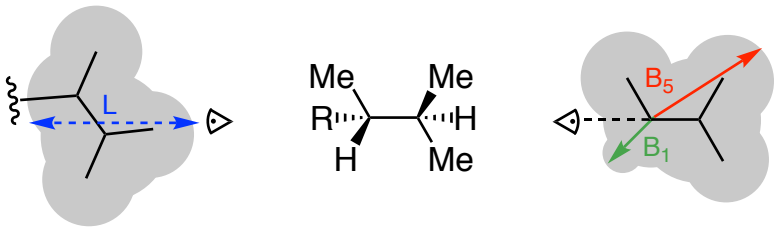

L: length along a defined axis
B_1: minimum width along a defined axixs
B_5: maximum width along a defined axis

When we revisited catalytic additions to ketones for which electronic factors alone could not explain the observed enantioselectivity trends, use of the Sterimol parameters proved considerably more satisfactory (Scheme 2.9). The two substituents to compare in this analysis are the phenyl group and the α-halomethyl group. The product with the largest difference in substituent size is the trifluoromethyl-substituted product **2.1** (Sterimol B_1: Ph = 1.71, CF_3 = 1.97, Δ = 0.26) and as such, this product was formed most enantioselectively.

Scheme 2.9. Sterimol Parameters Explain Variations in Enantioselectivity

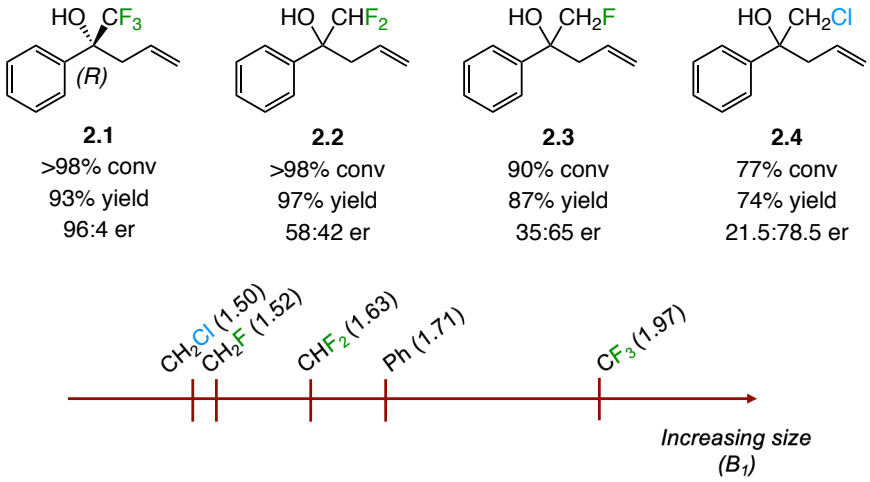

The next largest size difference corresponds to α-chloromethyl-substituted product **2.4** (Sterimol B_1: Ph = 1.71, CH_2Cl = 1.50, Δ = 0.21), followed by the α-monofluoromethyl-substituted product **2.3** (Sterimol B_1: Ph = 1.71, CH_2F = 1.52, Δ = 0.19), and the α-difluoromethyl-substituted product **2.2** (Sterimol B_1: Ph = 1.71, CHF_2 = 1.63, Δ = 0.08); enantiomeric ratios follow a similar trend. As we shall see, the use of these Sterimol parameters were proven to be key to understanding the origins of the selectivity trends that are presented below.

2.2.4. State-of-the-Art in Catalytic Enantioselective Additions to Halomethyl Ketones

Halocarbinols have several functional units that render them versatile fragments: a free alcohol, terminal olefin, and α-halomethyl group (Scheme 2.10). The halomethyl moiety can undergo nucleophilic substitution with a variety of nucleophiles. The terminal olefin may be converted to an alcohol or a 1,2-diol, or be used in an olefin metathesis reaction, to name a few sample possibilities. Notably, under basic conditions, the halocarbinol can readily be converted to a 1,1-disubstituted epoxide unit. Extant methods for synthesis of enantiomerically pure 1,1-disubstituted epoxides are limited in number and include the Shi[95] and Corey-Chaykovsky[96] strategies, which require the use of difficult to access catalysts and careful control of temperature and pH, in addition to being limited in scope.

[95] Shi, Y., *J. Org. Chem.* **2008**, *73*, 9539–9543.

[96] Shibasaki, M., *J. Am. Chem. Soc.* **2008**, *130*, 10078–10079.

Scheme 2.10. Halocarbinols as Precursors to Versatile Products

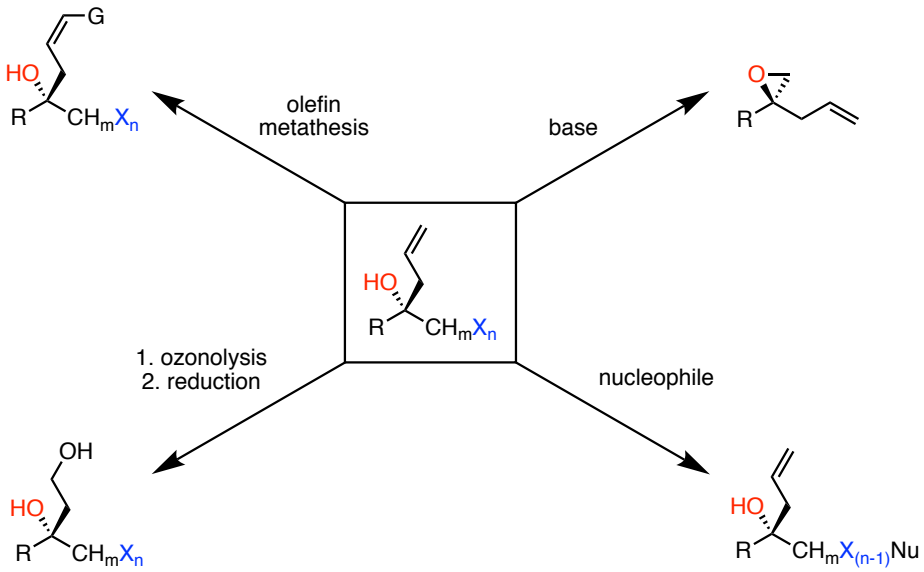

Despite their broad synthetic utility, there are less than a handful of enantioselective methods for synthesis of these homoallylic halocarbinols. One was reported by Schaus and coworkers in 2006 and involves a (*S*)-BINOL catalyst to obtain high enantioselectivity for addition to α-chloroacetophenone (Scheme 2.11).[97] The only other reported example is a Nozaki-Hiyama-Kishi allyl addition to α-chloroacetophenone, disclosed by Sigman *et al.* in 2007 (Scheme 2.11).[98] Clearly, a more general set of catalytic and enantioselective processes would be a welcome addition.

[97] Lou, S.; Moquist, P. N.; Schaus, S. E. *J. Am. Chem. Soc.* **2006**, *128*, 12660–12661.

[98] Miller, J. J.; Sigman, M. S. *J. Am. Chem. Soc.* **2007**, *129*, 2752–2753.

Scheme 2.11. Reported Catalytic Enantioselective Allyl Additions to α-Chloroacetophenone

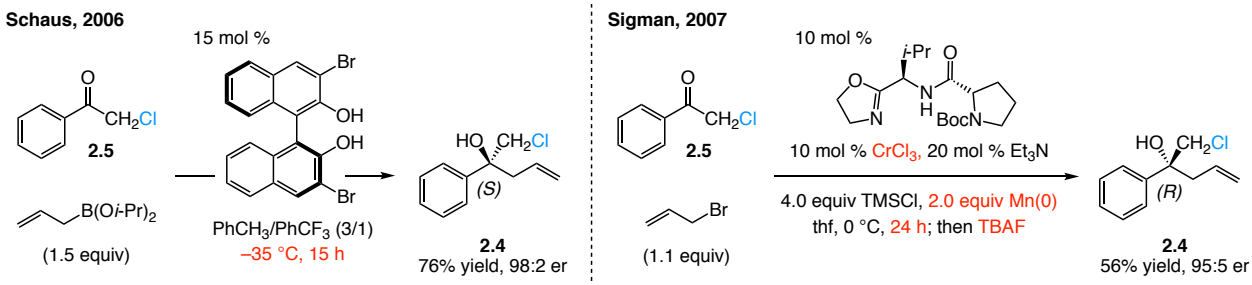

2.2.5. Initial Considerations and the Key Goals of the Study

An important reason why we decided to study additions to α-tri-, α-di-, and α-monohalomethyl ketones was to gain mechanistic insight regarding the steric and electronic parameters that distinguish C–F, C–Cl, and C–Br bonds (Scheme 2.12). Another impetus was to introduce a set of more broadly applicable methods for enantioselective preparation of homoallylic tertiary alcohols that contain various halomethyl groups. Such approaches would be valuable to preparation of bioactive compounds. This could be highlighted in a formal synthesis of anti-inflammatory agent, Boscartin F, as well as halogenated analogs of triazole-containing molecules such as leukotriene biosynthesis inhibitor and Banzel.

Scheme 2.12. Overview of the Method

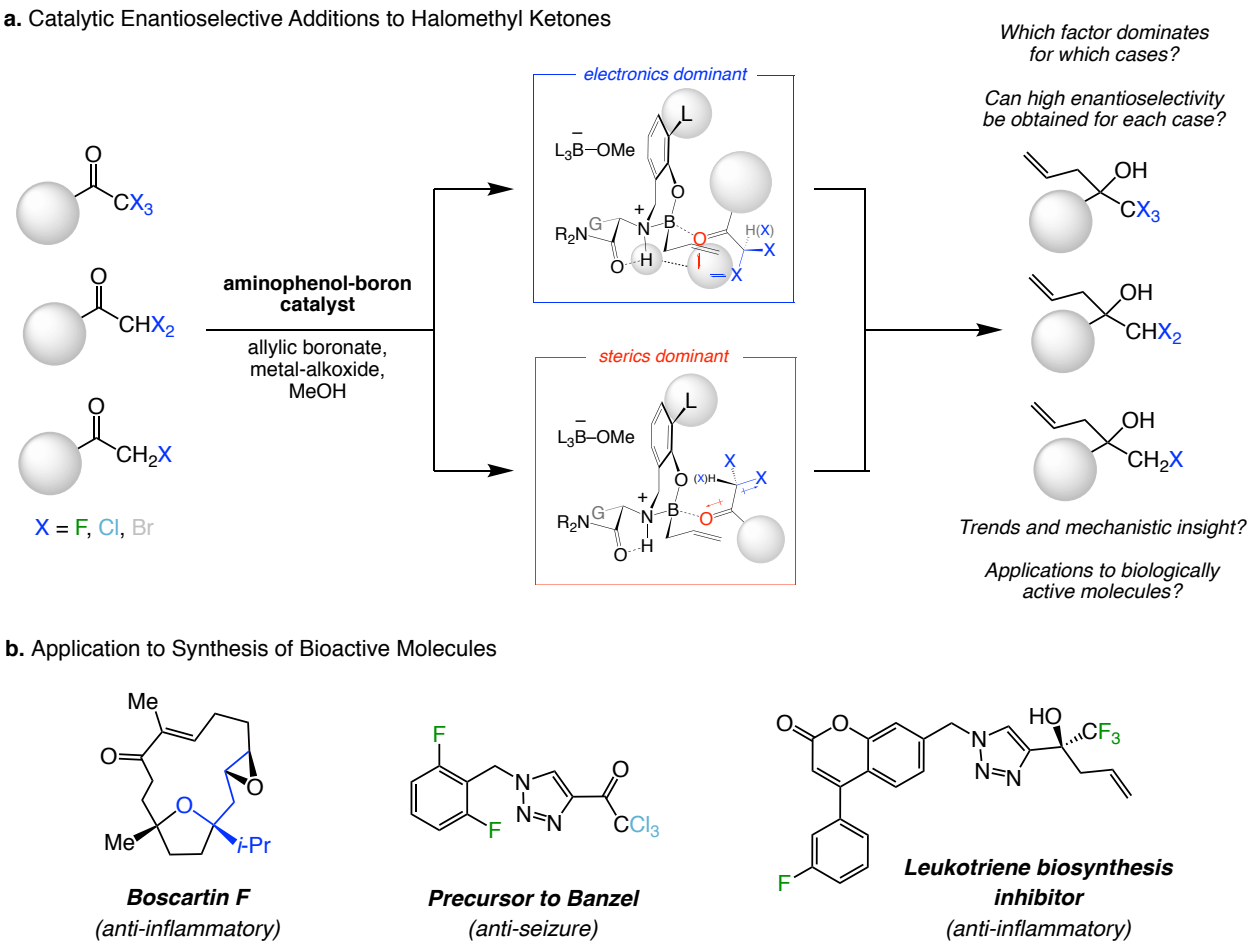

2.3. Catalytic Enantioselective Allyl Additions to Trihalomethyl Ketones

Catalytic enantioselective reduction of trichloromethyl-substituted ketones was systematically investigated by Corey and Link for the synthesis of unnatural α-amino acids,[99] but there are limited reports regarding the tribromomethyl variants. Equally important would be products that contain a combination of different halogen atoms; however, these types of substrates have received scant attention.

[99] Corey, E. J.; Link, J. O., *J. Am. Chem. Soc.* **1992**, *114*, 1906–1908.

2.3.1. Initial Results and Analysis of Stereochemical Models

When designing the course of our investigations, we encountered the following key questions. 1) Could the halogen atom of a C–Cl or a C–Br bond, similar to that of a C–F bond, participate in electrostatic interaction with an ammonium group? 2) How competitive would the uncatalyzed background reaction be? 3) Would steric factors play a larger role with chloro- or bromo-substituted ketones (vs. fluoro-substituted)? After all, there is a significant difference in the Sterimol values of various trihalomethyl moieties (Sterimol B_1: Ph = 1.71, CCl_3 = 2.64, CBr_3 = 2.87). Would such differences reinforce or counter electrostatic associations, if any (**IX** vs **X**, Scheme 2.13)?

Scheme 2.13. Stereochemical Models for Allyl Addition to Trihalomethyl Ketones

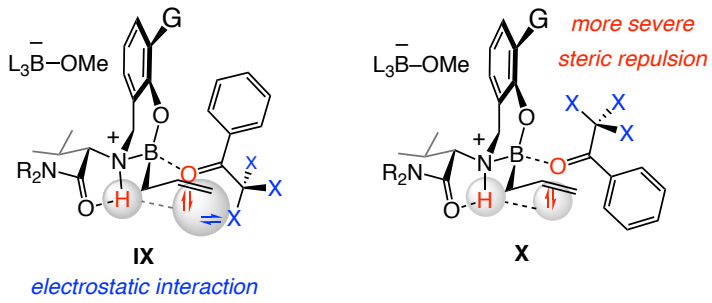

Reaction with trichloromethyl ketone **2.6a**, did not lead to any of the desired product (<2% conv with NaO*t*-Bu). In stark contrast, use of more a Lewis acidic $Zn(OMe)_2$ co-catalyst afforded **2.7a** in >98% conv, 91% yield, and 95:5 er, despite a highly competitive uncatalyzed background reaction (~70% conv in the absence of **ap-2**, Scheme 2.14).

Scheme 2.14. Initial Experiments for Allyl Addition to a Trichloromethyl Ketone[a]

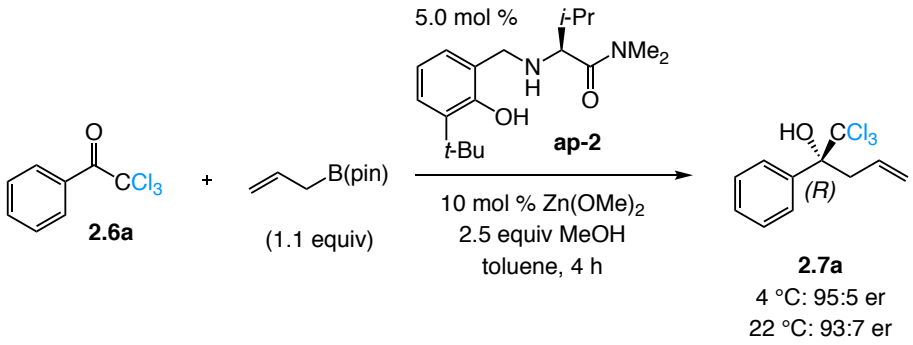

[a] Reactions performed under N_2 atm. Conv determined by analysis of ^{1}H NMR spectra of unpurified mixtures; conv (±2%) refers to disappearance of the ketone starting material. Yield of isolated and purified material (±5%). Enantioselectivity determined by HPLC analysis (±1%). See Experimental Section for details.

Scheme 2.15. Absolute Stereochemistry for Allyl Addition to Trihalomethyl Ketones

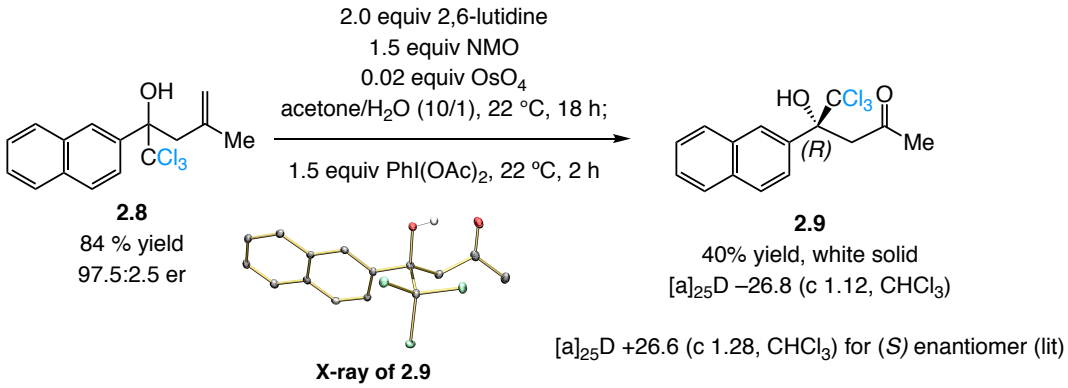

Use of 2-methylallyl–B(pin) afforded **2.8** in 97.5:2.5 er, and subsequent transformation to **2.9**, a compound reported in the literature,[100] provided proof of absolute stereochemistry (Scheme 2.15). The high enantioselectivity and preferential formation of the (*R*)-enantiomer indicates that addition to the trichloromethyl ketone is largely controlled by electrostatic interaction, similar to what we observed with the aforementioned trifluoromethyl ketones (**IX, S**cheme 2.13).

[100] Nicolaou, K. C.; Adsool, V. A.; Hale, C. R. H. *Org. Lett.* **2010**, *12*, 1552–1555.

2.3.2. Reaction Optimization and Aminophenol Ligand Screening

Further optimization began with performing the reaction at ambient temperature; however, this led to a decrease in enantioselectivity (93:7 vs 95:5 er). We then screened different aminophenol ligands (Scheme 2.16). Transformation in the presence of aryloxide **ap-3** afforded the product in 88:5:11.5 (vs 93:7 er), and with methyl-substituted aryloxide **ap-4** or triphenylsilyl-substituted **ap-1**, **2.7a** was generated in 90:10 er. These ligand screening data show that steric factors play a minor role, as enantioselectivities vary no more than 3–5%, despite the significant change in the size of the aminophenol aryl substituent.

Scheme 2.16. Ligand Screening for Allyl Additions to Trichloromethyl Ketones[a]

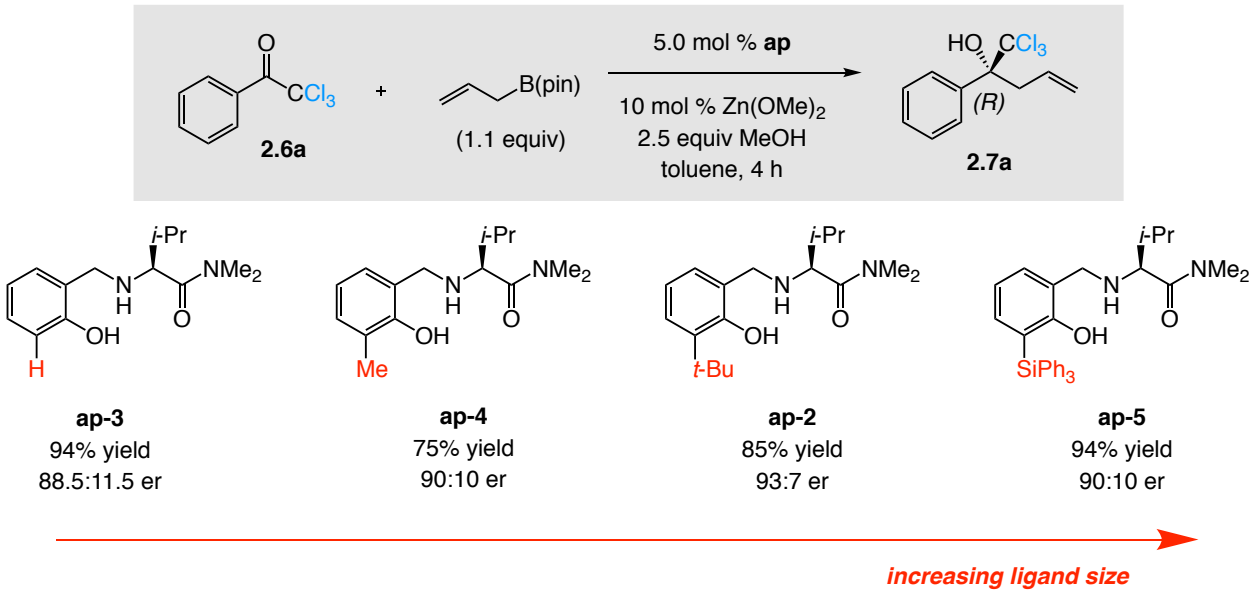

[a] Reactions performed under N_2 atm. Conv determined by analysis of ^{1}H NMR spectra of unpurified mixtures; conv (±2%) refers to disappearance of the ketone starting material. Yield of isolated and purified material (±5%). Enantioselectivity determined by HPLC analysis (±1%). See Experimental Section for details.

2.3.3. Scope for Allyl Additions to Trihalomethyl Ketones

A broad range of trichloromethyl ketones may be used. Substrates bearing aryl groups with an electron-withdrawing or an electron-donating substituent were suitable (**2.7b** and **2.7c**, Scheme 2.17). With more sterically demanding aryl groups, such as an *ortho*-substituted variant,

enantioselectivities were lower (90.5:9.5 er for **2.7d** vs 78.5:21.5 er for **2.7e**, Scheme 2.17). 2-Naphthyl-substituted **2.7f** and homoallylic alcohol **2.7g** were isolated with similarly high yields and enantioselectivities.

Scheme 2.17. Scope of Catalytic Enantioselective Allyl Additions to Trichloromethyl Ketones[a]

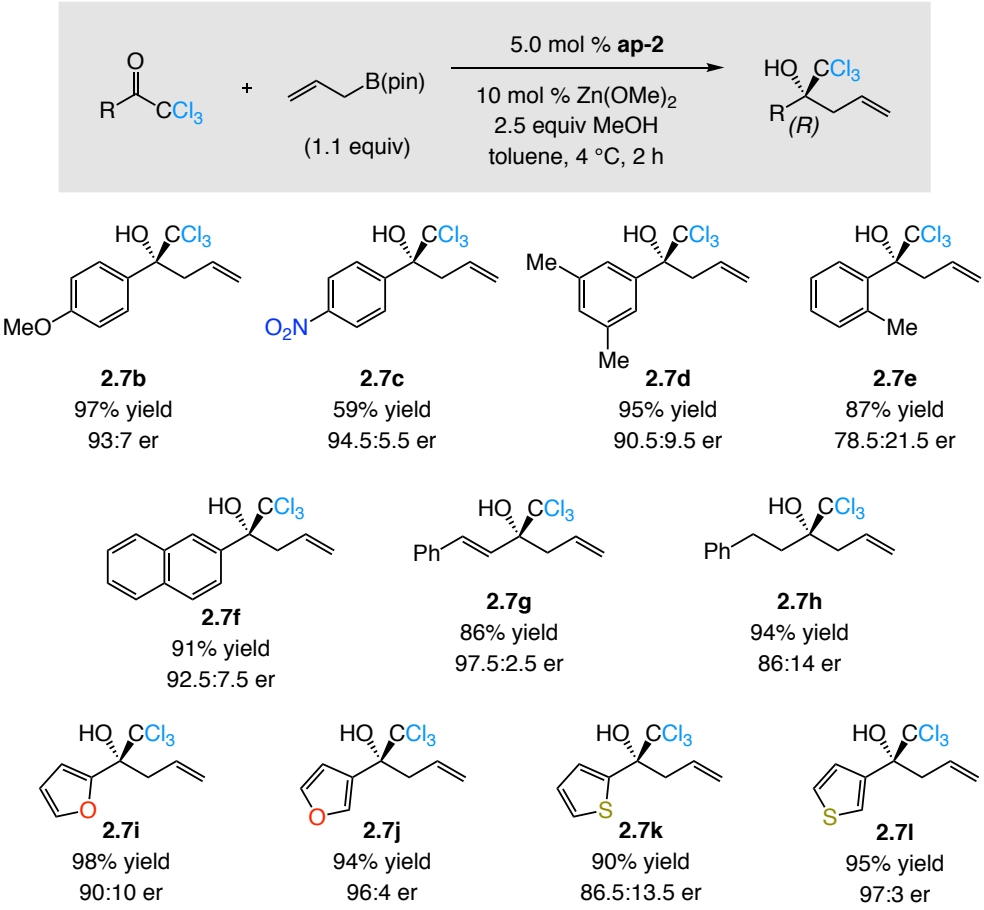

[a] Reactions performed under N_2 atm. Conv determined by analysis of ^{1}H NMR spectra of unpurified mixtures; conv (±2%) refers to disappearance of the ketone starting material. Yield of isolated and purified material (±5%). Enantioselectivity determined by HPLC analysis (±1%). See Experimental Section for details.

The lower enantioselectivity for alkyl-substituted **2.7h**, compared to **2.7g** (86:14 vs 97.5:2.5 er, respectively), may be attributed to the extended and flexible alkyl chain, which leads to lower enantioselectivity as a result of increased steric repulsion in the more favored mode of

addition. In other words, the L value for the Sterimol parameter likely becomes more crucial (Sterimol L values: Ph = 6.28, phenethyl = 8.47).

Heterocyclic ketones were equally effective starting materials. However, enantioselectivity fluctuated depending on the precise identity of the heterocycle. This can occur because the heteroatom (either oxygen or sulfur) can establish an electrostatic interaction with the catalyst's ammonium group,[6c] involving a transition state that leads to formation of the minor enantiomer. However, in contrast to the corresponding transformations involving trifluoromethyl ketones, the larger size of the trichloromethyl group (Sterimol B_1: CF_3 = 1.97, CCl_3 = 2.64) causes minimization of steric repulsion to be the primary factor (**XI** vs **XII**, Scheme 2.18).

Scheme 2.18. Heteroatoms Compete for Electrostatic Interaction: Low Enantioselectivity

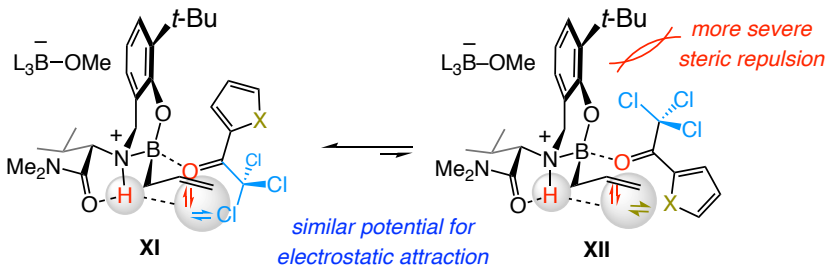

The above findings, namely, the fact that the same carbonyl group enantiotopic face undergoes reaction in a both trifluoromethyl and trichloromethyl ketones, and the fact that the major enantiomers are opposite to that formed with non-halogenated variants, point to similarity in strength of electrostatic interaction between an ammonium moiety and a C–F and a C–Cl bond of a trihalomethyl group. For further insight, we examined substrates that contained both fluorine and chlorine atoms on either side of the carbonyl group. We obtained 64.5:35.5 and 60:40 er for **2.7m** and **2.7n,** respectively (Scheme 2.19). These low enantioselectivities imply that a C–Cl bond

can establish electrostatic interaction equally as well as a C–F bond (**XIII** vs **XIV**, **XV** vs **XVI**, Scheme 2.19).

Scheme 2.19. Fluorine and Chlorine Can Participate in Electrostatic Interaction[a]

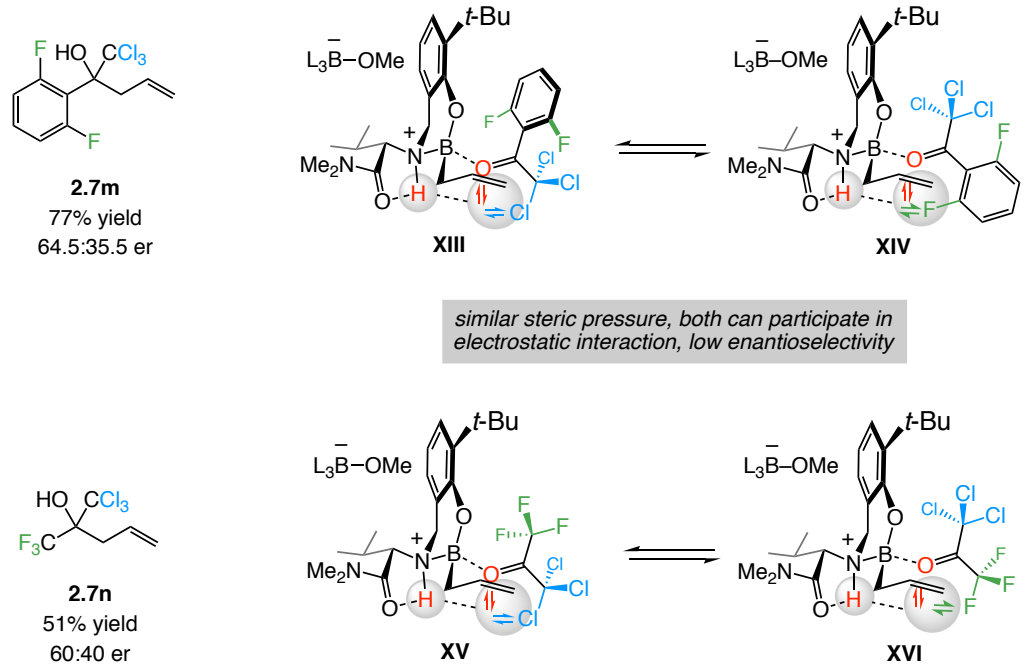

[a] Reactions performed under N_2 atm. Conv determined by analysis of ^{1}H NMR spectra of unpurified mixtures; conv (±2%) refers to disappearance of the ketone starting material. Yield of isolated and purified material (±5%). Enantioselectivity determined by HPLC analysis (±1%). See Experimental Section for details.

Scheme 2.20. Catalytic Enantioselective Allyl Addition to a Tribromomethyl Ketone[a]

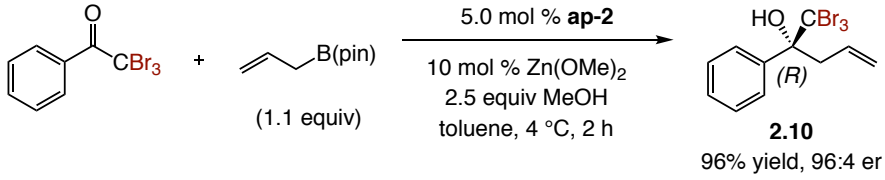

[a] Reaction performed under N_2 atm. Conv determined by analysis of ^{1}H NMR spectra of unpurified mixture; conv (±2%) refers to disappearance of the ketone starting material. Yield of isolated and purified material (±5%). Enantioselectivity determined by HPLC analysis (±1%). See Experimental Section for details.

Notably, under the same conditions, tribromomethyl halocarbinol **2.10** was afforded in 96% yield and 96:4 er (Scheme 2.20). Along these lines, we wondered what would happen if the substrate had a mixture of different halogen atoms at their α-carbon. In the event, we isolated **2.11**

and **2.12** in 91:9 and 92:8 er, respectively (Scheme 2.21). These comparatively low enantioselectivities to when halogen atoms are all the same (CF_3 = 96:4 er, CCl_3 = 95:5 er, CBr_3 = 96:4 er), might originate from the difference in the degree of steric pressure caused by different C–X bonds.

Scheme 2.21. Catalytic Enantioselective Allyl Additions to Mixed Trihalomethyl Ketones[a]

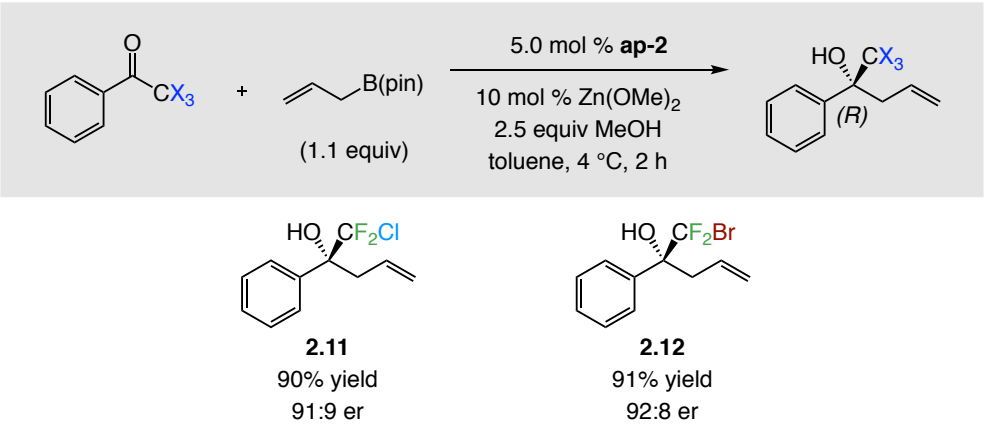

2.11
90% yield
91:9 er

2.12
91% yield
92:8 er

[a] Reactions performed under N_2 atm. Conv determined by analysis of ^{1}H NMR spectra of unpurified mixtures; conv (±2%) refers to disappearance of the ketone starting material. Yield of isolated and purified material (±5%). Enantioselectivity determined by HPLC analysis (±1%). See Experimental Section for details.

2.4. Catalytic Enantioselective Allyl Additions to Monohalomethyl Ketones

We next focused on allyl addition to various monohalomethyl ketones. The question was to what extent would there be a weakening of electrostatic attraction with the ammonium moiety as a result of minimization of dipolar repulsion, and to what degree would steric factors begin to exert control?

2.4.1. Initial Results and Analysis of Stereochemical Models

Catalytic enantioselective allyl addition to monohalomethyl ketones posed the following intriguing questions: 1) since the size differences between the ketone substituents are relatively small (Sterimol B_1: Ph = 1.71, CH_2F = 1.52, CH_2Cl = 1.50, CH_2Br = 1.50), would it be possible to

achieve high enantioselectivity? Might we design a ligand to differentiate between enantiotopic faces? 2) Monohalomethyl ketones are more stable in a conformer where dipolar repulsion is minimized. Will reaction by way of electrostatic interaction be possible? 3) How competitive would the uncatalyzed background reaction be?

Scheme 2.22. Stereochemical Models for Allyl Addition to Monohalomethyl Ketones

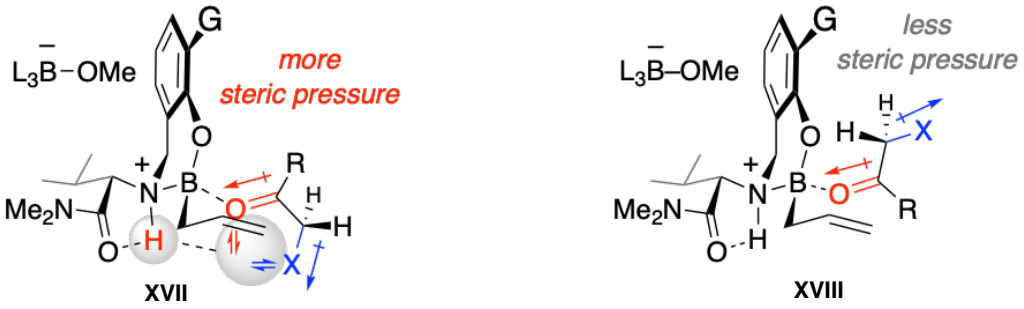

Scheme 2.23. Initial Experiments for Allyl Additions to Monohalomethyl Ketones[a]

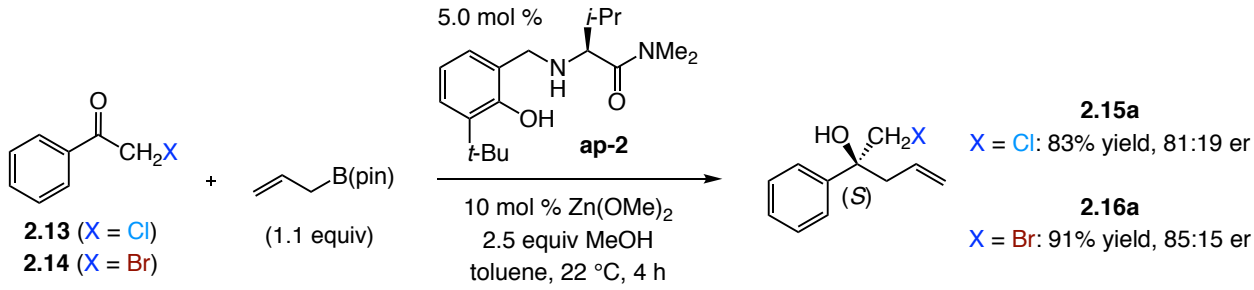

[a] Reactions performed under N_2 atm. Conv determined by analysis of ^{1}H NMR spectra of unpurified mixtures; conv (±2%) refers to disappearance of the ketone starting material. Yield of isolated and purified material (±5%). Enantioselectivity determined by HPLC analysis (±1%). See Experimental Section for details.

Examination of stereochemical models led us to predict that the major enantiomer would be obtained by reaction through **XVIII**, as this would allow for alleviation of dipolar as well as steric repulsion (Scheme 2.22). It appeared to us that the alternative mode of reaction (**XVII**) would suffer from a greater degree of steric pressure, owing to the pseudo-axially oriented aryl

moiety and dipolar repulsion. In the event, homoallylic alcohols **2.15a** and **2.16a** were generated in 81:19 and 85:15 er, respectively (Scheme 2.23).

Under appropriately basic conditions, monochloro- and monobromomethyl-substituted homoallylic alcohols can be converted to the corresponding 1,1-disubstituted epoxides (Scheme 2.24). We were able to use this protocol to determine the absolute stereochemistry of the products through comparison of the physical data regarding epoxide **2.17a** to those reported previously.[101] Comparison of optical rotations to a previously reported epoxide confirmed that the major enantiomer arises from addition to the opposite enantiotopic face of the ketone, compared to a trihalomethyl ketone. This in turn implied that such transformations are largely under steric control.

Scheme 2.24. One-Pot Synthesis of Enantiomerically Enriched 1,1-Disubstituted Epoxides[a]

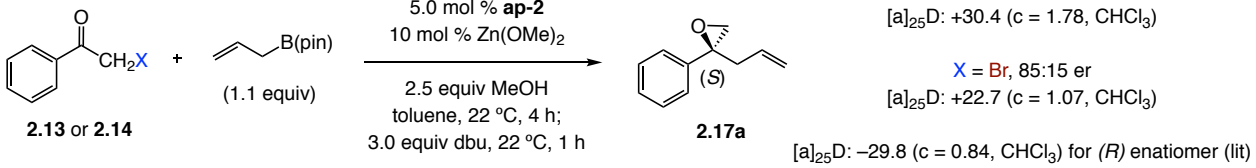

[a] Reactions performed under N_2 atm. Conv determined by analysis of ^{1}H NMR spectra of unpurified mixtures; conv (±2%) refers to disappearance of the ketone starting material. Yield of isolated and purified material (±5%). Enantioselectivity determined by HPLC analysis (±1%). See Experimental Section for details.

2.4.2. Optimization Studies

A survey of aminophenol ligands revealed that a bulkier aryloxide substituent resulted in improved enantioselectivity (Scheme 2.25), and the triphenylsilyl-substituted ligand **ap-1** was the most enantioselective. To probe whether further ligand modification might lead to higher enantioselectivity, we substituted the *N*-dimethyl terminus with an *N*-pyrrolidine amide group (i.e., **ap-1** vs **ap-5**, Scheme 2.26), leading to some improvement (>99:1 er). Use of 4-*tert*-butylphenyl-

[101] Wu, T. R.; Shen, L.; Chong, J. M. *Org. Lett.* **2004**, *6*, 2701–2704.

substituted ligand, **ap-6**, provided no improvement in enantioselectivity, nor did the use of the more three-dimensional adamantyl-substituted ligand, **ap-7**. What might be the origin of selectivity changes as a function of catalyst structure?

Scheme 2.25. Ligand Screening for Allyl Additions to Monohalomethyl Ketones[a]

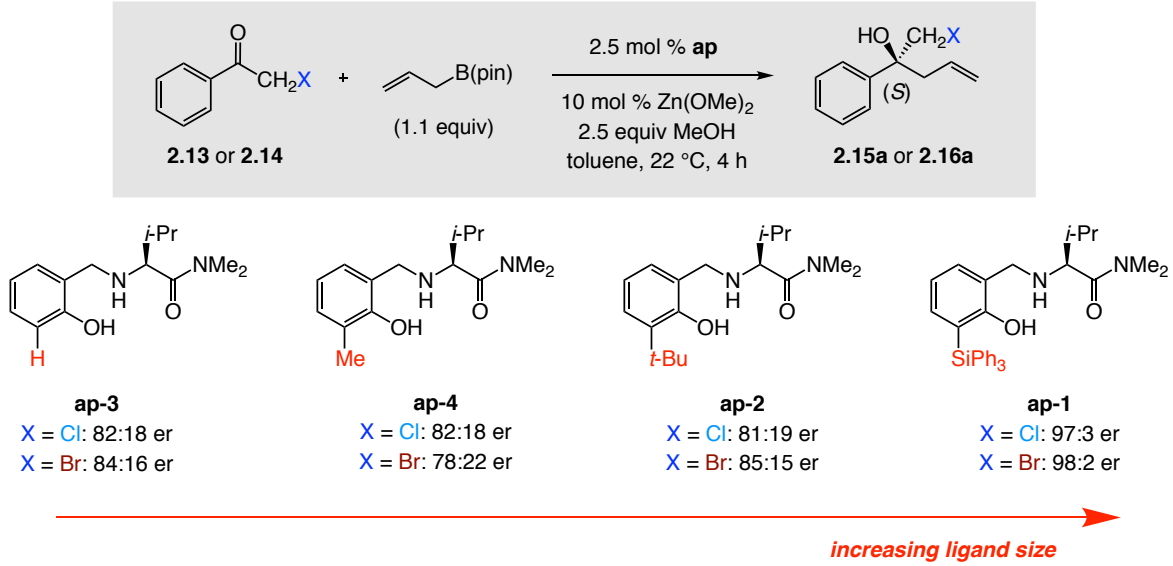

[a] Reactions performed under N_2 atm. Conv determined by analysis of ^{1}H NMR spectra of unpurified mixtures; conv (±2%) refers to disappearance of the ketone starting material. Yield of isolated and purified material (±5%). Enantioselectivity determined by HPLC analysis (±1%). See Experimental Section for details.

Scheme 2.26. Screening of Bulky Ligands for Allyl Additions to Monohalomethyl Ketones[a]

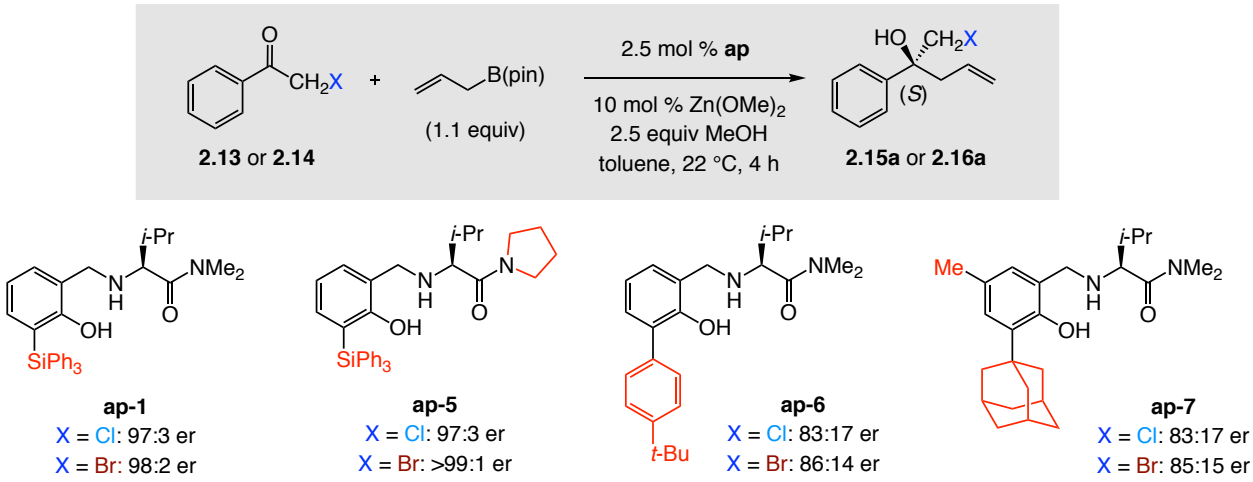

[a] Reactions performed under N_2 atm. Conv determined by analysis of ^{1}H NMR spectra of unpurified mixtures; conv (±2%) refers to disappearance of the ketone starting material. Yield of isolated and purified material (±5%). Enantioselectivity determined by HPLC analysis (±1%). See Experimental Section for details.

We considered several possibilities: 1) the longer length of a C–Si bond (1.86 Å versus 1.54 Å for a C–C bond) might place its aryl groups in closer proximity to the pseudo-axially oriented ketone substituent; 2) the triphenylsilyl group has a propeller-like shape that fills the rear pocket of the catalyst and disfavors substrate orientation where the aryl group is oriented pseudo-axially (as in Scheme 2.22); and 3) the increase in size of the amide further helps to tighten the catalyst pocket and differentiate enantiotopic faces. Final optimizations reduced ligand loading to just 0.5 mol % and the reactions can be run at ambient temperature in three hours.

2.4.3. Scope of Allyl Additions to Monochloro- and Monobromomethyl Ketones

Many monohalomethyl ketones are commercially available, allowing us to examine many cases. Reactions can be performed with electron-withdrawing (**b**), electron-donating (**c**), sterically hindered, alkyl (**2.16d**), alkenyl (**2.15d**), alkynyl, heterocyclic (**2.15e**, **2.15f**, **2.16f**), and carbonyl- or nitrile-containing (no competitive addition) starting materials (Scheme 2.27, note: all of the substrates in Scheme 2.28 have also been made as the homoallylic alcohols). The only incompatible functional groups we encountered were carboxylic acids and basic heterocycles such as triazoles and imidazoles. These substrates suffer from low efficiency and enantioselectivity, likely as a result of protodeboronation of the organoboron reagent and catalyst deactivation by deprotonation of the ammonium moiety, respectively. Interestingly, reaction of trifluoromethyl/monobromomethyl substrate **2.16e** was highly enantioselective. Previously, additions to such substrates were found to be minimally selective (**2.7m** and **2.7n**, Scheme 2.19). However, in this case, it might be proposed that because the monobromomethyl group is oriented pseudo-axially, the trifluoromethyl group is able to participate in electrostatic interaction with the

catalyst's ammonium group, thus favoring formation of the major enantiomer. This is analogous to the trend observed with the trihalomethyl-2-substituted heterocyclic ketones (see Scheme 2.17).

Scheme 2.27. Scope for Catalytic Enantioselective Allyl Additions to Monohalomethyl Ketones[a]

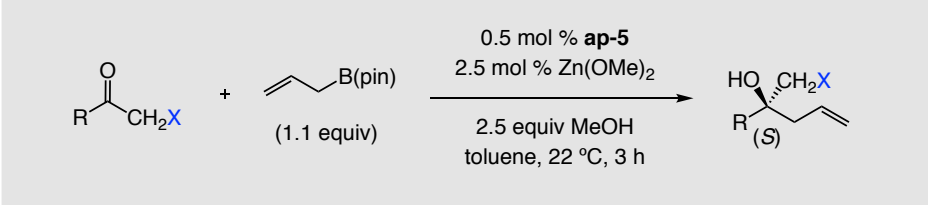

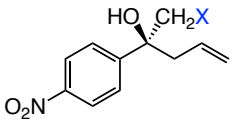

2.15b or **2.16b**
X = Cl: 81% yield, 94:6 er
X = Br: 93% yield, 88.5:11.5 er

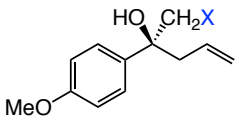

2.15c or **2.16c**
X = Cl: 93% yield, 95.5:3.5 er
X = Br: 71% yield, 95.5:4.5 er

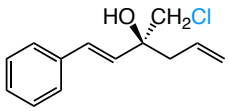

2.15d
73% yield, 96:4 er

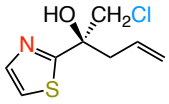

2.15e
95% yield, 90.5:9.5 er

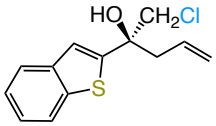

2.15f
84% yield, 95.5:4.5 er

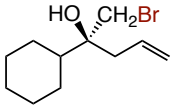

2.16d
81% yield, 95:5 er

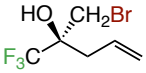

2.16e
54% yield, 97.5:2.5 er

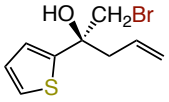

2.16f
91% yield, 99:1 er

[a] Reactions performed under N_2 atm. Conv determined by analysis of ^{1}H NMR spectra of unpurified mixtures; conv (±2%) refers to disappearance of the ketone starting material. Yield of isolated and purified material (±5%). Enantioselectivity determined by HPLC analysis (±1%). See Experimental Section for details.

2.4.4. Scope of 1,1-Disubstituted Epoxides

Next, we turned our attention to the one-pot allyl addition/cyclization protocol for synthesis of 1,1-disubstituted epoxides. Chlorine- and bromine-containing homoallylic alcohols were readily converted to the corresponding epoxides in high yield and enantioselectivity. Transformations were efficient with homoallylic alcohols bearing an electron-withdrawing (**2.17b-d**, **f**), a sterically hindered (**2.17j-n**), an alkyl (**2.17p**), or an alkynyl (**2.17o**) substituent (Scheme 2.28).

Scheme 2.28. Scope for Enantioselective One-Pot Synthesis of 1,1-Disubstituted Epoxides[a]

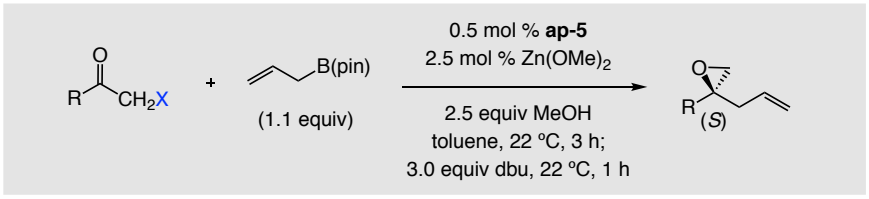

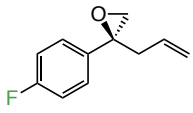

2.17b
X = Cl: 56% yield, 95:5 er
X = Br: 56% yield, 96:4 er

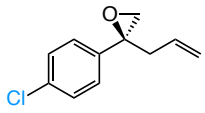

2.17c
X = Cl: 85% yield, 95.5:4.5 er
X = Br: 80% yield, 97:3 er

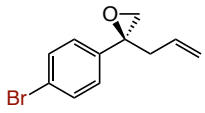

2.17d
X = Cl: 90% yield, 95:5 er
X = Br: 66% yield, 96.5:3.5 er

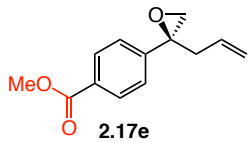

2.17e
X = Cl: 94% yield, 93.5:6.5 er

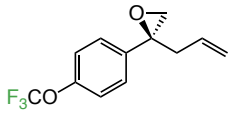

2.17f
X = Br: 72% yield, 96:4 er

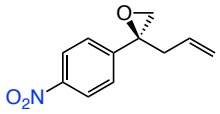

2.17g
X = Cl: 87% yield, 94:6 er
X = Br: 77% yield, 95:5 er

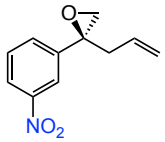

2.17h
X = Br: 79% yield, 96.5:3.5 er

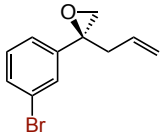

2.17i
X = Br: 53% yield, 97:3 er

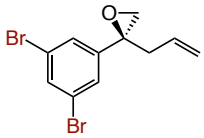

2.17j
X = Cl: 62% yield, 99:1 er
X = Br: 80% yield, 99.5:0.5 er

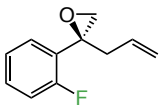

2.17k
X = Cl: 67% yield, 94:6 er
X = Br: 72% yield, 92:8 er

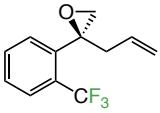

2.17l
X = Br: 52% yield, 98.5:2.5 er

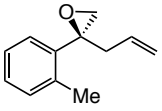

2.17m
X = Br: 86% yield, 99.5:0.5 er

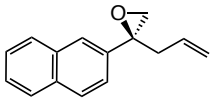

2.17n
X = Br: 88% yield, 96.5:3.5 er

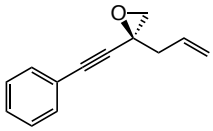

2.17o
X = Cl: 76% yield, 98:2 er

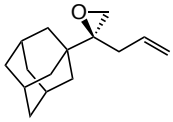

2.17p
X = Br: 86% yield, 89:11 er

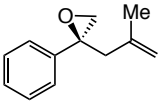

2.17q
X = Cl: 65% yield, 99:1 er
(1.0 mol % AP)

[a] Reactions performed under N_2 atm. Conv determined by analysis of ^{1}H NMR spectra of unpurified mixtures; conv (±2%) refers to disappearance of the ketone starting material. Yield of isolated and purified material (±5%). Enantioselectivity determined by HPLC analysis (±1%). See Experimental Section for details.

Unfortunately, homoallylic alcohols that contain an electron-rich or resonance-donating moiety decompose, likely through Meinwald rearrangement,[102] to generate a complex mixture of

[102] (a) Ranu, B. C.; Jana, U. *J. Org. Chem.* **1998**, *63*, 8212–8216. (b) Wang, Z. Meinwald Rearrangement. In *Comprehensive Organic Name Reactions and Reagents*, John Wiley & Sons, Inc.: Hoboken, NJ, 2010; pp 1880–1882.

products, including the corresponding aldehyde. It is worth noting that methods for enantioselective synthesis of 1,1-disubstituted epoxides are uncommon.[103]

2.4.5. Concise Formal Synthesis of Boscartin F

Boscartin F, a cembranoid diterpene natural product, was isolated from the gum resin of the *Boswellia carterii* tree and has anti-inflammatory properties.[104] A recent total synthesis involved 1,1-disubstituted epoxide **2.21**.[105]

Scheme 2.29. Sugita's Enantioselective Synthesis of 1,1-Disubstituted Epoxide

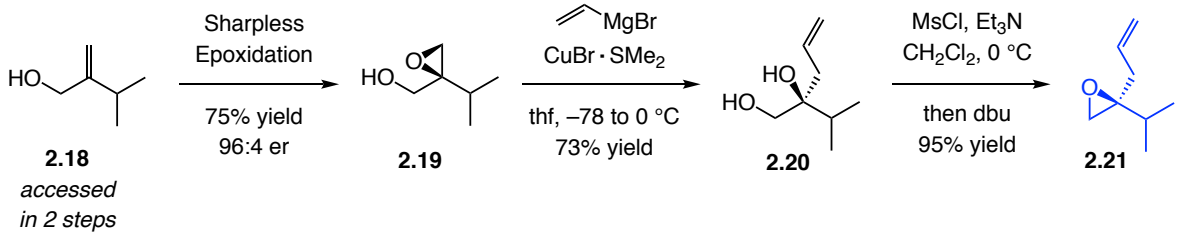

The synthesis of this key intermediate was accomplished in five-steps: two processes to obtain allylic alcohol **2.18** for Sharpless epoxidation, ring opening with vinylmagnesium bromide, and a one-pot alcohol activation/cyclization. The target epoxide was accordingly synthesized in 52% overall yield and 96:4 enantiomeric ratio (Scheme 2.30). We envisioned synthesizing epoxide **2.21** in a single step using our one-pot allyl addition/cyclization protocol. In the event,

(c) Karamé, I, Tommasino, M. L.; Lamaire, M. *Tetrahedron Lett.* **2003**, *44*, 7687–7689. (d) Robinson, M. W. C.; Pillinger, K. S.; Graham, A. E. *Tetrahedron Lett.* **2006**, *47*, 5919–5921.

[103] (a) Dexter, A. F.; Lakner, F. J.; Campbell, R. A.; Hager, L. P. *J. Am. Chem. Soc.* **1995**, *117*, 6412–6413. (b) Warren, J. D.; Shi, Y. *J. Org. Chem.* **1999**, *64*, 1675–1677. (c) Wang, B.; Wong, O. A.; Zhao, M.-X.; Shi, Y. *J. Org. Chem.* **2008**, *73*, 9539–9543. (d) Sone, T.; Yamaguchi, A.; Matsunaga, S.; Shibasaki, M. *Molecules* **2012**, *17*, 1617–1634.

[104] Byler, K. G.; Zeter, W. N. *Medicines* **2018**, *5*, 96.

[105] Sugita, X. X. *Org. Lett.* **2018**, *20*, 1031–1033.

commercially available ketone **2.22** was transformed to the desired epoxide in 91% yield and 95:5 er (Scheme 2.32).

Scheme 2.30. Our Enantioselective Formal Synthesis of Boscartin F[a]

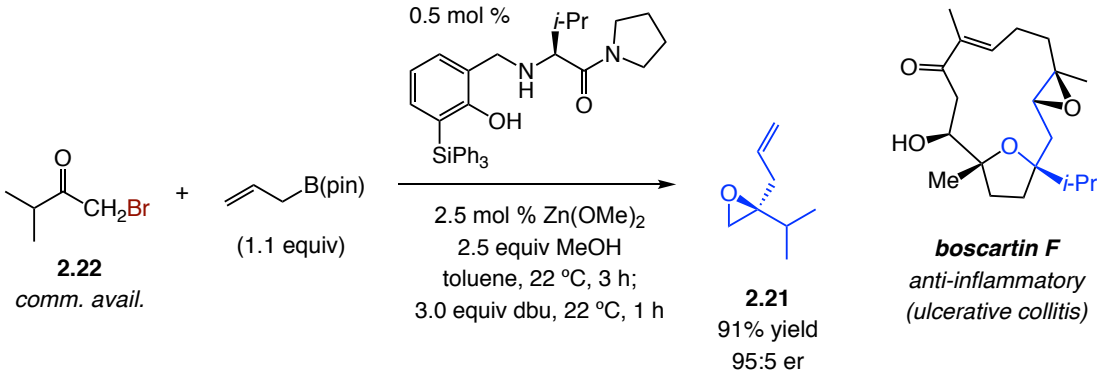

2.22
comm. avail.

2.21
91% yield
95:5 er

boscartin F
anti-inflammatory
(ulcerative collitis)

[a] Reactions performed under N_2 atm. Conv determined by analysis of ^{1}H NMR spectra of unpurified mixtures; conv (±2%) refers to disappearance of the ketone starting material. Yield of isolated and purified material (±5%). Enantioselectivity determined by HPLC analysis (±1%). See Experimental Section for details.

2.5. Catalytic Enantioselective Allyl Additions to Dihalomethyl Ketones

Enantioselectivity in additions to trihalomethyl and monohalomethyl ketones are entirely distinct: one is largely under electronic control while the latter is mostly governed by steric factors. Below, studies regarding additions to dihalomethyl ketones are described.

2.5.1. Initial Results and Analysis of Stereochemical Models

Analysis of the stereochemical models for addition to dihalomethyl ketones indicated that the corresponding transition states would be similar in energy (Scheme 2.31). We surmised this to be the case because we suspected that electrostatic attraction and minimization of dipolar repulsion would be equally favored, and the small difference in the Sterimol values for the ketone substituents should not result in high enantioselectivity (Sterimol B_1: Ph = 1.71, CHF_2 = 1.63, $CHCl_2$ = 1.65, $CHBr_2$ = 1.64).

Scheme 2.31. Stereochemical Models for Allyl Addition to Dihalomethyl Ketones

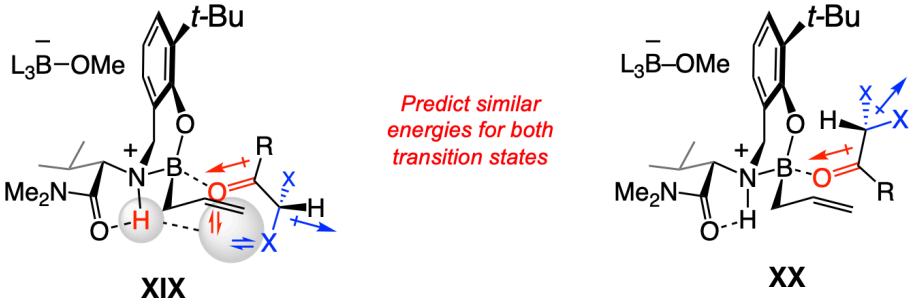

Initial experiments (same conditions used for additions to trifluoromethyl ketones, except at 22 °C) led us to isolate **2.25a** and **2.26a** in 73% yield and 86:14 er and 67% yield and 84:16 er, respectively (Scheme 2.32). Further studies revealed that with the more Lewis acidic $Zn(OMe)_2$, reaction efficiency and enantioselectivity improved (80% yield and 88:12 er, 82% yield and 91:9 er, respectively).

Scheme 2.32. Initial Studies for Allyl Additions to Dihalomethyl Ketones[a]

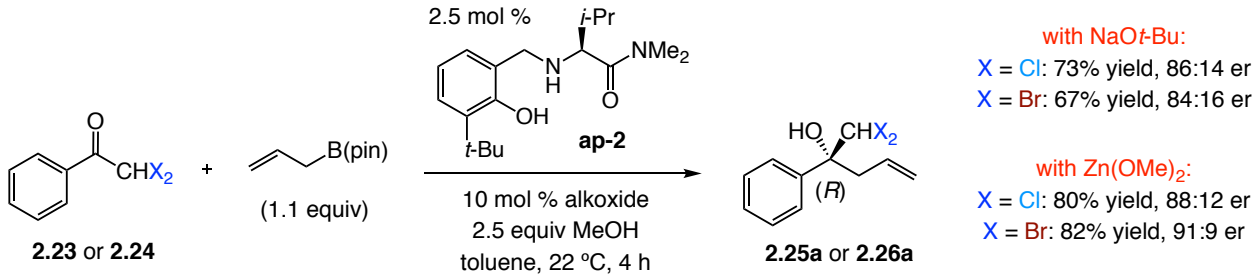

[a] Reactions performed under N_2 atm. Conv determined by analysis of ^{1}H NMR spectra of unpurified mixtures; conv (±2%) refers to disappearance of the ketone starting material. Yield of isolated and purified material (±5%). Enantioselectivity determined by HPLC analysis (±1%). See Experimental Section for details.

To confirm the identity of the major enantiomer, a halogen abstraction reaction was performed on **2.26a** to afford **2.16a** (Scheme 2.33). The optical rotations and HPLC traces of the two samples were then compared and revealed that additions to dihalomethyl ketones afford the same enantiomer as that of the trihalomethyl ketones. We were surprised that enantioselectivities

were higher than had been expected. Clearly, these findings show that enantioselectivity in catalytic allyl additions to dihalomethyl ketones can be impacted to a considerable degree by electronic factors.

Scheme 2.33. Absolute Stereochemistry for Allyl Additions to Dihalomethyl Ketones

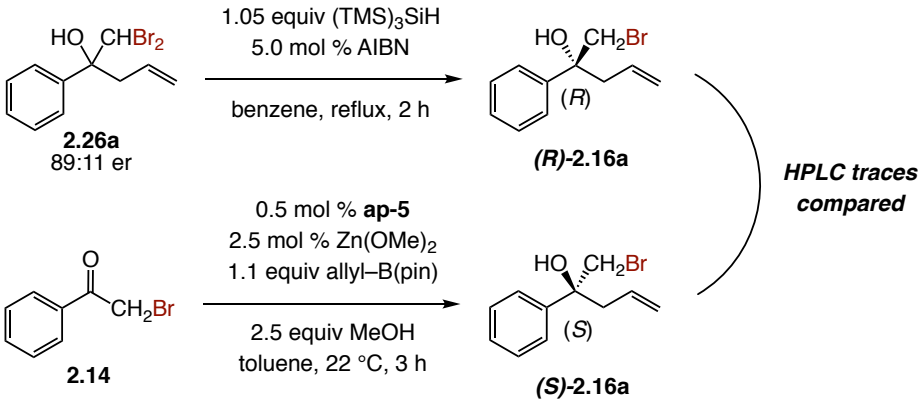

2.5.2. Optimization Studies

Performing the reaction to –40 °C for 18 hours with **ap-2** resulted in formation of the chloro- and bromomethyl homoallylic alcohols in 90:10 and 94:6 er, respectively (Scheme 2.34). Changing the amide to a larger pyrrolidine amide did not have much of an effect (**ap-2** vs **ap-8**). With triphenylsilyl-substituted ligand **ap-5**, which we had found to be optimal for additions to monohalomethyl ketones, there was a decrease in enantioselectivity, supporting the proposition that a ketone's aryl group is likely positioned pseudo-axially (Sterimol L value: Ph = 6.28, CHF_2 = 2.39, $CHCl_2$ = 3.85, $CHBr_2$ = 4.04). Further optimization led us to determine that additions may proceed to completion with 1.0 mol % **ap-2** and 2.5 mol % $Zn(OMe)_2$.

Scheme 2.34. Ligand Screening for Allyl Additions to Dihalomethyl Ketones[a]

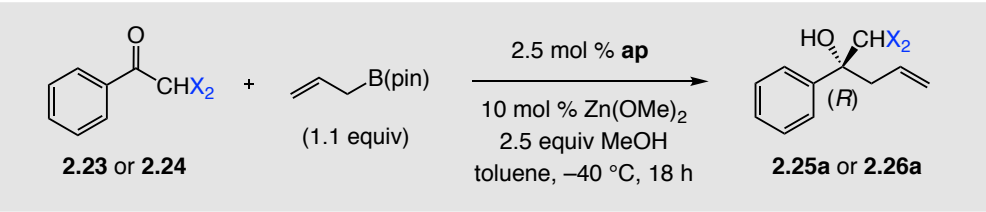

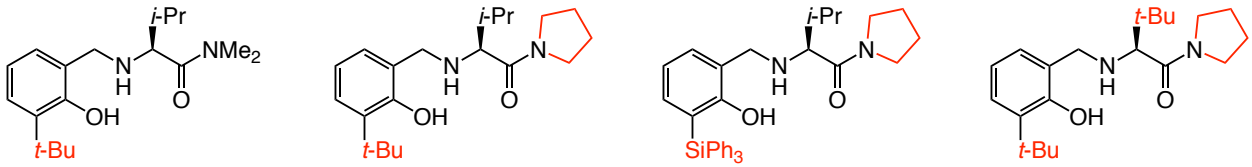

ap-2	**ap-8**	**ap-5**	**ap-9**
X = Cl: 90:10 er	X = Cl: 88.5:11.5 er	X = Cl: 84:16 er	X = Cl: 86:14 er
X = Br: 94:6 er	X = Br: 94:6 er	X = Br: 87:13 er	X = Br: 94:6 er

[a] Reactions performed under N_2 atm. Conv determined by analysis of ^{1}H NMR spectra of unpurified mixtures; conv (±2%) refers to disappearance of the ketone starting material. Yield of isolated and purified material (±5%). Enantioselectivity determined by HPLC analysis (±1%). See Experimental Section for details.

2.5.3. Scope of the Method

Reactions may be carried out with a dihalomethyl ketone that contains an electron-withdrawing (**b-d**), an electron-donating (**e-f**), a sterically hindered (**2.25h-i**), a heterocyclic (**g**), and an alkyl (**2.26h-i**) substituent (Scheme 2.35). Enantioselectivities for *p*-chloro, *p*-methoxy, and *p*-tolyl substrates (**b**, **e**, **f**) were slightly lower due to a higher level of uncatalyzed background reaction. The electron-rich carbonyls may form a stronger association with the allyl–B(pin) to facilitate this background reaction, while the electron-poor substrate is simply more electrophilic. As before, enantioselectivities were not as high with alkyl substrates (**2.26h-i**).

Scheme 2.35. Scope for Catalytic Enantioselective Allyl Additions to Dihalomethyl Ketones[a]

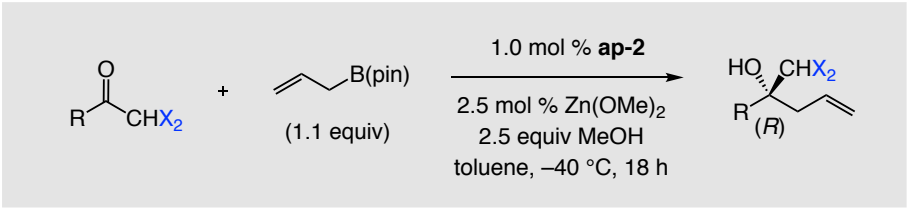

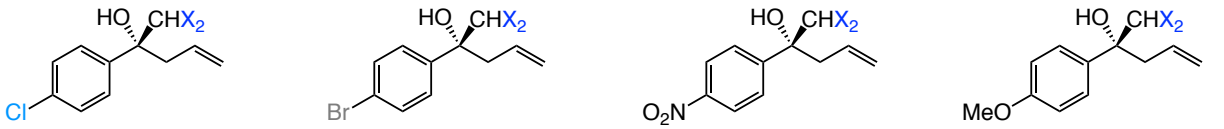

2.25b or **2.26b**
X = Cl: 92% yield, 88:12 er
X = Br: 79% yield, 94:6 er

2.25c or **2.26c**
X = Cl: 85% yield, 91.5:8.5 er
X = Br: 74% yield, 98:2 er

2.25d or **2.26d**
X = Cl: 78% yield, 96:4 er
X = Br: 92% yield, 94:6 er

2.25e or **2.26e**
X = Cl: 95% yield, 82:18 er
X = Br: 93% yield, 90:10 er

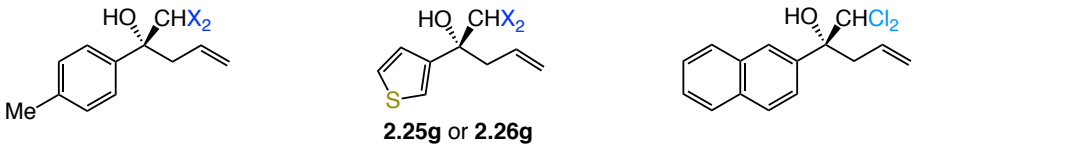

2.25f or **2.26f**
X = Cl: 92% yield, 87:13 er
X = Br: 88% yield, 85:15 er

2.25g or **2.26g**
X = Cl: 83% yield, 94.5:5.5 er
X = Br: 82% yield, 92:8 er

2.25h
87% yield, 88:12 er

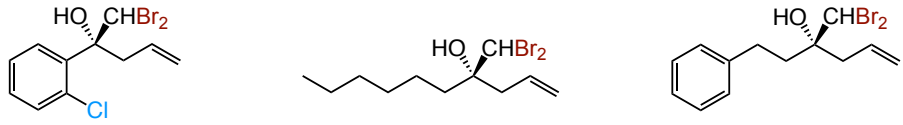

2.25i
82% yield, 95:5 er

2.26h
92% yield, 69:31 er

2.26i
92% yield, 62.5:37.5 er

[a] Reactions performed under N_2 atm. Conv determined by analysis of ^{1}H NMR spectra of unpurified mixtures; conv (±2%) refers to disappearance of the ketone starting material. Yield of isolated and purified material (±5%). Enantioselectivity determined by HPLC analysis (±1%). See Experimental Section for details.

2.5.4. Conversion to Aldehydes Bearing a Halogen-Substituted Quaternary Carbon Stereogenic Center

We wondered whether we could convert a dihalomethyl-substituted tertiary homoallylic alcohol to the corresponding halogen-substituted epoxide, analogous to the monohalomethyl-substituted variants. The expected epoxides were readily formed upon exposure of the homoallylic alcohol to mildly basic conditions (Scheme 2.26). Subsequent addition of a Lewis acid promoted halogen migration to afford aldehydes **2.27** or **2.28**, with complete enantiospecificity (Scheme

2.36).[106] These otherwise difficult-to-access aldehydes have several handles for further functionalization: the aldehyde itself, an olefin, and a halogen. A recent review detailed the applications of this type of aldehyde in natural product synthesis.[107]

Scheme 2.36. Synthesis of Enantiomerically Enriched Aldehydes

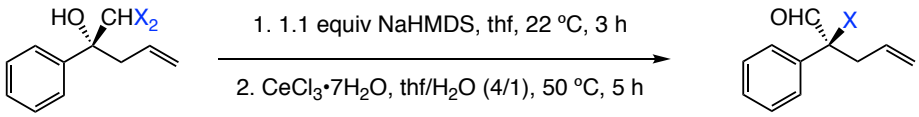

2.25a or **2.26a**
X = Cl: 90:10 er
X = Br: 93:7 er

2.27 or **2.28**
X = Cl: 76% yield, 90:10 er
X = Br: 58% yield, 93:7 er

[a] Reactions performed under N_2 atm. Conv determined by analysis of ^{1}H NMR spectra of unpurified mixtures; conv (±2%) refers to disappearance of the ketone starting material. Yield of isolated and purified material (±5%). Enantioselectivity determined by HPLC analysis (±1%). See Experimental Section for details.

2.6. Catalytic Enantioselective Allyl Additions to Mono- and Difluoromethyl Ketones

Previous studies had shown that additions to mono- and difluoromethyl ketones are minimally enantioselective.[6c] As noted earlier, we attribute this to minimization of dipolar repulsion preventing electrostatic interaction between the haloalkyl moieties and the catalyst's ammonium group. We wondered if we could use a combination of steric and electronic factors, which have been delineated above, to identify conditions for catalytic enantioselective allyl additions to mono- and difluoromethyl ketones.

[106] Arasaki, H.; Iwata, M.; Nishimura, D.; Itoh, A.; Masaki, Y. *Synlett* **2004**, *3*, 546–548.
[107] Britton, R.; Kang, B. *Nat. Prod. Rep.* **2013**, *30*, 227–236.

2.6.1. Optimization Studies

Analysis of the stereochemical models for addition to α-difluoromethyl ketones would appear to be similar in energy (Scheme 2.31). Reaction through electrostatic interaction would be similar in energy to minimization of dipolar repulsion (**XIX** vs **XX**) and the size difference between an aryl group and a difluoromethyl group is small (Sterimol B_1 values: phenyl = 1.71, CHF_2 = 1.63).

In the presence of **ap-2**, under the conditions used for allyl additions to trifluoromethyl ketones, **2.31a** was generated in 58:42 er (Scheme 2.37). Significant improvement was seen when the reaction was performed at –40 °C, affording **2.31a** in 81:19 er. Aminophenol screening indicated that increasing the bulk of the aryl substituent leads to some improvement in enantioselectivity (**ap-10** and **ap-11**, Scheme 2.37). Thus, with 5.0 mol % **ap-11** after eighteen hours at –40 °C, **2.31a** was isolated in 80% yield and 85.5:14.5 er.

Scheme 2.37. Ligand Screening for Allyl Addition to Difluoromethyl Ketones[a]

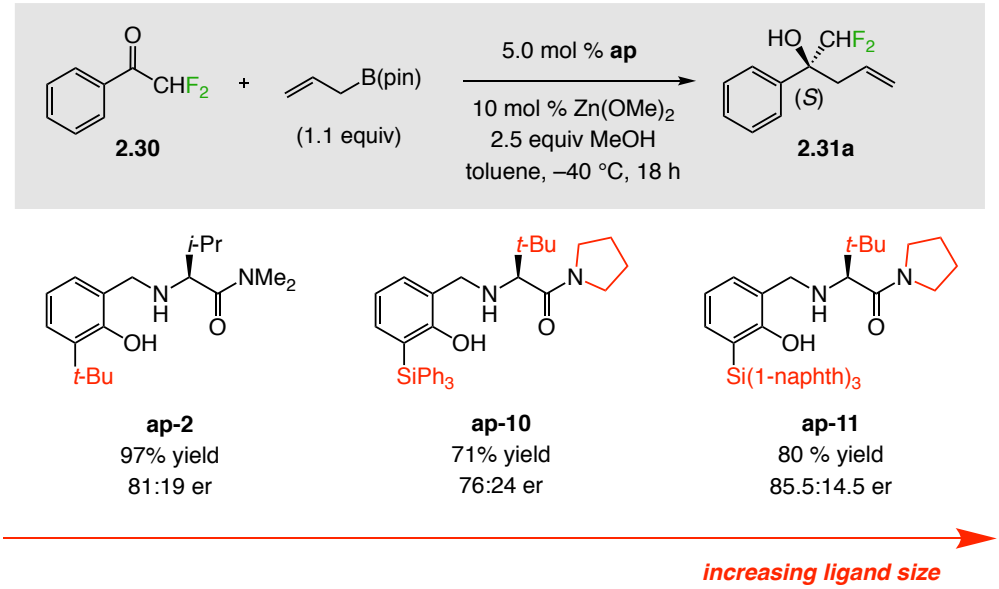

[a] Reactions performed under N_2 atm. Conv determined by analysis of ^{1}H NMR spectra of unpurified mixtures; conv (±2%) refers to disappearance of the ketone starting material. Yield of isolated and purified material (±5%). Enantioselectivity determined by HPLC analysis (±1%). See Experimental Section for details.

In order to identify whether electronic or steric factors were predominant in additions to difluoromethyl ketones, the HPLC traces of **2.31a** and the product of halogen abstraction from **2.12** were compared (Scheme 2.38). This analysis revealed that additions to difluoromethyl-substituted ketones occur to the opposite enantiotopic face as that of the trihalo-, dichloro-, and dibromomethyl-substituted ketones. The use of sterically encumbered aminophenol ligand **ap-11** proved successful in obtaining high enantioselectivity for additions to difluoromethyl-substituted ketones (**XX**, Scheme 2.31).

Scheme 2.38. Absolute Stereochemistry for Allyl Addition to Difluoromethyl Ketones

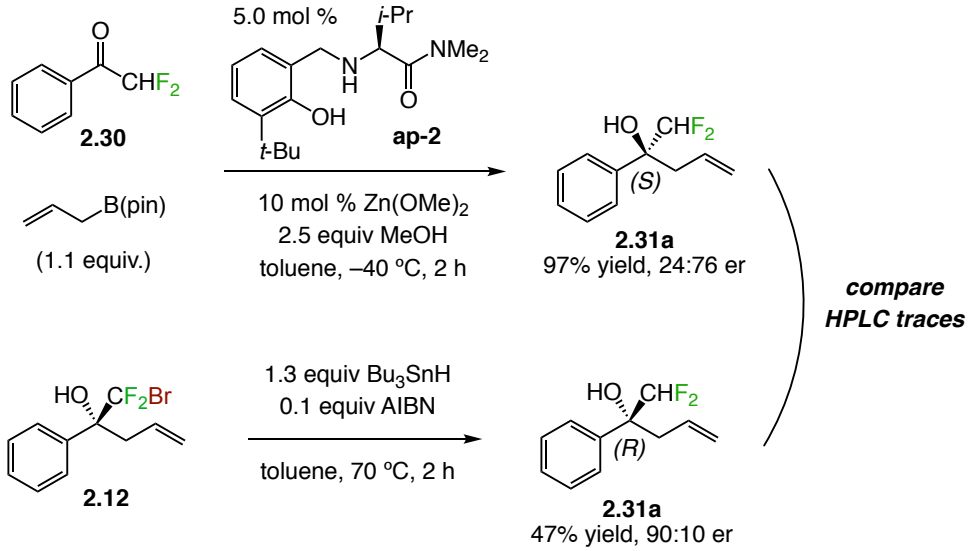

2.6.2. Scope of Allyl Additions to Difluoromethyl Ketones

A wide variety of difluoromethyl ketones were converted to the desired homoallylic alcohols in up to >98% yield and >99:1 er (Scheme 2.39). The lower enantioselectivity for **2.31b** is likely a result of a highly competitive background reaction, and the lower enantioselectivity for **2.31e** compared to **2.31d** supports the dominance of steric factors in controlling enantioselectivity. As noted earlier, the heteroatom in **2.31d** can establish electrostatic interaction with the catalyst's ammonium group, causing diminution in enantioselectivity (**XXI**, Scheme 2.40a). For

homoallylic alcohol **2.31e**, such interactions are not possible. What is more, a thienyl group is smaller than an aryl ring, and consequently, transition states **XXIII** and **XXIV** become similar in energy (Scheme 2.40b).

Scheme 2.39. Scope for Catalytic Enantioselective Allyl Additions to Difluoromethyl Ketones[a]

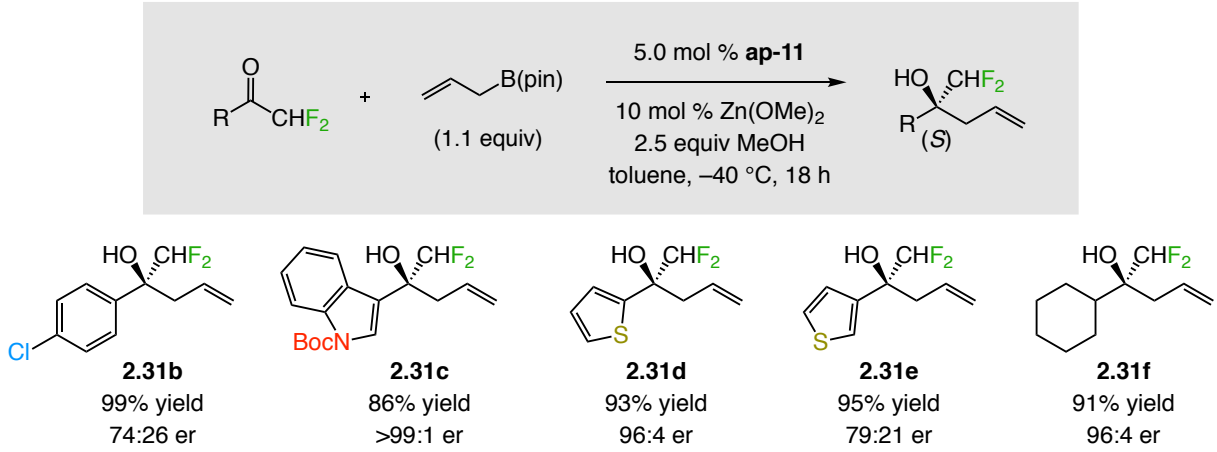

[a] Reactions performed under N_2 atm. Conv determined by analysis of ^{1}H NMR spectra of unpurified mixtures; conv (±2%) refers to disappearance of the ketone starting material. Yield of isolated and purified material (±5%). Enantioselectivity determined by HPLC analysis (±1%). See Experimental Section for details.

Scheme 2.40. Transition States for 2- and 3-Thienyl Substrates

a. Origin of high enantioselectivity for addition to 2-thienyl ketone:

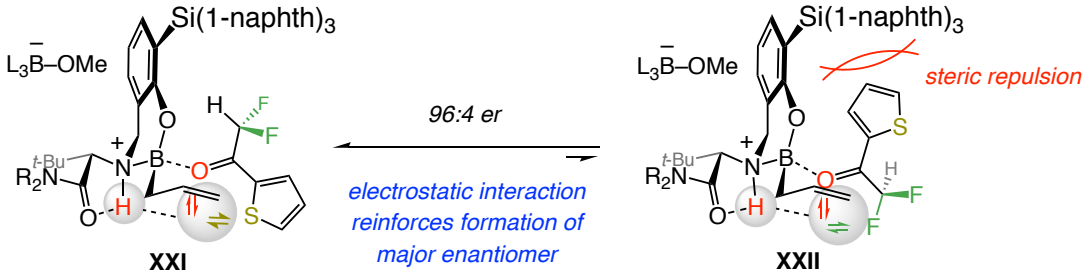

b. Origin of low enantioselectivity for addition to 3-thienyl ketone:

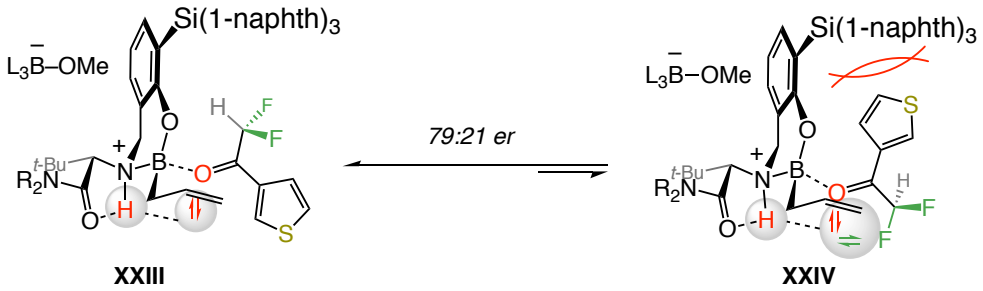

2.6.3. Optimization Studies for Allyl Additions to Monofluoromethyl Ketones

As shown in Scheme 2.22, addition to monofluoromethyl ketones is predicted to go through the sterically-controlled transition state due to minimization of steric and dipolar repulsion. However, monofluoromethyl ketones have the smallest size difference between its substituents, making enantiotopic face differentiation more challenging than monochloro- and monobromomethyl variants (Sterimol B_1 values: Ph = 1.71, CH_2F = 1.52, CH_2Cl = 1.50, CH_2Br = 1.50).

We began by screening a variety of aminophenols, leading us to determine that silyl-containing **ap-11** is the most effective (Scheme 2.41). The homoallylic alcohol product **2.33a** was thus isolated in 83% yield and 92.5:7.5 er. The higher enantioselectivity compared to the corresponding difluoromethyl derivative is probably because electrostatic interactions play a minimal role, if any, and thus the process is largely controlled by steric factors.

Scheme 2.41. Ligand Screening for Allyl Addition to Difluoromethyl Ketones[a]

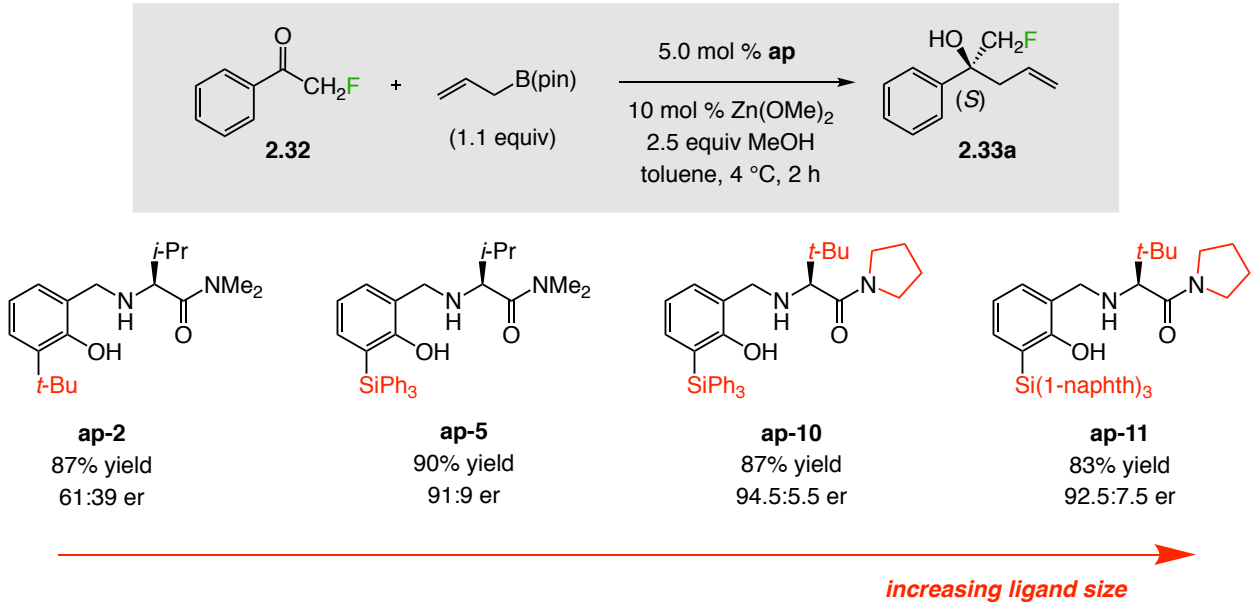

[a] Reactions performed under N_2 atm. Conv determined by analysis of ^{1}H NMR spectra of unpurified mixtures; conv (±2%) refers to disappearance of the ketone starting material. Yield of isolated and purified material (±5%). Enantioselectivity determined by HPLC analysis (±1%). See Experimental Section for details.

Identification of the major product enantiomer was carried out by comparison to a previously reported compound[62b] and revealed that additions to monofluoromethyl ketones afford the same enantiomer as additions to monochloromethyl, monobromomethyl, and difluoromethyl ketones (Scheme 2.42).

Scheme 2.42. Absolute Stereochemistry for Allyl Addition to Monofluoromethyl Ketones

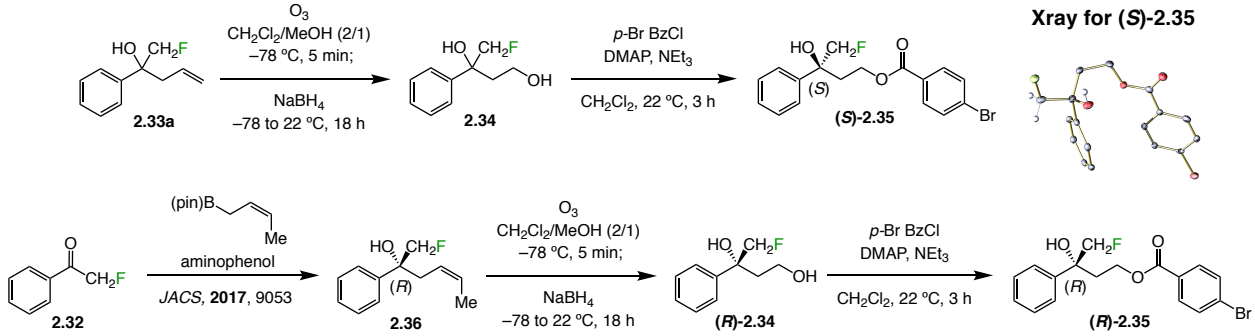

2.6.4. Scope of Allyl Additions to Monofluoromethyl Ketones

The method has broad scope; electron-donating aryl (**2.33b**), electron-withdrawing aryl (**2.33c**), sterically hindered (**2.33d-e**), heterocyclic (**2.33f**), and alkyl-substituted (**2.33g**) ketones were converted to the corresponding tertiary alcohols efficiently and with high enantioselectivity (Scheme 2.43). The slightly lower enantioselectivity observed for **2.33d** might arise from competitive uncatalyzed addition to the more electrophilic ketone. The high enantioselectivity observed for 2-thienyl substrate **2.33f** is in accordance with previous examples (see Scheme 2.40a).

Scheme 2.43. Scope of Catalytic Enantioselective Allyl Additions to Monofluoromethyl Ketones[a]

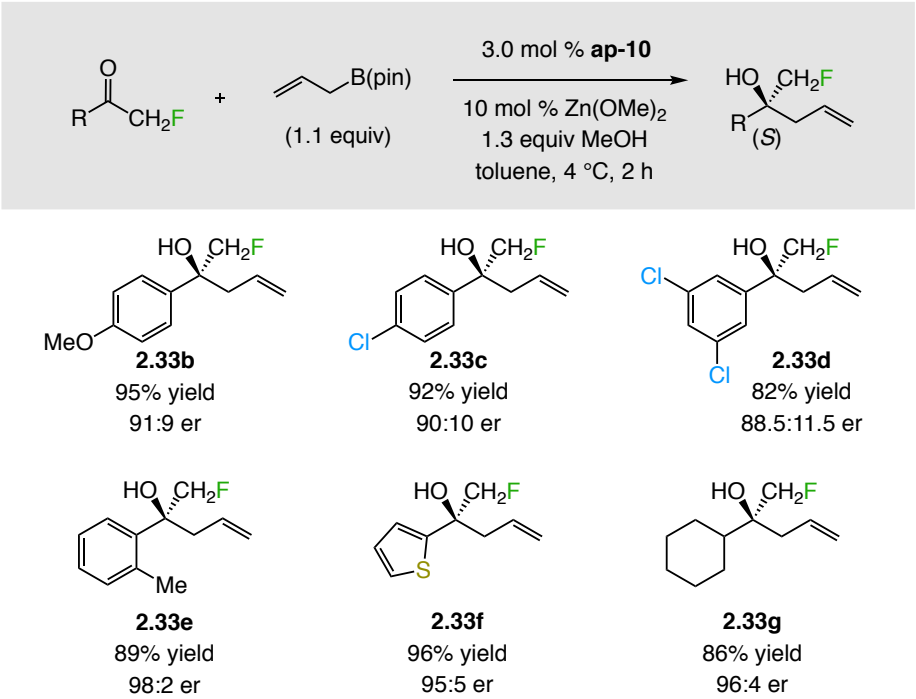

[a] Reactions performed under N_2 atm. Conv determined by analysis of ^{1}H NMR spectra of unpurified mixtures; conv (±2%) refers to disappearance of the ketone starting material. Yield of isolated and purified material (±5%). Enantioselectivity determined by HPLC analysis (±1%). See Experimental Section for details.

2.6.5. Representative Functionalization

Triazole-containing molecules are important in drug discovery.[108] Leukotriene biosynthesis inhibitor contains a trifluoromethyl homoallylic alcohol and the precursor to anti-seizure medication, Banzel, is a trichloromethyl ketone. We envisioned synthesizing a family of analogs with different numbers of halogens on the α-carbon. However, triazole-substituted alcohols **2.38** and **2.39** were generated in 62:38 and 60:40 er, respectively (Scheme 2.44). We

[108] (a) Kharb, R.; Sharma, P. C.; Yar, M. S. *J. Enzyme Inhib. Med. Chem.* **2011**, *26*, 1–21. (b) Zhou, C.-H.; Wang, Y. *Curr. Med. Chem.* **2012**, *19*, 239–280. (c) Dheer, D.; Singh, V.; Shankar, R. *Bioorg. Chem.* **2017**, *71*, 30–54. (d) Bozorov, K.; Zhao, J.; Aisa, H. A. *Bioorg. Med. Chem.* **2019**, *27*, 3511–3531. (e) Malik, M. S.; Ahmed, S. A.; Althagafi, I. I.; Ansari, M. A.; Kamal, A. *RSC Med. Chem.* **2020**, *11*, 327–348.

attributed this low level of enantioselectivity to competitive electrostatic interaction between the catalyst's ammonium moiety, the trihalomethyl group, and the triazole ring.

Scheme 2.44. Initial Attempts at Enantioselective Synthesis of Triazole-Substituted Tertiary Homoallylic Alcohols[a]

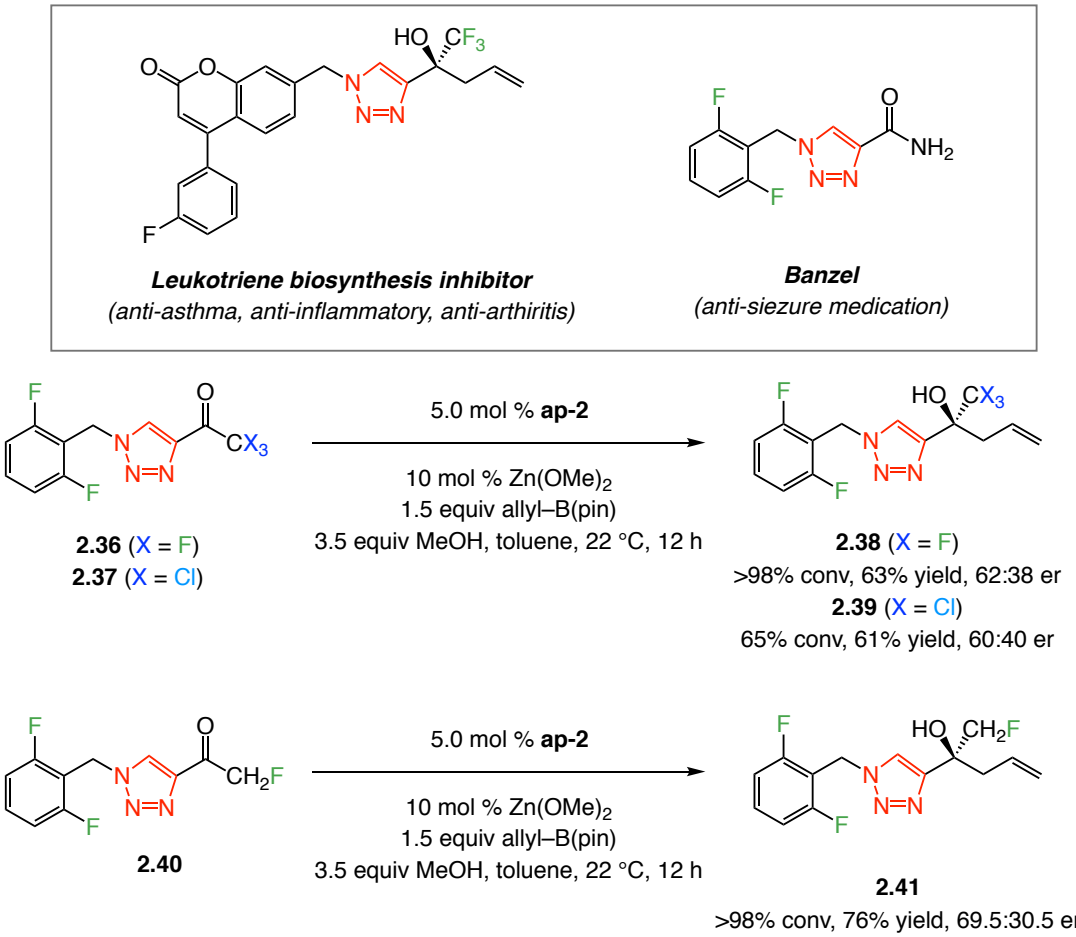

[a] Reactions performed under N_2 atm. Conv determined by analysis of ^{1}H NMR spectra of unpurified mixtures; conv (±2%) refers to disappearance of the ketone starting material. Yield of isolated and purified material (±5%). Enantioselectivity determined by HPLC analysis (±1%). See Experimental Section for details.

We predicted that allyl addition to monofluoromethyl ketone **2.40**, where electrostatic interactions are far less influential, would be more enantioselective. However, somewhat to our surprise, homoallylic alcohol **2.41** was obtained in 69.5:30.5 er (Scheme 2.44). Subsequent control

experiments revealed that basic moieties such as triazoles and imidazoles inhibit catalytic activity, perhaps by serving as a base and quenching the ammonium moiety of the catalyst.

As an alternative approach, we chose to install the triazole moiety after the allyl addition. Accordingly, as illustrated in Scheme 2.45, catalytic enantioselective allyl addition followed by [3+2]-cycloaddition ("click reaction"[109]) allowed us to isolate **2.41** and **2.45** in 86% and 89% yield and 99:1 and >99:1 er. A crystal structure of **2.45** allowed us to further confirm the identity of the major enantiomer.

Scheme 2.45. One-Pot Catalytic Enantioselective Allyl Addition/Dipolar Cycloaddition

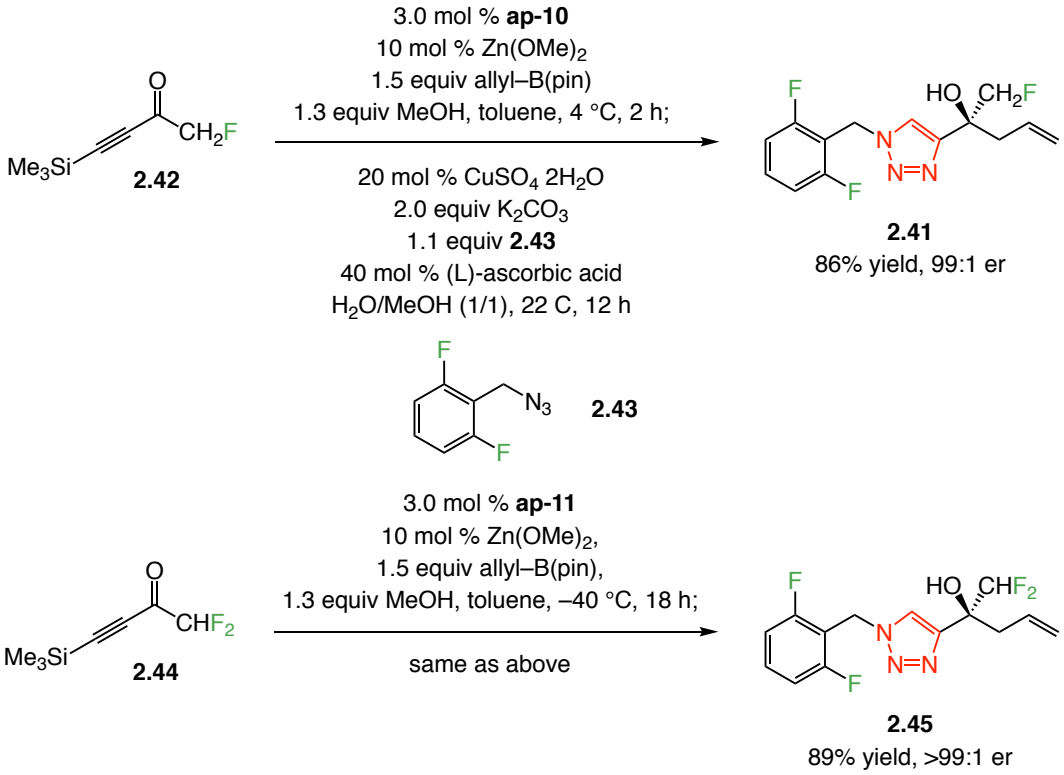

[a] Reactions performed under N_2 atm. Conv determined by analysis of ^{1}H NMR spectra of unpurified mixtures; conv (±2%) refers to disappearance of the ketone starting material. Yield of isolated and purified material (±5%). Enantioselectivity determined by HPLC analysis (±1%). See Experimental Section for details.

[109] (a) Rostovtsev, V. V.; Green, L. G.; Fokin, V. V.; Sharpless, K. B. *Angew. Chem., Int. Ed.* **2002**, *41*, 2596–2599. (b) Himo, F.; Lovell, T.; Hilgraf, R.; Rostovtsev, V. V.; Noodleman, L.; Sharpless, K. B.; Fokin, V. V. *J. Am. Chem. Soc.* **2005**, *127*, 210–216. (c) Worell, B. T.; Malik, J. A.; Fokin, V. V. *Science* **2013**, *340*, 457–460.

2.7. Summary and Conclusion

In brief, we have developed a set of catalytic enantioselective methods for addition of an allyl group to a range of tri-, di- and monohalomethyl ketones. The tertiary homoallylic alcohol products are readily modifiable, as illustrated through conversion to various enantiomerically enriched epoxides and α-halogenated quaternary aldehydes. None of the aforementioned compounds can be readily accessed by an alternative approach. Application to preparation of bioactive molecules, such as the one-pot formal synthesis of a 1,1-disubstituted epoxide for synthesis of anti-inflammatory compound, Boscartin F, and triazole-containing drug analogs, underscore the considerable utility of the advances described in this Chapter. Equally important are the mechanistic principles that served as the foundation of the investigation described herein, and the results have shed valuable light on the different fundamental attributes of carbon–halogen bonds.

2.8. Experimental Section

2.8.1. Experimental

2.8.1.1. General

Infrared (IR) spectra were recorded on a Bruker alpha spectrophotometer, $\square_{max}$ in cm^{-1}. Bands are characterized as broad (br), strong (s), medium (m), and weak (w). ^{1}H NMR spectra were recorded on a Varian Unity INOVA 400 (400 MHz) spectrometer. Chemical shifts are reported in ppm from tetramethylsilane with the solvent resonance as the internal standard ($CDCl_3$: δ 7.26 ppm). Data are reported as follows: chemical shift, integration, multiplicity (s = singlet, d = doublet, t = triplet, q = quartet, sept = septet, br = broad, m = multiplet), and coupling constants (Hz). ^{13}C NMR spectra were recorded on a Varian Unity INOVA 400 (100 MHz) with complete proton decoupling. Chemical shifts are reported in ppm from tetramethylsilane with the solvent resonance as the internal standard ($CDCl_3$: δ 77.16 ppm). Data are reported as follows: chemical shift, multiplicity (singlet unless otherwise noted), and coupling constants (Hz). High-resolution mass spectrometry was performed on a JEOL AccuTOF-DART (positive mode) at the Mass

Spectrometry Facility, Boston College. Enantiomeric ratio (er) values were determined by HPLC analysis using either a Shimadzu LC-2010AHT or SCL-10AVP chromatograph (Chiral Technologies Chiralcel OD-H (4.6 x 250 mm), Chiral Technologies Chiralcel OJ-H (4.6 x 250 mm), Chiral Technologies Chiralpak AD-H (4.6 x 250 mm), Chiral Technologies Chiralpak AZ-H (4.6 x 250 mm), Chiral Technologies Chiralpak AS-H (4.6 x 250 mm) columns), or GLPC (gas-liquid partition chromatography) with an Agilent chromatograph (Alltech Associated Chiraldex β-DM (30 m x 0.25 mm). Specific rotations were measured on a Rudolph Research Analytical Autopol IV Polarimeter. Melting points were determined using a Thomas Hoover Uni-melt capillary melting point apparatus. Unless otherwise noted, reactions were carried out under an atmosphere of dry N_2 in oven-dried (135 ºC) glassware with the appropriate oven-dried (65 ºC) Teflon cap.

2.8.1.2. Solvents

Unless otherwise noted, solvents were purged with Argon and purified under a positive pressure of dry Argon by a modified Innovative Technologies purification system. Toluene (Fisher, ACS Grade) was passed successively through activated copper and alumina columns. Dichloromethane (Fisher, ACS Grade) and diethyl ether (Aldrich, Chromasolv®) were passed successively through two activated alumina columns. Tetrahydrofuran was purified by distillation from sodium benzophenone ketyl immediately prior to use. $CDCl_3$ was purchased from Cambridge Isotope Laboratories and stored over activated 4Å molecular sieves prior to use. All work-up and purification procedures were carried out in air with reagent grade solvents (purchased from Fisher).

2.8.1.3. Reagents

Allylboronates: Allylboronic acid pinacol ester was purchased from Frontier Scientific and distilled prior to use. 2-Methyl-1-propenylboronic acid pinacol ester was synthesized and purified in accordance with a procedure in the literature.[110]

Ammonium Chloride was purchased from Fisher Scientific and used as received.

(L)-Ascorbic acid was purchased from Fisher and used as received.

9-Borabicyclo[3.3.1]nonane dimer was purchased from Alfa Aesar and used as received.

Benzyl bromide was purchased from Aldrich and used as received.

Boc-Tle-OH was purchased from Advanced ChemTech and used as received.

Boc-Val-OH was purchased from Advanced ChemTech and used as received.

1-Bromonaphthalene was purchased from Aldrich and used as received.

***N*-Bromosuccinimide** was purchased from Alfa Aesar and used as received.

---

[110] Zhang, P.; Roundtree, I. A.; Morken, J. P. *Org. Lett.* **2012**, *14*, 1416–1419.

***n*-Butyllithium (2.5M in hexanes)** was purchased from Aldrich and titrated with *N*-Benzylbenzamide prior to use.

3-*tert*-Butyl-2-hydroxybenzaldehyde was purchased from Aldrich and used as received.

***tert*-Butyllithium solution (1.7M in pentane)** was purchased from Aldrich and titrated with *N*-Benzylbenzamide in thf prior to use.

Cerium (III) chloride heptahydrate was purchased from Strem and used as received.

Cesium fluoride was purchased from Strem and used as received.

Chloroacetyl chloride was purchased from Oakwood and used as received.

***N*-Chlorosuccinimide** was purchased from Aldrich and used as received.

Chlorotrimethylsilane was purchased from Oakwood and used as received.

Chlorotriphenylsilane was purchased from Oakwood and was used as received.

Copper (II) sulfate pentahydrate was purchased from Aldrich and used as received.

18-Cr-6 was purchased from TCI and used as received.

Dess-Martin periodinane was purchased from Oakwood and used as received.

1,8-Diazabicycloundec-7-ene (DBU) was purchased from Aldrich and distilled from calcium hydride prior to use.

1,3-Dibromo-5,5-dimethylhydantoin was purchased from TCI and used as received.

2,6-Dibromophenol was purchased from Oakwood and used as received.

1,3-Dichloro-5,5-dimethylhydantoin was purchased from Oakwood and used as received.

(Difluoromethyl)trimethylsilane was purchased from Oakwood and used as received.

***N,N*-Diisopropylethylamine** was purchased from Alfa Aesar and used as received.

Dimethoxyethane was purchased from Aldrich and distilled from calcium hydride prior to use.

Dimethylamine (40 wt % in H_2O) was purchased from Aldrich and used as received.

Dimethylaminopyridine was purchased from Oakwood and used as received.

Dimethylformamide was purchased from Aldrich and used as received.

***N,O*-Dimethylhydroxylamine** was purchased from Aldrich and used as received.

Dimethylsulfoxide was purchased from Aldrich and used as received.

Ethanol was purchased from Fisher and used as received.

Ethyl bromodifluoroacetate was purchased from Oakwood and used as received.

Ethyl chlorodifluoroacetate was purchased from Oakwood and used as received.

Ethyl difluoroacetate was purchased from Oakwood and used as received.

Ethyl fluoroacetate was purchased from TCI and used as received.

1-Ethyl-3-(3-dimethylaminopropyl)carbodiimide Hydrochloride (EDC•HCl) was purchased from Advanced ChemTech and used as received.

Ethyl trimethylsilylacetate was purchased from Aldrich and used as received.

Ethynyltrimethylsilane was purchased from Oakwood and used as received.

Ethyl vinyl ether was purchased from Alfa Aesar and used as received.

Hydrochloric acid (4.0 M in 1,4-dioxane) was purchased from Aldrich and used as received.

1-Hydroxy-benzotriazole Hydrate (HOBt•H_2O) was purchased from Advanced ChemTech and used as received.

Imidazole was purchased from Oakwood and used as received.

Iron (III) chloride hexahydrate was purchased from Strem and used as received.

Magnesium sulfate was purchased from Fisher and flame-dried under vacuum prior to use.

Magnesium turnings were purchased from Oakwood and used as received.

Methanol was purchased from Aldrich (99.8% anhydrous) and distilled from magnesium prior to use or used as received.

Oxone® was purchased from AK Scientific and used as received.

Phenylacetylene was purchased from Oakwood and used as received.

Phenylmagnesium bromide was purchased from Aldrich and used as received.

Potassium bromide was purchased from Strem and used as received.

Potassium carbonate was purchased from Fisher and used as received.

Potassium chloride was purchased from Fisher and used as received.

Potassium *tert*-butoxide was purchased from Aldrich and used as received.

Potassium fluoride was purchased from Strem and used as received.

Pyrrolidine was purchased from Aldrich and used as received.

Silicon tetrachloride was purchased from Aldrich and used as received.

Sodium azide was purchased from Oakwood and used as received.

Sodium bis(trimethylsilyl)amide was purchased from Aldrich and used as received.

Sodium borohydride was purchased from Aldrich and used as received.

Sodium *tert*-butoxide was purchased from Strem Chemicals and used as received.

Sodium dichromate was purchased from Aldrich and used as received.

Sodium hydroxide was purchased from Oakwood and used as received.

Sodium trichloroacetate was purchased from Aldrich and used as received.

Tetrabutylammonium bromide was purchased from Combi Blocks and used as received.

Tetrabutylammonium fluoride was purchased from Oakwood and used as received.

***N*,*N*,*N*′,*N*′-Tetramethylethylenediamine** was purchased from Aldrich and used as received.

***p*-Toluenesulfonic acid monohydrate** was purchased from Oakwood and used as received.

Trichloroacetic acid was purchased from Aldrich and used as received.

(*E*)-1,1,1-Trichloro-4-ethoxybut-3-en-2-one was purchased from Synquest and used as received.

Triethylamine was purchased from Aldrich and distilled from to use.

Trifluoroacetic anhydride was purchased from Oakwood and used as received.

Triisopropylsilyl trifluoromethanesulfonate was purchased from Aldrich and used as received.

Trimethyl(phenylethynyl)silane was purchased from Aldrich and used as received.

Trimethylsilyl trifluoromethanesulfonate was purchased from Oakwood and used as received.

Zinc (II) fluoride was purchased from Acros and used as received.

Zinc (II) methoxide was purchased from Aldrich and used as received.

2.8.2. Substrates

2.8.2.1. Trihalomethyl ketones

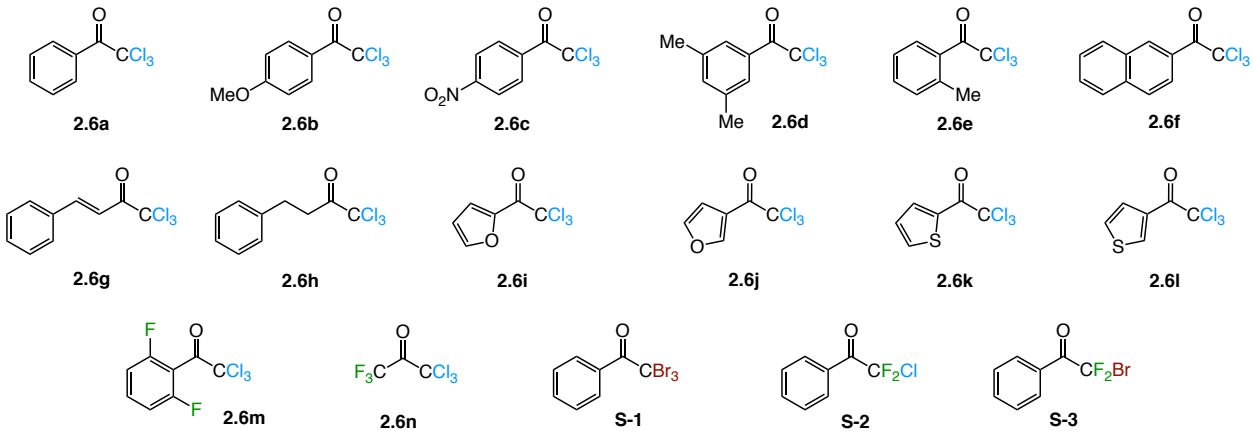

2,2,2-Trichloro-1-phenylethan-1-one (2.6a) was synthesized from 2,2,2-Trichloro-1-phenylethan-1-ol (purchased from Alfa Aesar) by oxidation in accordance to a procedure in the literature[111] and the analytical data are consistent with those reported previously.[112]

2,2,2-Trichloro-1-(4-methoxyphenyl)ethan-1-one (2.6b) was synthesized in accordance to a procedure in the literature[113,114] and analytical data are consistent with those reported previously.[112]

2,2,2-Trichloro-1-(4-nitrophenyl)ethan-1-one (2.6c) was synthesized in accordance to a procedure in the literature[113,114] and analytical data are consistent with those reported previously.[112]

2,2,2-Trichloro-1-(3,5-dimethylphenyl)ethan-1-one (2.6d) was synthesized in accordance to a procedure in the literature.[113,114] **IR (neat):** 1737 (s), 1594 (w), 1465 (w), 1383 (w), 1205 (m), 1034 (w), 981 (w), 908 (m), 854 (m), 806 (m), 774 (m), 732 (s), 691 (s), 596 (w), 527 (w), 398 (w) cm^{-1}; **^{1}H NMR (400 MHz, $CDCl_3$):** δ 7.26 (t, *J* = 7.7 Hz, 1H), 7.09 (d, *J* = 7.6 Hz, 2H), 2.37

[111] Ge, G.-C.; Mo, D.-L.; Ding, C.-H.; Dai, L.-X.; Hou, X.-L. *Org. Lett.* **2012**, *14*, 5756–5759.

[112] Ram, R. N.; Tittal, R. K. *Tetrahedron Lett.* **2016**, *57*, 2437–2440.

(s, 6H); **^{13}C NMR (100 MHz, $CDCl_3$):** δ 194.1, 136.2, 134.3, 130.0, 127.7, 94.8, 20.9; **HRMS (DART$^+$):** Calcd for $C_{10}H_{10}O_1Cl_3$ $[M+H]^+$: 250.9791; Found: 250.9801.

2,2,2-Trichloro-1-(*o*-tolyl)ethan-1-one (2.6e) was synthesized in accordance to a procedure in the literature[113,114] and analytical data are consistent with those reported previously.[112]

2,2,2-Trichloro-1-(naphthalen-2-yl)ethan-1-one (2.6f) was synthesized in accordance to a procedure in the literature[113,114] and analytical data are consistent with those reported previously.[115]

(*E*)-1,1,1-Trichloro-4-phenylbut-3-en-2-one (2.6g) was synthesized in accordance to a procedure in the literature and the analytical data are consistent with those reported previously.[116]

1,1,1-Trichloro-4-phenylbutan-2-one (2.6h) was synthesized in accordance to a procedure in the literature[113,115] and analytical data are consistent with those reported previously.[113]

2,2,2-Trichloro-1-(furan-2-yl)ethan-1-one (2.6i) was synthesized in accordance to a procedure in the literature.[113,114] **IR (neat):** 1740 (s), 1523 (w), 1465 (w), 1383 (w), 1205 (m), 1034 (w), 981 (w), 908 (m), 854 (m), 806 (m), 774 (m), 732 (s), 691 (s), 596 (w), 527 (w), 398 (w) cm^{-1}; **^{1}H NMR (400 MHz, $CDCl_3$):** δ 7.75 (s, 1H), 7.63 (d, J = 3.6 Hz, 1H), 6.65 (dd, J = 3.7, 1.7 Hz, 1H); **^{13}C NMR (100 MHz, $CDCl_3$):** δ 170.6, 148.9, 145.3, 124.2, 112.9, 94.4; **HRMS (DART$^+$):** Calcd for $C_6H_4O_2Cl_3$ $[M+H]^+$: 212.9271; Found: 212.9268.

2,2,2-Trichloro-1-(furan-3-yl)ethan-1-one (2.6j) was synthesized in accordance to a procedure in the literature[113,114] and analytical data are consistent with those reported previously.[117]

2,2,2-Trichloro-1-(thiophen-2-yl)ethan-1-one (S-1k) was synthesized in accordance to a procedure in the literature[113,114] and analytical data are consistent with those reported previously.[118]

2,2,2-Trichloro-1-(thiophen-3-yl)ethan-1-one (2.6l) was synthesized in accordance to a procedure in the literature.[113,114] **IR (neat):** 3117 (w), 1696 (s), 1500 (w), 1402 (w), 1235 (m), 1186 (m), 1080 (w), 1023 (w), 885 (m), 817 (s), 708 (s), 673 (s), 629 (m), 618 (m), 420 (w) cm^{-1}; **^{1}H NMR (400 MHz, $CDCl_3$):** δ 8.51 (dd, J = 3.0, 1.3 Hz, 1H), 7.77 (dd, J = 5.2, 1.3 Hz, 1H), 7.37 (dd, J = 5.2, 3.0 Hz, 1H); **^{13}C NMR (100 MHz, $CDCl_3$):** δ 175.7, 137.5, 131.9, 129.7, 126.1, 95.8; **HRMS (DART$^+$):** Calcd for $C_6H_4Cl_3OS$ $[M+H]^+$: 228.9048; Found: 228.9057.

2,2,2-Trichloro-1-(2,6-difluorophenyl)ethan-1-one (2.6m) was synthesized in accordance to a procedure in the literature.[113,115] **IR (neat):** 3117 (w), 1696 (s), 1500 (w), 1402 (w), 1235 (m), 1186 (m), 1080 (w), 1023 (w), 885 (m), 817 (s), 708 (s), 673 (s), 629 (m), 618 (m), 420 (w) cm^{-1}; **^{1}H NMR (400 MHz, $CDCl_3$):** δ 7.51 (tt, J = 8.5, 6.3 Hz, 1H), 7.03 (td, J = 8.5, 1.0 Hz, 2H); **^{13}C**

---

[113] Corey, E. J.; Link, J. O.; Shao, Y. *Tetrahedron Lett.* **1992**, *33*, 3435–3438.

[114] Perryman, M. S.; Harris, M. E.; Foster, J. L.; Joshi, A.; Clarkson, G. J.; Fox, D. J. *Chem. Commun.* **2013**, *49*, 10022–10024.

115] Cafiero, L. R.; Snowden, T. S. *Org. Lett.* **2008**, *10,* 3853–3856.

[116] Zhang, S.; Taylor, J. E.; Slawin, A. M. Z.; Smith, A. D. *Org. Lett.* **2018**, *20*, 5482–5485.

[117] Zanatta, N.; Faoro, D.; Silva, S. C.; Bonacorso, H. G.; Martins, M. A. P. *Tetrahedron Lett.* **2004**, *45*, 5689–5691.

118] Dohi, S.; Moriyama, K.; Togo, H. *Eur. J. Org. Chem.* **2013**, *34*, 7815–7822.

NMR (100 MHz, $CDCl_3$): δ 180.9 (t, *J* = 1.4 Hz), 160.1 (d, *J* = 6.8 Hz), 157.6 (d, *J* = 6.6 Hz), 133.6 (t, *J* = 9.8 Hz), 112.2 (t, *J* = 22.5 Hz), 112.1–111.8 (m), 94.9; **^{19}F NMR (376 MHz, $CDCl_3$):** –106.45 (t, *J* = 7.6 Hz, 2F); **HRMS (DART$^+$):** Calcd for $C_8H_4Cl_3OF_2$ $[M+H]^+$: 258.9290; Found: 258.9277.

1,1,1-Trichloro-3,3,3-trifluoropropan-2-one (2.6n) was purchased from Combi-Blocks and used as received.

2,2,2-Tribromo-1-phenylethan-1-one (S-1) was synthesized in accordance to a procedure in the literature and the analytical data are consistent with those reported previously.[119]

2-Chloro-2,2-difluoro-1-phenylethan-1-one (S-2) was purchased from Combi-Blocks and used as received.

2-Bromo-2,2-difluoro-1-phenylethan-1-one (S-3) was synthesized in accordance to a procedure in the literature and the analytical data are consistent with those reported previously.[120]

2.8.2.2. Dichloro- and Dibromomethyl ketones

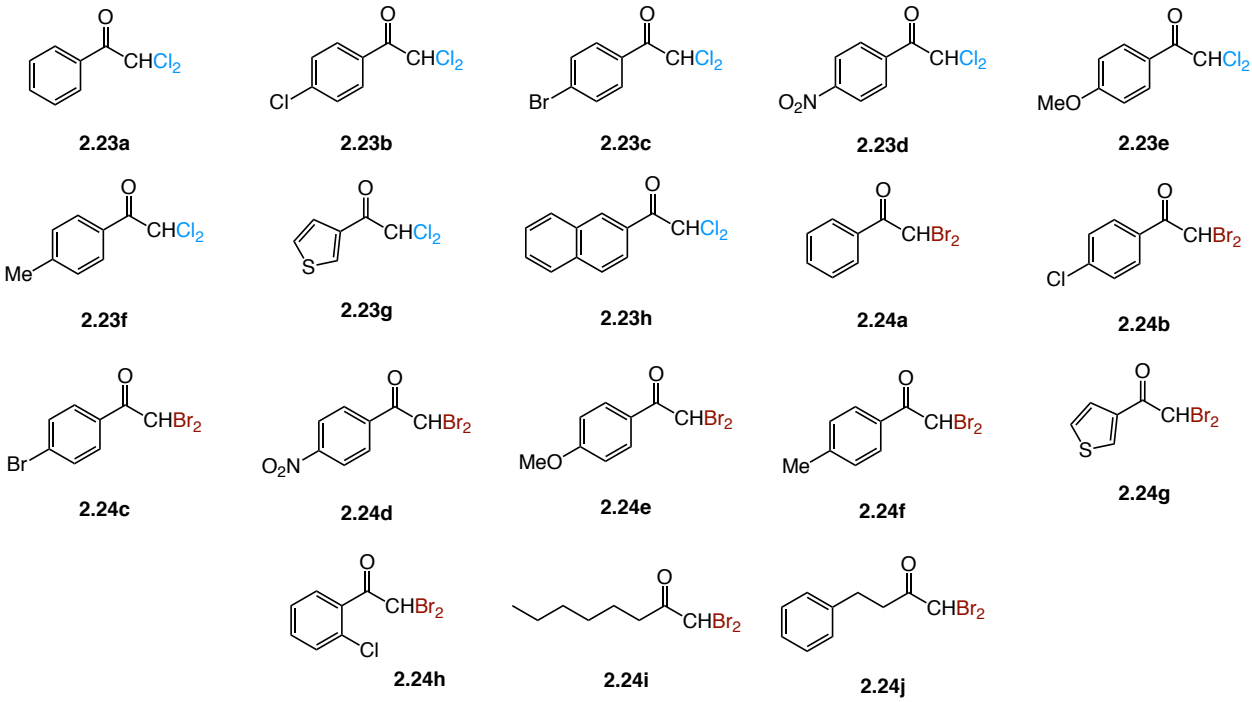

2.23a **2.23b** **2.23c** **2.23d** **2.23e**

2.23f **2.23g** **2.23h** **2.24a** **2.24b**

2.24c **2.24d** **2.24e** **2.24f** **2.24g**

2.24h **2.24i** **2.24j**

2,4'-Dichloroacetophenone (**2.23a**) was purchased from Aldrich and used as received.

2,2-Dichloro-1-(4-chlorophenyl)ethan-1-one (**2.23b**) was synthesized in accordance to a procedure in the literature and the analytical data are consistent with those reported previously.[121]

---

[119] Sriramoju, V.; Jillella, R.; Kurva, S.; Madabhushi, S. *Chem. Lett.* **2017**, *46*, 560–562.

[120] Nihei, T.; Iwai, N.; Matsuda, T.; Kitazume, T. *J. Org. Chem.* **2005**, *70*, 5912–5915.

[121] Zheng, Z.; Han, B.; Cheng, P.; Niu, J.; Wang, A. *Tetrahedron* **2014**, *70*, 9814–9818.

2,2-Dichloro-1-(4-bromophenyl)ethan-1-one (**2.23c**) was synthesized in accordance to a procedure in the literature and the analytical data are consistent with those reported previously.[122]

2,2-Dichloro-1-(4-nitrophenyl)ethan-1-one (**2.23d**) was synthesized in accordance to a procedure in the literature and the analytical data are consistent with those reported previously.[122]

2,2-Dichloro-1-(4-methoxyphenyl)ethan-1-one (**2.23e**) was synthesized in accordance to a procedure in the literature and the analytical data are consistent with those reported previously.[125]

2,2-Dichloro-1-(p-tolyl)ethan-1-one (**2.23f**) was synthesized in accordance to a procedure in the literature and the analytical data are consistent with those reported previously.[125]

2,2-Dichloro-1-(thiophen-3-yl)ethan-1-one (**2.23g**) was synthesized in accordance to a procedure in the literature and the analytical data are consistent with those reported previously.[123]

2,2-Dichloro-1-(naphthalen-2-yl)ethan-1-one (**2.23h**) was synthesized in accordance to a procedure in the literature and the analytical data are consistent with those reported previously.[124]

2,2-Dibromo-1-phenylethan-1-one (**2.24a**) was synthesized in accordance to a procedure in the literature and the analytical data are consistent with those reported previously.[125]

2,2-Dibromo-1-(4-chlorophenyl)ethan-1-one (**2.24b**) was synthesized in accordance to a procedure in the literature and the analytical data are consistent with those reported previously.[126]

2,2-Dibromo-1-(4-bromophenyl)ethan-1-one (**2.24c**) was synthesized in accordance to a procedure in the literature and the analytical data are consistent with those reported previously.[122]

2,2-Dibromo-1-(4-nitrophenyl)ethan-1-one (**2.24d**) was synthesized in accordance to a procedure in the literature[125] and the analytical data are consistent with those reported previously.[127]

2,2-Dibromo-1-(4-methoxyphenyl)ethan-1-one (**2.24e**) was synthesized in accordance to a procedure in the literature and the analytical data are consistent with those reported previously.[125]

2,2-Dibromo-1-(p-tolyl)ethan-1-one (**2.24f**) was synthesized in accordance to a procedure in the literature and the analytical data are consistent with those reported previously.[125]

2,2-Dibromo-1-(thiophen-3-yl)ethan-1-one (**2.24g**) was synthesized in accordance to a procedure in the literature and the analytical data are consistent with those reported previously.[125]

2,2-Dibromo-1-(2-chlorophenyl)ethan-1-one (**2.24h**) was synthesized in accordance to a procedure in the literature and the analytical data are consistent with those reported previously.[125]

---

[122] Zheng, Z.; Han, B.; Cheng, P.; Niu, J.; Wang, A. *Tetrahedron* **2014**, *70*, 9814–9818.

[123] Holzschneider, K.; Häring, A. P.; Haack, A.; Corey, D. J.; Benter, T.; Kirsch, S. F. *J. Org. Chem.* **2017**, *82*, 8242–8250.

[124] Zheng, Z.; Han, B.; Cheng, P.; Niu, J.; Wang, A. *Tetrahedron* **2014**, *70*, 9814–9818.

[125] Wu, C.; Xin, X.; Fu, Z.-M.; Xie, L.-Y.; Liu, K.-J.; Wang, Z.; Li, W.; Yuan, Z.-H.; He, W.-M. *Green Chem*. **2017**, *19*, 1983–1989.

[126] Zheng, Z.; Han, B.; Cheng, P.; Niu, J.; Wang, A. *Tetrahedron* **2014**, *70*, 9814–9818.

[127] Terent'ev, A. O.; Khodykin, S. V.; Krylov, I. B.; Ogibin, Y. N.; Nikishin, G. I. *Synthesis*, **2006**, *7*, 1087–1092.

1,1-Dibromooctan-2-one (**2.24i**) was synthesized according to a procedure in the literature and the analytical data are consistent with those reported previously.[128]

1,1-Dibromo-4-phenylbutan-2-one (**2.24j**) was synthesized according to a procedure in the literature and the analytical data are consistent with those reported previously.[129]

2.8.2.3. Monochloromethyl and Monobromomethyl ketones

a. Monochloromethyl Ketones

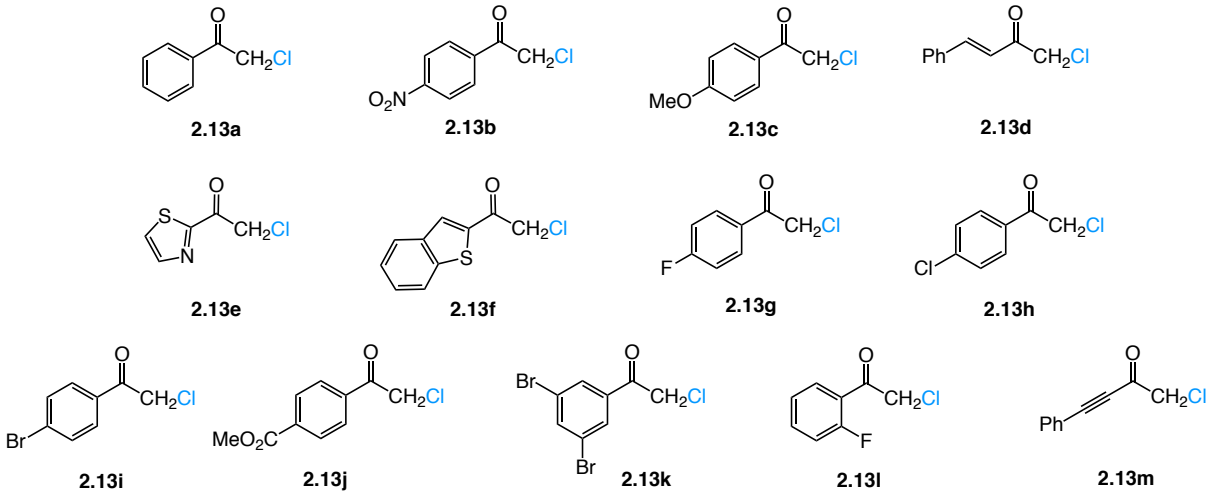

2-Chloro-1-phenylethan-1-one (2.13a) was purchased from Aldrich and used as received.

2-Chloro-1-(4-nitrophenyl)ethan-1-one (2.13b) was synthesized according to a procedure in the literature[130] and the analytical data are in accordance with those reported previously.[131]

2-Chloro-1-(4-methoxyphenyl)ethan-1-one (S2.13c) was purchased from Aldrich and used as received.

(*E*)-1-Chloro-4-phenylbut-3-en-2-one (2.13d) was synthesized according to a procedure in the literature[130] and the analytical data are in accordance with those reported previously.[132]

2-Chloro-1-(thiazol-2-yl)ethan-1-one (2.13e) was synthesized according to a procedure in the literature[134] and the analytical data are consistent with those reported previously.[133]

---

[128] Liu, J.; Li, W.; Wang, C.; Li, Y.; Li, Z. *Tetrahedron Lett.* **2011**, *52*, 4320–4323.

[129] Liu, J.; Li, W.; Wang, C.; Li, Y.; Li, Z. *Tetrahedron Lett.* **2011**, *52*, 4320–4323.

[130] Lim, B. Oh, E.-T.; Im, J.; Lee, K. S.; Jung, H.; Kim, M.; Kim, D.; Oh, J. T.; Bae, S.-H.; Chung, W.-J.; Ahn, K.-H.; Koo, S. *Eur. J. Org. Chem.* **2017**, *43*, 6390–6400.

[131] Shi, X.; Zhang, L.; Yang, P.; Sun, H.; Zhang, Y.; Xie, C.; Ou-yang, Z.; Wang, M. *Tetrahedron Lett.* **2018**, *59*, 1200–1203.

[132] Fraser, R. R. and Kong, F. *Syn. Commun.* **1988**, *18*, 1071–1077.

[133] Tanis, S. P.; Evans, B. R.; Nieman, J. A.; Parker, T. T.; Taylor, W. D.; Heasley, S. E.; Herrinton, P. M.; Perrault,

1-(Benzo[*b*]thiophen-2-yl)-2-chloroethan-1-one (2.13f) was synthesized according to a procedure in the literature[134] and the analytical data are consistent with those reported previously.[135]

2-Chloro-1-(4-fluorophenyl)ethan-1-one (2.13g) was purchased from Combi Blocks and used as received.

2,4'-Dichloroacetophenone (2.13h) was purchased from Alfa Aesar and used as received.

2-Chloro-1-(4-bromophenyl)ethan-1-one (2.13i) was purchased from Combi Blocks and used as received.

Methyl 4-(2-chloroacetyl)benzoate (2.13j) was synthesized according to a procedure in the literature and the analytical data are consistent with those reported previously.[136]

2-Chloro-1-(3,5-dibromophenyl)ethan-1-one (2.13k) was synthesized according to a literature procedure.[130] The title compound was purified by silica gel chromatography (0.1501 g, 0.5072 mmol, 10% yield). **IR (neat):** 3073 (w), 2938 (w), 1702 (s), 1552 (m), 1426 (m), 1393 (m), 1300 (w), 1199 (s), 1027 (w), 862 (m), 795 (m), 667 (m) cm^{-1}; **^{1}H NMR (400 MHz, $CDCl_3$):** δ 8.01 (s, 1H), 7.91 (s, 1H), 4.62 (s, 2H); **^{13}C NMR (100 MHz, $CDCl_3$):** δ 188.8, 139.1, 136.9, 130.3, 123.7, 45.4; **HRMS (DART$^+$):** Calcd for $C_8H_6OClBr_2$ $[M+H]^+$: 310.8469, Found: 310.8464.

2-Chloro-1-(2-fluorophenyl)ethan-1-one (2.13l) was synthesized according to a procedure in the literature[132] and the analytical data are consistent with those reported previously.[137]

1-Chloro-4-phenylbut-3-yn-2-one (2.13m) was synthesized in accordance to a procedure in the literature and the analytical data are consistent with those reported previously.[138]

W. R.; Hohler, R. A.; Dolak, L. A.; Hester, M. R.; Seest, E. P. *Tetrahedron: Asymmetry* **2006**, *17*, 2154–2182.

[134] Mátyus, P.; Huleatt, P.; Sperlágh, C. B.; Khoo, M. L.; Magyar, K.; Papp-behr, Á.; Deme, R.; Túrós, G.; Gyires, K.; WO2015/87094 A1, December 10, 2013.

[135] Huff, B. E.; Leffelman, C. L.; LeTourneau, M. E.; Sullivan, K. A.; Ward, J. A.; Stille, J. R. *Heterocycles,* **1997**, *45*, 1363–1384.

[136] Giboulot, S.; Liron, F.; Prestat, G.; Wahl, B.; Sauthier, M.; Castanet, Y.; Mortreux, A.; Poli, G. *Chem. Commun.* **2012**, *48*, 5889–5891.

[137] Rosen, J.; Steinhuebel, D.; Palucki, M.; Davies, I. *Org. Lett.* **2007**, *9*, 667–669.

[138] Raghavan, S.; Mustafa, S.; Sridhar, B. *J. Org. Chem.* **2009**, *74*, 4499–4507.

b. Monobromomethyl Ketones

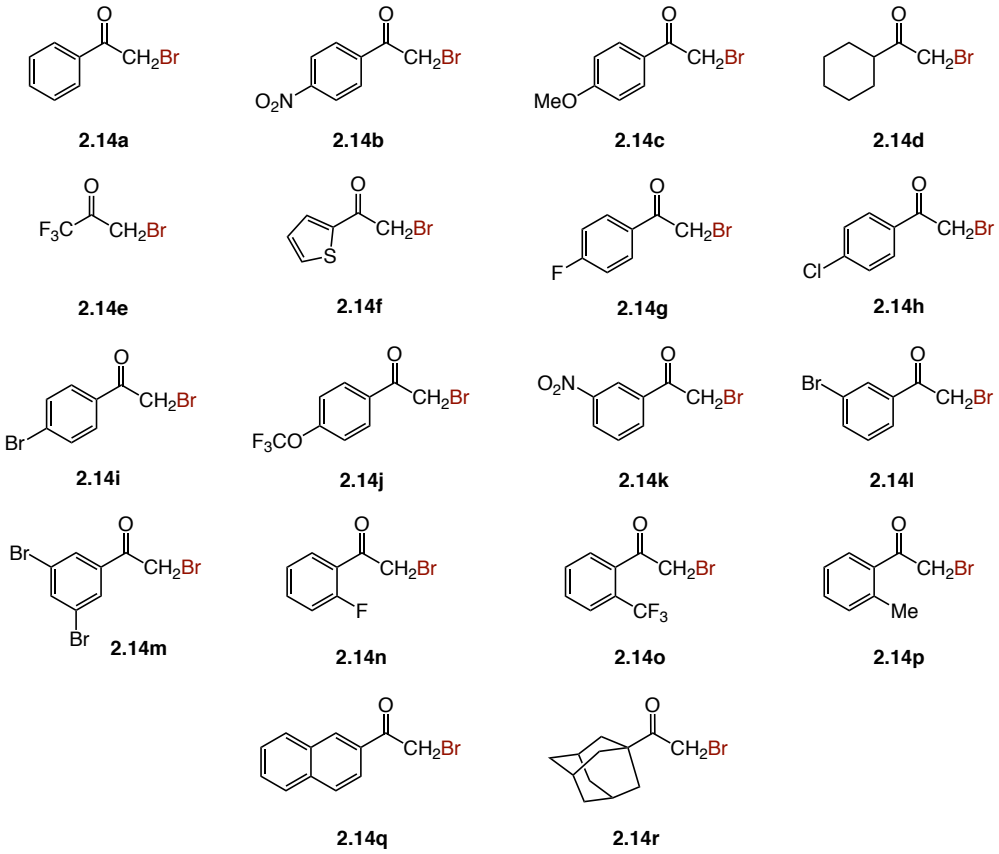

2-Bromo-1-phenylethan-1-one (2.14a) was purchased from Aldrich and used as received.

2-Bromo-4'-nitroacetopheone (2.14b) was purchased from Aldrich and used as received.

2-Bromo-1-(4-methoxyphenyl)ethan-1-one (2.14c) was synthesized according to a procedure in the literature[139] and the analytical data are consistent with those reported previously.[140]

2-Bromo-1-cyclohexylethan-1-one (2.14d) was prepared in accordance to a procedure in the literature and analytical data are consistent with those reported previously.[125]

3-Bromo-1,1,1-trifluoroacetone (2.14e) was purchased from Aldrich and used as received.

2-Bromo-1-(thiophen-2-yl)ethan-1-one (2.14f) was purchased from Oakwood and used as received.

2-Bromo-1-(4-fluorophenyl)ethan-1-one (2.14g) was prepared according to a literature procedure.[139] The analytical data are fully consistent with those previously reported.[141]

2-Bromo-1-(4-chlorophenyl)ethan-1-one (2.14h) was purchased from Aldrich and used as received.

---

[139] Borzęcka, W.; Lavandera, I.; Gotor, V. *J. Org. Chem.* **2013**, *78*, 7312–7317.

[140] Maji, T.; Karmakar, A.; Reiser, O. *J. Org. Chem.* **2011**, *76*, 736–739.

[141] Macharla, A. K.; Nappunni, R. C.; Marri, M. R.; Peraka, S.; Nama, N. *Tetrahedron Lett.* **2012**, *53*, 191–195.

2-Bromo-1-(4-bromophenyl)ethan-1-one (2.14i) was purchased from Aldrich and used as received.

2-Bromo-1-(4-(trifluoromethoxy)phenyl)ethan-1-one (2.14j) was purchased from Combi Blocks and used as received.

2-Bromo-1-(3-nitrophenyl)ethan-1-one (2.14k) was purchased from Combi Blocks and used as received.

2-Bromo-1-(3-bromophenyl)ethan-1-one (2.14l) was purchased from Aldrich and used as received.

2-Bromo-1-(3,5-dibromophenyl)ethan-1-one (2.14m) was synthesized according to a procedure in the literature[142] and the analytical data are consistent with those reported previously.[143]

2-Bromo-1-(2-fluorophenyl)ethan-1-one (2.14n) was synthesized according to a procedure in the literature[139] and the analytical data are consistent with those reported previously.[144]

2-Bromo-1-(2-(trifluoromethyl)phenyl)ethan-1-one (2.14o) was synthesized according to a procedure in the literature[139] and the analytical data are consistent with those reported previously.[145]

2-Bromo-1-(*o*-tolyl)ethan-1-one (2.14p) was purchased from Alfa Aesar and used as received.

2-Bromo-1-(naphthalen-2-yl)ethan-1-one (2.14q) was synthesized according to a procedure in the literature[146] and the analytical data are consistent with those reported previously.[147]

1-Adamantyl bromomethyl ketone (2.14r) was purchased from Astatech, Inc. and used as received.

2.8.2.4. Difluoromethyl ketones

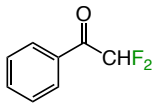

2.30a

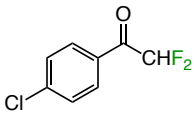

2.30b

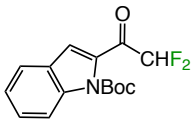

2.30c

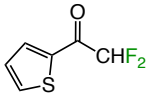

2.30d

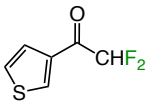

2.30e

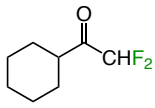

2.30f

[142] Chundawat, T. S.; Kumari, P.; Sharma, N.; Bhagat, S. *Med. Chem. Res.* **2016**, *25*, 2335–2348.

[143] Lintnerová, L.; García-Caballero, M.; Gregán, F.; Melicherčík, M.; Quesada, A. R.; Dobiaš, J.; Lác, J.; Sališová, M.; Bohác, A. *Eur. J. Med. Chem.* **2014**, *72*, 146–159.

[144] Chong, W. K. M.; Chu, S.; Duvadie, R. K.; Li, L.; Na, J.; Schaffer, L.; Yang, Y. PCT Int. Appl. WO 2004/072070 A1, August 26, 2004.

[145] Chen, Z.-W.; Ye, D.-N.; Ye, M.; Zhou, Z.-G.; Li, S.-H.; Liu, L.-X. *Tetrahedron Lett.* **2014**, *55*, 1373–1375.

[146] Reddy, P. O. V.; Mishra, S.; Tantak, M. P.; Nikhil, K.; Sadana, R.; Shah, K.; Kumar, D. *Bioorg. Med. Chem. Lett.* **2017**, *27*, 1379–1384.

[147] Kourounakis, A. P.; Matralis, A. N.; Nikitakis, A. *Bioorg. Med. Chem.* **2010**, *18*, 7402–7412.

2,2-Difluoro-1-phenylethan-1-one (2.30a) was purchased from Matrix Scientific and used as received.

1-(4-Chlorophenyl)-2,2-difluoroethan-1-one (2.30b) was synthesized according to a procedure in the literature[148] and the analytical data are consistent with the literature.[149]

***tert*-Butyl 2-(2,2-difluoroacetyl)-1*H*-indole-1-carboxylate (2.30c)** was synthesized according to a procedure in the literature and the analytical data are consistent with those reported previously.[149]

2,2-Difluoro-1-(thiophen-2-yl)ethan-1-one (2.30d) was synthesized according to a procedure in the literature and the analytical data are consistent with those reported previously.[148]

2,2-Difluoro-1-(thiophen-3-yl)ethan-1-one (2.30e) was synthesized according to a procedure in the literature and the analytical data are consistent with those reported previously.[150]

1-Cyclohexyl-2,2-difluoroethan-1-one (2.30f) was synthesized according to a procedure in the literature and the analytical data are consistent with those reported previously.[148]

2.8.2.5. Monofluoromethyl ketones

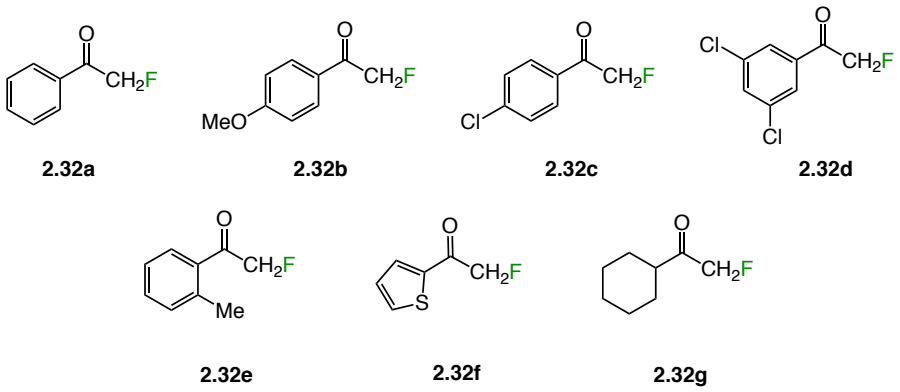

2.32a **2.32b** **2.32c** **2.32d**

2.32e **2.32f** **2.32g**

2-Fluoro-1-phenylethan-1-one (2.32a) was synthesized according to a procedure in the literature and the analytical data are consistent with those reported previously.[151]

2-Fluoro-1-(4-methoxyphenyl)ethan-1-one (2.32b) was synthesized by fluorination of the corresponding, commercially available, α-bromoketone according to a procedure in the literature[152] and the analytical data are consistent with the literature.[153]

---

[148] Yu, X.; Bai, H.; Wang, D.; Qin, Z.; Li, J.-Q.; Fu, B. *RSC Adv.* **2018**, *8*, 19402–19408.

[149] Prakash, G. K. S.; Hu, J.; Olah, G. A. *J. Fluor. Chem.* **2001**, *112*, 355–360.

[150] Pravst, I.; Zupan, M.; Stavber, S. *Synthesis*, **2005**, *18*, 3140–3146.

[151] Wei, Z.-L.; Li, Z.-Y.; Lin, G.-Q. *Tetrahedron* **1998**, *54*, 13059–13072.

[152] Kelly, C. B.; Mercadante, M. A.; Hamlin, T. A.; Fletcher, M. H.; Leadbeater, N. E. *J. Org. Chem.* **2012**, *77*, 8131–8141.

[153] Chen, D.; Ni, C.; Zhao, Y.; Cai, X.; Li, X.; Xiao, P.; Hu, J. *Angew. Chem., Int. Ed.* **2016**, *55*, 12632–12636.

1-(4-Chlorophenyl)-2-fluoroethan-1-one (2.32c) was synthesized according to a procedure in the literature and the analytical data are consistent with those reported previously.[154]

1-(3,5-Dichlorophenyl)-2-fluoroethan-1-one (2.32d) was synthesized by fluorination of the corresponding, commercially available α-bromoketone according to a procedure in the literature.[152] **IR (neat):** 3080 (w), 2932 (w), 2257 (w), 1715 (m), 1567 (m), 1429 (m), 1226 (m), 1133 (m), 1092 (m), 1047 (m), 1012 (s), 905 (s), 864 (m), 802 (s), 726 (s), 670 (s), 563 (w) cm^{-1}; **^{1}H NMR (400 MHz, $CDCl_3$):** δ 7.74 (dd, *J* = 1.9, 0.5 Hz, 2H), 7.57 (s, 1H), 5.50 (s, 1H), 5.38 (s, 1H); **^{13}C NMR (100 MHz, $CDCl_3$):** δ 191.6 (d, *J* = 16.6 Hz), 136.1, 136.0 (d, *J* = 1.1 Hz), 126.5 (d, *J* = 3.4 Hz), 84.6, 82.7; **^{19}F NMR (376 MHz, $CDCl_3$):** δ –76.31 (t, 1F); **HRMS (DART$^+$):** Calcd for $C_8H_6Cl_2FO$ $[M+H]^+$: 206.978; Found: 206.9783.

2-Fluoro-1-(*o*-tolyl)ethan-1-one (2.32e) was synthesized by fluorination of the corresponding, commercially available, α-bromoketone through procedure in the literature.[153] The analytical data are consistent with the literature.[155]

2-Fluoro-1-(thiophen-2-yl)ethan-1-one (2.32f) was synthesized by fluorination of the corresponding, commercially available α-bromoketone according to a procedure in the literature.[152] The analytical data are consistent with the literature.[156]

1-Cyclohexyl-2-fluoroethan-1-one (2.32g) was synthesized by fluorination of the corresponding, commercially available □-bromoketone according to a procedure in the literature. The analytical data are consistent with those reported previously.[157]

2.8.3. Aminophenol Ligands

(*S*)-2-((3-(*tert*-Butyl)-2-hydroxybenzyl)amino)-*N*,*N*,3-trimethylbutanamide (ap-2): The title compound was synthesized in accordance to a procedure in the literature and the analytical data are consistent with those reported previously.[158]

(*S*)-2-((2-Hydroxy-3-(triphenylsilyl)benzyl)amino)-*N*,*N*,3-trimethylbutanamide (ap-5): The title compound was synthesized in accordance to a procedure in the literature and the analytical data are consistent with those reported previously.[159]

---

[154] Fuglseth, E.; Thvedt, T. H. K.; Møll, M. F.; Hoff, B. H. *Tetrahedron* **2008**, *64*, 7318–7323.

[155] Yang, Q.; Mao, L.-L.; Yang, B.; Yang, S.-D. *Org. Lett.* **2014**, *16*, 3460–3463.

[156] Stavber, S.; Jereb, M.; Zupan, M. *Synthesis* **2002**, *17*, 2609–2615.

[157] Leroy, J. *J. Org. Chem.* **1981**, *46*, 206–209.

[45] Silverio, D. L.; Torker, S.; Pilyugina, T.; Vieira, E. M.; Snapper, M. L.; Haeffner, F.; Hoveyda, A. H. *Nature* **2013**, *494*, 216–221.

[159] Robbins, D. W.; Lee, K.; Silverio, D. L.; Volkov, A.; Torker, S.; Hoveyda, A. H. *Angew. Chem., Int. Ed.* **2016**, *55*, 9610–9614.

(*S*)-2-((2-Hydroxy-3-(triphenylsilyl)benzyl)amino)-3-methyl-1-(pyrrolidin-1-yl)butan-1-one (ap-1): The title compound was synthesized in accordance to a procedure in the literature and the analytical data are consistent with those reported previously.[159]

(*S*)-2-((2-Hydroxy-3-(triphenylsilyl)benzyl)amino)-3,3-dimethyl-1-(pyrrolidin-1-yl)butan-1-one (ap-3): The title compound was synthesized analogously to **ap-1** in accordance to a procedure in the literature.[159] **IR (neat):** 3305 (w), 3064 (w), 3045 (m), 2953 (w), 2242 (w), 1628 (m), 1426 (s), 1107 (s), 908 (m), 731 (m), 680 (s), 438 (m) cm^{-1}; **^{1}H NMR (400 MHz, $CDCl_3$):** δ 10.71 (s, 1H), 7.62 (dt, *J* = 8.0, 1.9 Hz, 6H), 7.44–7.28 (m, 9H), 7.26 (d, *J* = 2.1 Hz, 1H), 7.12 (d, *J* = 7.4 Hz, 1H), 6.98 (d, *J* = 7.4 Hz, 1H), 6.73 (td, *J* = 7.3, 2.0 Hz, 1H), 4.22 (d, *J* = 14.0 Hz, 1H), 3.65 (s, 1H), 3.47 (d, *J* = 12.9 Hz, 2H), 3.24 (d, *J* = 8.5 Hz, 1H), 3.04 (s, 2H), 1.87 (d, *J* = 7.0 Hz, 4H), 0.86 (d, *J* = 2.1 Hz, 9H); **^{13}C NMR (100 MHz, $CDCl_3$):** δ 171.3, 163.3, 137.9, 136.3, 135.0, 131.1, 129.1, 127.6, 121.7, 120.8, 118.9, 64.5, 50.6, 47.0, 45.5, 34.2, 26.8, 26.2, 24.2; **HRMS (DART$^+$):** Calcd for $C_{35}H_{41}N_2O_2Si$ $[M+H]^+$: 549.2922; Found: 549.2932; **Specific Rotation:** $[\alpha]^{24}_D$ –196.2 (*c* 0.08, $CHCl_3$).

Chlorotri(naphthalen-1-yl)silane: The title compound was synthesized in accordance to a procedure in the literature and the analytical data are consistent with those reported previously.[160]

2-Hydroxy-3-(tri(naphthalen-1-yl)silyl)benzaldehyde: The title compound was synthesized analogous to **ap-1.** The silyl-protected phenol was used directly without purification. **IR (neat):** 3050 (w), 2922 (w), 2845 (w), 2245 (w), 1726 (m), 1653 (m), 1572 (m), 1466 (m), 1216 (m), 979 (s), 757 (s), 442 (s) cm^{-1}; **^{1}H NMR (400 MHz, $CDCl_3$):** δ 11.07 (s, 1H), 9.80 (s, 1H), 7.98 (s, 3H), 7.91 (d, *J* = 8.2 Hz, 3H), 7.85 (d, *J* = 8.5 Hz, 3H), 7.80 (dd, *J* = 6.4, 3.3 Hz, 4H), 7.60 (dd, *J* = 7.7, 1.7 Hz, 1H), 7.42 (t, *J* = 7.8 Hz, 3H), 7.30 (t, *J* = 7.5 Hz, 3H), 7.03 (t, *J* = 7.9 Hz, 3H), 6.95 (t, *J* = 7.5 Hz, 1H); **^{13}C NMR (100 MHz, $CDCl_3$):** δ 196.6, 166.7, 146.3, 137.8, 137.6, 136.4, 133.6, 132.5, 130.9, 129.2, 129.0, 125.6, 125.4, 125.1, 124.7, 120.2, 120.1; **HRMS (ESI$^+$):** Calcd for $C_{37}H_{26}O_2Si$ $[M+H]^+$: 530.1697; Found: 530.1686.

(*S*)-2-((2-Hydroxy-3-(tri(naphthalen-1-yl)silyl)benzyl)amino)-3,3-dimethyl-1-(pyrrolidin-1-yl)butan-1-one (ap-11): The title compound was synthesized analogously to **ap-2** in accordance to a procedure in the literature.[159] **IR (neat):** 3050 (w), 2951 (w), 2870 (w), 2241 (w), 1941 (m), 1716 (m), 1623 (m), 1579 (w), 1426 (w), 1392 (w), 1275 (w), 1023 (s), 979 (s), 948 (s), 725 (s), 668 (m), 544 (w), 452 (s), 435 (s) cm^{-1}; **^{1}H NMR (400 MHz, $CDCl_3$):** δ 7.90 (dd, *J* = 17.8, 8.4 Hz, 8H), 7.82–7.69 (m, 4H), 7.45 (dd, *J* = 7.5, 1.7 Hz, 2H), 7.28 (s, 4H), 6.99 (d, *J* = 7.9 Hz, 3H), 6.97–6.85 (m, 2H), 6.71 (t, *J* = 7.4 Hz, 1H), 4.24 (s, 1H), 3.51 (d, *J* = 7.1 Hz, 1H), 3.43 (d, *J* = 14.1 Hz, 1H), 3.34 (d, *J* = 7.7 Hz, 1H), 2.41 (d, *J* = 36.2 Hz, 1H), 2.34–2.06 (m, 2H), 1.90–1.47 (m, 5H), 0.24 (s, 9H); **^{13}C NMR (100 MHz, $CDCl_3$):** δ 170.6, 138.2, 137.7, 133.6, 131.3, 130.5, 129.5, 128.9, 125.6, 125.1, 122.0, 121.4, 119.3, 50.3, 47.0, 45.4, 33.6, 26.3, 26.1, 24.3; **HRMS (ESI$^+$):** Calcd for $C_{47}H_{47}N_2O_2Si$ $[M+H]^+$: 699.9800; Found: 699.3406; **Specific Rotation:** $[\alpha]^{24}_D$ –227.0 (*c* 0.03, $CHCl_3$).

---

[160] Gilman, H.; Brannen, C. G. *J. Am. Chem. Soc.* **1951**, *73*, 4640–4644.

2.8.4. Screening Data for Catalytic Enantioselective Allyl Additions to Halomethyl Ketones

2.8.4.1. Metal Alkoxide Screening

Figure S1. Metal Alkoxide Screening for Catalytic Enantioselective Allyl Addition to Monochloromethyl Ketone

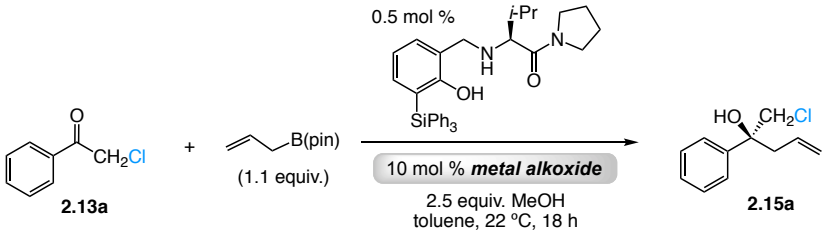

Entry	Base	Conv. (%)	er
1	None	30	59:41
2	$Zn(OMe)_2$	>98	97:3
3	LiOMe	58	88:12
4	CaOMe	98	96:4
5	NaOMe	68	94:6
6	KOMe	98	tbd
7	$Zn(Ot\text{-}Bu)_2$	98	95.5:4.5
8	LiOt-Bu	52	90:10
9	NaOt-Bu	98	95:5
10	KOt-Bu	98	96:4
11	ZnF_2	34	72.5:27.5
12	$ZnCl_2$	65	50:50
13	$Zn(HMDS)_2$	80	94:6
14	$Zn(OTF)_2$	83	50:50

2.8.4.2. Screening of Conditions for Epoxide Formation

Solvent and bases were screened using conditions reported in the literature.[161]

[161] (a) Rychnovsky, S. D.; Griesgraber, G.; Zeller, S.; Skalitzky, D. J. *J. Org. Chem.* **1991**, *56*, 5161–5169. (b) Gramlich, W. M.; Theryo, G.; Hillmyer, M. A. *Polym. Chem.* **2012**, *3*, 1510–1516. (c) Wang, Z. M.; Sharpless, B. K. *Synlett* **1993**, *8*, 603–604. (d) Shin, J. A.; Choi, K. I.; Pae, A. N.; Koh, H. Y.; Kang, H.-Y.; Cho, Y. S. *J. Chem. Soc., Perkins Trans.* **2001**, *1*, 946–948.

Figure S2. Condition Screening for Epoxide Formation

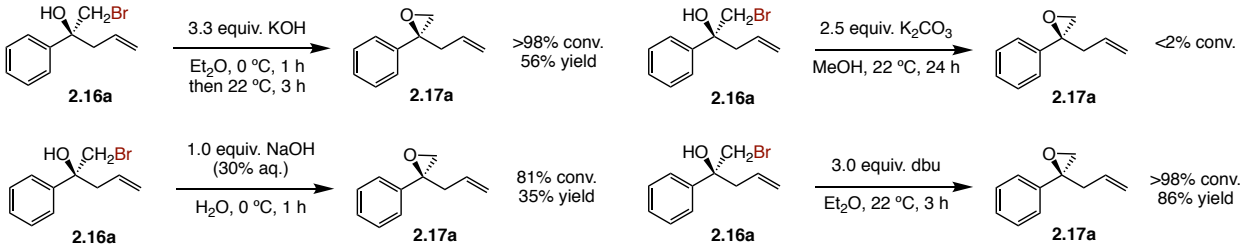

2.8.5. Catalytic Enantioselective Additions to Trihalomethyl ketones

In a N_2-filled glove box, aminophenol **ap-2** (7.66 mg, 0.025 mmol), $Zn(OMe)_2$ (6.37 mg, 0.05 mmol), methanol (51 μL, 1.25 mmol) and toluene (2.5 mL) were added to a two-dram vial equipped containing a stir bar. The solution was allowed to stir for 5 min at which time a two-dram vial equipped with a stir bar was charged with 0.5 mL of the solution. Trichloromethyl ketone (0.1 mmol) was added and the vial was capped and allowed to cool in a –40 ºC freezer for 30 min. Allylboronic acid pinacol ester (21 μL, 0.11 mmol) was also allowed to cool to –40 ºC for 30 min at which time it was added to the mixture. The vial was sealed with a cap, placed in a 4 ºC cold room, and allowed to stir at 4 ºC for 2 h. Conversion was determined by analysis of the ^{1}H NMR spectrum of an aliquot. The solution was then concentrated *in vacuo* and the resulting residue purified by silica gel chromatography, eluting with 10:1 hexanes:EtOAc, to afford the desired product as colorless oil.

(*R*)-1,1,1-Trichloro-2-phenylpent-4-en-2-ol (2.7a): 24.1 mg, 0.091 mmol, 91% yield. **IR (neat):** 3558 (br, w), 3062 (w), 2979 (w), 2928 (w), 1724 (w), 1640 (w), 1495 (w), 1448 (w), 1350 (w), 1226 (w), 1169 (w), 1104 (w), 993 (w), 908 (m), 817 (m), 792 (s), 733 (s), 704 (s), 618 (m), 475 (w) cm^{-1}; **^{1}H NMR (400 MHz, $CDCl_3$):** δ 7.80–7.69 (m, 2H), 7.43–7.32 (m, 3H), 5.58–5.43 (m, 1H), 5.30–5.02 (m, 2H), 3.55 (dd, J = 14.5, 5.8 Hz, 1H), 3.06 (dd, J = 14.5, 8.2 Hz, 1H), 2.93 (s, 1H); **^{13}C NMR (100 MHz, $CDCl_3$):** δ 136.6, 132.3, 129.3, 128.6, 127.6, 120.8, 107.6, 84.5, 41.2; **HRMS (DART$^+$):** Calcd for $C_{11}H_{10}Cl_3$ $[M+H–H_2O]^+$: 246.9848; Found: 246.9842; **Specific Rotation:** $[\alpha]^{24}_D$ +29.2 (*c* 2.26, $CHCl_3$) for a 95:5 er sample. The enantiomeric purity of this compound was determined by HPLC analysis in comparison with authentic racemic material (Chiralpak AD-H, 98:2 hexanes:*i*-PrOH, 0.5 mL/min, 220 nm).

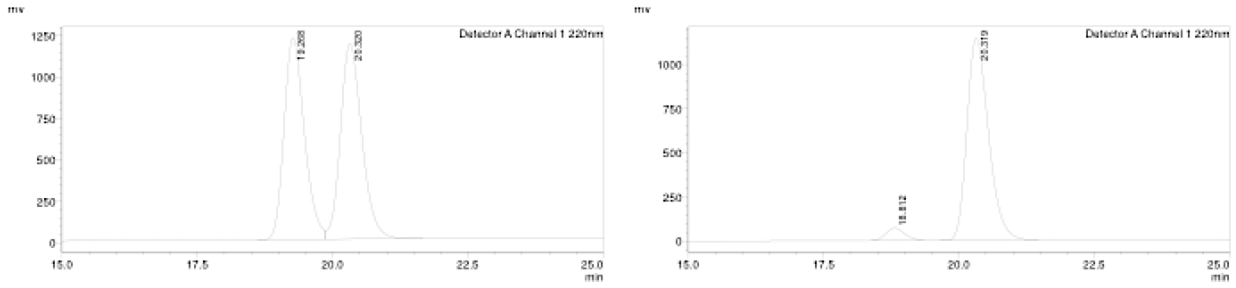

<Peak Table>
Detector A Channel 1 220nm

Peak#	Ret. Time	Area	Area%	Height
1	19.268	31668666	49.467	1211898
2	20.320	32351307	50.533	1175695
Total		64019973	100.000	2387592

<Peak Table>
Detector A Channel 1 220nm

Peak#	Ret. Time	Area	Area%	Height
1	18.812	1687230	5.033	70300
2	20.319	31835644	94.967	1143852
Total		33522874	100.000	1214152

Peak #	Ret. Time	Area	Area %	Peak #	Ret. Time	Area	Area %
1	19.3 min	31668666	49.467	1	18.8 min	1687230	5.033
2	20.3 min	32351307	50.533	2	20.3 min	31835644	94.967

(*S*)-1,1,1-Trichloro-4-methyl-2-(naphthalen-2-yl)pent-4-en-2-ol (2.8): 31.9 mg, 0.0970 mmol, 97% yield. **IR (neat):** 3532 (br, w), 3059 (w), 2972 (w), 1642 (w), 1439 (w), 1375 (w), 1362 (w), 1121 (w), 898 (w), 856 (w), 820 (m), 784 (m), 749 (s), 706 (w), 522 (w), 478 (m) cm^{-1}; **^{1}H NMR (400 MHz, $CDCl_3$):** δ 8.32 (d, *J* = 2.0 Hz, 1H), 8.00–7.80 (m, 4H), 7.57–7.46 (m, 2H), 4.94–4.90 (dt, *J* = 2.0, 1.0 Hz, 2H), 3.58 (dd, *J* = 14.3, 1.0 Hz, 1H), 3.30 (s, 1H), 3.24 (dd, *J* = 14.3, 0.9 Hz, 1H), 1.36 (s, 3H); **^{13}C NMR (100 MHz, $CDCl_3$):** δ 141.2, 135.0, 133.2, 132.5, 129.1, 128.8, 127.6, 126.8, 126.8, 126.5, 126.3, 117.8, 108.5, 83.5, 44.6, 23.8; **HRMS (DART$^+$):** Calcd for $C_{16}H_{14}Cl_3$ $[M+H–H_2O]^+$: 311.0161; Found: 311.0173; **Specific Rotation:** $[\alpha]^{24}_D$ –12.8 (*c* 2.98, $CHCl_3$) for a 97:3 er sample. The enantiomeric purity of this compound was determined by HPLC analysis in comparison with authentic racemic material (Chiralcel OD-H, 98:2 hexanes:*i*-PrOH, 0.5 mL/min, 220 nm).

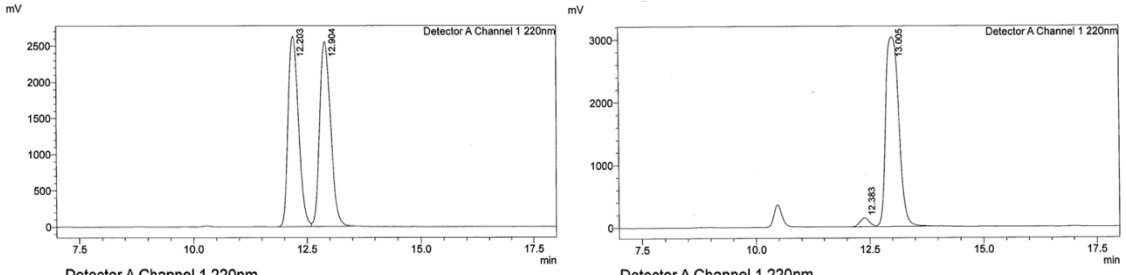

Detector A Channel 1 220nm

Peak#	Ret. Time	Area	Area%	Height
1	12.203	42078969	49.410	2625350
2	12.904	43084718	50.590	2546460
Total		85163687	100.000	5171809

Detector A Channel 1 220nm

Peak#	Ret. Time	Area	Area%	Height
1	12.383	2012546	3.204	140812
2	13.005	60795238	96.796	3029761
Total		62807784	100.000	3170573

Peak #	Ret. Time	Area	Area %	Peak #	Ret. Time	Area	Area %
1	12.2 min	42078969	49.410	1	12.4 min	2012546	3.204
2	12.9 min	43084718	50.590	2	13.0 min	60795238	96.796

(*R*)-1,1,1-Trichloro-2-(4-methoxyphenyl)pent-4-en-2-ol (2.7b): 28.6 mg, 0.0991 mmol, 97% yield. The analytical data are consistent with those reported previously.[162] **^{1}H NMR (400 MHz, $CDCl_3$):** δ 7.64 (d, J = 9.1 Hz, 1H), 6.90 (d, J = 9.1 Hz, 1H), 5.52 (dddd, J = 17.1, 10.1, 8.1, 5.8 Hz, 1H), 5.30–5.06 (m, 2H), 3.83 (s, 2H), 3.51 (ddt, J = 14.5, 5.8, 1.5 Hz, 1H), 3.03 (ddt, J = 14.6, 8.1, 1.0 Hz, 1H), 2.89 (s, 1H); **Specific Rotation:** $[\alpha]^{24}_D$ +16.3 (*c* 2.85, $CHCl_3$) for a 93:7 er sample. The enantiomeric purity of this compound was determined by HPLC analysis in comparison with authentic racemic material (Chiralpak AS-H, 98:2 hexanes:*i*-PrOH, 0.5 mL/min, 220 nm).

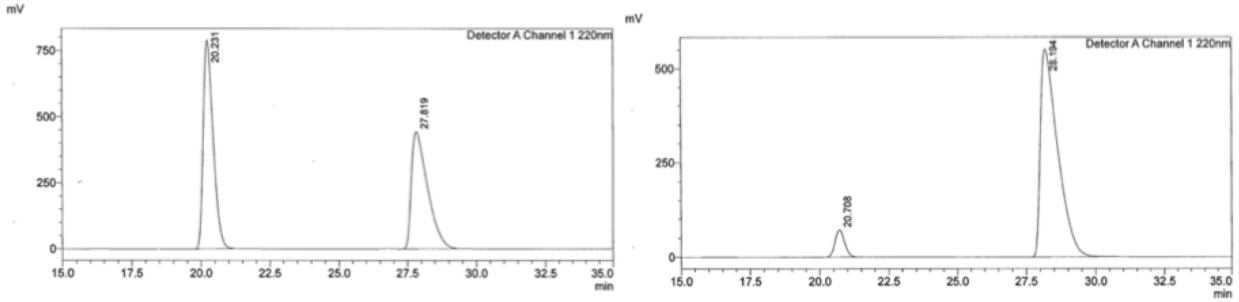

Detector A Channel 1 220nm

Peak#	Ret. Time	Area	Area%	Height
1	20.231	19819227	52.319	789357
2	27.819	18062612	47.681	442749
Total		37881839	100.000	1232106

Detector A Channel 1 220nm

Peak#	Ret. Time	Area	Area%	Height
1	20.708	1751932	6.848	71806
2	28.194	23832071	93.152	552960
Total		25584002	100.000	624766

Peak #	Ret. Time	Area	Area %	Peak #	Ret. Time	Area	Area %
1	20.2 min	19819227	52.319	1	20.7 min	1751932	6.848
2	27.8 min	18062612	47.681	2	28.2 min	23832071	93.152

(*R*)-1,1,1-Trichloro-2-(4-nitrophenyl)pent-4-en-2-ol (2.7c): 18.4 mg, 0.0592 mmol, 59% yield. **IR (neat):** 3513 (br, w), 3078 (w), 3020 (w), 1641 (w), 1605 (w), 1520 (m), 1348 (s), 1214 (w), 1169 (w), 1111 (w), 1077 (w), 1015 (w), 992 (w), 927 (w), 856 (w), 818 (w), 792 (w), 745 (s), 718 (m), 668 (w) cm^{-1}; **^{1}H NMR (400 MHz, $CDCl_3$):** δ 8.31–8.11 (m, 2H), 8.03–7.78 (m, 2H), 5.45 (dddd, *J* = 17.4, 10.0, 7.6, 6.3 Hz, 1H), 5.32–5.05 (m, 2H), 3.53 (ddt, *J* = 14.8, 6.3, 1.4 Hz, 1H), 3.10 (ddt, *J* = 14.8, 7.6, 1.2 Hz, 1H), 3.06 (s, 1H); **^{13}C NMR (100 MHz, $CDCl_3$):** δ 148.0, 143.8, 131.1, 130.5, 122.7, 121.6, 106.5, 84.5, 41.3; **HRMS (DART$^+$):** Calcd for $C_{11}H_{11}NO_3Cl_3$ $[M+H]^+$: 309.9799; Found: 309.9796; **Specific Rotation:** $[\alpha]^{24}_D$ +13.5 (*c* 1.71, $CHCl_3$) for a 94.5:5.5 er sample. The enantiomeric purity of this compound was determined by HPLC analysis in comparison with authentic racemic material (Chiralcel OD-H, 98:2 hexanes:*i*-PrOH, 0.5 mL/min, 220 nm).

[162] Bao, Z. J.; Lu, J.; Ji, S. J. *Chin. Chem. Lett.* **2007**, *18*, 1061–1063.

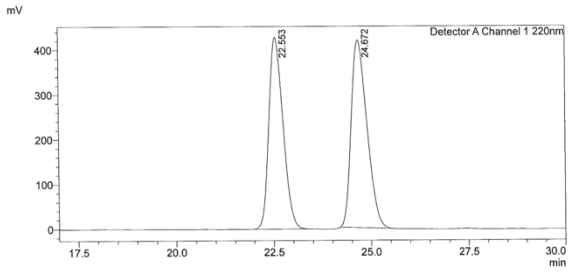

Detector A Channel 1 220nm

Peak#	Ret. Time	Area	Area%	Height
1	22.553	10828064	47.769	428754
2	24.672	11839659	52.231	419654
Total		22667724	100.000	848407

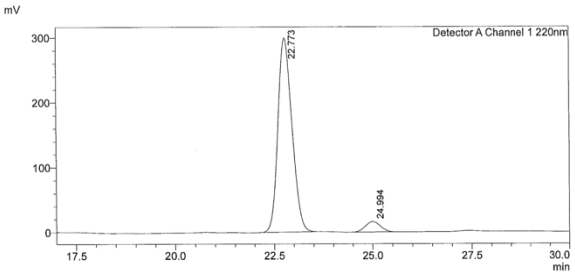

Detector A Channel 1 220nm

Peak#	Ret. Time	Area	Area%	Height
1	22.773	7526232	94.533	299174
2	24.994	435295	5.467	16223
Total		7961527	100.000	315398

Peak #	Ret. Time	Area	Area %	Peak #	Ret. Time	Area	Area %
1	22.6 min	10828064	47.769	1	22.8 min	7526232	94.533
2	24.7 min	11839659	52.231	2	25.0 min	435295	5.467

(*R*)-1,1,1-Trichloro-2-(3,5-dimethylphenyl)pent-4-en-2-ol (2.7d): 27.8 mg, 0.0946 mmol, 95% yield. **IR (neat):** 3552 (br, w), 2978 (w), 1606 (w), 1442 (w), 1220 (w), 1156 (w), 1037 (w), 992 (w), 921 (w), 898 (w), 950 (m), 807 (m), 784 (s), 737 (s), 684 (w), 646 (m), 577 (w), 538 (w) cm^{-1}; **^{1}H NMR (400 MHz, $CDCl_3$):** δ 7.39–7.30 (m, 2H), 7.00 (dt, *J* = 1.5, 0.8 Hz, 1H), 5.51 (dddd, *J* = 17.1, 10.0, 8.4, 5.5 Hz, 1H), 5.34–5.06 (m, 2H), 3.51 (ddt, *J* = 14.4, 5.5, 1.5 Hz, 1H), 3.02 (ddt, *J* = 14.4, 8.4, 1.0 Hz, 1H), 2.88 (s, 1H), 2.35 (m, 6H); **^{13}C NMR (100 MHz, $CDCl_3$):** δ 137.0, 136.5, 132.6, 130.3, 127.0, 120.6, 107.7, 84.4, 41.2, 21.7; **HRMS (DART$^+$):** Calcd for $C_{13}H_{14}Cl_3$ $[M+H–H_2O]^+$: 275.0161; Found: 275.0161; **Specific Rotation:** $[\alpha]^{24}_D$ +25.8 (*c* 2.71, $CHCl_3$) for a 90.5:9.5 er sample. The enantiomeric purity of this compound was determined by HPLC analysis in comparison with authentic racemic material (Chiralcel OD-H, 98:2 hexanes:*i*-PrOH, 0.5 mL/min, 220 nm).

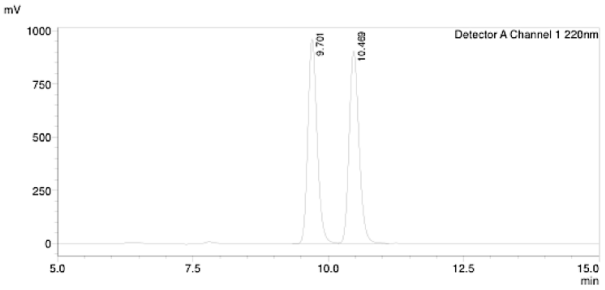

<Peak Table>
Detector A Channel 1 220nm

Peak#	Ret. Time	Area	Area%	Height
1	9.701	11418026	50.114	960427
2	10.469	11366121	49.886	903667
Total		22784147	100.000	1864094

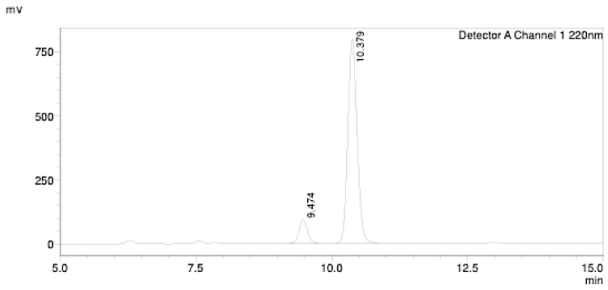

<Peak Table>
Detector A Channel 1 220nm

Peak#	Ret. Time	Area	Area%	Height
1	9.474	966070	9.354	91225
2	10.379	9362139	90.646	793710
Total		10328209	100.000	884935

Peak #	Ret. Time	Area	Area %	Peak #	Ret. Time	Area	Area %
1	9.7 min	11418026	50.114	1	9.5 min	966070	9.354
2	10.5 min	11366121	49.886	2	10.4 min	9362139	90.646

(*R*)-1,1,1-Trichloro-2-(*o*-tolyl)pent-4-en-2-ol (2.7e): The title compound was synthesized analogous to **1a** with an extended reaction time of 24 hours (24.2 mg, 0.0886 mmol, 87% yield).

IR (neat): 3559 (br, w), 3064 (w), 3023 (w), 2969 (w), 2931 (w), 1730 (w), 1639 (w), 1601 (w), 1488 (w), 1454 (w), 1352 (w), 993 (w), 821 (m), 804 (m), 790 (m), 735 (s), 702 (m), 627 (w) cm^{-1}; **^{1}H NMR (400 MHz, $CDCl_3$):** δ 7.65 (s, 1H), 7.36–7.21 (m, 3H), 5.63 (tdd, *J* = 13.7, 6.9, 4.0 Hz, 1H), 5.26 (dd, *J* = 37.8, 13.6 Hz, 2H), 3.68 (d, *J* = 14.6 Hz, 1H), 3.04 (dd, *J* = 14.9, 7.9 Hz, 1H), 2.98 (s, 1H), 2.80 (s, 3H); **^{13}C NMR (100 MHz, $CDCl_3$):** δ 140.6, 133.8, 132.6, 131.3, 128.7, 124.9, 120.6, 109.0, 88.5, 77.4, 43.4, 24.9; **HRMS (DART$^+$):** Calcd for $C_{12}H_{12}Cl_3$ $[M+H–H_2O]^+$: 261.0005; Found: 260.9994; **Specific Rotation:** $[\alpha]^{24}_D$ +11.7 (*c* 1.42, $CHCl_3$) for a 78.5:21.5 er sample. The enantiomeric purity of this compound was determined by HPLC analysis in comparison with authentic racemic material (Chiralcel OD-H, 98:2 hexanes:*i*-PrOH, 0.5 mL/min, 220 nm).

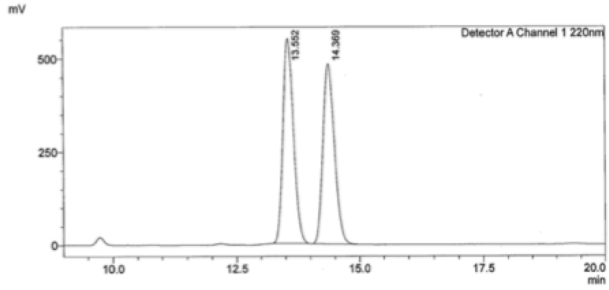

Detector A Channel 1 220nm

Peak#	Ret. Time	Area	Area%	Height
1	13.552	8261927	51.173	549634
2	14.369	7883153	48.827	483168
Total		16145081	100.000	1032802

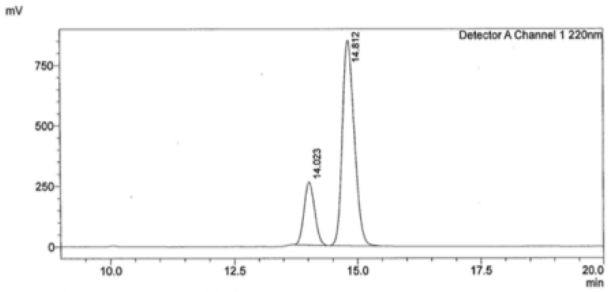

Detector A Channel 1 220nm

Peak#	Ret. Time	Area	Area%	Height
1	14.023	3895352	21.429	260025
2	14.812	14282662	78.571	848259
Total		18178014	100.000	1108284

Peak #	Ret. Time	Area	Area %	Peak #	Ret. Time	Area	Area %
1	13.5 min	8261927	51.173	1	14.0 min	3895352	21.429
2	14.4 min	7883153	48.827	2	14.8 min	14282662	78.571

(*R*)-1,1,1-Trichloro-2-(naphthalen-2-yl)pent-4-en-2-ol (2.7f): 28.6 mg, 0.0906 mmol, 91% yield. **IR (neat):** 3552 (br, w), 3058 (w), 1638 (w), 1599 (w), 1508 (w), 1443 (w), 1337 (w), 1264 (w), 1225 (w), 1160 (w), 1131 (w), 1097 (w), 992 (w), 923 (w), 853 (m), 812 (m), 787 (s), 750 (s), 686 (m), 642 (w), 623 (w), 476 (m) cm^{-1}; **^{1}H NMR (400 MHz, $CDCl_3$):** δ 8.25 (q, *J* = 0.9 Hz, 1H), 7.94–7.78 (m, 4H), 7.58–7.45 (m, 2H), 5.52 (dddd, *J* = 17.1, 10.1, 8.2, 5.7 Hz, 1H), 5.27 (dtd, *J* = 17.1, 1.7, 1.1 Hz, 1H), 5.12 (ddt, *J* = 10.1, 2.0, 1.0 Hz, 1H), 3.69 (ddt, *J* = 14.5, 5.7, 1.5 Hz, 1H), 3.13 (ddt, *J* = 14.6, 8.2, 1.0 Hz, 1H), 3.04 (s, 1H); **^{13}C NMR (100 MHz, $CDCl_3$):** δ 134.2, 133.1, 132.6, 132.2, 129.4, 128.8, 127.6, 127.0, 126.9, 126.4, 126.3, 120.9, 107.7, 84.6, 41.3; **HRMS (DART$^+$):** Calcd for $C_{15}H_{12}Cl_3$ $[M+H–H_2O]^+$: 297.0005; Found: 297.0005; **Specific Rotation:** $[\alpha]^{24}_D$ +33.1 (*c* 2.71, $CHCl_3$) for a 92.5:7.5 er sample. The enantiomeric purity of this compound was determined by HPLC analysis in comparison with authentic racemic material (Chiralcel OD-H, 98:2 hexanes:*i*-PrOH, 0.5 mL/min, 220 nm).

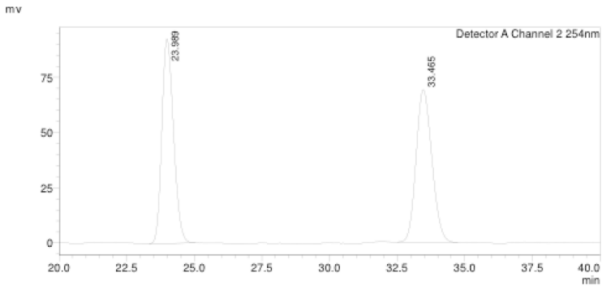

<Peak Table>
Detector A Channel 2 254nm

Peak#	Ret. Time	Area	Area%	Height
1	23.989	2782112	49.762	92575
2	33.465	2808704	50.238	69113
Total		5590817	100.000	161689

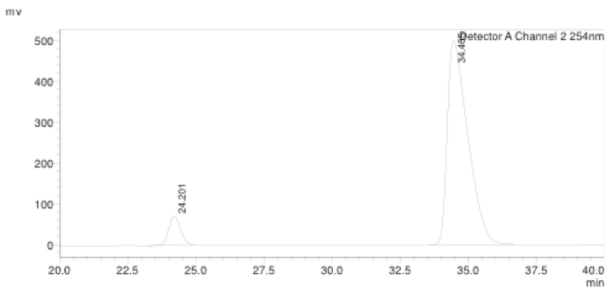

<Peak Table>
Detector A Channel 2 254nm

Peak#	Ret. Time	Area	Area%	Height
1	24.201	2101662	7.468	70736
2	34.465	26039982	92.532	498413
Total		28141644	100.000	569149

Peak #	Ret. Time	Area	Area %	Peak #	Ret. Time	Area	Area %
1	24.0 min	2782112	49.762	1	24.2 min	2101662	7.468
2	33.5 min	2808704	50.238	2	34.5 min	26039982	92.532

(*R*,*E*)-1-Phenyl-3-(trichloromethyl)hexa-1,5-dien-3-ol (2.7g): 24.8 mg, 0.0856 mmol, 86% yield. **IR (neat):** 3556 (br, w), 3078 (w), 2924 (w), 2331 (w), 1963 (w), 1640 (m), 1598 (m), 1068 (s), 902 (s), 794 (s), 688 (s), 649 (s) cm^{-1}; **^{1}H NMR (400 MHz, $CDCl_3$):** δ 7.45 (dd, *J* = 8.1, 1.4 Hz, 2H), 7.34 (m, 3H), 6.87 (d, *J* = 15.9 Hz, 1H), 6.50 (d, *J* = 15.9 Hz, 1H), 5.92–5.74 (m, 1H), 5.41–4.85 (m, 2H), 3.26–2.75 (m, 2H), 2.69 (s, 1H); **^{13}C NMR (100 MHz, $CDCl_3$):** δ 136.0, 134.2, 132.2, 128.8, 128.4, 127.0, 126.2, 120.2, 107.5, 84.1, 40.4; **HRMS(DART$^+$):** Calcd for $C_{13}H_{12}Cl_3$ $[M+H–H_2O]^+$: 272.9991; Found: 273.0146; **Specific Rotation:** $[\alpha]^{24}_D$ +5.9 (*c* 1.55, $CHCl_3$) for a 97.5:2.5 er sample. The enantiomeric purity of this compound was determined by HPLC analysis in comparison with authentic racemic material (Chiralpak AD-H, 98:2 hexanes:*i*-PrOH, 0.5 mL/min, 254 nm).

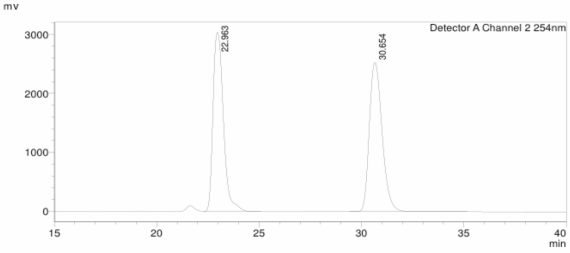

<Peak Table>
Detector A Channel 2 254nm

Peak#	Ret. Time	Area	Height	Area%
1	22.963	107185399	3036679	49.394
2	30.654	109814139	2529638	50.606
Total		216999538	5566316	100.000

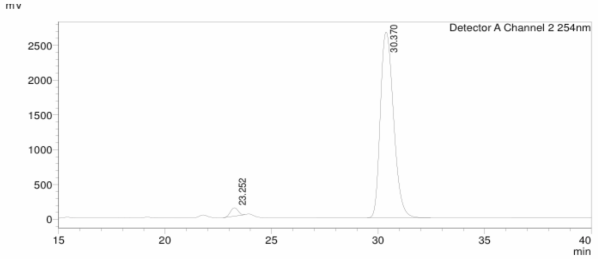

<Peak Table>
Detector A Channel 2 254nm

Peak#	Ret. Time	Area	Height	Area%
1	23.252	3041282	120664	2.571
2	30.370	115246068	2666757	97.429
Total		118287350	2787421	100.000

Peak #	Ret. Time	Area	Area %	Peak #	Ret. Time	Area	Area %
1	23.0 min	107185399	49.394	1	23.2 min	3041282	2.571
2	30. 7min	109814139	50.606	2	30.4 min	2666757	97.429

(*S*)-1-Phenyl-3-(trichloromethyl)hex-5-en-3-ol (2.7h): 27.6 mg, 0.0940 mmol, 94% yield. **IR (neat):** 3543 (br, w), 3081 (w), 3063 (w), 3026 (w), 2975 (w), 2942 (w), 1751 (w), 1639 (w), 1602 (w), 1495 (w), 1454 (w), 1347 (w), 999 (w), 921 (w), 818 (m), 787 (s), 745 (m), 698 (s), 657 (w), 558 (w) cm^{-1}; **^{1}H NMR (400 MHz, $CDCl_3$):** δ 7.35–7.19 (m, 5H), 6.14–5.97 (m, 1H), 5.35–5.22

(m, 2H), 2.96–2.81 (m, 4H), 2.57 (s, 1H), 2.42–2.24 (m, 2H); **^{13}C NMR (100 MHz, $CDCl_3$):** δ 141.7, 133.0, 128.7, 128.5, 126.3, 120.0, 109.6, 83.0, 40.1, 37.5, 31.0; **HRMS (DART$^+$):** Calcd for $C_{13}H_{14}Cl_3$ $[M+H–H_2O]^+$: 275.0156; Found: 275.0148; **Specific Rotation:** $[\alpha]^{24}_D$ –4.0 (*c* 2.80, $CHCl_3$) for a 86:14 er sample. The enantiomeric purity of this compound was determined by HPLC analysis in comparison with authentic racemic material (Chiralpak AD-H, 98:2 hexanes:*i*-PrOH, 0.5 mL/min, 220 nm).

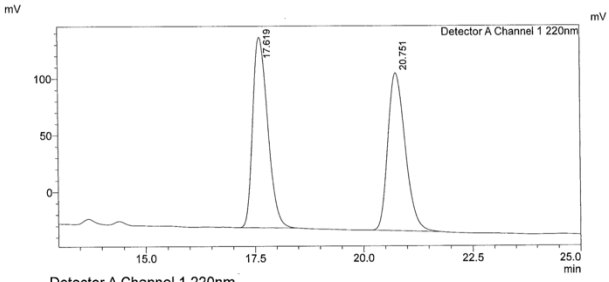

Detector A Channel 1 220nm

Peak#	Ret. Time	Area	Area%	Height
1	17.619	4067675	51.184	167967
2	20.751	3879495	48.816	139121
Total		7947170	100.000	307088

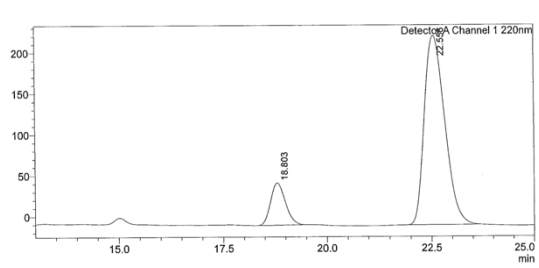

Detector A Channel 1 220nm

Peak#	Ret. Time	Area	Area%	Height
1	18.803	1294551	14.072	51666
2	22.556	7905186	85.928	231167
Total		9199737	100.000	282832

Peak #	Ret. Time	Area	Area %	Peak #	Ret. Time	Area	Area %
1	17.6 min	4067675	51.184	1	18.8 min	1294551	14.072
2	20.7 min	3879495	48.816	2	22.6 min	7905186	85.928

(*R*)-1,1,1-Trichloro-2-(furan-2-yl)pent-4-en-2-ol (2.7i): 25.0 mg, 0.0978 mmol, 98% yield. **IR (neat):** 3556 (br, w), 3081 (w), 1641 (w), 1348 (w), 1348 (w), 1158 (w), 1070 (w), 1009 (w), 993 (w), 913 (w), 886 (w), 819 (m), 790 (s), 740 (s), 678 (m), 647 (m), 595 (w), 545 (w), 499 (w) cm^{-1}; **^{1}H NMR (400 MHz, $CDCl_3$):** δ 7.49–7.43 (m, 1H), 6.55 (dt, *J* = 3.4, 0.6 Hz, 1H), 6.43 (dd, *J* = 3.4, 1.8 Hz, 1H), 5.64–5.52 (m, 1H), 5.24–5.12 (m, 2H), 3.34 (m 2H), 3.00 (ddt, *J* = 14.2, 7.6, 1.2 Hz, 1H); **^{13}C NMR (100 MHz, $CDCl_3$):** δ 150.3, 142.9, 131.9, 120.5, 111.6, 111.0, 106.2, 83.2, 39.7; **HRMS (DART$^+$):** Calcd for $C_9H_8Cl_3O$ $[M+H–H_2O]^+$: 236.9641; Found: 236.9644; **Specific Rotation:** $[\alpha]^{24}_D$ +13.9 (*c* 2.30, $CHCl_3$) for a 90:10 er sample. The enantiomeric purity of this compound was determined by HPLC analysis in comparison with authentic racemic material (Chiralpak AD-H, 98:2 hexanes:*i*-PrOH, 0.5 mL/min, 220 nm).

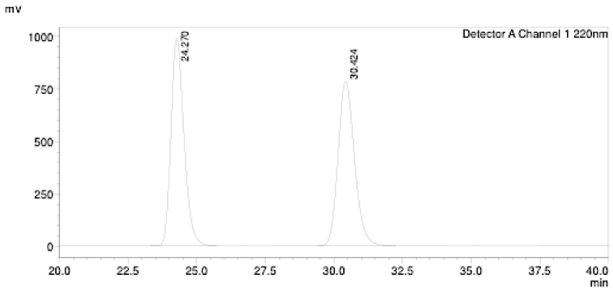

<Peak Table>
Detector A Channel 1 220nm

Peak#	Ret. Time	Area	Area%	Height
1	24.270	32499429	49.929	985079
2	30.424	32591386	50.071	778765
Total		65090815	100.000	1763844

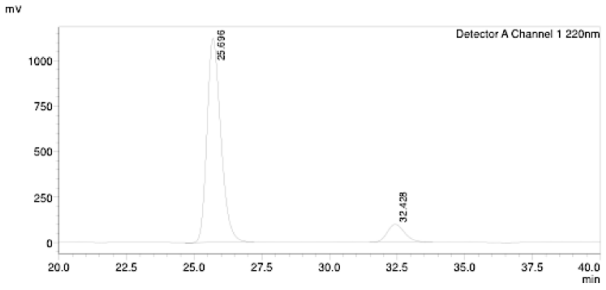

<Peak Table>
Detector A Channel 1 220nm

Peak#	Ret. Time	Area	Area%	Height
1	25.696	39875189	90.038	1121486
2	32.428	4411758	9.962	98601
Total		44286947	100.000	1220087

Peak #	Ret. Time	Area	Area %	Peak #	Ret. Time	Area	Area %
1	24.3 min	32499429	49.929	1	25.7 min	39875189	90.038
2	30.4 min	32591386	50.071	2	32.4 min	4411758	9.963

(*R*)-1,1,1-Trichloro-2-(furan-3-yl)pent-4-en-2-ol (2.7j): 23.2 mg, 0.0908 mmol, 94% yield. **IR (neat):** 3552 (br, w), 3153 (w), 3080 (w), 2980 (w), 1723 (w), 1640 (w), 1589 (w), 1438 (w), 1354 (w), 1248 (w), 1220 (w), 1169 (m), 1075 (w), 1034 (w), 1016 (w), 993 (w), 874 (m), 804 (s), 732 (s), 671 (m), 637 (m), 600 (w) cm^{-1}; **^{1}H NMR (400 MHz, $CDCl_3$):** δ 7.57 (ddd, *J* = 1.5, 0.9, 0.4 Hz, 1H), 7.43–7.38 (m, 1H), 6.55 (ddd, *J* = 1.9, 0.9, 0.4 Hz, 1H), 5.69–5.57 (m, 1H), 5.25–5.12 (m, 2H), 3.22–3.13 (m, 1H), 2.97 (ddt, *J* = 14.2, 8.1, 1.1 Hz, 1H), 2.81 (d, *J* = 0.4 Hz, 1H); **^{13}C NMR (100 MHz, $CDCl_3$):** δ 143.0, 142.8, 132.2, 124.0, 120.7, 110.8, 107.3, 82.6, 41.4; **HRMS (DART$^+$):** Calcd for $C_9H_8Cl_3O$ $[M+H–H_2O]^+$: 236.9641; Found: 236.9644; **Specific Rotation:** $[\alpha]^{24}_D$ +23.3 (*c* 1.82, $CHCl_3$) for a 96:4 er sample. The enantiomeric purity of this compound was determined by HPLC analysis in comparison with authentic racemic material (Chiralpak AD-H, 98:2 hexanes:*i*-PrOH, 0.5 mL/min, 220 nm).

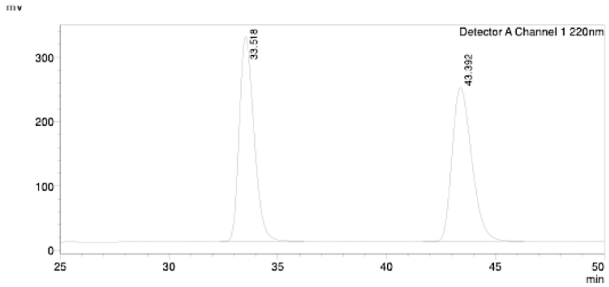

<Peak Table>
Detector A Channel 1 220nm

Peak#	Ret. Time	Area	Area%	Height
1	33.518	14977525	49.810	318376
2	43.392	15091622	50.190	239380
Total		30069148	100.000	557756

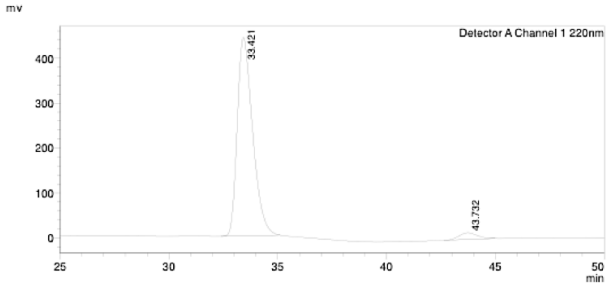

<Peak Table>
Detector A Channel 1 220nm

Peak#	Ret. Time	Area	Area%	Height
1	33.421	21691293	96.219	441536
2	43.732	852443	3.781	14632
Total		22543736	100.000	456168

Peak #	Ret. Time	Area	Area %	Peak #	Ret. Time	Area	Area %
1	33.5 min	14977525	49.810	1	33.4 min	21691293	96.219
2	43.4 min	15091622	50.190	2	43.7 min	852443	3.781

(*R*)-1,1,1-Trichloro-2-(thiophen-2-yl)pent-4-en-2-ol (2.7k): 23.2 mg, 0.0850 mmol, 90% yield. The analytical data are consistent with those reported previously.[162] **^{1}H NMR (400 MHz, $CDCl_3$):** δ 7.36 (dd, *J* = 5.1, 1.2 Hz, 1H), 7.27 (d, *J* = 1.2 Hz, 13H), 7.03 (dd, *J* = 5.1, 3.7 Hz, 1H), 5.58 (dddd, *J* = 17.1, 10.0, 8.4, 5.7 Hz, 1H), 5.34–5.11 (m, 2H), 3.34 (ddt, *J* = 14.1, 5.7, 1.5 Hz, 1H), 3.15 (s, 1H), 3.08 (ddt, *J* = 14.2, 8.4, 1.0 Hz, 1H); **Specific Rotation:** $[\alpha]^{24}_D$ +27.7 (*c* 2.16, $CHCl_3$) for a 86.5:13.5 er sample. The enantiomeric purity of this compound was determined by HPLC analysis in comparison with authentic racemic material (Chiralcel OD-H, 98:2 hexanes:*i*-PrOH, 0.5 mL/min, 220 nm.

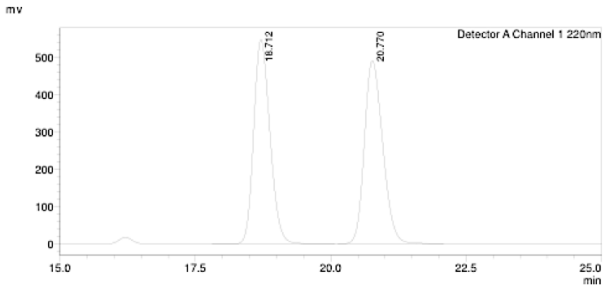

<Peak Table>
Detector A Channel 1 220nm

Peak#	Ret. Time	Area	Area%	Height
1	18.712	11450626	49.821	547076
2	20.770	11532892	50.179	489656
Total		22983518	100.000	1036732

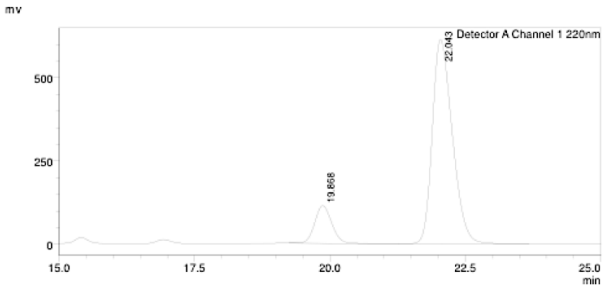

<Peak Table>
Detector A Channel 1 220nm

Peak#	Ret. Time	Area	Area%	Height
1	19.868	2469369	13.505	113042
2	22.043	15815007	86.495	613296
Total		18284376	100.000	726338

Peak #	Ret. Time	Area	Area %	Peak #	Ret. Time	Area	Area %
1	18.7 min	11450626	49.821	1	19.9 min	2469369	13.505
2	20.8 min	11532892	50.179	2	22.0 min	15815007	86.495

(*R*)-1,1,1-Trichloro-2-(thiophen-3-yl)pent-4-en-2-ol (2.7l): 25.2 mg, 0.0928 mmol, 95% yield. **IR (neat):** 3553 (br, w), 3113 (w), 3080 (w), 2980 (w), 2925 (w), 1719 (w), 1639 (w), 1438 (w), 1411 (w), 1334 (w), 1234 (w), 1154 (w), 1087 (w), 1019 (w), 992 (w), 923 (w), 887 (w), 865 (m), 804 (s), 797 (s), 727 (s), 669 (m), 604 (w) cm^{-1}; **^{1}H NMR (400 MHz, $CDCl_3$):** δ 7.53 (t, *J* = 2.2 Hz, 1H), 7.29 (d, *J* = 2.2 Hz, 2H), 5.53 (dddd, *J* = 17.1, 10.1, 8.3, 5.7 Hz, 1H), 5.28–5.08 (m, 2H), 3.37 (ddt, *J* = 14.3, 5.8, 1.4 Hz, 1H), 3.02 (dd, *J* = 14.3, 8.3 Hz, 1H), 2.93 (s, 1H); **^{13}C NMR (100 MHz, $CDCl_3$):** δ 138.8, 132.2, 128.2, 126.2, 124.8, 120.7, 107.3, 84.0, 41.8; **HRMS (DART$^+$):** Calcd for $C_9H_8Cl_3S$ $[M+H–H_2O]^+$: 252.9412; Found: 252.9418; **Specific Rotation:** $[\alpha]^{24}_D$ +22.2 (*c* 2.36, $CHCl_3$) for a 97:3 er sample. The enantiomeric purity of this compound was determined by HPLC analysis in comparison with authentic racemic material (Chiralpak AD-H, 98:2 hexanes:*i*-PrOH, 0.5 mL/min, 220 nm).

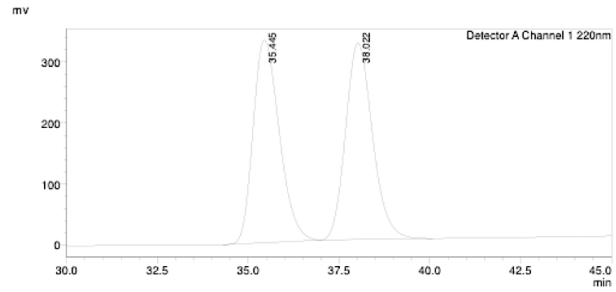

<Peak Table>
Detector A Channel 1 220nm

Peak#	Ret. Time	Area	Area%	Height
1	35.445	16604629	50.023	331298
2	38.022	16589376	49.977	321211
Total		33194005	100.000	652508

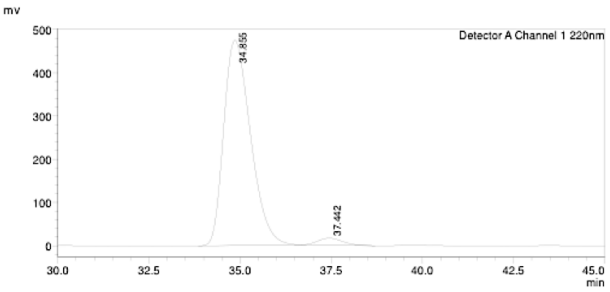

<Peak Table>
Detector A Channel 1 220nm

Peak#	Ret. Time	Area	Area%	Height
1	34.855	24238142	96.983	474904
2	37.442	753997	3.017	16096
Total		24992140	100.000	491000

Peak #	Ret. Time	Area	Area %	Peak #	Ret. Time	Area	Area %
1	35.4 min	16604629	50.023	1	34.9 min	24238142	96.983
2	38.0 min	16589376	49.977	2	37.4 min	753997	3.017

(*R*)-1,1,1-Trichloro-2-(2,6-difluorophenyl)pent-4-en-2-ol (2.7m): 23.2 mg, 0.0769 mmol, 77% yield. **IR (neat):** 3604 (br, w), 2926 (w), 1621 (w), 1464 (m), 1343 (w), 1269 (w), 1220 (m), 1077

(w), 983 (m), 922 (w), 779 (s), 689 (m), 582 (w), 520 (m), 446 (w) cm^{-1}; **^{1}H NMR (400 MHz, $CDCl_3$):** δ 7.36 (tt, *J* = 8.4, 6.0 Hz, 1H), 6.94 (m, 2H), 5.86–5.63 (m, 1H), 5.27 (dtt, *J* = 17.1, 2.1, 1.1 Hz, 1H), 5.05 (dtd, *J* = 10.2, 1.9, 0.8 Hz, 1H), 4.81 (ddd, *J* = 23.8, 3.5, 0.6 Hz, 1H), 3.69–3.39 (m, 1H), 2.98 (dtd, *J* = 14.3, 3.9, 2.0 Hz, 1H); **^{13}C NMR (100 MHz, $CDCl_3$):** δ 163.0 (d, *J* = 249.5 Hz), 160.0 (d, *J* = 251.3 Hz), 132.6, 131.4 (t, *J* = 12.9 Hz), 119.1, 113.9 (t, *J* = 10.9 Hz), 113.3 (d, *J* = 28.5 Hz), 107.4 (t, *J* = 2.1 Hz), 88.4 (t, *J* = 7.7 Hz), 40.4 (d, *J* = 11.4 Hz); **^{19}F NMR (376 MHz, $CDCl_3$):** –98.04 (s, 1F), –108.63 (s, 1F); **HRMS (DART$^+$):** Calcd for $C_{11}H_{13}Cl_3F_2ON$ $[M+NH_4]^+$: 318.0031; Found: 318.0038; **Specific Rotation:** $[\alpha]^{24}_D$ –15.4 (*c* 1.30, $CHCl_3$) for a 64.5:35.5 er sample. The enantiomeric purity of this compound was determined by HPLC analysis in comparison with authentic racemic material (Chiralcel OZ-H, 98:2 hexanes:*i*-PrOH, 0.5 mL/min, 220 nm).

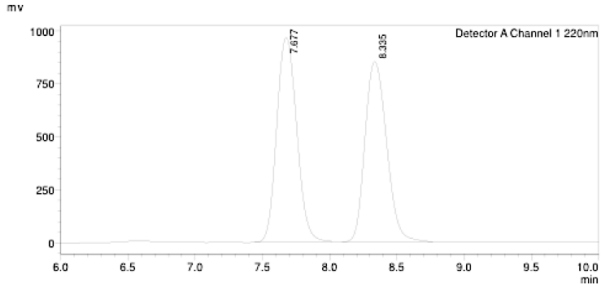

<Peak Table>
Detector A Channel 1 220nm

Peak#	Ret. Time	Area	Area%	Height
1	7.677	9964276	51.180	966021
2	8.335	9504877	48.820	850718
Total		19469153	100.000	1816739

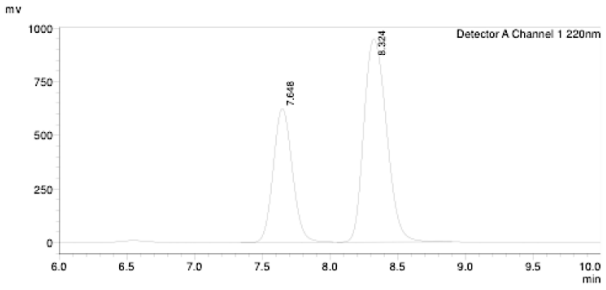

<Peak Table>
Detector A Channel 1 220nm

Peak#	Ret. Time	Area	Area%	Height
1	7.648	6107082	35.647	623124
2	8.324	11025043	64.353	946648
Total		17132125	100.000	1569772

Peak #	Ret. Time	Area	Area %	Peak #	Ret. Time	Area	Area %
1	7.7 min	9964276	51.180	1	7.6 min	6107082	35.647
2	8.3 min	19504877	48.820	2	8.3 min	11025043	64.353

(*R*)-1,1,1-Trichloro-2-(trifluoromethyl)pent-4-en-2-ol (2.7n): 23.5 mg, 0.0916 mmol, 51% yield. The title compound was synthesized in an analogous manner as **1a**, except for the following changes: 1) thf was used as solvent to increase conversion. The same reaction in toluene gave low conversion (~60%). 2) The reaction was performed for 5 h at 22 ºC. 3) The scale was 0.18 mmol. **IR (neat):** 3553 (br, w), 3113 (w), 3080 (w), 2980 (w), 2925 (w), 1719 (w), 1639 (w), 1438 (w), 1411 (w), 1334 (w), 1234 (w), 1154 (w), 1087 (w), 1019 (w), 992 (w), 923 (w), 887 (w), 865 (m), 804 (s), 797 (s), 727 (s), 669 (m), 604 (w) cm^{-1}; **^{1}H NMR (400 MHz, $CDCl_3$):** δ 6.01–5.79 (m, 1H), 5.46–5.31 (m, 2H), 3.31 (s, 1H), 3.11–2.93 (m, 2H); **^{13}C NMR (100 MHz, $CDCl_3$):** δ 130.3 (d, *J* = 2.1 Hz), 124.0 (q, *J* = 289.6 Hz), 123.3, 101.2, 82.2 (q, *J* = 27.1 Hz), 37.7; **^{19}F NMR (376 MHz, $CDCl_3$):** –65.35 (s, 3F); **HRMS (DART$^+$):** Calcd for $C_6H_7OF_3Cl_3$ $[M+H]^+$: 256.9509; Found: 256.9515; **Specific Rotation:** $[\alpha]^{24}_D$ +1.3 (*c* 0.98, $CHCl_3$) for a 60:40 er sample The enantiomeric purity was determined by HPLC analysis in comparison with authentic racemic material after benzoylation[163] (Chiralcel OD-H, 99:1 hexanes:*i*-PrOH, 0.5 mL/min, 254 nm).

[163] Rao, W.; Koh, M. J.; Li, D.; Hirao, H.; Chan, P. W. H. *J. Am. Chem. Soc.* **2013**, *135*, 7926–7932.

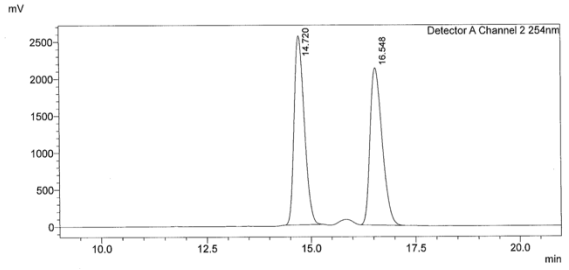

Detector A Channel 2 254nm

Peak#	Ret. Time	Area	Area%	Height
1	14.720	43641180	50.593	2558591
2	16.548	42618017	49.407	2127967
Total		86259197	100.000	4686558

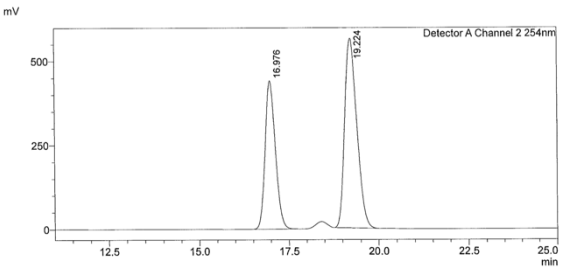

Detector A Channel 2 254nm

Peak#	Ret. Time	Area	Area%	Height
1	16.976	8869320	40.248	441074
2	19.224	13167304	59.752	564033
Total		22036624	100.000	1005107

Peak #	Ret. Time	Area	Area %	Peak #	Ret. Time	Area	Area %
1	14.7 min	43641180	50.593	1	17.0 min	8869320	40.248
2	16.5 min	42618017	49.407	2	19.2 min	13167304	59.752

(*R*)-1,1,1-Tribromo-2-phenylpent-4-en-2-ol (2.10): 38.2 mg, 0.0958 mmol, 96% yield. **IR (neat):** 3545 (br, w), 3077 (w), 3060 (w), 3019 (w), 1697 (w), 1639 (w), 1494 (w), 1446 (w), 1348 (w), 1214 (m), 1166 (w), 1069 (w), 991 (w), 924 (w), 892 (w), 758 (s), 701 (s), 669 (s), 605 (w), 544 (w) cm^{-1}; **^{1}H NMR (400 MHz, $CDCl_3$):** δ 7.88–7.81 (m, 2H), 7.40–7.33 (m, 3H), 5.56–5.39 (m, 1H), 5.15 (m, 2H), 3.77–3.62 (m, 1H), 3.13 (ddd, J = 14.5, 8.1, 1.0 Hz, 1H), 3.01 (s, 1H); **^{13}C NMR (100 MHz, $CDCl_3$):** δ 135.9, 132.8, 129.9, 128.6, 127.4, 120.6, 83.8, 61.6, 41.6; **HRMS (DART$^+$):** Calcd for $C_{11}H_{10}Br_3$ $[M+H–H_2O]^+$: 378.8338; Found: 378.8333; **Specific Rotation:** $[\alpha]^{24}_D$ +6.9 (*c* 1.45, $CHCl_3$) for a 96:4 er sample. The enantiomeric purity of this compound was determined by HPLC analysis in comparison with authentic racemic material (Chiralpak AD-H, 99:1 hexanes:*i*-PrOH, 0.5 mL/min, 220 nm).

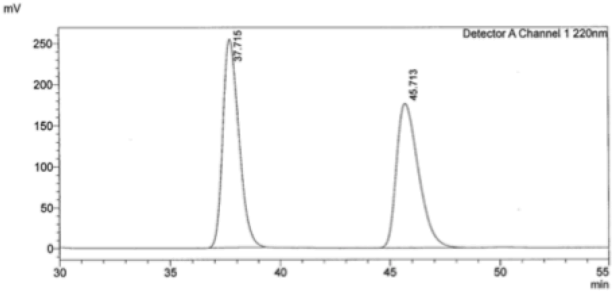

Detector A Channel 1 220nm

Peak#	Ret. Time	Area	Area%	Height
1	37.715	12993213	51.642	254414
2	45.713	12167001	48.358	176491
Total		25160214	100.000	430905

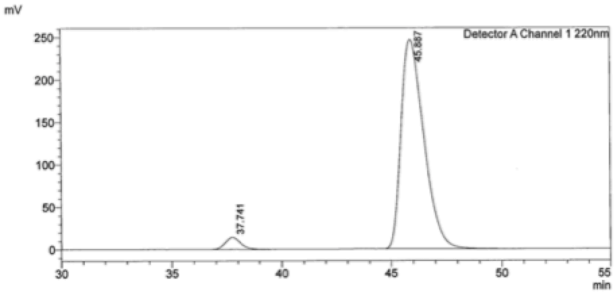

Detector A Channel 1 220nm

Peak#	Ret. Time	Area	Area%	Height
1	37.741	715735	3.888	14301
2	45.887	17691321	96.112	246523
Total		18407057	100.000	260823

Peak #	Ret. Time	Area	Area %	Peak #	Ret. Time	Area	Area %
1	37.7 min	12993213	51.642	1	37.7 min	715735	3.888
2	45.7 min	1267001	48.358	2	45.9 min	17691321	96.112

(*R*)-1-Chloro-1,1-difluoro-2-phenylpent-4-en-2-ol (2.11): 20.9 mg, 0.0898 mmol, 90% yield. **IR (neat):** 3552 (br, w), 3065 (w), 1640 (w), 1448 (w), 1171 (w), 1116 (m), 1073 (w), 1025 (m), 998

(m), 972 (m), 924 (m), 893 (w), 824 (m), 761 (w), 719 (s), 696 (s), 616 (m) cm^{-1}; **^{1}H NMR (400 MHz, $CDCl_3$):** δ 7.60 (ddq, *J* = 7.0, 2.2, 1.1 Hz, 2H), 7.49–7.34 (m, 3H), 5.60–5.46 (m, 1H), 5.28–5.15 (m, 2H), 3.14–3.06 (m, 1H), 2.94–2.84 (m, 1H), 2.69 (s, 1H); **^{13}C NMR (100 MHz, $CDCl_3$):** δ 137.4, 134.4, 131.4, 131.0, 128.6, 128.3, 127.1 (t, *J* = 1.7 Hz), 79.6 (t, *J* = 24.4 Hz), 40.6 (d, *J* = 1.8 Hz); **^{19}F NMR (376 MHz, $CDCl_3$):** –63.59 (d, *J* = 28.1 Hz, 2F); **HRMS (DART$^+$):** Calcd for $C_{11}H_{10}Cl_1F_2$ $[M+H–H_2O]^+$: 215.0439; Found: 215.0450; **Specific Rotation:** $[\alpha]^{24}_D$ +49.0 (*c* 1.02, $CHCl_3$) for a 91:9 er sample. The enantiomeric purity of this compound was determined by HPLC analysis in comparison with authentic racemic material (Chiralpak AS-H, 98:2 hexanes:*i*-PrOH, 0.5 mL/min, 220 nm).

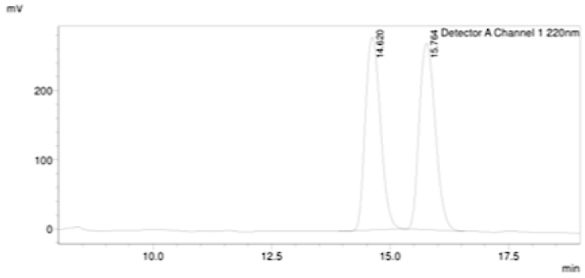

<Peak Table>
Detector A Channel 1 220nm

Peak#	Ret. Time	Area	Height	Area%
1	14.620	6222617	278638	49.427
2	15.764	6366997	269568	50.573
Total		12589613	548206	100.000

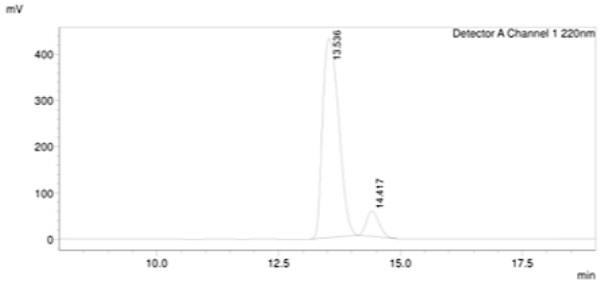

<Peak Table>
Detector A Channel 1 220nm

Peak#	Ret. Time	Area	Area%	Height
1	13.536	9932280	90.975	430526
2	14.417	985289	9.025	54707
Total		10917569	100.000	485233

Peak #	Ret. Time	Area	Area %	Peak #	Ret. Time	Area	Area %
1	14.6 min	6222617	49.427	1	13.5 min	9932280	90.975
2	15.8 min	6366997	50.573	2	14.4 min	985289	9.025

(*R*)-1-Bromo-1,1-difluoro-2-phenylpent-4-en-2-ol (2.12): 25.2 mg, 0.0909 mmol, 91% yield. **IR (neat):** 3542 (br, w), 3064 (w), 1640 (w), 1496 (w), 1448 (w), 1166 (m), 1114 (m), 1072 (m), 1018 (m), 993 (m), 967 (m), 919 (m), 888 (w), 840 (w), 802 (m), 761 (m), 714 (s), 696 (s), 660 (m), 608 (w) cm^{-1}; **^{1}H NMR (400 MHz, $CDCl_3$):** δ 7.58 (ddt, *J* = 8.1, 2.4, 1.1 Hz, 2H), 7.45–7.36 (m, 3H), 5.57–5.41 (m, 1H), 5.26–5.13 (m, 2H), 3.13–3.03 (m, 1H), 2.88 (ddd, *J* = 14.3, 8.1, 0.9 Hz, 1H), 2.68 (s, 1H); **^{13}C NMR (100 MHz, $CDCl_3$):** δ 137.5 (d, *J* = 1.7 Hz), 131.0, 128.7, 128.3, 127.5 (t, *J* = 315.1 Hz), 127.1 (t, *J* = 1.8 Hz), 121.6, 80.4 (t, *J* = 22.3 Hz), 40.7 (t, *J* = 1.8 Hz); **^{19}F NMR (376 MHz, $CDCl_3$):** –56.01 to –57.53 (m); **HRMS (DART$^+$):** Calcd for $C_{11}H_{10}BrF_2$ $[M+H–H_2O]^+$: 258.9934; Found: 258.9942; **Specific Rotation:** $[\alpha]^{24}_D$ +39.6 (*c* 2.02, $CHCl_3$) for a 92:8 er sample. The enantiomeric purity of this compound was determined by HPLC analysis in comparison with authentic racemic material (Chiralpak AS-H, 98:2 hexanes:*i*-PrOH, 0.5 mL/min, 220 nm).

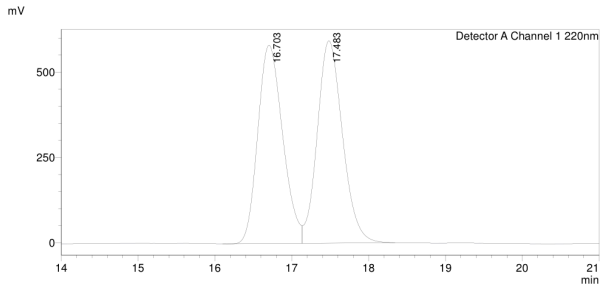

<Peak Table>
Detector A Channel 1 220nm

Peak#	Ret. Time	Area	Area%	Height
1	16.703	13096193	49.125	581534
2	17.483	13562710	50.875	593334
Total		26658903	100.000	1174869

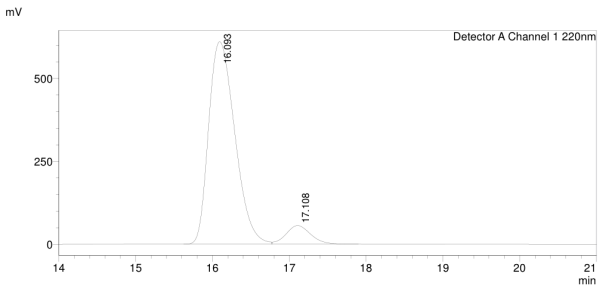

<Peak Table>
Detector A Channel 1 220nm

Peak#	Ret. Time	Area	Area%	Height
1	16.093	14467780	92.028	609740
2	17.108	1253227	7.972	55970
Total		15721007	100.000	665710

Peak #	Ret. Time	Area	Area %	Peak #	Ret. Time	Area	Area %
1	16.7 min	13096193	49.125	1	16.1 min	14467780	92.028
2	17.5 min	13562710	50.875	2	17.1 min	1253227	7.972

2.8.6. Catalytic Enantioselective Additions to Monochloro- and Monobromomethyl ketones

Allyl addition: In a N_2-filled glove box, aminophenol **ap-5** (0.27 mg, 0.0005 mmol), $Zn(OMe)_2$ (0.32 mg, 0.0025 mmol) and toluene (0.5 mL) were added to a two-dram vial equipped with a stir bar and allowed to stir for 5 min. Ketone (0.10 mmol, 1.0 equiv), (pinacolato)allylboron (0.020 mL, 0.11 mmol), and MeOH (0.010 mL, 0.25 mmol, 2.5 equiv) were added sequentially. The vessel was sealed with a Teflon cap, removed from the glove box, and allowed to stir for 3 h at 22 °C. Conversion was determined by analysis of ^{1}H NMR spectrum of an aliquot. The solution mixture was directly loaded onto a silica gel column eluted with hexanes/Et_2O to afford the product.

One-pot synthesis of 1,1-disubstituted epoxides: The latter procedure was followed and after 3 h, diazabicyclo[5.4.0]undec-7-ene (42 μL, 15 mmol, 3.0 equiv) was added and the mixture allowed to stir at 22°C for 0.5–3 h. Conversion was determined by analysis of ^{1}H NMR spectrum of an aliquot. The solution mixture was directly loaded onto a silica gel column eluted with hexanes/Et_2O to afford the product.

(*S*)-1-Chloro-2-phenylpent-4-en-2-ol (2.15a): 18.9 mg, 0.0960 mmol, 96% yield, colorless oil. The analytical data are consistent with those reported previously.[164] **^{1}H NMR (400 MHz, $CDCl_3$):** δ 7.46–7.35 (m, 4H), 7.33–7.27 (m, 1H), 5.71–5.47 (m, 1H), 5.24–5.03 (m, 2H), 3.97–3.69 (m, 2H), 2.77–2.64 (m, 2H), 2.58 (d, J = 0.8 Hz, 1H); **Specific Rotation:** $[\alpha]^{24}_D$ –13.4 (*c* 1.28, $CHCl_3$) for a 97:3 er sample. The enantiomeric purity of this compound was determined by HPLC analysis

[164] Fandrick, K. R.; Fandrick, D. R.; Gao, J. J.; Reeves, J. T.; Tan, Z.; Li, W.; Song, J. J.; Lu, B.; Yee, N. K.; Senanayake, C. H. *Org. Lett*. **2010**, *12*, 3748–3751.

in comparison with authentic racemic material (Chiralpak AD-H, 98:2 hexanes:*i*-PrOH, 0.5 mL/min, 220 nm).

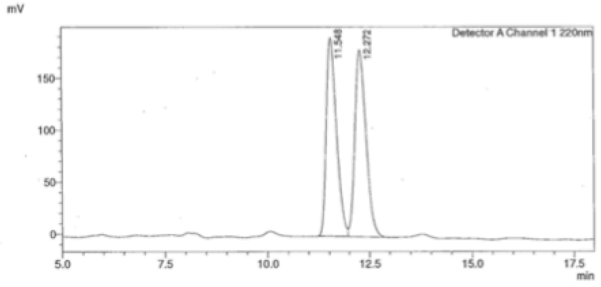

Detector A Channel 1 220nm

Peak#	Ret. Time	Area	Height	Area%
1	11.548	3374071	190821	49.548
2	12.272	3435629	179723	50.452
Total		6809701	370544	100.000

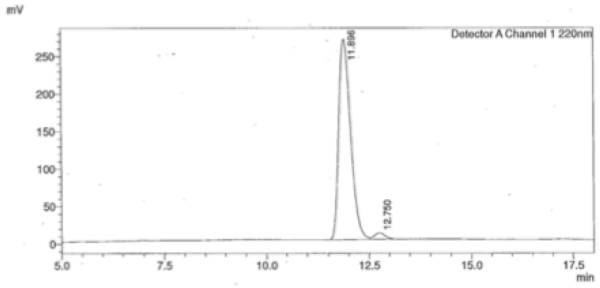

Detector A Channel 1 220nm

Peak#	Ret. Time	Area	Area%	Height
1	11.896	5368018	97.189	267212
2	12.750	155244	2.811	8510
Total		5523262	100.000	275722

Peak #	Ret. Time	Area	Area %	Peak #	Ret. Time	Area	Area %
1	11.5 min	3374071	49.548	1	11.9 min	5368018	97.189
2	12.3 min	3435629	50.542	2	12.8 min	155244	2.811

(*S*)-1-Bromo-2-phenylpent-4-en-2-ol (2.16a): 23.4 mg, 0.0970 mmol, 97% yield, yellow oil. The analytical data are consistent with those reported previously.[165] **^{1}H NMR (400 MHz, $CDCl_3$):** δ 7.45–7.35 (m, 4H), 7.32–7.27 (m, 1H), 5.60 (ddt, *J* = 17.2, 10.1, 7.2 Hz, 1H), 5.20–5.03 (m, 2H), 3.77 (d, *J* = 2.4 Hz, 2H), 2.74 (dt, *J* = 7.8, 0.9 Hz, 2H), 2.62–2.47 (m, 1H). **Specific Rotation:** $[\alpha]^{24}_D$ –11.0 (*c* 0.10, $CHCl_3$) for a 86:14 er sample. The enantiomeric purity was determined by HPLC analysis in comparison with authentic racemic material (Chiralcel OJ-H, 98:2 hexanes:*i*-PrOH, 0.5 mL/min, 220 nm).

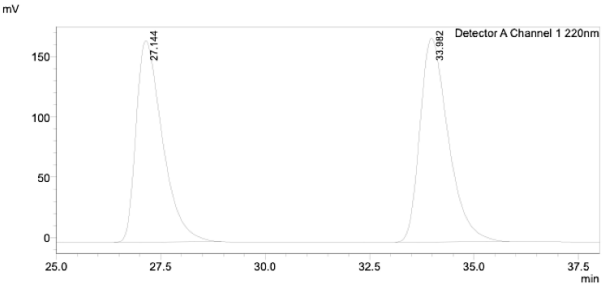

<Peak Table>
Detector A Channel 1 220nm

Peak#	Ret. Time	Area	Height	Area%
1	27.144	7336991	166933	47.862
2	33.982	7992511	169040	52.138
Total		15329502	335973	100.000

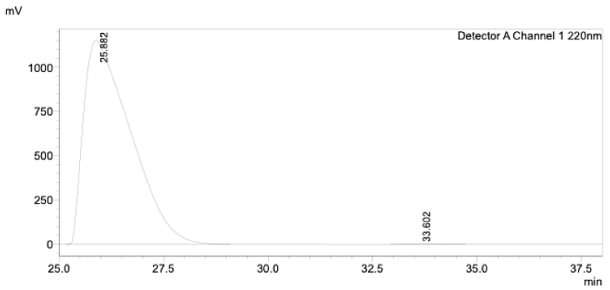

<Peak Table>
Detector A Channel 1 220nm

Peak#	Ret. Time	Area	Height	Area%
1	25.882	90409294	1153305	99.856
2	33.602	130127	2707	0.144
Total		90539420	1156012	100.000

Peak #	Ret. Time	Area	Area %	Peak #	Ret. Time	Area	Area %
1	27.1 min	7336991	47.862	1	25.9 min	90409294	99.856
2	33.0 min	7992511	52.138	2	33.6 min	130127	0.144

[165] Lin, M.-H.; Kuo, C.-K.; Lin, W.-C.; Huang, Y.-C.; Tsai, Y.-T.; Liang, K.-Y.; Li, Y.-S.; Chuang, T.-H. *Tetrahedron* **2013,** *69*, 8263–8268.

(*S*)-2-Allyl-2-phenyloxirane (2.17a): The title compound was synthesized according to the aforementioned procedure and purified by silica gel chromatography to afford **2.17a**. The analytical data are consistent with those reported previously.[166] **^{1}H NMR (400 MHz, $CDCl_3$):** δ 7.48–7.44 (m, 2H), 7.26–7.23 (m, 2H), 5.75 (ddt, *J* = 17.2, 10.3, 6.9 Hz, 1H), 5.18–5.05 (m, 2H), 3.00 (d, *J* = 5.3 Hz, 1H), 2.93–2.78 (m, 1H), 2.72 (dd, *J* = 5.3, 0.5 Hz, 1H), 2.61 (dd, *J* = 15.0, 7.2 Hz, 1H).

From X = Cl: 13.0 mg, 0.0811 mmol, 81% yield, colorless oil. **Specific Rotation:** $[\alpha]^{24}_D$ +30.4 (*c* 1.78, $CHCl_3$) for a 97:3 er sample. The enantiomeric purity of this compound was determined by HPLC analysis in comparison with authentic racemic material (Chiralcel OJ-H, 98:2 hexanes:*i*-PrOH, 0.5 mL/min, 220 nm).

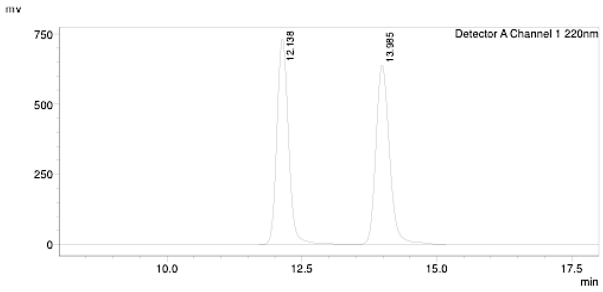

<Peak Table>
Detector A Channel 1 220nm

Peak#	Ret. Time	Area	Area%	Height
1	12.138	10919413	49.510	732335
2	13.985	11135762	50.490	638622
Total		22055175	100.000	1370957

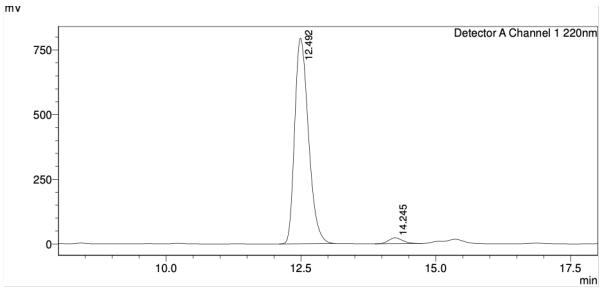

<Peak Table>
Detector A Channel 1 220nm

Peak#	Ret. Time	Area	Area%	Height
1	12.492	14113645	97.186	795677
2	14.245	408704	2.814	22584
Total		14522349	100.000	818261

Peak #	Ret. Time	Area	Area %	Peak #	Ret. Time	Area	Area %
1	12.1 min	10919413	49.510	1	12.5 min	14113645	97.186
2	14.0 min	11135762	50.490	2	14.2 min	408704	2.814

From X = Br: 15.1 mg, 0.0967 mmol, 97% yield, colorless oil. **Specific Rotation:** $[\alpha]^{24}_D$ +25.7 (*c* 1.07, $CHCl_3$) for a 96.5:3.5 er sample. The enantiomeric purity of this compound was determined by HPLC analysis in comparison with authentic racemic material (Chiralcel OJ-H, 98:2 hexanes:*i*-PrOH, 0.5 mL/min, 220 nm).

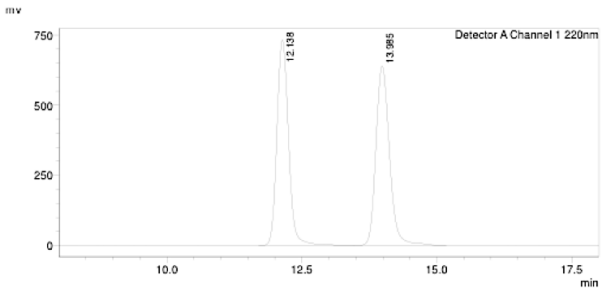

<Peak Table>
Detector A Channel 1 220nm

Peak#	Ret. Time	Area	Area%	Height
1	12.138	10919413	49.510	732335
2	13.985	11135762	50.490	638622
Total		22055175	100.000	1370957

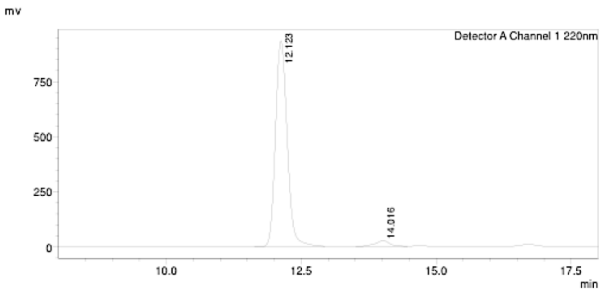

<Peak Table>
Detector A Channel 1 220nm

Peak#	Ret. Time	Area	Area%	Height
1	12.123	14084627	96.418	934541
2	14.016	523291	3.582	26469
Total		14607918	100.000	961010

[166] Fan, L.; Zhang, M.; Zhang, S. *Org. Biomol. Chem.* **2012**, *10*, 3182–3184.

Peak #	Ret. Time	Area	Area %	Peak #	Ret. Time	Area	Area %
1	12.1 min	10919413	49.510	1	12.1 min	14084627	96.418
2	14.0 min	11135762	50.490	2	14.0 min	523291	3.582

(*S*)-1-Chloro-2-(4-nitrophenyl)pent-4-en-2-ol (2.15b): 20.8 mg, 0.0861 mmol, 81% yield, colorless oil. **Specific Rotation:** $[\alpha]^{24}_{D}$ –2.0 (*c* 1.01, $CHCl_3$) for a 90:10 er sample. The enantiomeric purity was determined by HPLC analysis in comparison with authentic racemic material (Chiralpak AS-H, 98:2 hexanes:*i*-PrOH, 0.5 mL/min, 254 nm).

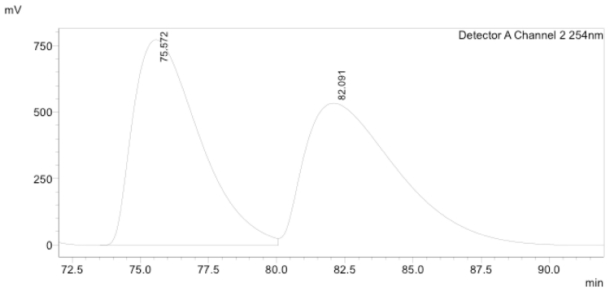

<Peak Table>
Detector A Channel 2 254nm

Peak#	Ret. Time	Area	Height	Area%
1	75.572	130909695	774825	50.578
2	82.091	127915238	535900	49.422
Total		258824933	1310725	100.000

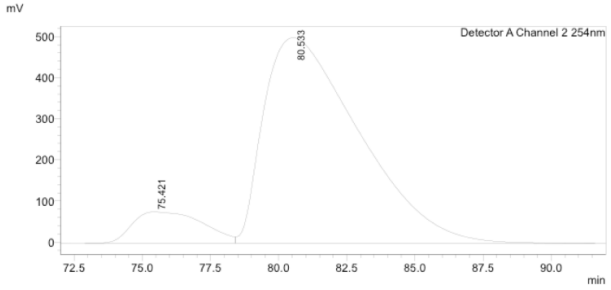

<Peak Table>
Detector A Channel 2 254nm

Peak#	Ret. Time	Area	Height	Area%
1	75.421	13759866	76346	10.141
2	80.533	121927605	500069	89.859
Total		135687471	576415	100.000

Peak #	Ret. Time	Area	Area %	Peak #	Ret. Time	Area	Area %
1	75.6 min	130909695	50.578	1	75.4 min	13759866	10.141
2	82.1 min	127915238	49.422	2	80.5 min	121927605	89.859

(*S*)-1-Bromo-2-(4-nitrophenyl)pent-4-en-2-ol (2.16b): 26.6 mg, 0.0939 mmol, 93% yield, colorless oil. The analytical data are fully consistent with those reported previously.[**Error! Bookmark not defined.**] **Specific Rotation:** $[\alpha]^{24}_{D}$ +5.7 (*c* 1.00, $CHCl_3$) for a 88:12 er sample. The enantiomeric purity was determined by HPLC analysis in comparison with authentic racemic material (Chiralpak AS-H, 98:2 hexanes:*i*-PrOH, 0.5 mL/min, 254 nm).

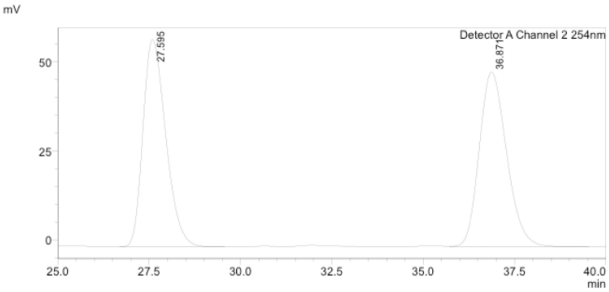

<Peak Table>
Detector A Channel 2 254nm

Peak#	Ret. Time	Area	Height	Area%
1	27.595	2523856	58156	49.798
2	36.871	2544370	48905	50.202
Total		5068227	107061	100.000

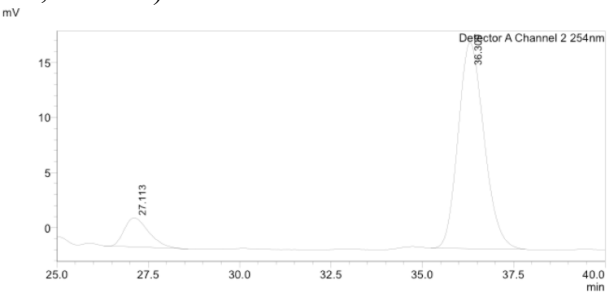

<Peak Table>
Detector A Channel 2 254nm

Peak#	Ret. Time	Area	Height	Area%
1	27.113	122807	2639	11.734
2	36.309	923773	18699	88.266
Total		1046580	21338	100.000

Peak #	Ret. Time	Area	Area %	Peak #	Ret. Time	Area	Area %
1	27.6 min	2523856	49.798	1	27.1 min	122807	11.734
2	36.9 min	2544370	50.202	2	36.3 in	923773	88.266

(*S*)-1-Chloro-2-(4-methoxyphenyl)pent-4-en-2-ol (2.15c): 33.5 mg, 0.0931 mmol, 93% yield, colorless oil. **IR (neat):** 3548 (br, w), 3476 (br, w), 3071 (w), 2837 (w), 1640 (w), 1610 (m), 1583 (s), 1246 (s), 1178 (m), 1031 (m), 830 (s), 801 (m), 572 (m), 546 (m) cm^{-1}; **^{1}H NMR (400 MHz, $CDCl_3$):** δ 7.35 (d, *J* = 8.8 Hz, 2H), 6.90 (d, *J* = 8.9 Hz, 2H), 5.62 (ddt, *J* = 17.3, 10.2, 7.2 Hz, 1H), 5.22–5.03 (m, 2H), 3.89–3.71 (m, 5H), 2.70 (dt, *J* = 7.3, 1.2 Hz, 2H), 2.56 (s, 1H); **^{13}C NMR (100 MHz, $CDCl_3$):** δ 159.0, 134.8, 132.7, 126.9, 119.7, 113.8, 75.2, 55.4, 54.1, 44.3; **HRMS (DART$^+$):** Calcd for $C_{12}H_{14}OCl$ $[M+H–H_2O]^+$: 209.0728, Found: 207.0715; **Specific Rotation:** $[\alpha]^{24}_D$ –12.5 (*c* 2.13, $CHCl_3$) for a 96.5:3.5 er sample. The enantiomeric purity of this compound was determined by HPLC analysis in comparison with authentic racemic material (Chiralpak AD-H, 98:2 hexanes:*i*-PrOH, 0.5 mL/min, 220 nm).

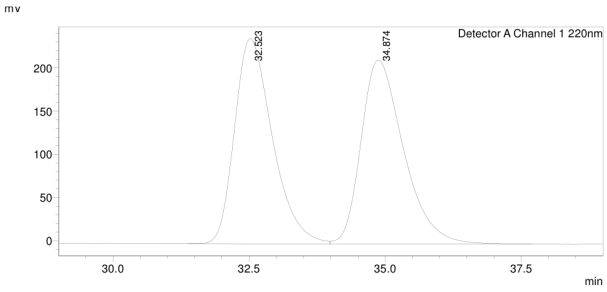

<Peak Table>
Detector A Channel 1 220nm

Peak#	Ret. Time	Area	Area%	Height
1	32.523	11482505	49.821	237381
2	34.874	11565179	50.179	212892
Total		23047683	100.000	450273

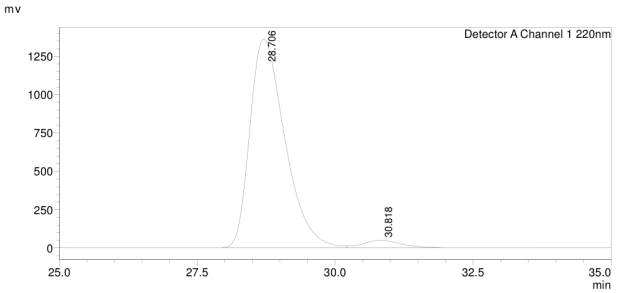

<Peak Table>
Detector A Channel 1 220nm

Peak#	Ret. Time	Area	Area%	Height
1	28.706	59951801	96.530	1360768
2	30.818	2154857	3.470	47899
Total		62106658	100.000	1408668

Peak #	Ret. Time	Area	Area %	Peak #	Ret. Time	Area	Area %
1	32.5 min	11482505	49.821	1	28.7 min	59951801	96.530
2	34.9 min	11565179	50.179	2	30.8 min	2154857	3.470

(*S*)-1-Bromo-2-(4-methoxyphenyl)pent-4-en-2-ol (2.16c): 19.2 mg, 0.0708 mmol, 71% yield, colorless oil. The analytical data are consistent with those reported previously.[165] **^{1}H NMR (400 MHz, $CDCl_3$):** δ 7.40 (dd, *J* = 9.0, 5.3 Hz, 2H), 7.05 (dd, *J* = 9.0, 8.5 Hz, 2H), 5.69–5.48 (m, 1H), 5.17–5.03 (m, 2H), 3.74 (d, *J* = 0.7 Hz, 3H), 2.72 (dt, *J* = 7.2, 1.2 Hz, 2H), 2.56 (s, 1H); **Specific Rotation:** $[\alpha]^{24}_D$ –30.0 (*c* 1.00, $CHCl_3$) for a 95.5:4.5 er sample. The enantiomeric purity was determined by HPLC analysis in comparison with authentic racemic material (Chiralpak OJ-H, 98:2 hexanes:*i*-PrOH, 0.5 mL/min, 254 nm).

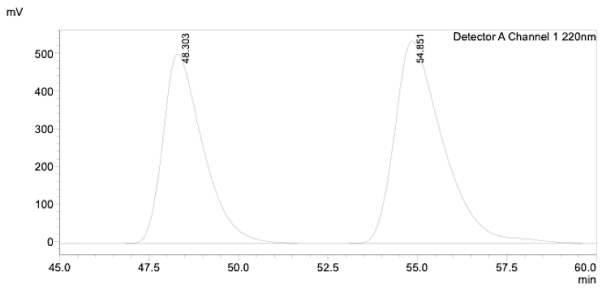

<Peak Table>
Detector A Channel 1 220nm

Peak#	Ret. Time	Area	Height	Area%
1	48.303	39099147	502180	43.721
2	54.851	50329197	536473	56.279
Total		89428344	1038653	100.000

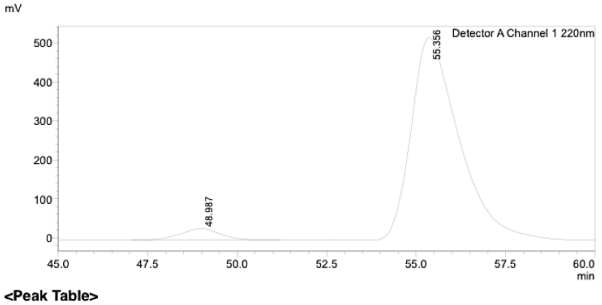

<Peak Table>
Detector A Channel 1 220nm

Peak#	Ret. Time	Area	Height	Area%
1	48.987	2265525	28984	4.473
2	55.356	48382388	519743	95.527
Total		50647913	548727	100.000

Peak #	Ret. Time	Area	Area %	Peak #	Ret. Time	Area	Area %
1	48.3 min	39099147	43.721	1	49.0 min	2265525	4.473
2	54.9 min	50329197	56.279	2	55.4 min	48382388	95.527

(*S*,*E*)-3-(Chloromethyl)-1-phenylhexa-1,5-dien-3-ol (2.15d): 16.2 mg, 0.0727 mmol, 73% yield, colorless oil. **IR (neat):** 3551 (br), 3027 (w), 2924 (w), 1640 (w), 1494 (m), 1335 (m), 1268 (m), 1028 (m), 970 (s), 921 (s), 746 (s), 693 (s) cm^{-1}; **^{1}H NMR (400 MHz, $CDCl_3$):** δ 7.43–7.38 (m, 2H), 7.37–7.30 (m, 2H), 7.29–7.21 (m, 1H), 6.76 (d, *J* = 16.0 Hz, 1H), 6.23 (d, *J* = 16.0 Hz, 1H), 5.97–5.61 (m, 1H), 5.35–5.03 (m, 2H), 3.65 (d, *J* = 2.1 Hz, 2H), 2.54 (dd, *J* = 7.4, 1.4 Hz, 2H), 2.34 (s, 1H); **^{13}C NMR (101 MHz,$CDCl_3$):** δ 136.6, 132.5, 131.1, 131.0, 128.8, 128.1, 126.8, 120.1, 74.3, 52.8, 43.5; **HRMS (DART$^+$):** Calcd for $C_{13}H_{16}ClO_3$ $[M+H]^+$: 255.0788, Found: 255.0784; **Specific Rotation:** $[\alpha]^{24}_D$ –2.3 (*c* 1.44, $CHCl_3$) for a 96:4 er sample. The enantiomeric purity of this compound was determined by HPLC analysis in comparison with authentic racemic material (Chiralcel OJ-H, 98:2 hexanes:*i*-PrOH, 0.5 mL/min, 220 nm).

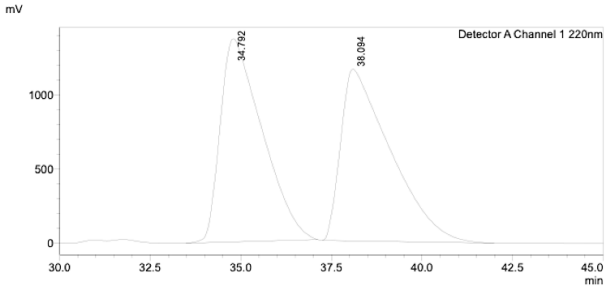

<Peak Table>
Detector A Channel 1 220nm

Peak#	Ret. Time	Area	Height	Area%
1	34.792	110457651	1373429	49.862
2	38.094	111070283	1162054	50.138
Total		221527935	2535484	100.000

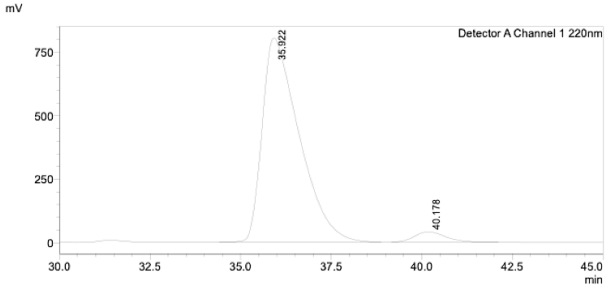

<Peak Table>
Detector A Channel 1 220nm

Peak#	Ret. Time	Area	Height	Area%
1	35.922	57191538	805079	95.842
2	40.178	2481401	41316	4.158
Total		59672939	846395	100.000

Peak #	Ret. Time	Area	Area %	Peak #	Ret. Time	Area	Area %
1	34.8 min	110457651	49.862	1	35.9 min	57191538	95.842
2	38.1 min	111070283	50.138	2	40.2 min	2481401	4.158

(*S*)-1-Chloro-2-(thiazol-2-yl)pent-4-en-2-ol (2.15e): 19.3 mg, 0.095 mmol, 95% yield, colorless oil. **IR (neat):** 3271 (br, w), 3083 (w), 1640 (w), 1477 (w), 1429 (w), 1287 (w), 1214 (m), 1179 (w), 1158 (w), 1124 (w), 1056 (w), 994 (w), 734 (s), 668 (m), 571 (w), 546 (w), 450 (w) cm^{-1}; **^{1}H NMR (400 MHz, $CDCl_3$):** δ 7.77 (d, *J* = 3.2 Hz, 2H), 7.32 (d, *J* = 3.2 Hz, 2H), 5.71 (dddd, *J* = 16.7, 10.6, 7.7, 6.8 Hz, 1H), 5.24–4.93 (m, 2H), 4.04 (d, *J* = 11.2 Hz, 1H), 3.89 (d, *J* = 11.2 Hz, 1H), 3.51 (s, 1H), 2.93–2.67 (m, 2H); **^{13}C NMR (100 MHz, $CDCl_3$):** δ 174.3, 142.8, 131.5, 120.4, 120.0, 76.7, 52.7, 44.2; **HRMS (DART$^+$):** Calcd for $C_8H_{11}ClSNO$ $[M+H–H_2O]^+$: 204.025; Found: 204.025. **Specific Rotation:** $[\alpha]^{24}_D$ –118.5 (*c* 1.32, $CHCl_3$) for a 90.5:9.5 er sample. The enantiomeric purity of this compound was determined by HPLC analysis in comparison with authentic racemic material (Chiralcel OD-H, 98:2 hexanes:*i*-PrOH, 0.5 mL/min, 220 nm).

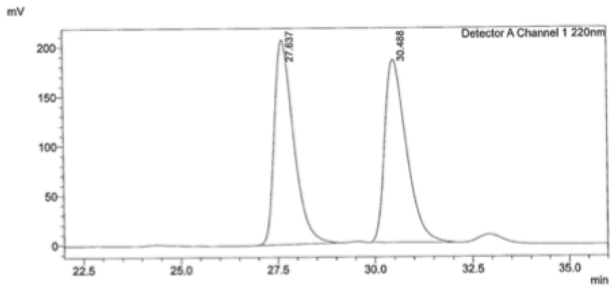

Detector A Channel 1 220nm

Peak#	Ret. Time	Area	Area%	Height
1	27.637	7209847	50.159	206636
2	30.488	7164157	49.841	184575
Total		14374004	100.000	391211

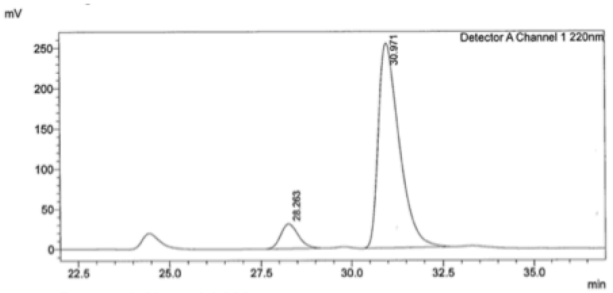

Detector A Channel 1 220nm

Peak#	Ret. Time	Area	Area%	Height
1	28.263	1041952	9.269	30712
2	30.971	10199765	90.731	254578
Total		11241717	100.000	285290

Peak #	Ret. Time	Area	Area %	Peak #	Ret. Time	Area	Area %
1	27.6 min	7209847	50.159	1	28.3 min	1041952	9.269
2	30.5 min	7164157	49.841	2	31.0 min	10199765	90.731

(*S*)-2-(Benzo[b]thiophen-2-yl)-1-chloropent-4-en-2-ol (2.15f): 21.2 mg, 0.084 mmol, 84% yield, colorless oil. **IR (neat):** 3530 (br, w), 3072 (w), 3057 (w), 2978 (w), 2913 (w), 1663 (w), 1639 (w), 1434 (w), 1332 (w), 1306 (w), 1249 (w), 1155 (w), 1110 (w), 1060 (w), 995 (w), 923 (w), 859 (w), 829 (w), 744 (s), 725 (m), 697 (w), 673 (w), 584 (w), 430 (w) cm^{-1}; **^{1}H NMR (400 MHz, $CDCl_3$):** δ 7.82 (dd, *J* = 7.9, 1.3 Hz, 1H), 7.77–7.69 (m, 1H), 7.34 (ddd, *J* = 9.2, 7.5, 1.4 Hz, 2H), 7.22 (s, 1H), 5.87–5.64 (m, 1H), 5.33–5.08 (m, 2H), 3.94–3.85 (m, 2H), 2.92 (s, 1H), 2.81 (dd, *J* = 7.3, 1.2 Hz, 2H); **^{13}C NMR (100 MHz, $CDCl_3$):** δ 148.2, 139.8, 139.6, 131.9, 124.5, 124.4, 123.7, 122.5, 121.0, 120.6, 75.2, 53.4, 44.8; **HRMS (DART$^+$):** Calcd for $C_{13}H_{12}ClS$ $[M+H–H_2O]^+$: 235.0348; Found: 235.0349; **Specific Rotation:** $[\alpha]^{24}_D$ –25.6 (*c* 0.91, $CHCl_3$) for a 95.5:4.5 er sample. The enantiomeric purity of this compound was determined by HPLC analysis in comparison with authentic racemic material (Chiralpak AS-H, 98:2 hexanes:*i*-PrOH, 0.5 mL/min, 220 nm).

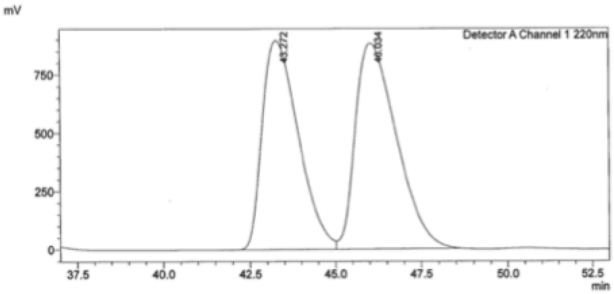

Detector A Channel 1 220nm

Peak#	Ret. Time	Area	Area%	Height
1	43.272	66076450	47.366	896542
2	46.034	73426570	52.634	882616
Total		139503020	100.000	1779158

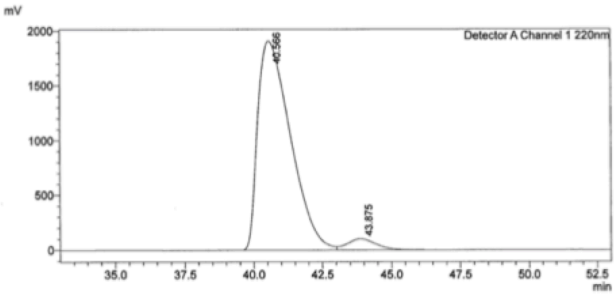

Detector A Channel 1 220nm

Peak#	Ret. Time	Area	Area%	Height
1	40.566	157875443	95.344	1908173
2	43.875	7709673	4.656	103118
Total		165585116	100.000	2011291

Peak #	Ret. Time	Area	Area %	Peak #	Ret. Time	Area	Area %
1	43.3 min	66076450	47.366	1	40.6 min	157875443	95.344
2	46.0 min	73426570	52.634	2	43.9 min	7709673	4.656

(*S*)-1-Bromo-2-cyclohexylpent-4-en-2-ol (2.16d): 20.8 mg, 0.0841 mmol, 81% yield, colorless oil. **IR (neat):** 3552 (br), 2927 (s), 2853 (s), 1710 (m), 1448 (m), 1229 (m), 998 (m), 894 (s), 840 (m), 768 (m), 635 (s), 517 (s) cm^{-1}; **^{1}H NMR (400 MHz, $CDCl_3$):** δ 5.94–5.74 (m, 1H), 5.22–5.06 (m, 2H), 3.63–3.44 (m, 1H), 2.49–2.31 (m, 2H), 2.20–1.92 (m, 1H), 1.80 (q, J = 7.1, 5.7 Hz, 4H), 1.72–1.53 (m, 2H), 1.25–1.15 (m, 1H), 1.15–1.04 (m, 2H); **^{13}C NMR (100 MHz, $CDCl_3$):** δ 133.2, 119.3, 74.2, 44.3, 42.6, 39.8, 27.3, 26.8, 26.8, 26.8, 26.5; **HRMS (DART$^+$):** Calcd for $C_{11}H_{23}BrON$ $[M+NH_4]^+$: 264.0963, Found: 264.0966; **Specific Rotation:** $[\alpha]^{24}_D$ –16.4 (*c* 1.26, $CHCl_3$) for a 95:5 er sample. The enantiomeric purity of this compound was determined by GLC analysis in comparison with authentic racemic material (Chiraldex CDB/DM, 15 psi, 110 °C): t_R: 15.1 (major) and 15.8 (minor).

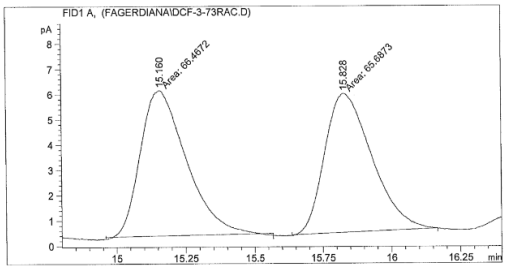

Peak #	RetTime [min]	Type	Width [min]	Area [pA*s]	Height [pA]	Area %
1	15.160	MM	0.1923	66.46724	5.76157	50.29510
2	15.828	MM	0.1990	65.68726	5.50119	49.70490

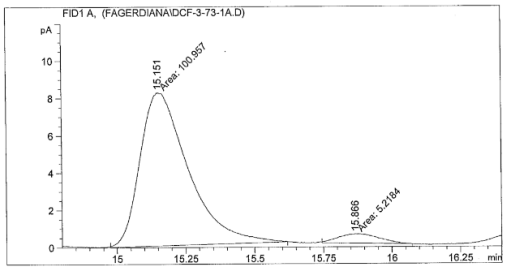

Peak #	RetTime [min]	Type	Width [min]	Area [pA*s]	Height [pA]	Area %
1	15.151	MM	0.2046	100.95725	8.22511	95.08513
2	15.866	MM	0.1723	5.21840	5.04747e-1	4.91487

Peak #	Ret. Time	Area	Area %	Peak #	Ret. Time	Area	Area %
1	15.1 min	66.46724	50.295	1	15.2 min	100.95725	95.085
2	15.8 min	65.68726	49.705	2	15.9 min	5.21840	4.915

(*R*)-2-(Bromomethyl)-1,1,1-trifluoropent-4-en-2-ol (2.16e): The title compound was synthesized analogous to **10a** and purified by silica gel chromatography to afford **14** (12.6 mg, 0.0540 mmol, 54% yield) as clear oil. **IR (neat):** 2921 (w), 2850 (m), 2590 (w), 2540 (s), 2339 (s), 2279 (m), 2224 (m), 2165 (w), 668 (m), 579 (s), 533 (m) cm^{-1}; **^{1}H NMR (400 MHz, $CDCl_3$):** δ 5.97–5.71 (m, 1H), 5.43–5.20 (m, 2H), 3.73–3.47 (m, 2H), 2.77–2.53 (m, 3H); **^{13}C NMR (101 MHz,$CDCl_3$):** δ 130.0, 124.8 (q, J = 287.2 Hz), 121.8, 73.7 (q, J = 27.4 Hz), 38.0, 34.0; **^{19}F NMR (376 MHz, $CDCl_3$):** δ –78.02 (s, 3F); **HRMS (DART$^+$):** Calcd for $C_6H_9OF_3Br$ $[M+H]^+$: 232.9783, Found: 232.9779; **Specific Rotation:** $[\alpha]^{24}_D$ –28.0 (*c* 1.25, $CHCl_3$) for a 98:2 er sample. The enantiomeric purity of this compound was determined by GLC analysis in comparison with authentic racemic material (Chiraldex CDB/DM, 15 psi, 70 °C).

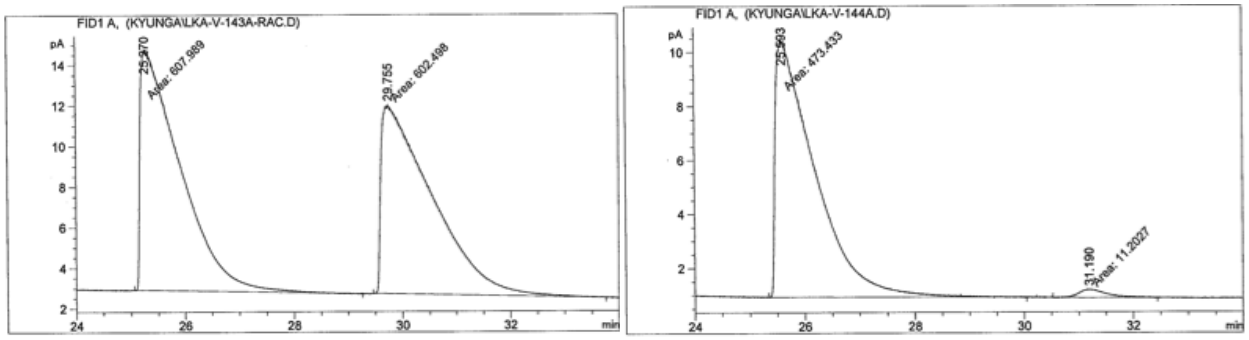

Peak #	RetTime [min]	Type	Width [min]	Area [pA*s]	Height [pA]	Area %
1	25.270	MM	0.8515	607.98859	11.89974	50.22679
2	29.755	MM	1.0779	602.49811	9.31566	49.77321
Totals :				1210.48669	21.21541	

Peak #	RetTime [min]	Type	Width [min]	Area [pA*s]	Height [pA]	Area %
1	25.593	MM	0.8281	473.43323	9.52808	97.68844
2	31.190	MM	0.6077	11.20266	3.07251e-1	2.31156
Totals :				484.63589	9.83534	

Peak #	Ret. Time	Area	Area %	Peak #	Ret. Time	Area	Area %
1	25.3 min	607.98859	50.22679	1	25.6 min	473.43323	97.68844
2	29.8 min	602.49811	49.77321	2	31.2 min	11.20266	2.31157

(*S*)-1-Bromo-2-(thiophen-2-yl)pent-4-en-2-ol (2.16f): 22.5 mg, 0.0910 mmol, 91% yield, colorless oil. **IR (neat):** 3527 (br), 3072 (w), 2975 (w), 1638 (w), 1530 (m), 1228 (m), 995 (m), 877 (m), 830 (m), 749 (m), 696 (s), 531 (w) cm^{-1}; **^{1}H NMR (400 MHz, $CDCl_3$):** δ 7.56 (dd, *J* = 5.1, 1.3 Hz, 1H), 7.40–7.19 (m, 2H), 6.01 (dddd, *J* = 17.2, 10.2, 7.7, 6.8 Hz, 1H), 5.63–5.36 (m, 2H), 4.29–3.74 (m, 2H), 3.41–2.70 (m, 3H); **^{13}C NMR (100 MHz, $CDCl_3$):** δ 147.7, 132.2, 127.1, 125.02, 124.0, 120.4, 74.2, 45.6, 44.1; **HRMS (DART$^+$):** Calcd for $C_9H_{10}SBr$ $[M+H–H_2O]^+$: 228.9681, Found: 228.9673; **Specific Rotation:** $[\alpha]^{24}_D$ +6.8 (*c* 2.25, $CHCl_3$) for a >99:1 er sample. The enantiomeric purity of this compound was determined by HPLC analysis in comparison with authentic racemic material (Chiralpak AZ-H, 98:2 hexanes:*i*-PrOH, 0.5 mL/min, 220 nm).

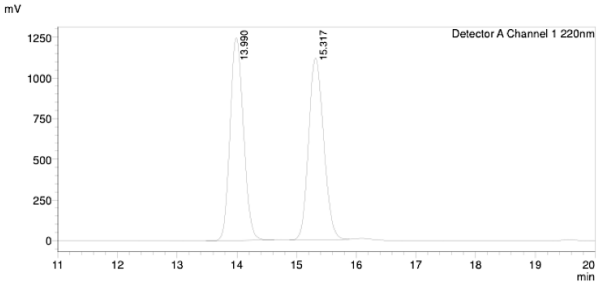

<Peak Table>
Detector A Channel 1 220nm

Peak#	Ret. Time	Area	Area%	Height
1	13.990	19400143	49.731	1243964
2	15.317	19610381	50.269	1116494
Total		39010524	100.000	2360458

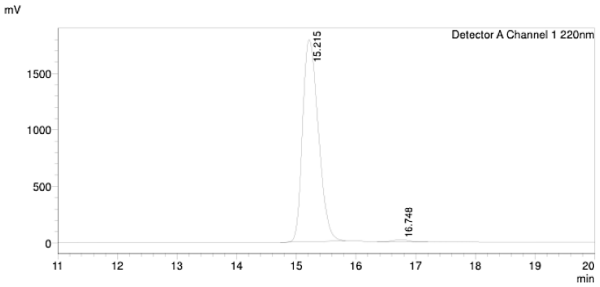

<Peak Table>
Detector A Channel 1 220nm

Peak#	Ret. Time	Area	Area%	Height
1	15.215	32864753	99.110	1787395
2	16.748	294959	0.890	17743
Total		33159712	100.000	1805138

Peak #	Ret. Time	Area	Area %	Peak #	Ret. Time	Area	Area %
1	14.0 min	19400143	49.731	1	15.2 min	32864753	99.110
2	15.3 min	19610381	50.269	2	16.7 min	294959	0.890

(*S*)-2-Allyl-2-(4-fluorophenyl)oxirane (2.17b): The title compound was synthesized analogous to **12a** and purified by silica gel chromatography to afford **12p.** The analytical data are fully consistent with those reported previously. The enantiomeric purity was determined by HPLC analysis in comparison with authentic racemic material.

From X = Cl: Colorless oil (11.9 mg, 0.0670 mmol, 67% yield). **Specific Rotation:** $[\alpha]^{24}_{D}$ +26.3 (*c* 0.86, $CHCl_3$ for a 95:4 er sample. The enantiomeric purity was determined by HPLC analysis in comparison with authentic racemic material (Chiralpak OJ-H, 99:1 hexanes:*i*-PrOH, 0.5 mL/min, 220 nm).

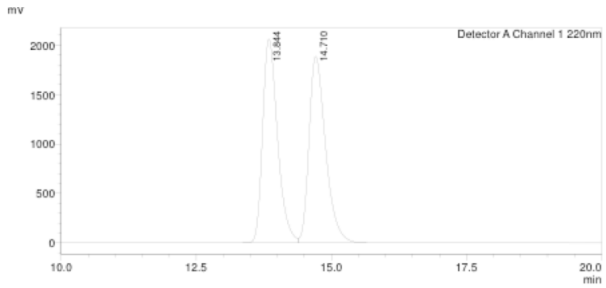

<Peak Table>
Detector A Channel 1 220nm

Peak#	Ret. Time	Area	Area%	Height
1	13.844	39545761	49.631	2057429
2	14.710	40133281	50.369	1881961
Total		79679042	100.000	3939390

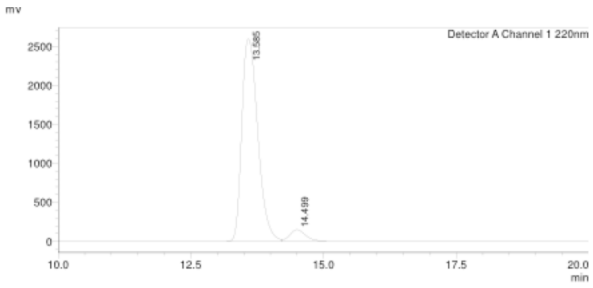

<Peak Table>
Detector A Channel 1 220nm

Peak#	Ret. Time	Area	Area%	Height
1	13.585	54161340	94.815	2593954
2	14.499	2961949	5.185	147113
Total		57123289	100.000	2741067

Peak #	Ret. Time	Area	Area %	Peak #	Ret. Time	Area	Area %
1	13.8 min	39545761	49.631	1	13.6 min	54161340	94.815
2	14.7 min	40133281	50.369	2	14.5 min	2961949	5.185

From X = Br: Colorless oil (4.4 mg, 0.0247 mmol, 56% yield). **Specific Rotation:** $[\alpha]^{24}_{D}$ +1.5 (*c* 2.12, $CHCl_3$ for a 96:4 er sample. The enantiomeric purity was determined by HPLC analysis in comparison with authentic racemic material (Chiralpak OJ-H, 98:2 hexanes:*i*-PrOH, 0.5 mL/min, 220 nm).

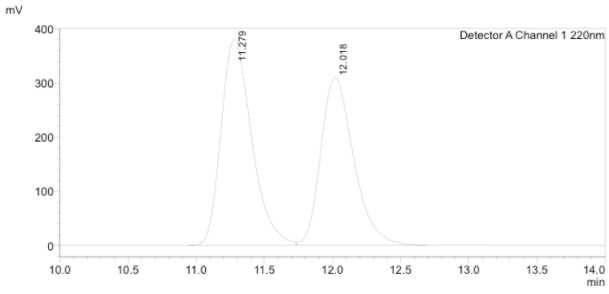

<Peak Table>
Detector A Channel 1 220nm

Peak#	Ret. Time	Area	Height	Area%
1	11.279	5956238	379752	53.425
2	12.018	5192644	310186	46.575
Total		11148882	689938	100.000

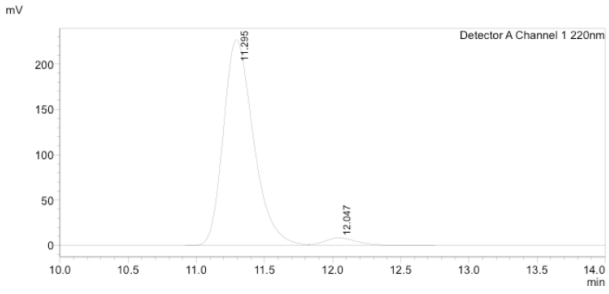

<Peak Table>
Detector A Channel 1 220nm

Peak#	Ret. Time	Area	Height	Area%
1	11.295	3495946	226749	96.063
2	12.047	143278	8592	3.937
Total		3639224	235342	100.000

Peak #	Ret. Time	Area	Area %	Peak #	Ret. Time	Area	Area %
1	11.3 min	5956238	53.425	1	11.295	3495946	96.063
2	12.0 min	5192644	46.575	2	12.0 min	143278	3.937

(*S*)-2-Allyl-2-(4-chlorophenyl)oxirane (2.17c): The title compound was synthesized analogous to **12a** and purified by silica gel chromatography to afford **12q** (16.5 mg, 0.0848 mmol, 85% yield) as colorless oil. The analytical data are fully consistent with those reported previously.[165] **Specific Rotation:** $[\alpha]^{24}_{D}$ +10.2 (*c* 1.24, $CHCl_3$) for a 96:4 er sample. The enantiomeric purity was determined by HPLC analysis in comparison with authentic racemic material (Chiralpak OJ-H, 99.5:0.5 hexanes:*i*-PrOH, 0.1 mL/min, 220 nm).

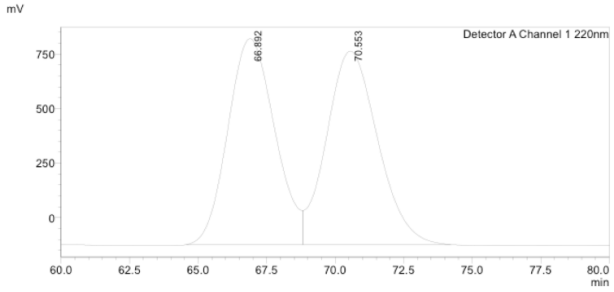

<Peak Table>
Detector A Channel 1 220nm

Peak#	Ret. Time	Area	Height	Area%
1	66.892	112348999	943549	49.301
2	70.553	115533704	886386	50.699
Total		227882703	1829934	100.000

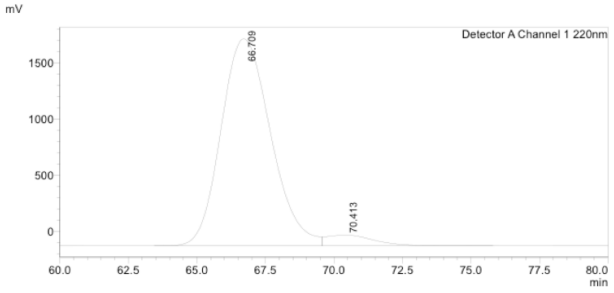

<Peak Table>
Detector A Channel 1 220nm

Peak#	Ret. Time	Area	Height	Area%
1	66.709	232117048	1842372	95.383
2	70.413	11235329	94960	4.617
Total		243352377	1937333	100.000

Peak #	Ret. Time	Area	Area %	Peak #	Ret. Time	Area	Area %
1	66.9 min	112348999	49.301	1	66.7 min	232117048	95.383
2	70.6 min	115533704	50.699	2	70.413 min	11235329	4.617

(*S*)-2-Allyl-2-(4-bromophenyl)oxirane (2.17d): The title compound was synthesized analogous to **12a** and purified by silica gel chromatography to afford **12e.** The analytical data are consistent with those reported previously.[167] **^{1}H NMR (400 MHz, $CDCl_3$):** δ7.49–7.43 (m, 2H), 7.26–7.20 (m, 2H), 5.86–5.60 (m, 1H), 5.19–5.03 (m, 2H), 3.00 (d, *J* = 5.3 Hz, 1H), 2.94–2.79 (m, 1H), 2.72 (d, *J* = 5.3 Hz, 1H), 2.68–2.51 (m, 1H).

From X = Cl: 21.6 mg, 0.0903 mmol, 90% yield, colorless oil. **Specific Rotation:** $[\alpha]^{24}_{D}$ +28.0 (*c* 1.07, $CHCl_3$) for a 95:5 er sample. The enantiomeric purity was determined by HPLC analysis in comparison with authentic racemic material (Chiralcel OJ-H, 99:1 hexanes:*i*-PrOH, 0.5 mL/min, 220 nm).

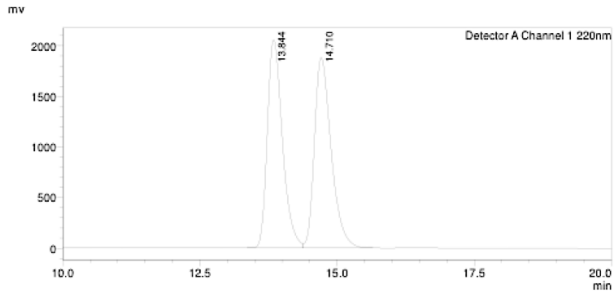

<Peak Table>
Detector A Channel 1 220nm

Peak#	Ret. Time	Area	Area%	Height
1	13.844	39545761	49.631	2057429
2	14.710	40133281	50.369	1881961
Total		79679042	100.000	3939390

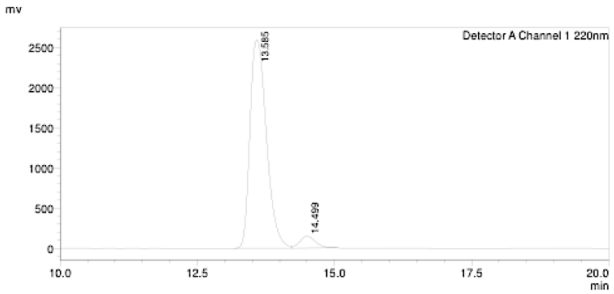

<Peak Table>
Detector A Channel 1 220nm

Peak#	Ret. Time	Area	Area%	Height
1	13.585	54161340	94.815	2593954
2	14.499	2961949	5.185	147113
Total		57123289	100.000	2741067

[167] Zhang, M.; Hu, Y.; Zhang, S. *Chem. Eur. J.* **2009**, *15*, 10732–10735.

Peak #	Ret. Time	Area	Area %	Peak #	Ret. Time	Area	Area %
1	13.8 min	39545761	49.631	1	13.6 min	54161340	94.815
2	14.7 min	40133281	50.369	2	14.5 min	2961949	5.815

From X = Br: 10.3 mg, 0.0431 mmol, 66% yield, colorless oil. **Specific Rotation:** $[\alpha]^{24}_{D}$ +18.0 (*c* 0.77, $CHCl_3$) for a 96:4 er sample. The enantiomeric purity was determined by HPLC analysis in comparison with authentic racemic material (Chiralpak OJ-H, 98:2 hexanes:*i*-PrOH, 0.5 mL/min, 220 nm).

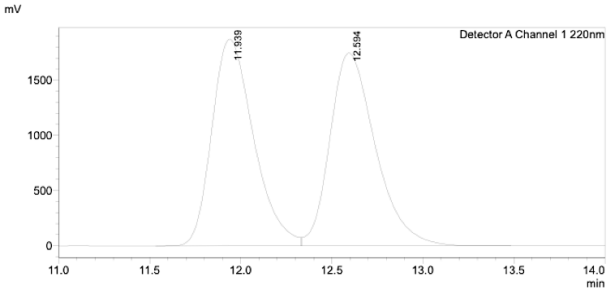

<Peak Table>
Detector A Channel 1 220nm

Peak#	Ret. Time	Area	Height	Area%
1	11.939	29935316	1873310	49.636
2	12.594	30374486	1748188	50.364
Total		60309802	3621498	100.000

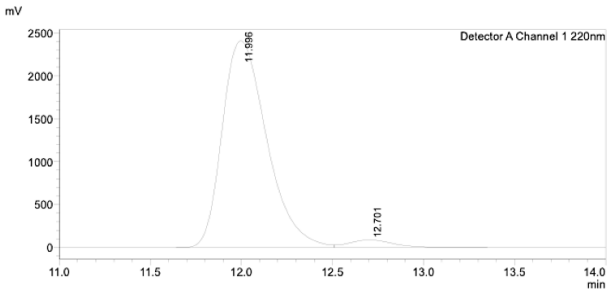

<Peak Table>
Detector A Channel 1 220nm

Peak#	Ret. Time	Area	Height	Area%
1	11.996	41067760	2409064	96.340
2	12.701	1560164	90422	3.660
Total		42627924	2499486	100.000

Peak #	Ret. Time	Area	Area %	Peak #	Ret. Time	Area	Area %
1	11.9 min	29935316	49.636	1	12.0 min	41067760	96.340
2	12.6 min	30374486	50.364	2	12.7 min	1560164	3.660

(*S*)-4-(2-Allyloxiran-2-yl) methyl benzoate (2.17e): 17.2 mg, 0.0788 mmol, 94% yield, colorless oil. **IR (neat):** 2952 (w), 2923 (w), 2852 (w), 1720 (s), 1435 (m), 1275 (s), 1111 (m), 1018 (w), 918 (w), 854 (w), 771 (m), 731 (m) cm^{-1}; **^{1}H NMR (400 MHz, $CDCl_3$):** δ 8.11–7.90 (m, 2H), 7.55–7.34 (m, 2H), 5.76 (ddddd, *J* = 17.4, 10.3, 7.2, 6.6, 0.6 Hz, 1H), 5.25–4.96 (m, 2H), 3.91 (t, *J* = 0.7 Hz, 3H), 3.04 (dd, *J* = 5.4, 0.6 Hz, 1H), 2.93 (ddt, *J* = 15.0, 6.6, 1.5 Hz, 1H), 2.75 (d, *J* = 5.3 Hz, 1H), 2.64 (ddt, *J* = 15.1, 7.3, 1.3 Hz, 1H); **^{13}C NMR (100 MHz, $CDCl_3$):** δ 166.9, 147.9, 132.0, 129.7, 129.5, 125.8, 120.2, 75.7, 53.6, 52.3, 44.5; **HRMS (DART$^+$):** Calcd for $C_{13}H_{15}O_3$ $[M+H]^+$: 219.1021, Found: 219.1025; **Specific Rotation:** $[\alpha]^{24}_{D}$ +20.6 (*c* 1.38, $CHCl_3$) for a 93.5:6.5 er sample. The enantiomeric purity of this compound was determined by HPLC analysis in comparison with authentic racemic material (Chiralcel OJ-H, 98:2 hexanes:*i*-PrOH, 0.5 mL/min, 220 nm).

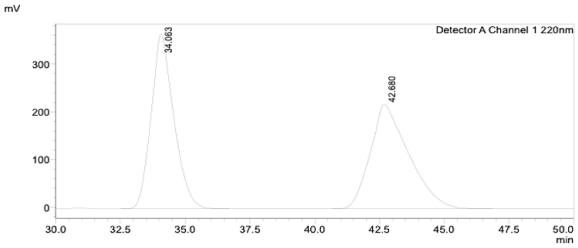

<Peak Table>
Detector A Channel 1 220nm

Peak#	Ret. Time	Area	Height	Area%
1	34.063	22200244	366135	49.691
2	42.680	22476387	218980	50.309
Total		44676631	585115	100.000

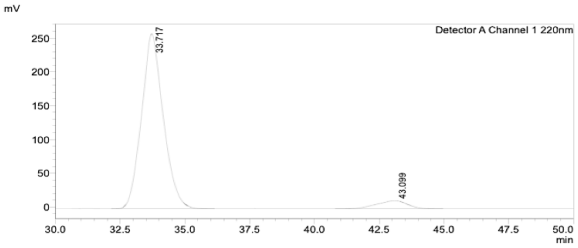

<Peak Table>
Detector A Channel 1 220nm

Peak#	Ret. Time	Area	Height	Area%
1	33.717	15152651	258931	93.721
2	43.099	1015219	12322	6.279
Total		16167870	271252	100.000

Peak #	Ret. Time	Area	Area %	Peak #	Ret. Time	Area	Area %
1	34.1 min	22200244	49.691	1	33.7 min	15152651	93.721
2	42.7 min	22476387	50.309	2	43.1 min	1015219	6.279

(*S*)-2-Allyl-2-(4-(trifluoromethoxy)phenyl)oxirane (2.17f): 17.7 mg, 0.0720 mmol, 72% yield, colorless oil. **IR (neat):** 3082 (w), 3052 (w), 2984 (w), 2913 (w), 1643 (w), 1511 (m), 1253 (s), 1157 (s), 1056 (m), 1018 (m), 847 (m), 557 (m) cm^{-1}; **^{1}H NMR (400 MHz, $CDCl_3$):** δ 7.53–7.31 (m, 2H), 7.22–7.07 (m, 2H), 6.03–5.48 (m, 1H), 5.31–4.98 (m, 2H), 3.02 (dt, *J* = 5.2, 1.2 Hz, 1H), 2.88 (dddt, *J* = 15.0, 6.5, 2.7, 1.4 Hz, 1H), 2.74 (dt, *J* = 5.3, 1.2 Hz, 1H), 2.70–2.54 (m, 1H); **^{13}C NMR (100 MHz, $CDCl_3$):** δ 148.7, 138.9, 132.5, 127.6, 120.9, 120.6 (d, *J* = 257.2 Hz), 119.0, 59.0, 55.0, 39.6; **^{19}F NMR (376 MHz, $CDCl_3$):** –92.01 (s, 3F); **HRMS (DART$^+$):** Calcd for $C_{15}H_{11}F_3O_2$ $[M]^+$: 245.0781, Found: 245.0789; **Specific Rotation:** $[\alpha]^{24}_D$ –63.8 (*c* 0.27, $CHCl_3$) for a 96:4 er sample. The enantiomeric purity of this compound was determined by HPLC analysis in comparison with authentic racemic material (Chiralcel OJ-H, 100:0 hexanes:*i*-PrOH, 0.5 mL/min, 220 nm).

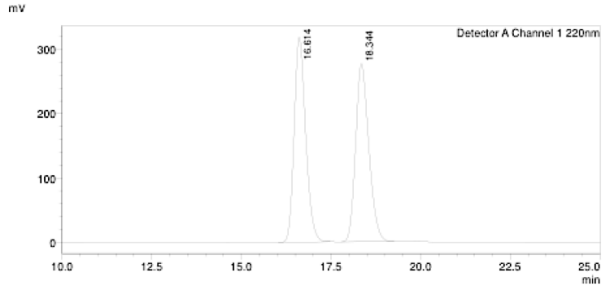

<Peak Table>
Detector A Channel 1 220nm

Peak#	Ret. Time	Area	Area%	Height
1	16.614	7108944	50.098	318605
2	18.344	7081145	49.902	276862
Total		14190089	100.000	595467

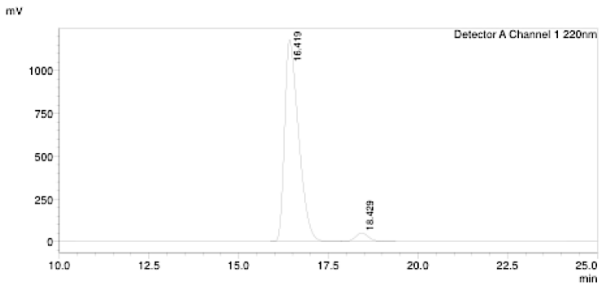

<Peak Table>
Detector A Channel 1 220nm

Peak#	Ret. Time	Area	Area%	Height
1	16.419	32072796	96.196	1182505
2	18.429	1268361	3.804	50167
Total		33341158	100.000	1232672

Peak #	Ret. Time	Area	Area %	Peak #	Ret. Time	Area	Area %
1	16.6 min	7108944	50.098	1	16.4 min	32072796	96.196
2	18.3 min	7081145	49.902	2	18.4 min	1268361	3.804

(*S*)-2-Allyl-2-(4-nitrophenyl)oxirane (2.17g): The title compound was synthesized analogous to **2.17a** and purified by silica gel chromatography to afford **2.17b**. The analytical data are consistent with those reported previously.[165] **^{1}H NMR (400 MHz, $CDCl_3$):** δ 8.25–8.13 (m, 2H), 7.60–7.48

(m, 2H), 5.84–5.61 (m, 1H), 5.22–5.05 (m, 2H), 3.08 (dd, *J* = 5.2, 1.1 Hz, 1H), 2.96 (ddt, *J* = 15.1, 6.6, 1.4 Hz, 1H), 2.75 (d, *J* = 5.2 Hz, 1H), 2.65 (ddt, *J* = 15.1, 7.1, 1.3 Hz, 1H).

From X = Cl: 17.9 mg, 0.0872 mmol, 87% yield, colorless oil. **Specific Rotation:** $[\alpha]^{24}_{D}$ +22.8 (*c* 0.41, $CHCl_3$) for a 94:6 er sample. The enantiomeric purity was determined by HPLC analysis in comparison with authentic racemic material (Chiralcel OJ-H, 98:2 hexanes:*i*-PrOH, 0.5 mL/min, 220 nm).

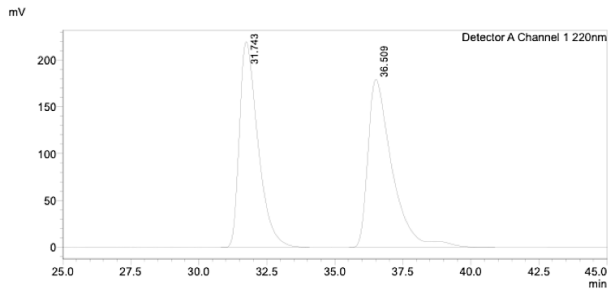

<Peak Table>
Detector A Channel 1 220nm

Peak#	Ret. Time	Area	Height	Area%
1	31.743	10406581	219601	48.493
2	36.509	11053176	179562	51.507
Total		21459757	399163	100.000

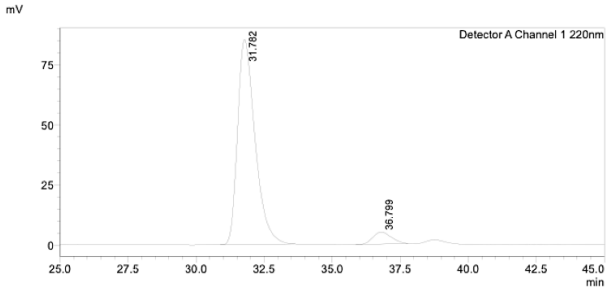

<Peak Table>
Detector A Channel 1 220nm

Peak#	Ret. Time	Area	Height	Area%
1	31.782	3829680	85353	94.127
2	36.799	238958	5016	5.873
Total		4068638	90369	100.000

Peak #	Ret. Time	Area	Area %	Peak #	Ret. Time	Area	Area %
1	31.7 min	10406581	48.493	1	31.8 min	3829680	94.127
2	36.5 min	11053176	51.507	2	36.8 min	238958	5.873

From X = Br: 15.8 mg, 0.770 mmol, 77% yield, colorless oil. **Specific Rotation:** $[\alpha]^{24}_{D}$ +42.4 (*c* 2.46, $CHCl_3$) for a 95:5 er sample. The enantiomeric purity was determined by HPLC analysis in comparison with authentic racemic material (Chiralcel OJ-H, 98:2 hexanes:*i*-PrOH, 0.5 mL/min, 220 nm).

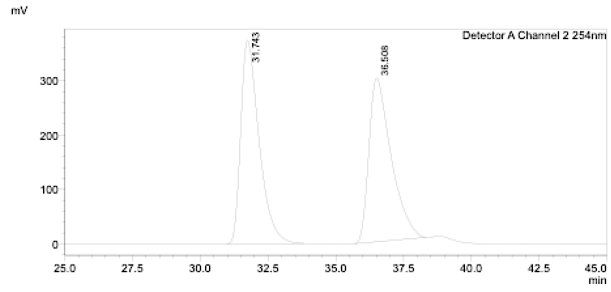

<Peak Table>
Detector A Channel 2 254nm

Peak#	Ret. Time	Area	Height	Area%
1	31.743	17539823	373935	50.495
2	36.508	17195609	300564	49.505
Total		34735432	674499	100.000

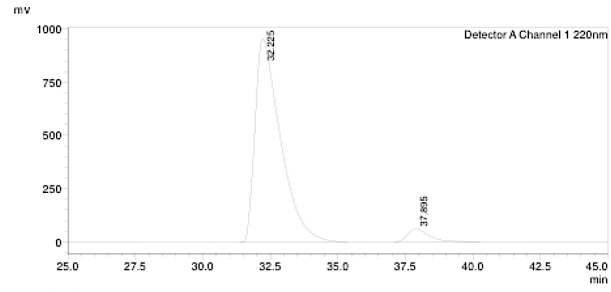

<Peak Table>
Detector A Channel 1 220nm

Peak#	Ret. Time	Area	Height	Area%
1	32.225	62804575	955756	94.789
2	37.895	3452605	61407	5.211
Total		66257180	1017162	100.000

Peak #	Ret. Time	Area	Area %	Peak #	Ret. Time	Area	Area %
1	31.7 min	17539823	50.495	1	32.2 min	62804575	94.789
2	36.5 min	17195609	49.505	2	37.9 min	61407	5.211

(*S*)-2-Allyl-2-(3-nitrophenyl)oxirane (2.17h): 16.3 mg, 0.0794 mmol, 79% yield, colorless oil. **IR (neat):** 3079 (w), 2981 (w), 2915 (w), 1729 (w), 1642 (w), 1526 (s), 1482 (w), 1433 (w), 1347

(s), 1311 (w), 1101 (w), 998 (w), 921 (m), 887 (w), 842 (w), 736 (m), 633 (w) cm^{-1}; **^{1}H NMR (400 MHz, $CDCl_3$):** δ 8.24 (t, *J* = 2.0 Hz, 1H), 8.13 (ddd, *J* = 8.1, 2.2, 1.0 Hz, 1H), 7.71 (ddd, *J* = 7.8, 1.8, 1.0 Hz, 1H), 7.52 (t, *J* = 8.0 Hz, 1H), 5.93–5.59 (m, 1H), 5.29–5.03 (m, 2H), 3.07 (dd, *J* = 5.2, 0.7 Hz, 1H), 2.94 (ddd, *J* = 15.1, 6.7, 1.4 Hz, 1H), 2.76 (d, *J* = 5.1 Hz, 1H), 2.67 (ddd, *J* = 15.1, 7.1, 1.2 Hz, 1H); **^{13}C NMR (100 MHz, $CDCl_3$):** δ 148.5, 142.5, 132.2, 132.0, 129.5, 122.7, 121.3, 119.5, 58.8, 55.1, 39.2; **HRMS (DART$^+$):** Calcd for $C_{11}H_{12}N_1O_3$ $[M+H]^+$: 206.0817; Found: 206.0821; **Specific Rotation:** $[\alpha]^{24}_D$ +18.1 (*c* 1.38, $CHCl_3$) for a 98:2 er sample. The enantiomeric purity of this compound was determined by HPLC analysis in comparison with authentic racemic material (Chiralcel OJ-H, 98:2 hexanes:*i*-PrOH, 0.5 mL/min, 220 nm): t_R: 32 min (major) and 35 min (minor).

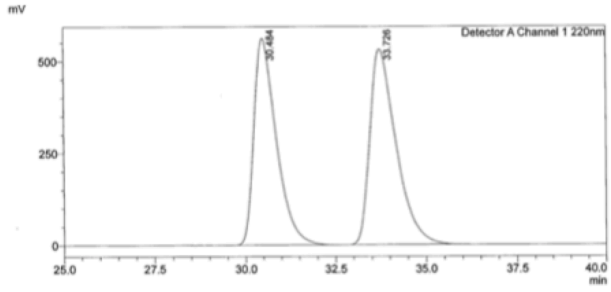

Detector A Channel 1 220nm

Peak#	Ret. Time	Area	Area%	Height
1	30.484	24724533	47.962	561518
2	33.726	26825644	52.038	531082
Total		51550177	100.000	1092600

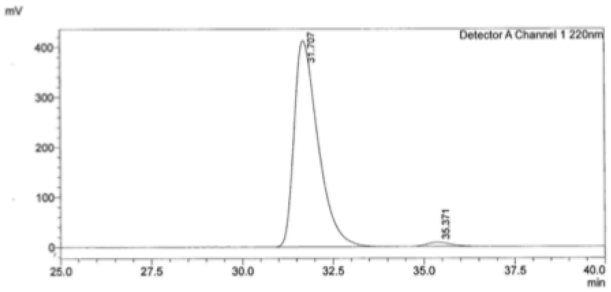

Detector A Channel 1 220nm

Peak#	Ret. Time	Area	Area%	Height
1	31.707	18953888	97.944	412523
2	35.371	397835	2.056	8475
Total		19351723	100.000	420997

Peak #	Ret. Time	Area	Area %	Peak #	Ret. Time	Area	Area %
1	30.5 min	24724533	47.962	1	31.7 min	18953888	97.944
2	33.7 min	26825644	52.038	2	35.4 min	397835	2.056

(*S*)-2-Allyl-2-(3-bromophenyl)oxirane (2.17i): 12.7 mg, 0.0531 mmol, 53% yield, colorless oil. The analytical data are consistent with those reported previously.[165] **^{1}H NMR (400 MHz, $CDCl_3$):** δ 7.53–7.52 (m, 1H), 7.41 (ddd, *J* = 7.9, 2.0, 1.1 Hz, 1H), 7.31 (ddd, *J* = 7.8, 1.7, 1.1 Hz, 1H), 7.20 (td, *J* = 7.8, 0.4 Hz, 1H), 5.75 (dddd, *J* = 17.4, 10.2, 7.3, 6.5 Hz, 1H), 5.22–5.01 (m, 2H), 3.00 (d, *J* = 5.3 Hz, 1H), 2.88 (ddt, *J* = 15.0, 6.5, 1.5 Hz, 1H), 2.73 (dd, *J* = 5.3, 0.4 Hz, 1H), 2.61 (ddt, *J* = 15.1, 7.3, 1.3 Hz, 1H); **Specific Rotation:** $[\alpha]^{24}_D$ +11.5 (*c* 0.77, $CHCl_3$) for a 97:3 er sample. The enantiomeric purity was determined by HPLC analysis in comparison with authentic racemic material (Chiralpak AS-H, 99.5:0.5 hexanes:*i*-PrOH, 0.5 mL/min, 220 nm).

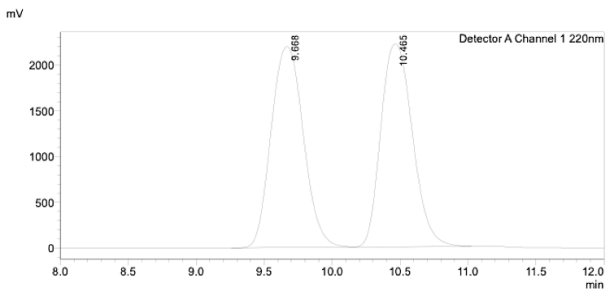

<Peak Table>
Detector A Channel 1 220nm

Peak#	Ret. Time	Area	Height	Area%
1	9.668	36275121	2197005	50.203
2	10.465	35981243	2223474	49.797
Total		72256364	4420480	100.000

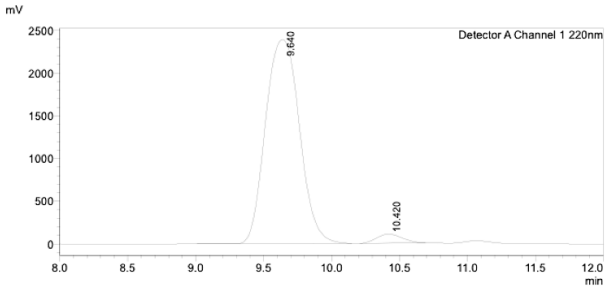

<Peak Table>
Detector A Channel 1 220nm

Peak#	Ret. Time	Area	Height	Area%
1	9.640	41540030	2386196	96.883
2	10.420	1336655	104940	3.117
Total		42876686	2491136	100.000

Peak #	Ret. Time	Area	Area %	Peak #	Ret. Time	Area	Area %
1	9.7 min	36275121	50.203	1	9.6 min	4150030	96.883
2	10.5 min	35981243	49.797	2	10.4 min	1336655	3.117

(*S*)-2-Allyl-2-(3,5-dibromophenyl)oxirane (2.17j): 25.3 mg, 0.0796 mmol, 80% yield, colorless oil. **IR (neat):** 2954 (m), 2923 (s), 2853 (m), 2034 (w), 1589 (m), 1461 (w), 1411 (w), 1260 (w), 921 (w), 856 (m), 740 (m), 686 (w) cm^{-1}; **^{1}H NMR (400 MHz, $CDCl_3$):** δ 7.57 (t, *J* = 1.8 Hz, 1H), 7.45 (d, *J* = 1.8 Hz, 2H), 5.72 (dddd, *J* = 17.0, 10.3, 7.3, 6.5 Hz, 1H), 5.18–5.06 (m, 2H), 2.99 (d, *J* = 5.3 Hz, 1H), 2.94–2.79 (m, 1H), 2.70 (d, *J* = 5.3 Hz, 1H), 2.64–2.52 (m, 1H); **^{13}C NMR (100 MHz, $CDCl_3$):** δ 144.4, 133.5, 132.0, 128.1, 123.2, 119.5, 58.6, 55.0, 39.2; **HRMS (DART$^+$):** Calcd for $C_{11}H_{11}OBr_2$ $[M+H]^+$: 316.9177, Found: 316.9186; **Specific Rotation:** $[\alpha]^{24}_D$ +0.9 (*c* 0.61, $CHCl_3$) for a >99:1 er sample. The enantiomeric purity of this compound was determined by HPLC analysis in comparison with authentic racemic material (Chiralcel OD-H, 100:0 hexanes:*i*-PrOH, 1.2 mL/min, 220 nm).

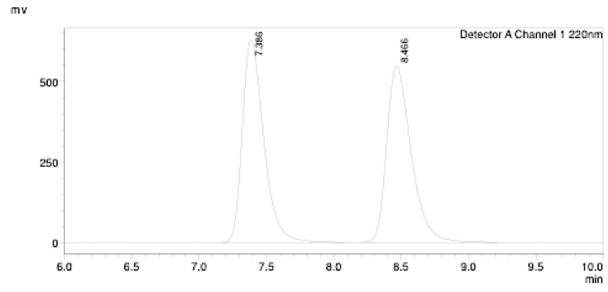

<Peak Table>
Detector A Channel 1 220nm

Peak#	Ret. Time	Area	Height	Area%
1	7.386	6946970	628459	50.165
2	8.466	6901173	546820	49.835
Total		13848142	1175279	100.000

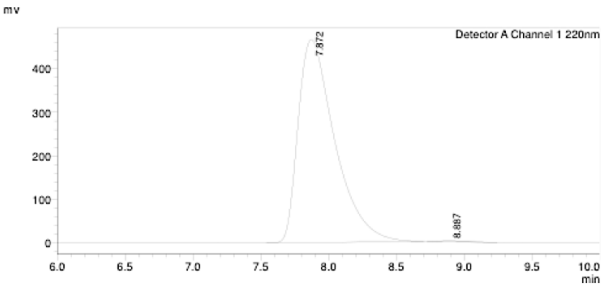

<Peak Table>
Detector A Channel 1 220nm

Peak#	Ret. Time	Area	Height	Area%
1	7.872	8760583	465805	99.631
2	8.887	32457	2228	0.369
Total		8793040	468033	100.000

Peak #	Ret. Time	Area	Area %	Peak #	Ret. Time	Area	Area %
1	7.4 min	6946970	50.165	1	7.4 min	8760583	99.631
2	8.5 min	6901173	49.835	2	8.6 min	32457	0.369

(*S*)-2-Allyl-2-(2-fluorophenyl)oxirane (2.17k): The title compound was synthesized analogous to **12a** and purified by silica gel chromatography to afford **12j. IR (neat):** 3080 (w), 2981 (w), 2914 (w), 1643 (w), 1618 (w), 1583 (w), 1491 (s), 1371 (m), 1220 (m), 920 (m), 758 (s), 568 (w)

cm^{-1}; **^{1}H NMR (400 MHz, $CDCl_3$):** δ 7.37 (td, *J* = 7.5, 1.8 Hz, 1H), 7.31–7.21 (m, 1H), 7.11 (tt, *J* = 7.5, 1.0 Hz, 1H), 7.02 (ddd, *J* = 10.3, 8.3, 1.1 Hz, 1H), 5.72 (ddt, *J* = 17.1, 10.2, 7.1 Hz, 1H), 5.10–4.97 (m, 2H), 3.01 (d, *J* = 5.2 Hz, 1H), 2.92–2.78 (m, 2H), 2.56 (dd, *J* = 14.6, 7.4 Hz, 1H); **^{13}C NMR (100 MHz, $CDCl_3$):** δ 160.4 (d, *J* = 246.4 Hz), 132.3, 129.6 (d, *J* = 8.0 Hz), 128.8 (d, *J* = 4.2 Hz), 127.5 (d, *J* = 14.6 Hz), 124.1 (d, *J* = 3.4 Hz), 118.8, 115.4 (d, *J* = 21.4 Hz), 61.9 (d, *J* = 835.4 Hz), 53.1 (d, *J* = 0.8 Hz), 40.5 (d, *J* = 2.3 Hz); **^{19}F NMR (376 MHz, $CDCl_3$):** δ –116.34 (dt, *J* = 12.1, 6.1 Hz, 1H); **HRMS (DART^{+}):** Calcd for $C_{11}H_{12}FO$ $[M+H]^+$: 179.0872, Found: 179.0870.

From X = Cl: 9.7 mg, 0.540 mmol, 67% yield, colorless oil. **Specific Rotation:** $[\alpha]^{24}_D$ +3.4 (*c* 0.62, $CHCl_3$) for a 94:6 er sample. The enantiomeric purity of this compound was determined by HPLC analysis in comparison with authentic racemic material (OJ-H, 98:2 hexanes:*i*-PrOH, 0.5 mL/min, 220 nm).

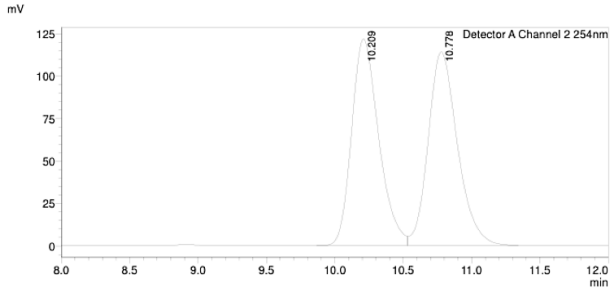

<Peak Table>
Detector A Channel 2 254nm

Peak#	Ret. Time	Area	Area%	Height
1	10.209	1679295	49.719	121682
2	10.778	1698268	50.281	114046
Total		3377563	100.000	235728

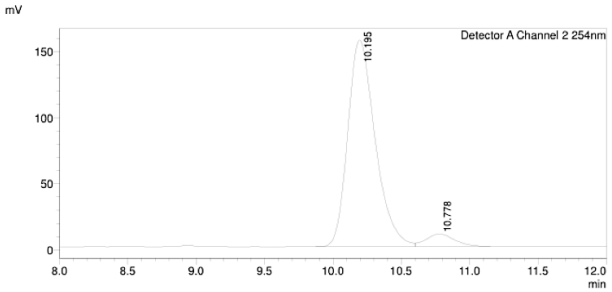

<Peak Table>
Detector A Channel 2 254nm

Peak#	Ret. Time	Area	Area%	Height
1	10.195	2180233	94.130	156307
2	10.778	135967	5.870	9409
Total		2316200	100.000	165716

Peak #	Ret. Time	Area	Area %	Peak #	Ret. Time	Area	Area %
1	10.2 min	1679295	49.719	1	10.2 min	2180233	94.103
2	10.8 min	1698268	50.281	2	10.8 min	135967	5.870

From X = Br: 12.9 mg, 0.0724 mmol, 72% yield, colorless oil. **Specific Rotation:** $[\alpha]^{24}_D$ +49.0 (*c* 0.34, $CHCl_3$) for a 91.5:8.5 er sample. The enantiomeric purity of this compound was determined by HPLC analysis in comparison with authentic racemic material (OD-H, 99.5:0.5 hexanes:*i*-PrOH, 0.1 mL/min, 220 nm).

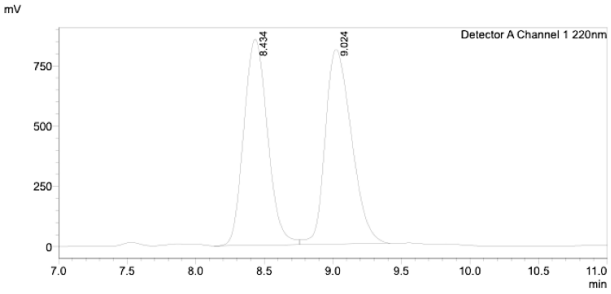

<Peak Table>
Detector A Channel 1 220nm

Peak#	Ret. Time	Area	Height	Area%
1	8.434	10326982	854422	48.931
2	9.024	10778260	807432	51.069
Total		21105242	1661855	100.000

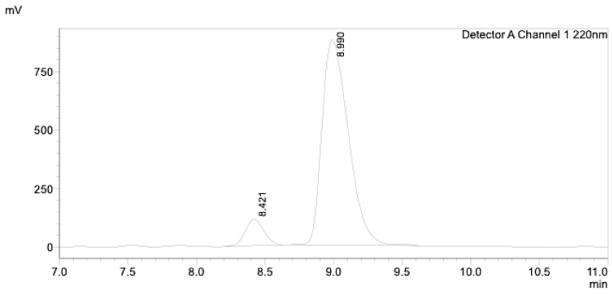

<Peak Table>
Detector A Channel 1 220nm

Peak#	Ret. Time	Area	Height	Area%
1	8.421	1075284	112083	8.389
2	8.990	11741829	876047	91.611
Total		12817113	988130	100.000

Peak #	Ret. Time	Area	Area %	Peak #	Ret. Time	Area	Area %
1	8.4 min	10326982	48.931	1	8.4 min	112083	8.389
2	9.0 min	10778260	51.069	2	9.0 min	11741829	91.611

(*S*)-2-Allyl-2-(2-(trifluoromethyl)phenyl)oxirane (2.17l): 3.50 mg, 0.0153 mmol, 52% yield, colorless oil. **IR (neat):** 2596 (m), 2924 (m), 2852 (w), 2167 (w), 1452 (w), 1316 (s), 1273 (m), 1174 (s), 1124 (s), 1037 (m), 929 (m), 769 (m) cm^{-1}; **^{1}H NMR (400 MHz, $CDCl_3$):** δ 7.65–7.58 (m, 2H), 7.56–7.50 (m, 1H), 7.41 (t, *J* = 7.7 Hz, 1H), 5.72 (ddt, *J* = 17.3, 10.3, 7.2 Hz, 1H), 5.17–4.91 (m, 2H), 3.10 (d, *J* = 4.9 Hz, 1H), 2.91 (d, *J* = 4.9 Hz, 1H), 2.84 (dd, *J* = 14.8, 7.1 Hz, 1H), 2.51 (dd, *J* = 14.8, 7.4 Hz, 1H); **^{13}C NMR (100 MHz, $CDCl_3$):** δ 138.6, 131.9 (d, *J* = 14.8 Hz), 130.1, 128.1, 127.3 (q, *J* = 31.5 Hz), 126.2 (q, *J* = 5.4 Hz), 124.5 (q, *J* = 273.7 Hz), 119.2, 59.8, 53.4 (q, *J* = 3.6 Hz), 41.2 (q, *J* = 2.0 Hz), 31.1; **^{19}F NMR (376 MHz, $CDCl_3$):** δ –58.18 (s, 3F); **HRMS (DART$^+$):** Calcd for $C_{12}H_{12}OF_3$ $[M+]^+$: 229.0840, Found: 229.0835; **Specific Rotation:** $[\alpha]^{24}_D$ +19.4 (*c* 0.15, $CHCl_3$) for a 98.5:1.5 er sample. The enantiomeric purity of this compound was determined by HPLC analysis in comparison with authentic racemic material (Chiralcel OD-H, 99.5:0.5 hexanes:*i*-PrOH, 1.2 mL/min, 254 nm).

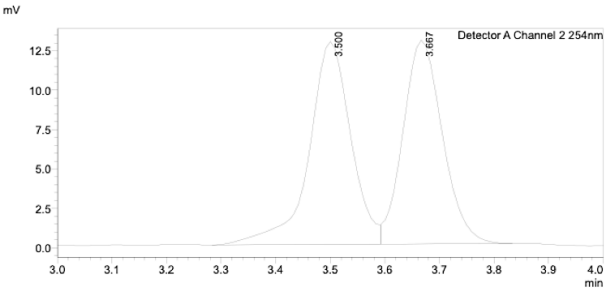

<Peak Table>
Detector A Channel 2 254nm

Peak#	Ret. Time	Area	Height	Area%
1	3.500	68835	12878	51.591
2	3.667	64589	12927	48.409
Total		133423	25805	100.000

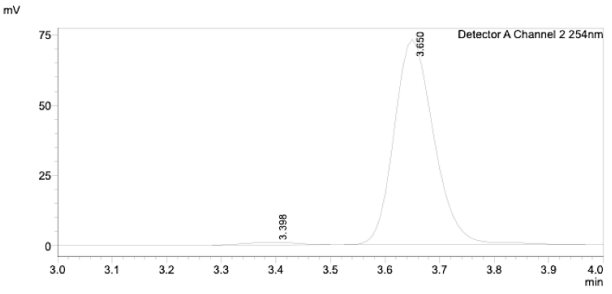

<Peak Table>
Detector A Channel 2 254nm

Peak#	Ret. Time	Area	Height	Area%
1	3.398	6250	976	1.660
2	3.650	370189	73094	98.340
Total		376439	74070	100.000

Peak #	Ret. Time	Area	Area %	Peak #	Ret. Time	Area	Area %
1	3.5 min	68835	51.591	1	3.4 min	6250	1.660
2	3.7 min	64589	48.409	2	3.7 min	370189	98.340

(*S*)-2-Allyl-2-(*o*-tolyl)oxirane (2.17m): 15.0 mg, 0.086 mmol, 86% yield, colorless oil. **IR (neat):** 3075 (w), 3056 (w), 3018 (w), 2981 (w), 2923 (w), 2164 (w), 2030 (w), 1643 (w), 1457 (w), 1432 (w), 1367 (w), 1285 (w), 1259 (w), 1039 (w), 997 (w), 966 (w), 918 (m), 862 (w), 795 (w), 762 (s), 729 (s), 700 (w), 623 (w), 562 (w), 455 (w), 633 (w) cm^{-1}; **^{1}H NMR (400 MHz, $CDCl_3$):** δ 7.31 (dd, *J* = 7.0, 1.9 Hz,1H), 7.24–7.06 (m, 3H), 5.89–5.63 (m, 1H), 5.11–4.99 (m, 2H), 3.03 (d, *J* = 5.3 Hz, 1H), 2.79 (d, *J* = 5.2 Hz, 1H), 2.73–2.64 (m, 1H), 2.56 (dd, *J* = 14.6, 7.7 Hz, 1H), 2.40 (s, 3H); **^{13}C NMR (100 MHz, $CDCl_3$):** δ 138.6, 135.5, 132.6, 130.2, 128.0, 127.7, 125.7, 118.6, 60.1, 52.7, 40.7, 19.3; **HRMS (DART$^+$):** Calcd for $C_{12}H_{15}O$ $[M+H]^+$: 175.1123; Found: 175.1125. **Specific Rotation:** $[\alpha]^{24}_D$ +232.9 (*c* 0.10, $CHCl_3$) for a >99:1 er sample. The enantiomeric purity of this compound was determined by HPLC analysis in comparison with authentic racemic material (Chiralpak AZ-H, 99:1 hexanes:*i*-PrOH, 0.5 mL/min, 254 nm).

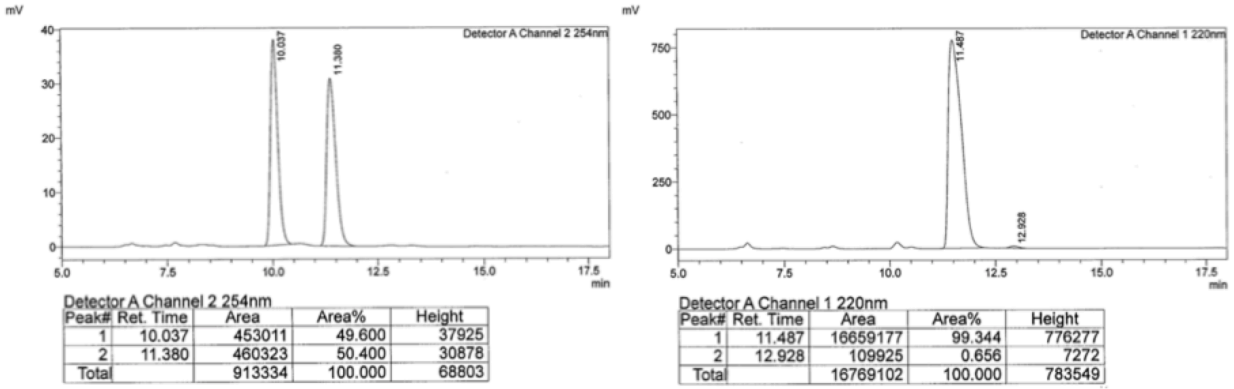

Detector A Channel 2 254nm

Peak#	Ret. Time	Area	Area%	Height
1	10.037	453011	49.600	37925
2	11.380	460323	50.400	30878
Total		913334	100.000	68803

Detector A Channel 1 220nm

Peak#	Ret. Time	Area	Area%	Height
1	11.487	16659177	99.344	776277
2	12.928	109925	0.656	7272
Total		16769102	100.000	783549

Peak #	Ret. Time	Area	Area %	Peak #	Ret. Time	Area	Area %
1	10.0 min	453011	49.600	1	11.5 min	16659177	99.344
2	11.4 min	460323	50.400	2	12.9 min	109925	0.656

(*S*)-2-Allyl-2-(naphthalen-2-yl)oxirane (2.17n): 12.8 mg, 0.0609 mmol, 88% yield, colorless oil. The analytical data are consistent with those reported previously.[165] **^{1}H NMR (400 MHz, $CDCl_3$):** δ 7.93–7.76 (m, 4H), 7.48 (ddd, *J* = 9.2, 3.9, 1.9 Hz, 3H), 5.93–5.72 (m, 1H), 5.24–5.03 (m, 2H), 3.08 (dt, *J* = 5.4, 1.0 Hz, 1H), 3.05–2.97 (m, 1H), 2.85 (dd, *J* = 5.3, 1.5 Hz, 1H), 2.74 (dd, *J* = 15.0, 7.3 Hz, 1H); **Specific Rotation:** $[\alpha]^{24}_D$ +15.7 (*c* 0.98, $CHCl_3$) for a 96.5:3.5 er sample. The enantiomeric purity was determined by HPLC analysis in comparison with authentic racemic material (Chiralcel OJ-H, 98:2 hexanes:*i*-PrOH, 0.5 mL/min, 254 nm).

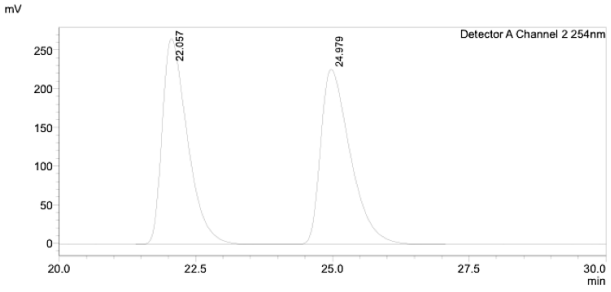

<Peak Table>
Detector A Channel 2 254nm

Peak#	Ret. Time	Area	Height	Area%
1	22.057	8552708	266002	50.094
2	24.979	8520772	226159	49.906
Total		17073480	492162	100.000

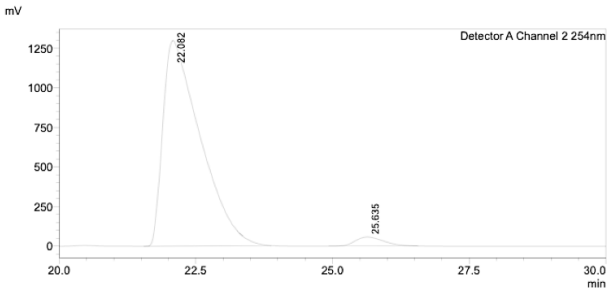

<Peak Table>
Detector A Channel 2 254nm

Peak#	Ret. Time	Area	Height	Area%
1	22.082	61920440	1297980	96.735
2	25.635	2089995	58092	3.265
Total		64010435	1356072	100.000

Peak #	Ret. Time	Area	Area %	Peak #	Ret. Time	Area	Area %
1	22.1 min	8552708	50.094	1	22.1 min	61920440	96.735
2	25.0 min	8520772	49.906	2	25.6 min	2089995	3.265

(*S*)-2-Allyl-2-(phenylethynyl)oxirane (2.17o): 10.6 mg, 0.0575 mmol, 76% yield, colorless oil. **IR (neat):** 2952 (m), 2922 (s), 2853 (m), 1491 (m), 1460 (m), 1444 (m), 1377 (w), 1360 (w), 918 (w), 818 (m), 733 (s), 690 (s) cm^{-1}; **^{1}H NMR (400 MHz, $CDCl_3$):** δ 7.52–7.37 (m, 2H), 7.37–7.27 (m, 3H), 5.92 (ddt, *J* = 17.2, 10.2, 7.0 Hz, 1H), 5.34–5.00 (m, 2H), 3.12 (dd, *J* = 5.6, 0.7 Hz, 1H), 2.90 (d, *J* = 5.5 Hz, 1H), 2.72–2.41 (m, 2H); **^{13}C NMR (100 MHz, $CDCl_3$):** δ 132.1, 132.1, 128.8, 128.4, 122.2, 119.0, 87.5, 83.5, 54.3, 50.6, 40.8; **HRMS (DART$^+$):** Calcd for $C_{13}H_{13}O$ $[M+H]^+$: 185.0966, Found: 185.0961; **Specific Rotation:** $[\alpha]^{24}_D$ +11.2 (*c* 0.36, $CHCl_3$) for a 98:2 er sample. The enantiomeric purity of this compound was determined by HPLC analysis in comparison with authentic racemic material (Chiralcel OD-H, 97:3 hexanes:*i*-PrOH, 0.3 mL/min, 220 nm).

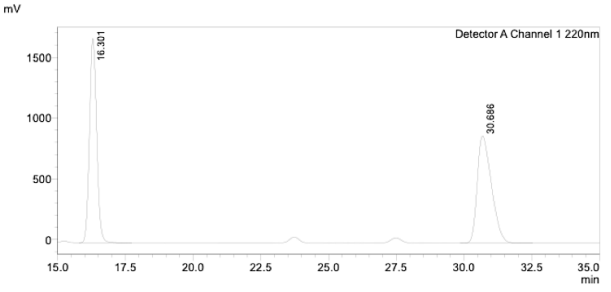

<Peak Table>
Detector A Channel 1 220nm

Peak#	Ret. Time	Area	Height	Area%
1	16.301	31060427	1680024	49.189
2	30.686	32084099	880938	50.811
Total		63144527	2560962	100.000

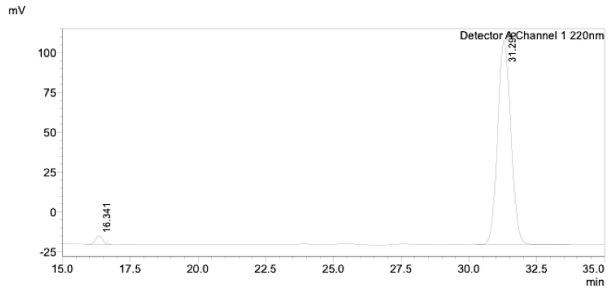

<Peak Table>
Detector A Channel 1 220nm

Peak#	Ret. Time	Area	Height	Area%
1	16.341	95503	5368	2.130
2	31.296	4388211	128627	97.870
Total		4483714	133995	100.000

Peak #	Ret. Time	Area	Area %	Peak #	Ret. Time	Area	Area %
1	16.3 min	31060427	49.189	1	16.3 min	95503	2.130
2	30.7 min	32084099	50.811	2	31.3 min	4388211	97.870

(*S*)-2-((3*S*,5*S*,7*S*)-Adamantan-1-yl)-2-allyloxirane (2.17p): The title compound was synthesized analogous to **12a** except **ap-4** (0.18 mg, 0.00025 mmol) was used. 17.9 mg, 0.082 mmol, 86% yield, colorless oil. **IR (neat):** 3075 (w), 3052 (w), 2902 (s), 2848 (m), 1640 (w), 1450 (m), 1357

(w),1344 (w), 1316 (w), 1211 (w), 1104 (w), 1054 (w), 982 (w), 912 (m), 810 (w), 758(w), 701 (w), 629 (w), 542 (w), 498 (w) cm^{-1}; **^{1}H NMR (400 MHz, $CDCl_3$):** δ 5.68 (dddd, *J* = 17.1, 10.2, 8.1, 6.1 Hz, 1H), 5.10–4.81 (m, 2H), 2.76 (d, *J* = 4.5 Hz, 1H), 2.59–2.35 (m, 3H), 1.99 (p, *J* = 3.2 Hz, 3H), 1.79–1.47 (m, 12H); **^{13}C NMR (100 MHz, $CDCl_3$):** δ 134.3, 117.6, 63.4, 47.3, 37.9, 37.1, 35.3, 34.1, 28.4; **HRMS (DART$^+$):** Calcd for $C_{15}H_{23}O$ $[M+H]^+$: 219.1749; Found: 219.1747; **Specific Rotation:** $[\alpha]^{24}_D$ +175.6 (*c* 1.08, $CHCl_3$) for a 89:11 er sample. The enantiomeric purity of this compound was determined by GLC analysis in comparison with authentic racemic material (Chiraldex CDB/DM, 15 psi, 100 °C).

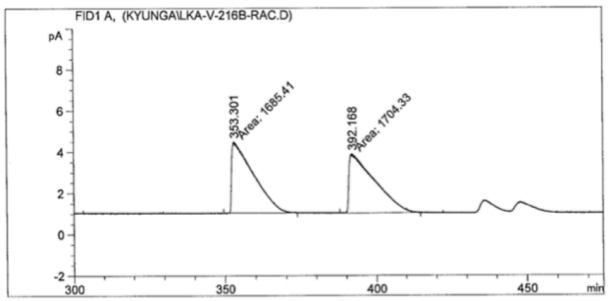

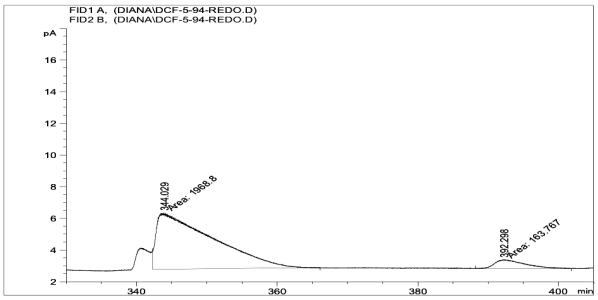

Peak #	RetTime [min]	Type	Width [min]	Area [pA*s]	Height [pA]	Area %
1	353.301	MM	8.1284	1685.41089	3.45582	49.72094
2	392.168	MM	9.8381	1704.32996	2.88730	50.27906
Totals :				3389.74084	6.34312	

Peak #	RetTime [min]	Type	Width [min]	Area [pA*s]	Height [pA]	Area %
1	344.029	FM	9.1748	1968.80310	3.57647	92.32069
2	392.298	MM	4.8256	163.76671	5.65614e-1	7.67931
Totals :				2132.56981	4.14209	

Peak #	Ret. Time	Area	Area %	Peak #	Ret. Time	Area	Area %
1	353 min	1685	49.721	1	344 min	1968	92.321
2	392 min	1704	50.279	2	392 min	163.8	7.679

(*S*)-2-(2-Methylallyl)-2-phenyloxirane (2.17q): The title compound was synthesized analogous to **12a** except 1.0 mol % of aminophenol was used. The title compound purified by silica gel chromatography to afford **12p** (11.3 mg, 0.065 mmol, 65% yield) as colorless oil. The analytical data are consistent with those reported previously.[168] **^{1}H NMR (400 MHz, $CDCl_3$):** δ 7.40–7.26 (m, 5H), 4.85–4.70 (m, 2H), 2.98 (d, *J* = 5.5 Hz, 1H), 2.89–2.82 (m, 1H), 2.78 (d, *J* = 5.5 Hz, 1H), 2.57 (d, *J* = 15.0 Hz, 1H), 1.74 (t, *J* = 1.1 Hz, 3H); **Specific Rotation:** $[\alpha]^{24}_D$ +8.5 (*c* 0.20, $CHCl_3$) for a 96.5:3.5 er sample. The enantiomeric purity of this compound was determined by HPLC analysis in comparison with authentic racemic material (Chiralcel OJ-H, 97:3 hexanes:*i*-PrOH, 0.5 mL/min, 254 nm).

[168] Capriati, V.; Florio, S.; Luisi, R.; Salomone, A. *Org. Lett.* **2002**, *4*, 2445–2448.

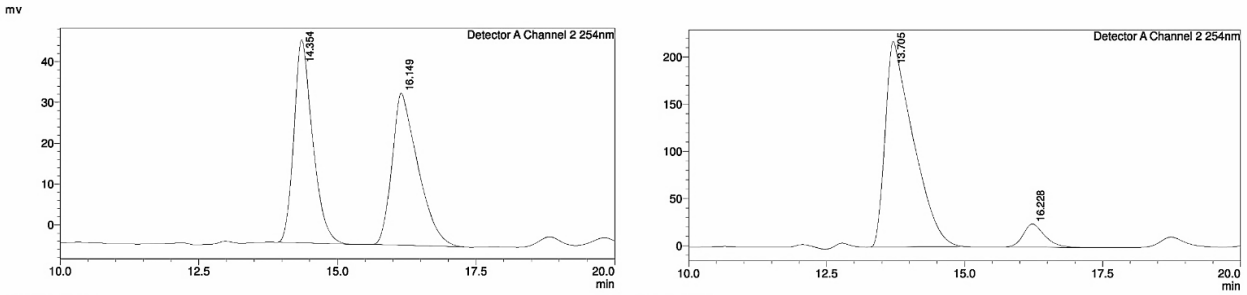

<Peak Table>
Detector A Channel 2 254nm

Peak#	Ret. Time	Area	Height	Area%
1	14.354	1168453	49711	49.149
2	16.149	1208915	37219	50.851
Total		2377368	86930	100.000

<Peak Table>
Detector A Channel 2 254nm

Peak#	Ret. Time	Area	Height	Area%
1	13.705	7662308	217896	92.101
2	16.228	657163	24398	7.899
Total		8319471	242293	100.000

Peak #	Ret. Time	Area	Area %	Peak #	Ret. Time	Area	Area %
1	14.4 min	1168453	49.149	1	13.7 min	217896	92.101
2	16.1 min	1209815	37219	2	16.2 min	657163	7.899

2.8.7. Formal Synthesis of Boscartin F

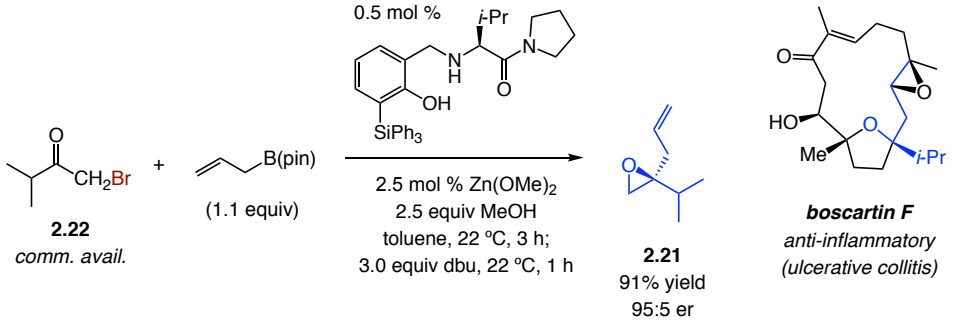

Gram-scale synthesis of (*S*)-2-Allyl-2-isopropyloxirane (2.21): In a N_2-filled glove box, **ap-5** (16.6 mg, 0.303 mmol, $Zn(OMe)_2$ (19.3 mg, 0.152 mmol), and toluene (30 mL) were added to an oven-dried round-bottom flask that contained a magnetic stir bar. Ketone (1.00g, 6.06 mmol), (pinacolato)allylboron (1.25 mL, 6.67 mmol), and MeOH (0.613 mL, 15.15 mmol) were added sequentially. The reaction vessel was sealed with a septum and then removed from the glove box; the mixture allowed to stir for 3 h at 22 °C. At this time, diazabicyclo[5.4.0]undec-7-ene (2.71 mL, 18.18 mmol) was added and the mixture allowed to stir at 22 °C for 2 h. The mixture was directly loaded onto a silica gel column and eluted with hexanes/Et_2O/EtOAc (100:0 hexanes/Et_2O–1:1 hexanes/Et_2O then 1:1 hexanes/EtOAc). The fractions containing **2.21**, as determined by tlc analysis, were combined to afford **2.21** as a solution in toluene, hexanes, Et_2O and EtOAc. Due to the volatility of this product, mass percent was used to determine percent yield based on careful analysis of the ^{1}H NMR spectrum (see Figure S1 for the details). **^{1}H NMR (400 MHz, toluene-d_8):** δ 5.81 (ddtd, J = 17.3, 10.2, 7.1, 1.0 Hz, 1H), 5.26–5.02 (m, 2H), 2.66 (s, 2H), 2.48 (dt, J = 7.1, 1.2 Hz, 2H), 1.90–1.72 (m, 1H), 1.06 (dd, J = 6.8, 0.9 Hz, 3H), 1.01 (dd, J = 7.0, 0.9 Hz, 3H); **^{13}C NMR (101 MHz, toluene-d_8):** δ 133.4, 117.8, 61.9, 50.0, 35.7, 32.3, 18.2, 17.8.

Figure S3. Determination of Percent Yield by Mass Percent

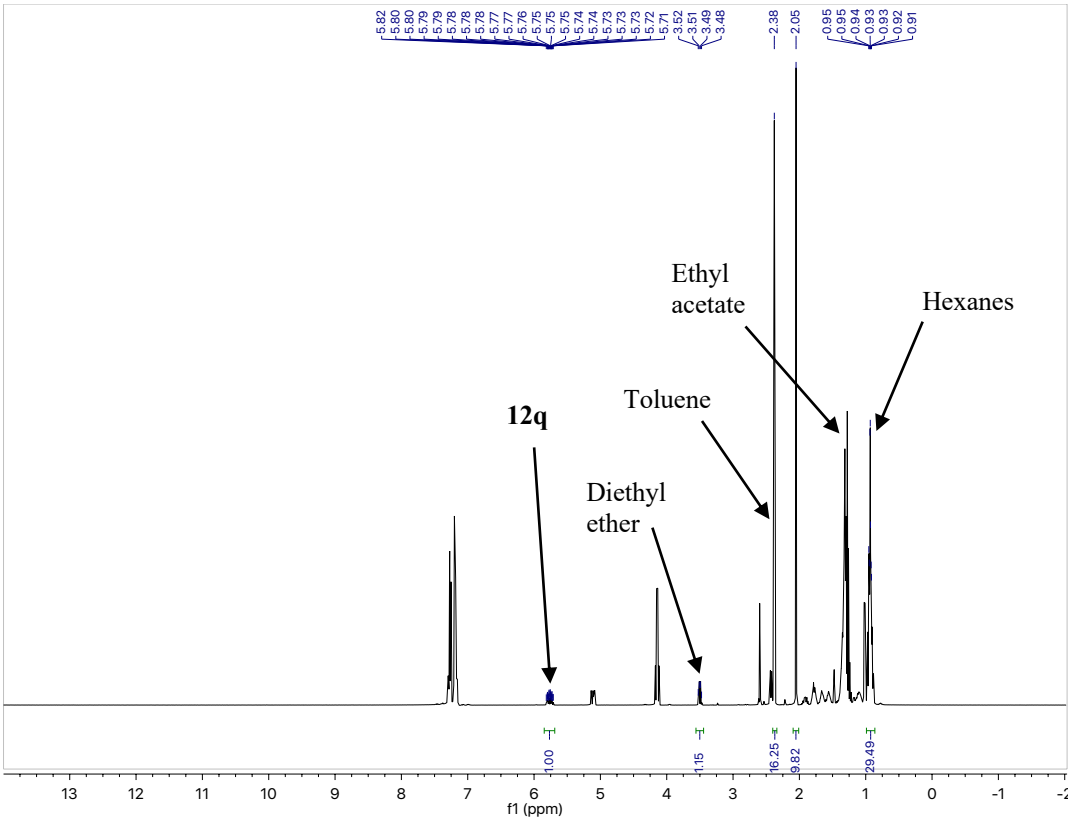

four solvents

	FW	integration	H eq.	total mass
material	126.20	1.0000	1	8.1670
EtOAc	88.11	9.8200	3	
Tol.	92.14	16.2500	3	
Et_2O	74.12	1.1500	4	
Hexane	86.18	29.4900	6	

	integration	sum	percent (%)	FW	corrected mass	mass %	total mass	mass	% yield
product	1.000	14.893	10.386	126.20	13.107	0.093	8.1670	0.7586	99.20
solvent	3.273		33.997	88.11	29.955	0.212		1.7338	
solvent	5.417		56.258	92.14	51.836	0.367		3.0002	
solvent	0.288		2.986	74.12	2.213	0.016		0.1281	
solvent	4.915		51.047	86.18	43.993	0.312		2.5463	

NMR Parameters for Determination of Yield by Mass Percent: The reaction was repeated on a 0.2 mmol scale to determine the relaxation constants for each integrated peak. Using these parameters and the resulting integrations, the yield was calculated analogous to that shown above. The yield was calculated to be 95%, within error of that of the gram-scale synthesis.

	Peak 1	Peak 2	Peak 3	Peak 4	Peak 5
ppm	5.75	3.48	2.38	1.33	0.95
T1	4.6410	4.4865	5.0550	4.1440	3.9600

Relaxation constants (T1):

Largest relaxation constant (T1): 5.0550 seconds

Relaxation delay: 26.0000 seconds

Benzyl-(*R*,*E*)-5-(bromomethyl)-5-hydroxy-6-methylhept-2-enoate (S-4):

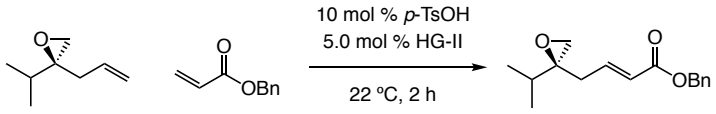

2.21 (4.0 equiv) **S-4**

>98% conv, >98:2 *E/Z*

95% yield, 92:8 er

To establish the enantiomeric purity of **2.21**, the product was converted to **S-4** by cross-metathesis by a single-vessel operation. Following the 3 h needed for allyl addition, **Ru-1** (3.14 mg, 0.005 mmol, 5.0 mol %) followed by benzyl acrylate (66 μL, 0.400 mmol, 4.0 equiv) were added and the mixture was allowed to stir at 22 °C for 2 h, after which the mixture was directly loaded on a silica gel column. Chromatography thus afforded as pale-yellow oil (25.3 mg, 0.741 mmol, 74% yield). **IR (neat):** 3488 (br), 3030 (w), 2962 (w), 2877 (w), 1706 (s), 1651 (m), 1267 (m), 1165 (s), 906 (m), 735 (m), 695 (s), 592 (w) cm^{-1}; **^{1}H NMR (400 MHz, $CDCl_3$):** δ 7.44–7.28 (m, 5H), 7.04 (dt, *J* = 15.5, 7.7 Hz, 1H), 5.99 (dd, *J* = 15.7, 1.5 Hz, 1H), 5.19 (s, 2H), 3.65–3.36 (m, 2H), 2.65–2.44 (m, 2H), 2.02 (dt, *J* = 13.8, 6.9 Hz, 1H), 1.91 (s, 1H), 0.97 (dd, *J* = 7.0, 1.8 Hz, 6H); **^{13}C NMR (101 MHz,$CDCl_3$):** δ 166.0, 144.3, 136.1, 128.7, 128.4, 124.6, 124.5, 74.8, 66.5, 42.3, 38.1, 34.1, 17.2, 16.7; **HRMS (DART$^+$):** Calcd for $C_{16}H_{22}O_3Br$ $[M+H]^+$: 341.0747, Found: 341.0752; **Specific Rotation:** $[\alpha]^{24}_D$ +9.7 (*c* 1.85, $CHCl_3$) for a 94.5:5.5 er sample. The enantiomeric purity was determined by HPLC analysis in comparison with authentic racemic material (Chiralcel OJ-H, 98:2 hexanes:*i*-PrOH, 0.5 mL/min, 220 nm).

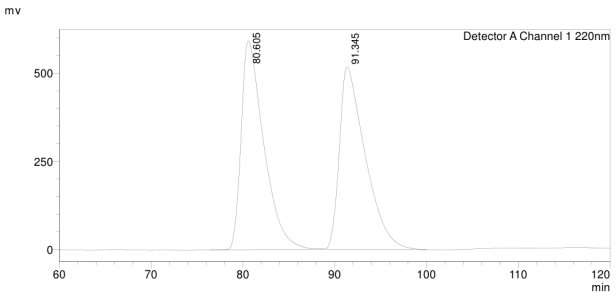

<Peak Table>
Detector A Channel 1 220nm

Peak#	Ret. Time	Area	Height	Area%
1	80.605	101099594	591822	50.046
2	91.345	100914623	516881	49.954
Total		202014217	1108703	100.000

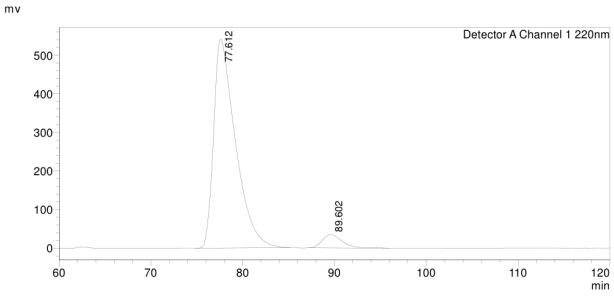

<Peak Table>
Detector A Channel 1 220nm

Peak#	Ret. Time	Area	Height	Area%
1	77.612	89369205	540563	94.521
2	89.602	5179995	34648	5.479
Total		94549200	575211	100.000

Peak #	Ret. Time	Area	Area %	Peak #	Ret. Time	Area	Area %
1	80.6 min	101099594	50.046	1	77.6 min	89369205	94.521
2	91.3 min	100914623	49.954	2	89.6 min	5179995	5.479

2.8.8. Catalytic Enantioselective Additions to Dihalomethyl ketones

In a N_2-filled glove box, **ap-2** (0.32 mg, 0.001 mmol), $Zn(OMe)_2$ (0.32 mg, 0.0025 mmol) and toluene (0.5 mL) were added to a two-dram vial equipped with a stir bar and allowed to stir for 5 min. Ketone (0.10 mmol), (pinacolato)allylboron (0.020 mL, 0.11 mmol) and MeOH (0.010 mL, 2.5 mmol, 2.5 equiv) were added sequentially. The vessel was sealed with a Teflon cap and allowed to stir for at –40 °C for 18 h. Conversion was determined by analysis of the ^{1}H NMR spectrum of an aliquot. The solution was loaded directly onto a silica gel column and eluted with hexanes/Et_2O to afford the desired product.

(*R*)-1,1-Dichloro-2-phenylpent-4-en-2-ol (2.25a): 22.6 mg, 0.0978 mmol, 98% yield, colorless oil. **IR (neat):** 3545 (br, w), 3077 (w), 2981 (w), 2919 (w), 1640 (w), 1495 (w), 1447 (w), 1334 (w), 1215 (w), 1173 (w), 1130 (w), 1068 (w), 1032 (w), 997 (w), 922 (m), 890 (w), 788 (s), 725 (m), 698 (s), 617 (m), 585 (w), 544 (w), 380 (w) cm^{-1}; **^{1}H NMR (400 MHz, $CDCl_3$):** δ 7.56–7.46 (m, 2H), 7.43–7.30 (m, 3H), 5.96 (s, 1H), 5.62–5.48 (m, 1H), 5.23–5.05 (m, 2H), 3.03–2.81 (m, 2H), 2.68 (s, 1H); **^{13}C NMR (100 MHz, $CDCl_3$):** δ 140.0, 131.9, 128.3, 128.2, 126.5, 120.5, 80.0, 79.3, 42.5; **HRMS (DART$^+$):** Calcd for $C_{11}H_{11}Cl_2$ $[M+H–H_2O]^+$: 213.0238; Found: 213.0242; **Specific Rotation:** $[\alpha]^{24}_D$ +1.6 (*c* 2.53, $CHCl_3$) for a 90:10 er sample. The enantiomeric purity of this compound was determined by HPLC analysis in comparison with authentic racemic material (Chiralcel OZ-H, 98:2 hexanes:*i*-PrOH, 0.5 mL/min, 220 nm).

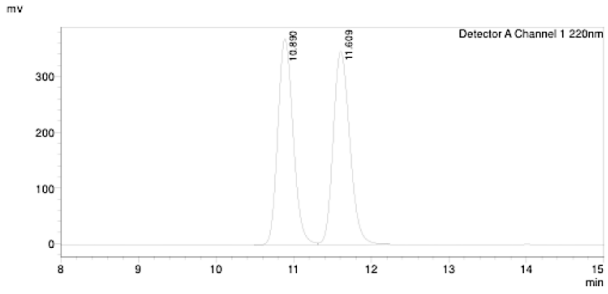

<Peak Table>
Detector A Channel 1 220nm

Peak#	Ret. Time	Area	Area%	Height
1	10.890	5079160	49.728	369865
2	11.609	5134711	50.272	346667
Total		10213871	100.000	716532

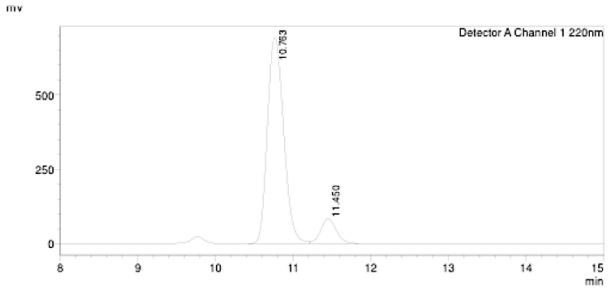

<Peak Table>
Detector A Channel 1 220nm

Peak#	Ret. Time	Area	Area%	Height
1	10.763	10074854	89.740	690621
2	11.450	1151819	10.260	83284
Total		11226672	100.000	773905

Peak #	Ret. Time	Area	Area %	Peak #	Ret. Time	Area	Area %
1	10.9 min	5079160	49.728	1	10.7 min	10074854	89.740
2	11.6 min	5134711	50.272	2	11.5 min	1151819	10.260

(*R*)-1,1-Dibromo-2-phenylpent-4-en-2-ol (2.26a): 30.4 mg, 0.0949 mmol, 95% yield, pale-yellow oil. **IR (neat):** 3539 (br), 3061 (m), 3026 (m), 2979 (m), 2920 (m), 1447 (m), 1096 (m), 1066 (m), 922 (s), 772 (s), 699 (s), 601 (s) cm^{-1}; **^{1}H NMR (400 MHz, $CDCl_3$):** δ 7.52–7.43 (m, 2H), 7.43–7.28 (m, 3H), 5.98 (d, *J* = 0.8 Hz, 1H), 5.59–5.43 (m, 1H), 5.20–5.03 (m, 2H), 3.04–2.85 (m, 2H), 2.72 (d, *J* = 1.3 Hz, 1H); **^{13}C NMR (100 MHz,$CDCl_3$):** δ 140.7, 132.5, 128.8, 128.54, 126.7, 120.7, 79.1, 57.7, 44.0; **HRMS (DART$^+$):** Calcd for $C_{11}H_{11}Br_2$ $[M+H–H_2O]^+$:

300.9228, Found: 300.9221; **Specific Rotation:** $[\alpha]^{24}_{D}$ –4.5 (*c* 1.33, $CHCl_3$) for a 94:6 er sample. The enantiomeric purity of this compound was determined by HPLC analysis in comparison with authentic racemic material (Chiralcel OJ-H, 98:2 hexanes:*i*-PrOH, 0.5 mL/min, 220 nm).

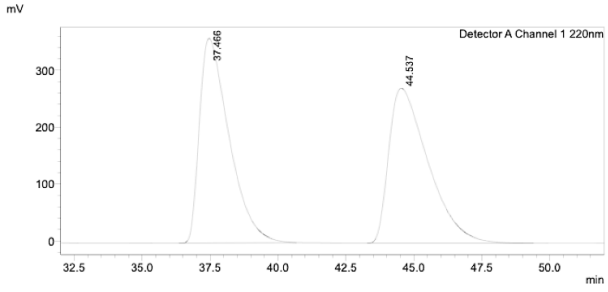

<Peak Table>
Detector A Channel 1 220nm

Peak#	Ret. Time	Area	Height	Area%
1	37.466	27340733	359496	49.846
2	44.537	27509339	272698	50.154
Total		54850072	632194	100.000

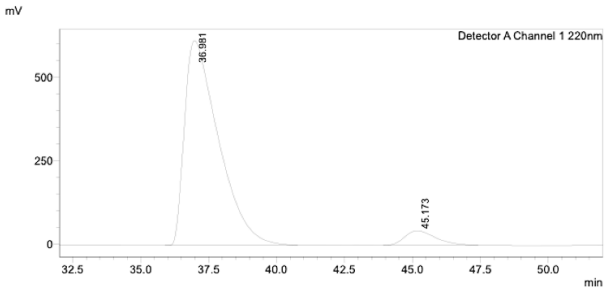

<Peak Table>
Detector A Channel 1 220nm

Peak#	Ret. Time	Area	Height	Area%
1	36.981	53267187	613410	93.968
2	45.173	3419490	43551	6.032
Total		56686677	656961	100.000

Peak #	Ret. Time	Area	Area %	Peak #	Ret. Time	Area	Area %
1	37.5 min	27340733	48.846	1	37.0 min	53267187	93.968
2	44.5 min	27509339	50.154	2	45.2 min	3419490	6.032

(*R*)-1,1-Dichloro-2-(4-chlorophenyl)pent-4-en-2-ol (2.25b): 24.5 mg, 0.0923 mmol, 92% yield, colorless oil. The analytical data are fully consistent with those reported previously.[170] **Specific Rotation:** $[\alpha]^{24}_{D}$ +1.7 (*c* 3.31, $CHCl_3$) for a 85:15 er sample. The enantiomeric purity of this compound was determined by HPLC analysis in comparison with authentic racemic material (OJ-H, 97:3 hexanes:*i*PrOH, 0.3 mL/min, 220 nm).

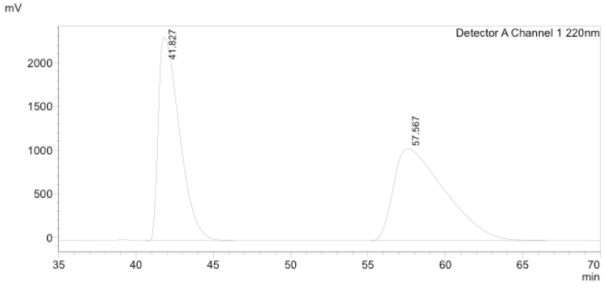

<Peak Table>
Detector A Channel 1 220nm

Peak#	Ret. Time	Area	Height	Area%
1	41.827	221665374	2325895	47.728
2	57.567	242772848	1051781	52.272
Total		464438222	3377676	100.000

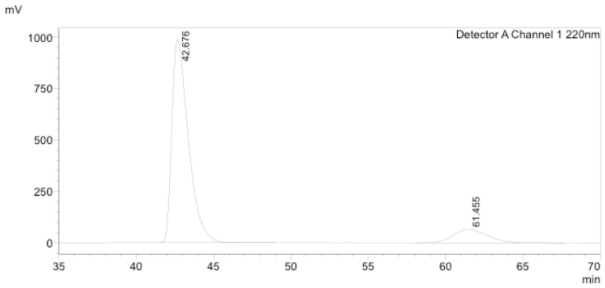

<Peak Table>
Detector A Channel 1 220nm

Peak#	Ret. Time	Area	Height	Area%
1	42.676	73176687	990288	88.085
2	61.455	9898730	65134	11.915
Total		83075417	1055422	100.000

Peak #	Ret. Time	Area	Area %	Peak #	Ret. Time	Area	Area %
1	41.8 min	221665374	47.728	1	42.7 min	73176687	88.085
2	57.6 min	242772848	52.272	2	61.5 min	9898730	11.915

(*R*)-1,1-Dibromo-2-(4-chlorophenyl)pent-4-en-2-ol (2.26b): 28.1 mg, 0.0792 mmol, 79% yield, as clear oil. **IR (neat):** 3541 (br), 2923 (m), 1640 (w), 1491 (s), 1400 (m), 1149 (m), 1094 (s), 1014 (s), 927 (m), 830 (s), 734 (s), 631 (m) cm^{-1}; **^{1}H NMR (400 MHz, $CDCl_3$):** δ 7.48 – 7.38 (m, 2H), 7.38 – 7.30 (m, 2H), 5.91 (d, *J* = 0.6 Hz, 1H), 5.51 (ddt, *J* = 17.2, 10.1, 7.1 Hz, 1H), 5.24 – 5.00 (m, 2H), 3.01 – 2.81 (m, 2H), 2.76 – 2.64 (m, 1H); **^{13}C NMR (100 MHz, $CDCl_3$):** δ 138.71,

134.08, 131.64, 128.45, 127.89, 120.64, 78.40, 56.56, 43.45; **HRMS (DART$^+$):** Calcd for $C_{11}H_{10}Br_2Cl$ $[M+H-H_2O]^+$: 334.8838, Found: 334.8842; **Specific Rotation:** $[\alpha]^{24}_D$ +5.0 (*c* 1.66, $CHCl_3$) for a 94:6 er sample. The enantiomeric purity of this compound was determined by HPLC analysis in comparison with authentic racemic material (OJ-H, 97:3 hexanes:*i*PrOH, 0.3 mL/min, 220 nm).

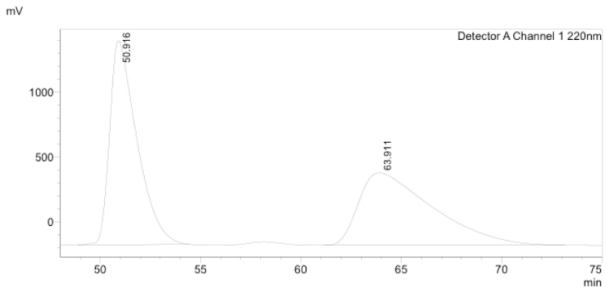

<Peak Table>
Detector A Channel 1 220nm

Peak#	Ret. Time	Area	Height	Area%
1	50.916	148363268	1572225	50.952
2	63.911	142819680	557645	49.048
Total		291182949	2129871	100.000

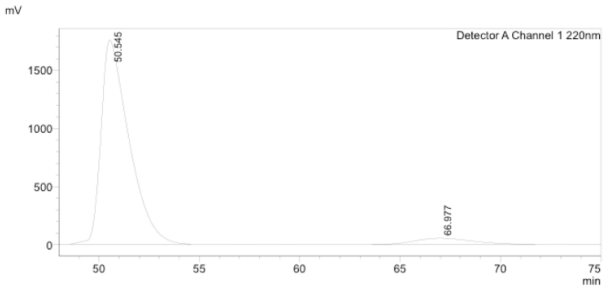

<Peak Table>
Detector A Channel 1 220nm

Peak#	Ret. Time	Area	Height	Area%
1	50.545	170225286	1758731	93.984
2	66.977	10896389	53615	6.016
Total		181121675	1812346	100.000

Peak #	Ret. Time	Area	Area %	Peak #	Ret. Time	Area	Area %
1	50.9 min	148363268	50.952	1	50.5 min	170225286	93.984
2	63.9 min	142819680	49.048	2	67.0 min	10896389	6.016

(*R*)-2-(4-Bromophenyl)-1,1-dichloropent-4-en-2-ol (2.25c): 26.4 mg, 0.0852 mmol, 85% yield, colorless oil. The analytical data are consistent with those reported previously.[169] **^{1}H NMR (400 MHz, $CDCl_3$):** δ 7.56–7.43 (m, 2H), 7.43–7.29 (m, 2H), 5.90 (d, *J* = 0.6 Hz, 1H), 5.65–5.43 (m, 1H), 5.25–5.04 (m, 3H), 3.02–2.73 (m, 3H), 2.68 (t, *J* = 0.9 Hz, 1H); **Specific Rotation:** $[\alpha]^{24}_D$ +2.9 (*c* 2.64, $CHCl_3$) for a 91.5:8.5 er sample. The enantiomeric purity of this compound was determined by HPLC analysis in comparison with authentic racemic material (OJ-H, 91:9 hexanes:*i*-PrOH, 0.3 mL/min, 220 nm).

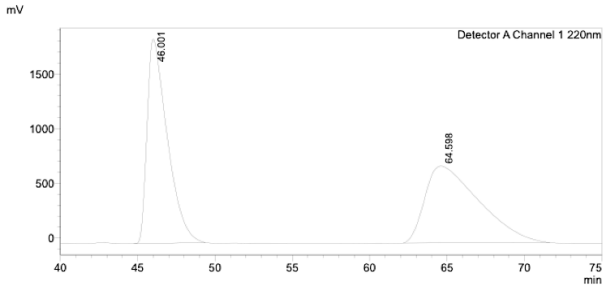

<Peak Table>
Detector A Channel 1 220nm

Peak#	Ret. Time	Area	Height	Area%
1	46.001	169596899	1862856	49.914
2	64.598	170183500	701027	50.086
Total		339780399	2563883	100.000

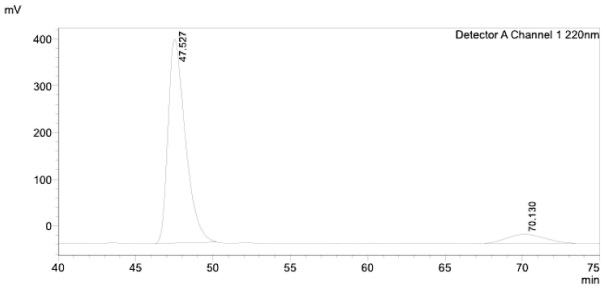

<Peak Table>
Detector A Channel 1 220nm

Peak#	Ret. Time	Area	Height	Area%
1	47.527	33817499	434951	91.413
2	70.130	3176706	19086	8.587
Total		36994205	454037	100.000

Peak #	Ret. Time	Area	Area %	Peak #	Ret. Time	Area	Area %
1	46.0 min	169596899	49.914	1	47.5 min	33817499	91.413
2	64.6 min	170183500	50.086	2	70.1 min	3176706	8.587

[169] Peppe, C.; Nobrega, J. A.; Drehmer, L. D.; Martins, M. A. P. *Lett. Org. Chem.* **2006**, *3*, 597–599.

(*R*)-1,1-Dibromo-2-(4-bromophenyl)pent-4-en-2-ol (2.26c): 29.5 mg, 0.0739 mmol, 74% yield, yellow oil. **IR (neat):** 3538 (br), 2923 (m), 1488 (s), 1396 (m), 1149 (w), 1075 (s), 1009 (s), 927 (m), 825 (m), 730 (m), 695 (m), 622 (m) cm^{-1}; **^{1}H NMR (400 MHz, $CDCl_3$):** δ 7.62–7.41 (m, 2H), 7.41–7.30 (m, 2H), 5.90 (t, *J* = 0.6 Hz, 1H), 5.50 (ddt, *J* = 16.0, 9.9, 7.0 Hz, 1H), 5.24–4.99 (m, 2H), 3.08–2.81 (m, 2H), 2.71 (s, 1H); **^{13}C NMR (100 MHz, $CDCl_3$):** δ 140.4, 132.2, 128.4, 128.2, 126.4, 120.3, 78.7, 57.3, 43.7; **HRMS (DART$^+$):** Calcd for $C_{11}H_{10}Br_3$ $[M+H–H_2O]^+$: 378.8333, Found: 378.8339; **Specific Rotation:** $[\alpha]^{24}_D$ –4.7 (*c* 2.48, $CHCl_3$) for a 97.5:2.5 er sample. The enantiomeric purity of this compound was determined by HPLC analysis in comparison with authentic racemic material (Chiralcel OJ-H, 97:3 hexanes:*i*-PrOH, 0.3 mL/min, 254 nm).

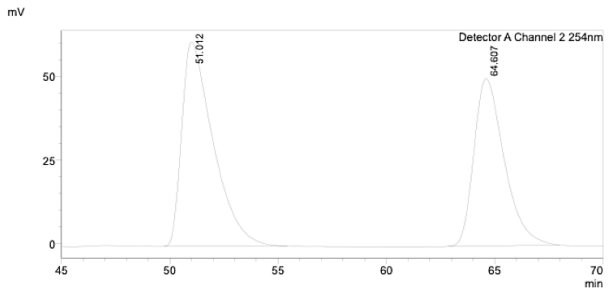

<Peak Table>
Detector A Channel 2 254nm

Peak#	Ret. Time	Area	Height	Area%
1	51.012	6171244	61175	55.817
2	64.607	4884898	50086	44.183
Total		11056142	111261	100.000

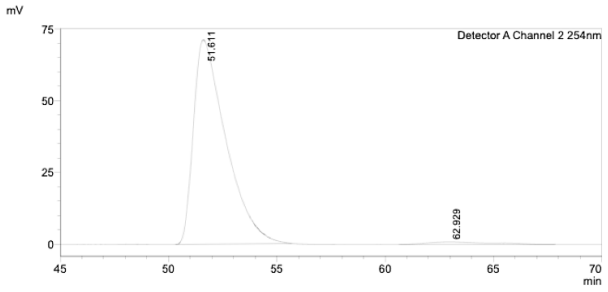

<Peak Table>
Detector A Channel 2 254nm

Peak#	Ret. Time	Area	Height	Area%
1	51.611	7424411	71260	97.614
2	62.929	181457	869	2.386
Total		7605868	72129	100.000

Peak #	Ret. Time	Area	Area %	Peak #	Ret. Time	Area	Area %
1	51.0 min	6171244	55.817	1	51.6 min	7424411	97.614
2	64.6 min	4884898	44.183	2	62.9 min	181457	2.386

(*R*)-1,1-Dichloro-2-(4-nitrophenyl)pent-4-en-2-ol (2.25d): 21.6 mg, 0.0782 mmol, 78% yield, pale-yellow solid. **Melting point:** 66–70 °C; **IR (neat):** 3534 (br), 3078 (w), 2923 (m), 2854 (w), 1602 (m), 1519 (s), 1348 (s), 855 (s), 786 (m), 750 (m), 733 (m), 705 (m) cm^{-1}; **^{1}H NMR (400 MHz, $CDCl_3$):** δ 8.28–8.19 (m, 2H), 7.74–7.65 (m, 2H), 5.95 (d, *J* = 1.1 Hz, 1H), 5.53 (ddt, *J* = 16.0, 10.1, 7.2 Hz, 1H), 5.23–5.11 (m, 2H), 3.02–2.86 (m, 2H), 2.82 (d, *J* = 0.9 Hz, 1H); **^{13}C NMR (100 MHz, $CDCl_3$):** δ 146.9, 130.6, 127.7, 123.3, 121.4, 79.2, 78.8, 42.6, 29.7; **HRMS (DART$^+$):** Calcd for $C_{11}H_{12}Cl_2NO_3$ $[M+H]^+$: 276.0194, Found: 276.0184; **Specific Rotation:** $[\alpha]^{24}_D$ +6.2 (*c* 1.62, $CHCl_3$) for a 95.5:4.5 er sample. The enantiomeric purity of this compound was determined by HPLC analysis in comparison with authentic racemic material (Chiralpak AD-H, 98:2 hexanes:*i*-PrOH, 0.5 mL/min, 254 nm).

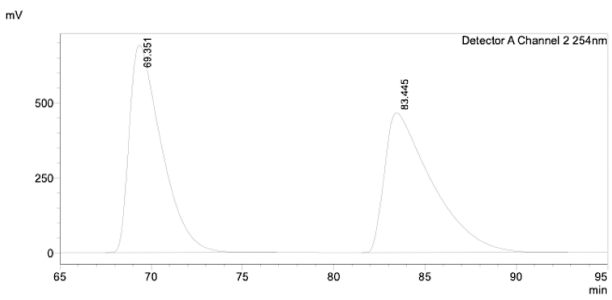

<Peak Table>
Detector A Channel 2 254nm

Peak#	Ret. Time	Area	Height	Area%
1	69.351	84491975	689656	50.171
2	83.445	83914365	465023	49.829
Total		168406340	1154679	100.000

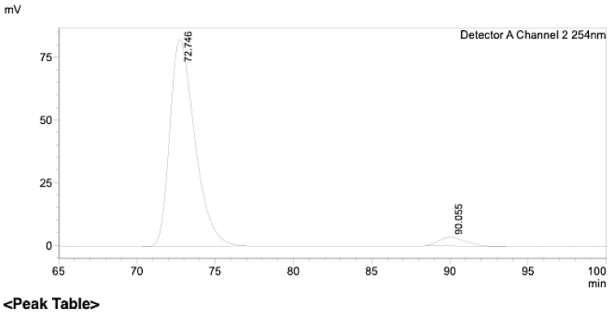

<Peak Table>
Detector A Channel 2 254nm

Peak#	Ret. Time	Area	Height	Area%
1	72.746	9162334	82584	95.695
2	90.055	412163	3455	4.305
Total		9574498	86039	100.000

Peak #	Ret. Time	Area	Area %	Peak #	Ret. Time	Area	Area %
1	69.4 min	84491975	50.171	1	72.7 min	9162334	95.695
2	83.4 min	83914365	49.829	2	90.1 min	412163	4.305

(*R*)-1,1-Dibromo-2-(4-nitrophenyl)pent-4-en-2-ol (2.26d): 33.5 mg, 0.0918 mmol, 92% yield, pale-yellow oil. **IR (neat):** 3527 (br), 2954 (w), 2921 (w), 2855 (w), 1494 (w), 1409 (s), 1347 (s), 1155 (s), 1084 (m), 1014 (w), 854 (m), 631 (m) cm^{-1}; **^{1}H NMR (400 MHz, $CDCl_3$):** δ 8.31–8.16 (m, 2H), 7.79–7.59 (m, 2H), 5.96 (s, 1H), 5.50 (ddt, *J* = 17.2, 10.1, 7.2 Hz, 1H), 5.26–5.01 (m, 2H), 2.95 (dt, *J* = 7.1, 1.2 Hz, 2H), 2.83 (s, 1H); **^{13}C NMR (100 MHz, $CDCl_3$):** δ 147.3, 130.8, 130.2, 127.5, 123.3, 121.2, 78.7, 55.2, 43.8; **HRMS (DART$^+$):** Calcd for $C_{11}H_{12}O_3NBr_2$ $[M+H]^+$: 363.9184, Found: 363.9191; **Specific Rotation:** $[\alpha]^{24}_D$ –5.3 (*c* 0.18, $CHCl_3$) for a 94:6 er sample. The enantiomeric purity of this compound was determined by HPLC analysis in comparison with authentic racemic material (Chiralpak AD-H, 98:2 hexanes:*i*-PrOH, 0.5 mL/min, 254 nm).

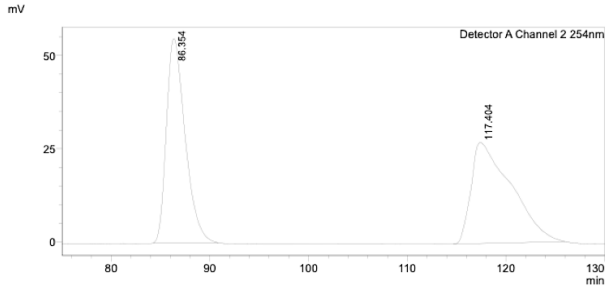

<Peak Table>
Detector A Channel 2 254nm

Peak#	Ret. Time	Area	Height	Area%
1	86.354	7243994	54818	48.676
2	117.404	7637953	27145	51.324
Total		14881947	81963	100.000

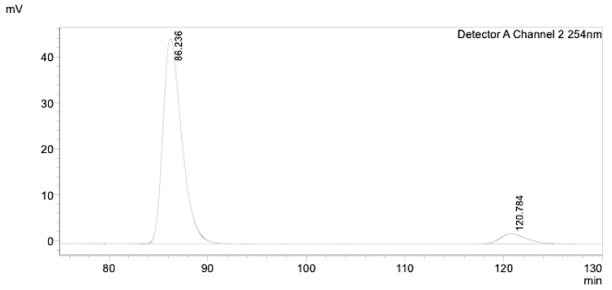

<Peak Table>
Detector A Channel 2 254nm

Peak#	Ret. Time	Area	Height	Area%
1	86.236	5912490	44535	93.826
2	120.784	389081	2180	6.174
Total		6301571	46715	100.000

Peak #	Ret. Time	Area	Area %	Peak #	Ret. Time	Area	Area %
1	86.4 min	7243994	48.676	1	86.2 min	5912490	93.826
2	117.4 min	7637953	51.324	2	120.8 min	389081	6.174

(*R*)-1,1-Dichloro-2-(4-methoxyphenyl)pent-4-en-2-ol (2.25e): 24.8 mg, 0.0950 mmol, 95% yield, colorless oil. The analytical data are fully consistent with those reported previously.[170] **Specific Rotation:** $[\alpha]^{24}_D$ –0.3 (*c* 1.93, $CHCl_3$) for a 82:18 er sample. The enantiomeric purity of

this compound was determined by HPLC analysis in comparison with authentic racemic material (AS-H, 98:2 hexanes:*i*PrOH, 0.5 mL/min, 220 nm).

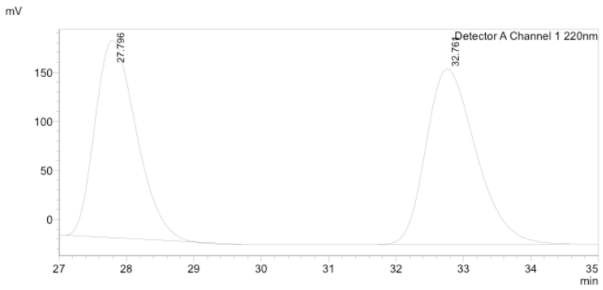

<Peak Table>
Detector A Channel 1 220nm

Peak#	Ret. Time	Area	Height	Area%
1	27.796	8568181	200911	48.279
2	32.761	9178906	178426	51.721
Total		17747086	379337	100.000

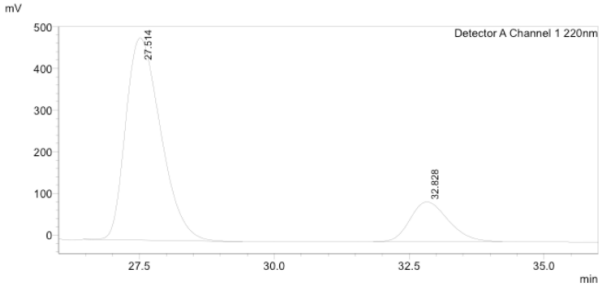

<Peak Table>
Detector A Channel 1 220nm

Peak#	Ret. Time	Area	Height	Area%
1	27.514	21974793	485979	82.308
2	32.828	4723498	95540	17.692
Total		26698291	581519	100.000

Peak #	Ret. Time	Area	Area %	Peak #	Ret. Time	Area	Area %
1	27.8 min	8568181	48.279	1	27.5 min	21974793	82.308
2	32.8 min	9178906	51.721	2	32.8 min	4723498	17.692

(*R*)-1,1-Dibromo-2-(4-methoxyphenyl)pent-4-en-2-ol (2.26e): 32.4 mg, 0.0926 mmol, 93% yield, pale-yellow oil. **IR (neat):** 3535 (br), 2956 (m), 2924 (m), 2854 (m), 2837 (m), 1610 (m), 1511 (s), 1252 (s), 1180 (m), 1033 (m), 832 (s), 579 (m) cm^{-1}; **^{1}H NMR (400 MHz, $CDCl_3$):** δ 7.45–7.30 (m, 2H), 6.98–6.81 (m, 2H), 5.92 (s, 1H), 5.54 (dddd, *J* = 16.9, 10.1, 7.6, 6.6 Hz, 1H), 5.24–5.00 (m, 2H), 3.82 (s, 3H), 2.93 (qdt, *J* = 14.2, 7.7, 1.2 Hz, 2H), 2.77–2.55 (m, 1H); **^{13}C NMR (100 MHz, $CDCl_3$):** δ 159.4, 132.4, 132.2, 127.8, 120.3, 113.7, 78.5, 57.8, 55.4, 43.3; **HRMS (DART$^+$):** Calcd for $C_{12}H_{13}Br_2O$ $[M+H–H_2O]^+$: 330.9333, Found: 330.9331; **Specific Rotation:** $[\alpha]^{24}_D$ –15.3 (*c* 2.17, $CHCl_3$) for a 89:11 er sample. The enantiomeric purity of this compound was determined by HPLC analysis in comparison with authentic racemic material (Chiralpak AZ-H, 97:3 hexanes:*i*-PrOH, 0.3 mL/min, 220 nm).

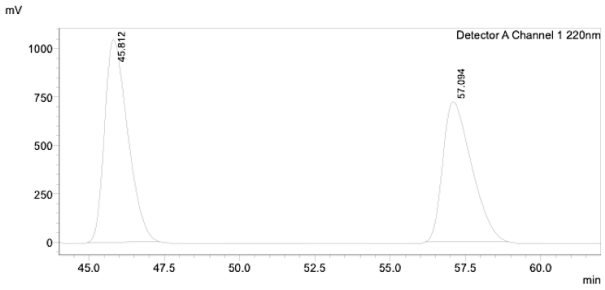

<Peak Table>
Detector A Channel 1 220nm

Peak#	Ret. Time	Area	Height	Area%
1	45.812	55966503	1045847	53.679
2	57.094	48294992	723718	46.321
Total		104261495	1769565	100.000

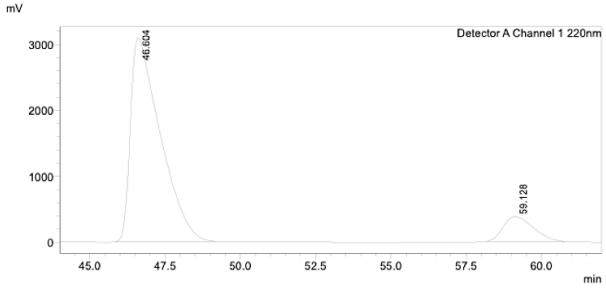

<Peak Table>
Detector A Channel 1 220nm

Peak#	Ret. Time	Area	Height	Area%
1	46.604	211913097	3092339	89.081
2	59.128	25976211	377531	10.919
Total		237889308	3469871	100.000

Peak #	Ret. Time	Area	Area %	Peak #	Ret. Time	Area	Area %
1	45.8 min	55966503	53.679	1	46.6 min	211913097	89.081
2	57.1 min	48294992	46.321	2	59.1 min	25976211	10.919

(*R*)-1,1-Dichloro-2-(*p*-tolyl)pent-4-en-2-ol (2.25f): 22.7 mg, 0.0925 mmol, 93% yield, colorless oil. The analytical data are fully consistent with those reported previously.[170] **Specific Rotation:** $[\alpha]^{24}_{D}$ +1.8 (*c* 1.76, $CHCl_3$) for a 93:7 er sample. The enantiomeric purity of this compound was determined by HPLC analysis in comparison with authentic racemic material (AZ-H, 87:13 hexanes:*i*PrOH, 0.3 mL/min, 220 nm).

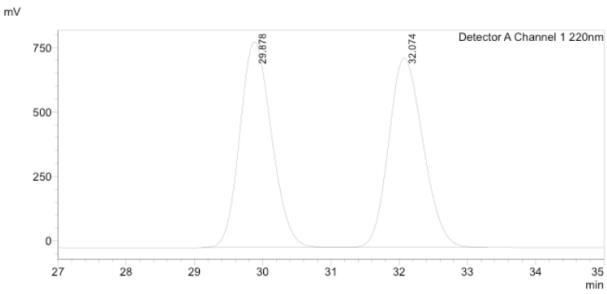

<Peak Table>
Detector A Channel 1 220nm

Peak#	Ret. Time	Area	Height	Area%
1	29.878	25836461	798288	50.020
2	32.074	25815687	734731	49.980
Total		51652148	1533019	100.000

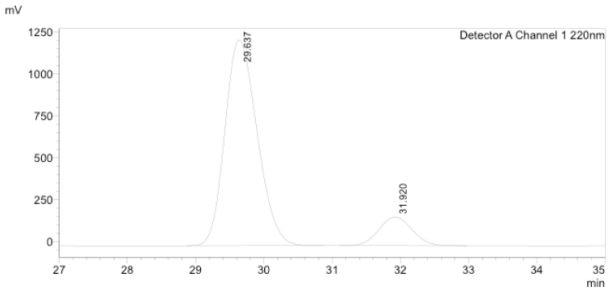

<Peak Table>
Detector A Channel 1 220nm

Peak#	Ret. Time	Area	Height	Area%
1	29.637	40424622	1227441	87.370
2	31.920	5843642	171595	12.630
Total		46268263	1399035	100.000

Peak #	Ret. Time	Area	Area %	Peak #	Ret. Time	Area	Area %
1	29.9 min	25836461	50.020	1	29.6 min	1227441	87.370
2	32.1 min	25815687	49.980	2	31.9 min	171595	12.630

(*R*)-1,1-Dibromo-2-(*p*-tolyl)pent-4-en-2-ol (2.26f): The title compound was synthesized analogous to **6a** and purified by silica gel chromatography to afford **S-7g** (28.8 mg, 0.0862 mmol, 88% yield) as clear oil. **IR (neat):** 3547 (br), 2922 (s), 2853 (m), 1457 (w), 1440 (w), 1147 (m), 922 (s), 816 (s), 736 (s), 722 (s), 653 (s), 574 (w) cm^{-1}; **^{1}H NMR (400 MHz, $CDCl_3$):** δ 7.38 – 7.31 (m, 2H), 7.21 – 7.15 (m, 2H), 5.95 (d, *J* = 0.5 Hz, 1H), 5.52 (dddd, *J* = 17.0, 10.1, 7.5, 6.7 Hz, 1H), 5.21 – 5.03 (m, 2H), 2.92 (ddt, *J* = 7.7, 6.4, 1.2 Hz, 2H), 2.75 (s, 1H), 2.35 (s, 3H); **^{13}C NMR (100 MHz, $CDCl_3$):** δ 137.83, 137.22, 132.22, 129.00, 126.19, 120.08, 78.54, 57.49, 43.40, 25.40; **HRMS (DART$^+$):** Calcd for $C_{12}H_{13}Br_2NO_3$ $[M+H-H_2O]^+$: 314.9384, Found: 314.9375; **Specific Rotation:** $[\alpha]^{24}_{D}$ +3.0 (*c* 0.81, $CHCl_3$) for a 85:15 er sample. The enantiomeric purity of this compound was determined by HPLC analysis in comparison with authentic racemic material (AZ-H, 97:3 hexanes:*i*PrOH, 0.3 mL/min, 220 nm).

[170] Peppe, C.; Nobrega, J. A.; Drehmer, L. D. Martins, M. A. *Letters in Organic Chemistry,* **2006**, *3*, 597–599.

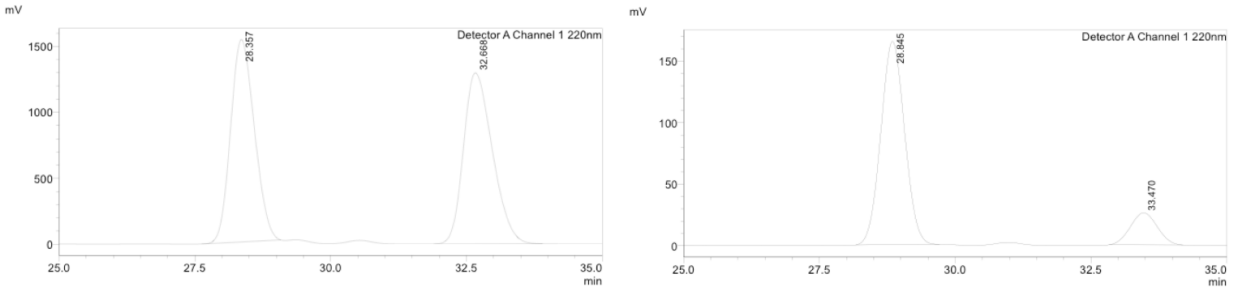

<Peak Table>
Detector A Channel 1 220nm

Peak#	Ret. Time	Area	Height	Area%
1	28.357	46795175	1533305	49.361
2	32.668	48006382	1295973	50.639
Total		94801556	2829278	100.000

<Peak Table>
Detector A Channel 1 220nm

Peak#	Ret. Time	Area	Height	Area%
1	28.845	5045011	165346	84.830
2	33.470	902183	26080	15.170
Total		5947194	191426	100.000

Peak #	Ret. Time	Area	Area %	Peak #	Ret. Time	Area	Area %
1	28.4 min	46795175	49.361	1	28.8 min	5045011	84.830
2	32.7 min	4806382	50.639	2	33.5 min	902183	15.170

(*R*)-1,1-Dichloro-2-(thiophen-3-yl)pent-4-en-2-ol (2.25g): 20.9 mg, 0.0825 mmol, 83% yield, colorless oil. **IR (neat):** 3543 (br, w), 3108 (w), 3109 (w), 3078 (w), 3020 (w), 2983 (w), 2187 (w), 2144 (w), 1639 (w), 1434 (w), 1413 (w), 1333 (w), 1214 (m), 1148 (w), 1086 (w), 995 (w), 927 (w), 858 (w), 789 (m), 742 (s), 667 (s), 589 (w) cm^{-1}; **^{1}H NMR (400 MHz, $CDCl_3$):** δ 7.37 (dd, *J* = 3.1, 1.4 Hz, 1H), 7.32 (dd, *J* = 5.1, 3.1 Hz, 1H), 7.11 (dd, *J* = 5.1, 1.4 Hz, 1H), 5.88 (s, 1H), 5.62 (dddd, *J* = 16.9, 10.1, 7.7, 6.6 Hz, 1H), 5.26–5.07 (m, 2H), 2.91 (dtdd, *J* = 15.2, 14.1, 7.2, 1.2 Hz, 2H), 2.78 (s, 1H); **^{13}C NMR (100 MHz, $CDCl_3$):** δ 141.9, 132.0, 126.1, 125.9, 123.4, 120.6, 78.0, 56.4, 43.4; **Specific Rotation:** $[\alpha]^{24}_D$ –24.1 (*c* 1.93, $CHCl_3$) for a 94.5:5.5 er sample. The enantiomeric purity of this compound was determined by HPLC analysis in comparison with authentic racemic material (Chiralpak AD-H, 98:2 hexanes:*i*-PrOH, 0.5 mL/min, 220 nm).

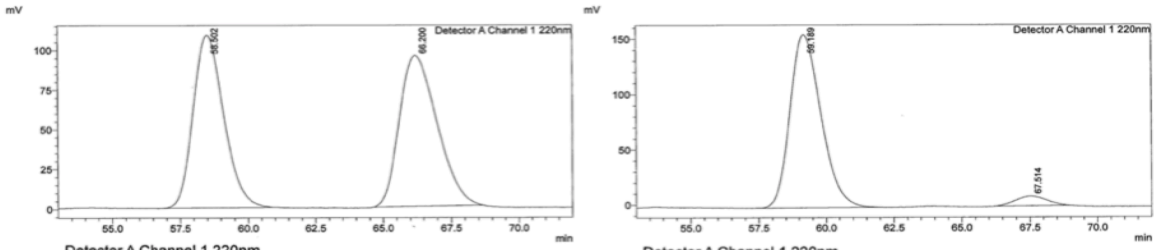

Detector A Channel 1 220nm

Peak#	Ret. Time	Area	Area%	Height
1	58.502	8469074	48.029	108384
2	66.200	9164206	51.971	94904
Total		17633280	100.000	203289

Detector A Channel 1 220nm

Peak#	Ret. Time	Area	Area%	Height
1	59.189	12598613	94.729	156338
2	67.514	701009	5.271	8799
Total		13299621	100.000	165137

Peak #	Ret. Time	Area	Area %	Peak #	Ret. Time	Area	Area %
1	58.5 min	8469074	48.029	1	59.2 min	12598613	94.729
2	66.2 min	9164206	51.971	2	67.5 min	701009	5.271

(*R*)-1,1-Dibromo-2-(thiophen-3-yl)pent-4-en-2-ol (2.26g): 31.8 mg, 0.0975 mmol, 98% yield, colorless oil. **IR (neat):** 3525 (br, w), 3073 (w), 2978 (w), 2912 (w), 1637 (w), 1529 (m), 1144 (m), 923 (m), 698 (s), 662 (s), 616 (w) cm^{-1}; **^{1}H NMR (400 MHz, $CDCl_3$):** δ 7.37 (dd, *J* = 3.1, 1.4 Hz, 1H), 7.32 (dd, *J* = 5.1, 3.1 Hz, 1H), 7.11 (dd, *J* = 5.1, 1.4 Hz, 1H), 5.89 (s, 1H), 5.62 (dddd,

J = 16.9, 10.1, 7.7, 6.6 Hz, 1H), 5.29 – 5.03 (m, 2H), 2.91 (qdt, *J* = 14.1, 7.8, 1.2 Hz, 2H), 2.78 (s, 1H); **^{13}C NMR (100 MHz, $CDCl_3$):** δ 141.9, 132.0, 126.1, 125. 9, 123.4, 120.6, 78.0, 56.5, 43.4; **Specific Rotation:** $[\alpha]^{24}_D$ –10.7 (*c* 2.60, $CHCl_3$) for a 92:8 er sample. The enantiomeric purity of this compound was determined by HPLC analysis in comparison with authentic racemic material (Chiralpak AD-H, 98:2 hexanes:*i*-PrOH, 0.5 mL/min, 220 nm).

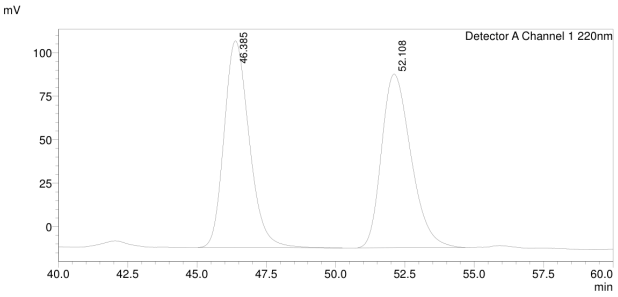

<Peak Table>
Detector A Channel 1 220nm

Peak#	Ret. Time	Area	Height	Area%
1	46.385	7509988	118836	50.449
2	52.108	7376182	99790	49.551
Total		14886170	218626	100.000

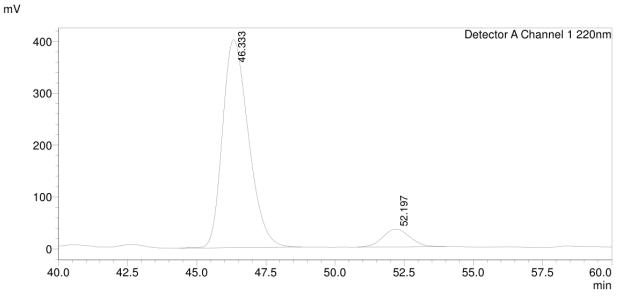

<Peak Table>
Detector A Channel 1 220nm

Peak#	Ret. Time	Area	Height	Area%
1	46.333	26252619	400881	91.817
2	52.197	2339681	34376	8.183
Total		28592300	435257	100.000

Peak #	Ret. Time	Area	Area %	Peak #	Ret. Time	Area	Area %
1	46.4 min	7509988	50.449	1	46.3 min	26252619	91.817
2	52.1 min	7376182	49.551	2	52.2 min	2339681	8.183

(*R*)-1,1-Dibromo-2-(2-chlorophenyl)pent-4-en-2-ol (2.26h): 29.4 mg, 0.0829 mmol, 82% yield, colorless oil. **IR (neat):** 3546 (br, w), 3074 (w), 2980 (w), 2919 (w), 1640 (w), 1591 (w), 1568 (w), 1466 (w), 1429 (w), 1336 (w), 1282 (w), 1214 (w), 1155 (m), 1072 (w), 1037 (m), 995 (w), 950 (m), 921 (w), 890 (w), 756 (s), 736 (s), 699 (m), 658 (m), 603 (m), 552 (w), 412 (w) cm^{-1}; **^{1}H NMR (400 MHz, $CDCl_3$):** δ 7.83–7.77 (m, 1H), 7.38–7.23 (m, 3H), 6.98 (s, 1H), 5.40 (ddt, *J* = 17.2, 10.1, 7.1 Hz, 1H), 5.15–4.85 (m, 2H), 3.39 (dddt, *J* = 14.4, 7.0, 1.6, 0.8 Hz, 1H), 3.01–2.72 (m, 2H); **^{13}C NMR (100 MHz, $CDCl_3$):** δ 138.1, 132.4, 131.3, 130.5, 129.7, 129.7, 127.2, 119.2, 79.7, 55.1, 41.8; **HRMS (DART$^+$):** Calcd for $C_{11}H_{10}Br_2Cl$ $[M+H–H_2O]^+$: 334.8838; Found: 334.8843; **Specific Rotation:** $[\alpha]^{24}_D$ +11.5 (*c* 3.03, $CHCl_3$) for a 95:5 er sample. The enantiomeric purity of this compound was determined by HPLC analysis in comparison with authentic racemic material (Chiralpak AD-H, 98:2 hexanes:*i*-PrOH, 0.5 mL/min, 220 nm).

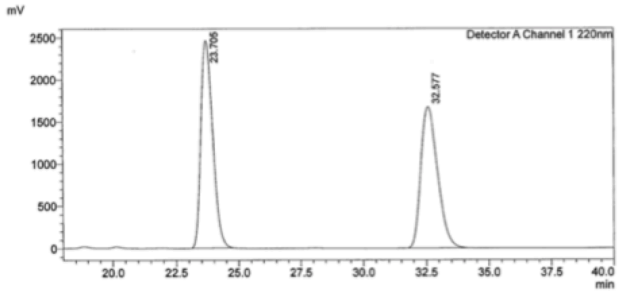

Detector A Channel 1 220nm

Peak#	Ret. Time	Area	Area%	Height
1	23.705	81337233	51.087	2460275
2	32.577	77875740	48.913	1673341
Total		159212974	100.000	4133616

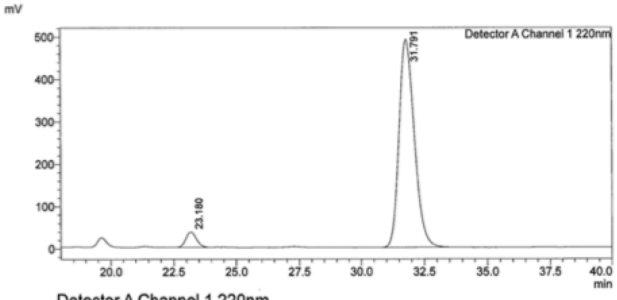

Detector A Channel 1 220nm

Peak#	Ret. Time	Area	Area%	Height
1	23.180	1068148	4.873	36462
2	31.791	20852713	95.127	491017
Total		21920861	100.000	527480

Peak #	Ret. Time	Area	Area %	Peak #	Ret. Time	Area	Area %
1	23.7 min	81337233	51.087	1	23.2 min	1068148	4.873
2	32.6 min	77875740	48.913	2	31.8 min	20852713	95.127

(*S*)-4-(Dibromomethyl)dec-1-en-4-ol (2.26i): 33.5 mg, 0.0918 mmol, 92% yield, clear oil. **IR (neat):** 3548 (br), 2954 (s), 2926 (s), 2857 (m), 1639 (w), 1465 (m), 1377 (m), 1187 (m), 998 (m), 919 (s), 712 (s), 523 (m) cm^{-1}; **^{1}H NMR (400 MHz, $CDCl_3$):** δ 5.89 – 5.69 (m, 2H), 5.35 – 5.09 (m, 2H), 2.70 – 2.43 (m, 2H), 2.07 (s, 1H), 1.99 – 1.63 (m, 2H), 1.48 – 1.16 (m, 8H), 1.02 – 0.79 (m, 3H); **^{13}C NMR (100 MHz, $CDCl_3$):** δ 132.24, 119.99, 76.81, 58.39, 40.13, 35.89, 31.91, 29.80, 23.13, 22.80, 14.27; **HRMS (DART$^+$):** Calcd for $C_{11}H_{24}ONBr_2$ $[M+NH_4]^+$: 344.02246, Found: 344.012361; **Specific Rotation:** $[\alpha]^{24}_D$ +0.9 (*c* 1.13, $CHCl_3$) for a 69:31 er sample. The enantiomeric purity of this compound was determined by GLC analysis in comparison with authentic racemic material (Chiraldex CDB/DM, 15 psi, 110 °C): t_R: 60.1 (major) and 63.5 (minor).

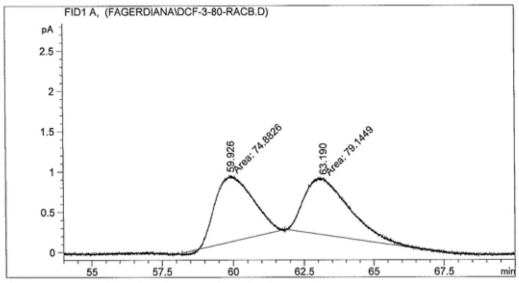

Peak #	RetTime Type	Width [min]	Area [pA*s]	Height [pA]	Area %
1	59.926 MM	1.5160	74.88264	8.23269e-1	48.61639
2	63.190 MM	1.8582	79.14494	7.09875e-1	51.38361

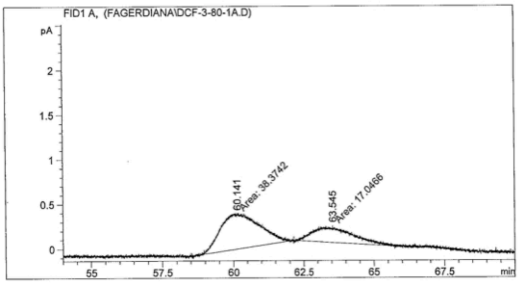

Peak #	RetTime Type	Width [min]	Area [pA*s]	Height [pA]	Area %
1	60.141 MM	1.5989	38.37424	4.00000e-1	69.24153
2	63.545 MM	1.4594	17.04660	1.94676e-1	30.75847

Peak #	Ret. Time	Area	Area %	Peak #	Ret. Time	Area	Area %
1	59.9 min	74.88264	48.61639	1	60.1 min	38.37424	69.24153
2	63.2 min	79.14494	51.38361	2	63.5 min	17.04660	30.75847

(*S*)-3-(Dibromomethyl)-1-phenylhex-5-en-3-ol (2.26j): 33.5 mg, 0.0918 mmol, 92% yield, colorless oil. **IR (neat):** 3543 (br), 3067 (m), 3023 (m), 2953 (w), 1639 (w), 1496 (m), 1346 (w), 1155 (w), 1053 (m), 921 (m), 698 (s), 589 (m) cm^{-1}; **^{1}H NMR (400 MHz, $CDCl_3$):** δ 7.36–7.27 (m, 2H), 7.26–7.18 (m, 3H), 6.04–5.76 (m, 2H), 5.48–5.14 (m, 2H), 2.92–2.56 (m, 4H), 2.36–1.94 (m, 3H); **^{13}C NMR (100 MHz, $CDCl_3$):** δ 142.0, 132.3, 129.1, 128.9, 126.7, 120.7, 77.0, 58.1, 40.5, 38.3, 30.3; **HRMS (DART$^+$):** Calcd for $C_{13}H_{20}ONBr_2$ $[M+NH_4]^+$: 363.9912, Found: 363.9928; **Specific Rotation:** $[\alpha]^{24}_D$ +0.3 (*c* 2.67, $CHCl_3$) for a 62.5:37.5 er sample. The enantiomeric purity of this compound was determined by HPLC analysis in comparison with authentic racemic material (Chiralcel OJ-H, 99.5:0.5 hexanes:*i*-PrOH, 0.3 mL/min, 220 nm).

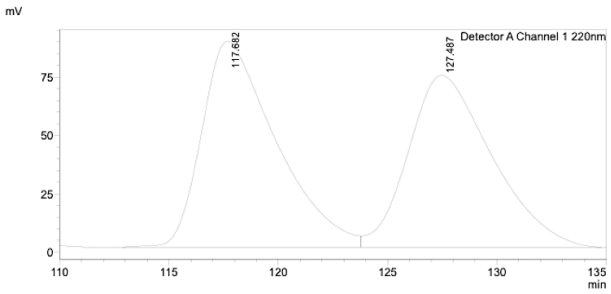

<Peak Table>
Detector A Channel 1 220nm

Peak#	Ret. Time	Area	Height	Area%
1	117.682	20832780	88261	51.567
2	127.487	19566343	73633	48.433
Total		40399123	161894	100.000

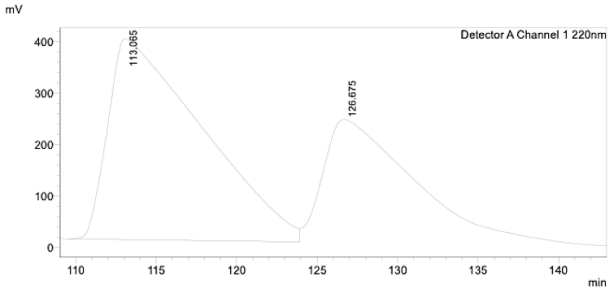

<Peak Table>
Detector A Channel 1 220nm

Peak#	Ret. Time	Area	Height	Area%
1	113.065	158955777	389288	62.630
2	126.675	94844881	238999	37.370
Total		253800658	628287	100.000

Peak #	Ret. Time	Area	Area %	Peak #	Ret. Time	Area	Area %
1	117.7 min	25836461	50.020	1	113.1 min	158955777	62.630
2	127.5 min	25815687	49.980	2	126.7 min	94844881	37.370

2.8.9. Synthesis of α-halo-γ,δ-unsaturated aldehydes

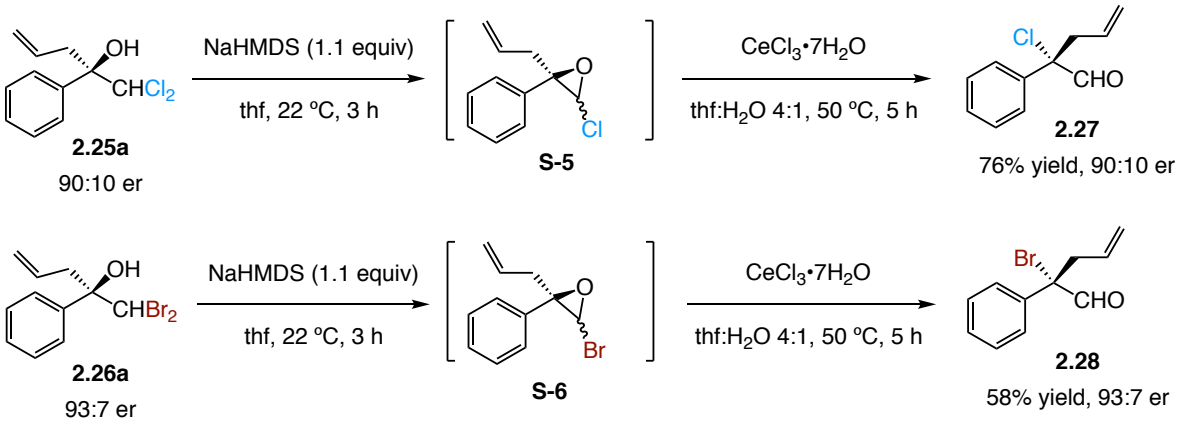

(*S*)-2-Chloro-2-phenylpent-4-enal (2.27): To a 4-dram vial equipped with a stir bar was added a solution of **2.25a** (23.8 mg, 0.10 mmol) in thf (1.0 mL). Sodium bis(trimethylsilyl)amide (21.0 mg, 0.011 mmol) was added and the mixture allowed to stir at 22 ºC for 3 h. Cerium (III) chloride heptahydrate (77 mg, 0.206 mmol) and 0.25 mL water were added and the mixture was allowed to stir at 22 ºC for 5 h. The mixture was diluted with EtOAc (5 mL) and the aqueous layer was washed with EtOAc (2x5 mL). The combined organic layers were dried over $MgSO_4$ and concentrated *in vacuo*. The resulting pale-yellow oil was purified by silica gel chromatography (eluted with 60:1 hexanes:EtOAc) to afford **2.27** as colorless oil (21.6 mg, 0.0782 mmol, 76% yield). **IR (neat):** 3082 (w), 3028 (w), 2983 (w), 2922 (w), 2828 (w), 2711 (w), 1730 (s), 1642 (w), 1583 (w), 1492 (w), 1446 (w), 1431 (w), 1375 (w), 1251 (w), 1106 (w), 993 (w), 953 (w), 922 (m), 758 (m), 696 (s), 646 (w), 597 (w), 530 (w) cm^{-1}; **^{1}H NMR (400 MHz, $CDCl_3$):** δ 9.40 (d, J = 1.5 Hz, 1H), 7.45–7.34 (m, 5H), 5.66 (dddd, J = 16.4, 13.9, 6.9, 1.6 Hz, 1H), 5.11 (ddt, J = 14.0, 3.5, 1.7 Hz, 2H), 3.12–2.91 (m, 2H); **^{13}C NMR (100 MHz, $CDCl_3$):** δ 191.8, 135.2, 131.4, 129.0, 128.9, 127.3,

120.1, 77.6, 42.6; **HRMS (DART$^+$):** Calcd for $C_{11}H_{11}O$ [M–Cl]$^+$: 159.2048; Found: 159.0842; **Specific Rotation:** $[\alpha]^{24}_D$ –64.4 (*c* 0.31, $CHCl_3$) for a 90:10 er sample. The enantiomeric purity of this compound was determined by HPLC analysis in comparison with authentic racemic material (Chiralpak AZ-H, 98:2 hexanes:*i*-PrOH, 0.5 mL/min, 220 nm).

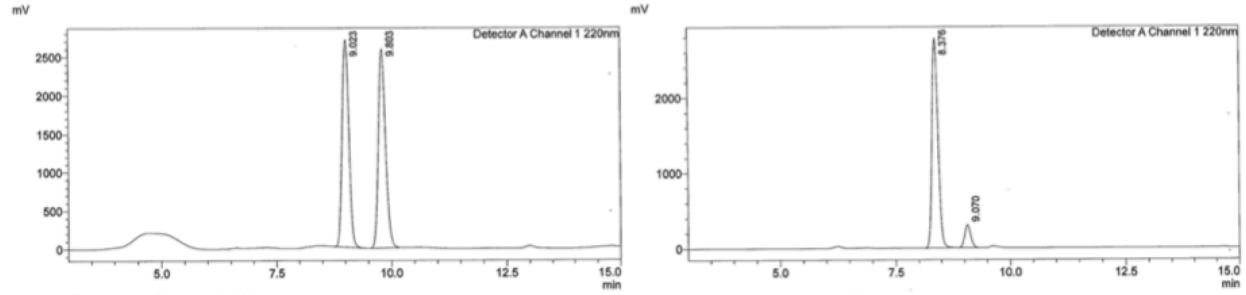

Detector A Channel 1 220nm

Peak#	Ret. Time	Area	Area%	Height
1	9.023	27256098	48.922	2697223
2	9.803	28457548	51.078	2590546
Total		55713646	100.000	5287769

Detector A Channel 1 220nm

Peak#	Ret. Time	Area	Area%	Height
1	8.376	25667265	90.139	2779515
2	9.070	2807804	9.861	302843
Total		28475069	100.000	3082359

Peak #	Ret. Time	Area	Area %	Peak #	Ret. Time	Area	Area %
1	9.0 min	27256098	48.922	1	8.4 min	25667265	90.139
2	9.8 min	28457548	51.978	2	9.1 min	2807804	9.861

(*S*)-2-Bromo-2-phenylpent-4-enal (2.28): The title compound was prepared analogous to **2.27** and purified by silica gel chromatography to afford **2.28** (12.5 mg, 0.0523 mmol, 58% yield) as pale-yellow oil. The analytical data are consistent with those reported previously.[171] **^{1}H NMR (400 MHz, $CDCl_3$):** δ 9.48 (s, 1H), 7.45–7.32 (m, 5H), 5.76–5.58 (m, 1H), 5.16–4.98 (m, 2H), 3.12 (dq, *J* = 6.9, 1.3 Hz, 2H); **Specific Rotation:** $[\alpha]^{24}_D$ –87.5 (*c* 0.57, $CHCl_3$) for a 93:7 er sample. The enantiomeric purity of this compound was determined by HPLC analysis in comparison with authentic racemic material (Chiralpak AZ-H, 98:2 hexanes:i-PrOH, 0.5 mL/min, 220 nm).

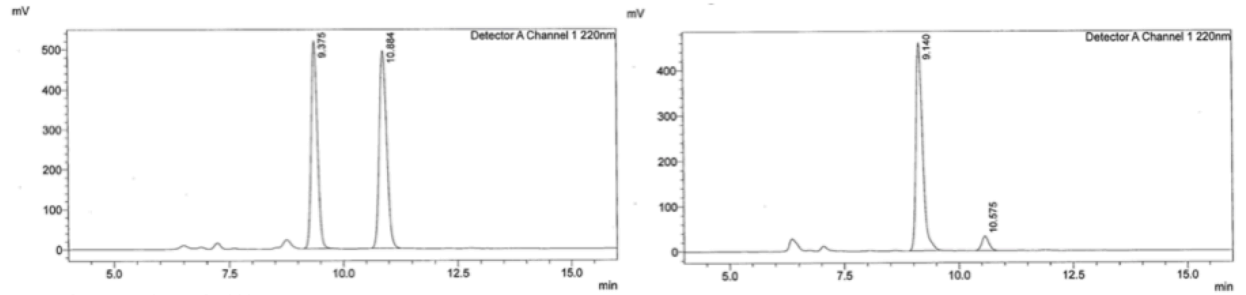

Detector A Channel 1 220nm

Peak#	Ret. Time	Area	Area%	Height
1	9.375	4993281	47.361	518457
2	10.884	5549819	52.639	493977
Total		10543101	100.000	1012434

Detector A Channel 1 220nm

Peak#	Ret. Time	Area	Area%	Height
1	9.140	4707071	92.891	458651
2	10.575	360209	7.109	32687
Total		5067280	100.000	491338

Peak #	Ret. Time	Area	Area %	Peak #	Ret. Time	Area	Area %
1	9.4 min	4993281	47.361	1	9.1 min	4707071	92.891
2	10.9 min	5549819	52.639	2	10.6 min	360209	7.109

[171] Wang, X.; Zhang, S. *Chin. J. Chem.* **2012**, *30*, 96–102.

2.8.10. Catalytic Enantioselective Allyl Additions to Fluoromethyl Ketones

2.8.10.1. Difluoromethyl ketones

In a N_2-filled glove box, **ap-11** (1.77 mg, 0.0025 mmol), $Zn(OMe)_2$ (1.27 mg, 0.01 mmol) and toluene (0.5 mL) were added to a two-dram vial equipped with a stir bar and the resulting solution was allowed to stir for 5 min. Ketone (0.10 mmol) and (pinacolato)allylboron (0.020 mL, 0.11 mmol) were added sequentially. The reaction vessel was sealed with a Teflon cap and the mixture was allowed to stir at –40 °C for 30 min. At this time, a sample of MeOH (0.010 mL, 0.25 mmol), which was in advance allowed to cool to –40 C for 30 min, was added to the solution. The vial was sealed with a Teflon cap and the mixture was allowed to stir for 18 h at –40 °C. Conversion was determined by analysis of the ^{1}H NMR spectrum of an aliquot. The mixture was directly loaded onto a silica gel column and eluted with hexanes/Et_2O to afford the desired product.

(*R*)-1,1-Difluoro-2-phenylpent-4-en-2-ol (2.31a): 15.9 mg, 0.0802 mmol, 80% yield, colorless oil. The analytical data are consistent with those reported previously.[172] **^{1}H NMR (400 MHz, $CDCl_3$):** δ 7.52 (d, *J* = 8.0 Hz, 2H), 7.40 (td, *J* = 7.7, 2.0 Hz, 2H), 7.33 (td, *J* = 7.2, 1.8 Hz, 1H), 5.90–5.52 (m, 2H), 5.32–5.07 (m, 3H), 2.80 (ddd, *J* = 81.9, 14.4, 7.3 Hz, 3H), 2.45 (d, *J* = 2.0 Hz, 1H); **Specific Rotation:** $[\alpha]^{24}_D$ +3.1 (*c* 0.54, $CHCl_3$) for a 85.5:14.5 er sample. The enantiomeric purity of this compound was determined by HPLC analysis in comparison with authentic racemic material (AS-H, 99:1 hexanes:*i*-PrOH, 0.5 mL/min, 220 nm).

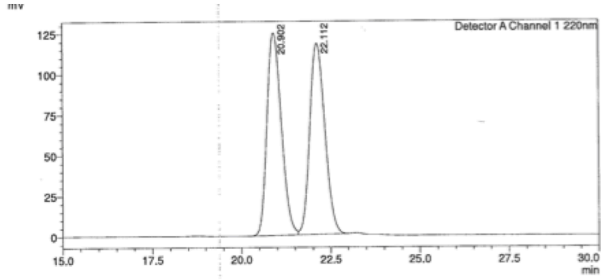

<Peak Table>
Detector A Channel 1 220nm

Peak#	Ret. Time	Area	Height	Area%
1	20.902	3516460	124842	50.112
2	22.112	3500722	117732	49.888
Total		7017182	242574	100.000

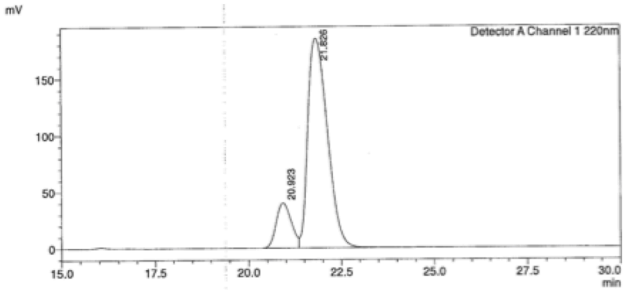

<Peak Table>
Detector A Channel 1 220nm

Peak#	Ret. Time	Area	Area%	Height
1	20.923	1138416	14.345	39908
2	21.826	6797478	85.655	185244
Total		7935894	100.000	225152

Peak #	Ret. Time	Area	Area %	Peak #	Ret. Time	Area	Area %
1	20.9 min	3516460	50.112	1	20.9 min	1138416	14.325
2	22.1 min	3500722	49.888	2	21.9 min	6797478	85.655

(*R*)-2-(4-Chlorophenyl)-1,1-difluoropent-4-en-2-ol (2.31b): 11.5 mg, 0.0494 mmol, 99% yield, colorless oil. **IR (neat):** 3549 (br), 3078 (w), 2978 (w), 1640 (w), 1491 (m), 1346 (m), 1066 (s), 955 (s), 926 (m), 798 (m), 699 (m), 558 (m) cm^{-1}; **^{1}H NMR (400 MHz, $CDCl_3$):** δ 7.46 (d, *J* = 8.2 Hz, 2H), 7.37 (dd, *J* = 8.5, 1.5 Hz, 2H), 5.86–5.52 (m, 2H), 5.29–5.13 (m, 2H), 2.78 (ddd, *J* = 57.6, 14.4, 7.3 Hz, 2H), 2.43 (s, 1H); **^{13}C NMR (101 MHz,$CDCl_3$):** δ 137.3, 134.4, 130.9, 128.7,

128.0, 121.6, 116.6 (t, J = 249.9 Hz), 75.3 (t, J = 21.6 Hz), 39.8 (t, J = 2.3 Hz); **^{19}F NMR (376 MHz, $CDCl_3$):** –127.23 to –132.31 (m, 2F); **HRMS (DART$^+$):** Calcd for $C_{11}H_{10}F_2Cl$ $[M+H–H_2O]^+$: 215.0434, Found: 215.0439; **Specific Rotation:** $[\alpha]^{24}_D$ –32.0 (*c* 1.08, $CHCl_3$) for a 74:26 er sample. The enantiomeric purity of this compound was determined by HPLC analysis in comparison with authentic racemic material (Chiralpak AS-H, 99:1 hexanes:*i*-PrOH, 0.5 mL/min, 220 nm).

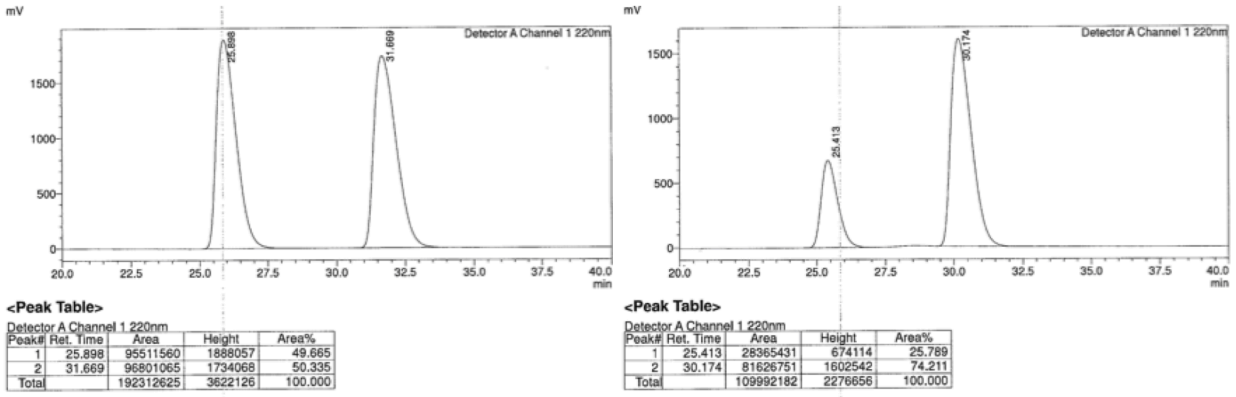

<Peak Table>
Detector A Channel 1 220nm

Peak#	Ret. Time	Area	Height	Area%
1	25.898	95511560	1888057	49.665
2	31.669	96801065	1734068	50.335
Total		192312625	3622126	100.000

<Peak Table>
Detector A Channel 1 220nm

Peak#	Ret. Time	Area	Height	Area%
1	25.413	28365431	674114	25.789
2	30.174	81626751	1602542	74.211
Total		109992182	2276656	100.000

Peak #	Ret. Time	Area	Area %	Peak #	Ret. Time	Area	Area %
1	25.9 min	95511560	49.665	1	25.4 min	28365431	25.789
2	31.7 min	96801065	50.335	2	30.2 min	1602542	74.211

***tert*-Butyl-(*R*)-2-(1,1-difluoro-2-hydroxypent-4-en-2-yl)-1*H*-indole-1-carboxylate (2.31c):** 16.0 mg, 0.0859 mmol, 86% yield, colorless oil. **IR (neat):** 3498 (br), 3079 (w), 2977 (w), 2926 (w), 1733 (m), 1450 (m), 1369 (s), 1251 (s), 1151 (s), 1066 (s), 746 (s), 556 (w) cm^{-1}; **^{1}H NMR (400 MHz, $CDCl_3$):** δ 8.19 (d, J = 8.7 Hz, 1H), 7.91–7.78 (m, 1H), 7.65 (s, 1H), 7.46–7.29 (m, 1H), 7.29–7.16 (m, 1H), 5.85 (m, 2H), 5.39–5.14 (m, 2H), 3.04 (dd, J = 14.3, 6.6 Hz, 1H), 2.81 (dd, J = 14.3, 8.2 Hz, 1H), 2.54 (s, 1H), 1.68 (s, 9H); **^{13}C NMR (101 MHz,$CDCl_3$):** δ 149.4, 136.0, 131.2, 127.9, 124.7, 124.5, 122.8, 121.2, 121.0, 118.8, 116.3 (t, J = 249.6 Hz), 115.4, 84.1, 74.3 (t, J = 22.8 Hz), 38.7, 28.2; **^{19}F NMR (376 MHz, $CDCl_3$):** δ –128.51 to –130.74 (m, 2F); **HRMS (DART$^+$):** Calcd for $C_{18}H_{22}NO_3F_2$ $[M+H]^+$: 338.1562, Found: 338.1562; **Specific Rotation:** $[\alpha]^{24}_D$ –27.6 (*c* 1.28, $CHCl_3$) for a >99:1 er sample. The enantiomeric purity of this compound was determined by HPLC analysis in comparison with authentic racemic material (Chiralpak AS-H, 99:1 hexanes:*i*-PrOH, 0.5 mL/min, 220 nm).

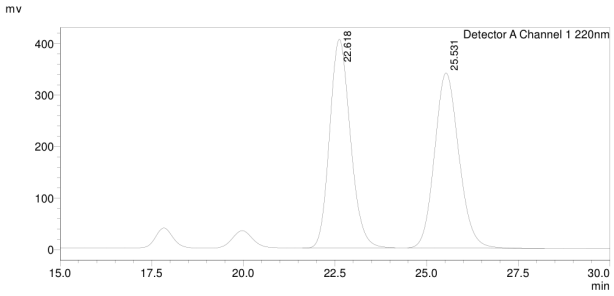

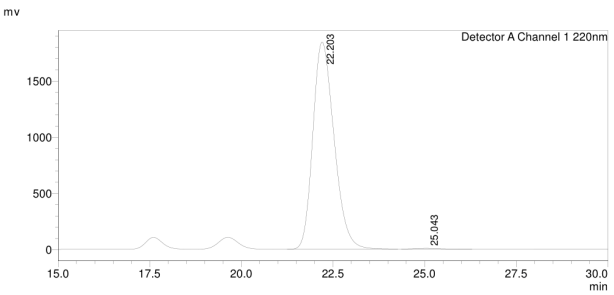

<Peak Table>

Detector A Channel 1 220nm

Peak#	Ret. Time	Area	Height	Area%
1	22.618	15966118	404913	50.463
2	25.531	15673291	339580	49.537
Total		31639410	744493	100.000

<Peak Table>

Detector A Channel 1 220nm

Peak#	Ret. Time	Area	Height	Area%
1	22.203	74370283	1843524	99.618
2	25.043	284855	6816	0.382
Total		74655138	1850340	100.000

Peak #	Ret. Time	Area	Area %	Peak #	Ret. Time	Area	Area %
1	22.6 min	15966118	50.463	1	22.2 min	1843524	99.618
2	25.5 min	15673291	49.537	2	25.0 min	284855	0.382

(*S*)-1,1-Difluoro-2-(thiophen-2-yl)pent-4-en-2-ol (2.31d): 10.4 mg, 0.0509 mmol, 93% yield, colorless oil. **IR (neat):** 3536 (br), 3076 (w), 2979 (w), 2849 (w), 1640 (w), 1436 (m), 1251 (m), 1134 (s), 1069 (s), 997 (m), 783 (s), 595 (w) cm^{-1}; **^{1}H NMR (400 MHz, $CDCl_3$):** δ 7.32 (dd, *J* = 5.0, 1.3 Hz, 1H), 7.14–6.93 (m, 2H), 5.74 (m, 2H), 5.36–5.17 (m, 2H), 3.18–2.68 (m, 2H), 2.65 (s, 1H); **^{13}C NMR (101 MHz,$CDCl_3$):** δ 143.1, 130.9, 127.4, 125.6 (d, *J* = 67.6 Hz), 121.7, 121.6, 116.0 (t, *J* = 252.5 Hz), 75.2 (t, *J* = 22.9 Hz), 40.6; **^{19}F NMR (376 MHz, $CDCl_3$):** δ –128.49 to –133.11 (m); **HRMS (DART^{+}):** Calcd for $C_9H_9F_2S$ $[M+H–H_2O]^{+}$: 187.0388, Found: 187.0394; **Specific Rotation:** $[\alpha]^{24}_{D}$ –7.9 (*c* 1.07, $CHCl_3$) for a 96:4 er sample. The enantiomeric purity of this compound was determined by HPLC analysis in comparison with authentic racemic material (Chiralpak AD-H, 98:2 hexanes:*i*-PrOH, 0.5 mL/min, 220 nm).

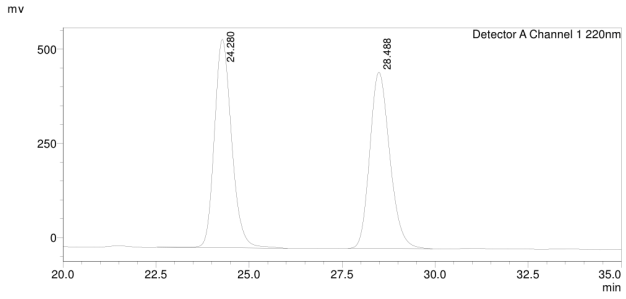

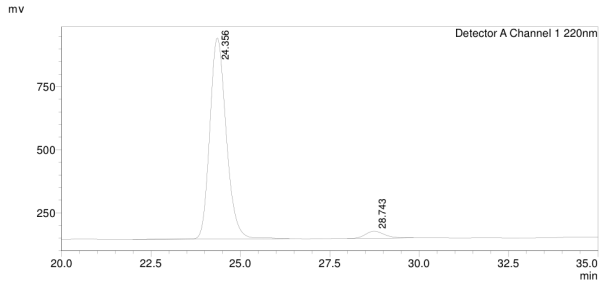

<Peak Table>

Detector A Channel 1 220nm

Peak#	Ret. Time	Area	Height	Area%
1	24.280	17823934	552549	50.465
2	28.488	17495190	467217	49.535
Total		35319124	1019767	100.000

<Peak Table>

Detector A Channel 1 220nm

Peak#	Ret. Time	Area	Height	Area%
1	24.356	25606920	796916	96.167
2	28.743	1020739	27664	3.833
Total		26627659	824580	100.000

Peak #	Ret. Time	Area	Area %	Peak #	Ret. Time	Area	Area %
1	24.2 min	17823934	50.465	1	24.4 min	25606920	96.167
2	28.5 min	17495190	49.535	2	28.7 min	1020739	3.833

(*S*)-1,1-Difluoro-2-(thiophen-3-yl)pent-4-en-2-ol (2.31e): 19.4 mg, 0.0950 mmol, 95% yield, yellow oil. **IR (neat):** 3460 (br), 3110 (w), 3078 (w), 2978 (w), 1639 (w), 1341 (m), 1233 (m),

1120 (m), 1063 (s), 994 (m), 823 (m), 657 (m) cm^{-1}; **^{1}H NMR (400 MHz, $CDCl_3$):** δ 7.37–7.32 (m, 1H), 7.12 (ddt, *J* = 4.8, 1.8, 0.9 Hz, 1H), 5.72 (t, *J* = 56.3 Hz, 1H), 5.72–5.60 (m, 1H), 5.28–5.14 (m, 2H), 2.83–2.64 (m, 2H), 2.48 (s, 1H); **^{13}C NMR (101 MHz,$CDCl_3$):** δ 140.43, 131.78 (d, *J* = 5.3 Hz), 130.27, 127.25 – 125.09 (m), 125.83 (dt, *J* = 166.5, 6.8 Hz), 122.87 (ddd, *J* = 184.4, 7.5, 4.0 Hz), 120.93 (td, *J* = 153.3, 152.8, 5.5 Hz), 117.30 (t, *J* = 249.7 Hz), 115.40 (t, *J* = 248.9 Hz), 74.77 (t, *J* = 23.2 Hz), 39.85 (t, *J* = 128.1 Hz); **^{19}F NMR (376 MHz, $CDCl_3$):** δ –128.79 to –131.33 (m); **HRMS (DART$^+$):** Calcd for $C_9H_9F_2S$ $[M+H–H_2O]^+$: 187.0388, Found: 187.0394; **Specific Rotation:** $[\alpha]^{24}_D$ –28.4 (*c* 1.61, $CHCl_3$) for a 79:21 er sample. The enantiomeric purity of this compound was determined by HPLC analysis in comparison with authentic racemic material (Chiralpak AD-H, 98:2 hexanes:*i*-PrOH, 0.5 mL/min, 220 nm).

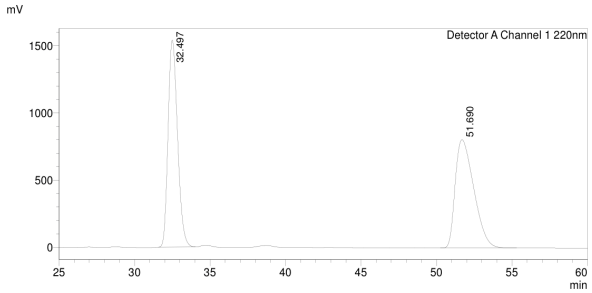

<Peak Table>
Detector A Channel 1 220nm

Peak#	Ret. Time	Area	Height	Area%
1	32.497	67085858	1538792	49.326
2	51.690	68919474	805738	50.674
Total		136005331	2344530	100.000

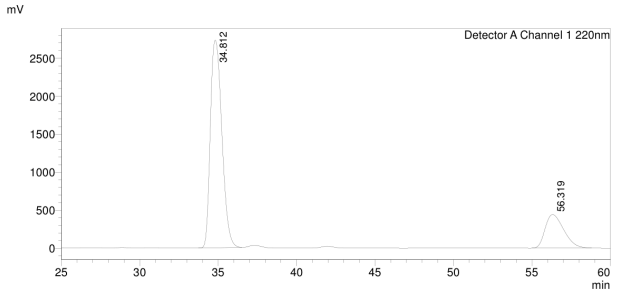

<Peak Table>
Detector A Channel 1 220nm

Peak#	Ret. Time	Area	Height	Area%
1	34.812	139500089	2732009	79.283
2	56.319	36453027	442001	20.717
Total		175953116	3174010	100.000

Peak #	Ret. Time	Area	Area %	Peak #	Ret. Time	Area	Area %
1	32.5 min	67085858	49.326	1	34.8 min	1395000089	79.283
2	51.7 min	68919474	50.674	2	56.3 min	36453027	20.717

(*R*)-2-Cyclohexyl-1,1-difluoropent-4-en-2-ol (2.31f): 9.3 mg, 0.0455 mmol, 91% yield, colorless oil. **IR (neat):** 3469 (br), 2928 (s), 2853 (m), 1640 (w), 1450 (m), 1339 (w), 1102 (s), 916 (m), 792 (w), 733 (m), 570 (w), 501 (w) cm^{-1}; **^{1}H NMR (400 MHz, $CDCl_3$):** δ 5.94–5.53 (m, 2H), 5.30–4.91 (m, 2H), 2.39 (qd, *J* = 14.3, 7.4 Hz, 2H), 1.93–1.72 (m, 5H), 1.63 (dd, *J* = 31.1, 12.3 Hz, 2H), 1.41–1.01 (m, 5H); **^{13}C NMR (101 MHz,$CDCl_3$):** δ 132.3, 120.1, 117.6, 43.3, 36.3, 26.9, 26.8, 26.8, 26.5; **^{19}F NMR (376 MHz, $CDCl_3$):** δ –126.11 to –132.74 (m, 2F); **HRMS (DART$^+$):** Calcd for $C_{11}H_{19}OF_2$ $[M+H]^+$: 205.1399, Found: 205.1390; **Specific Rotation:** $[\alpha]^{24}_D$ +1.4 (*c* 0.92, $CHCl_3$) for a 96:4 er sample. In order to determine the enantiomeric purity of this compound, the product was derivatized by cross-metathesis with **Ru-1** and benzyl acrylate (see **15** for experimental details). The er was determined by HPLC analysis of the product in comparison with authentic racemic material (Chiralpak AD-H, 98:2 hexanes:*i*-PrOH, 0.5 mL/min, 220 nm).

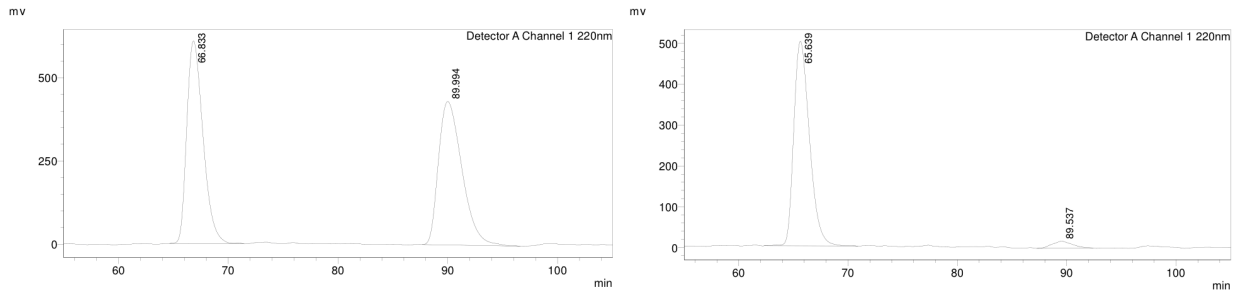

<Peak Table>
Detector A Channel 1 220nm

Peak#	Ret. Time	Area	Height	Area%
1	66.833	62839208	609338	49.447
2	89.994	64243536	431391	50.553
Total		127082744	1040729	100.000

<Peak Table>
Detector A Channel 1 220nm

Peak#	Ret. Time	Area	Height	Area%
1	65.639	50251700	501582	95.845
2	89.537	2178669	17158	4.155
Total		52430369	518740	100.000

Peak #	Ret. Time	Area	Area %	Peak #	Ret. Time	Area	Area %
1	66.8 min	62839208	49.447	1	65.6 min	50251700	95.845
2	90.0 min	64243536	50.553	2	89.5 min	2178669	4.155

2.8.10.2. Monofluoromethyl ketones

In a N_2-filled glove box, **ap-10** (1.64 mg, 0.003 mmol), $Zn(OMe)_2$ (1.27 mg, 0.01 mmol) and toluene (0.5 mL) were added to an two-dram vial equipped with a stir bar and allowed to stir for 5 min. Ketone (0.10 mmol) and (pinacolato)allylboron (0.020 mL, 0.11 mmol) were added sequentially. The reaction vessel was sealed with a Teflon cap and the mixture was allowed to stir at –40 °C for 30 min, after which MeOH (0.0052 mL, 0.13 mmol) was added. The vial was sealed with a Teflon cap and removed from the glove box and the mixture was allowed to stir for an additional 2 h at 4 °C. The mixture was directly loaded onto a silica gel column and eluted with hexanes/Et_2O to afford the desired product.

(*S*)-1-Fluoro-2-phenylpent-4-en-2-ol (2.33a): 15.3 mg, 0.0858 mmol, 87% yield, colorless oil. The analytical data are full consistent with those reported previously.[172] **^{1}H NMR (400 MHz, $CDCl_3$):** δ 7.48–7.44 (m, 2H), 7.42–7.35 (m, 2H), 7.33–7.27 (m, 1H), 5.73–5.54 (m, 1H), 5.22–5.07 (m, 2H), 4.49 (d, J = 47.7 Hz, 2H), 2.72 (ddt, J = 7.0, 5.8, 1.2 Hz, 2H), 2.44 (s, 1H); **Specific Rotation:** $[\alpha]^{24}_D$ –113.8 (*c* 1.29, $CHCl_3$) for a 92.5:7.5 er sample. The enantiomeric purity of this compound was determined by HPLC analysis in comparison with authentic racemic material (Chiralpak AZ-H, 98:2 hexanes:*i*-PrOH, 0.5 mL/min, 220 nm).

[172] Lee, K.; Silverio, D. L.; Torker, S.; Robbins, D. W.; Haeffner, F.; van der Mei, F. W.; Hoveyda, A. H. *Nat. Chem.* **2016**, *8*, 768–777.

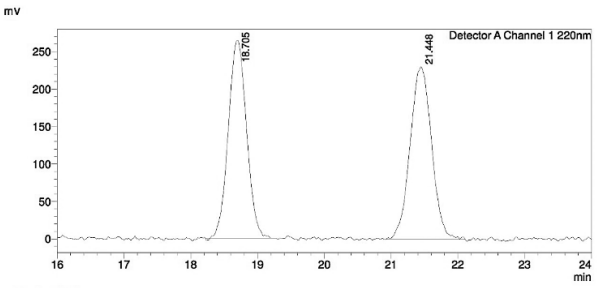

<Peak Table>
Detector A Channel 1 220nm

Peak#	Ret. Time	Area	Height	Area%
1	18.705	5001866	263658	49.051
2	21.448	5195351	230411	50.949
Total		10197216	494070	100.000

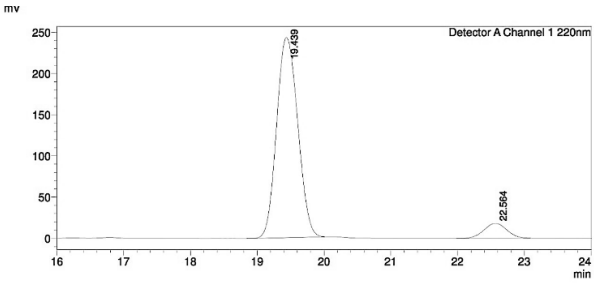

<Peak Table>
Detector A Channel 1 220nm

Peak#	Ret. Time	Area	Area%	Height
1	19.439	5346217	92.595	242883
2	22.564	427534	7.405	17936
Total		5773751	100.000	260819

Peak #	Ret. Time	Area	Area %	Peak #	Ret. Time	Area	Area %
1	18.7 min	5001866	49.051	1	19.4 min	5346217	92.595
2	21. 4 min	5195351	50.949	2	22.6 min	427534	7.405

(*S*)-1-Fluoro-2-(4-methoxyphenyl)pent-4-en-2-ol (2.33b): 20.0 mg, 0.0951 mmol, 95% yield, colorless oil. **IR (neat):** 3464 (br), 3077 (w), 2954 (w), 2838 (w), 1640 (m), 1513 (s), 1248 (s), 1179 (m), 1030 (m), 920 (m), 831 (m), 589 (m) cm^{-1}; **^{1}H NMR (400 MHz, $CDCl_3$):** δ 7.44–7.34 (m, 2H), 6.94–6.83 (m, 2H), 5.64 (ddddd, *J* = 17.0, 10.1, 7.7, 6.8, 0.8 Hz, 1H), 5.20–5.06 (m, 2H), 4.54–4.34 (m, 2H), 3.81 (s, 3H), 2.79–2.61 (m, 2H), 2.42 (s, 1H); **^{13}C NMR (101 MHz, $CDCl_3$):** δ 159.1, 133.7 (d, *J* = 4.1 Hz), 132.4, 126.9 (d, *J* = 1.1 Hz), 120.0, 113.9, 88.7 (d, *J* = 178.4 Hz), 74.9 (d, *J* = 18.0 Hz), 55.4, 42.5 (d, *J* = 3.1 Hz); **^{19}F NMR (376 MHz, $CDCl_3$):** δ –222.33 (t, 1F); **HRMS (DART$^+$):** Calcd for $C_{12}H_{14}FO$ $[M+H–H_2O]^+$: 193.10327, Found: 193.10287; **Specific Rotation:** $[\alpha]^{24}_D$ –29.3 (*c* 1.40, $CHCl_3$) for a 91:9 er sample. The enantiomeric purity of this compound was determined by HPLC analysis in comparison with authentic racemic material (Chiralpak AZ-H, 98:2 hexanes:*i*-PrOH, 0.5 mL/min, 220 nm).

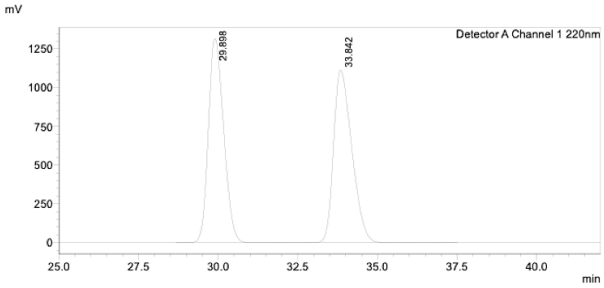

<Peak Table>
Detector A Channel 1 220nm

Peak#	Ret. Time	Area	Height	Area%
1	29.898	44051386	1316139	49.734
2	33.842	44522987	1113248	50.266
Total		88574373	2429388	100.000

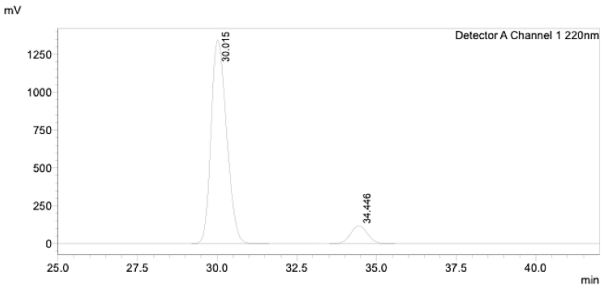

<Peak Table>
Detector A Channel 1 220nm

Peak#	Ret. Time	Area	Height	Area%
1	30.015	45596167	1346157	91.196
2	34.446	4401933	119018	8.804
Total		49998100	1465175	100.000

Peak #	Ret. Time	Area	Area %	Peak #	Ret. Time	Area	Area %
1	29.9 min	44051386	49.734	1	30.0 min	45596167	91.196
2	33.8 min	44522987	50.266	2	34.4 min	4401933	8.804

(*S*)-2-(4-Chlorophenyl)-1-fluoropent-4-en-2-ol (2.33c): 19.7 mg, 0.0918 mmol, 92% yield, colorless oil. **IR (neat):** 3568 (br), 3079 (w), 2297 (w), 2980 (w), 1641 (m), 1403 (w), 1347 (w), 1143 (m), 1014 (s), 923 (m), 829 (m), 762 (w) cm^{1}; **^{1}H NMR (400 MHz, $CDCl_3$):** δ 7.99–6.80 (m, 4H), 5.61 (ddt, *J* = 17.4, 10.3, 7.4 Hz, 1H), 5.42–4.94 (m, 2H), 4.46 (dd, *J* = 47.6, 1.0 Hz, 2H), 2.68 (dq, *J* = 7.6, 1.2 Hz, 2H), 2.47 (s, 1H); **^{13}C NMR (101 MHz,$CDCl_3$):** δ 140.3 (d, *J* = 3.6 Hz), 133.7, 131.9, 128.7, 127.2 (d, *J* = 1.1 Hz), 120.5, 88.4 (d, *J* = 178.4 Hz), 74.9 (d, *J* = 18.3 Hz), 42.6 (d, *J* = 3.4 Hz); **^{19}F NMR (376 MHz, $CDCl_3$):** δ –224.93 (t, *J* = 47.7 Hz, 1F); **HRMS (DART^{+}):** Calcd for $C_{11}H_{11}ClF$ $[M+H–H_2O]^{+}$: 197.0533, Found: 197.0538; **Specific Rotation:** $[\alpha]^{24}_{D}$ –51.2 (*c* 1.43, $CHCl_3$) for a 90:10 er sample. The enantiomeric purity of this compound was determined by HPLC analysis in comparison with authentic racemic material (Chiralpak AS-H, 98:2 hexanes:*i*-PrOH, 0.5 mL/min, 220 nm).

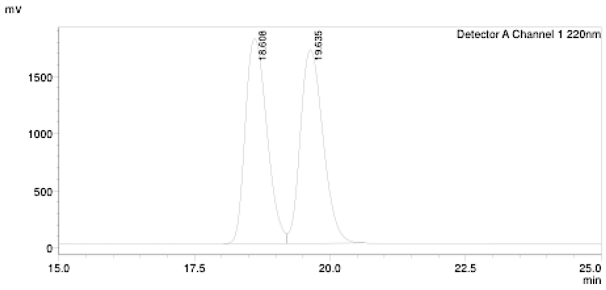

<Peak Table>
Detector A Channel 1 220nm

Peak#	Ret. Time	Area	Area%	Height
1	18.608	49658714	50.192	1792299
2	19.635	49279148	49.808	1693922
Total		98937862	100.000	3486222

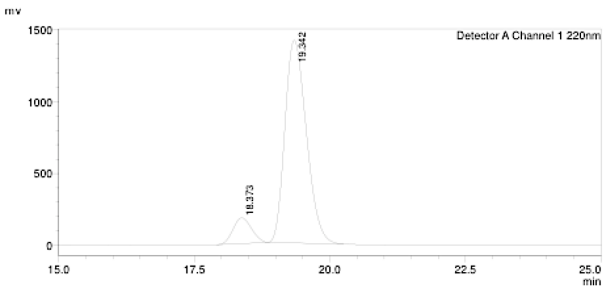

<Peak Table>
Detector A Channel 1 220nm

Peak#	Ret. Time	Area	Area%	Height
1	18.373	4232054	9.821	178358
2	19.342	38858687	90.179	1407393
Total		43090741	100.000	1585750

Peak #	Ret. Time	Area	Area %	Peak #	Ret. Time	Area	Area %
1	18.8 min	49658714	50.192	1	18.4 min	4232054	9.821
2	19.6 min	49279148	49.808	2	19.3 min	38858687	90.179

(*S*)-2-(3,5-Dichlorophenyl)-1-fluoropent-4-en-2-ol (2.33d): 19.3mg, 0.0775 mmol, 82% yield, colorless oil. **IR (neat):** 3565 (br), 3466 (br), 2957 (w), 2926 (w), 2857 (w), 1566 (m), 1417 (m), 1192 (m), 1098 (m), 1017 (m), 858 (m), 798 (s) cm^{-1}; **^{1}H NMR (400 MHz, $CDCl_3$):** δ 7.36 (d, *J* = 1.9 Hz, 2H), 7.30 (t, *J* = 1.9 Hz, 1H), 5.68–5.53 (m, 1H), 5.24–5.13 (m, 2H), 4.56–4.34 (m, 2H), 2.66 (dq, *J* = 7.3, 1.2 Hz, 2H), 2.50 (d, *J* = 0.8 Hz, 1H); **^{13}C NMR (101 MHz,$CDCl_3$):** δ 145.6 (d, *J* = 3.1 Hz), 135.3, 131.4, 127.93, 124.6, 121.2 (t, *J* = 2.5 Hz), 88.0 (d, *J* = 178.7 Hz), 74.7 (d, *J* = 18.4 Hz), 42.6 (d, *J* = 3.1 Hz); **^{19}F NMR (376 MHz, $CDCl_3$):** δ –71.76 (t, *J* = 47.1 Hz); **HRMS (DART^{+}):** Calcd for $C_{11}H_{10}Cl_2F$ $[M+H–H_2O]^{+}$: 231.0144, Found: 231.0153; **Specific Rotation:** $[\alpha]^{24}_{D}$ –50.4 (*c* 1.75, $CHCl_3$) for a 88.5:11.5 er sample. The enantiomeric purity of this compound was determined by HPLC analysis in comparison with authentic racemic material (Chiralpak AZ-H, 98:2 hexanes:*i*-PrOH, 0.5 mL/min, 220 nm).

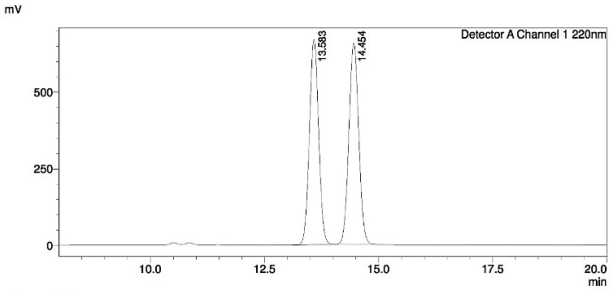

<Peak Table>
Detector A Channel 1 220nm

Peak#	Ret. Time	Area	Area%	Height
1	13.583	9398894	48.820	669701
2	14.454	9853293	51.180	656333
Total		19252187	100.000	1326034

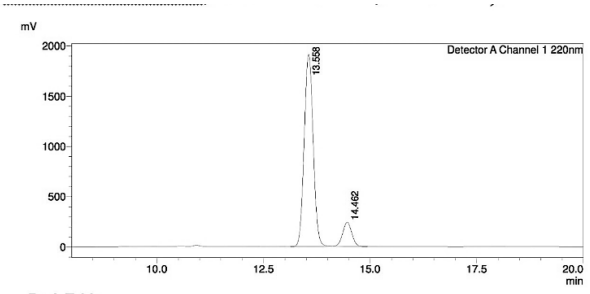

<Peak Table>
Detector A Channel 1 220nm

Peak#	Ret. Time	Area	Area%	Height
1	13.558	28077005	88.633	1911455
2	14.462	3600642	11.367	241220
Total		31677647	100.000	2152675

Peak #	Ret. Time	Area	Area %	Peak #	Ret. Time	Area	Area %
1	13.6 min	9398894	48.820	1	13.6 min	28077005	88.633
2	14.5 min	9853293	51.180	2	14.5 min	3600642	11.367

(*S*)-1-Fluoro-2-(*o*-tolyl)pent-4-en-2-ol (2.33e): 17.2 mg, 0.0885 mmol, 89% yield, colorless oil. **IR (neat):** 3555 (br), 3074 (w), 3074 (w), 2979 (w), 1639 (m), 1384 (m), 1260 (m), 977 (s), 917 (s), 760 (s), 728 (s), 595 (s) cm^{-1}; **^{1}H NMR (400 MHz, $CDCl_3$):** δ 7.49–7.37 (m, 1H), 7.24–7.13 (m, 3H), 5.72–5.54 (m, 1H), 5.22–5.07 (m, 2H), 4.78–4.47 (m, 2H), 2.95–2.62 (m, 2H), 2.56 (s, 3H), 2.52–2.37 (m, 1H); **^{13}C NMR (101 MHz,$CDCl_3$):** δ 138.9 (d, *J* = 3.4 Hz), 136.3, 133.1, 132.7, 127.9, 127.2 (d, *J* = 1.7 Hz), 126.0, 119.8 (t, *J* = 2.4 Hz), 87.6 (d, *J* = 176.6 Hz), 76.6 (d, *J* = 17.9 Hz), 41.5, 22.6; **^{19}F NMR (376 MHz, $CDCl_3$):** δ –225.60 (t, 1F); **HRMS (DART$^+$):** Calcd for $C_{12}H_{19}FON$ $[M+NH_4]^+$: 212.1443, Found: 212.1451; **Specific Rotation:** $[\alpha]^{24}_D$ –13.0 (*c* 0.83, $CHCl_3$) for a 98:2 er sample. The enantiomeric purity of this compound was determined by HPLC analysis in comparison with authentic racemic material (Chiralpak AZ-H, 98:2 hexanes:*i*-PrOH, 0.5 mL/min, 220 nm).

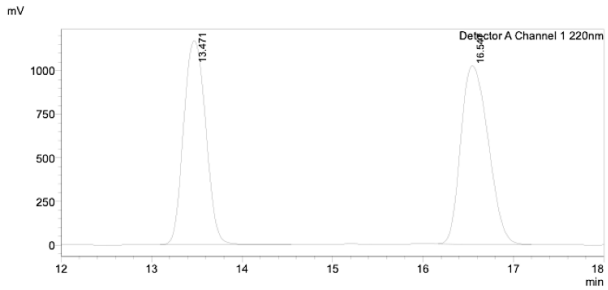

<Peak Table>
Detector A Channel 1 220nm

Peak#	Ret. Time	Area	Height	Area%
1	13.471	19931814	1171842	47.992
2	16.547	21599660	1023569	52.008
Total		41531474	2195412	100.000

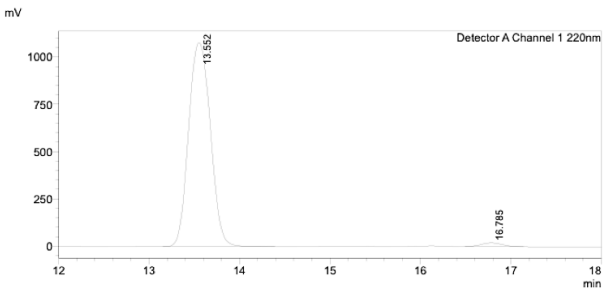

<Peak Table>
Detector A Channel 1 220nm

Peak#	Ret. Time	Area	Height	Area%
1	13.552	18067117	1079412	98.213
2	16.785	328750	19601	1.787
Total		18395867	1099014	100.000

Peak #	Ret. Time	Area	Area %	Peak #	Ret. Time	Area	Area %
1	13.5 min	19931814	47.992	1	13.6 min	18067117	98.213
2	16.5 min	21599660	52.008	2	16.8 min	328750	1.787

(*R*)-1-Fluoro-2-(thiophen-2-yl)pent-4-en-2-ol (2.33f): 18.0 mg, 0.0966 mmol, 96% yield, colorless oil. **IR (neat):** 3544 (br), 3074 (w), 2978 (w), 2949 (w), 1639 (w), 1532 (m), 1238 (m),

1045 (s), 997 (s), 847 (m), 699 (s), 563 (w) cm^{-1}; **^{1}H NMR (400 MHz, $CDCl_3$):** δ 7.27 (dd, *J* = 5.0, 1.3 Hz, 1H), 7.12–6.84 (m, 2H), 5.74 (ddt, *J* = 17.4, 10.3, 7.3 Hz, 1H), 5.46–4.87 (m, 2H), 4.87–4.07 (m, 2H), 2.74 (dq, *J* = 7.4, 1.3 Hz, 2H), 2.68 (s, 1H); **^{13}C NMR (101 MHz,$CDCl_3$):** δ 146.47 (d, *J* = 4.1 Hz), 131.99 (d, *J* = 2.4 Hz), 127.19, 125.15 (d, *J* = 3.0 Hz), 123.93, 120.67 (t, *J* = 6.1 Hz), 88.26 (d, *J* = 180.0 Hz), 74.58 (d, *J* = 19.1 Hz), 43.44 (d, *J* = 2.8 Hz); **^{19}F NMR (376 mHz, $CDCl_3$):** –222.30 to –223.63 (m, 1F); **HRMS (DART^{+}):** Calcd for $C_9H_{10}FS$ $[M+H–H_2O]^{+}$:169.0482, Found: 169.0474; **Specific Rotation:** $[\alpha]^{24}_D$ –20.1 (*c* 1.21, $CHCl_3$) for a 95:5 er sample. The enantiomeric purity of this compound was determined by HPLC analysis in comparison with authentic racemic material (Chiralpak AZ-H, 98:2 hexanes:*i*-PrOH, 0.5 mL/min, 220 nm).

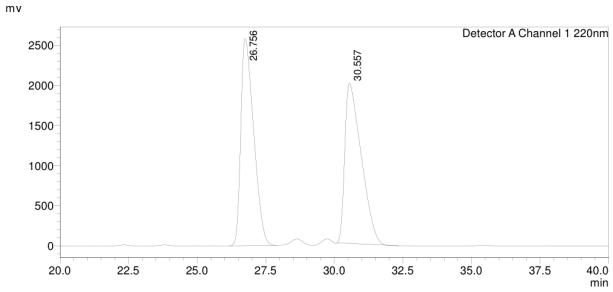

<Peak Table>
Detector A Channel 1 220nm

Peak#	Ret. Time	Area	Height	Area%
1	26.756	84228268	2584934	50.314
2	30.557	83177818	1998192	49.686
Total		167406086	4583126	100.000

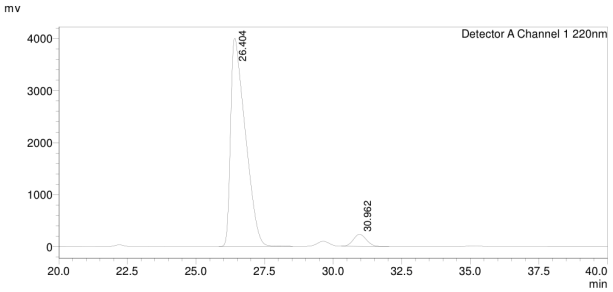

<Peak Table>
Detector A Channel 1 220nm

Peak#	Ret. Time	Area	Height	Area%
1	26.404	149220811	3995302	95.115
2	30.962	7664061	231194	4.885
Total		156884872	4226496	100.000

Peak #	Ret. Time	Area	Area %	Peak #	Ret. Time	Area	Area %
1	26.8 min	84228268	50.314	1	26.4 min	3995302	95.115
2	30.6 min	83177818	49.686	2	31.0 min	231194	4.885

(*S*)-2-Cyclohexyl-1-fluoropent-4-en-2-ol (2.33g): 16.0 mg, 0.0859 mmol, 86% yield, colorless oil. **IR (neat):** 3469 (br), 2924 (s), 2851 (m), 1713 (w), 1639 (w), 1449 (m), 1192 (w), 998 (m), 910 (s), 731 (s), 649 (w), 592 (w) cm^{-1}; **^{1}H NMR (400 MHz, $CDCl_3$):** δ 5.87 (ddt, *J* = 17.3, 10.3, 7.4 Hz, 1H), 5.35–4.98 (m, 2H), 4.62–4.12 (m, 2H), 2.33 (d, *J* = 7.5 Hz, 2H), 2.16–1.94 (m, 1H), 1.80 (d, *J* = 14.4 Hz, 4H), 1.74–1.45 (m, 2H), 1.31–1.03 (m, 5H); **^{13}C NMR (101 MHz,$CDCl_3$):** δ 133.0, 119.1, 86.6 (d, *J* = 172.4 Hz), 74.5 (d, *J* = 16.6 Hz), 43.7 (d, *J* = 3.0 Hz), 38.5 (d, *J* = 4.5 Hz), 26.8 (d, *J* = 1.0 Hz), 26.7 (d, *J* = 2.2 Hz), 26.4; **^{19}F NMR (376 MHz, $CDCl_3$):** δ –231.59 (t, *J* = 47.3 Hz, 1F); **HRMS (DART^{+}):** Calcd for $C_8H_{18}OF$ $[M+H–H_2O]^{+}$: 149.1336, Found: 149.1332; **Specific Rotation:** $[\alpha]^{24}_D$ –1.0 (*c* 1.03, $CHCl_3$) for a 96:4 er sample. The enantiomeric purity of this compound was determined by GLC analysis in comparison with authentic racemic material (Chiraldex CDB/DM, 10 psi, 80 °C).

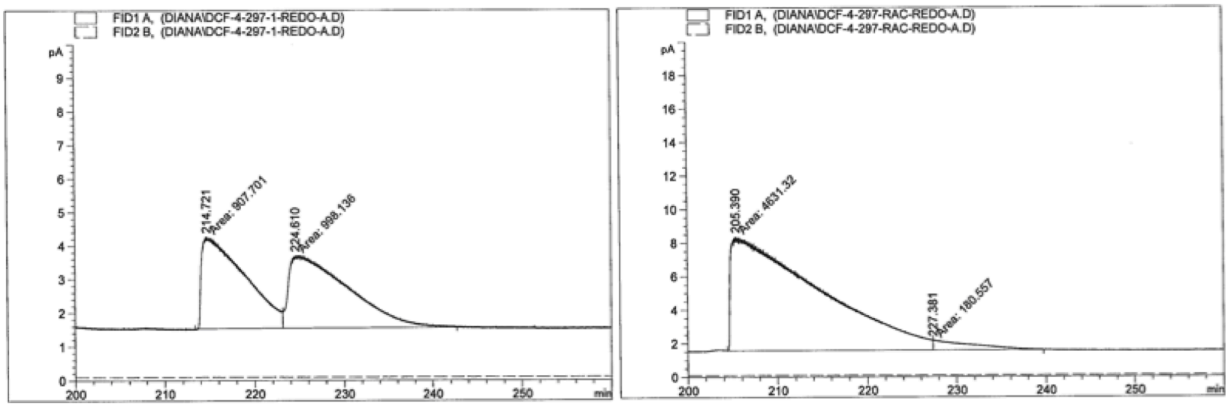

Peak #	RetTime [min]	Type	Width [min]	Area [pA*s]	Height [pA]	Area %
1	214.721	MF	5.5030	907.70093	2.74913	47.62742
2	224.610	FM	7.6424	998.13586	2.17676	52.37258
Totals :				1905.83679	4.92589	

Peak #	RetTime [min]	Type	Width [min]	Area [pA*s]	Height [pA]	Area %
1	205.390	MF	11.3117	4631.31982	6.82380	96.24767
2	227.381	FM	4.9397	180.55737	6.09202e-1	3.75233
Totals :				4811.87720	7.43300	

Peak #	Ret. Time	Area	Area %	Peak #	Ret. Time	Area	Area %
1	214.7 min	907.70093	47.62742	1	205.4 min	4631.31982	96.24767
2	224.6 min	998.13586	48.747	2	227.3 min	180.55737	3.75233

2.8.11. Synthesis of Analogs of Biologically Active Triazole-Containing Halomethyl Ketones

2.8.11.1. Additions to triazole-containing halomethyl ketones

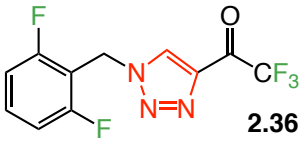

2.36

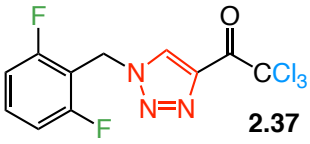

2.37

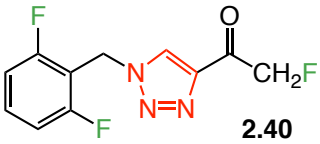

2.40

2,2,2-Trifluoro-1-(1-(2,6-difluorobenzyl)-1*H*-1,2,3-triazol-4-yl)ethan-1-one (2.36): The title compound was synthesized according to a previous procedure.[173] The analytical data are consistent with those reported previously and the melting point has been provided. **IR (neat):** 3152 (w), 2928 (w), 1725 (m), 1628 (m), 1595 (w), 1473 (s), 1264 (m), 1167 (m), 1037 (m), 914 (m), 738 (m), 703 (m) cm^{-1}; **^{19}F NMR (376 MHz, $CDCl_3$):** δ –74.92 (s, 3F), –113.97 (s, 2F).

2,2,2-Trichloro-1-(1-(2,6-difluorobenzyl)-1*H*-1,2,3-triazol-4-yl)ethan-1-one (2.37): The title compound was synthesized according to a previous procedure.[174] The analytical data are consistent with those reported previously and the melting point has been provided. **IR (neat):**

[173] Bonacorso, H. G.; Moraes, M. C.; Wiethan, C. W.; Luz, F. M.; Meyer, A. R.; Zanatta, N.; Martins, M. A. P. *J. Fluorine Chem*. **2013**, *156*, 112–119.

[174] Bonacorso, H. G.; Moraes, M. C.; Luz, F. M.; Quintana, P. S.; Zanatta, N.; Martins, M. A. P. *Tetrahedron Lett.* **2015**, *56*, 441–444.

3142 (w), 3011 (w), 1714 (s), 1627 (m), 1472 (s), 1236 (m), 1064 (m), 850 (m), 796 (s), 689 (m), 543 (w) cm^{-1}; **^{19}F NMR (376 MHz, $CDCl_3$):** δ –113.92 (t, *J* = 5.9 Hz, 2F).

1-(1-(2,6-Difluorobenzyl)-1*H*-1,2,3-triazol-4-yl)-2-fluoroethan-1-one (2.40): The title compound was synthesized according to a previous procedure.[175] **Melting point:** 113–118 °C; **IR (neat):** 3123 (w), 3093 (w), 2921 (w), 1707 (s), 1627 (m), 1471 (s), 1275 (m), 1039 (s), 959 (s), 796 (m), 767 (w), 551 (w) cm^{-1}; **^{1}H NMR (400 MHz, $CDCl_3$):** δ 8.18 (s, 1H), 7.42 (tt, *J* = 8.5, 6.5 Hz, 1H), 7.06–6.91 (m, 2H), 5.72 (s, 1H), 5.70 (s, 2H), 5.61 (s, 1H); **^{13}C NMR (101 MHz, $CDCl_3$):** δ 187.5 (d, *J* = 16.7 Hz), 162.5 (d, *J* = 6.7 Hz), 160.0 (d, *J* = 6.9 Hz), 144.7, 132.1 (t, *J* = 10.5 Hz), 126.0, 112.3–111.7 (m), 109.8 (t, *J* = 18.8 Hz), 83.4 (d, *J* = 181.4 Hz), 41.8; **^{19}F NMR (376 MHz, $CDCl_3$):** δ –111.93 (s, 1F) , –112.74 (d, *J* = 8.9 Hz, 2F); **HRMS (DART^{+}):** Calcd for $C_{11}H_9OF_3$ $[M+H]^+$: 256.0692, Found: 256.0686.

Procedure for allyl addition to triazole-containing halomethyl ketones:

In a N_2-filled glove box, **ap-2** (1.53 mg, 0.005 mmol), $Zn(OMe)_2$ (1.27 mg, 0.01 mmol) and toluene (0.5 mL) were added to a two-dram vial equipped with a stir bar. Ketone (34.10 mg, 0.10 mmol), (pinacolato)allylboron (0.027 mL, 0.15 mmol), and MeOH (0.014 mL, 0.35 mmol) were added sequentially. The vessel was sealed with a Teflon cap, removed from the glove box and the mixture was allowed to stir at 22 °C for 12 h. Conversion was determined by analysis of ^{1}H and ^{19}F NMR spectra of an aliquot. The mixture was loaded directly onto a silica gel column and eluted with hexanes/ethyl acetate to afford the product.

(*R*)-1,1,1-Trifluoro-2-(1-(2,6-difluorobenzyl)-1*H*-1,2,3-triazol-4-yl)pent-4-en-2-ol (2.38): 21.0 mg, 0.0630 mmol, 63% yield, white solid. The analytical data are consistent with those reported previously and the melting point has been provided.[176] **IR (neat):** 3350 (br), 2978 (w), 1627 (w), 1472 (s), 1334 (m), 1141 (s), 924 (w), 768 (s), 672 (m), 577 (w), 545 (w) cm^{-1}; **^{19}F NMR (376 MHz, $CDCl_3$):** δ –80.90 (s, 3F), –114.18 (t, *J* = 6.8 Hz, 2F); **Specific Rotation:** $[\alpha]^{24}_{D}$ –4.1 (*c* 1.22, $CHCl_3$) for a 56.5:43.5 er sample. The enantiomeric purity of this compound was determined by HPLC analysis in comparison with authentic racemic material (Chiralpak AD-H, 95:5 hexanes:*i*-PrOH, 0.8 mL/min, 220 nm).

---

[175] Andrade, F. C. D.; Pugnal, L. V. B. L.; Betim, H. L. I.; Vani, J. F.; Zukerman-Schpector, J.; Schwab, R. S. *Eur. J. Org. Chem*. **2018**, *40*, 5467–5476.

[176] Bonacorso, H. G.; Wiethan, C. W.; Belo, C. R.; Moraes, M. C.; Martins, M. A. P.; Zanatta, N. *Tetrahedron Lett.* **2014**, *55*, 2283–2285.

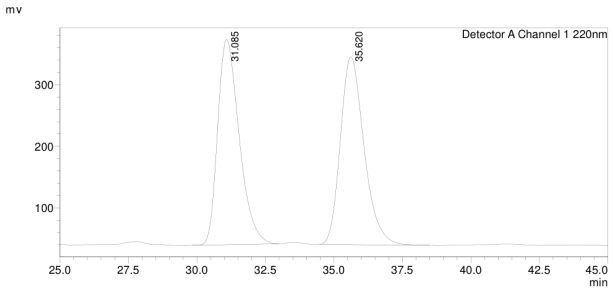

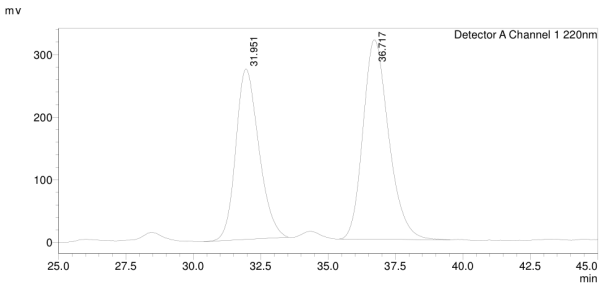

<Peak Table>
Detector A Channel 1 220nm

Peak#	Ret. Time	Area	Height	Area%
1	31.085	18262075	333831	49.840
2	35.620	18379401	305449	50.160
Total		36641476	639280	100.000

<Peak Table>
Detector A Channel 1 220nm

Peak#	Ret. Time	Area	Height	Area%
1	31.951	16222730	272147	43.411
2	36.717	21147197	318464	56.589
Total		37369927	590611	100.000

Peak #	Ret. Time	Area	Area %	Peak #	Ret. Time	Area	Area %
1	31.1 min	18262075	49.840	1	31.9 min	16222730	43.411
2	35.6 min	18379401	50.160	2	36.7 min	21147197	56.589

(*R*)-1,1,1-Trichloro-2-(1-(2,6-difluorobenzyl)-1*H*-1,2,3-triazol-4-yl)pent-4-en-2-ol (2.39): 25.8 mg, 0.0630 mmol, 67% yield, white solid. The analytical data are consistent with those reported previously and the melting point has been provided.[176] **^{19}F NMR (376 MHz, $CDCl_3$):** δ –114.24 (t, *J* = 6.9 Hz); **Specific Rotation:** $[\alpha]^{24}_D$ –3.3 (*c* 1.42, $CHCl_3$) for a 52:48 er sample. The enantiomeric purity of this compound was determined by HPLC analysis in comparison with authentic racemic material (Chiralpak AD-H, 95:5 hexanes:*i*-PrOH, 0.8 mL/min, 220 nm).

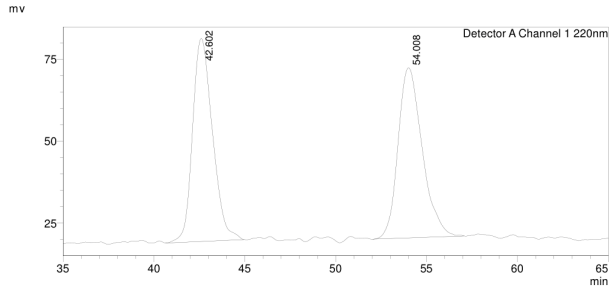

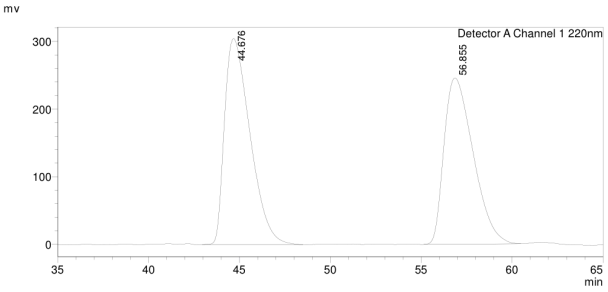

<Peak Table>
Detector A Channel 1 220nm

Peak#	Ret. Time	Area	Height	Area%
1	42.602	4733134	61910	49.631
2	54.008	4803431	51893	50.369
Total		9536565	113803	100.000

<Peak Table>
Detector A Channel 1 220nm

Peak#	Ret. Time	Area	Height	Area%
1	44.676	29691764	304469	51.981
2	56.855	27428780	245713	48.019
Total		57120544	550182	100.000

Peak #	Ret. Time	Area	Area %	Peak #	Ret. Time	Area	Area %
1	42.6 min	4733134	49.631	1	44.7 min	29691764	51.981
2	54.0 min	4803431	50.369	2	56.8 min	27428780	48.019

(*R*)-2-(1-(2,6-Difluorobenzyl)-1*H*-1,2,3-triazol-4-yl)-1-fluoropent-4-en-2-ol (2.40): 11.3 mg, 0.0380 mmol, 76% yield, white solid. **Melting point:** 55–58 °C; **IR (neat):** 3360 (br), 3073 (w), 2853 (w), 1627 (m), 1594 (w), 1472 (s), 1271 (m), 1236 (m), 1048 (m), 961 (s), 921 (m), 798 (s) cm^{-1}; **^{1}H NMR (400 MHz, $CDCl_3$):** δ 7.57 (s, 1H), 7.36 (tt, *J* = 8.5, 6.5 Hz, 1H), 6.96 (dd, *J* = 8.4, 7.3 Hz, 2H), 5.82–5.63 (m, 1H), 5.60 (d, *J* = 1.4 Hz, 2H), 5.20–5.03 (m, 2H), 4.67–4.38 (m, 2H), 3.11 (s, 1H), 2.82–2.55 (m, 2H); **^{13}C NMR (100 MHz, $CDCl_3$):** δ 161.4 (d, *J* = 244.9 Hz),

149.8, 131.8, 131.5 (t, J = 10.3 Hz), 121.5, 119.9, 112.0–111.6 (m), 110.6 (t, J = 18.8 Hz), 87.5 (d, J = 176.9 Hz), 72.0 (d, J = 18.7 Hz), 41.5 (d, J = 17.0 Hz); **^{19}F NMR (376 MHz, $CDCl_3$):** δ –114.0 (s, 2F), –114.7 (s, 1F); **HRMS (DART$^+$):** Calcd for $C_{14}H_{15}N_3OF_3$ $[M+H]^+$: 298.1160, Found: 298.1162; **Specific Rotation:** $[\alpha]^{24}_D$ +1.7 (*c* 2.10, $CHCl_3$) for a 69.5:30.5 er sample. The enantiomeric purity of this compound was determined by HPLC analysis in comparison with authentic racemic material (Chiralcel OD-H, 95:5 hexanes:*i*-PrOH, 0.8 mL/min, 220 nm).

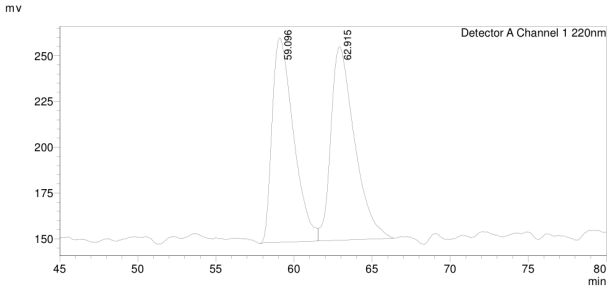

<Peak Table>
Detector A Channel 1 220nm

Peak#	Ret. Time	Area	Height	Area%
1	59.096	10653363	111664	48.759
2	62.915	11195692	105640	51.241
Total		21849055	217305	100.000

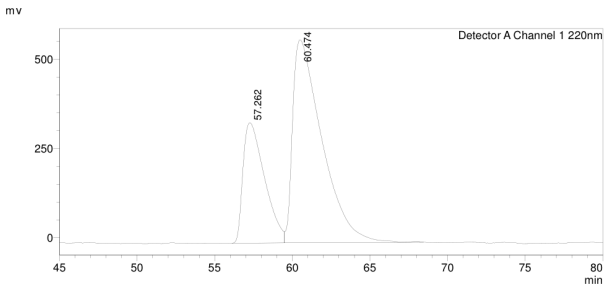

<Peak Table>
Detector A Channel 1 220nm

Peak#	Ret. Time	Area	Height	Area%
1	57.262	32522593	336763	30.353
2	60.474	74625939	567700	69.647
Total		107148531	904463	100.000

Peak #	Ret. Time	Area	Area %	Peak #	Ret. Time	Area	Area %
1	59.1 min	10653363	48.759	1	57.3 min	32522593	30.353
2	62.9 min	11195692	51.241	2	60.5 min	74625939	69.647

2.8.11.2. One-pot procedure for allyl addition and cycloaddition

In a N_2-filled glove box, **ap-10** (3.28 mg, 0.006 mmol) or **ap-11** (3.50 mg, 0.005 mmol), $Zn(OMe)_2$ (2.54 mg, 0.02 mmol) and toluene (1 mL) was added to an two-dram vial equipped with a stir bar and allowed to stir for 5 min. Ketone (31.6 mg, 0.20 mmol) and (pinacolato)allylboron (0.040 mL, 0.22 mmol) were added sequentially and the mixture was allowed to cool to –40 °C for 30 min, after which it was charged with MeOH (0.0104 mL, 0.26 mmol). The reaction vessel was sealed with a Teflon cap, removed from the glove box, and the resulting mixture was allowed to stir at 4 °C for 2 h (in the case of a monofluoromethyl ketone) or –40 °C for 18h (for a difluoromethyl ketone). The vial was then allowed to warm to 22 °C at which time K_2CO_3 (55.3 mg, 0.400 mmol), $CuSO_4$•$5H_2O$ (10.0 mg, 0.040 mmol), azide **2.43** (37.2 mg, 0.22 mmol), (L)-ascorbic acid (14.1 mg, 0.080 mmol), H_2O (0.5 mL) and MeOH (0.5 mL) were added sequentially. The vial was sealed with a Teflon cap and the mixture allowed to stir at 22 °C for 12 h, after which the reaction was quenched by the addition of a saturated aqueous solution of $NaHCO_3$ (2.0 mL). The layers were separated and the organic layer was washed with H_2O (5 mL) and brine (5 mL), dried over $MgSO_4$, filtered, and concentrated *in vacuo.* The desired product was isolated as white solid after purification by silica gel chromatography (elution with hexanes/EtOAc).

1-Fluoro-4-(trimethylsilyl)but-3-yn-2-one (2.42): The title compound was synthesized according to a previous procedure; the analytical data were fully consistent.[177] **^{1}H NMR (400 MHz, $CDCl_3$):** δ 4.86 (dd, *J* = 47.1, 2.2 Hz, 2H), 0.20 (dd, *J* = 7.3, 4.1 Hz, 9H).

2-(Azidomethyl)-1,3-difluorobenzene (2.43): The title compound was synthesized according to a previous procedure; the analytical data were fully consistent.[178] **^{1}H NMR (400 MHz, $CDCl_3$):** δ 7.33 (tt, *J* = 8.4, 6.4 Hz, 1H), 6.96 (td, *J* = 8.0, 4.3 Hz, 2H), 4.43 (s, 2H).

(*R*)-2-(1-(2,6-Difluorobenzyl)-1*H*-1,2,3-triazol-4-yl)-1-fluoropent-4-en-2-ol (2.41): 51.0 mg, 0.172 mmol, 86% yield, white solid. See page S65 for spectral data. Enantiomeric purity was determined by HPLC analysis in comparison with authentic racemic material (Chiralcel OD-H, 95:5 hexanes:*i*-PrOH, 0.8 mL/min, 220 nm).

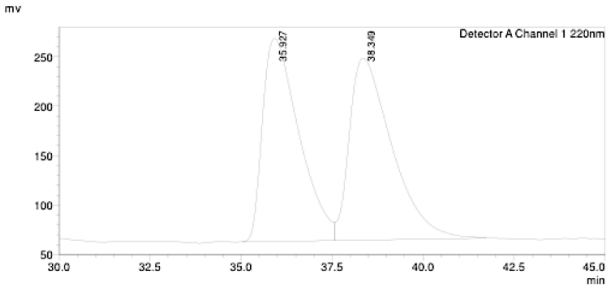

<Peak Table>
Detector A Channel 1 220nm

Peak#	Ret. Time	Area	Height	Area%
1	35.927	14236917	204878	48.801
2	38.349	14936379	183687	51.199
Total		29173297	388565	100.000

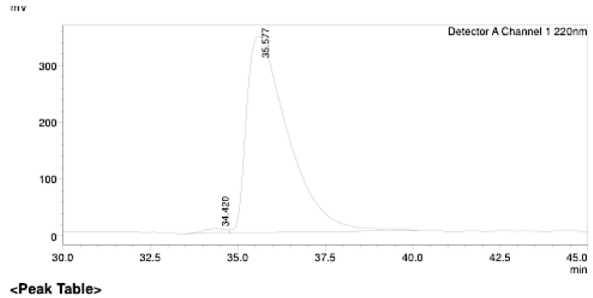

<Peak Table>
Detector A Channel 1 220nm

Peak#	Ret. Time	Area	Height	Area%
1	34.420	359629	8215	1.247
2	35.577	28478377	345842	98.753
Total		28838007	354057	100.000

Peak #	Ret. Time	Area	Area %	Peak #	Ret. Time	Area	Area %
1	36.0 min	14236917	48.801	1	34.4 min	359629	1.247
2	38.3 min	14936379	51.199	2	35.6 min	28478377	98.753

1,1-Difluoro-4-(trimethylsilyl)but-3-yn-2-one (2.44): The title compound was synthesized analogous to **24** and purified by silica gel chromatography to afford **25** (1.01g, 73% yield) as colorless oil. **IR (neat):** 2960 (w), 2253 (w), 1730 (w), 1700 (m), 1374 (m), 1252 (m), 1073 (m), 904 (s), 847 (s), 726 (s), 579 (m), 501 (w) cm^{-1}; **^{1}H NMR (400 MHz, $CDCl_3$):** δ 5.76 (t, *J* = 54.0 Hz, 1H), 0.29 (s, 9H); **^{13}C NMR (100 MHz, $CDCl_3$):** δ 175.0 (t, *J* = 29.7 Hz), 108.5 (t, *J* = 252.3 Hz), 108.3, 97.3, 1.1; **^{19}F NMR (376 MHz, $CDCl_3$):** δ –125.95 (d, *J* = 54.0 Hz, 2F); **HRMS (DART$^+$):** Calcd for $C_7H_{11}OF_2Si$ $[M+H]^+$: 177.0542, Found: 177.0533.

(*R*)-2-(1-(2,6-Difluorobenzyl)-1*H*-1,2,3-triazol-4-yl)-1,1-difluoropent-4-en-2-ol (2.45): 56.4 mg, 0.1789 mmol, 89% yield, white solid. **Melting point:** 57–62 °C; **IR (neat):** 3314 (br), 3152

[177] Shin, H. I.; Choi, W.; Heo, T. H.; Lee, K. W.; Lee, J. H.; Park, K. S. WO 2006090997, August, 31, 2006.

[178] Taylor, N. J.; Emer, E.; Preshlock, S.; Schedler, M.; Tredwell, M.; Verhoog, S.; Mercier, J.; Genicot, C.; Gouverneur, V. *J. Am. Chem. Soc.* **2017**, *139*, 8267–8276.

(w), 3079 (w), 2959 (w), 1627 (m), 1594 (m), 1472 (s), 1272 (m), 1072 (s), 1026 (s), 798 (s), 626 (w) cm^{-1}; **^{1}H NMR (400 MHz, $CDCl_3$):** δ 7.56 (s, 1H), 7.37 (tt, *J* = 8.4, 6.5 Hz, 1H), 6.97 (t, *J* = 7.9 Hz, 2H), 6.00–5.62 (m, 1H), 5.83 (t, *J* = 55.9 Hz, 1H), 5.62 (s, 1H), 5.30–4.99 (m, 2H), 3.33 (s, 1H), 2.85–2.42 (m, 2H); **^{13}C NMR (100 MHz, $CDCl_3$):** δ 162.6 (d, *J* = 7.1 Hz), 160.1 (d, *J* = 6.8 Hz), 146.4, 131.6 (t, *J* = 10.2 Hz), 130.8, 121.2 (d, *J* = 148.6 Hz), 115.7 (t, *J* = 249.6 Hz), 112.4–111.5 (m), 110.5 (t, *J* = 18.8 Hz), 72.7 (t, *J* = 21.9 Hz), 41.57, 39.6; **^{19}F NMR (376 MHz, $CDCl_3$):** δ –112.34 to –117.45 (m, 2F), –125.58 to –142.26 (m, 2F); **HRMS (DART^{+}):** Calcd for $C_{14}H_{14}N_3OF_4$ $[M+H]^+$: 316.1062, Found: 316.1068; **Specific Rotation:** $[\alpha]^{24}_D$ +1.8 (*c* 2.58, $CHCl_3$) for a >99:1 er sample. The enantiomeric purity of this compound was determined by HPLC analysis in comparison with authentic racemic material (Chiralpak AD-H, 95:5 hexanes:*i*-PrOH, 0.5 mL/min, 220 nm).

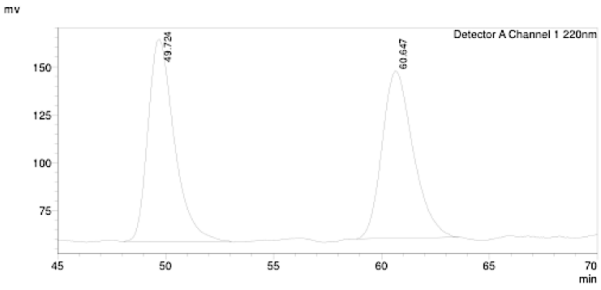

<Peak Table>
Detector A Channel 1 220nm

Peak#	Ret. Time	Area	Height	Area%
1	49.724	8985034	105605	50.708
2	60.647	8734113	87307	49.292
Total		17719147	192912	100.000

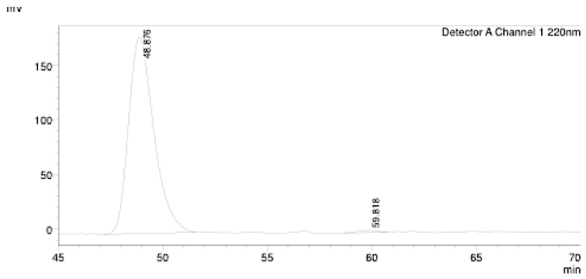

<Peak Table>
Detector A Channel 1 220nm

Peak#	Ret. Time	Area	Height	Area%
1	48.876	15188780	180239	99.108
2	59.818	136716	2133	0.892
Total		15325496	182372	100.000

Peak #	Ret. Time	Area	Area %	Peak #	Ret. Time	Area	Area %
1	49.7 min	8985034	50.708	1	48.9 min	15188780	99.108
2	60.6 min	8734113	49.292	2	59.8	2133	0.892

2.8.12. Determination of Absolute Stereochemistry

2.8.12.1. Trihalomethyl ketone products

The absolute stereochemistry of the tertiary alcohols resulting from allyl addition to trichloromethyl ketones was determined by converting **2.8** to **2.9**, a compound with known absolute stereochemistry.[179] Ketone **2.9** was synthesized according to a previous procedure; the corresponding analytical data were fully consistent with those reported.[180] The optical rotations and crystal structures of **2.9** and the literature compound were compared (see Section 8 for crystallographic information).

[179] Hara, N.; Tamura, R.; Funahashi, Y.; Nakamura, S. *Org. Lett.* **2011**, *13*, 1662–1665.

[180] Nicolaou, K. C.; Adsool, V. A.; Hale, C. R. H. *Org. Lett.* **2010**, *12*, 1552–1555.

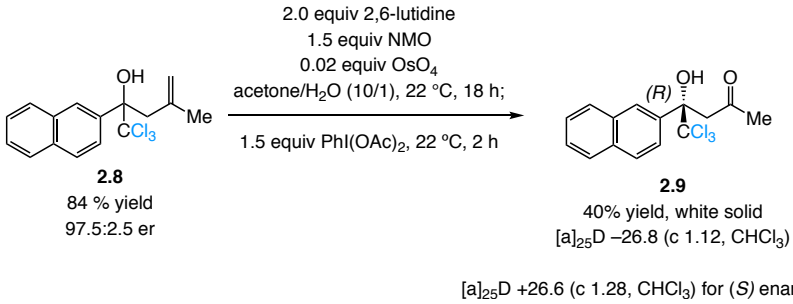

The absolute stereochemistry of the tertiary alcohols resulting from allyl addition to tribromomethyl ketones was determined by converting **2.10** to **S-7**, a compound with known absolute stereochemistry.[159] To a two-dram vial equipped with a stir bar was added **2.10** (13.4 mg, 0.034 mmol), toluene (0.34 mL), AIBN (5.6 mg, 0.034 mmol, 10 mol %), and tributyltin hydride (0.19 mL, 0.705 mmol, 20 equiv). The mixture was allowed to stir at 70 °C for 2 h at which time the reaction was quenched by the addition of a 5.0 % aqueous solution of KF (2 mL). The aqueous layer was washed with Et_2O (5 mL) and the organic layer washed with H_2O (2 mL). The combined organic layers were dried over $MgSO_4$ and concentrated *in vacuo* to afford **S-7** (4.2 mg, 0.026 mmol, 76% yield) as colorless oil. The HPLC traces of **(*R*)-S-7** and **(*S*)-S-7** were compared, thus confirming the assignment.

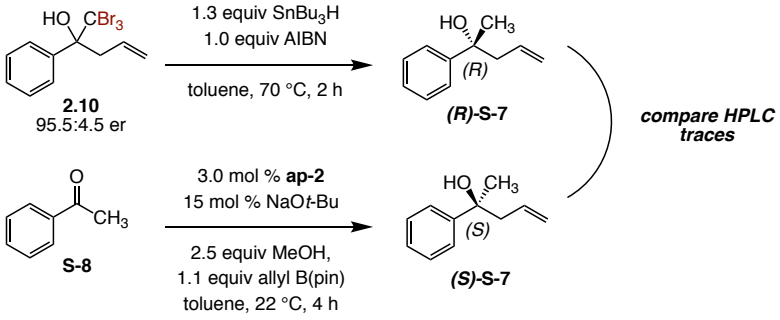

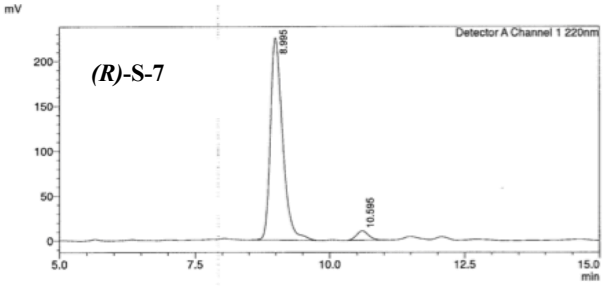

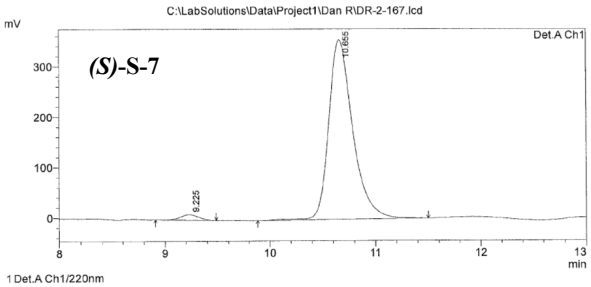

<Peak Table>
Detector A Channel 1 220nm

Peak#	Ret. Time	Area	Height	Area%
1	8.995	3574688	224794	95.659
2	10.595	162226	10404	4.341
Total		3736914	235198	100.000

PeakTable
Detector A Ch1 220nm

Peak#	Ret. Time	Area	Height	Area %	Height %
1	9.225	127712	11013	2.220	2.994
2	10.655	5623838	356809	97.780	97.006
Total		5751550	367822	100.000	100.000

Peak #	Ret. Time	Area	Area %	Peak #	Ret. Time	Area	Area %
1	9.0 min	3574688	95.659	1	9.2 min	127712	2.994
2	10.6 min	162226	4.341	2	10.6 min	356809	97.006

2.8.12.2. Dihalomethyl ketone products

The absolute stereochemistry of the tertiary alcohols resulting from allyl addition to dichloromethyl ketones was determined by X-ray crystallographic analysis of **2.25d** (see Section 8 for details). The absolute stereochemistry of the dibromomethyl ketones was determined by halogen abstraction from **2.26a** to afford **2.16a** through a previously reported procedure.[181] The HPLC traces of the two compounds were compared, confirming the assignment.

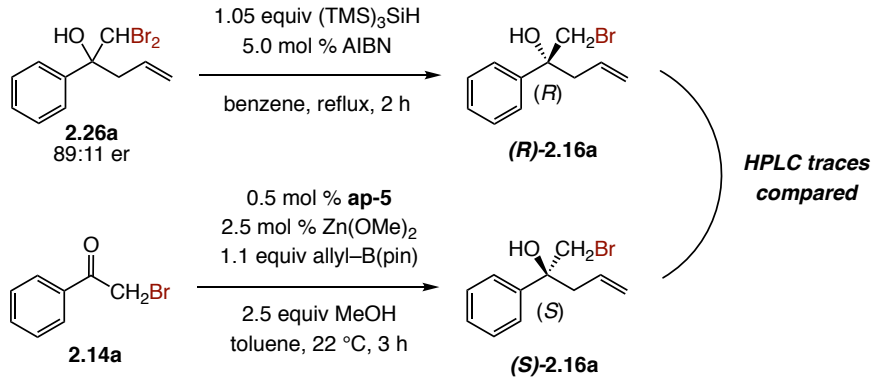

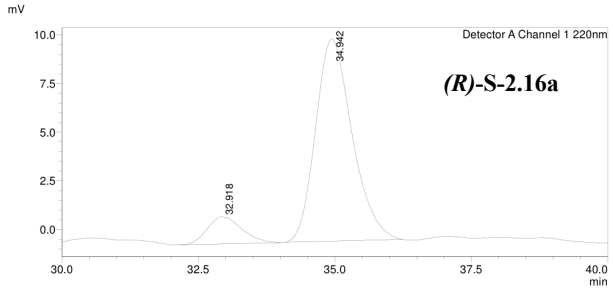

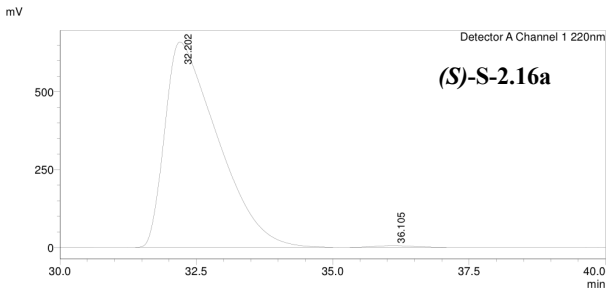

<Peak Table>
Detector A Channel 1 220nm

Peak#	Ret. Time	Area	Area%	Height
1	32.918	60994	11.194	1385
2	34.942	483891	88.806	10378
Total		544886	100.000	11763

<Peak Table>
Detector A Channel 1 220nm

Peak#	Ret. Time	Area	Height	Area%
1	32.202	44253906	659663	99.481
2	36.105	230669	5127	0.519
Total		44484576	664790	100.000

Peak #	Ret. Time	Area	Area %	Peak #	Ret. Time	Area	Area %
1	32.9 min	60994	11.194	1	32.2 min	44253906	99.481
2	34.9 min	483891	88.806	2	36.1 min	5127	0.519

The absolute stereochemistry of the tertiary alcohols resulting from allyl addition to difluoromethyl ketones was determined by converting **2.12**, a compound with known absolute stereochemistry, to ***(R)*-2.31a**. The optical rotations of the two compounds were compared, confirming the assignment.[172]

[181] Leung, A. E.; Blair, M; Forsyth, C. M.; Tuck, K. L. *Org. Lett.* **2013**, *15*, 2198–2201.

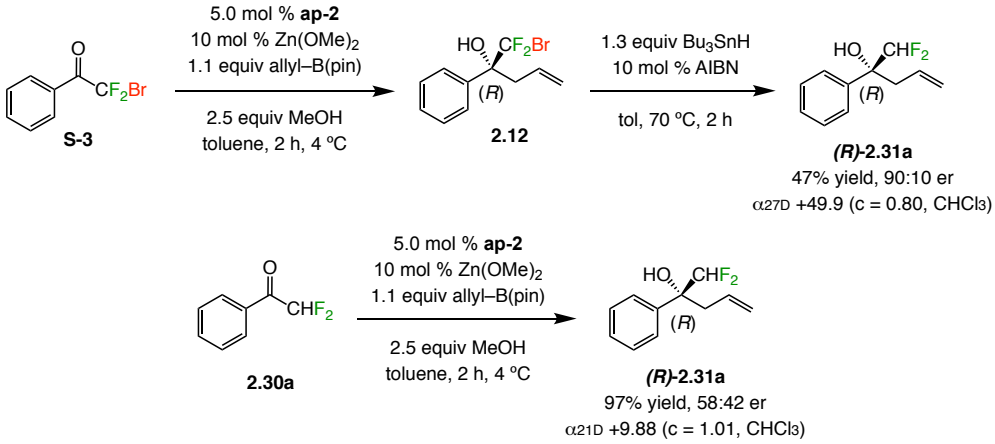

2.8.12.3. Monohalomethyl ketone products

The absolute stereochemistry of the epoxides resulting from allyl addition to monochloromethyl and monobromomethyl ketones was determined by comparison of the optical rotations of epoxide **2.17a** to that of the same epoxide with formerly determined absolute stereochemistry.[182]

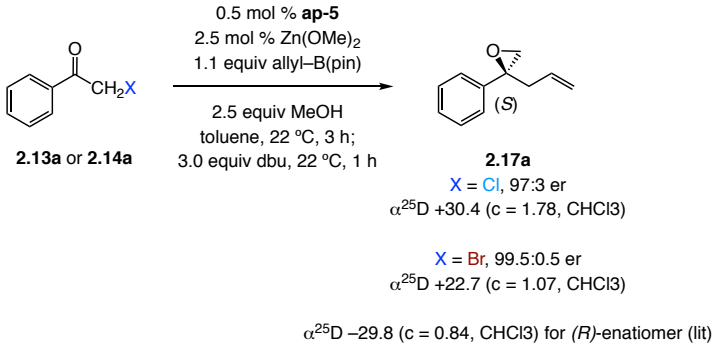

Additionally, the optical rotation of the epoxide resulting from addition of the 2-methylallyl reagent was compared to that reported for this compound previously.[168]

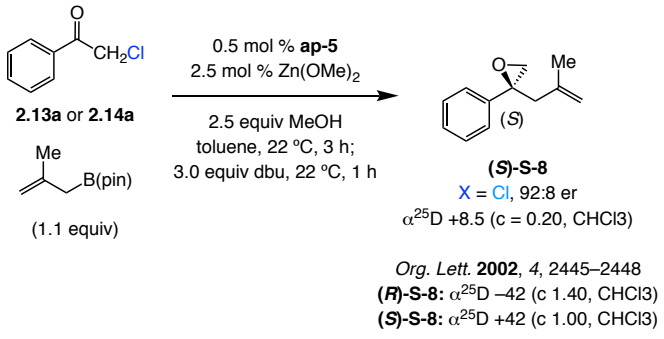

[182] Wu, T. R.; Shen, L.; Chong, J. M. *Org. Lett.* **2004**, *6*, 2701–2704.

For the monofluoromethyl ketones, **16a** was oxidized to **S-16**, a compound with known absolute stereochemistry by a previous procedure.[183] The HPLC traces of the intermediate diols **S-15a** and **S-15b** were compared. The crystal structures of **S-16** were compared (see Section 8 for details).

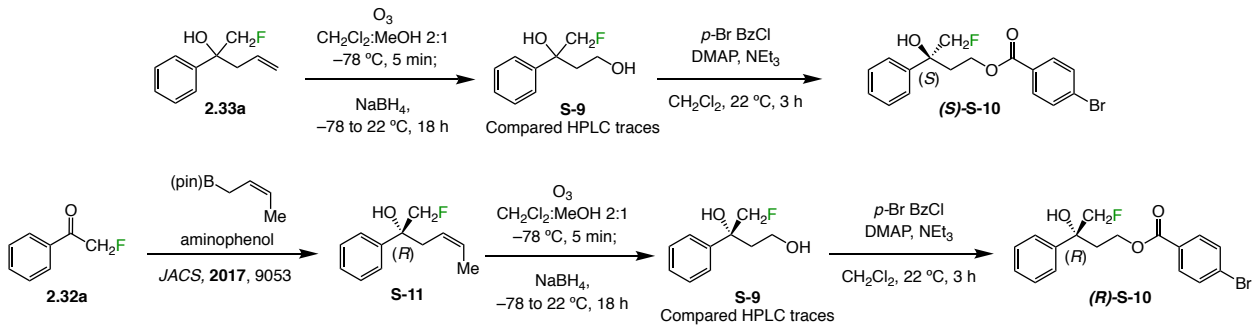

2.8.13. Calculation of Sterimol Values

The corresponding functional groups (capped by a hydrogen atom as R-H) have been optimized at the wB97XD/Def2SVP level in toluene as solvent (SMD solvation model). The thus obtained geometries have been processed with a program developed by Paton et al. as described in the following reference: Piou, T.; Romanov-Michailidis, F.; Romanova-Michaelides, M.; Jackson, K. E.; Semakul, N.; Taggart, T. D.; Newell, B. S.; Rithner, C. D.; Paton, R. S.; Rovis, T. Correlating reactivity and selectivity to cyclopentadienyl ligand properties in Rh(III)-catalyzed C-H activation reactions: an experimental and computational study. *J. Am. Chem. Soc.* **2017**, *139*, 1296–1310.

2.8.14. NMR Spectra

NMR spectra appear on the following pages:

[183] van der Mei, F. W.; Qin, C.; Morrison, R. J.; Hoveyda, A. H. *J. Am. Chem. Soc.* **2017**, *139*, 9053–9065.

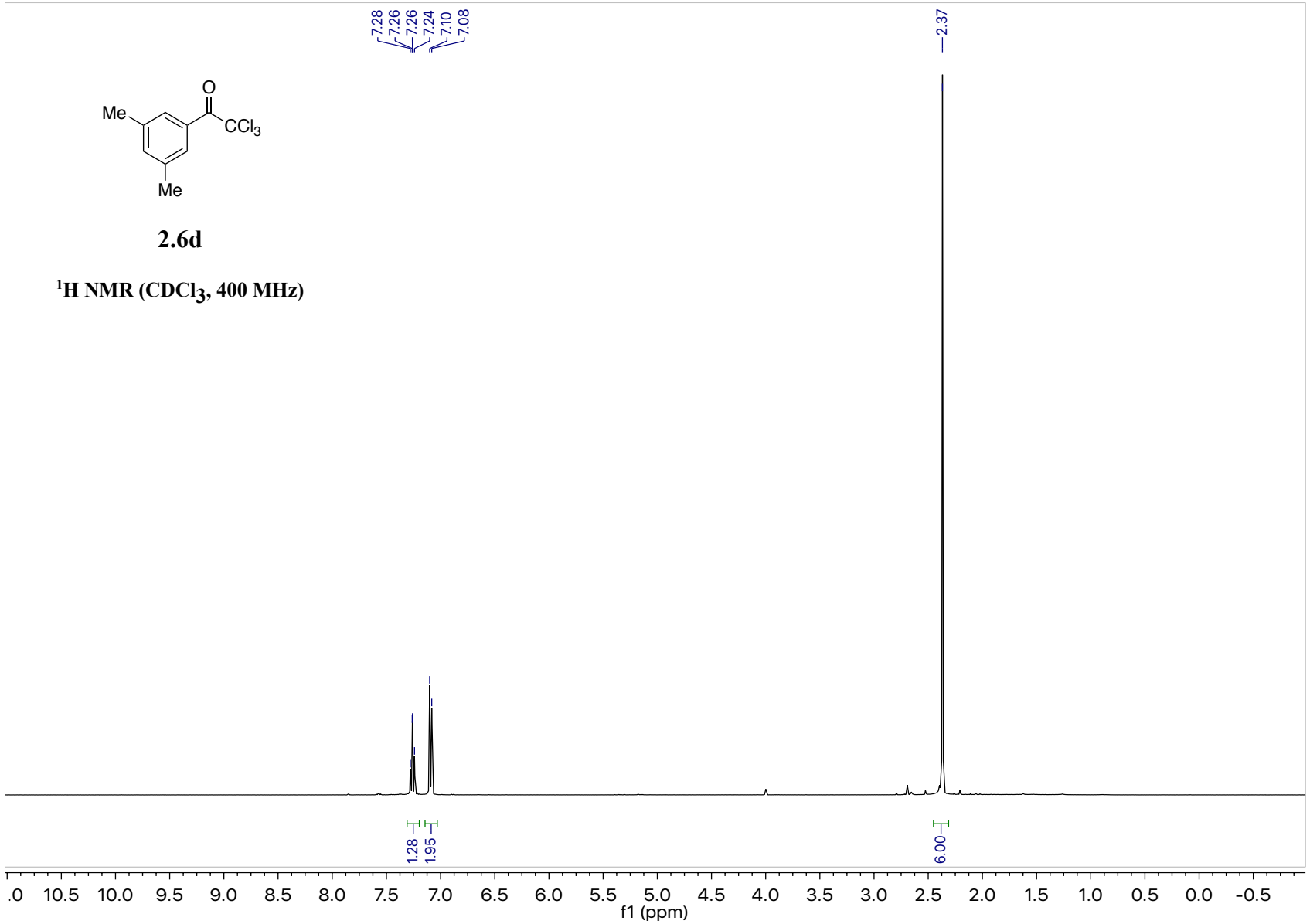

2.6d

^{1}H NMR ($CDCl_3$, 400 MHz)

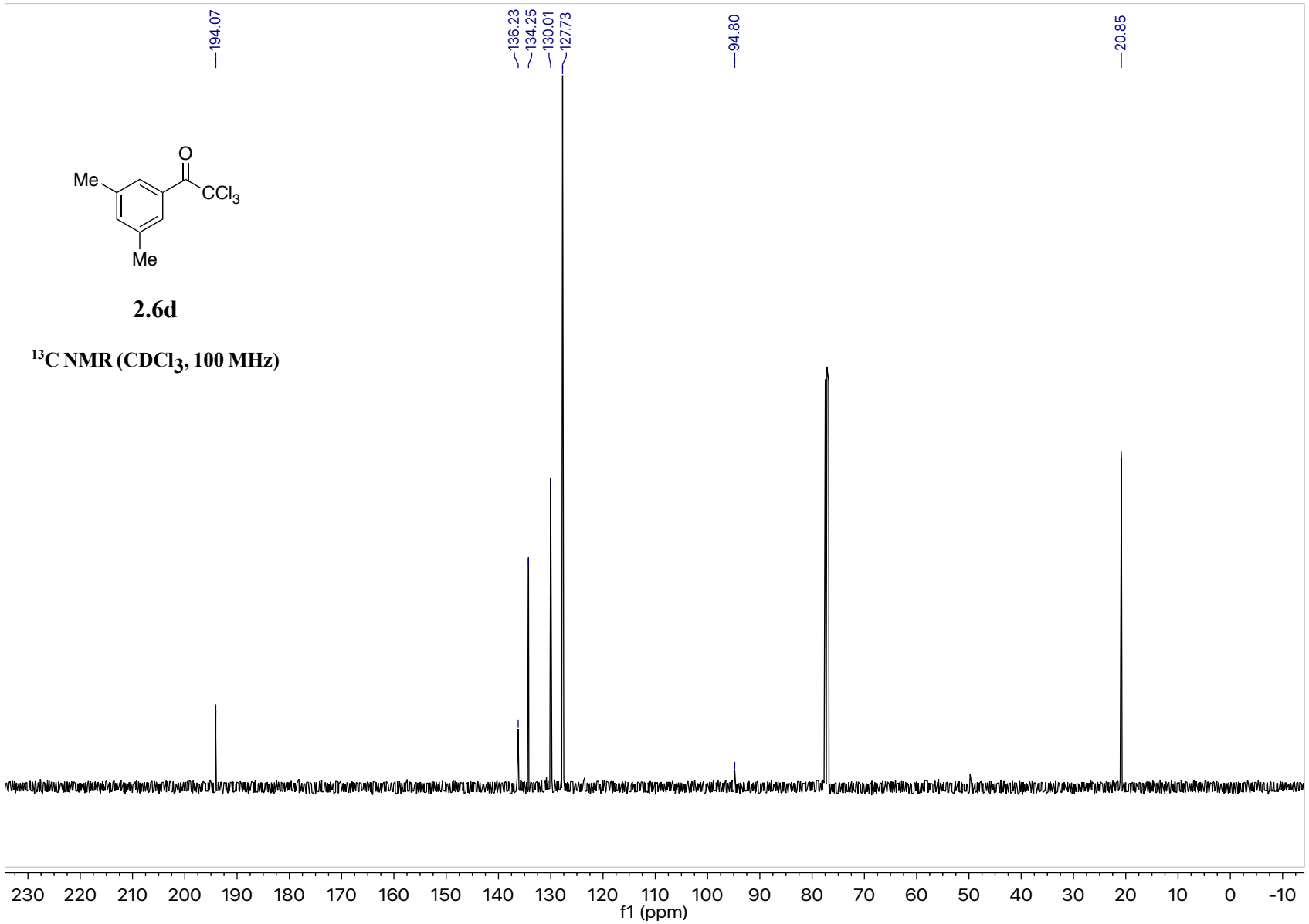
194.07
136.23
134.25
130.01
127.73
94.80
20.85
O
Me
CCl3
Me
2.6d
13C NMR (CDCl3, 100 MHz)
230 220 210 200 190 180 170 160 150 140 130 120 110 100 90 80 70 60 50 40 30 20 10 0 -10
f1 (ppm)

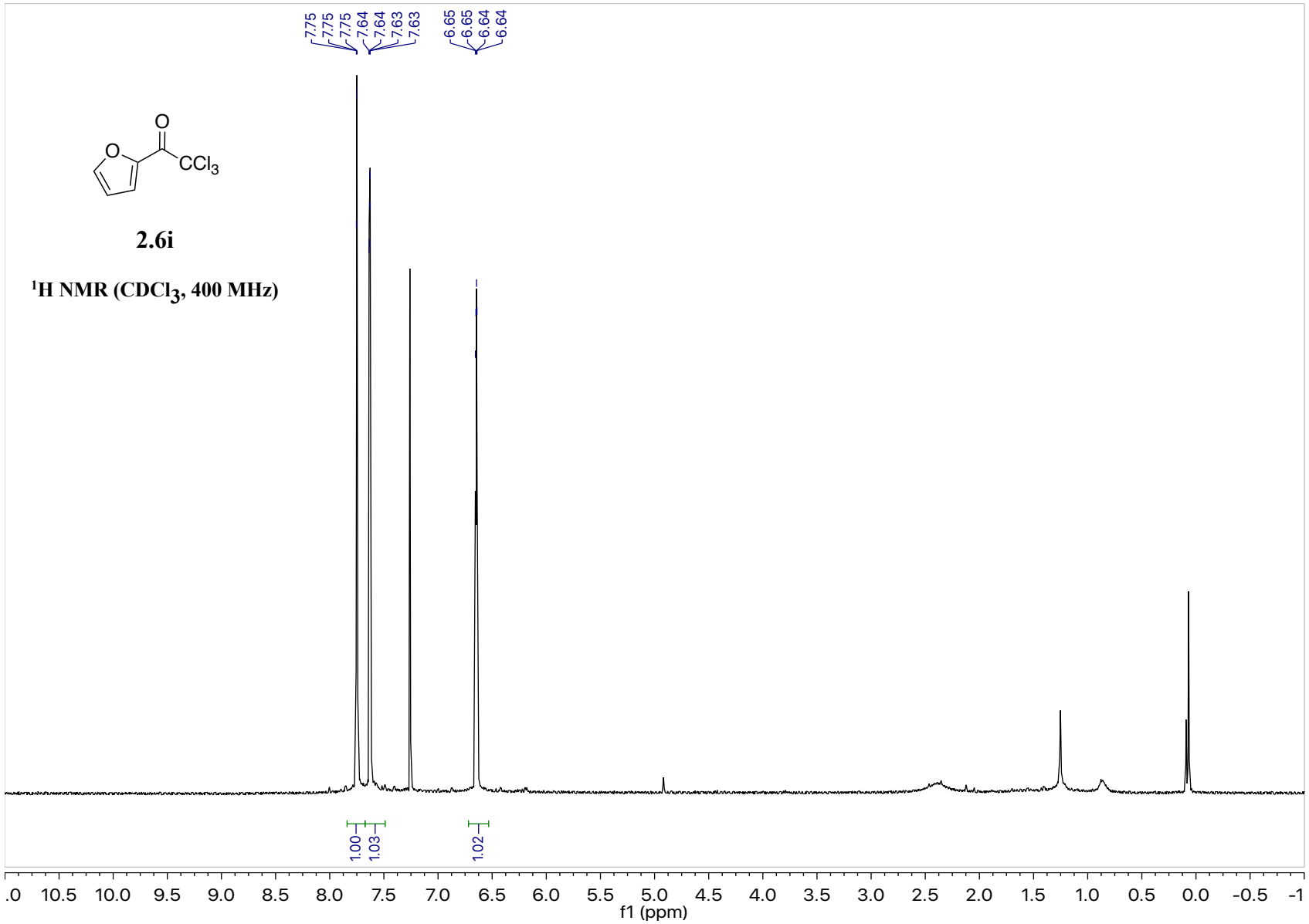
7.75
7.75
7.75
7.64
7.64
7.63
7.63
6.65
6.65
6.64
6.64
O
O
CCl3
2.6i
1H NMR (CDCl3, 400 MHz)
1.00
1.03
1.02
.0 10.5 10.0 9.5 9.0 8.5 8.0 7.5 7.0 6.5 6.0 5.5 5.0 4.5 4.0 3.5 3.0 2.5 2.0 1.5 1.0 0.5 0.0 -0.5 -1
f1 (ppm)

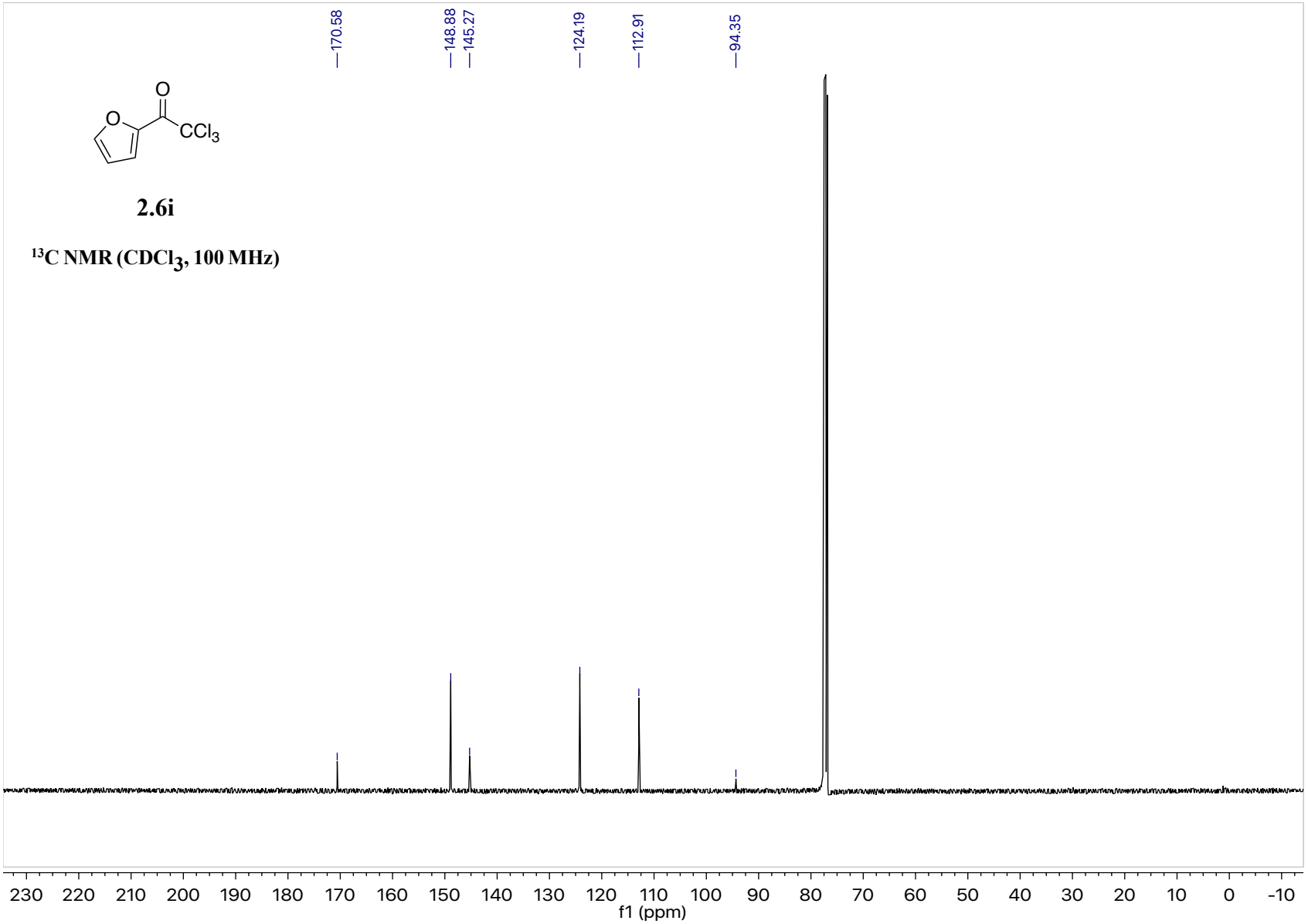

2.6i

^{13}C NMR ($CDCl_3$, 100 MHz)

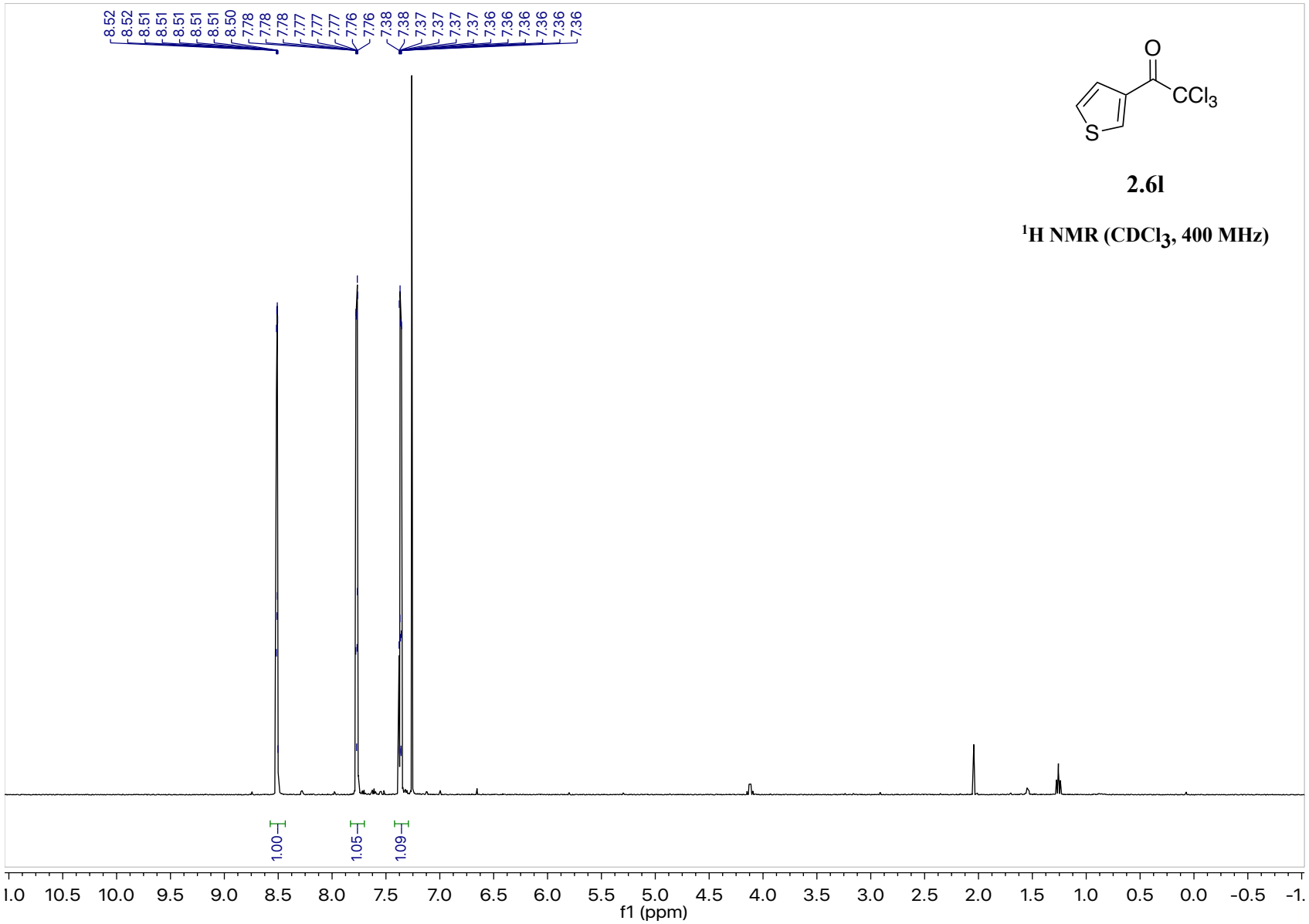
8.52
8.52
8.51
8.51
8.51
8.51
8.51
8.50
7.78
7.78
7.78
7.77
7.77
7.77
7.76
7.76
7.38
7.38
7.37
7.37
7.37
7.37
7.36
7.36
7.36
7.36
7.36
7.36
1.00
1.05
1.09
1.0
10.5
10.0
9.5
9.0
8.5
8.0
7.5
7.0
6.5
6.0
5.5
5.0
4.5
4.0
3.5
3.0
2.5
2.0
1.5
1.0
0.5
0.0
-0.5
-1.
f1 (ppm)
O
CCl3
S
2.6l
1H NMR (CDCl3, 400 MHz)

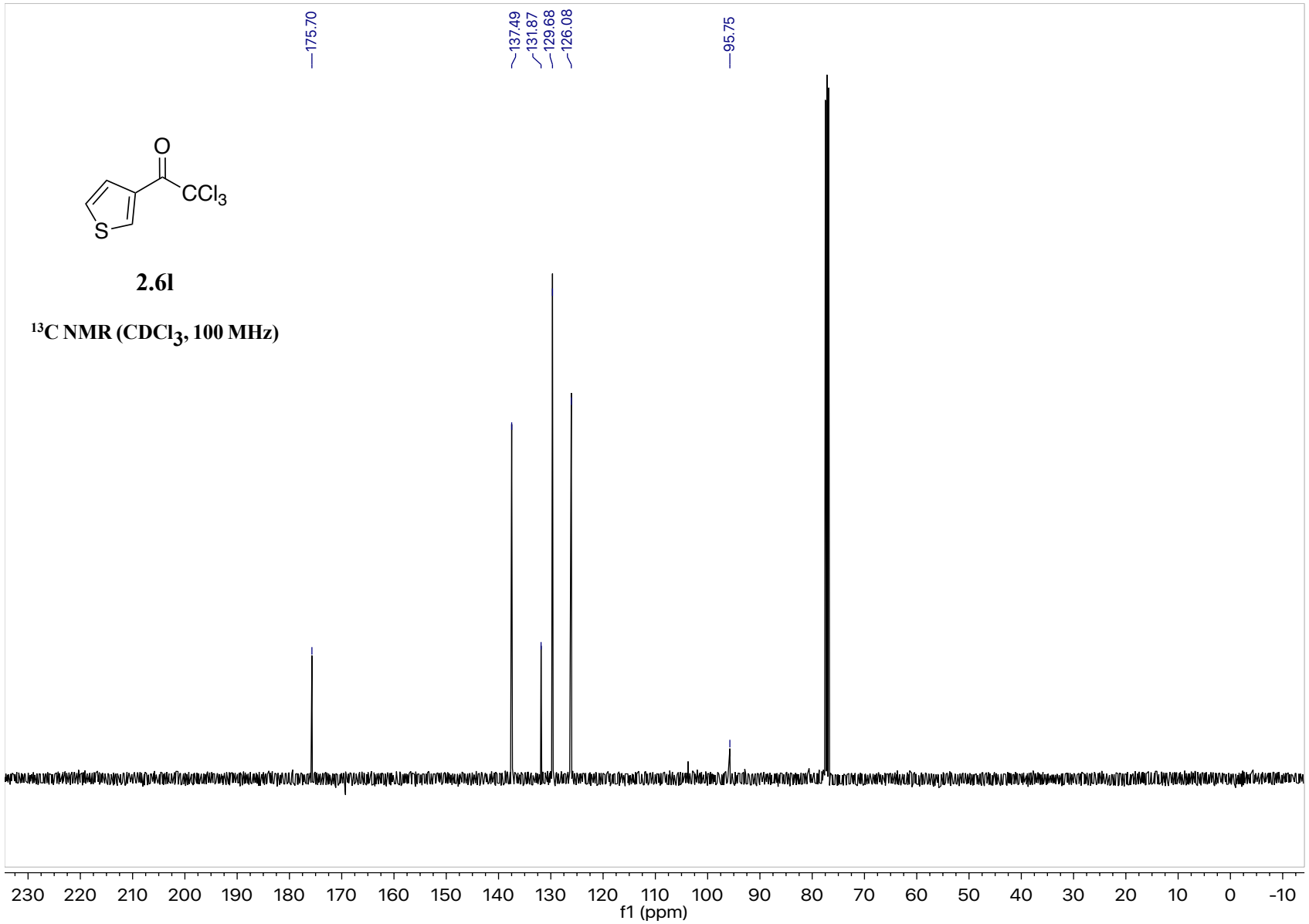
175.70
137.49
131.87
129.68
126.08
95.75
O
CCl3
S
2.6l
13C NMR (CDCl3, 100 MHz)
230 220 210 200 190 180 170 160 150 140 130 120 110 100 90 80 70 60 50 40 30 20 10 0 -10
f1 (ppm)

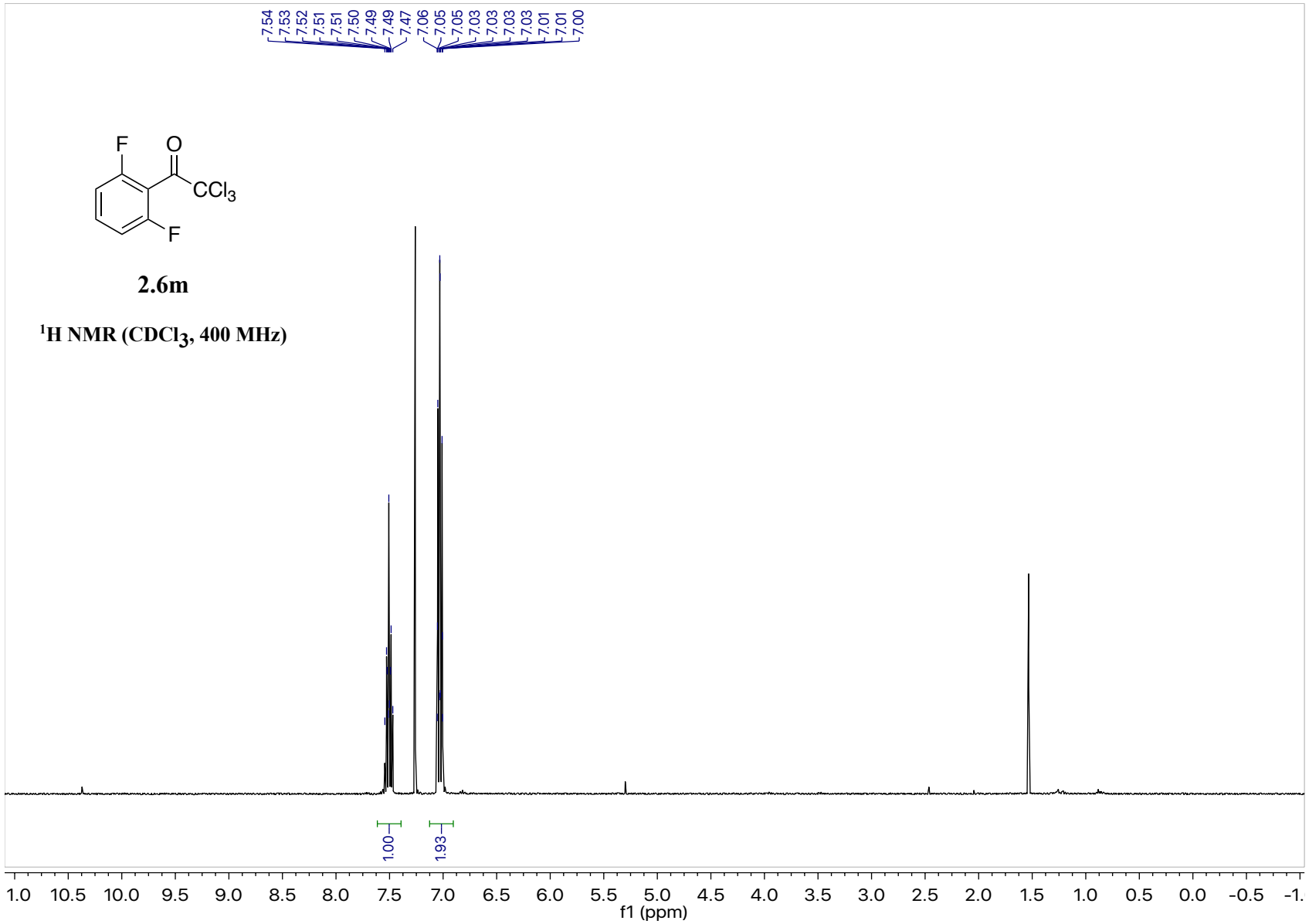
7.54
7.53
7.52
7.51
7.51
7.50
7.49
7.49
7.47
7.06
7.05
7.05
7.03
7.03
7.03
7.03
7.01
7.01
7.00
F
O
CCl3
F
2.6m
1H NMR (CDCl3, 400 MHz)
1.00
1.93
1.0 10.5 10.0 9.5 9.0 8.5 8.0 7.5 7.0 6.5 6.0 5.5 5.0 4.5 4.0 3.5 3.0 2.5 2.0 1.5 1.0 0.5 0.0 -0.5 -1.
f1 (ppm)

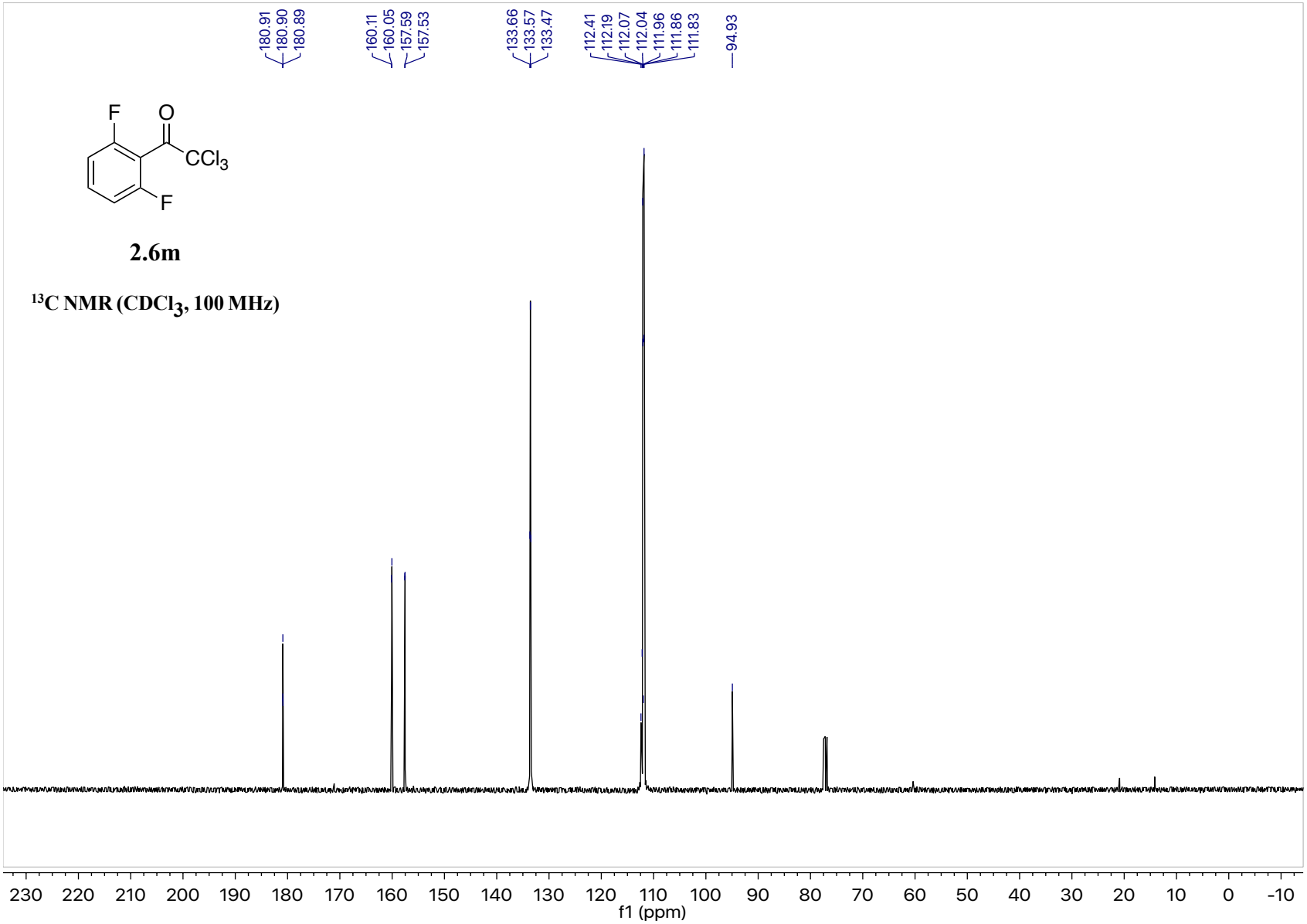
180.91
180.90
180.89
160.11
160.05
157.59
157.53
133.66
133.57
133.47
112.41
112.19
112.07
112.04
111.96
111.86
111.83
94.93
F
O
CCl3
F
2.6m
13C NMR (CDCl3, 100 MHz)
230 220 210 200 190 180 170 160 150 140 130 120 110 100 90 80 70 60 50 40 30 20 10 0 -10
f1 (ppm)

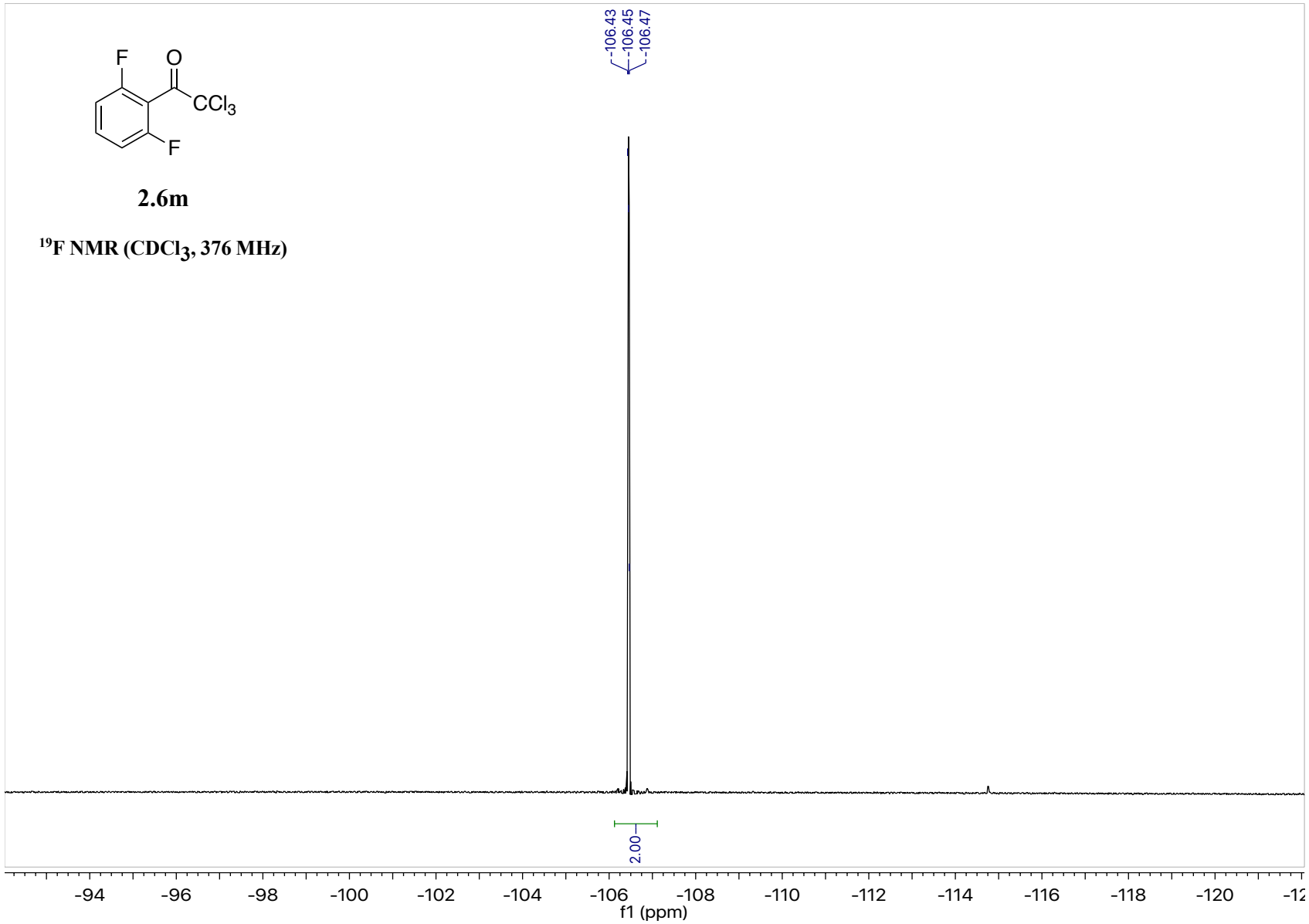

2.6m

^{19}F NMR ($CDCl_3$, 376 MHz)

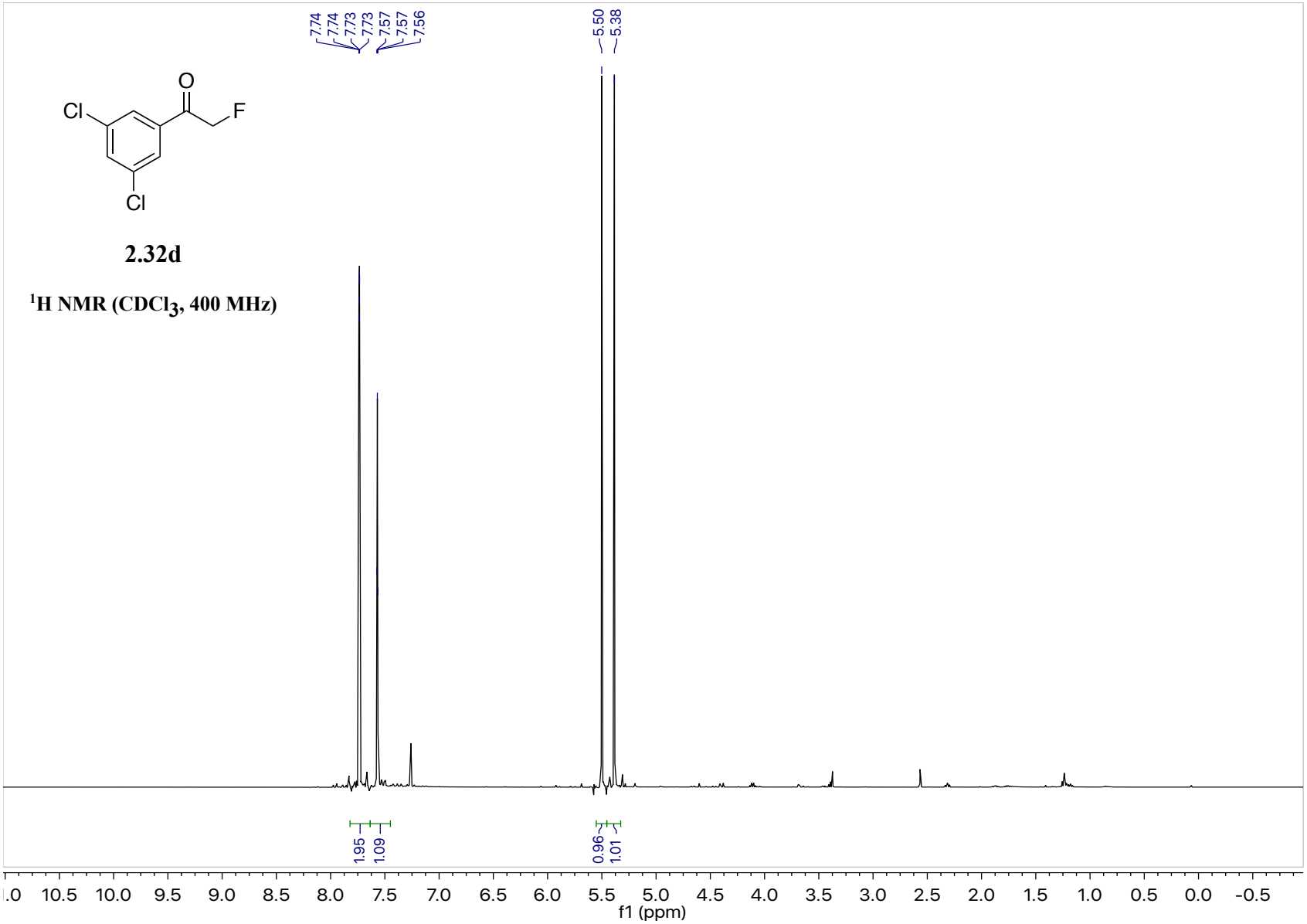
7.74
7.74
7.73
7.73
7.57
7.57
7.56
5.50
5.38
O
Cl
F
Cl
2.32d
1H NMR (CDCl3, 400 MHz)
1.95
1.09
0.96
1.01
f1 (ppm)

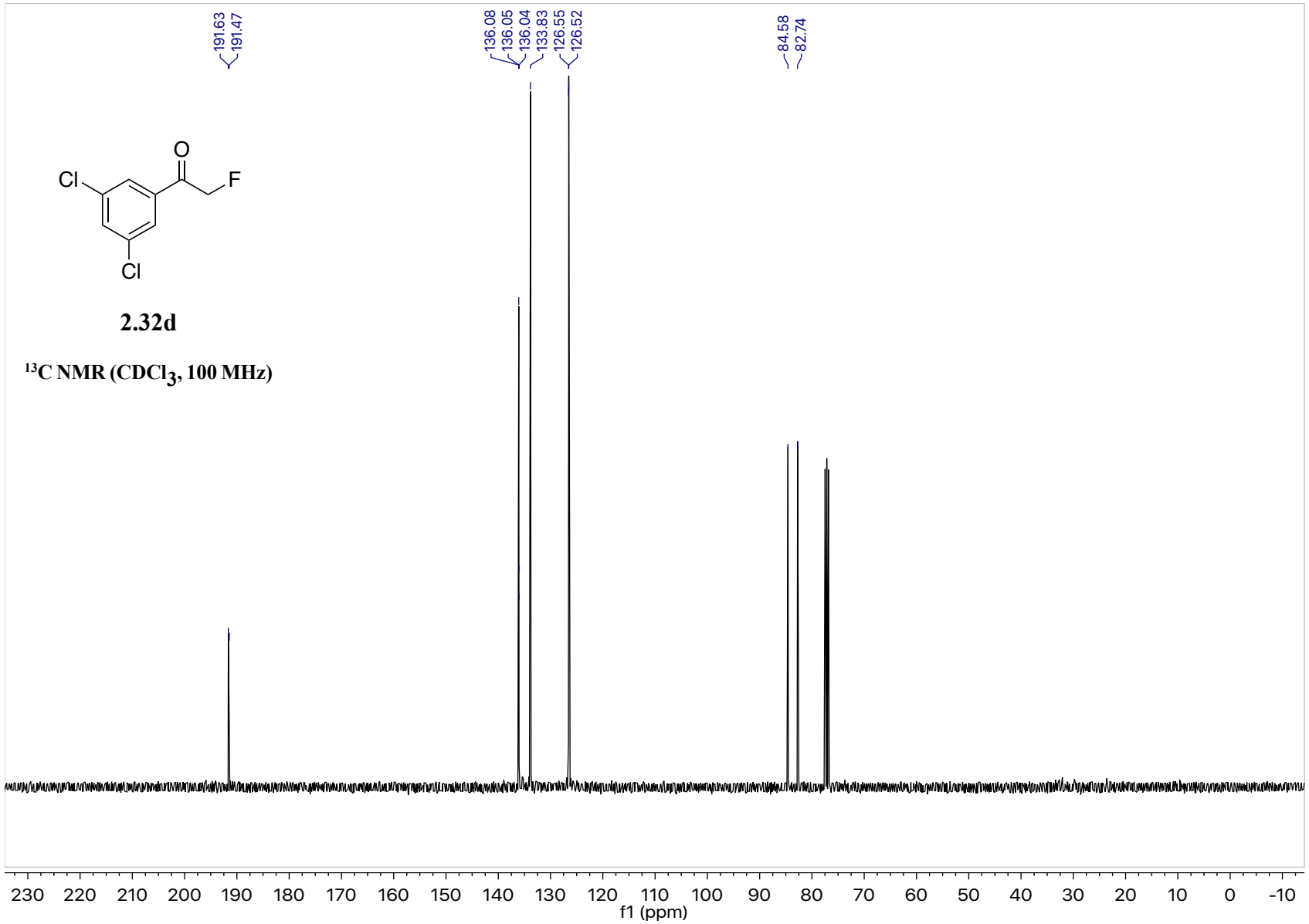
191.63
191.47
136.08
136.05
136.04
133.83
126.55
126.52
84.58
82.74
O
Cl
F
Cl
2.32d
13C NMR (CDCl3, 100 MHz)
230 220 210 200 190 180 170 160 150 140 130 120 110 100 90 80 70 60 50 40 30 20 10 0 -10
f1 (ppm)

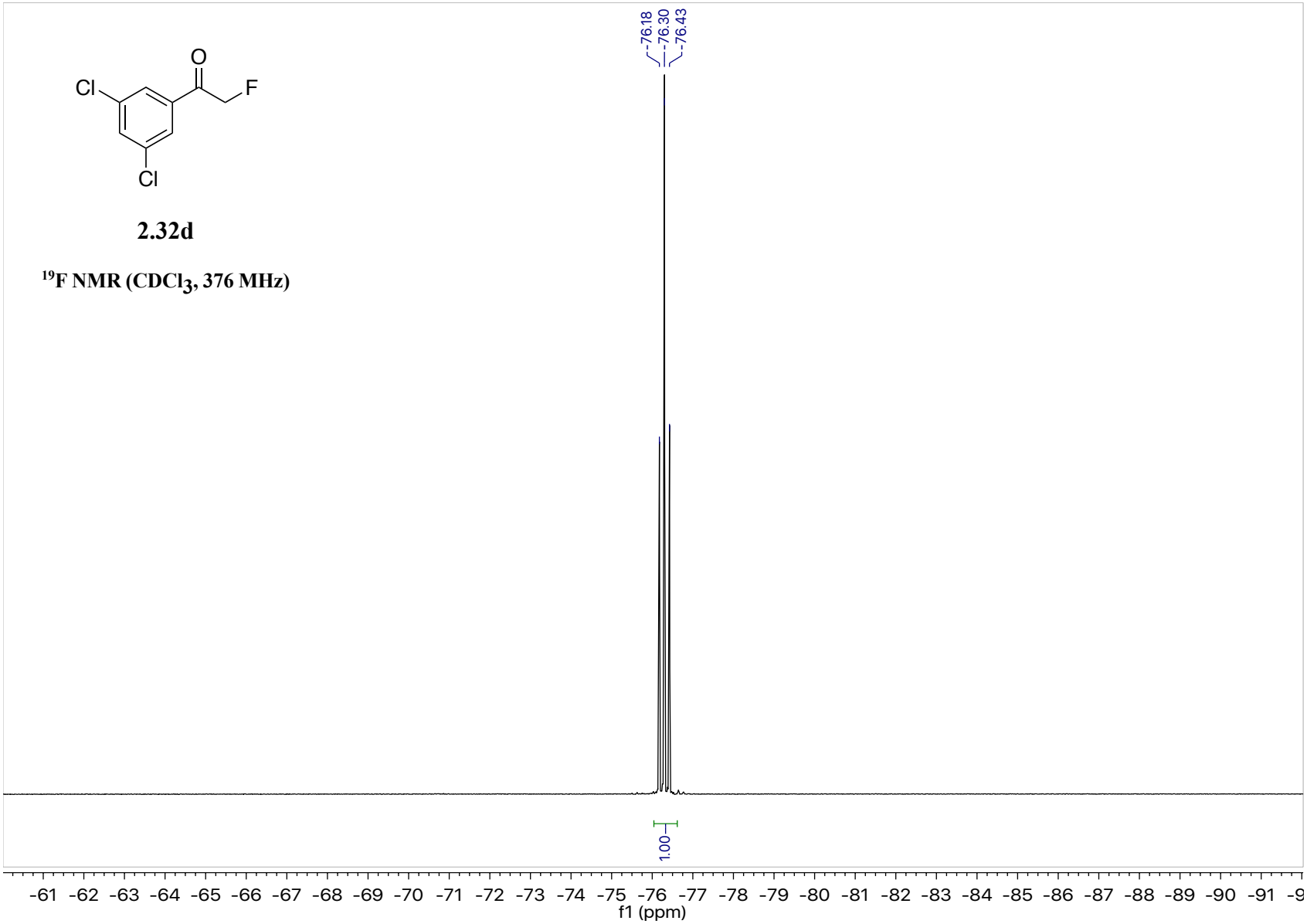

2.32d

^{19}F NMR ($CDCl_3$, 376 MHz)

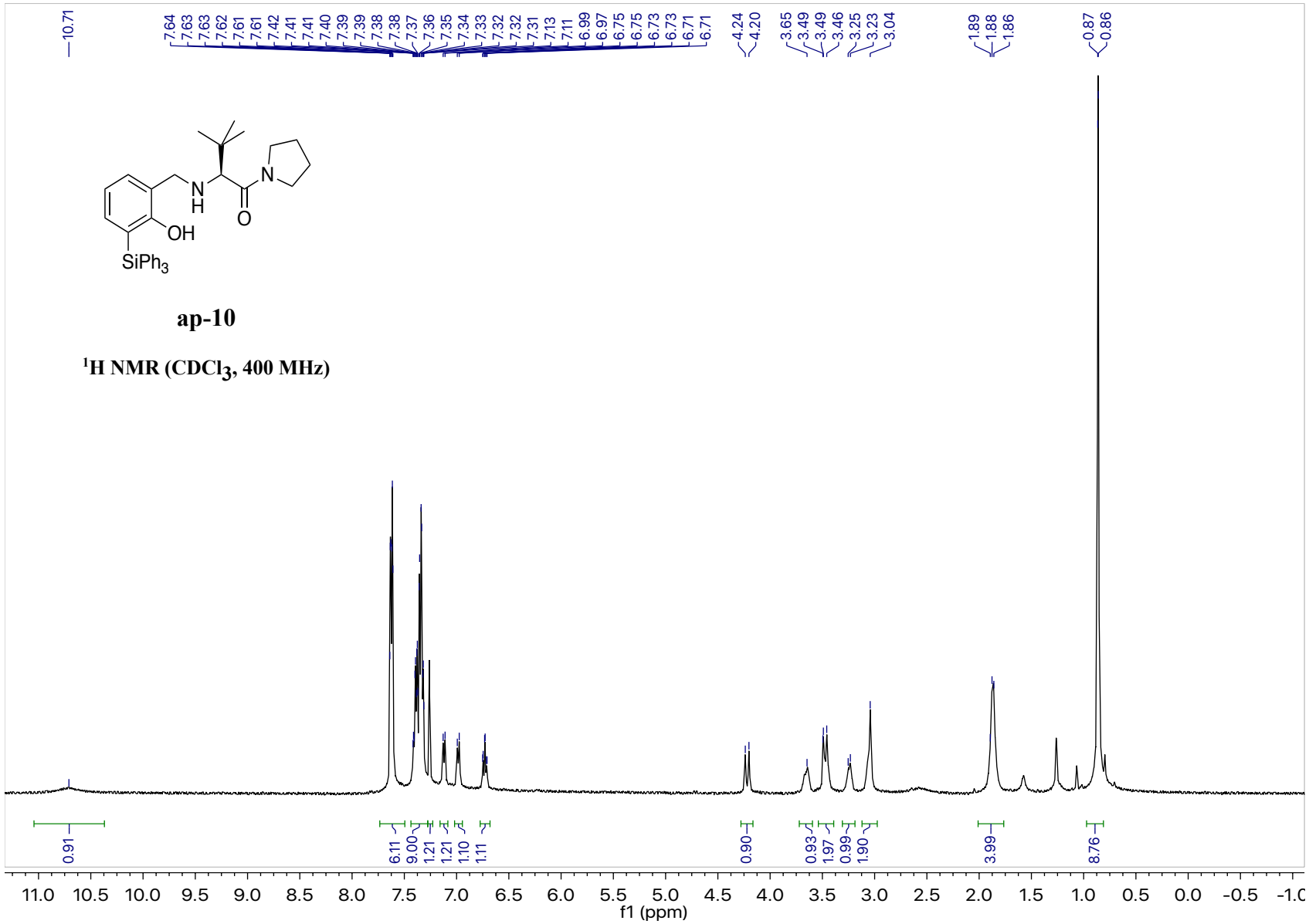

ap-10

^{1}H NMR ($CDCl_3$, 400 MHz)

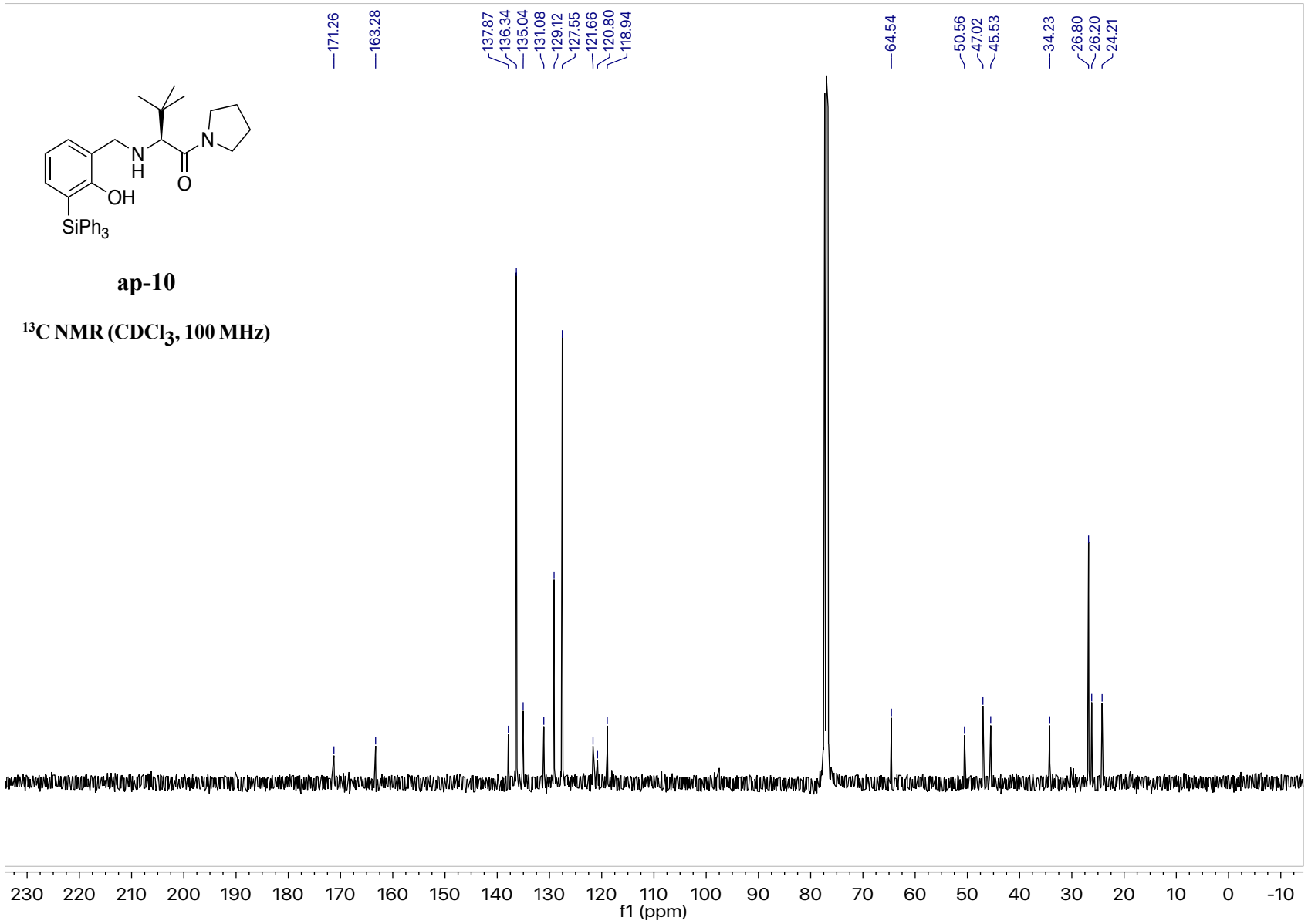
171.26
163.28
137.87
136.34
135.04
131.08
129.12
127.55
121.66
120.80
118.94
64.54
50.56
47.02
45.53
34.23
26.80
26.20
24.21
N
H
N
O
OH
SiPh3
ap-10
13C NMR (CDCl3, 100 MHz)
230 220 210 200 190 180 170 160 150 140 130 120 110 100 90 80 70 60 50 40 30 20 10 0 -10
f1 (ppm)

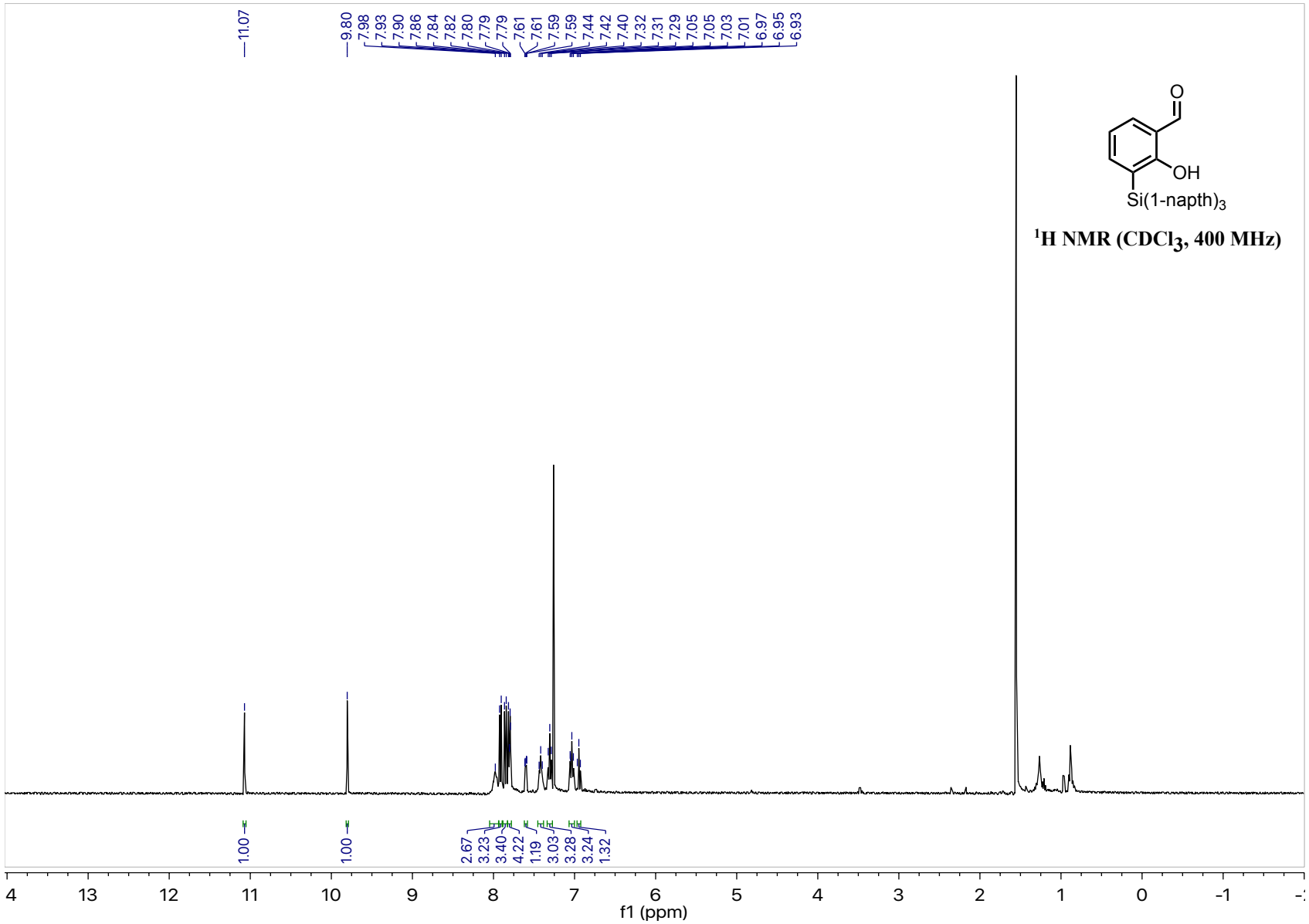
11.07
9.80
7.98
7.93
7.90
7.86
7.84
7.82
7.80
7.79
7.79
7.61
7.61
7.59
7.59
7.44
7.42
7.40
7.32
7.31
7.29
7.05
7.05
7.03
7.01
6.97
6.95
6.93
O
OH
Si(1-napth)3
1H NMR (CDCl3, 400 MHz)
1.00
1.00
2.67
3.23
3.40
4.22
1.19
3.03
3.28
3.24
1.32
f1 (ppm)

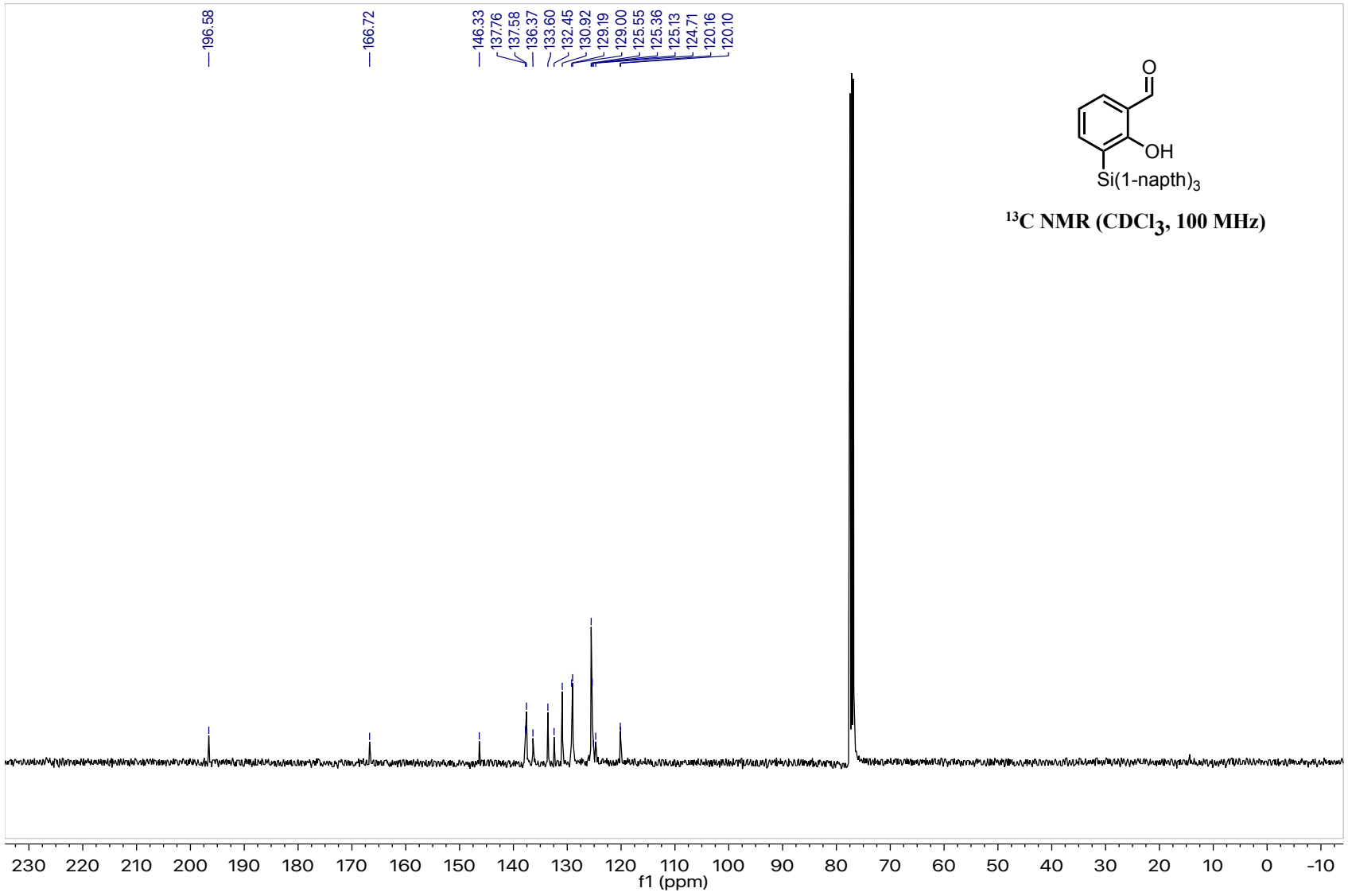

^{13}C NMR ($CDCl_3$, 100 MHz)

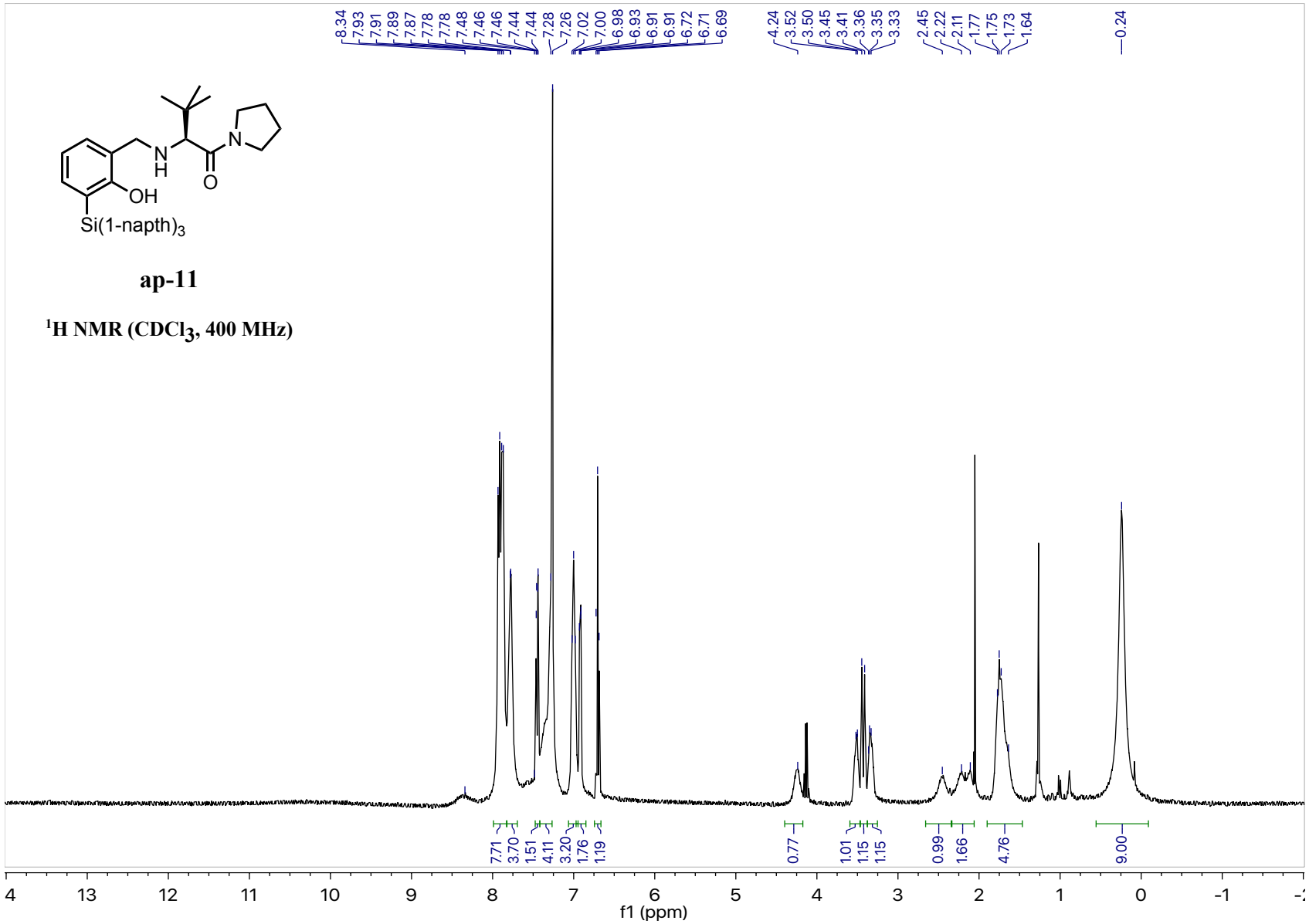

ap-11

^{1}H NMR ($CDCl_3$, 400 MHz)

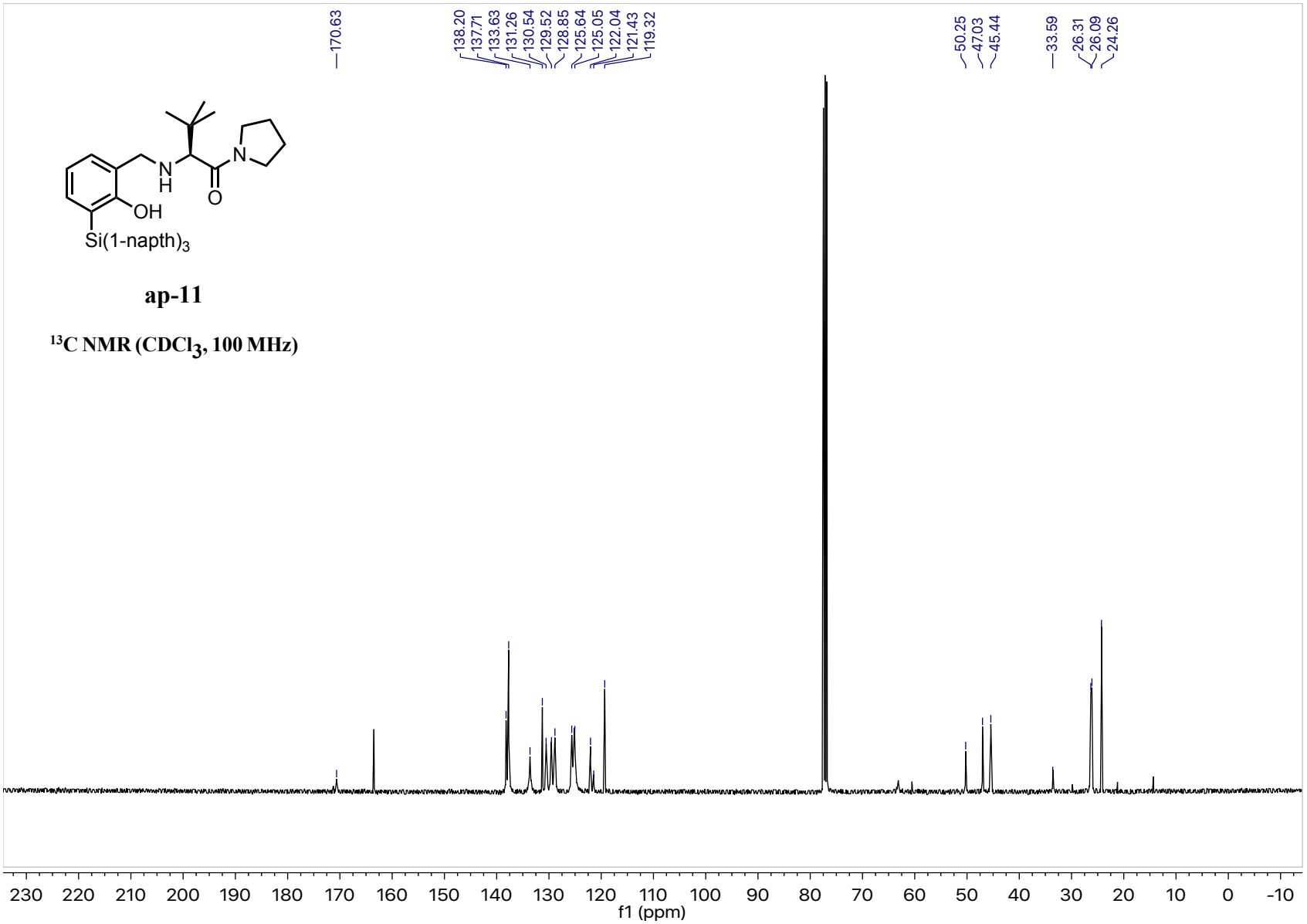

ap-11

^{13}C NMR ($CDCl_3$, 100 MHz)

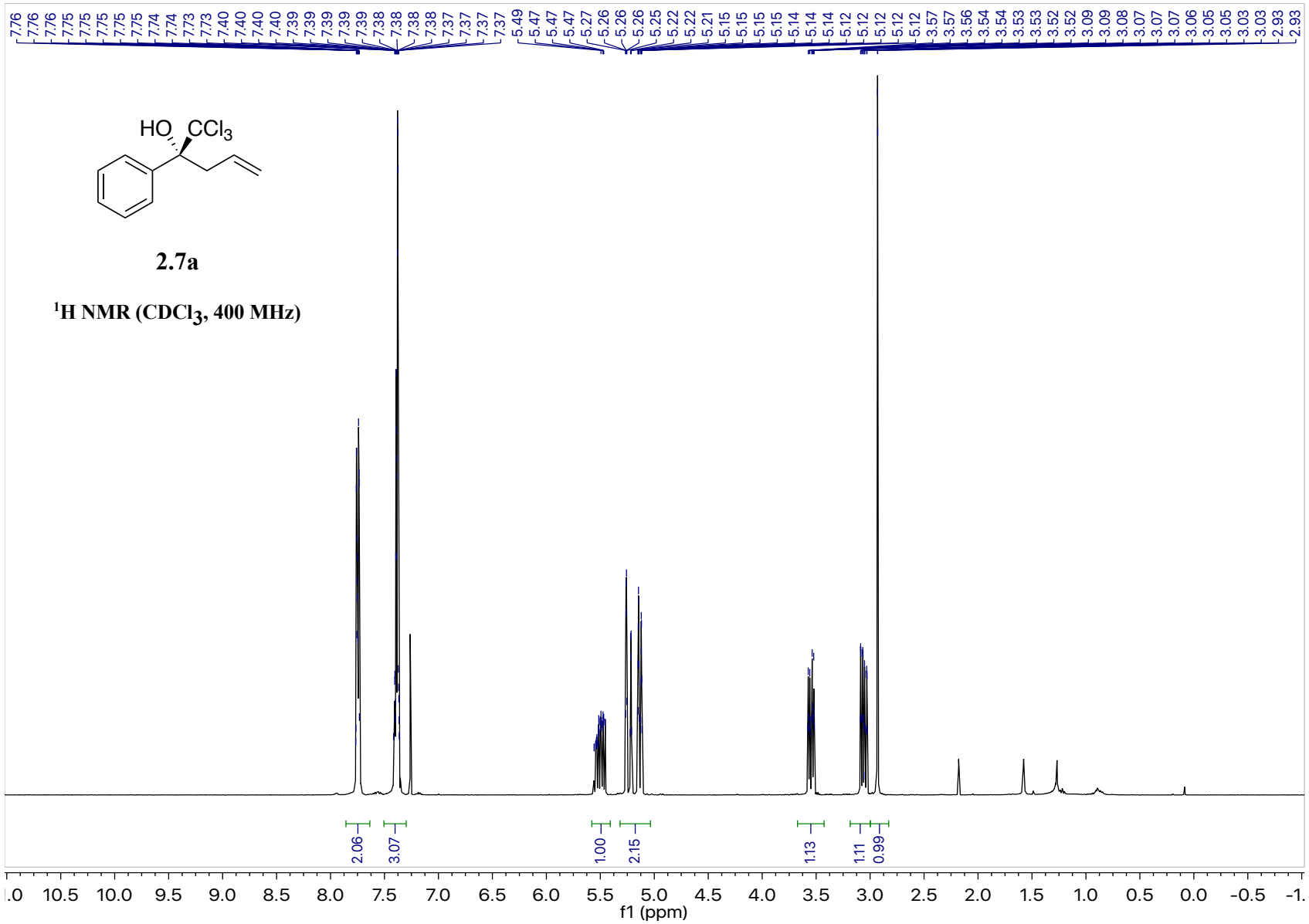
HO
CCl3
2.7a
1H NMR (CDCl3, 400 MHz)
2.06
3.07
1.00
2.15
1.13
1.11
0.99
f1 (ppm)

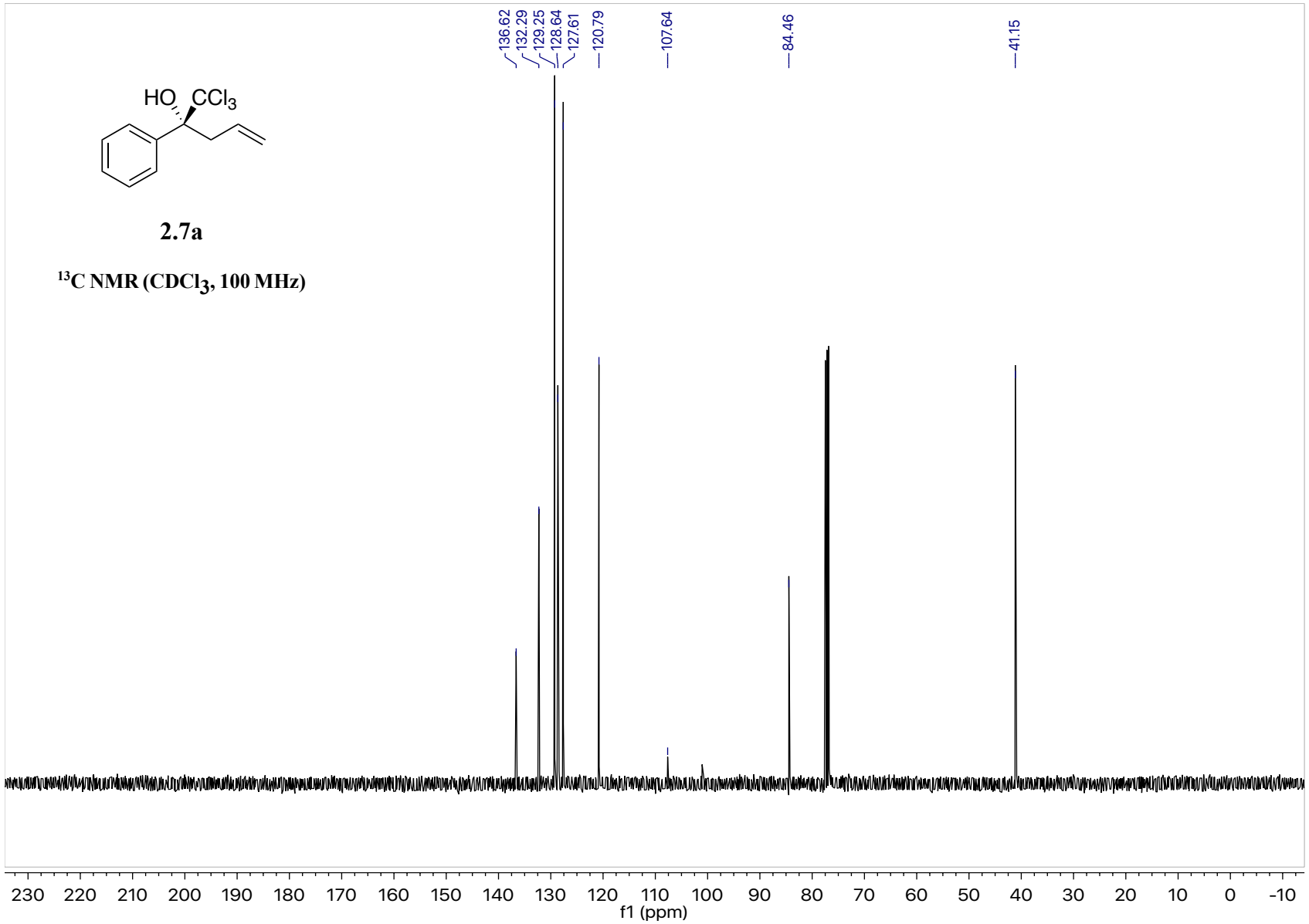
136.62
132.29
129.25
128.64
127.61
120.79
107.64
84.46
41.15
HO
CCl3
2.7a
13C NMR (CDCl3, 100 MHz)
230 220 210 200 190 180 170 160 150 140 130 120 110 100 90 80 70 60 50 40 30 20 10 0 -10
f1 (ppm)

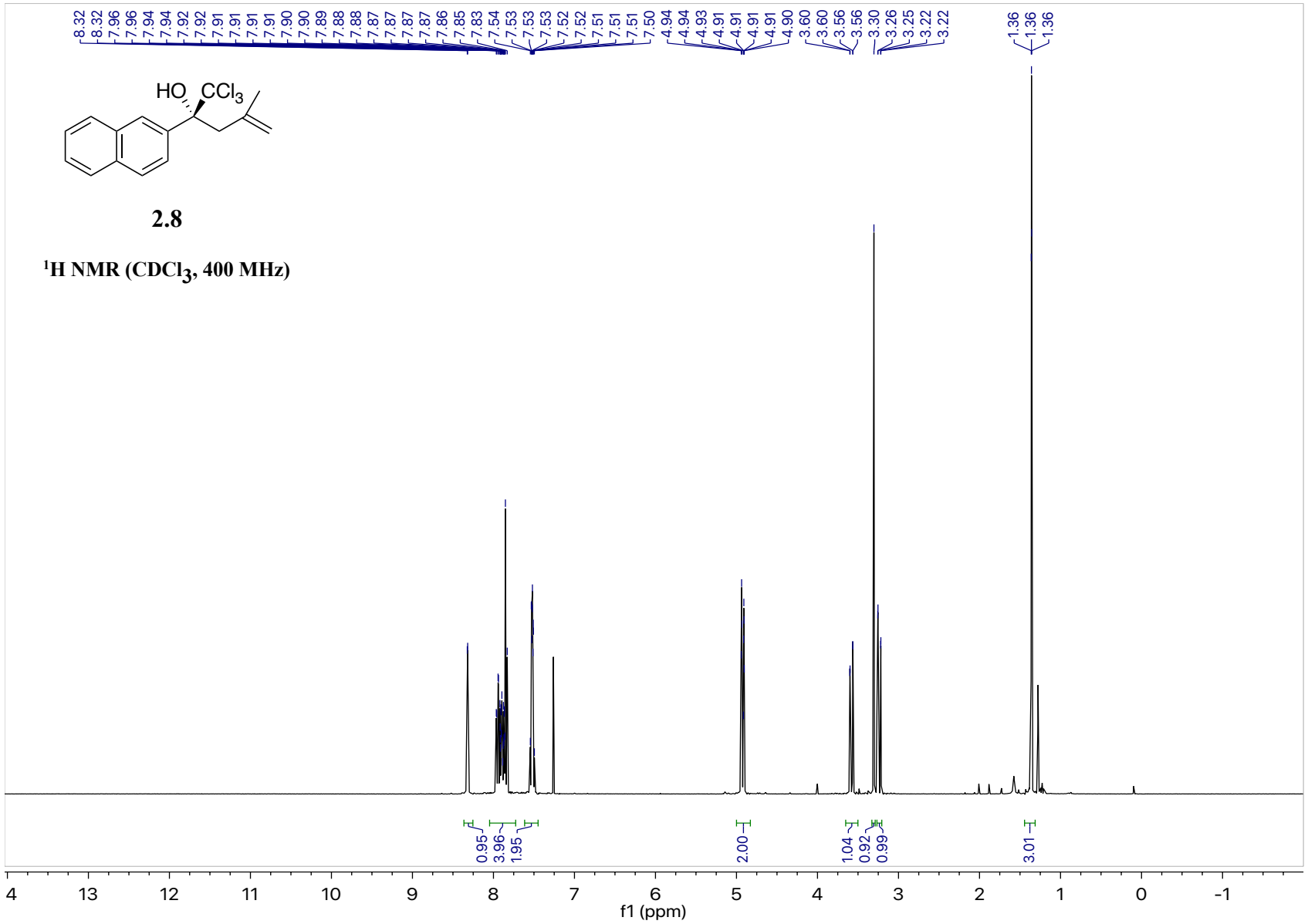
8.32
8.32
7.96
7.96
7.94
7.94
7.92
7.91
7.91
7.91
7.91
7.90
7.90
7.89
7.88
7.88
7.87
7.87
7.87
7.87
7.86
7.85
7.83
7.54
7.53
7.53
7.53
7.52
7.52
7.51
7.51
7.51
7.50
4.94
4.94
4.93
4.91
4.91
4.91
4.91
4.90
3.60
3.60
3.56
3.56
3.30
3.26
3.25
3.22
3.22
1.36
1.36
1.36
HO
CCl3
2.8
1H NMR (CDCl3, 400 MHz)
0.95
3.96
1.95
2.00
1.04
0.92
0.99
3.01
4
13
12
11
10
9
8
7
6
5
4
3
2
1
0
-1
f1 (ppm)

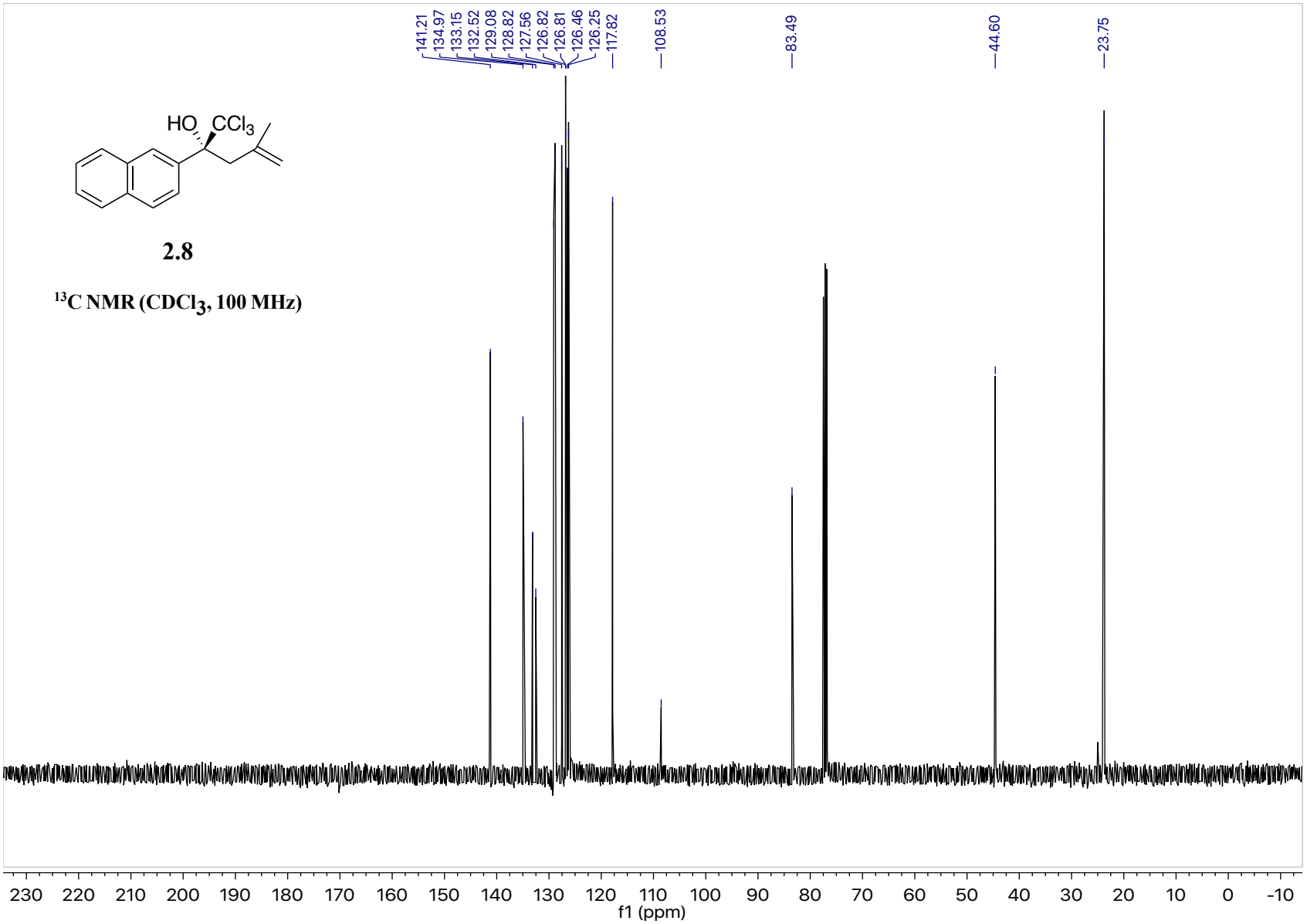
141.21
134.97
133.15
132.52
129.08
128.82
127.56
126.82
126.81
126.46
126.25
117.82
108.53
83.49
44.60
23.75
HO
CCl3
2.8
13C NMR (CDCl3, 100 MHz)
230 220 210 200 190 180 170 160 150 140 130 120 110 100 90 80 70 60 50 40 30 20 10 0 -10
f1 (ppm)

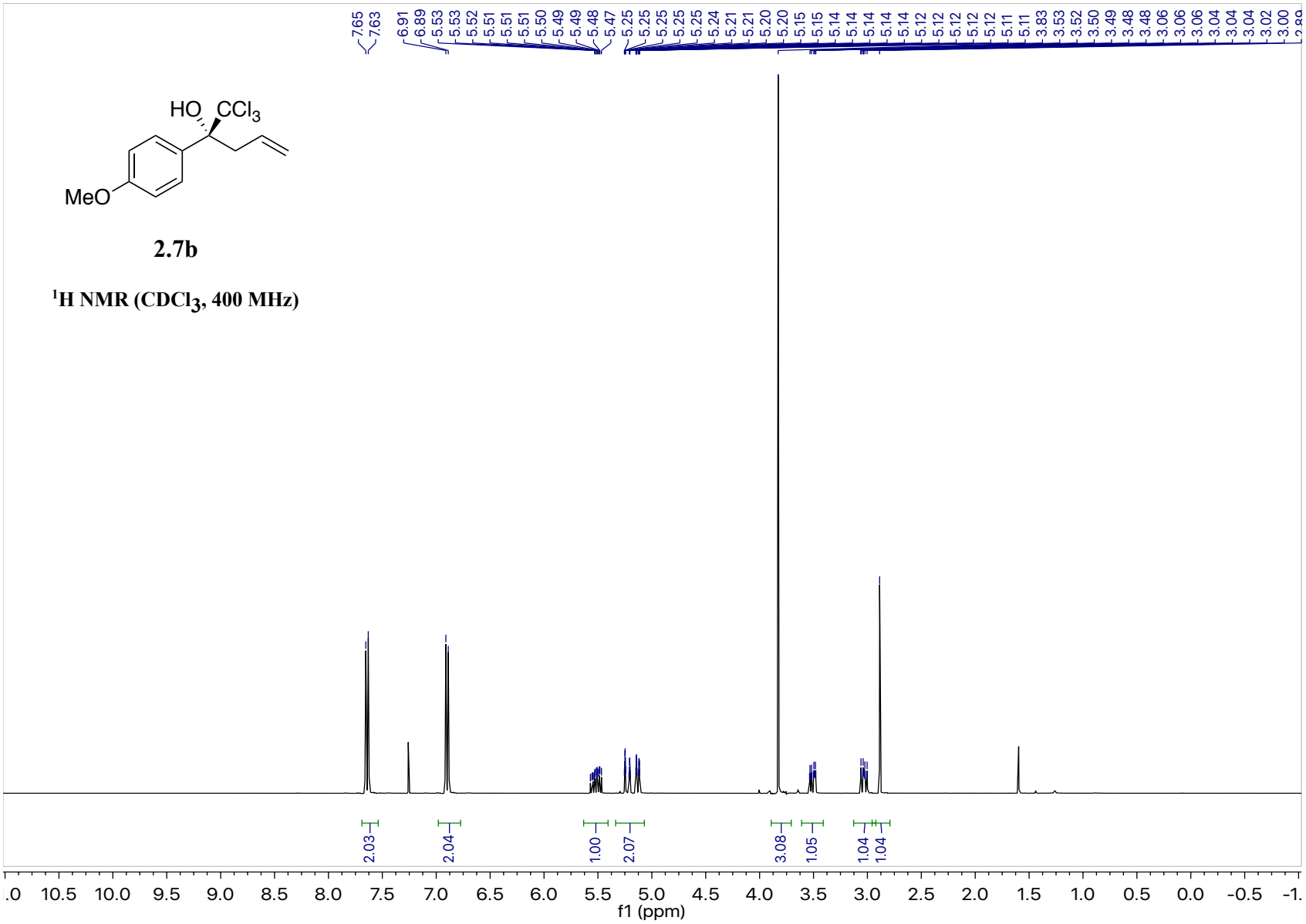
HO
CCl3
MeO
2.7b
1H NMR (CDCl3, 400 MHz)
7.65
7.63
6.91
6.89
5.53
5.52
5.51
5.51
5.51
5.50
5.49
5.49
5.48
5.47
5.25
5.25
5.25
5.25
5.24
5.21
5.21
5.20
5.20
5.15
5.15
5.14
5.14
5.14
5.14
5.12
5.12
5.12
5.12
5.11
5.11
3.83
3.53
3.52
3.50
3.49
3.48
3.48
3.06
3.06
3.06
3.04
3.04
3.04
3.02
3.00
2.03
2.04
1.00
2.07
3.08
1.05
1.04
1.04
f1 (ppm)

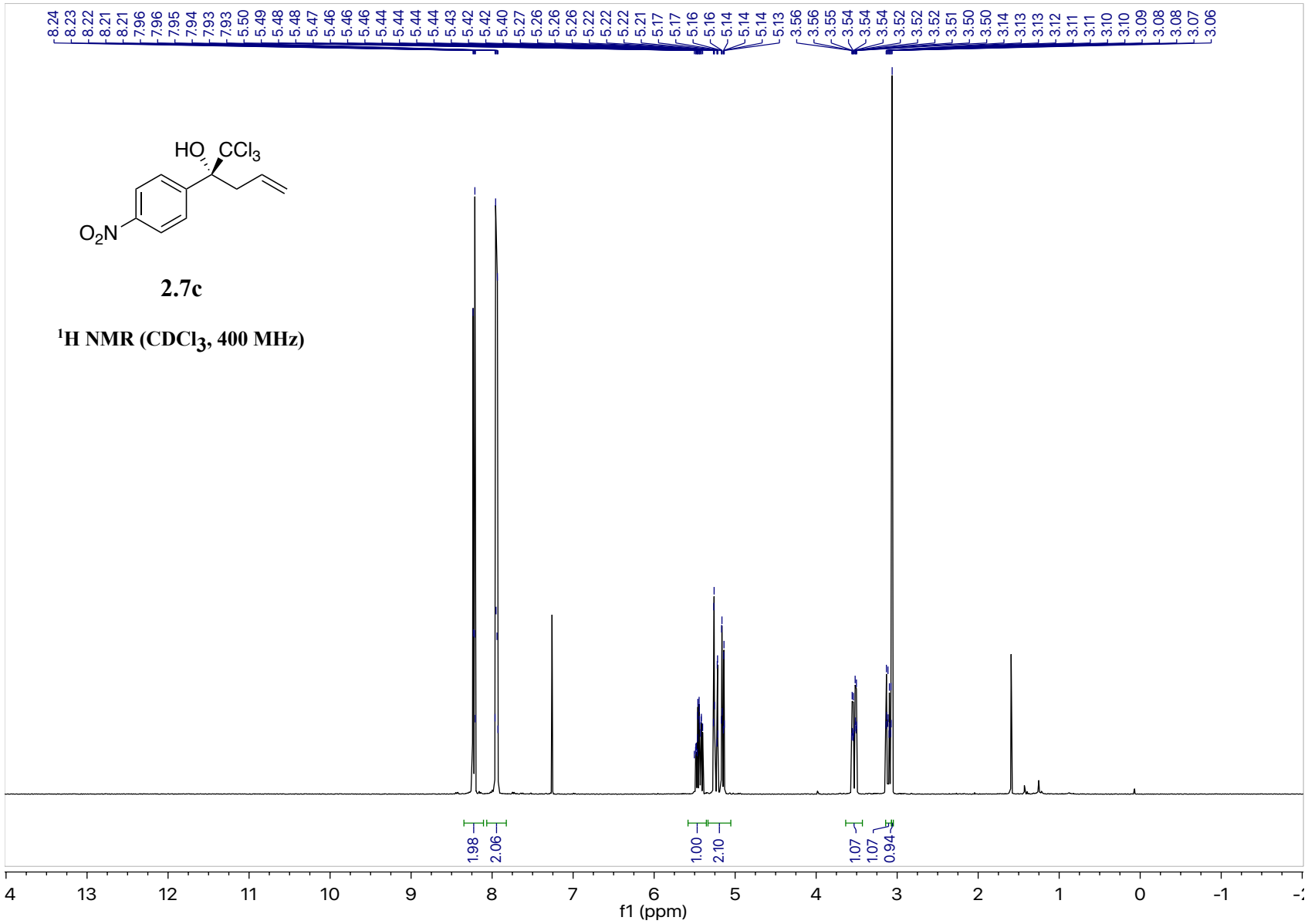
HO
CCl3
O2N
2.7c
1H NMR (CDCl3, 400 MHz)
8.24 8.23 8.22 8.21 8.21 7.96 7.96 7.95 7.94 7.93 7.93 5.50 5.49 5.48 5.48 5.47 5.46 5.46 5.46 5.44 5.44 5.44 5.44 5.43 5.42 5.42 5.40 5.27 5.26 5.26 5.26 5.22 5.22 5.22 5.21 5.17 5.17 5.16 5.16 5.14 5.14 5.14 5.13 3.56 3.56 3.55 3.54 3.54 3.54 3.52 3.52 3.52 3.51 3.50 3.50 3.14 3.13 3.13 3.12 3.11 3.11 3.10 3.10 3.09 3.08 3.08 3.07 3.06
1.98
2.06
1.00
2.10
1.07
1.07
0.94
f1 (ppm)

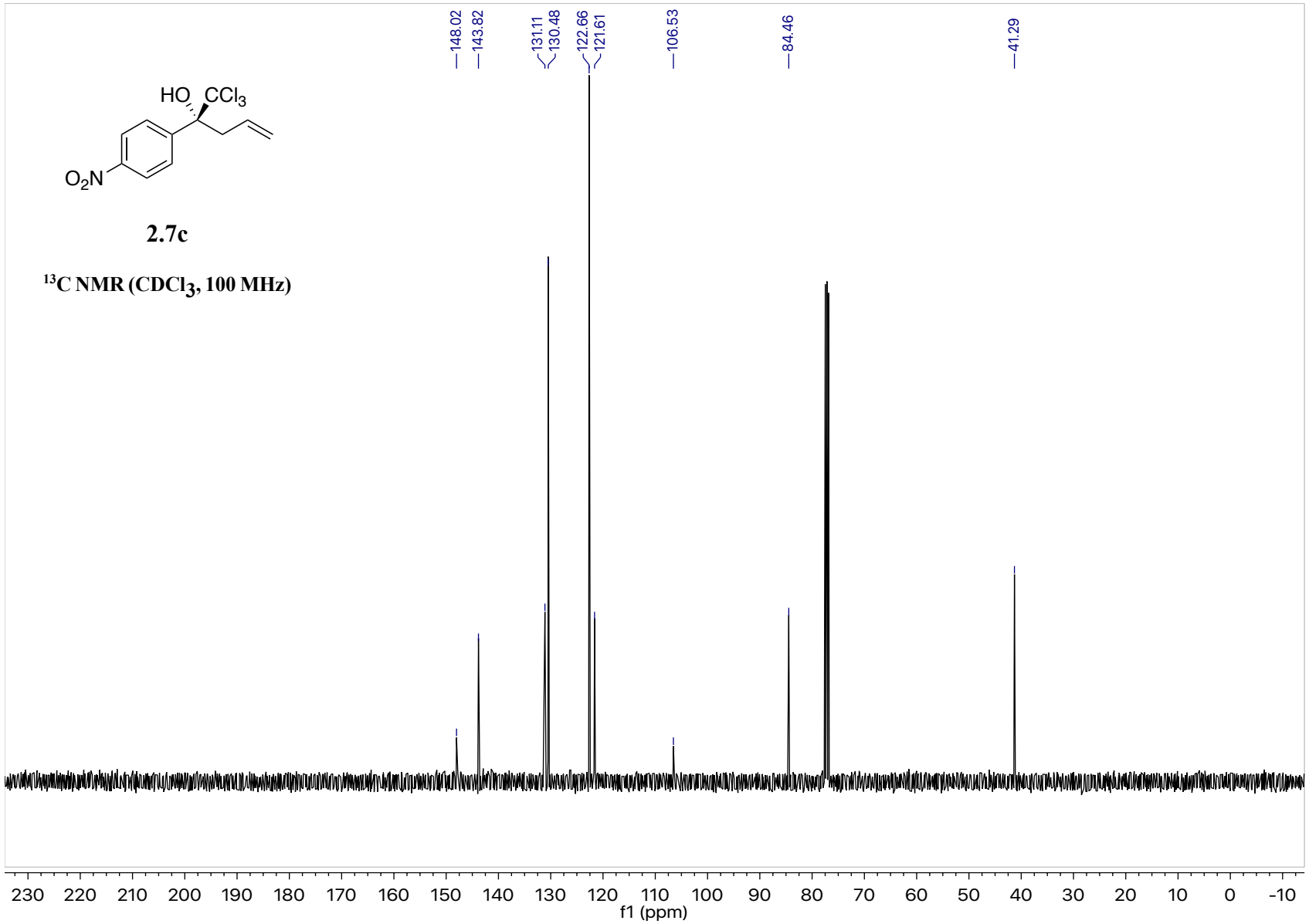
148.02
143.82
131.11
130.48
122.66
121.61
106.53
84.46
41.29
HO
CCl3
O2N
2.7c
13C NMR (CDCl3, 100 MHz)
230 220 210 200 190 180 170 160 150 140 130 120 110 100 90 80 70 60 50 40 30 20 10 0 -10
f1 (ppm)

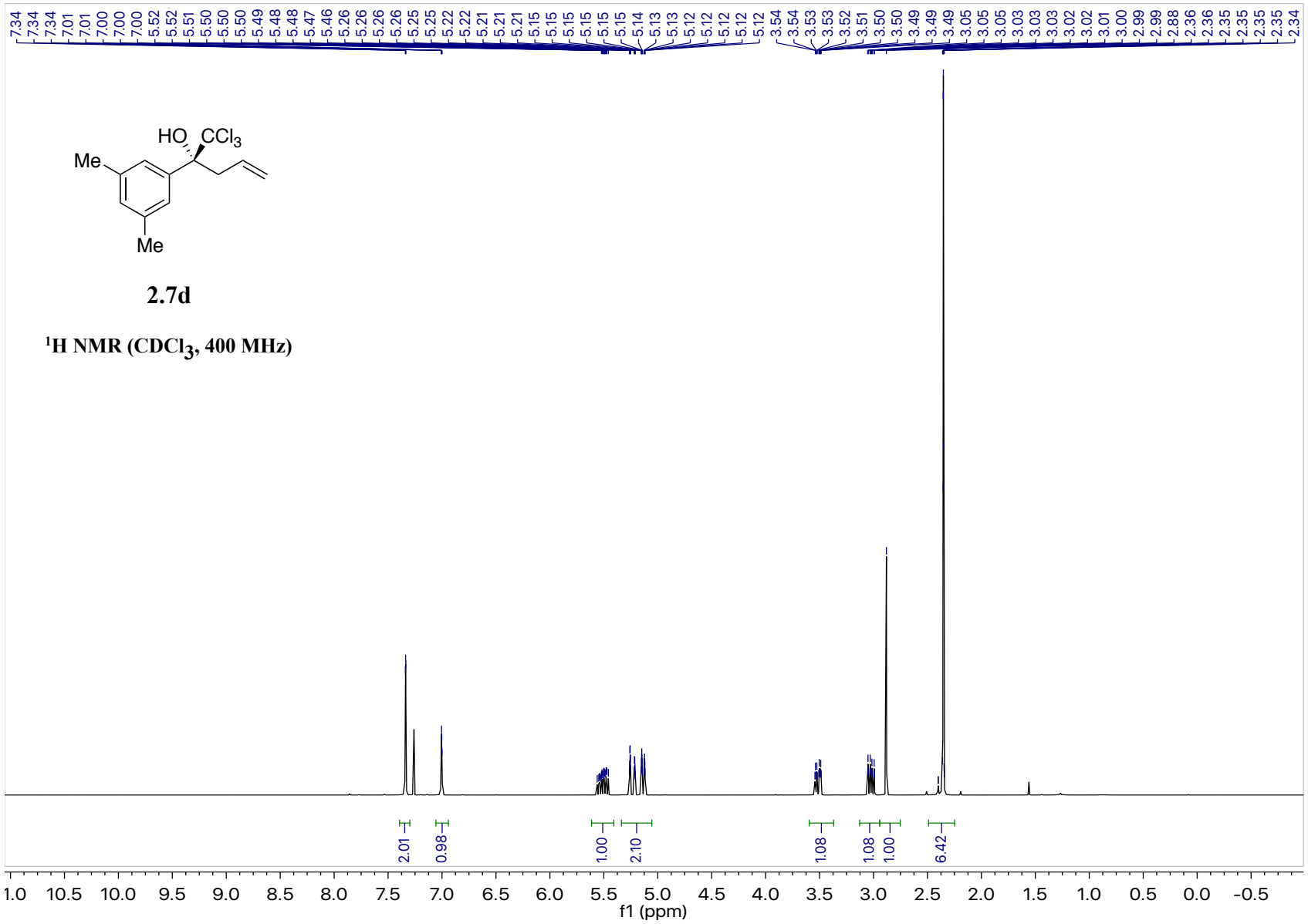
HO
CCl3
Me
Me
2.7d
1H NMR (CDCl3, 400 MHz)
2.01
0.98
1.00
2.10
1.08
1.08
1.00
6.42
f1 (ppm)

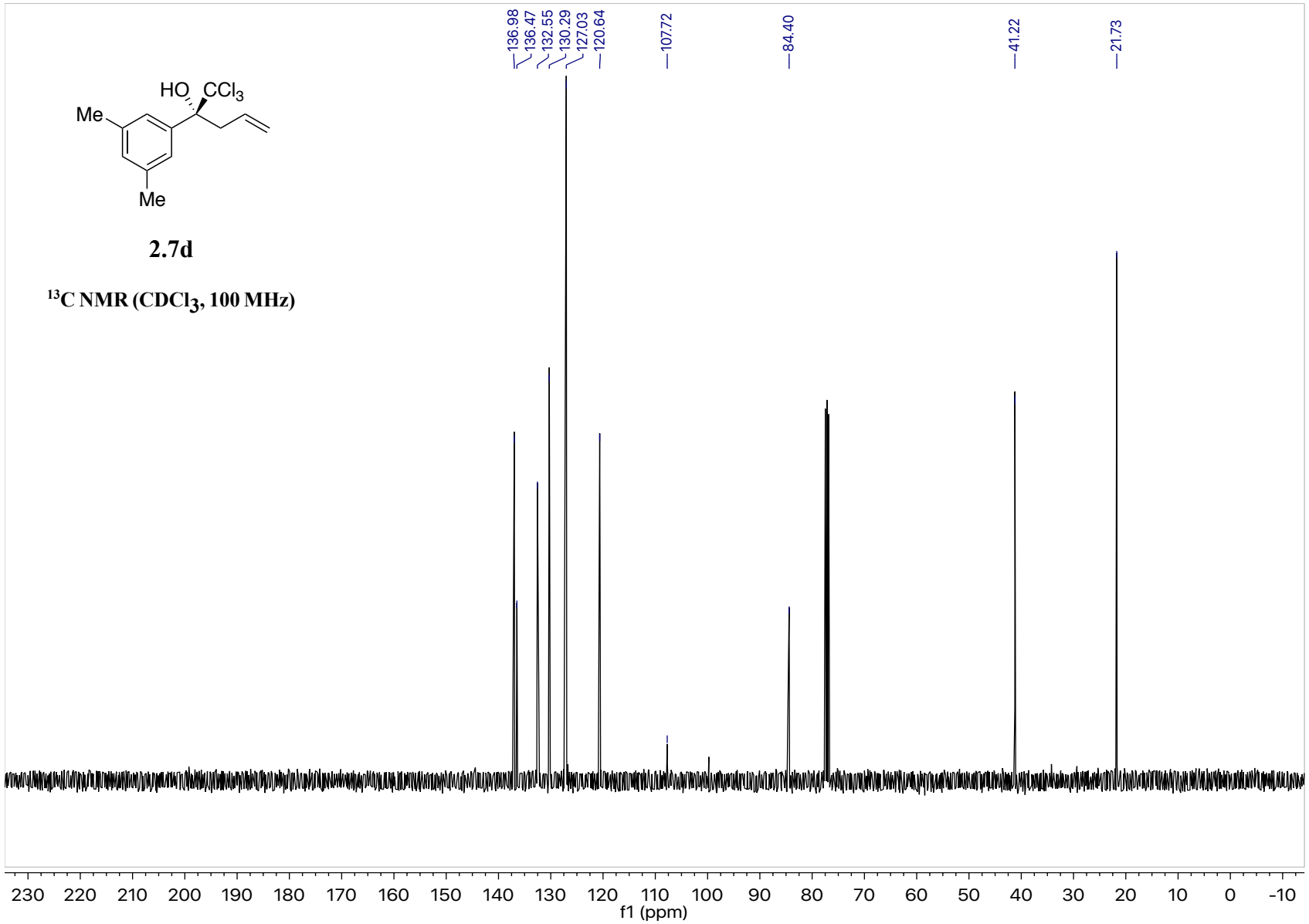
HO
CCl3
Me
Me
2.7d
13C NMR (CDCl3, 100 MHz)
136.98
136.47
132.55
130.29
127.03
120.64
107.72
84.40
41.22
21.73
230 220 210 200 190 180 170 160 150 140 130 120 110 100 90 80 70 60 50 40 30 20 10 0 -10
f1 (ppm)

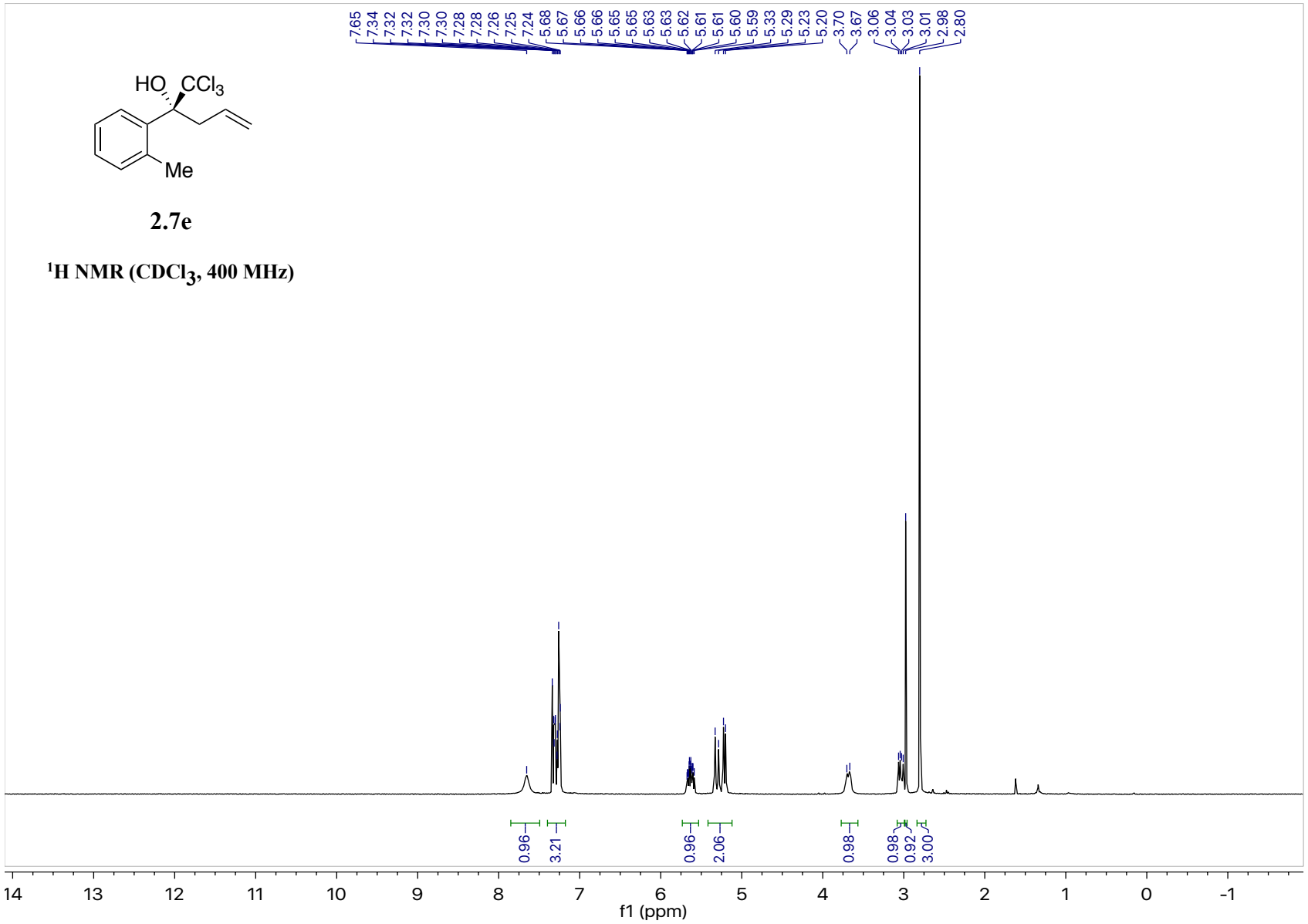

2.7e

^{1}H NMR ($CDCl_3$, 400 MHz)

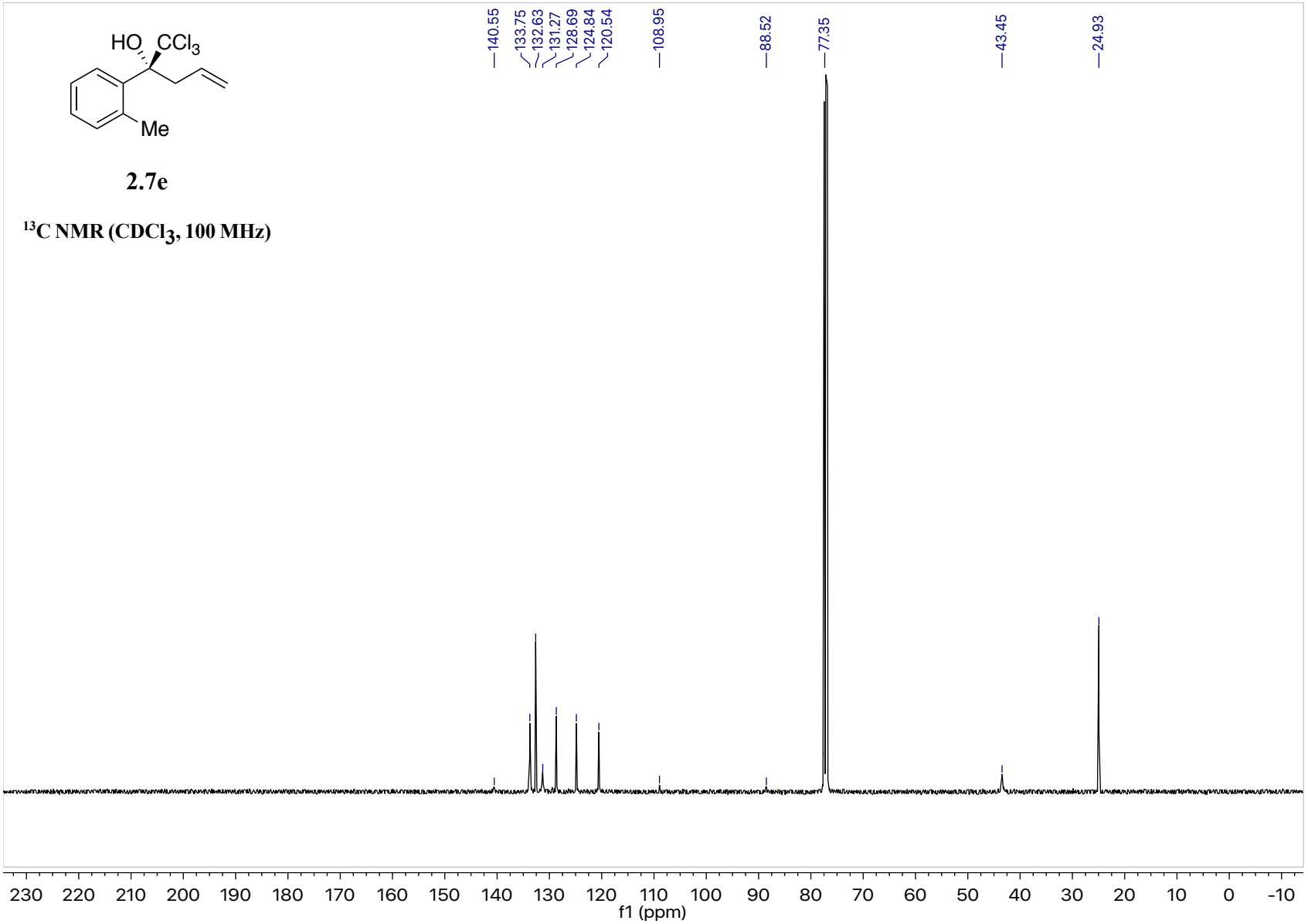

2.7e

^{13}C NMR ($CDCl_3$, 100 MHz)

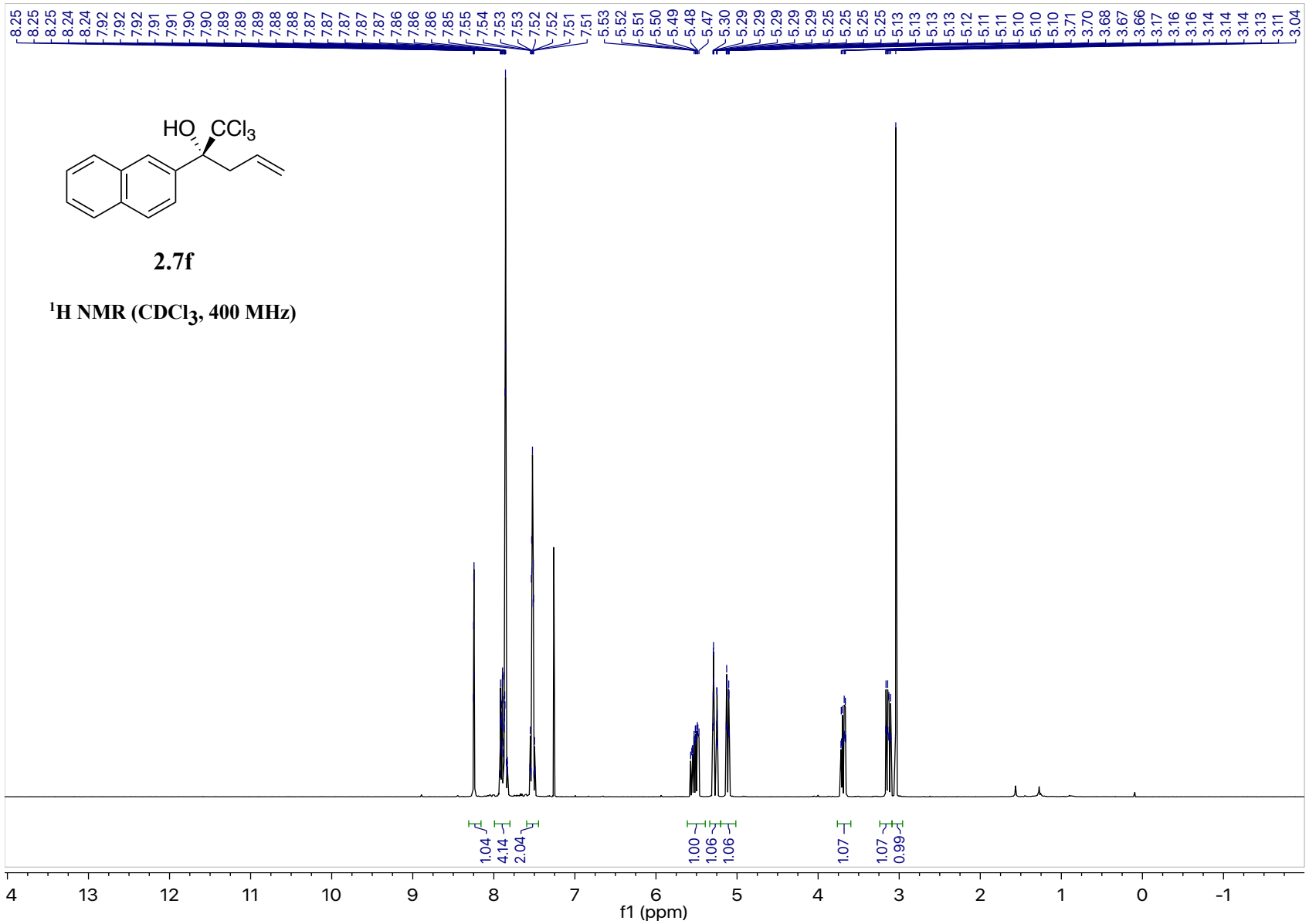
HO
CCl3
2.7f
1H NMR (CDCl3, 400 MHz)
f1 (ppm)

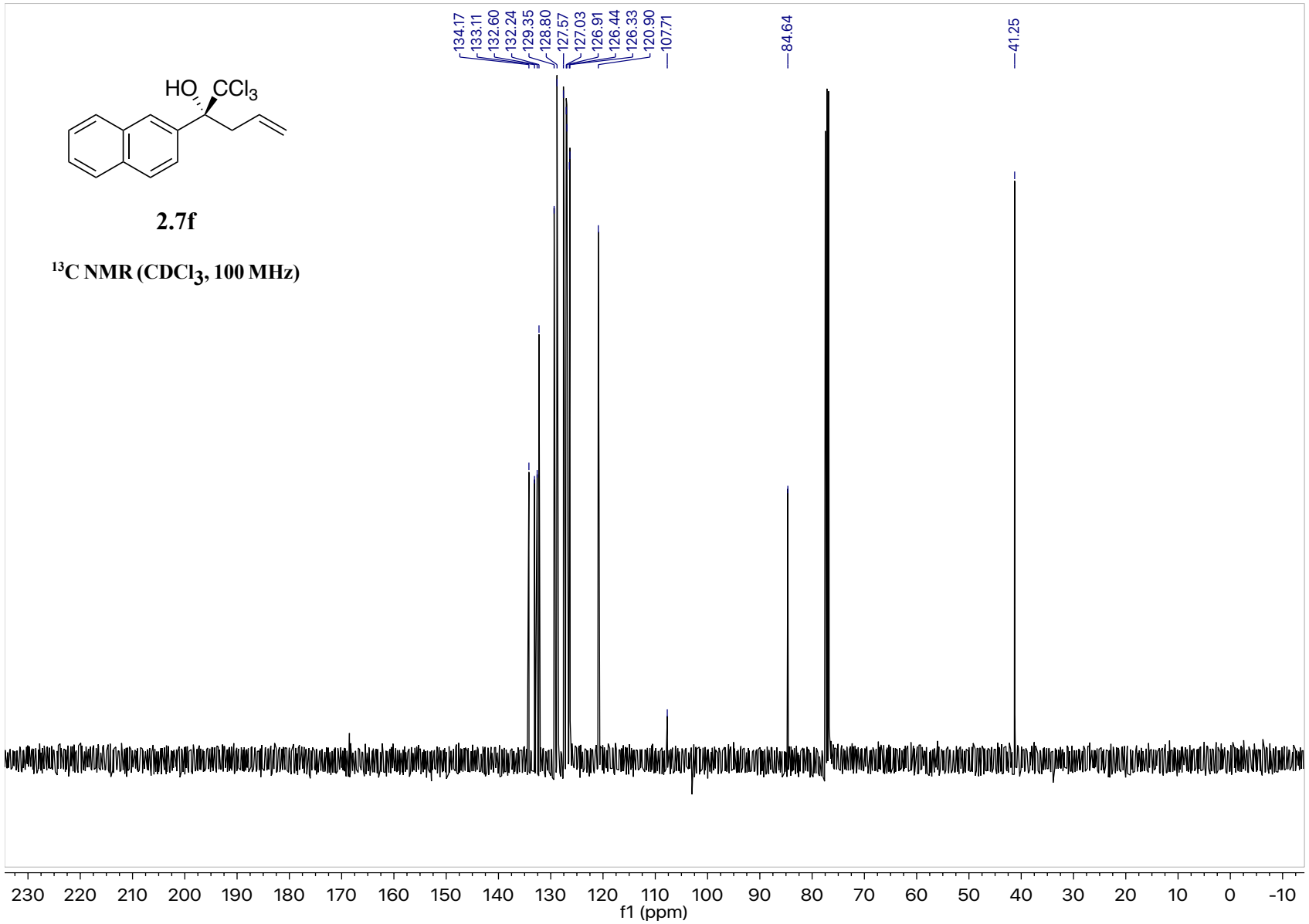
HO
CCl3
2.7f
13C NMR (CDCl3, 100 MHz)
134.17
133.11
132.60
132.24
129.35
128.80
127.57
127.03
126.91
126.44
126.33
120.90
107.71
84.64
41.25
230 220 210 200 190 180 170 160 150 140 130 120 110 100 90 80 70 60 50 40 30 20 10 0 -10
f1 (ppm)

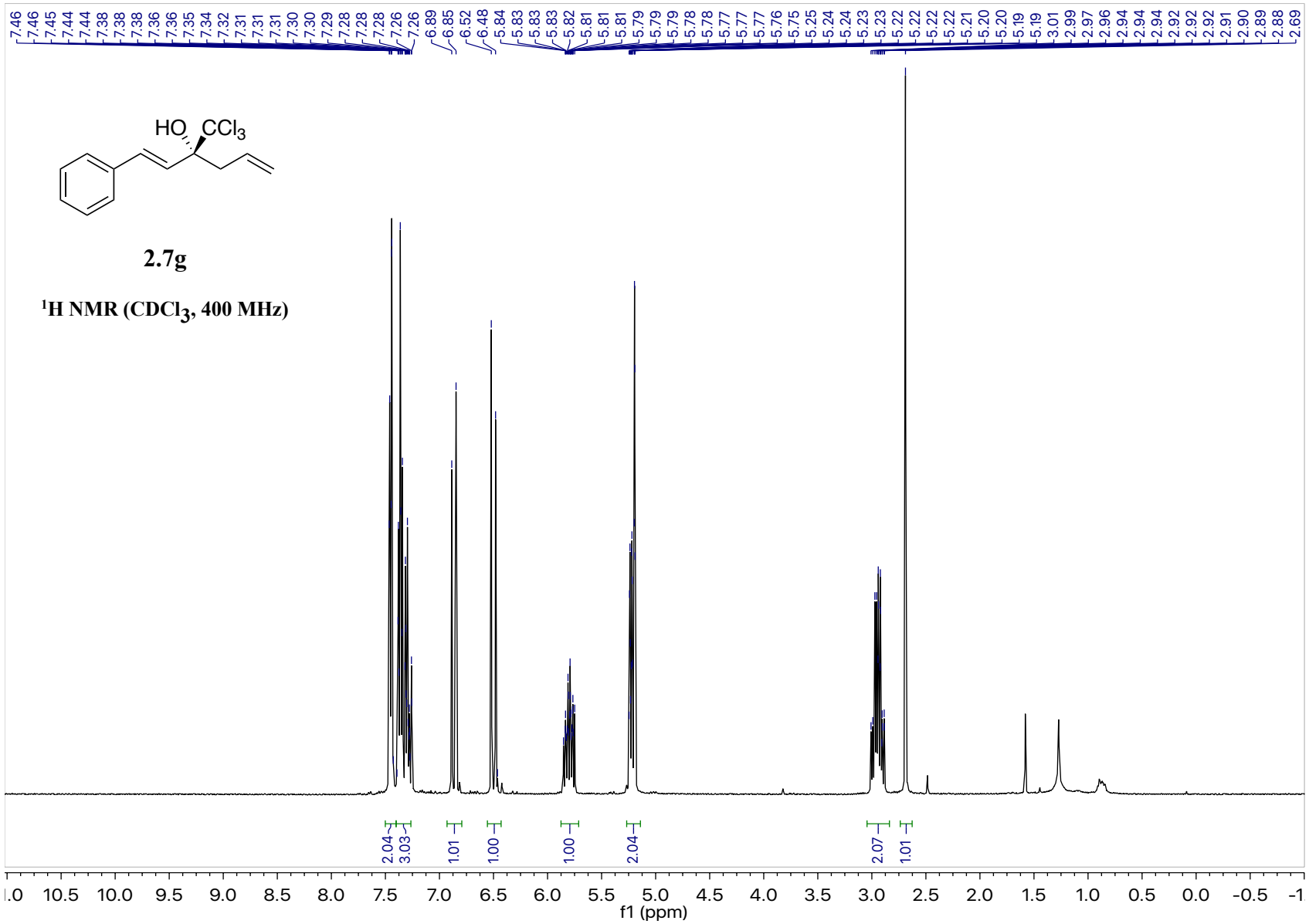
HO
CCl3
2.7g
1H NMR (CDCl3, 400 MHz)
2.04
3.03
1.01
1.00
1.00
2.04
2.07
1.01
f1 (ppm)

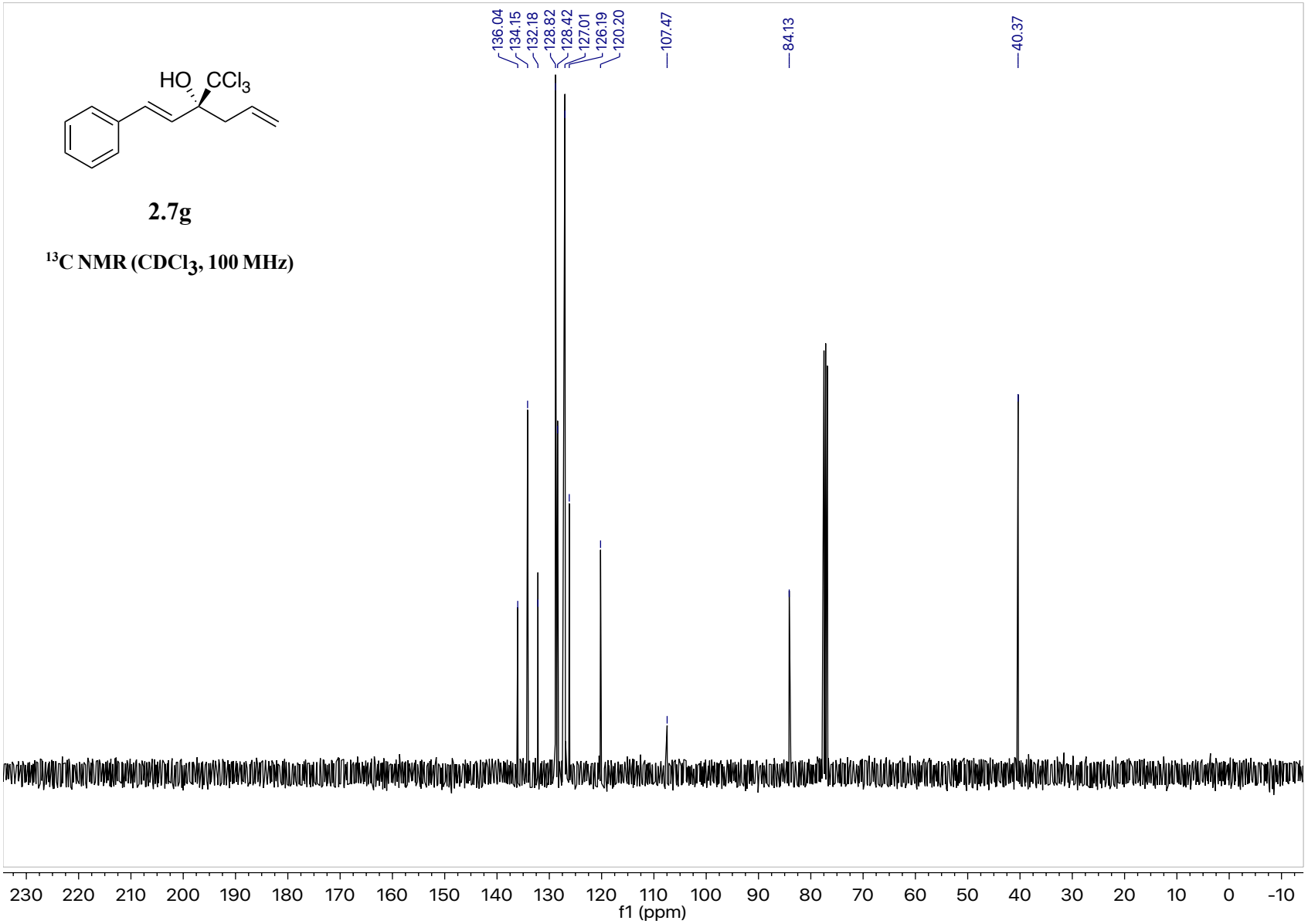
HO
CCl3
2.7g
13C NMR (CDCl3, 100 MHz)
136.04
134.15
132.18
128.82
128.42
127.01
126.19
120.20
107.47
84.13
40.37
230 220 210 200 190 180 170 160 150 140 130 120 110 100 90 80 70 60 50 40 30 20 10 0 -10
f1 (ppm)

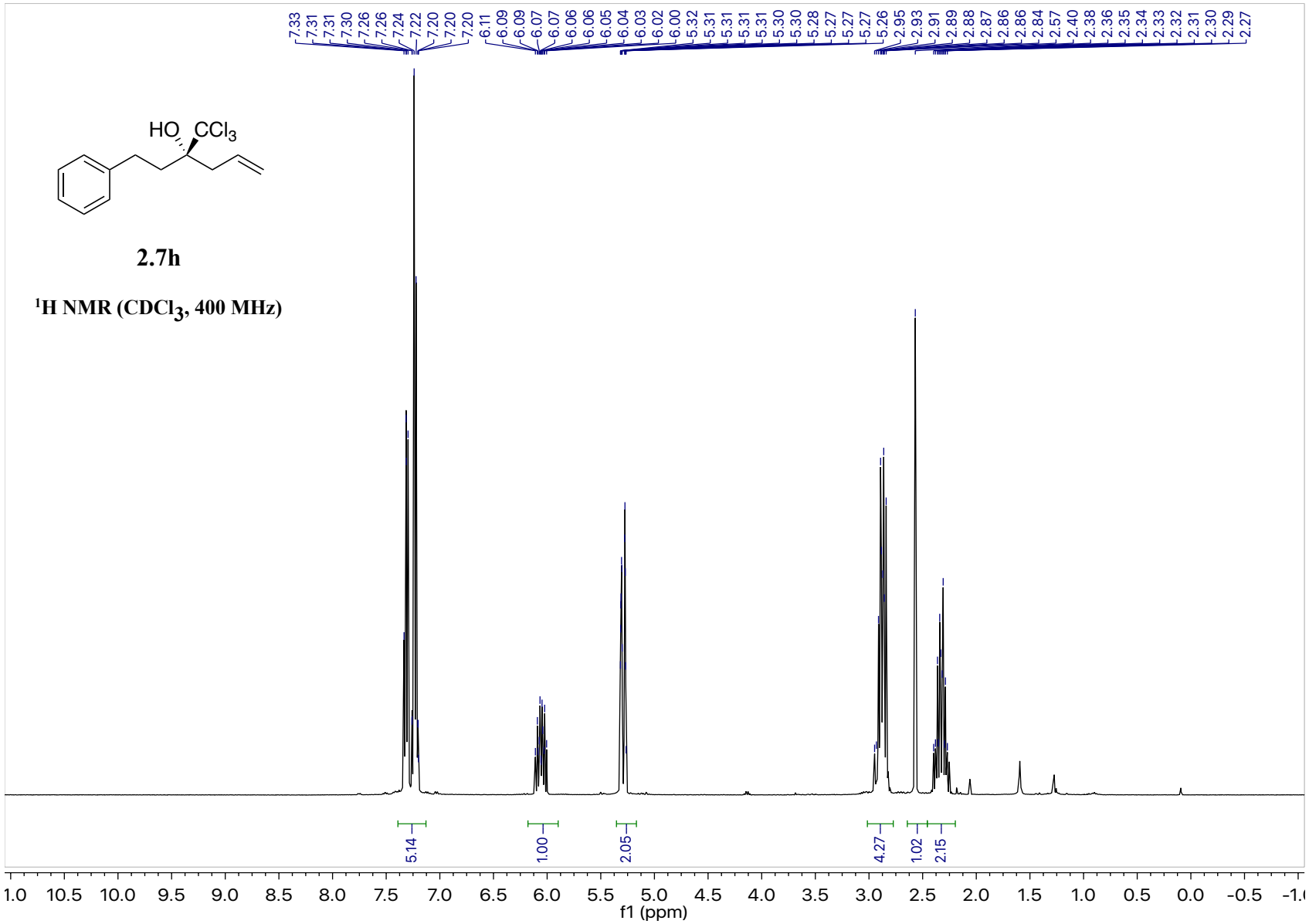
HO
CCl3
2.7h
1H NMR (CDCl3, 400 MHz)
7.33
7.31
7.31
7.30
7.26
7.26
7.24
7.22
7.20
7.20
7.20
6.11
6.09
6.09
6.07
6.07
6.06
6.06
6.05
6.04
6.03
6.02
6.00
5.32
5.31
5.31
5.31
5.30
5.30
5.28
5.27
5.27
5.27
5.26
2.95
2.93
2.91
2.89
2.88
2.87
2.86
2.86
2.84
2.57
2.40
2.38
2.36
2.35
2.34
2.33
2.32
2.31
2.30
2.29
2.27
5.14
1.00
2.05
4.27
1.02
2.15
1.0
10.5
10.0
9.5
9.0
8.5
8.0
7.5
7.0
6.5
6.0
5.5
5.0
4.5
4.0
3.5
3.0
2.5
2.0
1.5
1.0
0.5
0.0
-0.5
f1 (ppm)

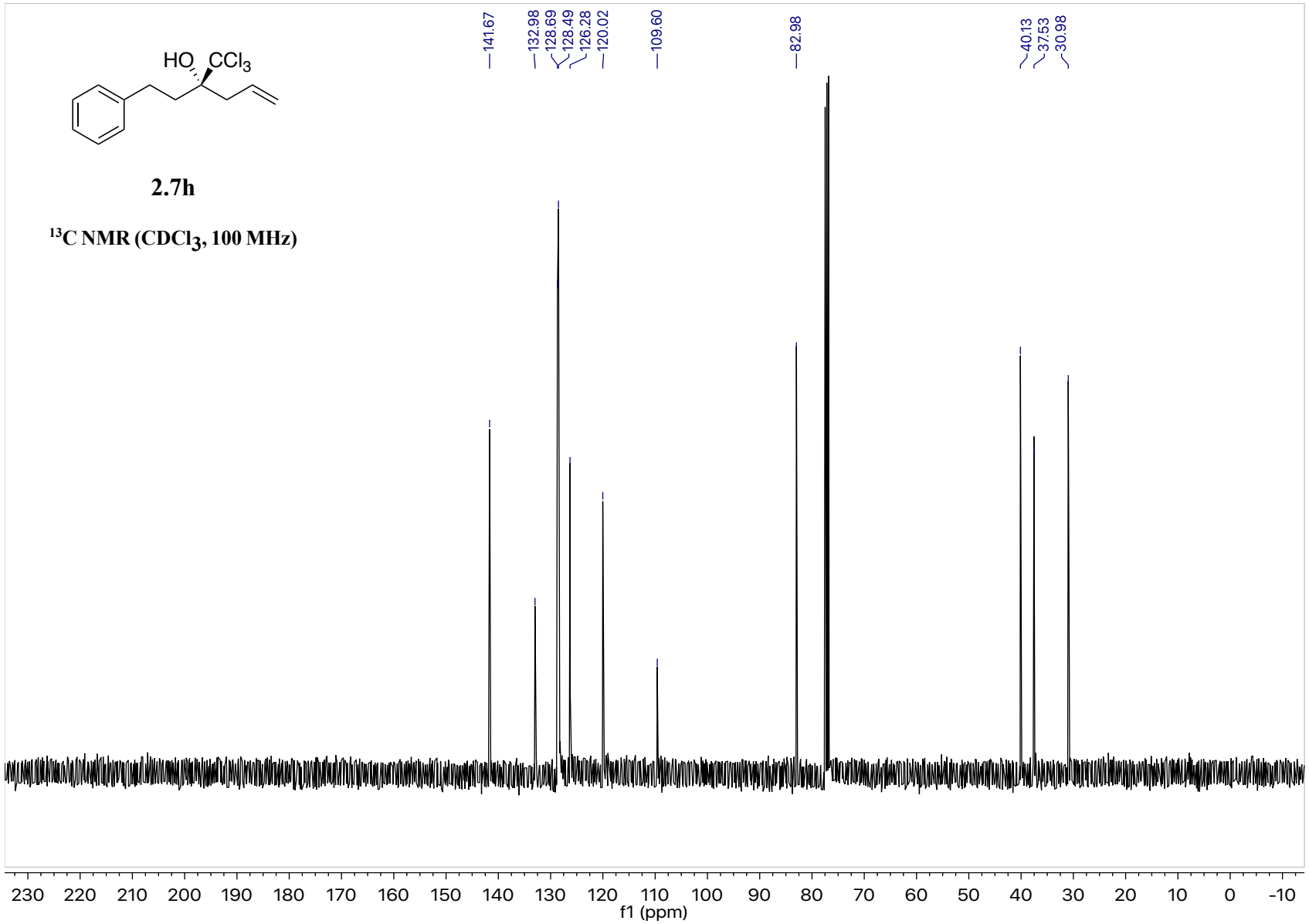

2.7h

^{13}C NMR ($CDCl_3$, 100 MHz)

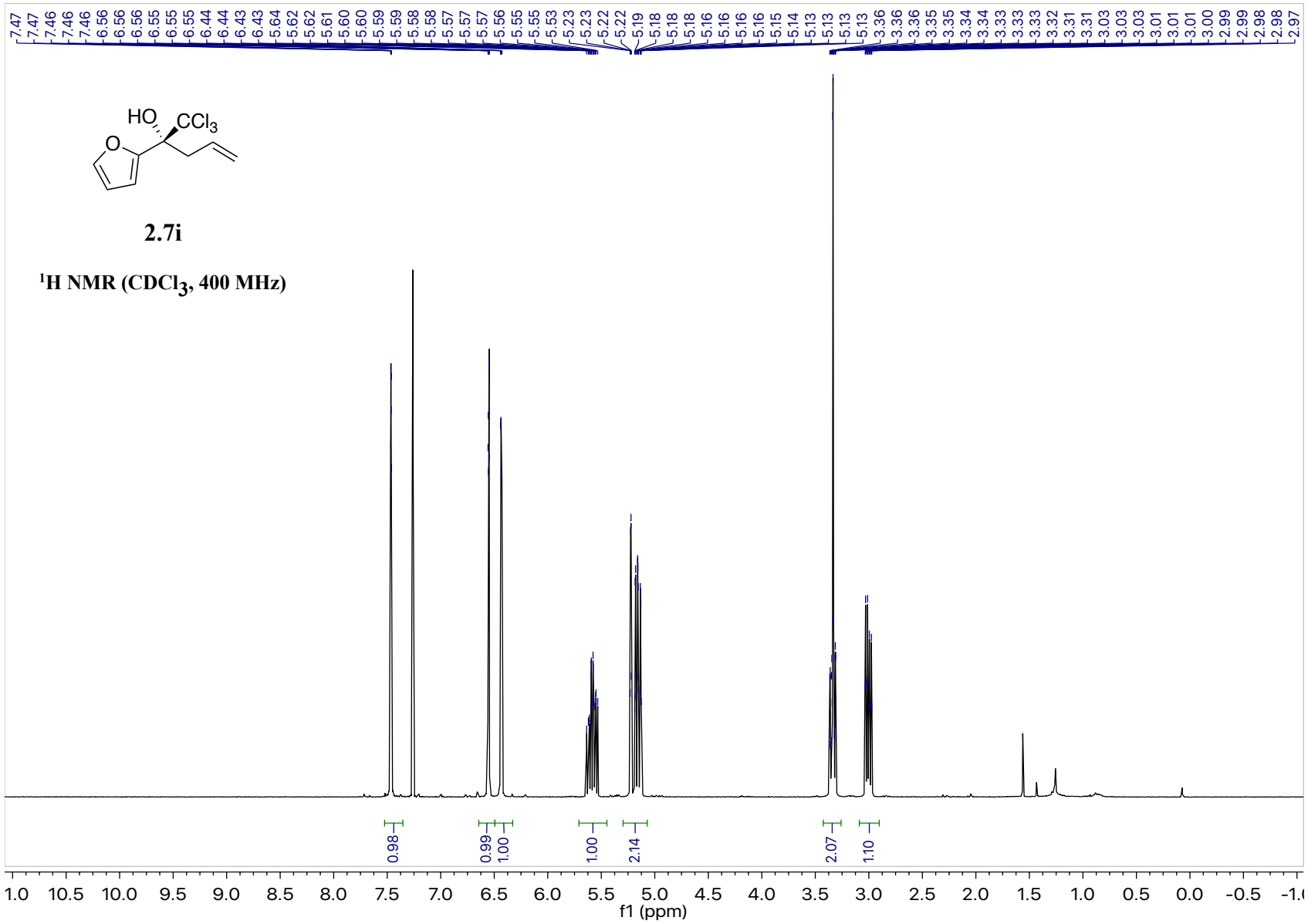
HO
CCl3
O
2.7i
1H NMR (CDCl3, 400 MHz)
0.98
0.99
1.00
1.00
2.14
2.07
1.10
f1 (ppm)

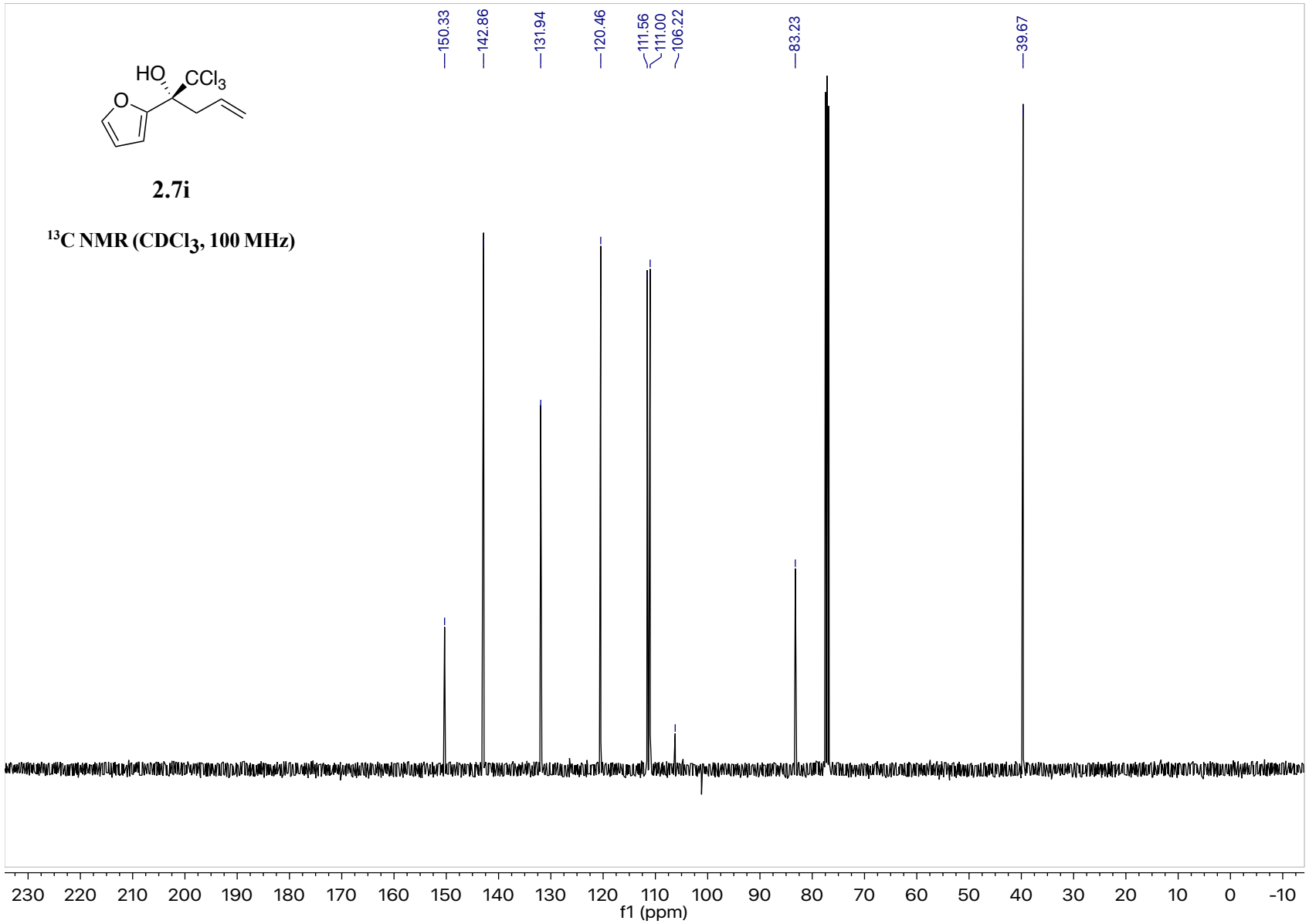

2.7i

^{13}C NMR ($CDCl_3$, 100 MHz)

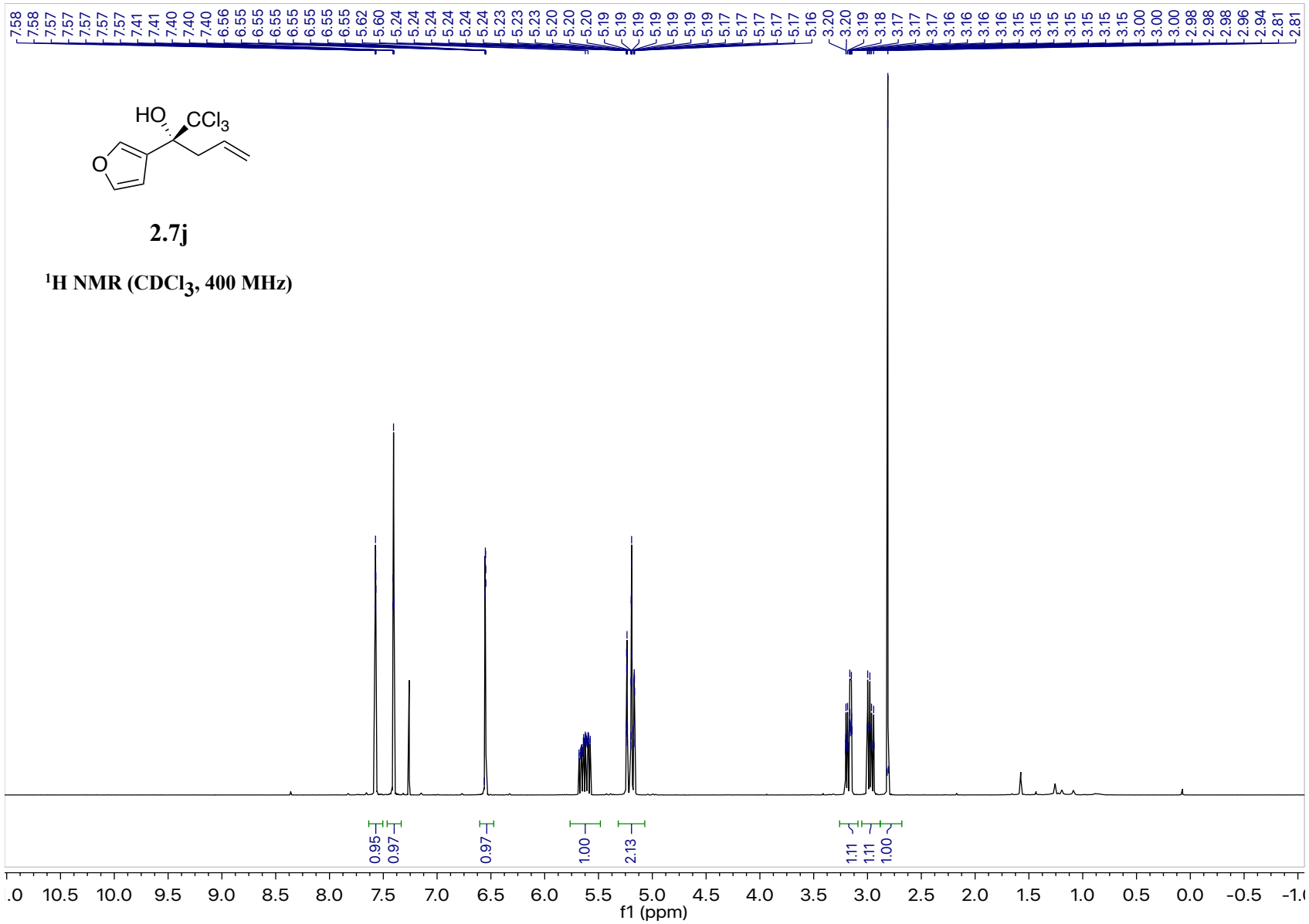
HO
CCl3
O
2.7j
1H NMR (CDCl3, 400 MHz)
f1 (ppm)

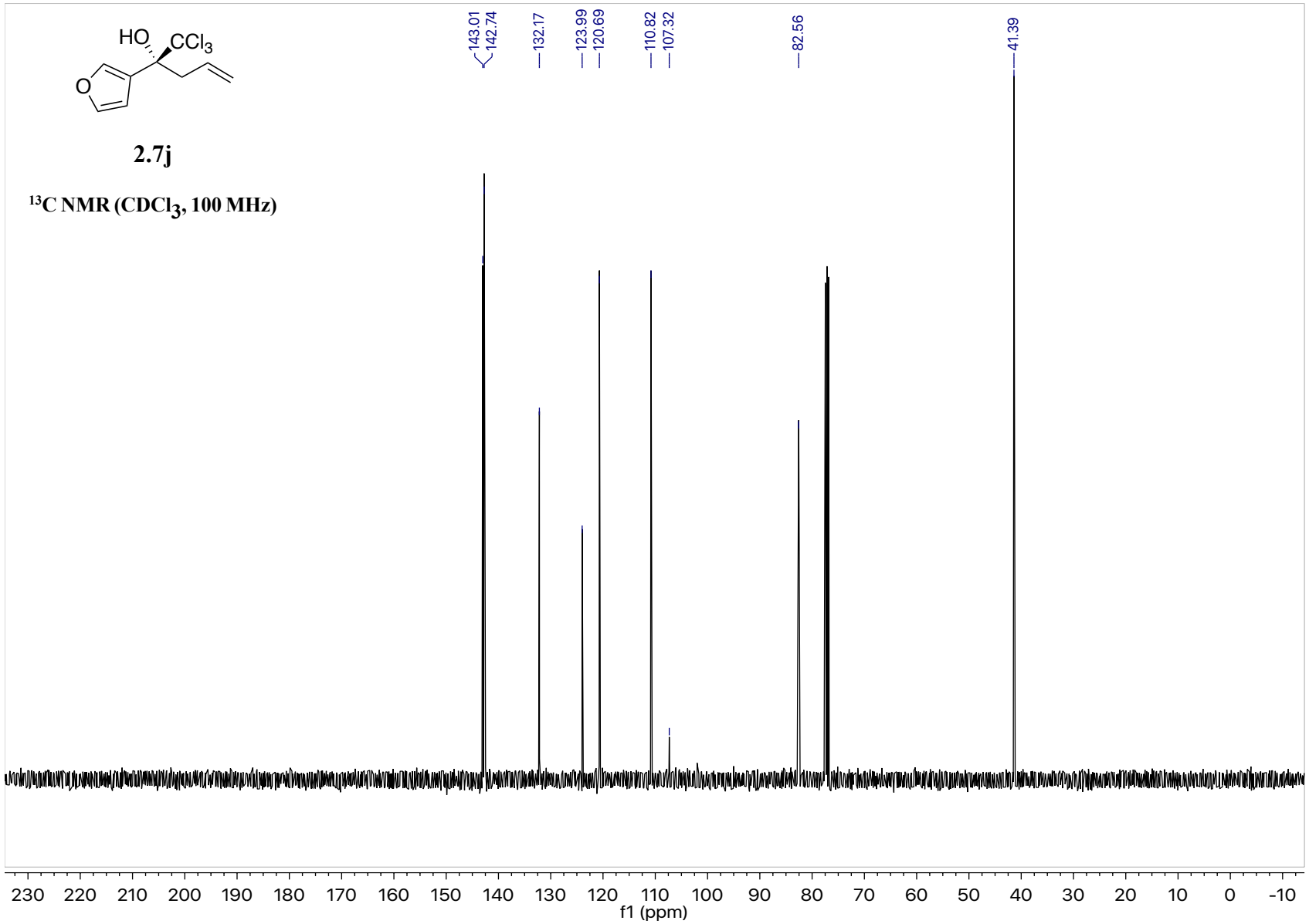
HO
CCl3
O
2.7j
13C NMR (CDCl3, 100 MHz)
143.01
142.74
132.17
123.99
120.69
110.82
107.32
82.56
41.39
230 220 210 200 190 180 170 160 150 140 130 120 110 100 90 80 70 60 50 40 30 20 10 0 -10
f1 (ppm)

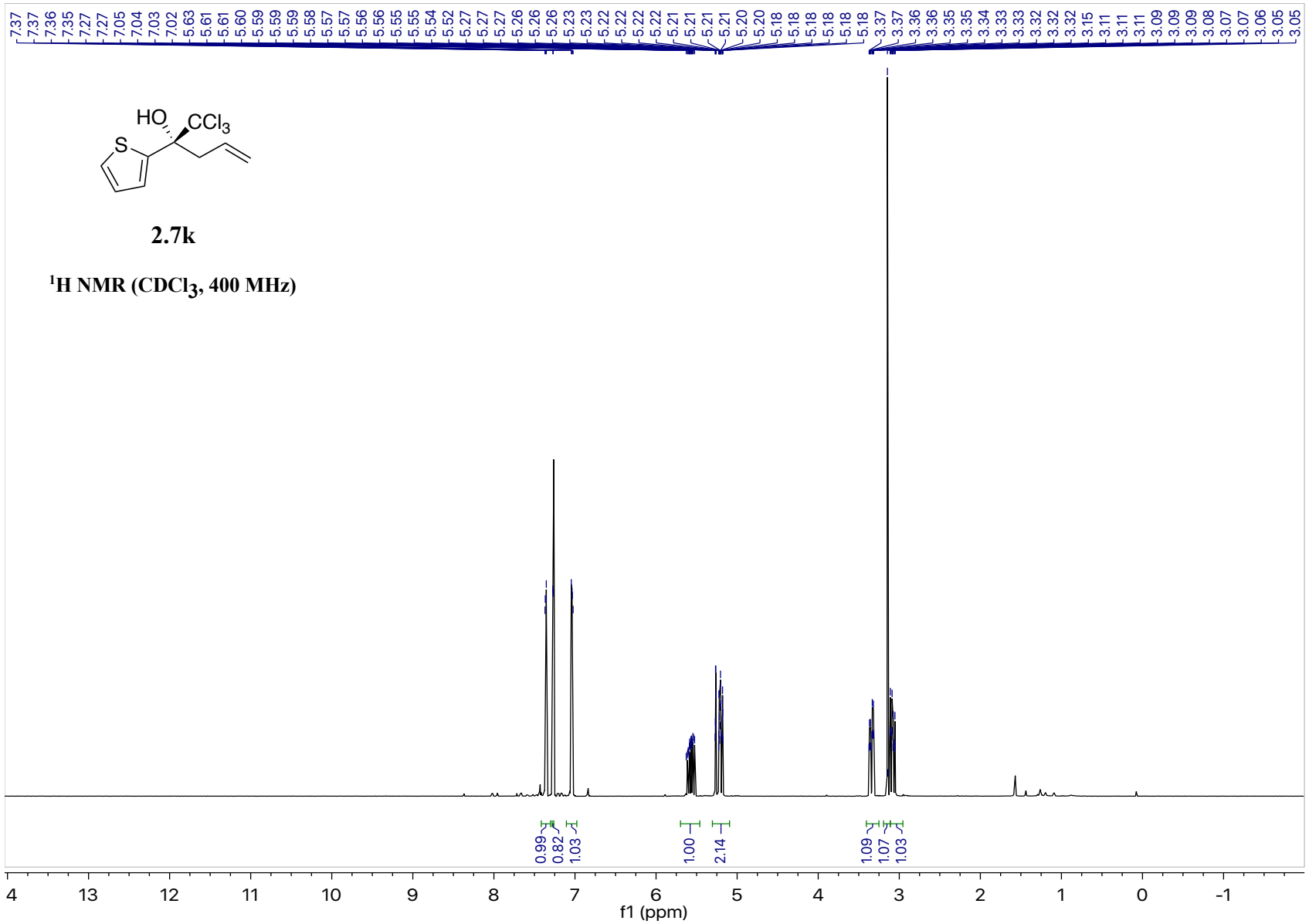

2.7k

^{1}H NMR ($CDCl_3$, 400 MHz)

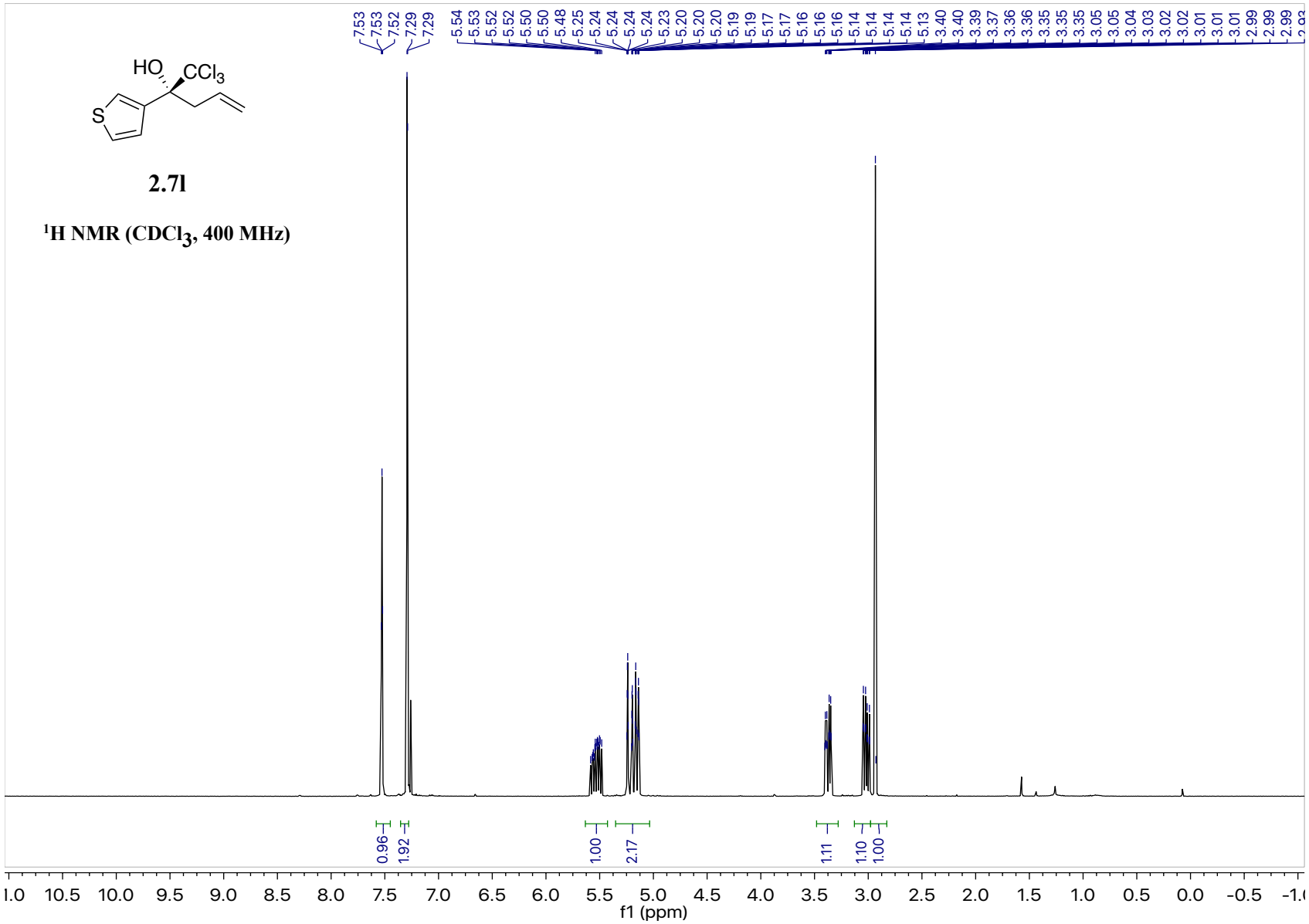
HO
CCl3
S
2.7l
1H NMR (CDCl3, 400 MHz)
7.53
7.53
7.52
7.29
7.29
5.54
5.53
5.52
5.52
5.50
5.50
5.48
5.25
5.24
5.24
5.24
5.24
5.23
5.20
5.20
5.20
5.19
5.19
5.17
5.17
5.16
5.16
5.16
5.14
5.14
5.14
5.13
3.40
3.40
3.39
3.37
3.36
3.36
3.35
3.35
3.35
3.05
3.05
3.04
3.03
3.02
3.02
3.01
3.01
3.01
2.99
2.99
2.99
0.96
1.92
1.00
2.17
1.11
1.10
1.00
f1 (ppm)

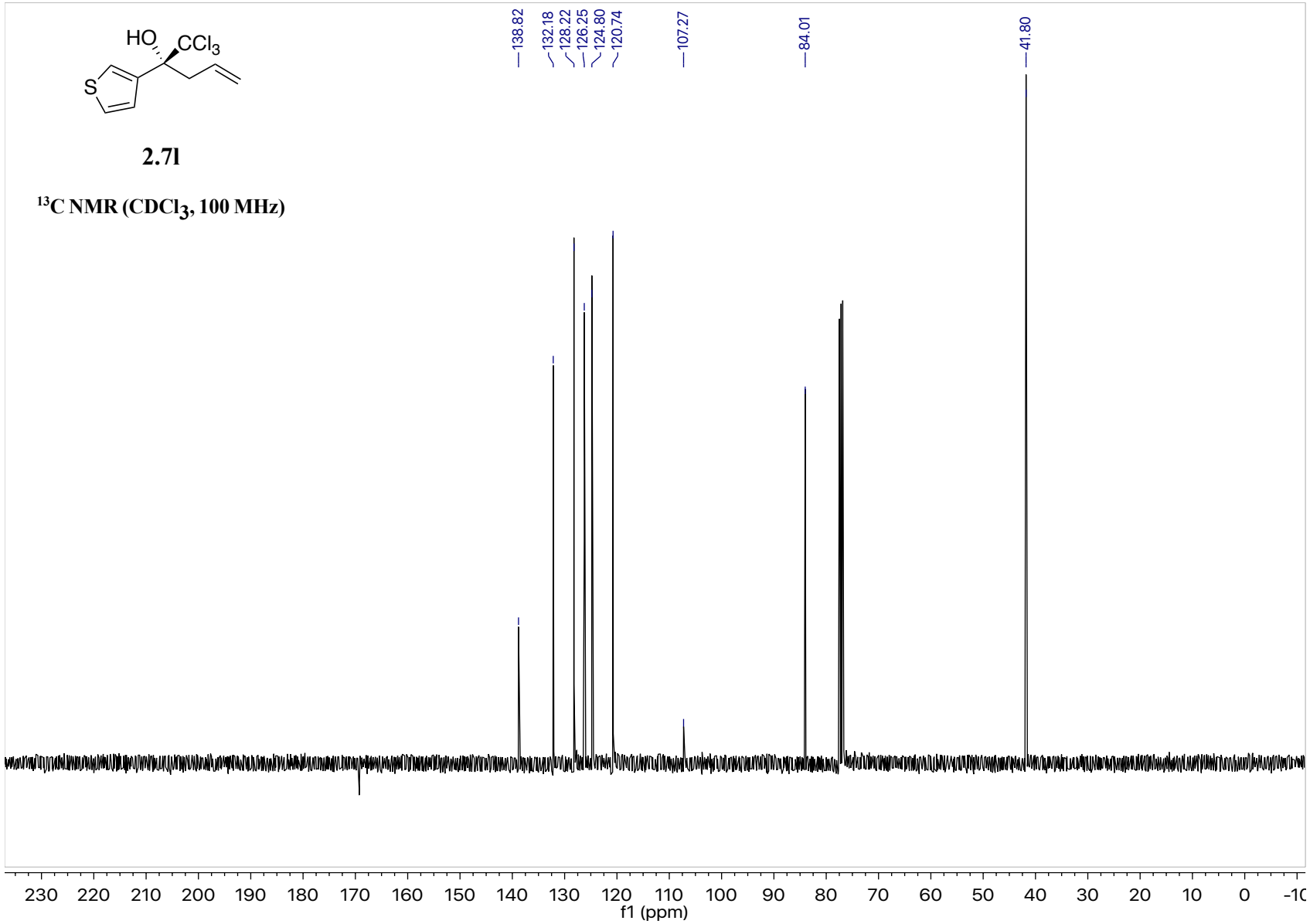
HO
CCl3
S
2.7l
13C NMR (CDCl3, 100 MHz)
138.82
132.18
128.22
126.25
124.80
120.74
107.27
84.01
41.80
230 220 210 200 190 180 170 160 150 140 130 120 110 100 90 80 70 60 50 40 30 20 10 0 -10
f1 (ppm)

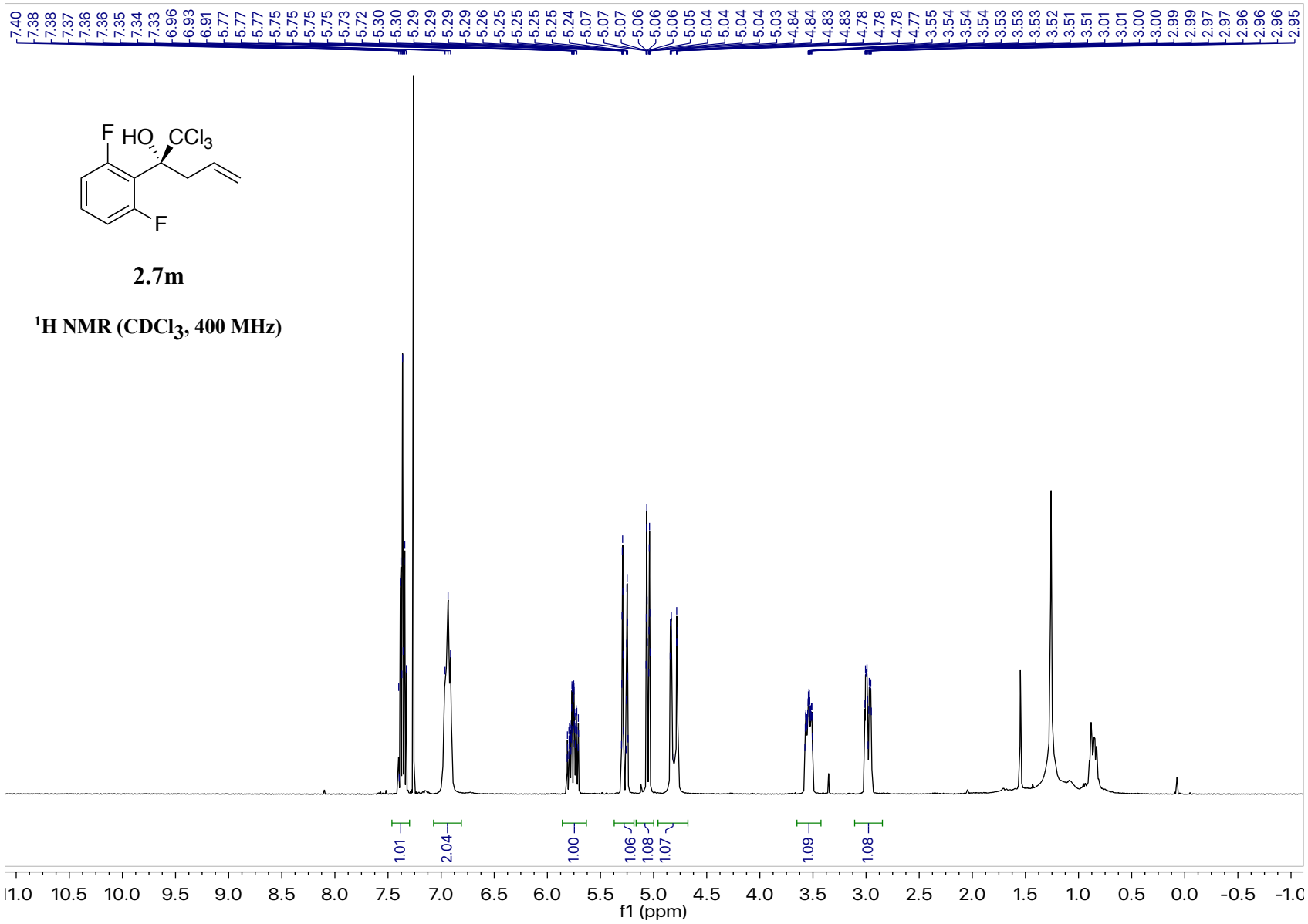
F
HO
CCl3
F
2.7m
1H NMR (CDCl3, 400 MHz)
7.40 7.38 7.38 7.37 7.36 7.36 7.35 7.34 7.33 6.96 6.93 6.91 5.77 5.77 5.77 5.75 5.75 5.75 5.75 5.73 5.72 5.30 5.30 5.29 5.29 5.29 5.29 5.26 5.25 5.25 5.25 5.24 5.07 5.07 5.07 5.06 5.06 5.06 5.05 5.04 5.04 5.04 5.04 5.03 4.84 4.84 4.83 4.78 4.78 4.78 4.77 3.55 3.54 3.54 3.54 3.53 3.53 3.52 3.51 3.51 3.01 3.01 3.00 3.00 2.99 2.99 2.97 2.97 2.96 2.96 2.95
1.01
2.04
1.00
1.06
1.08
1.07
1.09
1.08
11.0 10.5 10.0 9.5 9.0 8.5 8.0 7.5 7.0 6.5 6.0 5.5 5.0 4.5 4.0 3.5 3.0 2.5 2.0 1.5 1.0 0.5 0.0 -0.5 -1.0
f1 (ppm)

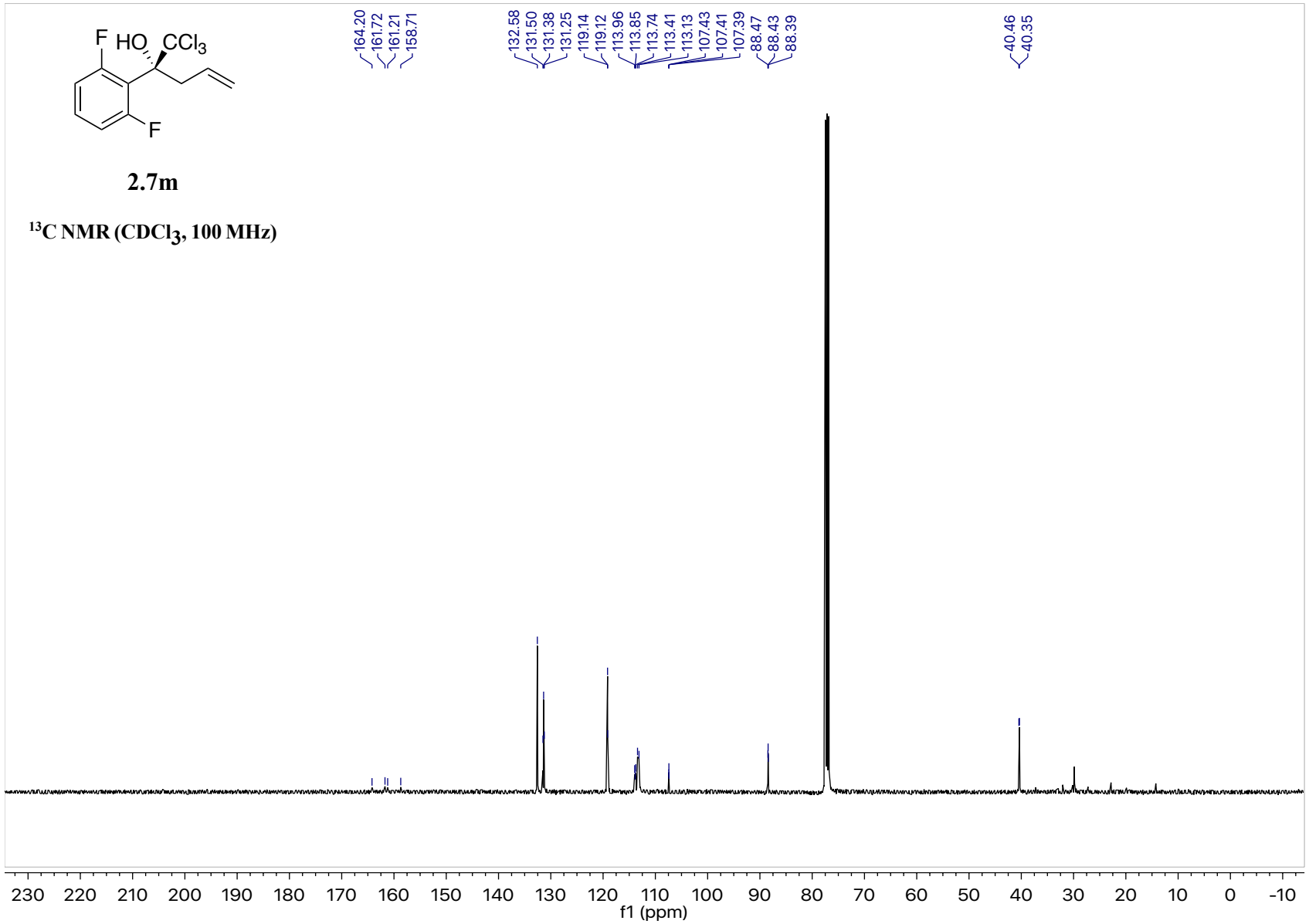

2.7m

^{13}C NMR ($CDCl_3$, 100 MHz)

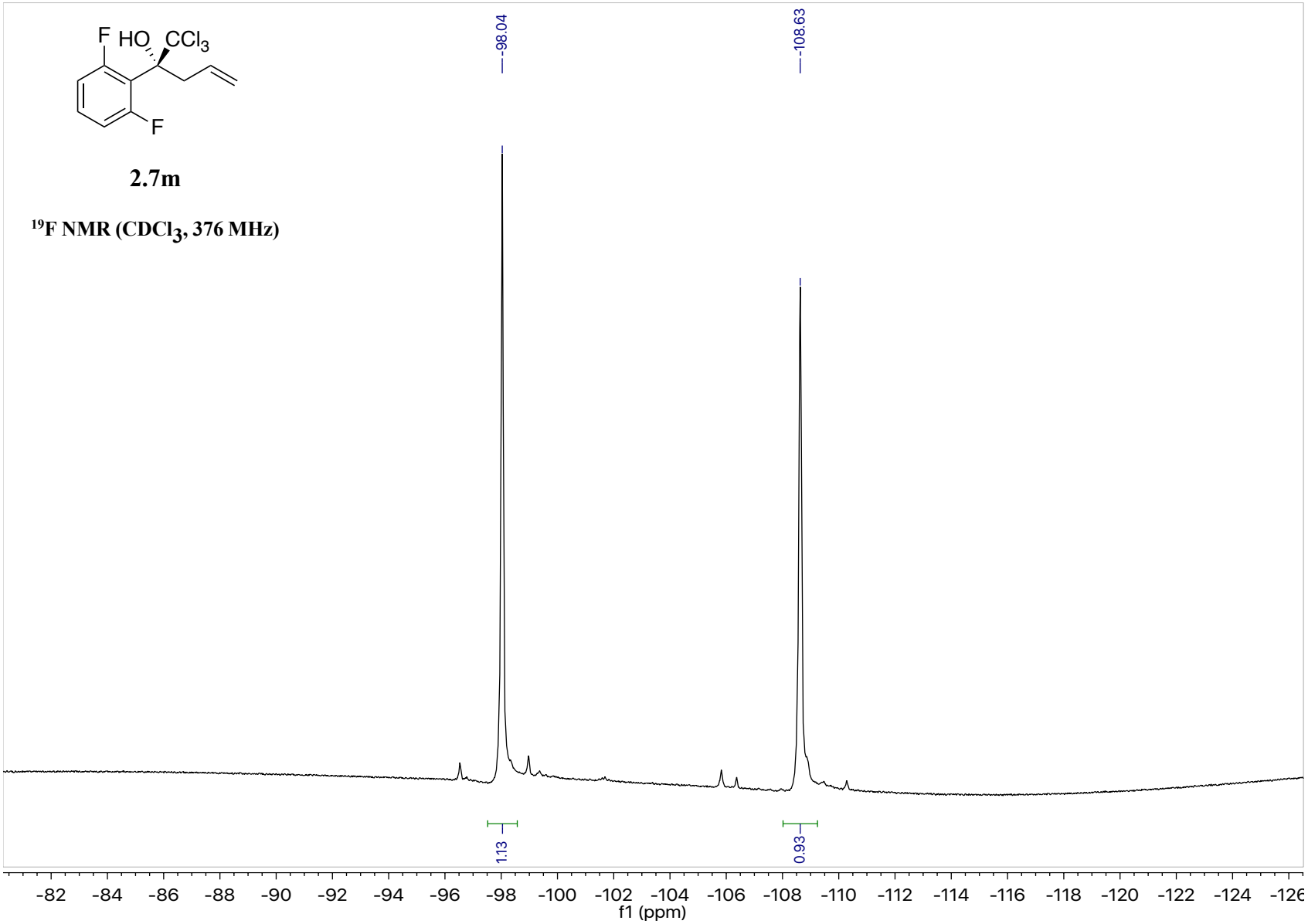
F
HO
CCl3
F
2.7m
19F NMR (CDCl3, 376 MHz)
-98.04
-108.63
1.13
0.93
-82 -84 -86 -88 -90 -92 -94 -96 -98 -100 -102 -104 -106 -108 -110 -112 -114 -116 -118 -120 -122 -124 -126
f1 (ppm)

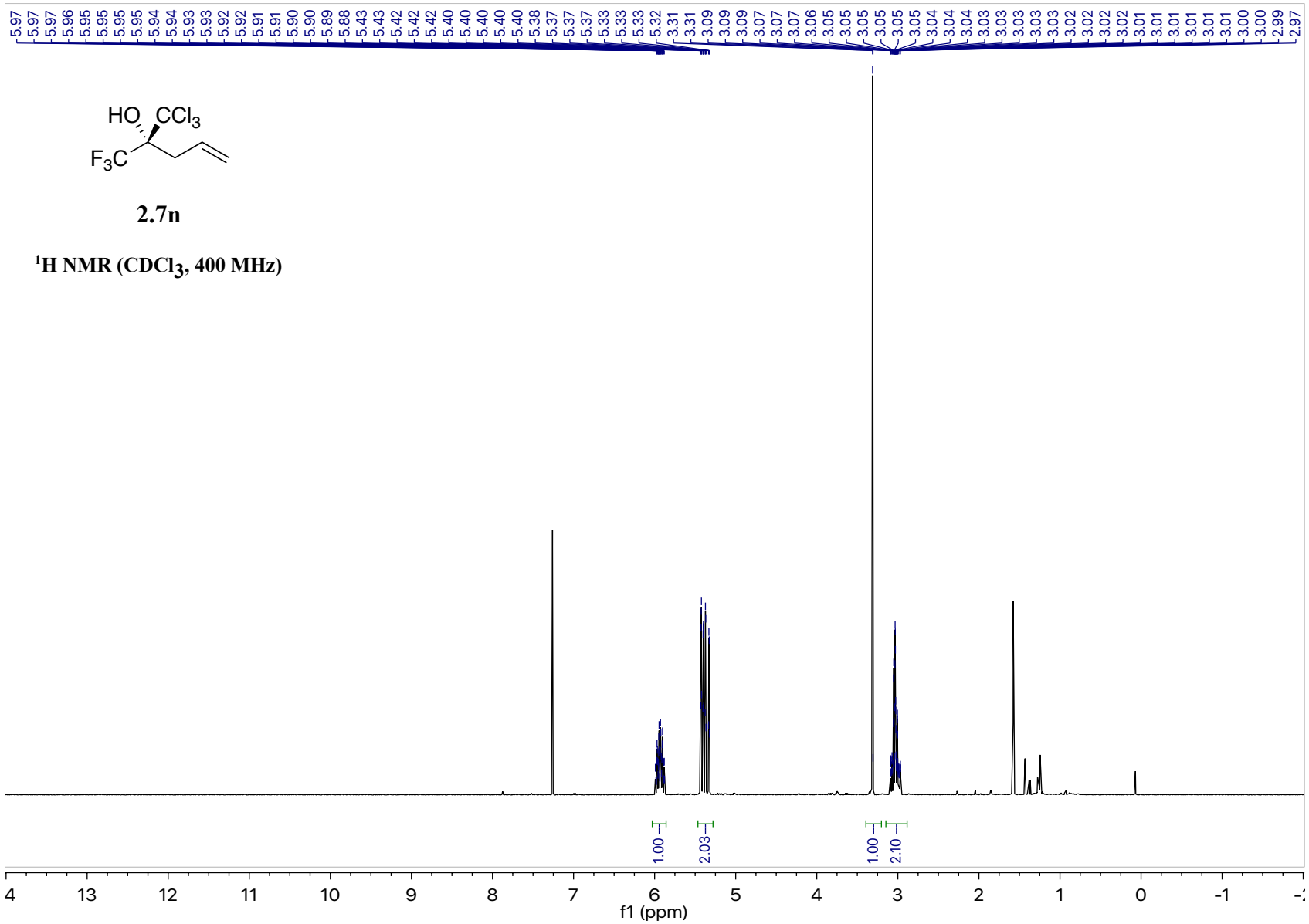
HO
CCl3
F3C
2.7n
1H NMR (CDCl3, 400 MHz)
1.00
2.03
1.00
2.10
f1 (ppm)

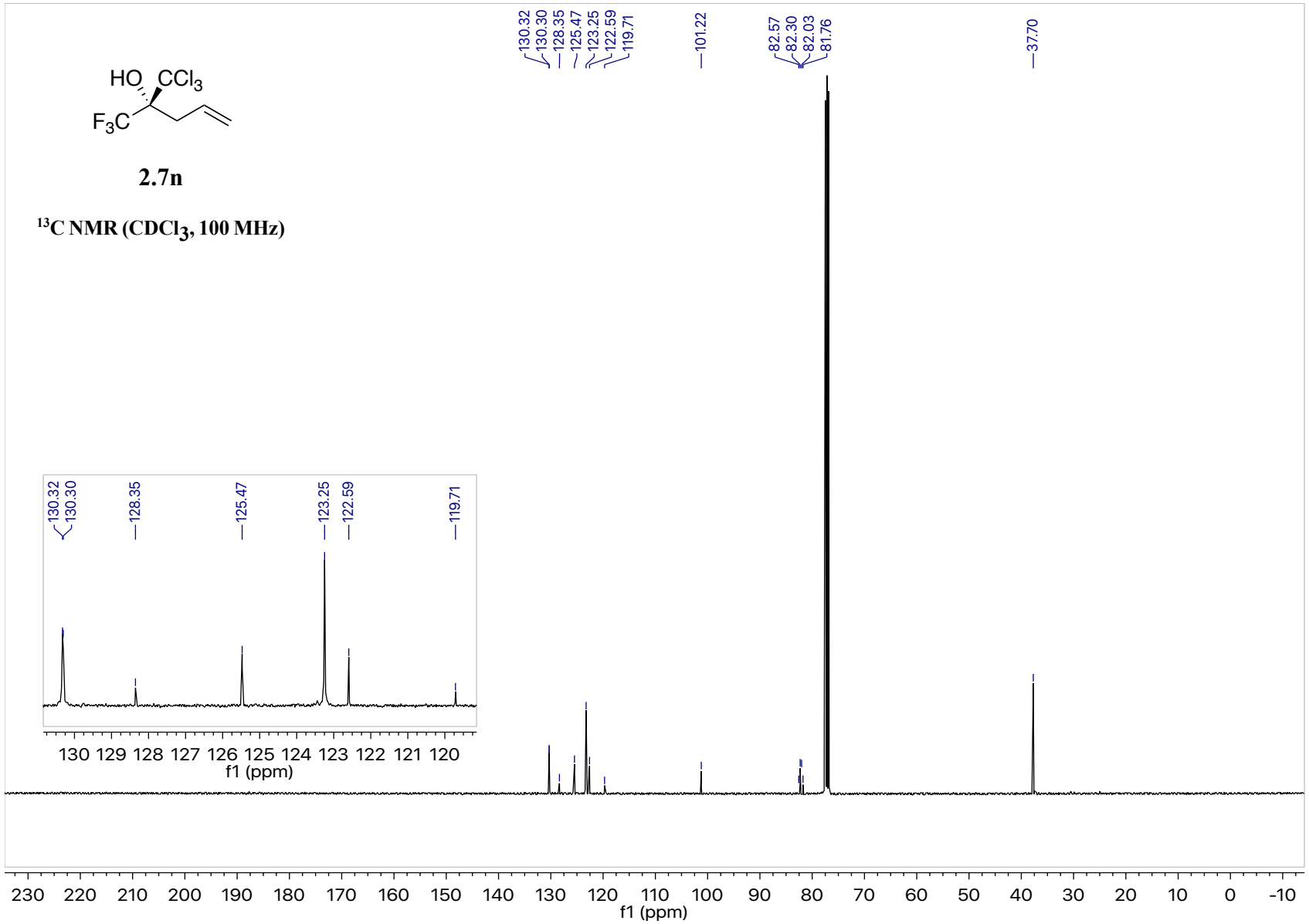
HO
CCl3
F3C
2.7n
13C NMR (CDCl3, 100 MHz)
130.32
130.30
128.35
125.47
123.25
122.59
119.71
101.22
82.57
82.30
82.03
81.76
37.70
f1 (ppm)

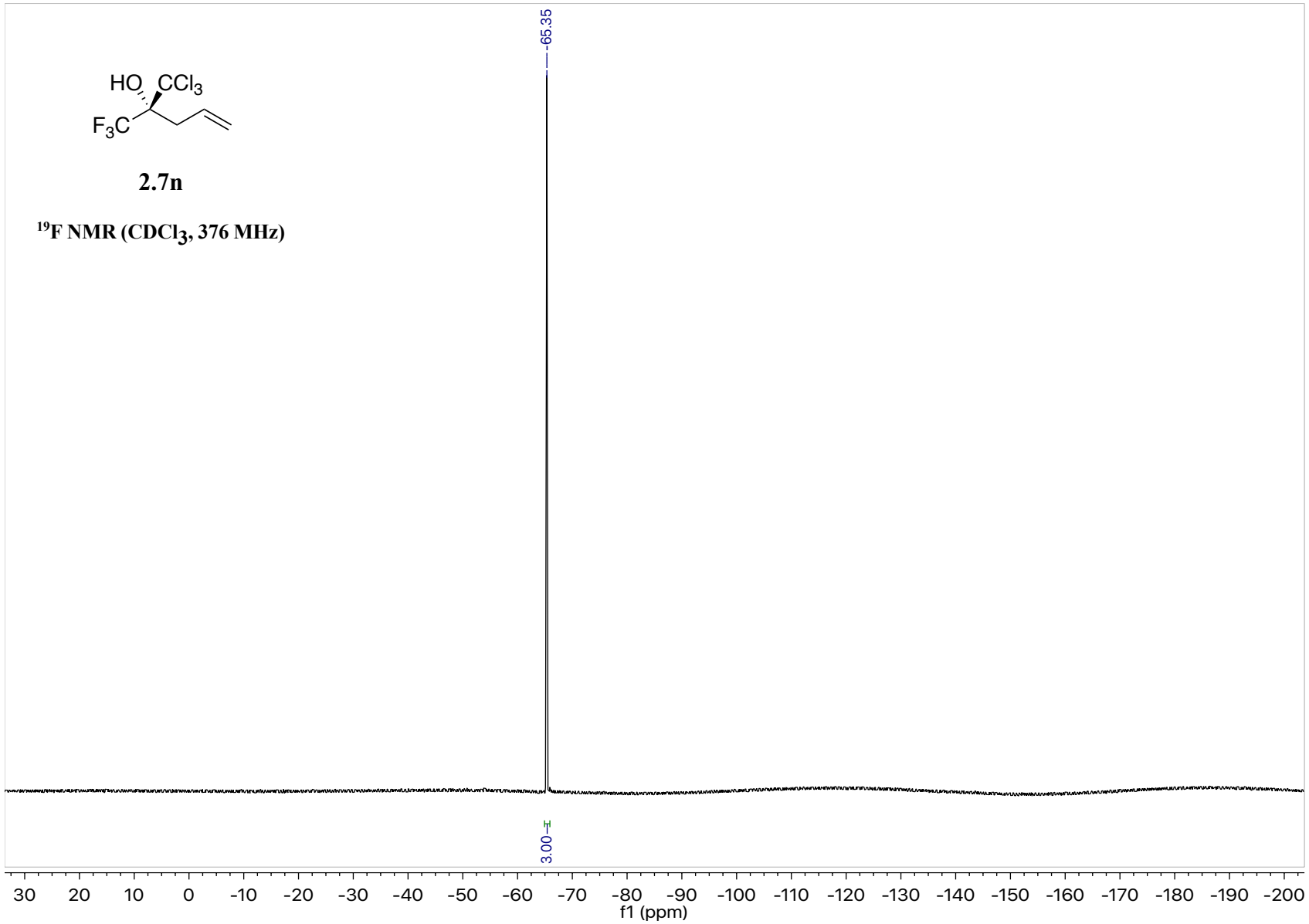
HO
CCl3
F3C
2.7n
19F NMR (CDCl3, 376 MHz)
-65.35
3.00
30 20 10 0 -10 -20 -30 -40 -50 -60 -70 -80 -90 -100 -110 -120 -130 -140 -150 -160 -170 -180 -190 -200
f1 (ppm)

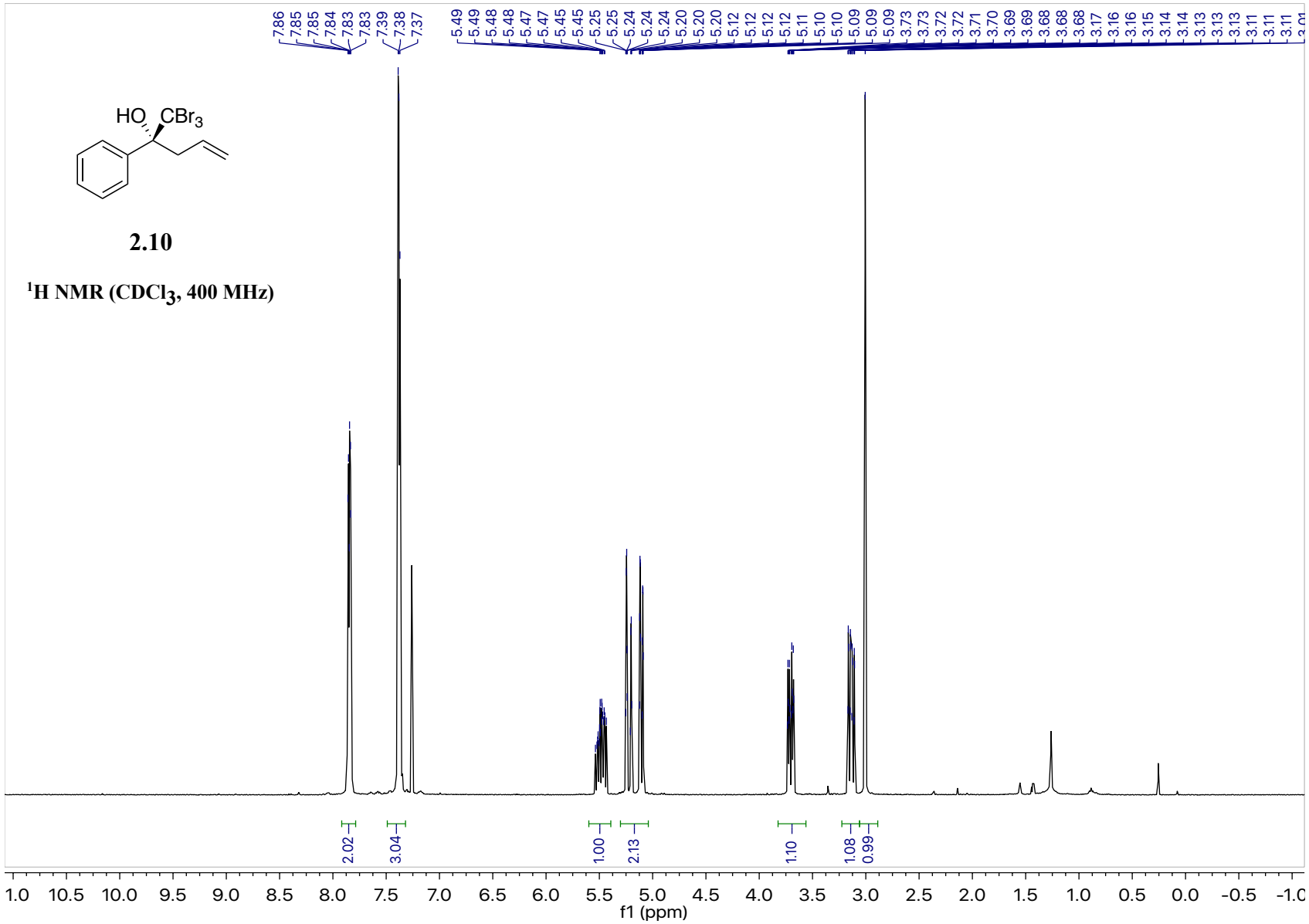
HO
CBr3
2.10
1H NMR (CDCl3, 400 MHz)
7.86 7.85 7.85 7.84 7.83 7.83 7.39 7.38 7.37
5.49 5.49 5.48 5.48 5.47 5.47 5.45 5.45 5.25 5.25 5.24 5.24 5.24 5.20 5.20 5.12 5.12 5.12 5.11 5.10 5.10 5.09 5.09 5.09
3.73 3.73 3.72 3.72 3.71 3.70 3.69 3.69 3.68 3.68 3.68 3.17 3.16 3.16 3.15 3.14 3.14 3.13 3.13 3.13 3.11 3.11 3.11
2.02
3.04
1.00
2.13
1.10
1.08
0.99
1.0 10.5 10.0 9.5 9.0 8.5 8.0 7.5 7.0 6.5 6.0 5.5 5.0 4.5 4.0 3.5 3.0 2.5 2.0 1.5 1.0 0.5 0.0 -0.5 -1.0
f1 (ppm)

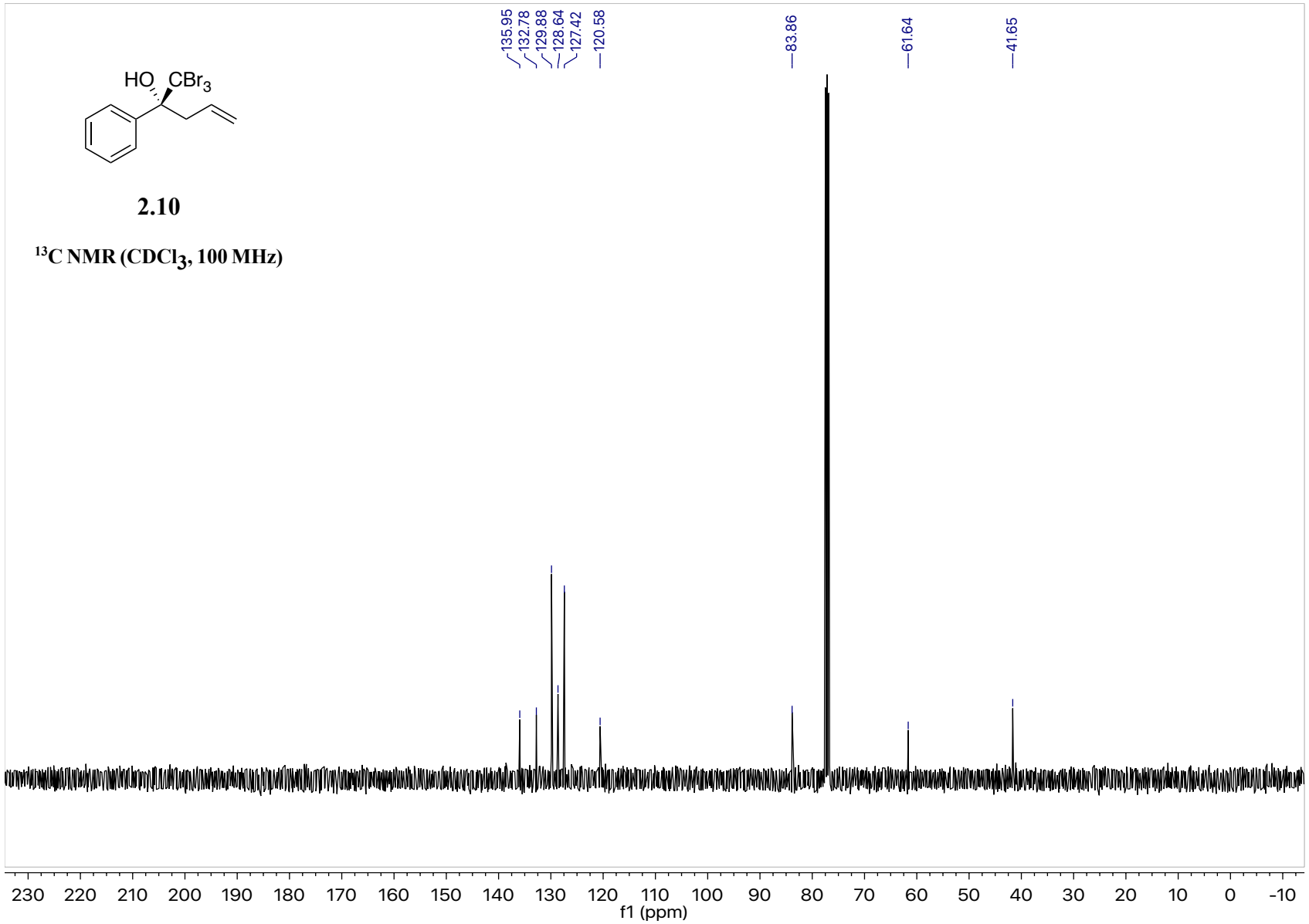

2.10

^{13}C NMR ($CDCl_3$, 100 MHz)

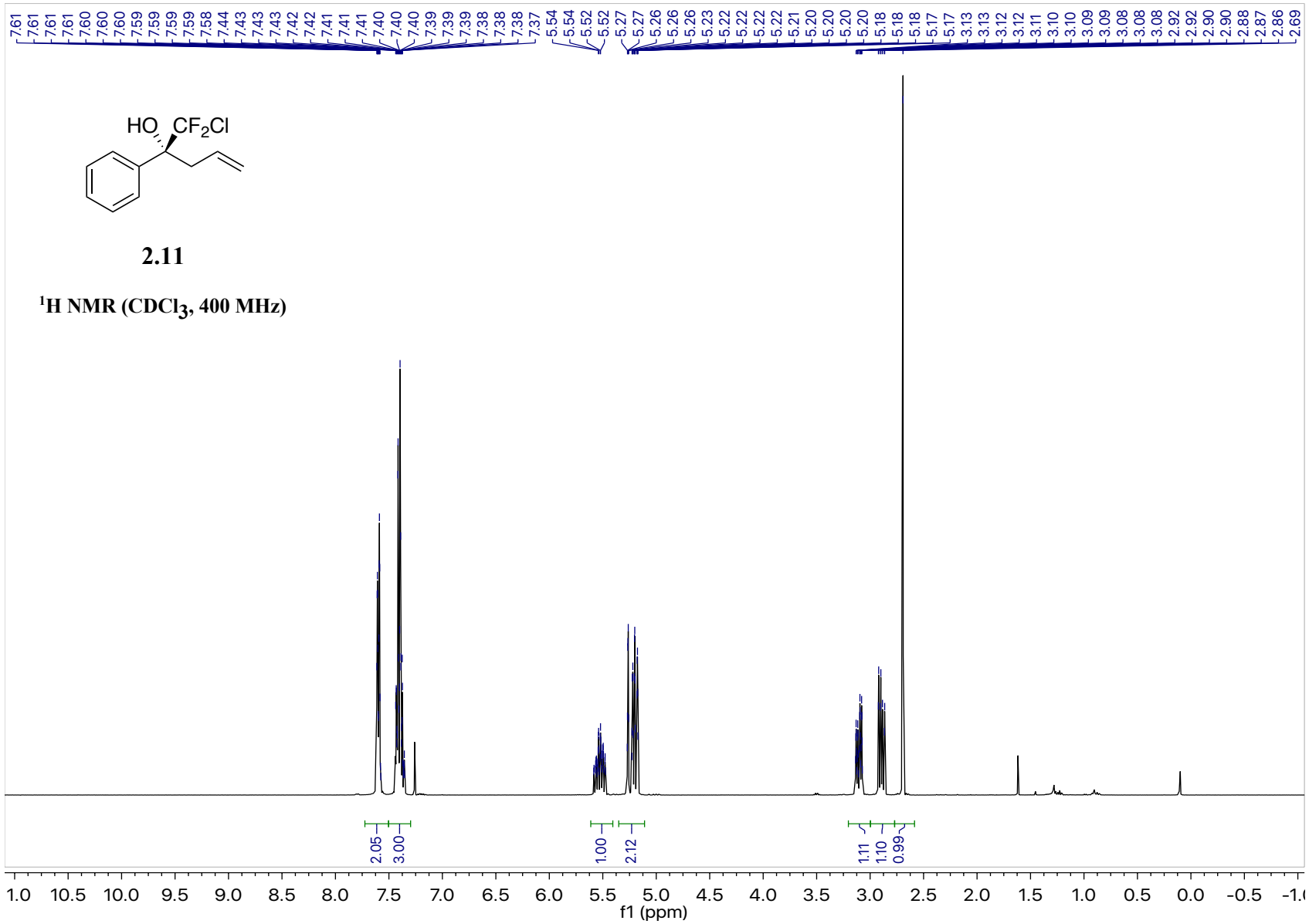
HO
CF2Cl
2.11
1H NMR (CDCl3, 400 MHz)
2.05
3.00
1.00
2.12
1.11
1.10
0.99
f1 (ppm)

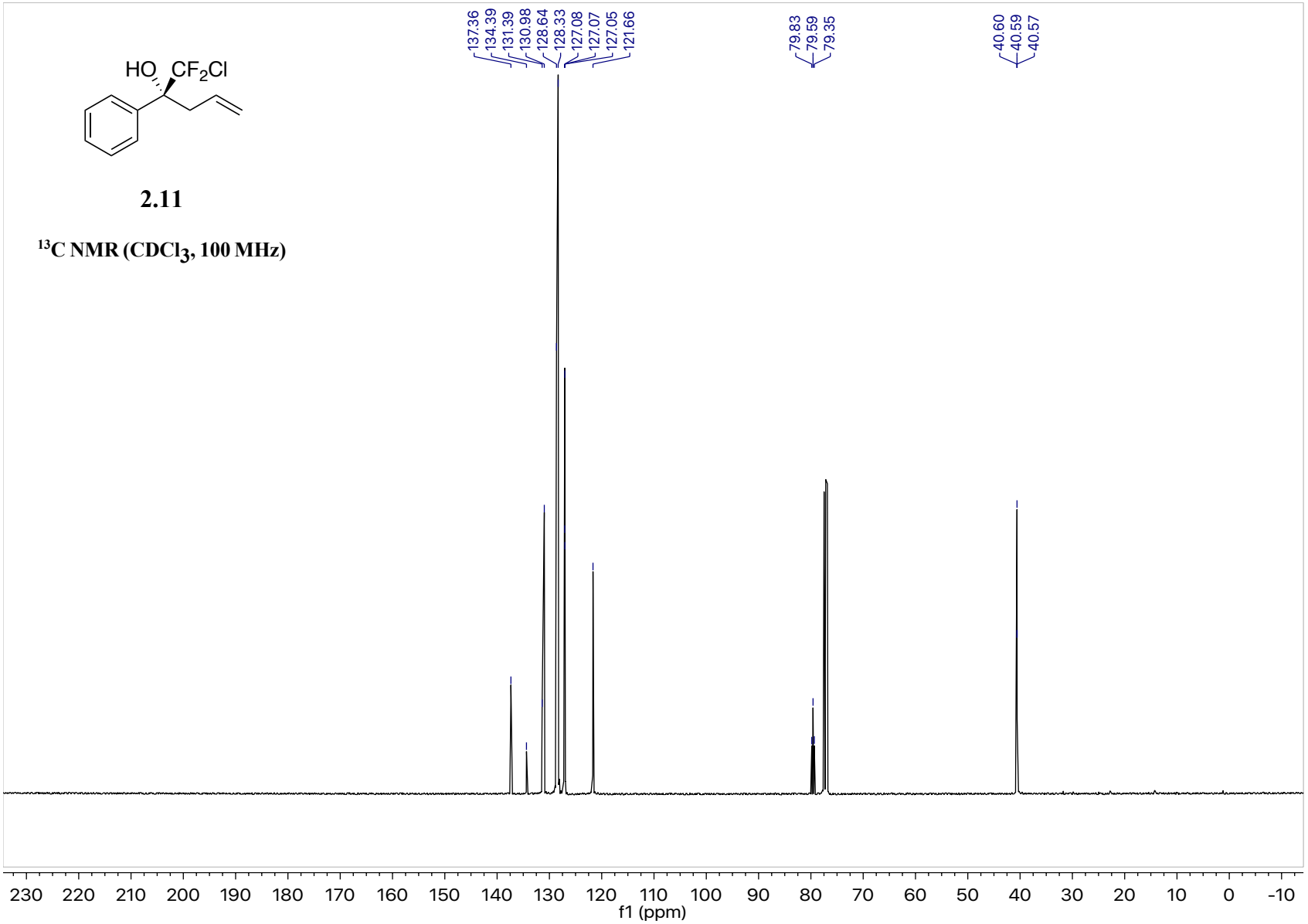

2.11

^{13}C NMR ($CDCl_3$, 100 MHz)

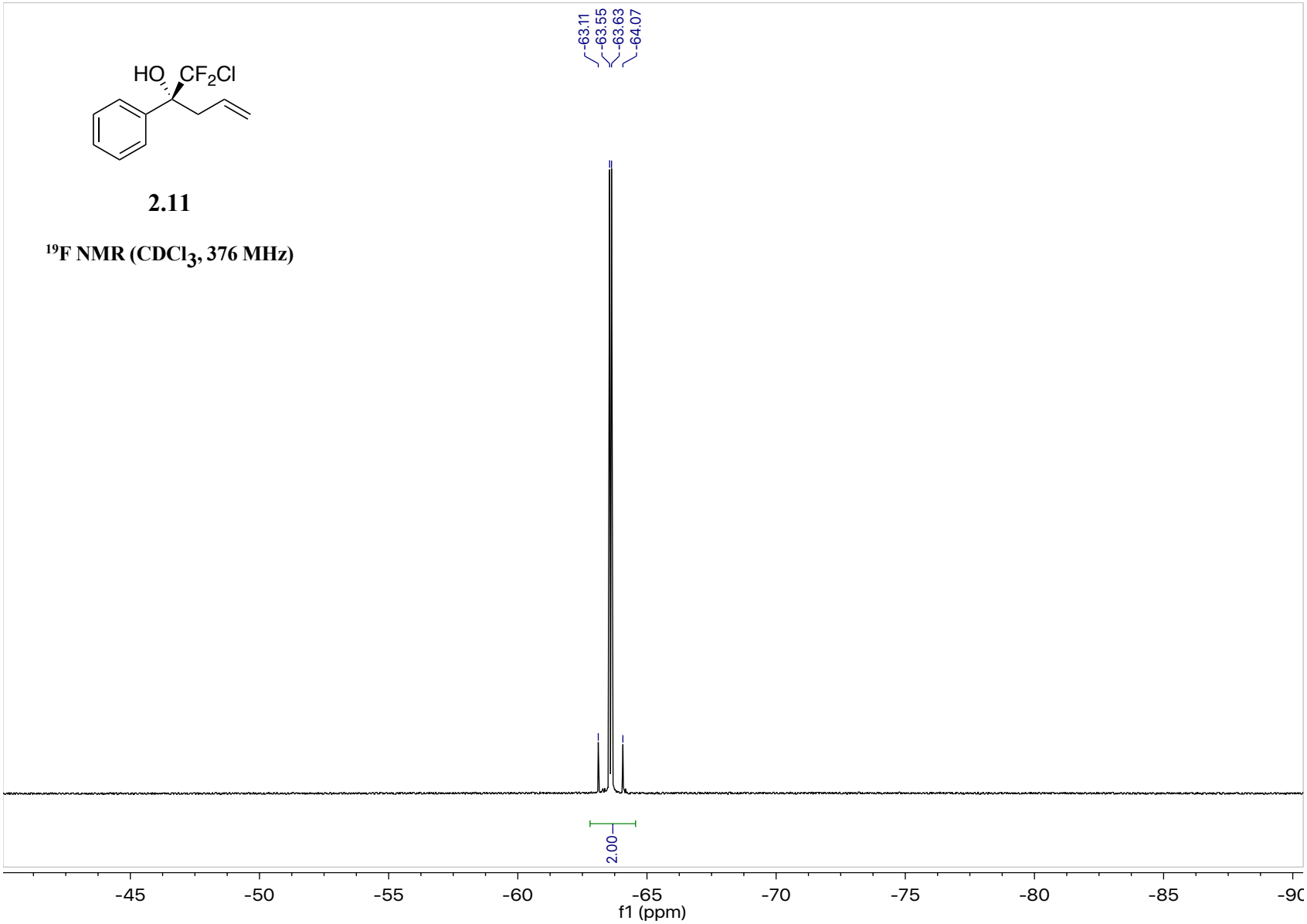

2.11

^{19}F NMR ($CDCl_3$, 376 MHz)

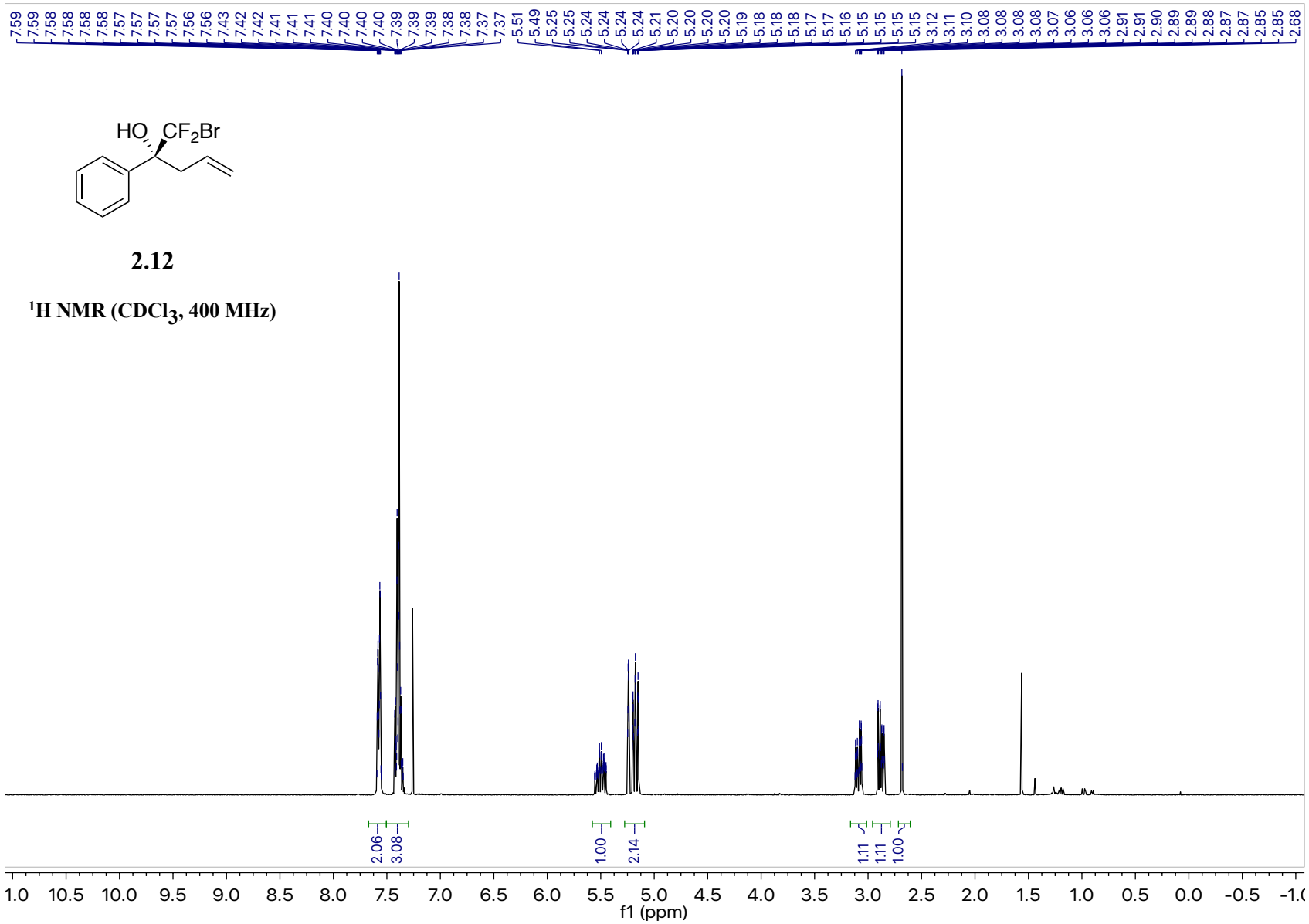
HO
CF2Br
2.12
1H NMR (CDCl3, 400 MHz)
2.06
3.08
1.00
2.14
1.11
1.11
1.00
f1 (ppm)

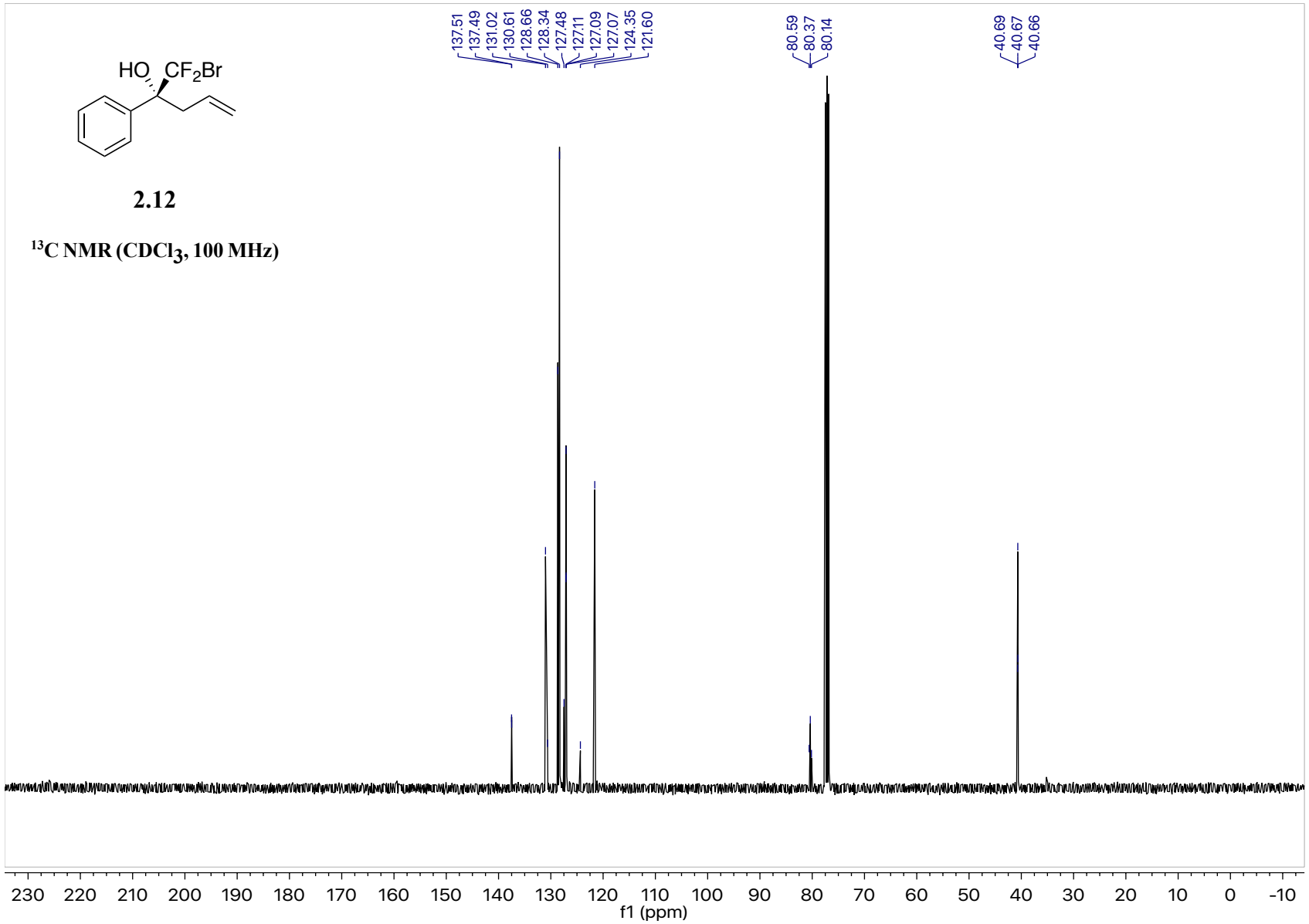

2.12

^{13}C NMR ($CDCl_3$, 100 MHz)

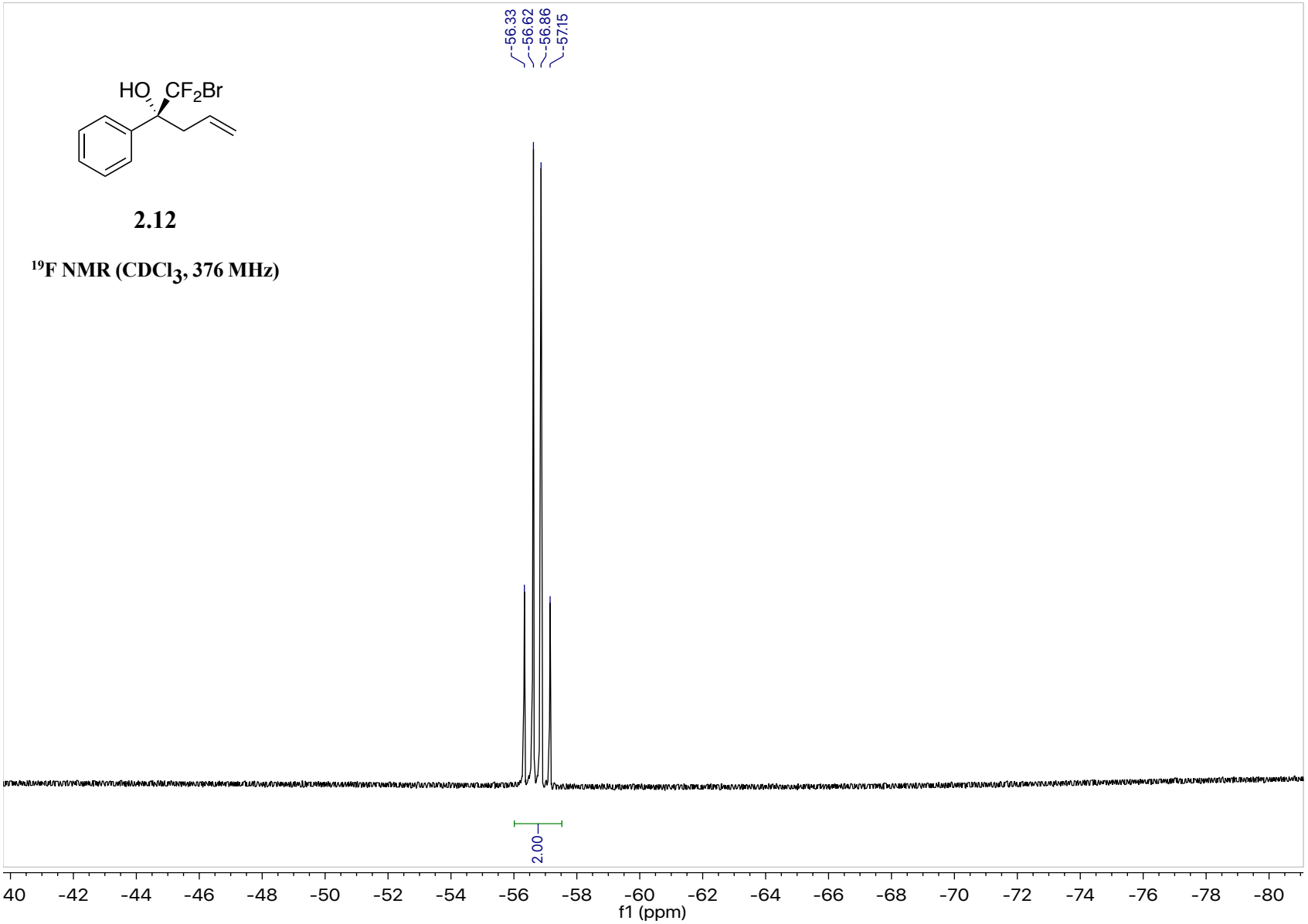

2.12

^{19}F NMR ($CDCl_3$, 376 MHz)

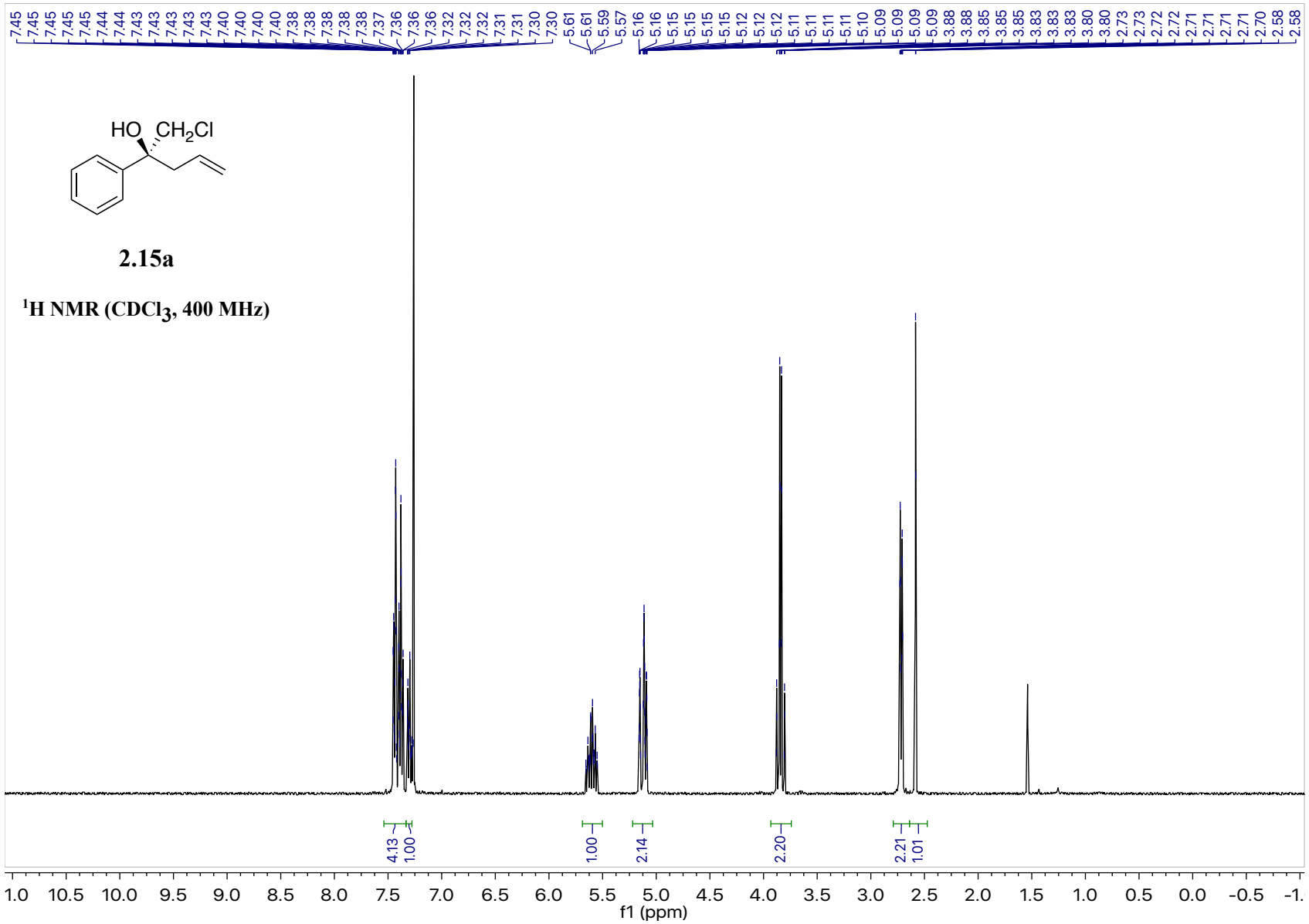
HO
CH2Cl
2.15a
1H NMR (CDCl3, 400 MHz)
4.13
1.00
1.00
2.14
2.20
2.21
1.01
f1 (ppm)

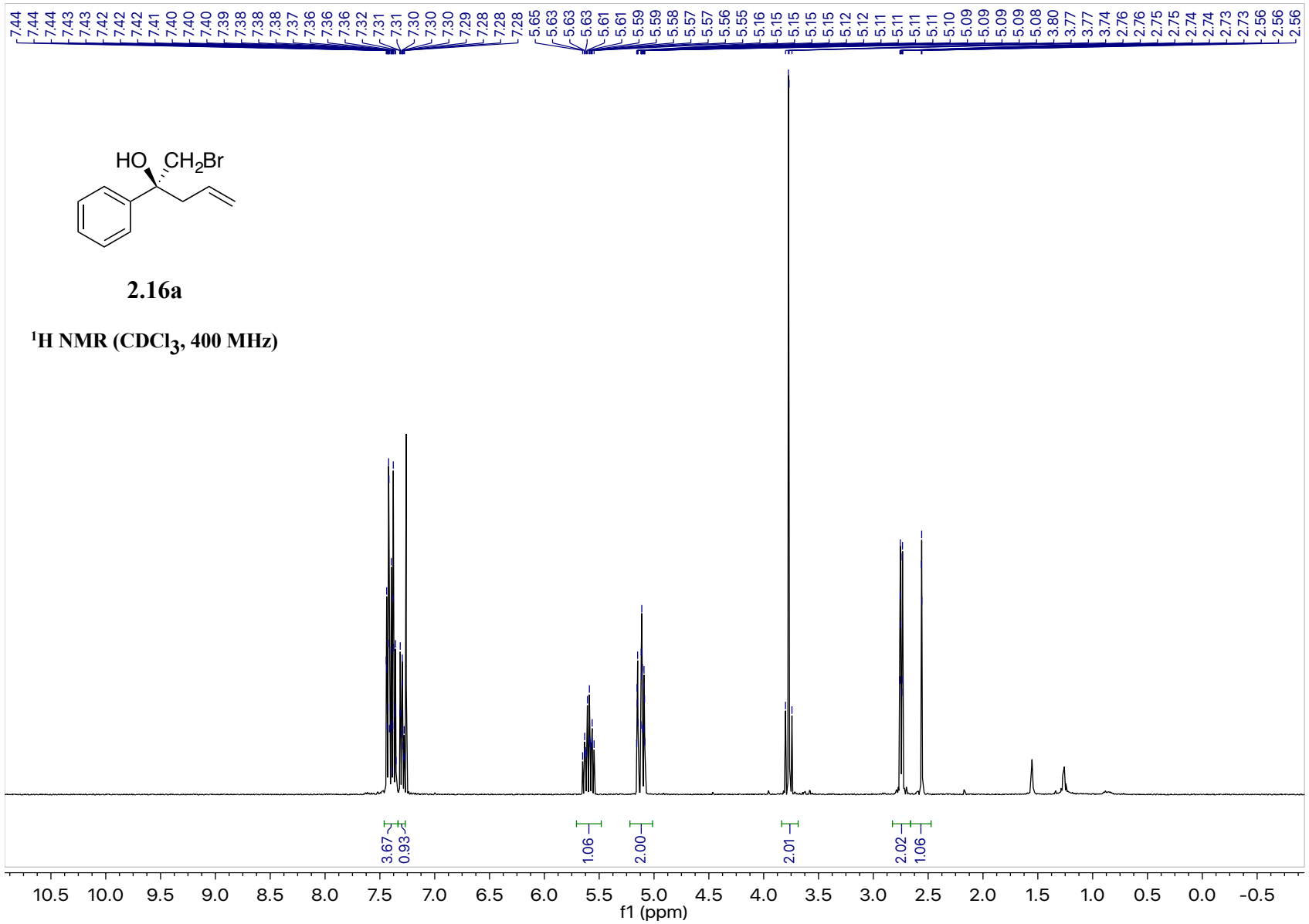

2.16a

^{1}H NMR ($CDCl_3$, 400 MHz)

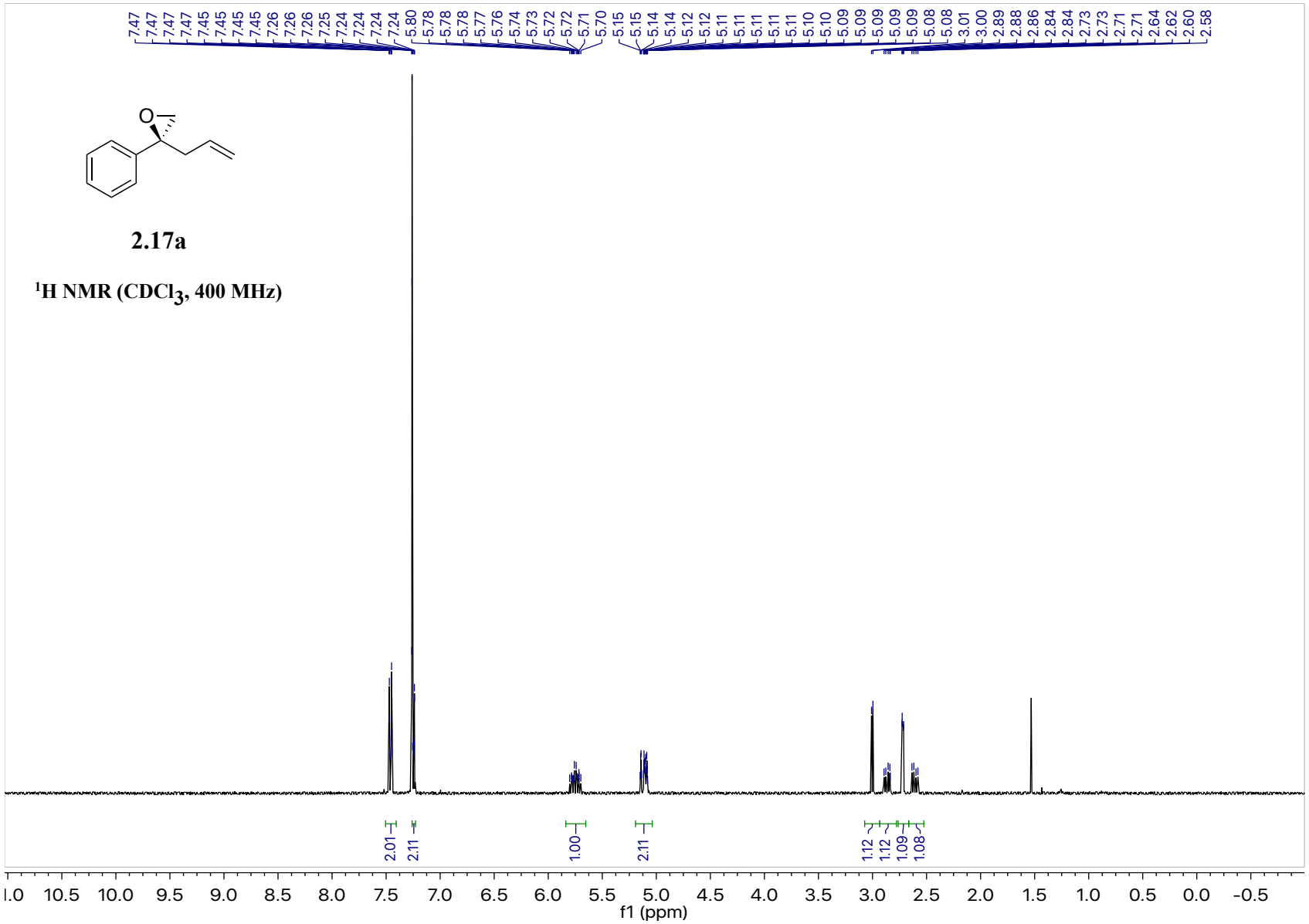
7.47 7.47 7.47 7.47 7.45 7.45 7.45 7.26 7.26 7.26 7.25 7.24 7.24 7.24 7.24 5.80 5.78 5.78 5.78 5.77 5.76 5.74 5.73 5.72 5.72 5.71 5.70 5.15 5.15 5.14 5.14 5.12 5.12 5.11 5.11 5.11 5.11 5.10 5.10 5.09 5.09 5.09 5.09 5.08 5.08 3.01 3.00 2.89 2.88 2.86 2.84 2.84 2.73 2.73 2.71 2.71 2.64 2.62 2.60 2.58
O
2.17a
1H NMR (CDCl3, 400 MHz)
2.01
2.11
1.00
2.11
1.12
1.12
1.09
1.08
10.5 10.0 9.5 9.0 8.5 8.0 7.5 7.0 6.5 6.0 5.5 5.0 4.5 4.0 3.5 3.0 2.5 2.0 1.5 1.0 0.5 0.0 -0.5
f1 (ppm)

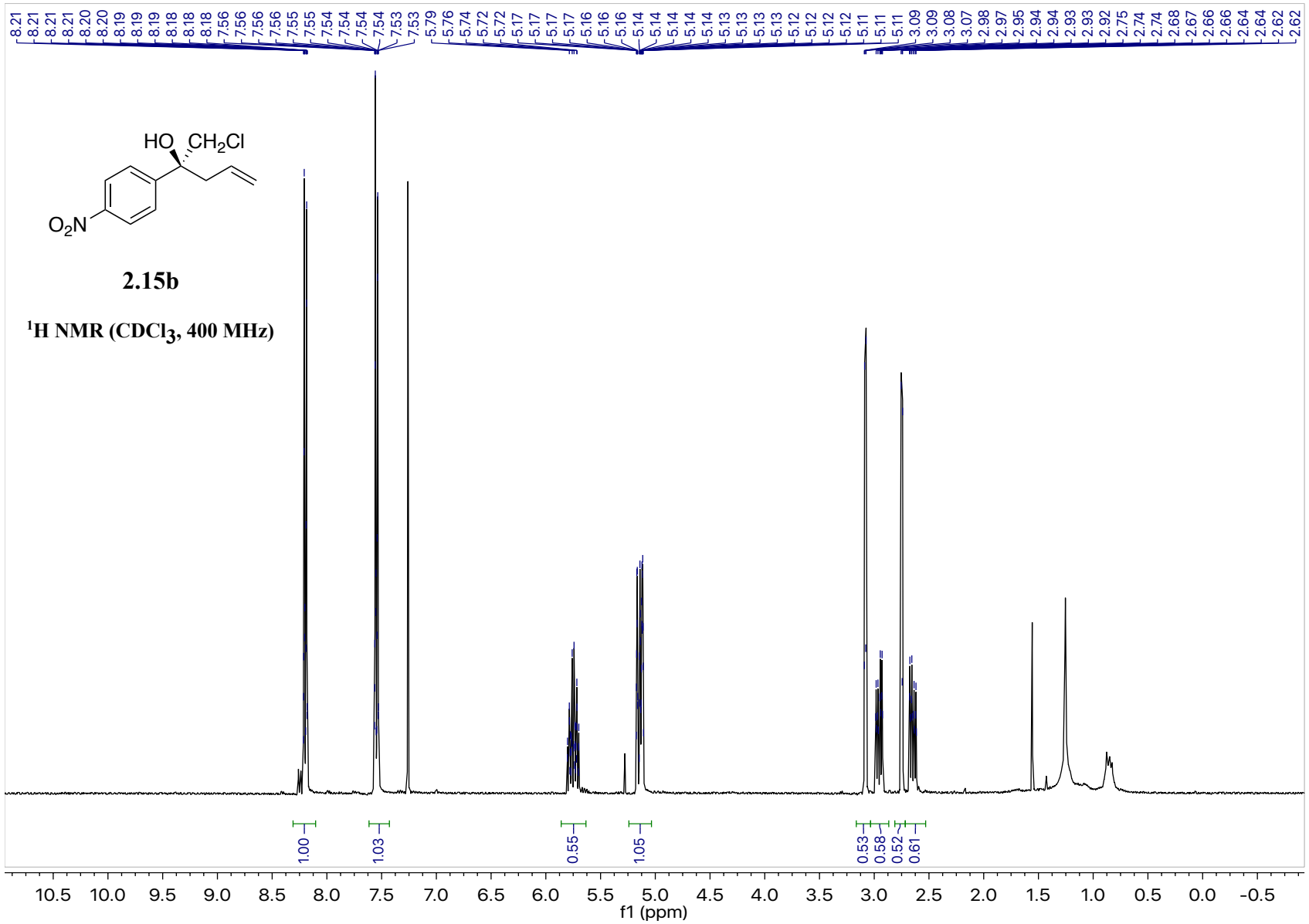
HO
CH2Cl
O2N
2.15b
1H NMR (CDCl3, 400 MHz)
f1 (ppm)

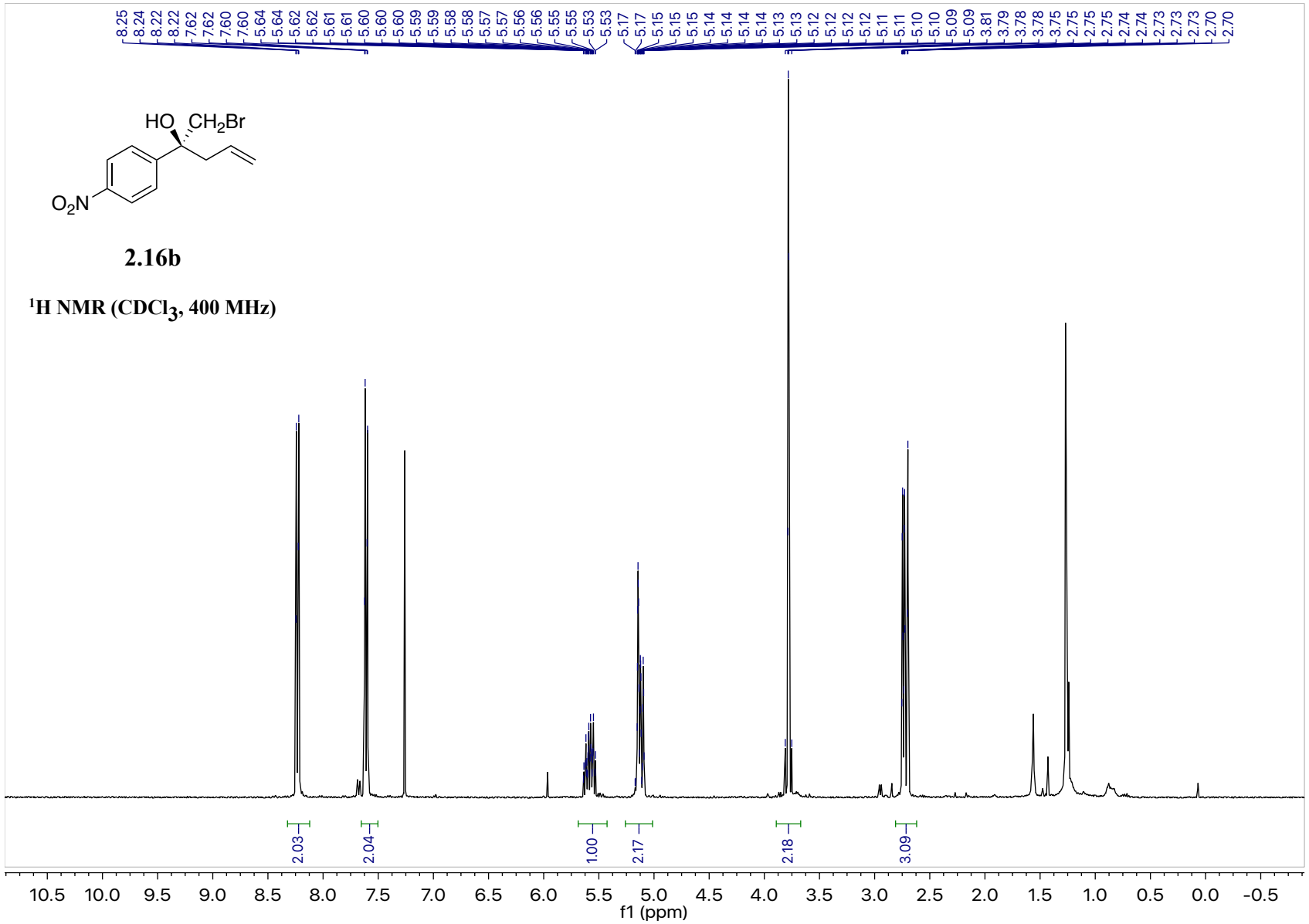
8.25 8.24 8.22 8.22 7.62 7.62 7.60 7.60 5.64 5.64 5.62 5.62 5.61 5.61 5.60 5.60 5.60 5.59 5.59 5.58 5.58 5.57 5.57 5.56 5.56 5.55 5.55 5.53 5.53 5.17 5.17 5.15 5.15 5.15 5.14 5.14 5.14 5.14 5.13 5.13 5.12 5.12 5.12 5.12 5.11 5.11 5.10 5.10 5.09 5.09 3.81 3.79 3.78 3.78 3.75 2.75 2.75 2.74 2.74 2.73 2.73 2.73 2.70 2.70
HO
CH2Br
O2N
2.16b
1H NMR (CDCl3, 400 MHz)
2.03
2.04
1.00
2.17
2.18
3.09
10.5 10.0 9.5 9.0 8.5 8.0 7.5 7.0 6.5 6.0 5.5 5.0 4.5 4.0 3.5 3.0 2.5 2.0 1.5 1.0 0.5 0.0 -0.5
f1 (ppm)

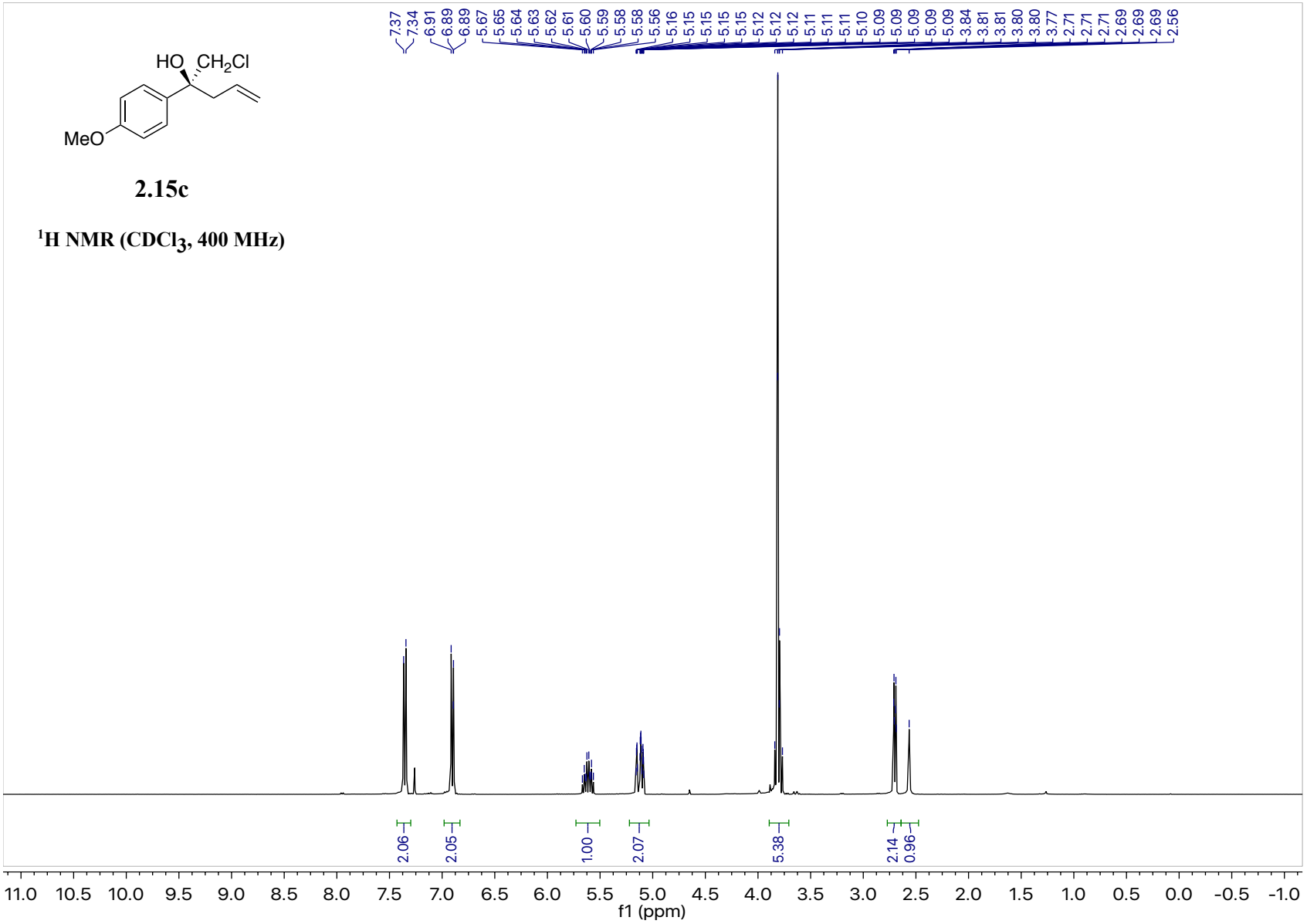

2.15c

^{1}H NMR ($CDCl_3$, 400 MHz)

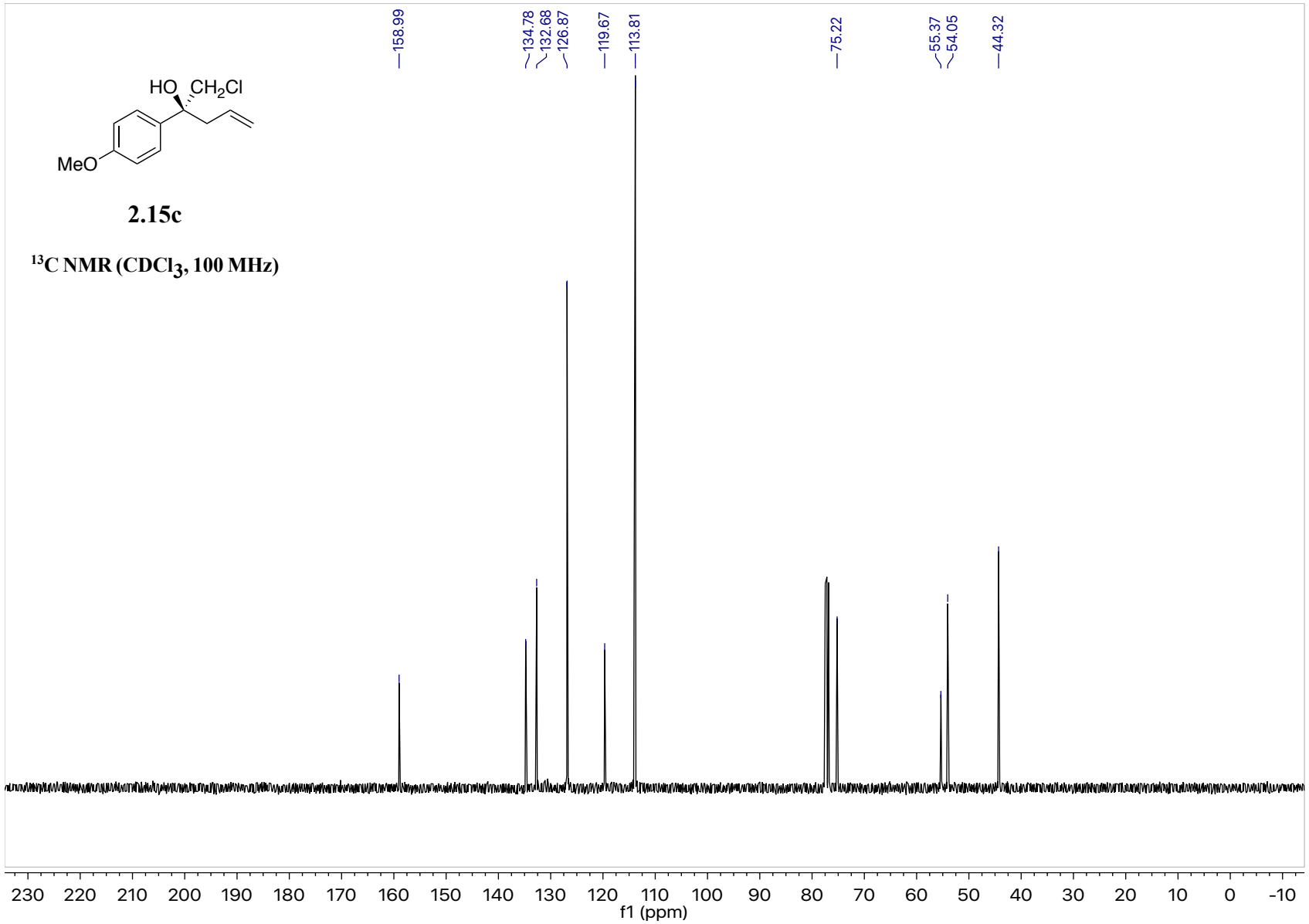
158.99
134.78
132.68
126.87
119.67
113.81
75.22
55.37
54.05
44.32
HO
CH2Cl
MeO
2.15c
13C NMR (CDCl3, 100 MHz)
230 220 210 200 190 180 170 160 150 140 130 120 110 100 90 80 70 60 50 40 30 20 10 0 -10
f1 (ppm)

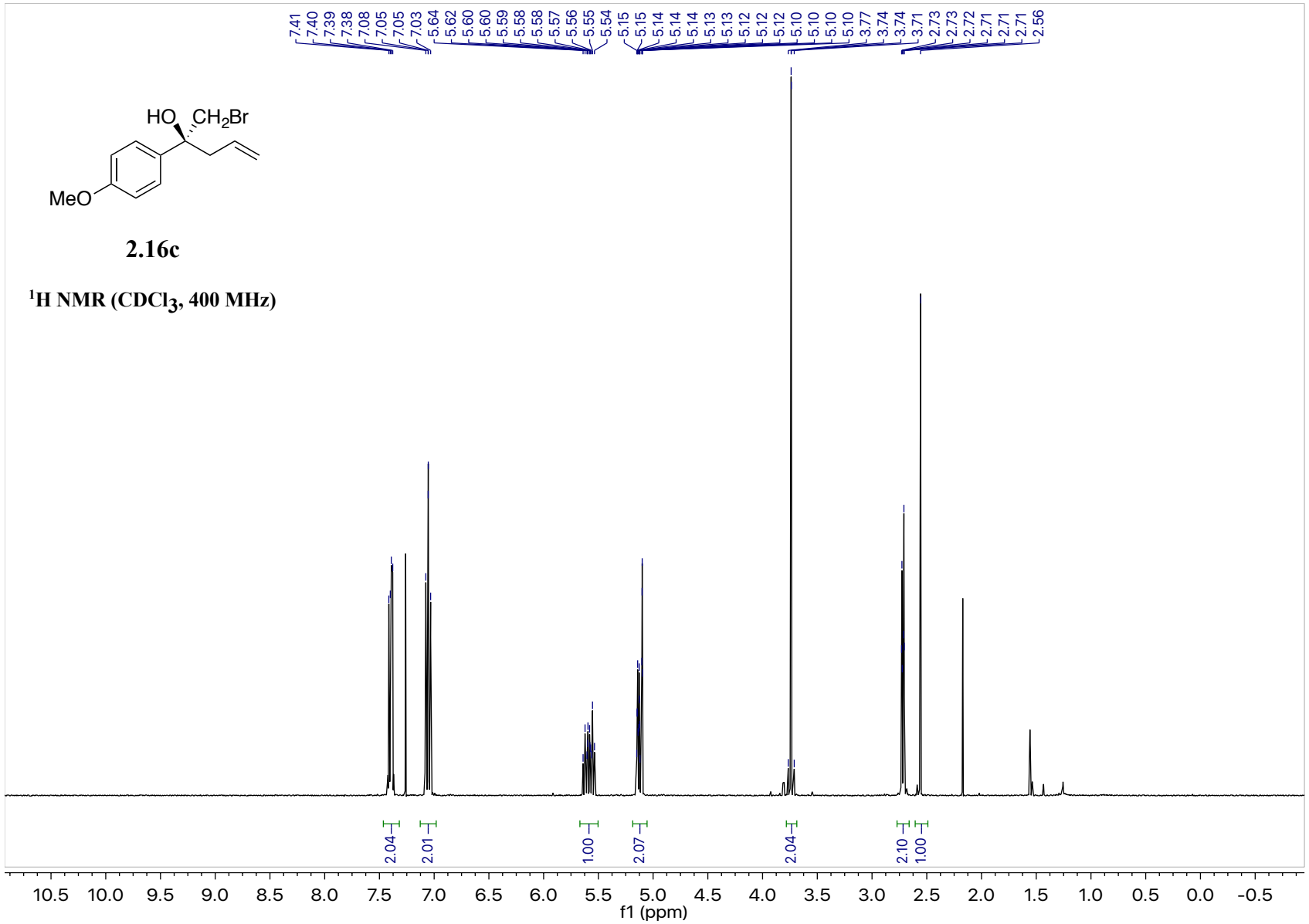

2.16c

^{1}H NMR ($CDCl_3$, 400 MHz)

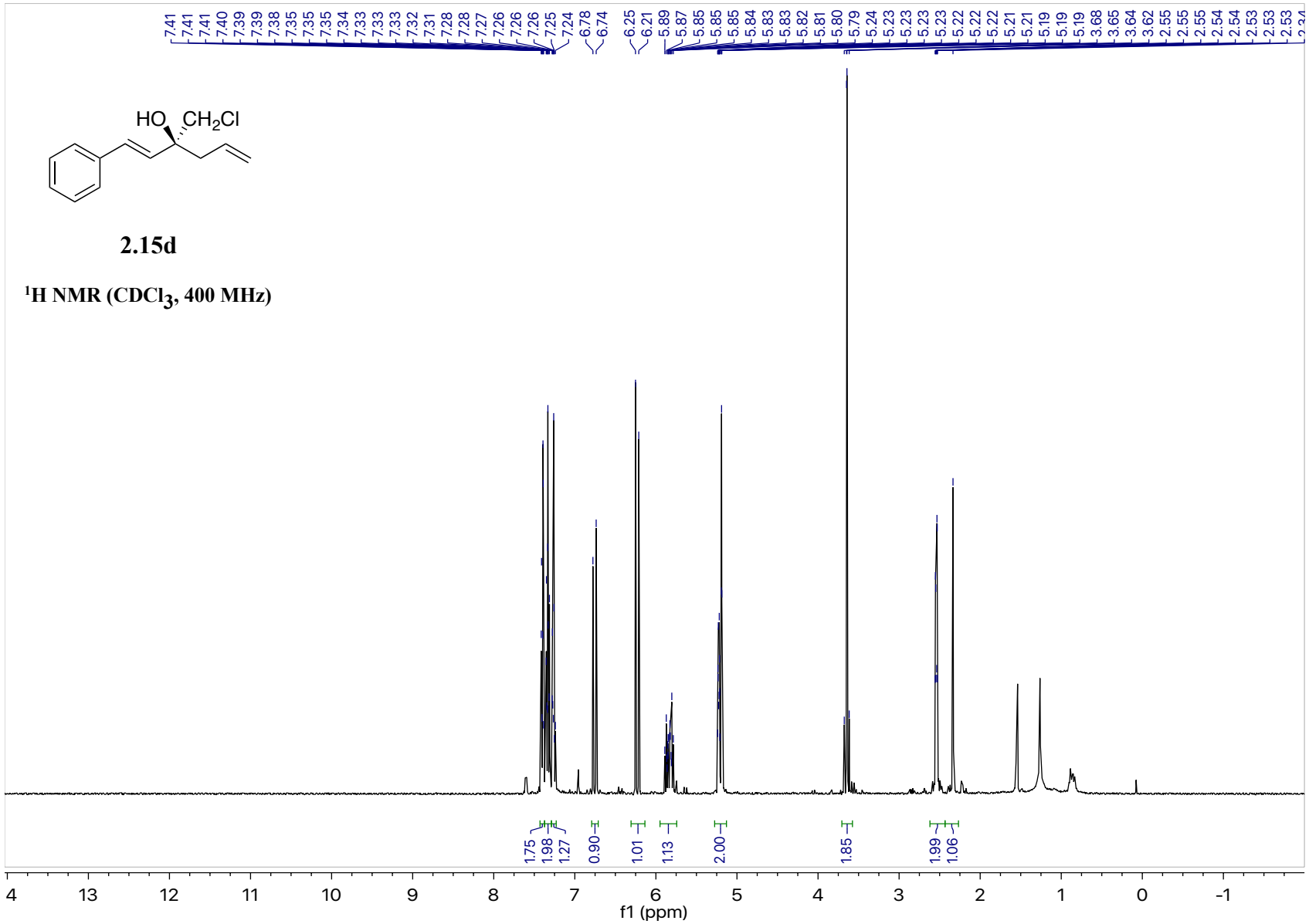
HO
CH2Cl
2.15d
1H NMR (CDCl3, 400 MHz)
f1 (ppm)

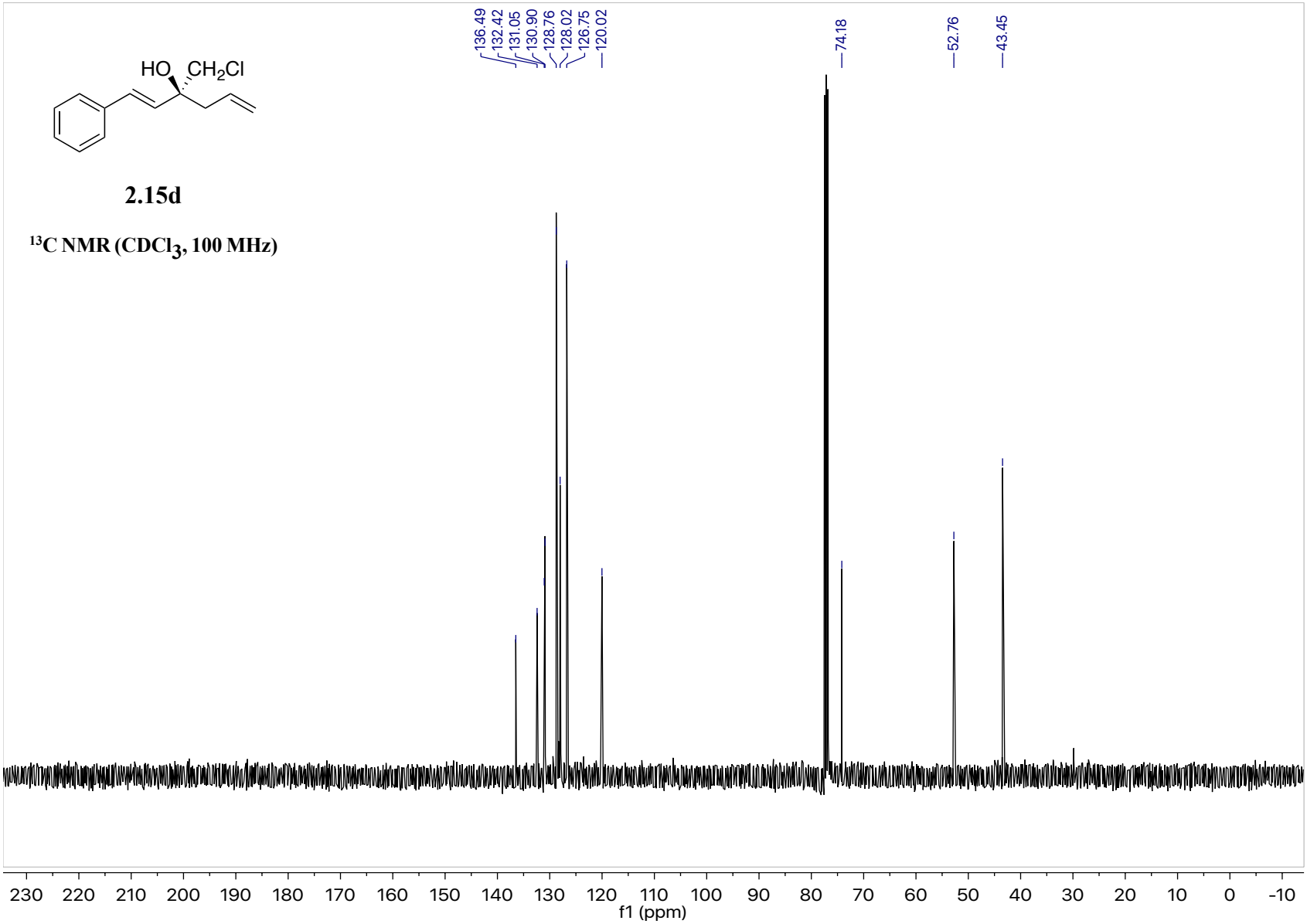
HO
CH2Cl
2.15d
13C NMR (CDCl3, 100 MHz)
136.49
132.42
131.05
130.90
128.76
128.02
126.75
120.02
74.18
52.76
43.45
230 220 210 200 190 180 170 160 150 140 130 120 110 100 90 80 70 60 50 40 30 20 10 0 -10
f1 (ppm)

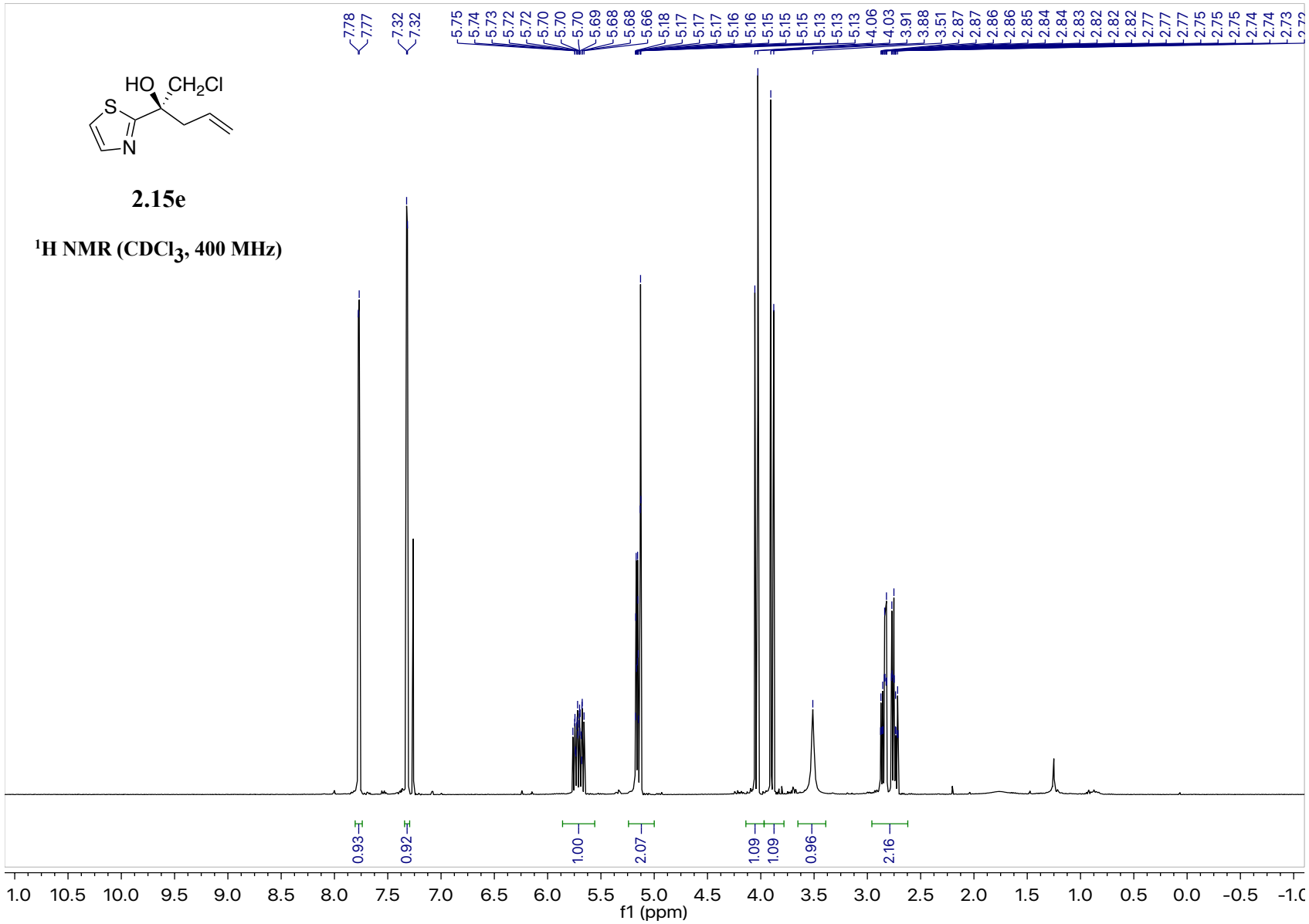
HO
CH2Cl
S
N
2.15e
1H NMR (CDCl3, 400 MHz)
f1 (ppm)

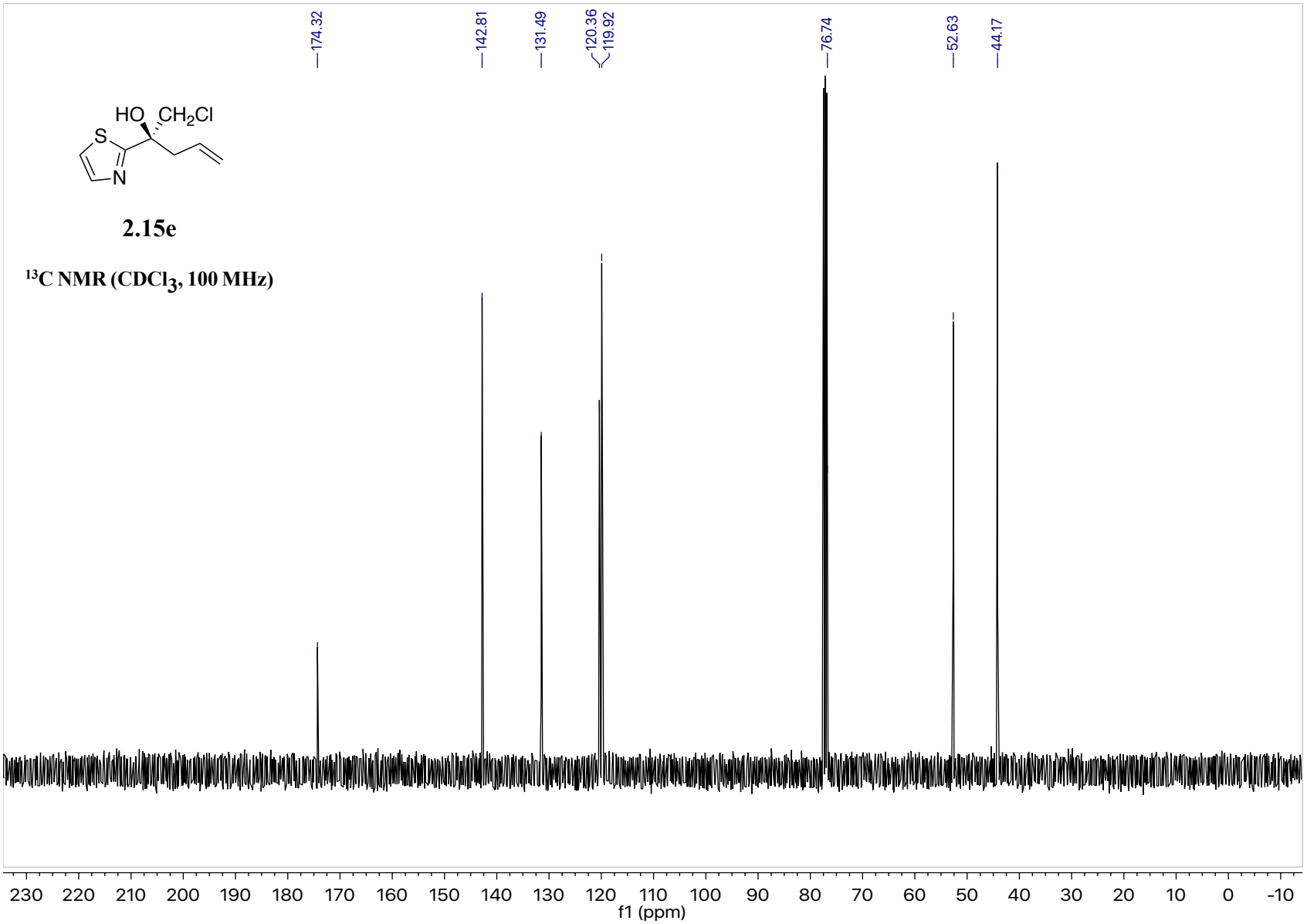
174.32
142.81
131.49
120.36
119.92
76.74
52.63
44.17
HO
CH2Cl
S
N
2.15e
13C NMR (CDCl3, 100 MHz)
230 220 210 200 190 180 170 160 150 140 130 120 110 100 90 80 70 60 50 40 30 20 10 0 -10
f1 (ppm)

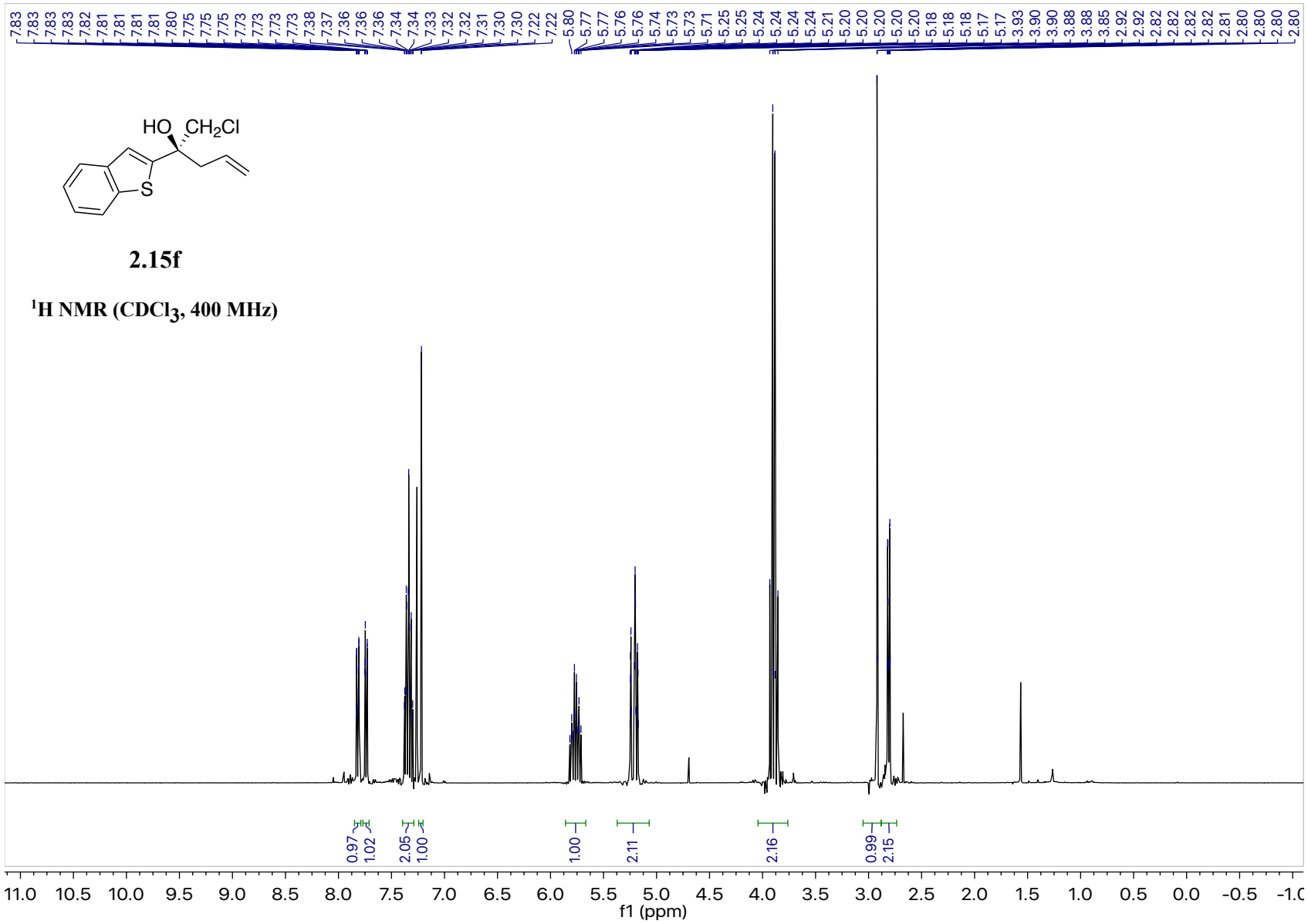
HO
CH2Cl
S
2.15f
1H NMR (CDCl3, 400 MHz)
7.83 7.83 7.83 7.82 7.81 7.81 7.81 7.81 7.80 7.75 7.75 7.75 7.73 7.73 7.73 7.73 7.38 7.37 7.36 7.36 7.36 7.34 7.34 7.33 7.32 7.32 7.31 7.30 7.30 7.22 7.22
5.80 5.77 5.77 5.76 5.76 5.74 5.73 5.73 5.71 5.25 5.25 5.24 5.24 5.24 5.24 5.21 5.20 5.20 5.20 5.20 5.20 5.18 5.18 5.18 5.17 5.17
3.93 3.90 3.90 3.88 3.88 3.85 2.92 2.92 2.82 2.82 2.82 2.82 2.81 2.80 2.80 2.80
0.97 1.02 2.05 1.00 1.00 2.11 2.16 0.99 2.15
11.0 10.5 10.0 9.5 9.0 8.5 8.0 7.5 7.0 6.5 6.0 5.5 5.0 4.5 4.0 3.5 3.0 2.5 2.0 1.5 1.0 0.5 0.0 -0.5 -1.0
f1 (ppm)

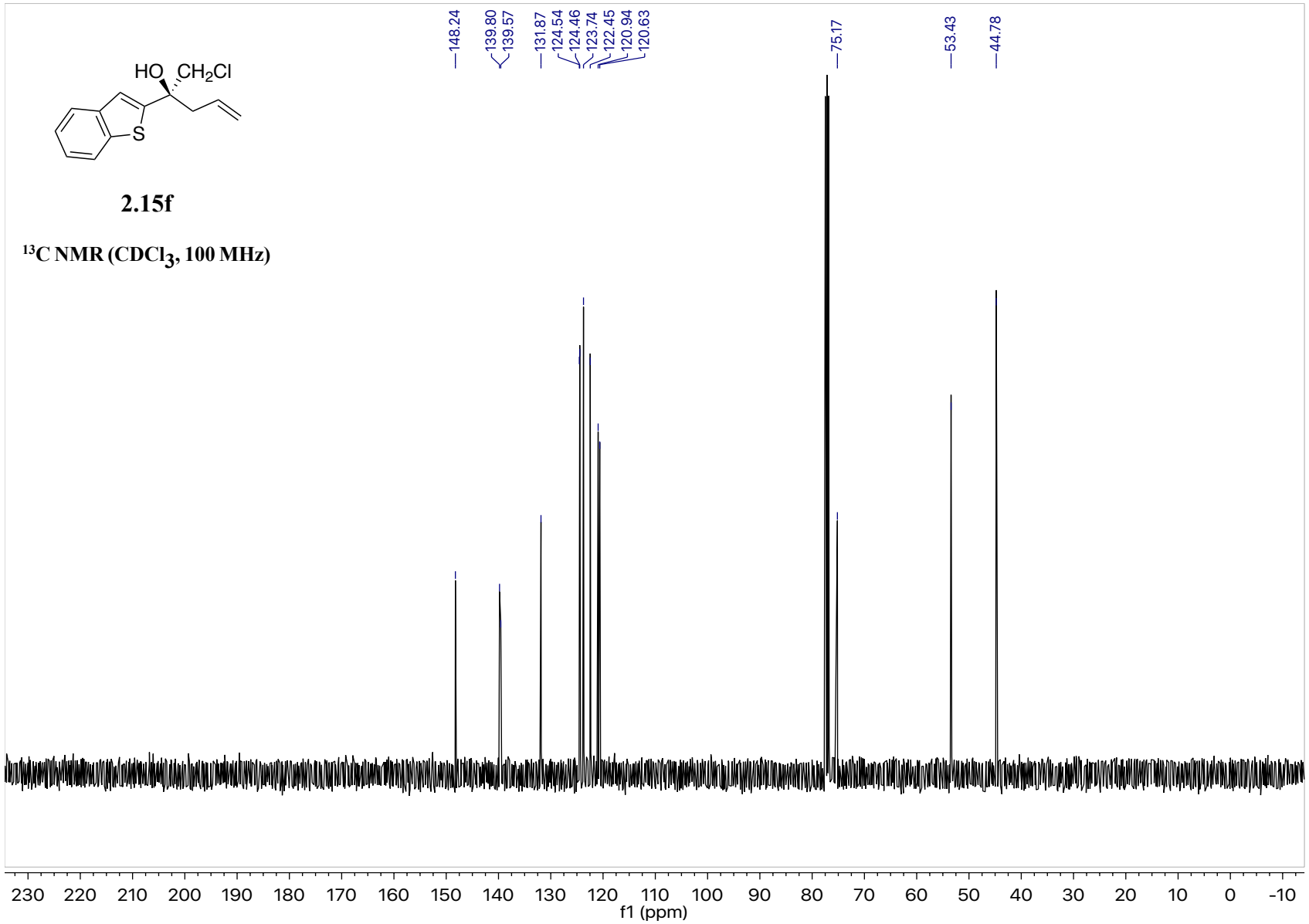
148.24
139.80
139.57
131.87
124.54
124.46
123.74
122.45
120.94
120.63
75.17
53.43
44.78
HO
CH2Cl
S
2.15f
13C NMR (CDCl3, 100 MHz)
230 220 210 200 190 180 170 160 150 140 130 120 110 100 90 80 70 60 50 40 30 20 10 0 -10
f1 (ppm)

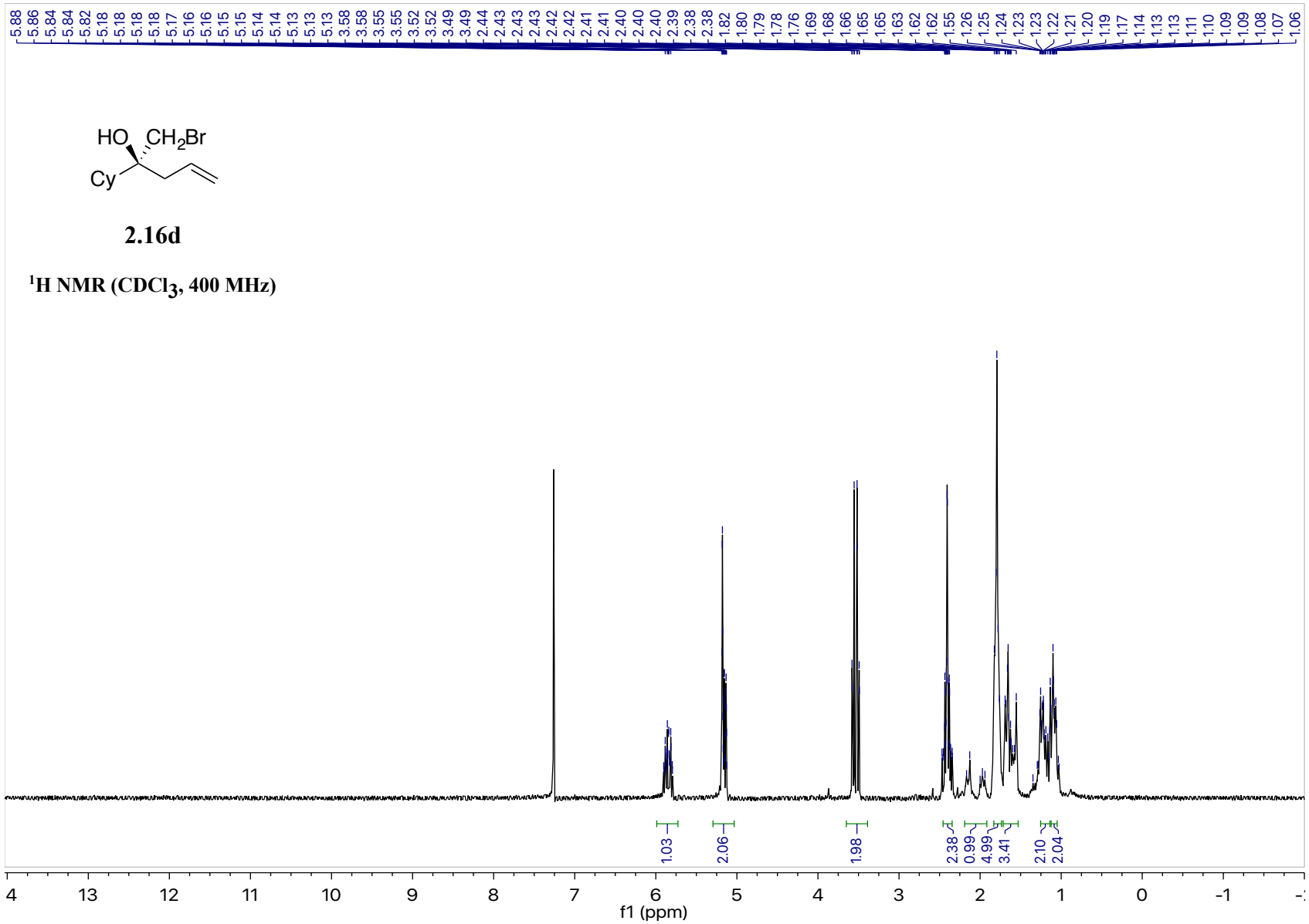

2.16d

^{1}H NMR ($CDCl_3$, 400 MHz)

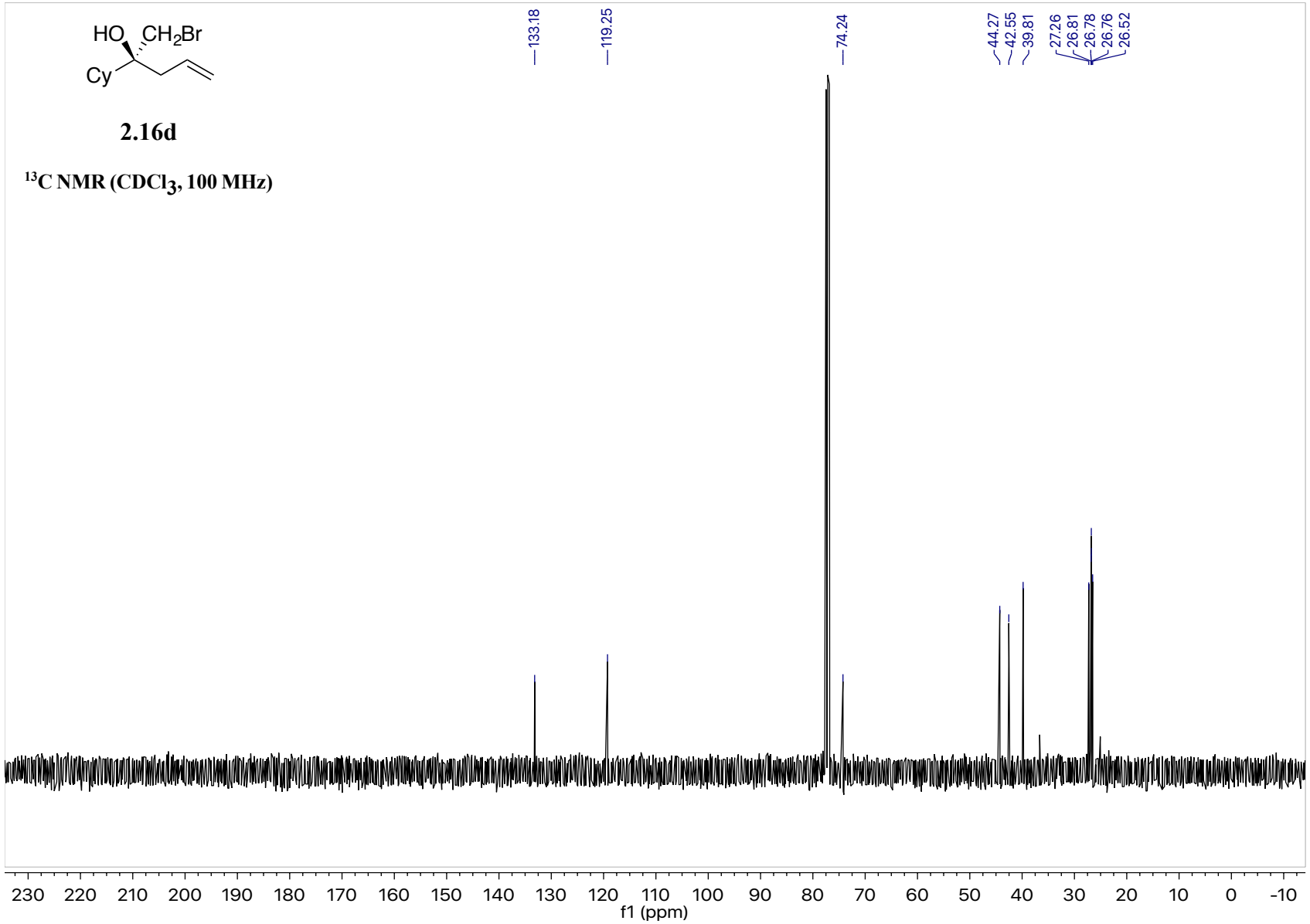
HO
CH2Br
Cy
2.16d
13C NMR (CDCl3, 100 MHz)
133.18
119.25
74.24
44.27
42.55
39.81
27.26
26.81
26.78
26.76
26.52
230 220 210 200 190 180 170 160 150 140 130 120 110 100 90 80 70 60 50 40 30 20 10 0 -10
f1 (ppm)

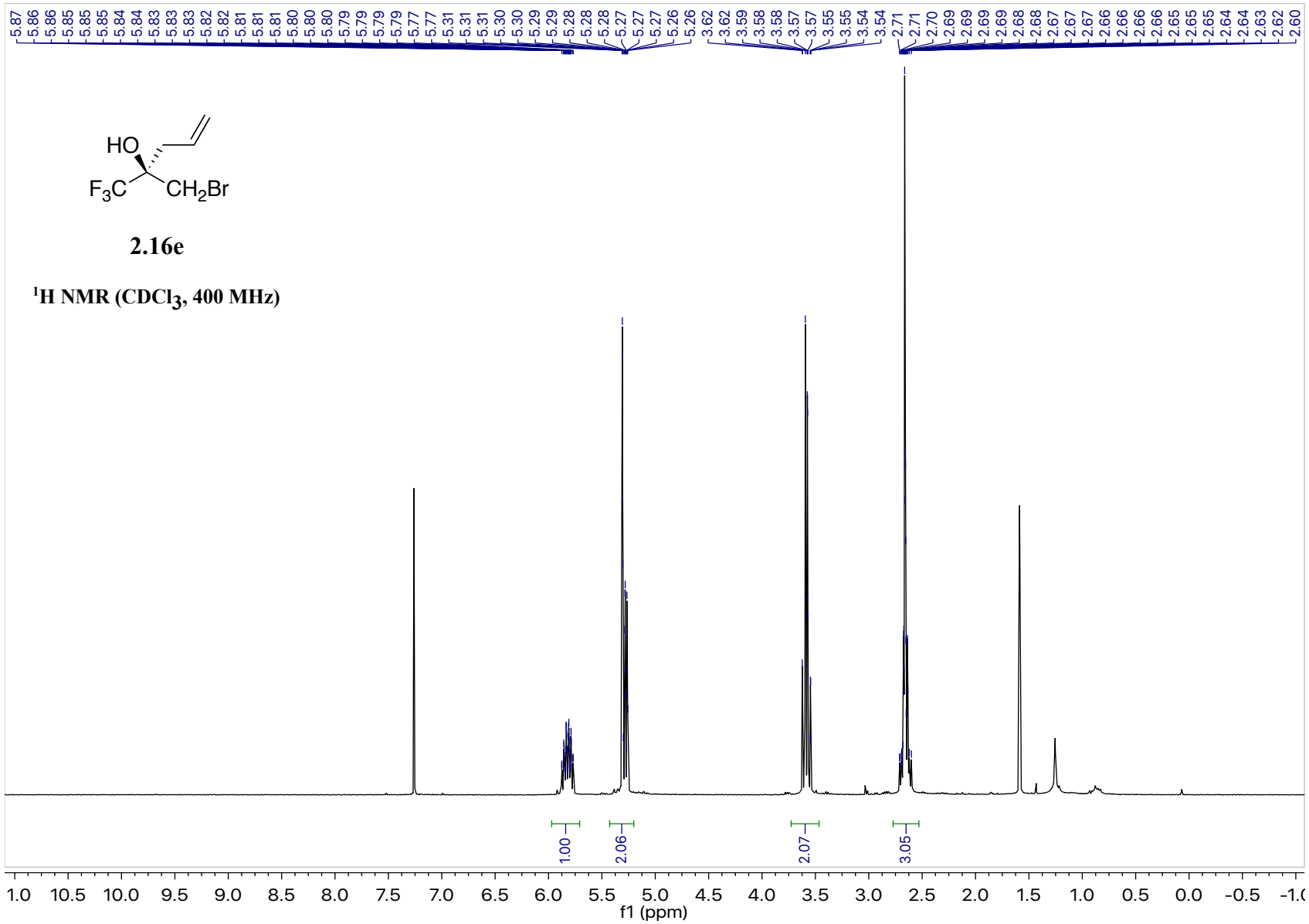
HO
F3C
CH2Br
2.16e
1H NMR (CDCl3, 400 MHz)
1.00
2.06
2.07
3.05
f1 (ppm)

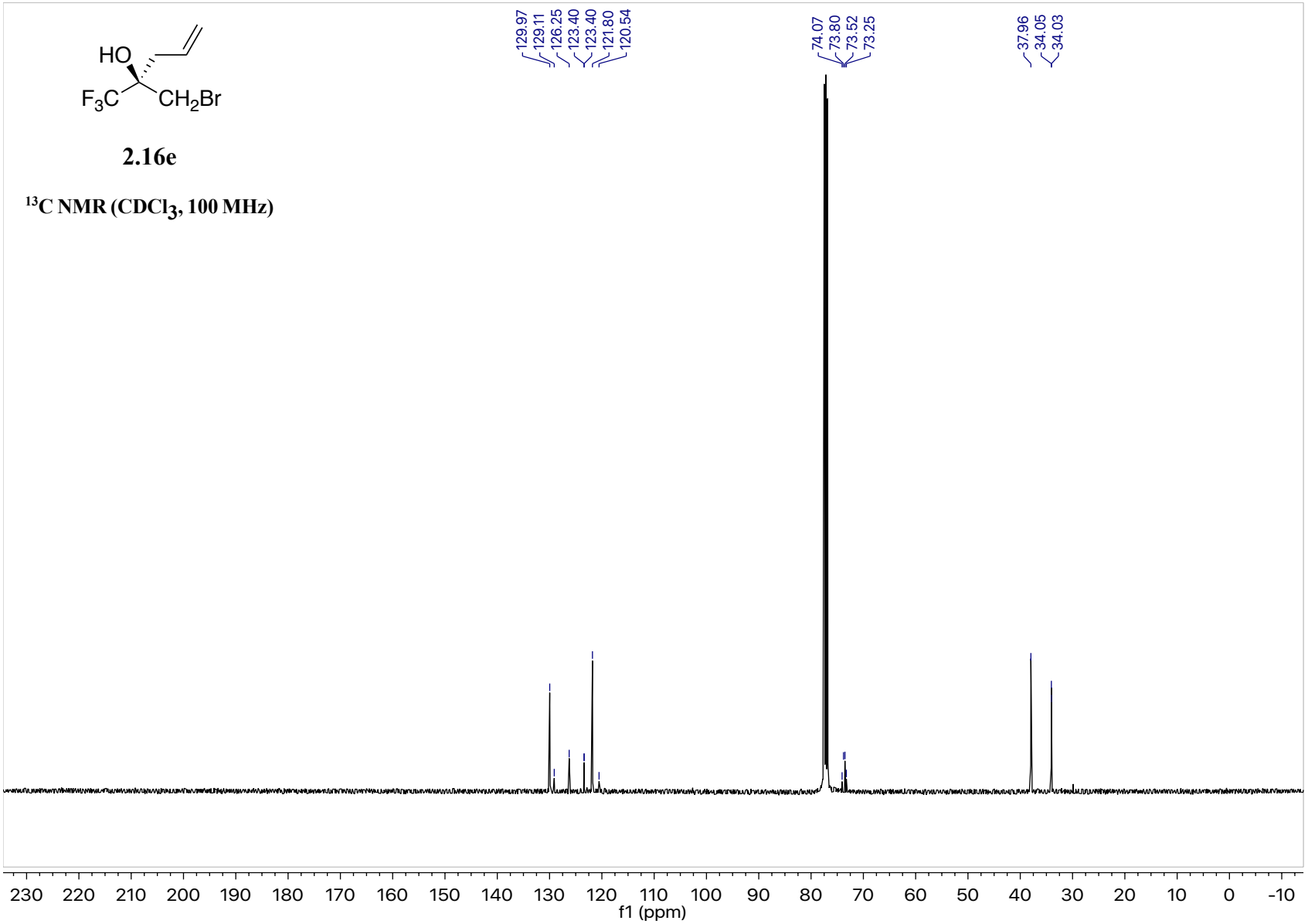
HO
F3C
CH2Br
2.16e
13C NMR (CDCl3, 100 MHz)
129.97
129.11
126.25
123.40
123.40
121.80
120.54
74.07
73.80
73.52
73.25
37.96
34.05
34.03
230 220 210 200 190 180 170 160 150 140 130 120 110 100 90 80 70 60 50 40 30 20 10 0 -10
f1 (ppm)

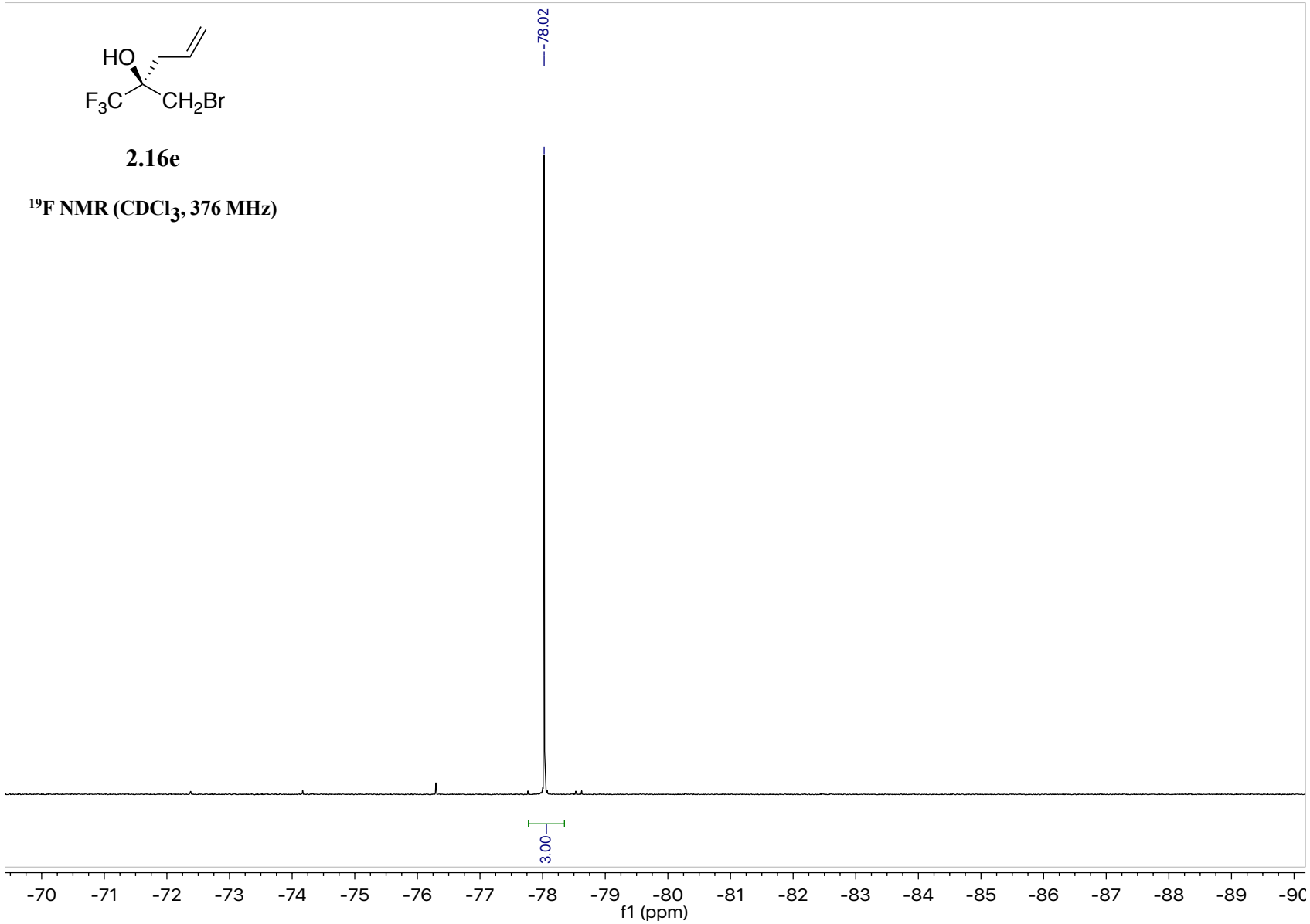
HO
F3C
CH2Br
2.16e
19F NMR (CDCl3, 376 MHz)
-78.02
3.00
-70 -71 -72 -73 -74 -75 -76 -77 -78 -79 -80 -81 -82 -83 -84 -85 -86 -87 -88 -89 -90
f1 (ppm)

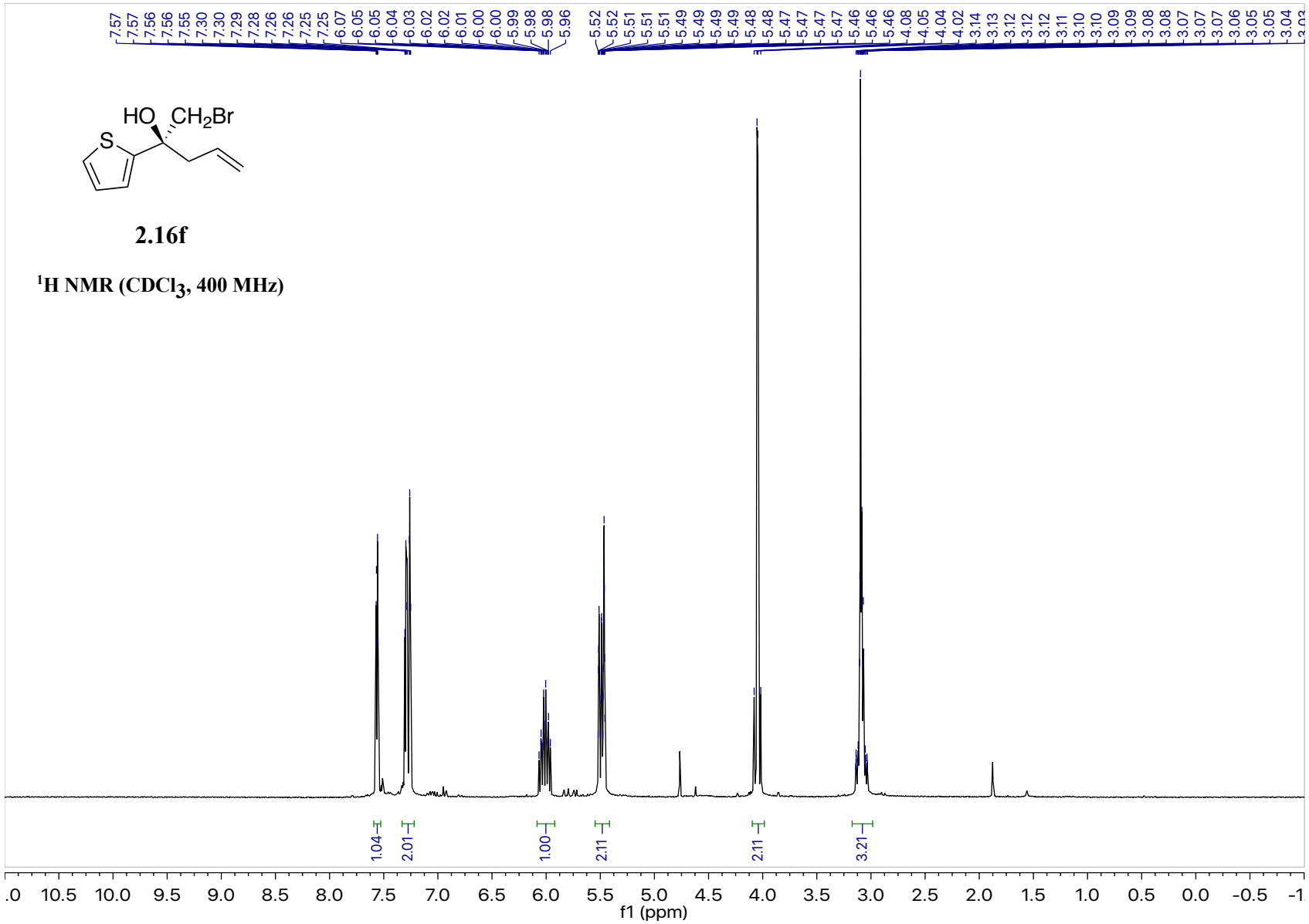

2.16f

^{1}H NMR ($CDCl_3$, 400 MHz)

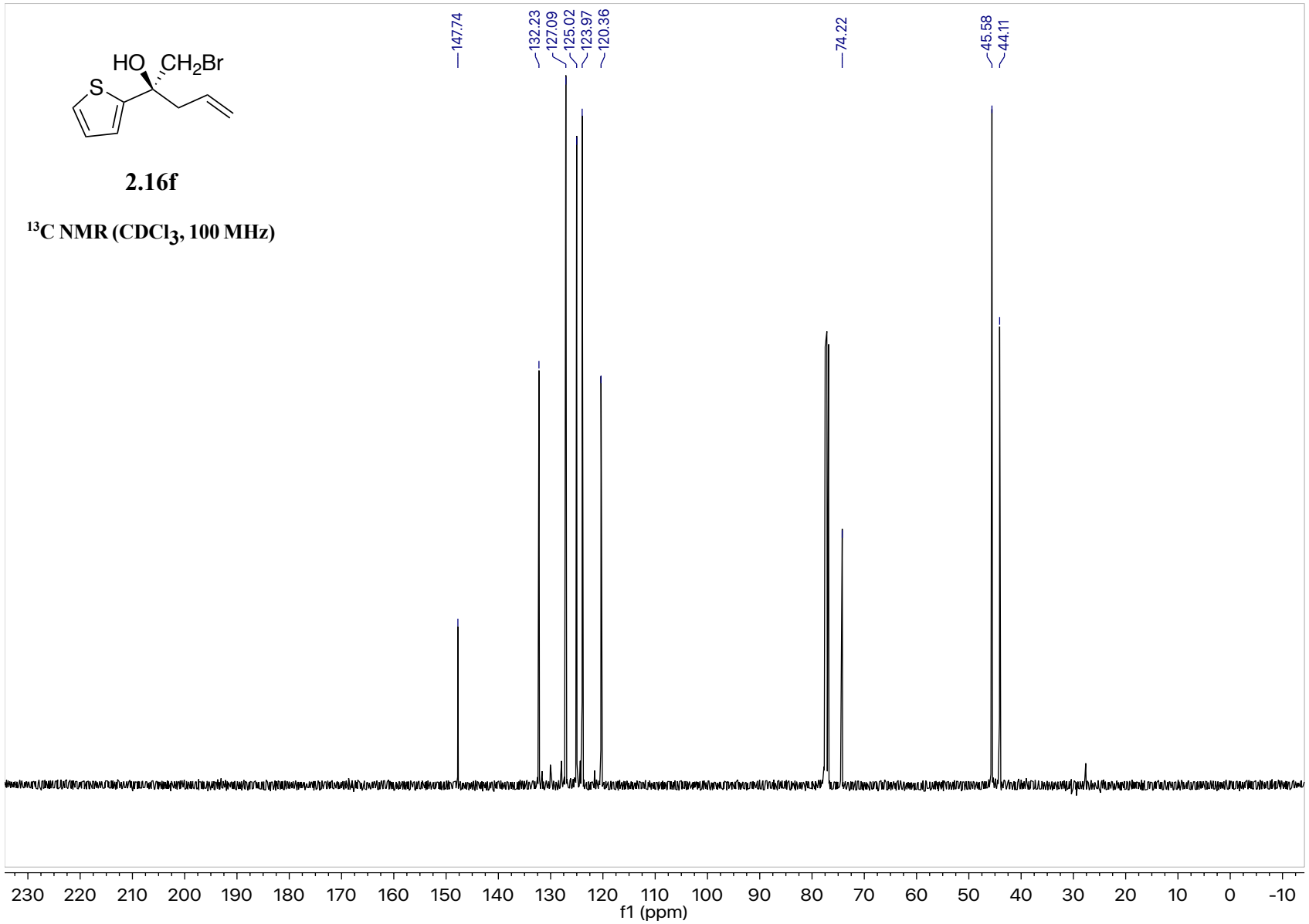

2.16f

^{13}C NMR ($CDCl_3$, 100 MHz)

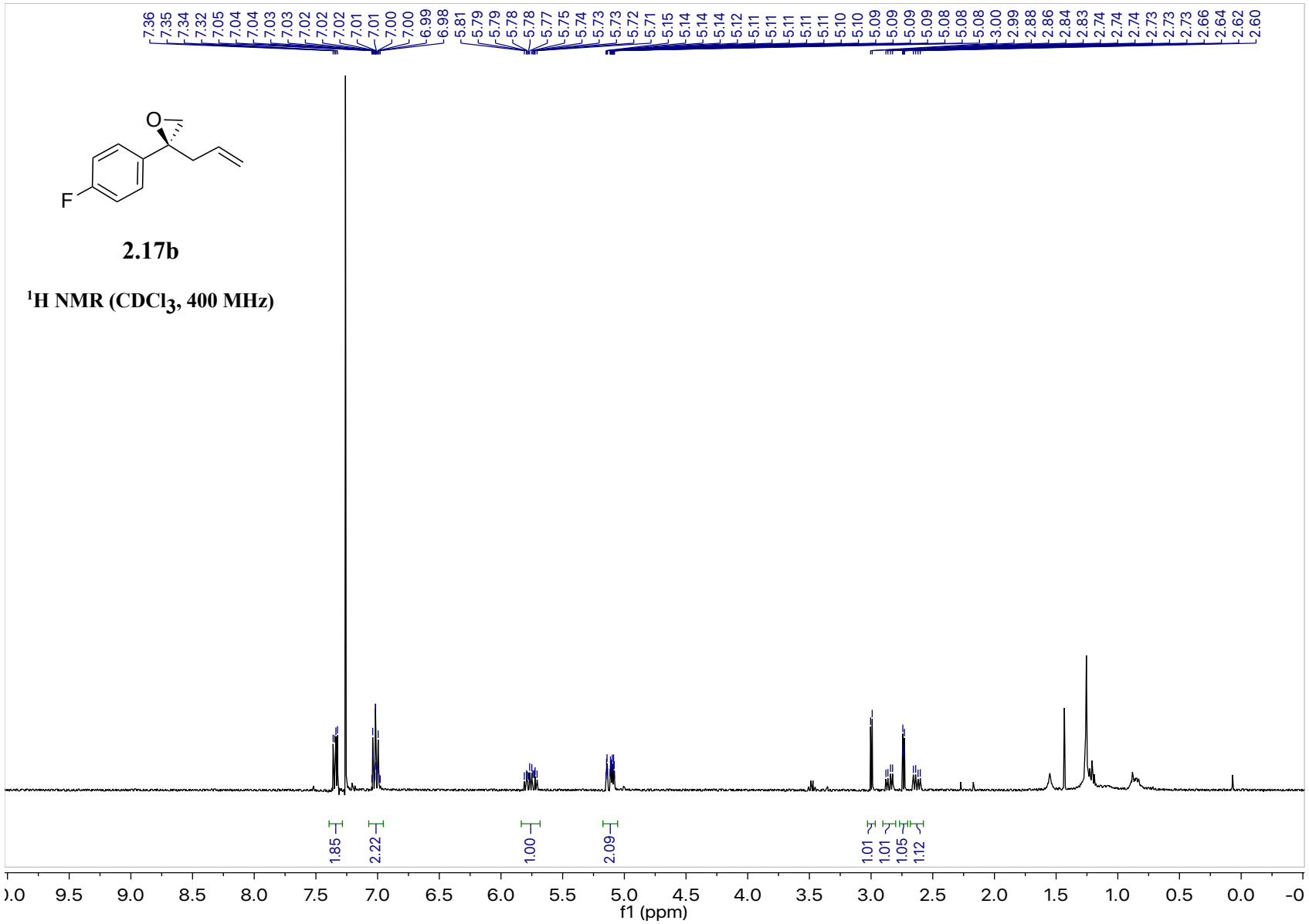
7.36 7.35 7.34 7.32 7.05 7.04 7.04 7.03 7.03 7.02 7.02 7.02 7.01 7.01 7.00 7.00 6.99 6.98 5.81 5.79 5.79 5.78 5.78 5.77 5.75 5.74 5.73 5.73 5.72 5.71 5.15 5.14 5.14 5.12 5.11 5.11 5.11 5.11 5.11 5.10 5.10 5.09 5.09 5.09 5.09 5.08 5.08 5.08 3.00 2.99 2.88 2.86 2.84 2.83 2.74 2.74 2.74 2.73 2.73 2.73 2.66 2.64 2.62 2.60
O
F
2.17b
1H NMR (CDCl3, 400 MHz)
1.85
2.22
1.00
2.09
1.01
1.01
1.05
1.12
f1 (ppm)

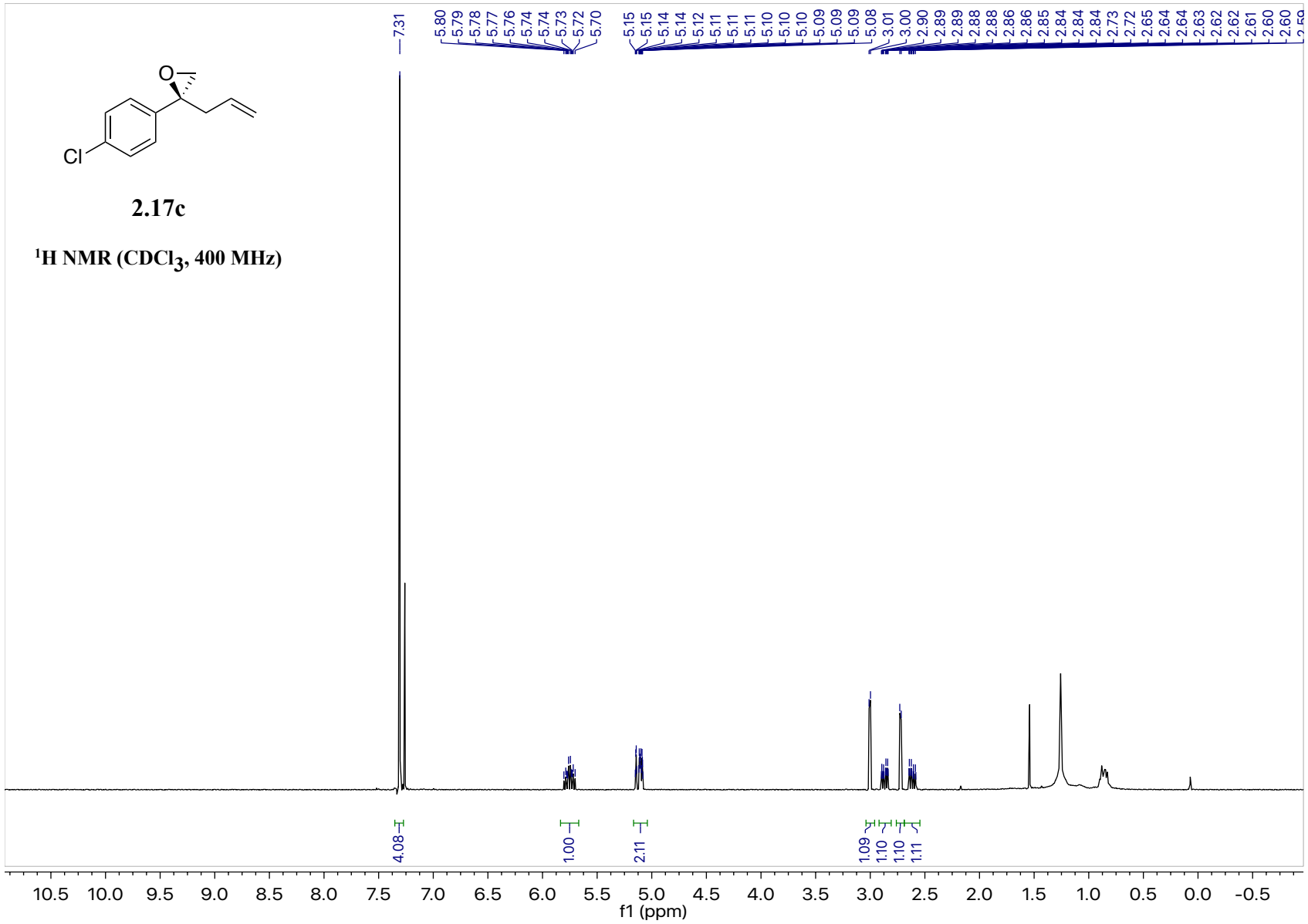
Cl
O
2.17c
^{1}H NMR (CDCl$_3$, 400 MHz)
7.31
5.80 5.79 5.78 5.77 5.76 5.74 5.74 5.73 5.72 5.70
5.15 5.15 5.14 5.14 5.12 5.11 5.11 5.11 5.10 5.10 5.10 5.09 5.09 5.09 5.08
3.01 3.00 2.90 2.89 2.89 2.88 2.88 2.86 2.86 2.85 2.84 2.84 2.84 2.73 2.72 2.65 2.64 2.64 2.63 2.62 2.62 2.61 2.60 2.60
4.08
1.00
2.11
1.09
1.10
1.10
1.11
10.5 10.0 9.5 9.0 8.5 8.0 7.5 7.0 6.5 6.0 5.5 5.0 4.5 4.0 3.5 3.0 2.5 2.0 1.5 1.0 0.5 0.0 -0.5
f1 (ppm)

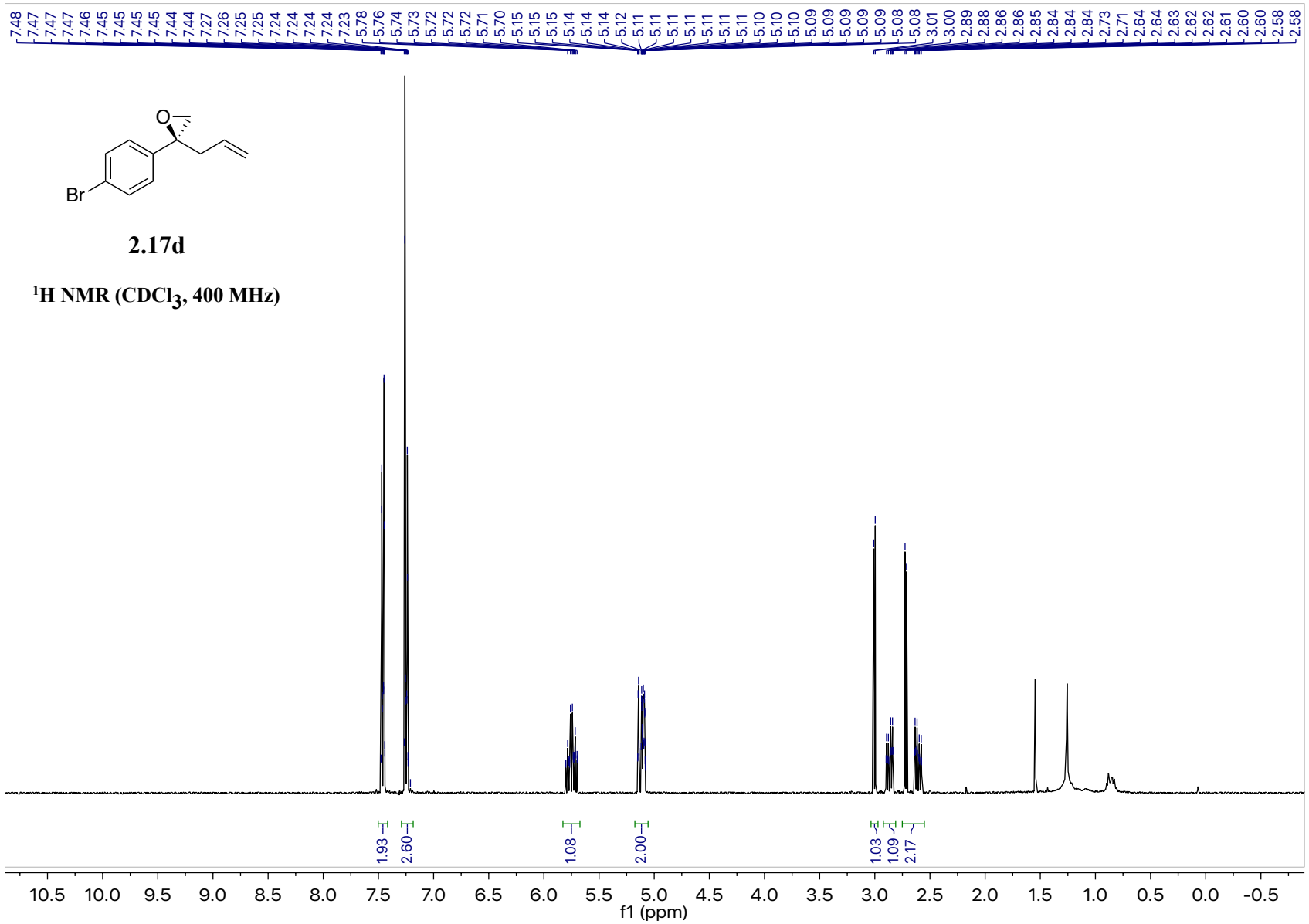
Br
O
2.17d
1H NMR (CDCl3, 400 MHz)
1.93
2.60
1.08
2.00
1.03
1.09
2.17
f1 (ppm)

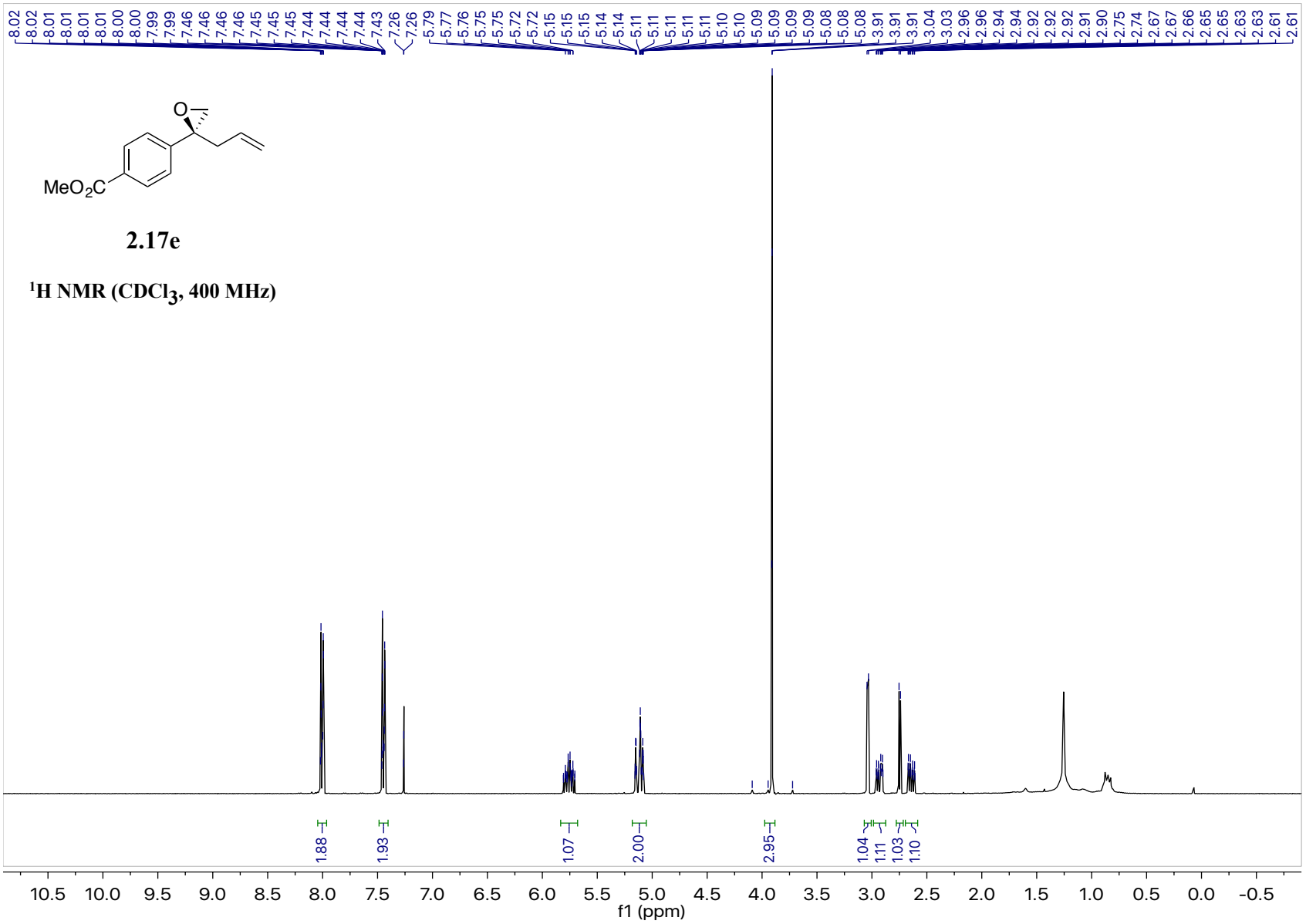

2.17e

^{1}H NMR ($CDCl_3$, 400 MHz)

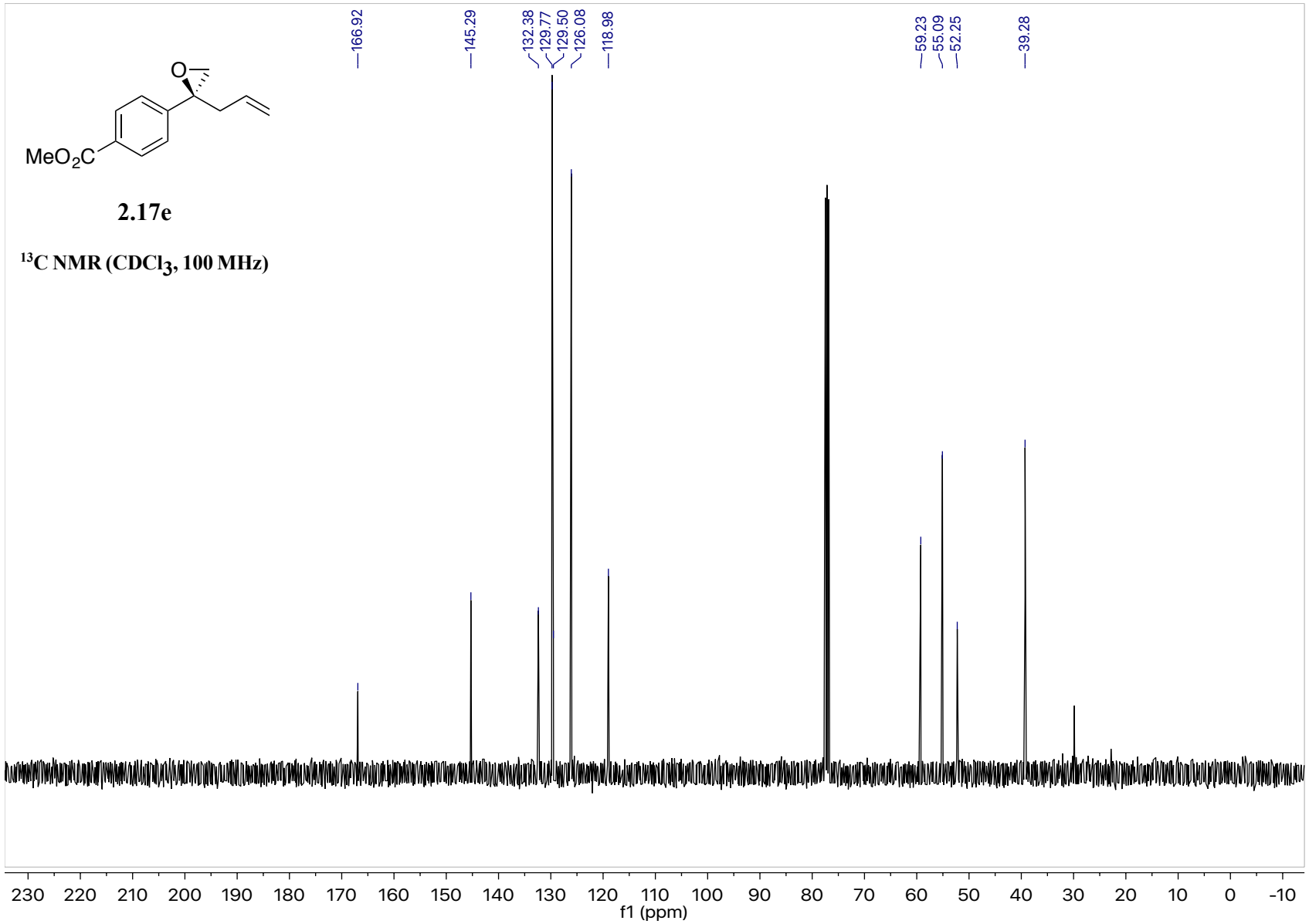

2.17e

^{13}C NMR ($CDCl_3$, 100 MHz)

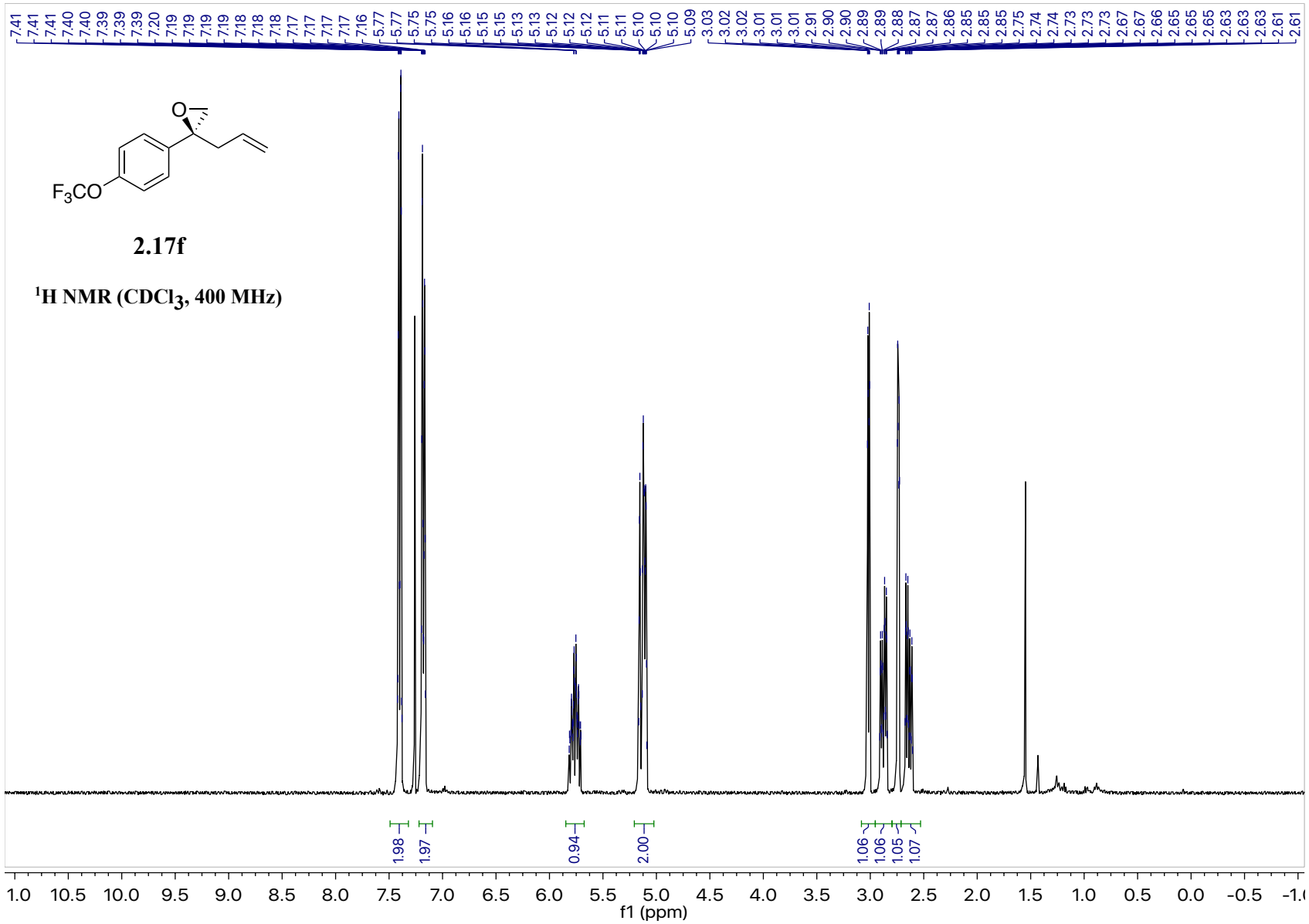
O
F3CO
2.17f
1H NMR (CDCl3, 400 MHz)
1.98
1.97
0.94
2.00
1.06
1.06
1.05
1.07
f1 (ppm)

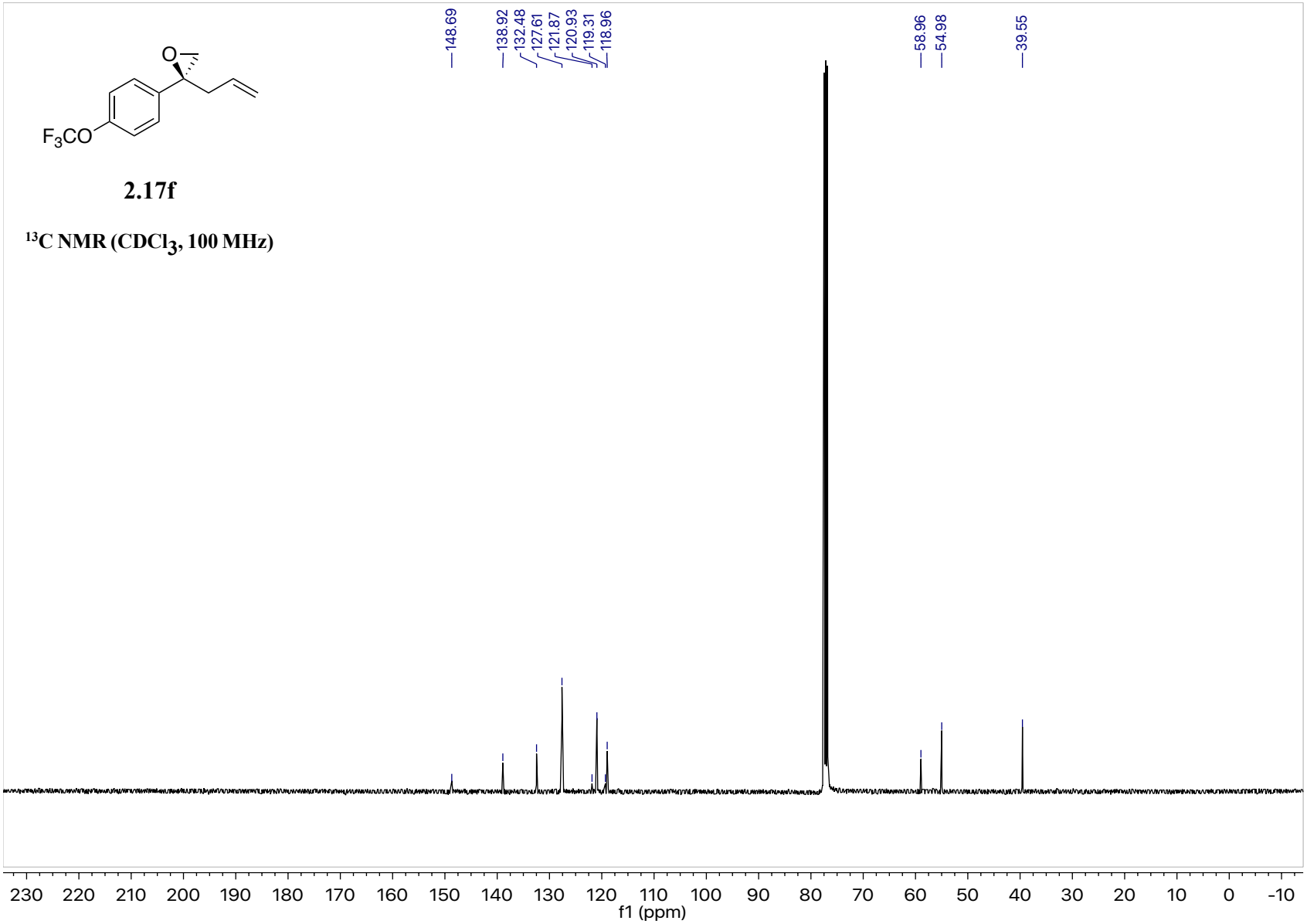

2.17f

^{13}C NMR ($CDCl_3$, 100 MHz)

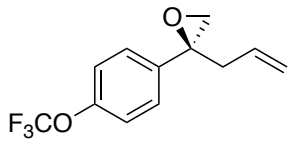

2.17f

^{19}F NMR ($CDCl_3$, 376 MHz)

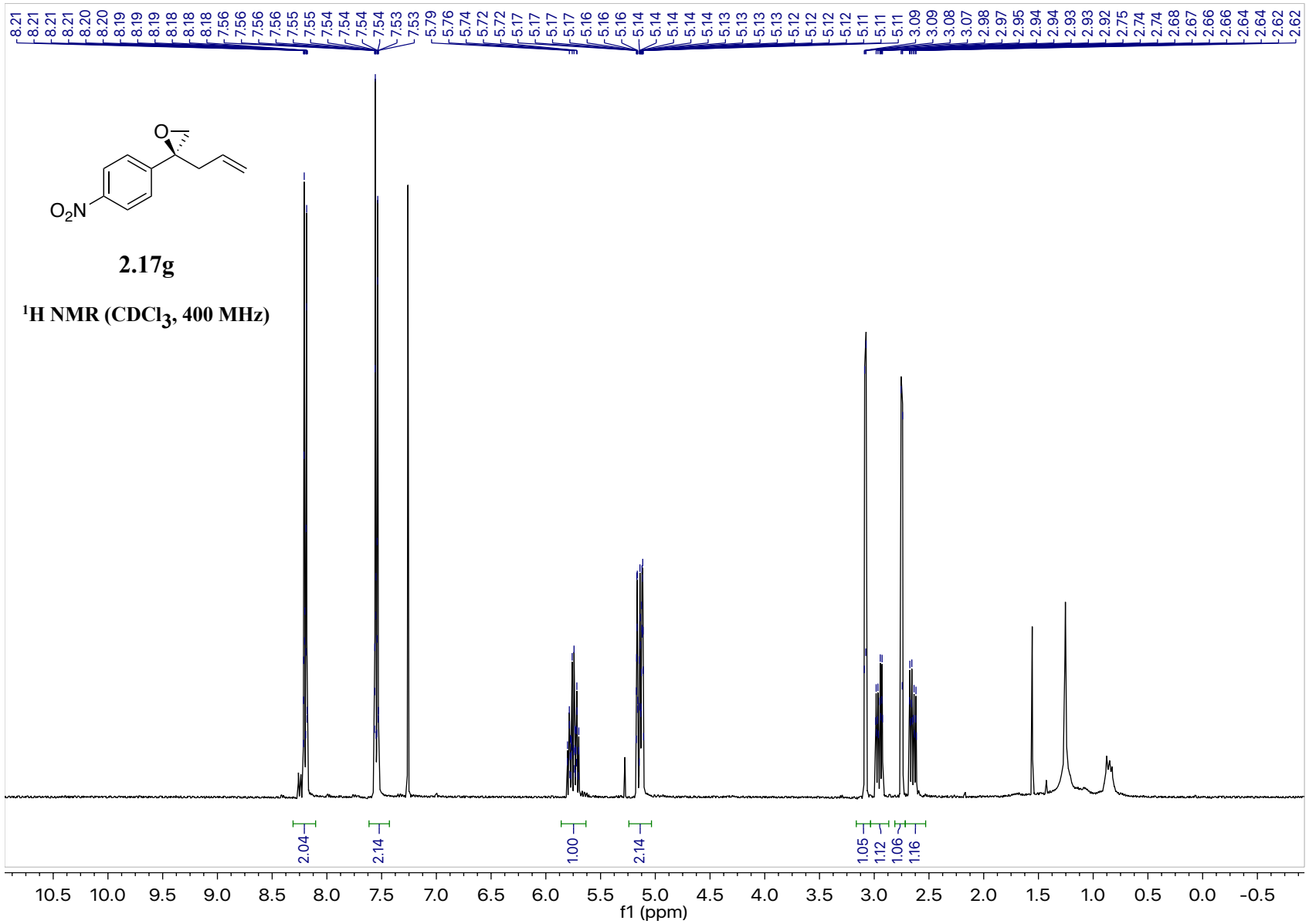
O
O2N
2.17g
1H NMR (CDCl3, 400 MHz)
2.04
2.14
1.00
2.14
1.05
1.12
1.06
1.16
f1 (ppm)

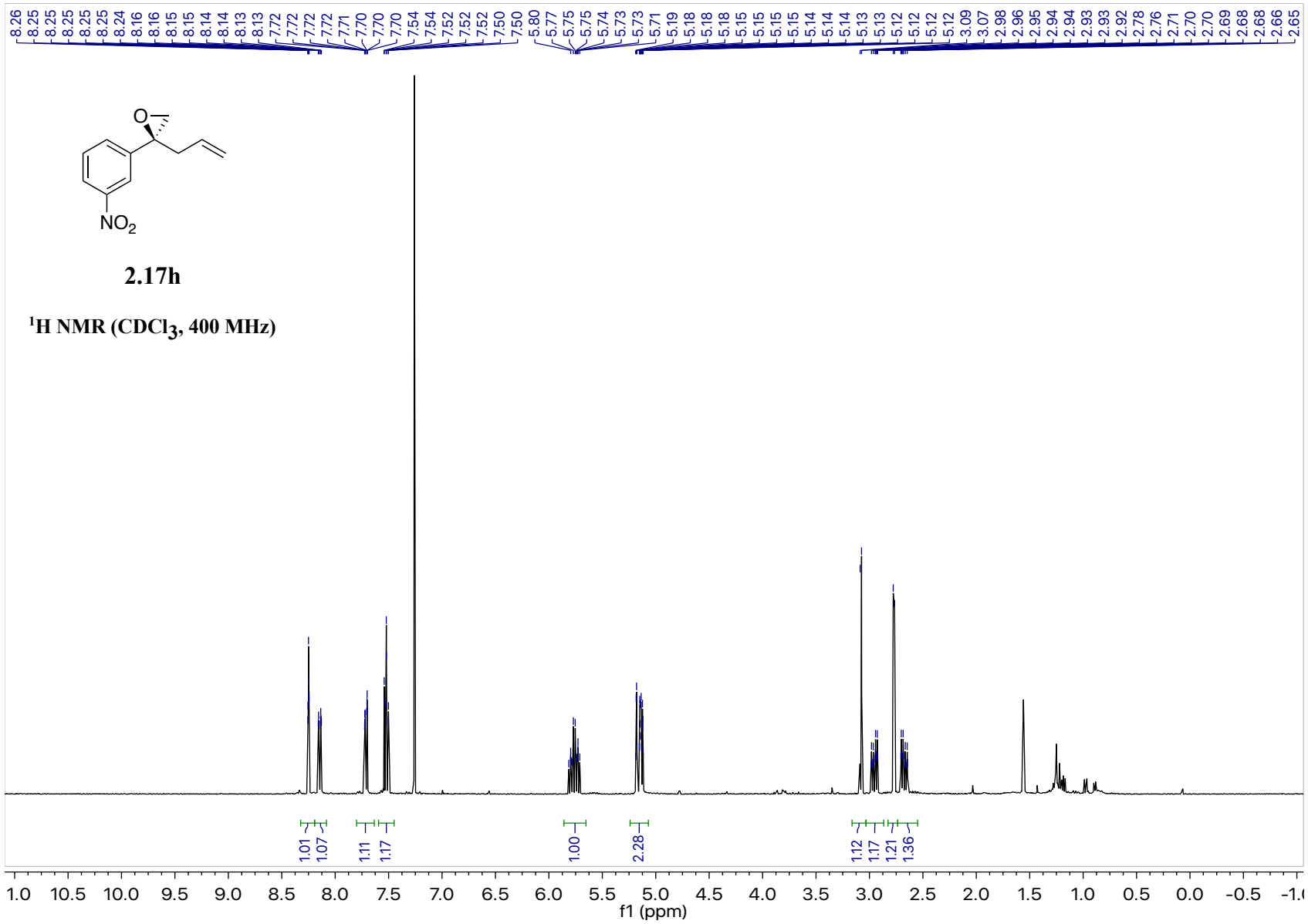
O
NO2
2.17h
1H NMR (CDCl3, 400 MHz)
f1 (ppm)

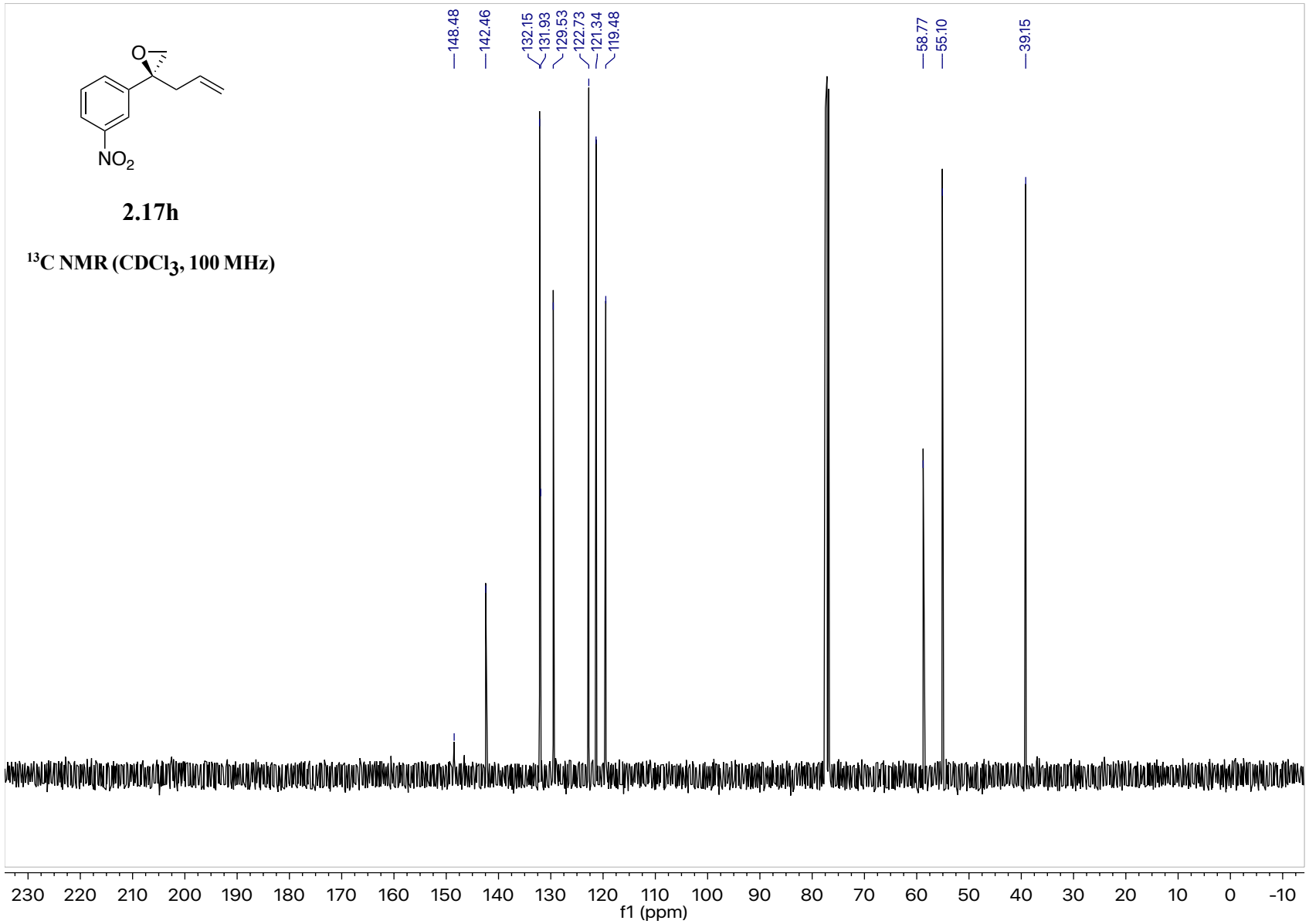

2.17h

^{13}C NMR ($CDCl_3$, 100 MHz)

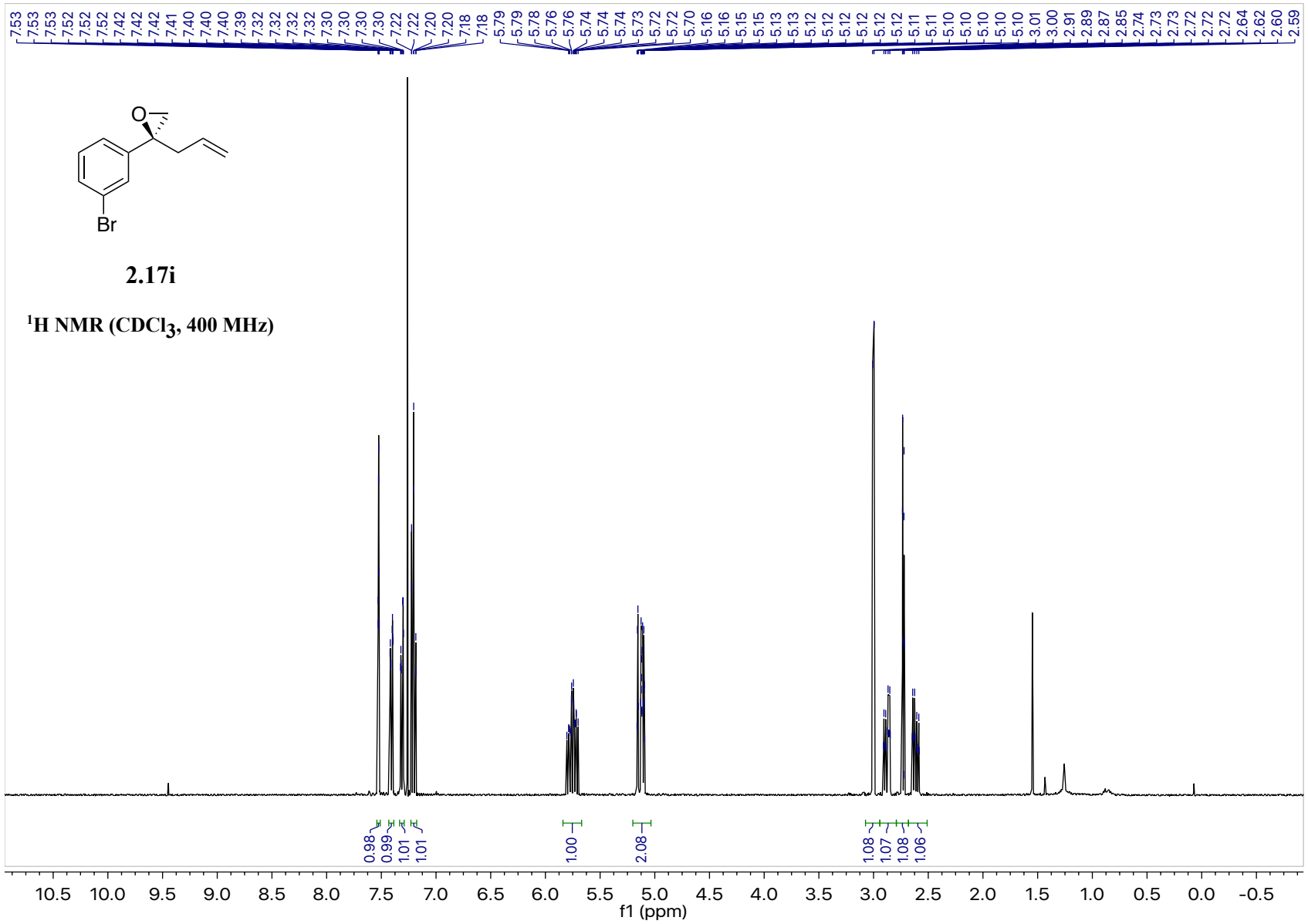
O
Br
2.17i
1H NMR (CDCl3, 400 MHz)
f1 (ppm)

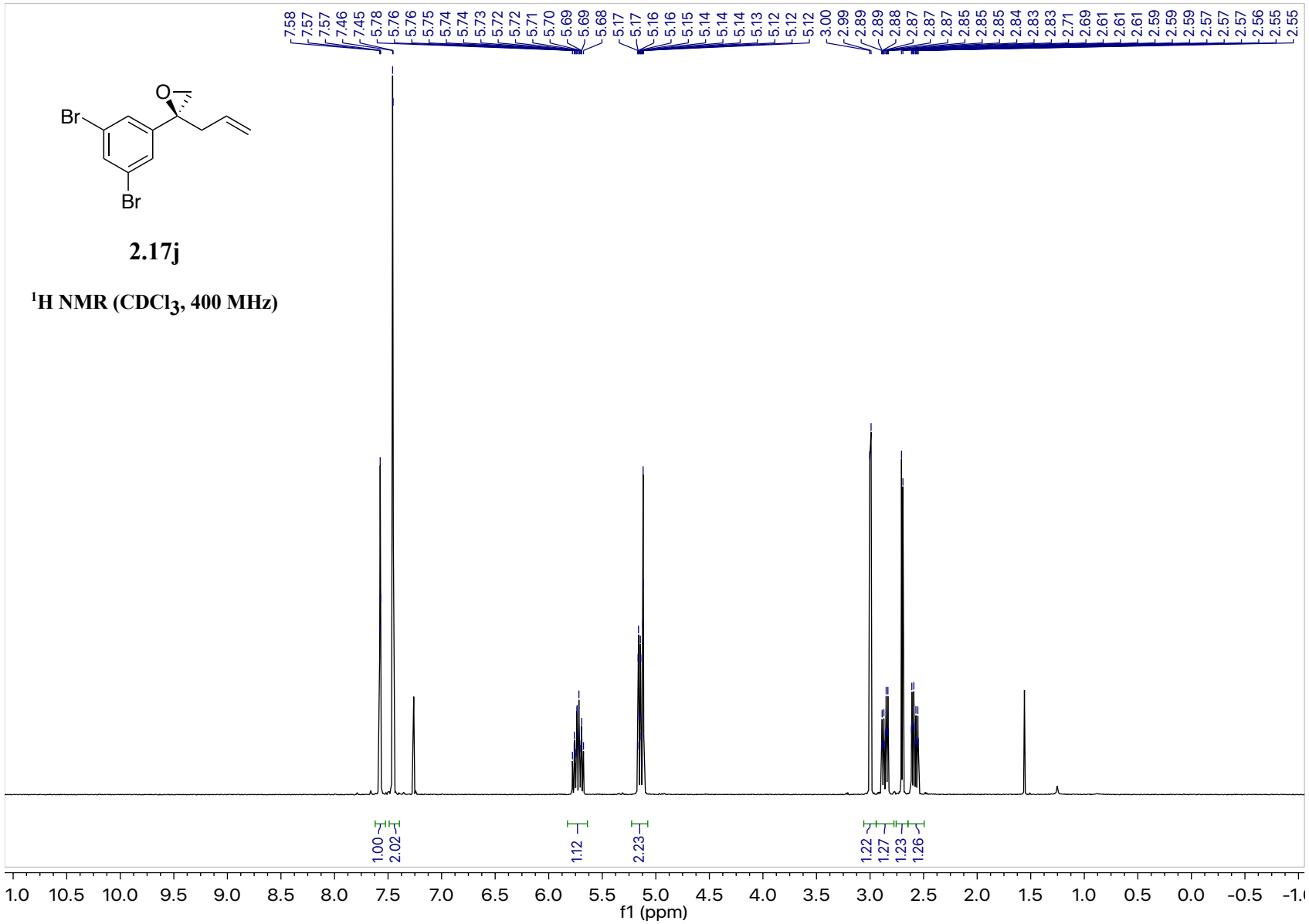
Br
O
Br
2.17j
^{1}H NMR (CDCl$_3$, 400 MHz)
7.58 7.57 7.57 7.46 7.45 5.78 5.76 5.76 5.75 5.74 5.74 5.73 5.72 5.72 5.71 5.70 5.69 5.69 5.68 5.17 5.17 5.16 5.16 5.15 5.14 5.14 5.13 5.12 5.12 5.12 3.00 2.99 2.89 2.89 2.88 2.87 2.87 2.87 2.85 2.85 2.85 2.84 2.83 2.83 2.71 2.69 2.61 2.61 2.61 2.59 2.59 2.59 2.57 2.57 2.57 2.56 2.55 2.55
1.00 2.02 1.12 2.23 1.22 1.27 1.23 1.26
1.0 10.5 10.0 9.5 9.0 8.5 8.0 7.5 7.0 6.5 6.0 5.5 5.0 4.5 4.0 3.5 3.0 2.5 2.0 1.5 1.0 0.5 0.0 -0.5
f1 (ppm)

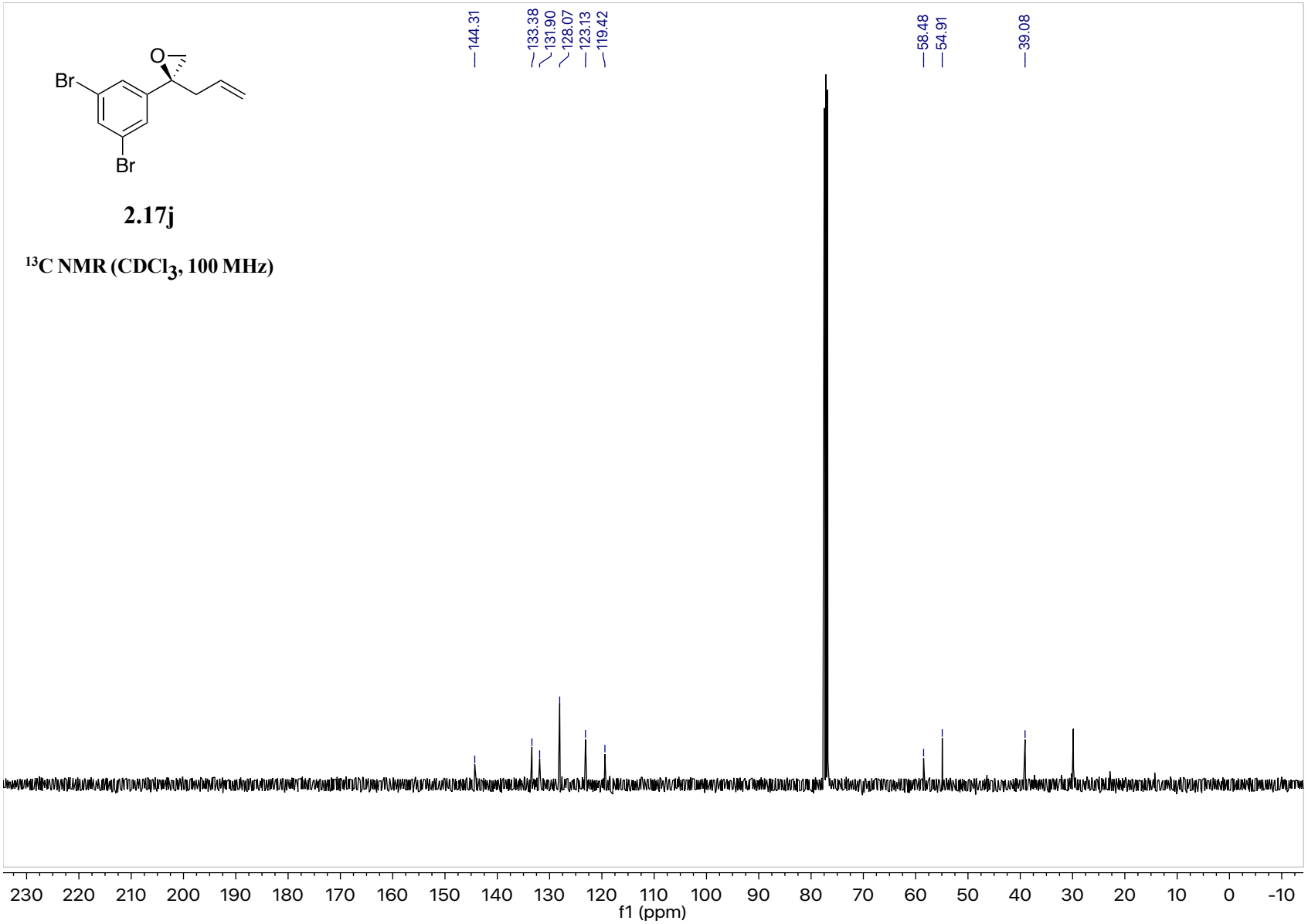

2.17j

^{13}C NMR ($CDCl_3$, 100 MHz)

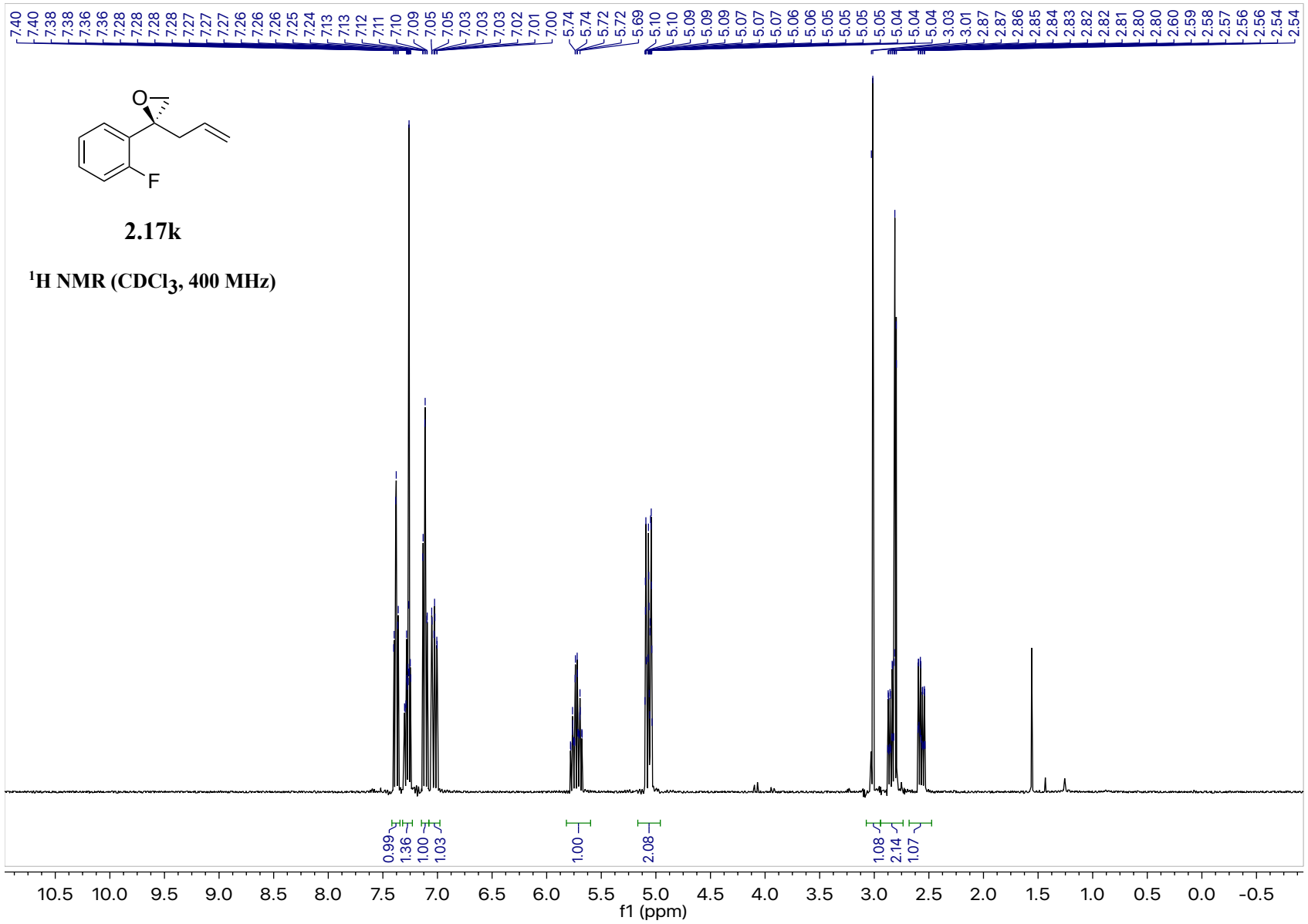
O
F
2.17k
1H NMR (CDCl3, 400 MHz)
0.99
1.36
1.00
1.03
1.00
2.08
1.08
2.14
1.07
f1 (ppm)

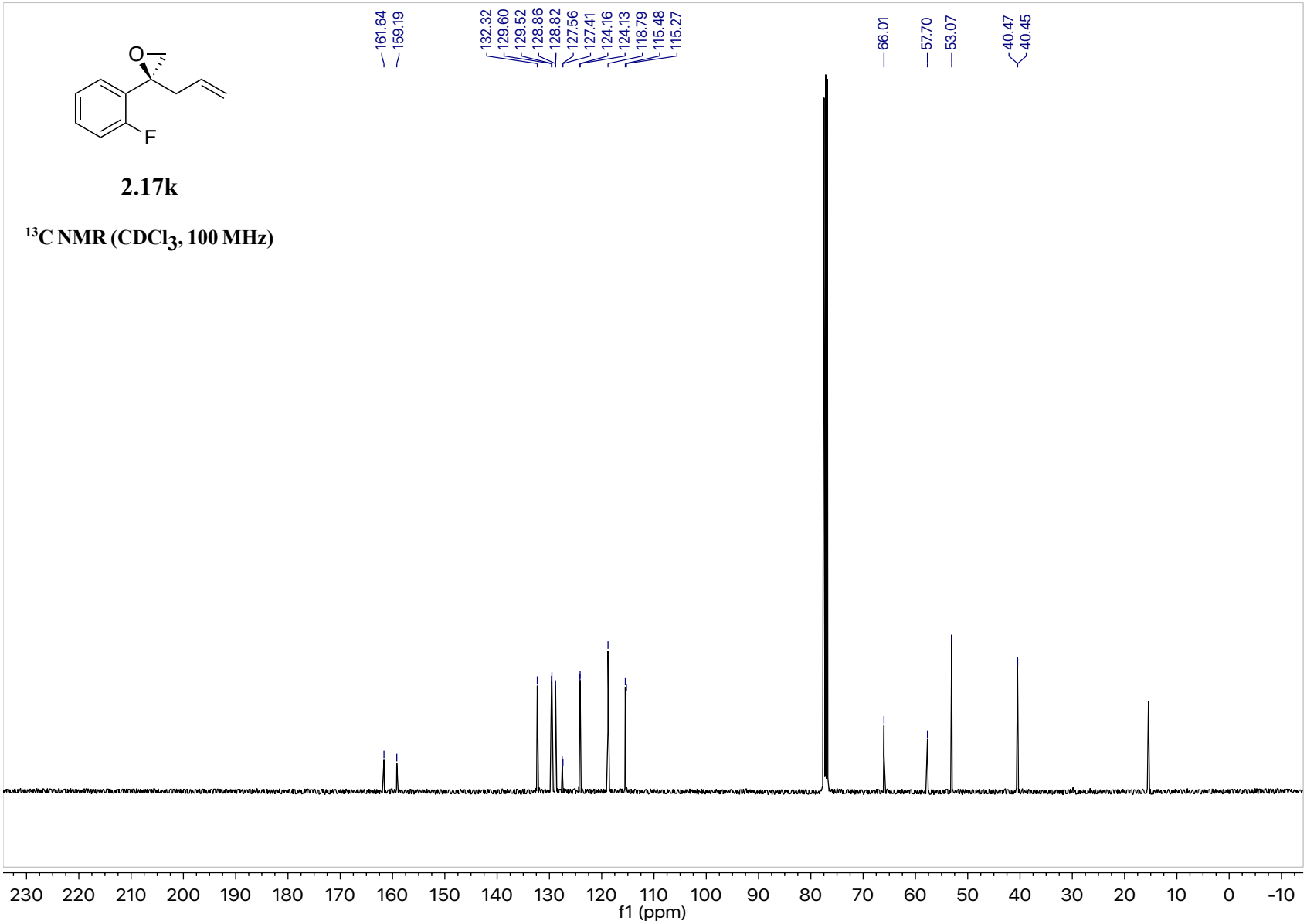

2.17k

^{13}C NMR ($CDCl_3$, 100 MHz)

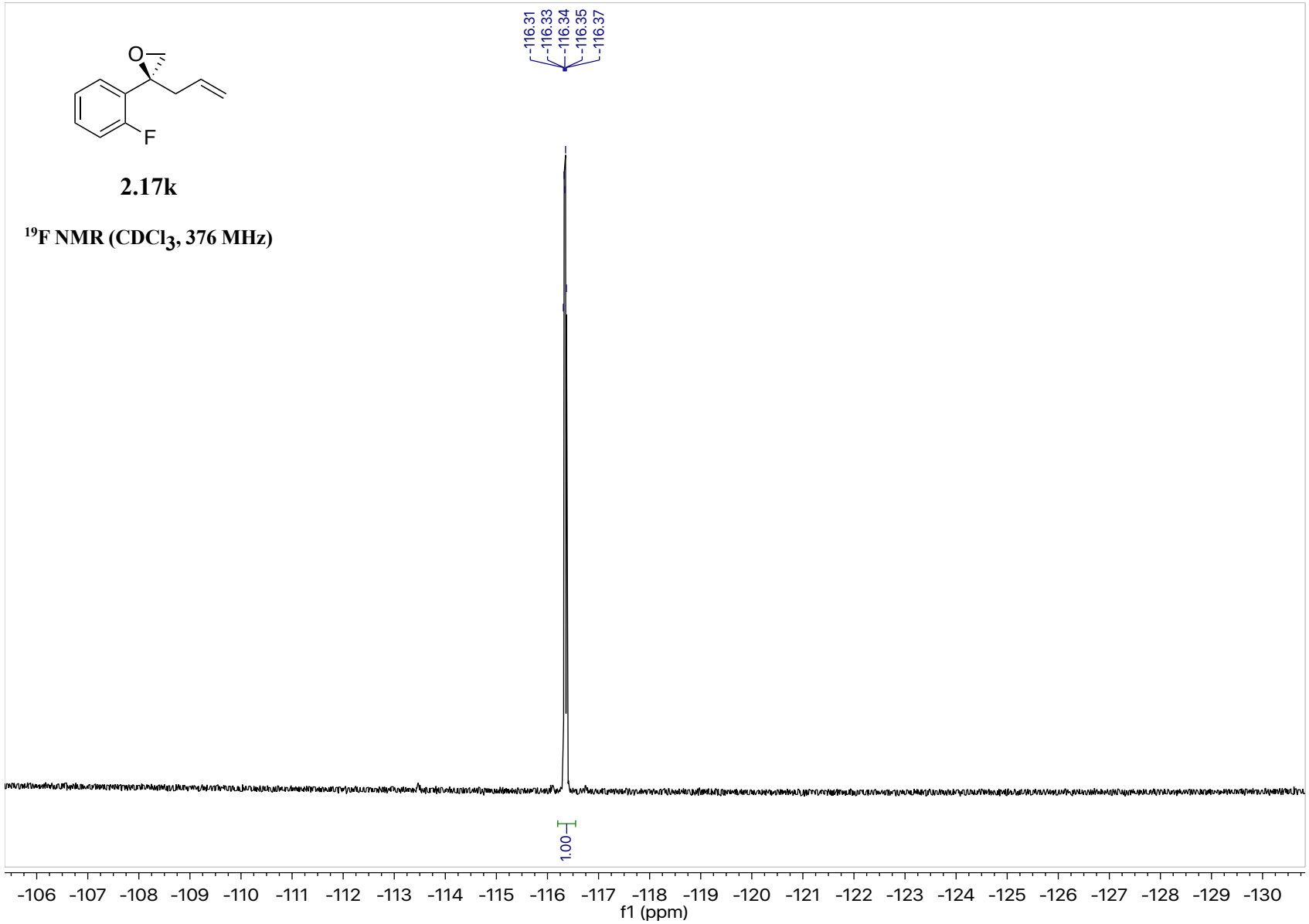

2.17k

^{19}F NMR ($CDCl_3$, 376 MHz)

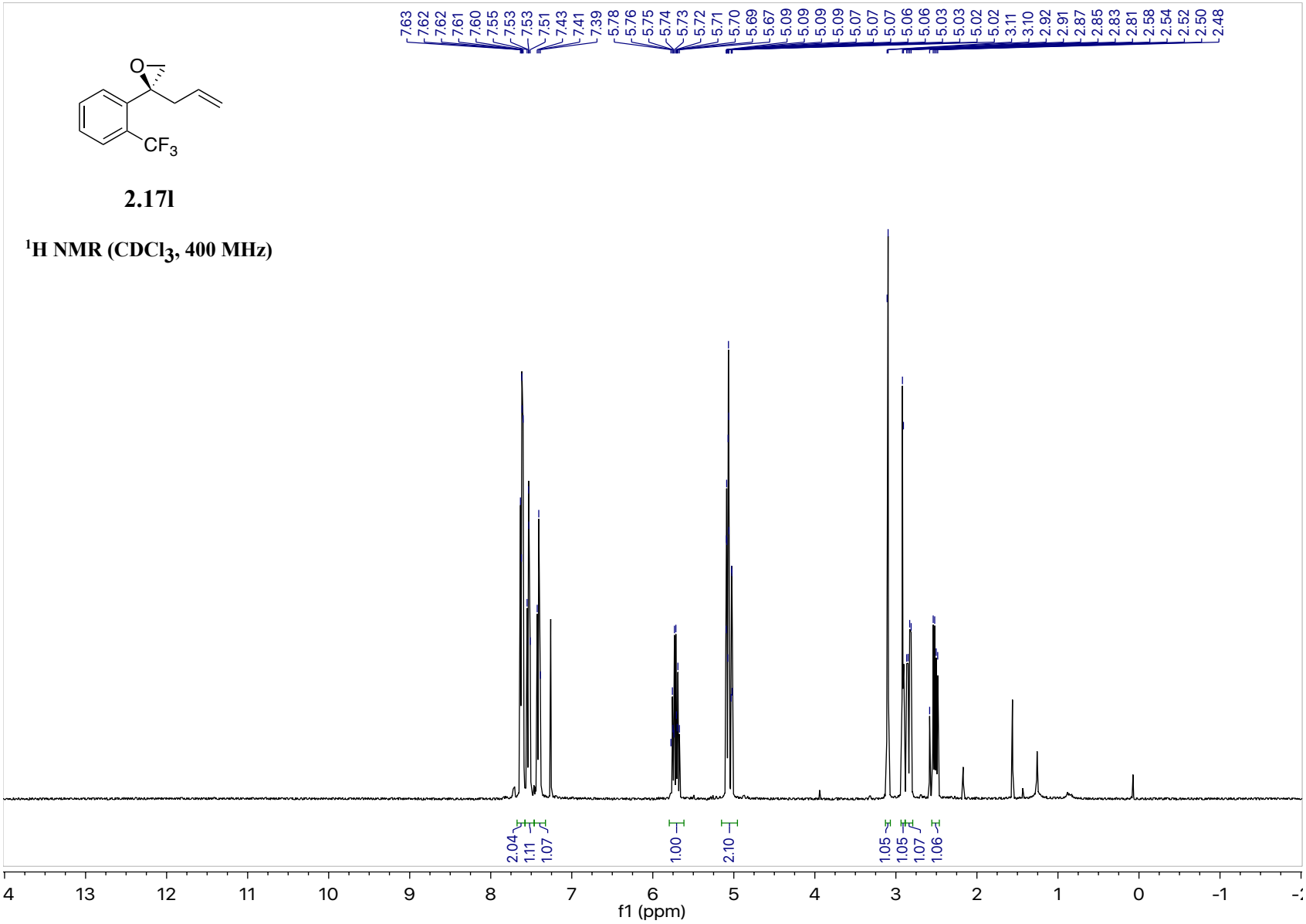
7.63
7.62
7.62
7.61
7.60
7.55
7.53
7.53
7.51
7.43
7.41
7.39
5.78
5.76
5.75
5.74
5.73
5.72
5.71
5.70
5.69
5.67
5.09
5.09
5.09
5.09
5.07
5.07
5.07
5.06
5.06
5.03
5.03
5.02
5.02
3.11
3.10
2.92
2.91
2.87
2.85
2.83
2.81
2.58
2.54
2.52
2.50
2.48
O
CF3
2.17l
1H NMR (CDCl3, 400 MHz)
2.04
1.11
1.07
1.00
2.10
1.05
1.05
1.07
1.06
4
13
12
11
10
9
8
7
6
5
4
3
2
1
0
-1
f1 (ppm)

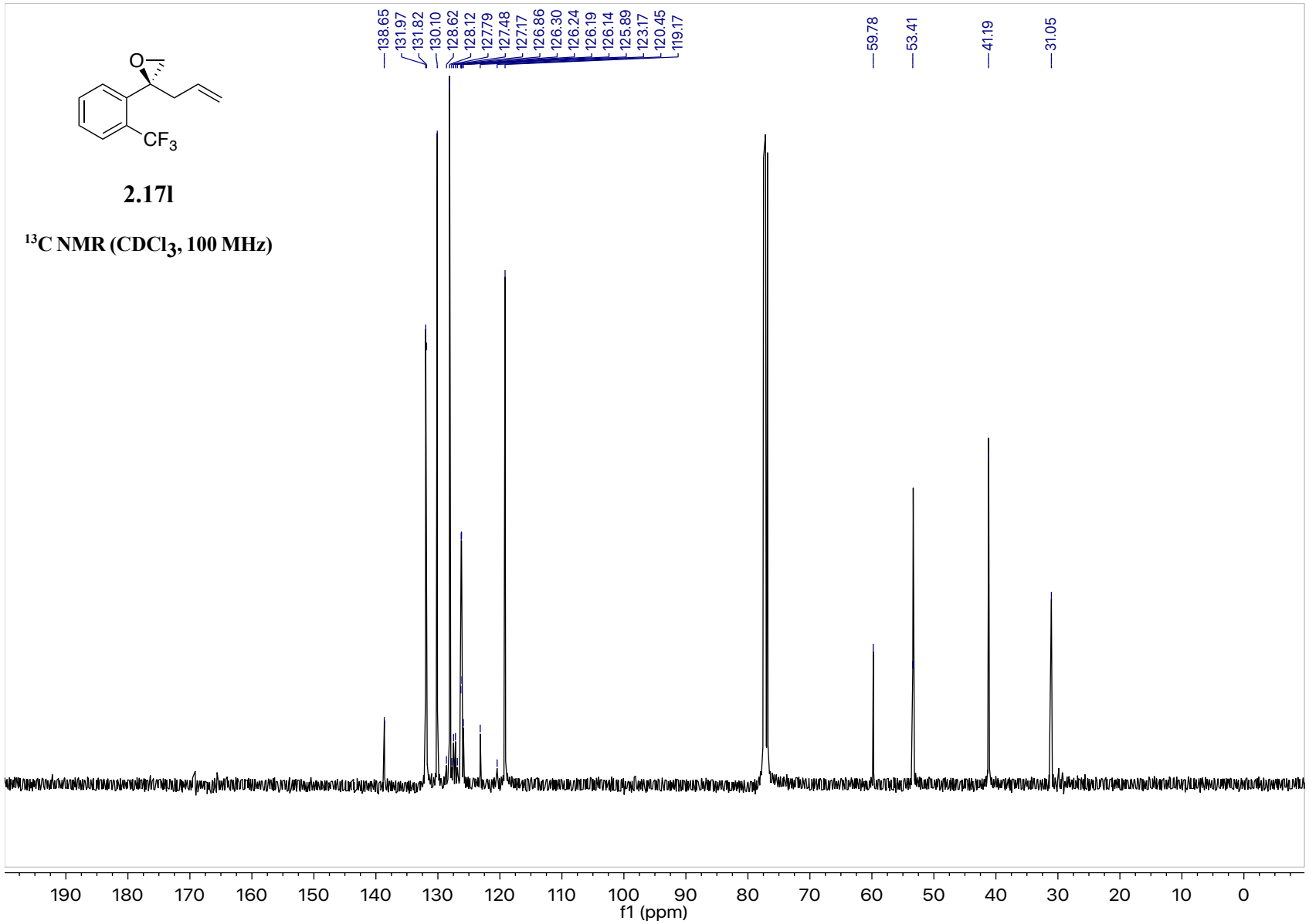

2.17l

^{13}C NMR ($CDCl_3$, 100 MHz)

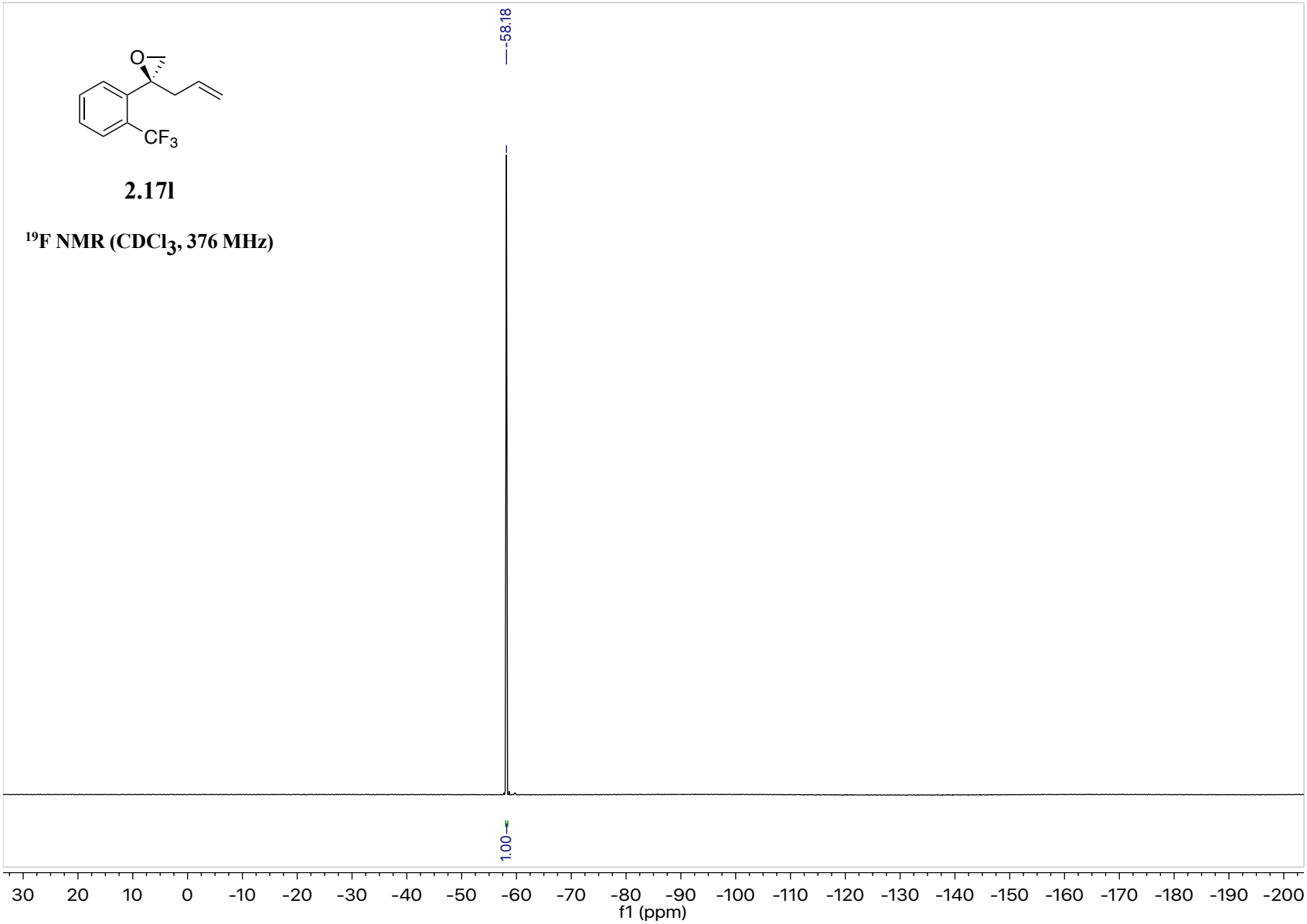
O
CF3
2.17l
19F NMR (CDCl3, 376 MHz)
-58.18
1.00
30 20 10 0 -10 -20 -30 -40 -50 -60 -70 -80 -90 -100 -110 -120 -130 -140 -150 -160 -170 -180 -190 -200
f1 (ppm)

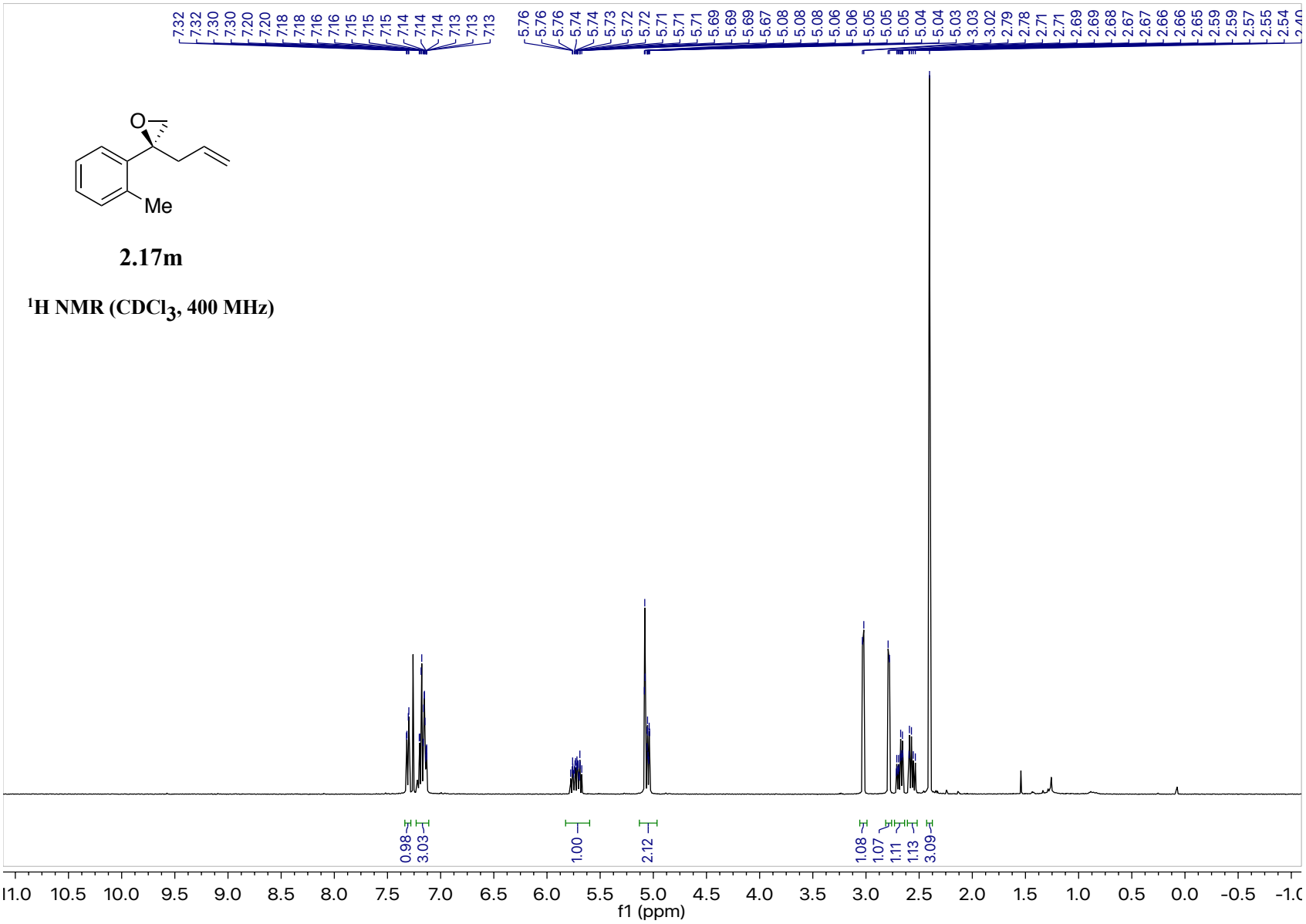

2.17m

^{1}H NMR ($CDCl_3$, 400 MHz)

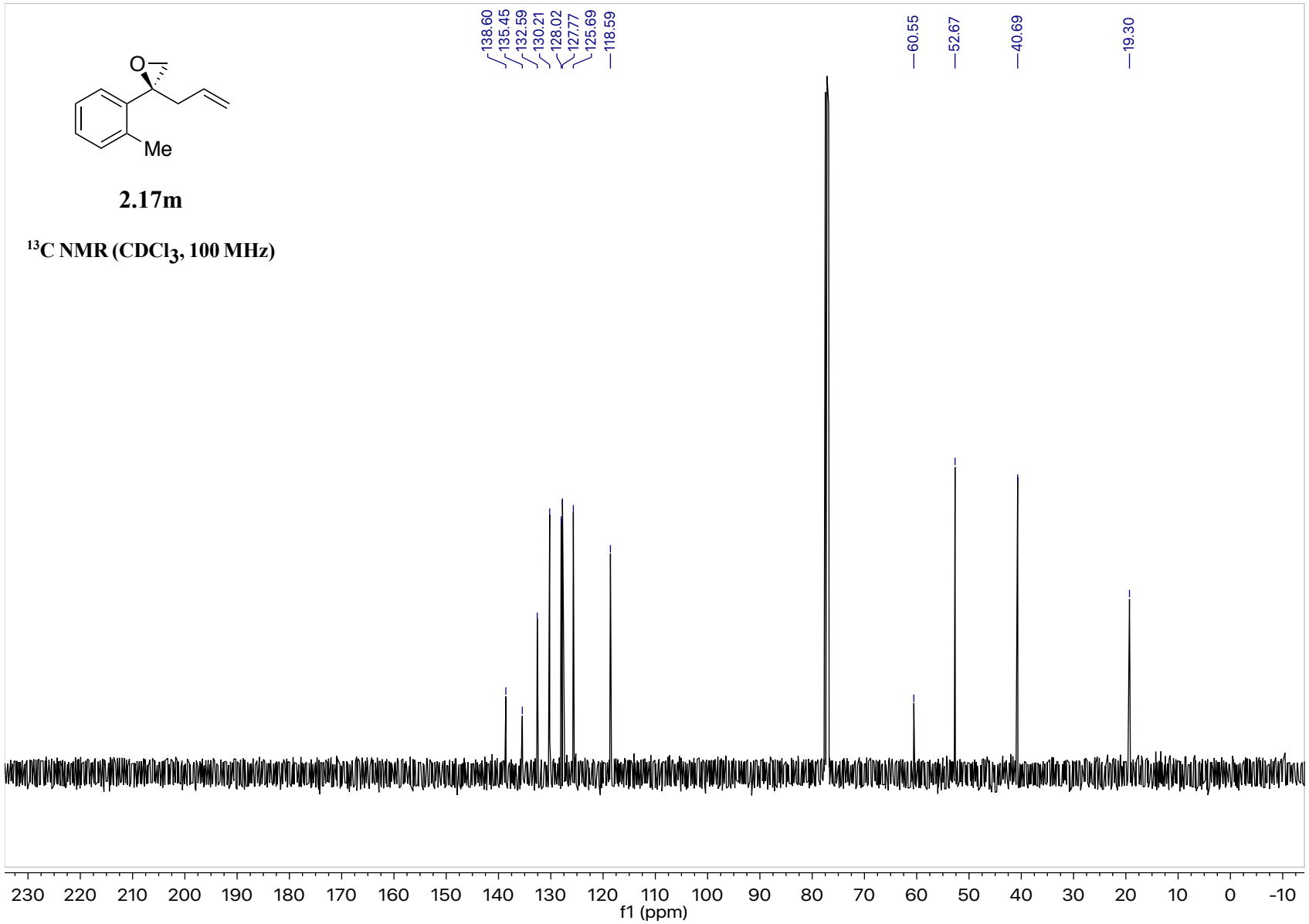

2.17m

^{13}C NMR ($CDCl_3$, 100 MHz)

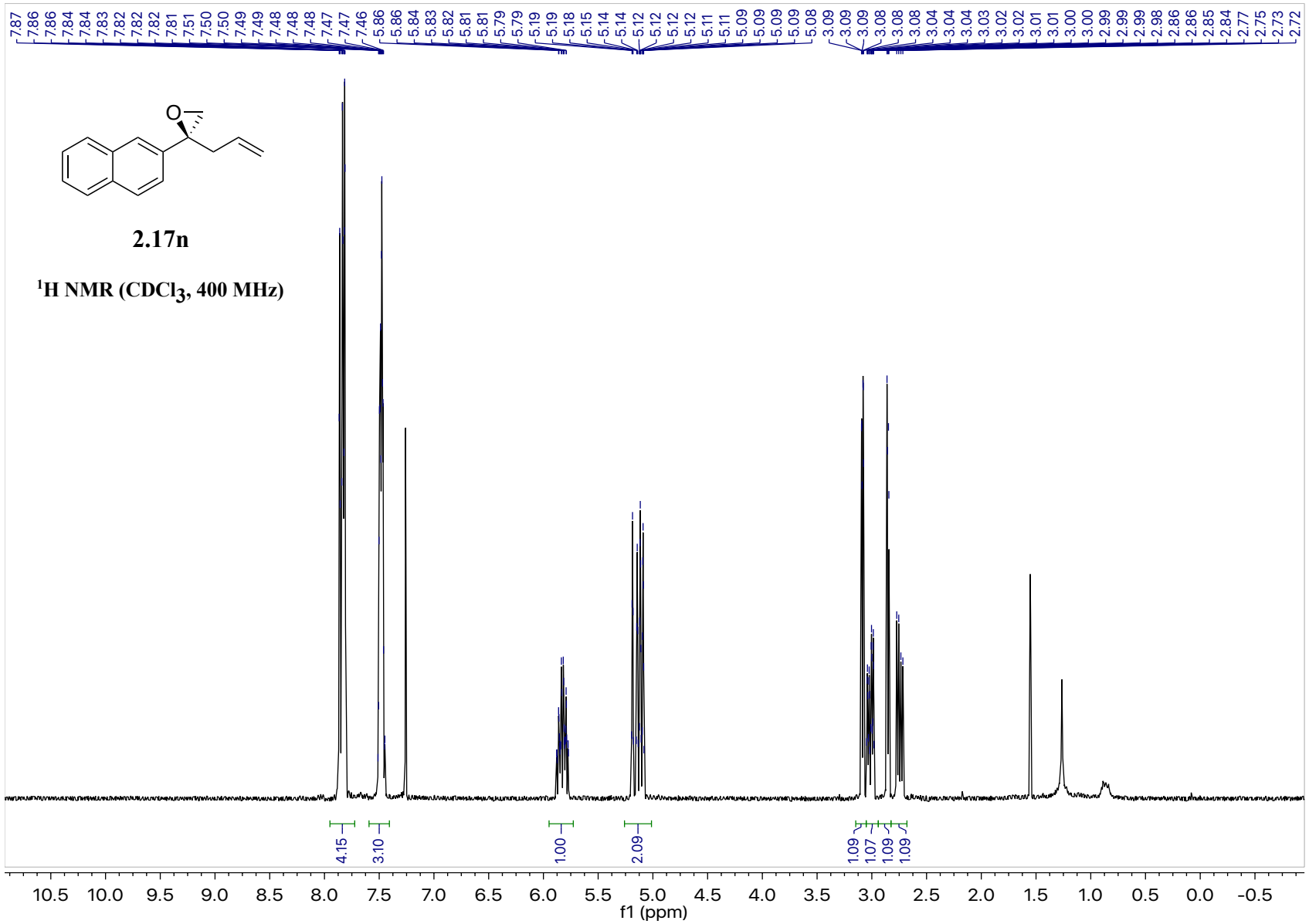
7.87 7.86 7.86 7.84 7.84 7.83 7.82 7.82 7.82 7.81 7.51 7.50 7.50 7.49 7.49 7.48 7.48 7.48 7.47 7.47 7.46 5.86 5.86 5.84 5.83 5.82 5.81 5.81 5.79 5.79 5.19 5.19 5.18 5.15 5.14 5.14 5.12 5.12 5.12 5.12 5.11 5.11 5.09 5.09 5.09 5.09 5.08 3.09 3.09 3.09 3.08 3.08 3.08 3.04 3.04 3.04 3.03 3.02 3.02 3.01 3.01 3.00 3.00 2.99 2.99 2.99 2.98 2.86 2.86 2.85 2.84 2.77 2.75 2.73 2.72
O
2.17n
^{1}H NMR ($CDCl_3$, 400 MHz)
4.15
3.10
1.00
2.09
1.09
1.07
1.09
1.09
10.5 10.0 9.5 9.0 8.5 8.0 7.5 7.0 6.5 6.0 5.5 5.0 4.5 4.0 3.5 3.0 2.5 2.0 1.5 1.0 0.5 0.0 -0.5
f1 (ppm)

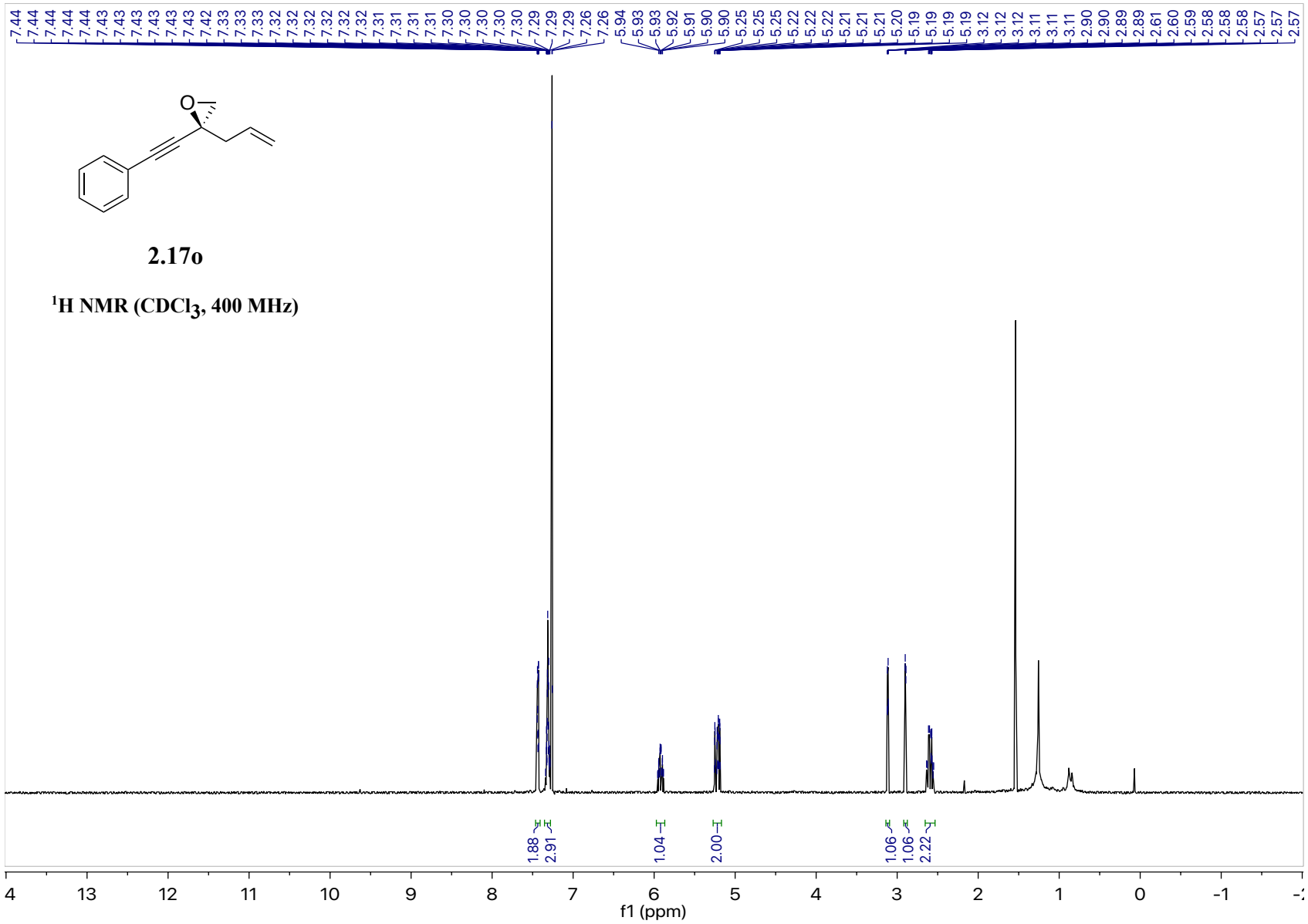
7.44 7.44 7.44 7.44 7.44 7.43 7.43 7.43 7.43 7.43 7.42 7.33 7.33 7.32 7.32 7.32 7.32 7.32 7.31 7.31 7.31 7.30 7.30 7.30 7.30 7.29 7.29 7.26 7.26
5.94 5.93 5.93 5.92 5.91 5.90 5.90 5.25 5.25 5.22 5.22 5.21 5.21 5.21 5.20 5.19 5.19 5.19 3.12 3.12 3.11 3.11 3.11 2.90 2.90 2.89 2.89 2.61 2.60 2.59 2.58 2.58 2.58 2.57 2.57 2.57
O
2.17o
1H NMR (CDCl3, 400 MHz)
1.88
2.91
1.04
2.00
1.06
1.06
2.22
4 13 12 11 10 9 8 7 6 5 4 3 2 1 0 -1
f1 (ppm)

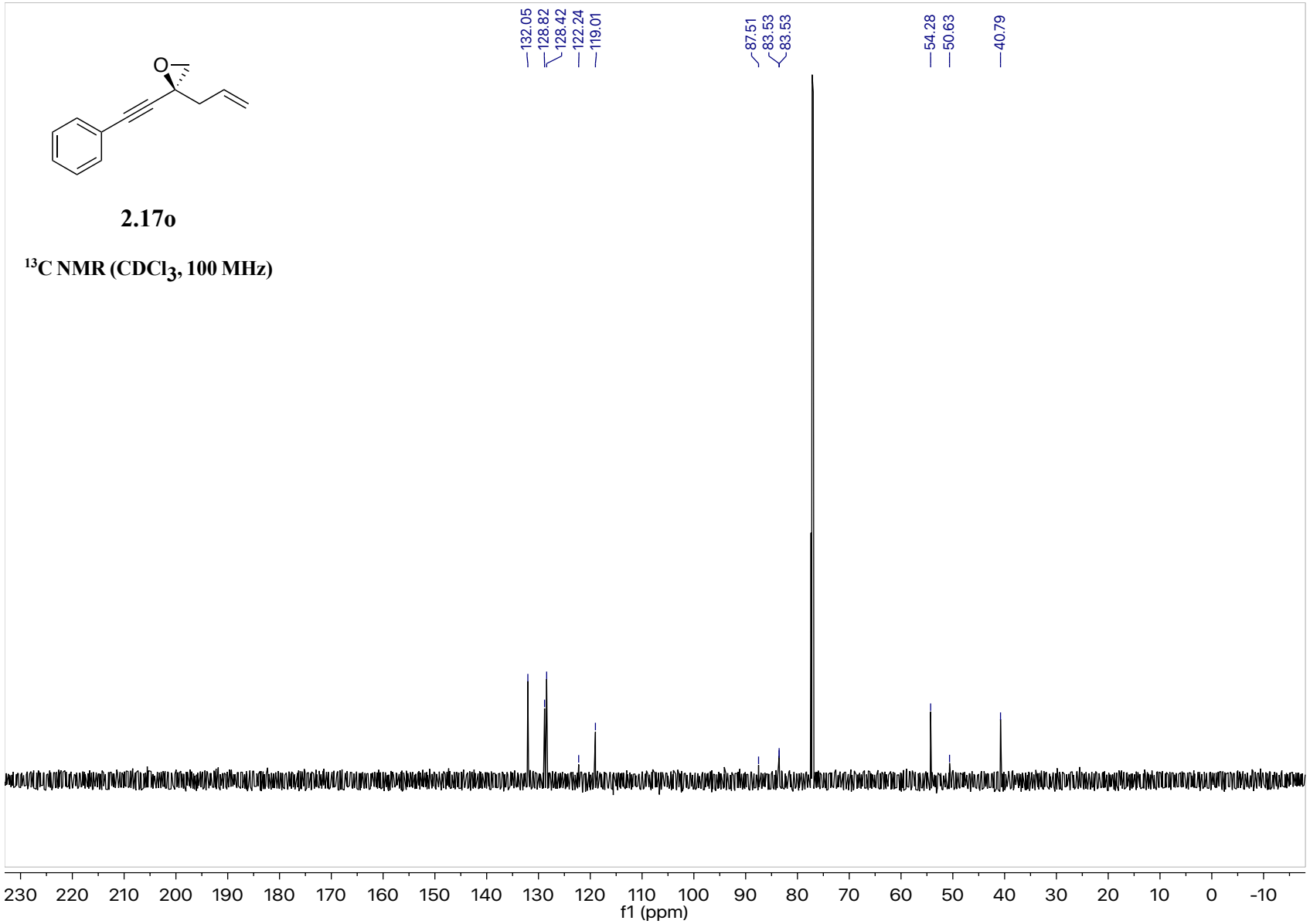

2.17o

^{13}C NMR ($CDCl_3$, 100 MHz)

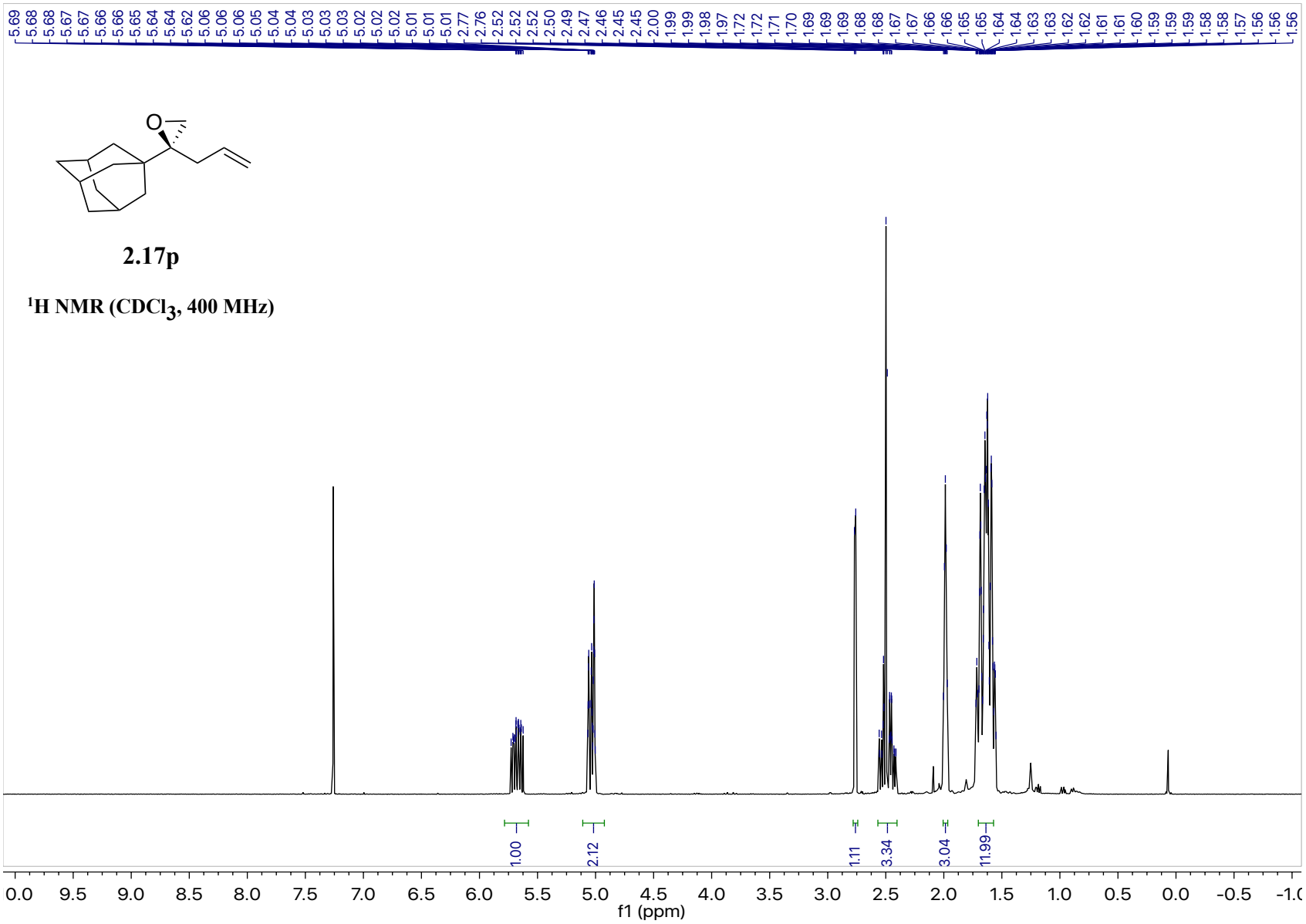
5.69 5.68 5.68 5.67 5.67 5.66 5.66 5.65 5.64 5.64 5.62 5.06 5.06 5.06 5.05 5.04 5.04 5.03 5.03 5.03 5.02 5.02 5.02 5.01 5.01 5.01 2.77 2.76 2.52 2.52 2.52 2.50 2.49 2.47 2.46 2.45 2.45 2.00 1.99 1.99 1.98 1.97 1.72 1.72 1.71 1.70 1.69 1.69 1.69 1.68 1.68 1.67 1.67 1.66 1.66 1.65 1.65 1.64 1.64 1.63 1.63 1.62 1.62 1.61 1.61 1.60 1.59 1.59 1.59 1.58 1.58 1.57 1.56 1.56 1.56
O
2.17p
^{1}H NMR (CDCl$_3$, 400 MHz)
1.00
2.12
1.11
3.34
3.04
11.99
0.0 9.5 9.0 8.5 8.0 7.5 7.0 6.5 6.0 5.5 5.0 4.5 4.0 3.5 3.0 2.5 2.0 1.5 1.0 0.5 0.0 -0.5 -1.0
f1 (ppm)

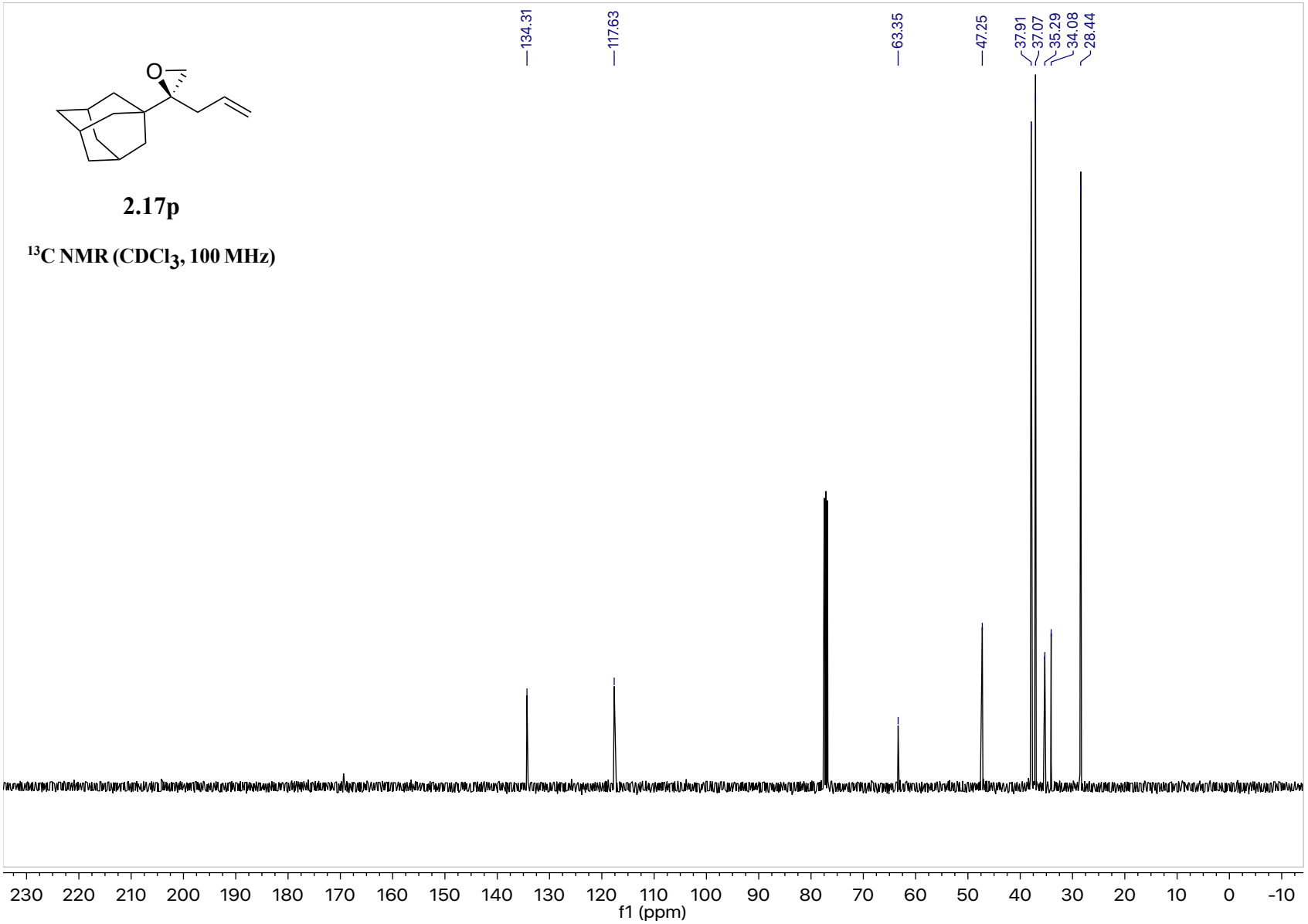
134.31
117.63
63.35
47.25
37.91
37.07
35.29
34.08
28.44
O
2.17p
13C NMR (CDCl3, 100 MHz)
230 220 210 200 190 180 170 160 150 140 130 120 110 100 90 80 70 60 50 40 30 20 10 0 -10
f1 (ppm)

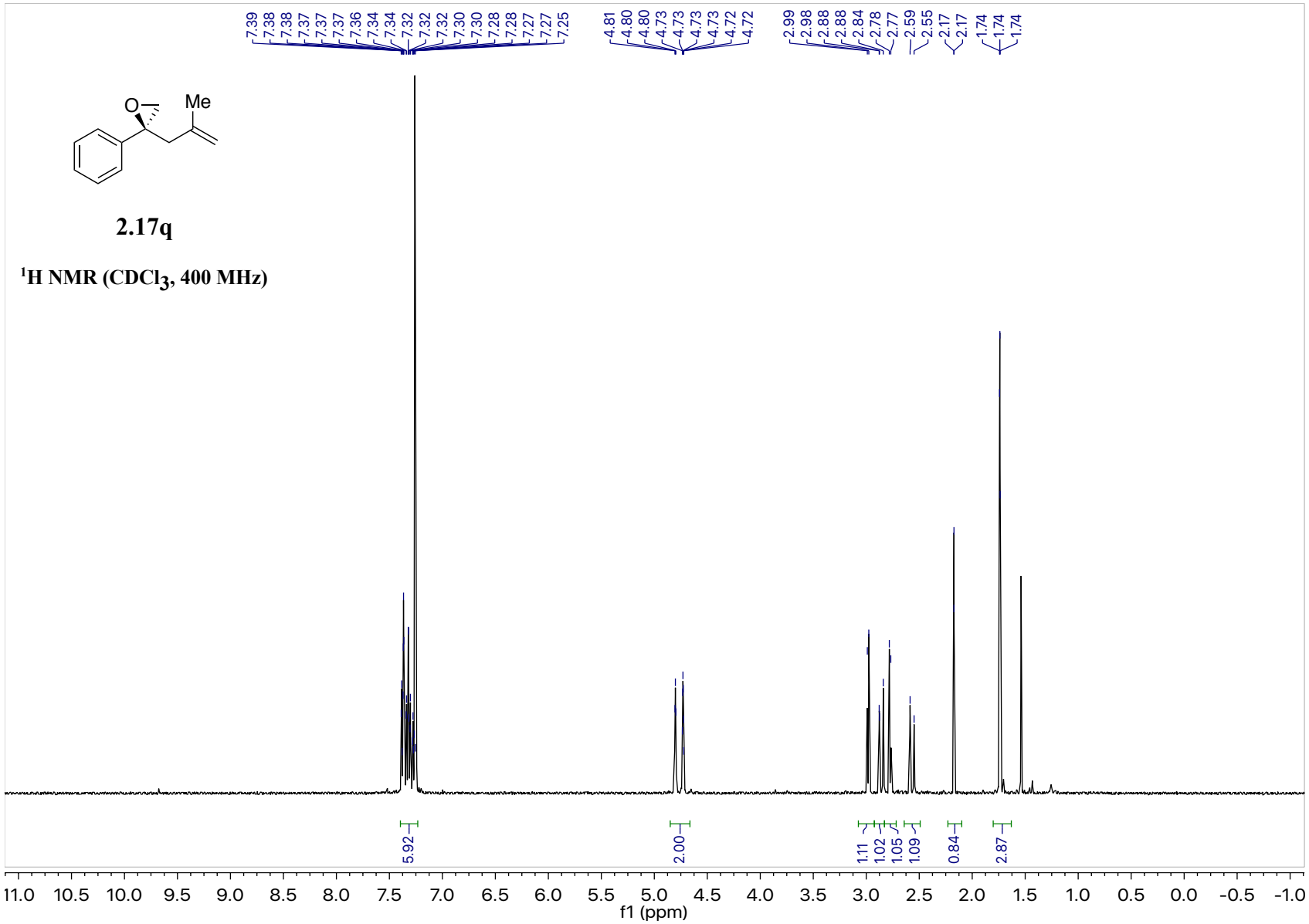
7.39
7.38
7.38
7.37
7.37
7.37
7.36
7.34
7.34
7.32
7.32
7.32
7.30
7.30
7.28
7.28
7.27
7.27
7.25
4.81
4.80
4.80
4.73
4.73
4.73
4.72
4.72
2.99
2.98
2.88
2.88
2.84
2.78
2.77
2.59
2.55
2.17
2.17
1.74
1.74
1.74
O
Me
2.17q
1H NMR (CDCl3, 400 MHz)
5.92
2.00
1.11
1.02
1.05
1.09
0.84
2.87
11.0 10.5 10.0 9.5 9.0 8.5 8.0 7.5 7.0 6.5 6.0 5.5 5.0 4.5 4.0 3.5 3.0 2.5 2.0 1.5 1.0 0.5 0.0 -0.5 -1.0
f1 (ppm)

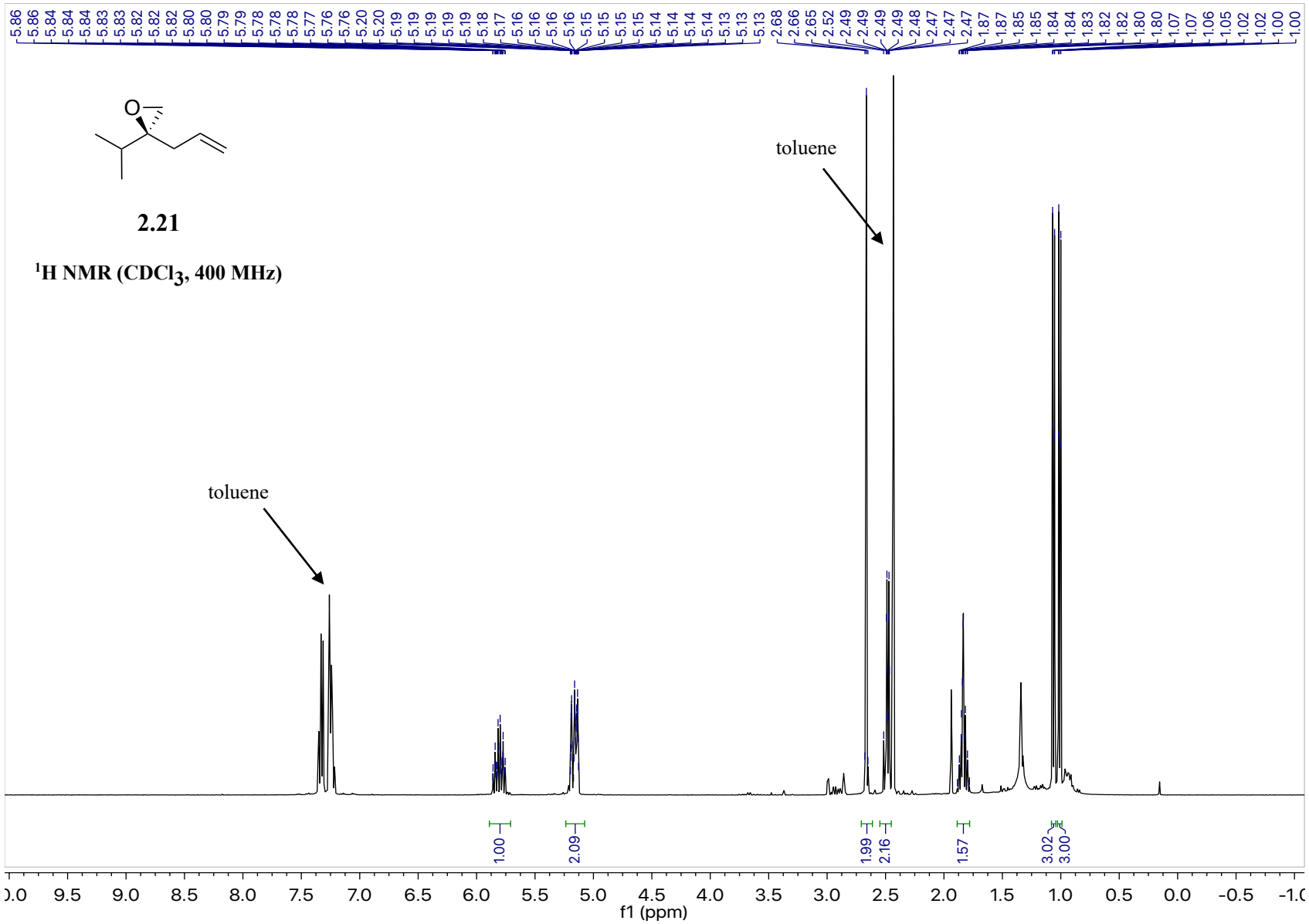
toluene
toluene
2.21
1H NMR (CDCl3, 400 MHz)
1.00
2.09
1.99
2.16
1.57
3.02
3.00
f1 (ppm)

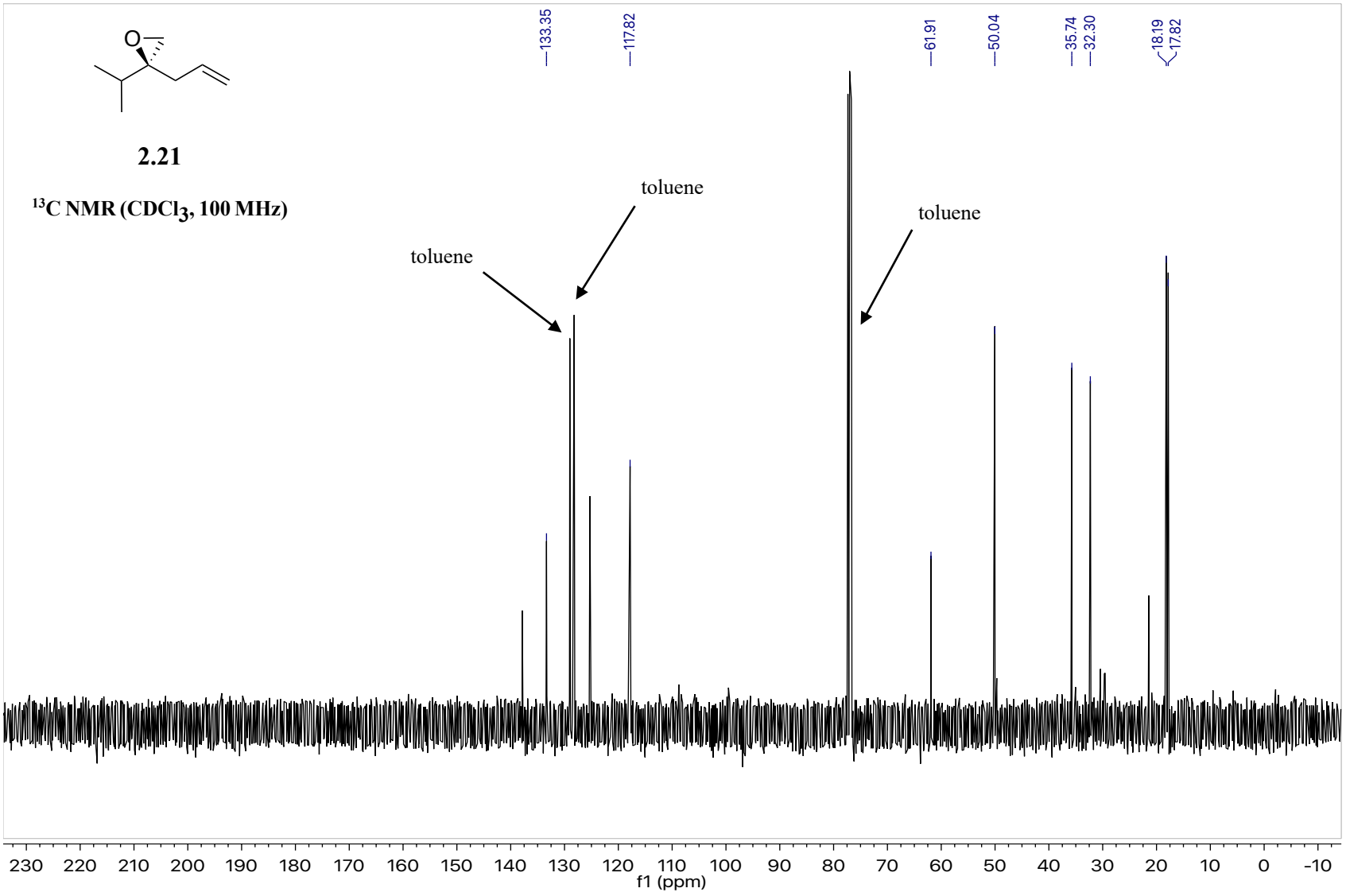
2.21
^{13}C NMR ($CDCl_3$, 100 MHz)
133.35
117.82
61.91
50.04
35.74
32.30
18.19
17.82
toluene
toluene
toluene
230 220 210 200 190 180 170 160 150 140 130 120 110 100 90 80 70 60 50 40 30 20 10 0 -10
f1 (ppm)

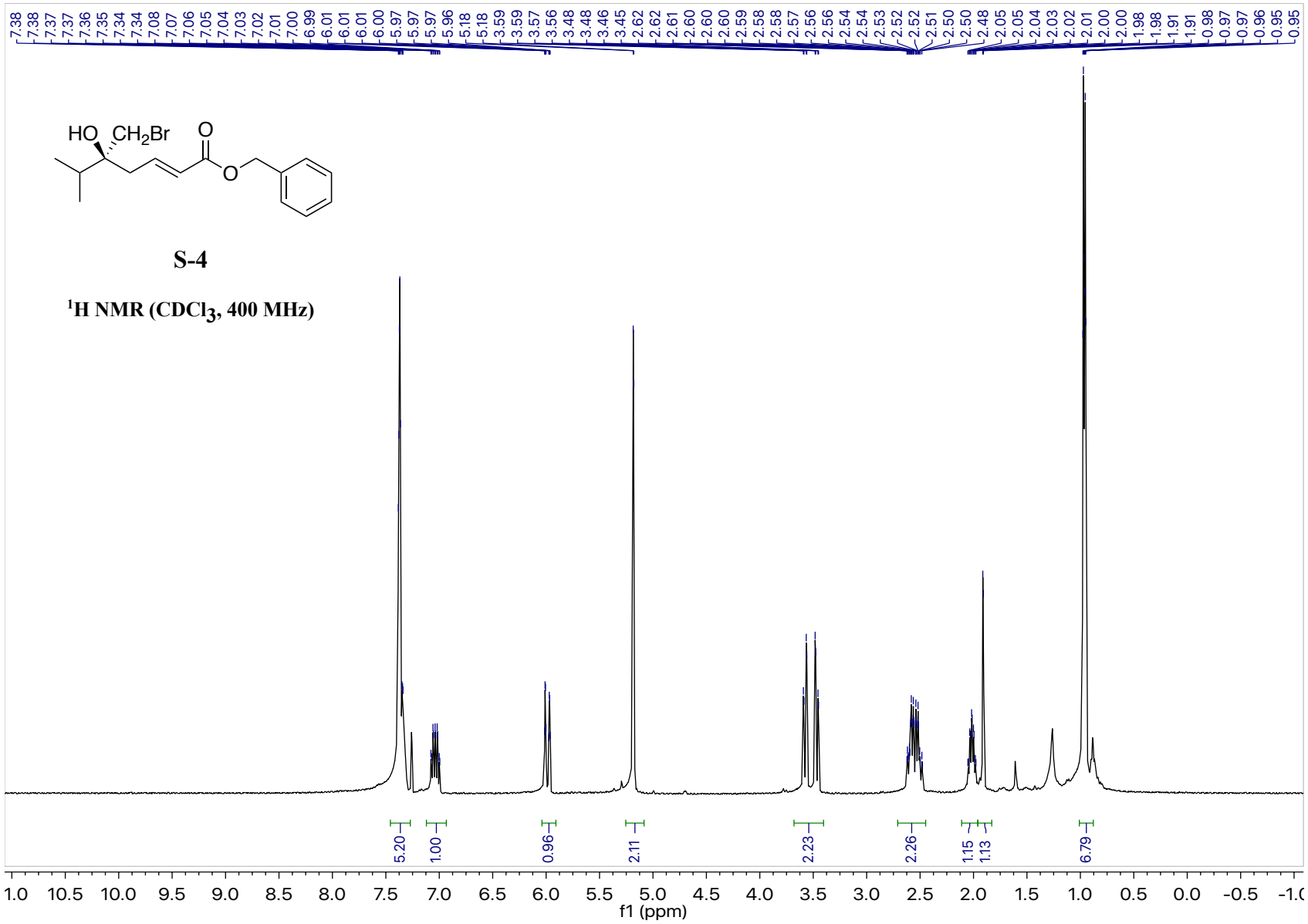
HO
CH2Br
O
O
S-4
1H NMR (CDCl3, 400 MHz)
5.20
1.00
0.96
2.11
2.23
2.26
1.15
1.13
6.79
f1 (ppm)

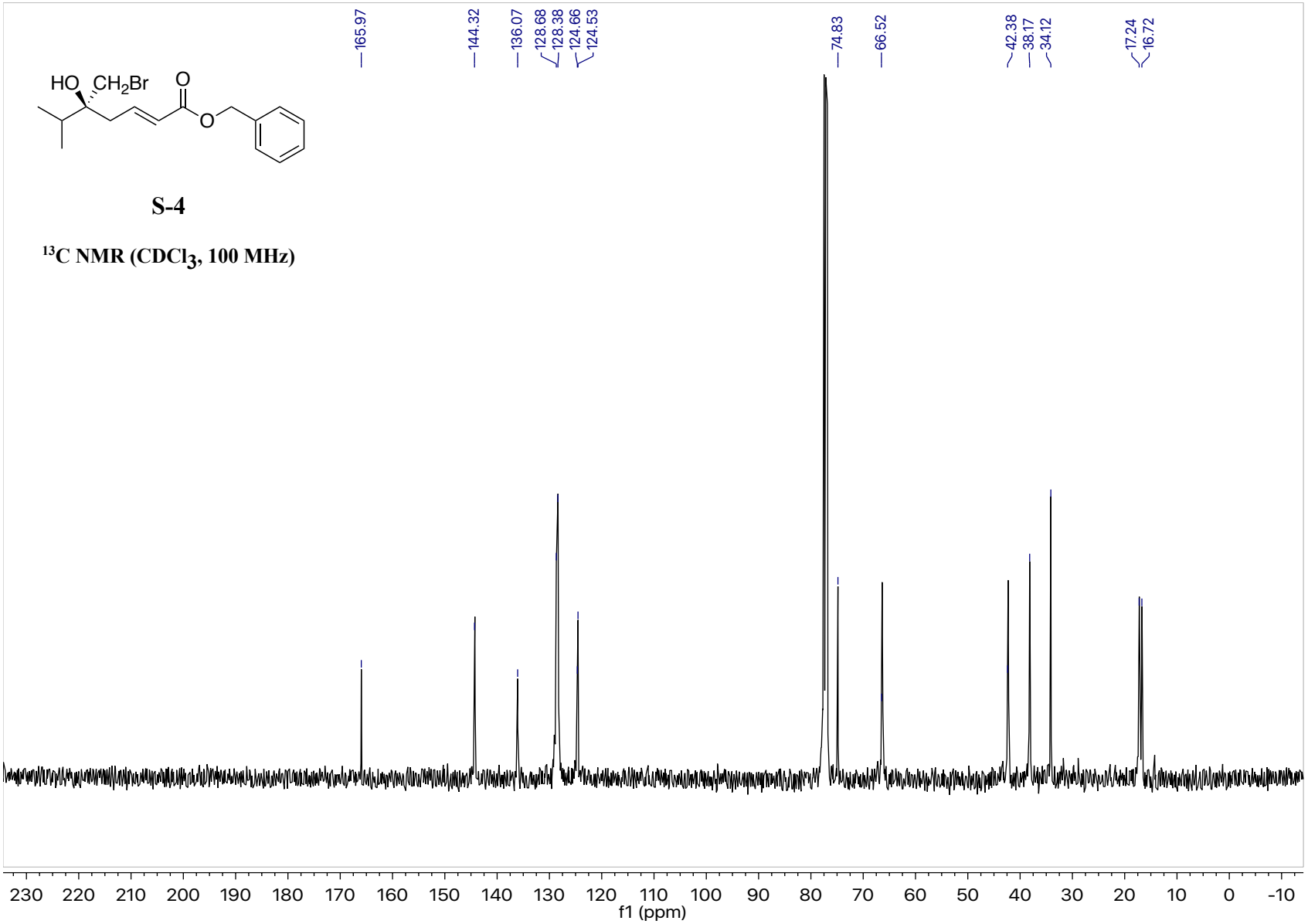

S-4

^{13}C NMR ($CDCl_3$, 100 MHz)

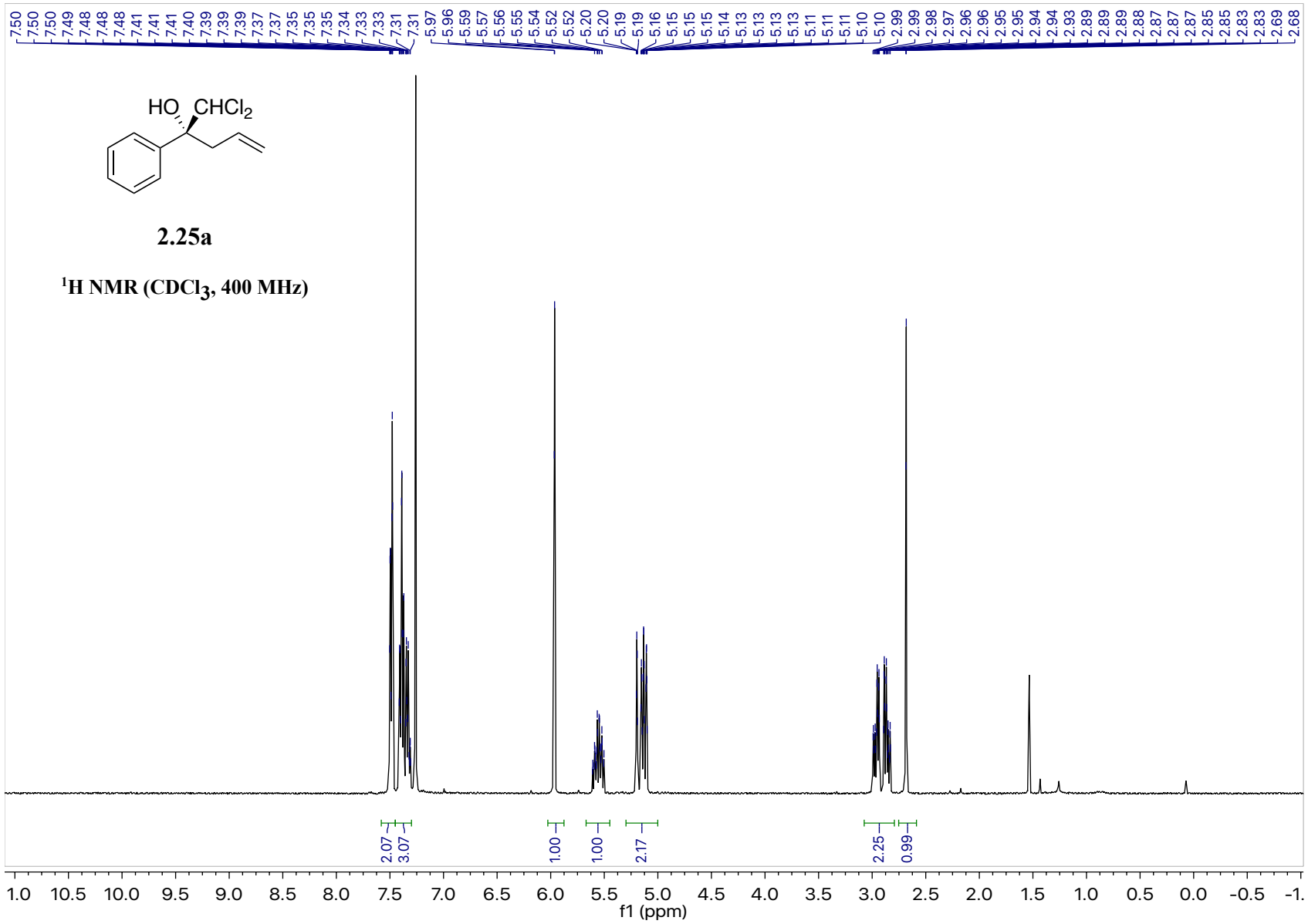
HO
CHCl2
2.25a
1H NMR (CDCl3, 400 MHz)
2.07
3.07
1.00
1.00
2.17
2.25
0.99
f1 (ppm)

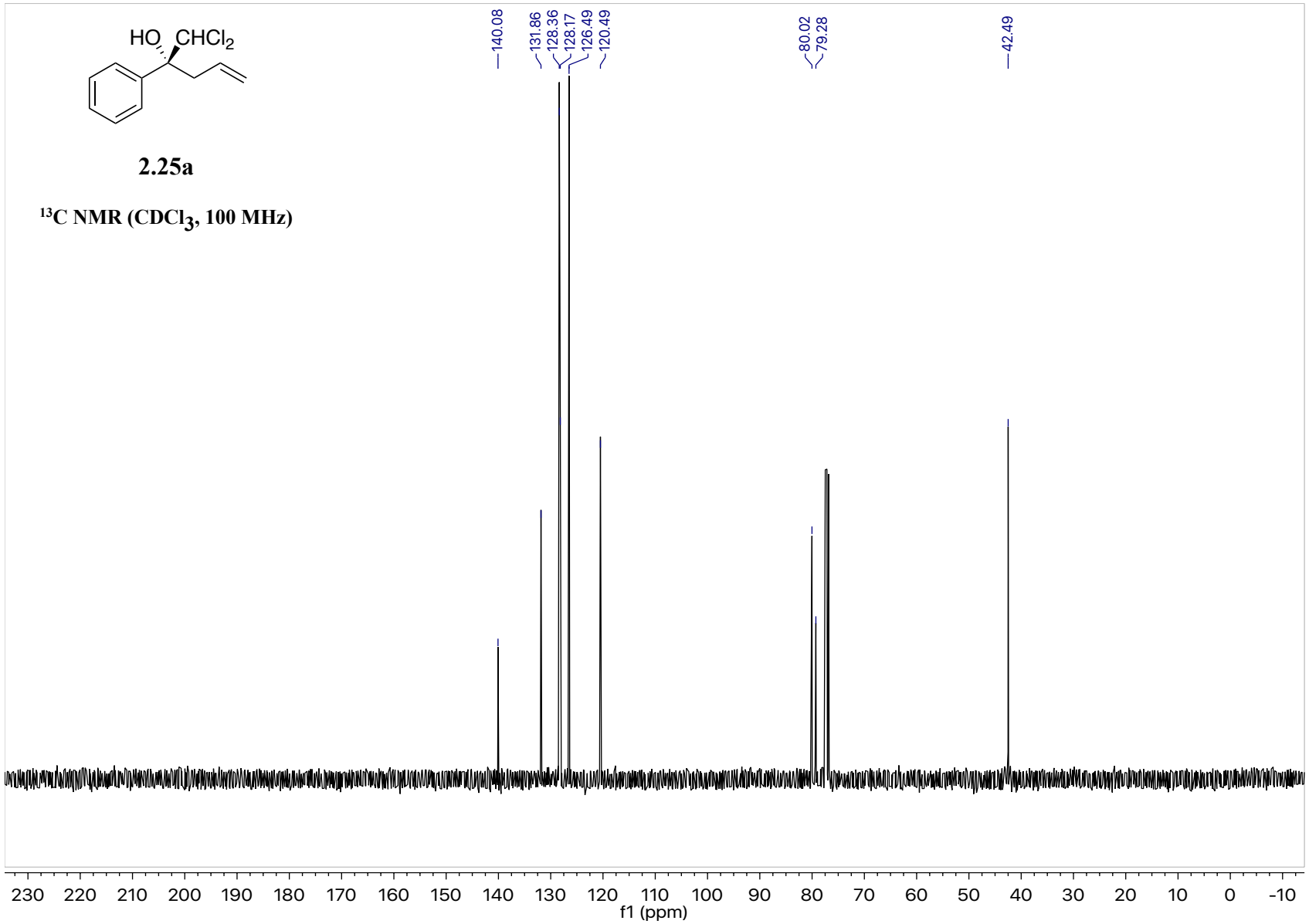

2.25a

^{13}C NMR ($CDCl_3$, 100 MHz)

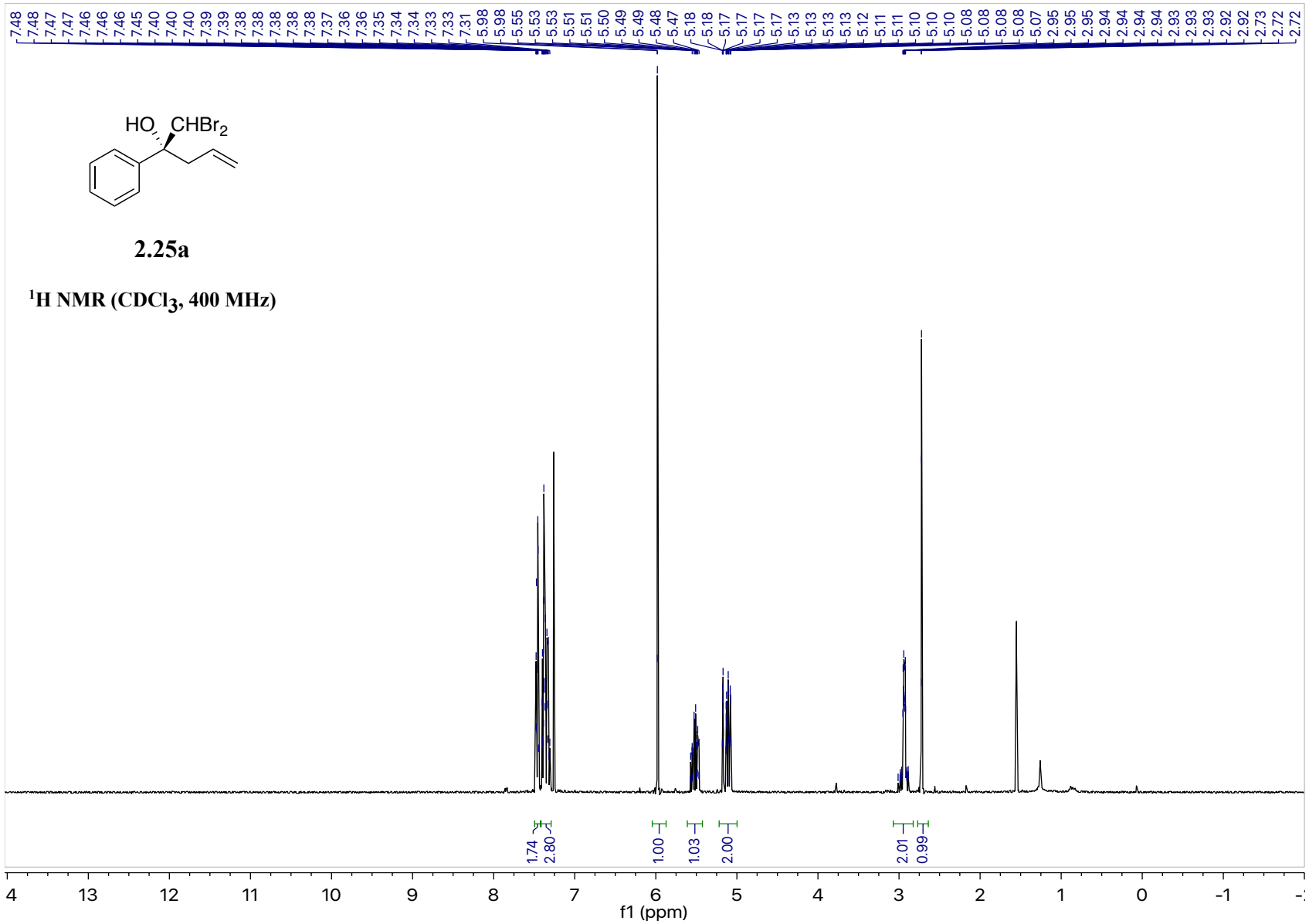
HO
CHBr2
2.25a
1H NMR (CDCl3, 400 MHz)
1.74
2.80
1.00
1.03
2.00
2.01
0.99
f1 (ppm)

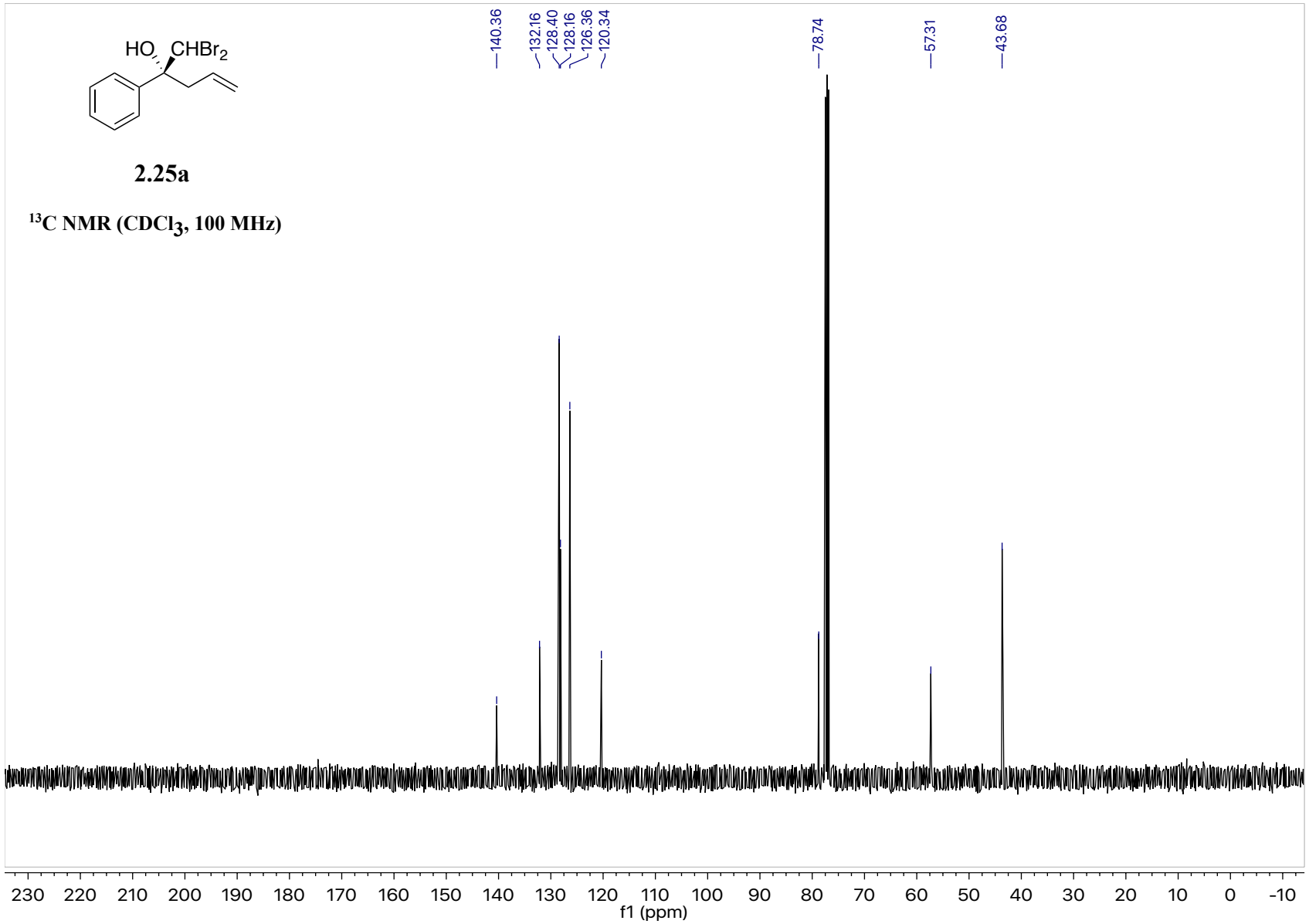

2.25a

^{13}C NMR ($CDCl_3$, 100 MHz)

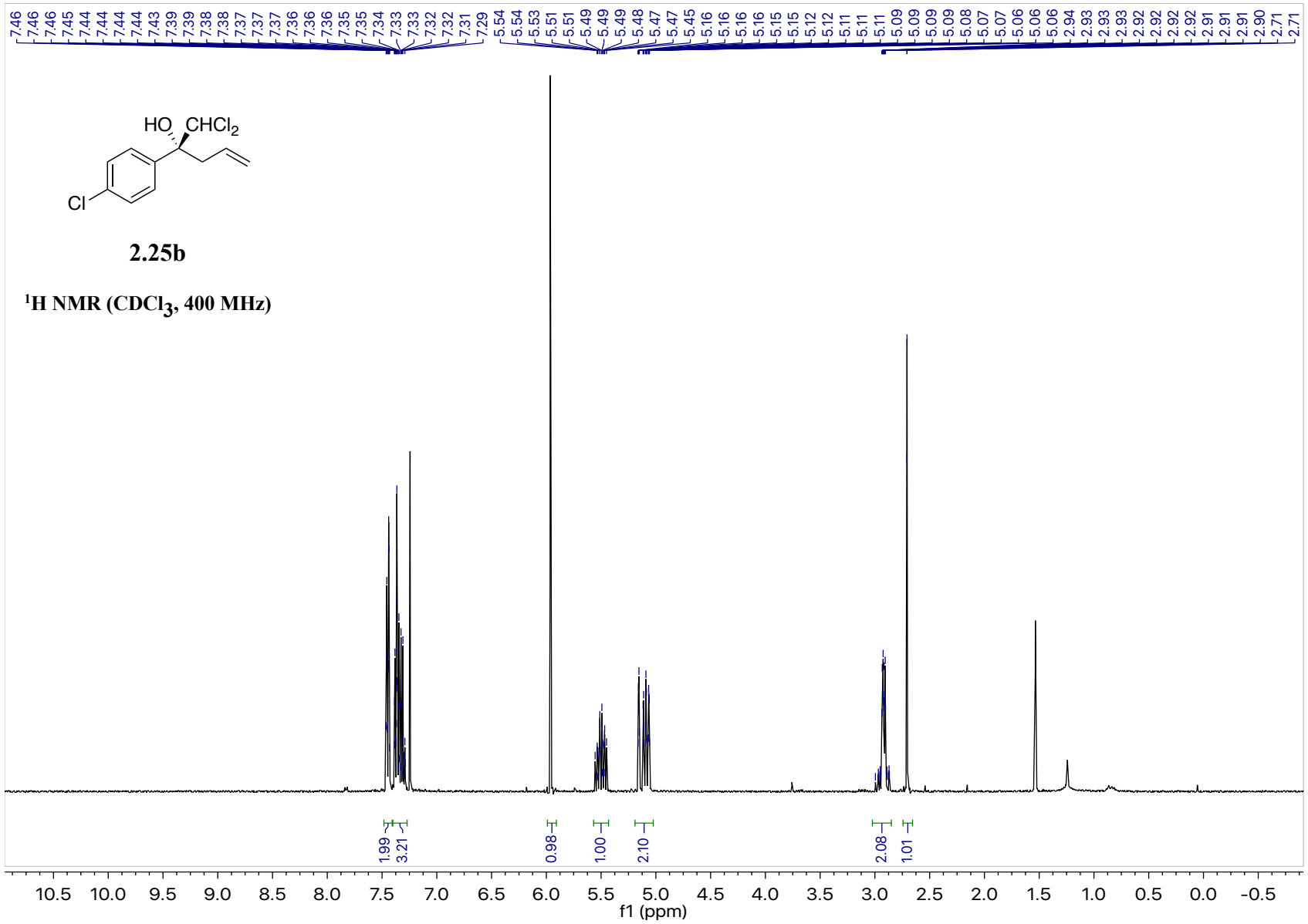
HO
CHCl2
Cl
2.25b
1H NMR (CDCl3, 400 MHz)
f1 (ppm)

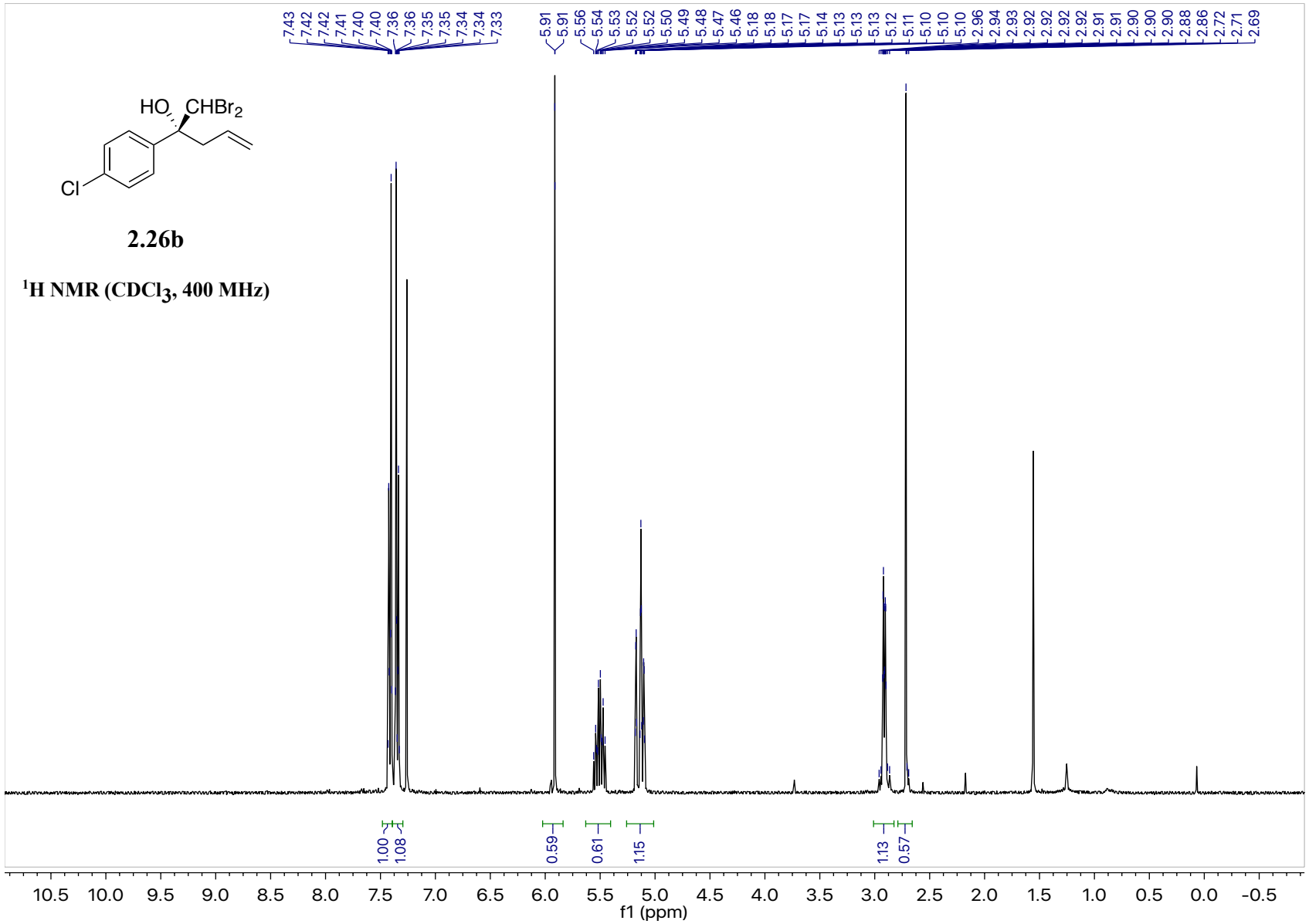
HO
CHBr2
Cl
2.26b
1H NMR (CDCl3, 400 MHz)
7.43 7.42 7.42 7.41 7.40 7.40 7.36 7.36 7.35 7.35 7.34 7.34 7.33
5.91 5.91 5.56 5.54 5.53 5.52 5.52 5.50 5.49 5.48 5.47 5.46 5.18 5.18 5.17 5.17 5.14 5.13 5.13 5.13 5.12 5.11 5.10 5.10 5.10 2.96 2.94 2.93 2.92 2.92 2.92 2.92 2.91 2.91 2.90 2.90 2.90 2.88 2.86 2.72 2.71 2.69
1.00
1.08
0.59
0.61
1.15
1.13
0.57
10.5 10.0 9.5 9.0 8.5 8.0 7.5 7.0 6.5 6.0 5.5 5.0 4.5 4.0 3.5 3.0 2.5 2.0 1.5 1.0 0.5 0.0 -0.5
f1 (ppm)

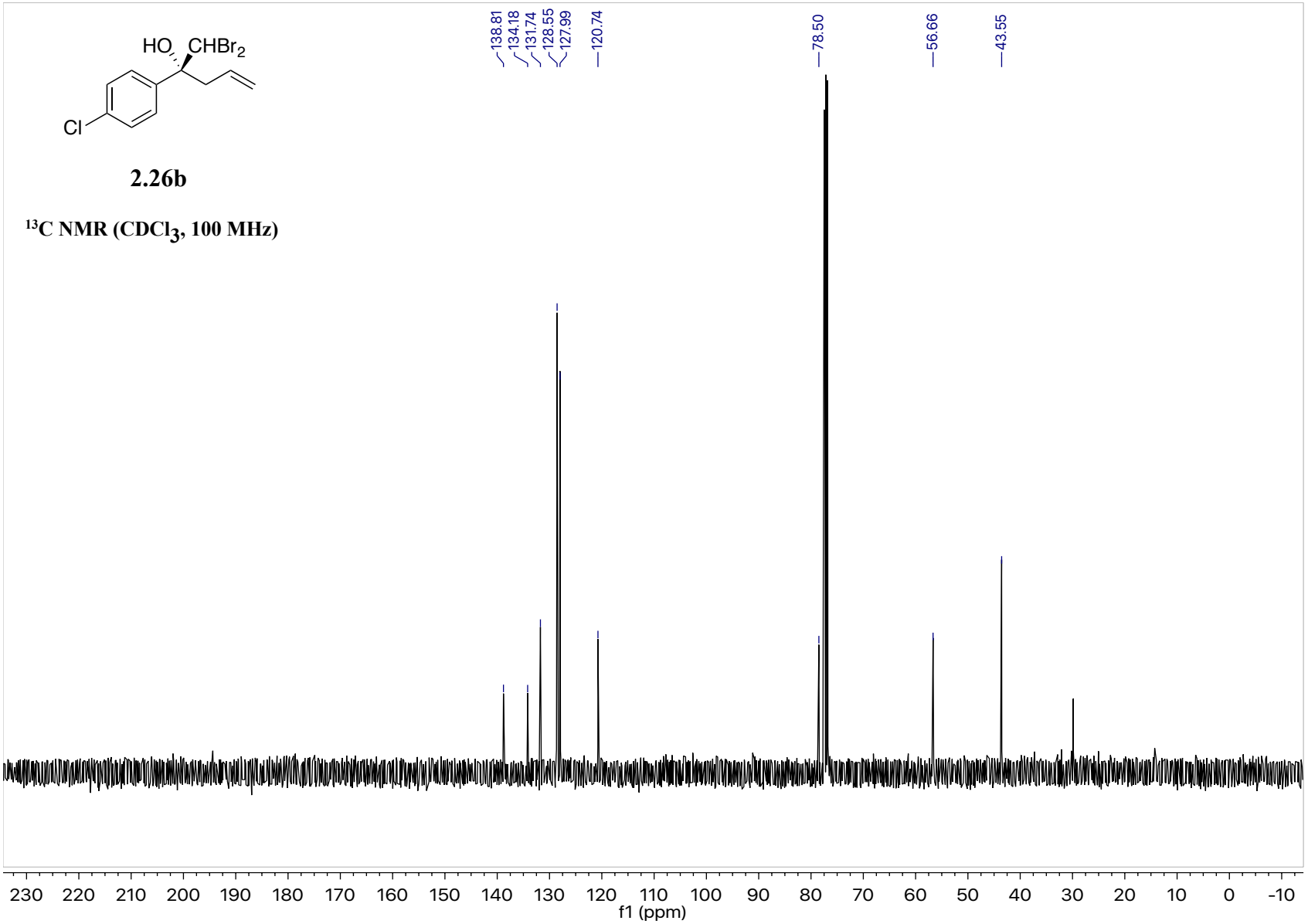
HO
CHBr2
Cl
2.26b
13C NMR (CDCl3, 100 MHz)
138.81
134.18
131.74
128.55
127.99
120.74
78.50
56.66
43.55
230 220 210 200 190 180 170 160 150 140 130 120 110 100 90 80 70 60 50 40 30 20 10 0 -10
f1 (ppm)

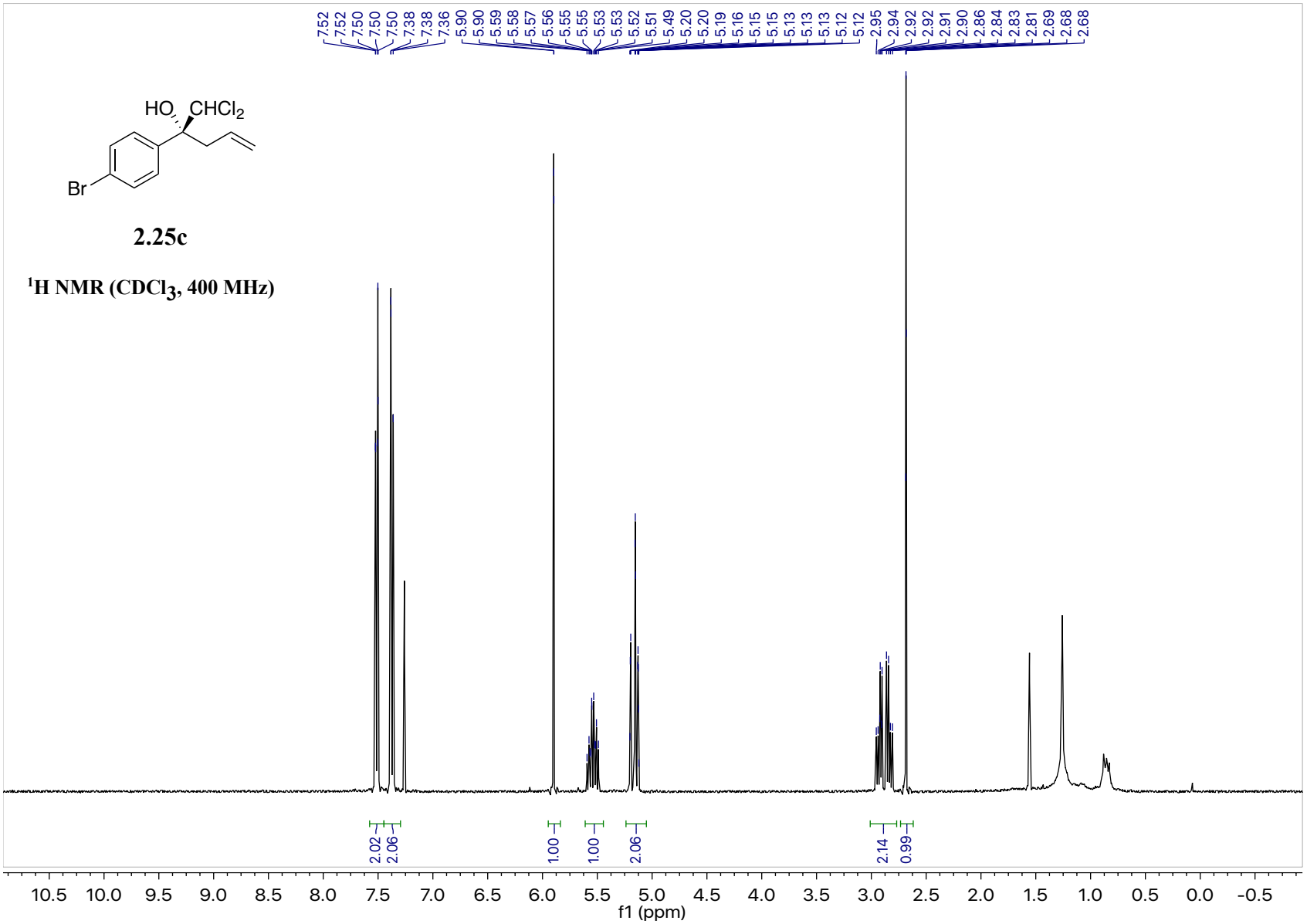
HO
CHCl2
Br
2.25c
1H NMR (CDCl3, 400 MHz)
7.52 7.52 7.50 7.50 7.50 7.38 7.38 7.36
5.90 5.90 5.59 5.58 5.57 5.56 5.55 5.55 5.53 5.53 5.52 5.51 5.49 5.20 5.20 5.19 5.16 5.15 5.15 5.13 5.13 5.13 5.12 5.12
2.95 2.94 2.92 2.92 2.91 2.90 2.86 2.84 2.83 2.81 2.69 2.68 2.68
2.02 2.06 1.00 1.00 2.06 2.14 0.99
10.5 10.0 9.5 9.0 8.5 8.0 7.5 7.0 6.5 6.0 5.5 5.0 4.5 4.0 3.5 3.0 2.5 2.0 1.5 1.0 0.5 0.0 -0.5
f1 (ppm)

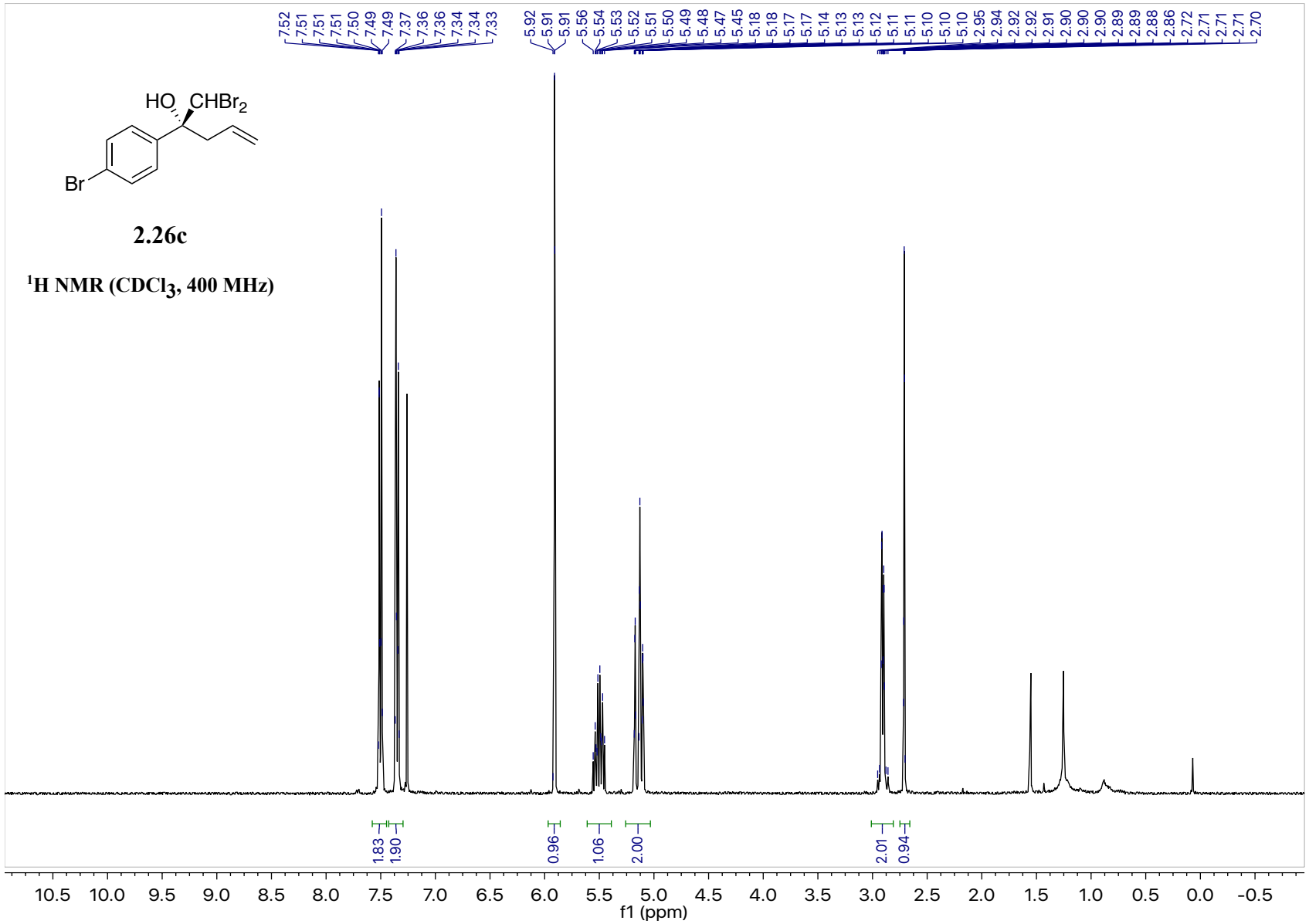
HO
CHBr2
Br
2.26c
1H NMR (CDCl3, 400 MHz)
7.52 7.51 7.51 7.51 7.50 7.49 7.49 7.37 7.36 7.36 7.34 7.34 7.33
5.92 5.91 5.91 5.56 5.54 5.53 5.52 5.51 5.50 5.49 5.48 5.47 5.45 5.18 5.18 5.17 5.17 5.14 5.13 5.13 5.12 5.11 5.11 5.10 5.10 5.10 2.95 2.94 2.92 2.92 2.91 2.90 2.90 2.90 2.89 2.89 2.88 2.86 2.72 2.71 2.71 2.71 2.70
1.83
1.90
0.96
1.06
2.00
2.01
0.94
10.5 10.0 9.5 9.0 8.5 8.0 7.5 7.0 6.5 6.0 5.5 5.0 4.5 4.0 3.5 3.0 2.5 2.0 1.5 1.0 0.5 0.0 -0.5
f1 (ppm)

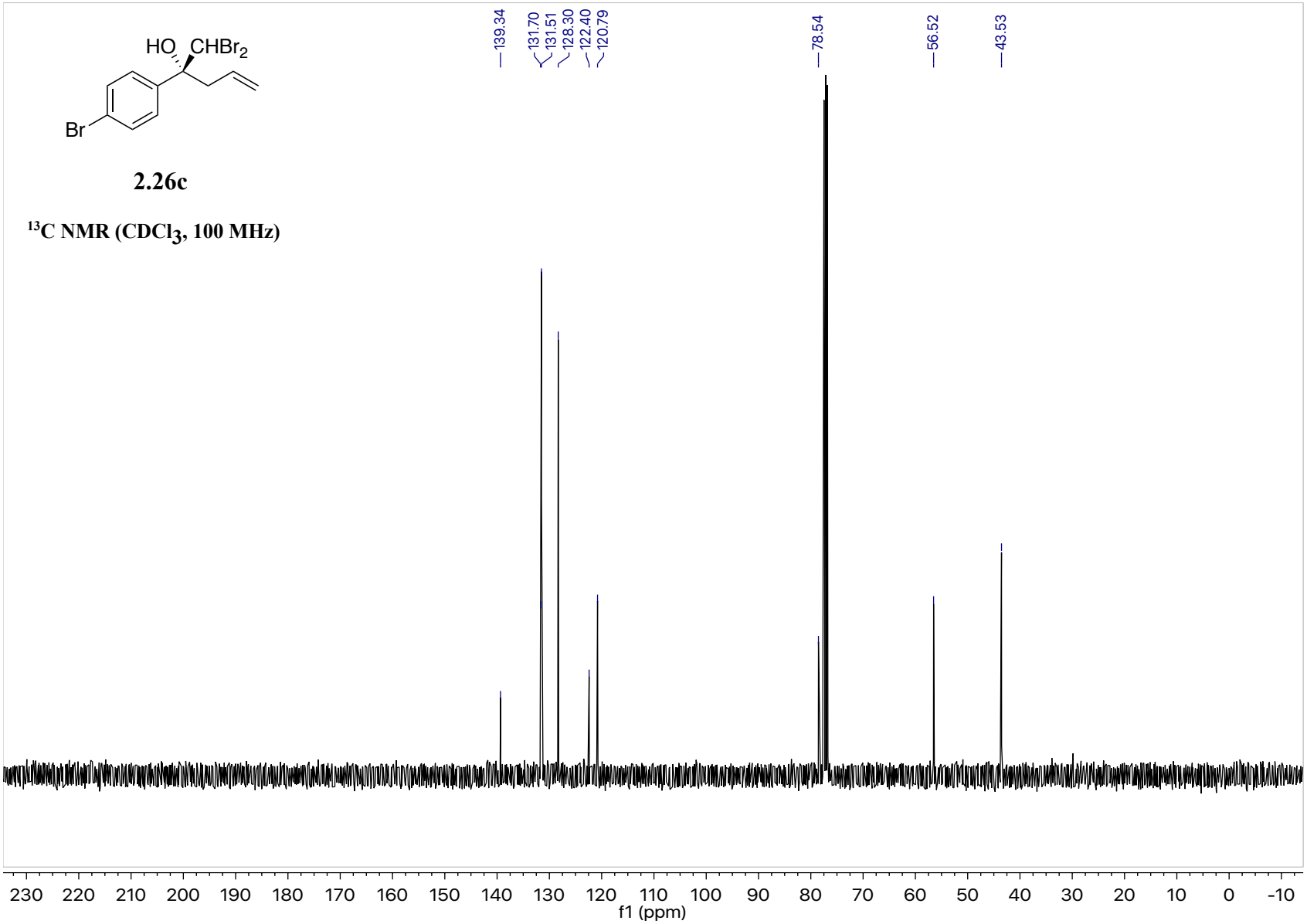
HO
CHBr2
Br
2.26c
13C NMR (CDCl3, 100 MHz)
139.34
131.70
131.51
128.30
122.40
120.79
78.54
56.52
43.53
230 220 210 200 190 180 170 160 150 140 130 120 110 100 90 80 70 60 50 40 30 20 10 0 -10
f1 (ppm)

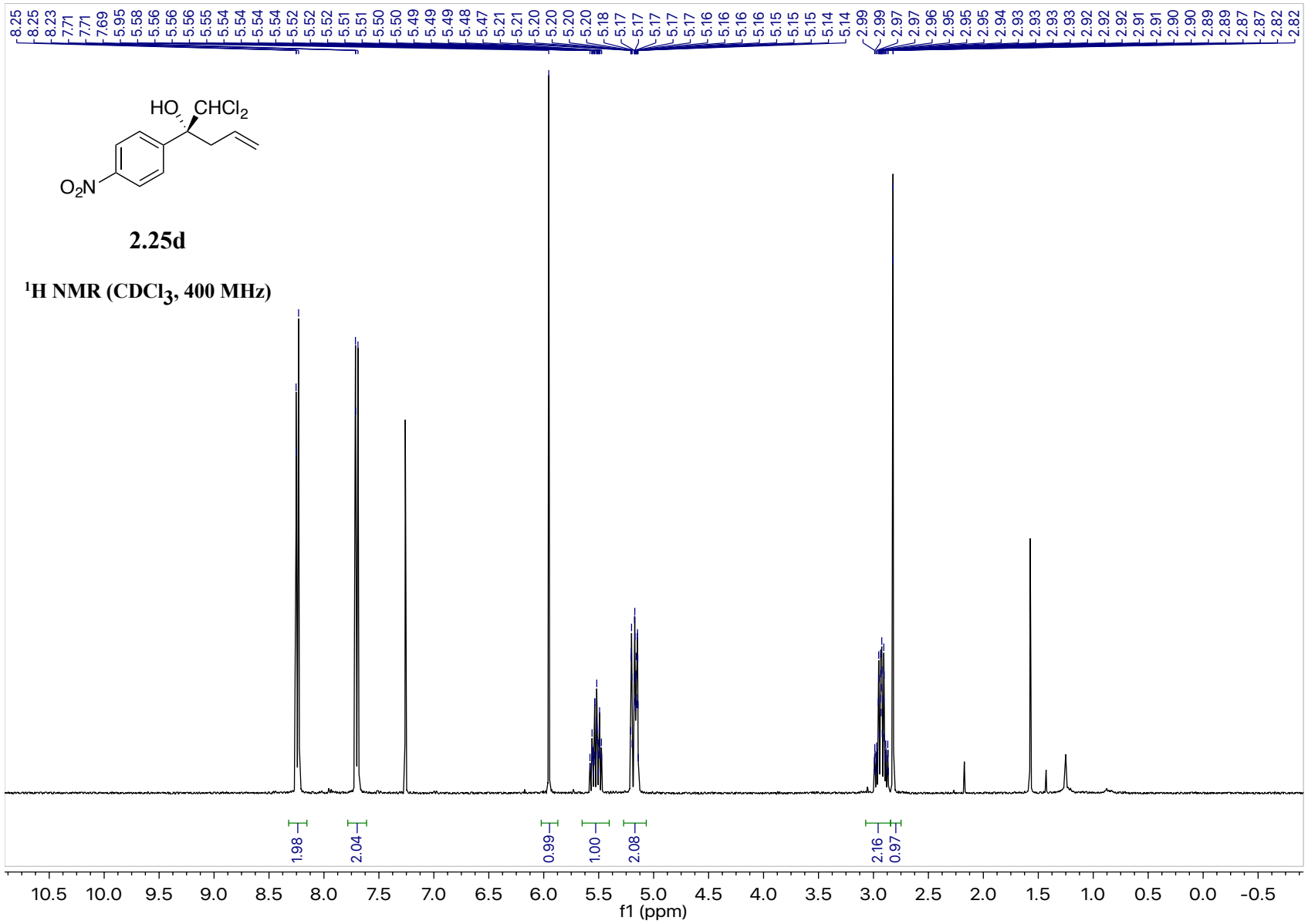
HO
CHCl2
O2N
2.25d
1H NMR (CDCl3, 400 MHz)
1.98
2.04
0.99
1.00
2.08
2.16
0.97
f1 (ppm)

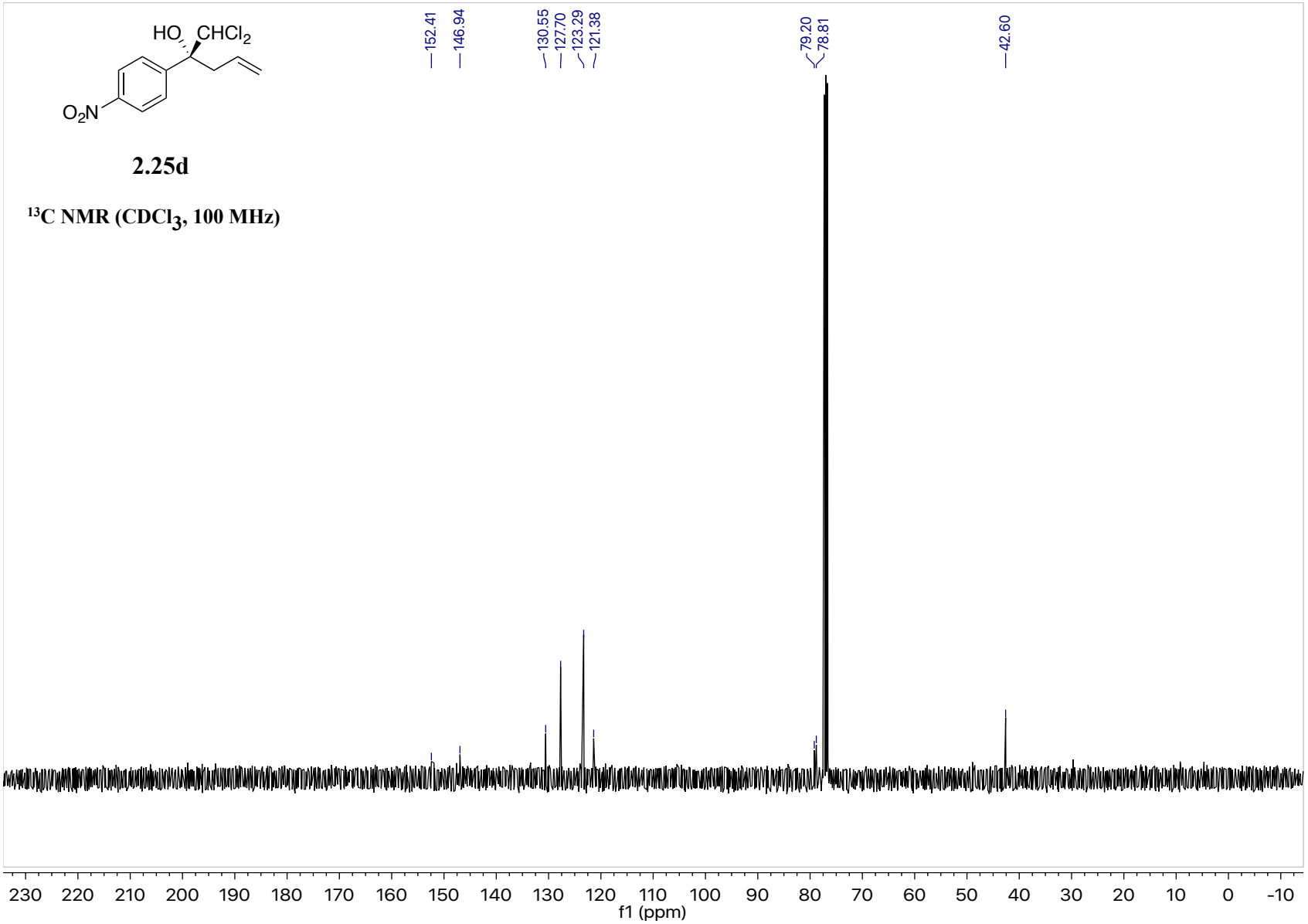

2.25d

^{13}C NMR ($CDCl_3$, 100 MHz)

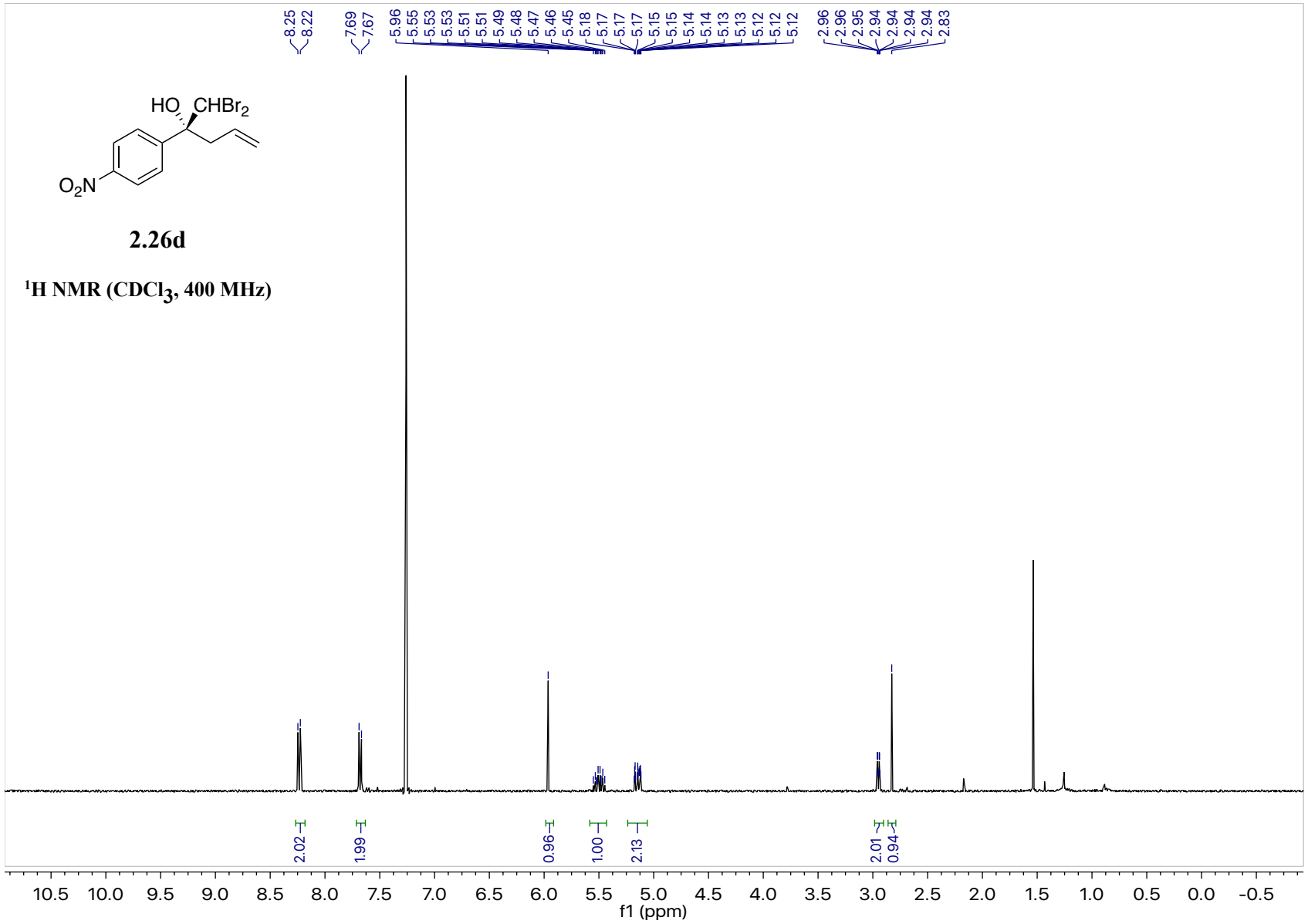
8.25
8.22
7.69
7.67
5.96
5.55
5.53
5.53
5.51
5.51
5.49
5.48
5.47
5.46
5.45
5.18
5.17
5.17
5.17
5.15
5.15
5.14
5.14
5.13
5.13
5.12
5.12
5.12
2.96
2.96
2.95
2.94
2.94
2.94
2.83
HO
CHBr2
O2N
2.26d
1H NMR (CDCl3, 400 MHz)
2.02
1.99
0.96
1.00
2.13
2.01
0.94
10.5
10.0
9.5
9.0
8.5
8.0
7.5
7.0
6.5
6.0
5.5
5.0
4.5
4.0
3.5
3.0
2.5
2.0
1.5
1.0
0.5
0.0
-0.5
f1 (ppm)

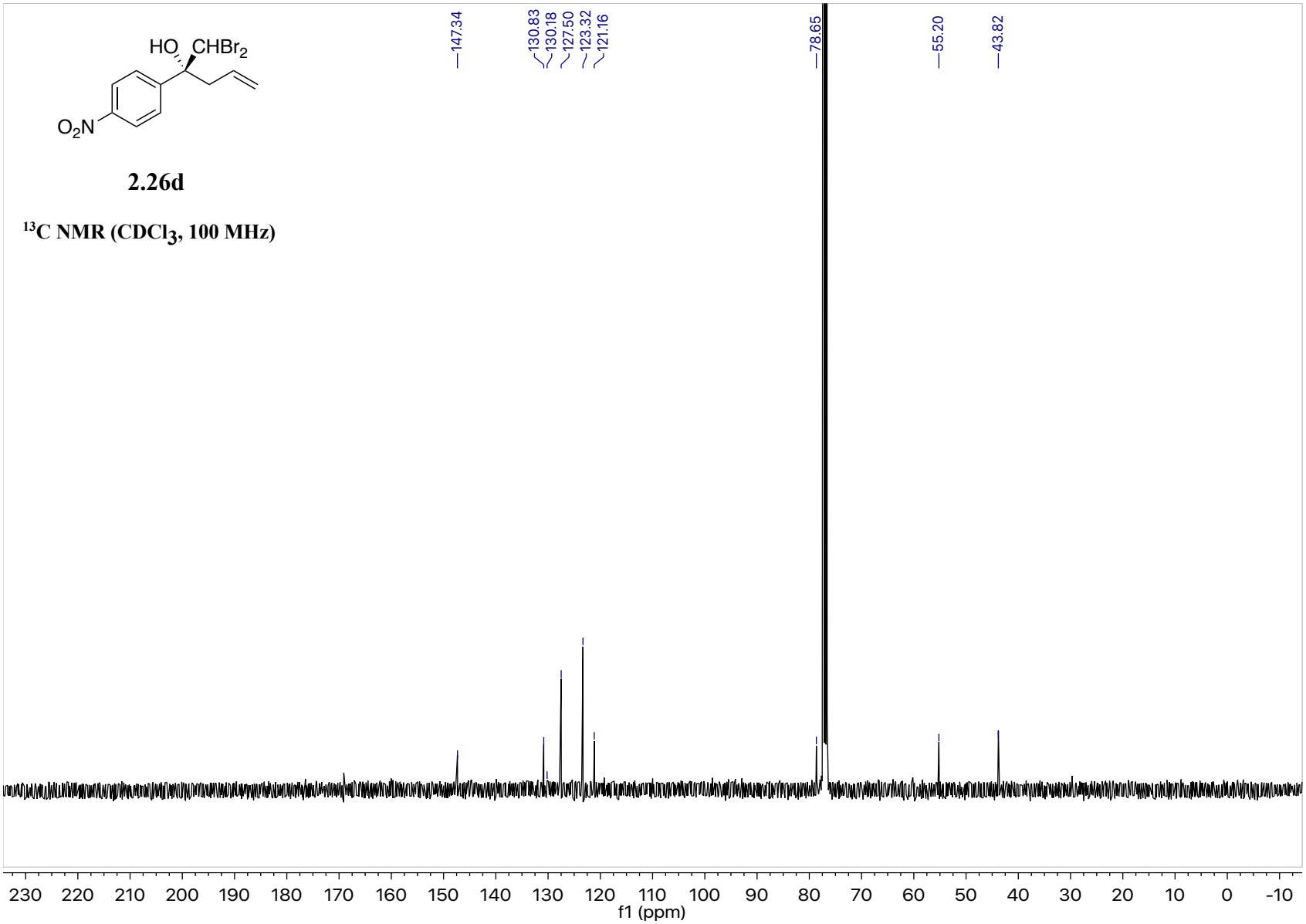

2.26d

^{13}C NMR ($CDCl_3$, 100 MHz)

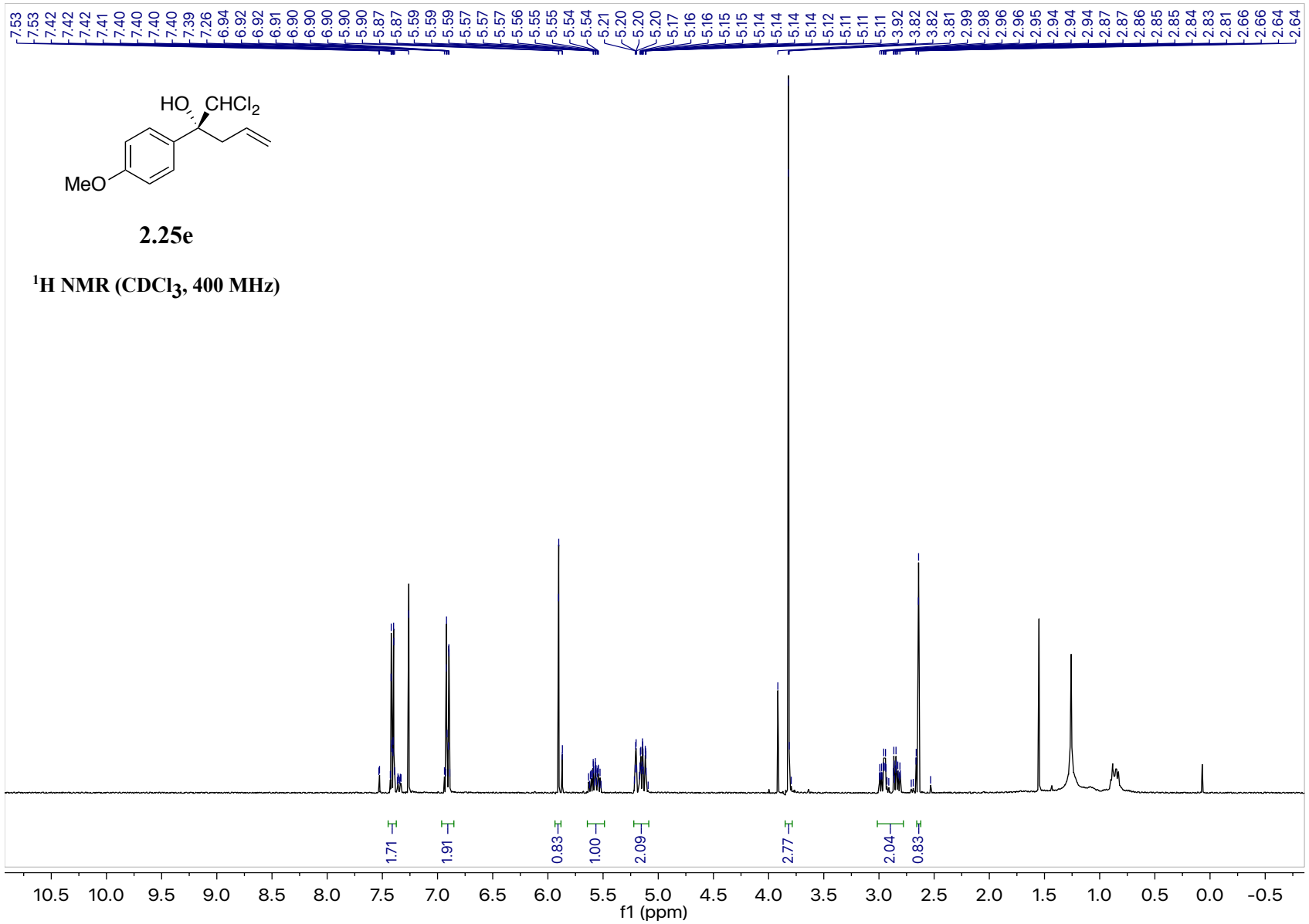
HO
CHCl2
MeO
2.25e
1H NMR (CDCl3, 400 MHz)
1.71
1.91
0.83
1.00
2.09
2.77
2.04
0.83
f1 (ppm)

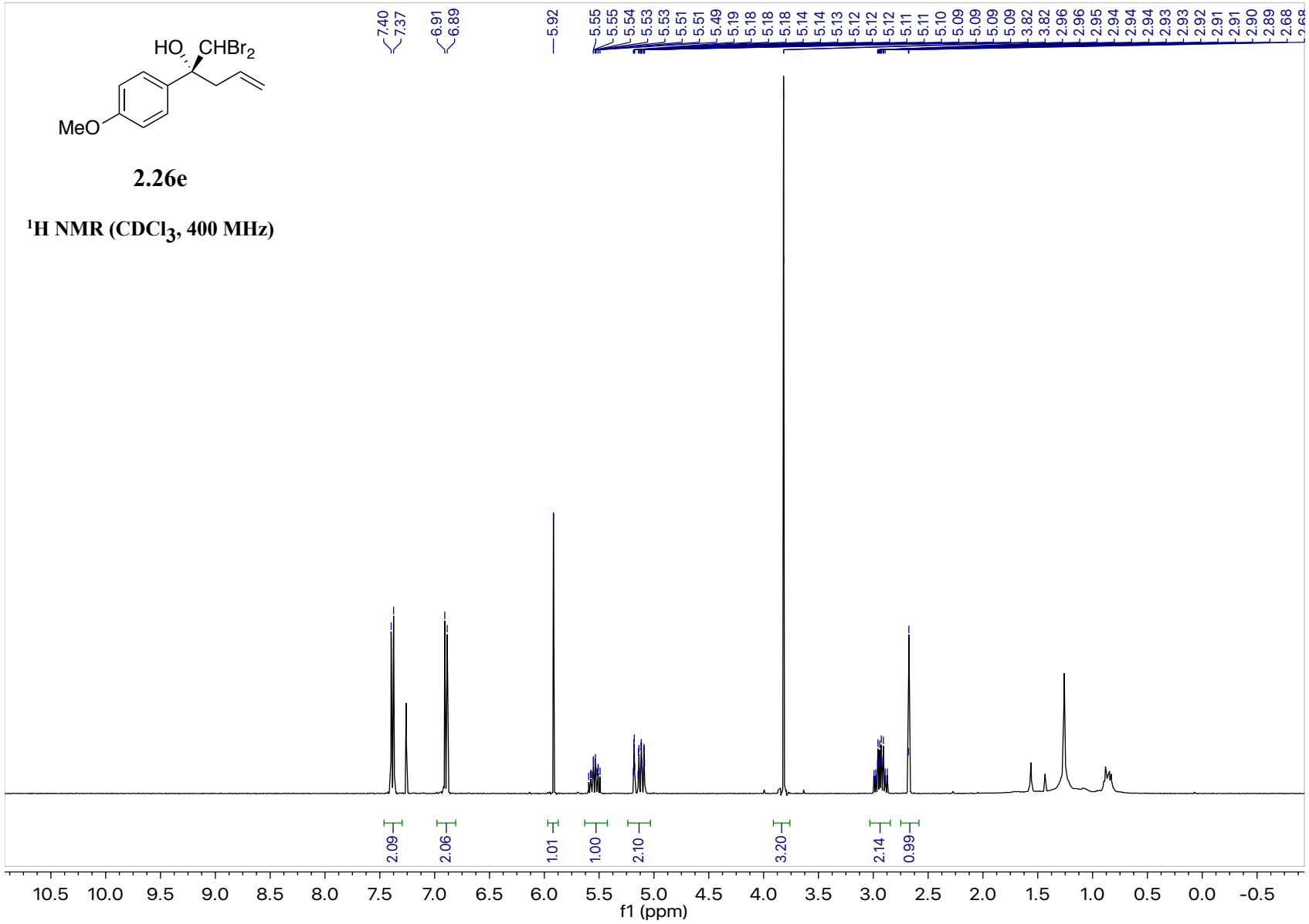
HO
CHBr2
MeO
2.26e
1H NMR (CDCl3, 400 MHz)
7.40
7.37
6.91
6.89
5.92
5.55
5.55
5.54
5.53
5.53
5.51
5.51
5.49
5.19
5.18
5.18
5.18
5.14
5.14
5.13
5.12
5.12
5.12
5.11
5.11
5.10
5.09
5.09
5.09
5.09
3.82
3.82
2.96
2.96
2.95
2.94
2.94
2.94
2.93
2.93
2.92
2.91
2.91
2.90
2.89
2.68
2.09
2.06
1.01
1.00
2.10
3.20
2.14
0.99
10.5
10.0
9.5
9.0
8.5
8.0
7.5
7.0
6.5
6.0
5.5
5.0
4.5
4.0
3.5
3.0
2.5
2.0
1.5
1.0
0.5
0.0
-0.5
f1 (ppm)

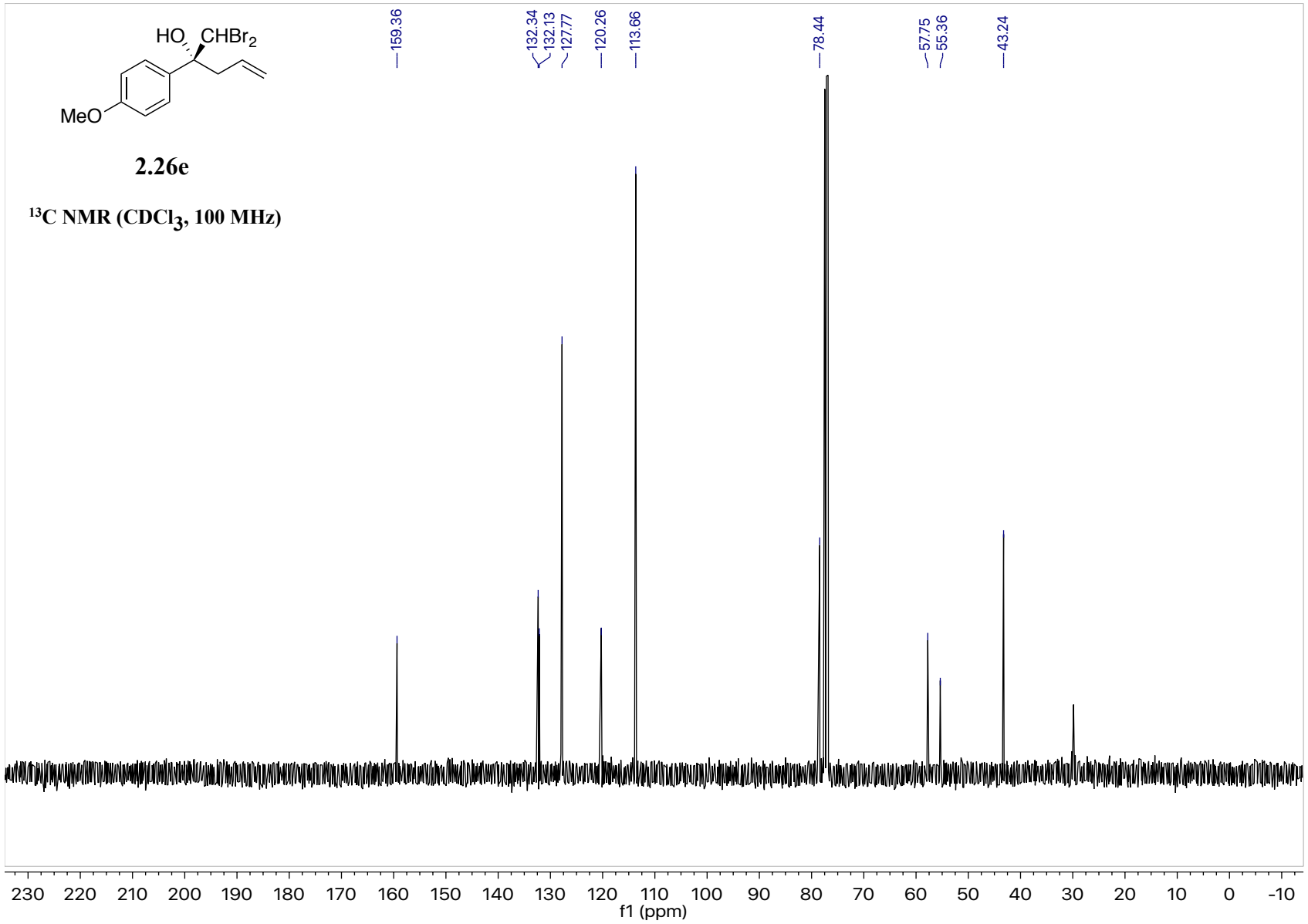

2.26e

^{13}C NMR ($CDCl_3$, 100 MHz)

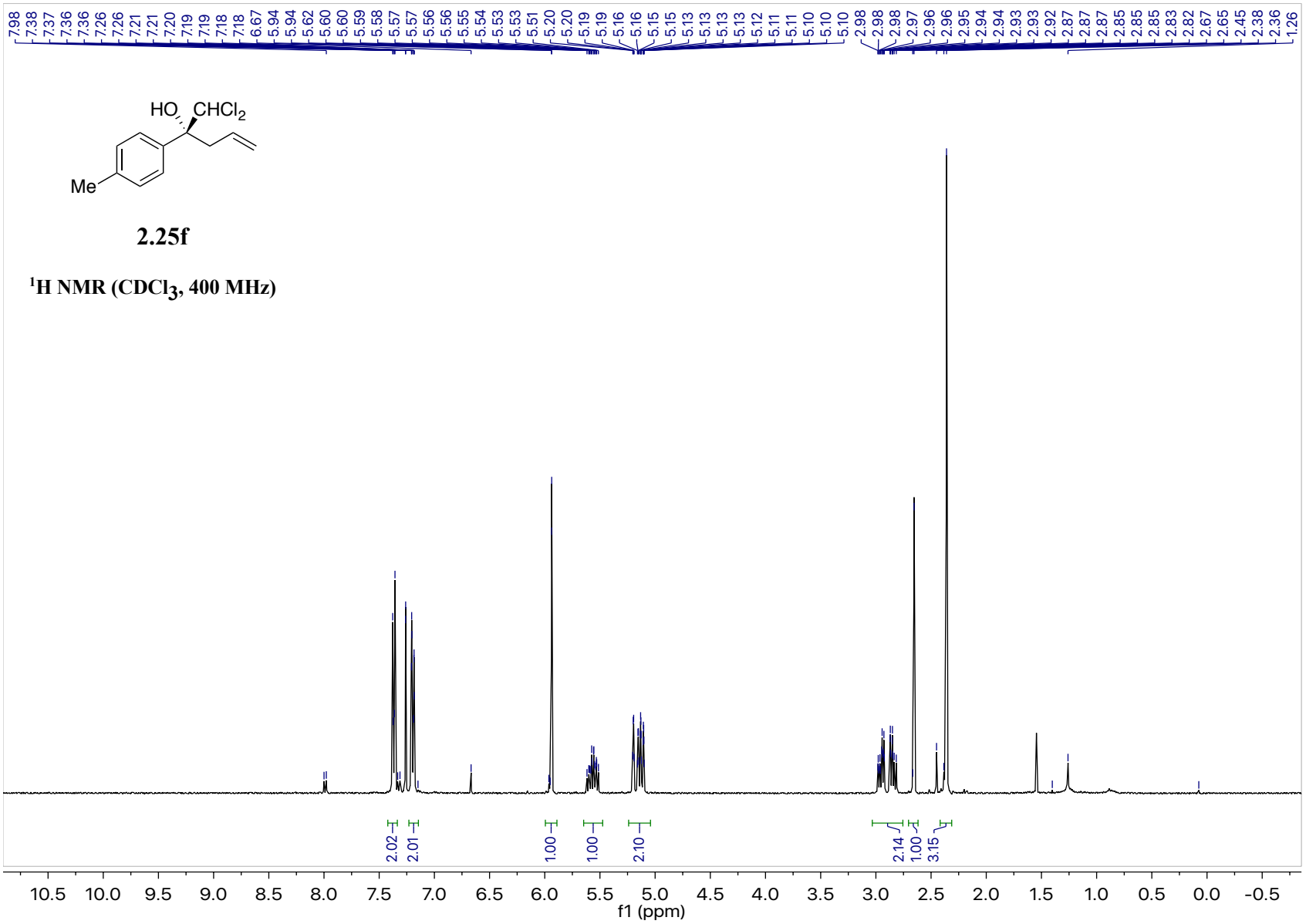
HO
CHCl2
Me
2.25f
1H NMR (CDCl3, 400 MHz)
f1 (ppm)

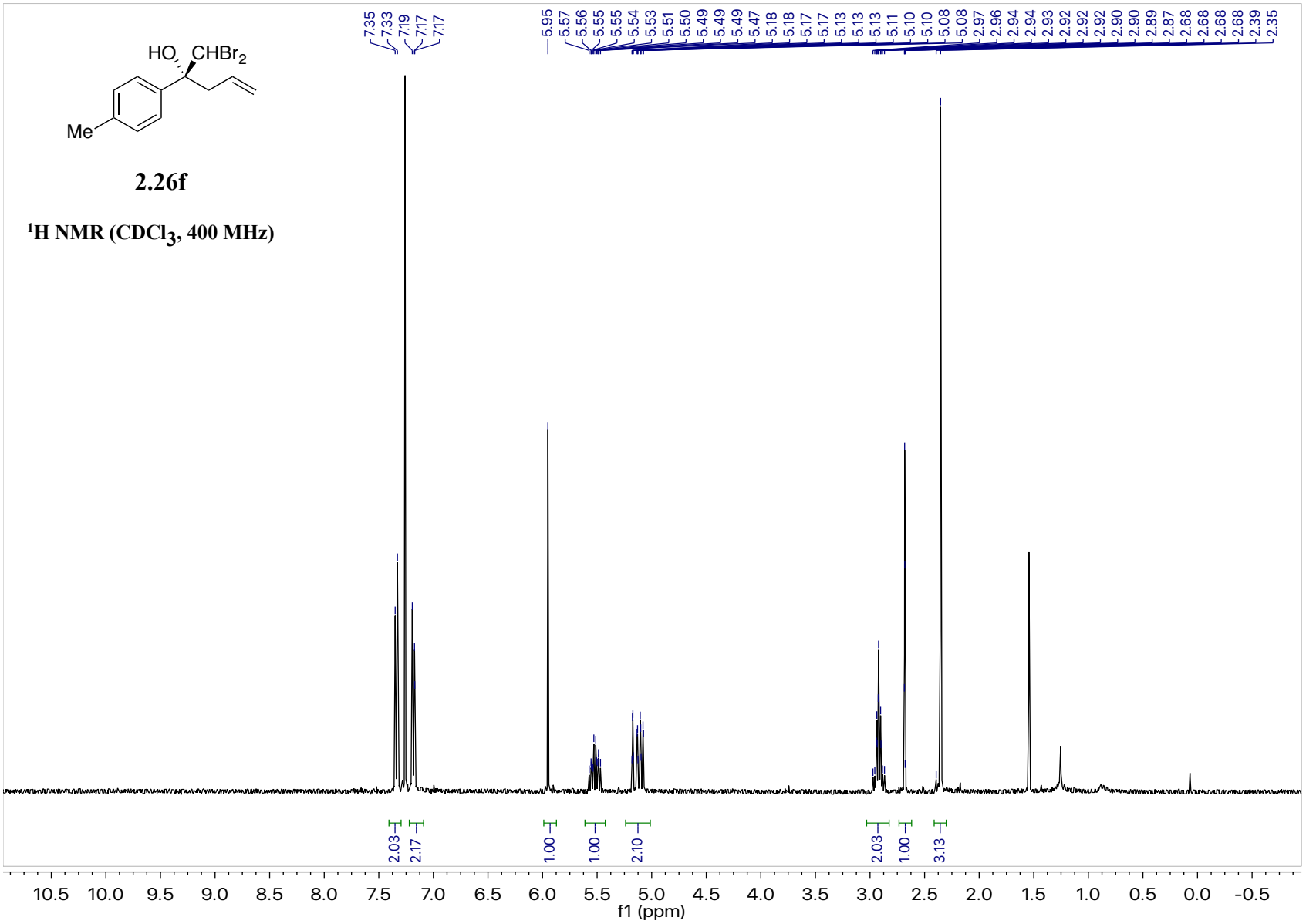
HO
CHBr2
Me
2.26f
1H NMR (CDCl3, 400 MHz)
7.35
7.33
7.19
7.17
7.17
5.95
5.57
5.56
5.55
5.55
5.54
5.53
5.51
5.50
5.49
5.49
5.47
5.18
5.18
5.17
5.17
5.13
5.13
5.13
5.11
5.10
5.10
5.08
5.08
2.97
2.96
2.94
2.94
2.93
2.92
2.92
2.92
2.90
2.90
2.89
2.87
2.68
2.68
2.68
2.68
2.39
2.35
2.03
2.17
1.00
1.00
2.10
2.03
1.00
3.13
10.5 10.0 9.5 9.0 8.5 8.0 7.5 7.0 6.5 6.0 5.5 5.0 4.5 4.0 3.5 3.0 2.5 2.0 1.5 1.0 0.5 0.0 -0.5
f1 (ppm)

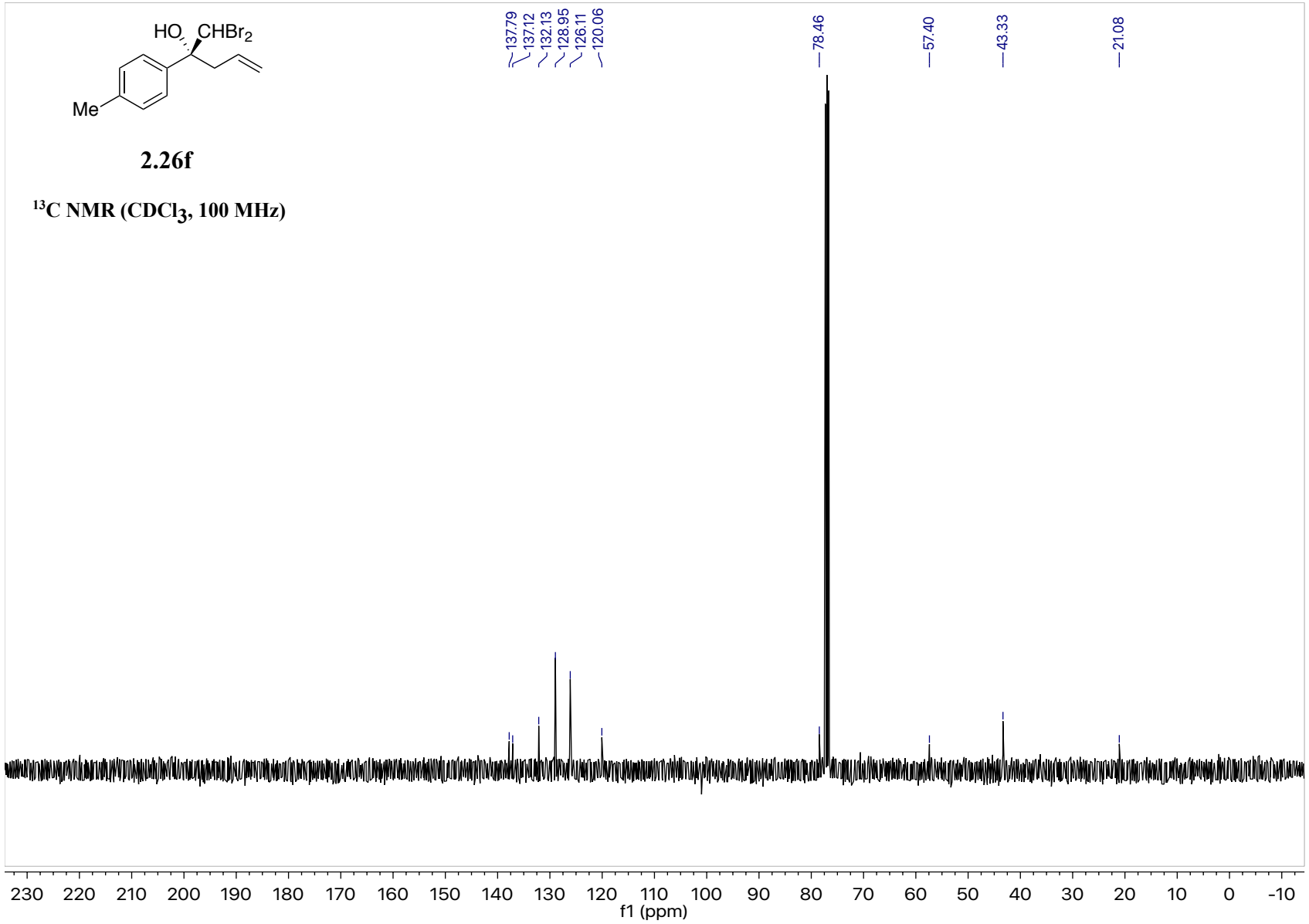

2.26f

^{13}C NMR ($CDCl_3$, 100 MHz)

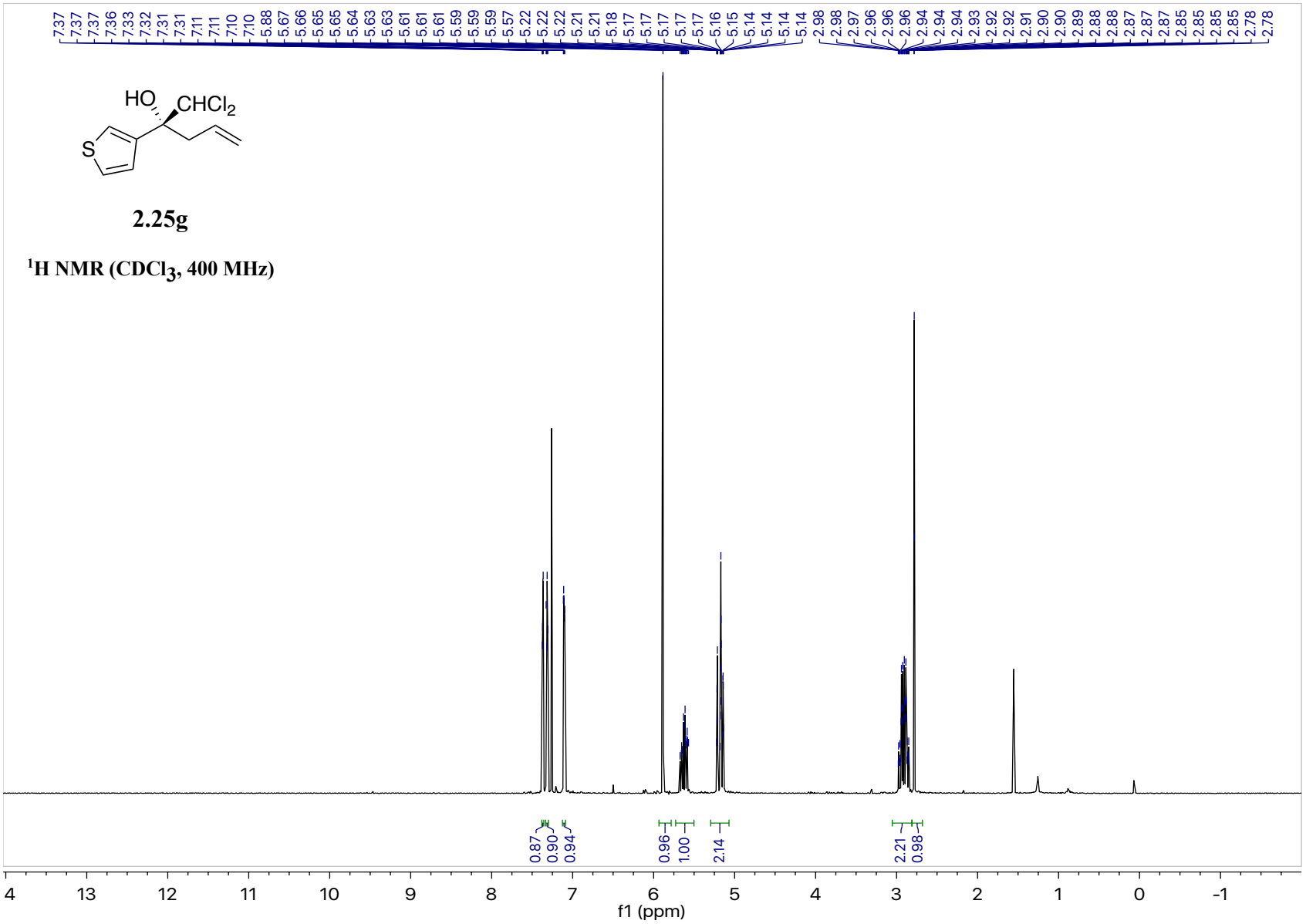
HO
CHCl2
S
2.25g
1H NMR (CDCl3, 400 MHz)
f1 (ppm)

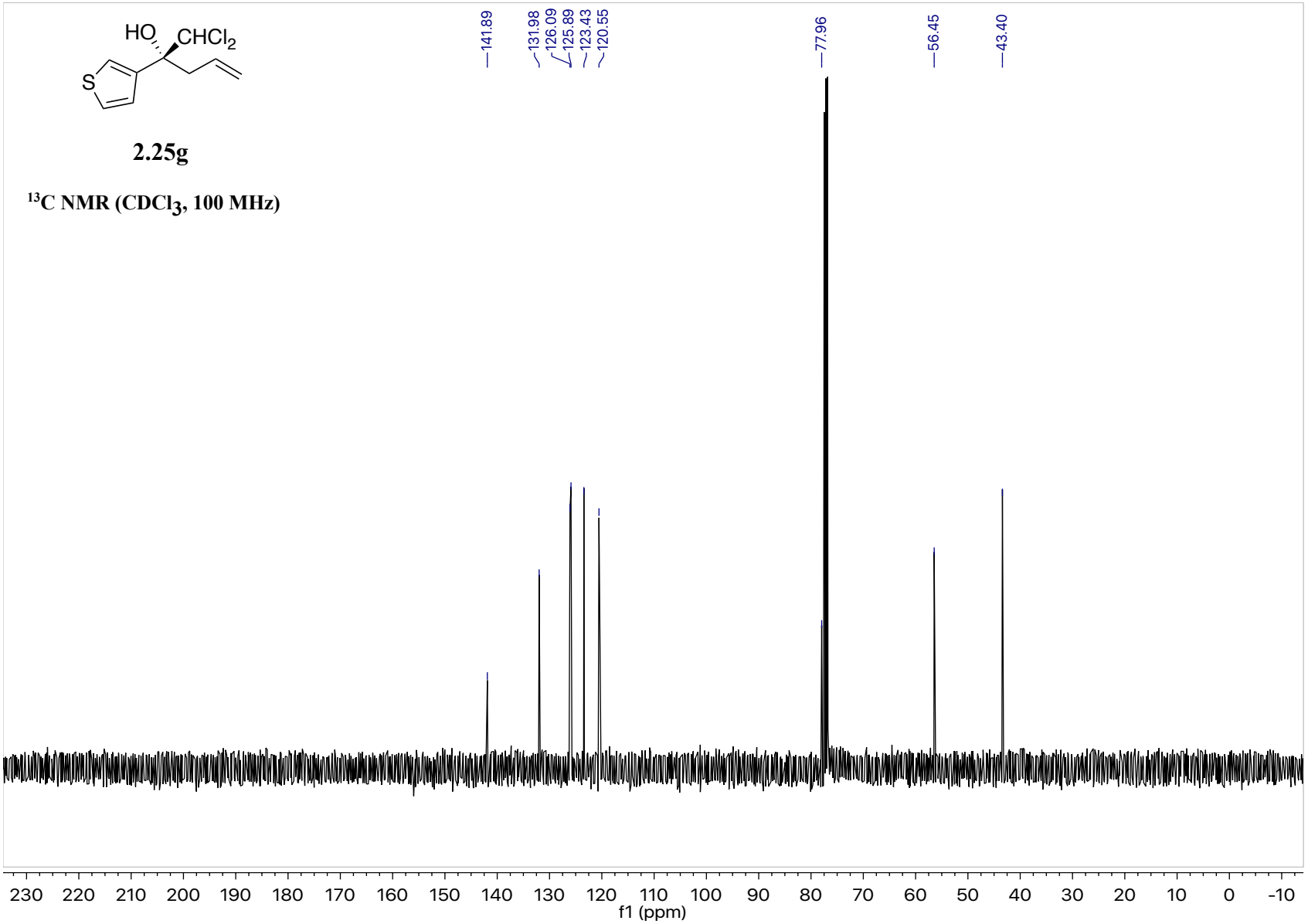

2.25g

^{13}C NMR ($CDCl_3$, 100 MHz)

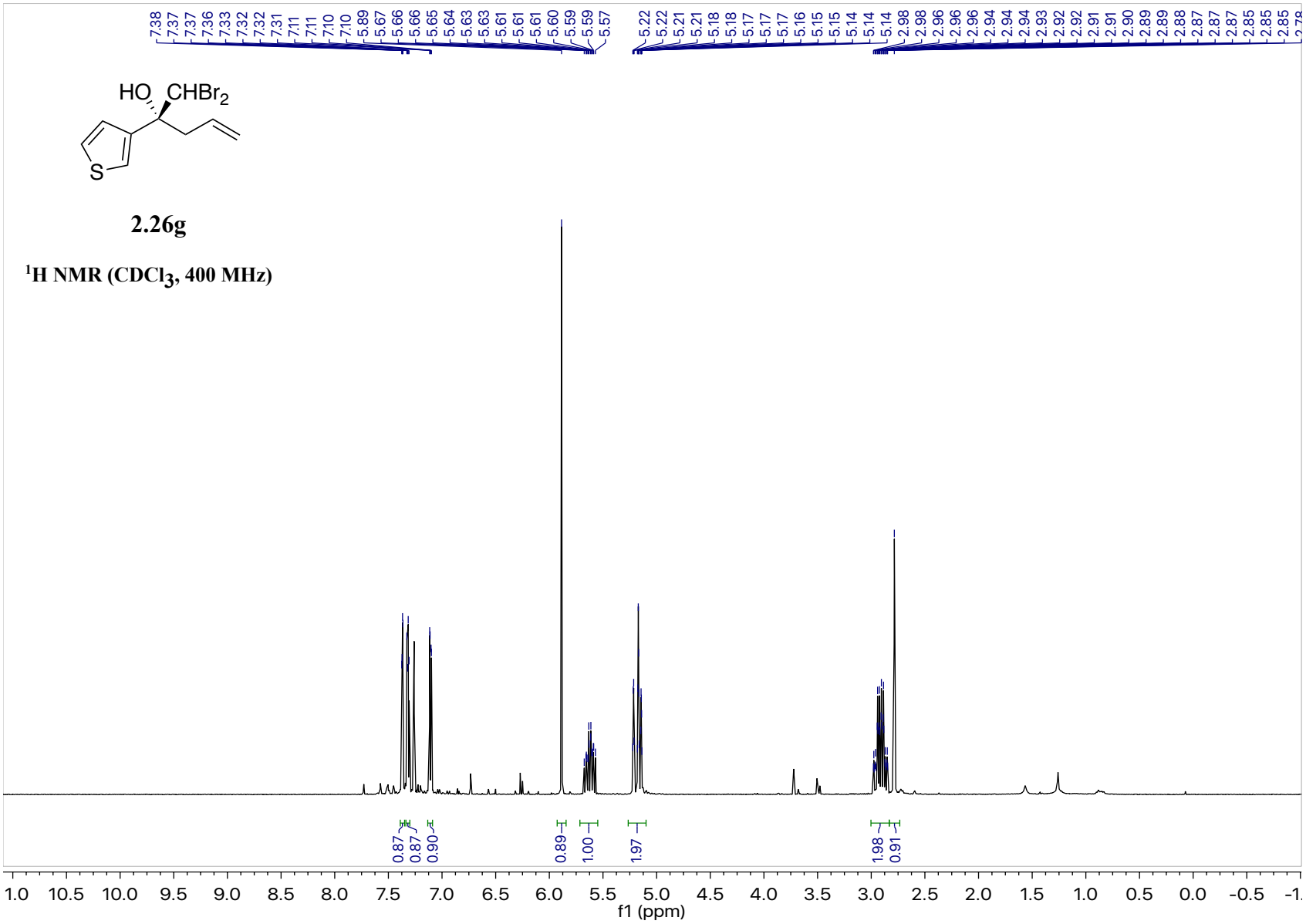

2.26g

^{1}H NMR ($CDCl_3$, 400 MHz)

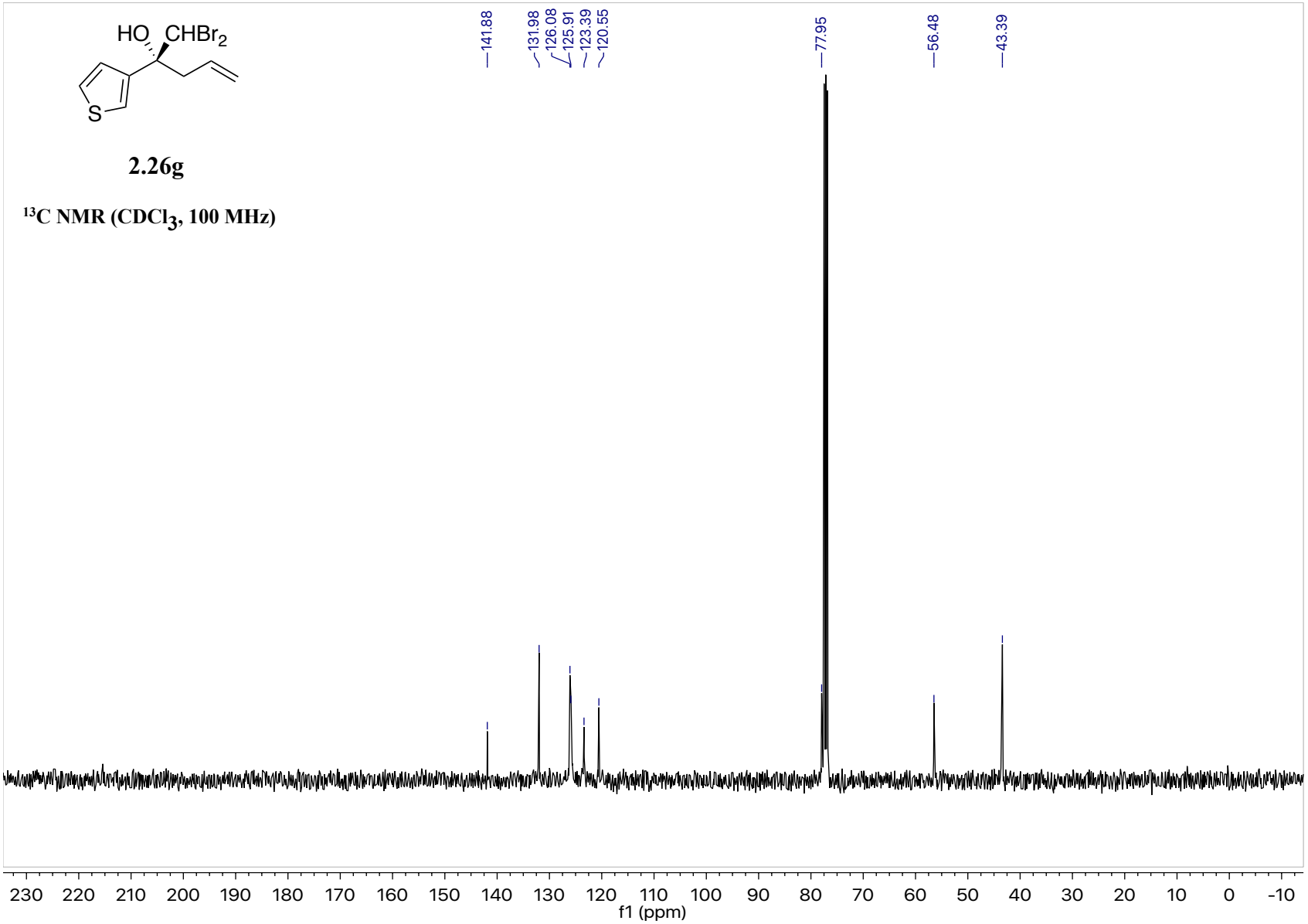

2.26g

^{13}C NMR ($CDCl_3$, 100 MHz)

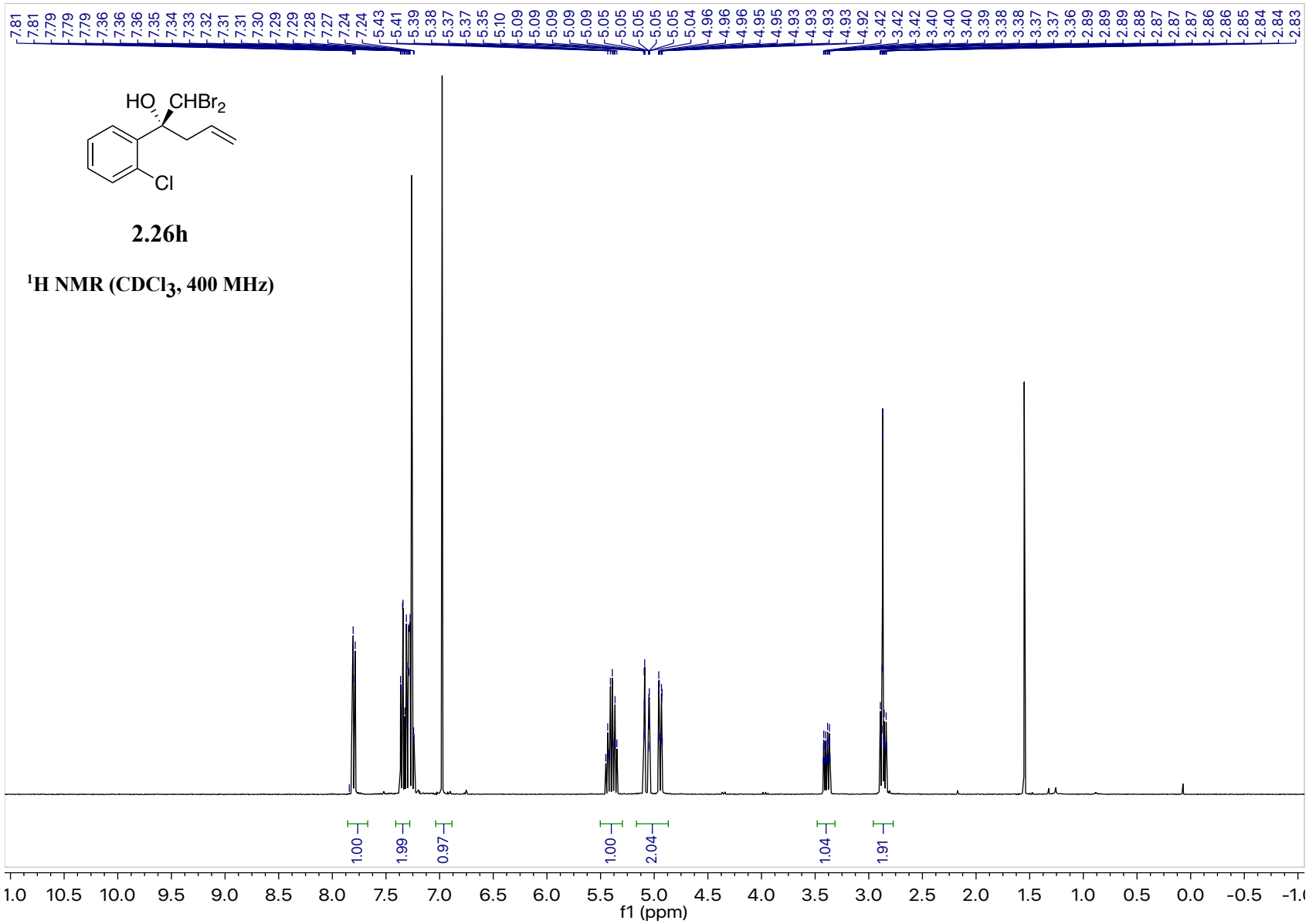
HO
CHBr2
Cl
2.26h
1H NMR (CDCl3, 400 MHz)
1.00
1.99
0.97
1.00
2.04
1.04
1.91
f1 (ppm)

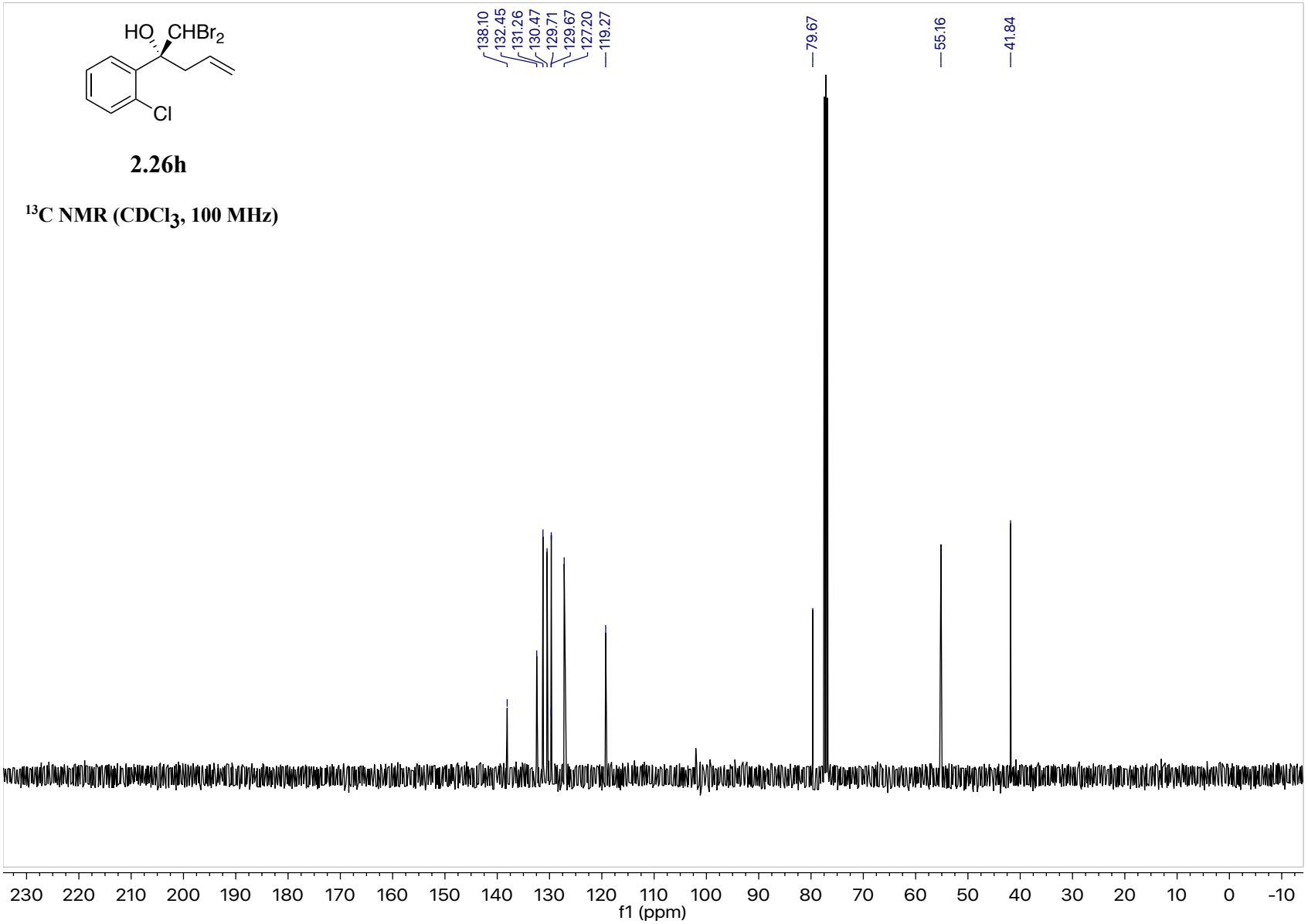
HO
CHBr2
Cl
2.26h
13C NMR (CDCl3, 100 MHz)
138.10
132.45
131.26
130.47
129.71
129.67
127.20
119.27
79.67
55.16
41.84
230 220 210 200 190 180 170 160 150 140 130 120 110 100 90 80 70 60 50 40 30 20 10 0 -10
f1 (ppm)

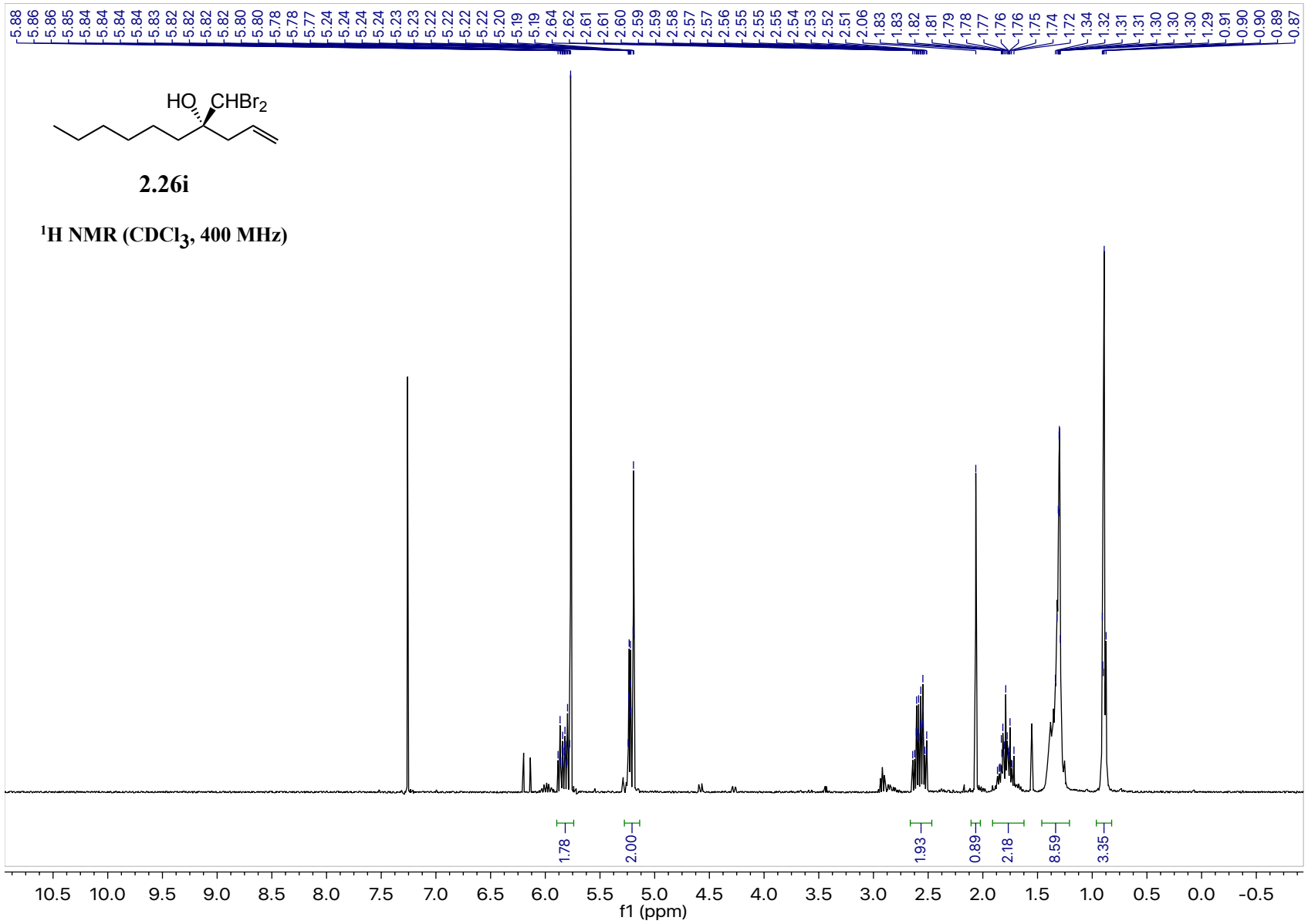
HO
CHBr2
2.26i
1H NMR (CDCl3, 400 MHz)
1.78
2.00
1.93
0.89
2.18
8.59
3.35
f1 (ppm)

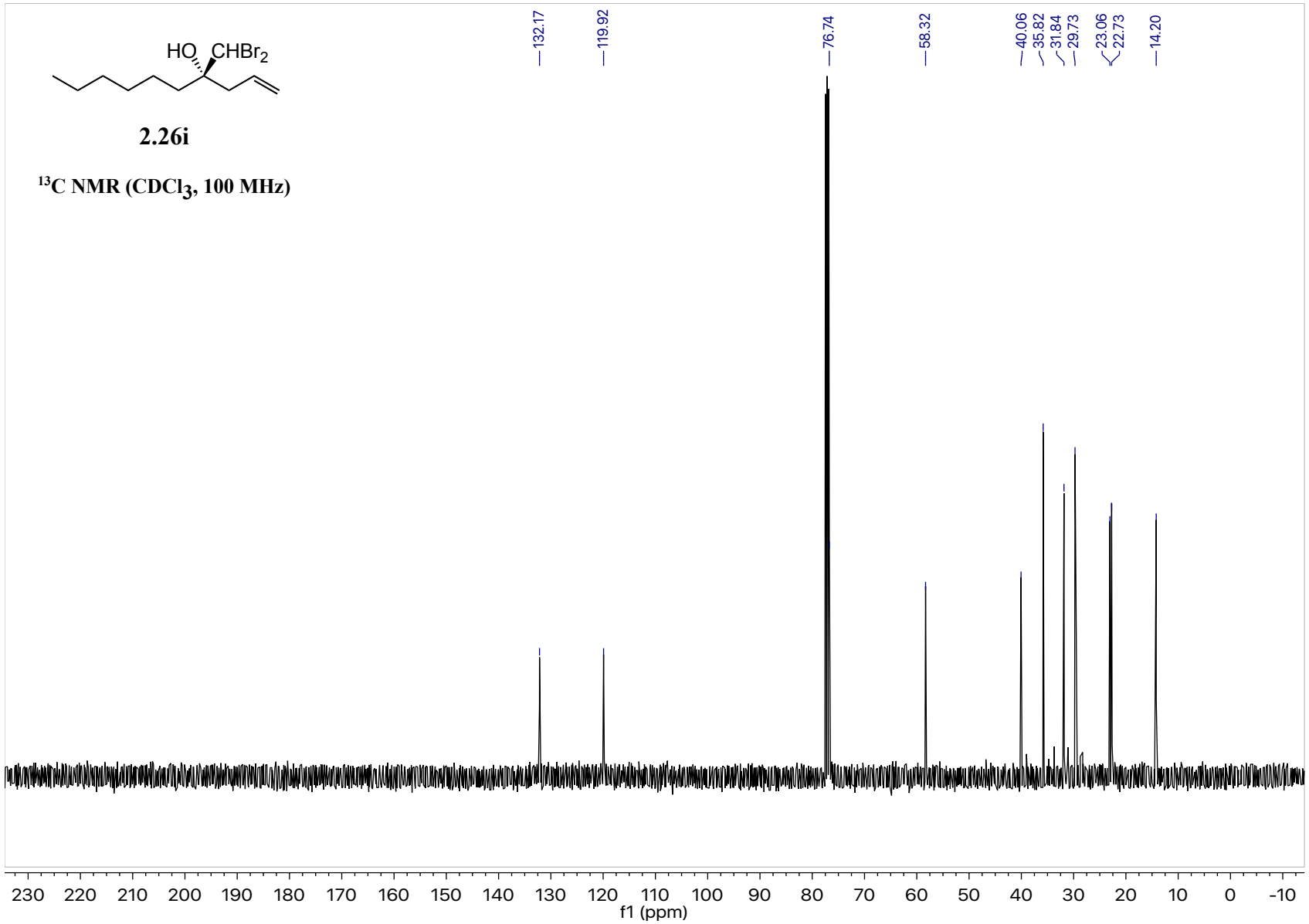
HO
CHBr2
2.26i
13C NMR (CDCl3, 100 MHz)
132.17
119.92
76.74
58.32
40.06
35.82
31.84
29.73
23.06
22.73
14.20
230 220 210 200 190 180 170 160 150 140 130 120 110 100 90 80 70 60 50 40 30 20 10 0 -10
f1 (ppm)

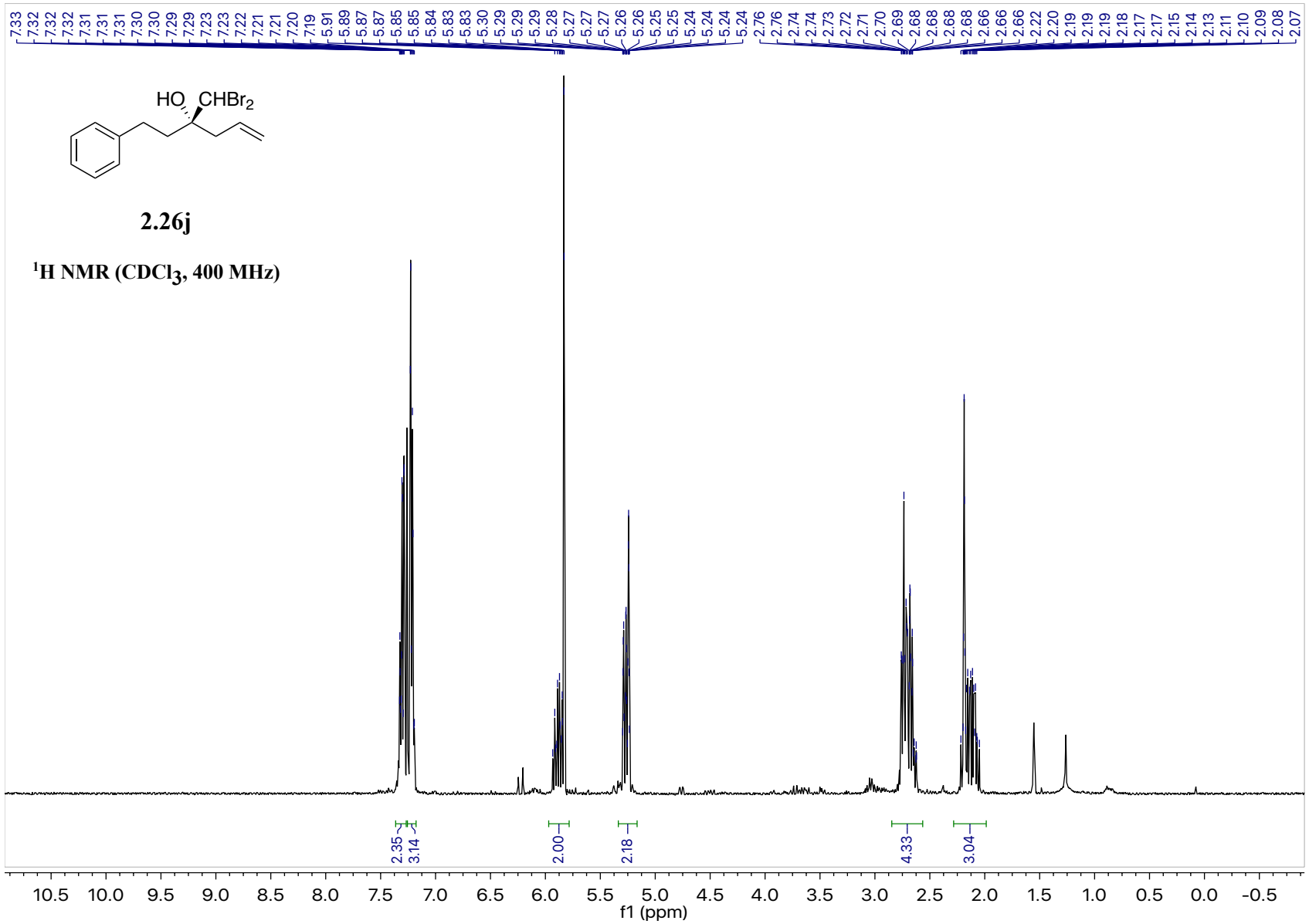
HO
CHBr2
2.26j
1H NMR (CDCl3, 400 MHz)
2.35
3.14
2.00
2.18
4.33
3.04
f1 (ppm)

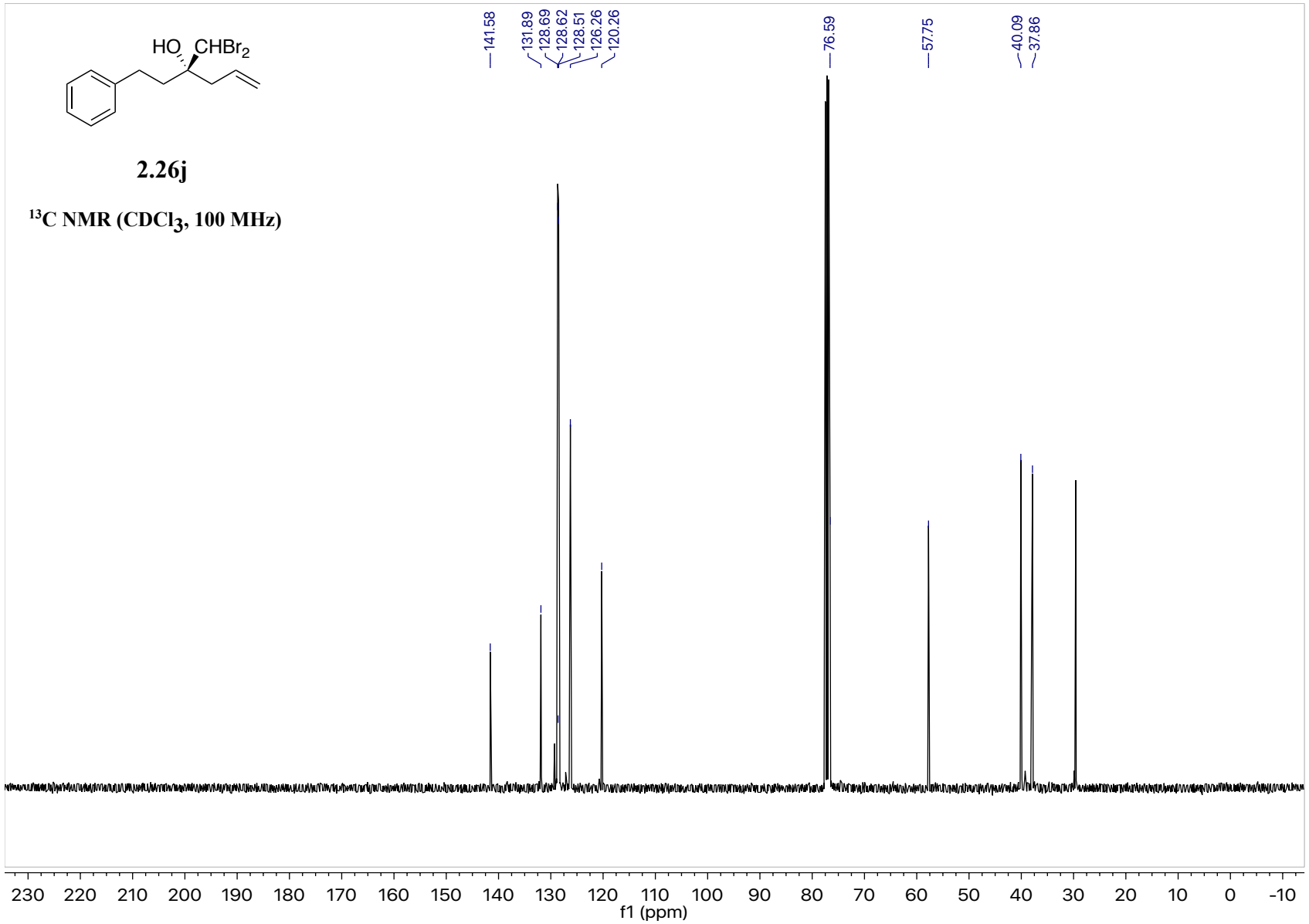

2.26j

^{13}C NMR ($CDCl_3$, 100 MHz)

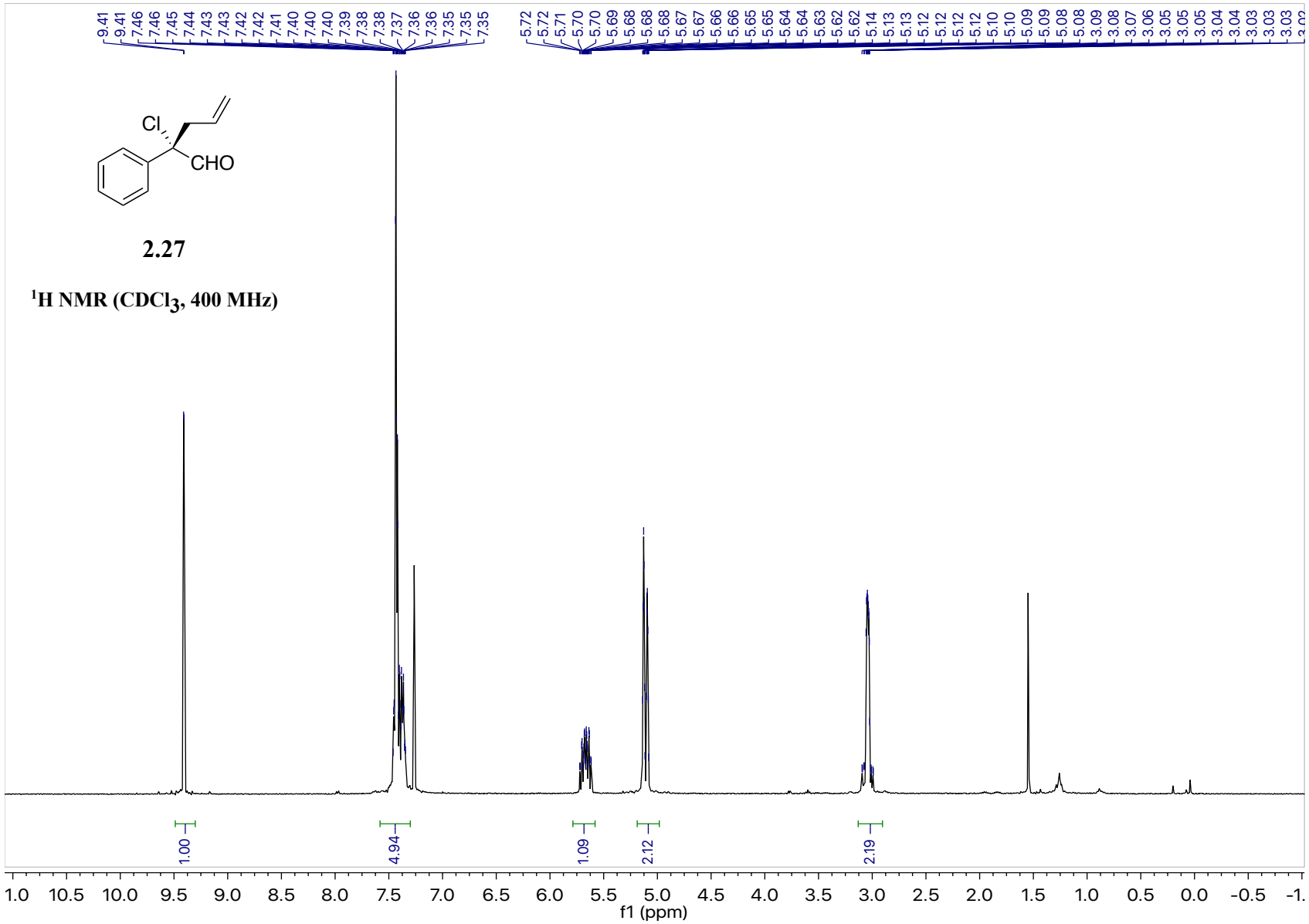
Cl
CHO
2.27
1H NMR (CDCl3, 400 MHz)
1.00
4.94
1.09
2.12
2.19
f1 (ppm)

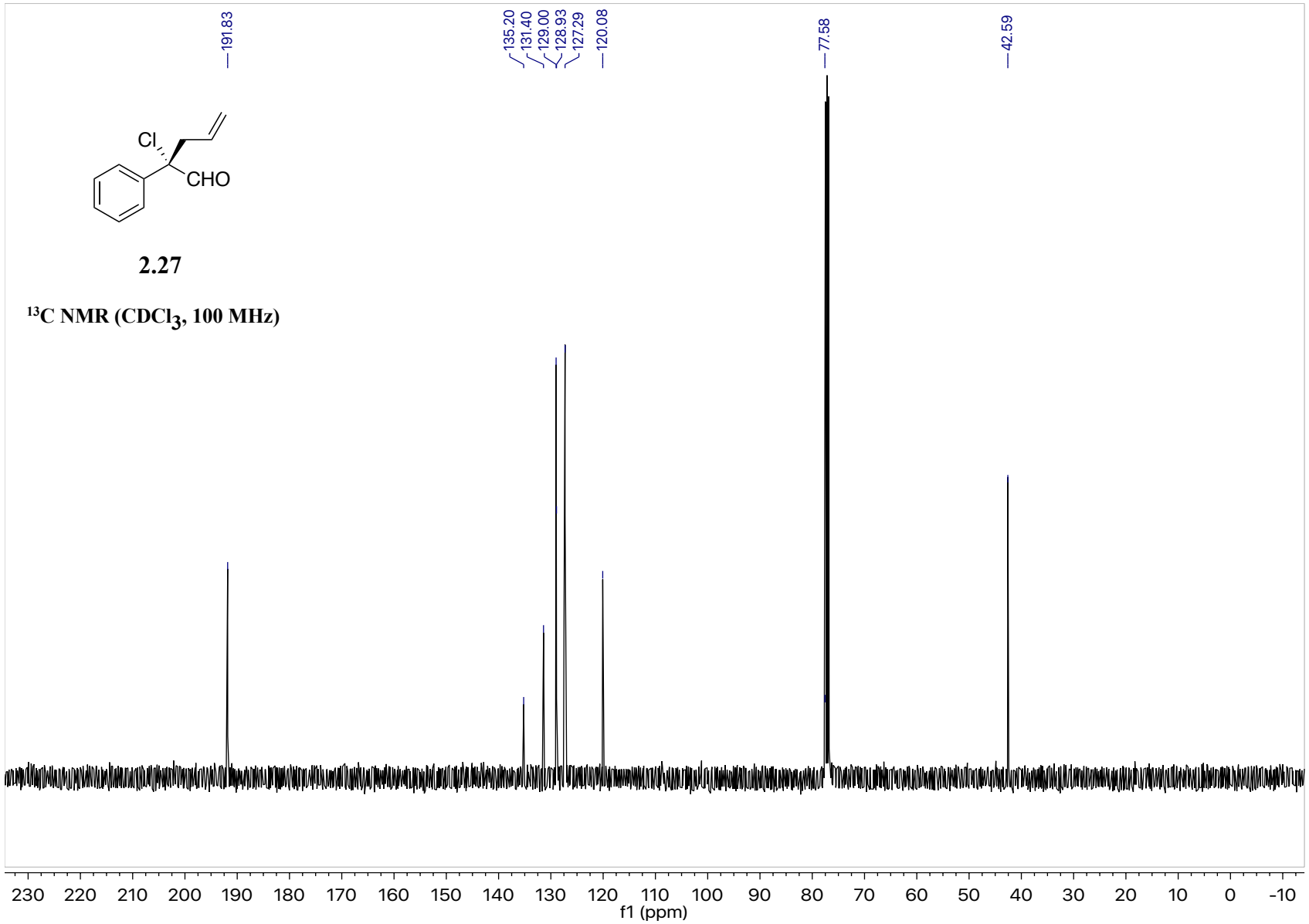
191.83
135.20
131.40
129.00
128.93
127.29
120.08
77.58
42.59
Cl
CHO
2.27
13C NMR (CDCl3, 100 MHz)
230 220 210 200 190 180 170 160 150 140 130 120 110 100 90 80 70 60 50 40 30 20 10 0 -10
f1 (ppm)

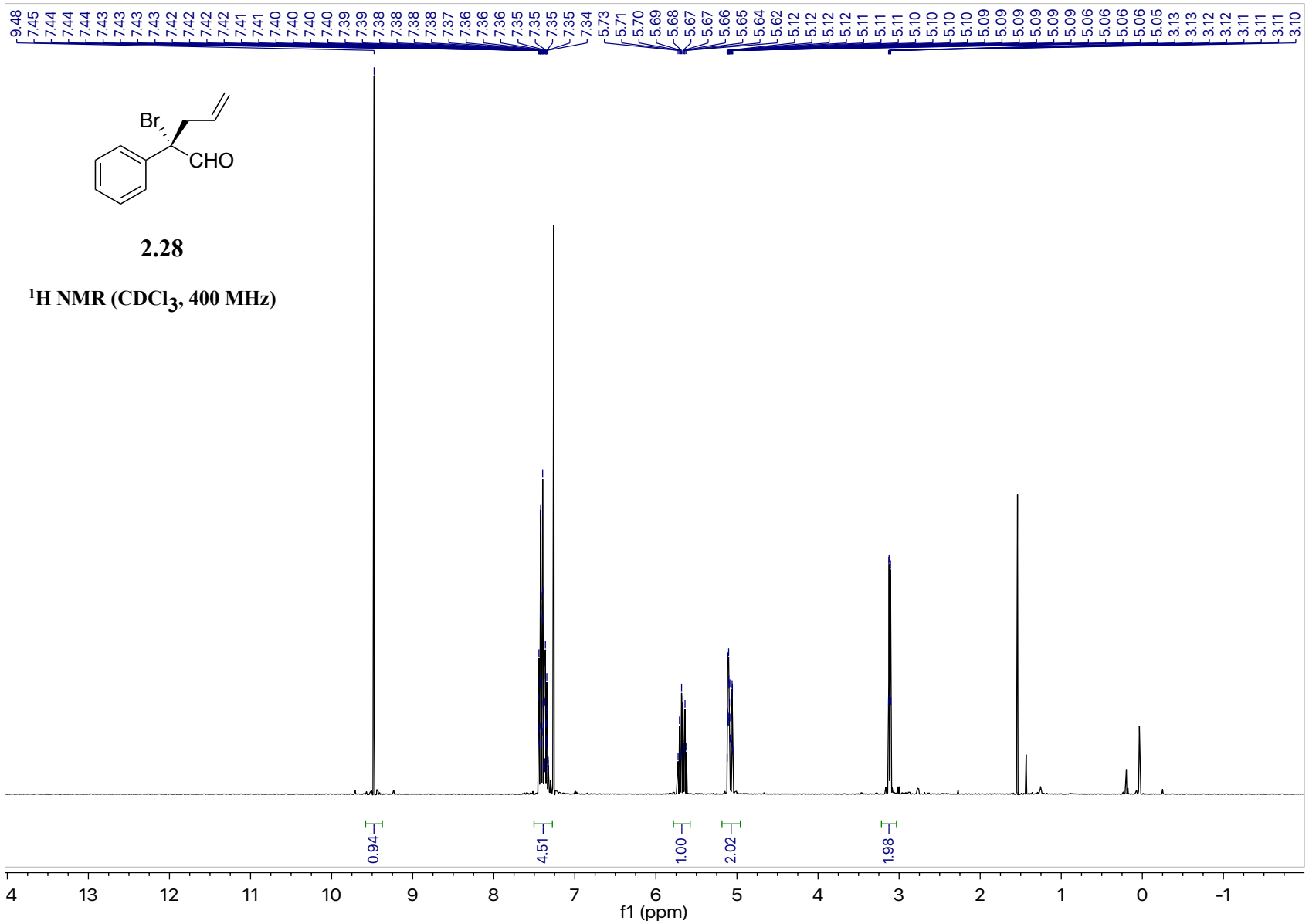
Br
CHO
2.28
^{1}H NMR ($CDCl_3$, 400 MHz)
0.94
4.51
1.00
2.02
1.98
f1 (ppm)

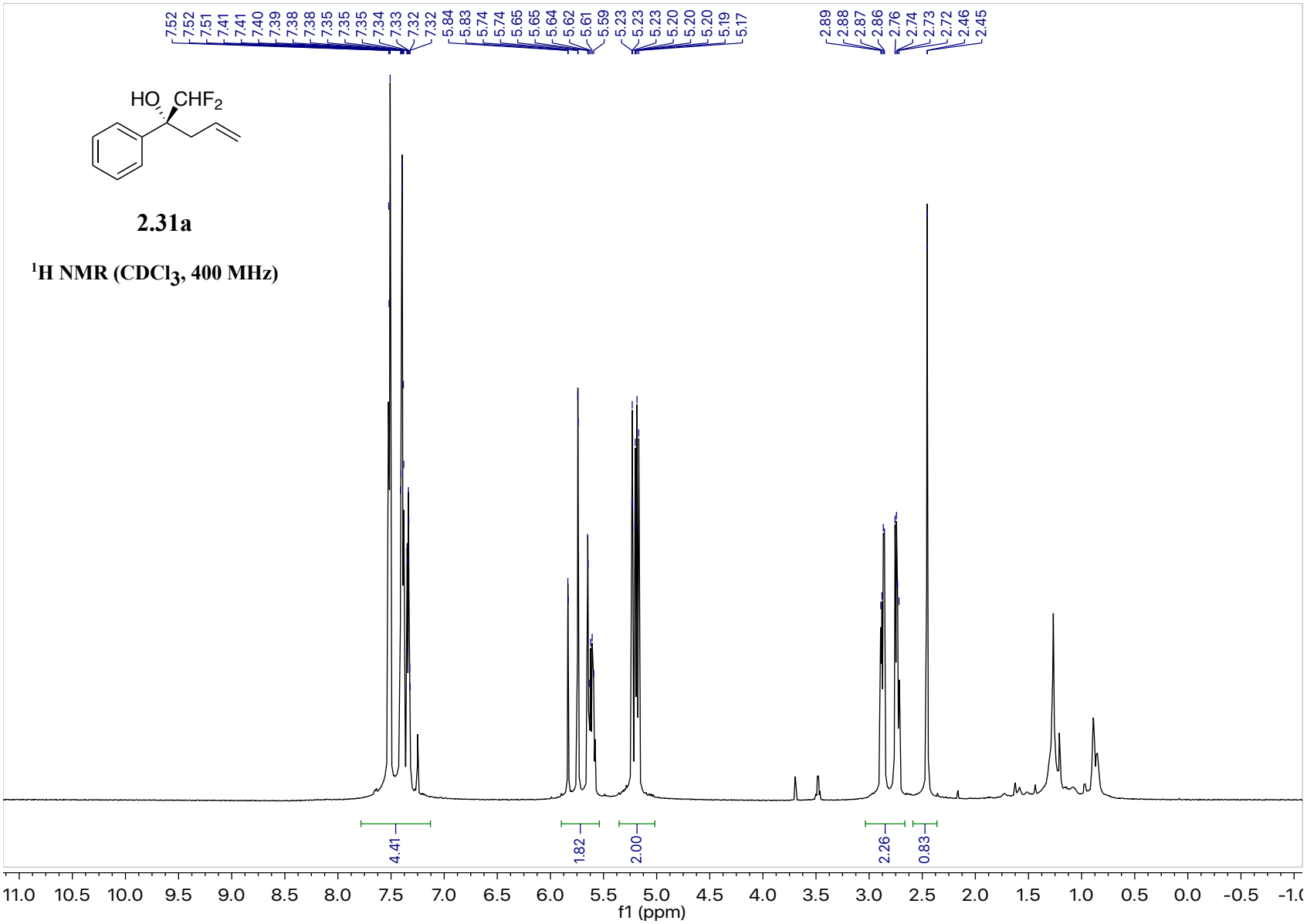
7.52
7.52
7.51
7.41
7.41
7.40
7.39
7.38
7.38
7.35
7.35
7.35
7.34
7.33
7.32
7.32
5.84
5.83
5.74
5.74
5.65
5.65
5.64
5.62
5.61
5.59
5.23
5.23
5.20
5.20
5.20
5.19
5.17
2.89
2.88
2.87
2.86
2.76
2.74
2.73
2.72
2.46
2.45
HO
CHF2
2.31a
1H NMR (CDCl3, 400 MHz)
4.41
1.82
2.00
2.26
0.83
11.0 10.5 10.0 9.5 9.0 8.5 8.0 7.5 7.0 6.5 6.0 5.5 5.0 4.5 4.0 3.5 3.0 2.5 2.0 1.5 1.0 0.5 0.0 -0.5 -1.0
f1 (ppm)

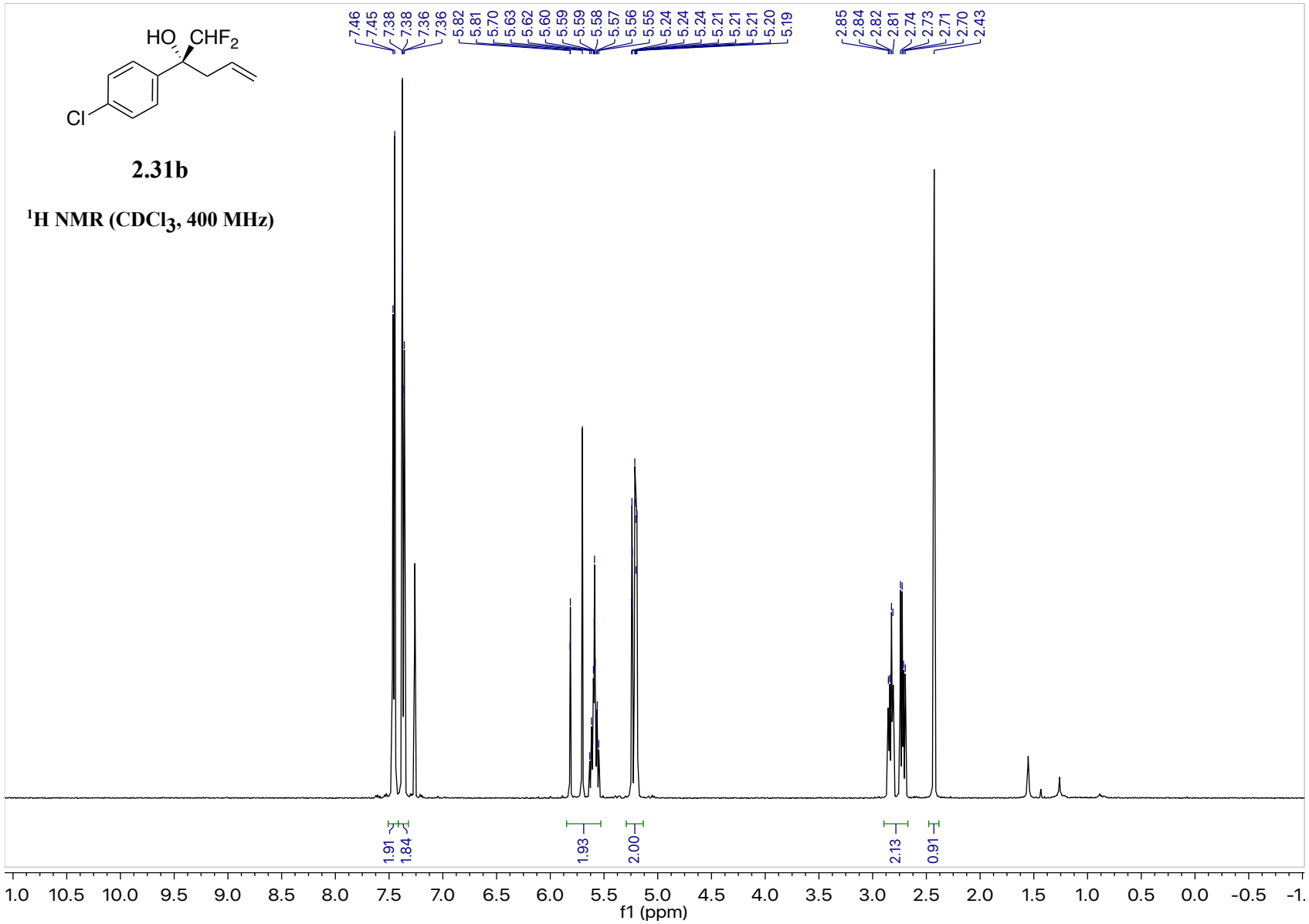
HO
CHF2
Cl
2.31b
1H NMR (CDCl3, 400 MHz)
7.46
7.45
7.38
7.38
7.36
7.36
5.82
5.81
5.70
5.63
5.62
5.60
5.59
5.59
5.58
5.57
5.56
5.55
5.24
5.24
5.21
5.21
5.21
5.20
5.19
2.85
2.84
2.82
2.81
2.74
2.73
2.71
2.70
2.43
1.91
1.84
1.93
2.00
2.13
0.91
1.0
10.5
10.0
9.5
9.0
8.5
8.0
7.5
7.0
6.5
6.0
5.5
5.0
4.5
4.0
3.5
3.0
2.5
2.0
1.5
1.0
0.5
0.0
-0.5
-1.
f1 (ppm)

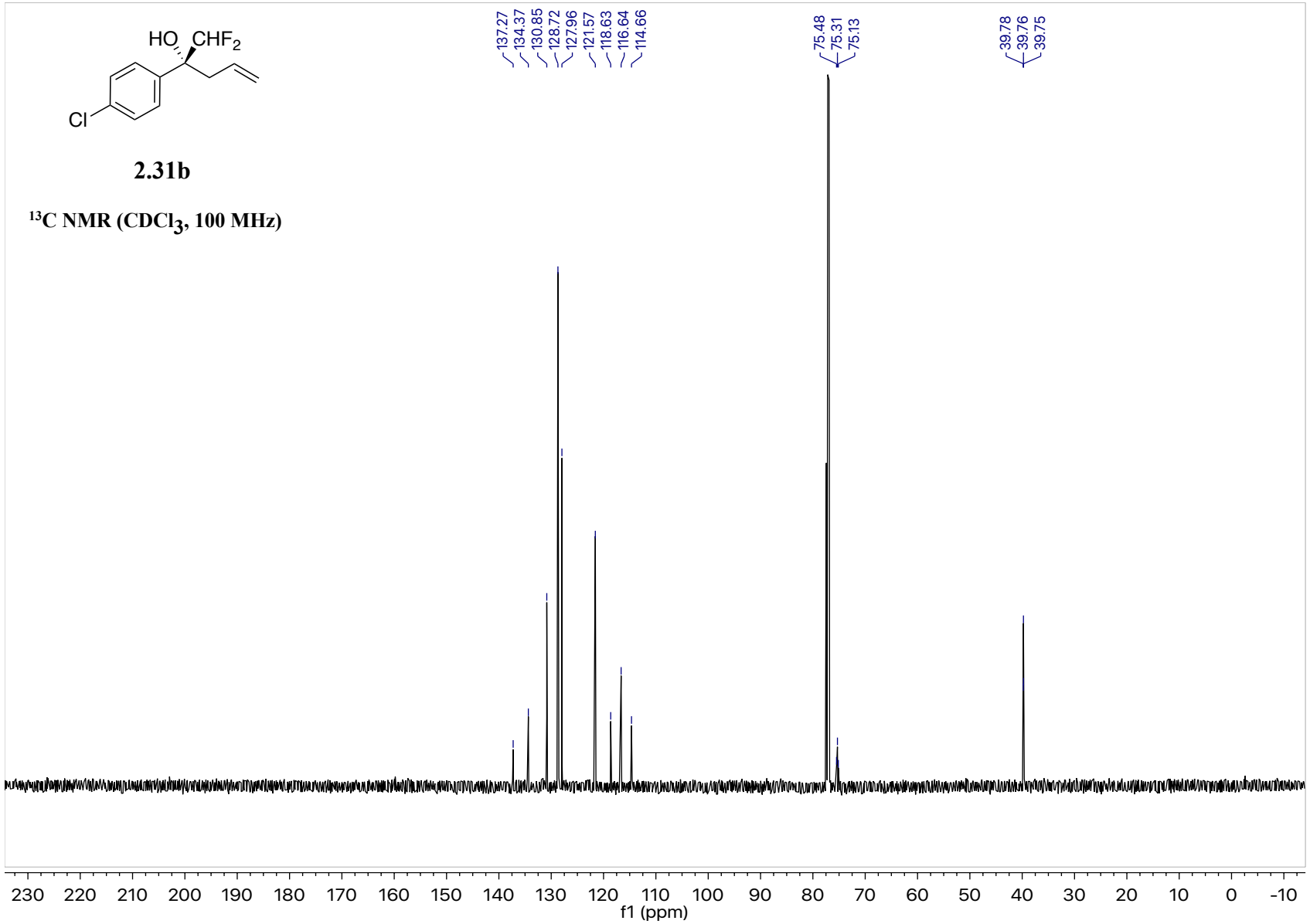

2.31b

^{13}C NMR ($CDCl_3$, 100 MHz)

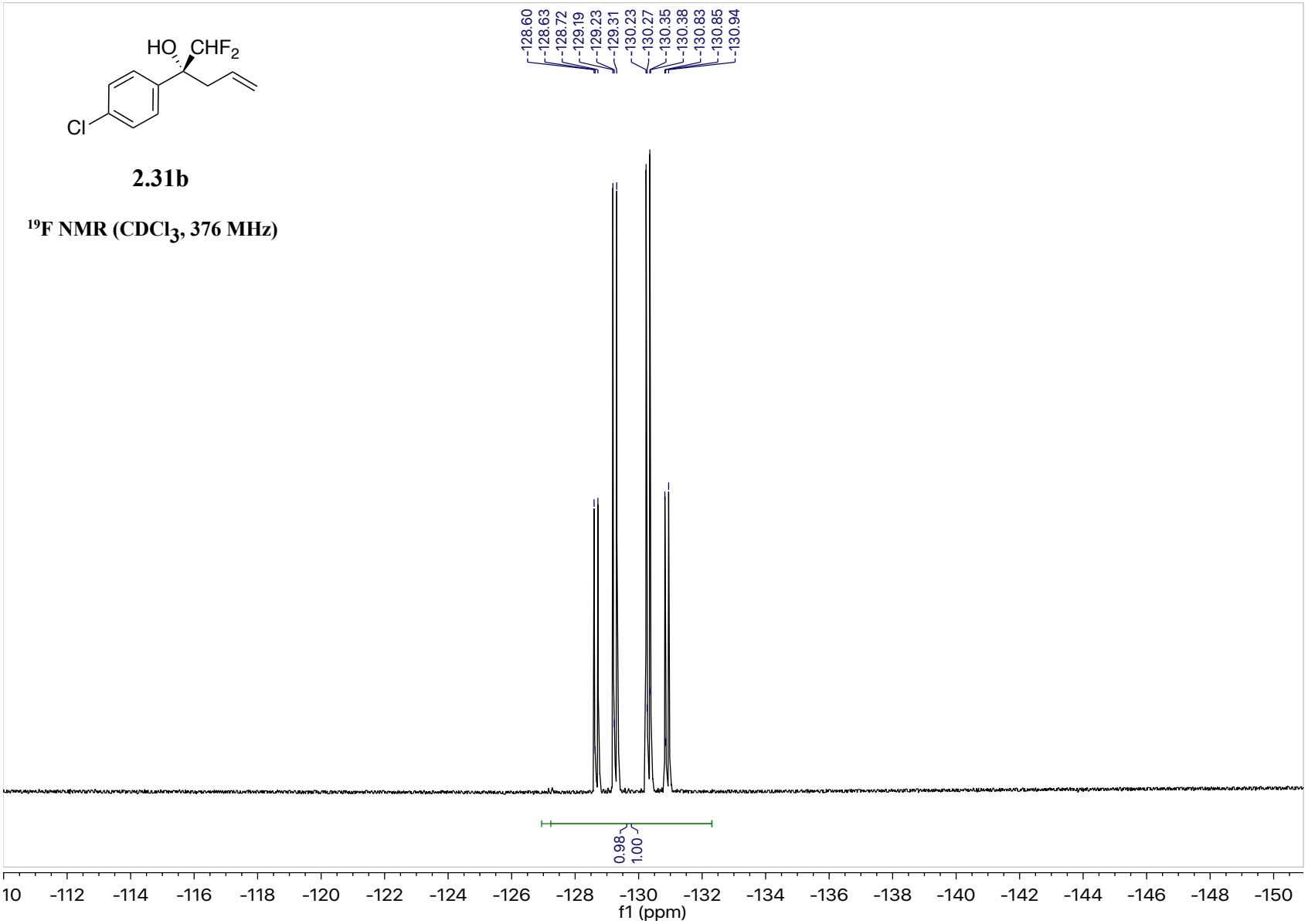

2.31b

^{19}F NMR ($CDCl_3$, 376 MHz)

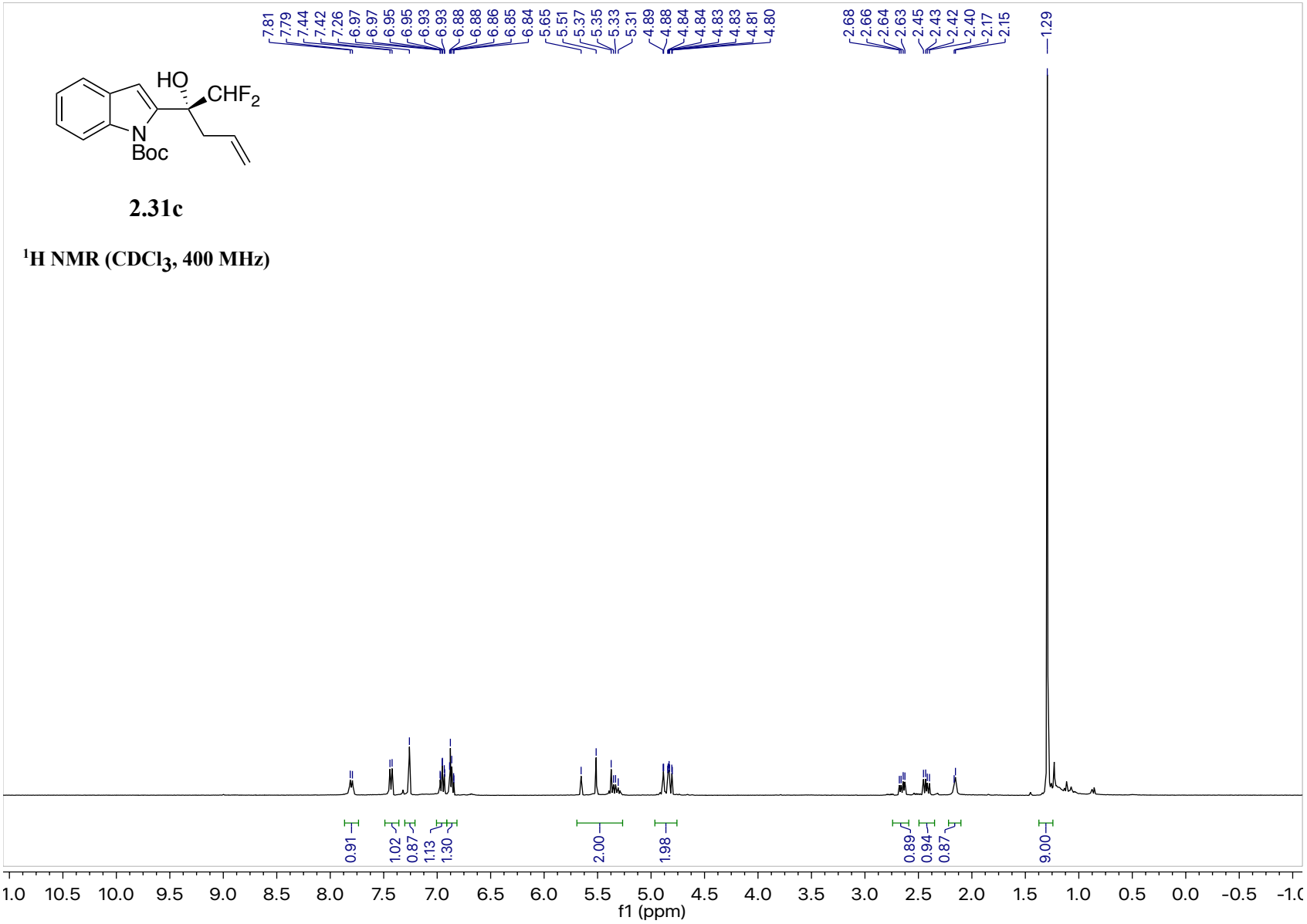

2.31c

^{1}H NMR ($CDCl_3$, 400 MHz)

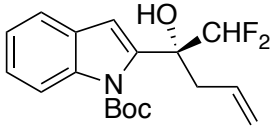

2.31c

^{13}C NMR ($CDCl_3$, 100 MHz)

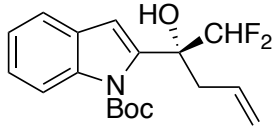

2.31c

^{19}F NMR ($CDCl_3$, 376 MHz)

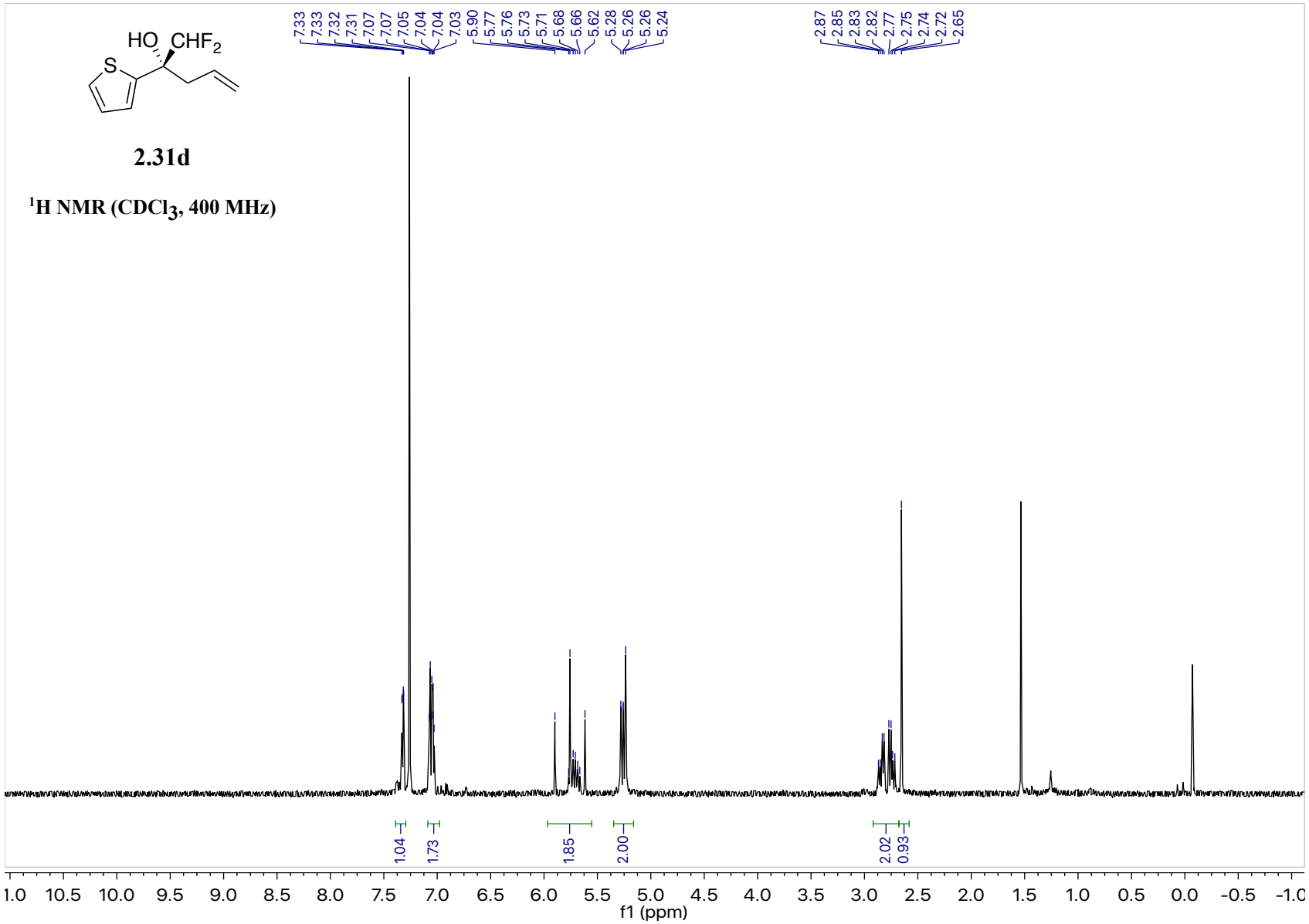
HO
CHF2
S
2.31d
1H NMR (CDCl3, 400 MHz)
7.33
7.33
7.32
7.31
7.07
7.07
7.05
7.04
7.04
7.03
5.90
5.77
5.76
5.73
5.71
5.68
5.66
5.62
5.28
5.26
5.26
5.24
2.87
2.85
2.83
2.82
2.77
2.75
2.74
2.72
2.65
1.04
1.73
1.85
2.00
2.02
0.93
f1 (ppm)

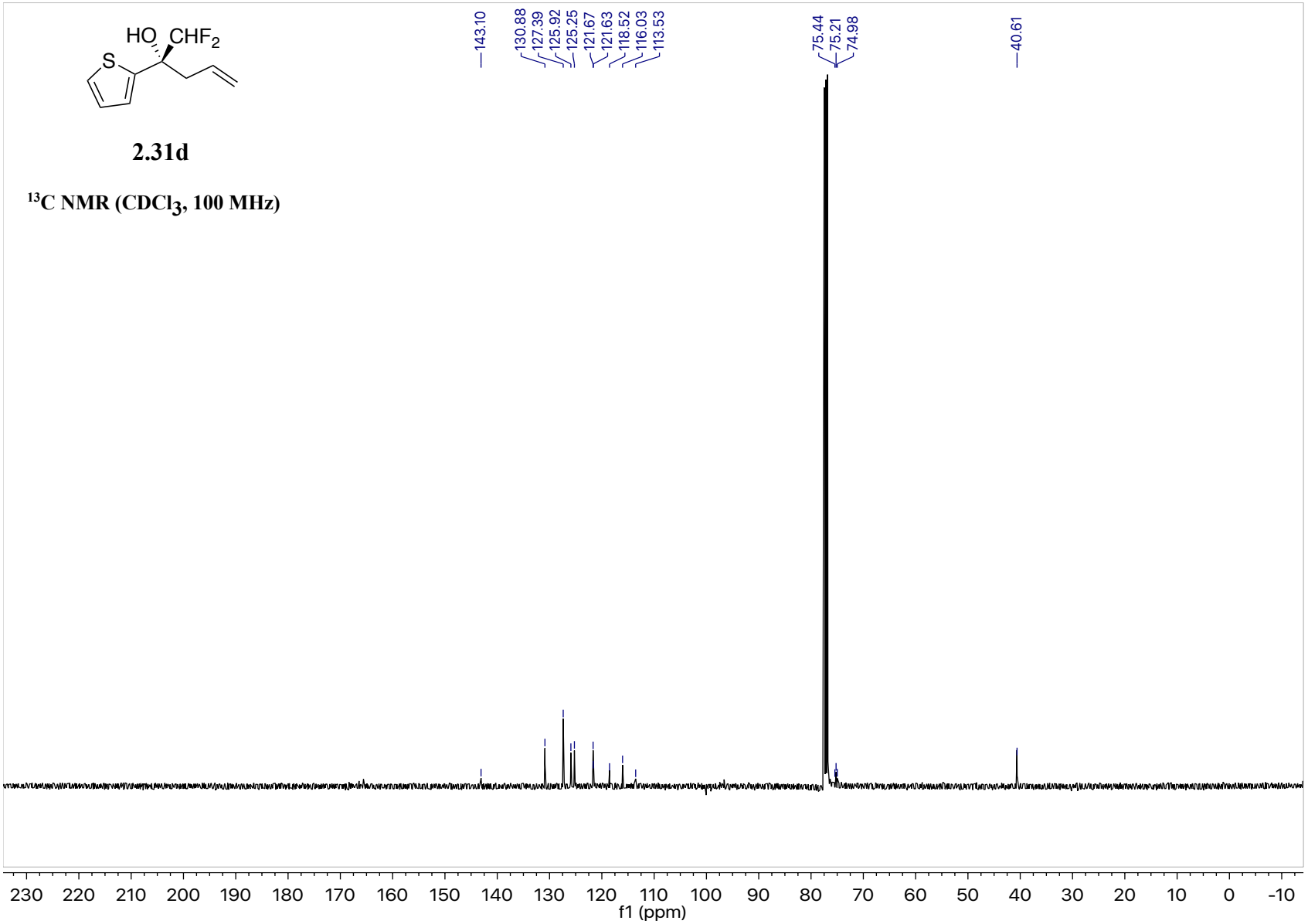

2.31d

^{13}C NMR ($CDCl_3$, 100 MHz)

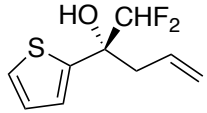

2.31d

^{19}F NMR ($CDCl_3$, 376 MHz)

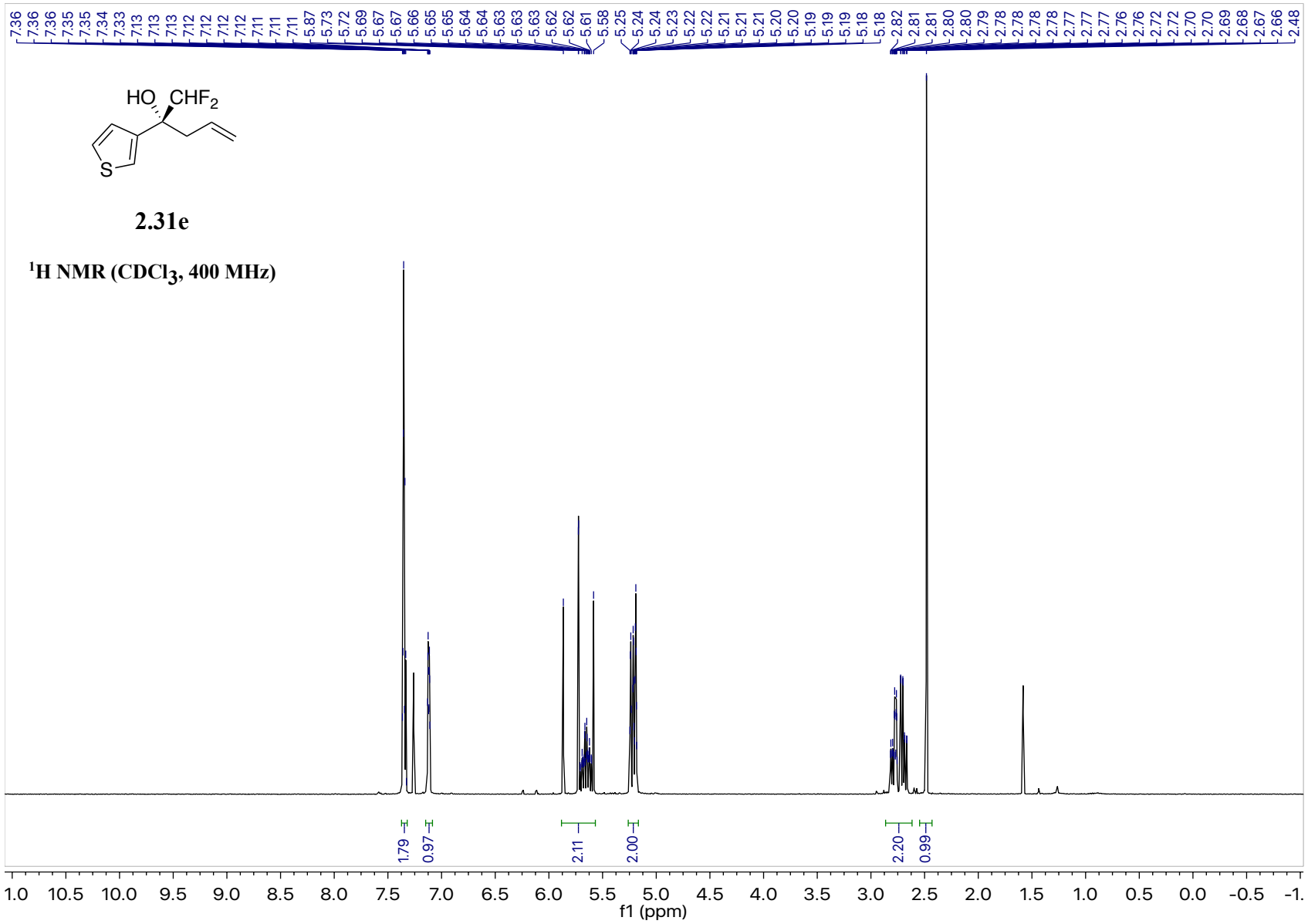
HO
CHF2
S
2.31e
1H NMR (CDCl3, 400 MHz)
1.79
0.97
2.11
2.00
2.20
0.99
f1 (ppm)

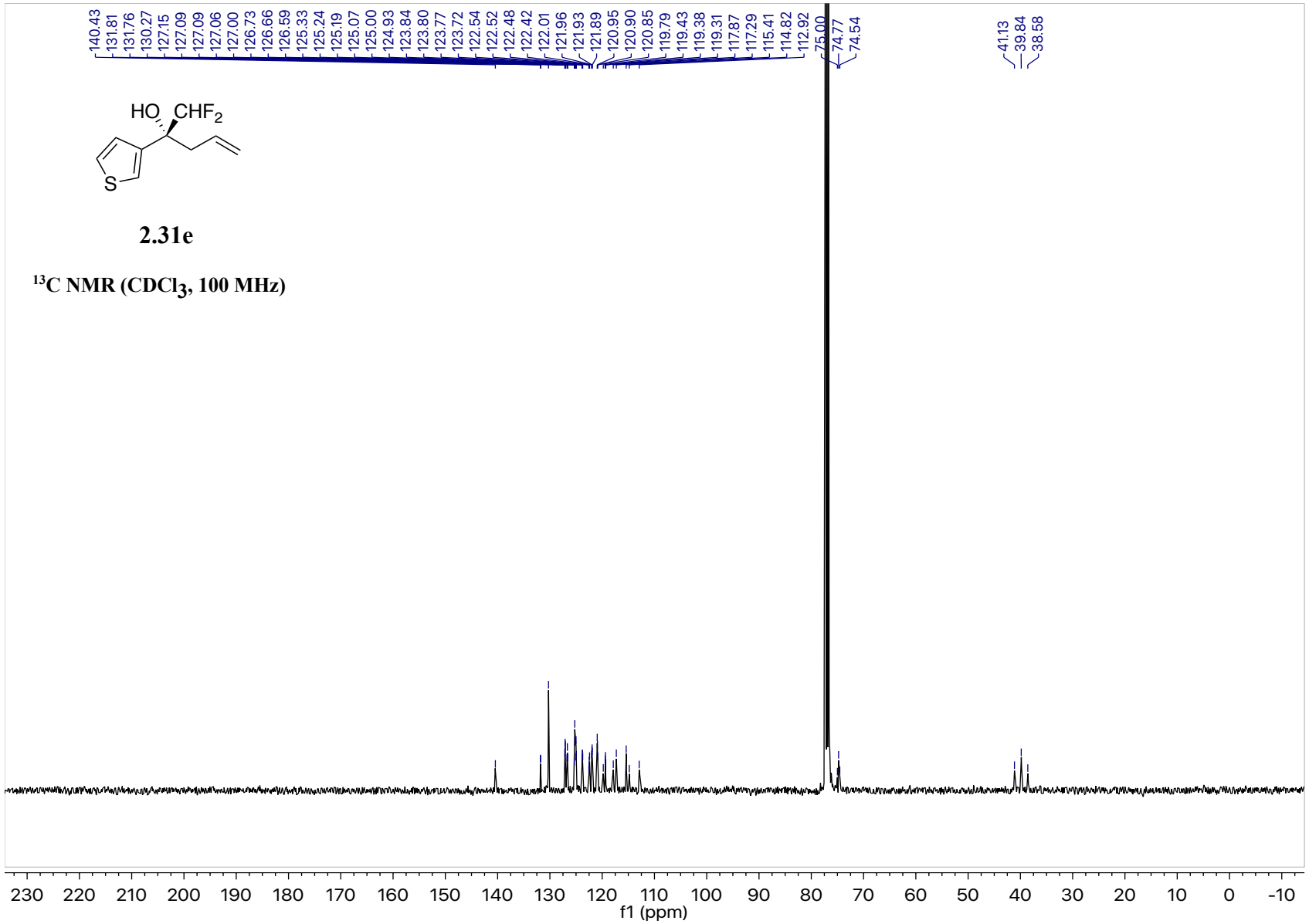

2.31e

^{13}C NMR ($CDCl_3$, 100 MHz)

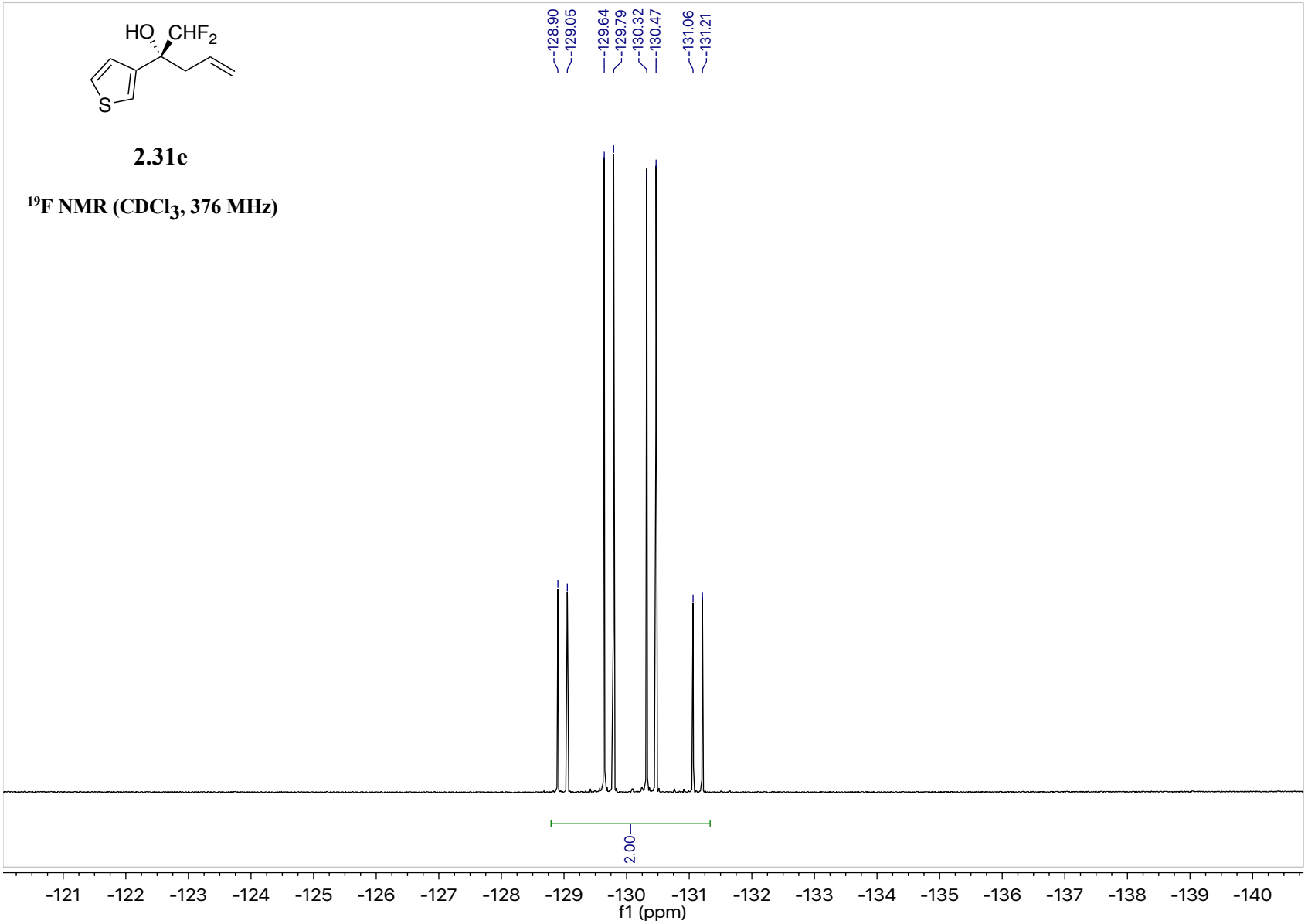

2.31e

^{19}F NMR ($CDCl_3$, 376 MHz)

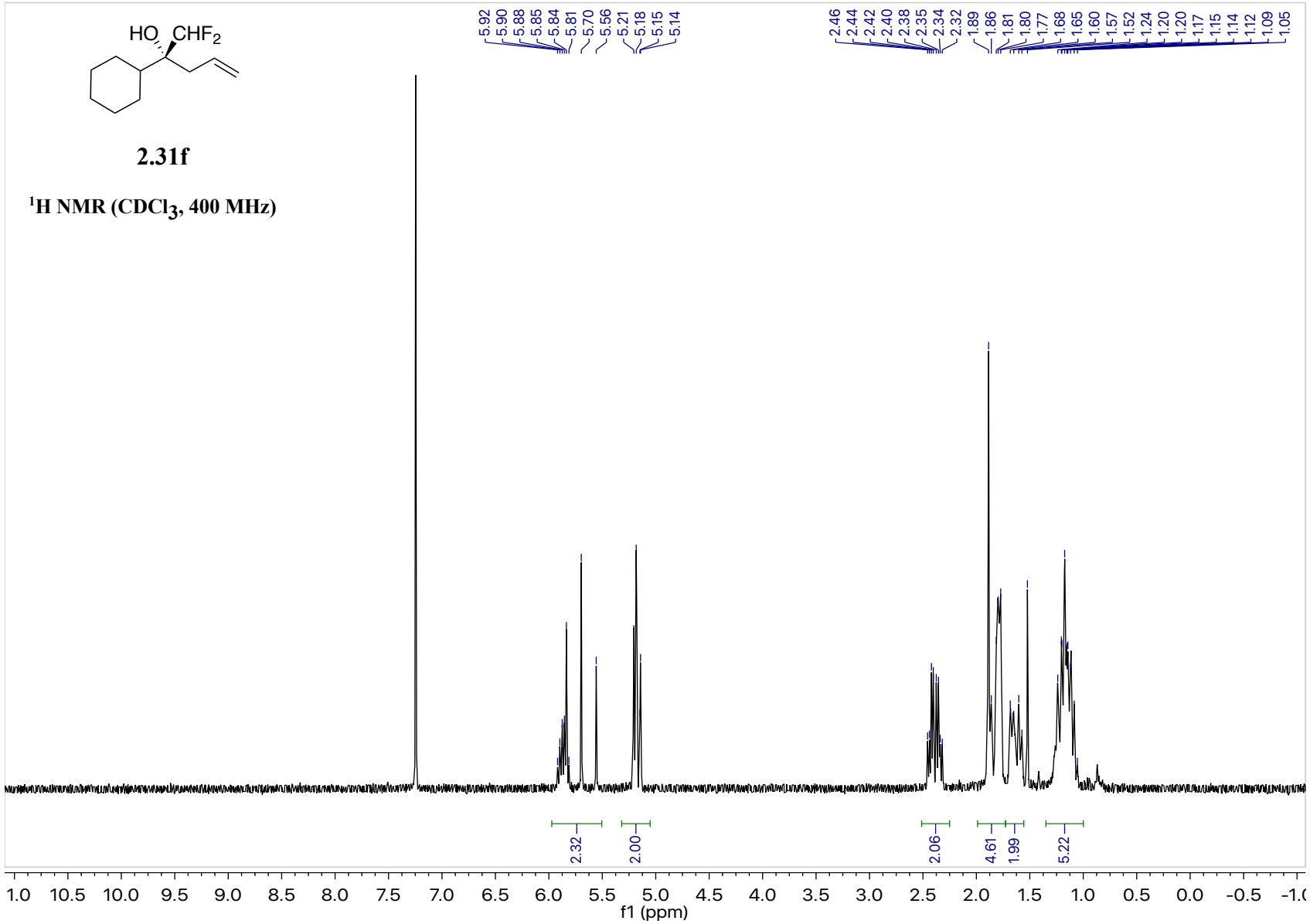

2.31f

^{1}H NMR ($CDCl_3$, 400 MHz)

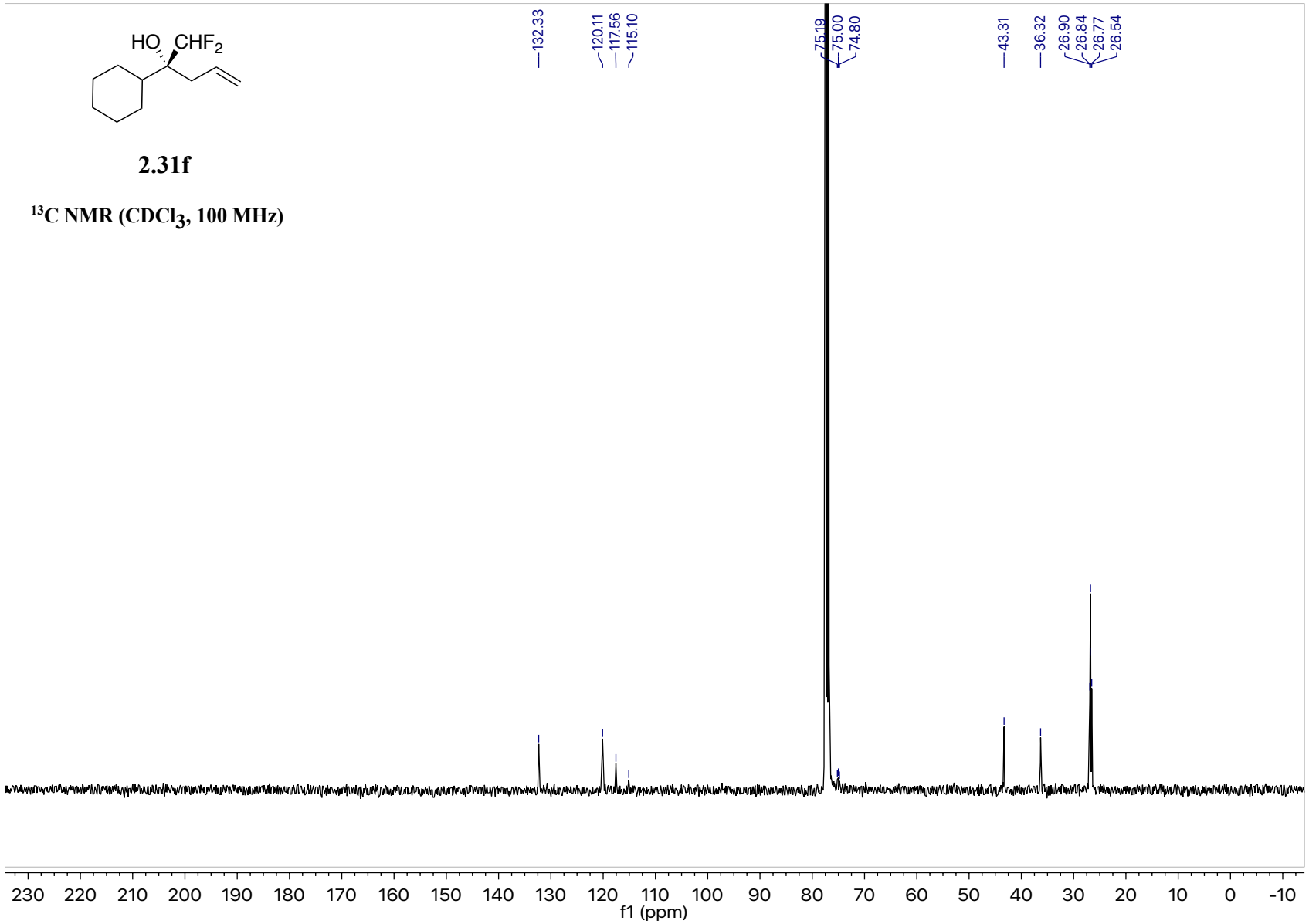

2.31f

^{13}C NMR ($CDCl_3$, 100 MHz)

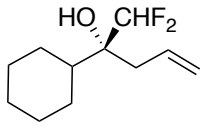

2.31f

^{19}F NMR ($CDCl_3$, 376 MHz)

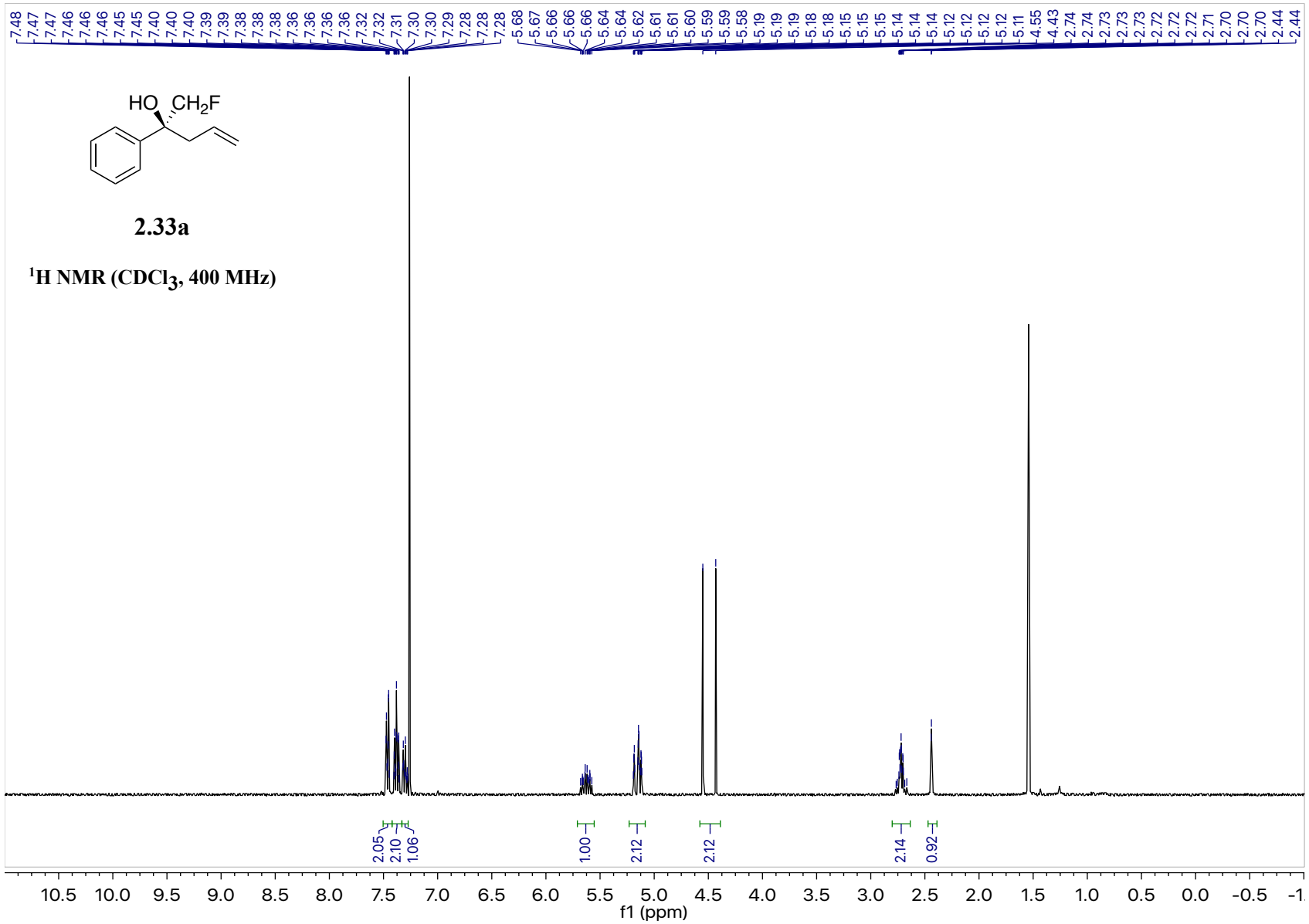
HO
CH2F
2.33a
1H NMR (CDCl3, 400 MHz)
2.05
2.10
1.06
1.00
2.12
2.12
2.14
0.92
f1 (ppm)

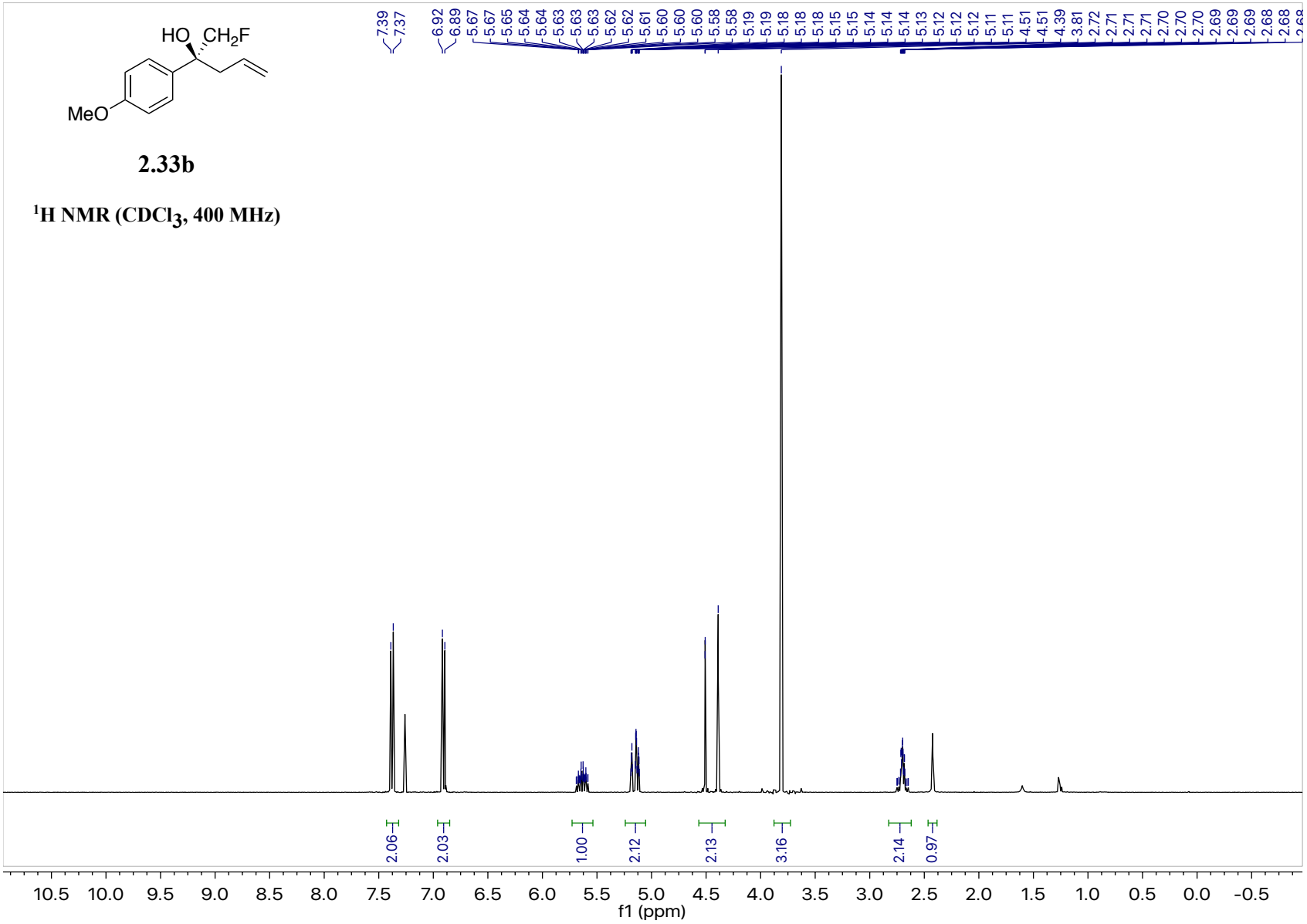
HO
CH2F
MeO
2.33b
1H NMR (CDCl3, 400 MHz)
7.39
7.37
6.92
6.89
5.67
5.67
5.65
5.64
5.64
5.63
5.63
5.63
5.62
5.62
5.61
5.60
5.60
5.60
5.58
5.58
5.19
5.19
5.18
5.18
5.18
5.15
5.15
5.14
5.14
5.14
5.13
5.12
5.12
5.12
5.11
5.11
4.51
4.51
4.39
3.81
2.72
2.71
2.71
2.71
2.70
2.70
2.70
2.69
2.69
2.69
2.68
2.68
2.06
2.03
1.00
2.12
2.13
3.16
2.14
0.97
10.5
10.0
9.5
9.0
8.5
8.0
7.5
7.0
6.5
6.0
5.5
5.0
4.5
4.0
3.5
3.0
2.5
2.0
1.5
1.0
0.5
0.0
-0.5
f1 (ppm)

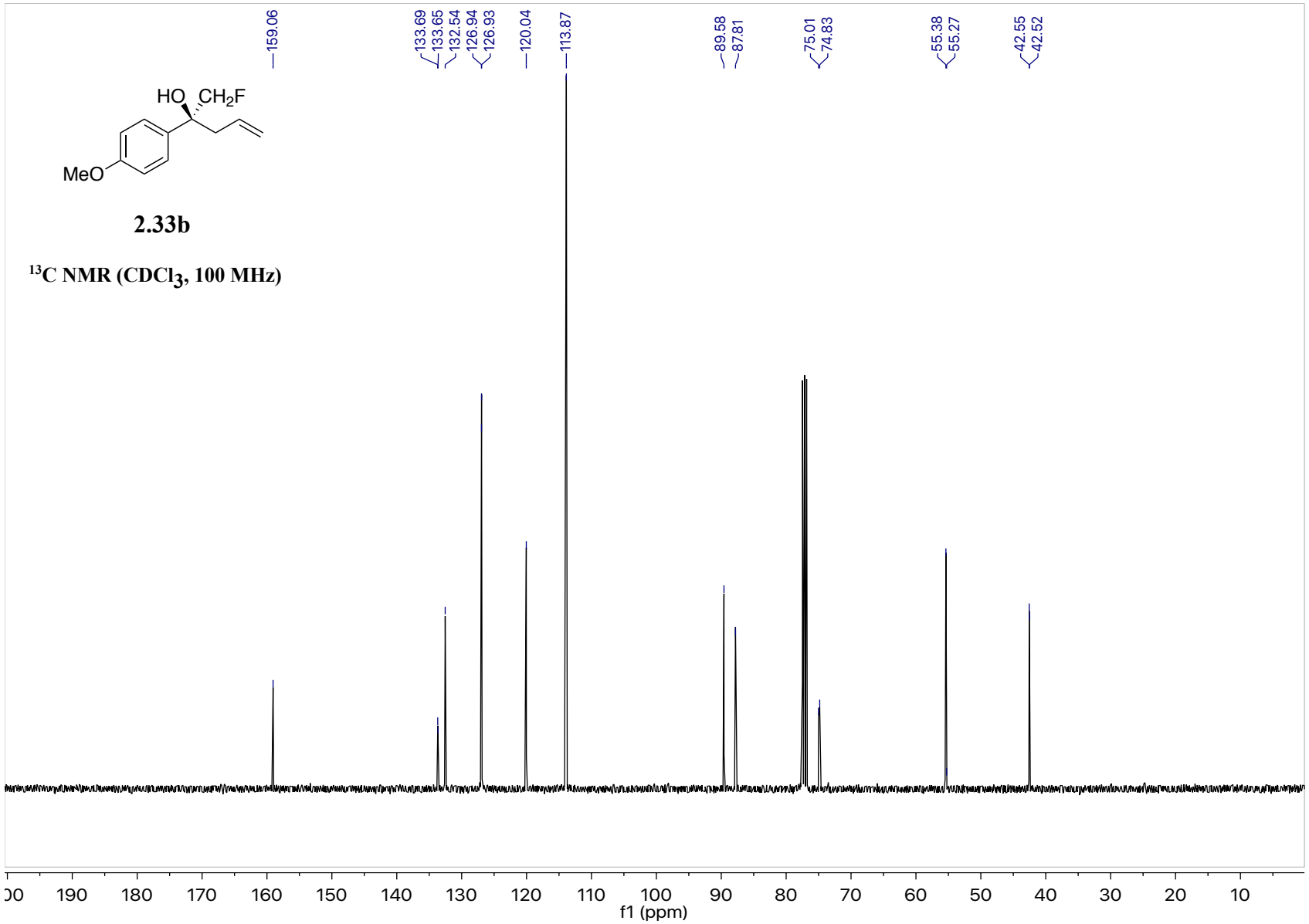
159.06
133.69
133.65
132.54
126.94
126.93
120.04
113.87
89.58
87.81
75.01
74.83
55.38
55.27
42.55
42.52
HO
CH2F
MeO
2.33b
13C NMR (CDCl3, 100 MHz)
f1 (ppm)

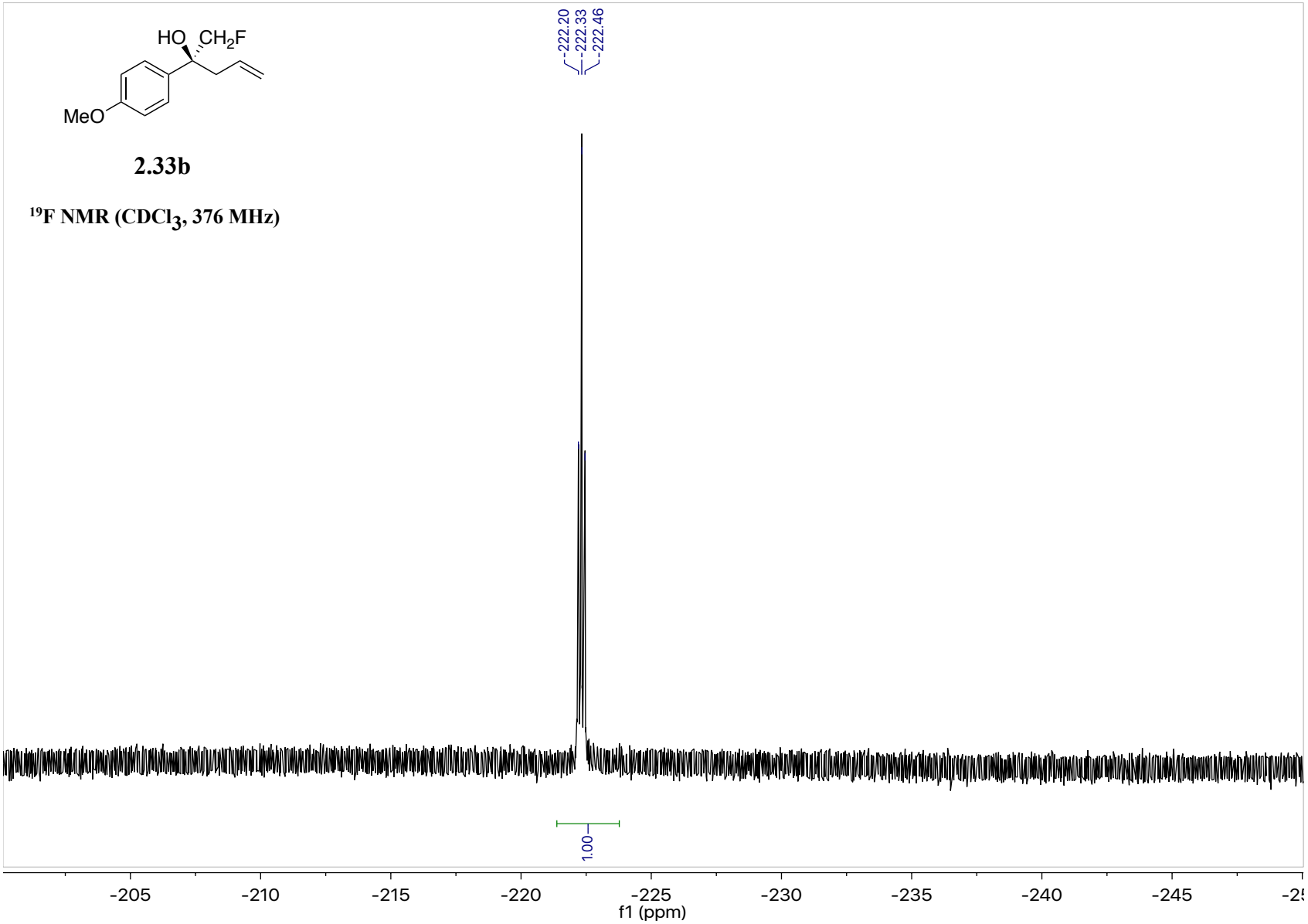
HO
CH2F
MeO
2.33b
19F NMR (CDCl3, 376 MHz)
-222.20
-222.33
-222.46
1.00
-205
-210
-215
-220
-225
-230
-235
-240
-245
f1 (ppm)

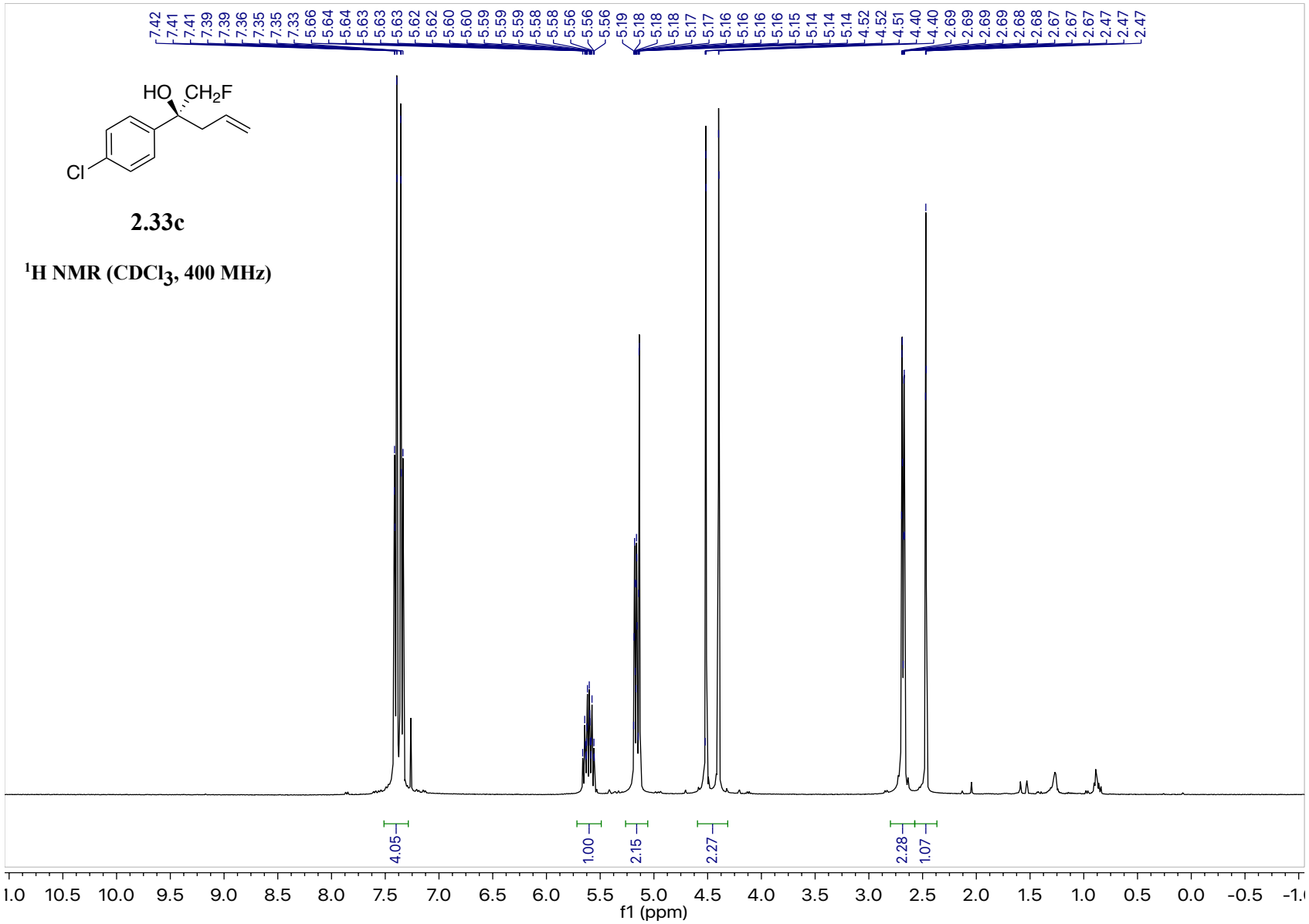
HO
CH2F
Cl
2.33c
1H NMR (CDCl3, 400 MHz)
7.42 7.41 7.41 7.39 7.39 7.36 7.35 7.35 7.33 5.66 5.64 5.64 5.63 5.63 5.62 5.62 5.60 5.60 5.59 5.59 5.59 5.58 5.58 5.56 5.56 5.56 5.19 5.18 5.18 5.18 5.17 5.17 5.16 5.16 5.16 5.15 5.14 5.14 5.14 4.52 4.52 4.51 4.40 4.40 2.69 2.69 2.69 2.68 2.68 2.67 2.67 2.67 2.47 2.47 2.47
4.05
1.00
2.15
2.27
2.28
1.07
f1 (ppm)

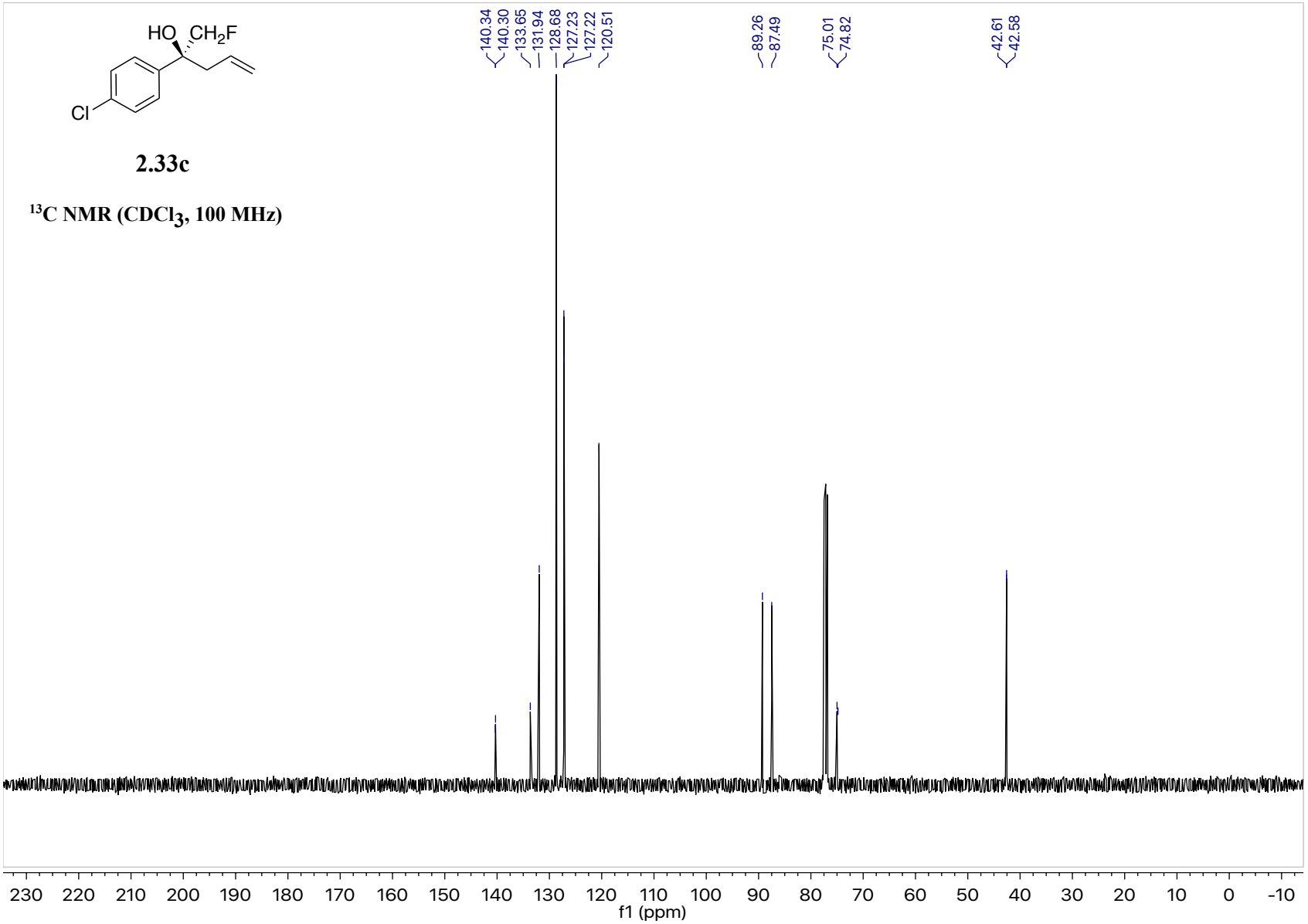

2.33c

^{13}C NMR ($CDCl_3$, 100 MHz)

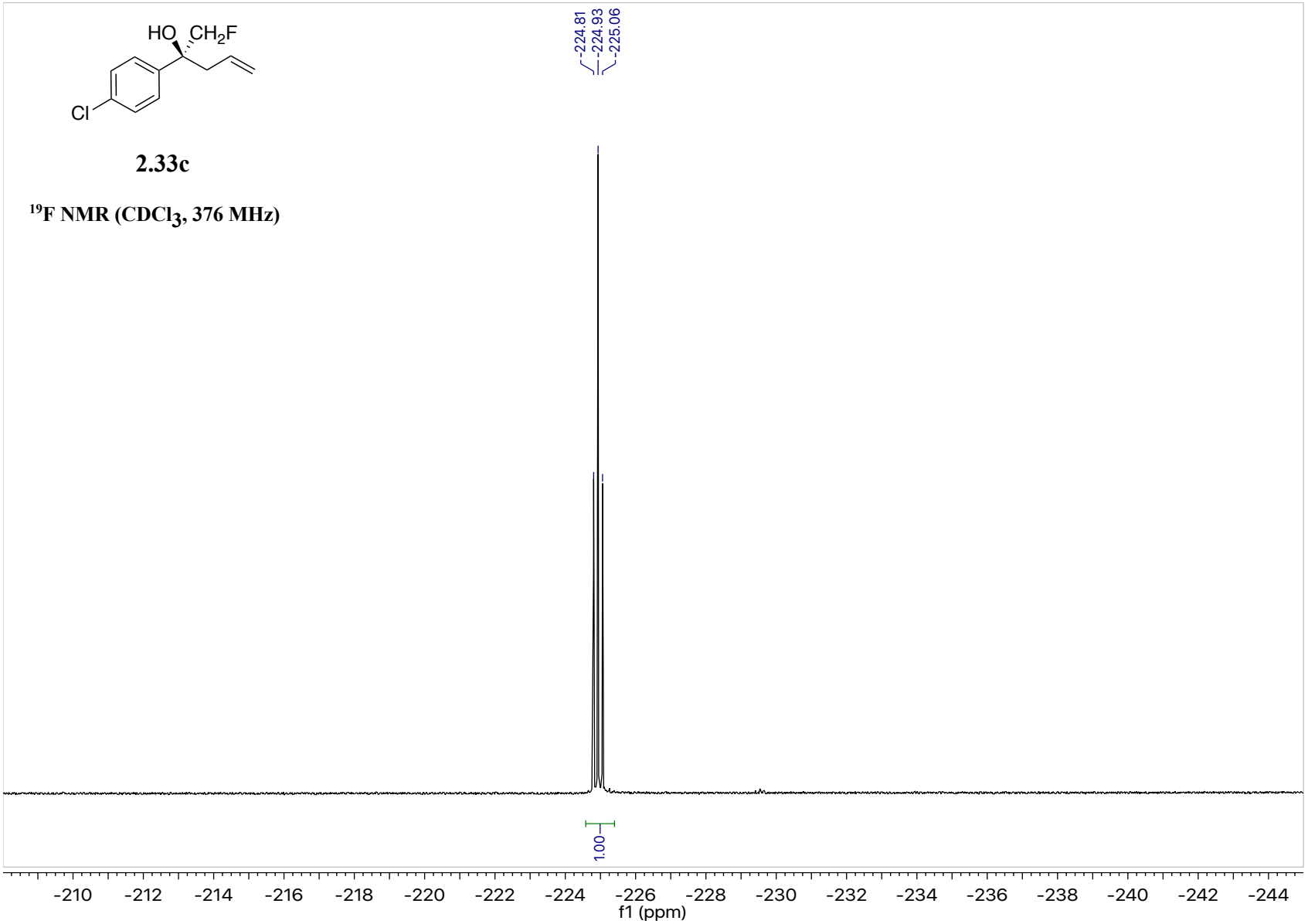

2.33c

^{19}F NMR ($CDCl_3$, 376 MHz)

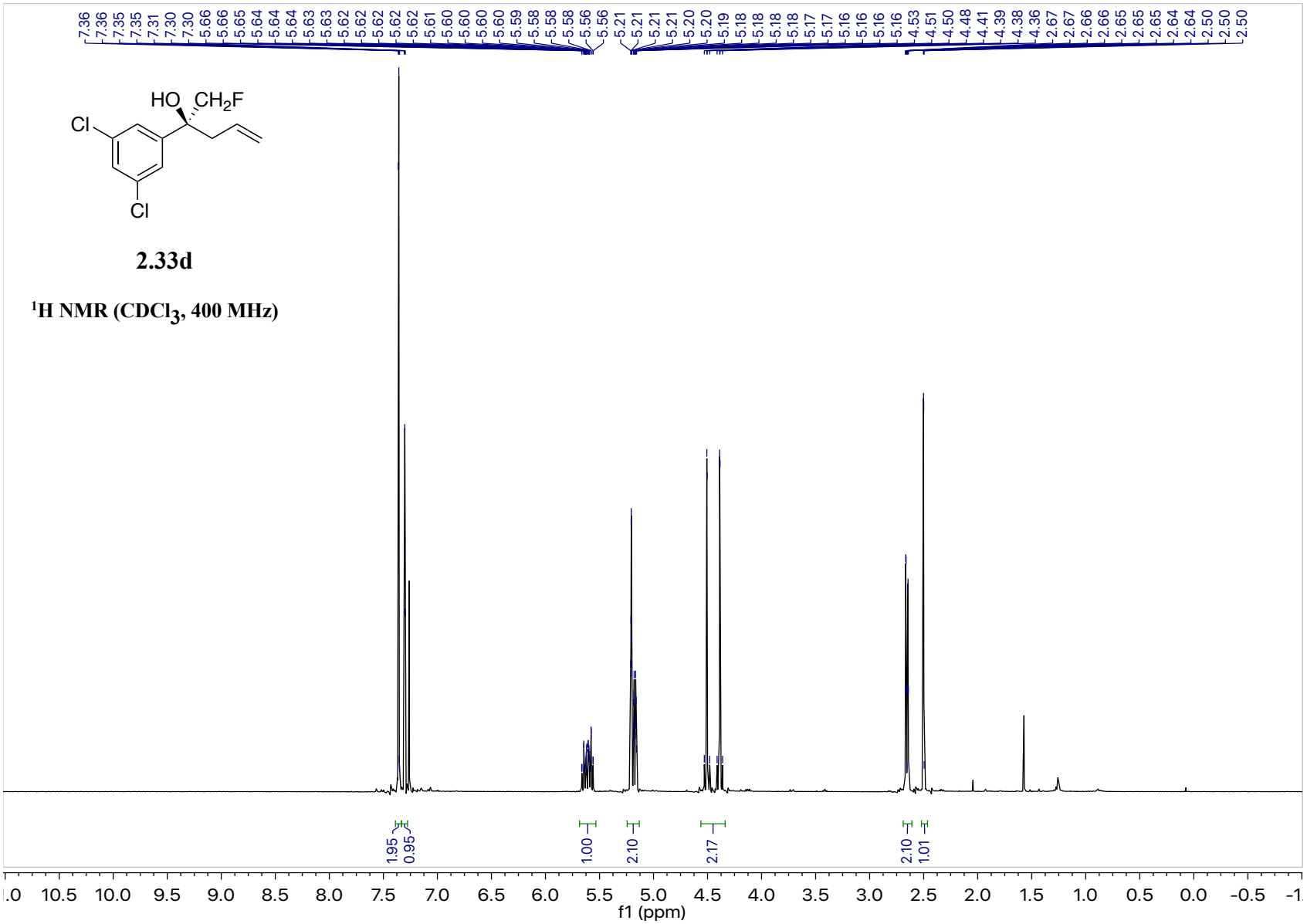
HO
CH2F
Cl
Cl
2.33d
1H NMR (CDCl3, 400 MHz)
f1 (ppm)

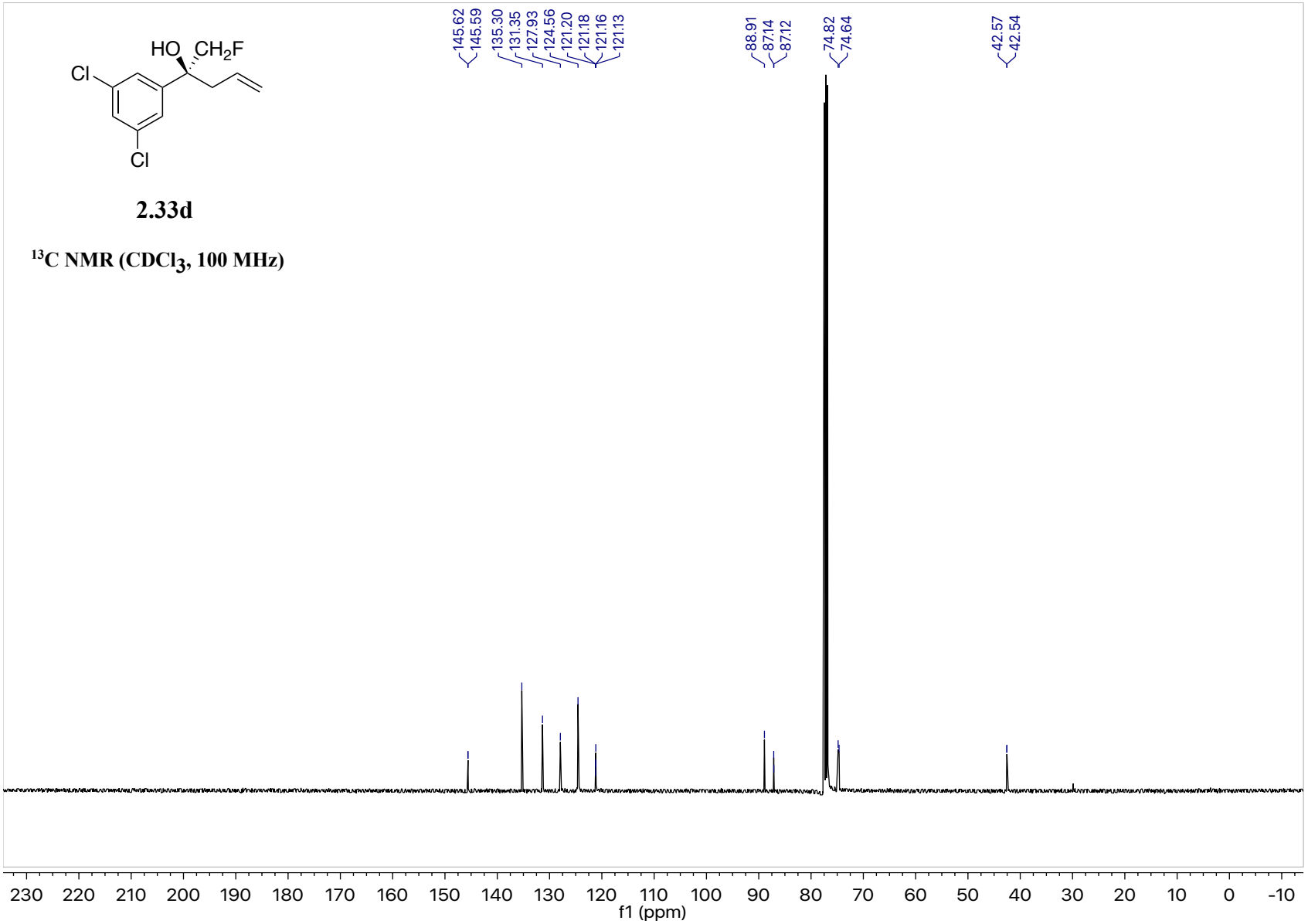

2.33d

^{13}C NMR ($CDCl_3$, 100 MHz)

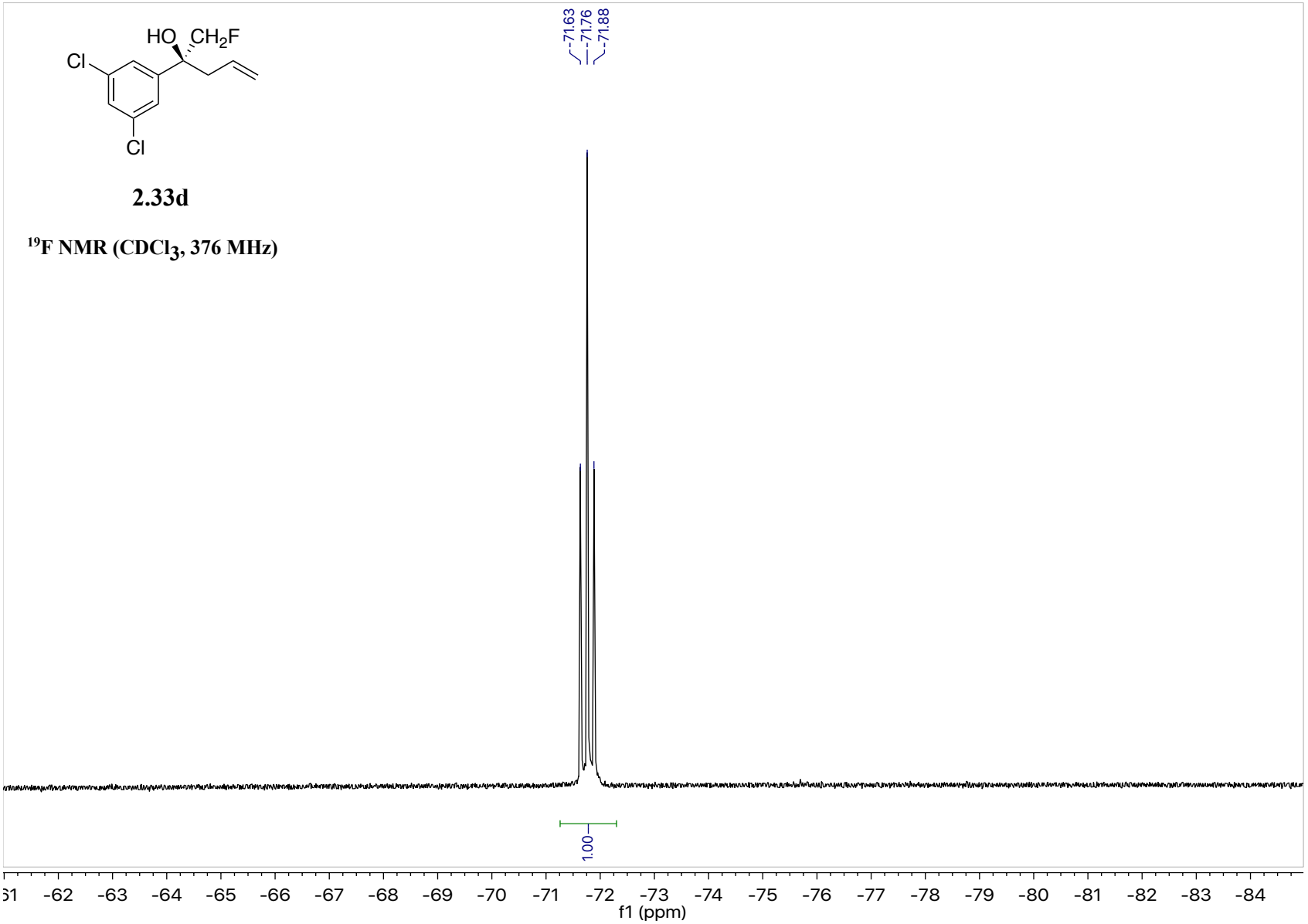

2.33d

^{19}F NMR ($CDCl_3$, 376 MHz)

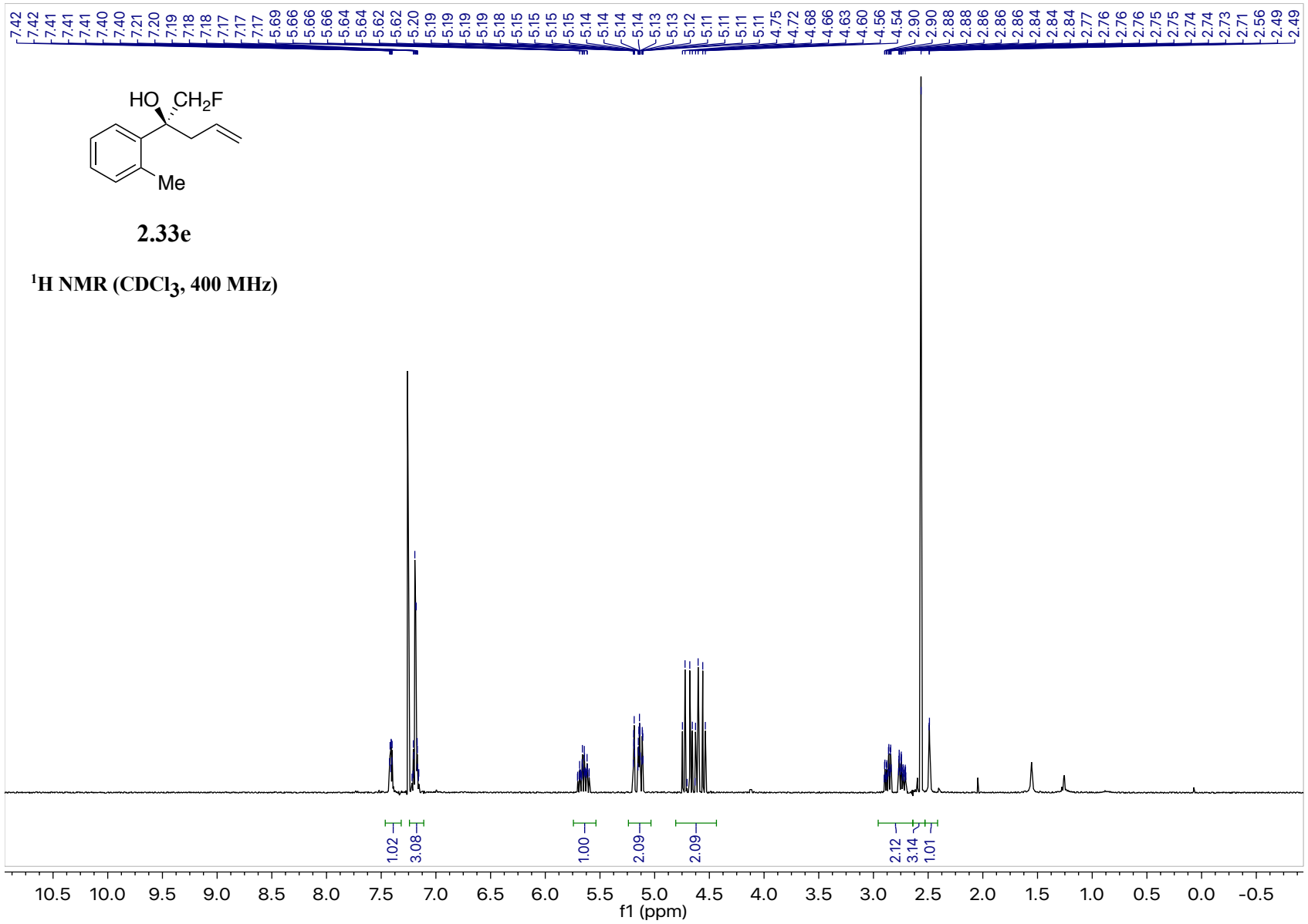

2.33e

^{1}H NMR ($CDCl_3$, 400 MHz)

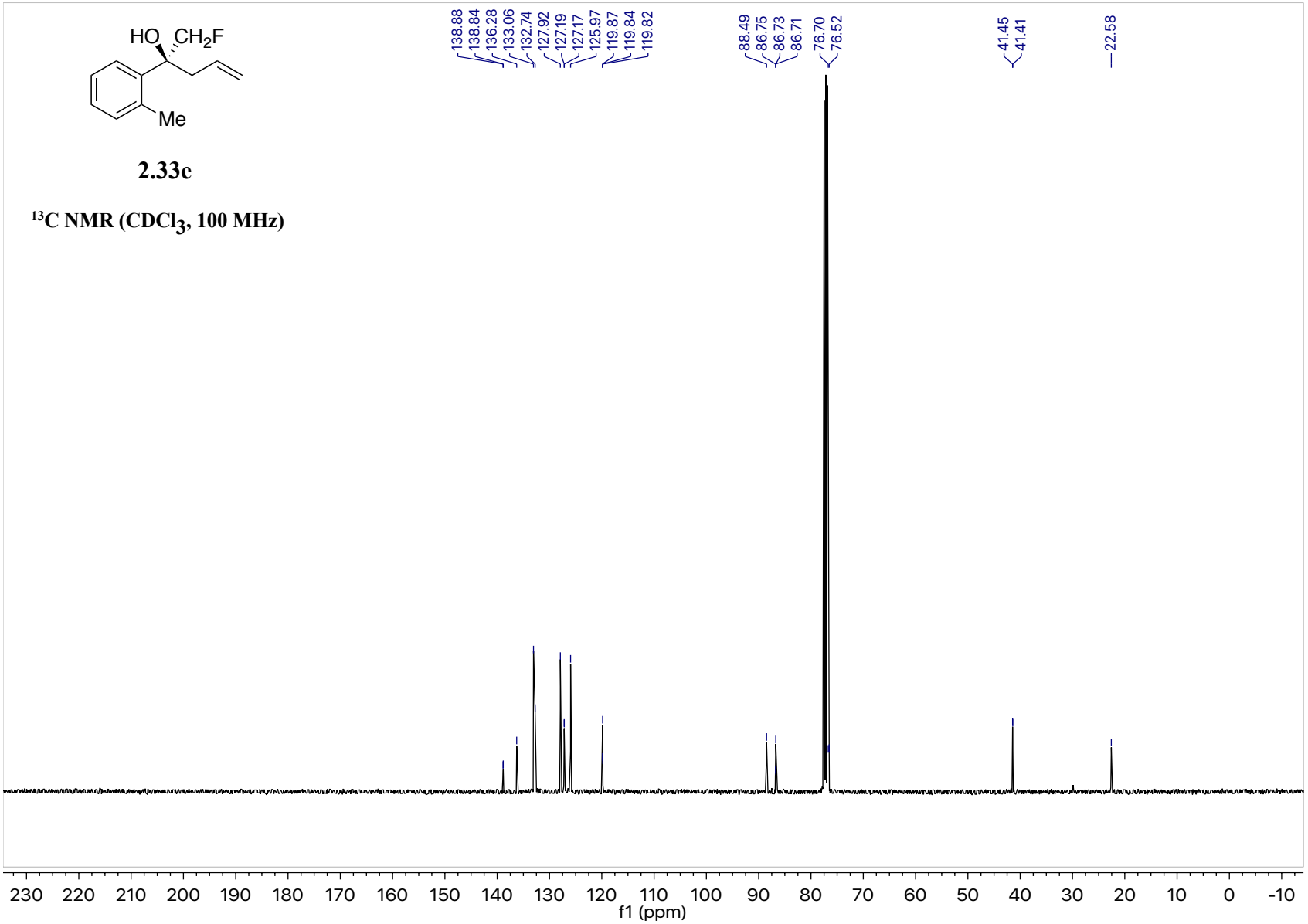

2.33e

^{13}C NMR ($CDCl_3$, 100 MHz)

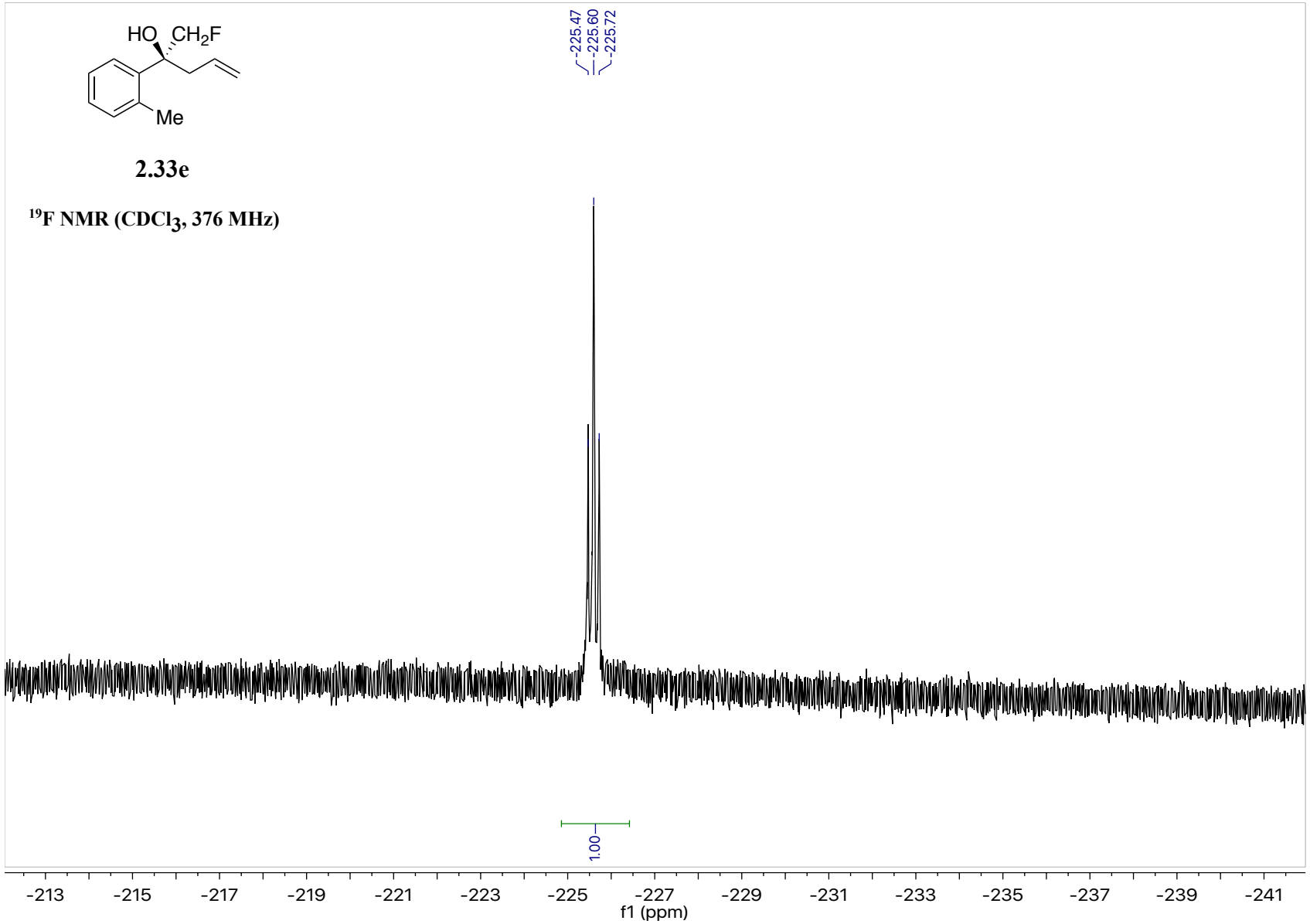

2.33e

^{19}F NMR ($CDCl_3$, 376 MHz)

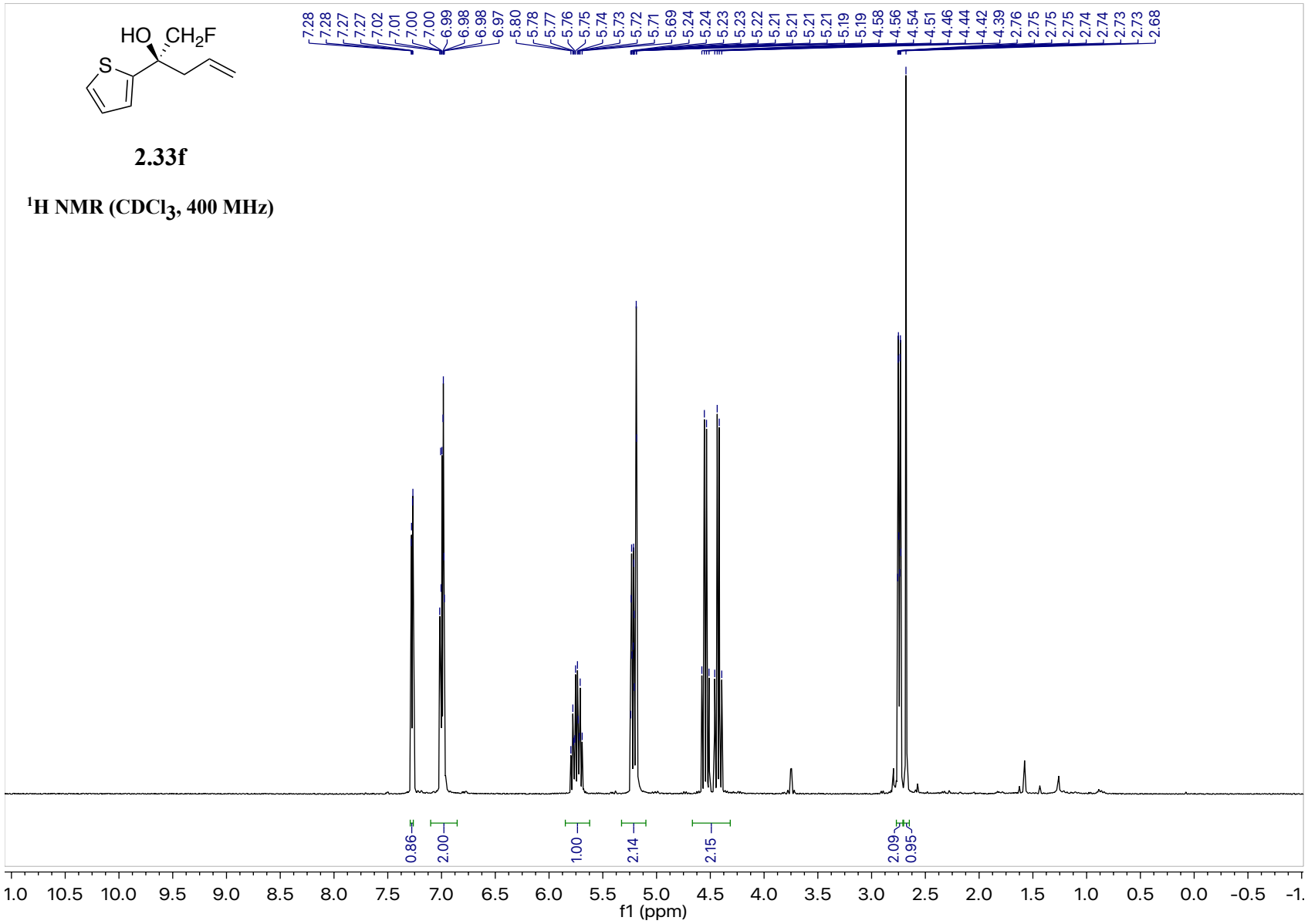
HO
CH2F
S
2.33f
1H NMR (CDCl3, 400 MHz)
7.28 7.28 7.27 7.27 7.02 7.01 7.00 7.00 6.99 6.98 6.98 6.97
5.80 5.78 5.77 5.76 5.75 5.74 5.73 5.72 5.71 5.69 5.24 5.24 5.23 5.22 5.21 5.21 5.21 5.21 5.19 5.19
4.58 4.56 4.54 4.51 4.46 4.44 4.42 4.39
2.76 2.75 2.75 2.75 2.74 2.74 2.73 2.73 2.68
0.86 2.00 1.00 2.14 2.15 2.09 0.95
1.0 10.5 10.0 9.5 9.0 8.5 8.0 7.5 7.0 6.5 6.0 5.5 5.0 4.5 4.0 3.5 3.0 2.5 2.0 1.5 1.0 0.5 0.0 -0.5 -1.
f1 (ppm)

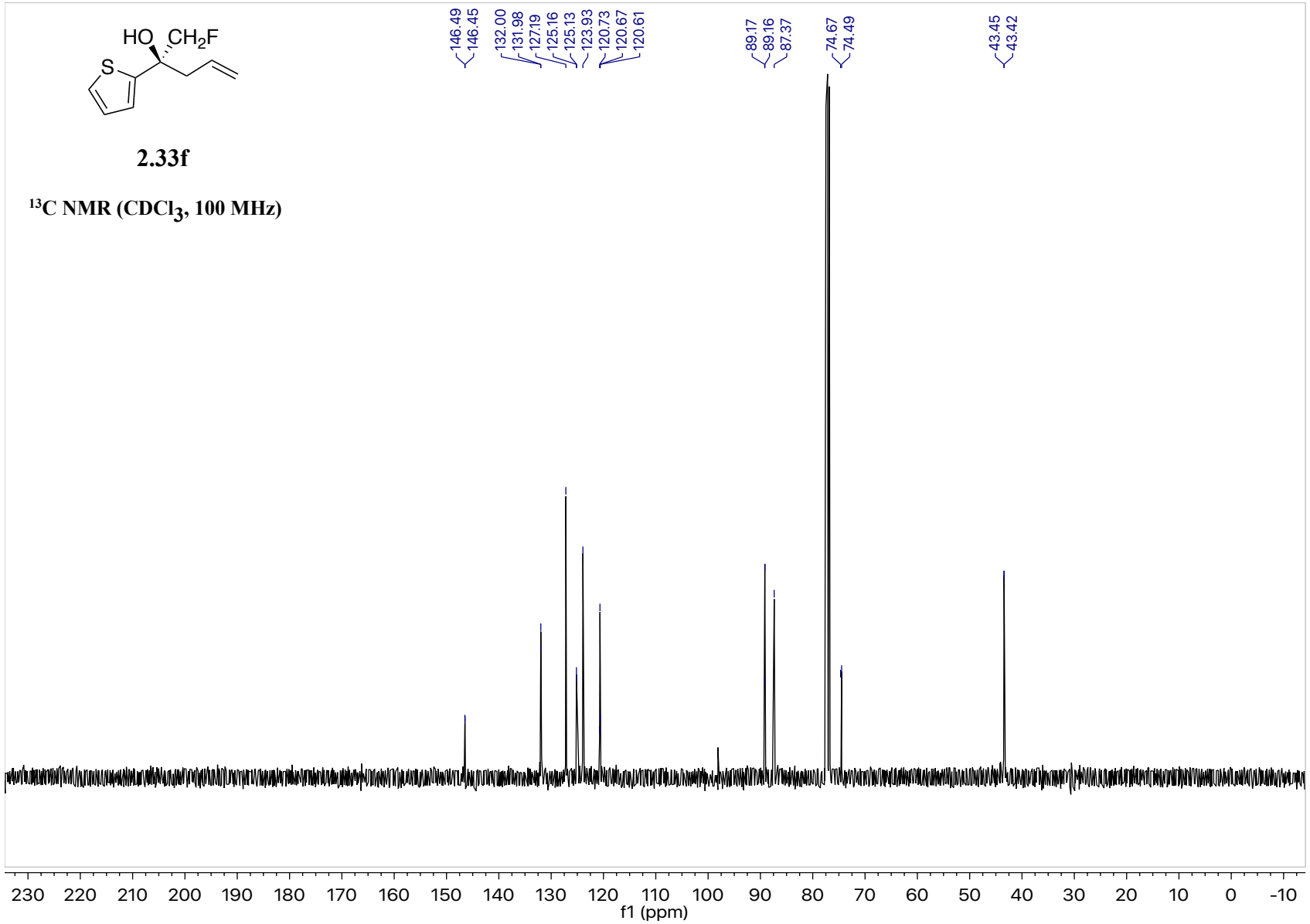
HO
CH2F
S
2.33f
13C NMR (CDCl3, 100 MHz)
146.49
146.45
132.00
131.98
127.19
125.16
125.13
123.93
120.73
120.67
120.61
89.17
89.16
87.37
74.67
74.49
43.45
43.42
230 220 210 200 190 180 170 160 150 140 130 120 110 100 90 80 70 60 50 40 30 20 10 0 -10
f1 (ppm)

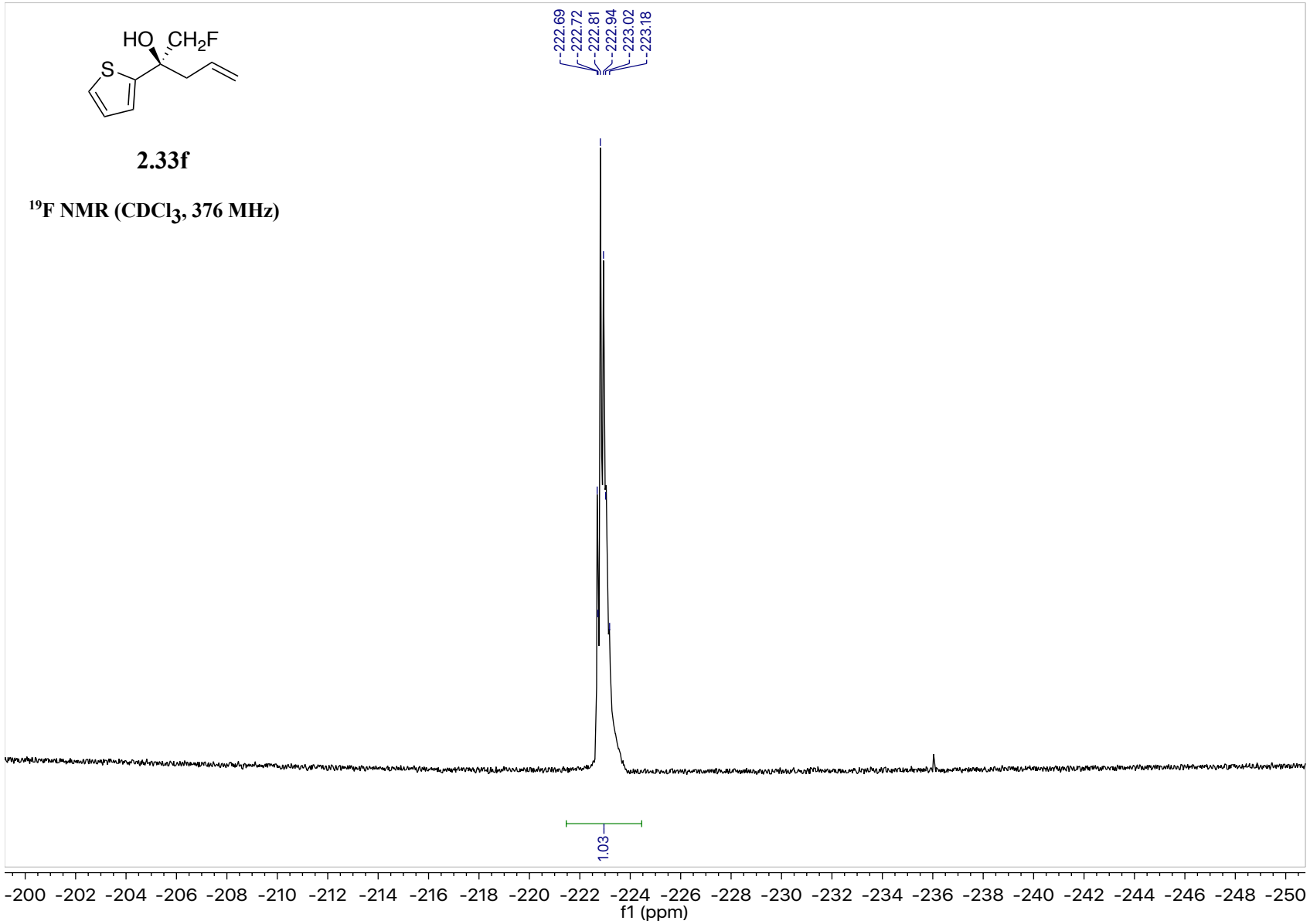
HO
CH2F
S
2.33f
19F NMR (CDCl3, 376 MHz)
-222.69
-222.72
-222.81
-222.94
-223.02
-223.18
1.03
-200 -202 -204 -206 -208 -210 -212 -214 -216 -218 -220 -222 -224 -226 -228 -230 -232 -234 -236 -238 -240 -242 -244 -246 -248 -250
f1 (ppm)

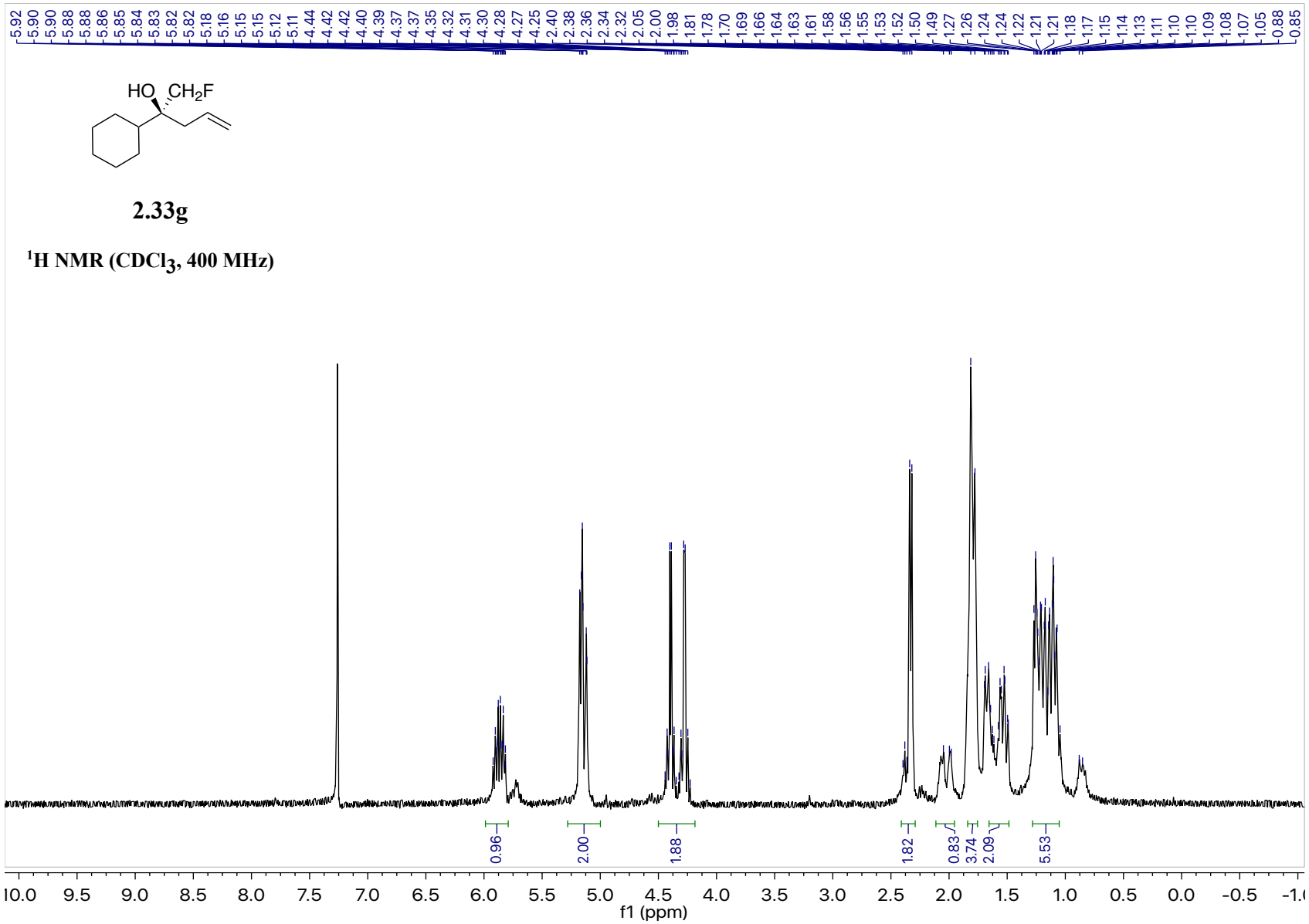

2.33g

^{1}H NMR ($CDCl_3$, 400 MHz)

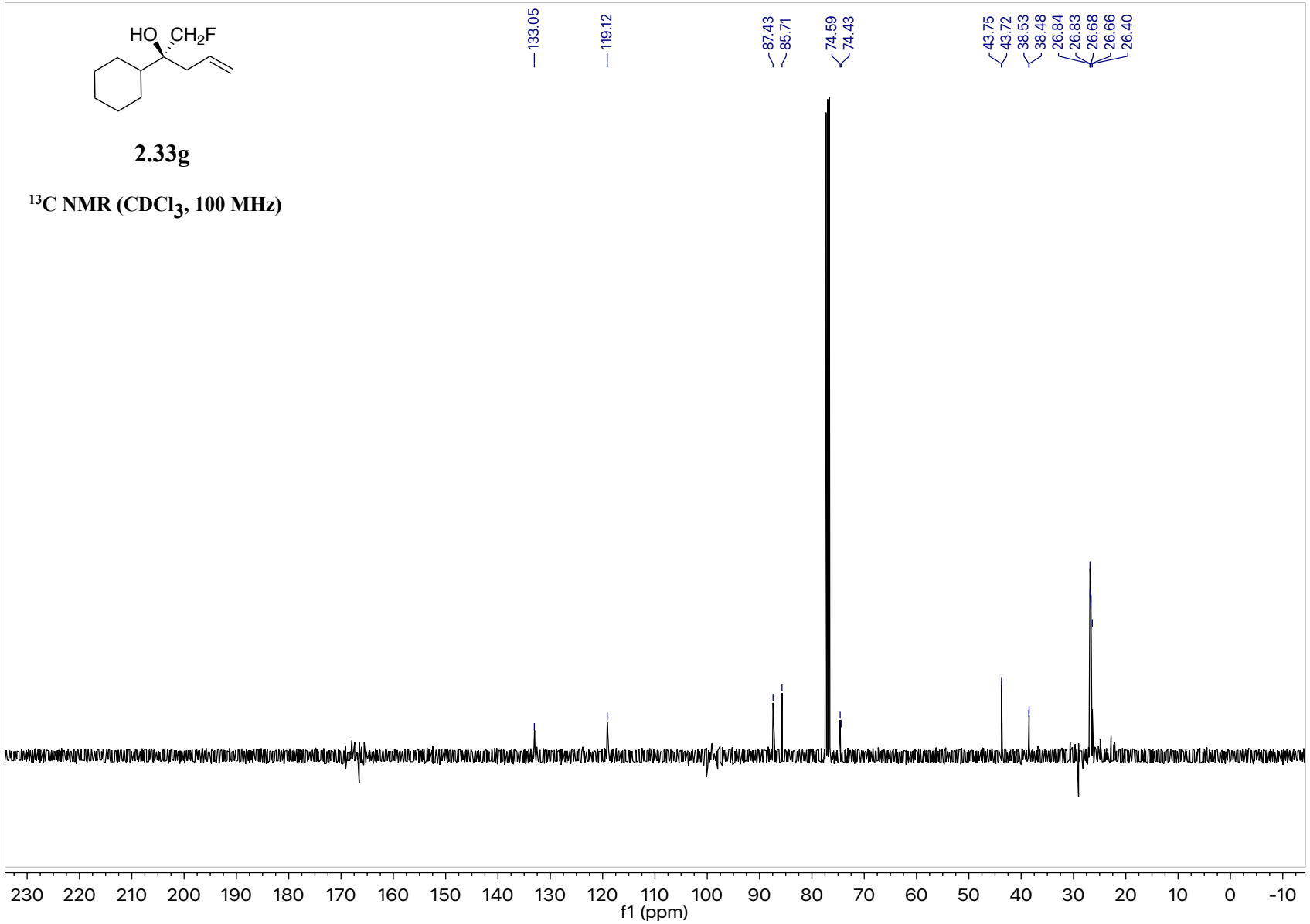
HO
CH2F
2.33g
13C NMR (CDCl3, 100 MHz)
133.05
119.12
87.43
85.71
74.59
74.43
43.75
43.72
38.53
38.48
26.84
26.83
26.68
26.66
26.40
230 220 210 200 190 180 170 160 150 140 130 120 110 100 90 80 70 60 50 40 30 20 10 0 -10
f1 (ppm)

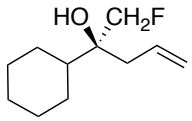

2.33g

^{19}F NMR ($CDCl_3$, 376 MHz)

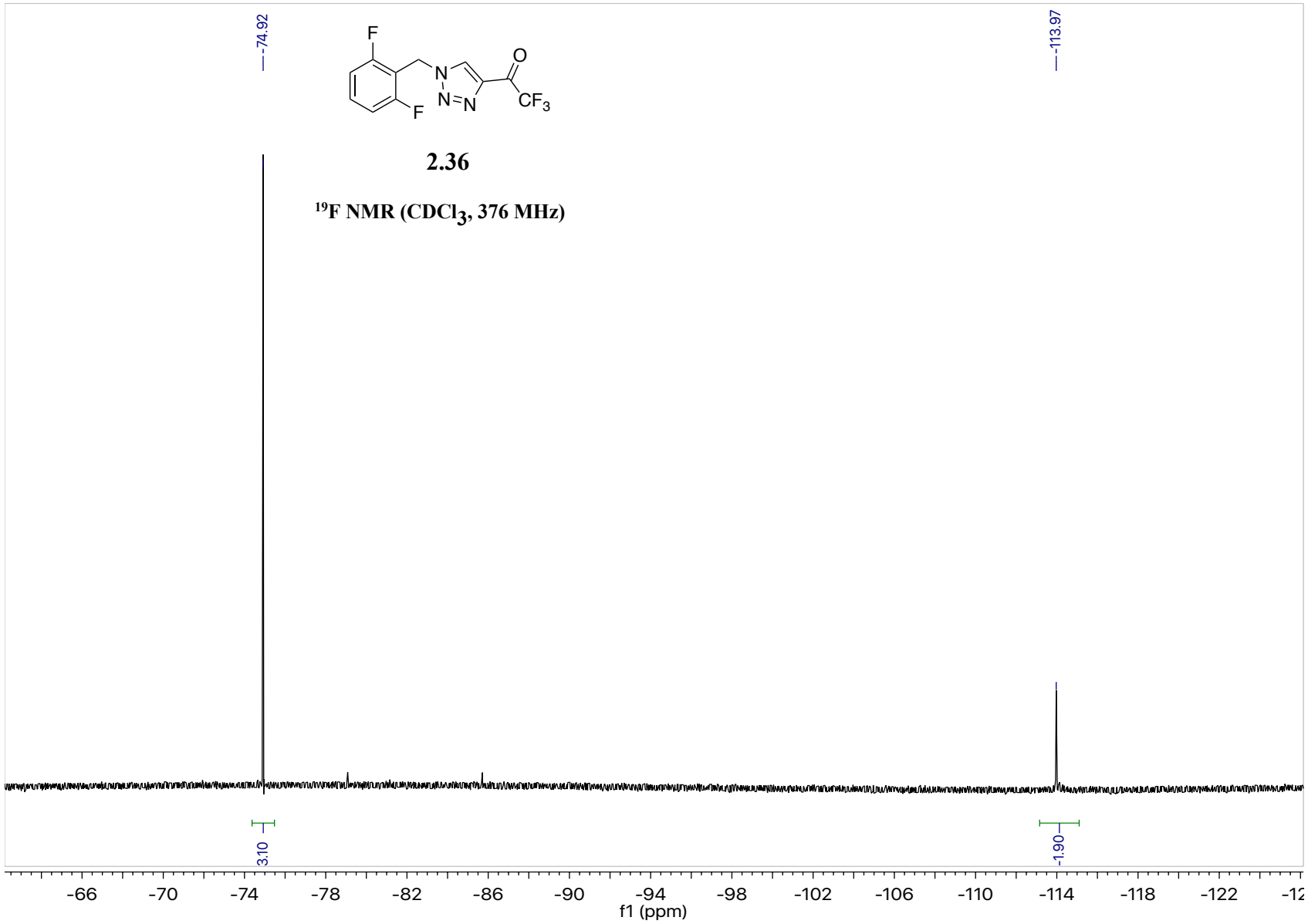

2.36

^{19}F NMR ($CDCl_3$, 376 MHz)

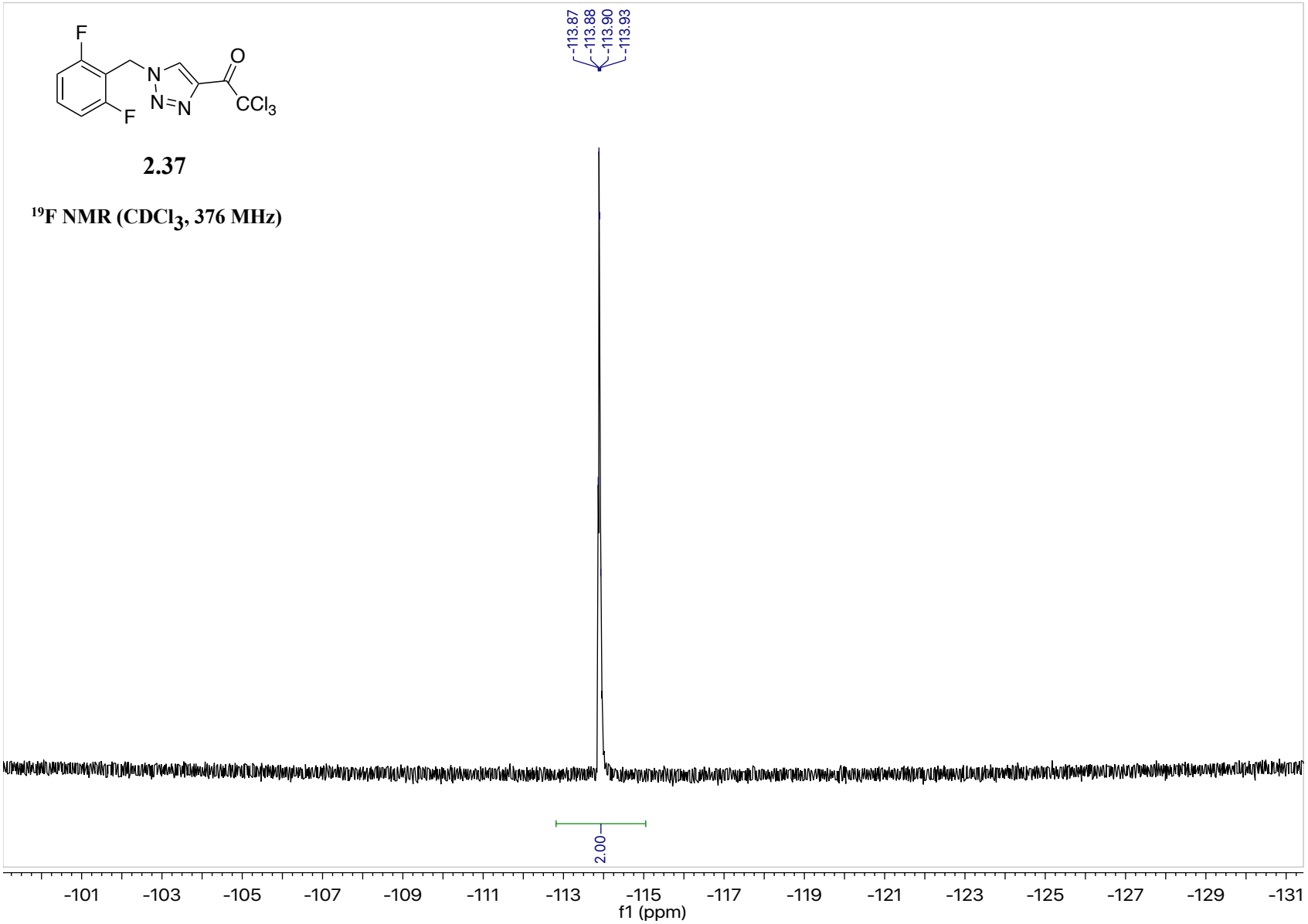

2.37

^{19}F NMR ($CDCl_3$, 376 MHz)

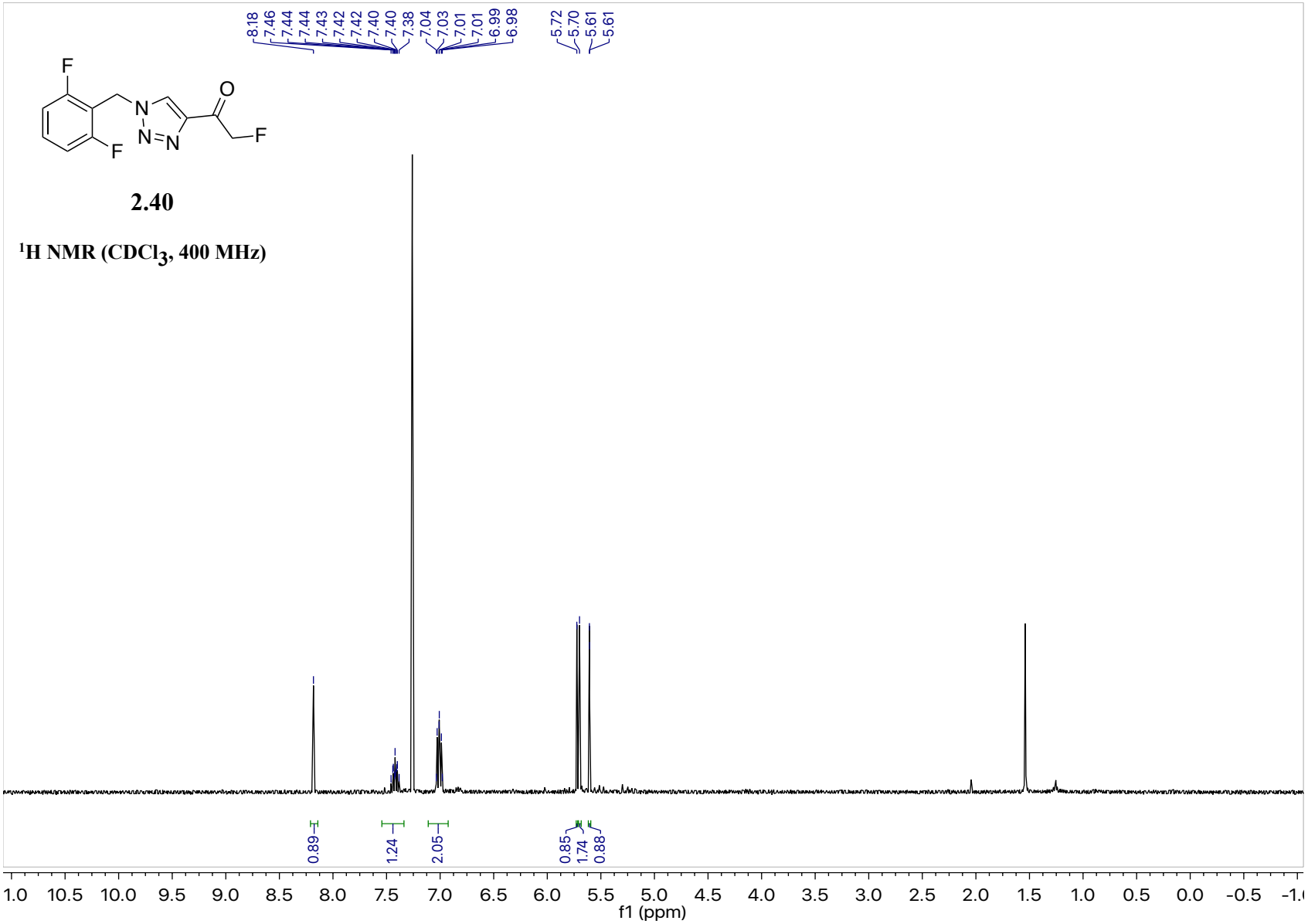

2.40

^{1}H NMR ($CDCl_3$, 400 MHz)

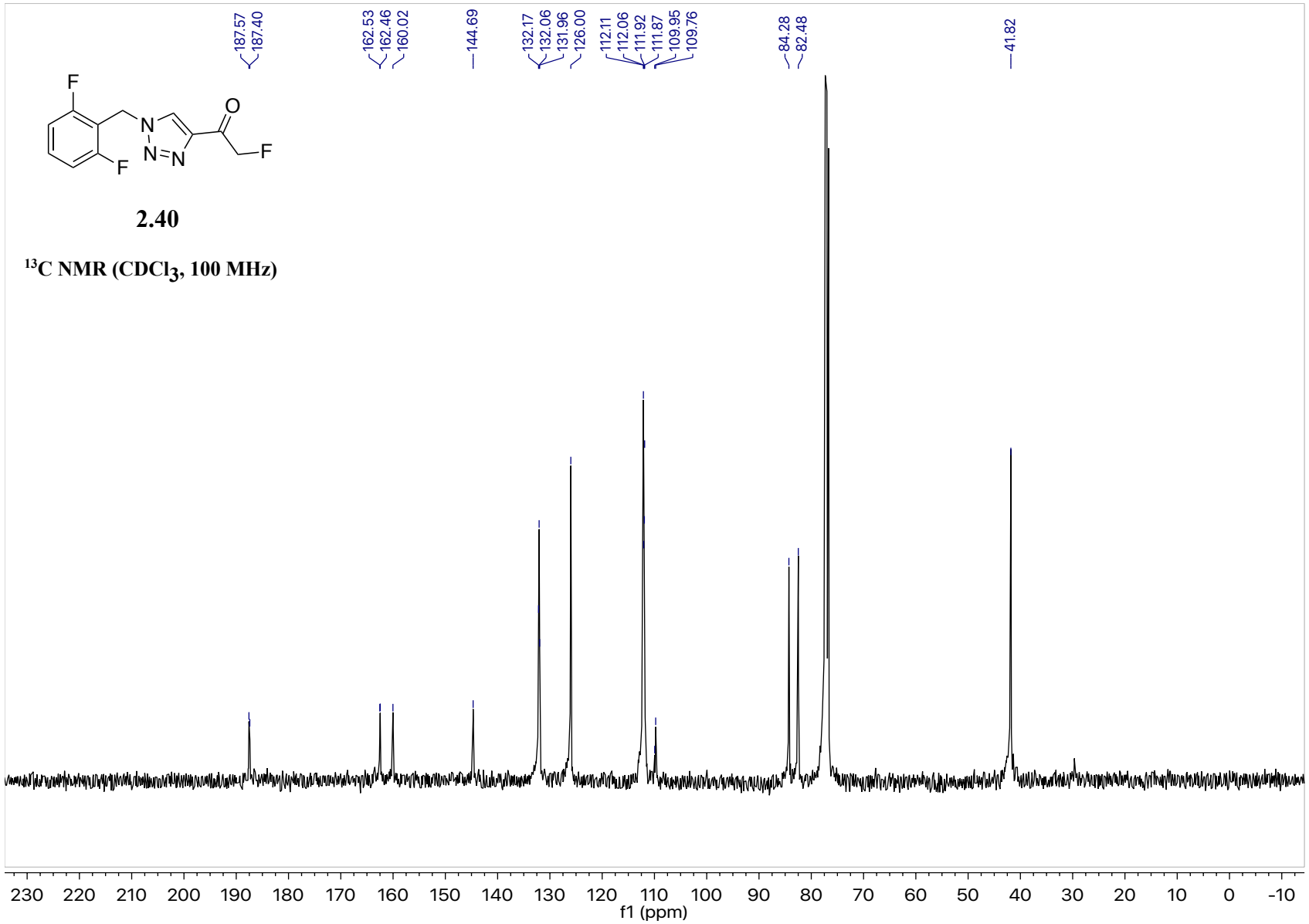

2.40

^{13}C NMR ($CDCl_3$, 100 MHz)

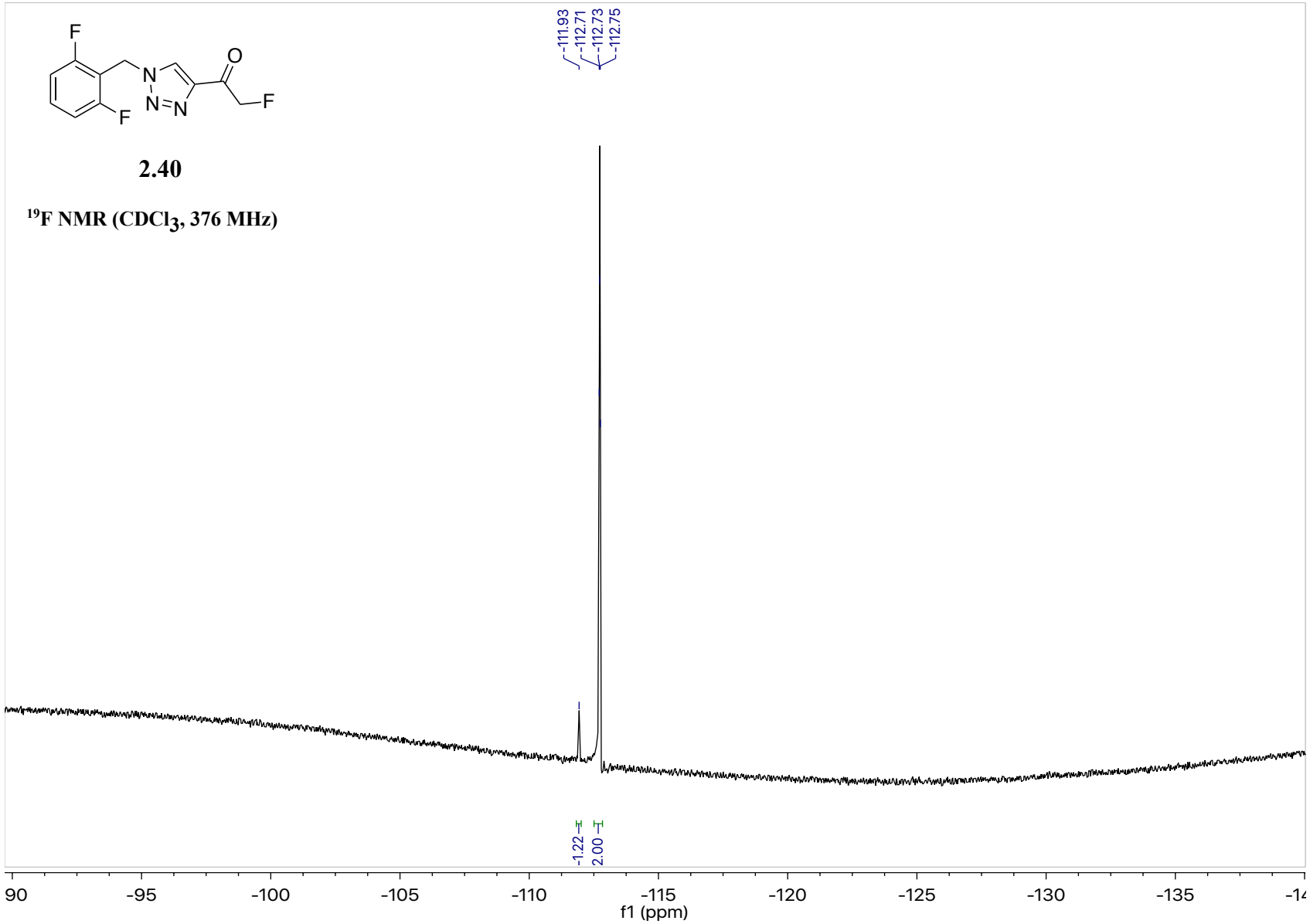

2.40

^{19}F NMR ($CDCl_3$, 376 MHz)

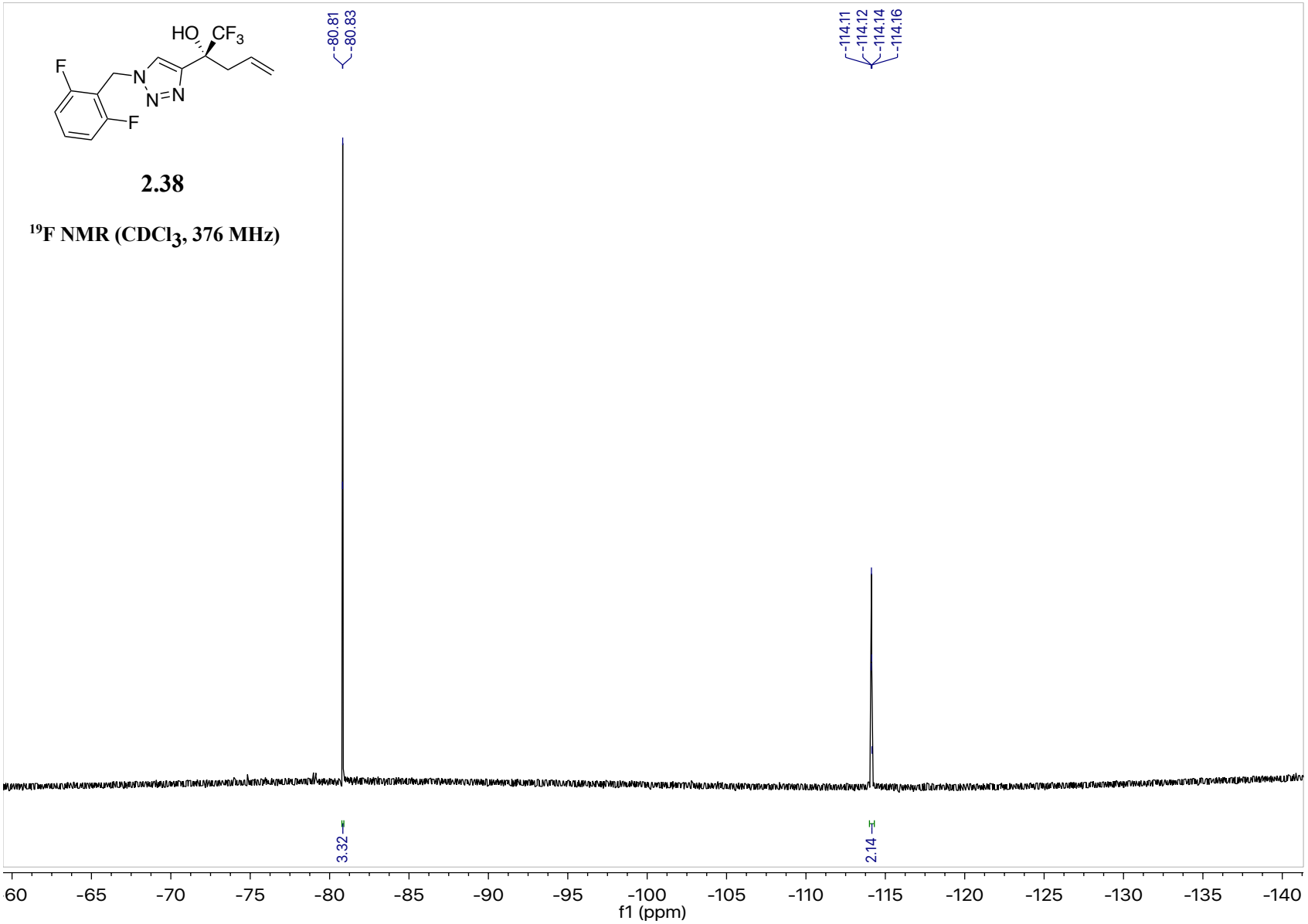

2.38

^{19}F NMR ($CDCl_3$, 376 MHz)

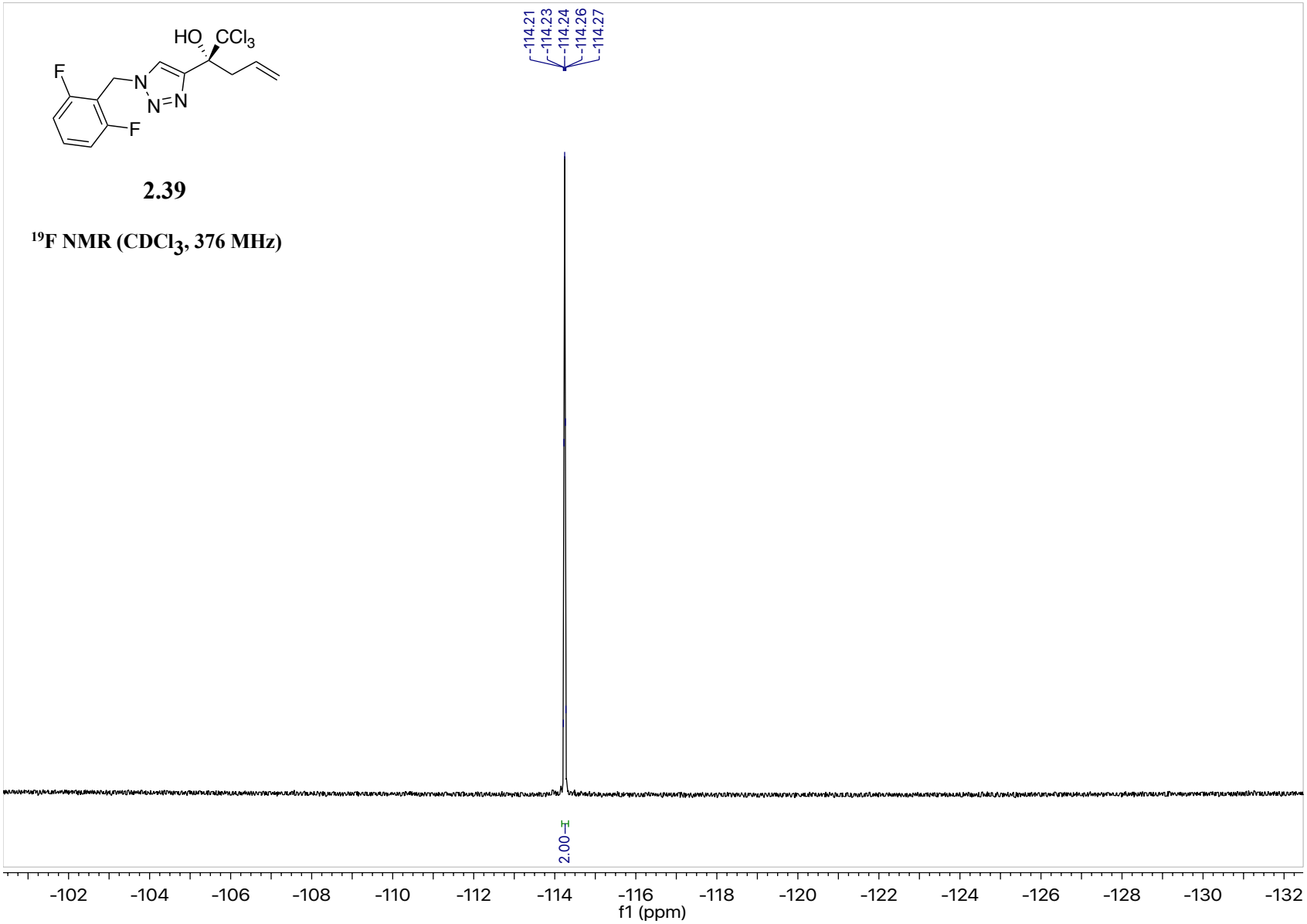

2.39

^{19}F NMR ($CDCl_3$, 376 MHz)

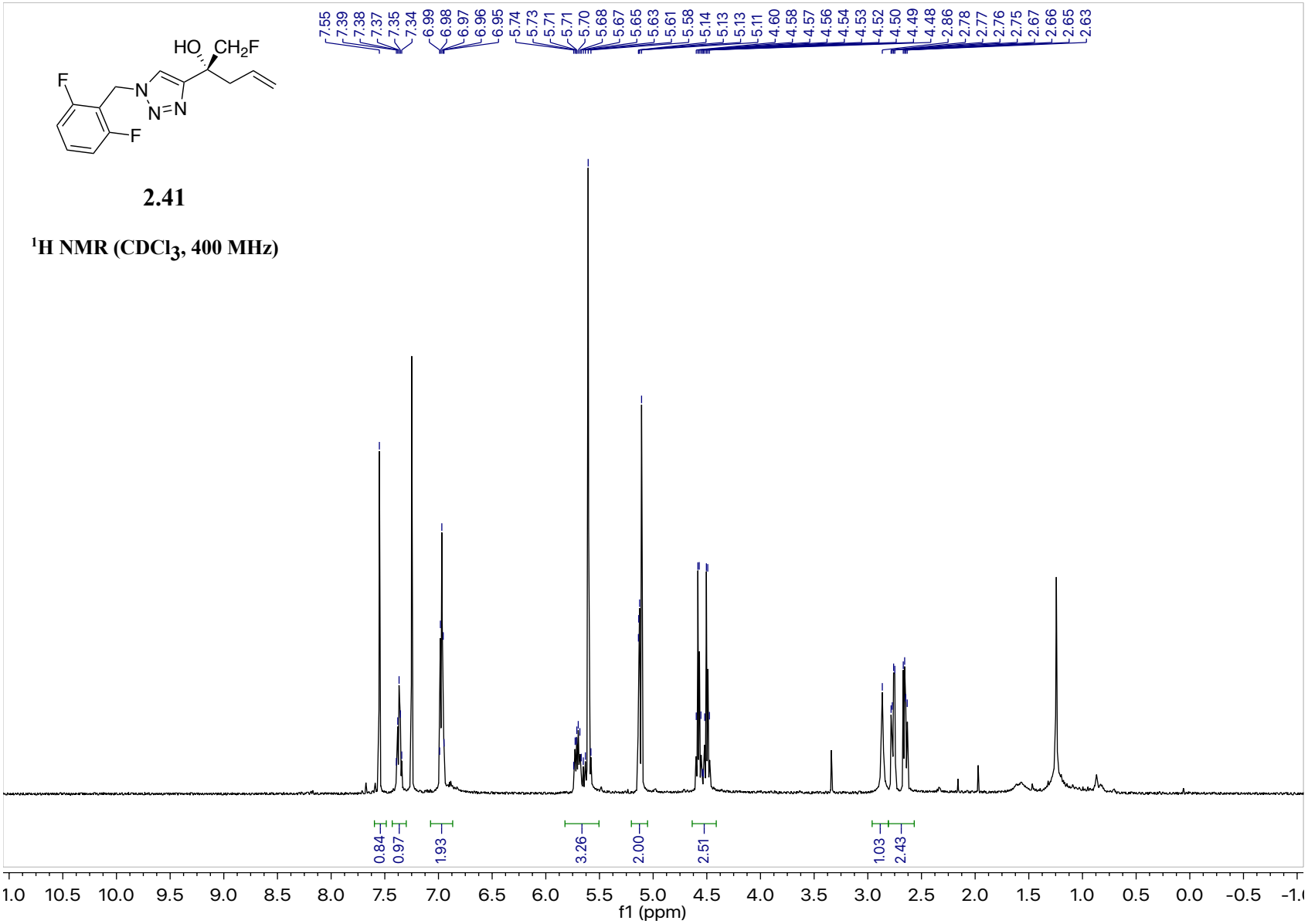

2.41

^{1}H NMR ($CDCl_3$, 400 MHz)

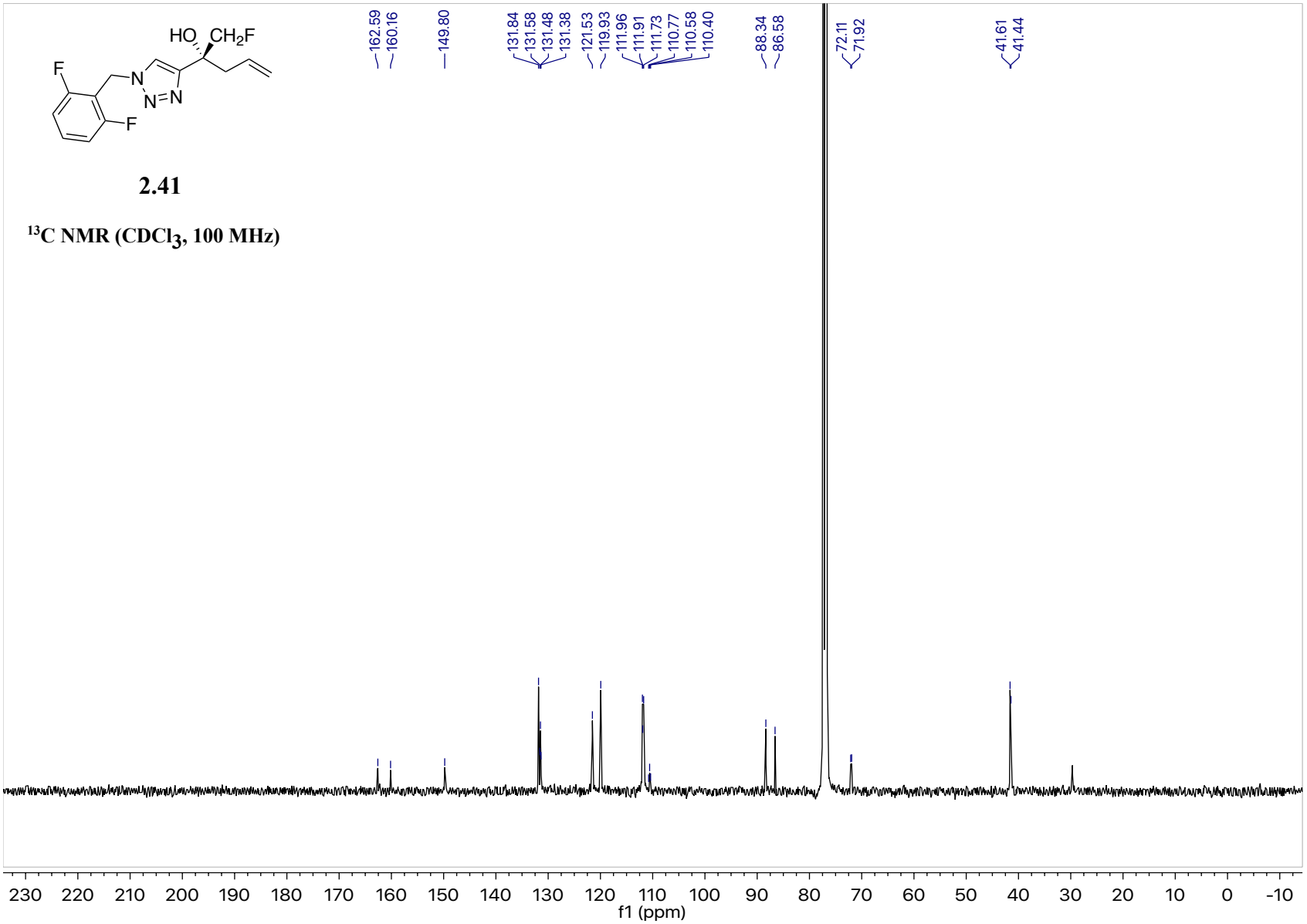

2.41

^{13}C NMR ($CDCl_3$, 100 MHz)

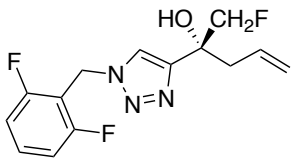

2.41

^{19}F NMR ($CDCl_3$, 376 MHz)

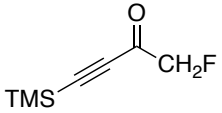

2.42

^{19}F NMR ($CDCl_3$, 376 MHz)

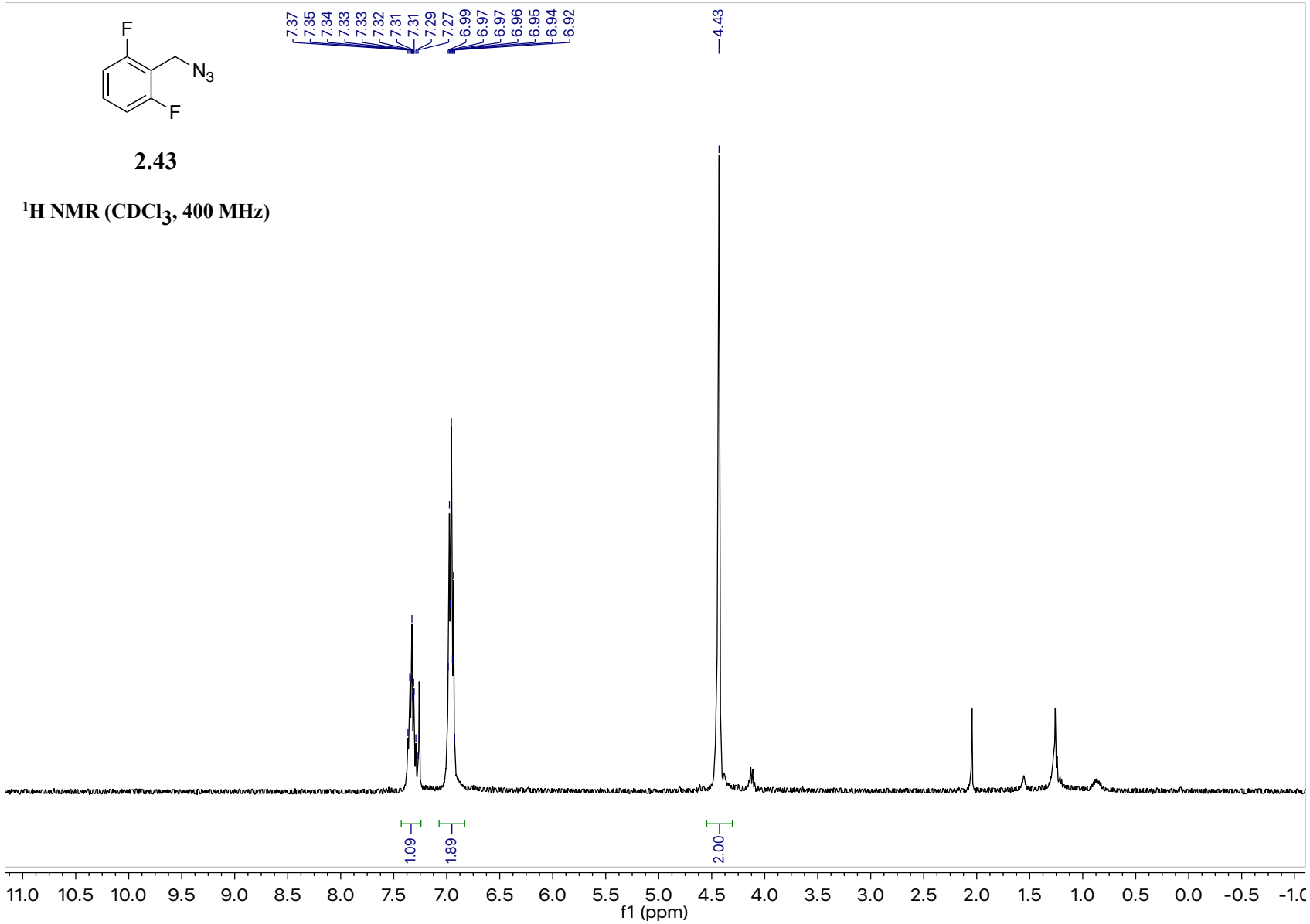

2.43

^{1}H NMR ($CDCl_3$, 400 MHz)

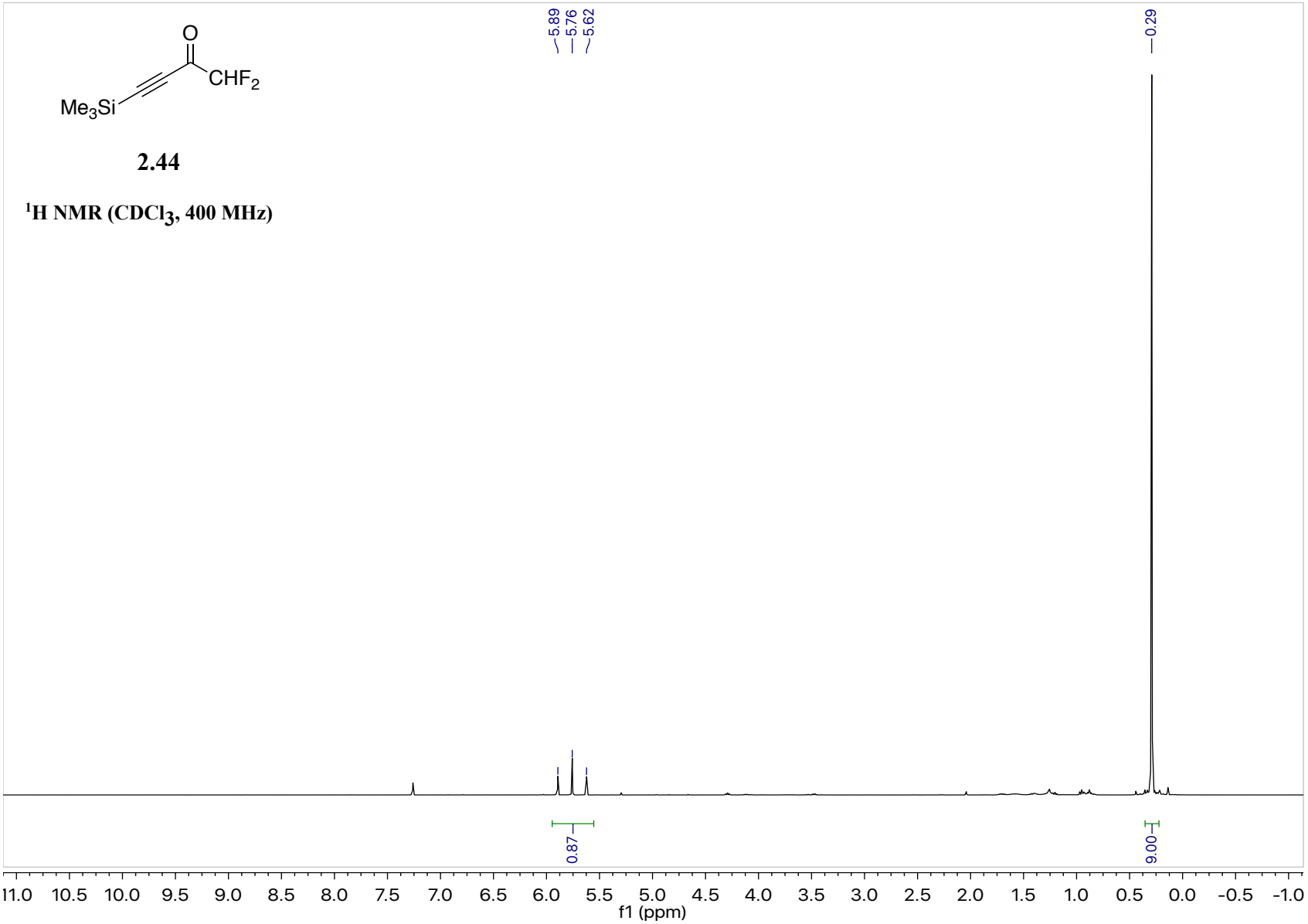

2.44

^{1}H NMR ($CDCl_3$, 400 MHz)

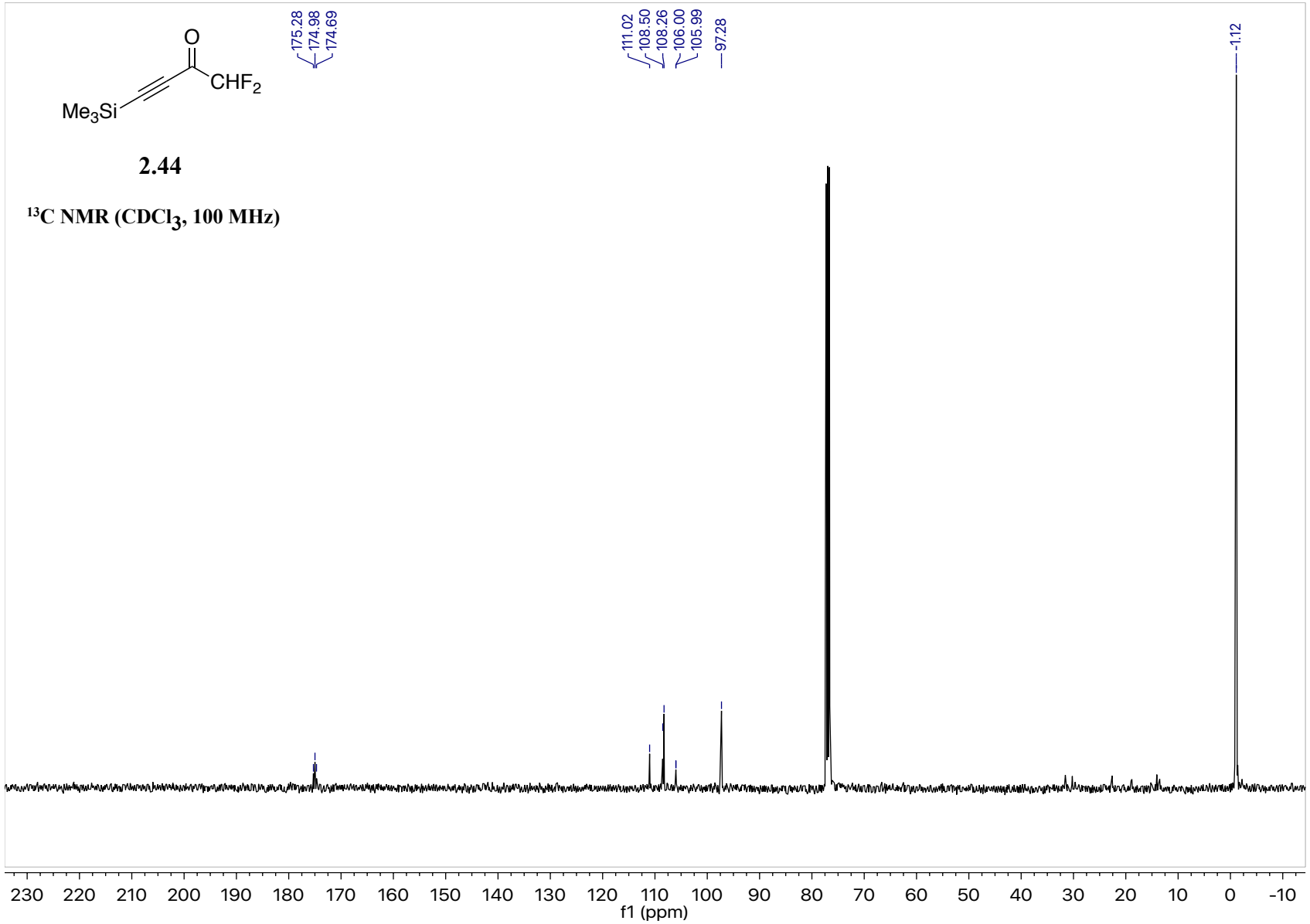

2.44

^{13}C NMR ($CDCl_3$, 100 MHz)

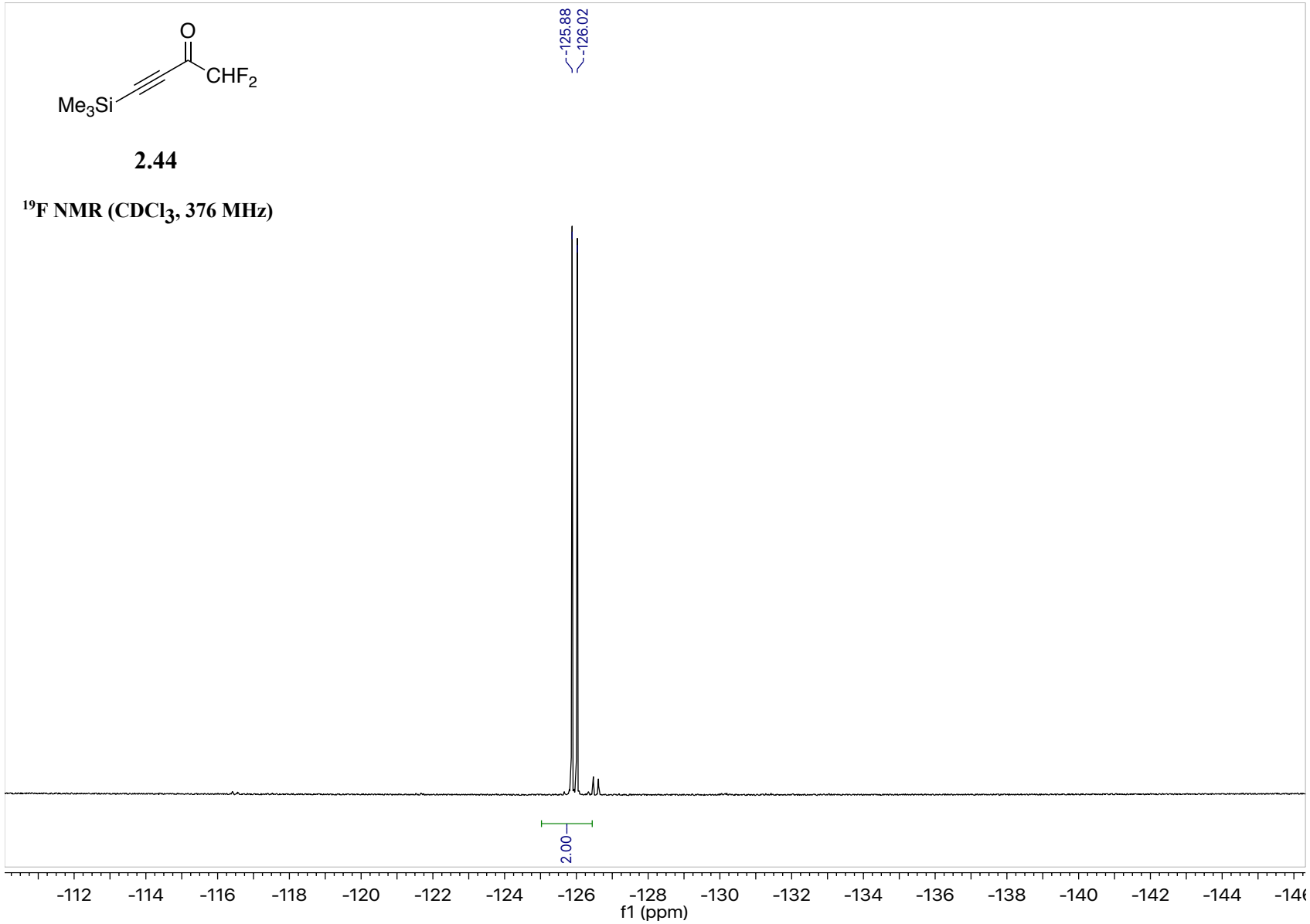
O
CHF2
Me3Si
2.44
19F NMR (CDCl3, 376 MHz)
-125.88
-126.02
2.00
-112
-114
-116
-118
-120
-122
-124
-126
-128
-130
-132
-134
-136
-138
-140
-142
-144
f1 (ppm)

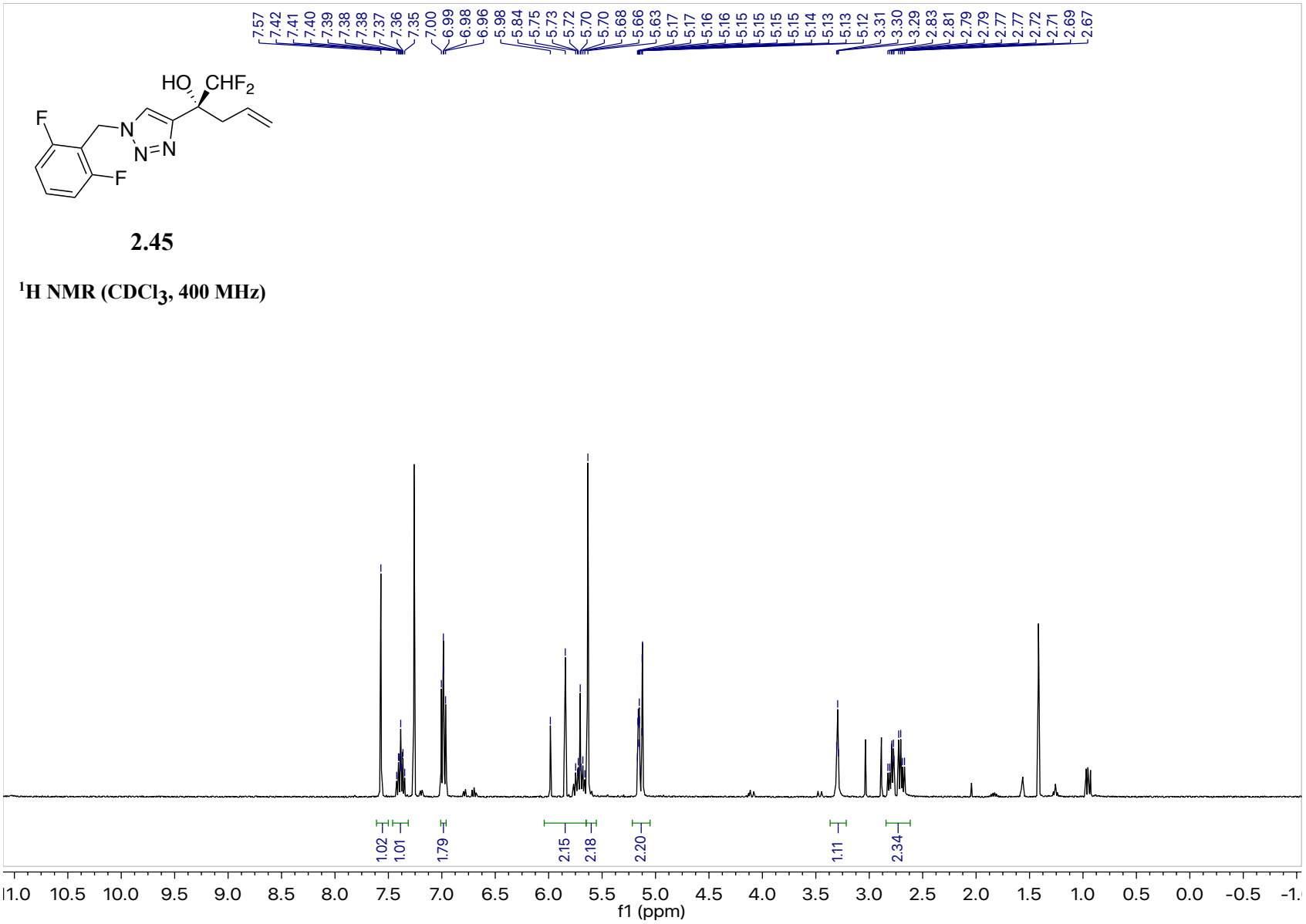

2.45

^{1}H NMR ($CDCl_3$, 400 MHz)

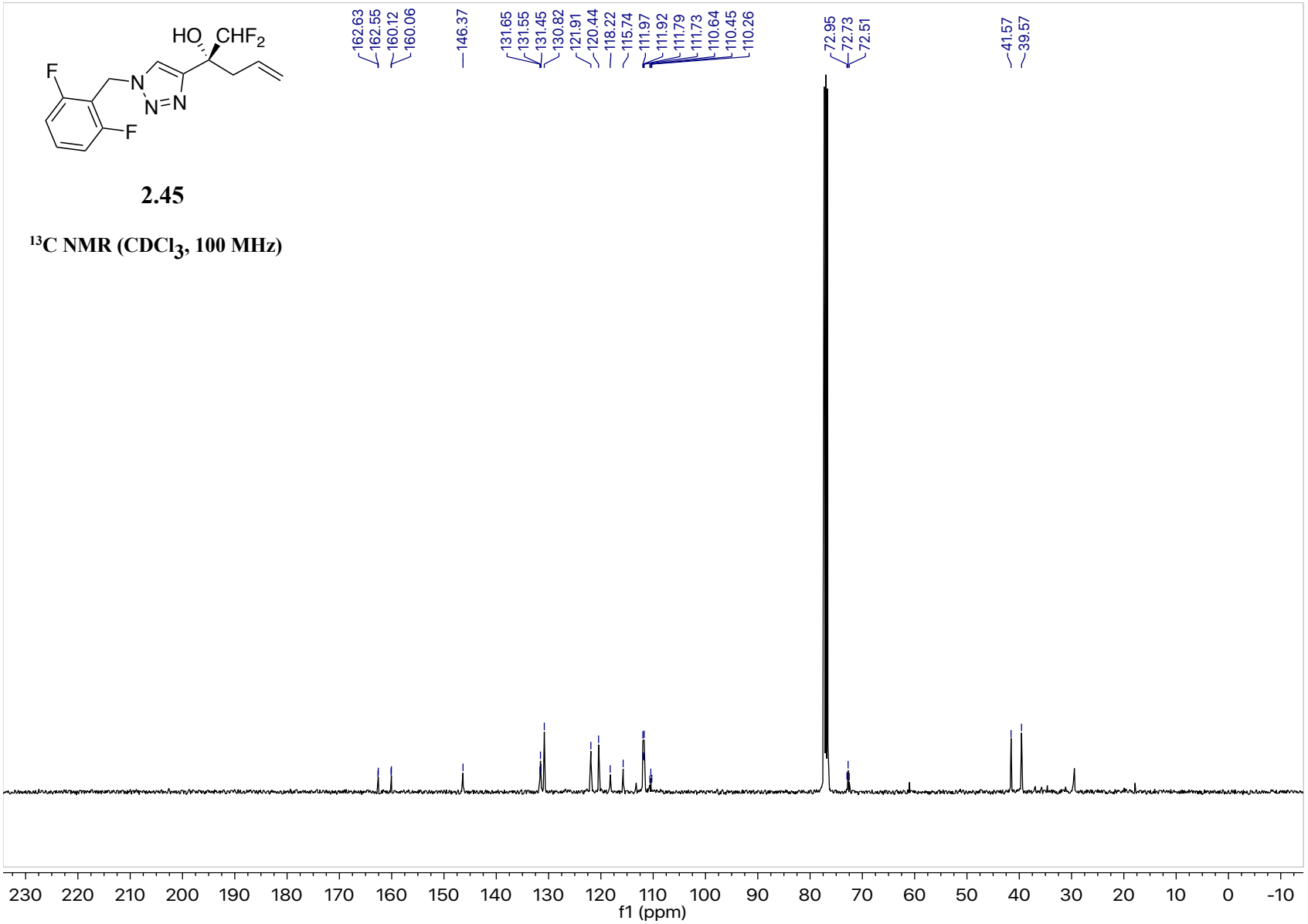
HO
CHF2
F
N
N=N
F
2.45
13C NMR (CDCl3, 100 MHz)
162.63
162.55
160.12
160.06
146.37
131.65
131.55
131.45
130.82
121.91
120.44
118.22
115.74
111.97
111.92
111.79
111.73
110.64
110.45
110.26
72.95
72.73
72.51
41.57
39.57
230 220 210 200 190 180 170 160 150 140 130 120 110 100 90 80 70 60 50 40 30 20 10 0 -10
f1 (ppm)

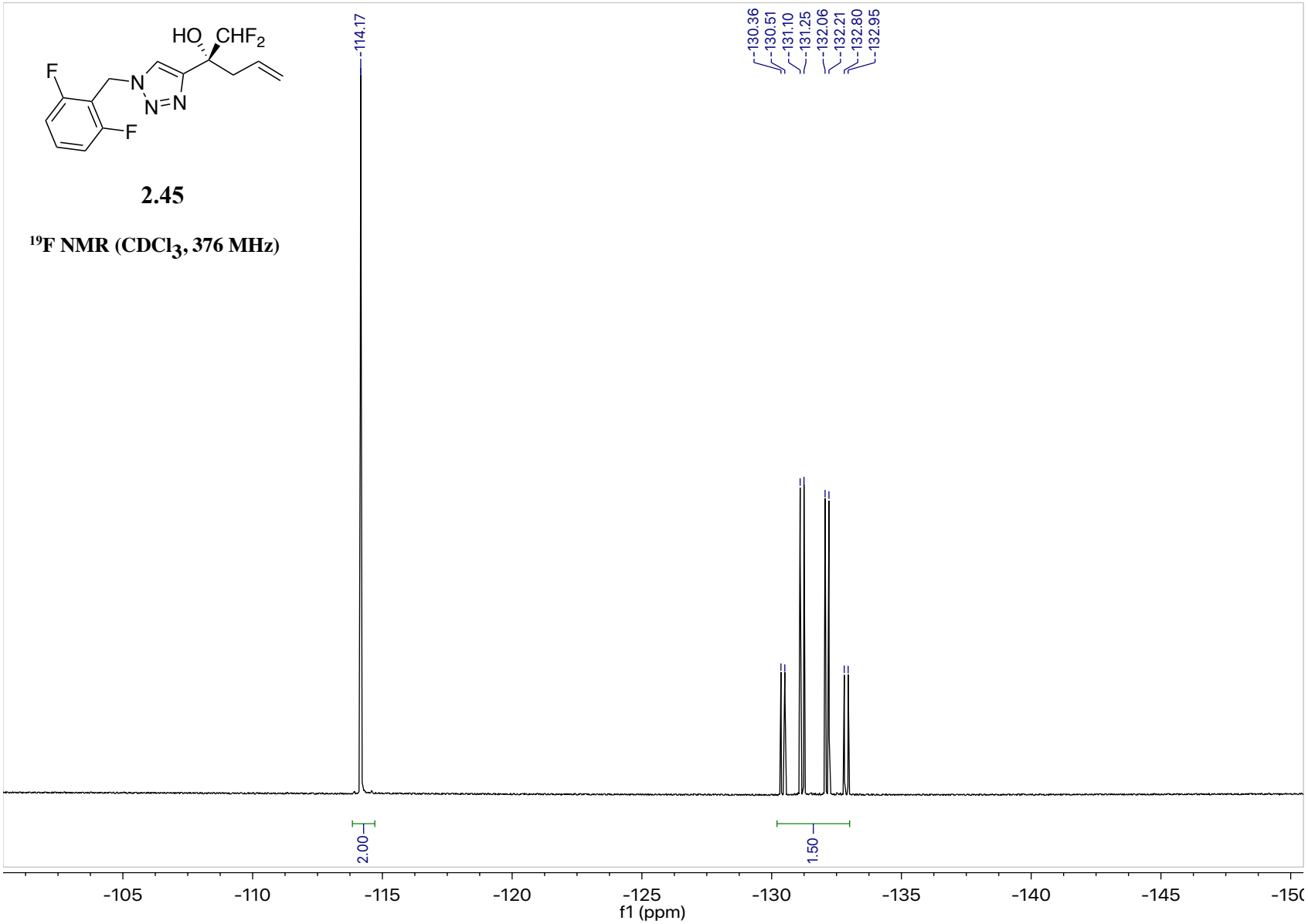
HO
CHF2
F
N
N=N
F
2.45
19F NMR (CDCl3, 376 MHz)
-114.17
-130.36
-130.51
-131.10
-131.25
-132.06
-132.21
-132.80
-132.95
2.00
1.50
-105
-110
-115
-120
-125
-130
-135
-140
-145
f1 (ppm)

2.8.15. Crystallographic Data

2.8.15.1. Crystallographic Data for (R)-5,5,5-Trichloro-4-hydroxy-4-(naphthalen-2-yl)pentan-2-one (2.9)

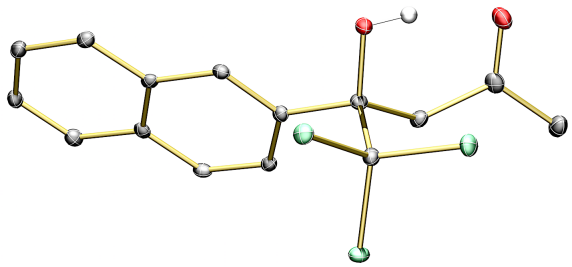

Table S1. Crystal data and structure refinement for C15H13Cl3O2

Identification code	C15H13Cl3O2
Empirical formula	C15 H13 Cl3 O2
Formula weight	331.60
Temperature	100(2) K
Wavelength	1.54178 Å
Crystal system	Monoclinic
Space group	$P2_1$
Unit cell dimensions	a = 8.0561(6) Å a= 90°.
	b = 6.0406(4) Å b= 98.325(2)°.
	c = 14.5291(10) Å g = 90°.
Volume	699.59(8) Å3
Z	2
Density (calculated)	1.574 Mg/m3
Absorption coefficient	5.913 mm-1
F(000)	340
Crystal size	0.600 x 0.300 x 0.180 mm3
Theta range for data collection	3.074 to 66.586°.
Index ranges	-9<=h<=9, -7<=k<=7, -17<=l<=17
Reflections collected	10919
Independent reflections	2470 [R(int) = 0.0493]

Completeness to theta = 66.586° 100.0 %
Absorption correction Semi-empirical from equivalents
Max. and min. transmission 0.7528 and 0.4327
Refinement method Full-matrix least-squares on F2
Data / restraints / parameters 2470 / 2 / 185
Goodness-of-fit on F2 1.109
Final R indices [I>2sigma(I)] R1 = 0.0673, wR2 = 0.1728
R indices (all data) R1 = 0.0674, wR2 = 0.1729
Absolute structure parameter 0.00(3)
Extinction coefficient n/a
Largest diff. peak and hole 0.375 and -0.350 e.Å-3

Table S2. Atomic coordinates (x104) and equivalent isotropic displacement parameters (Å2x 103) for C15H13Cl3O2. U(eq) is defined as one third of the trace of the orthogonalized Uij tensor

	x	y	z	U(eq)
Cl(1)	6942(2)	2070(2)	1766(1)	20(1)
Cl(2)	8285(2)	6502(2)	1890(1)	20(1)
Cl(3)	5500(2)	5452(2)	503(1)	21(1)
O(1)	1994(5)	7270(9)	1217(3)	28(1)
O(2)	4920(5)	7906(8)	2280(3)	19(1)
C(1)	1185(8)	3642(14)	704(5)	27(2)
C(2)	2218(7)	5272(12)	1306(4)	22(1)
C(3)	3471(7)	4318(11)	2089(4)	18(1)
C(4)	5147(7)	5597(12)	2360(4)	17(1)
C(5)	5929(6)	5078(11)	3363(4)	15(1)
C(6)	6907(6)	6664(10)	3860(4)	15(1)
C(7)	7649(7)	6256(12)	4792(4)	16(1)
C(8)	8717(7)	7852(11)	5301(4)	17(1)
C(9)	9427(7)	7439(11)	6204(4)	20(1)
C(10)	9064(7)	5422(12)	6637(4)	20(1)
C(11)	8059(7)	3858(12)	6165(4)	20(1)
C(12)	7327(7)	4238(11)	5222(4)	16(1)

C(13)	6304(7)	2639(10)	4705(4)	17(1)
C(14)	5641(7)	3031(11)	3795(4)	17(1)
C(15)	6418(7)	4923(11)	1670(4)	17(1)

Table S3. Bond lengths [Å] and angles [°] for C15H13Cl3O2.

Cl(1)-C(15)	1.775(6)
Cl(2)-C(15)	1.771(6)
Cl(3)-C(15)	1.777(6)
O(1)-C(2)	1.225(9)
O(2)-C(4)	1.409(9)
O(2)-H(2O)	0.84(3)
C(1)-C(2)	1.489(10)
C(1)-H(1A)	0.9800
C(1)-H(1B)	0.9800
C(1)-H(1C)	0.9800
C(2)-C(3)	1.521(9)
C(3)-C(4)	1.556(8)
C(3)-H(3A)	0.9900
C(3)-H(3B)	0.9900
C(4)-C(5)	1.533(7)
C(4)-C(15)	1.586(8)
C(5)-C(6)	1.377(8)
C(5)-C(14)	1.421(9)
C(6)-C(7)	1.419(7)
C(6)-H(6)	0.9500
C(7)-C(12)	1.411(9)
C(7)-C(8)	1.426(9)
C(8)-C(9)	1.377(8)
C(8)-H(8)	0.9500
C(9)-C(10)	1.420(10)
C(9)-H(9)	0.9500
C(10)-C(11)	1.363(10)

C(10)-H(10)	0.9500
C(11)-C(12)	1.430(8)
C(11)-H(11)	0.9500
C(12)-C(13)	1.413(9)
C(13)-C(14)	1.373(8)
C(13)-H(13)	0.9500
C(14)-H(14)	0.9500

C(4)-O(2)-H(2O)	102(7)
C(2)-C(1)-H(1A)	109.5
C(2)-C(1)-H(1B)	109.5
H(1A)-C(1)-H(1B)	109.5
C(2)-C(1)-H(1C)	109.5
H(1A)-C(1)-H(1C)	109.5
H(1B)-C(1)-H(1C)	109.5
O(1)-C(2)-C(1)	121.9(6)
O(1)-C(2)-C(3)	121.6(6)
C(1)-C(2)-C(3)	116.3(6)
C(2)-C(3)-C(4)	117.3(5)
C(2)-C(3)-H(3A)	108.0
C(4)-C(3)-H(3A)	108.0
C(2)-C(3)-H(3B)	108.0
C(4)-C(3)-H(3B)	108.0
H(3A)-C(3)-H(3B)	107.2
O(2)-C(4)-C(5)	108.2(5)
O(2)-C(4)-C(3)	111.9(5)
C(5)-C(4)-C(3)	111.2(5)
O(2)-C(4)-C(15)	106.8(5)
C(5)-C(4)-C(15)	109.5(4)
C(3)-C(4)-C(15)	109.1(5)
C(6)-C(5)-C(14)	119.4(5)
C(6)-C(5)-C(4)	118.8(5)
C(14)-C(5)-C(4)	121.8(5)
C(5)-C(6)-C(7)	120.6(6)

C(5)-C(6)-H(6)	119.7
C(7)-C(6)-H(6)	119.7
C(12)-C(7)-C(6)	119.6(6)
C(12)-C(7)-C(8)	119.4(5)
C(6)-C(7)-C(8)	121.1(6)
C(9)-C(8)-C(7)	120.5(6)
C(9)-C(8)-H(8)	119.7
C(7)-C(8)-H(8)	119.7
C(8)-C(9)-C(10)	119.6(5)
C(8)-C(9)-H(9)	120.2
C(10)-C(9)-H(9)	120.2
C(11)-C(10)-C(9)	121.2(5)
C(11)-C(10)-H(10)	119.4
C(9)-C(10)-H(10)	119.4
C(10)-C(11)-C(12)	120.2(6)
C(10)-C(11)-H(11)	119.9
C(12)-C(11)-H(11)	119.9
C(7)-C(12)-C(13)	119.0(5)
C(7)-C(12)-C(11)	119.1(6)
C(13)-C(12)-C(11)	121.8(6)
C(14)-C(13)-C(12)	120.6(6)
C(14)-C(13)-H(13)	119.7
C(12)-C(13)-H(13)	119.7
C(13)-C(14)-C(5)	120.6(5)
C(13)-C(14)-H(14)	119.7
C(5)-C(14)-H(14)	119.7
C(4)-C(15)-Cl(2)	110.9(4)
C(4)-C(15)-Cl(1)	111.6(4)
Cl(2)-C(15)-Cl(1)	108.8(3)
C(4)-C(15)-Cl(3)	109.9(4)
Cl(2)-C(15)-Cl(3)	107.5(3)
Cl(1)-C(15)-Cl(3)	108.1(3)

Symmetry transformations used to generate equivalent atoms:

Table S4. Anisotropic displacement parameters (Å2x 103) for C15H13Cl3O2. The anisotropic displacement factor exponent takes the form: -2p2[h2 a*2U11 + ... + 2 h k a* b* U12]

	U11	U22	U33	U23	U13	U12
Cl(1)	24(1)	14(1)	23(1)	0(1)	4(1)	2(1)
Cl(2)	17(1)	20(1)	24(1)	0(1)	4(1)	-4(1)
Cl(3)	23(1)	24(1)	16(1)	3(1)	1(1)	-1(1)
O(1)	22(2)	28(3)	33(3)	4(2)	-4(2)	3(2)
O(2)	19(2)	15(2)	21(2)	1(2)	-2(2)	0(2)
C(1)	19(3)	34(4)	28(3)	-9(3)	-1(2)	2(3)
C(2)	12(2)	29(4)	25(3)	0(3)	5(2)	1(3)
C(3)	16(3)	18(3)	22(3)	-4(3)	3(2)	-2(2)
C(4)	17(3)	13(3)	20(3)	2(2)	1(2)	-1(2)
C(5)	12(2)	17(3)	18(3)	-1(2)	2(2)	0(2)
C(6)	14(2)	13(3)	19(3)	1(2)	3(2)	1(2)
C(7)	13(2)	15(3)	18(3)	-3(2)	5(2)	2(2)
C(8)	15(2)	17(3)	19(3)	-2(2)	5(2)	-1(2)
C(9)	17(3)	20(3)	21(3)	-5(3)	0(2)	0(3)
C(10)	19(3)	23(3)	16(2)	0(2)	-1(2)	3(3)
C(11)	20(3)	22(3)	18(3)	1(3)	5(2)	3(3)
C(12)	12(2)	19(3)	19(3)	0(2)	3(2)	4(2)
C(13)	16(2)	12(3)	23(3)	2(2)	6(2)	0(2)
C(14)	15(3)	15(3)	20(3)	-3(2)	1(2)	0(2)
C(15)	18(2)	15(3)	18(2)	1(2)	0(2)	-2(3)

Table S5. Hydrogen coordinates (x104) and isotropic displacement parameters (Å2x103) for C15H13Cl3O2

	x	y	z	U(eq)
H(2O)	4000(60)	7990(170)	1920(50)	28

H(1A)	245	4407	333	41
H(1B)	752	2519	1095	41
H(1C)	1879	2925	289	41
H(3A)	3748	2793	1912	22
H(3B)	2910	4205	2649	22
H(6)	7088	8044	3578	18
H(8)	8941	9213	5014	20
H(9)	10155	8496	6537	24
H(10)	9532	5158	7265	24
H(11)	7843	2512	6464	24
H(13)	6073	1280	4990	20
H(14)	4984	1922	3451	21

Table S6. Torsion angles [°] for C15H13Cl3O2

O(1)-C(2)-C(3)-C(4)	-38.2(9)
C(1)-C(2)-C(3)-C(4)	146.6(5)
C(2)-C(3)-C(4)-O(2)	35.3(7)
C(2)-C(3)-C(4)-C(5)	156.4(5)
C(2)-C(3)-C(4)-C(15)	-82.7(7)
O(2)-C(4)-C(5)-C(6)	-27.7(7)
C(3)-C(4)-C(5)-C(6)	-150.9(5)
C(15)-C(4)-C(5)-C(6)	88.4(6)
O(2)-C(4)-C(5)-C(14)	151.0(5)
C(3)-C(4)-C(5)-C(14)	27.7(8)
C(15)-C(4)-C(5)-C(14)	-92.9(6)
C(14)-C(5)-C(6)-C(7)	1.0(8)
C(4)-C(5)-C(6)-C(7)	179.7(5)
C(5)-C(6)-C(7)-C(12)	-2.4(8)
C(5)-C(6)-C(7)-C(8)	177.5(5)
C(12)-C(7)-C(8)-C(9)	-0.1(8)
C(6)-C(7)-C(8)-C(9)	179.9(5)
C(7)-C(8)-C(9)-C(10)	-1.2(8)
C(8)-C(9)-C(10)-C(11)	1.7(9)

C(9)-C(10)-C(11)-C(12)	-0.8(9)
C(6)-C(7)-C(12)-C(13)	1.7(8)
C(8)-C(7)-C(12)-C(13)	-178.3(6)
C(6)-C(7)-C(12)-C(11)	-179.0(5)
C(8)-C(7)-C(12)-C(11)	1.0(8)
C(10)-C(11)-C(12)-C(7)	-0.6(8)
C(10)-C(11)-C(12)-C(13)	178.8(5)
C(7)-C(12)-C(13)-C(14)	0.5(8)
C(11)-C(12)-C(13)-C(14)	-178.8(5)
C(12)-C(13)-C(14)-C(5)	-1.9(8)
C(6)-C(5)-C(14)-C(13)	1.1(8)
C(4)-C(5)-C(14)-C(13)	-177.5(5)
O(2)-C(4)-C(15)-Cl(2)	54.1(5)
C(5)-C(4)-C(15)-Cl(2)	-62.8(6)
C(3)-C(4)-C(15)-Cl(2)	175.2(4)
O(2)-C(4)-C(15)-Cl(1)	175.5(4)
C(5)-C(4)-C(15)-Cl(1)	58.6(6)
C(3)-C(4)-C(15)-Cl(1)	-63.3(5)
O(2)-C(4)-C(15)-Cl(3)	-64.6(5)
C(5)-C(4)-C(15)-Cl(3)	178.5(4)
C(3)-C(4)-C(15)-Cl(3)	56.6(6)

Symmetry transformations used to generate equivalent atoms:

Table S7. Hydrogen bonds for C15H13Cl3O2 [Å and °]

D-H...A	d(D-H)	d(H...A)	d(D...A)	<(DHA)
O(2)-H(2O)...O(1)	0.84(3)	1.84(4)	2.652(6)	163(10)

Symmetry transformations used to generate equivalent atoms:

2.8.15.2. Crystallographic Data for (*R*)-1,1-Dichloro-2-(4-nitrophenyl)pent-4-en-2-ol (2.25d)

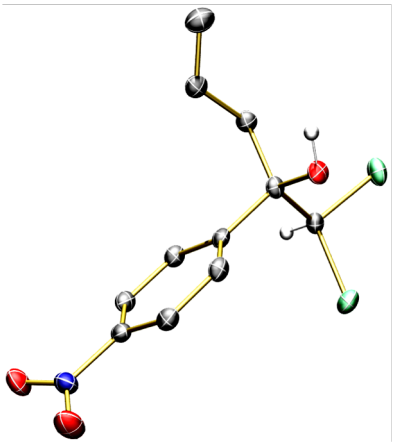

Table S8. Crystal data and structure refinement for C11H11Cl2NO3

Identification code C11H11Cl2NO3

Empirical formula C11 H11 Cl2 N O3

Formula weight 276.11

Temperature 100(2) K

Wavelength 1.54178 ≈

Crystal system Orthorhombic

Space group $P2_12_12_1$

Unit cell dimensions a = 7.9241(7) ≈ □= 90∞.

b = 9.4871(9) ≈ □= 90∞.

c = 16.0357(14) ≈ □ = 90∞.

Volume 1205.51(19) ≈3

Z 4

Density (calculated) 1.521 Mg/m3

Absorption coefficient 4.832 mm-1

F(000) 568

Crystal size 0.320 x 0.220 x 0.140 mm3

Theta range for data collection	5.417 to 70.756∞.
Index ranges	-7<=h<=9, -11<=k<=11, -19<=l<=19
Reflections collected	7863
Independent reflections	2253 [R(int) = 0.0286]
Completeness to theta = 67.679∞	99.9 %
Absorption correction	Semi-empirical from equivalents
Max. and min. transmission	0.7534 and 0.5587
Refinement method	Full-matrix least-squares on F2
Data / restraints / parameters	2253 / 1 / 159
Goodness-of-fit on F2	1.068
Final R indices [I>2sigma(I)]	R1 = 0.0218, wR2 = 0.0561
R indices (all data)	R1 = 0.0219, wR2 = 0.0562
Absolute structure parameter	0.036(15)
Extinction coefficient	n/a
Largest diff. peak and hole	0.299 and -0.161 e.≈-3

Table S9. Atomic coordinates (x104) and equivalent isotropic displacement parameters (≈2x103) for C11H11Cl2NO3. U(eq) is defined as one third of the trace of the orthogonalized Uij tensor

	x	y	z	U(eq)
Cl(1)	-1789(1)	3694(1)	8367(1)	25(1)
Cl(2)	-648(1)	4415(1)	6703(1)	23(1)
O(1)	1401(2)	5476(1)	8167(1)	19(1)
O(2)	7228(2)	2018(2)	5361(1)	28(1)
O(3)	6932(3)	4199(2)	4986(1)	35(1)
N(1)	6552(3)	3186(2)	5423(1)	22(1)
C(1)	4154(3)	3932(2)	9831(1)	28(1)

C(2)	3782(3)	3452(2)	9084(1)	20(1)
C(3)	2020(3)	3169(2)	8778(1)	18(1)
C(4)	1580(3)	4020(2)	7986(1)	16(1)
C(5)	-117(3)	3493(2)	7638(1)	17(1)
C(6)	2899(3)	3797(2)	7304(1)	15(1)
C(7)	3659(3)	4947(2)	6916(1)	18(1)
C(8)	4837(3)	4754(2)	6289(1)	19(1)
C(9)	5267(3)	3390(2)	6068(1)	18(1)
C(10)	4532(3)	2224(2)	6436(1)	18(1)
C(11)	3337(3)	2435(2)	7050(1)	18(1)

Table S10. Bond lengths [≈] and angles [∞] for C11H11Cl2NO3

Cl(1)-C(5)	1.777(2)
Cl(2)-C(5)	1.786(2)
O(1)-C(4)	1.419(2)
O(1)-H(1O)	0.81(2)
O(2)-N(1)	1.235(2)
O(3)-N(1)	1.228(2)
N(1)-C(9)	1.464(3)
C(1)-C(2)	1.315(3)
C(1)-H(1A)	0.9500
C(1)-H(1B)	0.9500
C(2)-C(3)	1.504(3)
C(2)-H(2)	0.9500
C(3)-C(4)	1.545(3)
C(3)-H(3A)	0.9900
C(3)-H(3B)	0.9900

C(4)-C(6)	1.528(3)
C(4)-C(5)	1.539(3)
C(5)-H(5)	1.0000
C(6)-C(7)	1.393(3)
C(6)-C(11)	1.398(3)
C(7)-C(8)	1.383(3)
C(7)-H(7)	0.9500
C(8)-C(9)	1.385(3)
C(8)-H(8)	0.9500
C(9)-C(10)	1.382(3)
C(10)-C(11)	1.382(3)
C(10)-H(10)	0.9500
C(11)-H(11)	0.9500

C(4)-O(1)-H(1O)	111(2)
O(3)-N(1)-O(2)	123.38(19)
O(3)-N(1)-C(9)	118.04(17)
O(2)-N(1)-C(9)	118.56(17)
C(2)-C(1)-H(1A)	120.0
C(2)-C(1)-H(1B)	120.0
H(1A)-C(1)-H(1B)	120.0
C(1)-C(2)-C(3)	124.5(2)
C(1)-C(2)-H(2)	117.7
C(3)-C(2)-H(2)	117.7
C(2)-C(3)-C(4)	112.61(17)
C(2)-C(3)-H(3A)	109.1
C(4)-C(3)-H(3A)	109.1
C(2)-C(3)-H(3B)	109.1

C(4)-C(3)-H(3B)	109.1
H(3A)-C(3)-H(3B)	107.8
O(1)-C(4)-C(6)	110.48(15)
O(1)-C(4)-C(5)	107.64(16)
C(6)-C(4)-C(5)	107.08(16)
O(1)-C(4)-C(3)	111.28(16)
C(6)-C(4)-C(3)	111.20(16)
C(5)-C(4)-C(3)	109.00(16)
C(4)-C(5)-Cl(1)	112.22(14)
C(4)-C(5)-Cl(2)	110.52(14)
Cl(1)-C(5)-Cl(2)	108.90(11)
C(4)-C(5)-H(5)	108.4
Cl(1)-C(5)-H(5)	108.4
Cl(2)-C(5)-H(5)	108.4
C(7)-C(6)-C(11)	119.13(18)
C(7)-C(6)-C(4)	120.46(17)
C(11)-C(6)-C(4)	120.40(17)
C(8)-C(7)-C(6)	120.83(18)
C(8)-C(7)-H(7)	119.6
C(6)-C(7)-H(7)	119.6
C(7)-C(8)-C(9)	118.40(19)
C(7)-C(8)-H(8)	120.8
C(9)-C(8)-H(8)	120.8
C(10)-C(9)-C(8)	122.36(19)
C(10)-C(9)-N(1)	119.21(18)
C(8)-C(9)-N(1)	118.43(18)
C(11)-C(10)-C(9)	118.48(18)
C(11)-C(10)-H(10)	120.8

C(9)-C(10)-H(10)	120.8
C(10)-C(11)-C(6)	120.77(18)
C(10)-C(11)-H(11)	119.6
C(6)-C(11)-H(11)	119.6

Symmetry transformations used to generate equivalent atoms:

Table S11. Anisotropic displacement parameters (≈2x 103) for C11H11Cl2NO3. The anisotropic displacement factor exponent takes the form: -2□2[h2 a*2U11 + ... + 2 h k a* b* U12]

	U11	U22	U33	U23	U13	U12
Cl(1)	17(1)	25(1)	33(1)	-2(1)	7(1)	-1(1)
Cl(2)	20(1)	25(1)	26(1)	3(1)	-6(1)	2(1)
O(1)	23(1)	13(1)	21(1)	-4(1)	-1(1)	1(1)
O(2)	34(1)	24(1)	27(1)	-1(1)	11(1)	5(1)
O(3)	46(1)	30(1)	28(1)	12(1)	14(1)	5(1)
N(1)	25(1)	24(1)	18(1)	1(1)	3(1)	0(1)
C(1)	34(1)	25(1)	25(1)	3(1)	-6(1)	-4(1)
C(2)	22(1)	16(1)	21(1)	4(1)	0(1)	-1(1)
C(3)	19(1)	16(1)	19(1)	2(1)	2(1)	-2(1)
C(4)	17(1)	11(1)	20(1)	-1(1)	1(1)	0(1)
C(5)	15(1)	16(1)	21(1)	1(1)	2(1)	1(1)
C(6)	14(1)	16(1)	16(1)	0(1)	-3(1)	1(1)
C(7)	18(1)	12(1)	23(1)	0(1)	-2(1)	0(1)
C(8)	17(1)	18(1)	21(1)	4(1)	-2(1)	-3(1)
C(9)	17(1)	21(1)	15(1)	1(1)	-2(1)	0(1)
C(10)	22(1)	15(1)	18(1)	-1(1)	-1(1)	2(1)

C(11)	19(1)	13(1)	20(1)	2(1)	-1(1)	-2(1)

Table S12. Hydrogen coordinates (x104) and isotropic displacement parameters (≈2x103) for C11H11Cl2NO3.

	x	y	z	U(eq)
H(1O)	1840(40)		5670(30)	8609(14) 34(8)
H(1A)	3279	4124	10220	34
H(1B)	5299	4087	9982	34
H(2)	4689	3272	8711	24
H(3A)	1207	3411	9224	22
H(3B)	1901	2151	8657	22
H(5)	-3	2468	7503	21
H(7)	3364	5875	7083	21
H(8)	5338	5539	6018	22
H(10)	4842	1298	6269	22
H(11)	2807	1646	7304	21

Table S13. Torsion angles [∞] for C11H11Cl2NO3

C(1)-C(2)-C(3)-C(4)	121.8(2)
C(2)-C(3)-C(4)-O(1)	-70.5(2)
C(2)-C(3)-C(4)-C(6)	53.1(2)
C(2)-C(3)-C(4)-C(5)	170.96(16)
O(1)-C(4)-C(5)-Cl(1)	-60.93(18)
C(6)-C(4)-C(5)-Cl(1)	-179.73(13)
C(3)-C(4)-C(5)-Cl(1)	59.88(18)

O(1)-C(4)-C(5)-Cl(2)	60.83(17)
C(6)-C(4)-C(5)-Cl(2)	-57.97(17)
C(3)-C(4)-C(5)-Cl(2)	-178.36(13)
O(1)-C(4)-C(6)-C(7)	-4.0(3)
C(5)-C(4)-C(6)-C(7)	112.94(19)
C(3)-C(4)-C(6)-C(7)	-128.09(19)
O(1)-C(4)-C(6)-C(11)	177.19(17)
C(5)-C(4)-C(6)-C(11)	-65.9(2)
C(3)-C(4)-C(6)-C(11)	53.1(2)
C(11)-C(6)-C(7)-C(8)	-0.3(3)
C(4)-C(6)-C(7)-C(8)	-179.07(18)
C(6)-C(7)-C(8)-C(9)	-1.2(3)
C(7)-C(8)-C(9)-C(10)	1.7(3)
C(7)-C(8)-C(9)-N(1)	-178.15(18)
O(3)-N(1)-C(9)-C(10)	165.0(2)
O(2)-N(1)-C(9)-C(10)	-16.8(3)
O(3)-N(1)-C(9)-C(8)	-15.1(3)
O(2)-N(1)-C(9)-C(8)	163.1(2)
C(8)-C(9)-C(10)-C(11)	-0.6(3)
N(1)-C(9)-C(10)-C(11)	179.21(18)
C(9)-C(10)-C(11)-C(6)	-0.9(3)
C(7)-C(6)-C(11)-C(10)	1.4(3)
C(4)-C(6)-C(11)-C(10)	-179.83(19)

Symmetry transformations used to generate equivalent atoms:

Table S14. Hydrogen bonds for C11H11Cl2NO3 [≈ and ∞]

D-H...A	d(D-H)	d(H...A)	d(D...A)	<(DHA)
O(1)-H(1O)...O(2)#1	0.81(2)	2.21(2)	2.982(2)	158(3)

Symmetry transformations used to generate equivalent atoms:

#1 -x+1,y+1/2,-z+3/2

2.8.15.3. Crystallographic Data for (S)-4-fluoro-3-hydroxy-3-phenylbutyl 4-bromobenzoate [(*S*)-2.35]

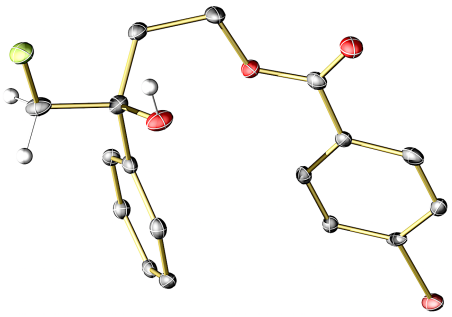

Table S15. Crystal data and structure refinement for C17H16BrFO3

Identification code	C17H16BrFO3
Empirical formula	C17H16BrFO3
Formula weight	367.21
Temperature	100(2) K
Wavelength	1.54178 ≈
Crystal system	Orthorhombic
Space group	$P2_12_12_1$
Unit cell dimensions	a = 5.7046(3) ≈ □= 90∞.

b = 7.4441(4) ≈ □= 90∞.

c = 35.724(2) ≈ □ = 90∞.

Volume 1517.06(14) ≈3

Z 4

Density (calculated) 1.608 Mg/m3

Absorption coefficient 3.889 mm-1

F(000) 744

Crystal size 0.440 x 0.340 x 0.080 mm3

Theta range for data collection 2.474 to 69.834∞.

Index ranges -6<=h<=6, -7<=k<=8, -43<=l<=42

Reflections collected 16996

Independent reflections 2841 [R(int) = 0.0471]

Completeness to theta = 67.679∞ 99.9 %

Absorption correction Semi-empirical from equivalents

Max. and min. transmission 0.7533 and 0.5277

Refinement method Full-matrix least-squares on F2

Data / restraints / parameters 2841 / 1 / 203

Goodness-of-fit on F2 1.300

Final R indices [I>2sigma(I)] R1 = 0.0444, wR2 = 0.1143

R indices (all data) R1 = 0.0445, wR2 = 0.1144

Absolute structure parameter -0.008(14)

Extinction coefficient n/a

Largest diff. peak and hole 0.907 and -0.774 e.≈-3

Table S16. Atomic coordinates (x104) and equivalent isotropic displacement parameters (≈2x103) for C17H16BrFO3. U(eq) is defined as one third of the trace of the orthogonalized Uij tensor

---

x y z U(eq)

Br(1)	10590(2)	10639(1)	2555(1)	34(1)
F(1)	4998(8)	1606(5)	4848(1)	34(1)
O(1)	8253(10)	3426(8)	4414(1)	32(1)
O(2)	7070(9)	7564(6)	4256(1)	28(1)
O(3)	10610(11)	8587(7)	4426(1)	35(1)
C(1)	7027(12)	3548(9)	3688(2)	23(1)
C(2)	6663(13)	3781(8)	3309(2)	24(1)
C(3)	4583(13)	4553(8)	3181(2)	23(1)
C(4)	2887(12)	5029(9)	3436(2)	24(1)
C(5)	3245(12)	4789(8)	3818(2)	22(1)
C(6)	5346(13)	4061(8)	3949(2)	22(1)
C(7)	5811(13)	3762(9)	4367(2)	23(1)
C(8)	5006(11)	5337(9)	4616(2)	25(2)
C(9)	6696(16)	6880(10)	4632(2)	34(2)
C(10)	9133(13)	8338(8)	4190(2)	24(1)
C(11)	9406(13)	8842(8)	3788(2)	21(1)
C(12)	11489(13)	9701(9)	3683(2)	28(2)
C(13)	11839(12)	10213(8)	3317(2)	25(1)
C(14)	10121(12)	9851(8)	3057(2)	23(2)
C(15)	8054(12)	8973(8)	3151(2)	21(1)
C(16)	7738(11)	8459(9)	3519(2)	21(1)
C(17)	4486(15)	2060(9)	4472(2)	29(2)

Table S17. Bond lengths [≈] and angles [∞] for C17H16BrFO3

Br(1)-C(14)	1.905(6)
F(1)-C(17)	1.417(7)

O(1)-C(7)	1.425(9)
O(1)-H(1O)	0.84(3)
O(2)-C(10)	1.331(9)
O(2)-C(9)	1.453(8)
O(3)-C(10)	1.206(9)
C(1)-C(2)	1.381(9)
C(1)-C(6)	1.392(9)
C(1)-H(1)	0.9500
C(2)-C(3)	1.395(10)
C(2)-H(2)	0.9500
C(3)-C(4)	1.375(10)
C(3)-H(3)	0.9500
C(4)-C(5)	1.391(9)
C(4)-H(4)	0.9500
C(5)-C(6)	1.396(9)
C(5)-H(5)	0.9500
C(6)-C(7)	1.532(8)
C(7)-C(17)	1.522(10)
C(7)-C(8)	1.543(9)
C(8)-C(9)	1.501(10)
C(8)-H(8A)	0.9900
C(8)-H(8B)	0.9900
C(9)-H(9A)	0.9900
C(9)-H(9B)	0.9900
C(10)-C(11)	1.496(8)
C(11)-C(16)	1.380(9)
C(11)-C(12)	1.400(10)
C(12)-C(13)	1.377(10)

C(12)-H(12) 0.9500

C(13)-C(14) 1.377(10)

C(13)-H(13) 0.9500

C(14)-C(15) 1.390(9)

C(15)-C(16) 1.380(9)

C(15)-H(15) 0.9500

C(16)-H(16) 0.9500

C(17)-H(17A) 0.9900

C(17)-H(17B) 0.9900

C(7)-O(1)-H(1O) 107(6)

C(10)-O(2)-C(9) 116.3(6)

C(2)-C(1)-C(6) 121.3(6)

C(2)-C(1)-H(1) 119.3

C(6)-C(1)-H(1) 119.3

C(1)-C(2)-C(3) 120.0(6)

C(1)-C(2)-H(2) 120.0

C(3)-C(2)-H(2) 120.0

C(4)-C(3)-C(2) 119.2(6)

C(4)-C(3)-H(3) 120.4

C(2)-C(3)-H(3) 120.4

C(3)-C(4)-C(5) 120.8(6)

C(3)-C(4)-H(4) 119.6

C(5)-C(4)-H(4) 119.6

C(4)-C(5)-C(6) 120.4(6)

C(4)-C(5)-H(5) 119.8

C(6)-C(5)-H(5) 119.8

C(1)-C(6)-C(5) 118.2(6)

C(1)-C(6)-C(7)	119.6(6)
C(5)-C(6)-C(7)	122.2(6)
O(1)-C(7)-C(17)	108.1(6)
O(1)-C(7)-C(6)	108.0(5)
C(17)-C(7)-C(6)	105.9(5)
O(1)-C(7)-C(8)	110.9(6)
C(17)-C(7)-C(8)	110.1(5)
C(6)-C(7)-C(8)	113.6(5)
C(9)-C(8)-C(7)	114.3(6)
C(9)-C(8)-H(8A)	108.7
C(7)-C(8)-H(8A)	108.7
C(9)-C(8)-H(8B)	108.7
C(7)-C(8)-H(8B)	108.7
H(8A)-C(8)-H(8B)	107.6
O(2)-C(9)-C(8)	109.1(5)
O(2)-C(9)-H(9A)	109.9
C(8)-C(9)-H(9A)	109.9
O(2)-C(9)-H(9B)	109.9
C(8)-C(9)-H(9B)	109.9
H(9A)-C(9)-H(9B)	108.3
O(3)-C(10)-O(2)	124.2(6)
O(3)-C(10)-C(11)	124.1(7)
O(2)-C(10)-C(11)	111.7(6)
C(16)-C(11)-C(12)	119.6(6)
C(16)-C(11)-C(10)	123.0(6)
C(12)-C(11)-C(10)	117.4(6)
C(13)-C(12)-C(11)	120.2(6)
C(13)-C(12)-H(12)	119.9

C(11)-C(12)-H(12)	119.9
C(14)-C(13)-C(12)	118.9(6)
C(14)-C(13)-H(13)	120.6
C(12)-C(13)-H(13)	120.6
C(13)-C(14)-C(15)	122.1(6)
C(13)-C(14)-Br(1)	118.3(5)
C(15)-C(14)-Br(1)	119.5(5)
C(16)-C(15)-C(14)	118.2(6)
C(16)-C(15)-H(15)	120.9
C(14)-C(15)-H(15)	120.9
C(11)-C(16)-C(15)	120.9(6)
C(11)-C(16)-H(16)	119.5
C(15)-C(16)-H(16)	119.5
F(1)-C(17)-C(7)	109.2(6)
F(1)-C(17)-H(17A)	109.8
C(7)-C(17)-H(17A)	109.8
F(1)-C(17)-H(17B)	109.8
C(7)-C(17)-H(17B)	109.8
H(17A)-C(17)-H(17B)	108.3

Symmetry transformations used to generate equivalent atoms:

Table S18. Anisotropic displacement parameters (≈2x 103) for C17H16BrFO3. The anisotropic displacement factor exponent takes the form: -2□2[h2 a*2U11 + ... + 2 h k a* b* U12]

	U11	U22	U33	U23	U13	U12
Br(1)	54(1)	26(1)	22(1)	2(1)	10(1)	-4(1)

F(1)	52(3)	30(2)	21(2)	7(2)	4(2)	-2(2)
O(1)	30(3)	46(3)	19(2)	3(2)	-1(2)	5(3)
O(2)	36(3)	26(2)	20(2)	1(2)	4(2)	-7(2)
O(3)	42(3)	38(3)	24(2)	1(2)	-3(3)	-7(3)
C(1)	23(3)	17(3)	30(3)	2(3)	-1(3)	-1(3)
C(2)	31(4)	17(3)	23(3)	-2(2)	7(3)	-2(3)
C(3)	34(3)	17(3)	19(3)	2(2)	-2(3)	-8(3)
C(4)	22(3)	24(3)	27(3)	2(3)	-3(3)	-1(3)
C(5)	21(3)	19(3)	26(3)	-2(2)	4(3)	3(3)
C(6)	31(4)	17(3)	20(3)	1(2)	0(3)	-7(3)
C(7)	21(3)	28(3)	21(3)	2(2)	1(3)	1(3)
C(8)	26(4)	31(4)	18(3)	2(2)	2(2)	-3(3)
C(9)	54(5)	31(4)	17(3)	-3(3)	5(3)	-15(4)
C(10)	32(4)	16(3)	24(3)	-2(2)	-1(3)	2(3)
C(11)	26(3)	15(3)	23(3)	-3(2)	5(3)	-1(3)
C(12)	40(4)	19(4)	26(3)	-4(3)	-2(3)	1(3)
C(13)	25(3)	20(3)	31(3)	-3(3)	8(3)	-2(3)
C(14)	39(4)	15(3)	15(3)	2(2)	7(3)	4(3)
C(15)	19(3)	18(3)	26(3)	-1(2)	1(3)	1(3)
C(16)	18(3)	17(3)	28(3)	-2(3)	0(3)	0(3)
C(17)	40(4)	29(3)	18(3)	5(2)	3(3)	9(4)

Table S19. Hydrogen coordinates (x104) and isotropic displacement parameters (≈2x 103) for C17H16BrFO3

	x	y	z	U(eq)
H(1O)	8450(140)	3180(110)	4640(9)	30(20)

H(1)	8453	3026	3772	28
H(2)	7830	3417	3135	28
H(3)	4341	4746	2921	28
H(4)	1452	5529	3350	29
H(5)	2054	5122	3990	26
H(8A)	3482	5784	4522	30
H(8B)	4752	4883	4874	30
H(9A)	6057	7844	4794	41
H(9B)	8204	6475	4740	41
H(12)	12665	9931	3865	34
H(13)	13243	10807	3245	30
H(15)	6890	8733	2968	25
H(16)	6354	7832	3589	25
H(17A)		2779	2256	4442	35
H(17B)		4958	1065	4304	35

Table S20. Torsion angles [∞] for C17H16BrFO3

C(6)-C(1)-C(2)-C(3)	0.3(10)
C(1)-C(2)-C(3)-C(4)	-1.7(9)
C(2)-C(3)-C(4)-C(5)	1.5(10)
C(3)-C(4)-C(5)-C(6)	0.2(10)
C(2)-C(1)-C(6)-C(5)	1.3(10)
C(2)-C(1)-C(6)-C(7)	179.5(6)
C(4)-C(5)-C(6)-C(1)	-1.6(9)
C(4)-C(5)-C(6)-C(7)	-179.6(6)
C(1)-C(6)-C(7)-O(1)	15.7(8)
C(5)-C(6)-C(7)-O(1)	-166.2(6)

C(1)-C(6)-C(7)-C(17) -99.9(7)

C(5)-C(6)-C(7)-C(17) 78.2(7)

C(1)-C(6)-C(7)-C(8) 139.2(6)

C(5)-C(6)-C(7)-C(8) -42.7(9)

O(1)-C(7)-C(8)-C(9) 40.7(8)

C(17)-C(7)-C(8)-C(9) 160.3(6)

C(6)-C(7)-C(8)-C(9) -81.2(8)

C(10)-O(2)-C(9)-C(8) -152.0(6)

C(7)-C(8)-C(9)-O(2) 58.7(8)

C(9)-O(2)-C(10)-O(3) -4.3(10)

C(9)-O(2)-C(10)-C(11) 174.9(5)

O(3)-C(10)-C(11)-C(16) 176.5(7)

O(2)-C(10)-C(11)-C(16) -2.8(9)

O(3)-C(10)-C(11)-C(12) -1.9(9)

O(2)-C(10)-C(11)-C(12) 178.8(6)

C(16)-C(11)-C(12)-C(13) 2.1(10)

C(10)-C(11)-C(12)-C(13) -179.4(6)

C(11)-C(12)-C(13)-C(14) -0.6(10)

C(12)-C(13)-C(14)-C(15) -0.5(10)

C(12)-C(13)-C(14)-Br(1) 178.0(5)

C(13)-C(14)-C(15)-C(16) 0.1(9)

Br(1)-C(14)-C(15)-C(16) -178.4(5)

C(12)-C(11)-C(16)-C(15) -2.5(9)

C(10)-C(11)-C(16)-C(15) 179.1(6)

C(14)-C(15)-C(16)-C(11) 1.4(9)

O(1)-C(7)-C(17)-F(1) 59.4(7)

C(6)-C(7)-C(17)-F(1) 174.9(6)

C(8)-C(7)-C(17)-F(1) -61.9(7)

Symmetry transformations used to generate equivalent atoms:

Table S21. Hydrogen bonds for C17H16BrFO3 [≈ and ∞]

D-H...A	d(D-H)	d(H...A)	d(D...A)	<(DHA)
O(1)-H(1O)...F(1)#1	0.84(3)	2.04(4)	2.819(6)	155(8)

2.8.15.4. Crystallographic Data for (*S*)-2-(1-(2,6-Difluorobenzyl)-1*H*-1,2,3-triazol-4-yl)-1,1-difluoropent-4-en-2-ol (2.45)

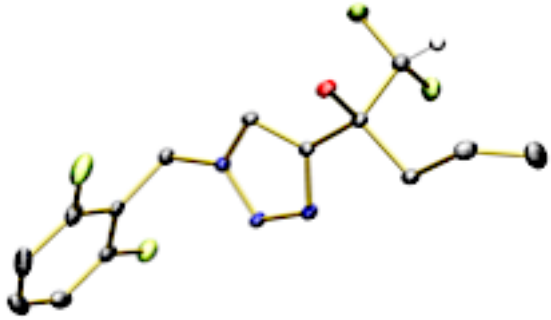

Table S22. Crystal data and structure refinement for C14H13F4N3O

Identification code	C14H13F4N3O
Empirical formula	C14 H13 F4 N3 O
Formula weight	315.27
Temperature	123(2) K
Wavelength	1.54178 ≈
Crystal system	Orthorhombic
Space group	$P2_12_12_1$
Unit cell dimensions	a = 5.3577(2) ≈ □= 90∞.
	b = 9.2921(4) ≈ □= 90∞.

c = 28.0870(12) ≈ □ = 90∞.

Volume 1398.29(10) ≈3

Z 4

Density (calculated) 1.498 Mg/m3

Absorption coefficient 1.168 mm-1

F(000) 648

Crystal size 0.580 x 0.120 x 0.080 mm3

Theta range for data collection 3.147 to 66.505∞.

Index ranges -6<=h<=6, -11<=k<=11, 0<=l<=33

Reflections collected 4855

Independent reflections 2465 [R(int) = 0.0304]

Completeness to theta = 66.505∞ 100.0 %

Absorption correction Semi-empirical from equivalents

Max. and min. transmission 0.7528 and 0.5837

Refinement method Full-matrix least-squares on F2

Data / restraints / parameters 2465 / 194 / 200

Goodness-of-fit on F2 1.073

Final R indices [I>2sigma(I)] R1 = 0.0570, wR2 = 0.1441

R indices (all data) R1 = 0.0577, wR2 = 0.1452

Extinction coefficient n/a

Largest diff. peak and hole 0.196 and -0.440 e.≈-3

Table S23. Atomic coordinates (x 104) and equivalent isotropic displacement parameters (≈2x103)

for C14H13F4N3O. U(eq) is defined as one third of the trace of the orthogonalized Uij tensor

x	y	z	U(eq)

F(1)	9039(5)	5283(2)	7857(1)	64(1)
F(2)	2367(4)	8504(2)	7991(1)	56(1)
F(3)	6999(4)	7702(2)	5473(1)	52(1)
F(4)	10706(4)	7649(2)	5798(1)	52(1)
O(1)	10286(4)	4704(2)	5975(1)	42(1)
N(1)	6508(5)	7032(3)	7044(1)	40(1)
N(2)	4278(5)	6564(3)	6898(1)	42(1)
N(3)	4603(5)	6009(3)	6471(1)	42(1)
C(1)	6410(10)	4144(4)	4746(1)	62(1)
C(2)	7346(6)	3986(4)	5170(1)	48(1)
C(3)	6273(5)	4639(3)	5614(1)	41(1)
C(4)	8154(5)	5572(3)	5887(1)	40(1)
C(5)	7057(5)	6133(3)	6348(1)	38(1)
C(6)	8267(6)	6794(3)	6719(1)	41(1)
C(7)	6780(6)	7792(3)	7502(1)	44(1)
C(8)	5789(6)	6942(3)	7915(1)	41(1)
C(9)	6971(7)	5739(4)	8091(1)	50(1)
C(10)	6150(11)	4991(4)	8487(1)	65(1)
C(11)	4011(9)	5482(4)	8717(1)	63(1)
C(12)	2731(7)	6672(4)	8556(1)	57(1)
C(13)	3641(6)	7355(4)	8157(1)	46(1)
C(14)	8972(6)	6814(3)	5568(1)	43(1)

Table S24. Bond lengths [≈] and angles [∞] for C14H13F4N3O

F(1)-C(9)	1.356(4)
F(2)-C(13)	1.350(4)
F(3)-C(14)	1.368(4)

F(4)-C(14)	1.371(3)
O(1)-C(4)	1.420(4)
O(1)-H(1)	0.8400
N(1)-C(6)	1.330(4)
N(1)-N(2)	1.336(4)
N(1)-C(7)	1.476(4)
N(2)-N(3)	1.318(4)
N(3)-C(5)	1.364(4)
C(1)-C(2)	1.300(5)
C(1)-H(1A)	0.9500
C(1)-H(1B)	0.9500
C(2)-C(3)	1.502(4)
C(2)-H(2)	0.9500
C(3)-C(4)	1.535(4)
C(3)-H(3A)	0.9900
C(3)-H(3B)	0.9900
C(4)-C(5)	1.512(4)
C(4)-C(14)	1.526(4)
C(5)-C(6)	1.373(4)
C(6)-H(6)	0.9500
C(7)-C(8)	1.501(4)
C(7)-H(7A)	0.9900
C(7)-H(7B)	0.9900
C(8)-C(9)	1.376(5)
C(8)-C(13)	1.391(5)
C(9)-C(10)	1.384(6)
C(10)-C(11)	1.392(7)
C(10)-H(10)	0.9500

C(11)-C(12)	1.378(6)
C(11)-H(11)	0.9500
C(12)-C(13)	1.377(5)
C(12)-H(12)	0.9500
C(14)-H(14)	1.0000

C(4)-O(1)-H(1)	109.5
C(6)-N(1)-N(2)	111.7(2)
C(6)-N(1)-C(7)	127.4(3)
N(2)-N(1)-C(7)	120.8(2)
N(3)-N(2)-N(1)	106.8(2)
N(2)-N(3)-C(5)	109.0(2)
C(2)-C(1)-H(1A)	120.0
C(2)-C(1)-H(1B)	120.0
H(1A)-C(1)-H(1B)	120.0
C(1)-C(2)-C(3)	124.6(3)
C(1)-C(2)-H(2)	117.7
C(3)-C(2)-H(2)	117.7
C(2)-C(3)-C(4)	113.1(2)
C(2)-C(3)-H(3A)	109.0
C(4)-C(3)-H(3A)	109.0
C(2)-C(3)-H(3B)	109.0
C(4)-C(3)-H(3B)	109.0
H(3A)-C(3)-H(3B)	107.8
O(1)-C(4)-C(5)	111.1(2)
O(1)-C(4)-C(14)	107.5(2)
C(5)-C(4)-C(14)	110.7(2)
O(1)-C(4)-C(3)	107.1(2)

C(5)-C(4)-C(3)	111.5(2)
C(14)-C(4)-C(3)	108.8(2)
N(3)-C(5)-C(6)	107.5(3)
N(3)-C(5)-C(4)	124.2(3)
C(6)-C(5)-C(4)	128.3(3)
N(1)-C(6)-C(5)	105.1(3)
N(1)-C(6)-H(6)	127.4
C(5)-C(6)-H(6)	127.4
N(1)-C(7)-C(8)	112.8(2)
N(1)-C(7)-H(7A)	109.0
C(8)-C(7)-H(7A)	109.0
N(1)-C(7)-H(7B)	109.0
C(8)-C(7)-H(7B)	109.0
H(7A)-C(7)-H(7B)	107.8
C(9)-C(8)-C(13)	115.4(3)
C(9)-C(8)-C(7)	122.9(3)
C(13)-C(8)-C(7)	121.7(3)
F(1)-C(9)-C(8)	117.1(3)
F(1)-C(9)-C(10)	119.5(4)
C(8)-C(9)-C(10)	123.4(4)
C(9)-C(10)-C(11)	118.0(4)
C(9)-C(10)-H(10)	121.0
C(11)-C(10)-H(10)	121.0
C(12)-C(11)-C(10)	121.5(4)
C(12)-C(11)-H(11)	119.3
C(10)-C(11)-H(11)	119.3
C(13)-C(12)-C(11)	117.4(4)
C(13)-C(12)-H(12)	121.3

C(11)-C(12)-H(12)	121.3
F(2)-C(13)-C(12)	117.9(3)
F(2)-C(13)-C(8)	117.9(3)
C(12)-C(13)-C(8)	124.3(3)
F(3)-C(14)-F(4)	105.9(2)
F(3)-C(14)-C(4)	110.4(2)
F(4)-C(14)-C(4)	110.3(2)
F(3)-C(14)-H(14)	110.0
F(4)-C(14)-H(14)	110.0
C(4)-C(14)-H(14)	110.0

Symmetry transformations used to generate equivalent atoms:

Table S25. Anisotropic displacement parameters (≈2x 103) for C14H13F4N3O. The anisotropic displacement factor exponent takes the form: -2□2[h2 a*2U11 + ... + 2 h k a* b* U12]

	U11	U22	U33	U23	U13	U12
F(1)	60(1)	66(1)	65(1)	-19(1)	-16(1)	22(1)
F(2)	46(1)	60(1)	62(1)	-9(1)	-7(1)	11(1)
F(3)	58(1)	48(1)	52(1)	5(1)	-7(1)	4(1)
F(4)	52(1)	51(1)	52(1)	2(1)	-3(1)	-15(1)
O(1)	33(1)	45(1)	50(1)	-2(1)	-2(1)	-1(1)
N(1)	34(1)	45(1)	41(1)	-1(1)	-3(1)	-1(1)
N(2)	34(1)	49(1)	43(1)	-4(1)	-1(1)	-2(1)
N(3)	33(1)	48(1)	43(1)	-4(1)	-2(1)	-1(1)
C(1)	78(3)	61(2)	47(2)	-6(2)	6(2)	-11(2)
C(2)	41(2)	47(2)	54(2)	-10(1)	2(1)	-3(1)

C(3)	33(1)	43(1)	46(2)	0(1)	1(1)	-4(1)
C(4)	34(1)	44(2)	41(1)	1(1)	0(1)	-1(1)
C(5)	32(1)	40(1)	41(1)	1(1)	-3(1)	0(1)
C(6)	33(1)	45(2)	44(1)	0(1)	-1(1)	-2(1)
C(7)	43(2)	47(2)	42(2)	-4(1)	-1(1)	-4(1)
C(8)	41(2)	44(2)	40(1)	-5(1)	-5(1)	-5(1)
C(9)	55(2)	46(2)	49(2)	-11(1)	-10(1)	3(2)
C(10)	96(3)	41(2)	58(2)	2(1)	-23(2)	-2(2)
C(11)	79(3)	63(2)	47(2)	-1(2)	0(2)	-22(2)
C(12)	56(2)	67(2)	49(2)	-12(2)	7(2)	-16(2)
C(13)	43(2)	49(2)	47(2)	-7(1)	-5(1)	-6(1)
C(14)	41(2)	44(2)	45(1)	-2(1)	-1(1)	-5(1)

Table S26. Hydrogen coordinates (x104) and isotropic displacement parameters (≈2x103) for C14H13F4N3O

	x	y	z	U(eq)
H(1)	11383	5197	6113	64
H(1A)	4946	4705	4702	74
H(1B)	7191	3699	4480	74
H(2)	8811	3418	5201	57
H(3A)	5681	3857	5826	49
H(3B)	4811	5236	5528	49
H(6)	9988	7031	6739	49
H(7A)	5881	8722	7484	53
H(7B)	8568	8003	7557	53
H(10)	7021	4167	8599	78

H(11)	3421	4985	8990	75
H(12)	1277	7009	8715	69
H(14)	9686	6433	5264	52

Table S27. Torsion angles [∞] for C14H13F4N3O

C(6)-N(1)-N(2)-N(3)	0.2(4)
C(7)-N(1)-N(2)-N(3)	176.6(3)
N(1)-N(2)-N(3)-C(5)	-0.1(4)
C(1)-C(2)-C(3)-C(4)	-124.1(4)
C(2)-C(3)-C(4)-O(1)	-54.7(3)
C(2)-C(3)-C(4)-C(5)	-176.4(3)
C(2)-C(3)-C(4)-C(14)	61.2(3)
N(2)-N(3)-C(5)-C(6)	0.0(4)
N(2)-N(3)-C(5)-C(4)	178.0(3)
O(1)-C(4)-C(5)-N(3)	-128.6(3)
C(14)-C(4)-C(5)-N(3)	112.1(3)
C(3)-C(4)-C(5)-N(3)	-9.2(4)
O(1)-C(4)-C(5)-C(6)	49.0(4)
C(14)-C(4)-C(5)-C(6)	-70.4(4)
C(3)-C(4)-C(5)-C(6)	168.4(3)
N(2)-N(1)-C(6)-C(5)	-0.2(3)
C(7)-N(1)-C(6)-C(5)	-176.3(3)
N(3)-C(5)-C(6)-N(1)	0.1(3)
C(4)-C(5)-C(6)-N(1)	-177.8(3)
C(6)-N(1)-C(7)-C(8)	-128.7(3)
N(2)-N(1)-C(7)-C(8)	55.5(4)
N(1)-C(7)-C(8)-C(9)	71.9(4)

N(1)-C(7)-C(8)-C(13) -110.4(3)

C(13)-C(8)-C(9)-F(1) 178.4(3)

C(7)-C(8)-C(9)-F(1) -3.8(4)

C(13)-C(8)-C(9)-C(10) -1.4(5)

C(7)-C(8)-C(9)-C(10) 176.4(3)

F(1)-C(9)-C(10)-C(11) -179.5(3)

C(8)-C(9)-C(10)-C(11) 0.3(5)

C(9)-C(10)-C(11)-C(12) 0.2(6)

C(10)-C(11)-C(12)-C(13) 0.4(5)

C(11)-C(12)-C(13)-F(2) 178.5(3)

C(11)-C(12)-C(13)-C(8) -1.6(5)

C(9)-C(8)-C(13)-F(2) -178.0(3)

C(7)-C(8)-C(13)-F(2) 4.1(4)

C(9)-C(8)-C(13)-C(12) 2.1(4)

C(7)-C(8)-C(13)-C(12) -175.7(3)

O(1)-C(4)-C(14)-F(3) -179.5(2)

C(5)-C(4)-C(14)-F(3) -58.0(3)

C(3)-C(4)-C(14)-F(3) 64.8(3)

O(1)-C(4)-C(14)-F(4) -62.8(3)

C(5)-C(4)-C(14)-F(4) 58.7(3)

C(3)-C(4)-C(14)-F(4) -178.4(2)

Symmetry transformations used to generate equivalent atoms:

Table S28. Hydrogen bonds for C14H13F4N3O [≈ and ∞]

D-H...A d(D-H) d(H...A) d(D...A) <(DHA)

O(1)-H(1)...N(3)#1	0.84	2.13	2.959(3)	167.4

Symmetry transformations used to generate equivalent atoms:

#1 x+1,y,z

2.8.16. Bibliography for Additions to Halomethyl Ketones

2.8.16.1. References for Preparing the Same Products in Racemic Form

[1] Jiang, S.; Agoston, G. E.; Chen, T.; Cabal, M-P.; Turos, E. *Organometallics* **1995**, *14*, 4697–4709.

[2] Cai, M. Z.; Song, C. S.; Huang, X. *Synthetic Communications*, **1997**, *27*, 3087–3093.

[3] Yasuda, M.; Tsuchida, M.; Baba, A. *Chem. Commun*. **1998**, 563–564.

[4] Shin, J. A.; Choi, K. I.; Pae, A. N.; Koh, H. Y.; Kang, H.-Y.; Cho, Y. S. *J. Chem. Soc., Perkins Trans.* **2001**, *1*, 946–948.

[5] Kamble, R. M.; Singh, V. K. *Tetrahedron Lett.* **2001**, *42*, 7525–7526.

[6] Yadav, J. S.; Reddy, B. V. S.; Krishna, A. D.; Sadasiv, K.; Chary, C. J. *Chem. Lett.* **2003**, *32*, 248–249.

[7] Peppe, C.; Nobrega, J. A.; Drehmer, L. D.; Martins, *Letters in Organic Chemistry* **2006**, *3,* 597–599.

[8] Lou, S.; Moquist, P. N.; Schaus, S. E. *J. Am. Chem. Soc.* **2006**, *128*, 12660–12661.

[9] Jian, Z.; Lu, J.; Ji, S. J. *Chin. Chem. Lett.* **2007**, *18*, 1061–1063.

[10] Miller, J. J.; Sigman, M. S. *J. Am. Chem. Soc.* **2007**, *129*, 2752–2753.

[11] Di, J.; Zhang, S. *Synlett*, **2008**, *10*, 1491–1494.

[12] Liu, X.; Zhang, S.; Di, J. *Synthesis*, **2009**, *16*, 2749–2755.

[13] Fandrick, K. R.; Fandrick, D. R.; Gao, J. J.; Reeves, J. T.; Tan, Z.; Li, W.; Song, J. J.; Lu, B.; Yee, N. K.; Senanayake, C. H. *Org. Lett.* **2010**, *12*, 3748–3751.

[14] Hara, N.; Tamura, R.; Funahashi, Y.; Nakamura, S. *Org. Lett*. **2011**, *13*, 1662–1665.

[15] Zhao, H.; Peng, J.; Xiao, R.; Hao, W.; Cai, M-Z. *J. Organomet. Chem.* **2011**, *696,* 2030–2034.

[16] Wang, X.; Zhang, S. *Chin. J. Chem.* **2012**, *30*, 96–102.

[17] Lin, M.-H.; Kuo, C.-K.; Lin, W.-C.; Huang, Y.-C.; Tsai, Y.-T.; Liang, K.-Y.; Li, Y.-S.; Chuang, T.-H. *Tetrahedron*, **2013**, *69*, 8263–8268.

2.8.16.2. References for Catalytic Enantioselective Additions to Halomethyl Ketones

[1] Yus, M.; Ramón, D. J.; Prieto, O. *Tetrahedron: Asymmetry* **2003**, *14*, 1103–1104.

[2] García, C.; Walsh, P. J. *Org. Lett.* **2003**, *5*, 3641–3644.

[3] Cozzi, P. G.; Alesi, S. *Chem. Commun.* **2004***,* 2448–2449.

[4] Suzuki, M.; Kato, N.; Kanai, M.; Shibasaki, M. *Org. Lett.* **2005**, *7*, 2527–2530.

[5] Forrat, V. J.; Prieto, O.; Ramón, D. J.; Yus, M. *Chem. Eur. J.* **2006**, *12*, 4431–4445.

[6] Zuend, S. J.; Jacobsen, E. N. *J. Am. Chem. Soc.* **2007**, *129*, 15872–15883.

[7] Yu, L.-T.; Ho, M.-T.; Chang, C.-Y.; Yang, T.-K. *Tetrahedron: Asymmetry* **2007**, *18*, 949–962.

[8] Forrat, V. J.; Ramón, D. J.; Yus, M. *Tetrahedron: Asymmetry* **2007**, *18*, 400–405.

[9] Chen, C.-A.; Wu, K.-H.; Gau, H.-M. *Angew. Chem., Int. Ed.* **2007**, *46*, 5373–5376.

[10] Zhou, S.; Wu, K.-H.; Chen, C.-A.; Gau, H.-M. *J. Org. Chem.* **2009**, *74*, 3500–3505.

[11] Nie, J.; Zhang, G.-W.; Wang, L.; Fu, A.; Zheng, Y.; Ma, J.-A. *Chem. Commun.* **2009**, 2356–2358.

[12] Benfatti, F.; Cozzi, P. G. *Tetrahedron: Asymmetry* **2010**, *21*, 1503–1506.

[13] Zhou, S.; Chen, C.-R.; Gau, H.-M. *Org. Lett.* **2010**, *12*, 48–51.

[14] Diebler, J.; von Langermann, J.; Mell, A.; Hein, M.; Langer, P.; Kragl, U. *ChemCatChem* **2014**, *6*, 987–991.

[15] Tamura, K.; Kumagai, N.; Shibasaki, M. *J. Org. Chem.* **2014**, *79*, 3272–3278.

[16] Shu, C.-C.; Zhou, S.; Gau, H.-M.; *RSC Adv.* **2015**, *5*, 98391–98398.

[17] Sasaki, S.; Yamaguchi, T.; Kanai, M.; Ishii, A.; Higashiyama, K. *Bull. Chem. Soc. Jpn.* **2015,** *88*, 200–208.

[18] Ito, J.-I.; Ubukata, S.; Muraoka, S.; Nishiyama, H. *Chem. Eur. J.* **2016**, *22*, 16801–16804.

[19] Xie, F.; Ni, T.; Zhao, J.; Pang, L.; Li, R.; Cai, Z.; Ding, Z.; Wang, T.; Yu, S.; Jin, Y.; Zhang, D.; Jiang, Y. *Bioorg. Med. Chem. Lett.* **2017**, *27*, 2171–2173.

[20] Neves-Garcia, T.; Vélez, A.; Martínez-Ilarduya, J. M.; Espinet, P. *Chem. Commun.* **2018**, *54*, 11809–11812.

[21] Karasawa, T.; Kumagai, N.; Shibasaki, M. *Org. Lett.* **2018**, *20*, 308–311.

[22] Cao, K.; Tan, S. M.; Lee, R.; Yang, S.; Jia, H.; Zhao, X.; Qiao, B.; Jiang, Z. *J. Am. Chem. Soc.* **2019**, *141*, 5437–5443.

[23] Gan, X.-C.; Yin, L. *J. Am. Chem. Soc.* **2019**, *21*, 931–936.

[24] Otrevel, J.; Svestka, D.; Bobal, P. *Org. Biomol. Chem.* **2019***, 17*, 5244–5248.

[25] Cai, L.; Zhao, Y.; Huang, T.; Meng, S.; Jia, X.; Chan, A. S. C.; Zhao, J. *Org. Lett.* **2019**, *21*, 3538–3542.

[26] Pluta, R.; Kumagai, N.; Shibasaki, M. *Angew. Chem., Int. Ed.* **2019**, *58*, 2459–2463.

[27] Matador, E.; Retamosa, M. G.; Jiménez-Sánchez, A.; Monge, D.; Fernández, R.; Lassaletta, J. M. *J. Org. Chem.* **2019**, 130–138.

Chapter Three

Catalytic Regio-, Z-, and Enantioselective Addition of Organoboron Compounds to Unprotected N–H Trifluoromethyl Ketimines

3.1. Introduction

The aminophenol-based boryl catalyst has been used for enantioselective additions of organoboron reagents to aldehydes,[184] ketones,[185] ketoesters,[2b] isatins,[186] and aldimines.[3,187] However, at the time we initiated our studies, additions to ketimines had not been reported. We wondered if these relatively unreactive compounds would be suitable substrates, considering the majority of reports required activating/directing groups.[188] We envisioned that, similar to trihalo-, dichloro-, and dibromomethyl ketones,[2e] electrostatic interaction involving a ketimine and a catalyst's ammonium group might lead to formation of α-tertiary amines enantioselectively.

---

[184] Morrison, R. J.; van der Mei, F. W.; Hoveyda, A. H. *J. Am. Chem. Soc.* **2020**, *142*, 436–447.

[185] (a) Lee, K.; Silverio, D. L.; Torker, S.; Haeffner, F.; Robbins, D. W.; van der Mei, F. W.; Hoveyda, A. H. *Nat. Chem.* **2016**, *8*, 768–777. (b) Robbins, D. W.; Lee, K.; Silverio, D. L.; Volkov, A.; Torker, S.; Hoveyda, A. H. *Angew. Chem., Int. Ed.* **2016**, *55*, 9610–9614. (c) Mszar, N. W.; Mikus, M. S.; Torker, S.; Haeffner, F.; Hoveyda, A. H. *Angew. Chem., Int. Ed.* **2017**, *56*, 8736–8741. (d) van der Mei, F. W.; Qin, C.; Morrison, R. J.; Hoveyda, A. H. *J. Am. Chem. Soc.* **2017**, *139*, 9053–9065. (e) Fager, D. C.; Lee, K.; Hoveyda, A. H. *J. Am. Chem. Soc.* **2018**, *141*, 16125–16138.

[186] Silverio, D. L.; Torker, S.; Pilyugina, T.; Vieira, E. M.; Snapper, M. L.; Haeffner, F.; Hoveyda, A. H. *Nature* **2013**, *494*, 216–221.

[187] (a) Wu, H.; Haeffner, F.; Hoveyda, A. H. *J. Am. Chem. Soc.* **2014**, *136*, 3780–3783. (b) van der Mei, F. W.; Miyamoto, H.; Silverio, D. L.; Hoveyda, A. H. *Angew. Chem., Int. Ed.* **2016**, *55*, 4701–4706. (c) Morrison, R. J.; Hoveyda, A. H. *Angew. Chem., Int Ed.* **2018**, *57*, 11654–11661.

[188] (a) Ishii, A.; Miyamoto, F.; Higashiyama, K.; Mikami, K. *Tetrahedron Lett.* **1998**, *39*, 1199–1202. (b) Guo, T.; Song, R.; Yuan, B.-H.; Chen, X.-Y.; Sun, X.-W.; Lin, G.-Q. *Chem Commun.* **2013**, *49*, 5402–5404. (c) Wu, Y.; Hu, L.; Deng, L. *Nature* **2015**, *523*, 445–450. (d) Lauson, C.; Charette, A. B. *Org. Lett.* **2006**, *8*, 2743–2745. (e) Liu, Y.-L.; Shi, T.-D.; Zhou, F.; Zhao, X.-L.; Wang, X.; Zhou, J. *Org. Lett.* **2011**, *13*, 3826–3829. (f) Sun, L.-H.; Liang, Z.-Q.; Jian, W.-Q.; Ye, S. *Angew. Chem., Int. Ed.* **2013**, *52*, 5803–5806.

Trifluoromethyl α-tertiary amines can be found in a range of biologically active molecules and as such, many methods are available for their synthesis.[189] We reasoned that development of a catalytic enantioselective method that obviates the need for protection/deprotection sequences and affords the H_2N-amine directly would be a valuable addition to the current state-of-the-art.

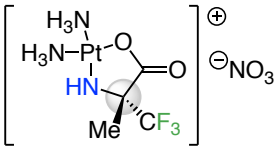

Cisplatin analog
(anti-cancer)

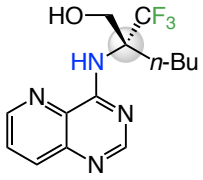

Toll-like receptor modulator
(anti-HIV)

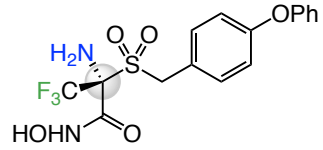

MMP inhibitor
(heart disease and anti-cancer)

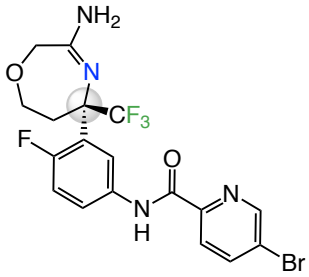

BACE-1 inhibitor
(anti-Alzheimer's)

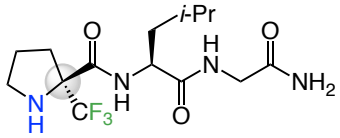

Allosteric MIF-1 activator
(anti-Parkinson's, antidepressant)

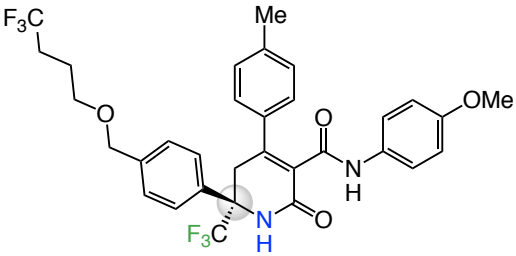

MGAT2 inhibitor
(anti-obesity)

[189] For methods for synthesis of trifluoromethyl α-tertiary amines, see: (a) Lauzon, C.; Charette, A. B. *Org. Lett.* **2006**, *8*, 2743–2745. (b) Fu, P.; Snapper, M. L.; Hoveyda, A. H. *J. Am. Chem. Soc.* **2008**, *130*, 5530–5541. (c) Jiang, B.; Dong, J. J.; Si, Y. G.; Zhao, X. L.; Huang, Z. G.; Xu, M. *Adv. Synth. Catal.* **2008**, *350*, 1360–1366. (d) Sukach, V. A.; Golovach, N. M.; Pirozhenko, V. V.; Rusanov, E. D.; Vovk, M. V. *Tetrahedron: Asymm.* **2008**, *19*, 761–764. (e) Hara, N.; Tamura, R.; Funahashi, Y.; Nakamura, S. *Org. Lett.* **2011**, *13*, 1662–1665. (f) Husmann, R.; Sugiono, E.; Mersmann, S.; Raabe, G.; Rueping, M.; Bolm, C. *Org. Lett.* **2011**, *13*, 1044–1047. (g) Huang, G.; Yang, J.; Zhang, X. *Chem. Commun.* **2011**, *47*, 5587–5589. (h) Liu, Y.-L.; Shi, T.-D.; Zhou, F.; Zhao, X.-L.; Wang, X.; Zhou, J. *Org. Lett.* **2011**, *13*, 3826–3829. (i) Sun, L.-H.; Liang, Z.-Q.; Jia, W.-Q.; Ye, S. *Angew. Chem., Int. Ed.* **2013**, *52*, 5803–5806. (j) Zhang, S.; Li, L.; Hu, Y.; Li, Y.; Yang, Y.; Zha, Z.; Wang, Z. *Org. Lett.* **2015**, *17*, 5036–5039. (k) Chen, P.; Yue, Z.; Zhang, J.; Lv, X.; Wang, L.; Zhang, J. *Angew. Chem., Int. Ed.* **2016**, *55*, 13316–13320. (l) Sawa, M.; Morisaki, K.; Kondo, Y.; Morimoto, H.; Ohshima, T. *Chem Eur. J.* **2017**, *23*, 17022–17028. (m) Chen, P.; Zhang, J. *Org. Lett.* **2017**, *19*, 6550–6553. (n) Trost, B. M.; Hung, C.-I.; Scharf, M. J. *Angew. Chem., Int. Ed.* **2018**, *57*, 11408–11412. (o) Yonesaki, R.; Kondo, Y.; Akkad, W.; Sawa, M.; Morisaki, K.; Morimoto, H.; Ohshima, T. *Chem. Eur. J.* **2018**, *24*, 15211–15214. (p) Miyagawa, M.; Yoshia, M.; Kiyota, Y.; Akiyama, T. *Chem. Eur. J.* **2019**, *25*, 5677–5681. (q) Zhu, J.; Huang, L.; Dong, W.; Li, N.; Yu, X.; Deng, W.-P.; Tang, W. *Angew. Chem., Int. Ed.* **2019**, *58*, 1–6.

3.2. Background

3.2.1. Synthesis of Trifluoromethyl α-Tertiary Amines

Due to the abundance of trifluoromethyl α-tertiary amines in biologically active molecules, there have been many reports for their preparation.[189] There are no reports for generating unprotected H_2N-amines directly by catalytic enantioselective allyl addition or methods that generate a terminally-substituted *Z* olefin. A monosubstituted olefin can be functionalized in a number of ways, but reaction of a *Z*-1,2-disubstituted alkene is more likely to be highly diastereoselective (the same comparison applies to the corresponding *E* olefins).[190] Finally, we were mindful of the fact that by finding a way to generate H_2N-amine products directly, there would be no need for deprotection, which at times require strongly basic or acidic conditions.[191]

3.2.1.1. Reactions of Enantiomerically Pure Ketimines

One common approach to the synthesis of α-tertiary amines relies on the use of enantiomerically pure ketimine substrates. In 1998, Mikami *et al.* reported the first addition to enantiomerically pure trifluoromethyl ketimines for synthesis of α-tertiary amines (Scheme 3.1).[192] Starting from trifluoromethyl ketone **3.1** and phenyl glycinol **(*R*)-3.2**, the *N,O*-acetal (**3.3**) was afforded in 1.6:1 diastereomeric ratio (dr). Separation of diastereomers and subsequent addition of an organolithium reagent (alkyl or vinyl) afforded the desired α-tertiary amines in >99:1

[190] Hoveyda, A. H.; Evans, D. A.; Fu, G. C. *Chem Rev.* **1993**, *93*, 1307–1370.

[191] (a) Ishii, A.; Miyamoto, F.; Higashiyama, K.; Mikami, K. *Tetrahedron Lett.* **1998**, 39, 1199–1202. (b) Chaume, G.; Van Severen, M.-C.; Marinkovic, S.; Brigaud, T. *Org. Lett.* **2006**, *8*, 6123–6126. (c) Min, Q.-Q.; He, C.-Y.; Zhoug, H.; Zhang, X. *Chem. Commun.* **2010**, *46*, 8029–8031. (d) Grellepois, F.; Jamaa, A. B.; Rosa, N. S. *Org. Biomol. Chem.* **2017**, *15*, 9696–9709.

[192] Ishii, A.; Miyamoto, F.; Higashiyama, K.; Mikami, K. *Tetrahedron Lett.* **1998**, *39*, 1199–1202.

diastereomeric ratio (**3.5**). Removal of the auxiliary by hydrogenolysis (H_2/Pd) or oxidative cleavage delivered the H_2N-α-tertiary amines (45-92% yield).

Scheme 3.1. Phenyl Glycinol Based Auxiliary Used in Diastereoselective Additions

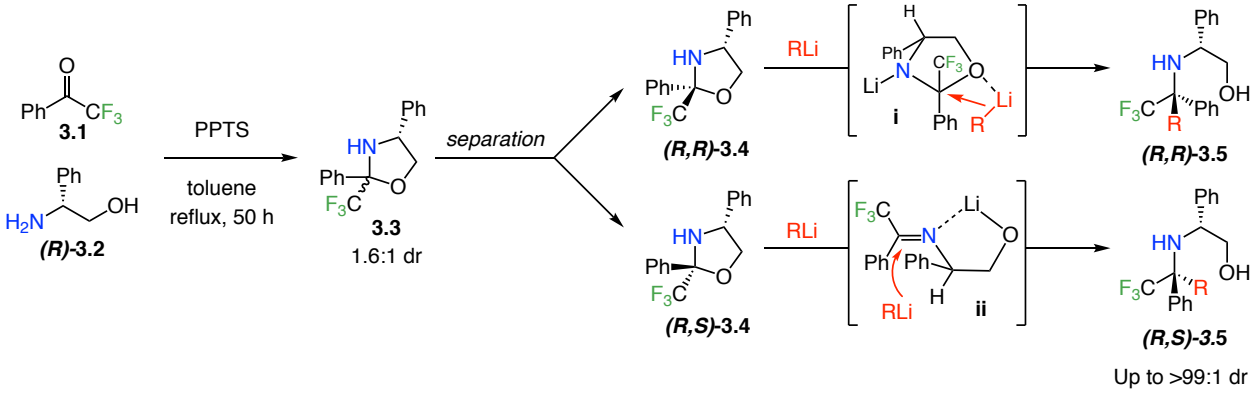

A few years later, Brigaud *et al.* used a silyl-protected phenyl glycinol auxiliary towards the same end.[193] Ensuing Lewis acid promoted allyl addition led to the formation of the homoallylic amines in up to 85:15 diastereomeric ratio through a transition state similar to **ii** (Scheme 3.1). This was followed by indium-mediated additions disclosed by Zhang *et al.* furnishing the amines in up to >20:1 diastereomeric ratio (**3.6** → **3.7**, Scheme 3.2).[194]

Scheme 3.2. Phenyl Glycinol Auxiliary for Diastereoselective Allyl and Crotyl Additions

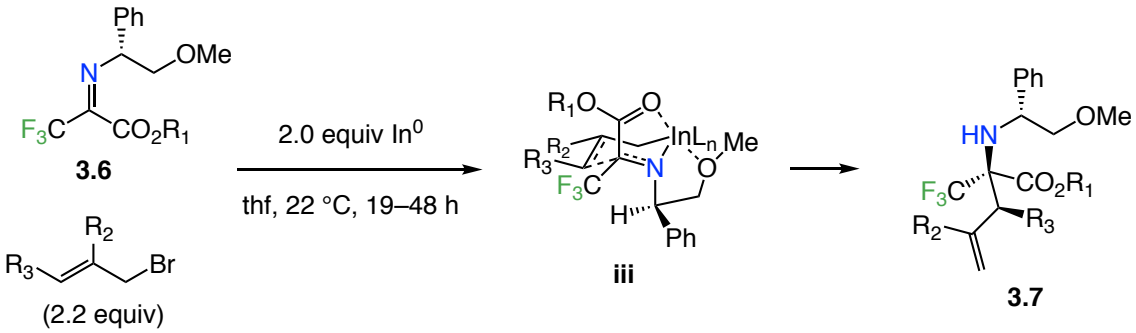

[193] Chaume, G.; Van Severen, M.-C.; Marinkovic, S.; Brigaud, T. *Org. Lett.* **2006**, *8*, 6123–6126.

[194] Min, Q.-Q.; He, C.-Y.; Zhou, H.; Zhang, X. *Chem. Commun.* **2010**, *46*, 8029–8031.

In 2013, Lin *et al.* used an Ellman auxiliary-based substrate to synthesize α-tertiary amines by Zn-mediated allyl addition, but diastereoselectivies did not exceed 85:15.[195] Later that year, Grellepois *et al.* reported diastereoselective additions of Grignard or organolithium reagents (alkyl, benzyl, allyl, and thienyl) to the same type of substrate with (70:30-98:2 dr, up to 83% yield).[196] Finally, in 2017, Grellepois *et al.* outlined two complementary methods: one involving a Zn-based complex (**iv**) and the other proceeding via an organoindium intermediate (**v**).[197] Homoallylic α-tertiary amines (**3.9**, Scheme 3.3) were thus isolated in up to >99:1 diastereomeric ratio and 77% yield. A limited number of crotyl-type additions were shown to afford products in 59:41 to 96:4 dr.

Scheme 3.3. Use of Ellman Auxiliary in Diastereoselective Allyl Additions

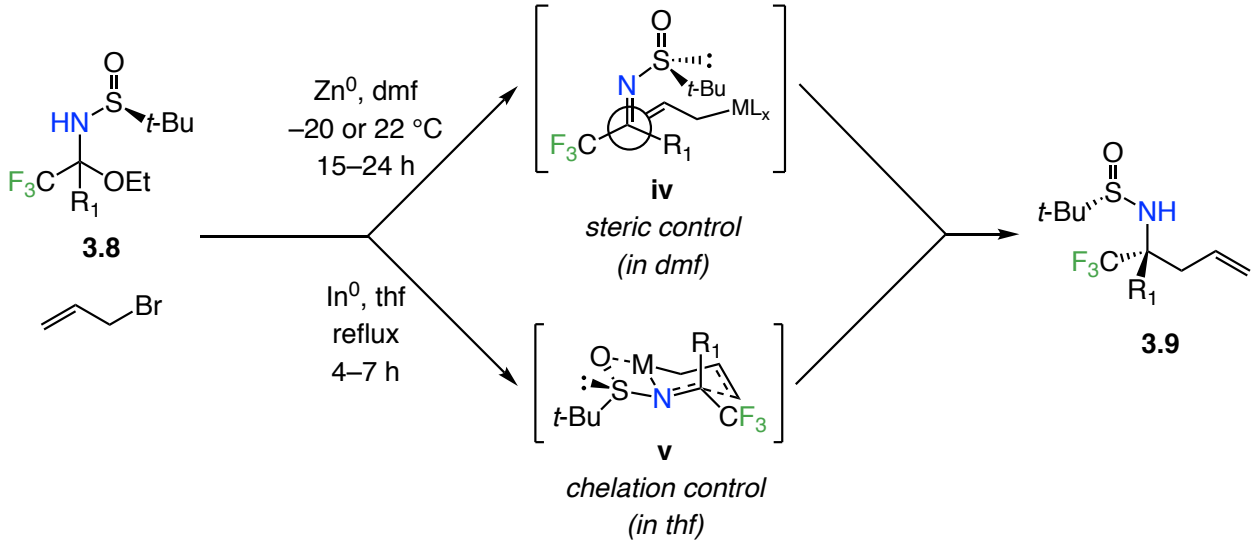

[195] Guo, T.; Song, R.; Yuan, B.-H.; Chen, X.-Y.; Sun, X.-W.; Lin, G.-Q. *Chem Commun.* **2013**, *49*, 5402–5404.

[196] Grellepois, F.; Jamaa, A. B.; Gassama, A. *Eur. J. Org. Chem.* **2013**, 6694–6701.

[197] Grellepois, F.; Jamaa, A. B.; Rosa, N. S. *Org. Biomol. Chem.* **2017**, *15*, 9696–9709.

3.2.1.2. Through Mannich-Type Processes

In 2008, Vovk *et al.* reported a L-proline-catalyzed (**pro-1**) Mannich-type reaction between a trifluoromethyl N–H ketimine (**3.10**) and acetone (Scheme 3.4).[198] Products were afforded in 87:13 to 96:4 er. However, reaction times were long, ranging from two to ten days, and in some cases never reaching full conversion. Soon after, Xu and coworkers showed that Mannich-type transformations could be performed with the imine core of antiviral agent, Efavirenz, and acetone with a substituted pyrrolidine as the catalyst.[199] Nonetheless, reaction times ranged from one to eight days and products were obtained in 65:35-89.5:10.5 er.

Scheme 3.4. Mannich-Type Reactions with Trifluoromethyl Ketimines

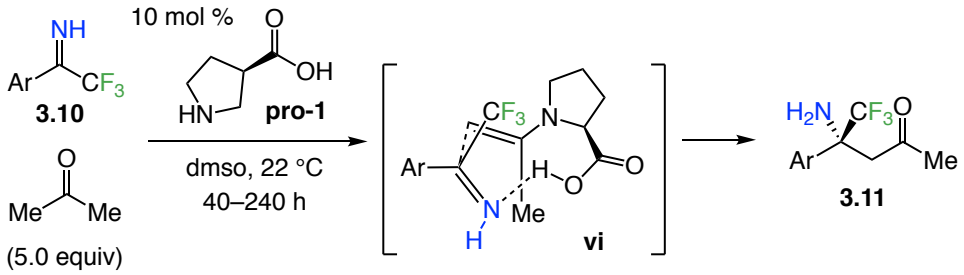

Scheme 3.5. Use of a Prolinamide Catalyst in Mannich-Type Processes

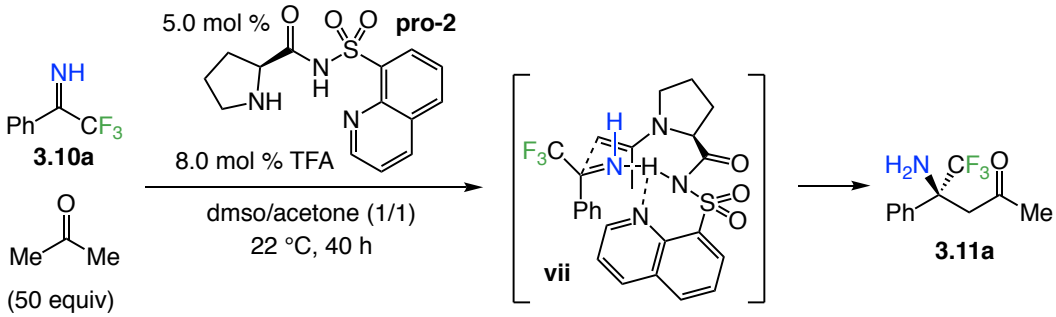

[198] Sukach, V. A.; Golovach, N. M.; Pirozhenko, V. V.; Rusanov, E. B.; Vovk, M. V. *Tetrahedron Asymm.* **2008**, *19*, 761–764.

[199] Jiang, B.; Dong, J. J.; Si, Y. G.; Zhao, X. L.; Huang, Z. G.; Xu, M. *Adv. Synth. Catal.* **2008**, *350*, 1360–1366.

In 2011, Nakamura *et al.* demonstrated that if *N*-(8-quinolinesulfonyl)prolinamide (**pro-2**) is used, there is complete conversion in 40 hours with enantioselectivities ranging from 88.5:11.5 to 96:4 (Scheme 3.5).[200] Most recently, Wang and coworkers reported processes involving benzosulfonimides (**3.12**) and ketones, promoted by a urea-based catalyst (**urea-1**), to generate products in 95.5:4.5 to >99:1 er in just 36 hours (Scheme 3.6).[201]

Scheme 3.6. Urea Catalysts for Mannich Reactions of Trifluoromethyl Ketimines

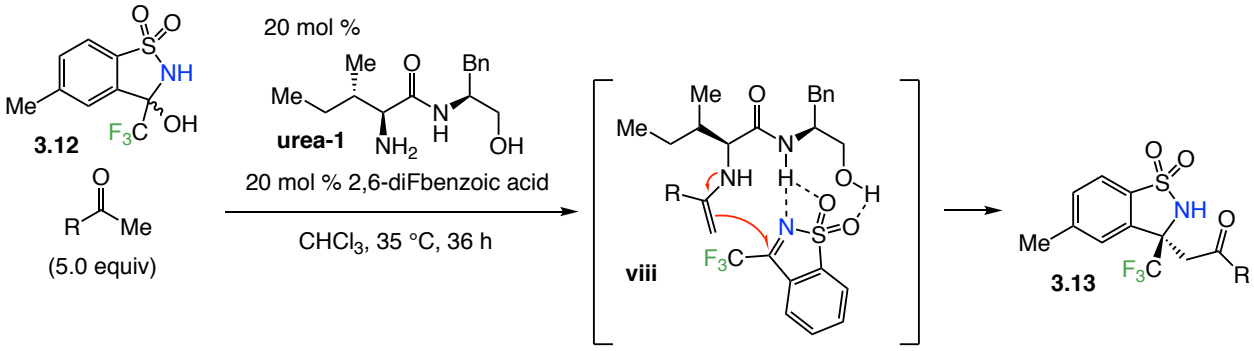

3.2.1.3. By Umpolung Strategies

Deng *et al.* have employed umpolung strategies toward development of methods for synthesis of trifluoromethyl α-tertiary amines (**3.17** and **3.18**, Scheme 3.7). Through the use of activated *N*-(4-nitrophenyl)benzyl ketimines (**3.14**) and a cinchona-alkaloid phase transfer catalyst (**cinch-1**), products were obtained in 89:11 to >99:1 er and 51–96% yield.[202] Substrates containing alkyl, alkenyl, aryl, electron-donating, and electron-withdrawing substituents on both the nucleophilic ketimine (**3.14**) and electrophiles (**3.15** or **3.16**) proved to be suitable.

---

[200] Hara, N.; Tamura, R.; Funahashi, Y.; Nakamura, S. *Org. Lett.* **2011**, *13*, 1662–1665.

[201] Zhang, S.; Li, L.; Hu, Y.; Yang, L.; Zha, Z.; Wang, Z. *Org. Lett.* **2015**, *17*, 5036–5039.

[202] (a) Wu, Y.; Hu, L.; Deng, L. *Nature* **2015**, *523*, 445–450. (b) Hu, L.; Wu, Y.; Deng, L. *J. Am. Chem. Soc.* **2016**, *138*, 15817–15820. (c) Li, Z.; Hu, B.; Wu, Y.; Fei, C.; Deng, L. *PNAS* **2018**, *115*, 1730–1735. (d) Hu, B.; Deng, L.; *J. Org. Chem.* **2019**, *84*, 94–105.

Scheme 3.7. An Umpolung Approach to Enantioselective Synthesis of α-Tertiary Amines

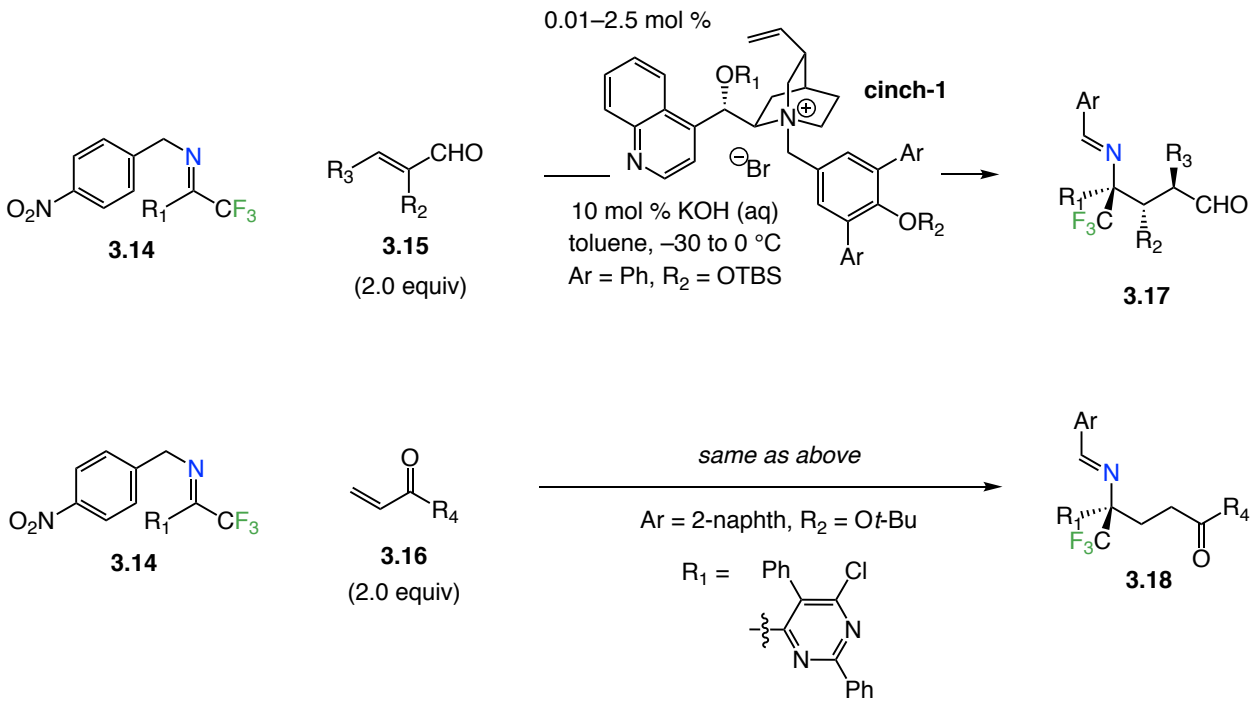

A related approach was reported by Zhang *et al.*, who utilized the same set of starting materials (**3.14**) in the presence of a substituted allyl ether (**3.19**) and a P-based catalyst (**phos-1**) to furnish ester-substituted homoallylic α-tertiary amines (**3.21**) in 70–91% yield and 95:5 to >99:1 er (Scheme 3.8). The approach is applicable to substrates bearing electron-donating and electron-withdrawing substituents in the *meta* and *para* positions of an aryl substrate. Equally effective were heterocyclic, alkyl, and alkenyl substrates. A few years later, the same group published on the use of allenoates (**3.20**) for synthesis of α-tertiary amines that contain an *E* enoate (**3.22** in 64–81% yield and 95:5 to 97.5:2.5 er, Scheme 3.8).

Scheme 3.8. Phosphine Catalysts for Umpolung Reactions of Trifluoromethyl Ketimines

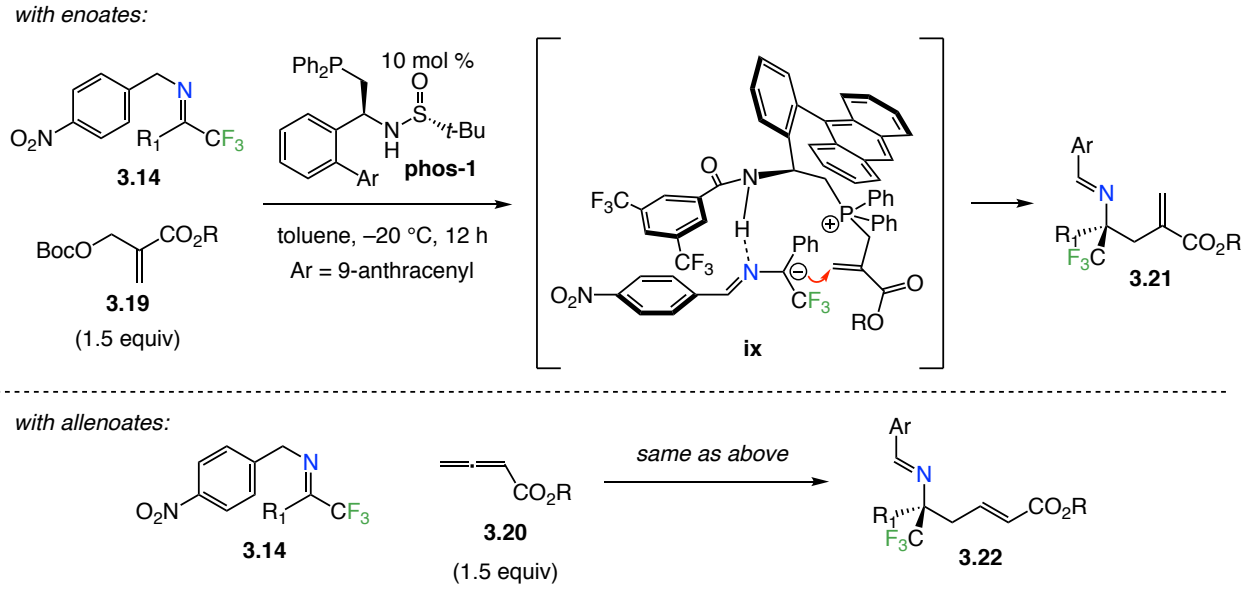

Most recently, the use of Fmoc imines were used for synthesis of α-tertiary amines. Consecutively, Wang[203] *et al.* and Niu[204] *et al.* disclosed enantioselective iridium-phosphine-catalyzed umpolung allyl addition/aza-cope cascades to afford trifluoromethyl α-tertiary amines. The reactions are tolerant of broad substitution on both the ketimines and allyl esters and afford products in 50–97% yield and 96:4 to >99:1 enantiomeric ratio.

3.2.1.4. Through Alkynyl Addition

Zhang *et al.* were able to develop a BINOL–Zn catalyzed enantioselective alkynyl addition of terminal alkynes to *o*-methoxyphenyl-substituted ketoesters.[205] Alkynes with electron-donating or electron-withdrawing substituents in the *meta* and *para* positions of the aryl ring as well as alkenyl, alkyl, silyl, and alkoxy substrates were converted to the desired products in 84–95% yield

[203] Shen, C.; Wang, R.-Q.; Wei, L.; Wang, Z.-F.; Tao, H.-Y.; Wang, C.-J. *Org. Lett.* **2019**, *21*, 6940–6945.
[204] Cao, C.-G.; He, B.; Fu, Z.; Niu, D. *Org. Process Res. Dev.* **2019**, *23*, 1758–1761.
[205] Huang, G.; Yang, J.; Zhang, X. *Chem. Commun.* **2011**, *47*, 5587–5589.

and 96:4 to 99:1 er. Ohshima and coworkers later disclosed a phosphoric acid catalyzed enantioselective alkynyl addition to trifluoromethyl N–H ketimines.[206] The scopes of the ketimines and alkynes were demonstrated to be broad and propargylamines were isolated in 82–99% yield and 71:29 to 83:17 er.

3.2.1.5. Through Alkyl Additions

Alkyl additions to *N*-phosphinoyl ketimines have been utilized to generate trifluoromethyl α-tertiary amines. Substrates were synthesized from the corresponding trifluoromethyl ketones by Lewis acid mediated condensation, requiring up to 96 hours reaction time, however. Charette *et al.* reported the copper-catalyzed enantioselective alkylation to such ketimines (71–89% yield and 95.5:4.5 to >99:1 er).[207]

3.2.1.6. By Strecker-Type Processes

Using *para*-methoxyphenyl (PMP) ketimines (**3.23**), Zhou and coworkers disclosed a strategy for enantioselective Strecker reaction, catalyzed by a urea catalyst (**urea-2**) and TMSCN and furnishing products in 88.5:11.5 to 98:2 er (Scheme 3.9).[208] Alkyl, electron-donating and electron-withdrawing aryl, and 2-thienyl substrates proved to be suitable. It was proposed that hydrogen-bonding between the catalyst's N–H bonds, the non-bonding electrons of the ketimine nitrogen, and those of a fluorine atom are key (**x**, Scheme 3.9). The catalyst's bulky quinoline

[206] Morisaki, K.; Morimoto, H.; Ohshima, T. *Chem Commun.* **2017**, *53*, 6319–6322.

[207] Lauson, C.; Charette, A. B. *Org. Lett.* **2006**, *8*, 2743–2745.

[208] Liu, Y.-L.; Shi, T.-D.; Zhou, F.; Zhao, X.-L.; Wang, X.; Zhou, J. *Org. Lett.* **2011**, *13*, 3826–3829.

moiety might thus prohibit addition to the *si* face of the ketimine in addition to participating in π-π stacking with the PMP moiety (**x**, Scheme 3.9).

Scheme 3.9. Thiourea Catalysts for Strecker-Type Reactions with Trifluoromethyl Ketimines

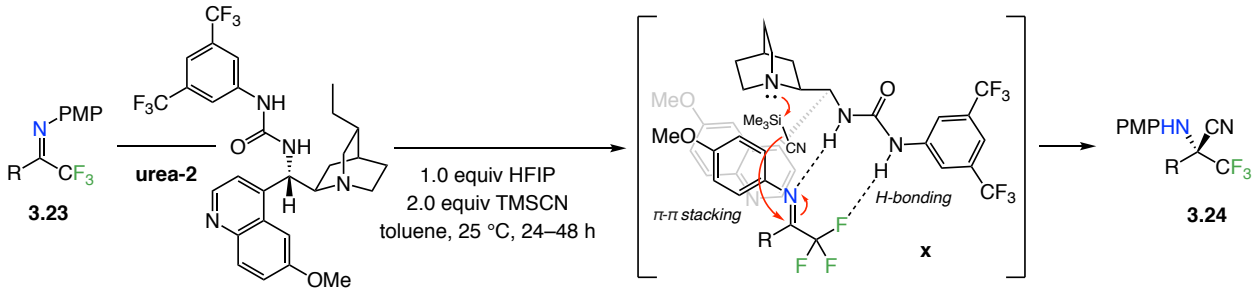

3.2.1.7. Through Aza-Benzoin Reaction

In 2013, Ye *et al.* reported an NHC-catalyzed (**triaz-1**) aza-benzoin approach involving cinnamaldehydes and *N*-Boc trifluoromethyl ketimines (**3.25**, Scheme 3.10).[209] Products (**3.26**) were obtained in 31 to 89% yield and 93.5:6.5-97.5:2.5 er. It was shown that a wide range of aldehydes, including those that are alkyl, aryl-, or heteroaryl-substituted may be used.

Scheme 3.10. NHC-Catalyzed Aza-Benzoin Reactions of Trifluoromethyl Ketimines

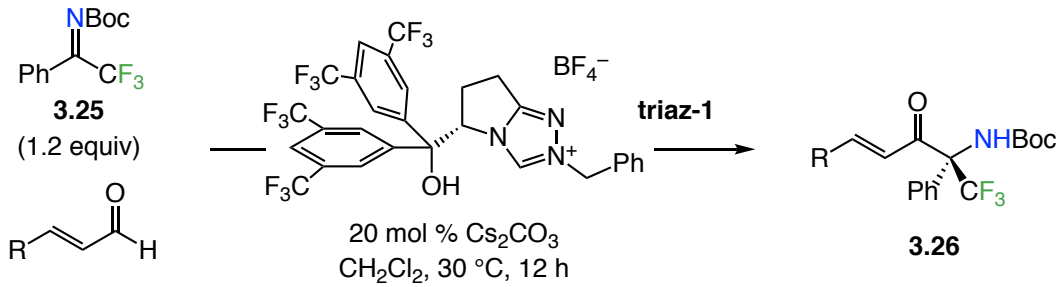

[209] Sun, L.-H.; Liang, Z.-Q.; Jian, W.-Q.; Ye, S. *Angew. Chem., Int. Ed.* **2013**, *52*, 5803–5806.

3.2.1.8. By Friedel-Crafts Alkyl Additions

In 2011, Bolm and coworkers outlined an enantioselective phosphoric acid catalyzed Friedel-Crafts reaction of indoles and *N*-Boc trifluoromethyl ketoesters, resulting in the formation of quaternary α-amino acids.[210] Reactions were efficient and products were isolated in high enantiomeric purity (up to 99% yield and 98:2). Notably, the *N*-Boc protecting group could be removed in 98% yield under relatively mild conditions.

3.2.2. Challenges Associated with Development of a Catalytic Method for Enantioselective Synthesis of Trifluoromethyl α-Tertiary Amines

The above advances underscore several persisting limitations. The majority of the syntheses require a chiral auxiliary or a protecting/activating group. Preparation of substrate N–H ketimines are at times low yielding, needing toxic and unstable reagents and/or are hampered by extensive hemiaminal formation.[211] Finally, the use of costly and/or precious metal salts (i.e., iridium and indium), extended reaction times, and heating or cooling limit application, particularly on larger scale.

3.3. Choosing an Appropriate Substrate and Initial Mechanistic Studies

We sought a substrate that was easy to synthesize and handle, did not have a directing or activating group, and would furnish an unprotected H_2N-amine product directly.

---

[210] Husmann, R.; Sugiono, E.; Mersmann, S.; Raabe, G.; Rueping, M.; Bolm, C. *Org. Lett.* **2011**, *13*, 1044–1047.

[211] (a) Koos, M; Mosher, H. S. *Tetrahedron* **1993**, *49*, 1541–1546. (b) Kende, A. S.; Liu, K. *Tetrahedron Lett.* **1995**, *36*, 4035–4038. (c) Gosselin, F.; O'Shea, P. D.; Roy, S.; Reamer, R. A.; Chen, C.; Volante, R. P. *Org. Lett.* **2005**, *7*, 355–358. (d) Morisaki, K.; Morimoto, H.; Ohshima, T. *Chem. Commun.* **2017**, *53*, 6319–6322.

3.3.1. *N*-Trimethylsilyl Ketimines

We found that *N*-trimethylsilyl ketimines may be easily synthesized from a trifluoromethyl ketone and LiHMDS without the need for purification (Scheme 3.11a). For electron-rich or hindered substrates, the trifluoromethyl ketone, *n*-BuLi, and HMDS were used and the silyl ketimine was distilled directly from the reaction flask (Scheme 3.11b). Silyl ketimines are stable for several months when stored in the freezer.

Scheme 3.11. Synthesis of *N*-Trimethylsilyl Ketimines

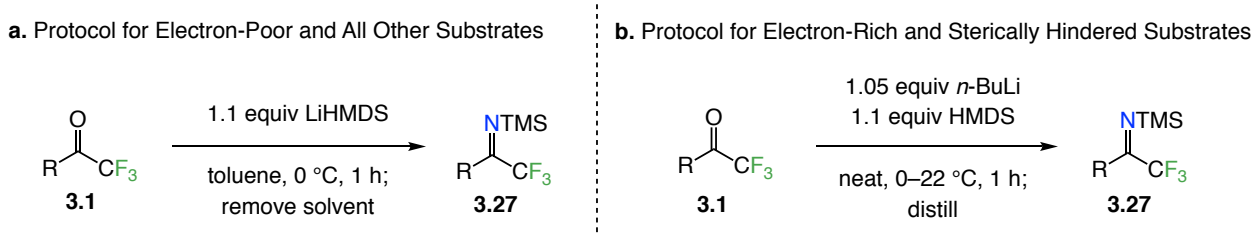

3.3.2. Spectroscopic Investigation of Silyl Removal

With a stable and readily available ketimine substrate in hand, we set out to study the lability of the *N*-trimethylsilyl group to verify that addition occurs to the N–H ketimine (**3.29**) to afford the H_2N-amine during the course of the reaction, and not upon silica gel purification. When we monitored reaction progress (Scheme 3.12a), we found that the silyl ketimine (**3.27a**) remained intact, nor was there any product formation (**3.28a**) without a fluoride source. When a catalytic amount of tetrabutylammonium difluorotriphenylsilicate (TBAT) was added to the mixture [no allyl–B(pin)], we observed two new ^{19}F NMR peaks, which we assigned as the *E*- and *Z*-N–H ketimine isomers (**3.29**, Scheme 3.12b). Over the course of one hour, the silyl ketimine was converted completely to the derived N–H ketimine. In the presence of TBAT and allyl–B(pin), the addition product was readily generated in four hours, indicating that addition occurs readily to

the in situ generated N–H ketimine (>98% conv; Scheme 3.12c). The above date clearly indicate that it is the N–H ketimine that undergoes allyl addition.

Scheme 3.12. Control Experiments and Spectroscopic Studies[a]

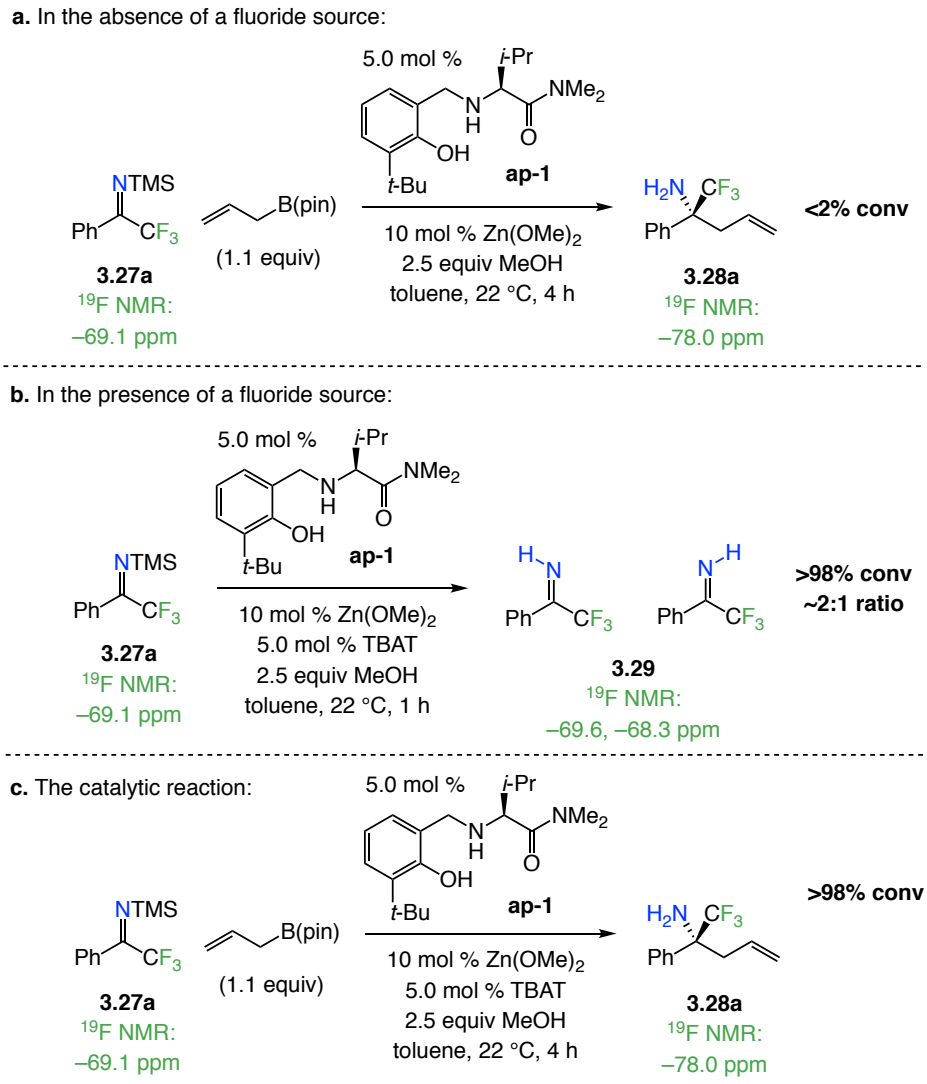

[a] Reactions performed under N_2 atm. Conv, dr, and α:γ ratios determined by analysis of ^{19}F NMR spectra of unpurified mixtures; conv (±2%) refers to disappearance of the silyl ketimine starting material. Yield of isolated and purified material (±5%). Enantioselectivity determined by HPLC analysis (±1%). See Experimental Section for details.

3.4. Catalytic Enantioselective Allyl Additions to N–H Trifluoromethyl Ketimines

After demonstrating the feasibility, we set out to optimize conditions to obtain the H_2N-amine with high enantioselectivity. Some challenges and questions to be addressed included: 1) which enantiomer will predominate? Namely, will the transformation be more largely influenced by steric or electronic factors? 2) How would the presence of *E*- and *Z*-isomers of the N–H ketimine impact efficiency and/or enantioselectivity? 3) Would it be possible to overcome the relatively facile non-catalytic process (~35% conv under otherwise identical conditions)?

3.4.1. Condition Optimization and Aminophenol Ligand Screening

We began by examining the stereochemical models for allyl addition to either the *E* or *Z* isomer of the N–H ketimine. We predicted that the *Z* ketimine isomer would react through transition state **II**, favored owing to attractive electrostatic interaction between a fluorine atom and the catalyst's ammonium group.[2a] In the reaction proceeding via the *E* isomer, on the other hand, there would be no such association due to the presence of the N–H, and there would be steric strain between the aryl group of the ketimine and the bulk of the aminophenol ligand (Scheme 3.13, **I** vs **II**). For formation of the minor enantiomer, we predicted that the *E* isomer would be the major contributor because of coulombic interaction involving the phenolic oxygen, the N–H proton, and a fluorine atom in **III** (Scheme 3.13). For the *Z* isomer leading to the minor enantiomer (**IV**), electron–electron repulsion between the phenolic oxygen and fluorine would likely increase the energy of this transition state (Scheme 3.13, **IV** versus **III**). In brief, we predicted that the major enantiomer would arise from an electronically-controlled transition state with the *Z* isomer of the N–H ketimine, with the minor enantiomer originating from an electronically-controlled transition state, involving an *E* N–H ketimine.

Scheme 3.13. Stereochemical Models for Allyl Addition to Trifluoromethyl Ketimines

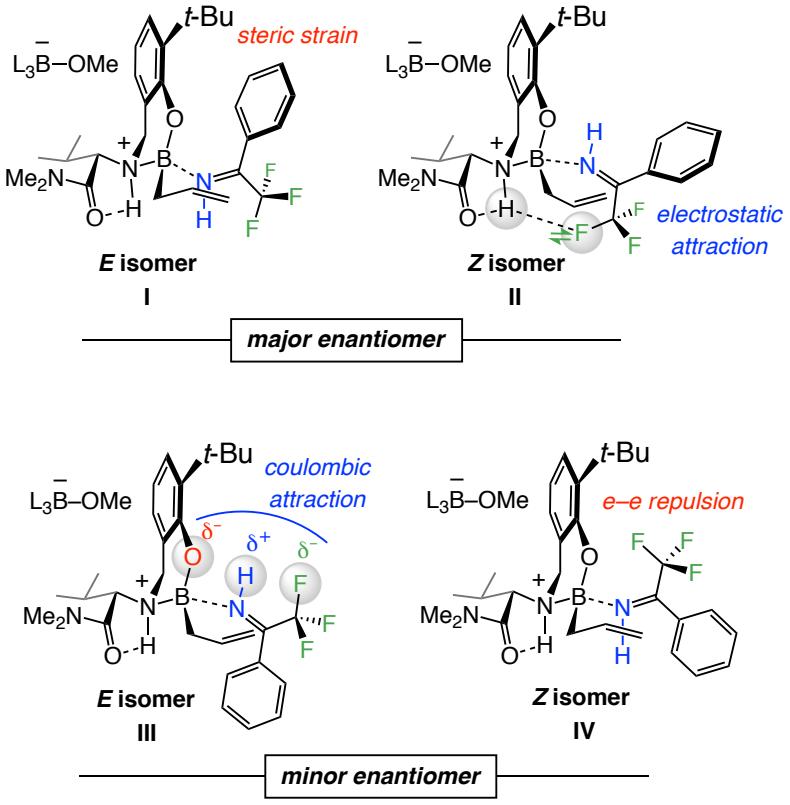

The highest enantioselectivity in our initial optimization studies was achieved with threonine-based **ap-4** as the ligand (Scheme 3.14), and by running the process at 4 °C, with 1.5 equivalents of allyl–B(pin) at 0.5 M concentration, and with isopropanol as the proton source. We opted to investigate **ap-4**, an aminophenol not formerly used, because we wondered whether an additional stereogenic center might lead to higher enantioselectivity. However, we were unable to increase the enantioselectivity further (e.g., by trying to minimize uncatalyzed addition by slow addition of the substrate).

Scheme 3.14. Aminophenol Ligand Screening for Allyl Addition to Trifluoromethyl Ketimines[a]

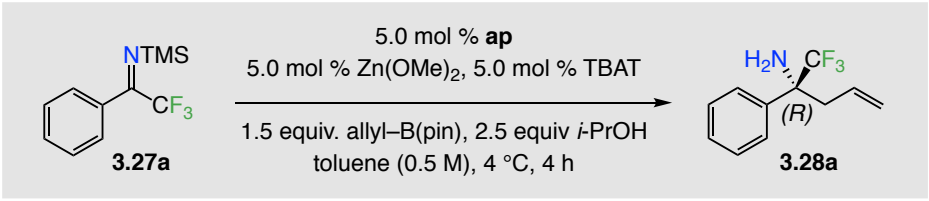

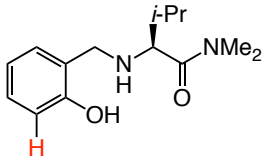

ap-2
94% conv
82:18 er

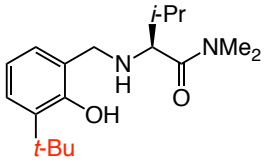

ap-1
>98% conv
86:14 er

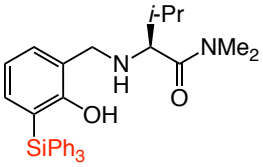

ap-3
>98% conv
81:19 er

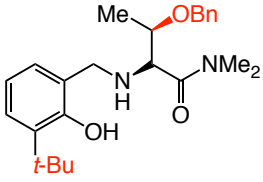

ap-4
>98% conv
91:9 er

[a] Reactions performed under N_2 atm. Conv, dr, and α:γ ratios determined by analysis of ^{19}F NMR spectra of unpurified mixtures; conv (±2%) refers to disappearance of the silyl ketimine starting material. Yield of isolated and purified material (±5%). Enantioselectivity determined by HPLC analysis (±1%). See Experimental Section for details.

3.4.2. Scope with Allyl–B(pin)

We then wondered whether reactions of other ketimines might prove to be more enantioselective (vs 91:9 er for **3.28a**). We found that enantioselectivities were lower with substrates that contain an electron-withdrawing substituent (**3.28d-e**), likely due to an increase in the uncatalyzed (background) reaction. Addition to electron-rich substrates (**3.28d**) were less efficient and resulted in large amounts of hemiaminal formation.

Scheme 3.15. Scope of Allyl Addition to Trifluoromethyl N–H Ketimines[a]

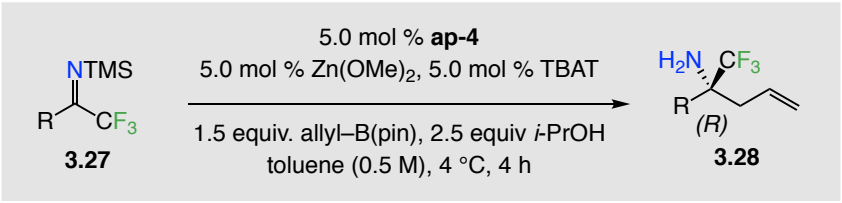

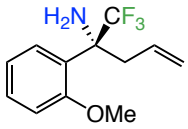

3.28b
67% conv
56% yield
91:9 er
(86.5:13.5 er at 22 °C)

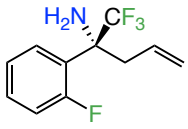

3.28c
>98% conv
68% yield
91:9 er

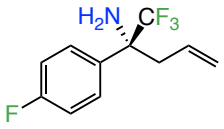

3.28d
>98% conv
47% yield
78:22 er

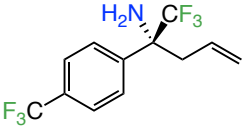

3.28e
>98% convr
32% yield
74:26 er

[a] Reactions performed under N_2 atm. Conv, dr, and α:γ ratios determined by analysis of ^{19}F NMR spectra of unpurified mixtures; conv (±2%) refers to disappearance of the silyl ketimine starting material. Yield of isolated and purified material (±5%). Enantioselectivity determined by HPLC analysis (±1%). See Experimental Section for details.

We found it interesting that enantioselectivities were significantly lower than those for the corresponding allyl additions to trifluoromethyl ketones (92.5:7.5–96:4 er).[2a] We reasoned that perhaps the presence of the N–H proton might diminish electrostatic attraction (**II** in Scheme 3.13 versus Scheme 2.5). This, together with a competitive uncatalyzed background reaction, can lead to reduced enantioselectivity. Upon re-examination of catalyst screening data, we noted the possible influence of steric factors. Specifically, with **ap-3** we noticed the lowering of enantioselectivity, which might be attributed to steric pressure in **I** and **II**, thus resulting in preference for transformation via **III** and **IV** (Scheme 3.13). Former investigations regarding additions of *Z*-substituted organoboron reagents to aldehydes[1] and ketones[2d] has indicated that the presence of an allylic substituent within a chiral allyl boronate intermediate can result in substantial improvement in enantioselectivity. Would the same be true for reactions involving trifluoromethyl ketimines?

3.5. Catalytic Regio-, Z-, and Enantioselective Additions to N–H Trifluoromethyl Ketimines

We had two principal questions to address: 1) would the catalytic processes be regio- and *Z*-selective? 2) Which enantiomer would predominate?

3.5.1. Controlling 1,3-Borotropic Shift

Examination of the stereochemical models revealed that allyl boronate intermediate **V** would be formed stereoretentively and subsequent coordination of the substrate and direct addition would afford **α-3.30a** (Scheme 3.16). If complex **V** were to isomerize by way of 1,3-borotropic shift to generate the lower energy and less sterically hindered complex **VII**, ensuing catalyst/ketimine complex generation and C–C bond formation would afford **γ-3.30a**. In the event, we obtained a product ratio of 82:18 α:γ with **ap-1**, indicating that substrate coordination and direct α-addition are comparatively facile. Upon purification by silica gel chromatography, we isolated pure **α-3.30a** in 73% yield, 98:2 *Z:E* ratio, and 96:4 er.

Scheme 3.16. The Impact of 1,3-Borotropic Shift on α-Selectivity

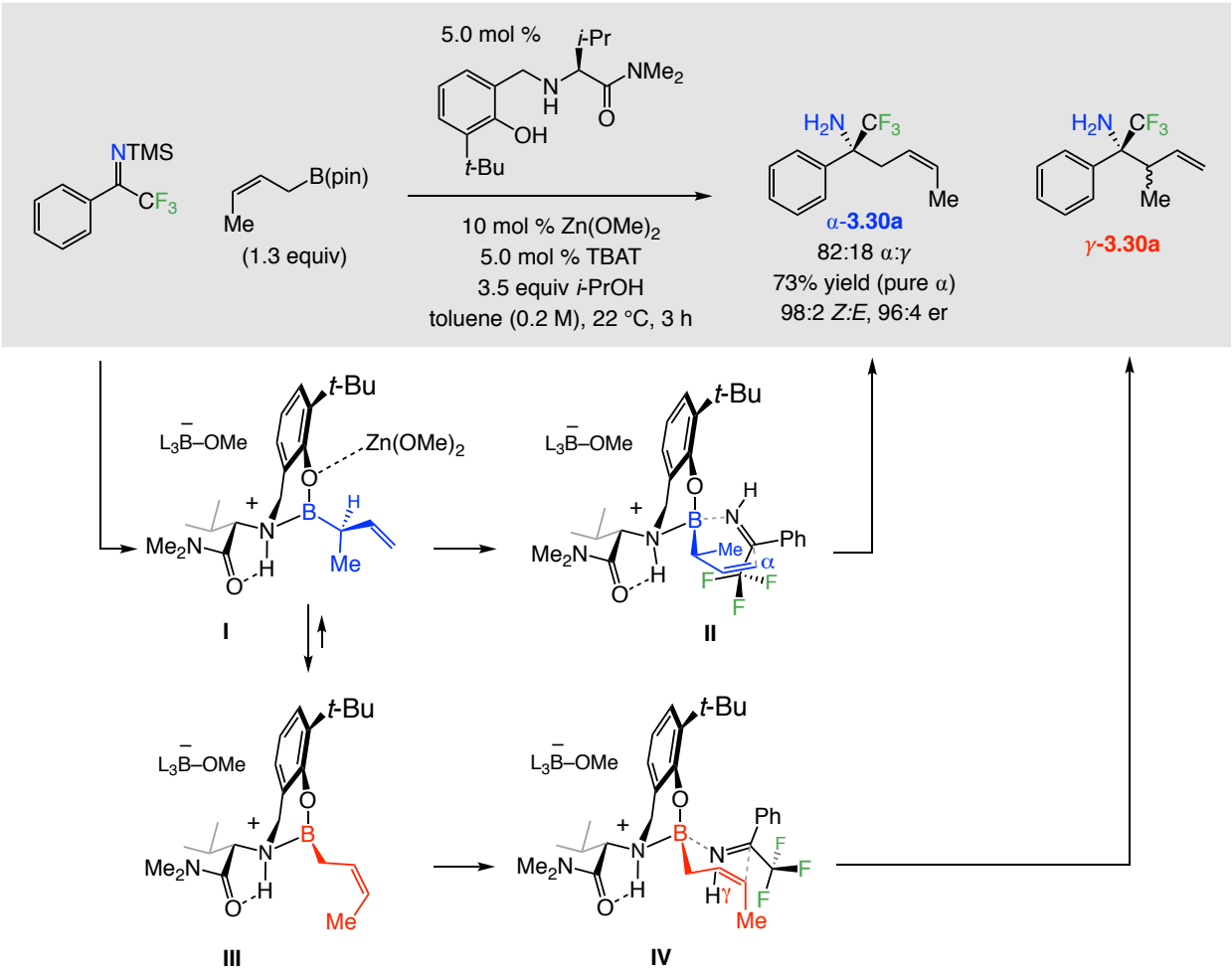

3.5.2. Condition Optimization and Aminophenol Screening

We needed an aminophenol-based boryl complex that could initiate quickly to outcompete the background reaction, enhance substrate coordination, and/or facilitate direct α-addition. Screening of aminophenol ligands (Scheme 3.17) revealed that increasing the size of the amide from *N*-dimethyl to *N*-pyrrolidine increased selectivity as a result of steric pressure between the catalyst's backbone and quaternary stereogenic center of the chiral allylboron, which in turn helps to drive direct α-addition. We then synthesized and tested a variety of threonine-based aminophenols, as they were previously effective for the allyl addition (Scheme 3.17).

Scheme 3.17. Aminophenol Screening Studies[a]

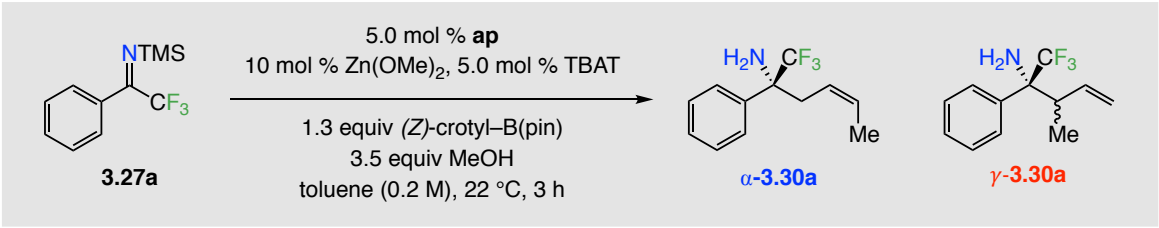

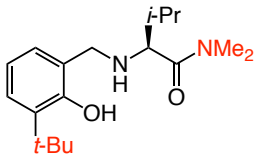

ap-1
82:18 α:γ, 93:7 *Z:E*
73% yield (pure α)
89:11 er

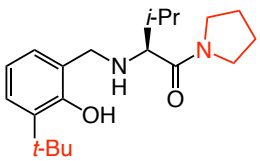

ap-5
93:7 α:γ, 98:2 *Z:E*
87% yield (pure α)
96:4 er

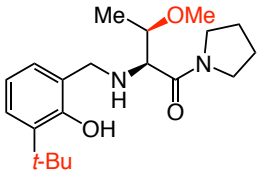

ap-6
97:3 α:γ, 98:2 *Z:E*
88% yield (pure α)
97:3 er

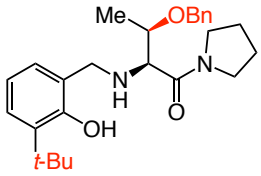

ap-7
88:12 α:γ, 88:12 *Z:E*
68% yield (pure α)
92:8 er

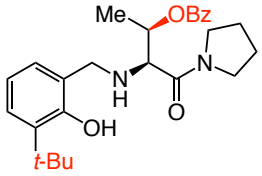

ap-8
88:12 α:γ, 95:5 *Z:E*
71% yield (pure α)
86:14 er

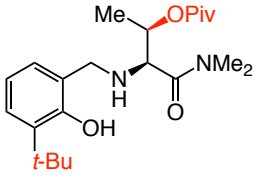

ap-9
97:3 α:γ, 95:5 *Z:E*
63% yield (pure α)
92:8 er

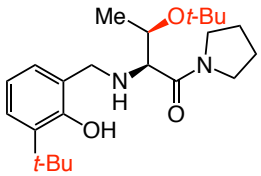

ap-10
73:27 α:γ, 97:3 *Z:E*
29% yield (pure α)
89:11 er

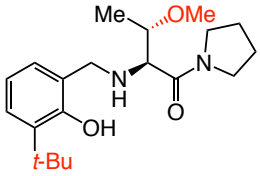

ap-11
89:11 α:γ, 97:3 *Z:E*
80% yield (pure α)
92:8 er

[a] Reactions performed under N_2 atm. Conv, dr, and α:γ ratios determined by analysis of ^{19}F NMR spectra of unpurified mixtures; conv (±2%) refers to disappearance of the silyl ketimine starting material. Yield of isolated and purified material (±5%). Enantioselectivity determined by HPLC analysis (±1%). See Experimental Section for details.

Reactions with ligands that contain a larger threonine substituent (**ap-7**, **ap-8**, **ap-9**, and **ap-10**) were less selective (Scheme 3.17). Importantly, reaction with methoxy-threonine ligands **ap-6** and **ap-11** afforded the product with better selectivity. Particularly noteworthy was that **α-3.30a** was obtained in 97:3 α:γ ratio and er with **ap-6**. We propose this is owing to a sterically favorable conformation and electronically activating σ C–N to σ* C–O hyperconjugative interaction that leads to an increase in the Lewis acidity of the boron center, thus leading to faster catalyst initiation, more facile substrate coordination, and a longer catalyst lifetime (**IX**, Scheme 3.18).

Scheme 3.18. Rationale for the Role of Threonine-Based Ligands

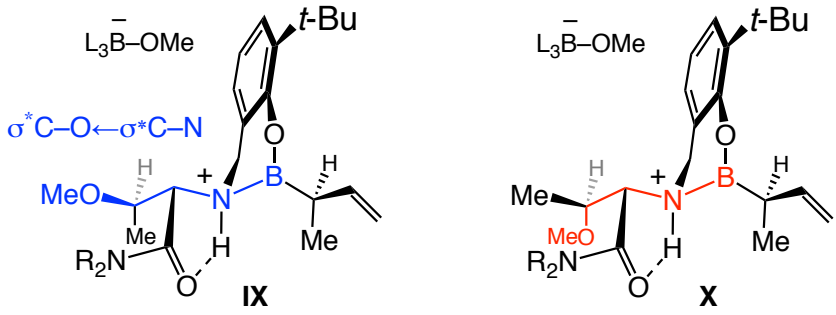

3.5.3. Scope with *(Z)*-Crotyl–B(pin)

The method is applicable to N–H ketimines that contain an electron-withdrawing (**3.30b-d**, **3.30f),** an electron-donating (**3.30f-h**), or a sterically demanding (**3.30i-m**) substituent (Scheme 3.19). Regioselectivities are lower in some instances likely as a result of reduced ketimine reactivity, which leaves time for 1,3-borotropic shift to occur, thus increasing the formation of the γ-addition product. In all cases, high *Z:E* ratios are observed.

Scheme 3.19. Regio- and Enantioselective Addition of (*Z*)-Crotyl–B(pin) to N–H Ketimines[a]

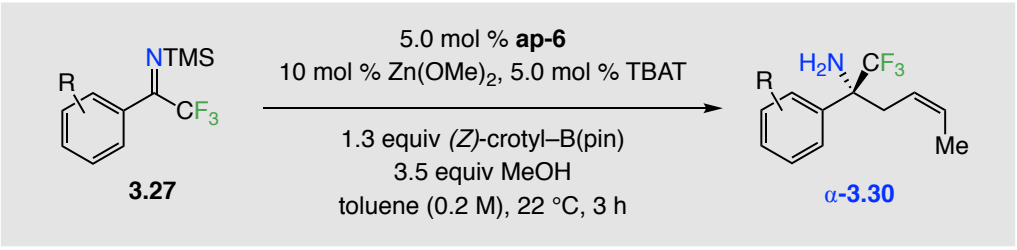

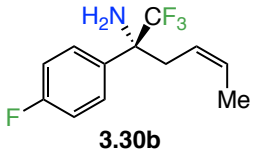

3.30b
93:7 α:γ, 98:2 Z:*E*
68% (pure α)
97:3 er

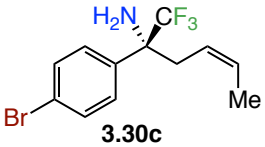

3.30c
96:4 α:γ, 97:3 Z:*E*
67% (pure α)
98:2 er

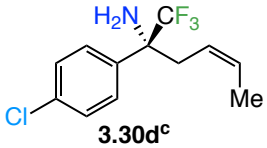

3.30d[c]
95:5 α:γ, 95:5 *Z:E*
87% yield
96:4 er

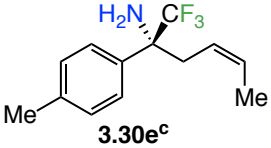

3.30e[c]
89:11 α:γ, 96:4 *Z:E*
71% yield
97:3 er

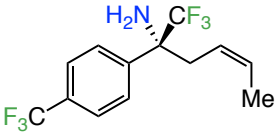

3.30f
98:2 α:γ, 96:4 Z:*E*
61% (pure α)
97:3 er

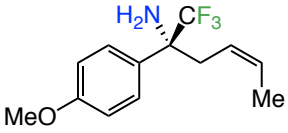

3.30g[c]
94:6 α:γ, 98:2 Z:*E*
78% yield
98:2 er

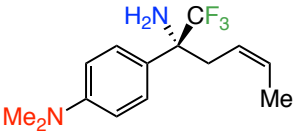

3.30h[b,d]
87:13 α:γ, 98:2 Z:*E*
50% (pure α)
98:2 er

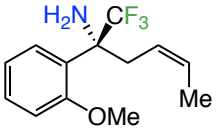

3.30i
96:4 α:γ, 98:2 Z:*E*
70% (pure α)
99:1 er

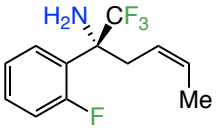

3.30j[c,e]
96:4 α:γ, 98:2 Z:*E*
89% yield
98.5:1.5 er

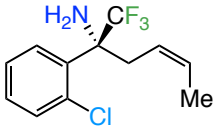

3.30k[b,c]
67:33 α:γ, 98:2 Z:*E*
79% yield
96:4 er

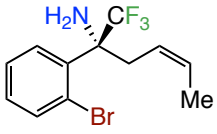

3.30l[c]
59:41 α:γ, 97:3 Z:*E*
53% yield
90:10 er

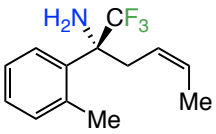

3.30m[b,c]
45:55 α:γ, 98:2 Z:*E*
52% yield
95:5 er

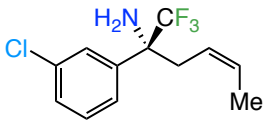

3.30n
>98:2 α:γ, 97:3 Z:*E*
90% (pure α)
96:4 er

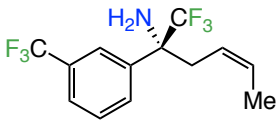

3.30o
98:2 α:γ, 98:2 Z:*E*
82% (pure α)
97:3 er

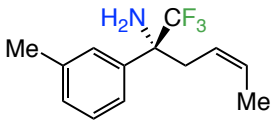

3.30p[c]
91:9 α:γ, >98:2 *Z:E*
67% yield
96:4 er

[a] Reactions performed under N_2 atm. Conv, dr, and α:γ ratios determined by analysis of ^{19}F NMR spectra of unpurified mixtures; conv (±2%) refers to disappearance of the silyl ketimine starting material. Yield of isolated and purified material (±5%). Enantioselectivity determined by HPLC analysis (±1%). [b] NH-Ketimine generated first. [c] Yield is for mixture of α- and γ-addition products. [d] Reaction time = 8 h. [e] The derived acetate was used. See Experimental Section for details.

The approach may be used for preparation of homoallylic α-tertiary amines with a heterocyclic (**3.30q-s**), an alkenyl- (**3.30t**), an alkynyl- (**3.30u**), or a polyfluoromethyl (**3.30v-w**) substituent (Scheme 3.20). The yield for **3.30r** was low because of significant decomposition upon silica gel chromatography. The methyl-substituent on the olefin of **3.30t** is required, as the corresponding unsubstituted olefin undergoes reaction to an unidentifiable byproduct. The regioselectivity for **3.30u** is lower as a result of hemiaminal formation. Electron-withdrawing groups on the polyfluoromethyl substrates afforded products selectively (**3.30v**). However, transformation with more electron-rich N–H ketimines were less selective (**3.30w**), probably because 1,3-borotropic shift is more facile that C–C bond formation.

Scheme 3.20. Additional Examples of Regio- and Enantioselective Additions of (*Z*)-Crotyl–B(pin) to N–H Ketimines[a]

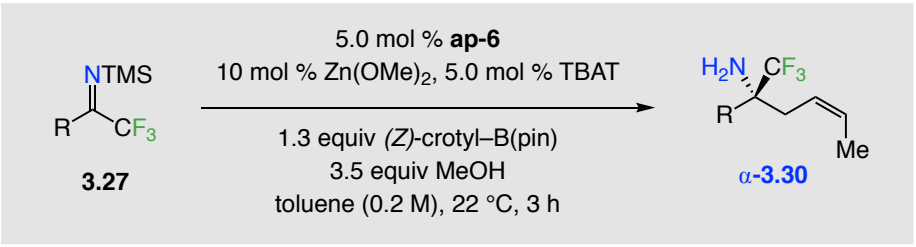

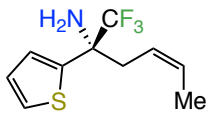

3.30q
98:2 α:γ, 97:3 Z:*E*
84% yield
93:7 er

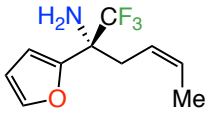

3.30r
89:11 α:γ, 98:2 Z:*E*
32% yield
97:3 er

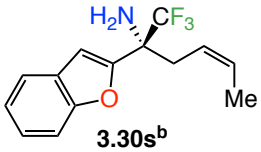

3.30s[b]
87:13 α:γ, >98:2 Z:*E*
77% yield
97.5:2.5 er

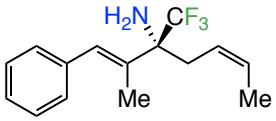

3.30t
91:9 α:γ, 96:4 Z:*E*
64% yield
98:2 er

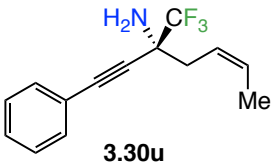

3.30u
80:20 α:γ, 96:4 Z:*E*
81% yield
93:7 er

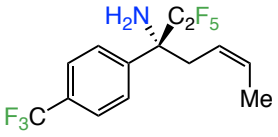

3.30v
98:2 α:γ, 98:2 Z:*E*
72% (pure α)
97:3 er

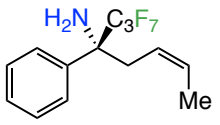

3.30w
88:12 α:γ, >98:2 *Z*:*E*
80% yield
78:22 er

[a] Reactions performed under N_2 atm. Conv, dr, and α:γ ratios determined by analysis of ^{19}F NMR spectra of unpurified mixtures; conv (±2%) refers to disappearance of the silyl ketimine starting material. Yield of isolated and purified material. Yield is for mixture of α- and γ-addition products (±5%). Enantioselectivity determined by HPLC analysis (±1%). [b] NH-Ketimine generated first. See Experimental Section for details.

3.5.4. Substrate Scope with Other Organoboron Reagents

Our group has previously developed several strategies for catalytic stereoretentive cross-metathesis that may be used for synthesis of (*Z*)-substituted allyl boronates. To enhance the scope of our method, we took advantage of this advance, and prepared a variety of other (*Z*)-allyl boronates and probed the corresponding reactions (Scheme 3.21).

Scheme 3.21. Regio- and Enantioselective Additions of (*Z*)-Substituted Allyl Boronates[a]

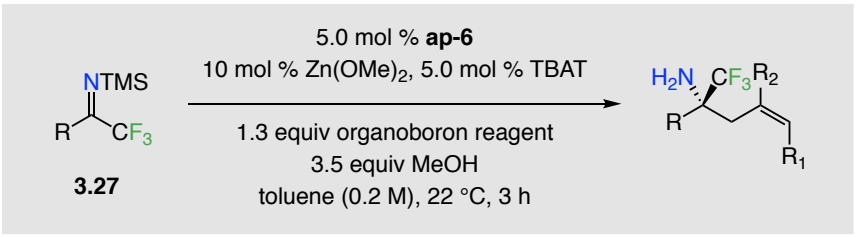

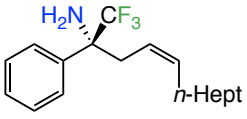

3.31
98:2 α:γ, 98:2 Z:*E*
86% yield (pure α)
97:3 er

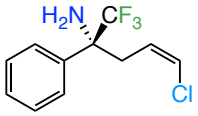

3.32a[b,c]
97:3 α:γ, >98:2 Z:*E*
91% yield
88:12 er

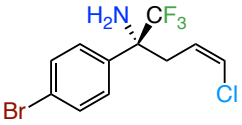

3.32b[b]
94:6 α:γ, >98:2 Z:*E*
81% (pure α)
92.5:7.5 er

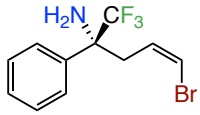

3.33a[b,d]
87:13 α:γ, >98:2 *Z:E*
35% yield (pure α)
89:11 er

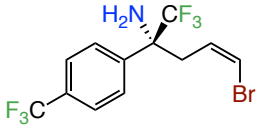

3.33b[b,c,d]
93:7 α:γ, >98:2 *Z:E*
76% yield
93:7 er

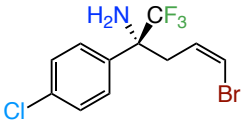

3.33c[b,d]
84:16 α:γ, >98:2 Z:*E*
74% yield (pure α)
89.5:10.5 er

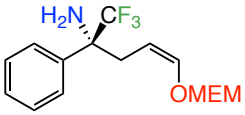

3.34[c]
98:2 α:γ, 98:2 *Z:E*
40% yield
90:10 er

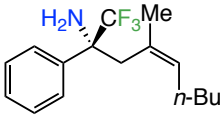

3.35a[c,d]
80:20 α:γ, 96:4 Z:*E*
81% yield
93:7 er

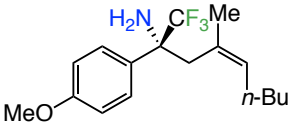

3.35b[d]
88:12 α:γ, >98:2 Z:*E*
62% (pure α)
92.5:7.5 er

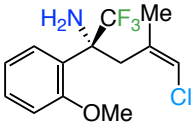

3.36[b,e]
97:3 α:γ, 97:3 Z:*E*
34% (pure α)
93:7 er

[a] Reactions performed under N_2 atm. Conv, dr, and α:γ ratios determined by analysis of ^{19}F NMR spectra of unpurified mixtures; conv (±2%) refers to disappearance of the silyl ketimine starting material. Yield of isolated and purified material (±5%). Enantioselectivity determined by HPLC analysis (±1%). [b] NH-Ketimine generated first. [c] Yield is for mixture of α- and γ-addition products. [d] Reaction time =14 h. [e] Reaction temperature = 50 °C. See Experimental Section for details.

Thus, reactions involving (*Z*)-chloro- and (*Z*)-bromo-substituted allyl boronates, generated through cross-metathesis of commercially available halogenated olefins and (*Z*)-crotyl–B(pin)[212], afforded **3.32a-b** and **3.33a-c** (Scheme 3.21). Trisubstituted alkenyl-chloride **3.36** was obtained in 34% yield owing to the reduced reactivity of the allyl boronate. Alkoxy-substituted homoallylic amine **3.34** was prepared by the use of an organoboron reagent previously used by us for synthesis of 1,2-amino alcohols.[213] (*Z*)-Alkyl di- and tri-substituted allylic boronates, were prepared according to a catalytic protocol developed by Morken *et al.*,[214] and were used to access **3.31** and **3.35a-b** (Scheme 3.22).

3.5.5. Formal Synthesis of BACE-1 Inhibitor

As noted earlier, trifluoromethyl α-tertiary amines may be found in many biologically active molecules. We envisioned applying the new method to a formal synthesis of a BACE-1 inhibitor developed by Novartis.[215] The published medicinal chemistry route was inefficient requiring a series of protection/deprotection sequences as well as a late stage crystallization to obtain the enantioenriched product. The key intermediate was isolated in the racemic form in 15% overall yield after six steps. Our formal synthesis was performed on gram-scale using a single-vessel crotyl addition/acylation sequence, affording **3.38** after two steps in 76% yield (1.21 g), and with 98.5:1.5 enantiomeric ratio (Scheme 3.22).

---

[212] Koh, M.J.; Nguyen, T. T.; Zhang, H.; Schrock, R. R.; Hoveyda, A. H. *Nature* **2016**, *531*, 459–465.

[213] Morrison, R. J.; Hoveyda, A. H. *Angew. Chem., Int. Ed.* **2018**, *57*, 11654–11661.

[214] See Experimental Section for details on the synthesis of these organoboron reagents.

[215] Oehlrich, D.; Prokopcova, H.; Gijsen, H. J. M. *Bioorg. Med. Chem. Lett.* **2014**, *24*, 2033–2045.

Scheme 3.22. A Concise Enantioselective Formal Synthesis of BACE-1 Inhibitor[a]

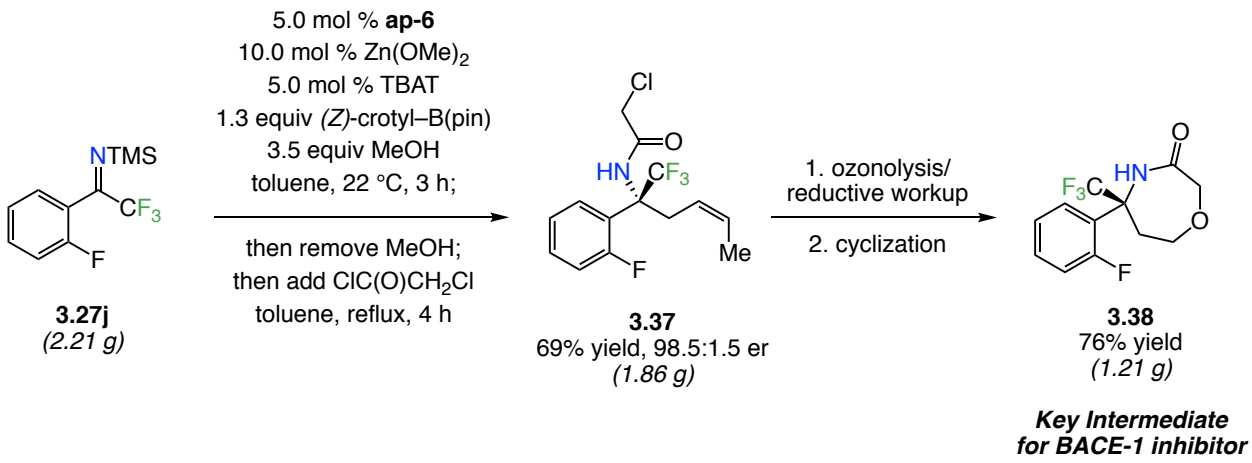

3.27j
(2.21 g)

3.37
69% yield, 98.5:1.5 er
(1.86 g)

3.38
76% yield
(1.21 g)

Key Intermediate for BACE-1 inhibitor

[a] Yield of isolated and purified material (±5%); enantioselectivity determined by HPLC analysis (±1%). See Experimental Section for details.

3.5.6. Diastereoselective Functionalizations

The *Z*-alkene within the trifluoromethyl-substituted α-tertiary amine allows for a wide range of highly diastereoselective modifications (Scheme 3.23). Directed epoxidation/cleavage[216] afforded the differentially protected diol **3.39** with >98:2 regioselectivity and 93:7 dr. Subsequent saponification (**3.40**), acetal formation, and amide formation (**3.41**) are representative additional functionalizations. The trisubstituted olefin product (**3.35a**) underwent oxidation/cleavage to generate **3.42** in 72% yield, with complete regioselectivity, and in 91:9 dr. It should be noted that the same sequence of events but involving a monosubstituted alkene was found to be non-selective (51:49 dr).

[216] Davies, S. G.; Fletcher, A. M.; Thomson, J. E. *Org. Biomol. Chem.* **2014**, *12*, 4544–4549.

Scheme 3.23. Diastereoselective Oxidation/Cleavage Processes Involving the *Z*-Alkene Unit[a]

a. Diastereoselective Transformation of a *Z* Olefin

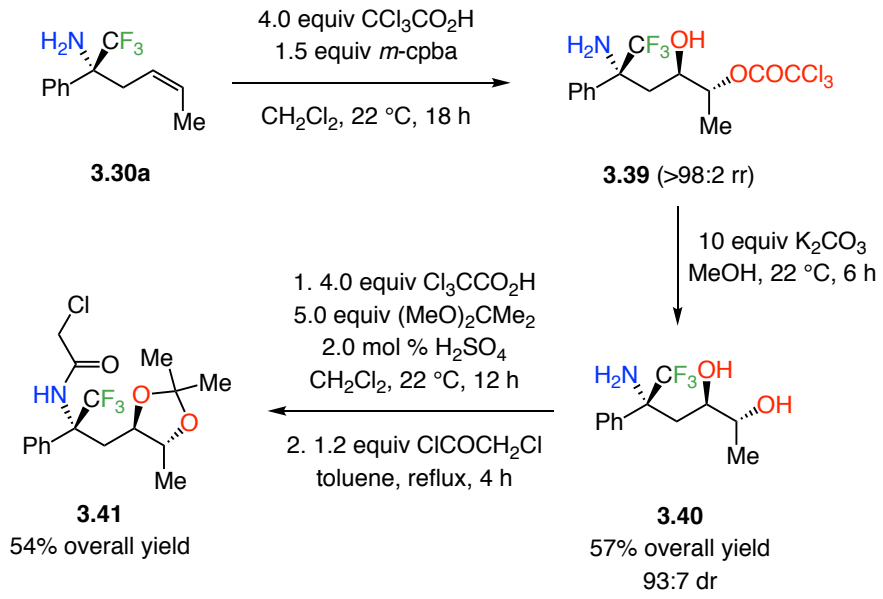

3.30a

3.39 (>98:2 rr)

3.41
54% overall yield

3.40
57% overall yield
93:7 dr

b. Diastereoselective Transformation of a Trisubstituted Olefin

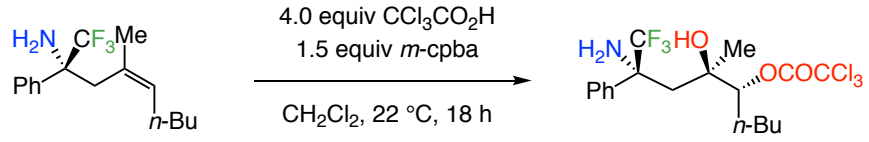

3.35a
98:2 α:γ, 88% yield (pure α)
98:2 *Z*:*E*, 88.5:11.5 er

3.42
72% yield
>98:2 rr, 91:9 dr

[a] Yield of isolated and purified material (±5%); enantioselectivity determined by HPLC analysis (±1%). See Experimental Section for details.

3.5.7. Chemoselective Cross-Coupling Reactions

Catalytic cross-coupling can transform an aryl or alkenyl halide to a variety of carbon-substituted derivatives.[217] In this context, we found that aryl bromide **3.32b** can be converted to **3.43** with complete chemoselectivity (<2% reaction with alkenyl–Cl; Scheme 3.24a). Along the same lines, alkenyl bromide **3.33b** was converted to **3.44** in >98:2 *Z/Z:Z/E* selectivity.

[217] Torborg, C.; Beller, M. *Adv. Synth. Catal.* **2009**, *351*, 3027–3043.

Scheme 3.24. Stereoretentive Cross-Coupling Reactions[a]

a. Aryl Bromide Cross-Coupling

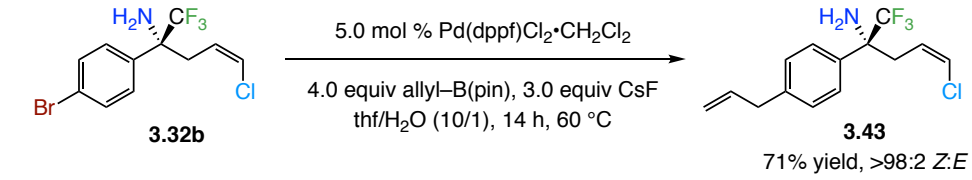

b. Stereoretentive Alkenyl Bromide Cross-Coupling

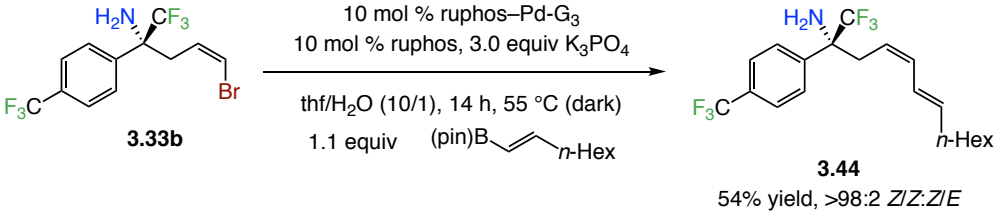

[a] Yield of isolated and purified material (±5%); enantioselectivity determined by HPLC analysis (±1%). See Experimental Section for details.

3.6. Conclusion and Summary

Through the use of a threonine-based aminophenol-boryl complex, we have been able to carry out catalytic regio-, *Z*-, and enantioselective addition of various allyl boronates to trifluoromethyl-substituted N–H ketimines. The ability to synthesize H_2N-amines directly obviates the need for the installation and subsequent removal of a protecting/activating group, operations that are not only wasteful, but can require oxidative/reductive conditions that translate to limited applicability. The products are otherwise difficult to access, and this is the first report of the synthesis of versatile α-tertiary amines that contain a *Z*-disubstituted or *Z*-trisubstituted alkene. A two-step enantioselective formal synthesis of a key intermediate of a BACE-1 inhibitor, highly diastereoselective functionalizations of the *Z*-alkenes, and chemoselective cross-coupling reactions serve to underscore the considerable utility of this advance.

3.7. Experimental Section

3.7.1. Experimental

3.7.1.1 General

Infrared (IR) spectra were recorded on a Bruker alpha spectrophotometer, λ_{max} in cm^{-1}. Bands are characterized as broad (br), strong (s), medium (m), and weak (w). ^{1}H NMR spectra were recorded on a Varian Unity INOVA 400 (400 MHz) or a Varian Premium Shielded 600 (600 MHz) spectrometer. Chemical shifts are reported in ppm from tetramethylsilane with the solvent resonance as the internal standard ($CDCl_3$: δ 7.26 ppm). Data are reported as follows: chemical shift, integration, multiplicity (s = singlet, d = doublet, t = triplet, q = quartet, br = broad, m = multiplet), and coupling constants (Hz). ^{13}C NMR spectra were recorded on a Varian Unity INOVA 400 (100 MHz) or a Varian Premium Shielded 600 (125 MHz) spectrometer with complete proton decoupling. ^{19}F NMR spectra were recorded on a Varian Unity INOVA 400 (376 MHz) or a Varian Premium Shielded 600 (564 MHz) spectrometer using trifluorotoluene as an external standard. Chemical shifts are reported in ppm from tetramethylsilane with the solvent resonance as the internal standard ($CDCl_3$: δ 77.16 ppm). Data are reported as follows: chemical shift, multiplicity (singlet unless otherwise noted), and coupling constant (Hz). High-resolution mass spectrometry was performed on a JEOL AccuTOF-DART (positive mode) at the Mass Spectrometry Facility, Boston College. Enantiomeric ratios (er) were determined by HPLC analysis through the use of either a Shimadzu LC-2010AHT or SCL-10AVP chromatograph (Chiral Technologies Chiralcel OD-H (4.6 x 250 mm), Chiral Technologies Chiralcel OJ-H (4.6 x 250 mm), Chiral Technologies Chiralpak AD-H (4.6 x 250 mm), Chiral Technologies Chiralpak AZ-H (4.6 x 250 mm), Chiral Technologies Chiralpak AS-H (4.6 x 250 mm) columns). Authentic racemic samples for HPLC analysis were obtained by performing the reaction with *rac*-**ap-1a**. Specific rotations were measured on a Rudolph Research Analytical Autopol IV Polarimeter. Melting points were determined by the use of a Thomas Hoover Uni-melt capillary melting point apparatus. Unless otherwise noted, reactions were carried out under an atmosphere of dry N_2 in oven-dried (135 ºC) glassware.

3.7.1.2. Solvents

Unless otherwise noted, solvents were purged with Argon and purified under a positive pressure of dry Argon by a modified Innovative Technologies purification system. Toluene (Fisher, ACS Grade) was passed successively through activated copper and alumina columns. Dichloromethane (Fisher, ACS Grade) and diethyl ether (Aldrich, Chromasolv®) were passed successively through two activated alumina columns. Tetrahydrofuran was purified by distillation from sodium benzophenone ketyl immediately prior to use. $CDCl_3$ was purchased from Cambridge

Isotope Laboratories and stored over activated 4Å molecular sieves prior to use. All work-up and purification procedures were carried out in air with reagent grade solvents (purchased from Fisher).

3.7.1.3. Reagents

1-(Benzofuran-2-yl)-2,2,2-trifluoroethan-1-one was synthesized according to a procedure in the literature and the analytical data are consistent with those reported previously.[218]

Bis(pinacolato)diboron was purchased from Frontier and recrystallized from pentane prior to use.

Bis(trimethylsilyl)amine was purchased from Acros and used as received.

Boc-D-Allo-Thr-OBn was purchased from Advanced ChemTech and used as received.

Boc-Ile-OH was purchased from Advanced ChemTech and used as received.

Boc-Thr-OH was purchased from ArkPharm and used as received.

Boc-Thr(Bzl)-OH was purchased from ArkPharm and used as received.

Boc-Thr(Me)-OH was purchased from Alfa Aesar and used as received.

Boc-Val-OH was purchased from Advanced ChemTech and used as received.

1-(2-Bromophenyl)-2,2,2-trifluoroethan-1-one was synthesized from the corresponding aldehyde (Aldrich, used as received).

4'-Bromo-2,2,2-trifluoroacetophenone was purchased from Combi Blocks and used as received.

1-Chloro-3-methyl-2-butene was purchased from Alfa Aesar and used as received.

1-(2-Chlorophenyl)-2,2,2-trifluoroethan-1-one was synthesized from the corresponding aldehyde (Aldrich, used as received).

1-(3-Chlorophenyl)-2,2,2-trifluoroethan-1-one was synthesized from the corresponding aldehyde (Aldrich, used as received).

4'-Chloro-2,2,2-trifluoroacetophenone was purchased from Oakwood and used as received.

Dess-Martin periodinane was purchased from Oakwood and used as received.

1,2-Dibromoethylene was purchased from Aldrich and used as received.

Dimethylamine (40 wt % in H_2O) was purchased from Aldrich and used as received.

4′-(Dimethylamino)-2,2,2-trifluoroacetophenone was purchased from Aldrich and used as received.

1-(2,5-Dimethyl-1*H*-pyrrol-1-yl)-1-(((1'*r*,3'*r*)-2,2'',4,4'',6,6''-hexaisopropyl-[1,1':3',1''-terphenyl]-2'-yl)oxy)-1-(2-methyl-2-phenylpropylidene)-*N*-(perfluorophenyl)molybdenumimine (Mo-1) was synthesized according to a procedure in the

[218] Debien, L.; Trost, B. M. *J. Am. Chem. Soc.* **2015**, *137*, 11606–11609.

literature and the analytical data are consistent with those reported previously.[219]

1-(2,5-Dimethyl-1*H*-pyrrol-1-yl)-1-(((1'*r*,3'*r*)-2,2'',4,4'',6,6''-hexamethyl-[1,1':3',1''-terphenyl]-2'-yl)oxy)-1-(2-methyl-2-phenylpropylidene)-*N*-(perfluorophenyl)molybdenumimine (Mo-2) was purchased from Strem and used as received.

1-Ethyl-3-(3-dimethylaminopropyl)carbodiimide Hydrochloride (EDC•HCl) was purchased from Advanced ChemTech and used as received.

2'-Fluorobenzaldehyde was purchased from Aldrich and used as received.

Hydrochloric Acid (4.0 M in 1,4-dioxane) was purchased from Aldrich and used as received.

1-Hydroxy-benzotriazole hydrate (HOBt•H_2O) was purchased from Advanced ChemTech and used as received.

Lithium bis(trimethylsilyl)amide (1.0 M in thf) was purchased from Aldrich and used as received.

Magnesium Sulfate was purchased from Fisher and flame-dried under vacuum prior to use.

Methanol (99.8% anhydrous) was purchased from Alfa Aesar and used as received.

2'-Methoxy-2,2,2-trifluoroacetophenone as purchased from Oakwood and used as received.

4'-Methoxy-2,2,2-trifluoroacetophenone was purchased from Aldrich and used as received.

***n*-Butyllithium (1.6 or 2.5 M in hexanes)** was purchased from Aldrich and titrated with *n*-benzylbenzamide prior to use.

Palladium on carbon was purchased from Strem and used as received.

2,2,3,3,3-Pentafluoro-1-(4-(trifluoromethyl)phenyl)propan-1-one was synthesized according to a procedure in the literature and the analytical data are consistent with those reported previously.[220]

Pyrrolidine was purchased from Aldrich and used as received.

Sodium Borohydride was purchased from Aldrich and used as received.

3-*tert*-Butyl-2-hydroxybenzaldehyde was purchased from Aldrich and used as received.

Tetrabutylammonium fluoride (1M in thf) was purchased from Oakwood and used as received.

2,2,2,4'-Tetrafluoroacetophenone was purchased from Oakwood and used as received.

Triethylamine was purchased from Aldrich and distilled from to use.

2,2,2-Trifluoroacetophenone was purchased from Oakwood and used as received.

4-(Trifluoroacetyl)toluene was purchased from Oakwood and used as received.

2,2,2-Trifluoro-1-(2-fluorophenyl)ethan-1-one was synthesized from the corresponding aldehyde (Aldrich, used as received).

---

[219] Zhang, H.; Yu, E.; Torker, S.; Schrock, R. R. .; Hoveyda, A. H. *J. Am. Chem. Soc.* **2014**, *136*, 16493–16496.

[220] Antúnez, D.-J. B.; Greenhalgh, M. D.; Brueckner, A. C.; Walden, D. M.; Elías-Rodríguez, P.; Roberts, P.; Young, B. G.; West, T. H.; Slawin, A. M. Z.; Cheong, P. H.-Y.; Smith, A. D. *Chem. Sci.* **2019**, *10*, 6162–6173.

2,2,2-Trifluoro-1-(furan-2-yl)ethan-1-one was purchased from Enamine and used as received.

(*E*)-1,1,1-Trifluoro-3-methyl-4-phenylbut-3-en-2-one was synthesized according to a procedure in the literature and the analytical data are consistent with those reported previously.[221]

1,1,1-Trifluoro-4-phenylbut-3-yn-2-one was synthesized according to a procedure in the literature and the analytical data are consistent with those reported previously.[222]

2,2,2-Trifluoro-1-(thiophen-2-yl)ethan-1-one was purchased from Oakwood and used as received.

2,2,2-Trifluoro-1-(*m*-tolyl)ethan-1-one was purchased from Oakwood and used as received.

2,2,2-Trifluoro-1-(*o*-tolyl)ethan-1-one was synthesized from the corresponding aldehyde (TCI America, used as received).

2,2,2-Trifluoro-4′-(trifluoromethyl)acetophenone was purchased from Oakwood and used as received.

2,2,2-Trifluoro-1-(3-(trifluoromethyl)phenyl)ethan-1-one was synthesized from the corresponding aldehyde (Aldrich, used as received).

Trifluoromethyltrimethylsilane was purchased from Oakwood and used as received.

Tris(dibenzylideneacetone)dipalladium(0) was purchased from Strem and used as received.

Zinc (II) methoxide was purchased from Aldrich and used as received.

3.7.2. Synthesis of N-trimethylsilyl ketimines

Two different methods were used to synthesize N-trimethylsilyl (N-TMS) ketimines. In general, ketones possessing electron-withdrawing substituents were synthesized by Method A, whereas condensation of electron-rich and/or hindered ketones were carried out under conditions outlined by Method B. Note: In some cases, hexamethyldisilazide co-distills along with the ketimine product, but this does not affect the catalytic transformation. Weight percent was determined and substrates were revised accordingly.

Method A: Condensation was carried out according to a procedure described by Gosselin *et. al*.[223] To an oven-dried six-dram vial equipped with a magnetic stir-bar was added ketone (1.0 equiv.) and toluene (1.0 M). The solution was cooled to 0 °C, then LiHMDS (1.0 M in thf, 1.1 equiv.) was added dropwise manner. The solution was allowed to stir at 0 °C for one h, then the reaction was quenched by the addition of water (5 mL). The organic layer was washed with water (2 x 10 mL), dried over $MgSO_4$, filtered, and concentrated under reduced pressure to afford the product as

[221] Buesking, A. W.; Ellman, J. A. *Chem. Sci.* **2014**, *5*, 1983–1987.

[222] Hung, C.-I.; Scharf, M. J.; Trost, B. M. *Angew. Chem., Int. Ed.* **2018**, *57*, 11408–11412.

[223] Gosselin, F.; O'Shea, P. D.; Roy, S.; Reamer, R. A.; Chen, C.; Volante, R. P. *Org. Lett.* **2005**, *7*, 355–358.

yellow oil, which was used without purification.

Method B: Condensation was carried out according to a procedure described by Hart *et. al*.[224] To an oven-dried six-dram vial equipped with a magnetic stir-bar was added HMDS (1.1 equiv.). The vial was allowed to cool to 0 °C for 10 min, then *n*-BuLi (2.6 M in hexanes, 1.05 equiv.) was added in a dropwise manner. The suspension was allowed to stir at 0 °C for five min and then allowed to warm to 22 °C for 10 min. After re-cooling to 0 °C again, trifluoromethyl ketone (1.0 equiv.) was added dropwise. The yellow solution was allowed to stir at 0 °C for one h, then concentrated under reduced pressure (rotary evaporator) and the desired ketimine was distilled directly form the reaction flask under vacuum to afford the product as colorless or yellow oil.

2,2,2-Trifluoro-1-phenyl-*N*-(trimethylsilyl)ethan-1-imine (3.27a) was synthesized according to Method A and the analytical data are consistent with those reported previously.[223] **^{1}H NMR (400 MHz, $CDCl_3$):** δ 7.57–7.51 (m, 2H), 7.50–7.38 (m, 3H), 0.17 (s, 9H).

2,2,2-Trifluoro-1-(4-fluorophenyl)-*N*-(trimethylsilyl)ethan-1-imine (3.27b) was synthesized according Method A. Yellow oil, 2.09 g, 80% yield, 7.92 mmol; **IR (neat):** 2961 (w), 1704 (m), 1602 (m), 1509 (m), 1237 (m), 1160 (s), 1129 (s), 862 (s), 840 (s) 687 (m), 528 (w) cm^{-1}; **^{1}H NMR (400 MHz, $CDCl_3$):** δ 7.64 (m, *J* = 7.1, 5.3, 0.9 Hz, 2H), 7.17–7.02 (m, 2H), 0.22 (s, 9H); **^{13}C NMR (100 MHz, $CDCl_3$):** δ 165.7, 163.2, 130.3 (dq, *J* = 8.7, 1.8 Hz), 117.8 (d, *J* = 287.9 Hz), 115.7, 115.5, 0.5; **^{19}F NMR (376 MHz, $CDCl_3$):** –68.5 (s, 3F), –108.9 (ddd, *J* = 8.2, 5.4, 3.1 Hz, 1F); **HRMS (DART):** Calcd for $C_{11}H_{14}F_4NSi$ $[M+H]^+$: 264.0832; Found: 264.0826.

(*Z*)-1-(4-Bromophenyl)-2,2,2-trifluoro-*N*-(trimethylsilyl)ethan-1-imine (3.27c) was synthesized according to Method A and the analytical data are consistent with those reported previously.[223]

(*Z*)-1-(4-Chlorophenyl)-2,2,2-trifluoro-*N*-(trimethylsilyl)ethan-1-imine (3.27d) was synthesized according to Method A. Yellow oil, 0.573 g, 77% yield, 2.05 mmol; **IR (neat):** 2960 (w), 1702 (m), 1609 (w), 1252 (m), 1174 (s), 1131 (s), 1023 (s), 952 (s), 726 (s), 528 (m) cm^{-1}; **^{1}H NMR (400 MHz, $CDCl_3$):** δ 7.62–7.51 (m, 2H), 7.47–7.33 (m, 2H), 0.21 (s, 9H); **^{13}C NMR (100 MHz, $CDCl_3$):** δ 156.5 (q, *J* = 33.8 Hz), 137.3, 133.9, 129.4 (q, *J* = 1.8 Hz), 128.8, 117.7 (q, *J* = 287.8 Hz), 0.5; **^{19}F NMR (376 MHz, $CDCl_3$):** –68.7 (d, *J* = 4.0 Hz, 3F); **HRMS (DART):** Calcd for $C_{11}H_{14}NF_3SiCl$ $[M+H]^+$: 260.1077; Found: 260.1072.

2,2,2-Trifluoro-1-(*p*-tolyl)-*N*-(trimethylsilyl)ethan-1-imine (3.27e) was synthesized according to Method #1. Yellow oil; **IR (neat):** 2961 (w), 1705 (s), 1591 (w), 1307 (m), 1186 (s), 1174 (s), 1131 (s), 927 (s), 863 (s), 840 (s), 622 (m) cm^{-1}; **^{1}H NMR (400 MHz, $CDCl_3$):** δ 7.52–7.39 (m, 2H), 7.23–7.15 (m, 2H), 2.40 (s, 3H), 0.18 (s, 9H); **^{13}C NMR (100 MHz, $CDCl_3$):** δ 158.6 (d, *J* = 33.3 Hz), 141.2, 133.0, 129.1, 127.9, 118.0 (q, *J* = 287.5 Hz), 21.6, 0.6; **^{19}F NMR (376 MHz, $CDCl_3$):** –69.11 (d, *J* = 7.3 Hz, 3F); **HRMS (DART):** Calcd for $C_{11}H_{14}NF_3Si$ $[M+H]^+$: 280.0531;

[224] Hart, D. J.; Kanai, K; Thomas, D. G.; Yang, T.-K. *J. Org. Chem.* **1983,** *48*, 289-294.

Found: 280.0543.

2,2,2-Trifluoro-1-(4-(trifluoromethyl)phenyl)-N-(trimethylsilyl)ethan-1-imine (3.27f) was synthesized according to Method A. Yellow oil, 0.480 g, 87% yield, 1.53 mmol; **IR (neat):** 2254 (w), 1712 (w), 1327 (m), 1188 (m), 1020 (m), 903 (s), 847 (s), 724 (s), 650 (m) cm^{-1}; **^{1}H NMR (400 MHz, $CDCl_3$):** δ 7.75–7.62 (m, 4H), 0.20 (s, 9H); **^{13}C NMR (100 MHz, $CDCl_3$):** δ 156.5 (q, *J* = 34.4 Hz), 138.7, 132.5 (q, *J* = 32.6 Hz), 128.9, 122.3 (q, *J* = 272.5 Hz), 117.5 (q, *J* = 287.3 Hz), 29.7, 0.2; **^{19}F NMR (376 MHz, $CDCl_3$):** –63.0 (d, *J* = 6.1 Hz, 3F), –69.1 (d, *J* = 6.3 Hz, 3F); **HRMS (DART):** Calcd for $C_{12}H_{14}NF_6Si$ $[M+H]^+$: 314.0800; Found: 314.0811.

2,2,2-Trifluoro-1-(4-methoxyphenyl)-*N*-(trimethylsilyl)ethan-1-imine (3.27g) was synthesized according to Method B. Yellow oil, 0.371 g, 55% yield, 1.35 mmol; **IR (neat):** 2957 (w), 2834 (w), 1697 (m), 1602 (m), 1577 (m), 1251 (s), 1164 (s), 1126 (s), 1032 (m), 862 (s), 837 (s), 761 (m), 560 (w) cm^{-1}; **^{1}H NMR (400 MHz, $CDCl_3$):** δ 7.62 (m, *J* = 7.8, 1.2 Hz, 2H), 7.01–6.78 (m, 2H), 3.85 (d, *J* = 1.2 Hz, 3H), 0.22 (s, 9H); **^{13}C NMR (100 MHz, $CDCl_3$):** δ 161.7, 156.6 (q, *J* = 33.1 Hz), 129.6 (q, *J* = 26.8 Hz), 128.0, 116.5 (q, *J* = 288.1 Hz), 113.5 (d, *J* = 13.2 Hz), 55.3 (q, *J* = 22.5 Hz), 0.5; **^{19}F NMR (376 MHz, $CDCl_3$):** –68.0 (s, 3F); **HRMS (DART):** Calcd for $C_{12}H_{17}NF_3SiO$ $[M+H]^+$: 276.1032; Found: 276.1044.

***N*,*N*-Dimethyl-4-(2,2,2-trifluoro-1-((trimethylsilyl)imino)ethyl)aniline (3.27h)** was synthesized according to Method B. Yellow solid, 0.349 g, 52% yield, 1.21 mmol; **M.p.** = 56–58 °C; **IR (neat):** 2956 (w), 2899 (w), 1690 (m), 1602 (s), 1527 (w), 1369 (m), 1164 (s), 1129 (s), 864 (m), 842 (m) cm^{-1}; **^{1}H NMR (400 MHz, $CDCl_3$):** δ 7.64 (d, *J* = 8.6 Hz, 2H), 6.65 (d, *J* = 8.9 Hz, 2H), 3.03 (s, 6H), 0.23 (s, 9H); **^{13}C NMR (100 MHz, $CDCl_3$):** δ 152.1, 129.8 (q, *J* = 26.2 Hz), 122.8, 118.0 (q, *J* = 289.0 Hz), 110.9, 110.8, 40.1, 40.0, 0.7; **^{19}F NMR (376 MHz, $CDCl_3$):** –66.9 (s, 3F); **HRMS (DART):** Calcd for $C_{13}H_{20}N_2F_3Si$ $[M+H]^+$: 289.1342; Found: 289.1334.

2,2,2-Trifluoro-1-(2-methoxyphenyl)-*N*-(trimethylsilyl)ethan-1-imine (3.27i) was synthesized according to Method B. Yellow oil, 0.624 g, 97% yield, 2.26 mmol; **IR (neat):** 2958 (w), 1702 (m), 1488 (m), 1247 (m), 1180 (s), 1125 (s), 944 (m), 802 (s), 751 (s), 657 (m), 575 (w) cm^{-1}; **^{1}H NMR (400 MHz, $CDCl_3$):** δ 7.38 (ddd, *J* = 8.4, 7.5, 1.8 Hz, 1H), 7.09 (m, 1H), 6.96 (td, *J* = 7.5, 0.9 Hz, 1H), 6.90 (dd, *J* = 8.4, 0.9 Hz, 1H), 3.81 (s, 3H), –0.01 (s, 9H); **^{13}C NMR (100 MHz, $CDCl_3$):** δ 156.7, 132.7, 131.2, 130.8 (q, *J* = 288.0 Hz), 128.5, 120.8, 120.4, 111.9, 111.0, 55.9 (q, *J* = 27.3 Hz), 1.5, -0.4; **^{19}F NMR (376 MHz, $CDCl_3$):** –73.9 (s, 3F); **HRMS (DART):** Calcd for $C_{12}H_{17}NOF_3Si$ $[M+H]^+$: 276.1026; Found: 276.1022.

2,2,2-Trifluoro-1-(2-fluorophenyl)-*N*-(trimethylsilyl)ethan-1-imine (3.27j) was synthesized according to Method B. Yellow oil, 0.895 g, 65% yield, 3.39 mmol; **IR (neat):** 2962 (w), 1708 (m), 1489 (m), 1452 (m), 1182 (s), 1133 (s), 822 (m), 758 (m), 744 (s), 612 (m) cm^{-1}; **^{1}H NMR (400 MHz, $CDCl_3$):** δ 7.43 (m, 1H), 7.25–7.15 (m, 2H), 7.11 (ddt, *J* = 9.4, 8.3, 1.0 Hz, 1H), 0.05 (s, 9H); **^{13}C NMR (100 MHz, $CDCl_3$):** δ 159.0 (d, *J* = 248.4 Hz), 156.7 (q, *J* = 36.8 Hz), 131.7 (d, *J* = 8.0 Hz), 129.0 (d, *J* = 3.2 Hz), 124.2 (d, *J* = 18.9 Hz), 124.1 (d, *J* = 3.6 Hz), 117.7 (q, *J* = 285.8 Hz), 115.9 (d, *J* = 21.4 Hz), –0.6; **^{19}F NMR (376 MHz, $CDCl_3$):** –74.0 (d, *J* = 5.1 Hz, 3F), –113.9 (dq, *J* = 10.8, 5.5 Hz, 1F); **HRMS (DART):** Calcd for $C_{11}H_{14}NF_4Si$ $[M+H]^+$: 264.0832;

Found: 264.0842.

1-(2-Chlorophenyl)-2,2,2-trifluoro-*N*-(trimethylsilyl)ethan-1-imine (3.27k) was synthesized according to Method B. Yellow oil, 0.338 g, 50% yield, 1.21 mmol; **IR (neat):** 2962 (w), 1708 (m), 1186 (s), 1126 (s), 1059 (m), 950 (s), 839 (s), 756 (s), 648 (m), 471 (m) cm^{-1}; **^{1}H NMR (400 MHz, $CDCl_3$):** δ 7.44–7.40 (m, 1H), 7.40–7.34 (m, 1H), 7.34–7.27 (m, 1H), 7.21–7.16 (m, 1H), 0.02 (s, 9H); **^{13}C NMR (100 MHz, $CDCl_3$):** δ 159.1, 135.8, 131.8, 131.0, 129.9, 128.8, 126.8, 117.9 (q, J = 284.7 Hz), –0.6; **^{19}F NMR (376 MHz, $CDCl_3$):** –73.5 (s, 3F); **HRMS (DART):** Calcd for $C_{11}H_{14}NF_3SiCl$ $[M+H]^+$: 280.0531; Found: 280.0533.

1-(2-Bromophenyl)-2,2,2-trifluoro-*N*-(trimethylsilyl)ethan-1-imine (3.27l) was synthesized according to Method #2. White solid; **IR (neat):** 2960 (w), 1709 (m), 1430 (w), 1251 (m), 1186 (s), 1130 (s), 933 (s), 841 (s), 705 (m), 621 (w) cm^{-1}; **^{1}H NMR (400 MHz, $CDCl_3$):** δ 7.71–7.66 (m, 1H), 7.59 (dd, J = 8.0, 1.2 Hz, 1H), 7.31–7.26 (m, 1H), 7.18 (dd, J = 7.4, 1.8 Hz, 1H), 0.01 (s, 9H); **^{13}C NMR (100 MHz, $CDCl_3$):** δ 134.1–131.9 (m), 131.1, 128.8, 128.4, 127.6, 127.4, 120.7 (d, J = 10.6 Hz), 1.5, –0.5; **^{19}F NMR (376 MHz, $CDCl_3$):** –73.1 (s, 1F); **HRMS (DART):** Calcd for $C_{11}H_{14}NF_3SiBr$ $[M+H]^+$: 324.0026; Found: 324.0017.

(*Z*)-2,2,2-Trifluoro-1-(*o*-tolyl)-*N*-(trimethylsilyl)ethan-1-imine (3.27m) was synthesized according to Method B. Yellow oil, 0.912 g, 89% yield, 3.52 mmol; **IR (neat):** 3051 (w), 1702 (w), 1420 (m), 1304 (m), 1263 (m), 1184 (m), 930 (m), 859 (m), 730 (s), 702 (m), 513 (w) cm^{-1}; **^{1}H NMR (400 MHz, $CDCl_3$):** δ 7.35–7.28 (m, 1H), 7.20 (m, 2H), 7.07 (d, J = 7.6 Hz, 1H), 2.25 (s, 3H), –0.02 (s, 9H); **^{13}C NMR (100 MHz, $CDCl_3$):** δ 163.7 (q, J = 35.5 Hz), 136.7, 135.2, 130.4, 129.6, 127.3, 125.7, 118.3 (q, J = 285 Hz), 19.7, –0.4; **^{19}F NMR (376 MHz, $CDCl_3$):** –73.6 (s, 3F); **HRMS (DART):** Calcd for $C_{12}H_{17}NF_3Si$ $[M+H]^+$: 260.1077; Found: 260.1072.

1-(3-Chlorophenyl)-2,2,2-trifluoro-*N*-(trimethylsilyl)ethan-1-imine (3.27n) was synthesized according to Method A. Yellow oil, 0.439 g, 66% yield, 1.57 mmol; **IR (neat):** 2957 (w), 1707 (m), 1568 (w), 1251 (m), 1224 (s), 1178 (s), 840 (s), 674 (m), 622 (m), 540 (w) cm^{-1}; **^{1}H NMR (400 MHz, $CDCl_3$):** δ 7.58 (m, 1H), 7.46 (m, 2H), 7.42–7.30 (m, 1H), 0.27–0.14 (m, 9H); **^{13}C NMR (100 MHz, $CDCl_3$):** δ 156.4 (q, J = 34.3 Hz), 137.2, 134.7, 131.0, 129.8, 128.1 (d, J = 1.8 Hz), 126.0 (d, J = 1.9 Hz), 117.7 (d, J = 287.3 Hz), 0.5; **^{19}F NMR (376 MHz, $CDCl_3$):** –68.9 (s, 3F); **HRMS (DART):** Calcd for $C_{11}H_{14}NF_3SiCl$ $[M+H]^+$: 280.0531; Found: 280.0533.

2,2,2-Trifluoro-1-(3-(trifluoromethyl)phenyl)-*N*-(trimethylsilyl)ethan-1-imine (3.27o) was synthesized according to Method A. Yellow oil, 0.303 g, 55% yield, 0.968 mmol; **IR (neat):** 2959 (w), 1960 (m), 1332 (m), 1165 (s), 1126 (s), 1099 (m), 863 (m), 842 (m), 648 (m) cm^{-1}; **^{1}H NMR (400 MHz, $CDCl_3$):** δ 7.57 (m, 1H), 7.46 (m, 2H), 7.35 (m, 1H), 0.23–0.18 (s, 9H); **^{13}C NMR (100 MHz, $CDCl_3$):** δ 156.4 (q, J = 34.3 Hz), 137.2, 134.7, 131.3 (q, J = 230.0 Hz), 131.1, 129.8, 128.1 (d, J = 1.6 Hz), 126.0 (q, J = 1.8 Hz), 117.7 (q, J = 288.9 Hz), 0.5 (d, J = 1.4 Hz); **^{19}F NMR (376 MHz, $CDCl_3$):** –68.9 (s, 3F), –62.9 (s, 3F); **HRMS (DART):** Calcd for $C_{12}H_{14}NF_6Si$ $[M+H]^+$: 314.0794; Found: 314.0806.

2,2,2-Trifluoro-1-(*m*-tolyl)-*N*-(trimethylsilyl)ethan-1-imine (3.27p) was synthesized according to Method #1. Yellow oil; **IR (neat):** 2961 (w), 1705 (m), 1252 (m), 1188 (m), 1131 (m), 905 (s),

863 (s), 725 (s), 622 (m) cm^{-1}; **^{1}H NMR (400 MHz, $CDCl_3$):** δ 7.31–7.27 (m, 2H), 7.27–7.21 (m, 2H), 2.36 (s, 3H), 0.13 (s, 9H); **^{13}C NMR (100 MHz, $CDCl_3$):** δ 162.3–155.4 (m), 138.0, 135.7, 131.3, 128.1, 124.7, 117.9 (d, *J* = 287.1 Hz), 21.4, 0.3; **^{19}F NMR (376 MHz, $CDCl_3$):** –69.6 (s, 3F); **HRMS (DART):** Calcd for $C_{12}H_{17}NOF_3Si$ $[M+H]^+$: 260.1077; Found: 260.1074.

2,2,2-Trifluoro-1-(thiophen-2-yl)-*N*-(trimethylsilyl)ethan-1-imine (3.27q) was synthesized according to Method B. Yellow oil, 0.289 g, 41% yield, 1.14 mmol; **IR (neat):** 2960 (w), 1682 (s), 1421 (m), 1251 (m), 1184 (s), 1136 (s), 1061 (m), 841 (s), 712 (s), 567 (m) cm^{-1}; **^{1}H NMR (400 MHz, $CDCl_3$):** δ 7.56–7.45 (m, 2H), 7.09 (dt, *J* = 5.1, 2.3 Hz, 1H), 0.28 (s, 9H); **^{13}C NMR (100 MHz, $CDCl_3$):** δ 142.9, 131.8, 130.01 (q, *J* = 3.2 Hz), 128.4, 117.1 (q, *J* = 289 Hz), 105.6, 0.7; **^{19}F NMR (376 MHz, $CDCl_3$):** –67.6 (s, 3F); **HRMS (DART):** Calcd for $C_9H_{13}NF_3Si$ $[M+H]^+$: 252.0485; Found: 252.0489.

2,2,2-Trifluoro-1-(furan-2-yl)-*N*-(trimethylsilyl)ethan-1-imine (3.27r) was synthesized according to Method A and the analytical data are consistent with those reported previously.[225]

1-(Benzofuran-2-yl)-2,2,2-trifluoro-*N*-(trimethylsilyl)ethan-1-imine (3.27s) was synthesized according to Method B. Yellow solid, 0.649 g, 79% yield, 2.25 mmol; **M.p.** = 59–61°C; **IR (neat):** 2958 (w), 1686 (s), 1407 (w), 1251 (s), 1200 (m), 1154 (s), 1129 (s), 982 (s), 905 (s), 843 (s), 743 (s), 626 (w) cm^{-1}; **^{1}H NMR (400 MHz, $CDCl_3$):** δ 7.71 (dt, *J* = 7.9, 0.9 Hz, 1H), 7.54 (dd, *J* = 8.3, 1.1 Hz, 1H), 7.44 (ddd, *J* = 8.4, 7.2, 1.2 Hz, 1H), 7.36–7.28 (m, 2H), 0.38 (s, 9H); **^{13}C NMR (100 MHz, $CDCl_3$):** δ 155.1, 147.6, 127.5, 127.4, 124.0, 123.3, 117.1 (q, *J* = 285.4 Hz), 111.6, 111.5, 111.5 (q, peaks overlapped), 0.7; **^{19}F NMR (376 MHz, $CDCl_3$):** –70.1 (d, *J* = 1.8 Hz, 3F); **HRMS (DART):** Calcd for $C_{13}H_{15}NOF_3Si$ $[M+H]^+$: 286.0870; Found: 286.0868.

(*E*)-1,1,1-Trifluoro-3-methyl-4-phenyl-*N*-(trimethylsilyl)but-3-en-2-imine (3.27t) was synthesized according to Method B. Yellow oil, 0.295 g, 52% yield, 1.04 mmol; **IR (neat):** 3298 (w), 2959 (w), 1696 (m), 1608 (m), 1184 (s), 1129 (s), 953 (s), 839 (s), 696 (s), 626 (m), 506 (w) cm^{-1}; **^{1}H NMR (400 MHz, $CDCl_3$):** δ 7.43–7.27 (m, 5H), 6.80 (s, 1H), 2.05 (dt, *J* = 1.6, 0.8 Hz, 3H), 0.27 (s, 9H); **^{13}C NMR (100 MHz, $CDCl_3$):** δ 161.7 (q, *J* = 32.6 Hz), 136.0, 134.7, 133.8 (q, *J* = 2.0 Hz), 129.2, 128.4, 127.8, 117.9 (q, *J* = 287.9 Hz), 15.7 (q, *J* = 1.5 Hz), 0.5; **^{19}F NMR (376 MHz, $CDCl_3$):** –68.4 (d, *J* = 5.8 Hz, 3F); **HRMS (DART):** Calcd for $C_{14}H_{19}NF_3Si$ $[M+H]^+$: 286.1233; Found: 286.1231.

1,1,1-Trifluoro-4-phenyl-*N*-(trimethylsilyl)but-3-yn-2-imine (3.27u) was synthesized according to Method B. Yellow oil, 0.434 g, 64% yield, 1.61 mmol; **IR (neat):** 2959 (w), 2199 (m), 1654 (m), 1319 (m), 1247 (s), 1196 (s), 1138 (s), 860 (s), 843 (s), 755 (s), 687 (m), 533 (m) cm^{-1}; **^{1}H NMR (400 MHz, $CDCl_3$):** δ 7.57–7.51 (m, 2H), 7.49–7.43 (m, 1H), 7.43–7.36 (m, 2H), 0.37 (s, 9H); **^{13}C NMR (100 MHz, $CDCl_3$):** δ 145.1 (q, *J* = 39.6 Hz), 132.4, 130.6, 128.7, 120.1, 117.1 (q, *J* = 281.9), 94.3, 82.2, –0.7; **^{19}F NMR (376 MHz, $CDCl_3$):** –74.5 (s, 3F); **HRMS (DART):** Calcd for $C_{13}H_{15}NF_3Si$ $[M+H]^+$: 270.0920; Found: 270.0922.

---

[225] Zhu, J.; Huang, L.; Dong, W.; Li, N.; Yu, X.; Deng, W.-P. T. W. *Angew. Chem., Int. Ed.* **2019**, *58*, 16119–16123.

(*Z*)-2,2,3,3,3-Pentafluoro-1-(4-(trifluoromethyl)phenyl)-*N*-(trimethylsilyl)propan-1-imine (3.27v) was synthesized according to Method #1. Yellow oil; **IR (neat):** 2963 (w), 1711 (m), 1410 (s), 1185 (s), 1130 (s), 1019 (m), 864 (m), 844 (m), 798 (m), 593 (w) cm^{-1}; **^{1}H NMR (400 MHz, $CDCl_3$):** δ 7.72–7.64 (m, 2H), 7.46–7.39 (m, 2H), 0.15–0.05 (m, 9H); **^{13}C NMR (100 MHz, $CDCl_3$):** δ 156.5 (q, J = 34.5 Hz), 138.3 (d, J = 84.1 Hz), 132.5 (q, J = 32.8 Hz), 129.0, 128.2 (d, J = 5.8 Hz), 126.0–124.7 (m), 117.5 (q, J = 287.4 Hz), 21.4, 0.2; **^{19}F NMR (376 MHz, $CDCl_3$):** –62.99 (s, 3F), –80.85 (s, 3F), –114.92 (s, 2F); **HRMS (DART):** Calcd for $C_{13}H_{14}NF_8Si$ $[M+H]^+$: 364.0762; Found: 364.0741.

3.7.3. Boronic ester reagents

2-Allyl-4,4,5,5-tetramethyl-1,3,2-dioxaborolane was purchased from Frontier Scientific and distilled from calcium hydride prior to use.

(*Z*)-2-(But-2-en-1-yl)-4,4,5,5-tetramethyl-1,3,2-dioxaborolane was purchased from Aldrich or Santa Cruz and used as received.

(*Z*)-1-(4,4,5,5-Tetramethyl-1,3,2-dioxaborolan-2-yl)dec-2-en-5-one (S-*Z*-1) was synthesized according to a procedure in the literature and the analytical data are consistent with those reported previously.[226]

(*Z*)-2-(3-Chloroallyl)-4,4,5,5-tetramethyl-1,3,2-dioxaborolane (S-*Z*-2) was synthesized according to a procedure in the literature and the analytical data are consistent with those reported previously.[227]

(*Z*)-2-(3-Bromoallyl)-4,4,5,5-tetramethyl-1,3,2-dioxaborolane (S-*Z*-3):

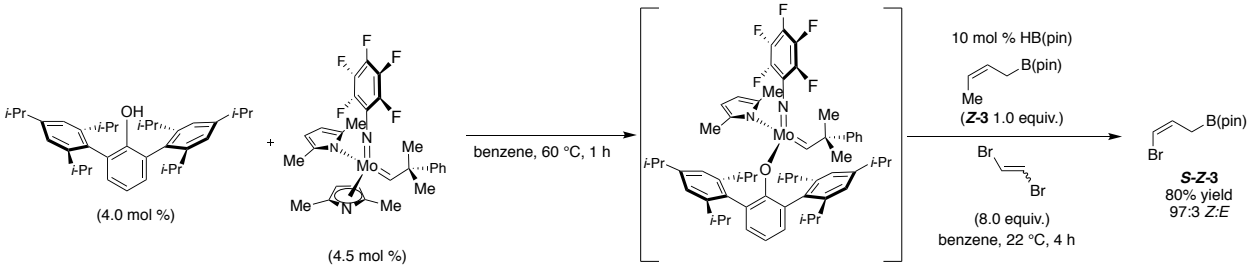

In a N_2-filled glovebox, an oven-dried one-dram vial was charged with aryl-oxide (24.9 mg, 0.05 mmol), bis-imidomolybdenum (33.7 mg, 0.055 mmol), and benzene (0.4 mL). The vial was sealed with a Teflon cap and the solution was allowed to stir at 60 °C for one h. A separate oven-dried one-dram vial was charged with ***Z*-3** (227.6 mg, 1.25 mmol), 1,2-dibromoethylene (mixture of *cis*- and *trans*-, 1.85 g, 10.0 mmol), HB(pin) (16.0 mg, 0.125 mmol) and benzene (0.1 mL). The solution was allowed to stir at 22 °C for 10 min. The freshly prepared catalyst solution was allowed to cool to 22 °C before it was added in a dropwise manner (0.3 mL) to the vial

[226] Ely, R. J.; Morken, J. P. *J. Am. Chem. Soc.* **2010**, *132*, 2534–2535.

[227] Koh, M. J.; Nguyen, T. T.; Zhang, H.; Schrock, R. R.; Hoveyda, A. H. *Nature* **2016**, *531*, 459–465.

containing the cross partners. The solution was allowed to stir at 22 °C for two h, after which the remaining catalyst stock solution (0.1 mL) was added. The solution was allowed to stir at 22 °C for an additional two 2, then reaction was quenched by the addition of $CDCl_3$ and analyzed by ^{1}H-NMR spectroscopy affording the desired allyl boron in 95% conv., 97:3 *Z*:*E*. The volatiles were removed in vacuo prior and the remaining brown oil was purified by Kugelrohr distillation (90–120 °C, 0.5 torr) to afford **S-*Z*-3** (247.3 mg, 1.00 mmol, 80% yield) as light brown oil. **IR (neat):** 2977 (m), 2930 (w), 1619 (w), 1468 (s), 1369 (s), 1302 (s), 1108 (s), 966 (m), 846 (m) 718 (m), 675 (m) cm^{-1}; **^{1}H NMR (400 MHz, $CDCl_3$):** δ 6.23 (td, *J* = 7.6, 6.8 Hz, 1H), 6.15 (dt, *J* = 6.8, 1.4 Hz, 1H), 1.86–1.83 (m, 2H), 1.26 (s, 12H); **^{13}C NMR (100 MHz, $CDCl_3$):** δ 130.7, 108.0, 83.7, 24.9, 24.7; **HRMS (DART):** Calcd for $C_9H_{17}BO_2Br$ $[M+H]^+$: 247.0500; Found: 247.0497.

(*Z*)-2-(3-((2-Methoxyethoxy)methoxy)allyl)-4,4,5,5-tetramethyl-1,3,2-dioxaborolane (S-*Z*-4) was prepared according to a reported procedure and the analytical data are consistent with those reportedly previously.[228]

(*Z*)-4,4,5,5-Tetramethyl-2-(2-methylhept-2-en-1-yl)-1,3,2-dioxaborolane (S-*Z*-5) was synthesized according to a procedure in the literature.[226] **IR (neat):** 2975 (m), 2924 (m), 1350 (s), 1320 (s), 1141 (s), 967 (m), 847 (m) cm^{-1}; **^{1}H NMR (400 MHz, $CDCl_3$):** δ 5.11 (tq, *J* = 7.1, 1.3 Hz, 1H), 1.94 (q, *J* = 6.6 Hz, 2H), 1.73 (q, *J* = 1.3 Hz, 3H), 1.65 (s, 2H), 1.30 (tt, *J* = 5.1, 2.4 Hz, 4H), 1.23 (s, 12H), 0.93 – 0.78 (m, 3H); **^{13}C NMR (150 MHz, $CDCl_3$):** δ 167.6, 131.8, 124.0 (d, *J* = 13.5 Hz) 97.6, 83.1, 32.0, 28.0, 25.7 (m), 24.7, 22.4, 14.1; **HRMS (DART):** Calcd for $C_{14}H_{28}BO_2$ $[M+H]^+$: 239.21769; Found: 239.21758.

(*Z*)-2-(3-Chloro-2-methylallyl)-4,4,5,5-tetramethyl-1,3,2-dioxaborolane (S-*Z*-6) was synthesized according to a procedure in the literature and the analytical data are consistent with those reportedly previously.[229]

3.7.4. Aminophenol ligands

(*S*)-2-((3-(*tert*-Butyl)-2-hydroxybenzyl)amino)-3-methyl-1-(pyrrolidin-1-yl)butan-1-one (ap-1) was synthesized in accordance to a procedure in the literature and the analytical data are consistent with those reported previously.[230]

(2*S*,3*R*)-3-(Benzyloxy)-2-((3-(*tert*-butyl)-2-hydroxybenzyl)amino)-1-(pyrrolidin-1-yl)butan-1-one (ap-4) was synthesized analogous to **ap-1** except Boc-Thr(Bzl)-OH was used as the starting material. Yellow oil; **IR (neat):** 3315 (w), 2955 (m, br), 1635 (s), 1435 (s), 1239 (m), 1054 (m),

---

[228] Morrison, R. J.; Hoveyda, A. H. *Angew. Chem., Int. Ed.* **2018**, *57*, 11654-1166.

[229] Nguyen, T. T.; Koh, M. J.; Mann, T. J.; Schrock, R. R.; Hoveyda, A. H. *Nature* **2017**, *552*, 347–354.

[230] Silverio, D. L.; Torker, S.; Pilyugina, T.; Vieira, E. M.; Snapper, M. L.; Haeffner, F.; Hoveyda, A. H. *Nature* **2013**, *494*, 216–221.

782 (m), 698 (m) cm^{-1}; **^{1}H NMR (400 MHz, $CDCl_3$):** δ 11.01 (s, 1H), 7.33–7.27 (m, 4H), 7.19 (dd, *J* = 7.8, 1.7 Hz, 1H), 6.79 (dd, *J* = 7.5, 1.6 Hz, 1H), 6.69 (t, *J* = 7.6 Hz, 1H), 4.66–4.39 (m, 2H), 4.10 (d, *J* = 13.4 Hz, 1H), 3.82–3.53 (m, 3H), 3.47 (d, *J* = 7.0 Hz, 2H), 3.26 (dt, *J* = 50.9, 7.6 Hz, 2H), 2.85 (s, 1H), 1.83 (h, *J* = 6.7 Hz, 4H), 1.42 (s, 9H), 1.22 (d, *J* = 6.3 Hz, 3H); **^{13}C NMR (100 MHz, $CDCl_3$):** δ 157.1, 138.0, 137.0, 128.3, 127.8, 127.6, 126.7, 126.1, 122.6, 118.3, 75.4, 71.2, 62.0, 51.1, 46.5, 45.9, 34.7, 29.5, 26.0, 24.1, 16.1; **HRMS (DART):** Calcd for $C_{26}H_{37}N_2O_3$ $[M+H]^+$: 425.2800; Found: 425.2784; **Specific rotation:** $[\alpha]^{24}_D$ –29.6 (*c* = 0.84, $CHCl_3$).

(2*S*,3*R*)-2-((3-(*tert*-Butyl)-2-hydroxybenzyl)amino)-3-methoxy-1-(pyrrolidin-1-yl)butan-1-one (ap-6) was synthesized analogous to **ap-1a** in accordance to a reported procedure except Boc-Thr(OMe)-OH was used as the starting material. Colorless oil; **IR (neat):** 3288 (w), 2949 (m, br), 1631 (s), 1434 (s), 1238 (m), 1090 (s), 877 (s), 748 (m), 619 (s), 509 (w) cm^{-1}; **^{1}H NMR (400 MHz, $CDCl_3$):** δ 7.20 (dd, *J* = 7.8, 1.7 Hz, 1H), 6.81 (dd, *J* = 7.4, 1.7 Hz, 1H), 6.70 (t, *J* = 7.6 Hz, 1H), 4.11 (d, *J* = 13.5 Hz, 1H), 3.68 (d, *J* = 13.5 Hz, 1H), 3.64 – 3.39 (m, 5H), 3.31 (s, 3H), 3.24 (dt, *J* = 10.5, 6.6 Hz, 1H), 1.89 (qt, *J* = 11.7, 5.1 Hz, 4H), 1.42 (s, 9H), 1.16 (d, *J* = 6.2 Hz, 3H); **^{13}C NMR (100 MHz, $CDCl_3$):** δ 169.7, 157.1, 137.0, 126.7, 126.1, 122.7, 118.3, 78.4, 61.5, 57.1, 51.2, 46.5, 45.9, 34.7, 29.5, 26.1, 24.1, 15.5; **HRMS (DART):** Calcd for $C_{20}H_{33}N_2O_3$ $[M+H]^+$: 349.2486; Found: 349.2478; **Specific rotation:** $[\alpha]^{24}_D$ –21.6 (*c* 1.41, $CHCl_3$).

(2*S*,3*S*)-2-((3-(*tert*-Butyl)-2-hydroxybenzyl)amino)-3-methoxy-1-(pyrrolidin-1-yl)butan-1-one (ap-11) was synthesized analogous to **ap-1a**. The requisite amino acid was obtained by alkylating Boc-allo-Thr-OBn with trimethyloxonium tetrafluoroborate (Meerwein's Salt) according to a reported procedure[231] and subsequent hydrolysis of the benzyl ester according to a known protocol.[232] Colorless oil; **IR (neat):** 3269 (w), 2948 (m, br), 1631 (s), 1434 (s), 1238 (m), 1103 (m), 841 (m), 749 (m) cm^{-1}; **^{1}H NMR (400 MHz, $CDCl_3$):** δ 10.78 (s, 1H), 7.20 (dd, *J* = 7.8, 1.7 Hz, 1H), 6.79 (dd, *J* = 7.4, 1.7 Hz, 1H), 6.71 (t, *J* = 7.5 Hz, 1H), 4.11 (d, *J* = 13.5 Hz, 1H), 3.65 – 3.36 (m, 5H), 3.35 – 3.28 (m, 1H), 3.24 (s, 3H), 3.14 (dt, *J* = 8.9, 6.6 Hz, 1H), 1.88 (dq, *J* = 6.2, 3.8, 2.2 Hz, 4H), 1.41 (s, 9H), 1.24 (d, *J* = 6.1 Hz, 3H); **^{13}C NMR (100 MHz, $CDCl_3$):** δ 171.1, 156.8, 137.0, 126.7, 126.1, 122.5, 118.4, 78.4, 62.2, 57.1, 50.8, 46.3, 45.9, 34.6, 29.4, 25.9, 24.3, 16.6; **HRMS (DART):** Calcd for $C_{20}H_{33}N_2O_3$ $[M+H]^+$: 349.2486; Found: 349.2475; **Specific rotation:** $[\alpha]^{24}_D$ –35.7 (*c* 2.35, $CHCl_3$).

---

[231] Kiho, T.; Nakayama, M.; Yasuda, K.; Miyakoshi, S.; Inukai, M.; Kogen, H. *Bioorg. Med. Chem.* **2004**, *12*, 337–361.

[232] Xiao, K.-J.; Chu, L.; Yu, J.-Q. *Angew. Chem., Int. Ed.* **2016**, *55*, 2856-2860.

3.7.4. Ligand Screening and Silyl Removal Studies

3.7.4.1. Screening of fluoride reagents

Table S1: Examination of different fluoride reagents.[a]

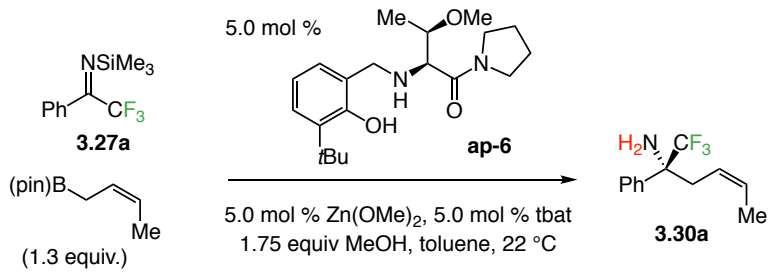

Entry	Reagent	N-H Ketimine (%)[b]	Conv. to **4a** (%)[b]	Hemiaminal (%)[b]	*Z*:*E* (α-add. isomer)[b]	e.r. (α-add. isomer)[c]
1	CsF	>98	36	19	>98:2	97:3
2	(nBu)$_4$NF (solid)	>98	58	15	84:16	97:3
3	(nBu)$_4$NF•H$_2$O (1.0 M, thf)	>98	88	<5	96:4	97:3
4	(Me)$_4$NF	>98	25	<10	>98:2	97:3
5	tbat	>98	>98	<10	>98:2	97:3

[a] All reactions were performed under N_2 atm. [b] Determined by analysis of ^{19}F NMR spectra of unpurified mixtures; conv. (±2%) refers to disappearance of the silyl ketimine. [c] Enantioselectivity was determined by HPLC analysis (±1%);

3.7.4.2. Spectroscopic investigations

In a N_2-filled glovebox, NTMS ketimine (0.1 mmol), tbat (5.0 mol %), and toluene (0.5 mL) were combined in a J-Young NMR tube. Immediately prior to placing the tube in the spectrometer, the solution was charged with *i*PrOH (2.5 equiv.) after which the tube was turned several times to ensure complete mixing. Spectra (^{19}F NMR) were collected every minute until complete disappearance of the N-TMS ketimine (~60 min). The signals corresponding to *E* and *Z* isomers of the N-H ketimine can be observed increasing in intensity at the left and right of the N-TMS ketimine peak. It was not determined which peak corresponds to the *E*- and *Z*-N–H imine isomers.

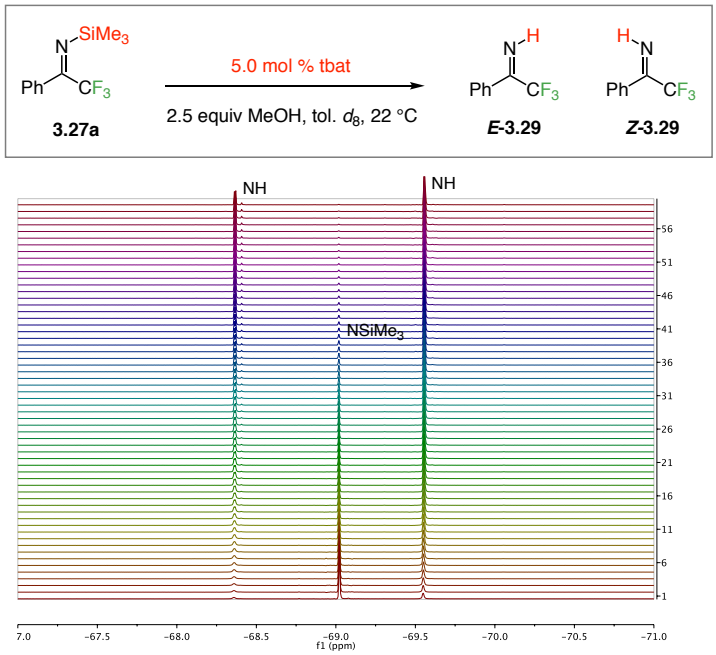

N-H ketimine generation and crotyl addition: In a N_2-filled glovebox, ketimine (0.1 mmol), tbat (5.0 mol %), and toluene (0.25 mL) were combined in a J-Young NMR tube, after which the solution was charged with a solution of aminophenol (5.0 mol %) and $Zn(OMe)_2$ (10.0 mol %) in toluene. (0.25 mL). Immediately prior to placement of the tube within the NMR instrument, MeOH (1.75 equiv.) was added and the tube was turned ~10 times to ensure complete mixing. (Note: MeOH (1.75 equiv.) so that formation of N-H ketimine and homoallylamine formation could be monitored.) Spectra (^{19}F NMR) were collected until complete disappearance of N–TMS ketimine and appearance of the final product.

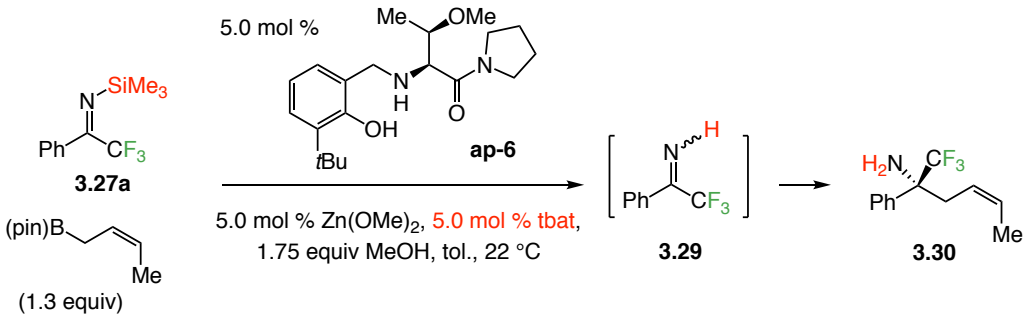

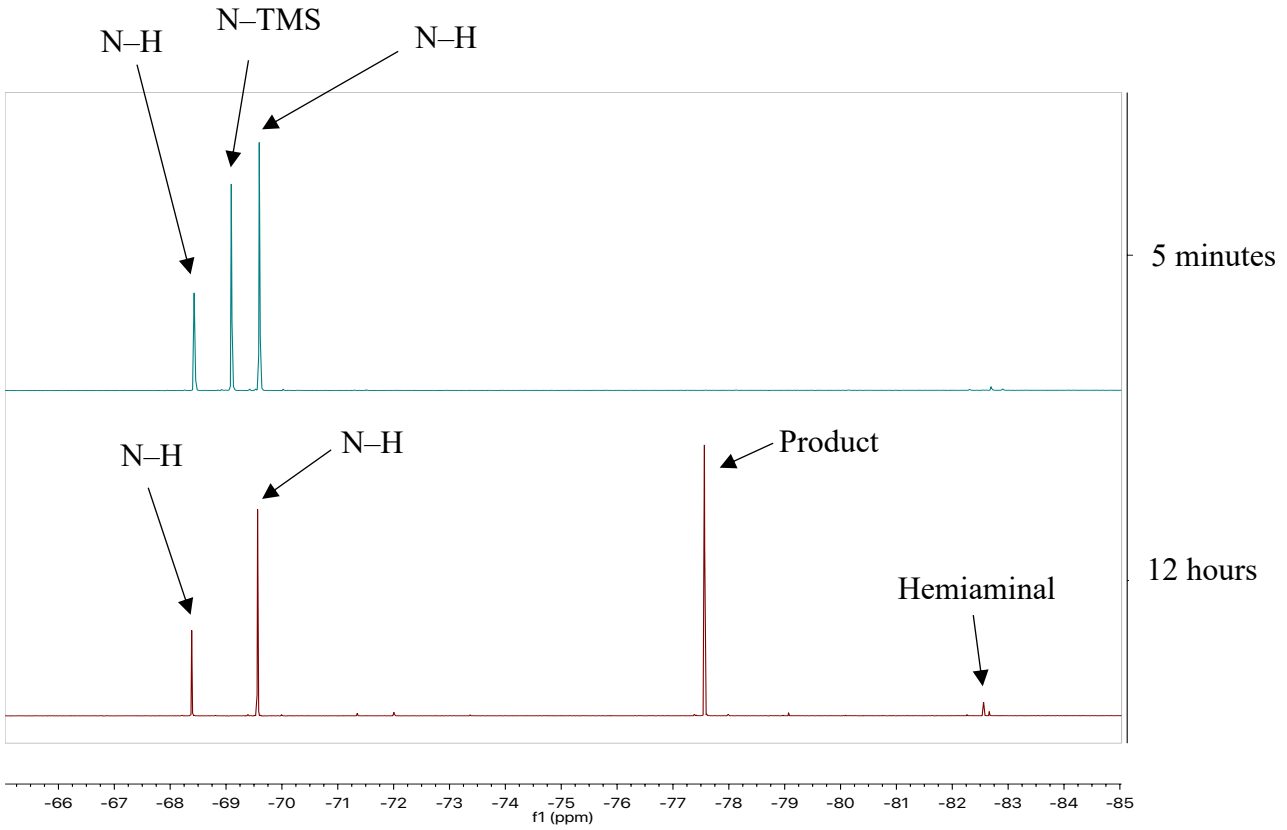

3.7.5. Additions of Allyl–B(pin) to Trifluoromethyl N-H Ketimines

General procedure for addition of allyl–B(pin): In a N_2-filled glovebox, an oven-dried two-dram vial equipped with a magnetic stir-bar was charged with **ap-4** (3.3 mg, 0.01 mmol), $Zn(OMe)_2$ (1.7 mg, 0.01 mmol) and the solids were dissolved in toluene (0.20 mL). A second oven-dried two-dram vial was charged with ketimine (0.1 mmol), toluene (0.10 mL), and tbat (2.7 mg, 0.005 mmol) to which was added the freshly prepared catalyst stock solution (0.1 mL) followed by allylboronic acid pinacol ester (25.3 mg, 0.15 mmol). The vial was sealed (septum and electrical tape), and removed from the glovebox, and the solution was allowed to cool to 4 °C in a cold room. To this solution was added *i*PrOH (19 μL, 0.25 mmol) and the mixture was allowed to stir for 3 h. Reaction progress (conv.) was monitored by ^{19}F NMR spectroscopy (aliquot removed). Once transformation reached completion, the mixture was loaded onto a silica gel column and eluted with hexanes/Et_2O to afford the α-tertiary amine as colorless oil.

(*R*)-1,1,1-Trifluoro-2-phenylpent-4-en-2-amine (3.28a): The title compound was synthesized according to the general procedure and purified by silica gel chromatography to afford the product as colorless oil. The analytical data are consistent with those reported previously.[233] Colorless oil, 20.2 mg, 94% yield, 0.094 mmol; **Specific Rotation:** $[\alpha]^{24}_D$ +38.7 (*c* 2.57, $CHCl_3$) for a 91:9

[233] Morisaki, K.; Kondo, Y.; Sawa, M.; Morimoto, H.; Ohshima, T. *Chem. Pharm. Bull.* **2017**, *65*, 1089–1092.

er sample. The enantiomeric purity was determined by HPLC analysis in comparison with authentic racemic material (Chiralpak AD-H, 99:1 hexanes:*i*PrOH, 0.7 mL/min, 220 nm) : t_R: 17.980 min (major) and 20.475 min (minor).

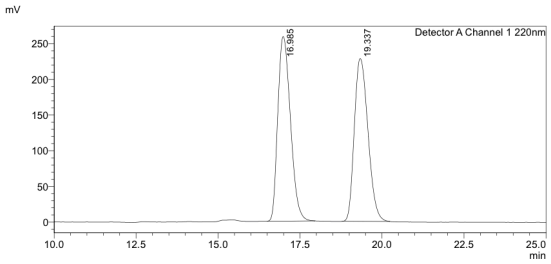

<Peak Table>
Detector A Channel 1 220nm

Peak#	Ret. Time	Area	Area%	Height
1	16.985	6930915	51.194	258584
2	19.337	6607487	48.806	228035
Total		13538401	100.000	486619

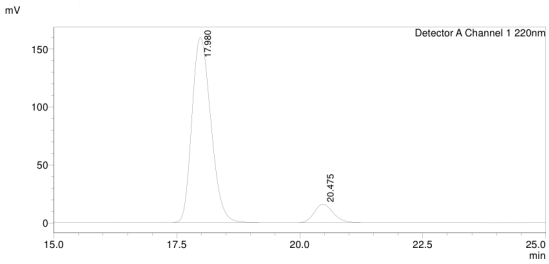

<Peak Table>
Detector A Channel 1 220nm

Peak#	Ret. Time	Area	Height	Area%
1	17.980	4271190	159486	91.006
2	20.475	422106	15899	8.994
Total		4693296	175384	100.000

Peak #	Ret. Time (min)	Area %	Peak #	Ret. Time (min)	Area %
1	16.985	51.194	1	17.980	91.006
2	19.337	48.806	2	20.475	8.994

(*R*)-1,1,1-Trifluoro-2-(2-methoxyphenyl)pent-4-en-2-amine (3.28b): Colorless oil, 16.4 mg, 67% yield, 0.067 mmol; **IR (neat):** 2254 (w), 2014 (w), 1495 (w), 1381 (w), 903 (s), 723 (s), 650 (m), 543 (w) cm^{-1}; **^{1}H NMR (400 MHz, $CDCl_3$):** δ 7.46–7.40 (m, 1H), 7.32 (ddd, *J* = 8.2, 7.3, 1.7 Hz, 1H), 7.01–6.92 (m, 2H), 5.73–5.61 (m, 1H), 5.24–5.07 (m, 2H), 3.86 (s, 3H), 3.30 (ddt, *J* = 14.5, 6.3, 1.5 Hz, 1H), 2.61 (dd, *J* = 14.6, 7.9 Hz, 1H), 2.35 (br, 2H); **^{13}C NMR (100 MHz, $CDCl_3$):** δ 159.1, 132.5, 130.2, 130.0, 127.2 (q, *J* = 286.7 Hz), 120.7, 119.7, 112.7, 62.0 (q, *J* = 26.6 Hz), 55.8, 39.4; **^{19}F NMR (376 MHz, $CDCl_3$):** –78.44 (s, 3F); **HRMS (DART):** Calcd for $C_{12}H_{15}NOF_3$ $[M+H]^+$: 246.1106; Found: 246.1118; **Specific rotation:** $[\alpha]^{24}_D$ = +18.8 (*c* 2.08, $CHCl_3$) for a 91.5:8.5 er sample. The enantiomeric purity was determined by HPLC analysis in comparison with authentic racemic material (Chiralpak AD-H, 99:1 hexanes:*i*PrOH, 0.7 mL/min, 220 nm): t_R: 19.536 min (major) and 23.252 min (minor).

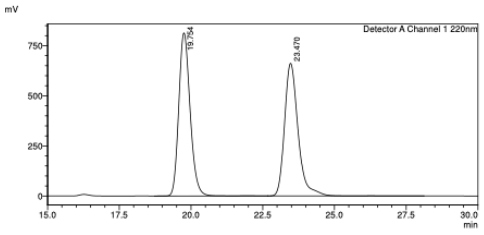

<Peak Table>
Detector A Channel 1 220nm

Peak#	Ret. Time	Area	Height	Area%
1	19.754	22308615	812925	50.671
2	23.470	21718038	661467	49.329
Total		44026654	1474392	100.000

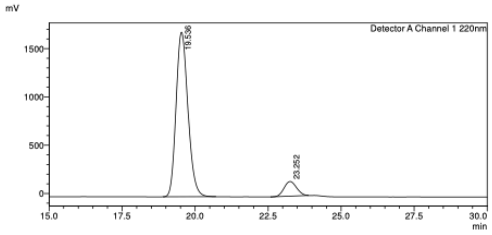

<Peak Table>
Detector A Channel 1 220nm

Peak#	Ret. Time	Area	Height	Area%
1	19.536	48230817	1702737	91.455
2	23.252	4506163	151715	8.545
Total		52736980	1854452	100.000

Peak #	Ret. Time (min)	Area %	Peak #	Ret. Time (min)	Area %
1	19.754	50.671	1	19.536	91.455
2	23.470	49.329	2	23.252	8.545

(*R*)-1,1,1-Trifluoro-2-(2-fluorophenyl)pent-4-en-2-amine (3.28c): Colorless oil, 15.9 mg, 68% yield, 0.068 mmol; **IR (neat):** 3444 (w), 3084 (w), 2933 (w), 1642 (m), 1489 (m), 1219 (m), 1149 (s), 818 (m), 757 (s), 573 (w) cm^{-1}; **^{1}H NMR (400 MHz, $CDCl_3$):** δ 7.58–7.51 (m, 1H), 7.36 (ddd, *J* = 14.0, 10.6, 4.5 Hz, 1H), 7.22–7.14 (m, 1H), 7.08 (ddd, *J* = 13.1, 8.3, 1.5 Hz, 1H), 5.76–5.52 (m, 1H), 5.31–5.05 (m, 2H), 3.30 (dd, *J* = 14.5, 6.4 Hz, 1H), 2.61 (dd, *J* = 14.5, 7.8 Hz, 1H), 1.87 (s, 2H); **^{13}C NMR (100 MHz, $CDCl_3$):** δ 161.4 (d, *J* = 249.6 Hz), 135.1, 131.5, 130.6, 130.1, 129.3 (q, *J* = 278.3 Hz), 124.3 (d, *J* = 3.5 Hz), 120.4, 117.0 (d, *J* = 25.4 Hz), 61.2 (q, *J* = 20.0 Hz), 39.1 (d, *J* = 6.2 Hz); **^{19}F NMR (376 MHz, $CDCl_3$):** δ –79.2 (d, *J* = 15.0 Hz, 3F), –108.5 (dt, *J* = 21.3, 12.4 Hz, 1F); **HRMS (DART):** Calcd for $C_{11}H_{12}F_4N$ $[M+H]^+$: 234.0906; Found: 234.0905; **Specific rotation:** $[\alpha]^{24}_D$ = +28.1 (*c* 1.42, $CHCl_3$) for a 91:9 er sample. The enantiomeric purity was determined by HPLC analysis in comparison with authentic racemic material (Chiralpak AD-H, 99:1 hexanes:*i*PrOH, 0.7 mL/min, 220 nm): t_R: 17.544 min (minor) and 19.618 min (major).

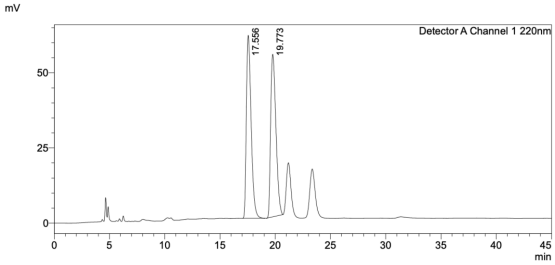

<Peak Table>
Detector A Channel 1 220nm

Peak#	Ret. Time	Area	Height	Area%
1	17.556	1824963	60867	50.556
2	19.773	1784848	54080	49.444
Total		3609811	114947	100.000

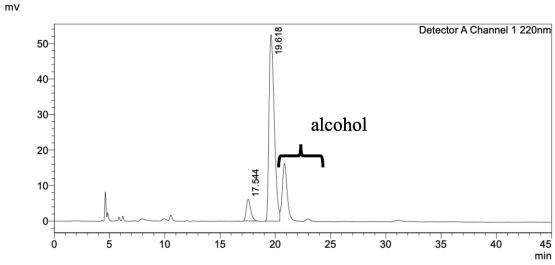

<Peak Table>
Detector A Channel 1 220nm

Peak#	Ret. Time	Area	Height	Area%
1	17.544	168514	6098	8.805
2	19.618	1745224	52511	91.195
Total		1913738	58609	100.000

Peak #	Ret. Time	Area	Area %	Peak #	Ret. Time	Area	Area %
1	17.6 min	1824963	50.556	1	17.5 min	168514	8.805
2	19.8 min	1784848	49.444	2	10.6 min	1745224	91.195

(*R*)-1,1,1-Trifluoro-2-(4-fluorophenyl)pent-4-en-2-amine (3.28d): Colorless oil, 15.6 mg, 67% yield, 0.067 mmol; **IR (neat):** 2047 (w), 3083 (w), 2985 (w), 1642 (m), 1510 (m), 1147 (s), 830 (s), 735 (m), 583 (m) cm^{-1}; **^{1}H NMR (400 MHz, $CDCl_3$):** δ 7.55 (dd, *J* = 8.4, 5.4 Hz, 2H), 7.06 (dd, *J* = 9.0, 1.9 Hz, 2H), 5.50 (dq, *J* = 16.8, 7.9 Hz, 1H), 5.17–5.05 (m, 2H), 2.88 (dd, *J* = 14.4, 6.6 Hz, 1H), 2.63 (dd, *J* = 14.4, 7.8 Hz, 1H), 1.73 (br, 2H); **^{13}C NMR (100 MHz, $CDCl_3$):** δ 162.6 (d, *J* = 247.6 Hz), 134.3 (d, *J* = 171.1 Hz), 131.0, 128.8 (d, *J* = 8.2 Hz), 126.9 (q, *J* = 285.2 Hz), 120.5, 115.4 (d, *J* = 21.4 Hz), 60.9 (q, *J* = 26.0 Hz), 41.1; **^{19}F NMR (376 MHz, $CDCl_3$):** –78.20 (d, *J* = 13.8 Hz, 3F), –114.48 (s, 1F); **HRMS (DART):** Calcd for $C_{11}H_{12}F_4N$ $[M+H]^+$: 234.0906; Found: 234.0911; **Specific rotation:** $[\alpha]^{24}_D$ = +34.8 (*c* 1.35, $CHCl_3$) for a 86:14 er sample. The enantiomeric purity was determined by HPLC analysis in comparison with authentic racemic material (Chiralpak AD-H, 99:1 hexanes:*i*-PrOH, 0.7 mL/min, 220 nm): t_R: 9.508 min (major) and 12.461 min (minor).

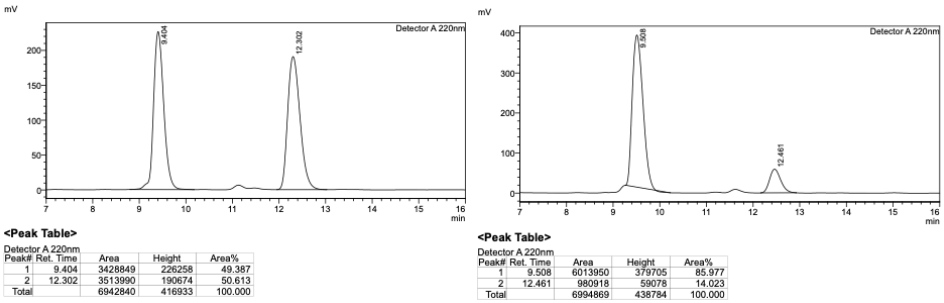

Peak #	Ret. Time (min)	Area %	Peak #	Ret. Time (min)	Area %
1	9.404	49.387	1	9.508	85.977
2	12.302	50.613	2	12.461	14.023

(*R*)-1,1,1-Trifluoro-2-(4-(trifluoromethyl)phenyl)pent-4-en-2-amine (3.28e): Colorless oil, 9.06 mg, 32% yield, 0.032 mmol; **IR (neat):** 2991 (w), 2942 (w), 2849 (w), 2053 (w), 1622 (m), 1325 (s), 1117 (s), 1068 (s), 1019 (s), 839 (m), 579 (w) cm^{-1}; **^{1}H NMR (400 MHz, $CDCl_3$):** δ 7.74 (d, *J* = 8.3 Hz, 2H), 7.69–7.57 (m, 2H), 5.49 (ddd, *J* = 16.9, 9.5, 7.2 Hz, 1H), 5.24–5.05 (m, 2H), 2.91 (dd, *J* = 14.4, 6.8 Hz, 1H), 2.69 (dd, *J* = 14.4, 7.6 Hz, 1H), 1.79 (s, 2H); **^{13}C NMR (100 MHz, $CDCl_3$):** δ 141.8, 135.6, 130.7, 130.1 (q, *J* = 22.7 Hz), 127.6, 125.4 (d, *J* = 4.2 Hz), 124.6 (q, *J* = 274.2 Hz), 120.9, 61.4 (q, *J* = 26.6 Hz), 41.1; **^{19}F NMR (376 MHz, $CDCl_3$):** δ –62.79 (s, 3F), –77.63 (s, 3F); **HRMS (DART):** Calcd for $C_{12}H_{12}F_6N$ $[M+H]^+$: 284.0874; Found: 284.0882; **Specific rotation:** $[\alpha]^{24}_D$ = +26.6 (*c* 0.93, $CHCl_3$) for a 89:11 er sample. The enantiomeric purity was determined by HPLC analysis in comparison with authentic racemic material (Chiralpak AD-H, 99:1 hexanes:*i*PrOH, 0.7 mL/min, 220 nm): t_R: 8.993 min (major) and 13.258 min (minor).

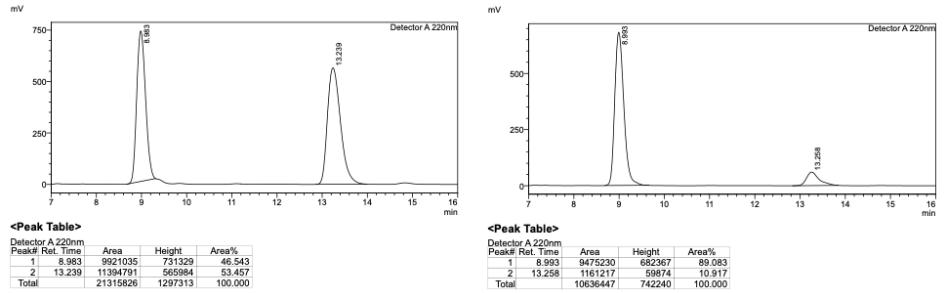

Peak #	Ret. Time (min)	Area %	Peak #	Ret. Time (min)	Area %
1	8.983	46.543	1	8.993	89.083
2	13.239	53.457	2	13.258	10.917

3.7.6. Additions of Other Allyl Boronates to Trifluoromethyl N-H Ketimines

3.7.6.1. With (*Z*)-2-(but-2-en-1-yl)-4,4,5,5-tetramethyl-1,3,2-dioxaborolane

In a N_2-filled glovebox, an oven-dried two-dram vial was charged with a stock solution of aminophenol **ap-6** (3.5 mg, 0.01 mmol), $Zn(OMe)_2$ (2.6 mg, 0.02 mmol), and toluene (0.5 mL). A separate oven-dried two-dram vial equipped with a magnetic stir-bar was charged with ketimine (0.1 mmol), toluene (0.25 mL), and tbat (2.7 mg, 0.005 mmol), followed by the freshly prepared stock solution of the catalyst (0.25 mL) and *(Z)*-crotyl–B(pin) (27 μL, 0.13 mmol) and MeOH (14 μL, 0.35 mmol). The mixture was allowed to stir for five min after which the vial was capped, removed from the glovebox, and the mixture was allowed to stir for 3 h at 22 °C. Conversion and α:γ ratio were determined by spectroscopic analysis (^{19}F NMR) of an aliquot sample. The mixture was loaded onto silica gel and eluted with 100:0 → 3:1 hexanes:Et_2O, resulting in the isolation of α-tertiary amine as colorless oil. Note: In some cases, and as explicitly indicated in the body of the manuscript, yields of isolated products are reported as mixtures of α and γ isomers. The minor γ isomer accounts for the minor signals in the corresponding NMR spectra.

(*R,Z*)-1,1,1-Trifluoro-2-phenylhex-4-en-2-amine (3.30a): Colorless oil, 19.9 mg, 80% yield, 0.080 mmol; **IR (neat):** 2254 (w), 1156 (w), 903 (s), 722 (s), 650 (s), 543 (m) cm^{-1}; **^{1}H NMR (400 MHz, $CDCl_3$):** δ 7.61–7.53 (m, 2H), 7.52–7.31 (m, 3H), 5.60 (m, 1H), 5.25–5.03 (m, 1H), 2.88 (dd, *J* = 14.9, 6.7 Hz, 1H), 2.82–2.63 (m, 1H), 1.77 (s, 2H), 1.62 (ddt, *J* = 6.9, 1.8, 0.9 Hz, 3H); **^{13}C NMR (100 MHz, $CDCl_3$):** δ 137.8, 128.7, 128.4, 128.2, 127.3 (q, *J* = 285.3 Hz), 126.1 (q, *J* = 1.6 Hz), 123.0, 61.6 (q, *J* = 25.8 Hz), 33.6, 13.3; **^{19}F NMR (376 MHz, $CDCl_3$):** –77.9 (s, 3F); **HRMS (DART):** Calcd for $C_{12}H_{15}NF_3$ $[M+H]^+$: 230.1151; Found: 230.1156; **Specific rotation:** $[\alpha]^{24}_D$ = –6.1 (*c* 1.40, $CHCl_3$) for a 97:3 er sample; The enantiomeric purity was determined by HPLC analysis in comparison with authentic racemic material (Chiralpak AD-H, 99:1 hexanes:*i*PrOH, 0.7 mL/min, 220 nm): t_R: 10.631 min (major) and 11.843 min (minor).

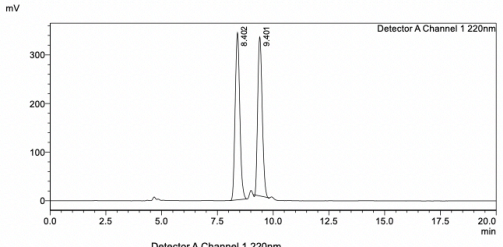

Detector A Channel 1 220nm

Peak#	Ret. Time	Area	Area%
1	8.402	4979793	51.910
2	9.401	4613273	48.090
Total		9593065	100.000

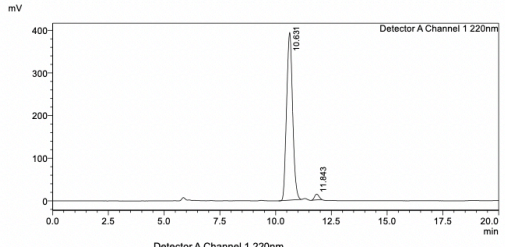

Detector A Channel 1 220nm

Peak#	Ret. Time	Area	Area%
1	10.631	7386910	97.547
2	11.843	185720	2.453
Total		7572630	100.000

Peak #	Ret. Time (min)	Area %	Peak #	Ret. Time (min)	Area %
1	8.402	51.910	1	10.631	97.547
2	9.401	48.090	2	11.843	2.453

(*R,Z*)-1,1,1-Trifluoro-2-(4-fluorophenyl)hex-4-en-2-amine (3.30b): Colorless oil, 16.8 mg, 68% yield, 0.068 mmol; **IR (neat):** 2924 (w), 1606 (m), 1511 (s), 1237 (m), 1145 (s), 831 (s), 737 (m) cm^{-1}; **^{1}H NMR (400 MHz, $CDCl_3$):** δ 7.62–7.45 (m, 2H), 7.17–6.98 (m, 2H), 5.72–5.54 (m, 1H), 5.25–5.07 (m, 1H), 2.84 (dd, *J* = 15.0, 6.9 Hz, 1H), 2.70 (dd, *J* = 15.0, 7.6 Hz, 1H), 1.74 (s, 2H), 1.61 (ddt, *J* = 6.8, 1.9, 0.9 Hz, 3H); **^{13}C NMR (100 MHz, $CDCl_3$):** δ 162.6 (d, *J* = 247.5 Hz), 133.6 (d, *J* = 3.2 Hz), 129.0, 128.9, 127.2 (q, *J* = 285.2 Hz), 122.7, 115.3 (d, *J* = 21.3 Hz), 61.4 (q, *J* = 25.9 Hz), 33.7, 13.2; **^{19}F NMR (376 MHz, $CDCl_3$):** δ –78.2 (s, 3F), –114.6 (s, 1F); **HRMS (DART):** Calcd for $C_{12}H_{14}NF_4$ $[M+H]^+$: 248.1057; Found: 248.1064; **Specific rotation:** $[\alpha]^{25.1}_D$ +14.6 (*c* 0.77, $CHCl_3$) for a 97:3 er sample. Enantiomeric purity was determined by HPLC analysis in comparison with authentic racemic material (Chiralpak AD-H, 99:1 hexanes:*i*PrOH, 0.7 mL/min, 220 nm): t_R: 12.251 min (major) and 15.020 min (minor).

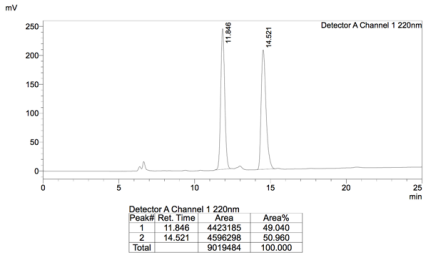

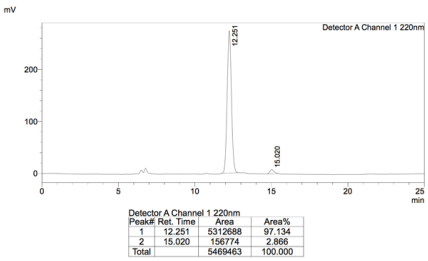

Peak #	Ret. Time (min)	Area %	Peak #	Ret. Time (min)	Area %
1	11.846	49.040	1	12.251	97.134
2	14.521	50.960	2	15.020	2.866

(*R,Z*)-2-(4-Bromophenyl)-1,1,1-trifluorohex-4-en-2-amine (3.30c): Colorless oil, 20.6 mg, 67% yield, 0.067 mmol; **IR (neat):** 3026 (w), 1591 (m), 1490 (m), 1250 (m), 1137 (s), 1010 (m), 818 (m), 751 (m) cm^{-1}; **^{1}H NMR (400 MHz, $CDCl_3$):** δ 7.54–7.48 (m, 2H), 7.48–7.43 (m, 2H), 5.61 (m, 1H), 5.24–4.99 (m, 1H), 2.83 (dd, *J* = 15.0, 6.9 Hz, 1H), 2.79–2.61 (m, 1H), 1.73 (s, 2H), 1.61 (ddt, *J* = 6.8, 1.8, 0.9 Hz, 3H).; **^{13}C NMR (100 MHz, $CDCl_3$):** δ 137.0, 131.6, 129.1, 129.0 (q, *J* = 1.5 Hz), 127.01 (q, *J* = 285.4 Hz), 122.6, 122.5, 61.6 (q, *J* = 26.0 Hz), 33.6, 13.3; **^{19}F NMR (376 MHz, $CDCl_3$):** δ –78.0 (s, 3F); **HRMS (DART):** Calcd for $C_{12}H_{14}NF_3Br$ $[M+H]^+$: 308.0256; Found: 308.0252; **Specific rotation:** $[\alpha]^{25.2}_D$ +31.0 (*c* 1.3, $CHCl_3$) for a 98:2 er sample. Enantiomeric purity was determined by HPLC analysis in comparison with authentic racemic material (Chiralpak AD-H, 99:1 hexanes:*i*PrOH, 0.7 mL/min, 220 nm): t_R: 13.500 min (major) and 18.184 min (minor).

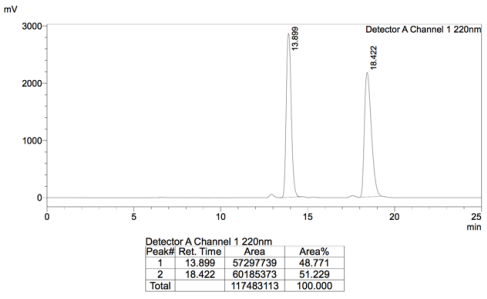

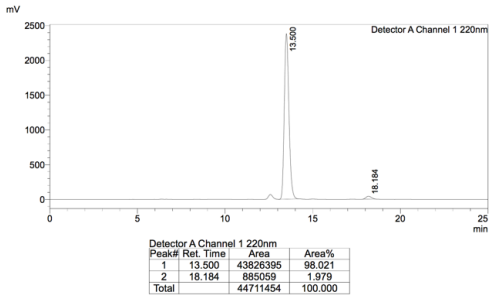

Peak #	Ret. Time (min)	Area %	Peak #	Ret. Time (min)	Area %
1	13.809	48.771	1	13.500	98.021
2	18.422	51.229	2	18.184	1.979

(*R*,*Z*)-2-(4-Chlorophenyl)-1,1,1-trifluorohex-4-en-2-amine (3.30d): Colorless oil, 22.9 mg, 87% yield, 0.087 mmol; **IR (neat):** 3397 (w), 3025 (w), 2925 (w), 1597 (m), 1493 (m), 1525 (m), 1148 (s), 1096 (s), 820 (m), 692 (m) cm^{-1}; **^{1}H NMR (400 MHz, $CDCl_3$):** δ 7.52 (d, *J* = 8.4 Hz, 2H), 7.35 (d, *J* = 8.7 Hz, 2H), 5.61 (m, 1H), 5.14 (m, 1H), 2.83 (dd, *J* = 15.0, 6.9 Hz, 1H), 2.70 (dd, *J* = 14.9, 7.6 Hz, 1H), 1.72 (s, 2H), 1.61 (ddt, *J* = 6.9, 2.0, 1.0 Hz, 3H); **^{13}C NMR (100 MHz, $CDCl_3$):** δ 136.4, 134.3, 129.0, 128.6, 128.6, 127.1 (q, *J* = 143.5 Hz), 122.5, 61.5 (q, *J* = 26.3Hz), 33.7, 13.3; **^{19}F NMR (376 MHz, $CDCl_3$):** δ –78.0 (s, 3F); **HRMS (DART):** Calcd for $C_{12}H_{14}NF_3Cl$ $[M+H]^+$: 264.0761; Found: 264.0760; **Specific rotation:** $[\alpha]^{24.3}_D$ +18.9 (*c* 2.1, $CHCl_3$) for a 96:4 er sample. Enantiomeric purity was determined by HPLC analysis in comparison with authentic racemic material (Chiralpak AS-H, 98:2 hexanes:*i*PrOH, 0.5 mL/min, 220 nm): t_R: 17.953 min (major) and 23.319 min (minor).

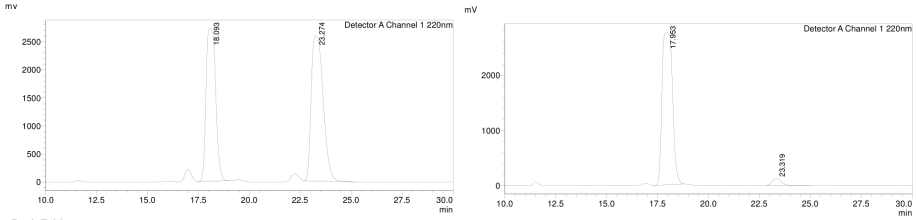

<Peak Table>
Detector A Channel 1 220nm

Peak#	Ret. Time	Area	Height	Area%
1	18.093	88995742	2718014	45.821
2	23.274	105231015	2594724	54.179
Total		194226757	5312738	100.000

<Peak Table>
Detector A Channel 1 220nm

Peak#	Ret. Time	Area	Height	Area%
1	17.953	97749502	2764486	95.991
2	23.319	4082876	127681	4.009
Total		101832378	2892167	100.000

Peak #	Ret. Time (min)	Area %	Peak #	Ret. Time (min)	Area %
1	18.093	45.821	1	17.953	95.991
2	23.274	54.179	2	23.319	4.009

(*R*,*Z*)-1,1,1-Trifluoro-2-(*p*-tolyl)hex-4-en-2-amine (3.30e): Clear oil, 17.2 mg, 71% yield, 0.071 mmol; **IR (neat):** 3397 (w), 3025 (w), 2924 (w), 1616 (w), 1514 (w), 1523 (m), 1150 (s), 812 (m), 651 (m) cm^{-1}; **^{1}H NMR (400 MHz, $CDCl_3$):** δ 7.45 (d, *J* = 8.0 Hz, 2H), 7.18 (s, 2H), 5.67–5.52 (m, 1H), 5.15 (q, *J* = 8.2 Hz, 1H), 2.79 (ddd, *J* = 59.5, 15.0, 7.2 Hz, 2H), 2.35 (s, 3H), 1.69 (s, 1H), 1.65–1.60 (m, 1H); **^{13}C NMR (100 MHz, $CDCl_3$):** δ 137.97, 134.74, 129.15, 128.63, 126.95, 127.26 (q, *J* = 143.1 Hz), 123.08, 61.55 (q, *J* = 26.3 Hz), 33.53, 21.13, 13.30; **^{19}F NMR (376 MHz, $CDCl_3$):** –77.9 (s, 3F); **HRMS (DART):** Calcd for $C_{13}H_{17}NF_3$ $[M+H]^+$: 244.1308; Found: 244.1303; **Specific rotation:** $[\alpha]^{24.3}_D$ +7.5 (*c* = 1.1, $CHCl_3$) for a 96:4 er sample. Enantiomeric purity was determined by HPLC analysis in comparison with authentic racemic material (Chiralpak OJ-H, 97:3 hexanes:*i*PrOH, 0.5 mL/min, 220 nm): t_R: 16.653 min (major) and 18.860 min (minor).

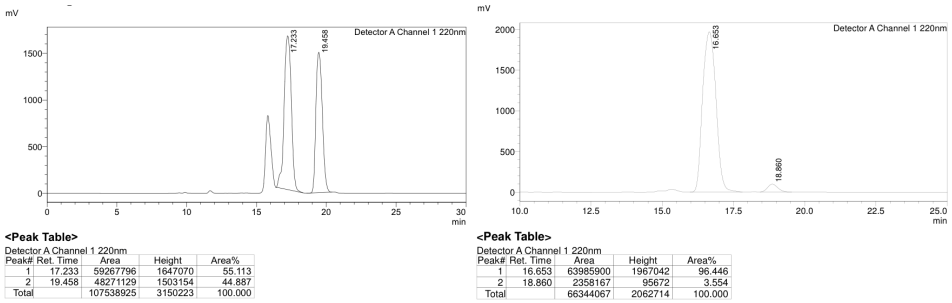

<Peak Table>
Detector A Channel 1 220nm

Peak#	Ret. Time	Area	Height	Area%
1	17.233	59267796	1647070	55.113
2	19.458	48271129	1503154	44.887
Total		107538925	3150223	100.000

<Peak Table>
Detector A Channel 1 220nm

Peak#	Ret. Time	Area	Height	Area%
1	16.653	63985900	1967042	96.446
2	18.860	2358167	95672	3.554
Total		66344067	2062714	100.000

Peak #	Ret. Time (min)	Area %	Peak #	Ret. Time (min)	Area %
1	17.233	55.113	1	16.653	96.446
2	19.458	44.887	2	18.860	3.554

(*R*,*Z*)-1,1,1-Trifluoro-2-(4-(trifluoromethyl)phenyl)hex-4-en-2-amine (3.30f): Colorless oil, 18.1 mg, 61% yield, 0.061 mmol; **IR (neat):** 2939 (w), 1622 (m), 1325 (s), 1152 (s), 1070 (s), 1018 (m), 834 (m), 733 (m) cm^{-1}; **^{1}H NMR (400 MHz, $CDCl_3$):** δ 7.82–7.69 (m, 2H), 7.64 (d, *J* = 8.3 Hz, 2H), 5.62 (m, 1H), 5.22–5.07 (m, 1H), 2.87 (dd, *J* = 15.0, 7.0 Hz, 1H), 2.73 (dd, *J* = 15.1, 7.5 Hz, 1H), 1.77 (s, 2H), 1.61 (ddt, *J* = 6.9, 1.9, 0.9 Hz, 3H); **^{13}C NMR (100 MHz, $CDCl_3$):** δ 142.0, 130.5 (q, *J* = 32.6 Hz), 129.3, 127.6 (q, *J* = 1.7 Hz), 127.0, 125.4 (q, *J* = 3.8 Hz), 124.1, 122.3 (q, *J* = 274 Hz), 61.9 (q, *J* = 26.1 Hz), 33.8, 13.3; **^{19}F NMR (376 MHz, $CDCl_3$):** δ –62.8 (s, 3F), –77.7 (s, 3F); **HRMS (DART):** Calcd for $C_{13}H_{14}NF_6$ $[M+H]^+$: 298.1025; Found: 298.1035; **Specific rotation:** $[\alpha]^{26.0}_D$ +19.9 (*c* 1.5, $CHCl_3$) for a 97.5:2.5 er sample. Enantiomeric purity was determined by HPLC analysis in comparison with authentic racemic material (Chiralpak AD-H, 99:1 hexanes:*i*PrOH, 0.7 mL/min, 220 nm): t_R: 11.572 min (major) and 14.955 min (minor).

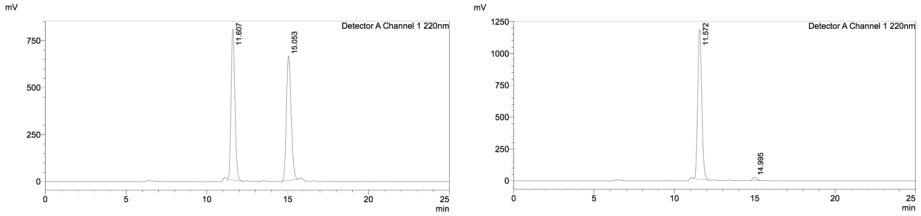

Detector A Channel 1 220nm

Peak#	Ret. Time	Area	Area%
1	11.607	13222387	49.194
2	15.053	13655692	50.806
Total		26878079	100.000

Detector A Channel 1 220nm

Peak#	Ret. Time	Area	Area%
1	11.572	20621210	97.672
2	14.995	491469	2.328
Total		21112680	100.000

Peak #	Ret. Time (min)	Area %	Peak #	Ret. Time (min)	Area %
1	11.607	49.194	1	11.572	97.672
2	15.053	50.806	2	14.995	2.328

(*R*,*Z*)-1,1,1-Trifluoro-2-(4-methoxyphenyl)hex-4-en-2-amine (3.30g): Colorless oil, 20.2 mg, 78% yield, 0.078 mmol; **IR (neat):** 2937 (w), 2839 (w), 1612 (m), 1515 (s), 1254 (s), 1149 (s), 1035 (m), 829 (m) cm^{-1}; **^{1}H NMR (400 MHz, $CDCl_3$):** δ 7.58–7.38 (m, 2H), 7.03–6.81 (m, 2H), 5.74–5.49 (m, 1H), 5.27–5.07 (m, 1H), 3.81 (s, 3H), 2.85 (dd, *J* = 15.0, 6.7 Hz, 1H), 2.70 (dd, *J* = 14.9, 7.7 Hz, 1H), 1.72 (s, 2H), 1.63 (ddt, *J* = 6.9, 1.9, 0.9 Hz, 3H); **^{13}C NMR (100 MHz, $CDCl_3$):** δ 159.4, 129.7 (br), 128.6, 128.4 (q, *J* = 1.3 Hz), 127.3 (q, *J* = 285 Hz), 123.1, 113.7, 61.2 (q, *J* =

26.0 Hz), 53.4, 35.6, 13.3; **^{19}F NMR (376 MHz, $CDCl_3$):** δ –78.4 (s, 3F); **HRMS (DART):** Calcd for $C_{13}H_{17}NOF_3$ $[M+H]^+$: 260.1257; Found: 260.1261; **Specific rotation:** $[\alpha]^{24.2}_D$ +23.6 (*c* 1.3, $CHCl_3$) for a 98:2 er sample. Enantiomeric purity was determined by HPLC analysis in comparison with authentic racemic material (Chiralpak AD-H, 99:1 hexanes:*i*PrOH, 0.7 mL/min, 220 nm): t_R: 16.220 min (major) and 19.445 min (minor).

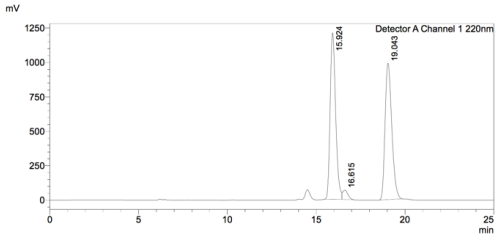

Detector A Channel 1 220nm

Peak#	Ret. Time	Area	Area%
1	15.924	26050564	48.768
2	16.615	1376459	2.577
3	19.043	25990583	48.655
Total		53417607	100.000

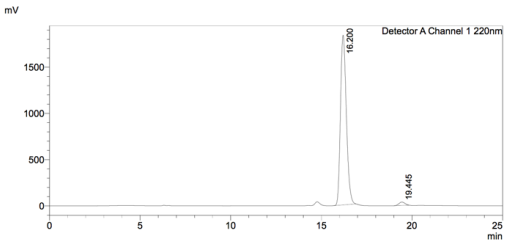

Detector A Channel 1 220nm

Peak#	Ret. Time	Area	Area%
1	16.200	41331980	97.996
2	19.445	845435	2.004
Total		42177414	100.000

Peak #	Ret. Time (min)	Area %	Peak #	Ret. Time (min)	Area %
1	15.924	48.768	1	16.200	97.996
2	19.043	48.655	2	19.445	2.004

(*R*,*Z*)-4-(2-Amino-1,1,1-trifluorohex-4-en-2-yl)-*N*,*N*-dimethylaniline (3.30h): Pale yellow oil, 13.6 mg, 50% yield, 0.050 mmol; **IR (neat):** 2890 (w), 1614 (m), 1523 (m), 1355 (m), 1139 (s), 947 (m), 909 (m), 813 (m), 734 (m) cm^{-1}; **^{1}H NMR (400 MHz, $CDCl_3$):** δ 7.52–7.25 (m, 2H), 6.71 (d, *J* = 9.0 Hz, 2H), 5.74–5.46 (m, 1H), 5.34–4.99 (m, 1H), 2.96 (s, 6H), 2.90–2.77 (m, 1H), 2.70 (dddd, *J* = 14.9, 7.8, 1.6, 0.8 Hz, 1H), 1.71 (s, 2H), 1.64 (dt, *J* = 6.9, 1.0 Hz, 3H); **^{13}C NMR (100 MHz, $CDCl_3$):** δ 150.0, 128.2, 127.7, 127.3 (q, *J* = 285 Hz), 124.7, 123.3, 111.8, 60.9 (q, *J* = 25.7 Hz), 40.3, 33.2, 13.2; **^{19}F NMR (376 MHz, $CDCl_3$):** δ –78.6 (s, 3F); **HRMS (DART):** Calcd for $C_{14}H_{20}N_2F_3$ $[M+H]^+$: 273.1573; Found: 273.1580; **Specific rotation:** $[\alpha]^{24.2}_D$ +23.6 (*c* 1.3, $CHCl_3$) for a 96.5:3.5 er sample. Enantiomeric purity was determined by HPLC analysis in comparison with authentic racemic material (Chiralpak AD-H, 99:1 hexanes:*i*PrOH, 0.7 mL/min, 220 nm): t_R: 13.506 min (major) and 14.847 min (minor).

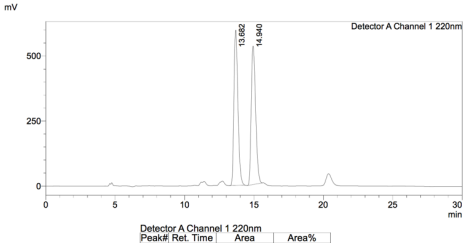

Detector A Channel 1 220nm

Peak#	Ret. Time	Area	Area%
1	13.682	11707795	50.335
2	14.940	11552163	49.665
Total		23259958	100.000

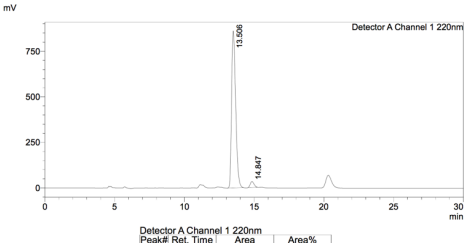

Detector A Channel 1 220nm

Peak#	Ret. Time	Area	Area%
1	13.506	17315969	96.559
2	14.847	617070	3.441
Total		17933040	100.000

Peak #	Ret. Time (min)	Area %	Peak #	Ret. Time (min)	Area %
1	13.682	50.335	1	13.506	96.559
2	14.940	49.665	2	14.847	3.441

(*R*,*Z*)-1,1,1-Trifluoro-2-(2-methoxyphenyl)hex-4-en-2-amine (3.30i): Colorless oil, 18.1 mg, 70% yield, 0.070 mmol; **IR (neat):** 2941 (w, br), 1601 (w), 1492 (m), 1244 (m), 1218 (s), 1026 (m) cm^{-1}; **^{1}H NMR (400 MHz, $CDCl_3$):** δ 7.51 (td, *J* = 8.1, 1.8 Hz, 1H), 7.34 (dddd, *J* = 8.1, 7.3, 4.8, 1.7 Hz, 1H), 7.17 (td, *J* = 7.7, 1.3 Hz, 1H), 7.07 (m, 1H), 5.69–5.55 (m, 1H), 5.23 (m, 1H), 3.86 (s, 3H), 3.29–3.12 (m, 1H), 2.78–2.57 (m, 1H), 2.00 (s, 2H), 1.76–1.58 (m, 3H)**; ^{13}C NMR (100 MHz, $CDCl_3$):** δ 159.2, 130.3, 129.9, 127.4 (q, *J* = 286.8 Hz), 127.9, 124.7, 124.2, 120.7, 112.7, 62.6 (q, *J* = 26.6 Hz), 55.8, 32.3, 13.4; **^{19}F NMR (376 MHz, $CDCl_3$):** δ –78.5 (s, 3F); **HRMS (DART):** Calcd for $C_{12}H_{14}NF_4$ $[M+H]^+$: 248.1057; Found: 248.1068; **Specific rotation:** $[\alpha]^{24.8}_D$ –4.2 (*c* 1.6, $CHCl_3$) for a 99:1 er sample. Enantiomeric purity was determined by HPLC analysis in comparison with authentic racemic material (Chiralpak AD-H, 99:1 hexanes:*i*PrOH, 0.7 mL/min, 220 nm): t_R: 12.692 min (major) and 14.106 min (minor).

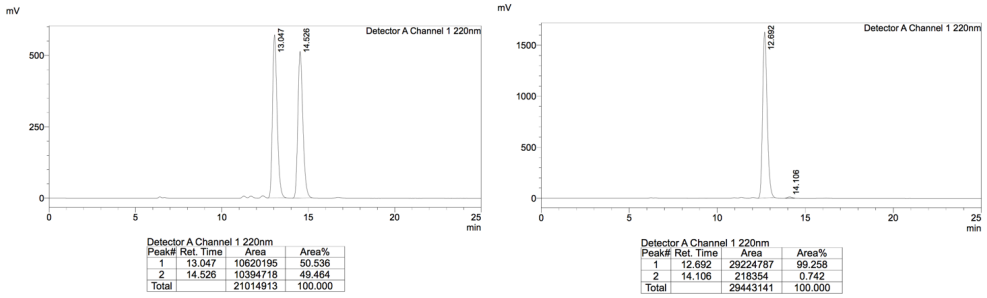

Peak #	Ret. Time (min)	Area %	Peak #	Ret. Time (min)	Area %
1	13.047	50.536	1	12.692	99.258
2	14.536	49.464	2	14.106	0.742

(*R*,*Z*)-1,1,1-Trifluoro-2-(2-fluorophenyl)hex-4-en-2-amine (3.30j): Colorless oil, 22.0 mg, 89% yield, 0.089 mmol; **IR (neat):** 3030 (w), 2158 (w), 1614 (m), 1489 (m), 1445 (m), 1221 (s), 1151 (s), 759 (s) cm^{-1}; **^{1}H NMR (400 MHz, $CDCl_3$):** δ 7.51 (td, *J* = 8.1, 1.8 Hz, 1H), 7.34 (dddd, *J* = 8.1, 7.3, 4.8, 1.7 Hz, 1H), 7.17 (td, *J* = 7.7, 1.3 Hz, 1H), 7.07 (ddd, *J* = 13.0, 8.2, 1.3 Hz, 1H), 5.69–5.55 (m, 1H), 5.23 (m, 1H), 3.29–3.12 (m, 1H), 2.78–2.57 (m, 1H), 2.00 (s, 2H), 1.76–1.58 (m, 3H); **^{13}C NMR (100 MHz, $CDCl_3$):** δ 161.6 (d, *J* = 249.5 Hz), 138.0 (d, *J* = 74.0 Hz), 130.6 (d, *J* = 9.3 Hz), 130.2 (d, *J* = 3.8 Hz), 128.8, 126.9 (q, *J* = 286.1 Hz), 124.2 (d, *J* = 3.4 Hz), 123.1, 117.0 (d, *J* = 25.4 Hz), 61.6 (q, *J* = 26.7 Hz), 32.0 (d, *J* = 5.7 Hz), 13.3; **^{19}F NMR (376 MHz, $CDCl_3$):** δ –79.2 (d, *J* = 15.0 Hz, 3F), –108.7 (ddt, *J* = 26.5, 18.5, 9.4 Hz, 1F); **HRMS (DART):** Calcd for $C_{12}H_{14}NF_4$ $[M+H]^+$: 248.1057; Found: 248.1068; **Specific rotation:** $[\alpha]^{24.0}_D$ +16.0 (*c* 1.4, $CHCl_3$) for a 98.5:1.5 er sample. Enantiomeric purity was determined by HPLC analysis of the derived chloroacetamide in comparison with authentic racemic material (Chiralpak AD-H, 99:1 hexanes:*i*PrOH, 0.7 mL/min, 220 nm): t_R: 13.658 min (minor) and 15.671 min (major).

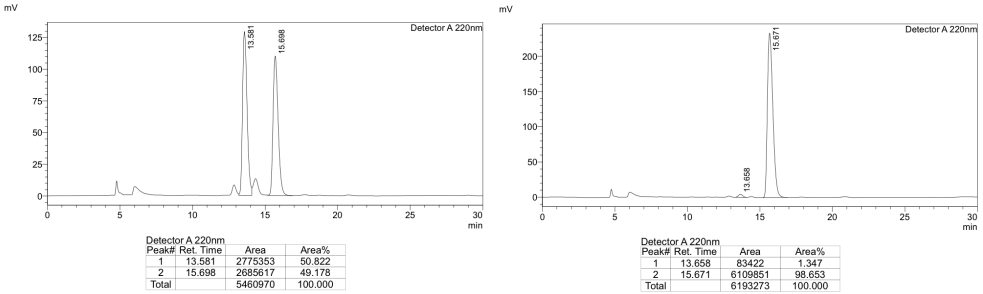

Peak #	Ret. Time (min)	Area %	Peak #	Ret. Time (min)	Area %
1	13.581	50.822	1	13.658	1.347
2	15.698	49.178	2	15.671	98.563

(*R,Z*)-2-(2-Chlorophenyl)-1,1,1-trifluorohex-4-en-2-amine (3.30k): Colorless oil, 20.8 mg, 79% yield, 0.079 mmol; **IR (neat):** 2981 (w), 2160 (w), 1429 (m), 1245 (m), 1153 (s), 1042 (m), 755 (m) cm^{-1}; **^{1}H NMR (400 MHz, $CDCl_3$):** δ 7.75–7.48 (m, 1H), 7.47–7.36 (m, 1H), 7.32–7.23 (m, 2H), 5.62 (m, 1H), 5.39–5.15 (m, 1H), 3.39 (ddt, *J* = 15.6, 6.5, 1.5 Hz, 1H), 2.93–2.69 (m, 1H), 2.24 (s, 2H), 1.69 (ddt, *J* = 6.8, 1.9, 1.0 Hz, 3H); **^{13}C NMR (100 MHz, $CDCl_3$):** δ 137.6, 134.2, 132.6, 131.1 (q, *J* = 1.5 Hz), 130.48 (q, *J* = 156.6 Hz), 129.5, 128.6, 126.7, 123.1, 63.3 (q, *J* = 26.6 Hz), 32.6, 13.2; **^{19}F NMR (376 MHz, $CDCl_3$):** δ –76.8 (s, 3F); **HRMS (DART):** Calcd for $C_{12}H_{14}NF_3Cl$ $[M+H]^+$: 264.0761; Found: 264.0770; **Specific rotation:** $[\alpha]^{24.9}_D$ +7.4 (*c* 1.2, $CHCl_3$) for a 96.5:3.5 er sample. Enantiomeric purity was determined by HPLC analysis in comparison with authentic racemic material (Chiralcel OJ-H, 99:1 hexanes:*i*PrOH, 0.7 mL/min, 220 nm): t_R: 10.447 min (minor) and 10.963 min (major).

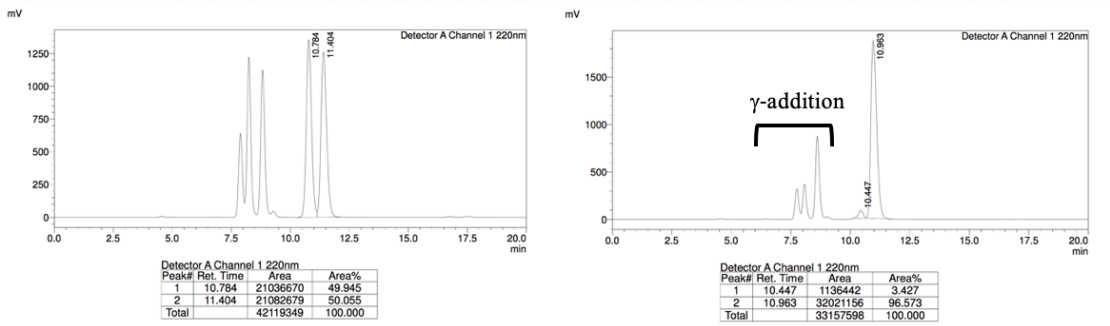

Peak #	Ret. Time (min)	Area %	Peak #	Ret. Time (min)	Area %
1	10.784	49.945	1	10.447	3.427
2	11.404	50.055	2	10.963	96.573

(*Z*)-2-(2-Bromophenyl)-1,1,1-trifluorohex-4-en-2-amine (3.30l): Clear oil, 16.3 mg, 53% yield, 0.053 mmol; **IR (neat):** 2984 (w,), 1621 (w), 1464 (m), 1424 (m), 1244 (m), 1155 (s), 1019 (m), 755 (m) cm^{-1}; **^{1}H NMR (400 MHz, $CDCl_3$):** δ 7.78 (d, *J* = 8.0 Hz, 1H), 7.67 7.66f (m, 1H), 7.64–7.60 (m, 1H), 7.33 (dtd, *J* = 8.6, 7.3, 1.4 Hz, 2H), 7.16 (m, 1H, peaks overlapped with γ-addition product), 5.75–5.56 (m, 1H), 5.34–5.17 (m, 1H, peaks overlapped with γ-addition product),), 3.38 (dd, *J* = 15.7, 6.5 Hz, 1H), 2.84 (dd, *J* = 15.7, 7.4 Hz, 1H), 2.29 (s, 2H), 1.69 (ddt, *J* = 6.9, 2.0, 1.0

Hz, 3H)**; ^{13}C NMR (100 MHz, $CDCl_3$):** δ 137.8, 136.7, 131.5 (q, *J* = 1.9 Hz), 129.8, 128.7, 127.1 (q, *J* = 285 Hz), 127.3, 123.3, 117.7, 63.8 (q, *J* = 26.3 Hz), 32.9 (q, *J* =1.3 Hz), 13.4; **^{19}F NMR (376 MHz, $CDCl_3$):** –76.1 (s, 3F), –106.2 (m, 2F); **HRMS (DART):** Calcd for $C_{12}H_{14}NF_3Br$ $[M+H]^+$: 308.0256; Found: 308.0248; **Specific rotation:** $[\alpha]^{24.6}_D$ +1.5 (*c* = 1.1, $CHCl_3$) for a 97:3 er sample. Enantiomeric purity was determined by HPLC analysis in comparison with authentic racemic material (Chiralcel OZ-H, 99:1 hexanes:*i*PrOH, 0.7 mL/min, 220 nm): t_R: 6.278 min (major) and 6.584 min (minor).

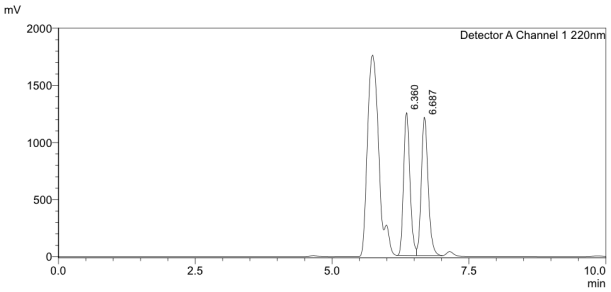

<Peak Table>
Detector A Channel 1 220nm

Peak#	Ret. Time	Area	Area%	Height
1	6.360	9995624	48.648	1250476
2	6.687	10551083	51.352	1209830
Total		20546707	100.000	2460306

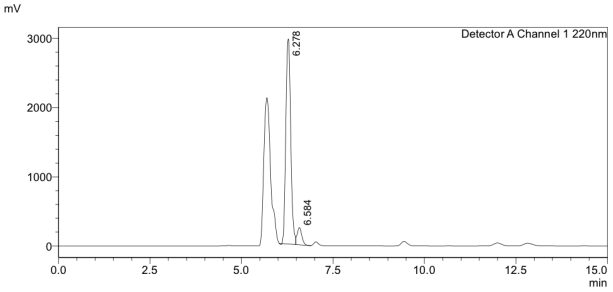

<Peak Table>
Detector A Channel 1 220nm

Peak#	Ret. Time	Area	Area%	Height
1	6.278	27681317	92.634	2963272
2	6.584	2201194	7.366	248668
Total		29882511	100.000	3211939

Peak #	Ret. Time (min)	Area %	Peak #	Ret. Time (min)	Area %
1	6.360	48.648	1	6.278	92.634
2	6.687	51.352	2	6.584	7.366

(*R*,*Z*)-1,1,1-Trifluoro-2-(*o*-tolyl)hex-4-en-2-amine (3.30m): Colorless oil, 12.7 mg, 52% yield, 0.052 mmol; **IR (neat):** 3315 (w, br), 2956 (w), 1762 (m), 1449 (m), 1239 (s), 1151 (s), 989 (m), 676 (s), 623 (s), 573 (w) cm^{-1}; **^{1}H NMR (400 MHz, $CDCl_3$):** δ 7.50 (m, 1H), 7.24–7.13 (m, 3H), 5.75–5.46 (m, 1H), 5.33–5.06 (m, 1H, overlapped with γ-addition product), 3.16 (dd, *J* = 15.8, 6.4 Hz, 1H), 2.70 (dd, *J* = 15.7, 7.5 Hz, 1H), 2.64 (s, 3H), 1.81 (s, 2H, overlapped with γ-addition product), 1.68 (m, 3H); **^{13}C NMR (100 MHz, $CDCl_3$):** δ 138.2, 135.1, 133.7, 129.5, 128.5, 128.3, 127.6 (q, *J* = 286.1 Hz), 125.9, 123.6, 63.6 (q, *J* = 25.8 Hz), 34.0, 23.7, 13.4; **^{19}F NMR (376 MHz, $CDCl_3$):** δ –77.4 (s, 3F); **HRMS (DART):** Calcd for $C_{13}H_{17}NF_3$ $[M+H]^+$: 244.1308; Found: 244.1319; **Specific rotation:** $[\alpha]^{26.0}_D$ +29.5 (*c* 1.48, $CHCl_3$) for a 95.5:4.5 er sample. Enantiomeric purity was determined by HPLC analysis in comparison with authentic racemic material (Chiralcel OJ-H, 99:1 hexanes:*i*PrOH, 0.7 mL/min, 220 nm): t_R: 11.463 min (major) and 12.557 min (minor).

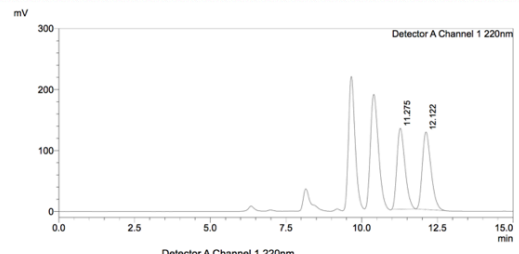

Detector A Channel 1 220nm

Peak#	Ret. Time	Area	Area%
1	11.275	2473974	49.404
2	12.122	2533673	50.596
Total		5007647	100.000

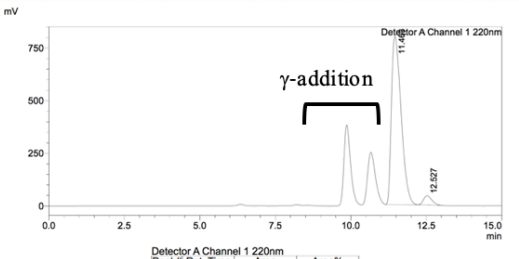

Detector A Channel 1 220nm

Peak#	Ret. Time	Area	Area%
1	11.463	17780260	95.445
2	12.527	848456	4.555
Total		18628716	100.000

Peak #	Ret. Time (min)	Area %	Peak #	Ret. Time (min)	Area %
1	11.275	49.404	1	11.463	95.445
2	12.122	50.596	2	12.527	4.555

(*R,Z*)-2-(3-Chlorophenyl)-1,1,1-trifluorohex-4-en-2-amine (3.30n): Colorless oil, 23.7 mg, 90% yield, 0.090 mmol; **IR (neat):** 2232 (w), 2032 (w), 1573 (m), 1251 (m), 1141 (s), 780 (s), 700 (s) cm^{-1}; **^{1}H NMR (400 MHz, $CDCl_3$):** δ 7.60 (m, 1H), 7.47 (m, 1H), 7.36–7.29 (m, 2H), 5.78–5.41 (m, 1H), 5.22–4.94 (m, 1H), 2.83 (dd, *J* = 14.9, 7.0 Hz, 1H), 2.71 (dddd, *J* = 14.9, 7.7, 1.7, 0.9 Hz, 1H), 1.74 (s, 2H), 1.67–1.49 (m, 3H); **^{13}C NMR (100 MHz, $CDCl_3$):** δ 139.9, 134.4, 129.5, 129.0, 128.3, 127.4 (q, *J* = 1.4 Hz), 126.8 (q, *J* = 285.5 Hz), 125.1 (q, *J* = 1.8 Hz), 122.3, 61.6 (q, *J* = 26.0 Hz), 33.5, 13.1; **^{19}F NMR (376 MHz, $CDCl_3$):** δ –77.8 (s, 3F); **HRMS (DART):** Calcd for $C_{12}H_{14}NF_3Cl$ $[M+H]^+$: 264.0761; Found: 264.0770; **Specific rotation:** $[\alpha]^{24.9}_D$ +25.6 (*c* 1.2, $CHCl_3$) for a 96.5:3.5 er sample. Enantiomeric purity was determined by HPLC analysis in comparison with authentic racemic material (Chiralcel OZ-H, 99:1 hexanes:*i*PrOH, 0.7 mL/min, 220 nm): t_R: 7.991 min (major) and 8.728 min (minor).

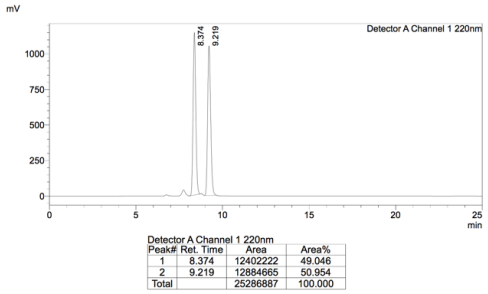

Detector A Channel 1 220nm

Peak#	Ret. Time	Area	Area%
1	8.374	12402222	49.046
2	9.219	12884665	50.954
Total		25286887	100.000

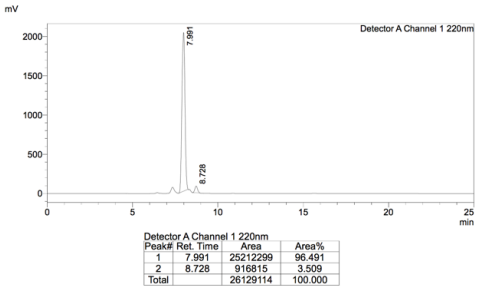

Detector A Channel 1 220nm

Peak#	Ret. Time	Area	Area%
1	7.991	25212299	96.491
2	8.728	916815	3.509
Total		26129114	100.000

Peak #	Ret. Time (min)	Area %	Peak #	Ret. Time (min)	Area %
1	8.374	49.046	1	7.991	96.491
2	9.219	50.954	2	8.728	3.509

(*R,Z*)-1,1,1-Trifluoro-2-(3-(trifluoromethyl)phenyl)hex-4-en-2-amine (3.30o): Colorless oil, 24.4 mg, 82% yield, 0.082 mmol; **IR (neat):** 2926 (w), 1617 (m), 1444 (m), 1329 (s), 1129 (s), 1079 (m), 802 (m), 703 (m) cm^{-1}; **^{1}H NMR (400 MHz, $CDCl_3$):** δ 7.61 (m, 1H), 7.50–7.42 (m, 1H), 7.38–7.27 (m, 2H), 5.74–5.51 (m, 1H), 5.27–4.97 (m, 1H), 2.83 (dd, *J* = 14.9, 7.0 Hz, 1H), 2.71 (dddd, *J* = 14.9, 7.7, 1.7, 0.9 Hz, 1H), 1.74 (s, 2H), 1.69–1.45 (m, 3H); **^{13}C NMR (100 MHz, $CDCl_3$):** δ 139.1, 130.9 (q, *J* = 32.1 Hz), 130.6 (m), 129.3, 128.9, 126.9 (q, *J* = 269.2 Hz), 125.2 (q, *J* = 3.8 Hz), 124.2 (q, *J* = 272.3 Hz), 124.1 (m), 122.2, 61.8 (q, *J* = 26.0 Hz), 33.8 (q, *J* =1.4 Hz), 13.2; **^{19}F NMR (376 MHz, $CDCl_3$):** δ –62.6 (s, 3F), –77.8 (s, 3F); **HRMS (DART):** Calcd for $C_{13}H_{14}NF_6$ $[M+H]^+$: 298.1025; Found: 298.1038; **Specific rotation:** $[\alpha]^{24.3}_D$ +20.9 (*c* 1.4, $CHCl_3$) for a 98:2 er sample. Enantiomeric purity was determined by HPLC analysis in comparison with authentic racemic material (Chiralpak OZ-H, 99:1 hexanes:*i*PrOH, 0.7 mL/min, 220 nm): t_R: 7.816 min (major) and 8.668 min (minor).

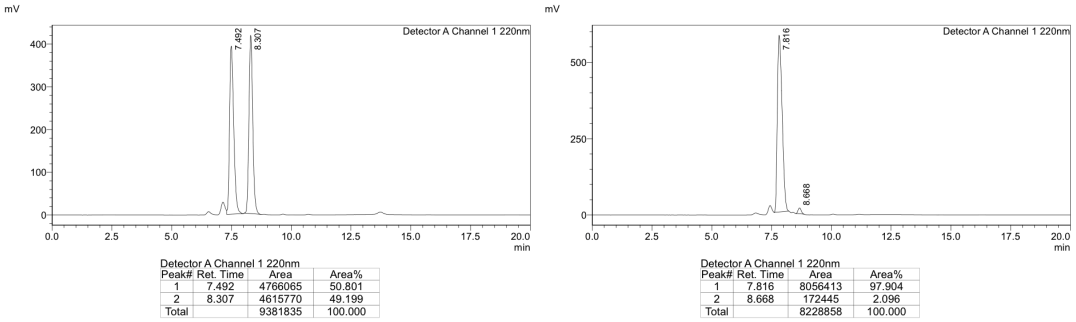

Peak #	Ret. Time (min)	Area %	Peak #	Ret. Time (min)	Area %
1	7.492	50.801	1	7.816	97.904
2	8.307	49.199	2	8.668	2.096

(*R*,*Z*)-1,1,1-Trifluoro-2-(*m*-tolyl)hex-4-en-2-amine (3.30p): Clear oil, 16.3 mg, 67% yield, 0.067 mmol; **IR (neat):** 3397 (w), 3027 (w), 2923 (w), 1608 (w), 1446 (m), 1252 (m), 1142 (s), 839 (s), 785 (s), 717 (s), 532 (m) cm^{-1}; **^{1}H NMR (400 MHz, $CDCl_3$):** δ 7.40 – 7.31 (m, 2H), 7.26 (t, *J* = 7.6 Hz, 1H), 7.14 (d, *J* = 7.4 Hz, 1H), 5.59 (dddd, *J* = 11.6, 8.6, 5.9, 3.5 Hz, 1H), 5.15 (q, *J* = 8.1 Hz, 1H), 2.79 (ddd, *J* = 56.1, 14.9, 7.2 Hz, 2H), 2.37 (s, 3H), 1.73 (s, 2H), 1.68 – 1.55 (m, 3H); **^{13}C NMR (100 MHz, $CDCl_3$):** δ 138.00, 137.68, 128.94, 128.66, 128.27, 127.71, 127.1 (q, *J* = 219.1 Hz), 124.12, 123.06, 61.55 (q, *J* = 27.7, 27.0 Hz), 33.64, 21.79, 13.28; **^{19}F NMR (376 MHz, $CDCl_3$):** –77.9 (s, 3F); **HRMS (DART):** Calcd for $C_{13}H_{17}NF_3$ $[M+H]^+$: 244.1308; Found: 244.1303; **Specific rotation:** $[\alpha]^{24.3}_D$ +18.4 (*c* = 1.3, $CHCl_3$) for a 96:4 er sample. Enantiomeric purity was determined by HPLC analysis in comparison with authentic racemic material (Chiralpak OJ-H, 97:3 hexanes:*i*PrOH, 0.5 mL/min, 220 nm): t_R: 12.058 min (major) and 10.325 min (minor).

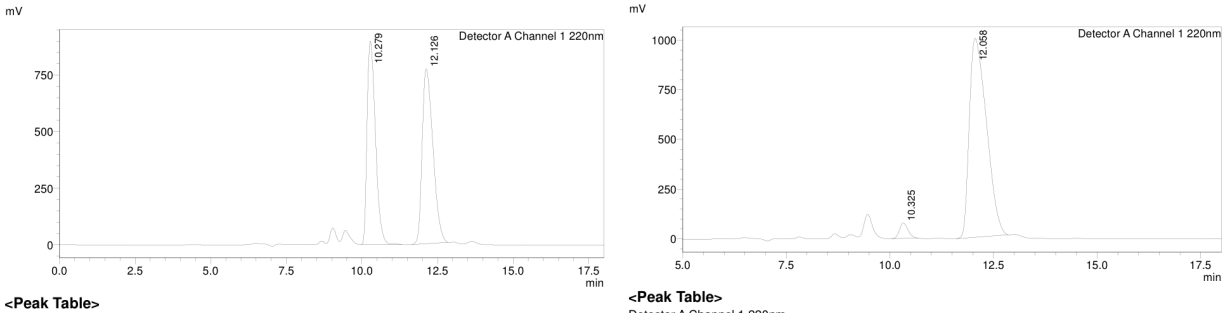

Peak #	Ret. Time (min)	Area %	Peak #	Ret. Time (min)	Area %
1	10.279	47.612	1	10.325	3.736
2	12.126	52.388	2	12.058	96.264

(*R*,*Z*)-1,1,1-Trifluoro-2-(thiophen-2-yl)hex-4-en-2-amine (3.30q): Pale yellow oil, 19.8 mg, 84% yield, 0.084 mmol; **IR (neat):** 3026 (w), 1617 (m), 1436 (m), 1143 (s), 1052 (m), 832 (m),

701 (s) cm^{-1}; **^{1}H NMR (400 MHz, $CDCl_3$):** δ 7.35–7.25 (m, 1H), 7.11 (m, 1H), 7.02 (dd, *J* = 5.1, 3.7 Hz, 1H), 5.67 (m, 1H), 5.43–5.14 (m, 1H), 2.76 (d, *J* = 7.4 Hz, 2H), 1.91 (s, 2H), 1.72–1.31 (m, 3H); **^{13}C NMR (100 MHz, $CDCl_3$):** δ 143.1, 129.2, 127.2, 126.4 (q, *J* = 285.2 Hz), 125.5 (q, *J* = 1.4 Hz), 125.4, 122.3, 61.0 (q, *J* = 27.1 Hz), 34.7, 13.1; **^{19}F NMR (376 MHz, $CDCl_3$):** δ –79.2 (s, 3F); **HRMS (DART):** Calcd for $C_{10}H_{13}NF_3S$ $[M+H]^+$: 236.0715; Found: 236.0717; **Specific rotation:** $[\alpha]^{26.0}_D$ –20.0 (*c* 0.5, $CHCl_3$) for a 93:7 er sample. Enantiomeric purity was determined by HPLC analysis in comparison with authentic racemic material (Chiralcel OJ-H, 99:1 hexanes:*i*PrOH, 0.7 mL/min, 220 nm): t_R: 14.853 min (minor) and 15.650 min (major).

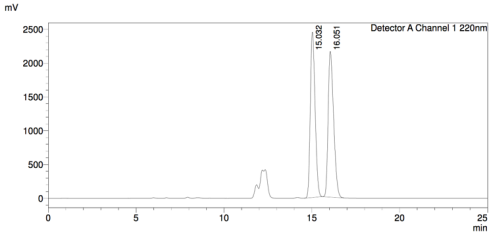

Detector A Channel 1 220nm

Peak#	Ret. Time	Area	Area%
1	15.032	46233175	49.672
2	16.051	46844537	50.328
Total		93077711	100.000

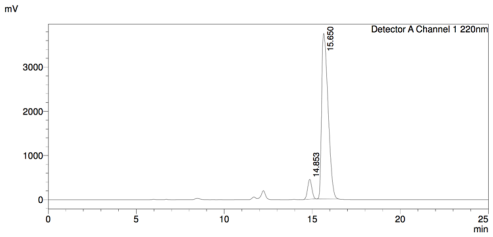

Detector A Channel 1 220nm

Peak#	Ret. Time	Area	Area%
1	14.853	7383342	7.153
2	15.650	95834624	92.847
Total		103217966	100.000

Peak #	Ret. Time (min)	Area %	Peak #	Ret. Time (min)	Area %
1	15.032	49.672	1	14.853	7.153
2	16.051	50.328	2	15.650	92.847

(*R*,*Z*)-1,1,1-Trifluoro-2-(furan-2-yl)hex-4-en-2-amine (3.30r): Pale yellow oil, 7.01 mg, 32% yield, 0.032 mmol; **IR (neat):** 3999 (w, br), 3025 (w), 1759 (w), 1616 (m), 1257 (m), 1144 (s), 1016 (m), 738 (s), 556 (m) cm^{-1}; **^{1}H NMR (400 MHz, $CDCl_3$):** δ 7.42 (s, 1H), 6.55 – 6.01 (m, 2H), 5.81 – 5.58 (m, 1H), 5.35 – 5.10 (m, 1H), 2.82 (dd, *J* = 14.6, 6.6 Hz, 1H), 2.70 (dd, *J* = 14.4, 8.1 Hz, 1H), 1.81 (s, 2H), 1.64 (dt, *J* = 6.9, 0.9 Hz, 3H); **^{13}C NMR (100 MHz, $CDCl_3$):** δ 151.6, 142.9, 129.4, 126.1 (q, *J* = 285.4 Hz), 122.4, 110.6, 108.8, 59.8 (q, *J* = 27.3 Hz), 31.4, 13.2; **^{19}F NMR (376 MHz, $CDCl_3$):** δ –79.3 (s, 3F); **HRMS (DART):** Calcd for $C_{10}H_{13}NOF_3$ $[M+H]^+$: 220.0944; Found: 220.0940; **Specific rotation:** $[\alpha]^{26.0}_D$ +27.9 (*c* 1.72, $CHCl_3$) for a 97:3 er sample. Enantiomeric purity was determined by HPLC analysis in comparison with authentic racemic material (Chiralcel OJ-H, 99:1 hexanes:*i*PrOH, 0.7 mL/min, 220 nm): t_R: 10.198 min (minor) and 10.820 min (minor).

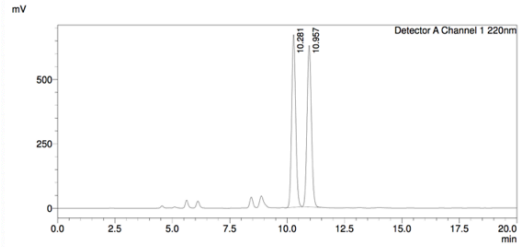

Detector A Channel 1 220nm

Peak#	Ret. Time	Area	Area%
1	10.281	8207254	49.800
2	10.957	8273339	50.200
Total		16480593	100.000

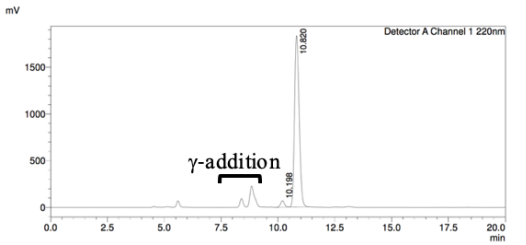

Detector A Channel 1 220nm

Peak#	Ret. Time	Area	Area%
1	10.198	825703	3.064
2	10.820	26063368	96.936
Total		26887071	100.000

Peak #	Ret. Time (min)	Area %	Peak #	Ret. Time (min)	Area %
1	10.281	49.800	1	10.198	3.064
2	10.957	50.200	2	10.820	96.936

(*R*,*Z*)-2-(Benzofuran-2-yl)-1,1,1-trifluorohex-4-en-2-amine (3.30s): Pale yellow oil, 20.7 mg, 77% yield, 0.077 mmol; **IR (neat):** 3400 (w), 3025 (w), 1705 (w), 1473 (m), 1138 (s), 1004 (m), 739 (s), 629 (m), 429 (m) cm^{-1}; **^{1}H NMR (400 MHz, $CDCl_3$):** δ 7.57 (ddd, *J* = 7.6, 1.5, 0.8 Hz, 1H), 7.49 (dq, *J* = 8.2, 0.9 Hz, 1H), 7.30 (ddd, *J* = 8.3, 7.2, 1.5 Hz, 1H), 7.23 (dd, *J* = 7.4, 1.1 Hz, 1H), 6.80 (d, *J* = 0.9 Hz, 1H), 5.67 (m, 1H), 5.33–5.17 (m, 1H), 2.95 (dd, *J* = 14.6, 6.6 Hz, 1H), 2.79 (dd, *J* = 14.6, 8.2 Hz, 1H), 1.95 (s, 2H), 1.66 (ddt, *J* = 6.9, 1.9, 0.9 Hz, 3H); **^{13}C NMR (125 MHz, $CDCl_3$):** δ 155.0, 154.3, 129.5, 127.8, 124.6, 124.4 (q, *J* = 204.4 Hz), 123.0, 122.0, 121.2, 111.4, 105.7, 60.2 (q, *J* = 22.6 Hz), 31.3, 13.1; **^{19}F NMR (376 MHz, $CDCl_3$):** δ –78.7 (s, 3F); **HRMS (DART):** Calcd for $C_{14}H_{15}NOF_3$ $[M+H]^+$: 270.1100; Found: 270.1098; **Specific rotation:** $[\alpha]^{26.0}_D$ +37.9 (*c* 10.7, $CHCl_3$) for a 97:3 er sample. Enantiomeric purity was determined by HPLC analysis in comparison with authentic racemic material (Chiralpak AD-H, 99:1 hexanes:*i*PrOH, 0.7 mL/min, 220 nm): t_R: 11.248 min (major) and 12.690 min (minor).

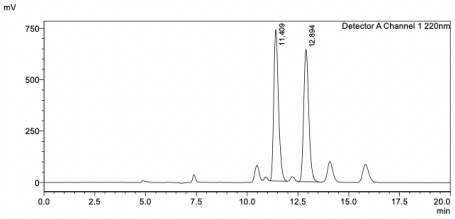

Detector A Channel 1 220nm

Peak#	Ret. Time	Area	Area%
1	11.409	11863591	51.383
2	12.894	11225147	48.617
Total		23088738	100.000

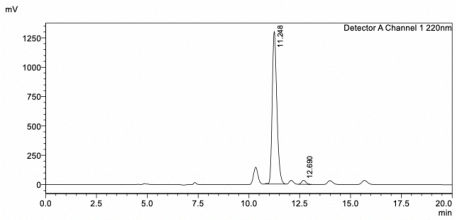

Detector A Channel 1 220nm

Peak#	Ret. Time	Area	Area%
1	11.248	20562082	97.487
2	12.690	530143	2.513
Total		21092225	100.000

Peak #	Ret. Time (min)	Area %	Peak #	Ret. Time (min)	Area %
1	11.409	51.383	1	11.248	97.487
2	12.894	48.617	2	12.690	2.513

(*R*,1*E*,5*Z*)-2-Methyl-1-phenyl-3-(trifluoromethyl)hepta-1,5-dien-3-amine (3.30t): Colorless oil, 17.2 g, 64% yield, 0.064 mmol; **IR (neat):** 3024 (w), 2935 (w), 1444 (m), 1250 (m), 1147 (m), 1003 (m), 700 (m) cm^{-1}; **^{1}H NMR (600 MHz, $CDCl_3$):** δ 7.34 (m, 2H), 7.26–7.22 (m, 3H), 6.90 (s, 1H), 5.78–5.62 (m, 1H), 5.37 (m, 1H), 2.71 (dd, *J* = 15.1, 6.7 Hz, 1H), 2.51 (dd, *J* = 15.1, 7.5 Hz, 1H), 1.90 (t, *J* = 1.3 Hz, 3H), 1.71 (dt, *J* = 6.8, 1.1 Hz, 3H), 1.57 (s, 2H); **^{13}C NMR (100 MHz, $CDCl_3$):** δ 137.7, 134.3, 129.8, 129.1, 128.2, 128.1, 127.3 (q, *J* = 286.8 Hz), 126.7, 122.9, 62.9 (q, *J* = 25.0 Hz), 30.9, 15.0, 13.2; **^{19}F NMR (376 MHz, $CDCl_3$):** δ –76.8 (s, 3F); **HRMS (DART):** Calcd for $C_{15}H_{19}NF_3$ $[M+H]^+$: 270.1464; Found: 270.1474; **Specific rotation:** $[\alpha]^{24.8}_D$ +4.4 (*c* 0.9, $CHCl_3$) for a 98.5:1.5 er sample. Enantiomeric purity was determined by HPLC analysis in comparison with authentic racemic material (Chiralpak AD-H, 99:1 hexanes:*i*PrOH, 0.7 mL/min, 220 nm): t_R: 8.587 min (minor) and 9.560 min (major).

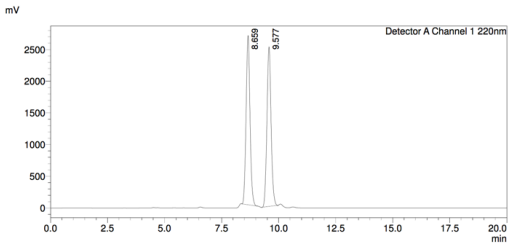

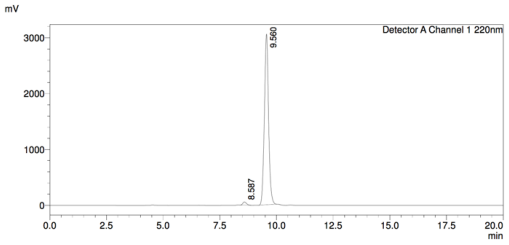

Peak #	Ret. Time (min)	Area %	Peak #	Ret. Time (min)	Area %
1	8.659	50.025	1	8.587	1.602
2	9.577	49.975	2	9.560	98.398

(*R*,*Z*)-1-Phenyl-3-(trifluoromethyl)hept-5-en-1-yn-3-amine (3.30u): Colorless oil, 20.5 mg, 81% yield, 0.081 mmol; **IR (neat):** 3026 (w), 1617 (m), 1436 (m), 1143 (s), 1052 (m), 832 (m), 701 (s) cm^{-1}; **^{1}H NMR (600 MHz, $CDCl_3$):** δ 7.52–7.37 (m, 2H), 7.36–7.27 (m, 3H), 5.84 (dqt, *J* = 12.3, 6.8, 1.5 Hz, 1H), 5.68 (td, *J* = 9.0, 6.8 Hz, 1H), 2.63 (d, *J* = 7.4 Hz, 2H), 1.83 (s, 2H), 1.72 (dq, *J* = 6.7, 0.9 Hz, 3H); **^{13}C NMR (150 MHz, $CDCl_3$):** δ 140.8 (q, *J* = 15.1 Hz), 134.5, 132.3, 131.5, 128.9 (q, *J* = 190.1 Hz), 125.1, 124.5, 88.5, 87.8, 59.2 (q, *J* = 29.1 Hz), 35.5, 15.8; **^{19}F NMR (376 MHz, $CDCl_3$):** δ –80.5 (s, 3F); **HRMS (DART):** Calcd for $C_{14}H_{15}NF_3$ $[M+H]^+$: 254.1151; Found: 254.1153; **Specific rotation:** $[\alpha]^{26.0}_D$ +11.4 (*c* 1.85, $CHCl_3$) for a 96.5:3.5 er sample. Enantiomeric purity was determined by HPLC analysis in comparison with authentic racemic material (Chiralpak AD-H, 99:1 hexanes:*i*PrOH, 0.7 mL/min, 220 nm): t_R: 8.366 min (major) and 8.950 min (minor).

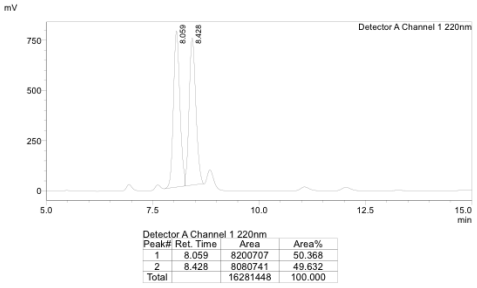

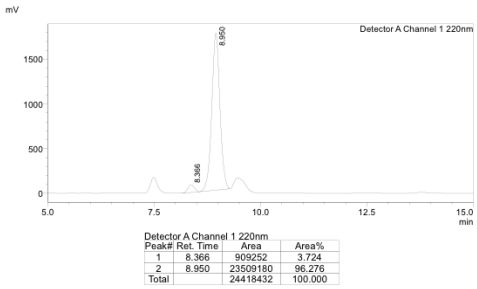

Peak #	Ret. Time (min)	Area %	Peak #	Ret. Time (min)	Area %
1	8.059	50.368	1	8.366	3.724
2	8.428	49.632	2	8.950	96.276

(*R*,*Z*)-1,1,1,2,2-Pentafluoro-3-(4-(trifluoromethyl)phenyl)hept-5-en-3-amine (3.30v): Pale yellow oil, 25.0 mg, 72% yield, 0.072 mmol; **IR (neat):** 3027 (w), 2919 (w), 1620 (m), 1324 (s), 1209 (m), 1164 (s), 1121 (s), 1069 (m), 751 (m), 599 (m) cm^{-1}; **^{1}H NMR (400 MHz, $CDCl_3$):** δ 7.72–7.58 (m, 4H), 5.61 (dtd, *J* = 12.0, 8.4, 7.8, 6.3 Hz, 1H), 4.97 (q, *J* = 8.6 Hz, 1H), 3.02–2.79 (m, 2H), 1.78 (s, 2H), 1.63 (ddt, *J* = 6.8, 1.7, 0.8 Hz, 3H); **^{13}C NMR (100 MHz, $CDCl_3$):** δ 141.66,

130.50 (dd, J = 65.6, 32.8 Hz), 129.71, 127.86, 125.30, 124.11 (q, J = 272.0 Hz), 122.05, 121.03 (t, J = 37.1 Hz), 115.99 (tq, J = 37.2 Hz, J = 33.6 Hz, J = 33.6 Hz, J = 36.8, 34.9 Hz), 61.70 (t, J = 21.3 Hz), 33.61, 13.35; **^{19}F NMR (376 MHz, $CDCl_3$):** –62.7 (s, 3F), –77.0 (s, 3F), –120.1 (dd, J = 73.8 Hz, J = 124.1 Hz, 2F); **HRMS (DART):** Calcd for $C_{14}H_{14}NF_8$ $[M+H]^+$: 348.0993; Found: 348.1002; **Specific rotation:** $[\alpha]^{26.0}_D$ +13.9 (c = 2.75, $CHCl_3$) for a 97:3 er sample. Enantiomeric purity was determined by HPLC analysis in comparison with authentic racemic material (Chiralcel AD-H, 97:3 hexanes:*i*PrOH, 0.7 mL/min, 220 nm): t_R: 6.673 min (minor) and 8.264 min (minor).

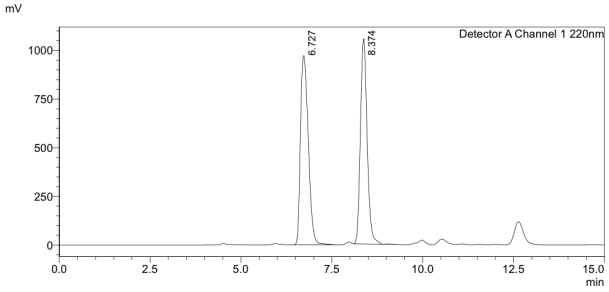

<Peak Table>
Detector A Channel 1 220nm

Peak#	Ret. Time	Area	Area%	Height
1	6.727	14507897	51.575	972360
2	8.374	13621924	48.425	1054252
Total		28129820	100.000	2026612

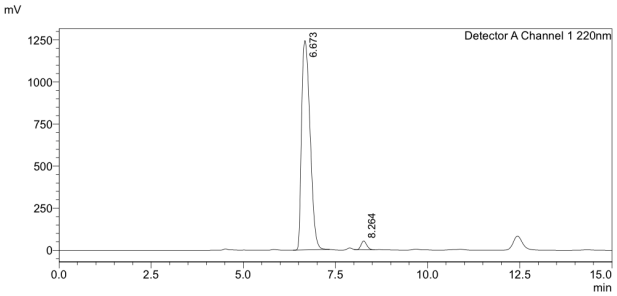

<Peak Table>
Detector A Channel 1 220nm

Peak#	Ret. Time	Area	Area%	Height
1	6.673	19942733	97.314	1244168
2	8.264	550433	2.686	52409
Total		20493165	100.000	1296577

Peak #	Ret. Time (min)	Area %	Peak #	Ret. Time (min)	Area %
1	6.727	51.574	1	6.673	97.314
2	8.374	48.425	2	8.264	2.686

3.7.6.2. With (*Z*)-1-(4,4,5,5-tetramethyl-1,3,2-dioxaborolan-2-yl)dec-2-en-5-one (S-*Z*-1)

In a N_2-filled glovebox, a stock solution of **ap-6** (3.5 mg, 0.01 mmol), $Zn(OMe)_2$ (2.6 mg, 0.02 mmol), and toluene (0.5 mL) was prepared. A separate oven-dried two-dram vial equipped with a magnetic stir-bar was charged with NTMS-ketimine (0.1 mmol), toluene (0.25 mL), and tbat (2.7 mg, 0.005 mmol). The freshly prepared catalyst stock solution (0.25 mL) was then added followed by (*Z*)-1-(4,4,5,5-Tetramethyl-1,3,2-dioxaborolan-2-yl)dec-2-en-5-one (34.6 mg, 0.13 mmol), and MeOH (14 µL, 0.35 mmol). The mixture was allowed to stir for five min before the vial was capped, removed from the glovebox, and the mixture was allowed to stir for 3 h at 22 °C. Conversion and α:γ ratio were determined by spectroscopic analysis (^{19}F NMR) of an aliquot sample. The mixture was loaded onto silica gel and eluted with 100:0 → 3:1 hexanes:Et_2O to afford the expected α-tertiary amine as colorless oil.

(*R*,*Z*)-1,1,1-Trifluoro-2-phenyldodec-4-en-2-amine (3.31): Colorless oil, 27.0 mg, 86% yield, 0.086 mmol; **IR (neat):** 2925 (m), 2855 (m), 1449 (m), 1252 (m), 1147 (s), 763 (m), 699 (s) cm^{-1}; **^{1}H NMR (400 MHz, $CDCl_3$):** δ 7.63–7.52 (m, 2H), 7.45–7.31 (m, 3H), 5.58–5.41 (m, 1H), 5.20–5.01 (m, 1H), 2.88 (dd, J = 15.1, 6.9 Hz, 1H), 2.79–2.64 (m, 1H), 2.13–1.95 (m, 2H), 1.74 (s, 2H), 1.38–1.18 (m, 10H), 1.00–0.76 (m, 3H); **^{13}C NMR (100 MHz, $CDCl_3$):** δ 137.8, 134.9, 128.4, 128.2, 127.3 (q, J = 285.4 Hz), 127.1 127.0, 121.7, 61.6 (q, J = 25.8 Hz), 32.0, 29.6, 29.4, 29.3,

27.7, 22.8, 14.2; **^{19}F NMR (376 MHz, $CDCl_3$):** δ –78.0 (s, 3F); **HRMS (DART):** Calcd for $C_{18}H_{27}NF_3$ $[M+H]^+$: 314.2090; Found: 314.2091; **Specific rotation:** $[\alpha]^{24.7}_D$ +16.4 (*c* 0.9, $CHCl_3$) for a 97:3 er sample. Enantiomeric purity was determined by HPLC analysis in comparison with authentic racemic material (Chiralcel OD-H, 99:1 hexanes:*i*PrOH, 0.7 mL/min, 220 nm): t_R: 6.114 min (minor) and 6.741 min (major).

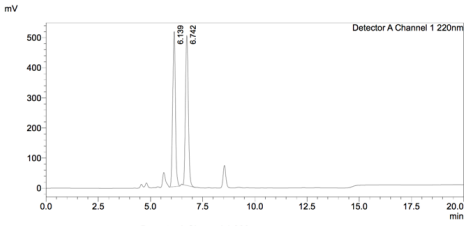

Detector A Channel 1 220nm

Peak#	Ret. Time	Area	Area%
1	6.139	4701018	49.817
2	6.742	4735486	50.183
Total		9436504	100.000

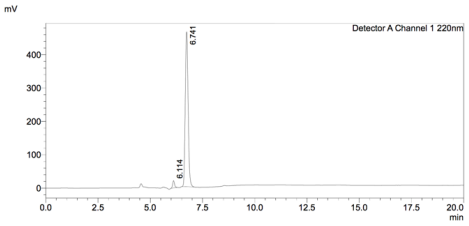

Detector A Channel 1 220nm

Peak#	Ret. Time	Area	Area%
1	6.114	136081	3.003
2	6.741	4394866	96.997
Total		4530946	100.000

Peak #	Ret. Time (min)	Area %	Peak #	Ret. Time (min)	Area %
1	6.139	49.817	1	6.114	3.003
2	6.742	50.183	2	6.741	96.997

3.7.6.3. With (*Z*)-2-(3-chloroallyl)-4,4,5,5-tetramethyl-1,3,2-dioxaborolane (S-*Z*-2)

In a N_2-filled glovebox, a stock solution of **ap-6** (3.5 mg, 0.01 mmol), $Zn(OMe)_2$ (2.6 mg, 0.02 mmol), and toluene (0.5 mL) was prepared. A separate oven-dried two-dram vial equipped with a magnetic stir-bar was charged with NTMS-ketimine (0.1 mmol), toluene (0.25 mL), tbat (2.7 mg, 0.005 mmol) and MeOH (7 μL, 0.175 mmol), and was subsequently charged with the freshly prepared catalyst stock solution (0.25 mL) followed by (*Z*)-2-(3-Chloroallyl)-4,4,5,5-tetramethyl-1,3,2-dioxaborolane (26.3 mg, 0.13 mmol), and MeOH (7 μL, 0.175 mmol). The mixture was allowed to stir for five min prior and then the vessel was capped, removed from the glovebox, and the solution was allowed to stir for 14 h at 22 °C. Conversion and α:γ ratio were determined by spectroscopic analysis (^{19}F NMR) of an aliquot sample. The mixture was directly loaded onto silica gel and eluted with 100:0 → 3:1 hexanes:Et_2O to afford the desired α-tertiary amine as colorless oil.

(*R,Z*)-5-Chloro-1,1,1-trifluoro-2-phenylpent-4-en-2-amine (3.32a): Colorless oil, 22.7 mg, 91% yield, 0.091 mmol; **IR (neat):** 2924 (m), 2853 (m), 1630 (m), 1449 (m), 1255 (m), 1152 (s), 756 (m) cm^{-1}; **^{1}H NMR (600 MHz, $CDCl_3$):** δ 7.60–7.52 (m, 2H), 7.45–7.32 (m, 3H), 6.10 (dt, *J* = 7.2, 1.7 Hz, 1H), 5.54 (q, *J* = 7.0 Hz, 1H), 3.11 (ddd, *J* = 15.5, 6.6, 1.8 Hz, 1H), 2.89 (ddd, *J* = 15.5, 7.2, 1.7 Hz, 1H), 1.81 (s, 2H); **^{13}C NMR (100 MHz, $CDCl_3$):** δ 136.6, 128.4, 128.3, 126.9 (q, *J* = 285.4 Hz), 126.8, 125.0, 121.7, 61.2 (q, *J* = 26.2 Hz), 33.8; **^{19}F NMR (564 MHz, $CDCl_3$):** δ –78.7 (s, 3F); **HRMS (DART):** Calcd for $C_{11}H_{12}NF_3Cl$ $[M+H]^+$: 250.0605; Found: 250.0616; **Specific rotation:** $[\alpha]^{24.5}_D$ +4.1 (*c* 1.3, $CHCl_3$) for a 88.5:11.5 er sample. Enantiomeric purity was determined by HPLC analysis in comparison with authentic racemic material (Chiralcel OJ-H,

99:1 hexanes:*i*PrOH, 0.7 mL/min, 220 nm): t_R: 16.891 min (minor) and 18.316 min (major).

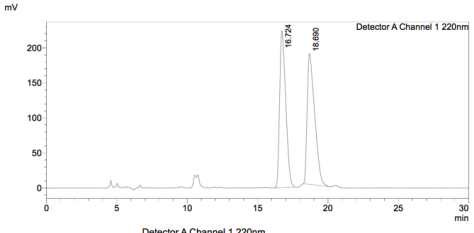

Detector A Channel 1 220nm

Peak#	Ret. Time	Area	Area%
1	16.724	6738880	49.341
2	18.690	6918774	50.659
Total		13657653	100.000

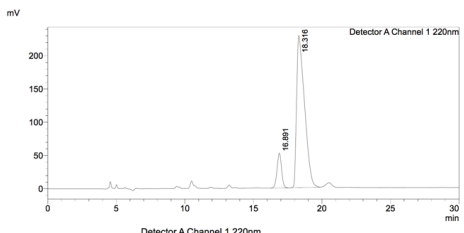

Detector A Channel 1 220nm

Peak#	Ret. Time	Area	Area%
1	16.891	1203011	11.552
2	18.316	9211025	88.448
Total		10414036	100.000

Peak #	Ret. Time (min)	Area %	Peak #	Ret. Time (min)	Area %
1	16.724	49.341	1	16.891	11.552
2	18.690	50.659	2	18.316	88.448

(*R*,*Z*)-5-Bromo-1,1,1-trifluoro-2-phenylpent-4-en-2-amine (3.32b): Clear oil, 26.6 mg, 81% yield, 0.081 mmol; **IR (neat):** 2977 (m), 2930 (m), 1619 (w), 1468 (s), 1369 (s), 1329 (s), 1214 (s), 966 (m), 882 (m), 718 (w) cm^{-1}; **^{1}H NMR** (400 MHz, $CDCl_3$) δ 7.59–7.53 (m, 2H), 7.44–7.32 (m, 3H), 6.25 (dt, *J* = 7.2, 1.7 Hz, 1H), 5.87 (q, *J* = 6.9 Hz, 1H), 3.08 (ddd, *J* = 15.5, 6.4, 1.8 Hz, 1H), 2.85 (ddd, *J* = 15.5, 7.0, 1.7 Hz, 1H), 1.78 (s, 2H); **^{13}C NMR (100 MHz, $CDCl_3$):** δ 136.71, 128.59, 128.54, 128.47, 127.1 (q, *J* = 286.8 Hz), 127.0 (d, *J* = 1.5 Hz), 111.71, 61.33 (q, *J* = 26.2 Hz), 36.62 (d, *J* = 1.8 Hz); **^{19}F NMR (564 MHz, $CDCl_3$):** –78.8 (s, 3F); **HRMS (DART):** Calcd for $C_{11}H_{12}NF_3Br$ $[M+H]^+$: 294.00997; Found: 294.00948; **Specific rotation:** $[\alpha]^{23.2}_D$ +2.3 (*c* = 0.5, $CHCl_3$) for a 89:11 er sample. Enantiomeric purity was determined by HPLC analysis in comparison with authentic racemic material (Chiralcel OJ-H, 99:1 hexanes:*i*PrOH, 0.7 mL/min, 220 nm): t_R: 17.987 min (minor) and 19.425 min (major).

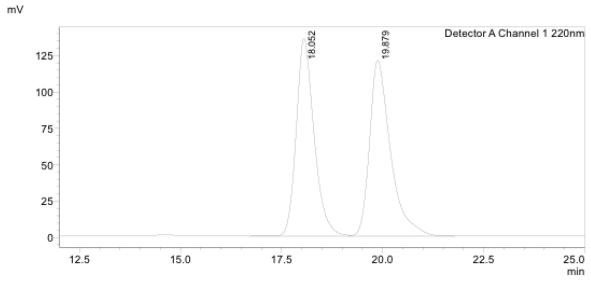

Detector A Channel 1 220nm

Peak#	Ret. Time	Area	Area%
1	18.052	4181758	48.960
2	19.879	4359438	51.040
Total		8541196	100.000

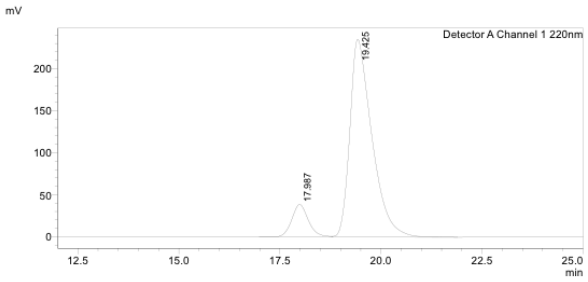

Detector A Channel 1 220nm

Peak#	Ret. Time	Area	Area%
1	17.987	1134654	11.207
2	19.425	8989411	88.793
Total		10124065	100.000

Peak #	Ret. Time (min)	Area %	Peak #	Ret. Time (min)	Area %
1	18.052	48.960	1	17.987	11.207
2	19.879	51.040	2	19.425	88.783

3.7.6.4. With (*Z*)-2-(3-Bromoallyl)-4,4,5,5-tetramethyl-1,3,2-dioxaborolane (S-*Z*-3)

In a N_2-filled glovebox, a stock solution of aminophenol **ap-6** (3.5 mg, 0.01 mmol), $Zn(OMe)_2$ (2.6 mg, 0.02 mmol), and toluene (0.5 mL) was prepared. A separate oven-dried two-dram vial equipped with a magnetic stir-bar was charged with NTMS-ketimine (0.1 mmol), toluene (0.25 mL), TBAT (2.7 mg, 0.005 mmol) and MeOH (7 μL, 0.175 mmol). The freshly prepared catalyst stock solution (0.25 mL) was then added followed by (*Z*)-2-(3-Bromoallyl)-4,4,5,5-tetramethyl-1,3,2-dioxaborolane (32.1 mg, 0.13 mmol), and MeOH (7 μL, 0.175 mmol). The mixture was allowed to stir for five minutes prior to being sealed with a Teflon cap, removed from the glovebox, and allowed to stir at 22 °C for 14 h. Conversion and α:γ ratio were determined by ^{19}F NMR of an aliquot. The mixture was loaded onto silica gel and eluted with 100:0 → 3:1 hexanes:Et_2O to afford the α-tertiary amine as colorless oil.

(*R*,*Z*)-5-Bromo-1,1,1-trifluoro-2-phenylpent-4-en-2-amine (3.33a): Clear oil, 10.3 mg, 35% yield, 0.035 mmol; **IR (neat):** 2977 (m), 2930 (m), 1619 (w), 1468 (s), 1369 (s), 1329 (s), 1214 (s), 966 (m), 882 (m), 718 (w) cm^{-1}; **^{1}H NMR** (400 MHz, $CDCl_3$) δ 7.59–7.53 (m, 2H), 7.44–7.32 (m, 3H), 6.25 (dt, *J* = 7.2, 1.7 Hz, 1H), 5.87 (q, *J* = 6.9 Hz, 1H), 3.08 (ddd, *J* = 15.5, 6.4, 1.8 Hz, 1H), 2.85 (ddd, *J* = 15.5, 7.0, 1.7 Hz, 1H), 1.78 (s, 2H); **^{13}C NMR (100 MHz, $CDCl_3$):** δ 136.71, 128.59, 128.54, 128.47, 127.1 (q, *J* = 286.8 Hz), 127.0 (d, *J* = 1.5 Hz), 111.71, 61.33 (q, *J* = 26.2 Hz), 36.62 (d, *J* = 1.8 Hz); **^{19}F NMR (564 MHz, $CDCl_3$):** –78.8 (s, 3F); **HRMS (DART):** Calcd for $C_{11}H_{12}NF_3Br$ $[M+H]^+$: 294.00997; Found: 294.00948; **Specific rotation:** $[\alpha]^{23.2}_D$ +2.3 (*c* = 0.5, $CHCl_3$) for a 89:11 er sample. Enantiomeric purity was determined by HPLC analysis in comparison with authentic racemic material (Chiralcel OJ-H, 99:1 hexanes:*i*PrOH, 0.7 mL/min, 220 nm): t_R: 17.987 min (minor) and 19.425 min (major).

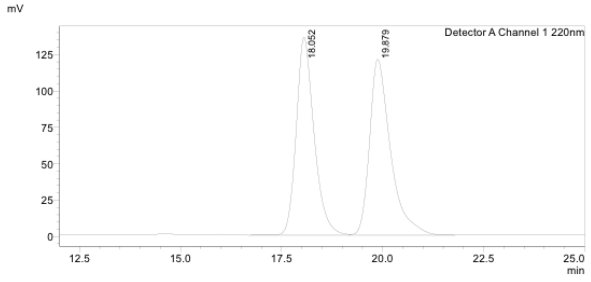

Detector A Channel 1 220nm

Peak#	Ret. Time	Area	Area%
1	18.052	4181758	48.960
2	19.879	4359438	51.040
Total		8541196	100.000

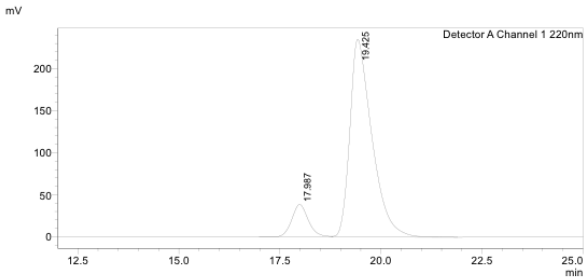

Detector A Channel 1 220nm

Peak#	Ret. Time	Area	Area%
1	17.987	1134654	11.207
2	19.425	8989411	88.793
Total		10124065	100.000

Peak #	Ret. Time (min)	Area %	Peak #	Ret. Time (min)	Area %
1	18.052	48.960	1	17.987	11.207
2	19.879	51.040	2	19.425	88.783

(*R*,*Z*)-5-Bromo-1,1,1-trifluoro-2-(4-(trifluoromethyl)phenyl)pent-4-en-2-amine (3.33b): Colorless oil, 27.5 mg, 76% yield, 0.076 mmol; **IR (neat):** 3401 (w), 2993 (w), 2855 (w), 1623

(w), 1324 (s), 1253 (m), 1158 (s), 1125 (s), 735 (m), 625 (m) cm^{-1}; **^{1}H NMR (400 MHz, $CDCl_3$):** δ 7.72 (d, *J* = 8.4 Hz, 2H), 7.66 (d, *J* = 8.4 Hz, 2H), 6.27 (dt, *J* = 7.3, 1.7 Hz, 1H), 5.85 (q, *J* = 6.9 Hz, 1H), 3.10 (ddd, *J* = 15.5, 6.8, 1.6 Hz, 1H), 2.85 (ddd, *J* = 15.5, 6.7, 1.7 Hz, 1H), 1.80 (s, 2H); **^{13}C NMR (100 MHz, $CDCl_3$):** δ 161.6 (d, *J* = 249.5 Hz), 130.6, 130.4 (q, *J* = 35.8 Hz), 128.8, 126.9 (q, *J* = 286.1 Hz), 124.2 (q, *J* = 3.4 Hz), 123.1, 117.0 (q, *J* = 25.4 Hz), 61.6 (q, *J* = 26.7 Hz), 32.0; **^{19}F NMR (564 MHz, $CDCl_3$):** δ –62.41 to –63.28 (m, 3F), –78.13 to –78.89 (m, 3F); **HRMS (DART):** Calcd for $C_{12}H_{11}NF_6Br$ $[M+H]^+$: 361.9974; Found: 361.9980; **Specific rotation:** $[\alpha]^{24.5}_D$ –6.2 (*c* 7.8, $CHCl_3$) for a 93:7 er sample. Enantiomeric purity was determined by HPLC analysis in comparison with authentic racemic material (Chiralcel OJ-H, 98:2 hexanes:*i*PrOH, 0.5 mL/min, 220 nm): t_R: 15.988 min (major) and 21.552 min (minor).

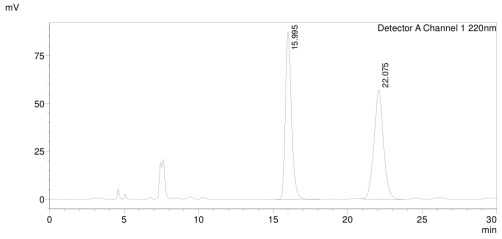

<Peak Table>
Detector A Channel 1 220nm

Peak#	Ret. Time	Area	Height	Area%
1	15.995	2504363	87792	49.717
2	22.075	2532849	57415	50.283
Total		5037212	145207	100.000

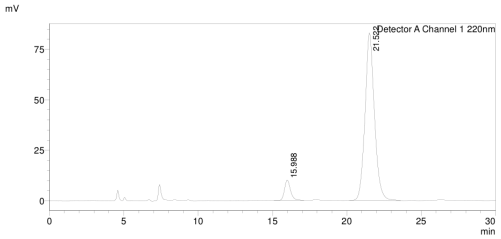

<Peak Table>
Detector A Channel 1 220nm

Peak#	Ret. Time	Area	Height	Area%
1	15.988	281278	10071	7.159
2	21.522	3647724	82920	92.841
Total		3929002	92991	100.000

Peak #	Ret. Time (min)	Area %	Peak #	Ret. Time (min)	Area %
1	15.995	49.717	1	15.988	7.159
2	22.075	50.283	2	21.552	92.841

(*R*,*Z*)-5-Bromo-2-(4-chlorophenyl)-1,1,1-trifluoropent-4-en-2-amine (3.33c): Yellow oil, 24.3 mg, 74 % yield, 0.074 mmol; **IR (neat):** 3402 (w), 3334 (w), 2926 (w), 1624 (w), 1494 (m), 1151 (s), 1075 (m), 824 (m), 699 (m), 581 (m) cm^{-1}; **^{1}H NMR (400 MHz, $CDCl_3$):** δ 7.51 (d, *J* = 8.3 Hz, 2H), 7.39–7.33 (m, 2H), 6.26 (dt, *J* = 7.3, 1.7 Hz, 1H), 5.86 (q, *J* = 6.9 Hz, 1H), 3.05 (dd, *J* = 15.5, 6.7 Hz, 1H), 2.82 (ddd, *J* = 15.4, 6.8, 1.7 Hz, 1H), 1.79 (s, 2H); **^{13}C NMR (100 MHz, $CDCl_3$):** δ 135.4, 134.7, 129.9, 128.6, 128.0, 126.8 (q, *J* = 285.8 Hz), 112.1, 62.1 (q, *J* = 26.4 Hz), 36.6; **^{19}F NMR (564 MHz, $CDCl_3$):** δ –78.8 (s, 3F); **HRMS (DART):** Calcd for $C_{11}H_{11}NF_3ClBr$ $[M+H]^+$: 327.9710; Found: 327.9718; **Specific rotation:** $[\alpha]^{24.5}_D$ –3.5 (*c* 0.85, $CHCl_3$) for a 92:8 er sample. Enantiomeric purity was determined by HPLC analysis in comparison with authentic racemic material (Chiralpak AD-H, 99:1 hexanes:*i*PrOH, 0.7 mL/min, 220 nm): t_R: 12.760 min (major) and 17.991 min (minor).

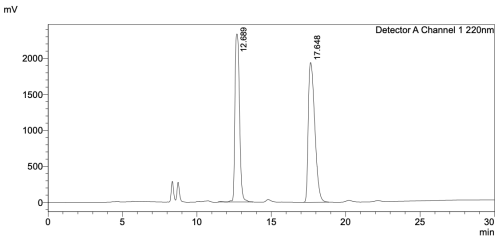

<Peak Table>
Detector A Channel 1 220nm

Peak#	Ret. Time	Area	Height	Area%
1	12.689	50119875	2334559	46.147
2	17.648	58488202	1940051	53.853
Total		108608076	4274609	100.000

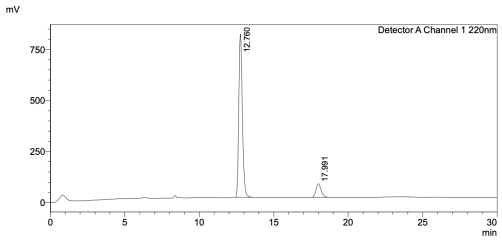

<Peak Table>
Detector A Channel 1 220nm

Peak#	Ret. Time	Area	Height	Area%
1	12.760	13433502	799630	89.499
2	17.991	1576140	66681	10.501
Total		15009642	866311	100.000

Peak #	Ret. Time (min)	Area %	Peak #	Ret. Time (min)	Area %
1	12.689	46.147	1	12.760	89.499
2	17.648	53.853	2	17.991	10.501

3.7.6.5. With (*Z*)-2-(3-((2-methoxyethoxy)methoxy)allyl)-4,4,5,5-tetramethyl-1,3,2-dioxaborolane (S-*Z*-4)

In a N_2-filled glovebox, a stock solution of aminophenol **ap-6** (3.5 mg, 0.01 mmol), $Zn(OMe)_2$ (2.6 mg, 0.02 mmol), and toluene (0.5 mL) was prepared. A separate oven-dried two-dram vial equipped with a magnetic stir-bar was charged with NTMS-ketimine (0.1 mmol), toluene (0.25 mL), tbat (2.7 mg, 0.005 mmol), and MeOH (7 μL, 0.175 mmol), which was charged with the freshly prepared catalyst stock solution (0.25 mL) followed by (Z)-2-(3-((2-methoxyethoxy)methoxy)allyl)-4,4,5,5-tetramethyl-1,3,2-dioxaborolane (35.4 mg, 0.13 mmol) and MeOH (4 μL, 0.0825 mmol). The mixture was allowed to stir for five min and then the vial was capped, removed from the glovebox, and the solution was allowed to stir for 14 h at 60 °C. Conversion and α:γ ratio were determined by ^{19}F NMR of an aliquot. The mixture was loaded onto silica gel and eluted with 100:0 → 3:1 hexanes:Et2O to afford the α-tertiary amine as colorless oil.

(*R*,*Z*)-1,1,1-Trifluoro-5-((2-methoxyethoxy)methoxy)-2-phenylpent-4-en-2-amine (3.34): Colorless oil, 21.7 mg, 68% yield, 0.068 mmol; **IR (neat):** 3325 (w, br), 2975 (m), 2929 (m), 1668 (w), 1472 (m), 1146 (s), 1040 (s), 850 (m), 757 (m), 674 (m) cm^{-1}; **^{1}H NMR (400 MHz, $CDCl_3$):** δ 7.59 (m, 2H), 7.43–7.30 (m, 3H), 6.25 (dd, *J* = 6.4, 1.4 Hz, 1H), 4.92–4.81 (m, 2H), 4.32–4.19 (m, 1H), 3.77–3.64 (m, 2H), 3.64–3.45 (m, 2H), 3.38 (d, *J* = 1.5 Hz, 3H), 3.00–2.78 (m, 2H), 1.81 (s, 2H); **^{13}C NMR (100 MHz, $CDCl_3$):** δ 145.8, 128.2, 127.2, 120.7 (q, *J* = 216.9 Hz), 100.8, 95.5, 71.7, 67.6, 61.6 (q, *J* = 26.3 Hz), 59.2, 31.0, 25.0, 24.7; **^{19}F NMR (564 MHz, $CDCl_3$):** δ –78.3 (s, 3F); **HRMS (DART):** Calcd for $C_{15}H_{21}NO_3F_3$ $[M+H]^+$: 320.1457; Found: 320.1480; **Specific rotation:** $[\alpha]^{24.5}_D$ +11.0 (*c* 1.9, $CHCl_3$) for a 88:12 er sample. Enantiomeric purity was determined by HPLC analysis in comparison with authentic racemic material (Chiralpak AD-H, 98:2 hexanes:*i*PrOH, 1.0 mL/min, 220 nm): t_R: 11.425 min (major) and 13.704 min (minor).

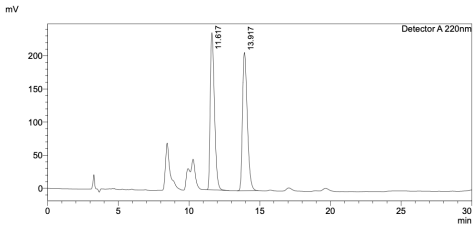

<Peak Table>
Detector A 220nm

Peak#	Ret. Time	Area	Height	Area%
1	11.617	4936239	237192	49.703
2	13.917	4995323	208753	50.297
Total		9931562	445946	100.000

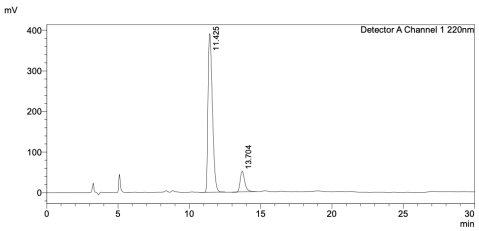

<Peak Table>
Detector A Channel 1 220nm

Peak#	Ret. Time	Area	Area%	Height
1	11.425	8409329	88.285	390335
2	13.704	1115881	11.715	51102
Total		9525209	100.000	441437

Peak #	Ret. Time (min)	Area %	Peak #	Ret. Time (min)	Area %
1	11.617	49.703	1	11.425	88.285
2	13.917	50.297	2	13.704	11.715

3.7.6.6. With (*Z*)-4,4,5,5-Tetramethyl-2-(2-methylhept-2-en-1-yl)-1,3,2-dioxaborolane (S-*Z*-5)

In a N_2-filled glovebox, a stock solution of aminophenol **ap-6** (3.5 mg, 0.01 mmol), $Zn(OMe)_2$ (2.6 mg, 0.02 mmol), and toluene (0.5 mL) was prepared. A separate oven-dried two-dram vial equipped with a magnetic stir-bar was charged with NTMS-ketimine (0.1 mmol), toluene (0.25 mL), and TBAT (2.7 mg, 0.005 mmol), which was charged with the freshly prepared catalyst stock solution (0.25 mL) followed by (*Z*)-4,4,5,5-tetramethyl-2-(2-methylhept-2-en-1-yl)-1,3,2-dioxaborolane (31.0 mg, 0.13 mmol), and MeOH (14 μL, 0.35 mmol). The mixture was allowed to stir for five min after which the vial was capped, removed from the glovebox, and the mixture was allowed to stir for 3 h at 22 °C. Conversion and α:γ ratio were determined by ^{19}F NMR of an aliquot The mixture was loaded onto silica gel and eluted with 100:0 → 3:1 hexanes:Et_2O to afford the α-tertiary amine as colorless oil.

(*R*,*Z*)-1,1,1-Trifluoro-4-methyl-2-phenylnon-4-en-2-amine (3.35a): Colorless oil, 25.1 mg, 88% yield, 0.088 mmol; **IR (neat):** 2955 (m), 2855 (m), 1603 (w), 1143 (s), 760 (m), 700 (s), 509 (m) cm^{-1}; **^{1}H NMR (400 MHz, $CDCl_3$):** δ 7.58 (d, *J* = 7.6 Hz, 2H), 7.43–7.28 (m, 3H), 5.56–5.44 (m, 1H), 5.11 (q, *J* = 7.8 Hz, 1H), 2.88 (dd, *J* = 14.9, 6.6 Hz, 1H), 2.77–2.66 (m, 1H), 2.02 (m, 2H), 1.75 (s, 1H), 1.28 (d, *J* = 8.3 Hz, 7H), 0.93–0.84 (m, 3H); **^{13}C NMR (100 MHz, $CDCl_3$):** δ 137.8, 134.9, 128.4, 128.2, 127.3 (q, *J* = 285.4 Hz), 127.1 (q, *J* = 1.5 Hz), 121.7, 61.6 (q, *J* = 25.9 Hz), 34.0 (d, *J* = 1.4 Hz), 32.0, 29.6, 29.4, 29.3, 27.7, 22.8; **^{19}F NMR (564 MHz, $CDCl_3$):** δ –78.0 (s, 3F); **HRMS (DART):** Calcd for $C_{16}H_{23}NF_3$ $[M+H]^+$: 286.1777; Found: 286.1778; **Specific rotation:** $[\alpha]^{24.5}_D$ +34.7 (*c* 1.77, $CHCl_3$) for a 88.5:11.5 er sample. Enantiomeric purity was determined by HPLC analysis in comparison with authentic racemic material (Chiralcel OJ-H, 99:1 hexanes:*i*PrOH, 0.7 mL/min, 220 nm): t_R: 16.891 min (minor) and 18.316 min (major).

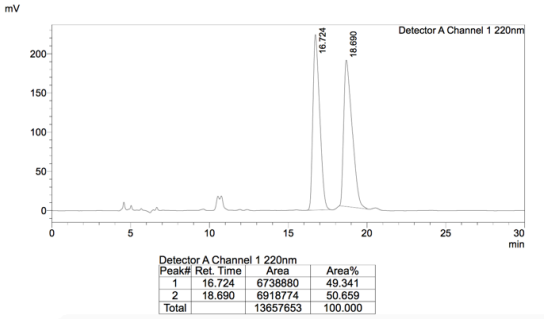

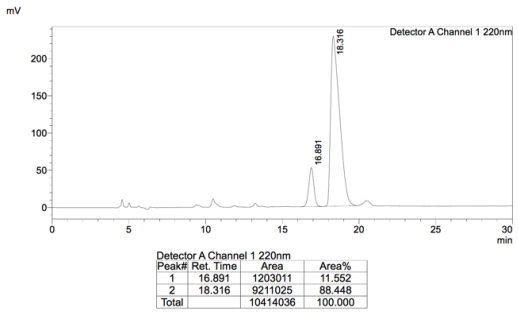

Peak #	Ret. Time (min)	Area %	Peak #	Ret. Time (min)	Area %
1	16.724	49.341	1	16.891	11.552
2	18.690	50.659	2	18.316	88.448

(*R*,*Z*)-1,1,1-Trifluoro-2-(4-methoxyphenyl)-4-methylnon-4-en-2-amine (3.35b): Colorless oil, 19.6 mg, 62% yield, 0.062 mmol; **IR (neat):** 3040 (w), 2930 (w), 1707 (w), 1514 (m), 1251 (s), 1148 (s), 1036 (m), 829 (m), 588 (w) cm^{-1}; **^{1}H NMR (400 MHz, $CDCl_3$):** δ 7.54 (d, *J* = 8.6 Hz, 2H), 6.92–6.85 (m, 2H), 5.34–5.26 (m, 1H), 3.81 (d, *J* = 1.1 Hz, 3H), 2.89–2.66 (m, 2H), 1.96 (q, *J* = 7.0 Hz, 2H), 1.69 (s, 2H), 1.31–1.19 (m, 7H), 0.89 (td, *J* = 6.7, 2.1 Hz, 3H); **^{13}C NMR (100 MHz, $CDCl_3$):** δ 159.4, 131.8, 130.8, 129.2, 128.1, 126.1 (q, *J* = 286.8 Hz), 113.6, 61.3 (q, *J* = 25.6, 25.2 Hz), 55.4, 37.9, 32.1, 28.3, 25.5, 22.6, 14.1; **^{19}F NMR (564 MHz, $CDCl_3$):** δ –78.3 (s, 3F); **HRMS (DART):** Calcd for $C_{17}H_{25}NOF_3$ $[M+H]^+$: 316.1883; Found: 316.1879; **Specific rotation:** $[\alpha]^{24.5}_D$ +70.5 (*c* = 2.4, $CHCl_3$) for a 92:8 er sample. Enantiomeric purity was determined by HPLC analysis in comparison with authentic racemic material (Chiralpak AZ-H, 98:2 hexanes:*i*PrOH, 0.3 mL/min, 220 nm): t_R: 13.924 min (major) and 14.724 min (minor).

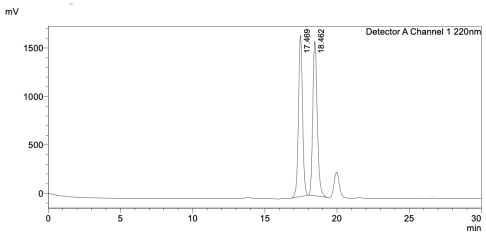

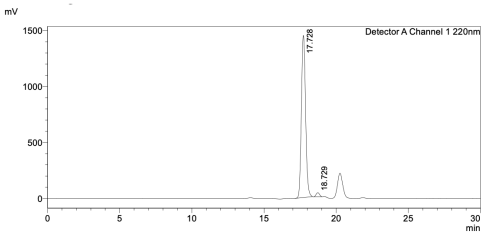

Peak #	Ret. Time (min)	Area %	Peak #	Ret. Time (min)	Area %
1	17.469	48.782	1	17.728	98.007
2	18.462	51.218	2	18.729	1.993

3.7.7. Gram-Scale Enantioselective Formal Synthesis of BACE-1 Inhibitor

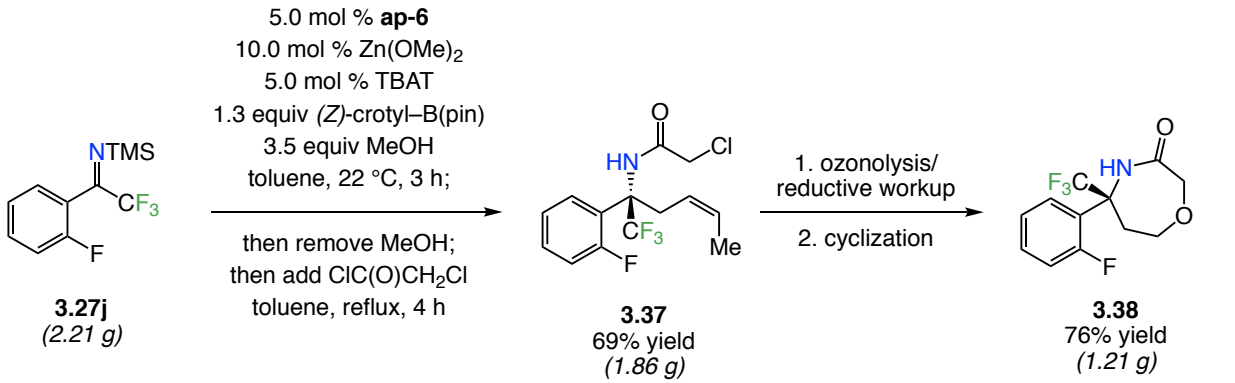

In a N_2-filled glovebox, an oven-dried vial containing a stir bar was charged with **ap-6** (0.146 g, 0.42 mmol) and $Zn(OMe)_2$ (0.107 g, 0.84 mmol). The solids were dissolved in toluene (42.0 mL) and the mixture was allowed to stir for 10 min, after which it was sequentially charged with NTMS-ketimine **3.27j** (2.21 g, 8.38 mmol), tbat (0.227 g, 0.42 mmol), *Z*-crotyl boronic pinacol ester (1.83 g, 10.1 mmol) and MeOH (0.940 g, 29.3 mmol). The solution was allowed to stir for five min in open vial and then the vial was capped and removed from the glovebox, after which the mixture was allowed to stir for three h at 22 °C. Reaction progress was monitored spectroscopically (^{19}F NMR) of aliquot samples until >98% conv. was reached. The volatiles were removed in vacuo to ~50 % of original volume (rotary evaporator), the solution was diluted with toluene (10 mL), and the volatiles were removed to ~50% volume; the azeotrope was carried out a total of three times. Toluene (5 mL) was added such that total volume was 20 mL and the resulting solution was allowed to cool to 0 °C (ice-bath). Chloroacetyl chloride (1.0 mL, 12.6 mmol) was added dropwise, the ice-bath was removed, and the mixture was allowed to heat for four h to 100 °C. The mixture was allowed to cool to 22 °C, the volatiles were removed in vacuo, and the resulting brown residue was purified by silica gel chromatography (hexanes → 2:1 hexanes:Et_2O) to afford white solid (1.86 g, 69% yield, 5.75 mmol).

(*R*,*Z*)-2-Chloro-*N*-(1,1,1-trifluoro-2-(2-fluorophenyl)hex-4-en-2-yl)acetamide (3.37): White solid, m.p. = 88–90 °C; **IR (neat):** 3298 (m), 3078 (m), 1682 (s), 1528 (s), 1490 (m), 1327 (m), 1227 (s), 759 (m) cm^{-1}; **^{1}H NMR (400 MHz, $CDCl_3$):** δ 7.43 (ddt, *J* = 8.4, 6.9, 1.3 Hz, 1H), 7.36 (dddd, *J* = 8.2, 7.4, 4.8, 1.7 Hz, 1H), 7.24–7.21 (m, 1H), 7.18 (ddd, *J* = 8.0, 7.4, 1.4 Hz, 1H), 7.08 (ddd, *J* = 13.1, 8.2, 1.4 Hz, 1H), 5.88–5.65 (m, 1H), 5.50–5.20 (m, 1H), 4.04 (s, 2H), 3.32–3.05 (m, 2H), 1.70 (ddt, *J* = 7.0, 1.9, 0.9 Hz, 3H); **^{13}C NMR (100 MHz, $CDCl_3$):** δ 164.8, 160.6 (d, *J* = 249.8 Hz), 130.7 (d, *J* = 9.5 Hz), 130.1, 128.9 (q, *J* = 88.9 Hz), 125.5 (q, *J* = 287.2 Hz), 124.4 (d, *J* = 3.4 Hz), 122.6 (d, *J* = 8.6 Hz), 122.2 (d, *J* = 1.6 Hz), 117.1 (d, *J* = 24.4 Hz), 63.7 (q, *J* = 27.7 Hz), 42.7, 31.4 (d, *J* = 3.4 Hz), 13.0; **^{19}F NMR (376 MHz, $CDCl_3$):** δ –72.9 (d, *J* = 8.6 Hz, 3F), –110.4 (dq, *J* = 13.6, 7.4 Hz, 1F); **HRMS (DART):** Calcd for $C_{14}H_{15}NF_4Cl$ $[M+H]^+$:

324.0773; Found: 324.0780; **Specific rotation:** $[\alpha]^{24.5}_{D}$ +14.7 (*c* 1.3, $CHCl_3$) for a 97:3 er sample.

The oxidation and cyclization steps were carried out according to a reported procedure.[234] An oven-dried flask equipped with a stir bar was charged with **3.37** (1.86 g, 5.75 mmol) and $NaHCO_3$ (0.745 g, 8.60 mmol). The solids were dissolved in CH_2Cl_2:MeOH (50.0:12.5 mL) and the resulting mixture was allowed to cool to –78 °C. Ozone was then introduced until blue color persisted (after ~ 45 min); the mixture was then purged with a stream of oxygen. At this time, $NaBH_4$ (435.1 mg, 11.5 mmol) was added (2 portions) and the solution was allowed to stir for 10 min, before allowing it to warm to 0 °C. The mixture was poured into a cold (0 °C) aqueous solution of 1M HCl (30 mL) and washed with Et_2O (3 x 25 mL). The combined organic layers were dried over Na_2SO_4, filtered, and concentrated in vacuo to afford colorless oil.

An oven-dried flask was charged with KO*t*-Bu (1.30 g, 11.6 mmol, 2.0 equiv.), *t*-BuOH (44 mL), and the solution was allowed to reach reflux (85 °C). A solution of the aforementioned alcohol, dissolved in thf (35 mL), was added slowly (over ~5 min), and the mixture was allowed to stir at reflux (85 °C) for 14 h before it allowed to cool to 0 °C. At this time, the reaction was quenched by addition of an aqueous solution of 1 M HCl (25 mL). The mixture was diluted with EtOAc (50 mL) and the organic layers were washed with brine (50 mL), dried over $MgSO_4$, and concentrated in vacuo to afford brown solid, which was purified by silica gel chromatography (100:0 → 1:2 hexanes:EtOAc) to afford **3.38** as white solid (1.21 g, 76% over 2 steps, 4.36 mmol).

(*R*)-5-(2-Fluorophenyl)-5-(trifluoromethyl)-1,4-oxazepan-3-one (3.38): White solid, m.p. = 129–131°C; **IR (neat):** 2953 (w), 2918 (w), 1628 (m), 1489 (m), 1247 (m), 1159 (s), 1009 (m), 819 (m), 784 (m), 643 (w) cm^{-1}; **^{1}H NMR (600 MHz, $CDCl_3$):** δ 7.55 (td, *J* = 8.0, 1.8 Hz, 1H), 7.44 (dddd, *J* = 8.2, 7.5, 4.8, 1.7 Hz, 1H), 7.29–7.24 (m, 1H), 7.14 (ddd, *J* = 12.5, 8.2, 1.3 Hz, 1H), 6.47 (s, 1H), 4.13 (q, *J* = 16.9 Hz, 2H), 3.91 (dd, *J* = 12.2, 6.1 Hz, 1H), 3.79–3.67 (m, 1H), 3.11 (dddt, *J* = 15.3, 4.6, 3.1, 1.6 Hz, 1H), 2.71 (tdd, *J* = 15.0, 6.2, 2.0 Hz, 1H); **^{13}C NMR (100 MHz, $CDCl_3$):** δ 174.6, 159.7 (d, *J* = 248.9 Hz), 130.1 (d, *J* = 3.4 Hz), 126.4, 125.0 (d, *J* = 3.4 Hz), 123.6, 121.7 (d, *J* = 12.0 Hz), 117.0 (d, *J* = 25.0 Hz), 70.0, 65.9, 63.7 (q, *J* = 28.9 Hz), 32.3 (d, *J* = 7.5 Hz); **^{19}F NMR (376 MHz, $CDCl_3$):** δ –79.9 (d, *J* = 16.1 Hz, 3F), –109.9 to –110.3 (m, 1F); **HRMS (DART):** Calcd for $C_{12}H_{12}NO_2F_4$ $[M+H]^+$: 278.0799; Found: 278.0805; **Specific rotation:** $[\alpha]^{25.0}_{D}$ +26.2 (*c* 1.7, $CHCl_3$).

(234) Badiger, S.; Chebrolu, M.; Frederiksen, M.; Holzer, P.; Hurth, K.; Li, L.; Liu, H.; Lueoend, R. M.; Machauer, R.; Moebitz, H.; Meumann, U.; Ramos, R.; Rueeger, H.; Schaefer, M.; Tintelnot-Blomley, M.; Veenstra, S. J.; Voegtle, M.; Xiong, X. PCT. Int. Appl. 2012006953.

3.7.8. Functionalization of Olefins

3.7.8.1. Directed epoxidation/ring-opening

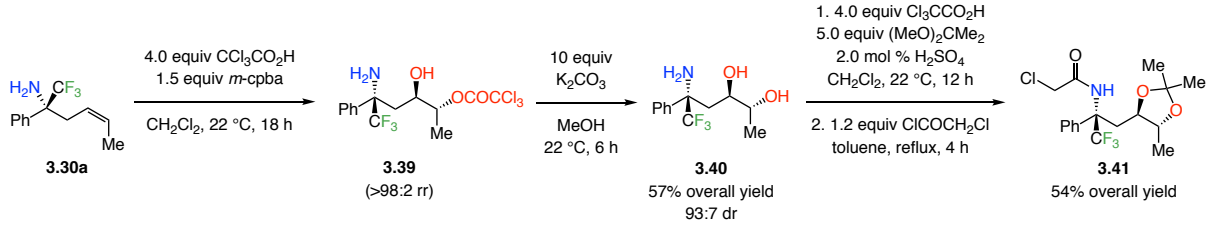

One-pot procedure (3.39): This sequence was carried out based on a procedure by Davies.[235] To a cooled (0 °C) solution of amine **3.30a** (126.0 mg, 0.55 mmol) in CH_2Cl_2 (2.0 mL) was added trichloroacetic acid (220 µL, 2.20 mmol) and the solution was allowed to stir for 30 min. The mixture was charged with *m*-cpba (188.7 mg, 0.82 mmol; single portion), after which it was allowed to warm to 22 °C, and stir for 18 h. The solution was diluted with CH_2Cl_2 (7.0 mL), and the reaction was quenched by the addition of a saturated aqueous solution of $NaHCO_3$ and $Na_2S_2O_3$. The pH was adjusted to 8 by the addition of a saturated solution of aqueous $NaHCO_3$. The aqueous layer was washed with CH_2Cl_2 (2 x 5.0 mL) and the combined organics were dried over Na_2SO_4 and concentrated to afford yellow residue which was purified by silica gel chromatography to afford the desired product as white solid.

(2*R*,3*R*,5*R*)-5-Amino-6,6,6-trifluoro-3-hydroxy-5-phenylhexan-2-yl-2,2,2-trichloroacetate (3.39): IR (neat): 3386 (w), 1760 (m), 1263 (m), 1155 (m), 1040 (w), 733 (s), 701 (s), 620 (m), 502 (m) cm^{-1}; **^{1}H NMR (600 MHz, $CDCl_3$):** δ 7.49 (d, *J* = 7.3 Hz, 2H), 7.45–7.33 (m, 3H), 4.94–4.84 (m, 1H), 3.46 (dd, *J* = 10.8, 3.6 Hz, 1H), 2.30 (d, *J* = 1.5 Hz, 1H), 2.26 (d, *J* = 1.5 Hz, 1H), 2.05 (dd, *J* = 14.2, 10.6 Hz, 2H), 1.36–1.28 (m, 3H); **^{13}C NMR (100 MHz, $CDCl_3$):** δ 166.1, 131.6, 129.8, 129.5, 127.3 (q, *J* = 157.3 Hz), 126.3, 94.5, 72.0, 70.8, 64.0 (q, *J* =27.3 Hz), 35.2, 19.4; **^{19}F NMR (376 MHz, $CDCl_3$):** δ –79.5 (s, 3F); **HRMS (DART):** Calcd for $C_{14}H_{16}NO_2F_3Cl_3$ $[M+H]^+$: 408.0142; Found: 408.0137; **Specific rotation:** $[\alpha]^{25.0}_D$ +9.4 (*c* 13.4, $CHCl_3$).

Trichloroacetate cleavage (3.40): To a solution of **3.39** in MeOH (8.0 mL) was added granular K_2CO_3 (304 mg, 5.5 mmol). The mixture was allowed to stir for 4 h at 22 °C, after which the volatiles were removed to ~10% of the original volume. The resulting yellow oil was passed through a (~5 cm) plug of silica gel eluting with Et_2O and then thoroughly flushed with EtOAc. The filtrate was concentrated, diluted with EtOAc, and dried over $MgSO_4$. The solids were filtered off and the filtrate was concentrated to afford yellow oil (82.5 mg, 57% yield, 0.314 mmol).

(235) Bond, C. W.; Cresswell, A. J.; Davies, S. G.; Fletcher, A. M.; Kurosawa, W.; Lee, J. A.; Roberts, P. M.; Russell, A. J.; Smith, A. D.; Thomson, J. E. *J.* Org. *Chem.* **2009**, *74*, 6735–6748.

(2*R*,3*R*,5*R*)-5-Amino-6,6,6-trifluoro-5-phenylhexane-2,3-diol (3.40): IR (neat): 3526 (br), 2920 (m), 1799 (m), 1763 (m), 1249 (s), 1153 (s), 644 (m) cm^{-1}; **^{1}H NMR (600 MHz, $CDCl_3$):** δ 7.55–7.32 (m, 5H), 5.12 (br, 1H), 3.52 (p, *J* = 6.1 Hz, 1H), 3.11 (ddd, *J* = 10.6, 5.0, 1.8 Hz, 1H), 2.38 (s, 1H), 2.22 (dd, *J* = 14.4, 1.8 Hz, 1H), 2.18 (s, 2H), 2.02 (dd, *J* = 14.4, 10.6 Hz, 1H), 1.07 (d, *J* = 6.3 Hz, 3H); **^{13}C NMR (100 MHz, $CDCl_3$):** δ 135.2, 129.0, 128.8, 126.6 (q, *J* = 286.8 Hz), 126.3 (q, *J* = 1.7 Hz), 72.2, 70.7, 62.3 (q, *J* = 26.4 Hz), 37.1, 19.2; **^{19}F NMR (376 MHz, $CDCl_3$):** δ –80.9 (s, 3F); **HRMS (DART):** Calcd for $C_{12}H_{17}NO_2F_3$ $[M+H]^+$: 264.1206; Found: 264.1208; **Specific rotation:** $[\alpha]^{25.0}_D$ +21.8 (*c* 2.3, $CHCl_3$).

Acetonide Formation (S-1): To a solution of diol **3.40** (82.2 mg, 0.30 mmol) in CH_2Cl_2 (0.6 mL) was added trichloroacetic acid (120 µL, 1.20 mmol) and the solution was allowed to stir for 30 min. Dimethoxypropane (183 µL, 1.50 mmol) was then added followed by conc. H_2SO_4 (25 µL). The solution was allowed to stir for 12 h, and then allowed to cool to 0 °C, after which the reaction was quenched by the addition of a saturated aqueous solution of $NaHCO_3$. At this point, NaOH (1M, 0.1 mL) was added until pH was ~9. The aqueous layer was washed with CH_2Cl_2 (2 x 5.0 mL) and the combined organic layers were washed with brine (5.0 mL), dried over Na_2SO_4, filtered and concentrated to afford yellow oil, which was purified by silica gel chromatography (gradient: 100:0 → 3:1 hexanes:Et_2O) to afford the desired product as colorless oil (72.8 mg, 80% yield, 0.24 mmol).

(*R*)-1,1,1-Trifluoro-2-phenyl-3-((4*R*,5*R*)-2,2,5-trimethyl-1,3-dioxolan-4-yl)propan-2-amine (S-1): IR (neat): 3413 (w), 2983 (w), 1616 (w), 1311 (m), 1148 (s), 1094 (s), 763 (m), 701 (s), 577 (w) cm^{-1}; **^{1}H NMR (600 MHz, $CDCl_3$):** δ 7.57 (d, *J* = 7.7 Hz, 2H), 7.40 (m, 3H), 3.77–3.66 (m, 1H), 3.18 (m, 1H), 2.42 (m, 1H), 2.12 (m, 3H), 2.08 (m, 1H), 1.37 (s, 3H), 1.25 (s, 3H), 1.10–1.02 (m, 3H); **^{13}C NMR (100 MHz, $CDCl_3$):** δ 137.6, 128.6, 128.4, 128.2 (q, *J* = 181.1 Hz), 127.2, 108.8, 78.4, 77.0, 61.8 (q, *J* =214.1 Hz), 38.0, 27.4, 27.3, 16.6; **^{19}F NMR (376 MHz, $CDCl_3$):** δ –79.2 (s, 3F): **HRMS (DART):** Calcd for $C_{15}H_{21}NO_2F_3$ $[M+H]^+$: 304.1519; Found: 304.1523; **Specific rotation:** $[\alpha]^{25.0}_D$ +32.6 (*c* 5.7, $CHCl_3$).

Amide (3.41): To a solution of **S-1** (22.5 mg, 0.074 mmol) in toluene (0.5 mL) was added dropwise chloroacetyl chloride (12.5 mg, 0.11 mmol), and the resulting solution was allowed to heat to 100 °C in a sealed vial for 4 h. The mixture was then allowed to cool to 22 °C, the volatiles were removed in vacuo, and the resulting brown residue was purified by silica gel chromatography (hexanes → 2:1 hexanes:Et_2O) to afford **3.41** (19.0 mg, 68% yield, 0.50 mmol) as white solid.

2-Chloro-*N*-((*R*)-1,1,1-trifluoro-2-phenyl-3-((4*R*,5*R*)-2,2,5-trimethyl-1,3-dioxolan-4-yl)propan-2-yl)acetamide (3.41): White solid, m.p. = 129–131°C; **IR (neat):** 3321 (br), 2982 (w), 1704 (m), 11542 (m), 1233 (s), 1165 (s), 1025 (m), 700 (m), 628 (w) cm^{-1}; **^{1}H NMR (600 MHz, $CDCl_3$):** δ 8.30 (s, 1H), 7.38 (m, 5H), 4.18–4.05 (m, 2H), 3.80–3.69 (m, 1H), 3.21 (t, *J* =

9.2 Hz, 1H), 2.30 (dd, *J* = 14.6, 9.8 Hz, 1H), 2.20 (d, *J* = 14.4 Hz, 1H), 1.43 (s, 3H), 1.37 (s, 3H), 1.03 (d, *J* = 6.0 Hz, 3H); **^{13}C NMR (100 MHz, $CDCl_3$):** δ 165.3, 134.1, 128.9, 128.7, 126.0, 124.8 (q, *J* = 122.1 Hz), 109.4, 77.7, 77.3, 62.4 (q, *J* = 44.1 Hz), 43.0, 39.1, 27.4, 27.2, 16.5; **^{19}F NMR (376 MHz, $CDCl_3$):** δ –68.5 (s, 3F); **HRMS (DART):** Calcd for $C_{17}H_{22}NO_3F_3Cl$ $[M+H]^+$: 380.1223; Found: 380.1229; **Specific rotation:** $[\alpha]^{25.0}_D$ +21.5 (*c* 1.9, $CHCl_3$).

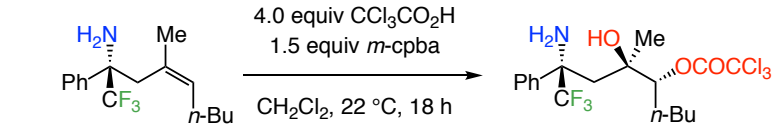

3.35a
98:2 *α*:*γ*, 88% yield (pure *α*)
98:2 *Z*:*E*, 88.5:11.5 er

3.42
72% yield
>98:2 rr, 91:9 dr

(2*R*,4*R*,5*R*)-2-Amino-1,1,1-trifluoro-4-hydroxy-4-methyl-2-phenylnonan-5-yl-2,2,2-trichloroacetate (3.42) was synthesized according to the above procedure to afford the product as yellow oil (66.9 mg, 72% yield, 0.144 mmol). **IR (neat):** 3383 (w), 2955 (m), 1761 (m), 1233 (s), 1155 (s), 990 (m), 825 (s), 737 (s), 704 (s), 676 (s), 576 (w) cm^{-1}; **^{1}H NMR (600 MHz, $CDCl_3$ & CD_2Cl_2):** δ 7.56–7.50 (m, 2H), 7.44–7.38 (m, 3H), 4.83 (dd, *J* = 10.7, 2.1 Hz, 1H), 2.38 (d, *J* = 14.7 Hz, 1H), 2.22 (d, *J* = 14.6 Hz, 1H), 1.42–1.28 (m, 6H), 1.27 (s, 2H), 0.93–0.90 (m, 3H), 0.63 (s, 3H); **^{13}C NMR (100 MHz, Acetone-d6):** δ 162.4, 138.1, 135.8, 129.7 (q, *J* = 93.9 Hz), 129.2, 128.2, 88.2, 74.4, 62.9 (q, *J* = 25.6 Hz), 55.1, 38.1, 29.2, 29.2, 24.6, 23.1, 14.3; **^{19}F NMR (376 MHz, acetone-d_6):** δ –79.5 (s, 3F); **HRMS (DART):** Calcd for $C_{18}H_{24}NO_3F_3Cl_3$ $[M+H]^+$: 464.0768; Found: 464.0774; **Specific rotation:** $[\alpha]^{25.0}_D$ +27.6 (*c* 7.3, $CHCl_3$).

3.7.8.2. Cross-coupling reactions

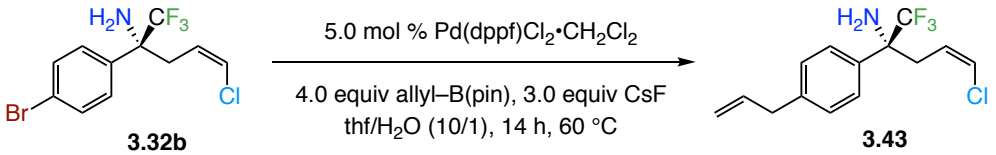

3.32b

3.43
71% yield, >98:2 *Z*:*E*

(*R*,*Z*)-2-(4-Allylphenyl)-5-chloro-1,1,1-trifluoropent-4-en-2-amine (3.43): In a N_2-filled glovebox, an oven-dried two-dram vial equipped with a stir bar was charged with amine **3.32b** (20.8 mg, 0.063 mmol), $Pd(dppf)Cl_2•CH_2Cl_2$ (1.3 mg, 0.00158 mmol) and thf (0.62 mL). The solution was stirred for five minutes at 22 °C, then allyl–B(pin) (47.3 μL, 0.252 mmol) and CsF (28.7 mg, 0.186 mmol) were added. The vial was sealed with a Teflon septa cap and removed from the glovebox. Water (0.6 mL) was added to the vial and the solution was allowed stir at 60 °C for 14 h. The solution was then allowed to cool to 22 °C, filtered through a small (~5 cm) plug of silica gel eluting with Et_2O after which the volatiles were removed in vacuo to afford brown

residue, which was purified by silica gel chromatography (gradient: 100:00 → 2:1 hexanes/Et_2O) to afford **17** as colorless oil (26.9 mg, 93% yield, 0.059 mmol). **IR (neat):** 3078 (m), 2921 (m), 2851 (m), 1637 (w), 1149 (s), 915 (m), 804 (m), 721 (m), 527 (w) cm^{-1}; **^{1}H NMR (600 MHz, $CDCl_3$):** δ 7.48 (d, *J* = 8.1 Hz, 2H), 7.22 (d, *J* = 8.0 Hz, 2H), 6.10 (d, *J* = 7.3 Hz, 1H), 5.97 (dq, *J* = 15.8, 7.2 Hz, 1H), 5.55 (q, *J* = 7.1 Hz, 1H), 5.14–5.04 (m, 2H), 3.40 (d, *J* = 6.7 Hz, 2H), 3.08 (dd, *J* = 15.5, 6.6 Hz, 1H), 2.87 (dd, *J* = 15.5, 7.1 Hz, 1H), 1.79 (s, 2H); **^{13}C NMR (100 MHz, $CDCl_3$):** δ 140.5, 137.1, 135.1, 130.3, 128.1, 126.7 (q, *J* = 287.9 Hz), 125.2, 121.8, 116.3, 61.2 (q, *J* = 26.7 Hz), 39.8, 33.9; **^{19}F NMR (376 MHz, $CDCl_3$):** δ –78.8 (s, 3F); **HRMS (DART):** Calcd for $C_{14}H_{16}NF_3Cl$ $[M+H]^+$: 290.0918; Found: 290.0914; **Specific rotation:** $[\alpha]^{25.0}_D$ +0.8 (*c* 1.1, $CHCl_3$).

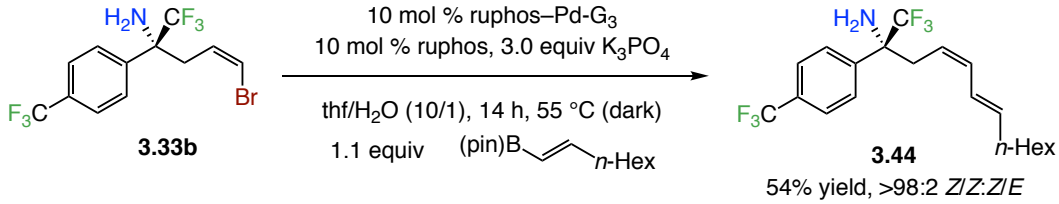

(*R*,4*Z*,6*E*)-1,1,1-Trifluoro-2-(4-(trifluoromethyl)phenyl)trideca-4,6-dien-2-amine (3.44): In a N_2-filled glovebox, an oven-dried two-dram vial equipped with a stir bar was charged with **3.33b** (20.9 mg, 0.058 mmol), alkenyl–B(pin) (16.5 mg, 0.69 mmol), and thf (0.53 mL). The mixture was allowed to stir for five min at 22 °C after which ruphos–Pd-G_3 (4.85 mg, 0.0058 mmol), ruPhos (2.71 mg, 0.0058 mmol), and K_3PO_4 (12.3 mg, 0.17 mmol) were added. The vial was capped and removed from the glovebox, after which water (53 μL) was added, and the vial was wrapped in aluminum foil. The solution was then allowed stir for 14 h at 60 °C, after which it was allowed to cool to room temperature, and % conv. determined by analysis of ^{1}H and ^{19}F NMR spectra. Removal of the volatiles in vacuo and purification of the orange oil by silica gel chromatography (elution with hexanes/Et_2O) to afford **3.44** as yellow oil (12.2 mg, 54% yield, 0.031 mmol). **IR (neat):** 2955 (m), 1621 (w), 1412 (w), 1325 (s), 1156 (s), 1125 (s), 1070 (s), 834 (m), 725 (w) cm^{-1}; **^{1}H NMR (600 MHz, $CDCl_3$):** δ 7.74 (d, *J* = 8.3 Hz, 2H), 7.64 (d, *J* = 8.4 Hz, 2H), 6.34–6.14 (m, 1H), 6.07 (dd, *J* = 11.8, 10.1 Hz, 1H), 5.73 (dt, *J* = 14.5, 7.0 Hz, 1H), 4.97 (q, *J* = 8.1 Hz, 1H), 2.99 (dd, *J* = 15.1, 7.1 Hz, 1H), 2.86 (dd, *J* = 15.1, 7.9 Hz, 1H), 2.10 (q, *J* = 7.2 Hz, 2H), 1.78 (s, 2H), 1.49–1.17 (m, 8H), 0.96–0.79 (m, 3H); **^{13}C NMR (100 MHz, $CDCl_3$):** δ 141.8, 138.0, 133.7, 130.6 (q, *J* = 32.7 Hz), 127.7, 125.4, 125.4 (q, *J* = 286.4 Hz), 124.73, 124.3 (q, *J* = 221.6 Hz), 120.2, 61.9 (q, *J* = 26.0 Hz), 34.4, 33.1, 31.9, 29.4, 29.1, 22.8, 14.2; **^{19}F NMR (376 MHz, $CDCl_3$):** δ –62.8 (s, 3F), –77.7 (s, 3F); **HRMS (DART):** Calcd for $C_{20}H_{26}NF_6$ $[M+H]^+$: 394.1964; Found: 394.1961; **Specific rotation:** $[\alpha]^{25.0}_D$ +16.0 (*c* 1.3, $CHCl_3$).

3.7.9. NMR Spectra

NMR spectra appear on the following pages:

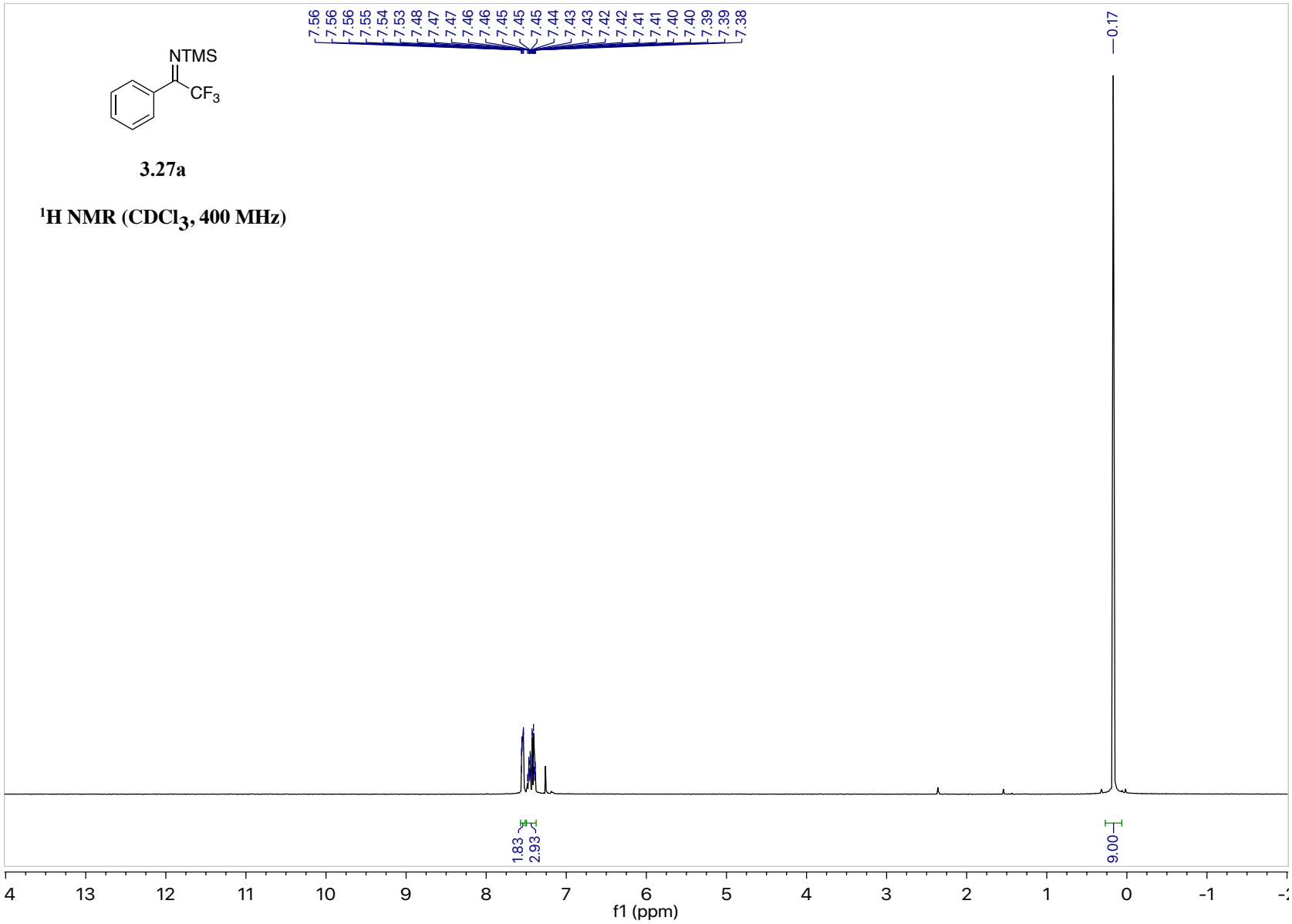
NTMS
CF3
3.27a
1H NMR (CDCl3, 400 MHz)
7.56
7.56
7.56
7.55
7.54
7.53
7.48
7.47
7.47
7.46
7.46
7.45
7.45
7.45
7.44
7.43
7.43
7.42
7.42
7.41
7.41
7.40
7.40
7.39
7.39
7.38
0.17
1.83
2.93
9.00
f1 (ppm)

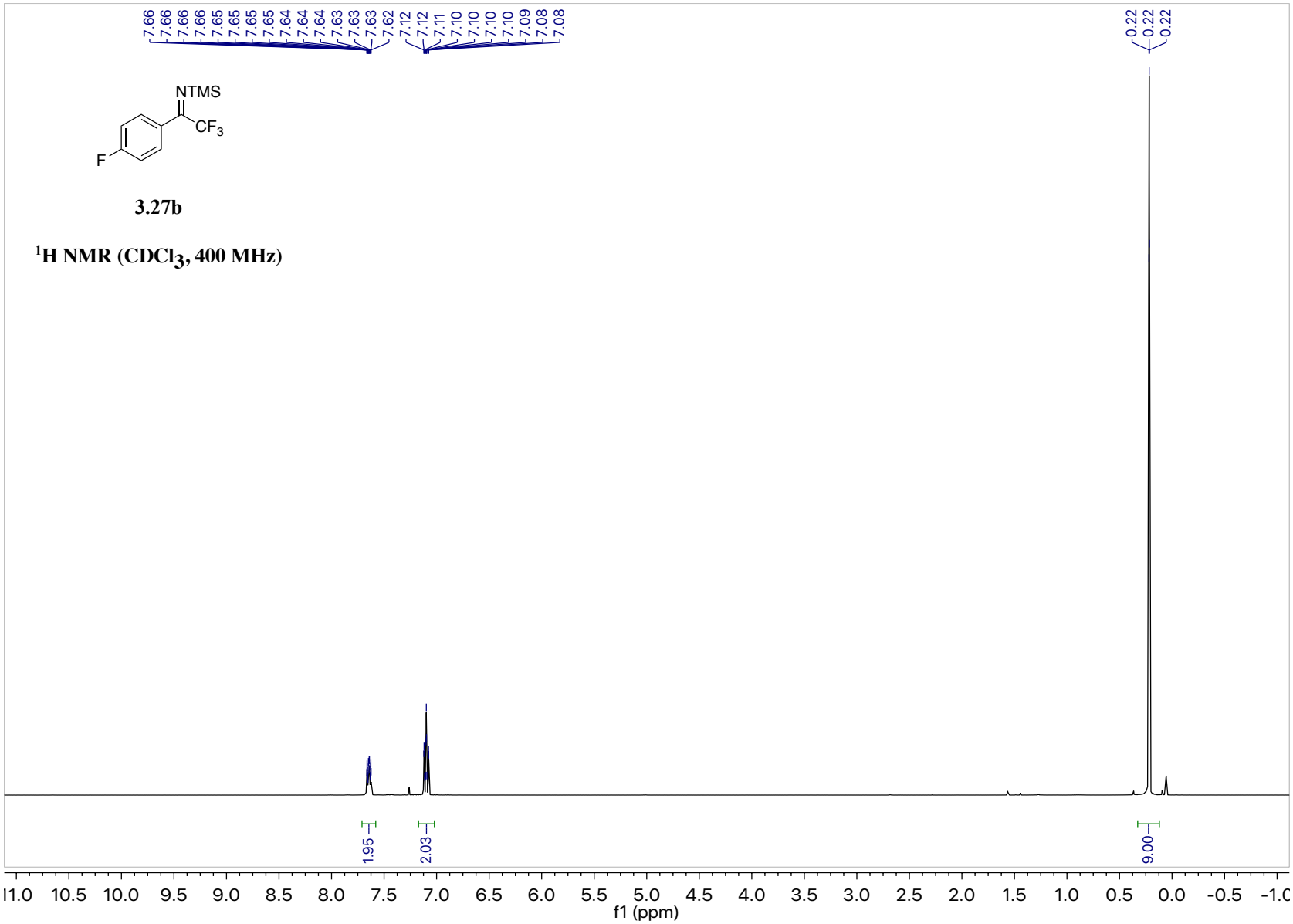

3.27b

^{1}H NMR ($CDCl_3$, 400 MHz)

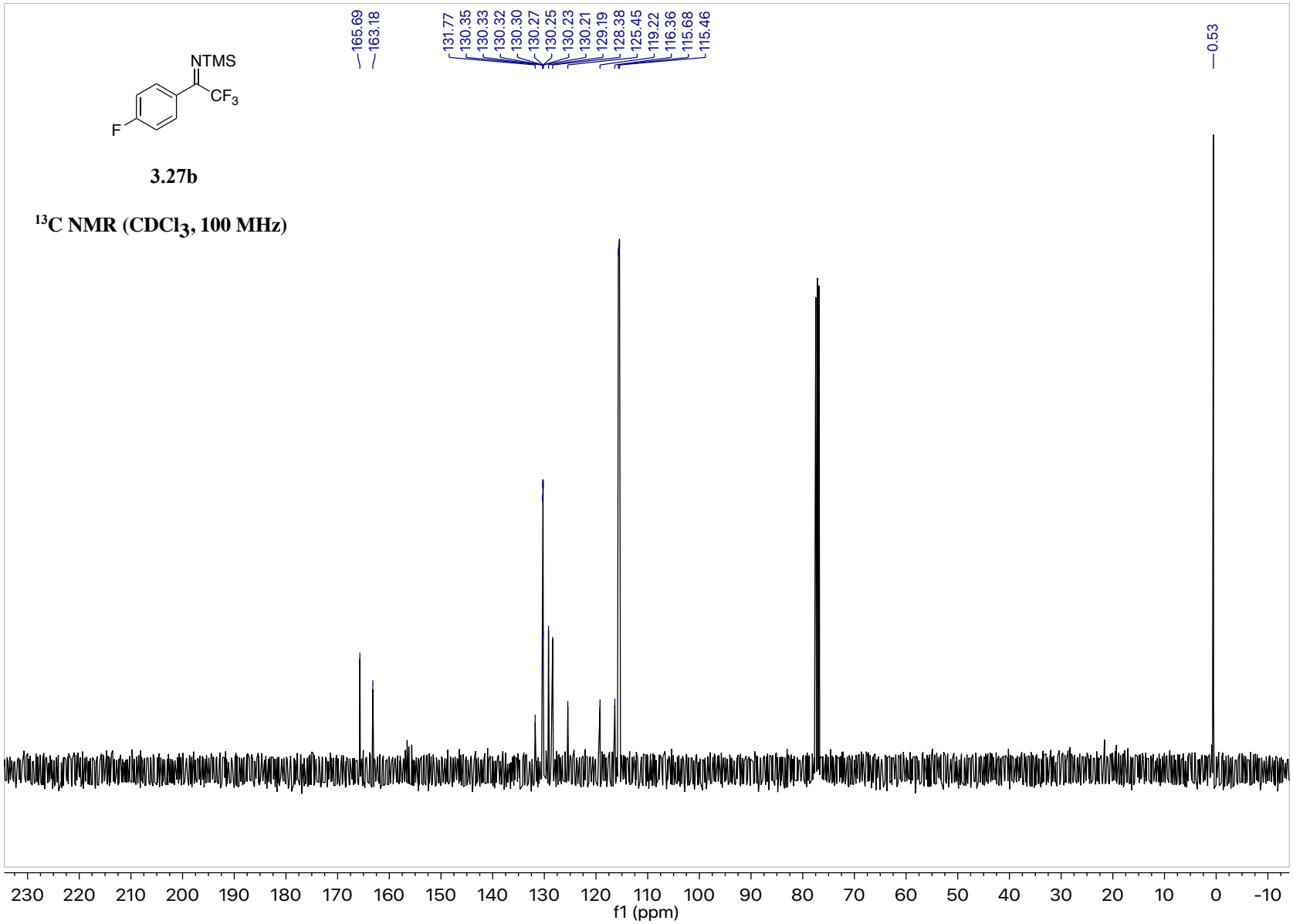
NTMS
CF3
F
3.27b
13C NMR (CDCl3, 100 MHz)
165.69
163.18
131.77
130.35
130.33
130.32
130.30
130.27
130.25
130.23
130.21
129.19
128.38
125.45
119.22
116.36
115.68
115.46
0.53
230 220 210 200 190 180 170 160 150 140 130 120 110 100 90 80 70 60 50 40 30 20 10 0 -10
f1 (ppm)

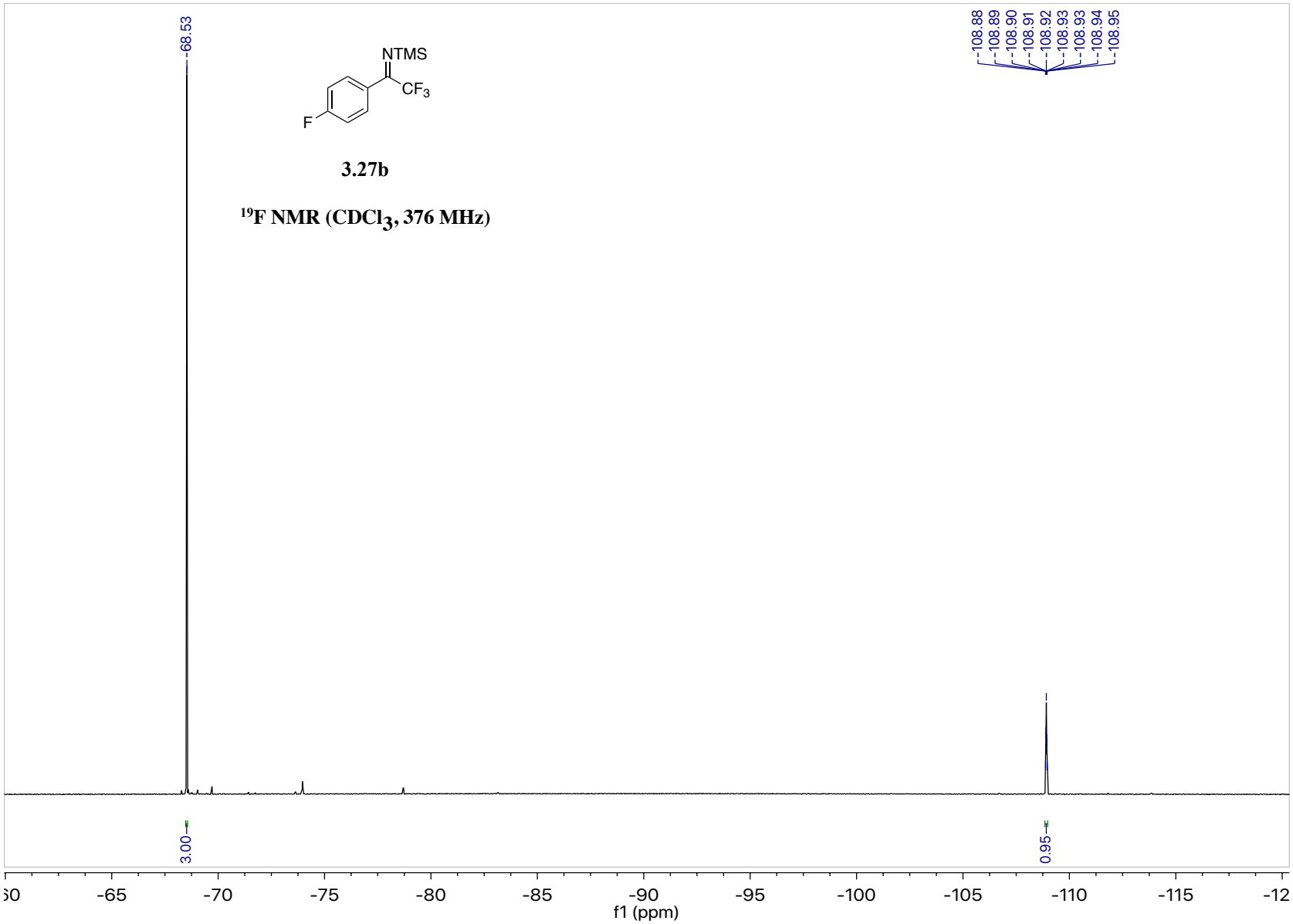

3.27b

^{19}F NMR ($CDCl_3$, 376 MHz)

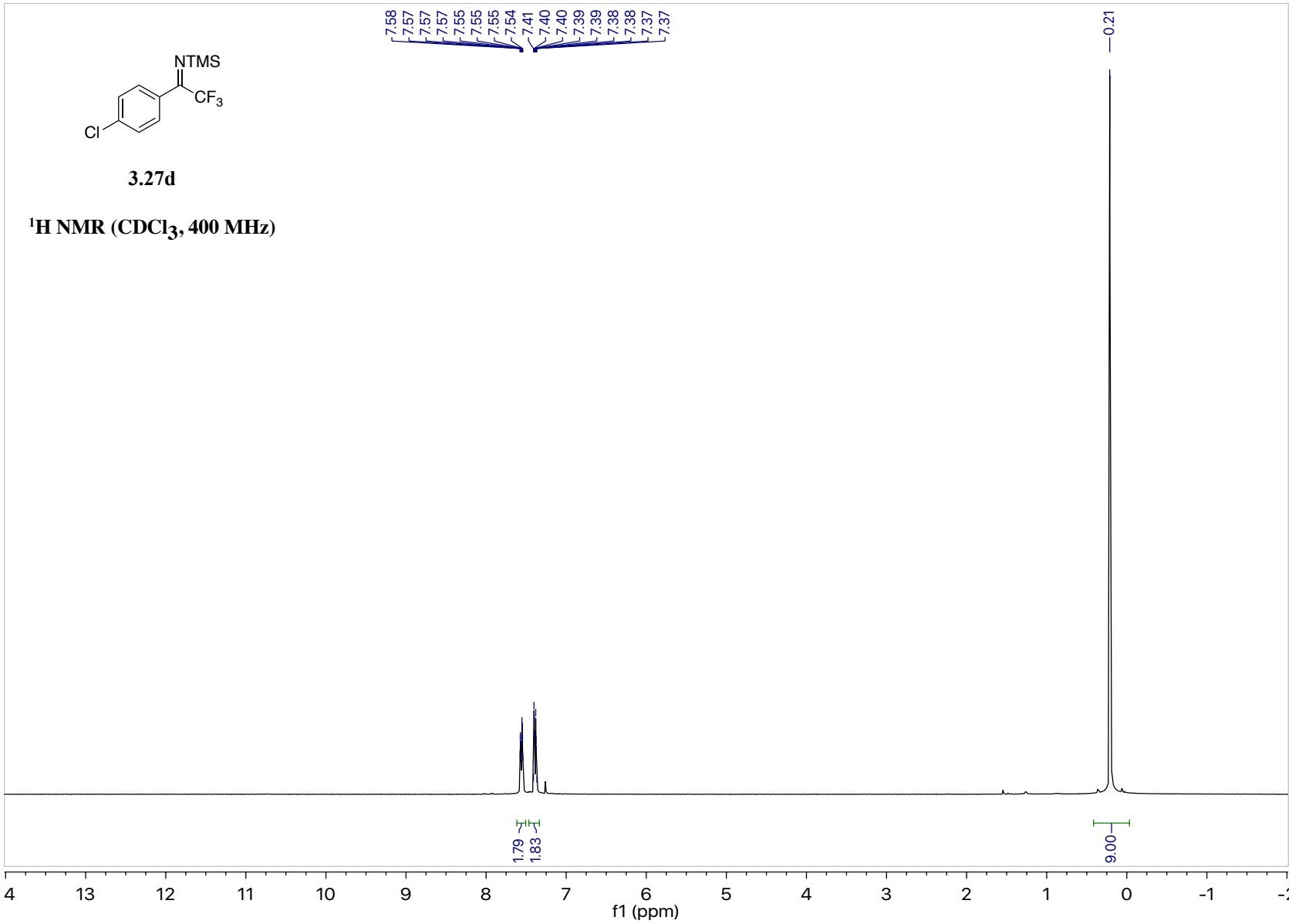
NTMS
CF3
Cl
3.27d
1H NMR (CDCl3, 400 MHz)
7.58
7.57
7.57
7.57
7.55
7.55
7.55
7.54
7.41
7.40
7.40
7.39
7.39
7.38
7.38
7.37
7.37
0.21
1.79
1.83
9.00
f1 (ppm)

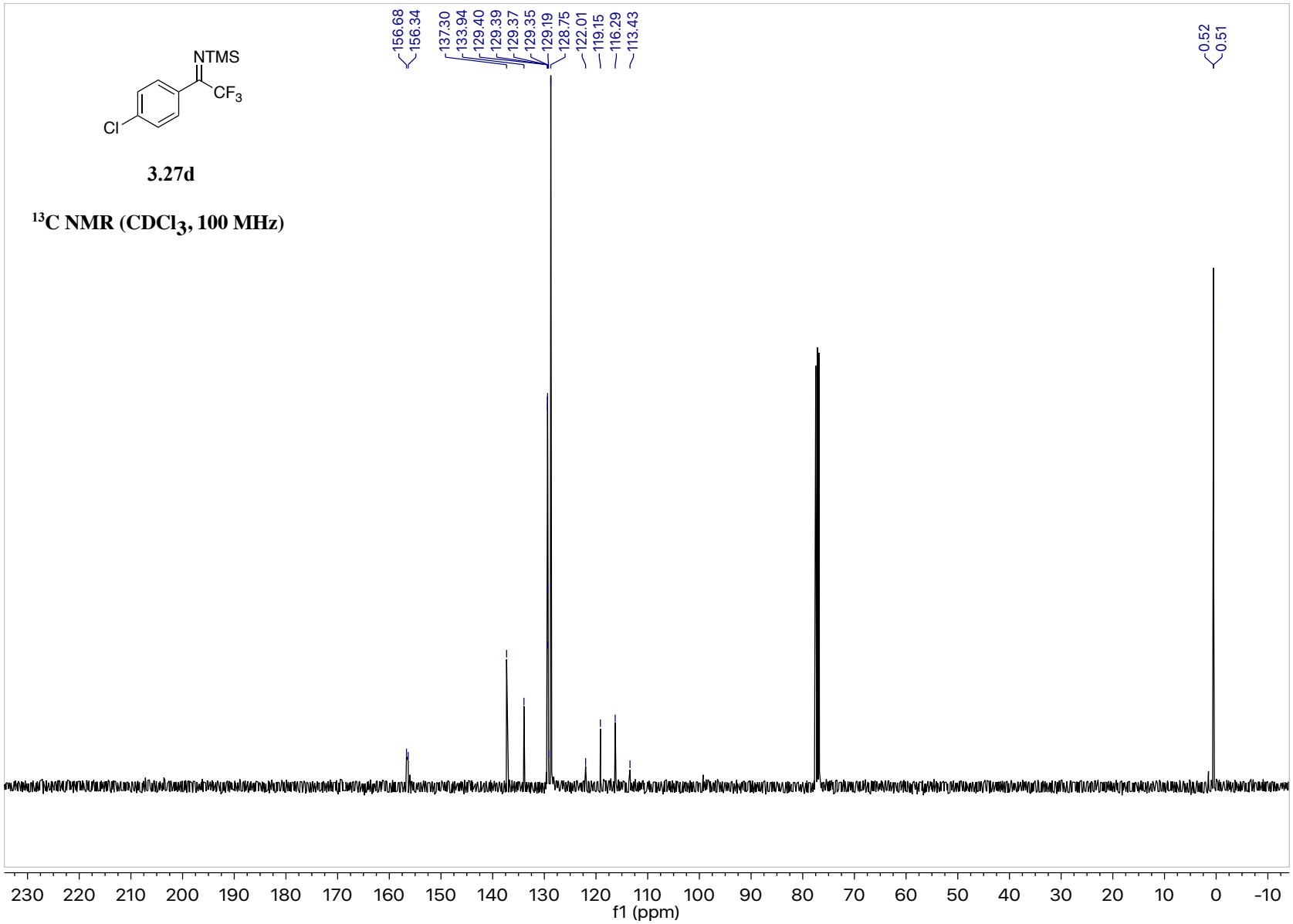
NTMS
CF3
Cl
3.27d
13C NMR (CDCl3, 100 MHz)
156.68
156.34
137.30
133.94
129.40
129.39
129.37
129.35
129.19
128.75
122.01
119.15
116.29
113.43
0.52
0.51
f1 (ppm)

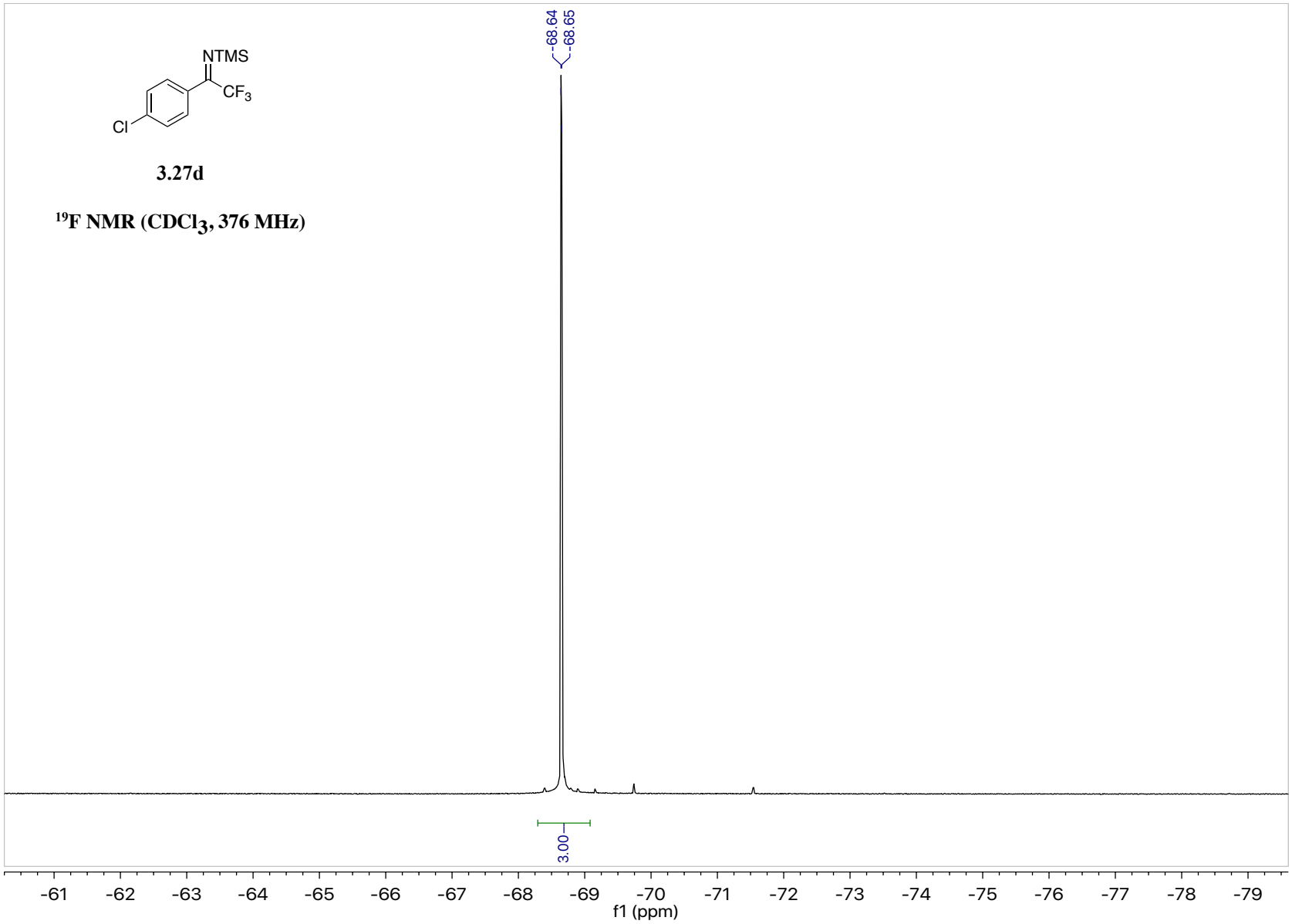
NTMS
CF3
Cl
3.27d
19F NMR (CDCl3, 376 MHz)
-68.64
-68.65
3.00
-61
-62
-63
-64
-65
-66
-67
-68
-69
-70
-71
-72
-73
-74
-75
-76
-77
-78
-79
f1 (ppm)

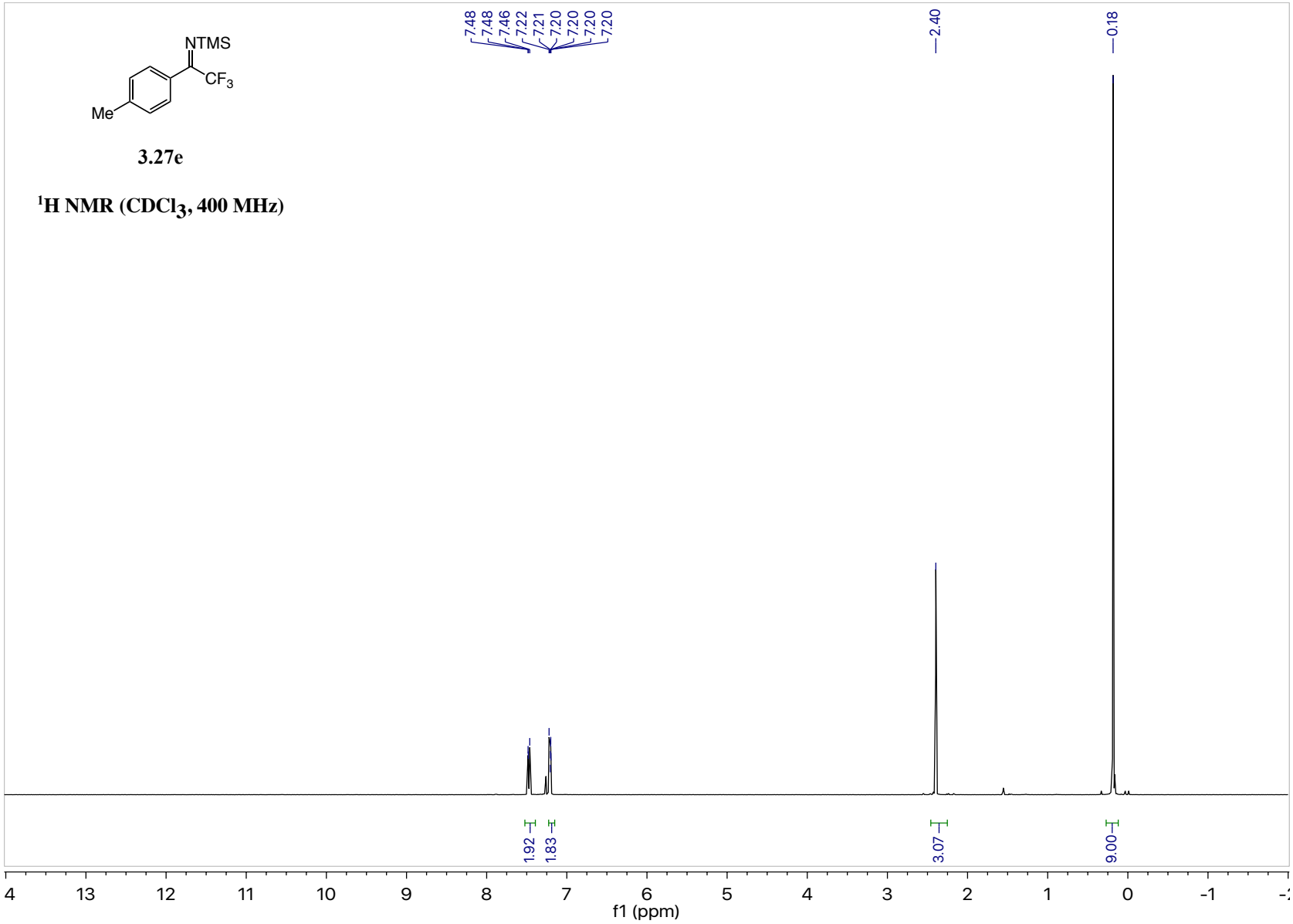

3.27e

^{1}H NMR ($CDCl_3$, 400 MHz)

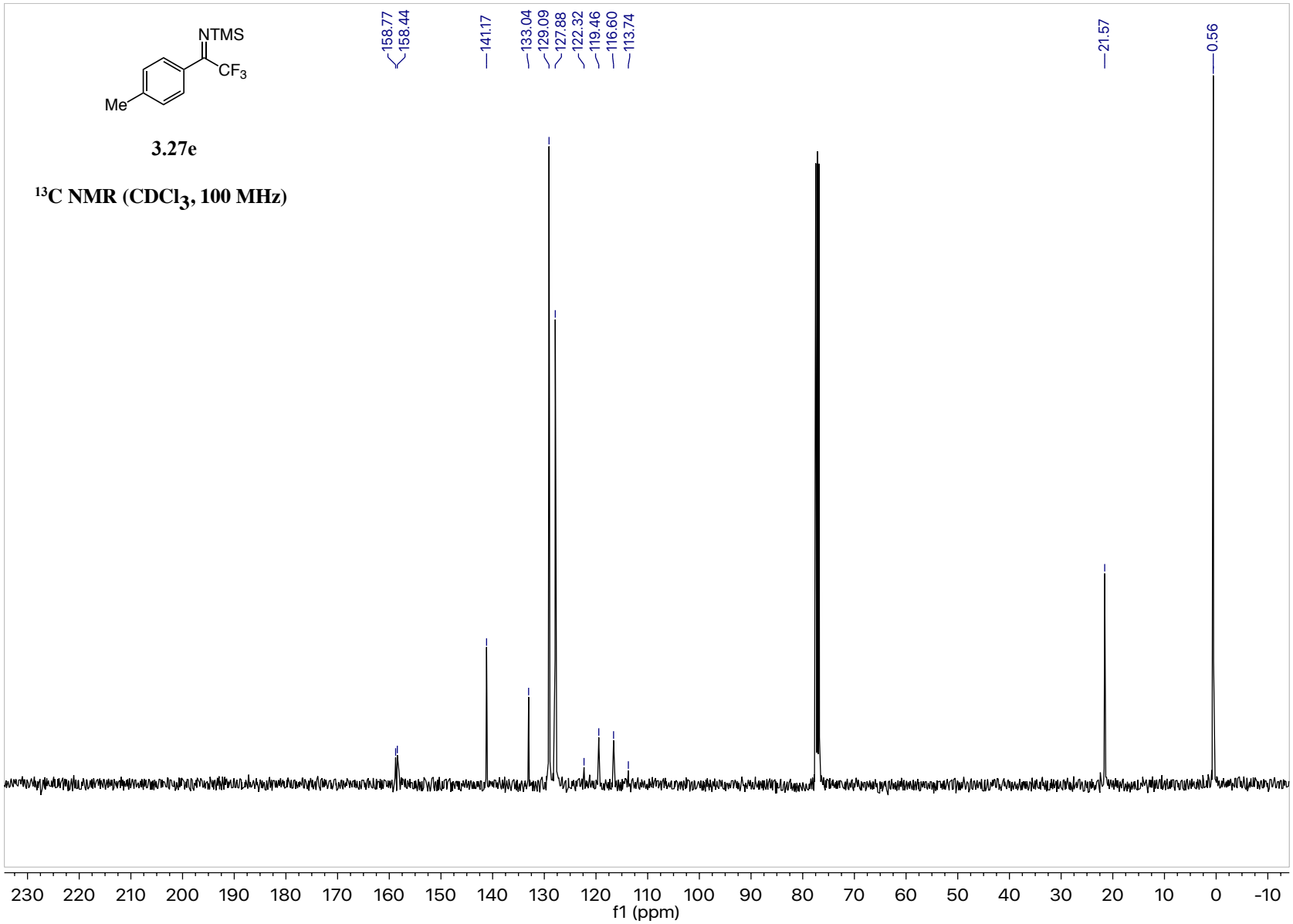
NTMS
CF3
Me
3.27e
13C NMR (CDCl3, 100 MHz)
158.77
158.44
141.17
133.04
129.09
127.88
122.32
119.46
116.60
113.74
21.57
0.56
230 220 210 200 190 180 170 160 150 140 130 120 110 100 90 80 70 60 50 40 30 20 10 0 -10
f1 (ppm)

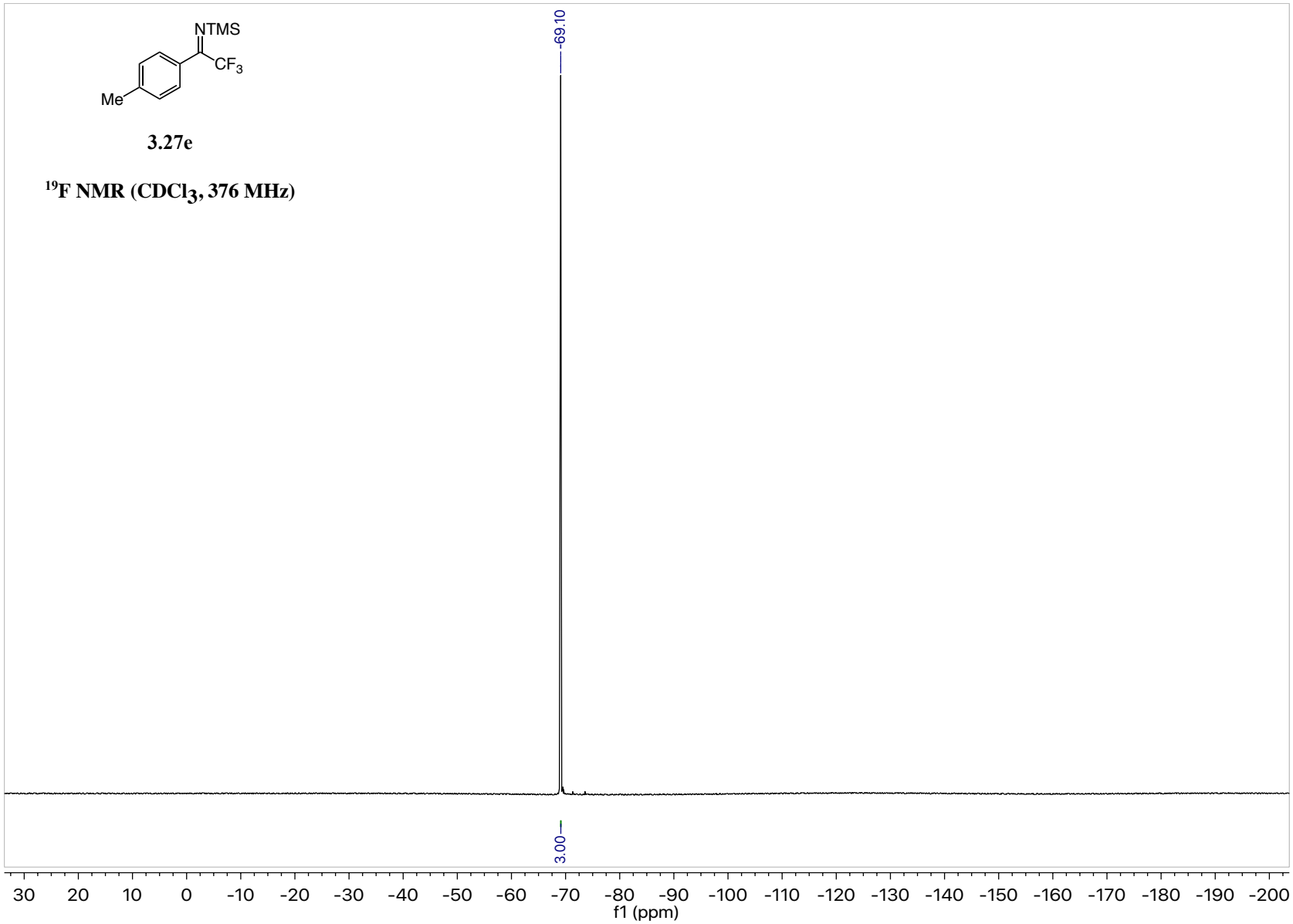
NTMS
CF3
Me
3.27e
19F NMR (CDCl3, 376 MHz)
-69.10
3.00
30 20 10 0 -10 -20 -30 -40 -50 -60 -70 -80 -90 -100 -110 -120 -130 -140 -150 -160 -170 -180 -190 -200
f1 (ppm)

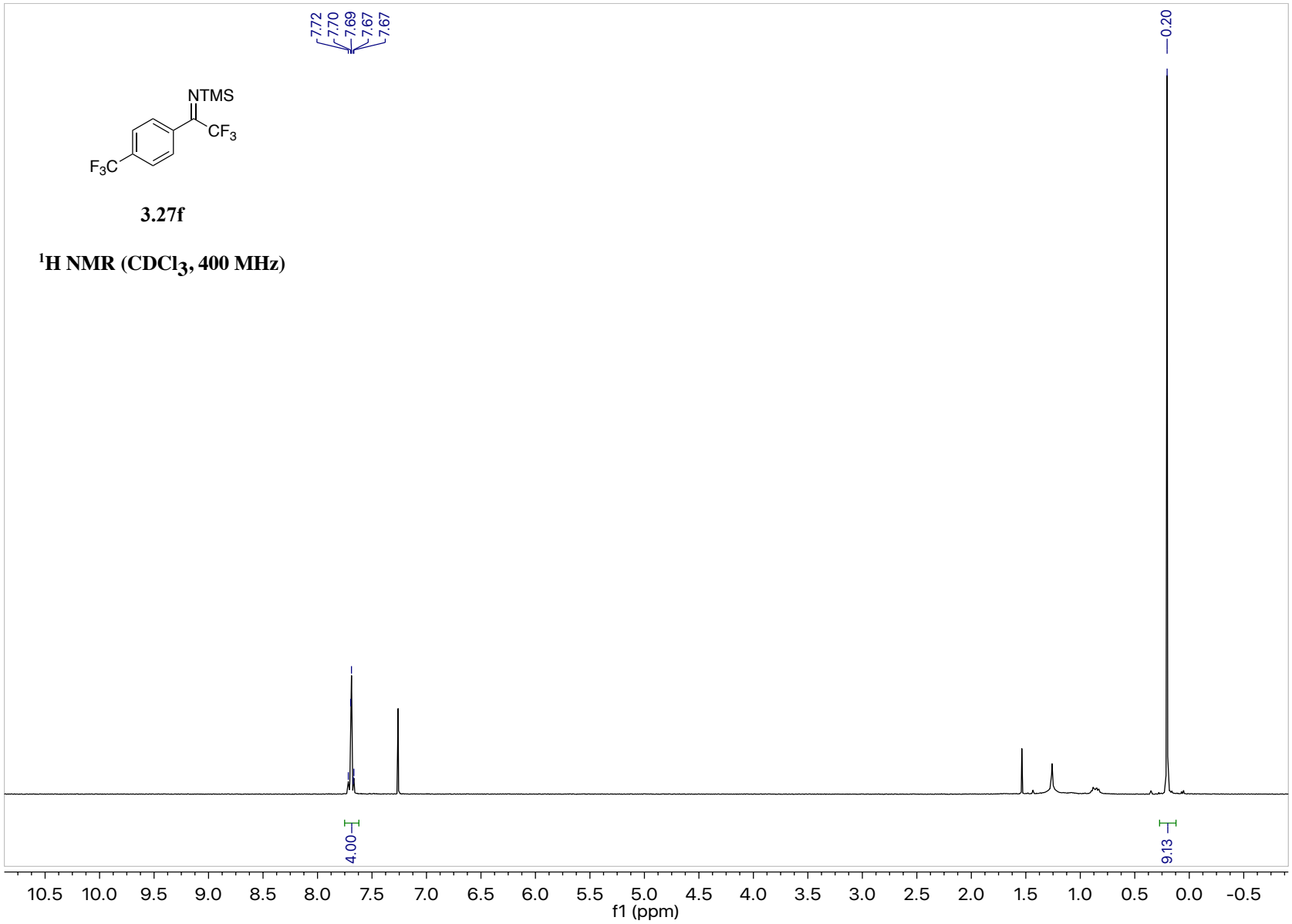

3.27f

^{1}H NMR ($CDCl_3$, 400 MHz)

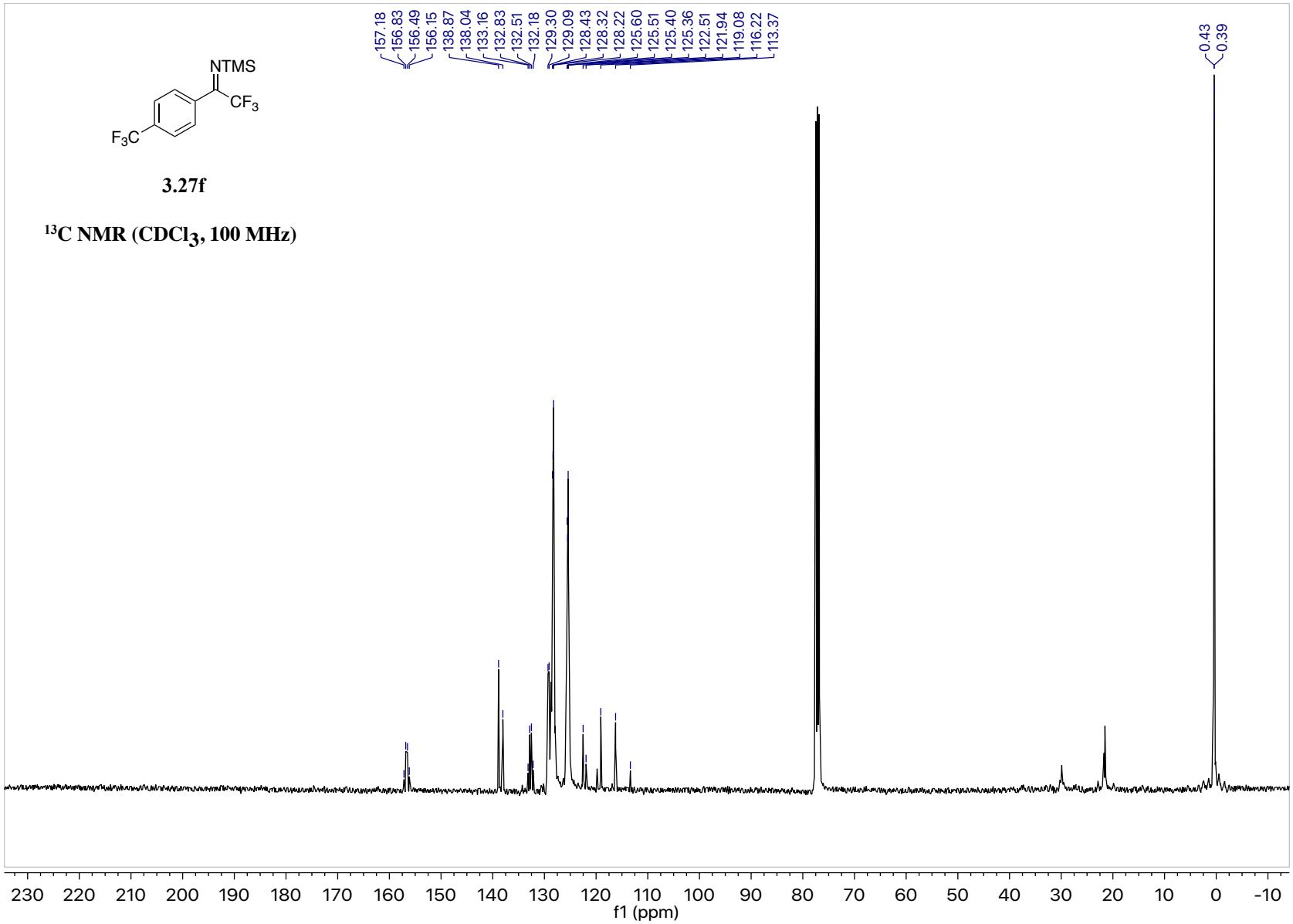

3.27f

^{13}C NMR ($CDCl_3$, 100 MHz)

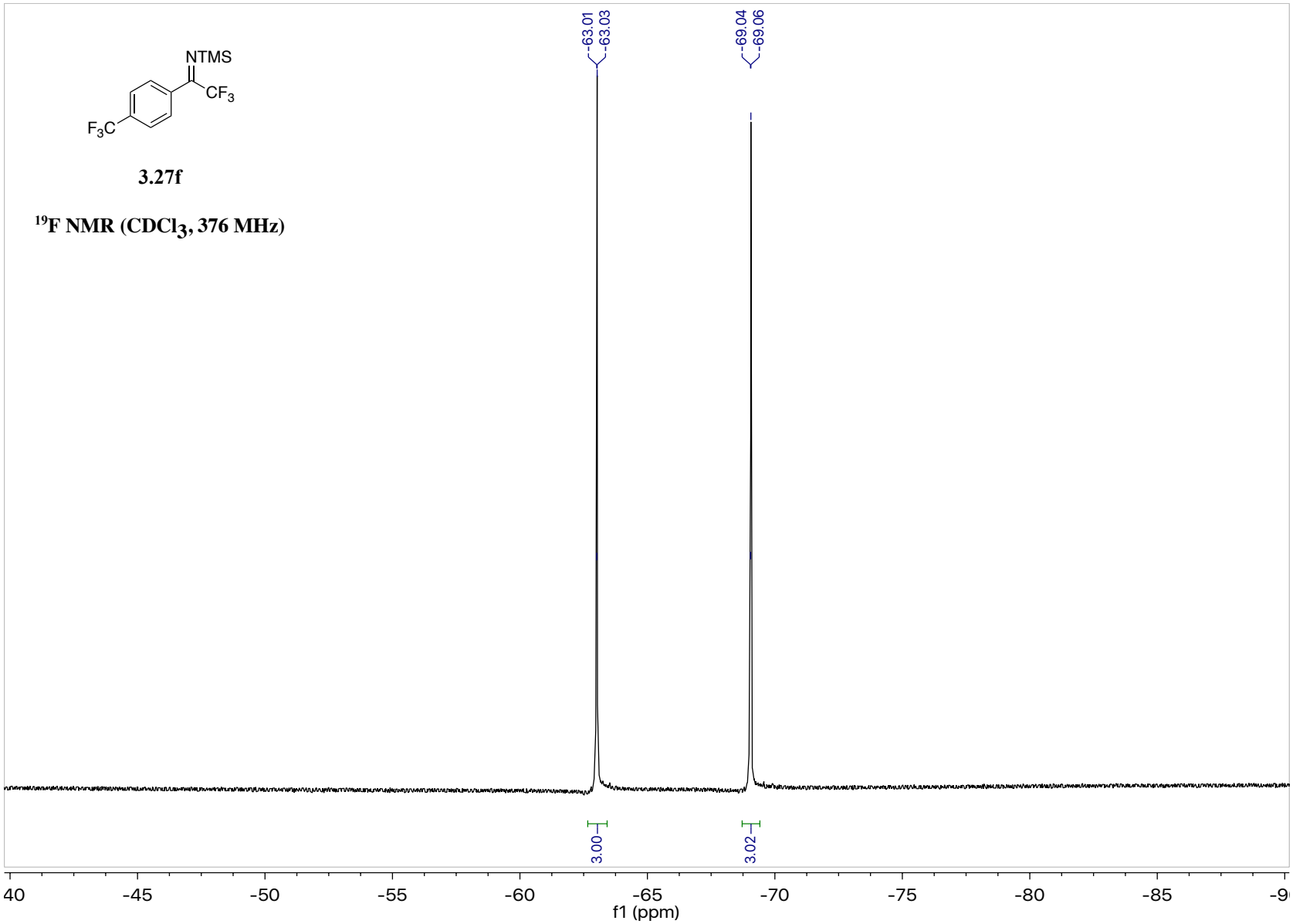

3.27f

^{19}F NMR ($CDCl_3$, 376 MHz)

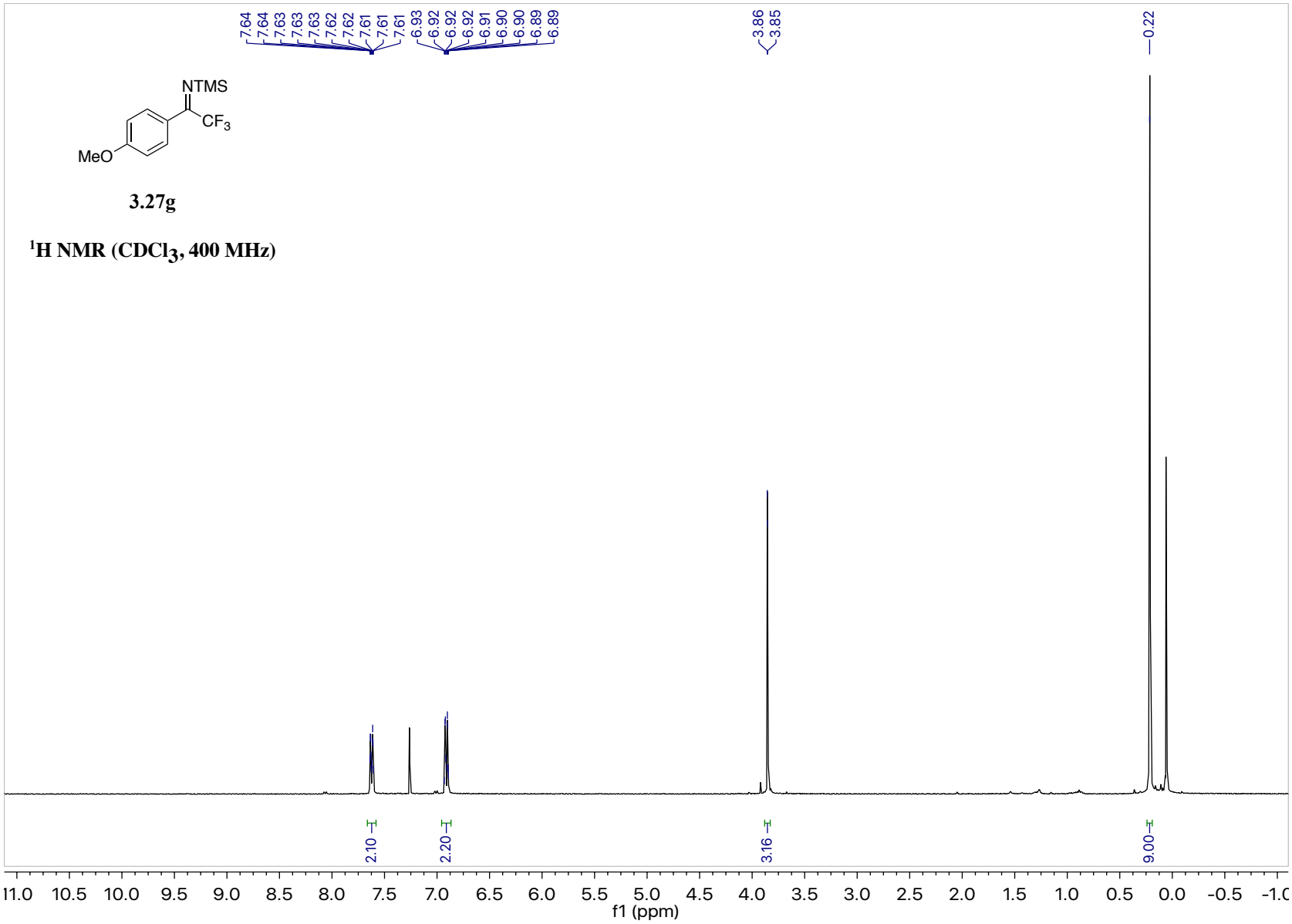

3.27g

^{1}H NMR ($CDCl_3$, 400 MHz)

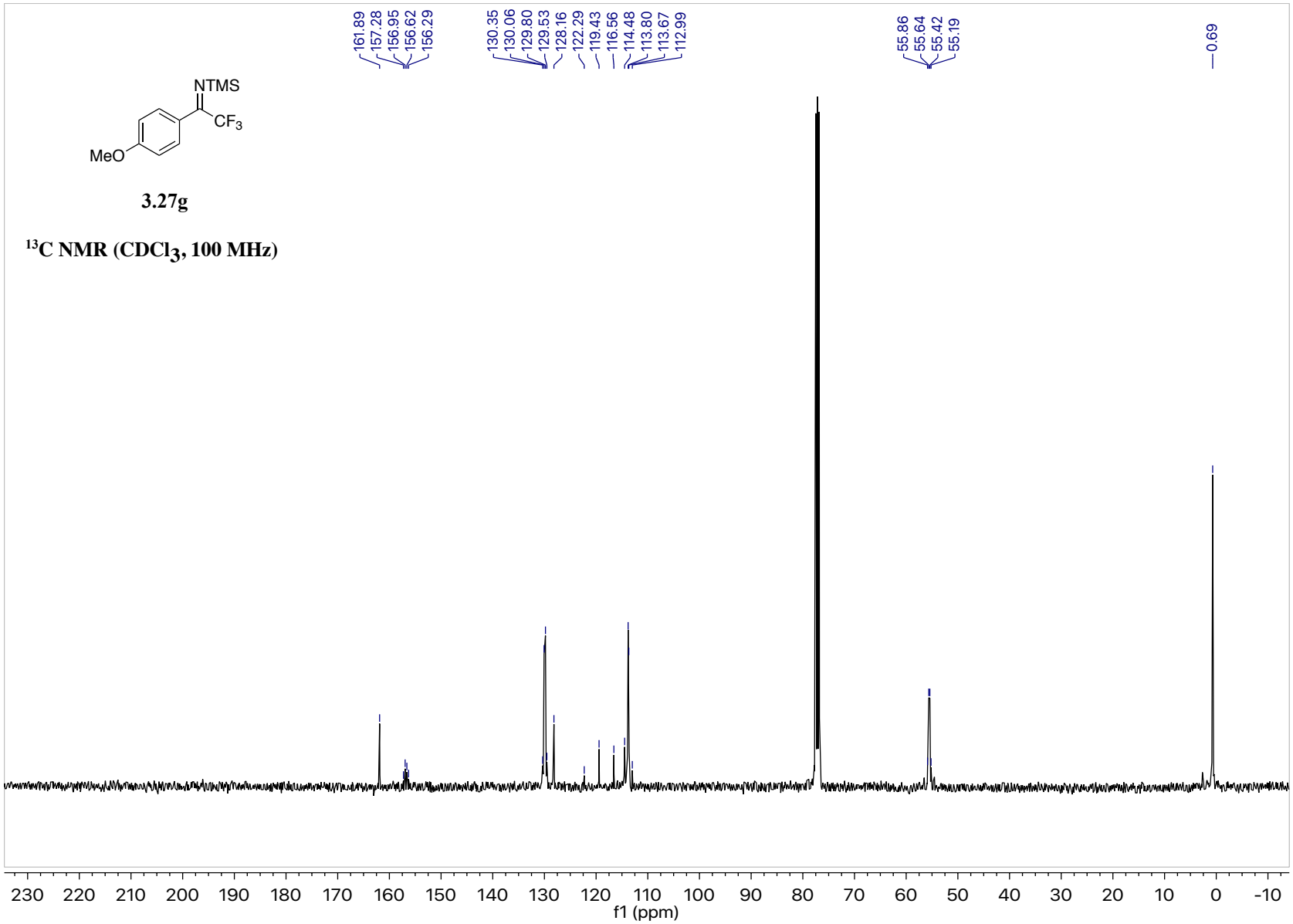

3.27g

^{13}C NMR ($CDCl_3$, 100 MHz)

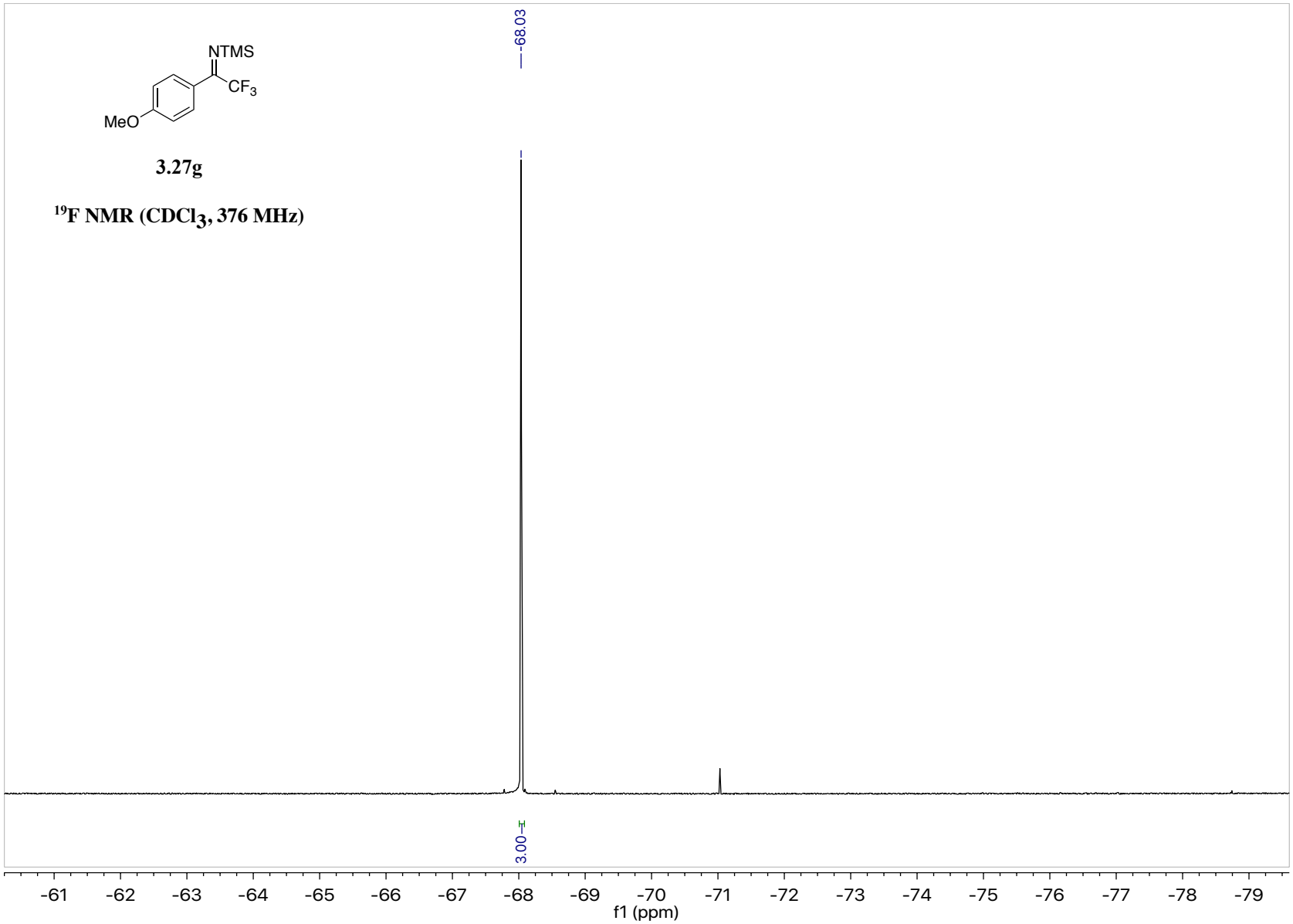

3.27g

^{19}F NMR ($CDCl_3$, 376 MHz)

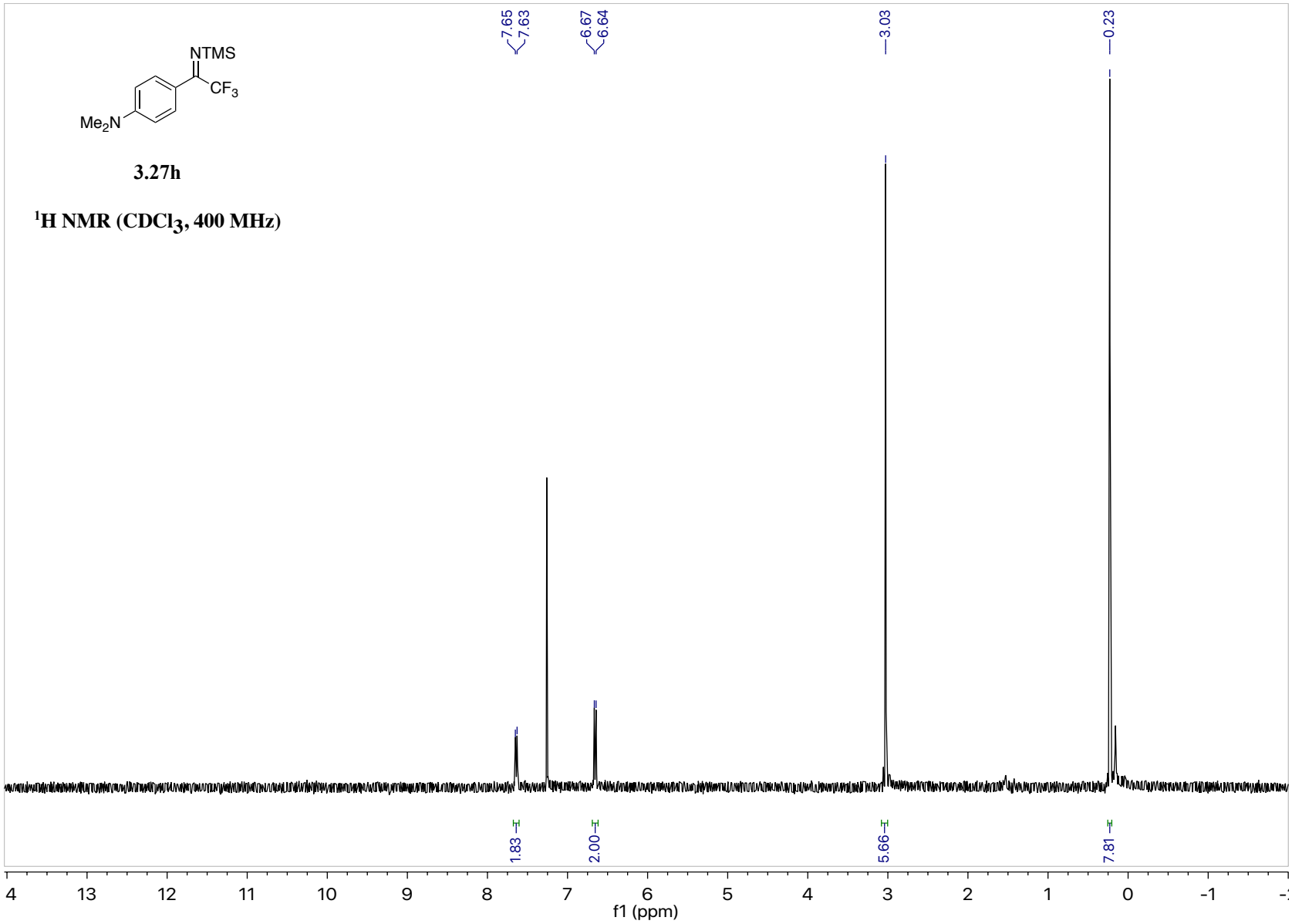

3.27h

^{1}H NMR ($CDCl_3$, 400 MHz)

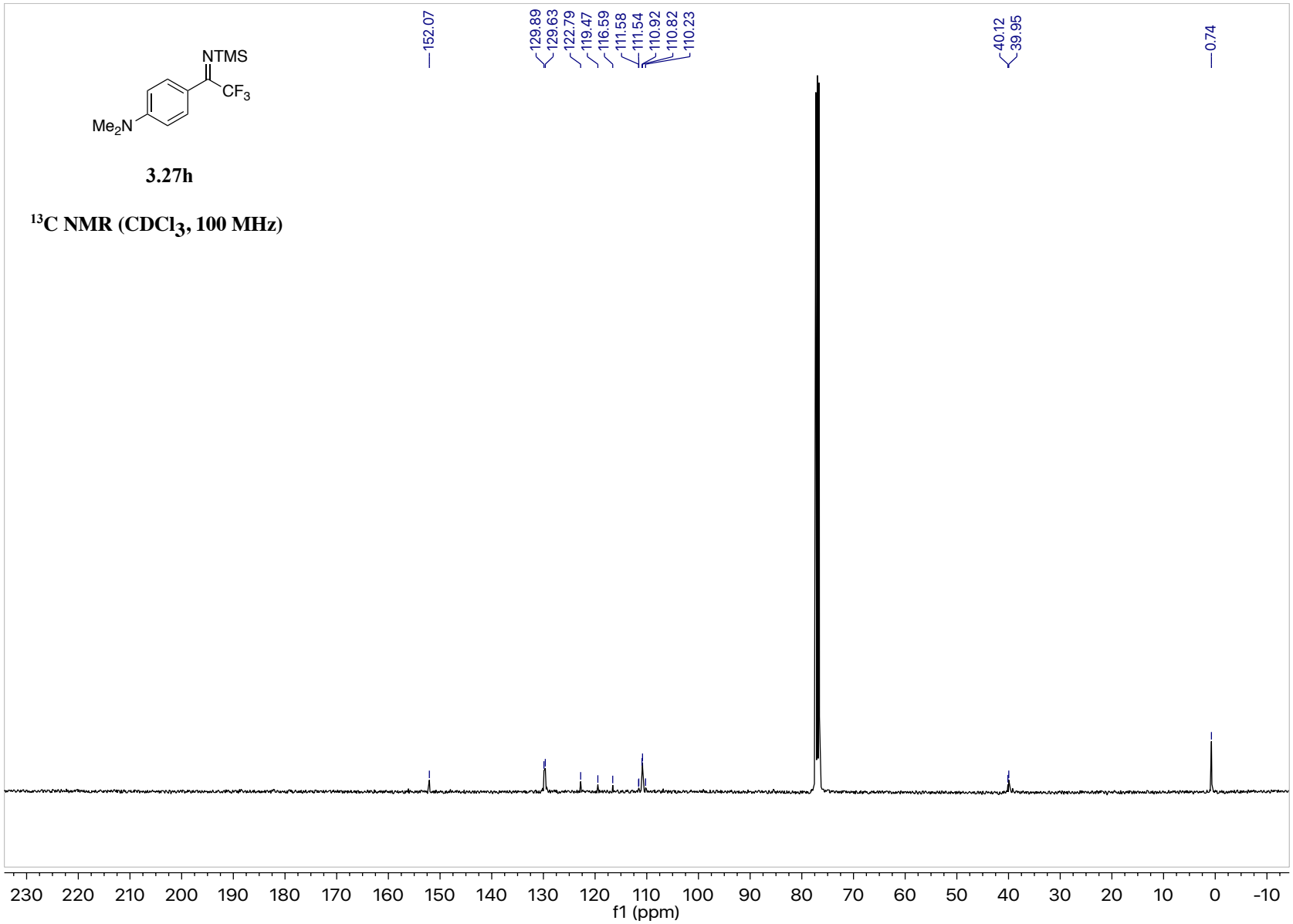

3.27h

^{13}C NMR ($CDCl_3$, 100 MHz)

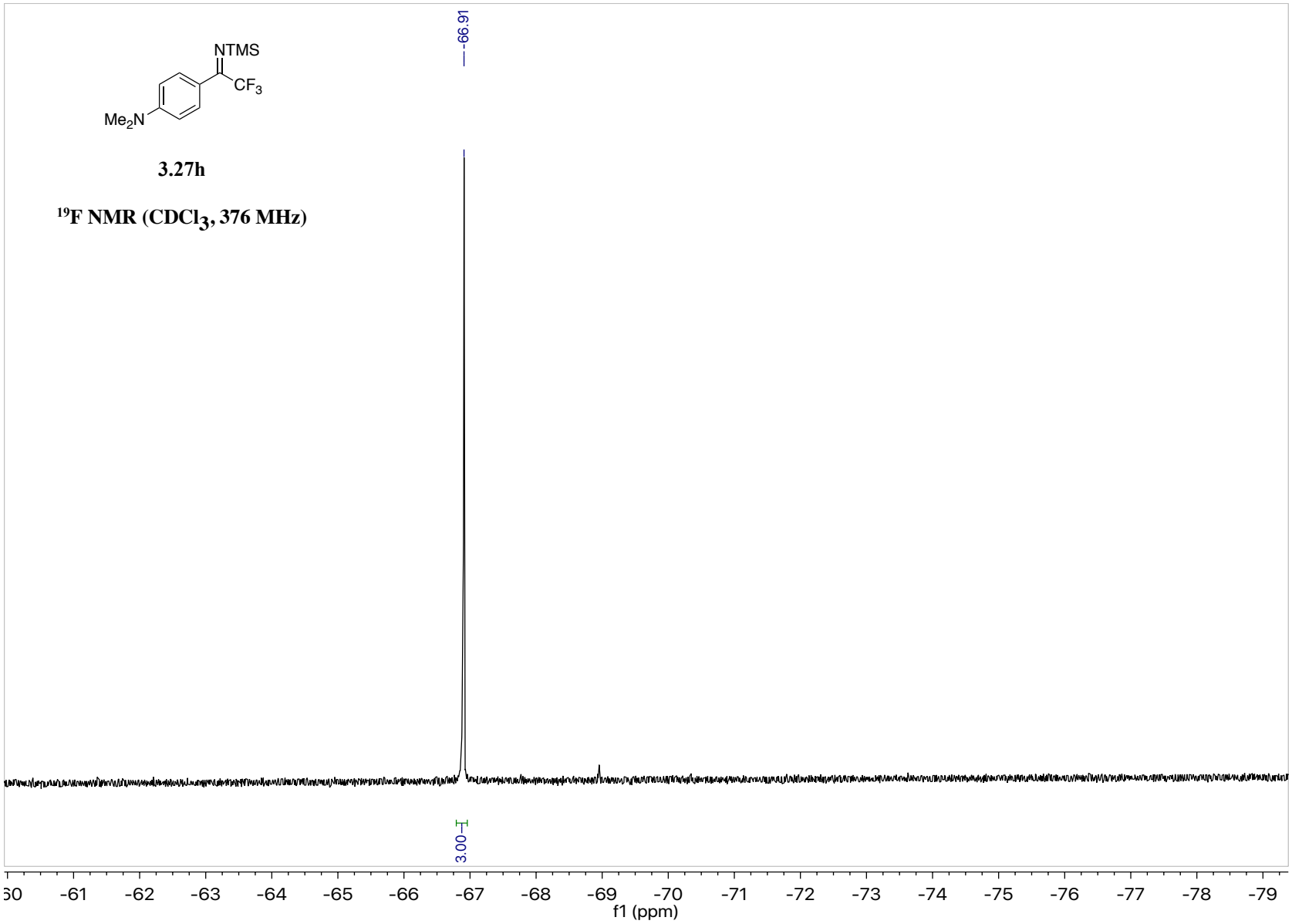
NTMS
CF3
Me2N
3.27h
19F NMR (CDCl3, 376 MHz)
-66.91
3.00
-60
-61
-62
-63
-64
-65
-66
-67
-68
-69
-70
-71
-72
-73
-74
-75
-76
-77
-78
-79
f1 (ppm)

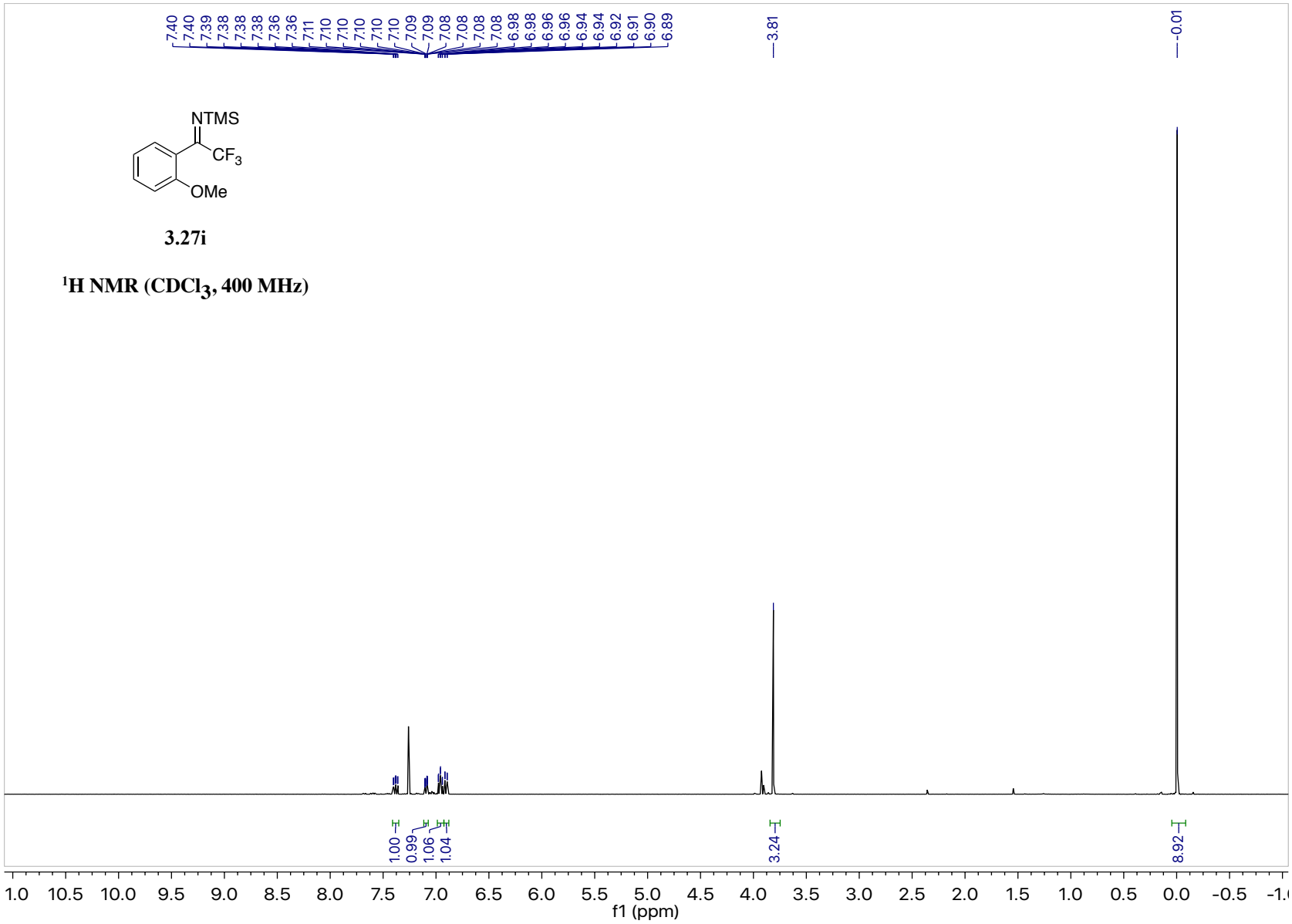

3.27i

^{1}H NMR ($CDCl_3$, 400 MHz)

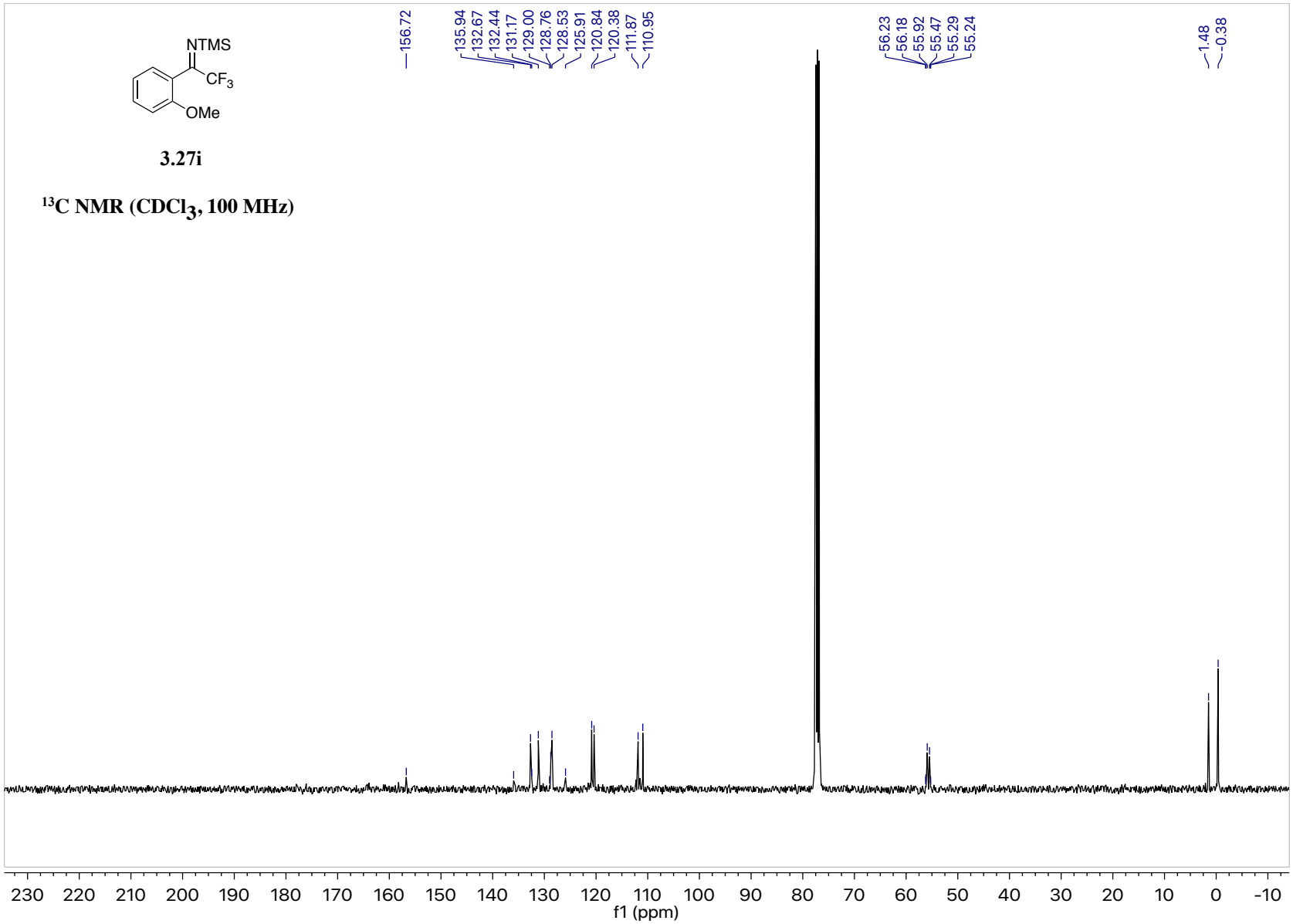

3.27i

^{13}C NMR ($CDCl_3$, 100 MHz)

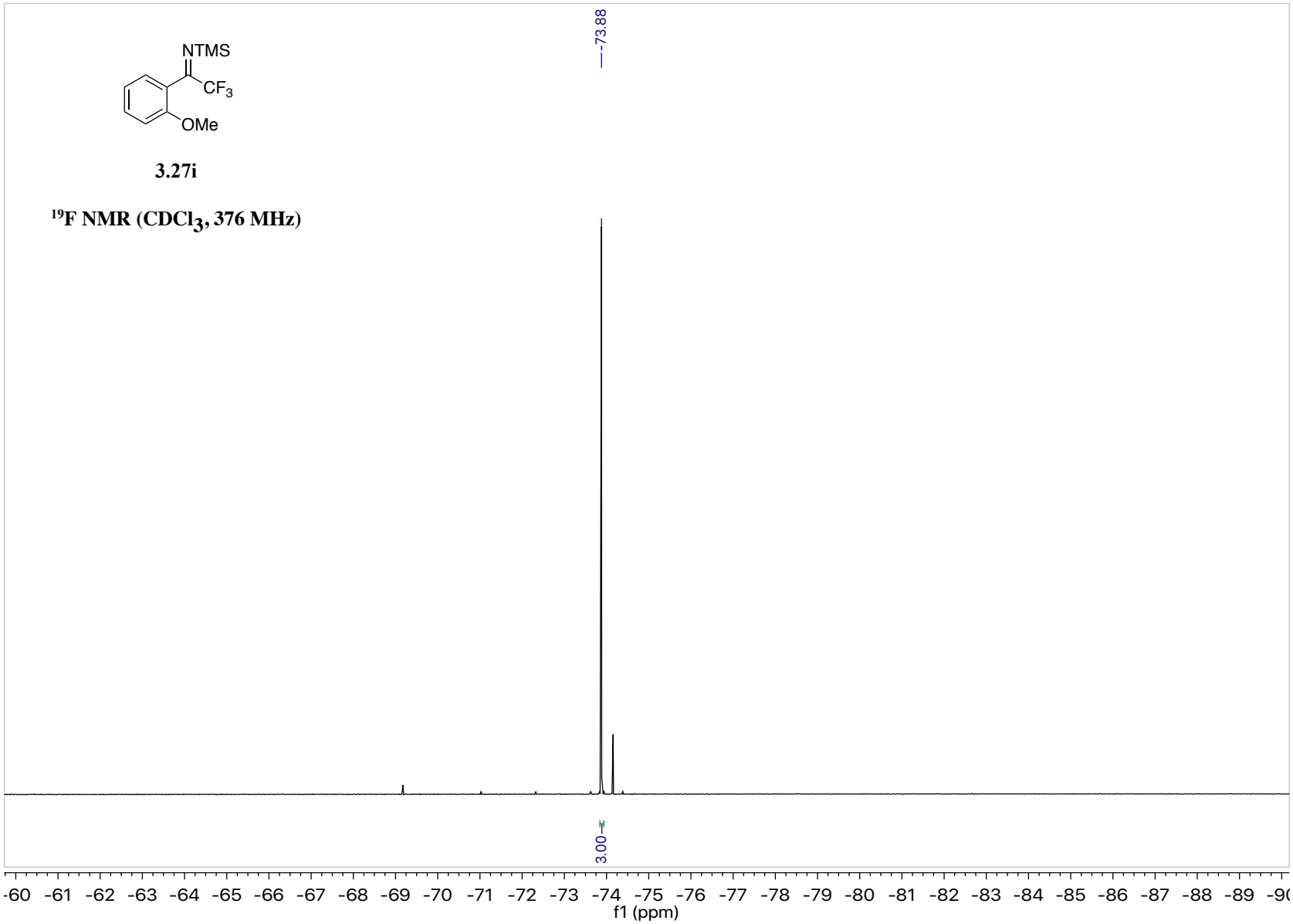

3.27i

^{19}F NMR ($CDCl_3$, 376 MHz)

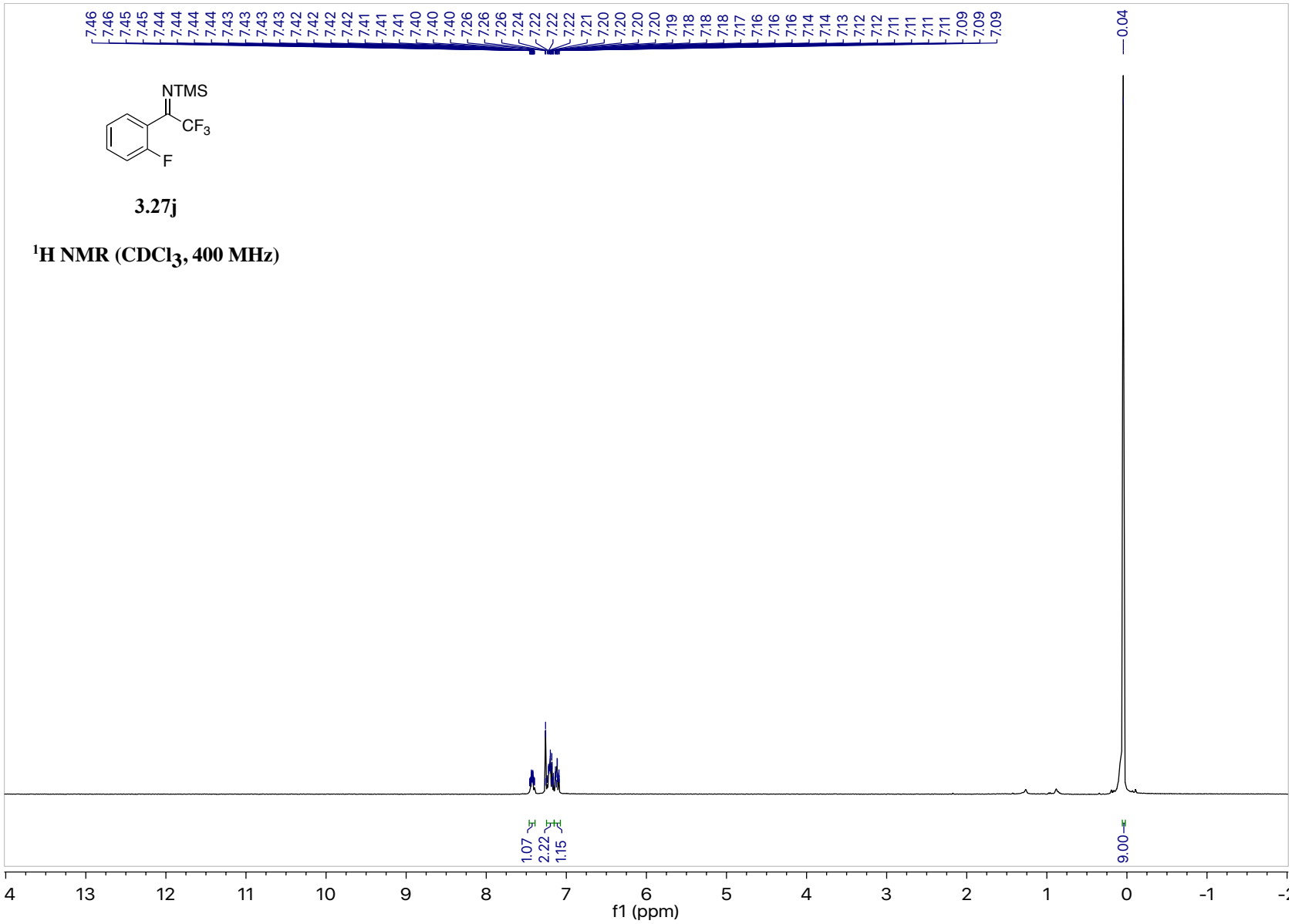

3.27j

^{1}H NMR ($CDCl_3$, 400 MHz)

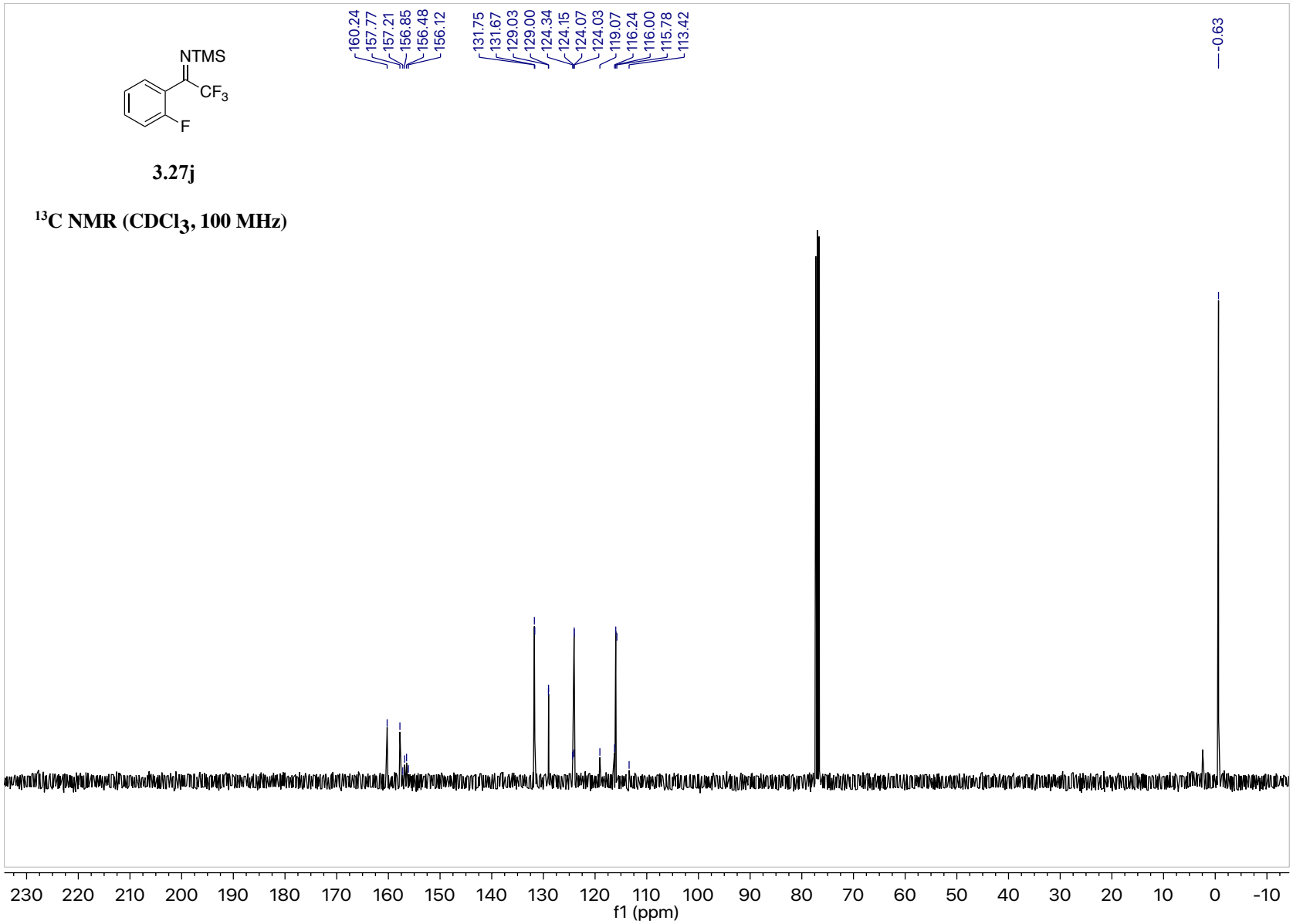
NTMS
CF3
F
3.27j
13C NMR (CDCl3, 100 MHz)
160.24
157.77
157.21
156.85
156.48
156.12
131.75
131.67
129.03
129.00
124.34
124.15
124.07
124.03
119.07
116.24
116.00
115.78
113.42
-0.63
230 220 210 200 190 180 170 160 150 140 130 120 110 100 90 80 70 60 50 40 30 20 10 0 -10
f1 (ppm)

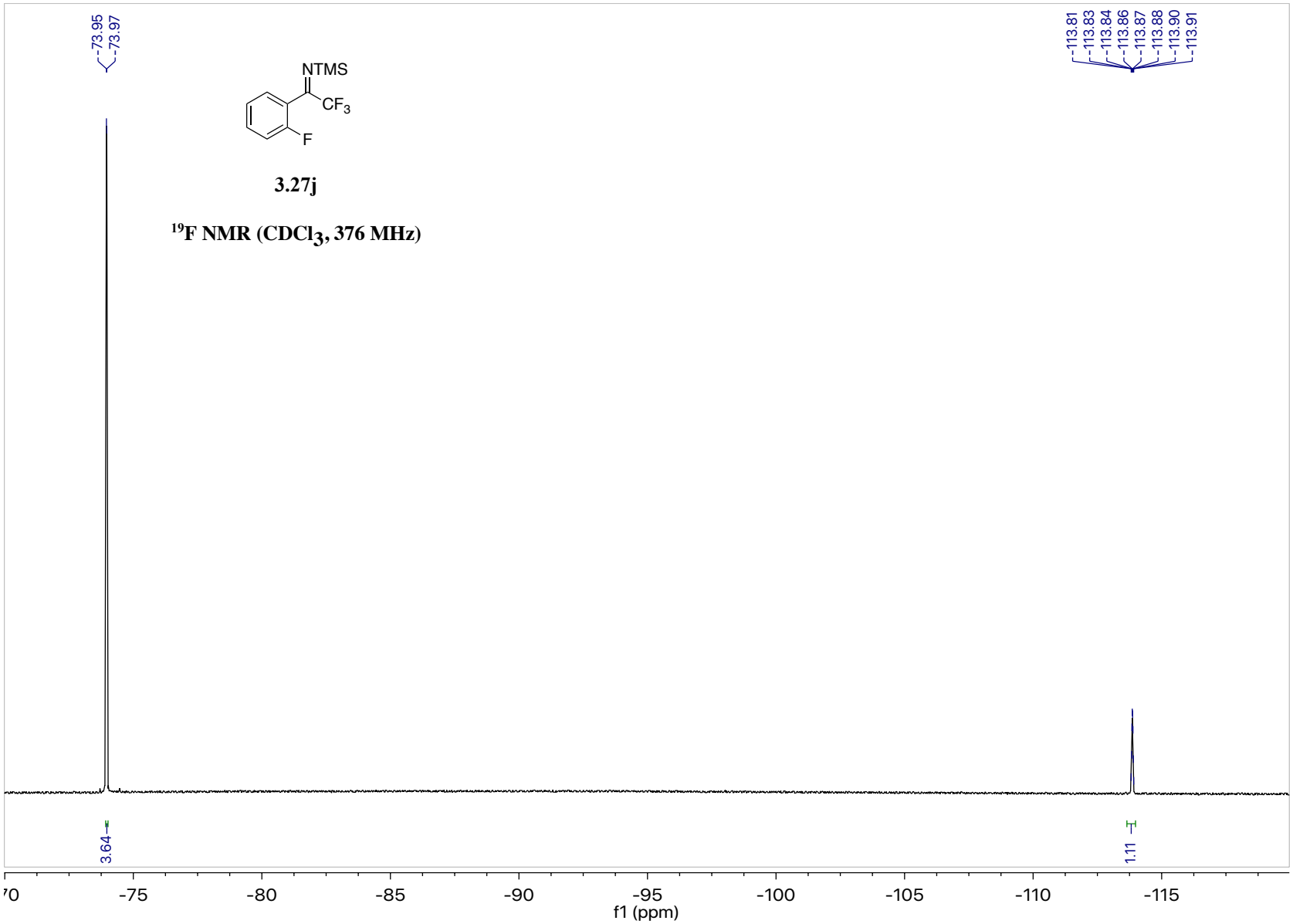

3.27j

^{19}F NMR ($CDCl_3$, 376 MHz)

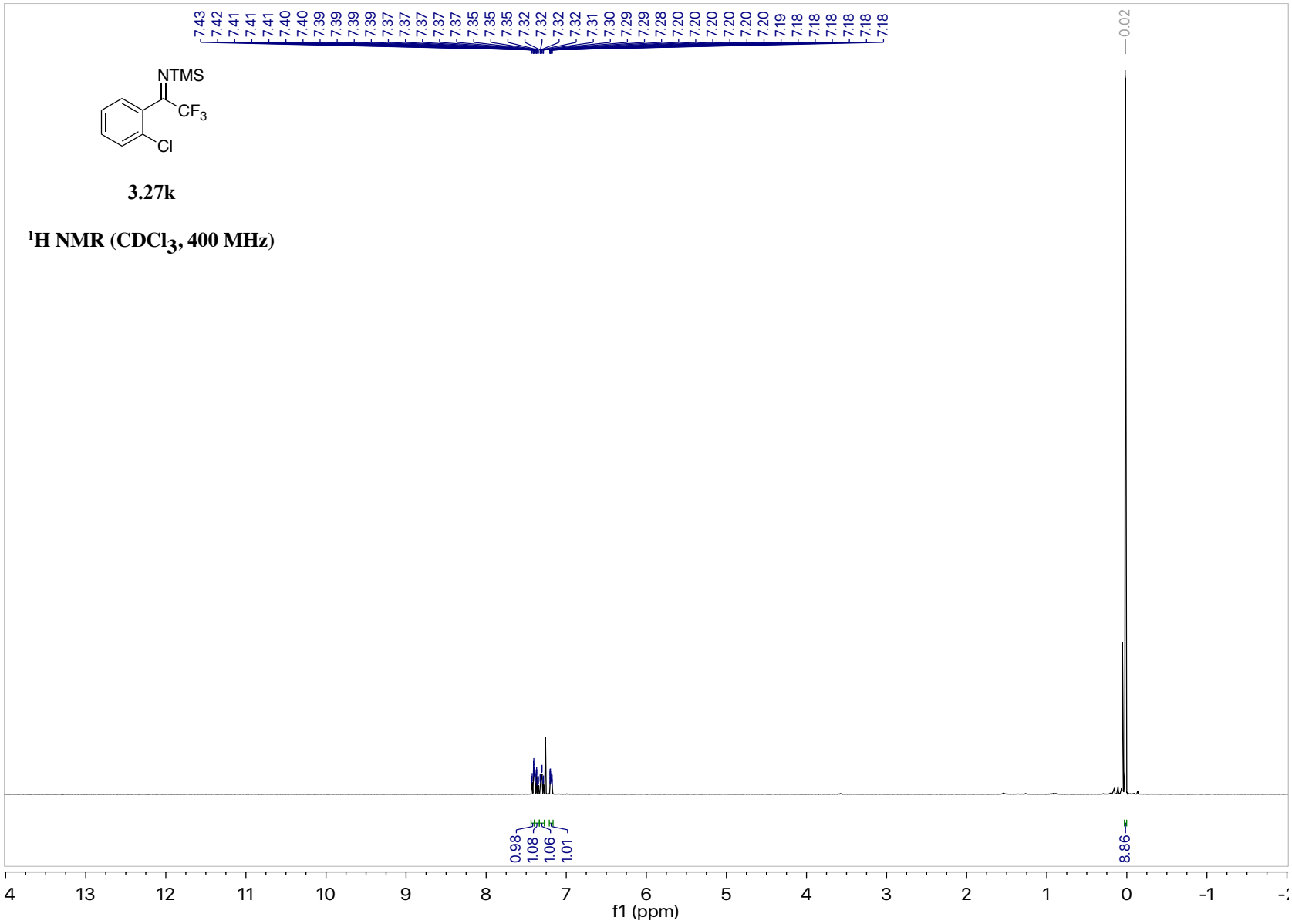

3.27k

^{1}H NMR ($CDCl_3$, 400 MHz)

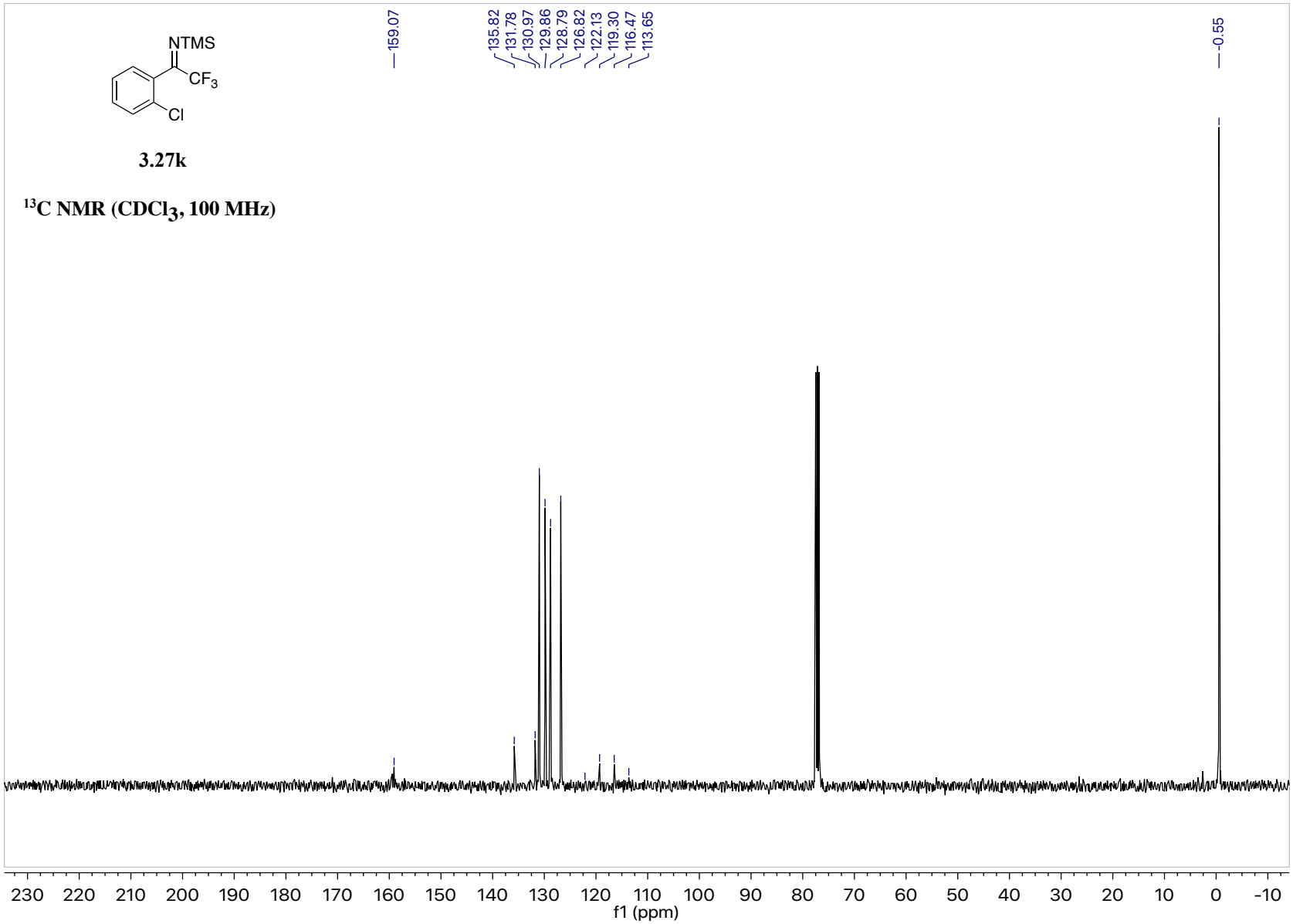
NTMS
CF3
Cl
3.27k
13C NMR (CDCl3, 100 MHz)
159.07
135.82
131.78
130.97
129.86
128.79
126.82
122.13
119.30
116.47
113.65
-0.55
230 220 210 200 190 180 170 160 150 140 130 120 110 100 90 80 70 60 50 40 30 20 10 0 -10
f1 (ppm)

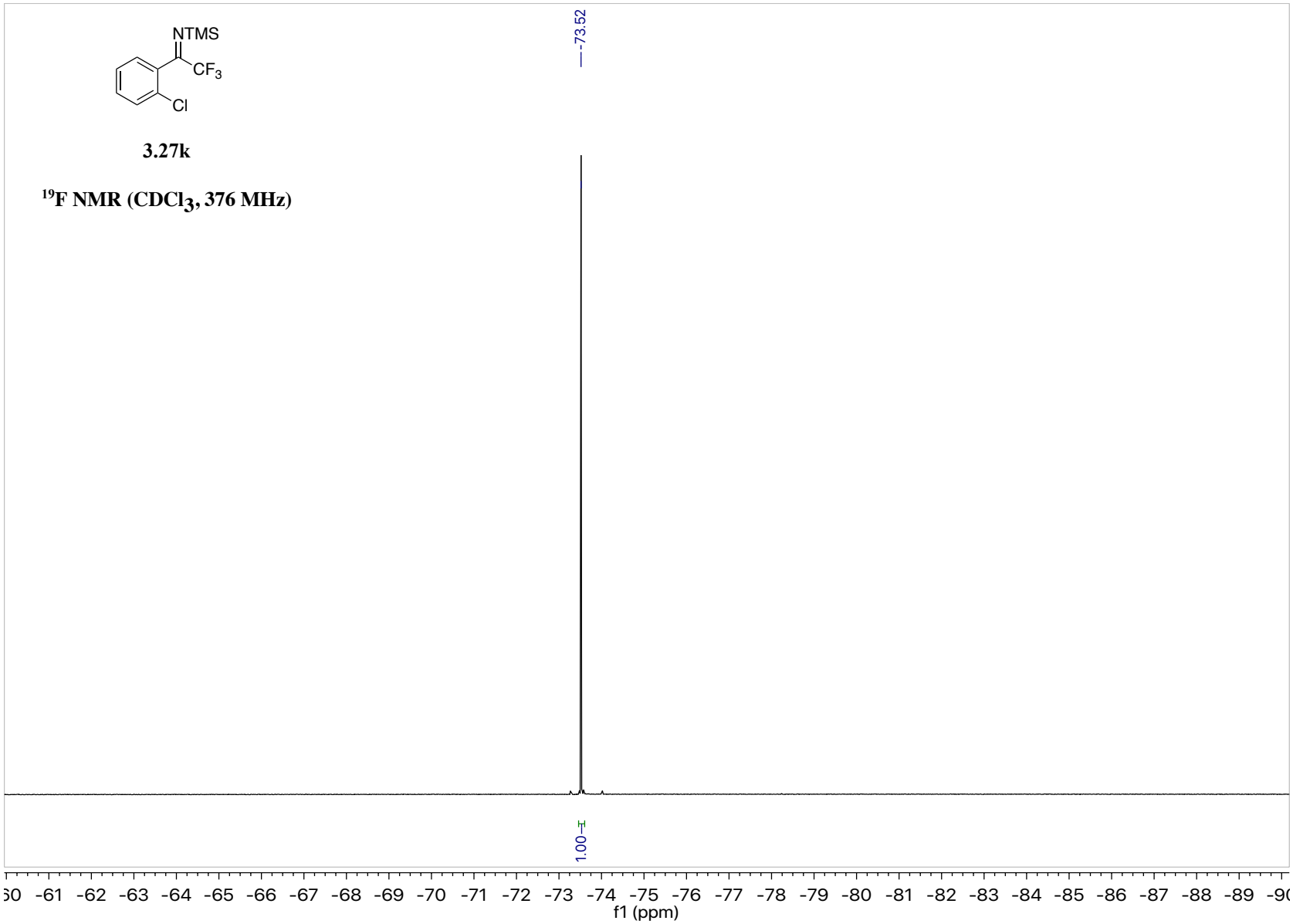
NTMS
CF3
Cl
3.27k
19F NMR (CDCl3, 376 MHz)
-73.52
1.00
-60 -61 -62 -63 -64 -65 -66 -67 -68 -69 -70 -71 -72 -73 -74 -75 -76 -77 -78 -79 -80 -81 -82 -83 -84 -85 -86 -87 -88 -89 -90
f1 (ppm)

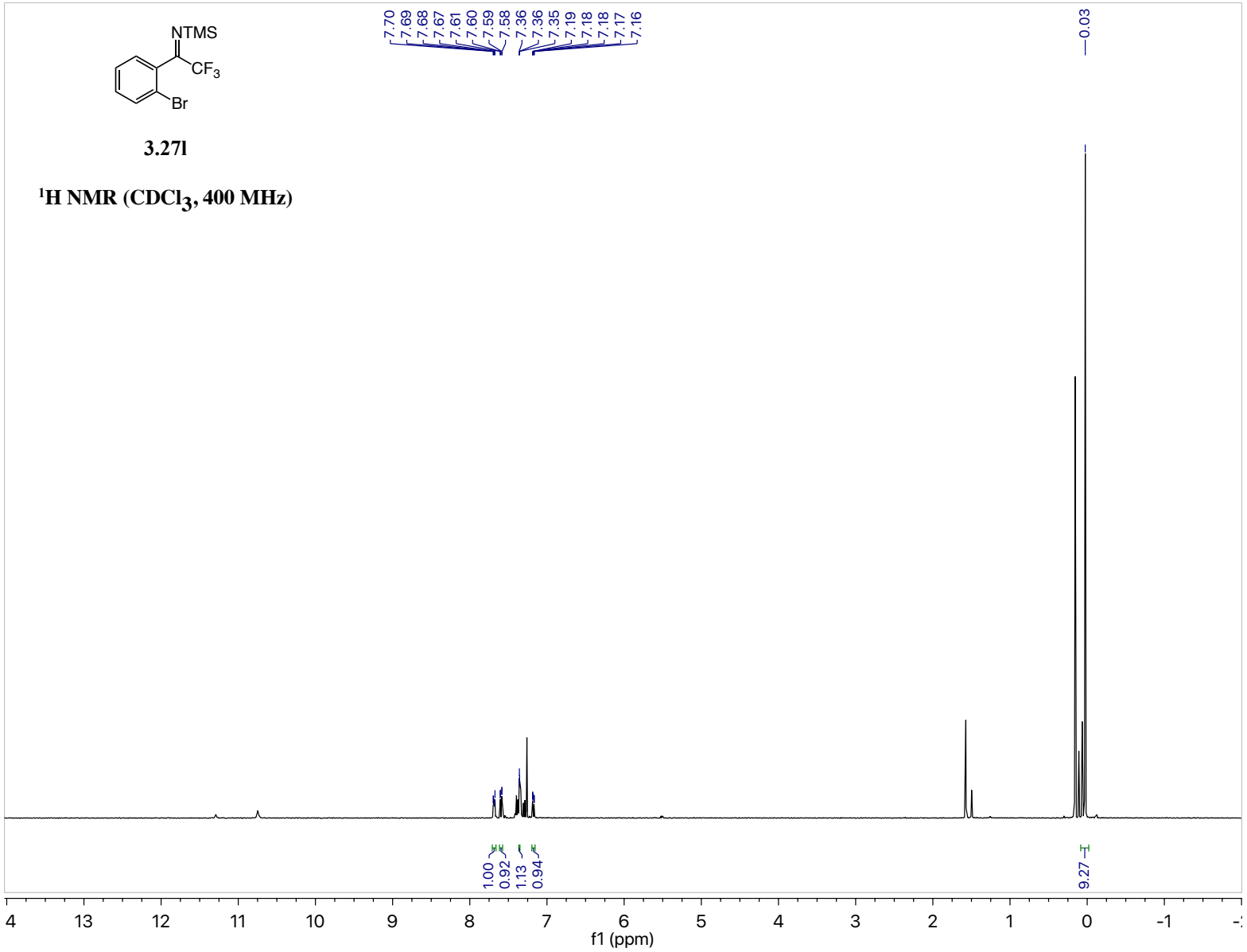
NTMS
CF3
Br
3.27l
1H NMR (CDCl3, 400 MHz)
7.70
7.69
7.68
7.67
7.61
7.60
7.59
7.58
7.36
7.36
7.35
7.19
7.18
7.18
7.17
7.16
0.03
1.00
0.92
1.13
0.94
9.27
f1 (ppm)

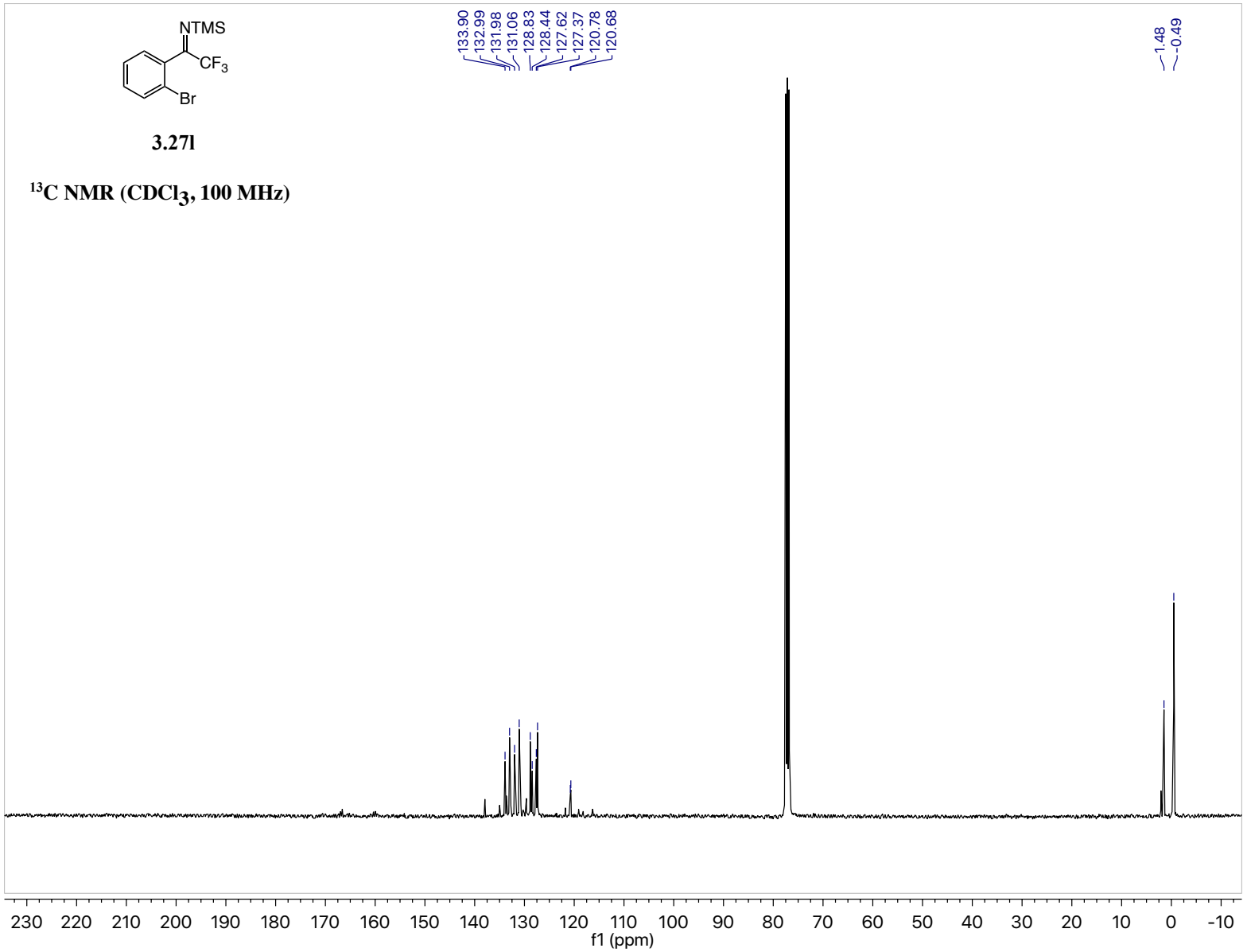
NTMS
CF3
Br
3.27l
13C NMR (CDCl3, 100 MHz)
133.90
132.99
131.98
131.06
128.83
128.44
127.62
127.37
120.78
120.68
1.48
-0.49
230 220 210 200 190 180 170 160 150 140 130 120 110 100 90 80 70 60 50 40 30 20 10 0 -10
f1 (ppm)

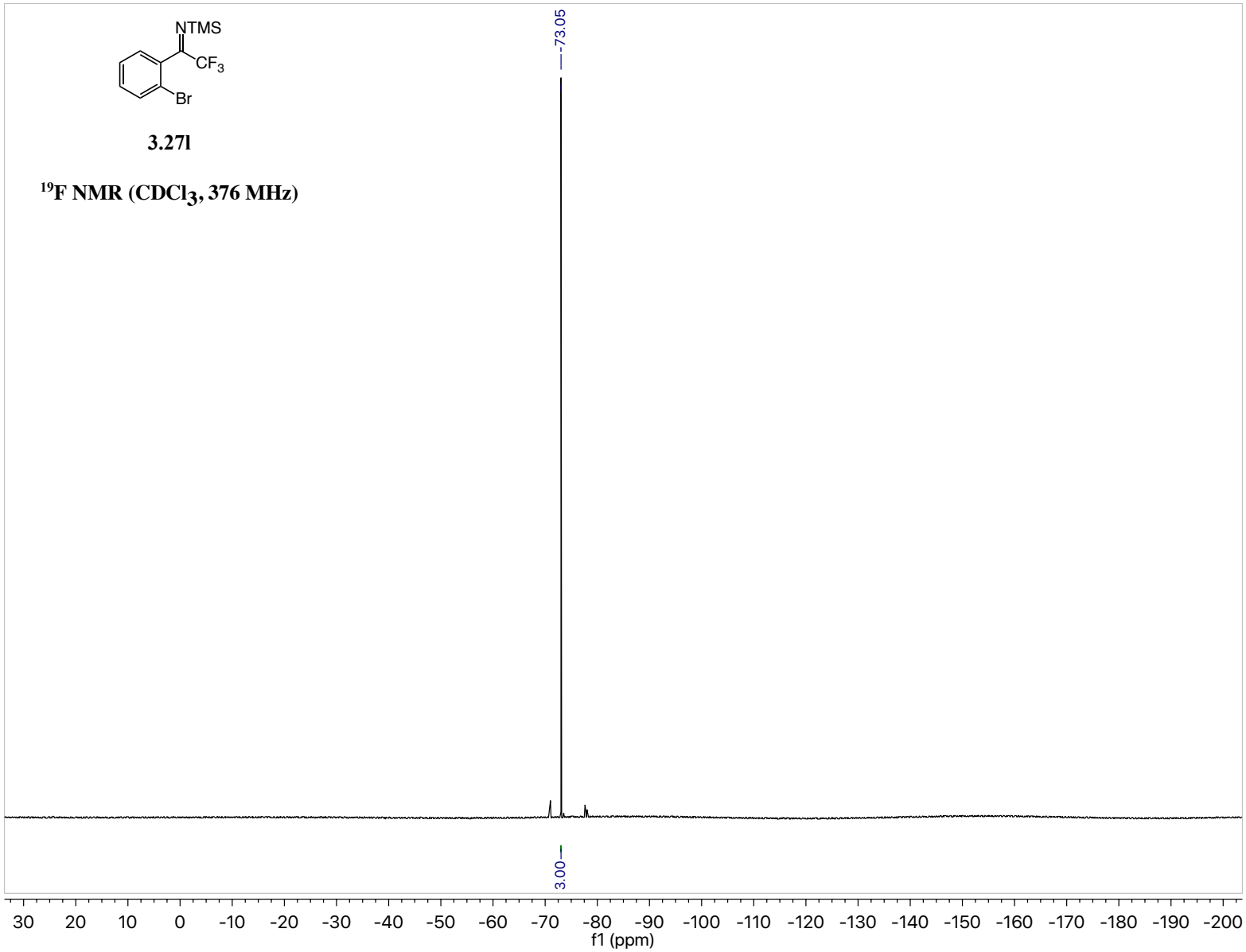
NTMS
CF3
Br
3.27l
19F NMR (CDCl3, 376 MHz)
-73.05
3.00
30 20 10 0 -10 -20 -30 -40 -50 -60 -70 -80 -90 -100 -110 -120 -130 -140 -150 -160 -170 -180 -190 -200
f1 (ppm)

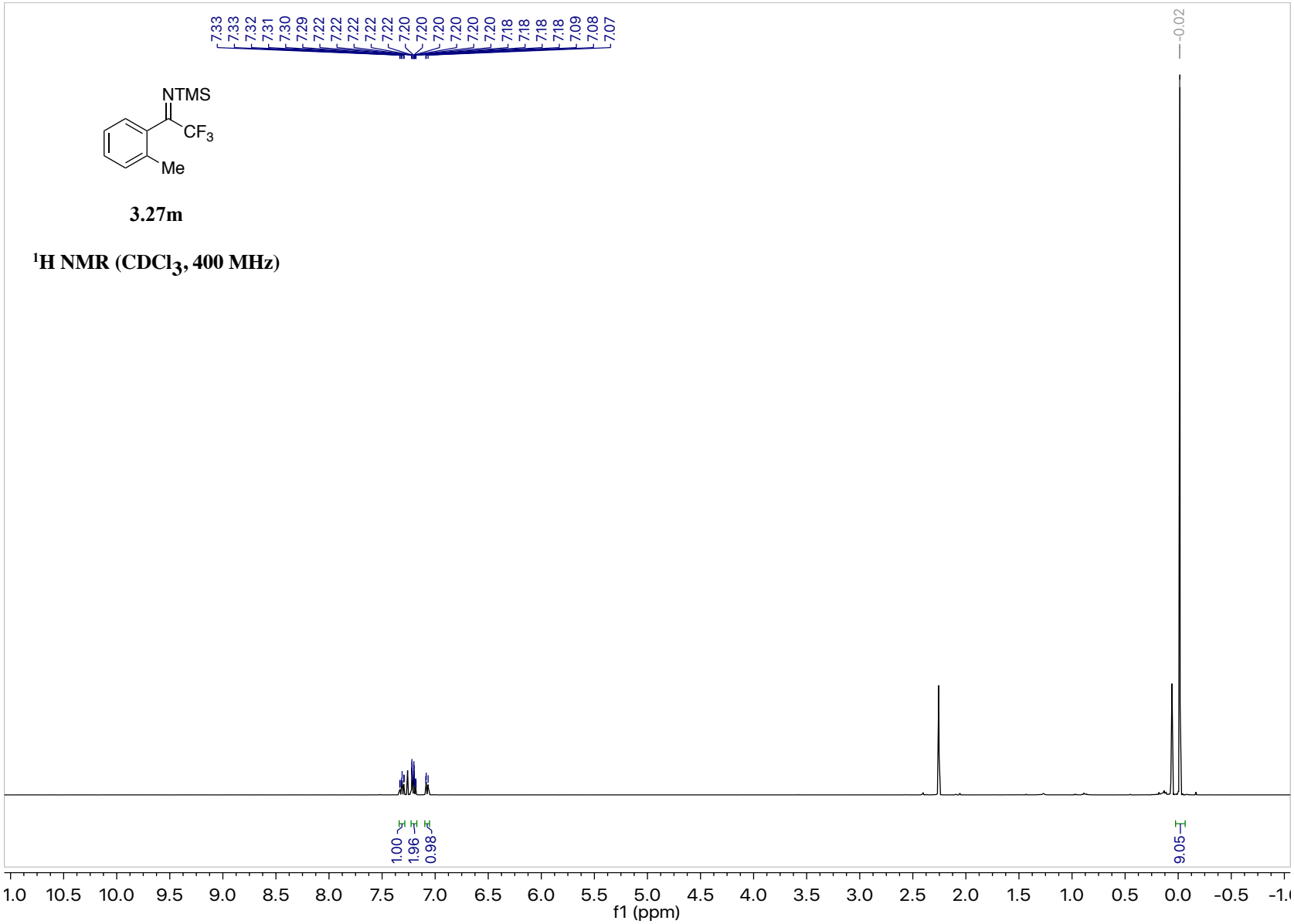

3.27m

^{1}H NMR ($CDCl_3$, 400 MHz)

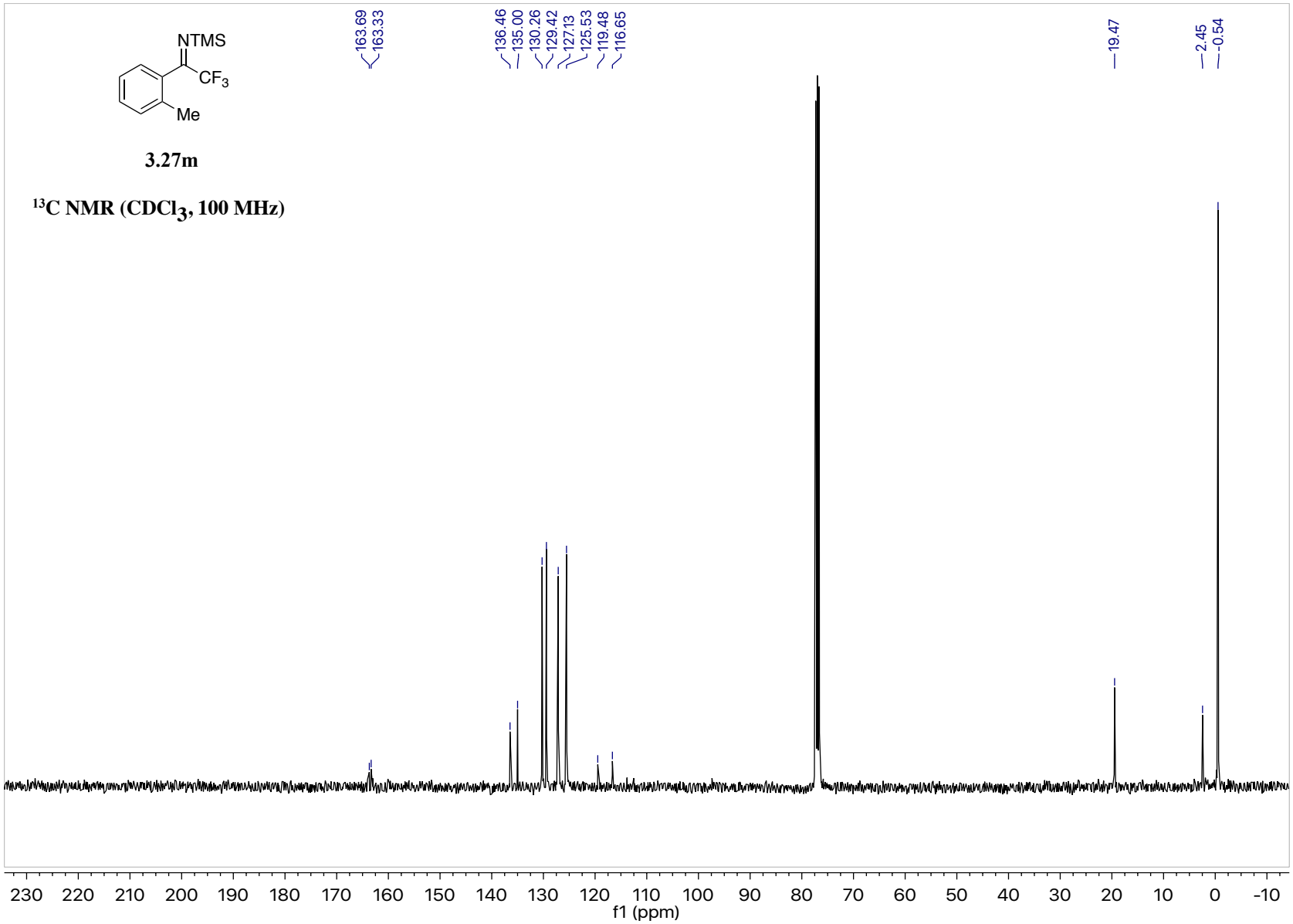
NTMS
CF3
Me
3.27m
13C NMR (CDCl3, 100 MHz)
163.69
163.33
136.46
135.00
130.26
129.42
127.13
125.53
119.48
116.65
19.47
2.45
-0.54
230 220 210 200 190 180 170 160 150 140 130 120 110 100 90 80 70 60 50 40 30 20 10 0 -10
f1 (ppm)

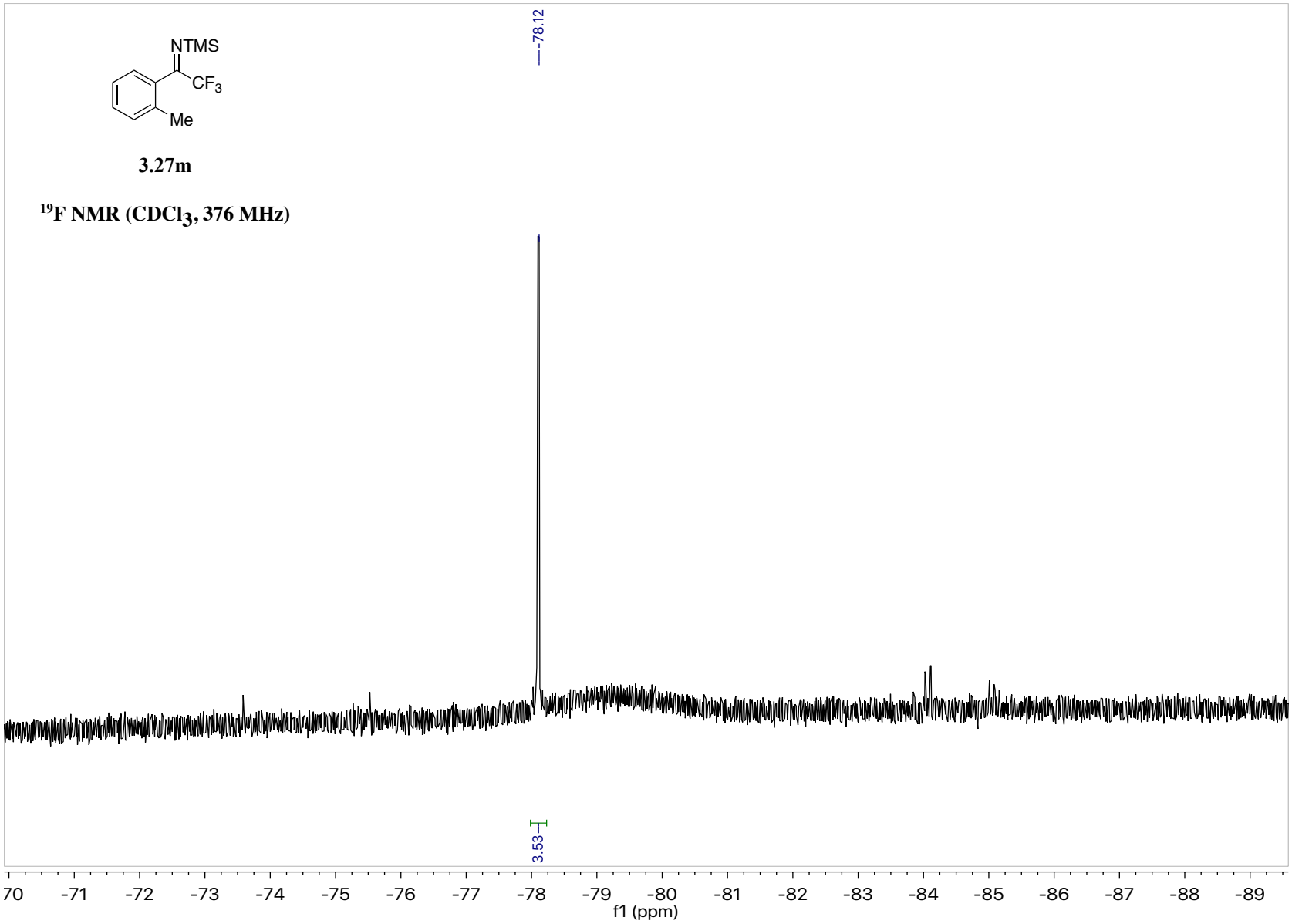
NTMS
CF3
Me
3.27m
19F NMR (CDCl3, 376 MHz)
-78.12
3.53
70 -71 -72 -73 -74 -75 -76 -77 -78 -79 -80 -81 -82 -83 -84 -85 -86 -87 -88 -89
f1 (ppm)

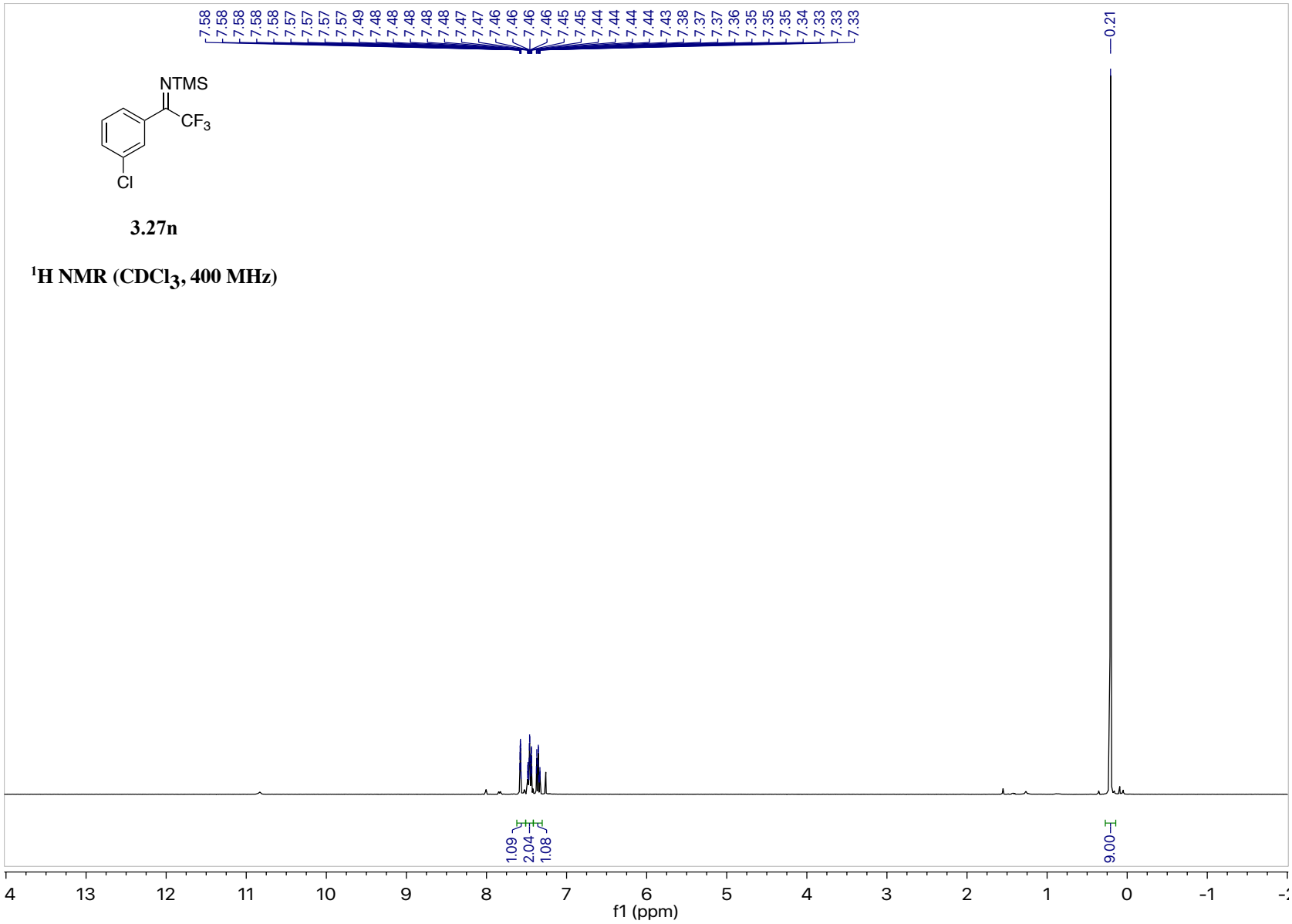

3.27n

^{1}H NMR ($CDCl_3$, 400 MHz)

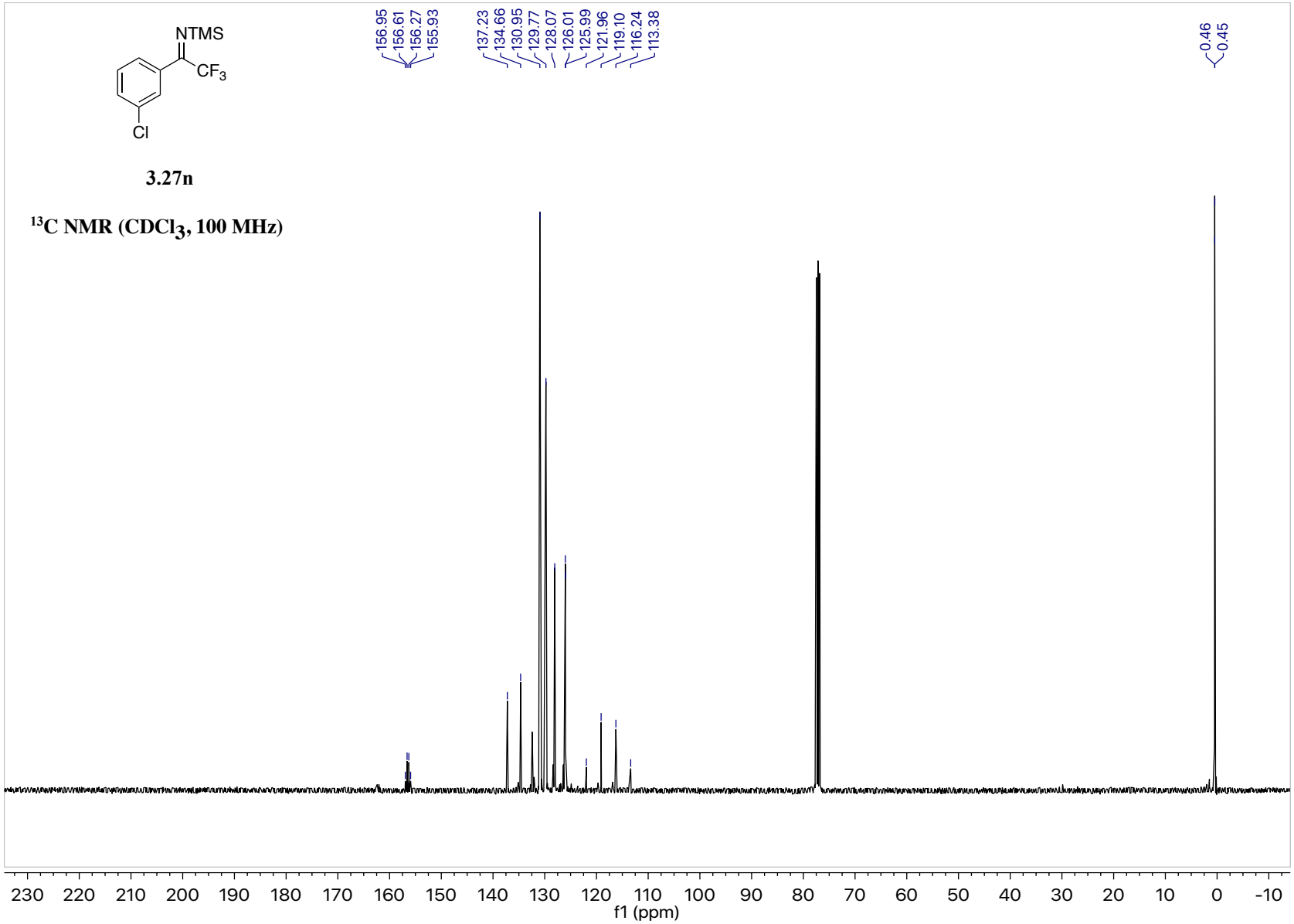

3.27n

^{13}C NMR ($CDCl_3$, 100 MHz)

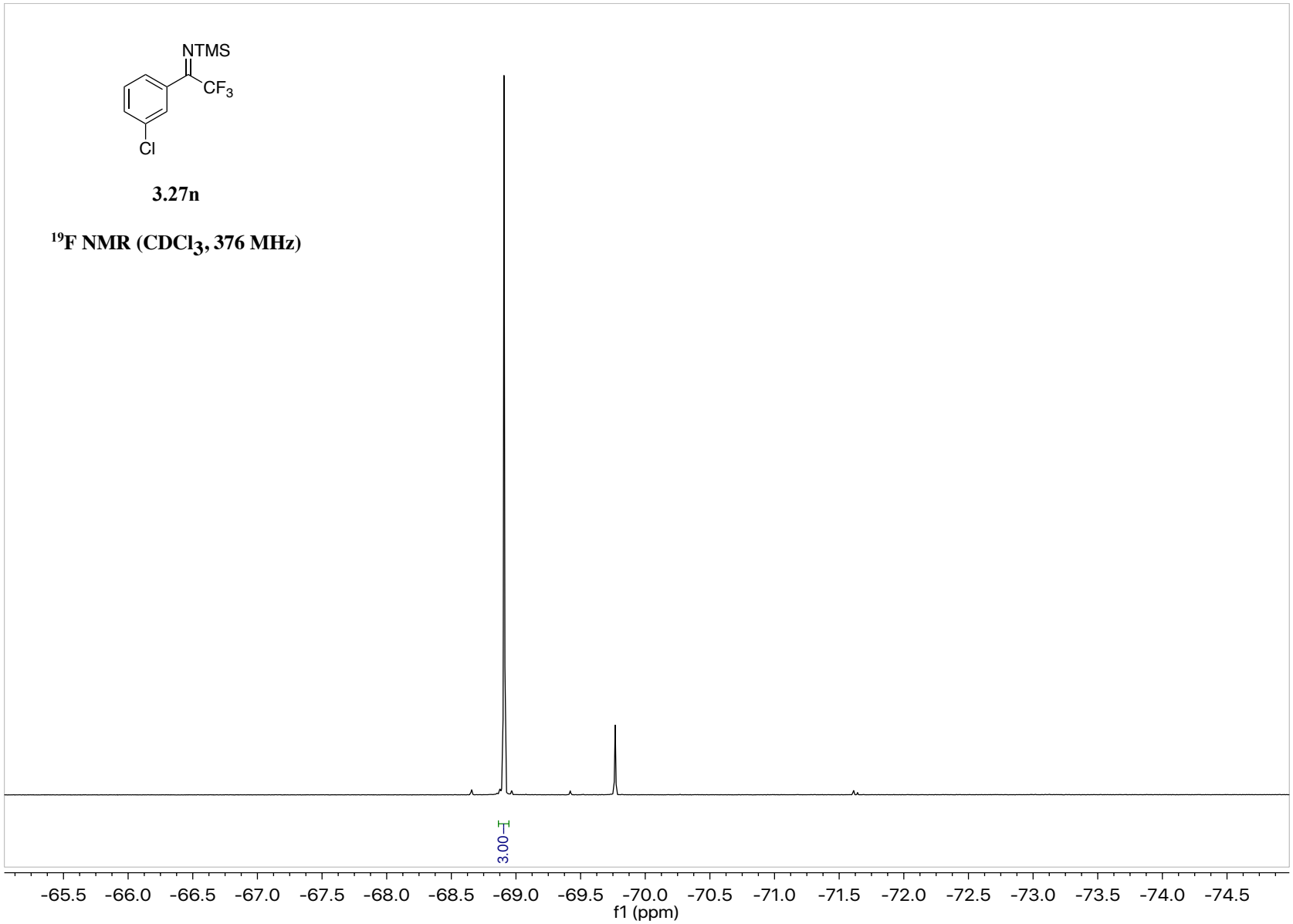

3.27n

^{19}F NMR ($CDCl_3$, 376 MHz)

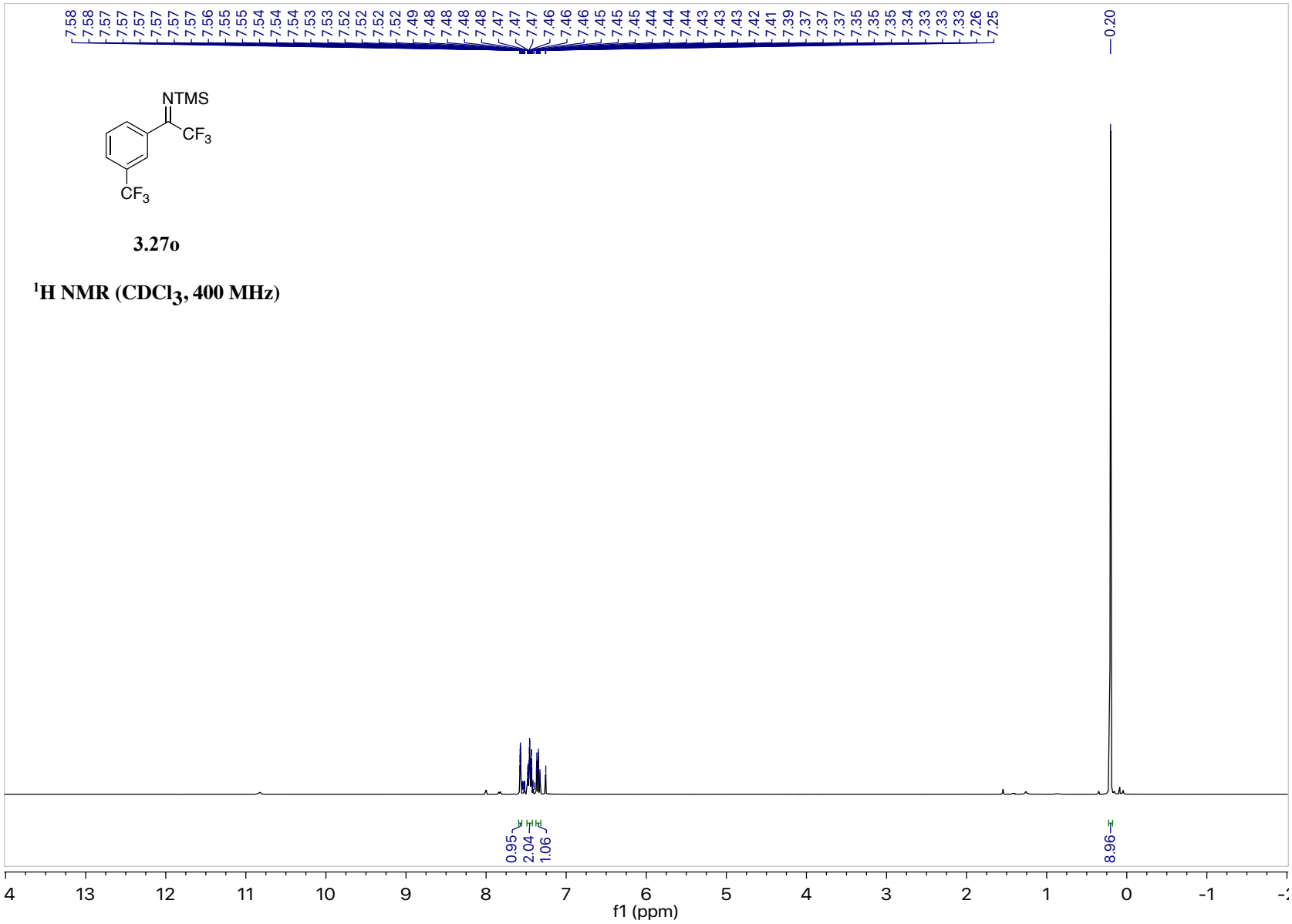

3.27o

^{1}H NMR ($CDCl_3$, 400 MHz)

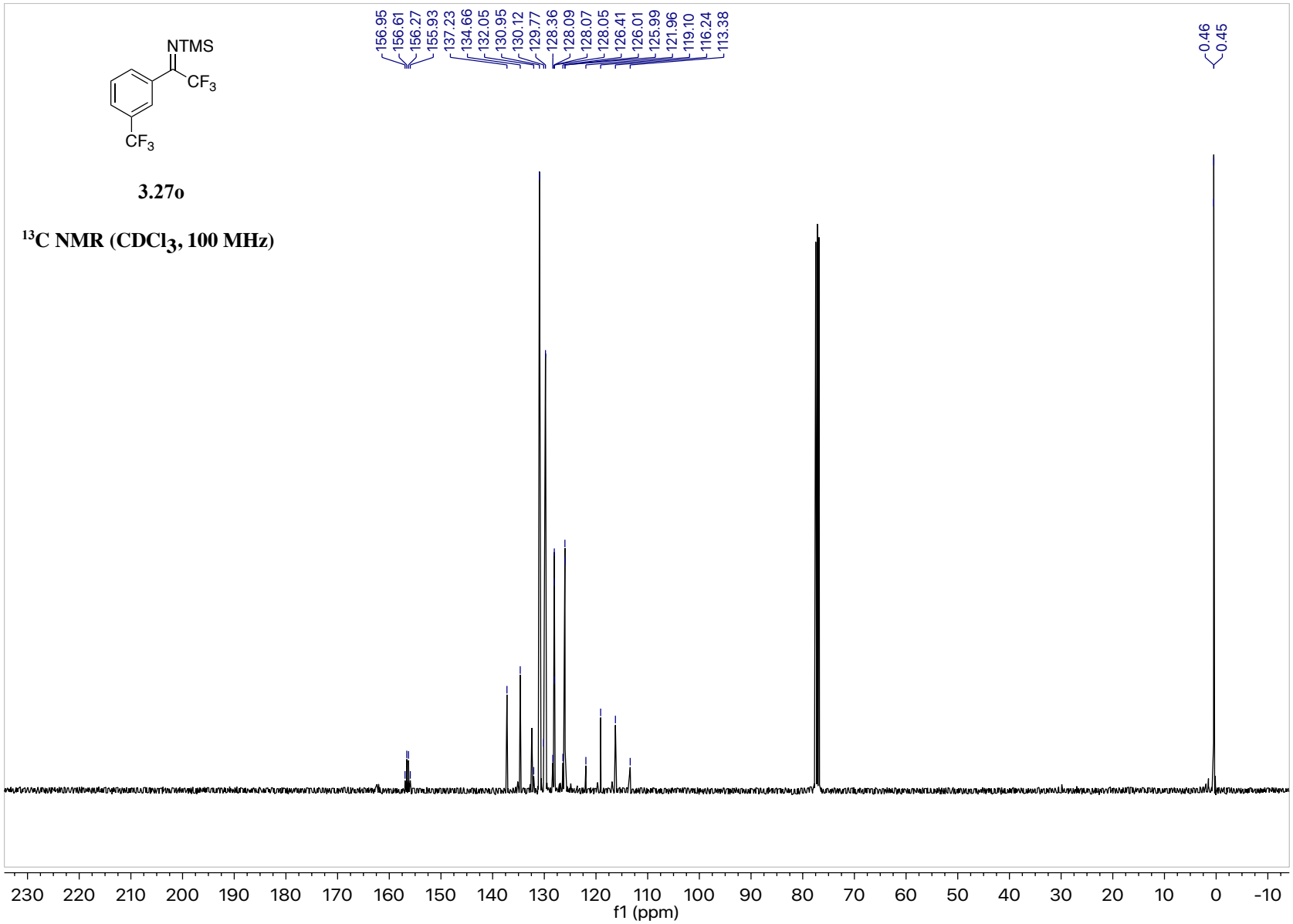

3.27o

^{13}C NMR ($CDCl_3$, 100 MHz)

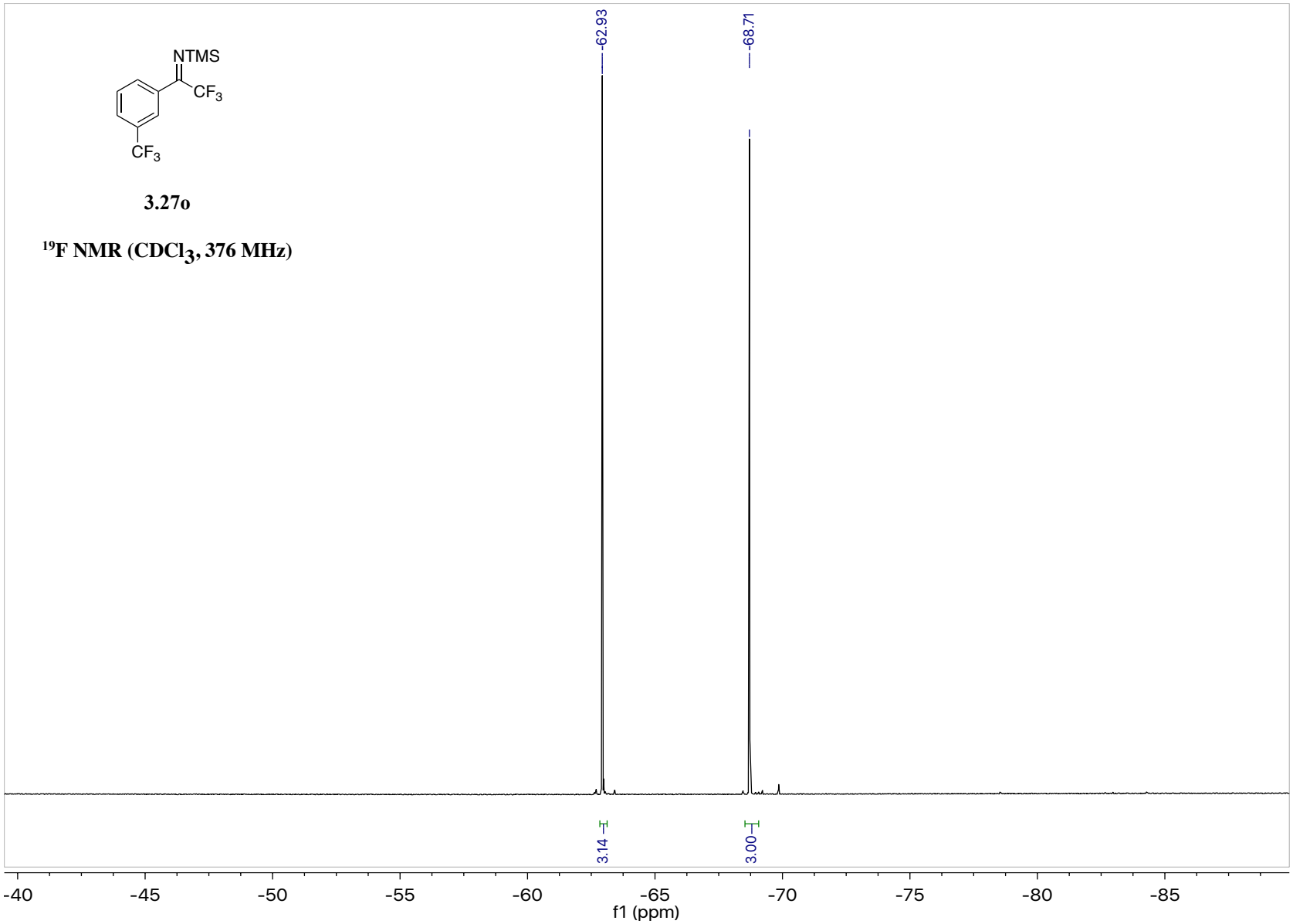

3.27o

^{19}F NMR ($CDCl_3$, 376 MHz)

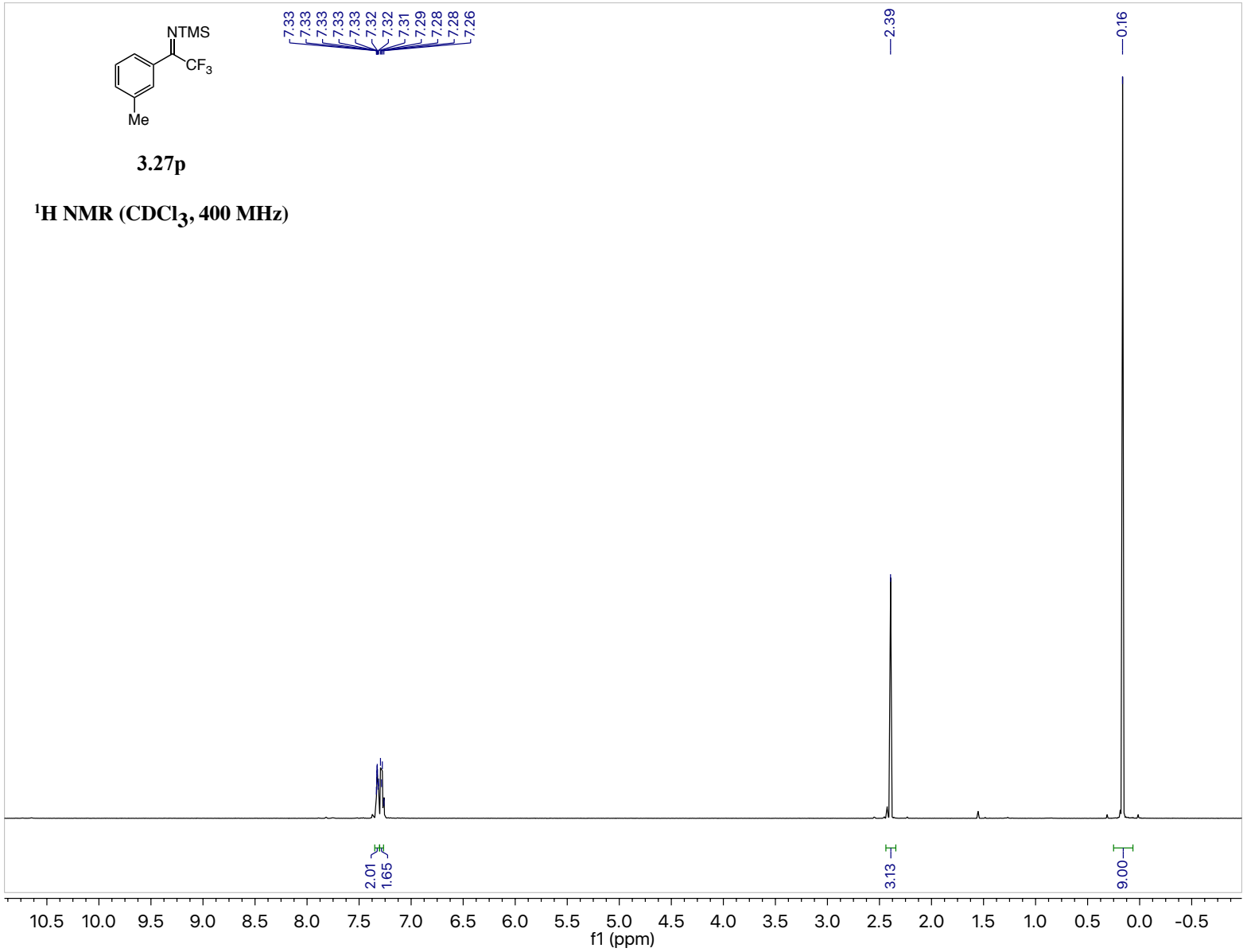

3.27p

^{1}H NMR ($CDCl_3$, 400 MHz)

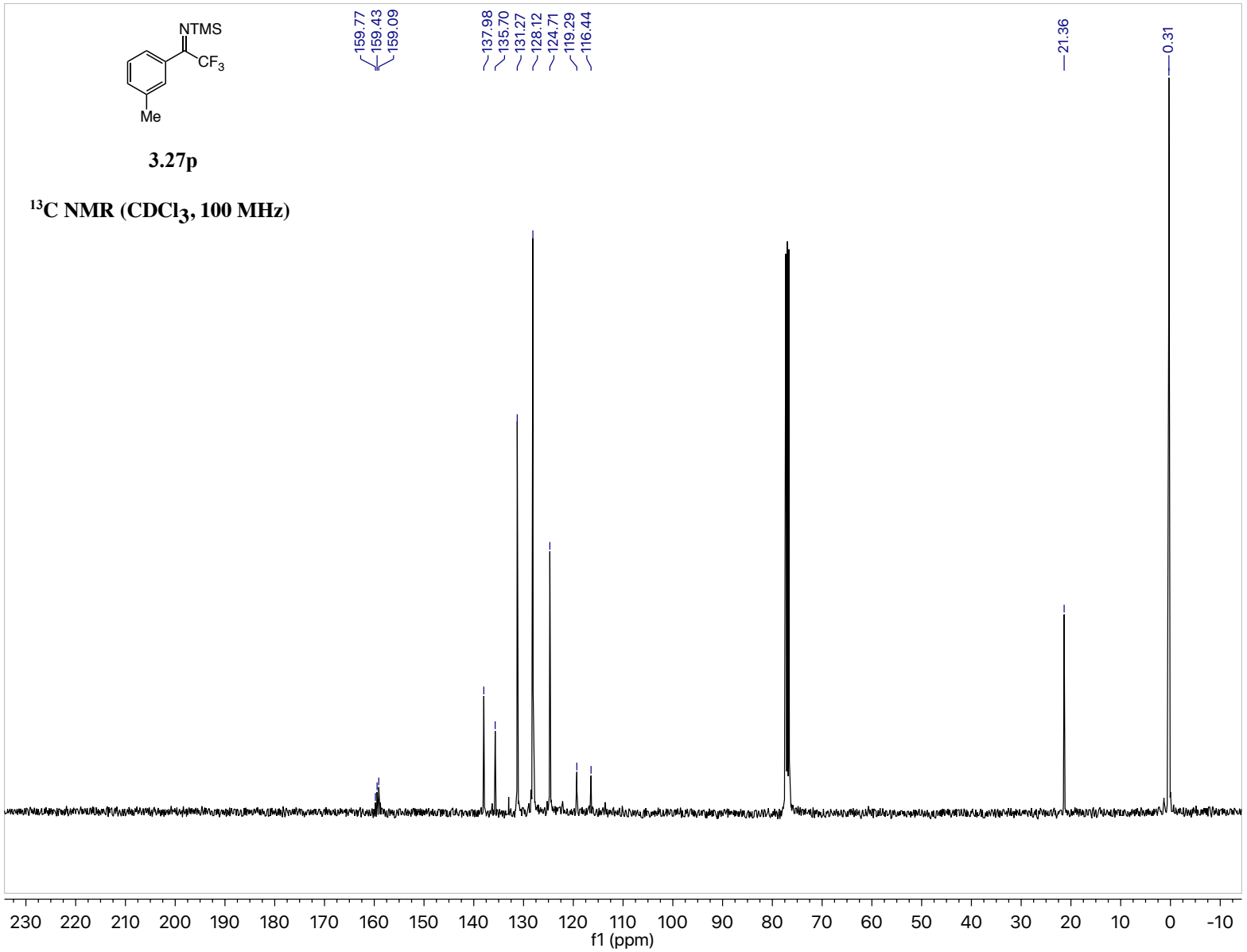
NTMS
CF3
Me
3.27p
13C NMR (CDCl3, 100 MHz)
159.77
159.43
159.09
137.98
135.70
131.27
128.12
124.71
119.29
116.44
21.36
0.31
230 220 210 200 190 180 170 160 150 140 130 120 110 100 90 80 70 60 50 40 30 20 10 0 -10
f1 (ppm)

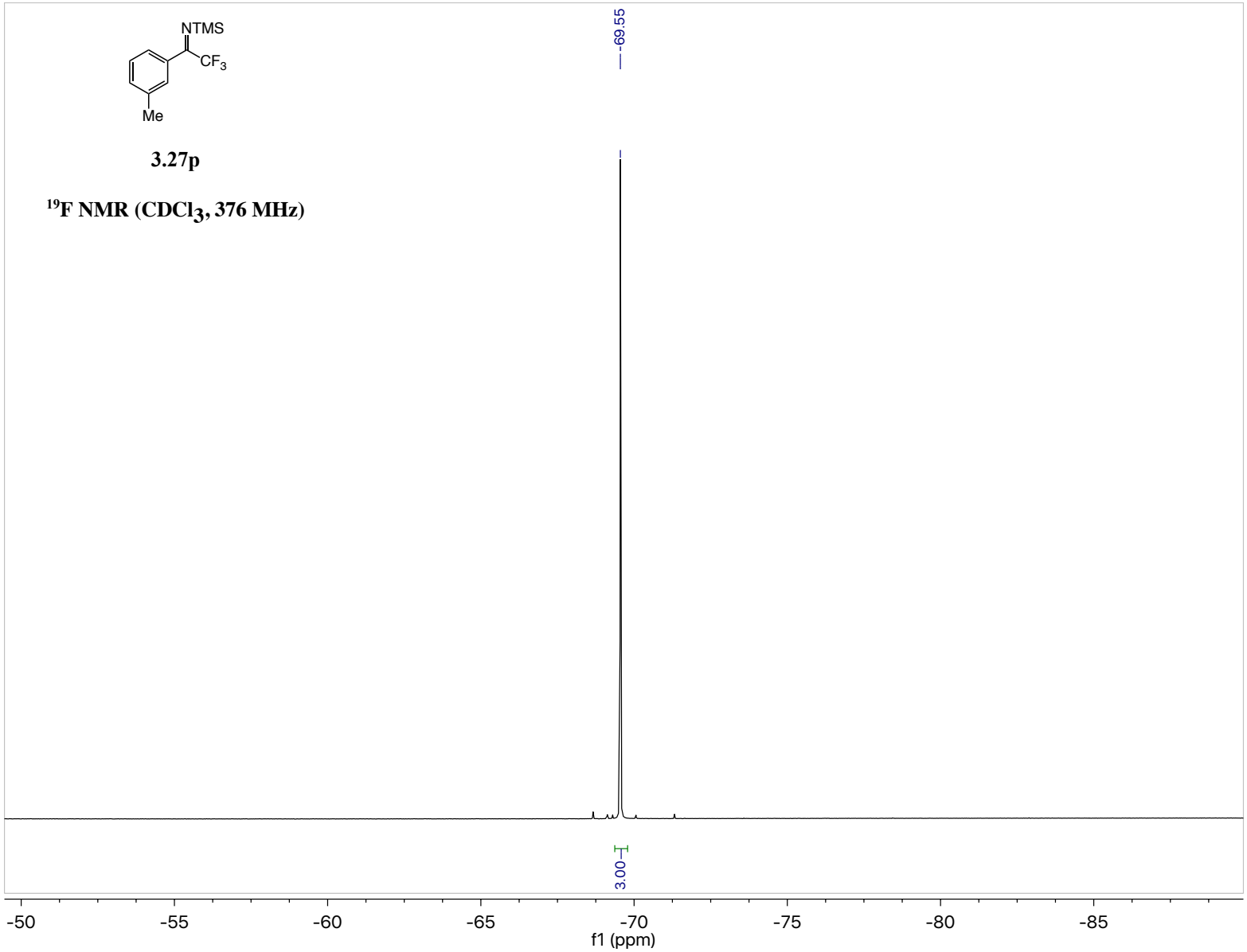

3.27p

^{19}F NMR ($CDCl_3$, 376 MHz)

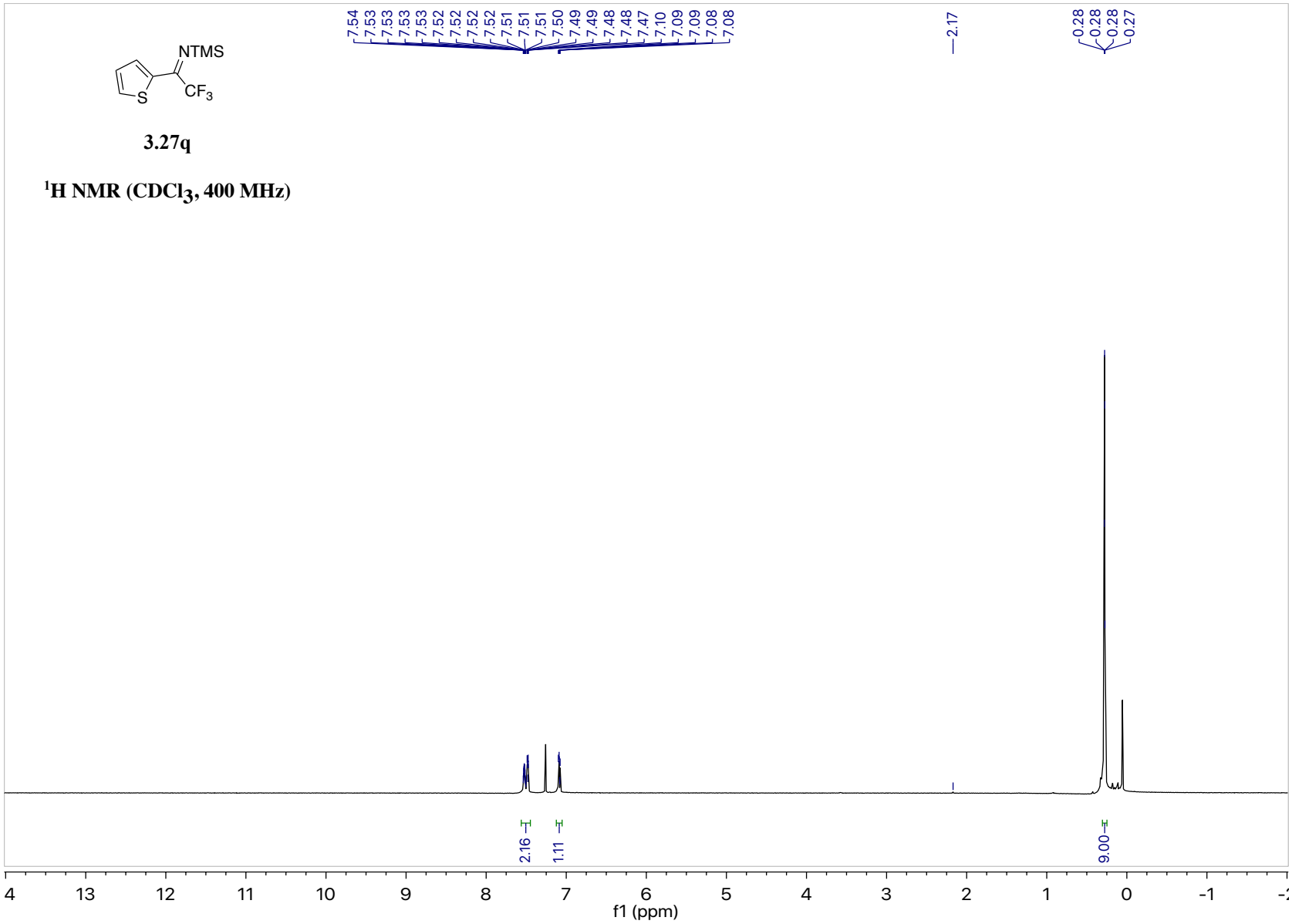

3.27q

^{1}H NMR ($CDCl_3$, 400 MHz)

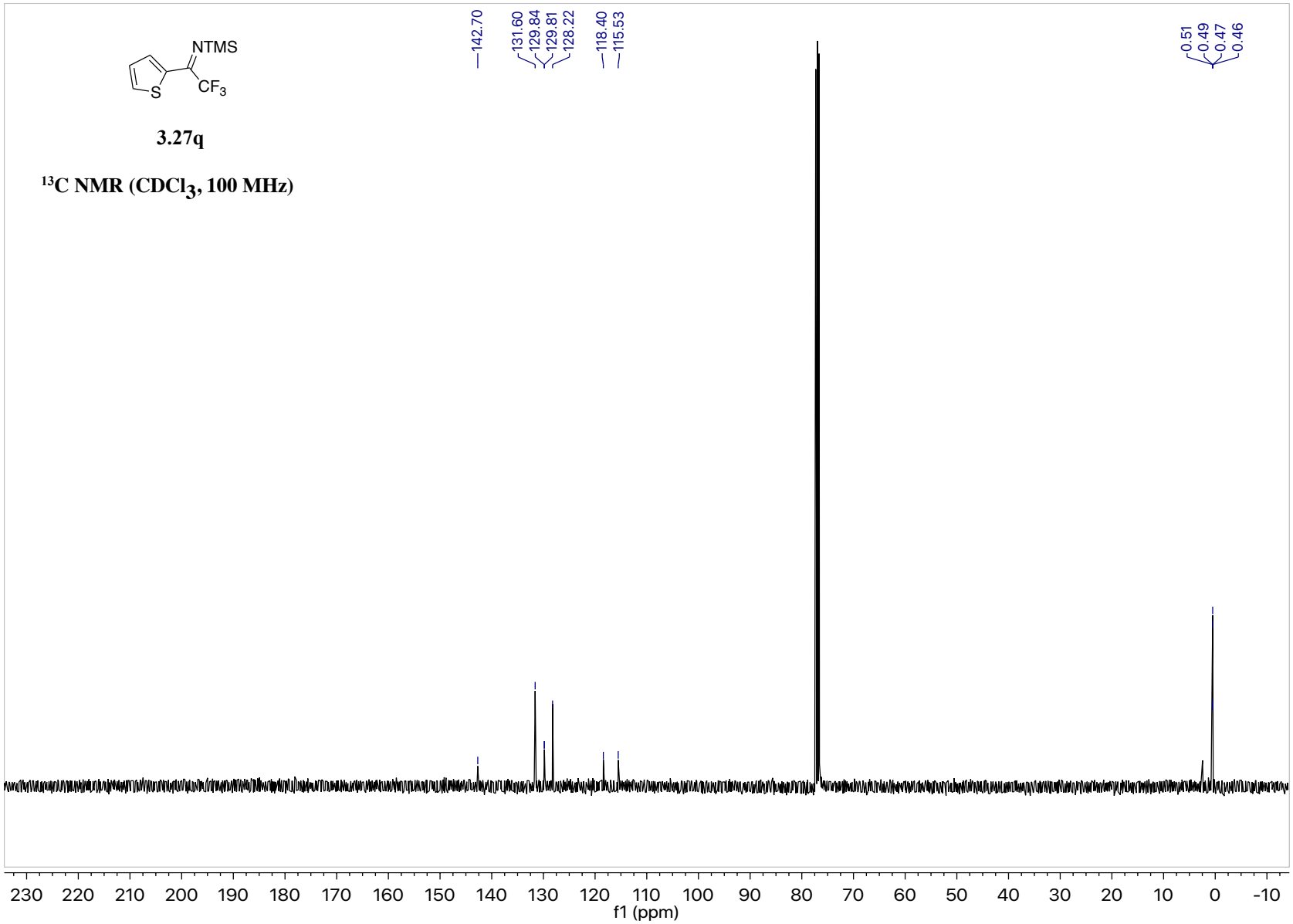

3.27q

^{13}C NMR ($CDCl_3$, 100 MHz)

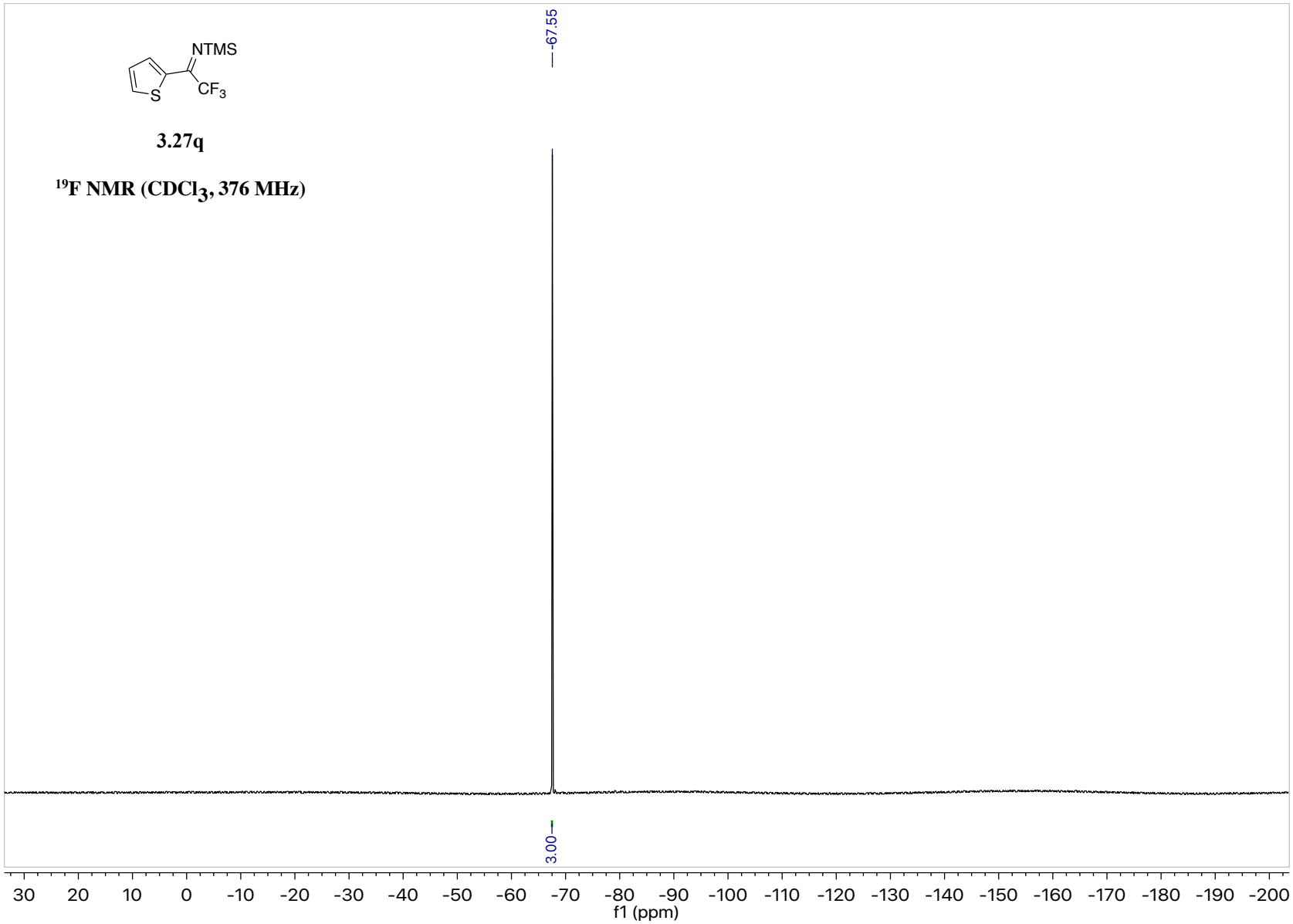

3.27q

^{19}F NMR ($CDCl_3$, 376 MHz)

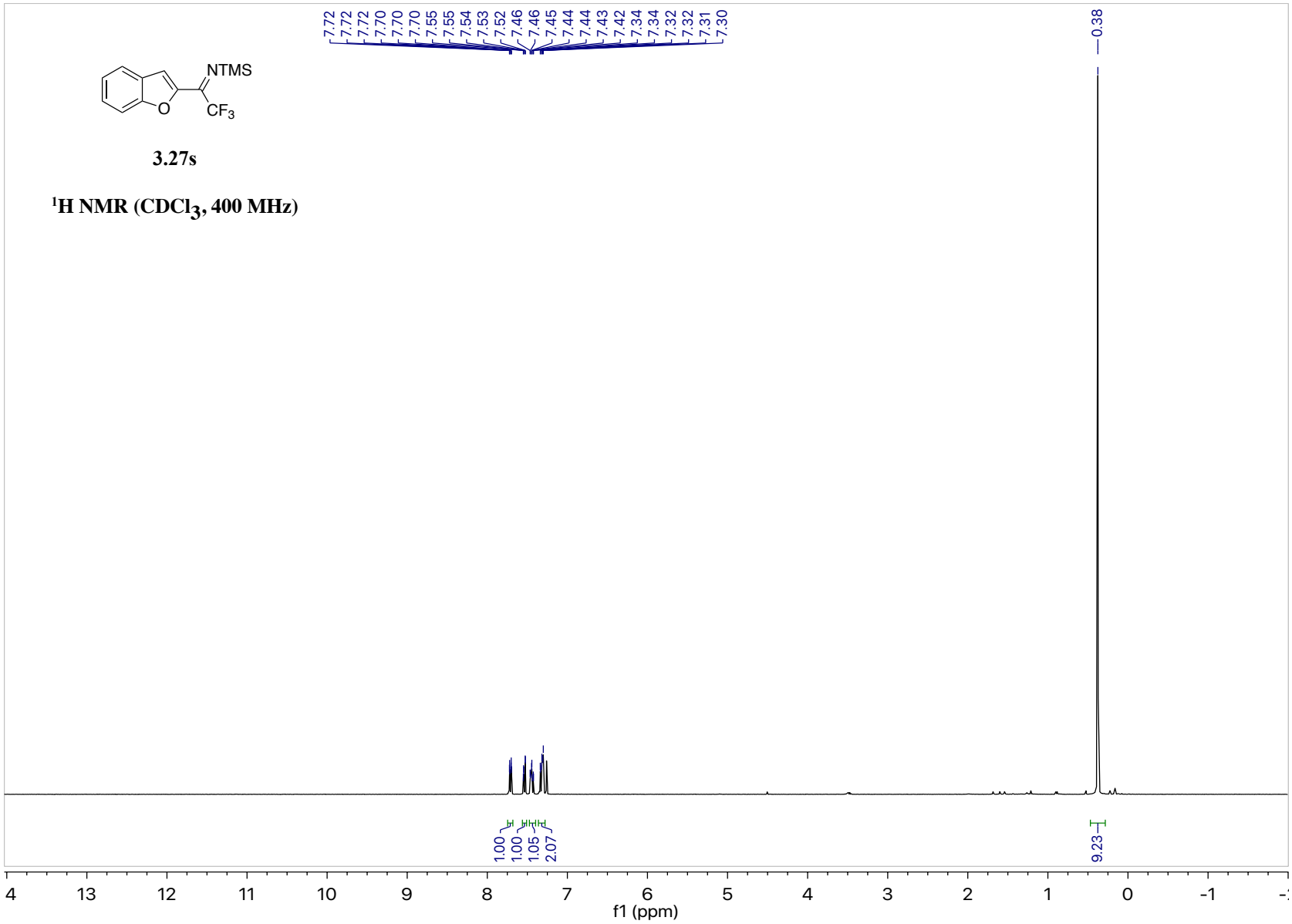
NTMS
O
CF3
3.27s
1H NMR (CDCl3, 400 MHz)
7.72
7.72
7.72
7.70
7.70
7.70
7.55
7.55
7.54
7.53
7.52
7.46
7.46
7.45
7.44
7.44
7.43
7.42
7.34
7.34
7.32
7.32
7.31
7.30
0.38
1.00
1.00
1.05
2.07
9.23
f1 (ppm)

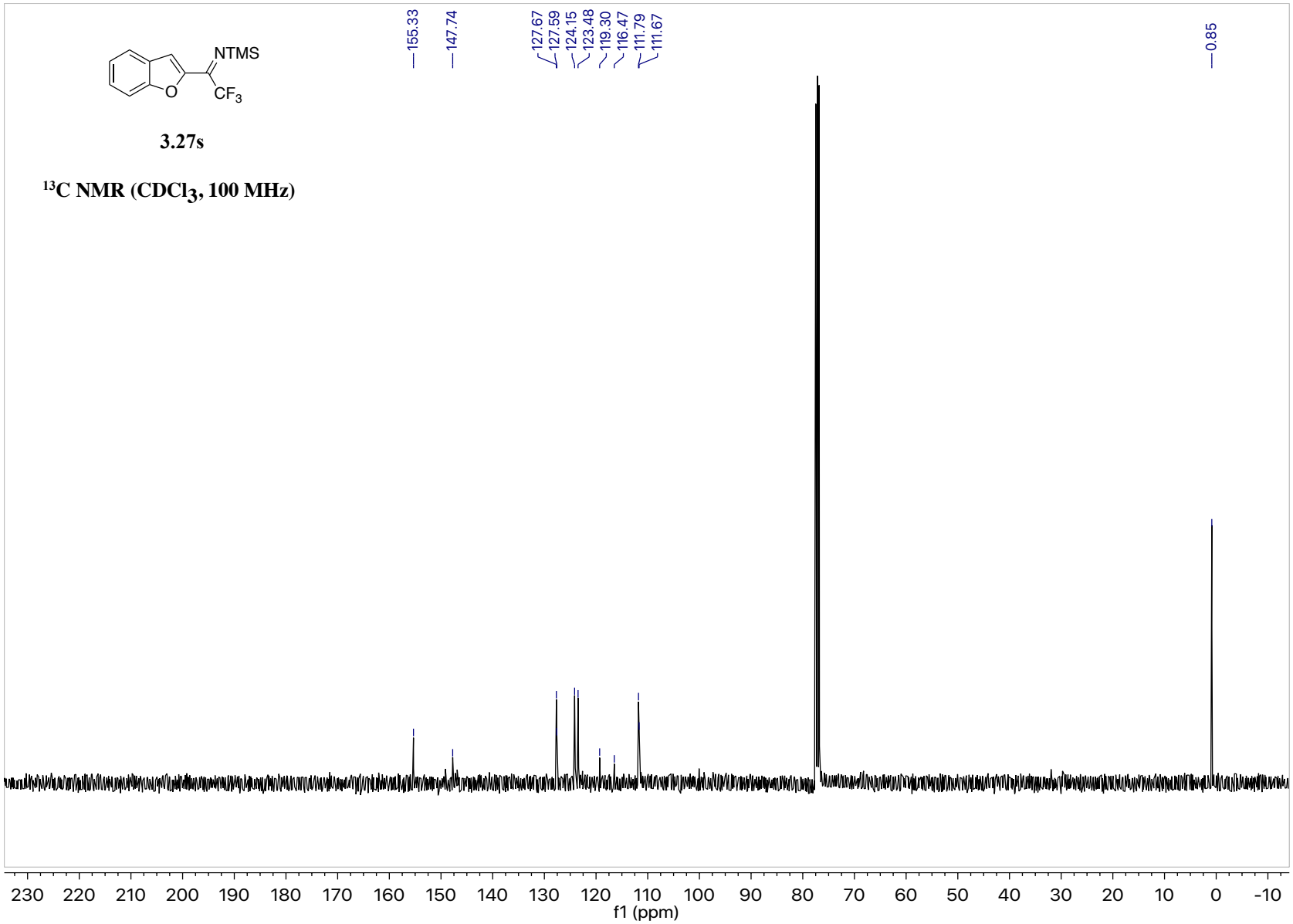

3.27s

^{13}C NMR ($CDCl_3$, 100 MHz)

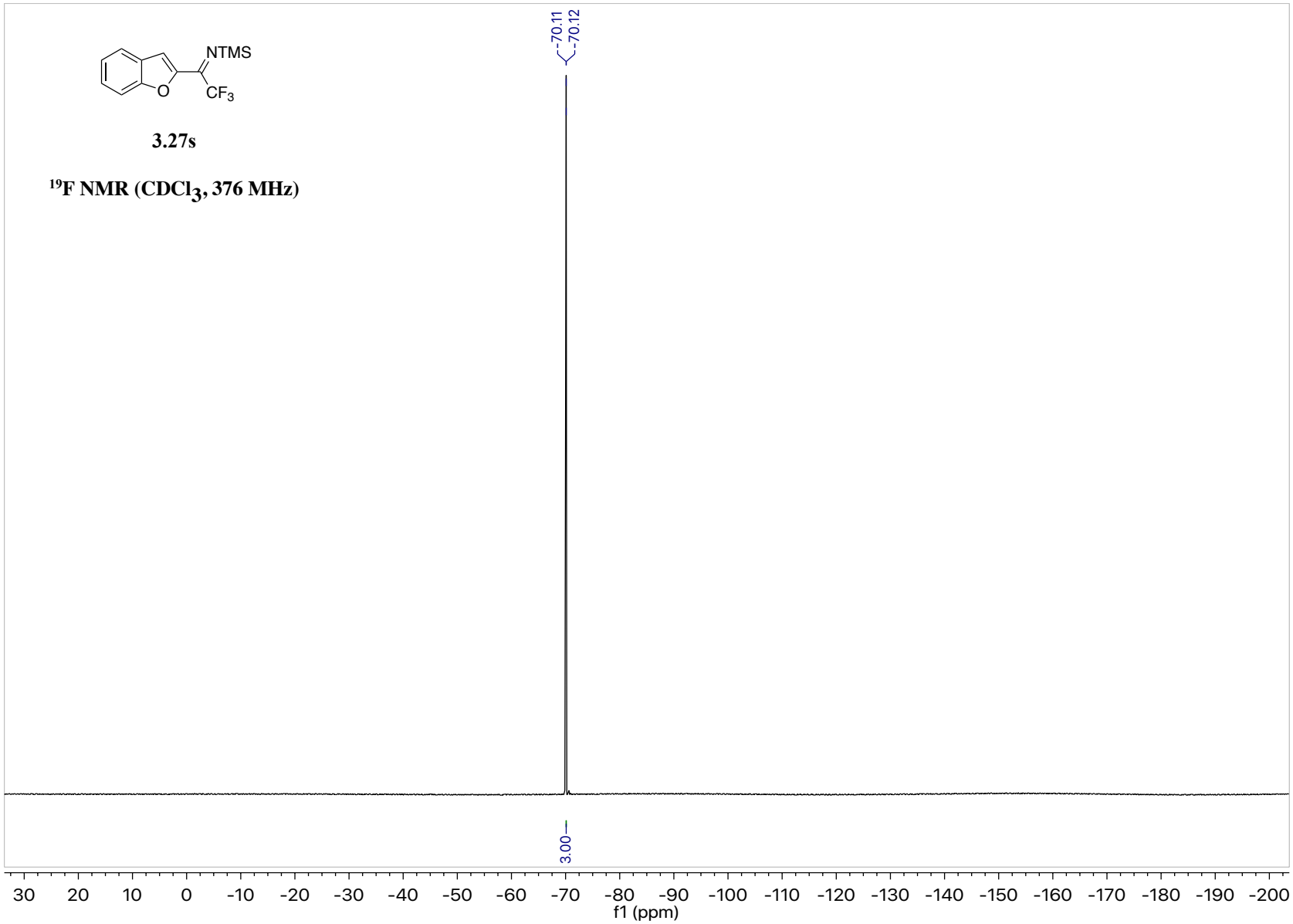
NTMS
O
CF3
3.27s
19F NMR (CDCl3, 376 MHz)
-70.11
-70.12
3.00
30 20 10 0 -10 -20 -30 -40 -50 -60 -70 -80 -90 -100 -110 -120 -130 -140 -150 -160 -170 -180 -190 -200
f1 (ppm)

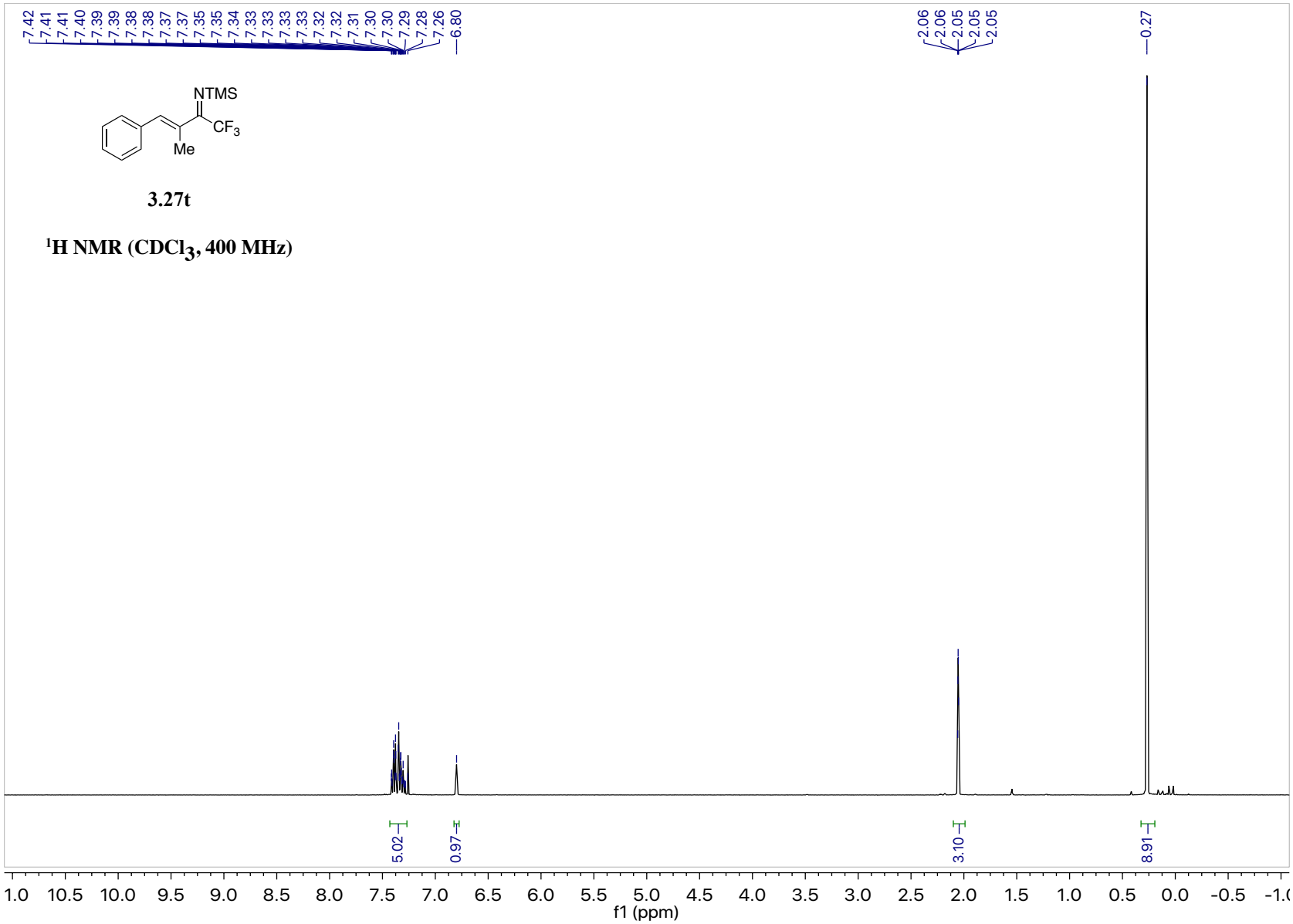

3.27t

^{1}H NMR ($CDCl_3$, 400 MHz)

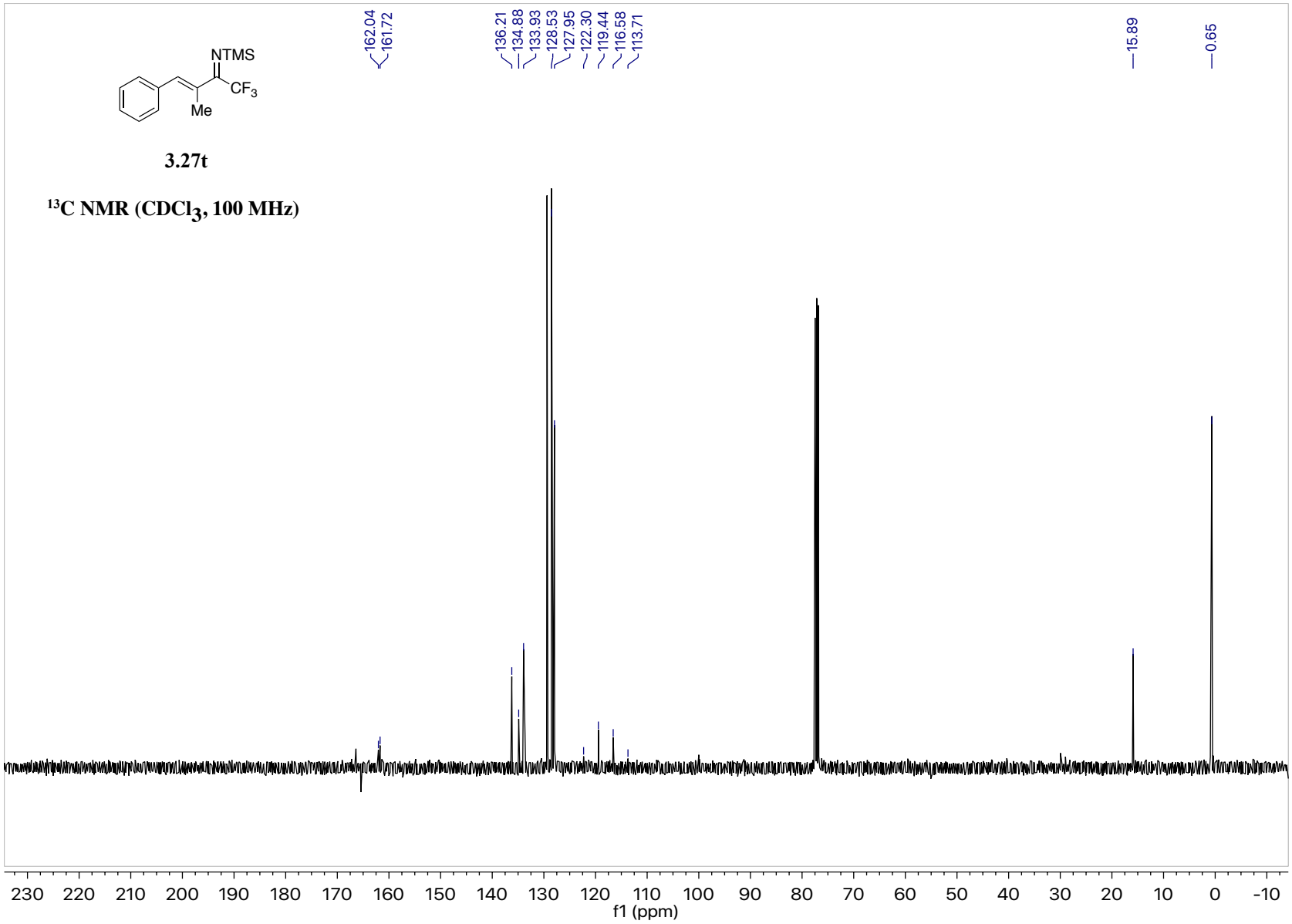
NTMS
CF3
Me
3.27t
13C NMR (CDCl3, 100 MHz)
162.04
161.72
136.21
134.88
133.93
128.53
127.95
122.30
119.44
116.58
113.71
15.89
0.65
230 220 210 200 190 180 170 160 150 140 130 120 110 100 90 80 70 60 50 40 30 20 10 0 -10
f1 (ppm)

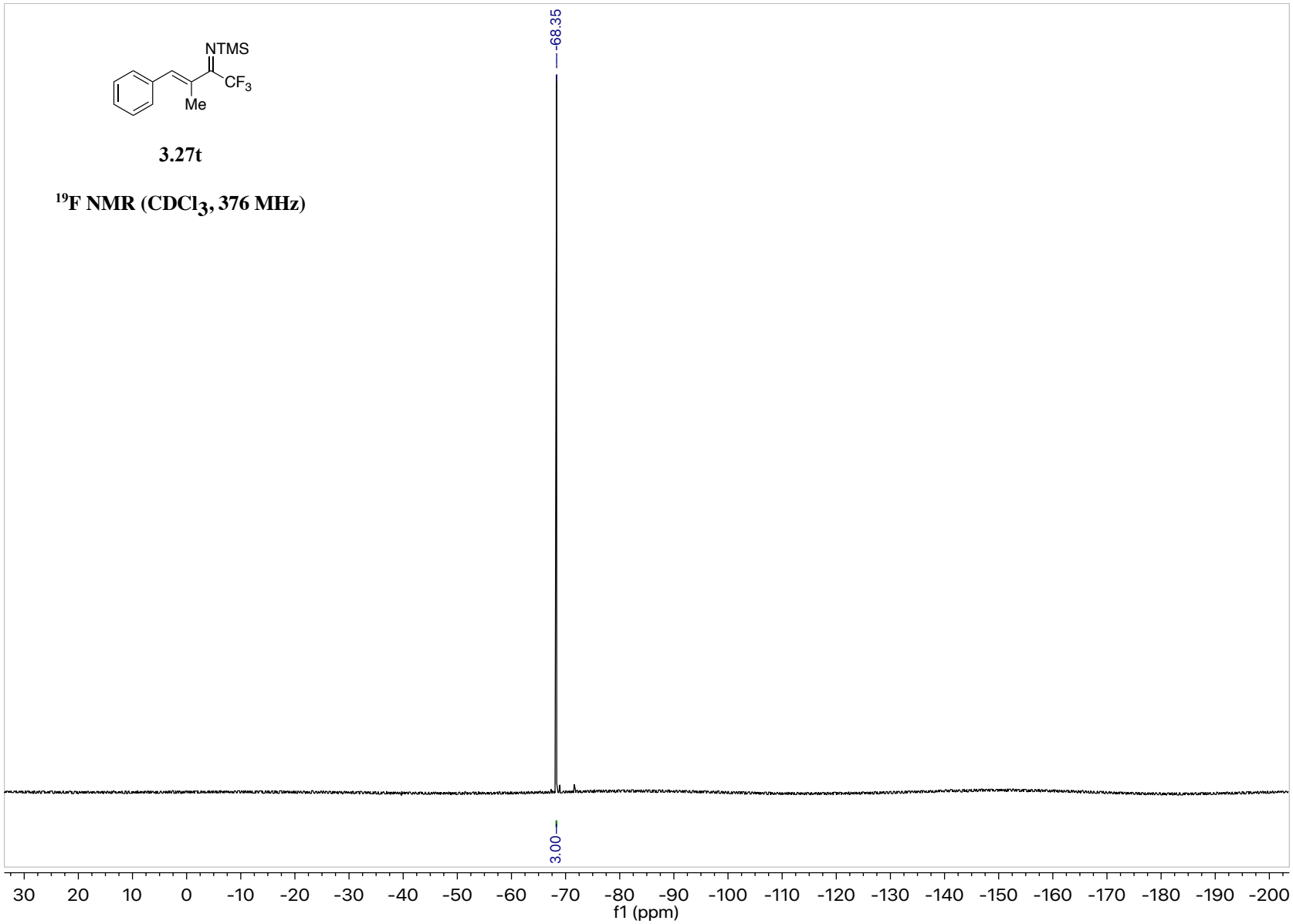
NTMS
CF3
Me
3.27t
19F NMR (CDCl3, 376 MHz)
-68.35
3.00
30 20 10 0 -10 -20 -30 -40 -50 -60 -70 -80 -90 -100 -110 -120 -130 -140 -150 -160 -170 -180 -190 -200
f1 (ppm)

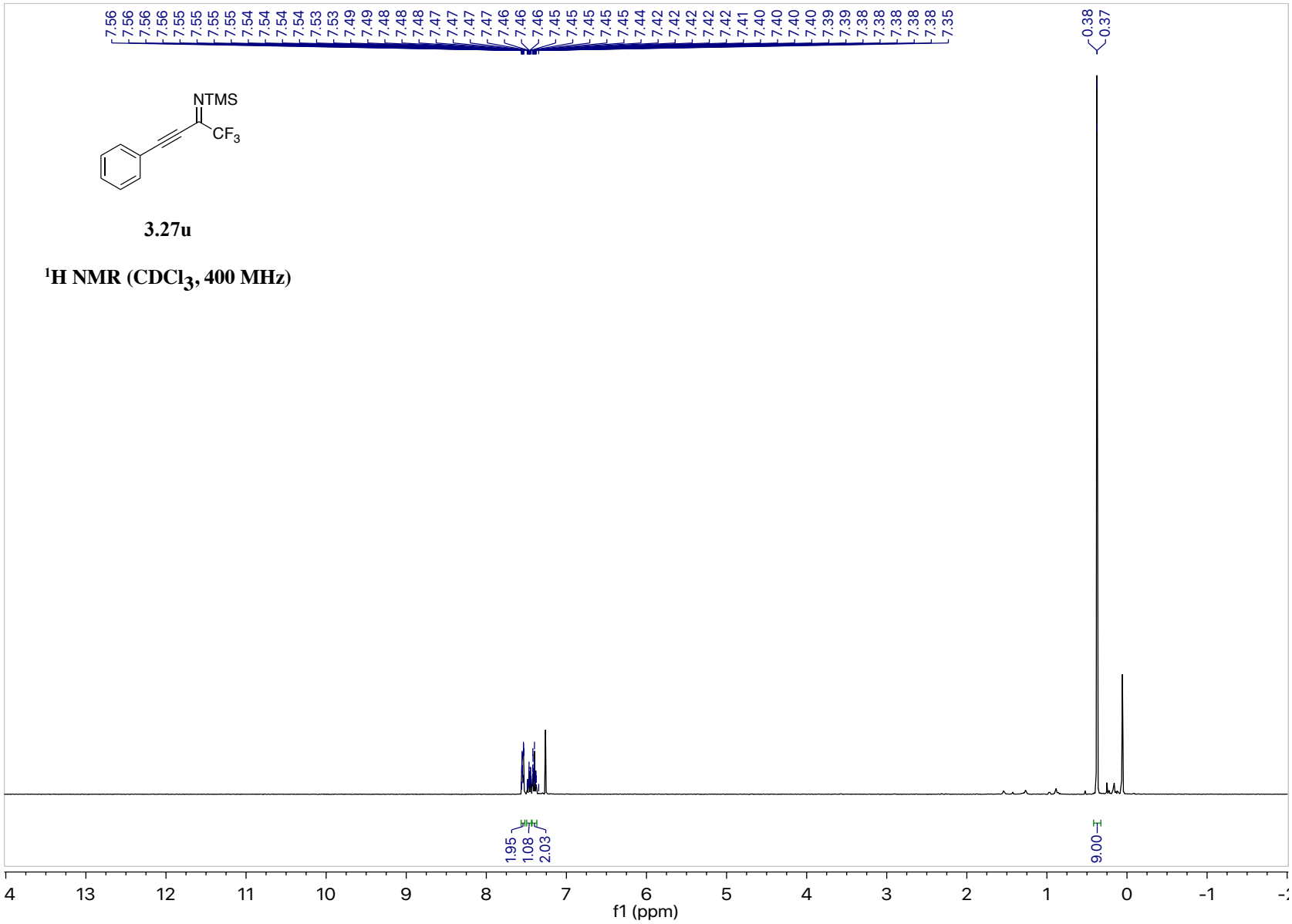

3.27u

^{1}H NMR ($CDCl_3$, 400 MHz)

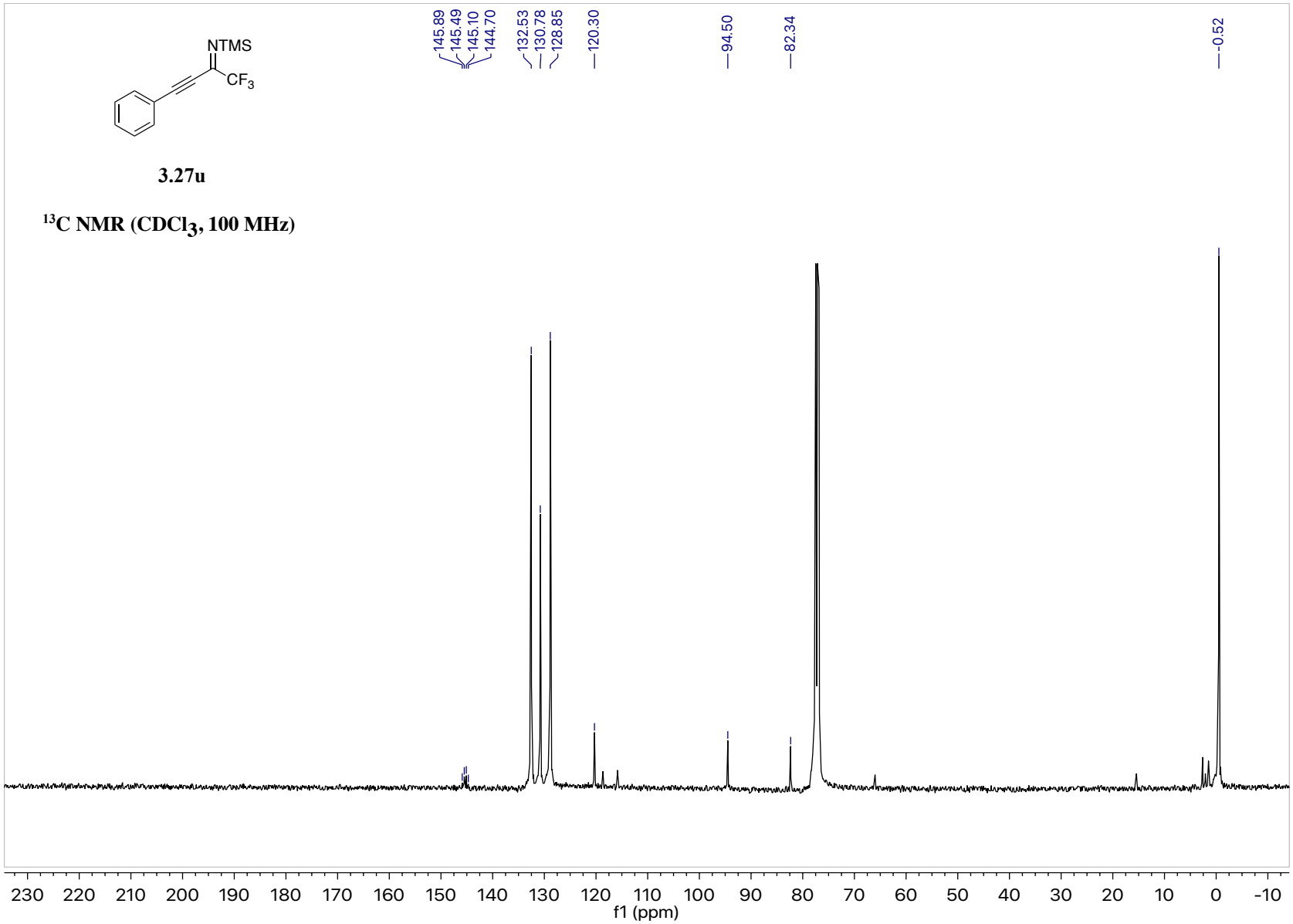

3.27u

^{13}C NMR ($CDCl_3$, 100 MHz)

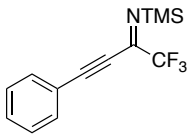

3.27u

^{19}F NMR ($CDCl_3$, 376 MHz)

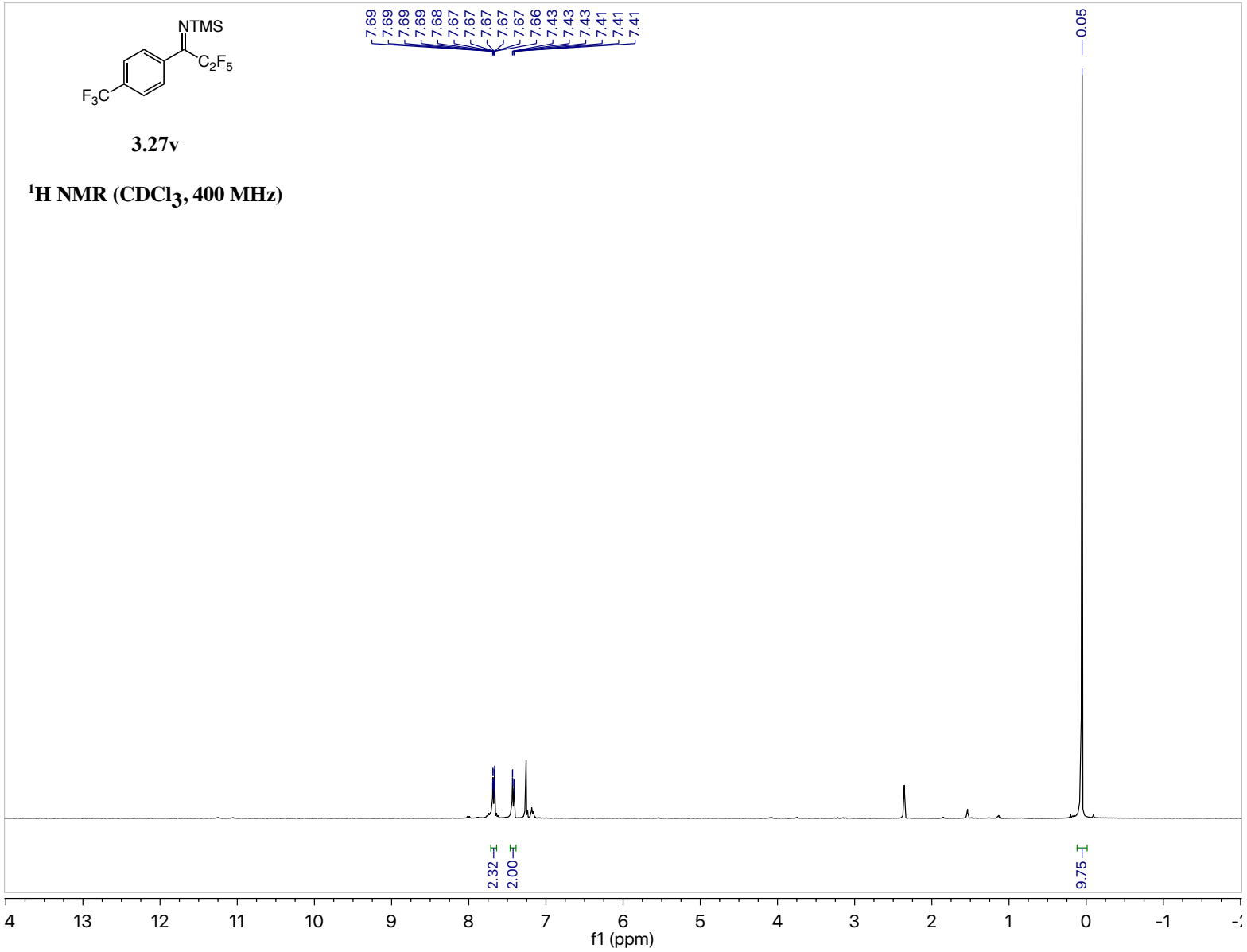

3.27v

^{1}H NMR ($CDCl_3$, 400 MHz)

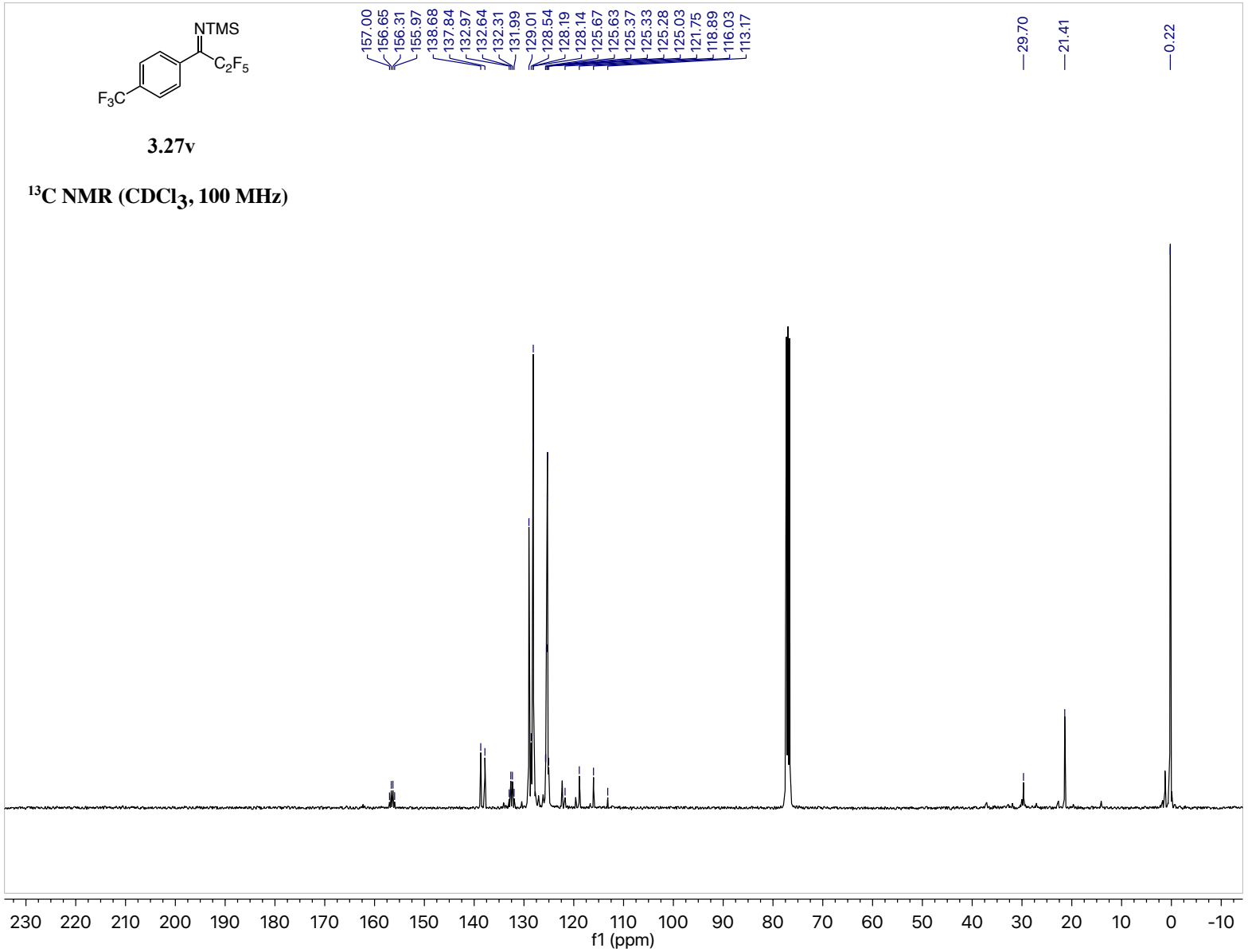

3.27v

^{13}C NMR ($CDCl_3$, 100 MHz)

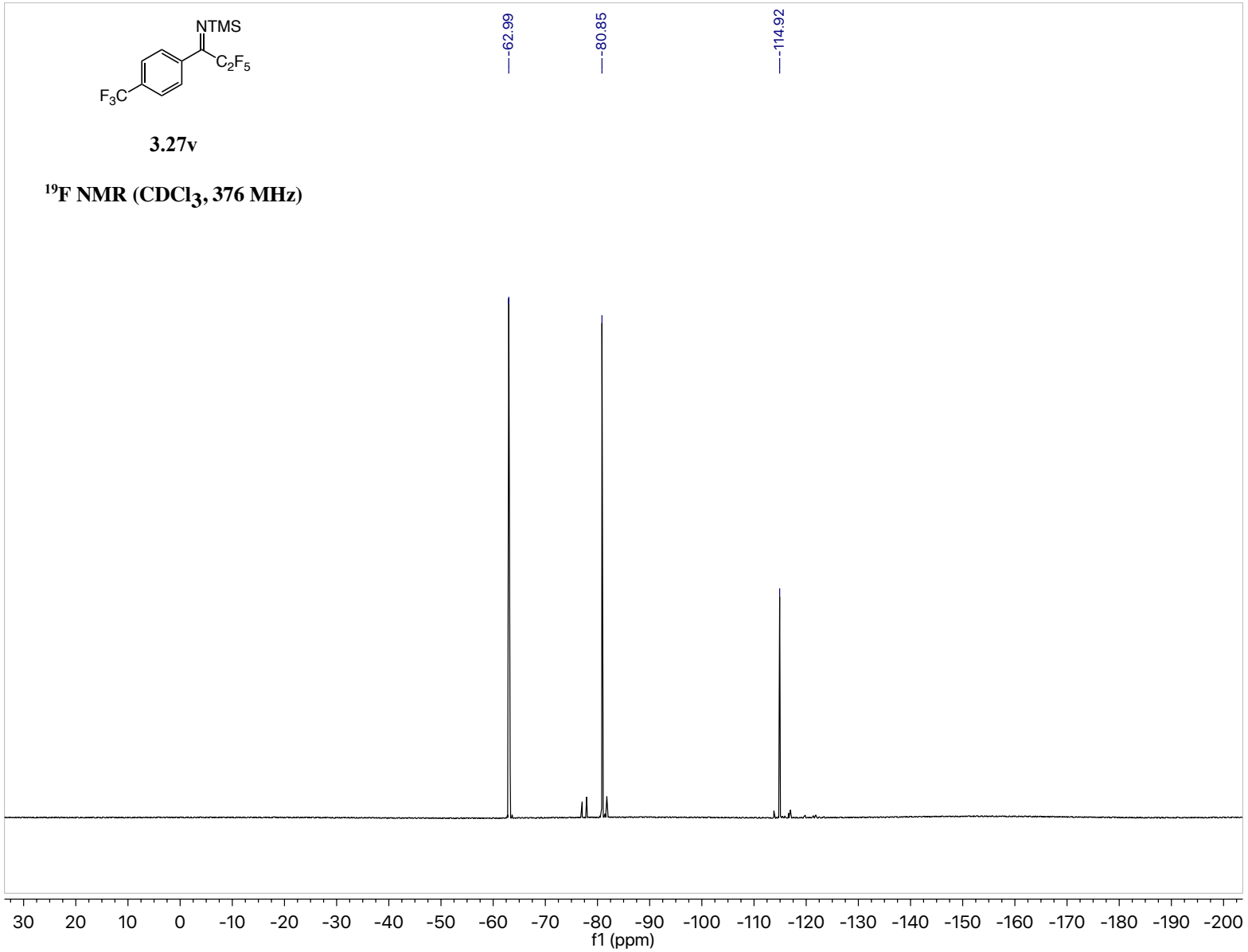

3.27v

^{19}F NMR ($CDCl_3$, 376 MHz)

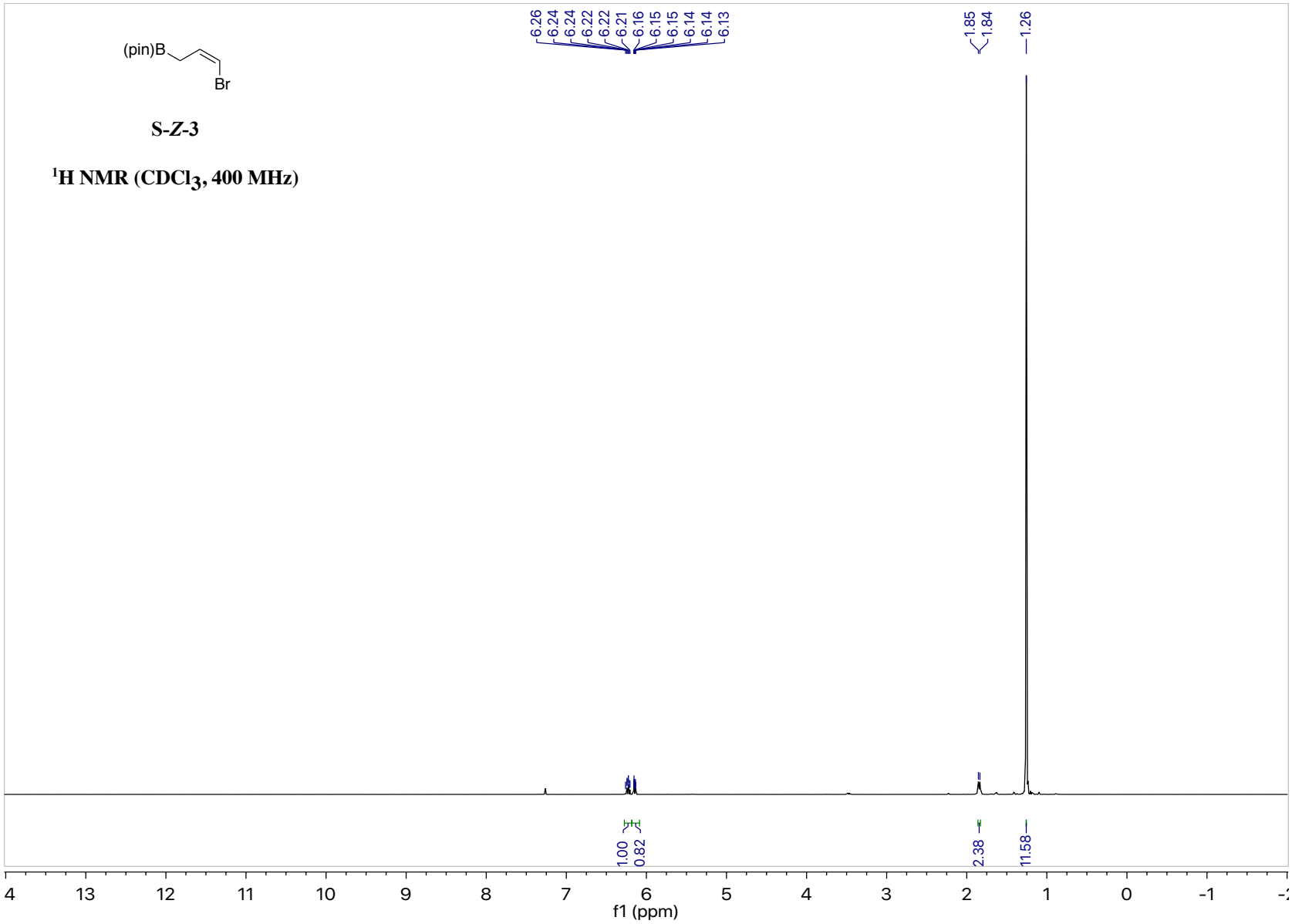

S-*Z*-3

^{1}H NMR ($CDCl_3$, 400 MHz)

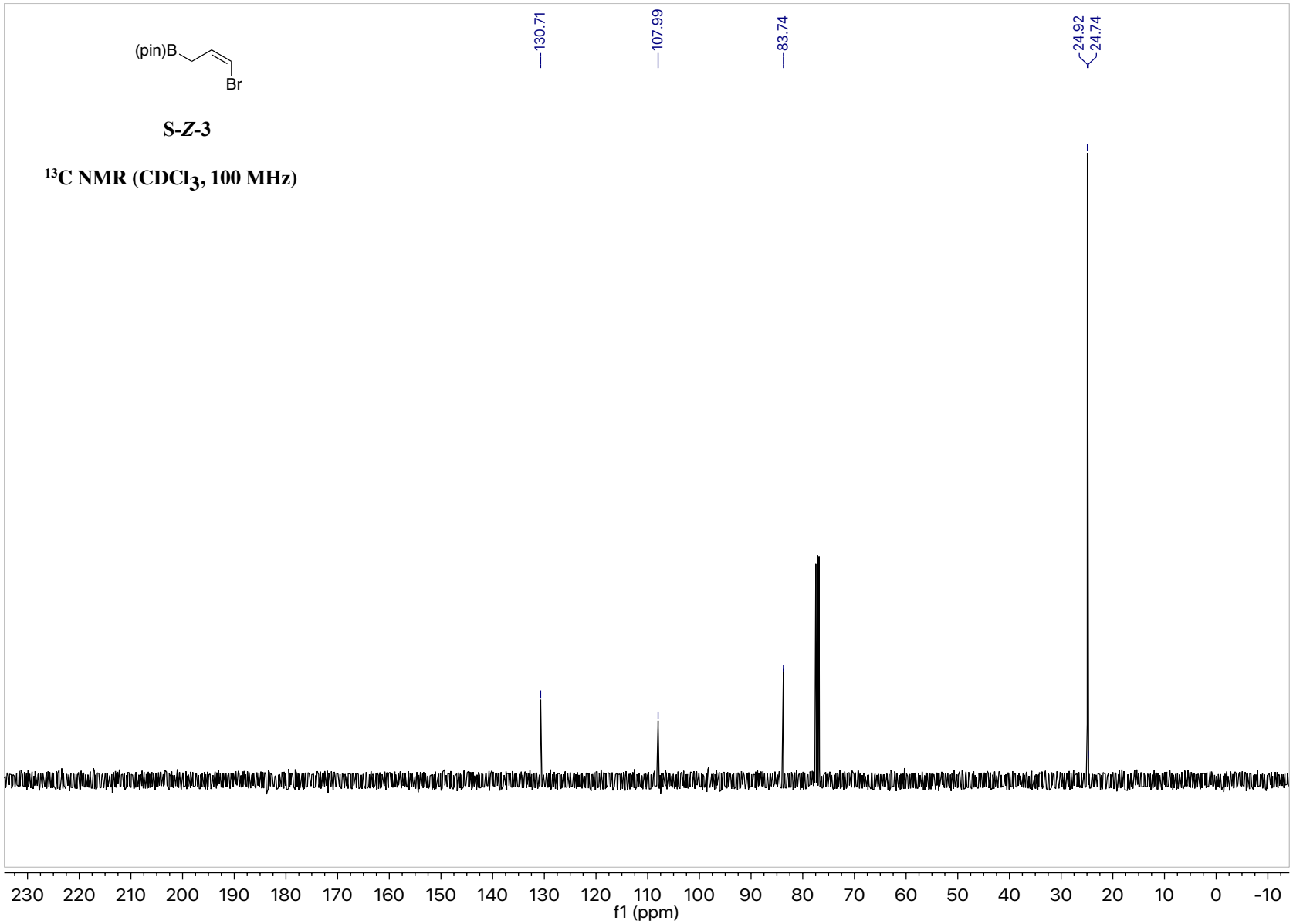

S-*Z*-3

^{13}C NMR ($CDCl_3$, 100 MHz)

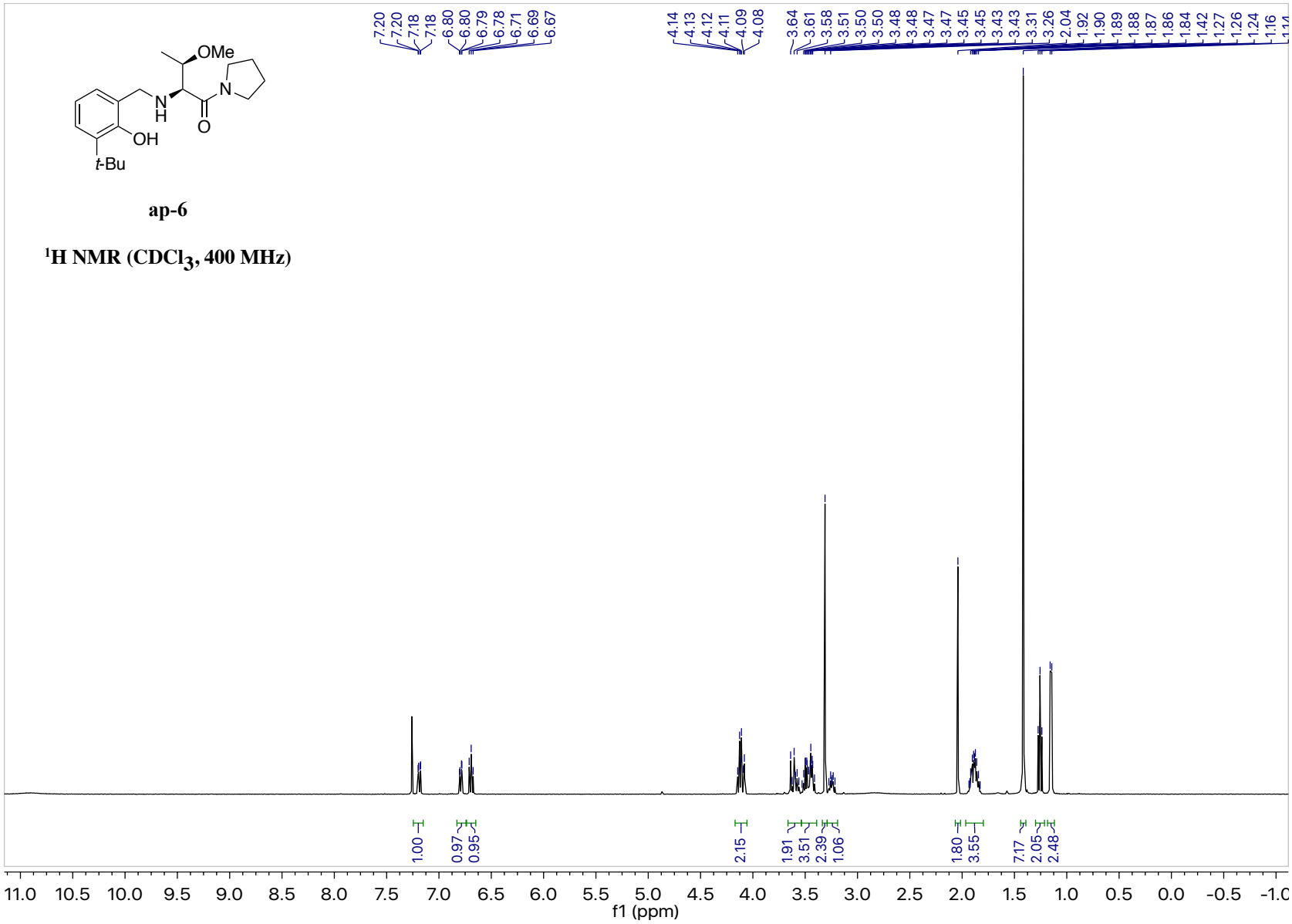

ap-6

^{1}H NMR ($CDCl_3$, 400 MHz)

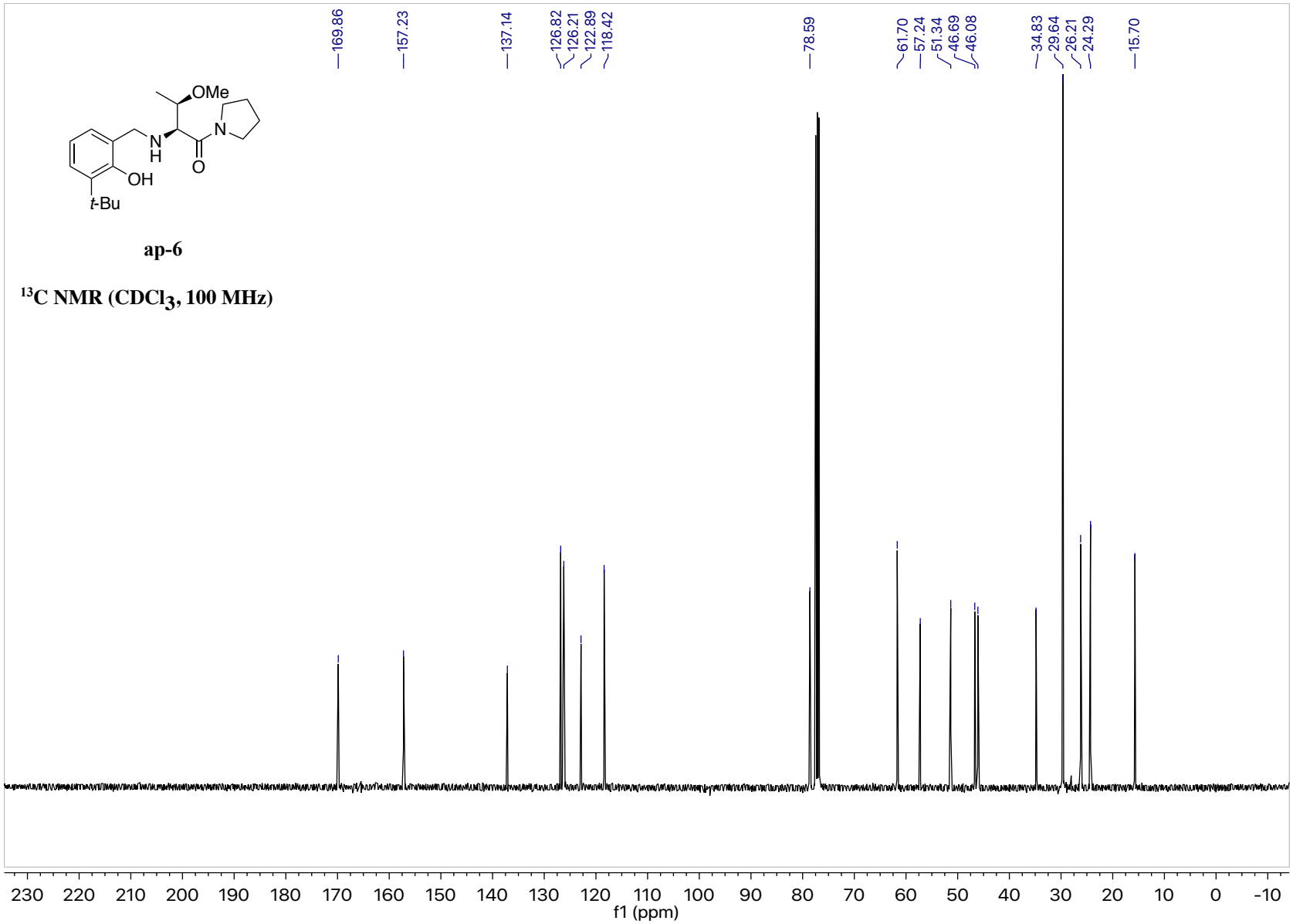

ap-6

^{13}C NMR ($CDCl_3$, 100 MHz)

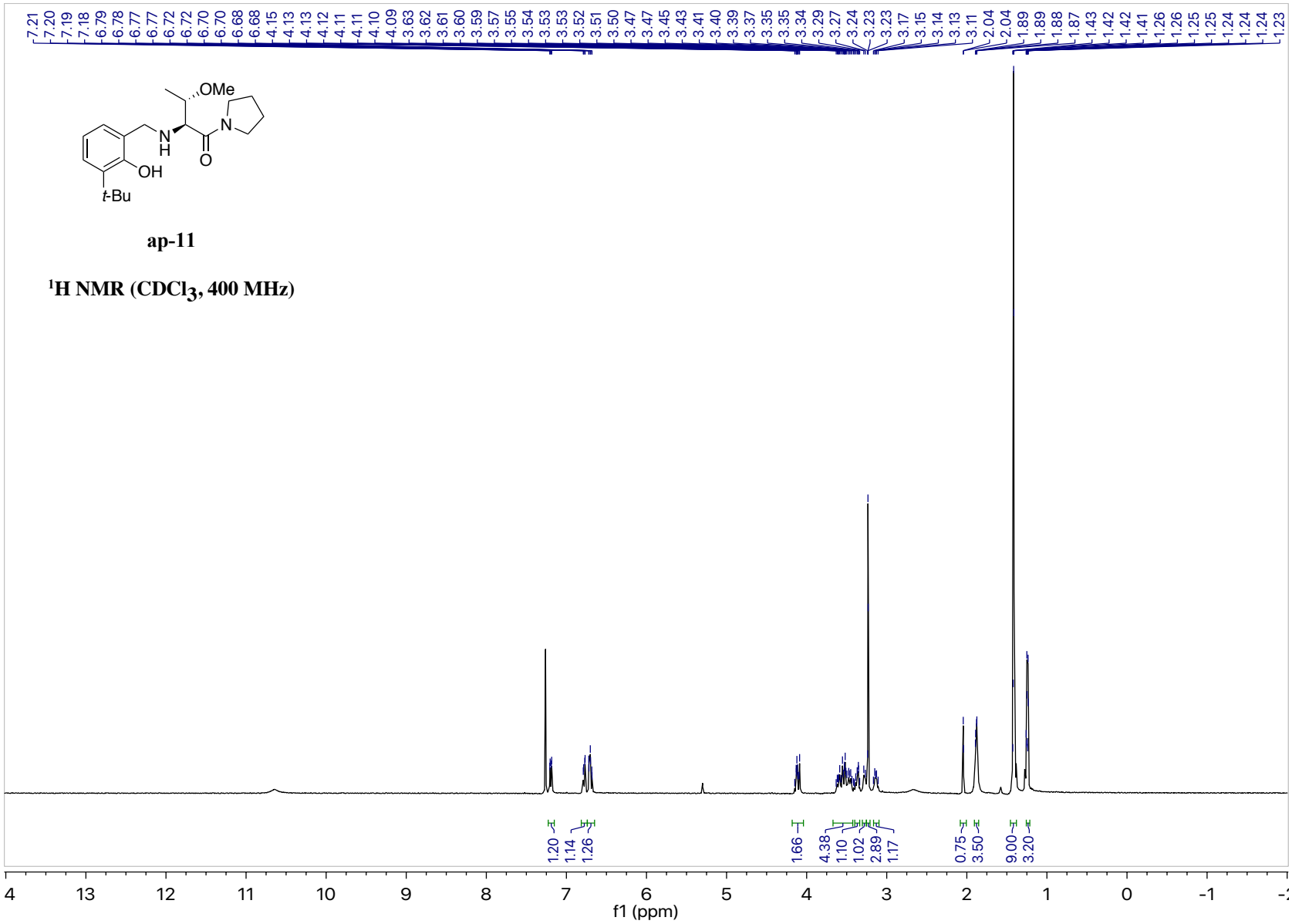

ap-11

^{1}H NMR ($CDCl_3$, 400 MHz)

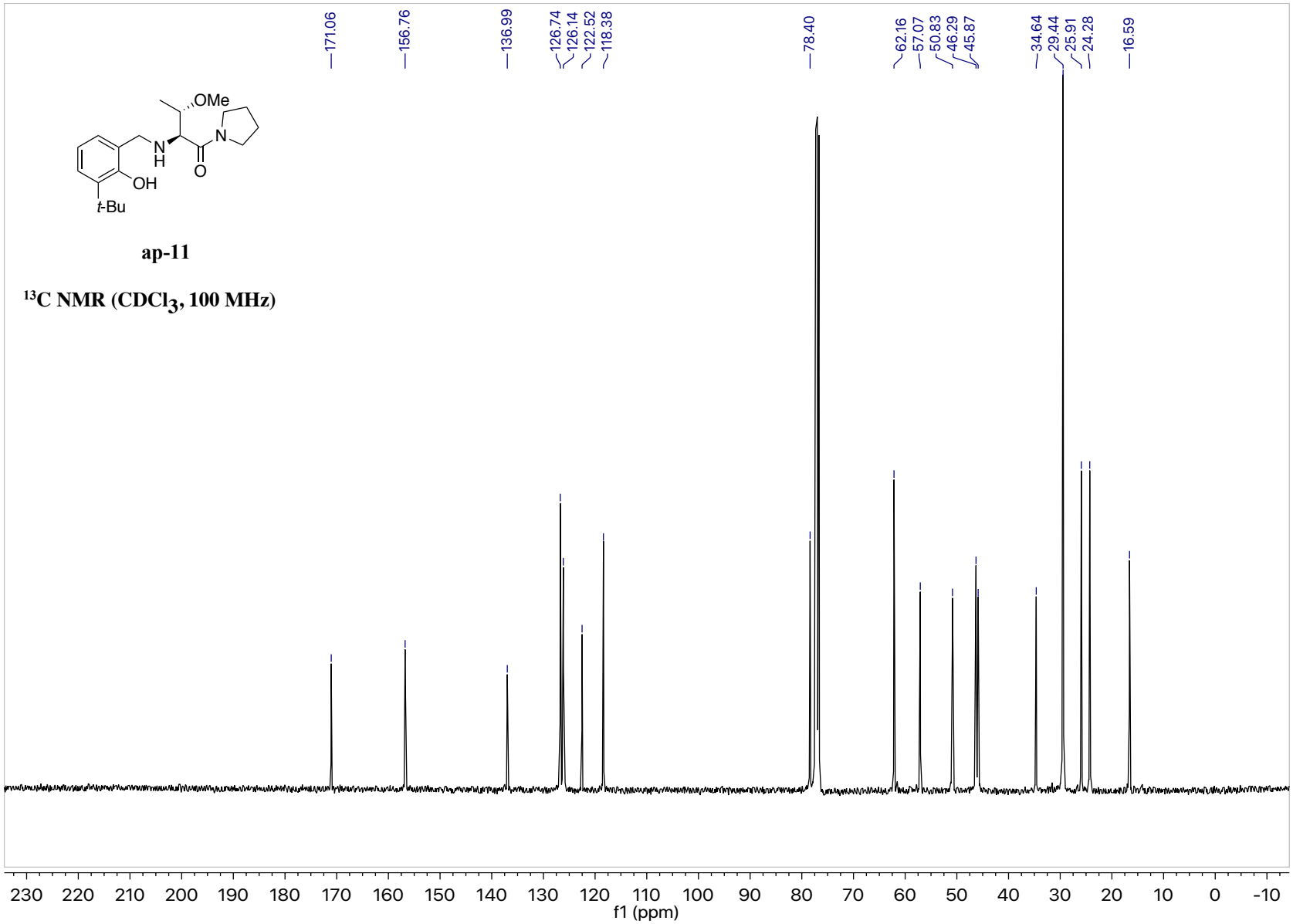

ap-11

^{13}C NMR ($CDCl_3$, 100 MHz)

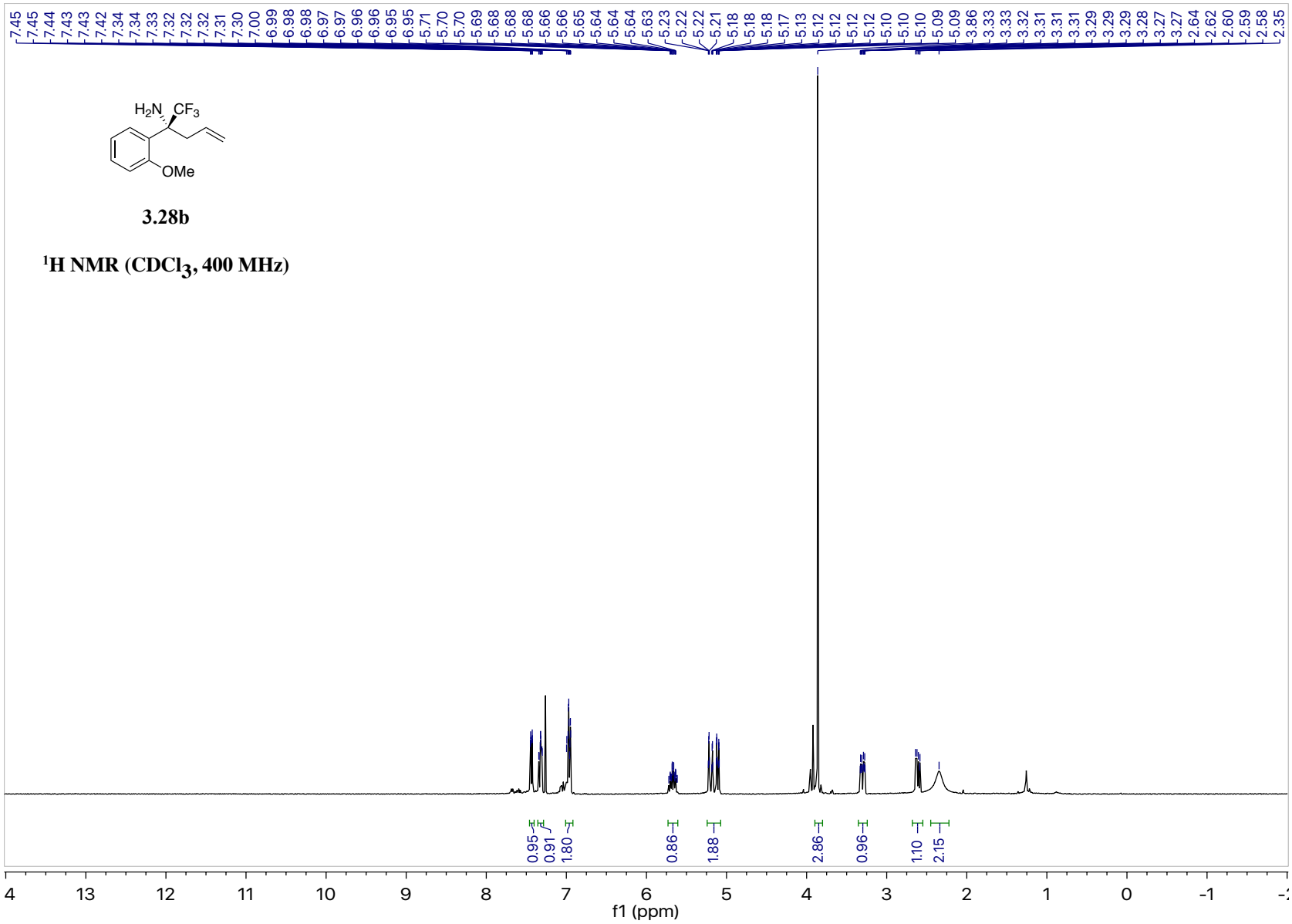

3.28b

^{1}H NMR ($CDCl_3$, 400 MHz)

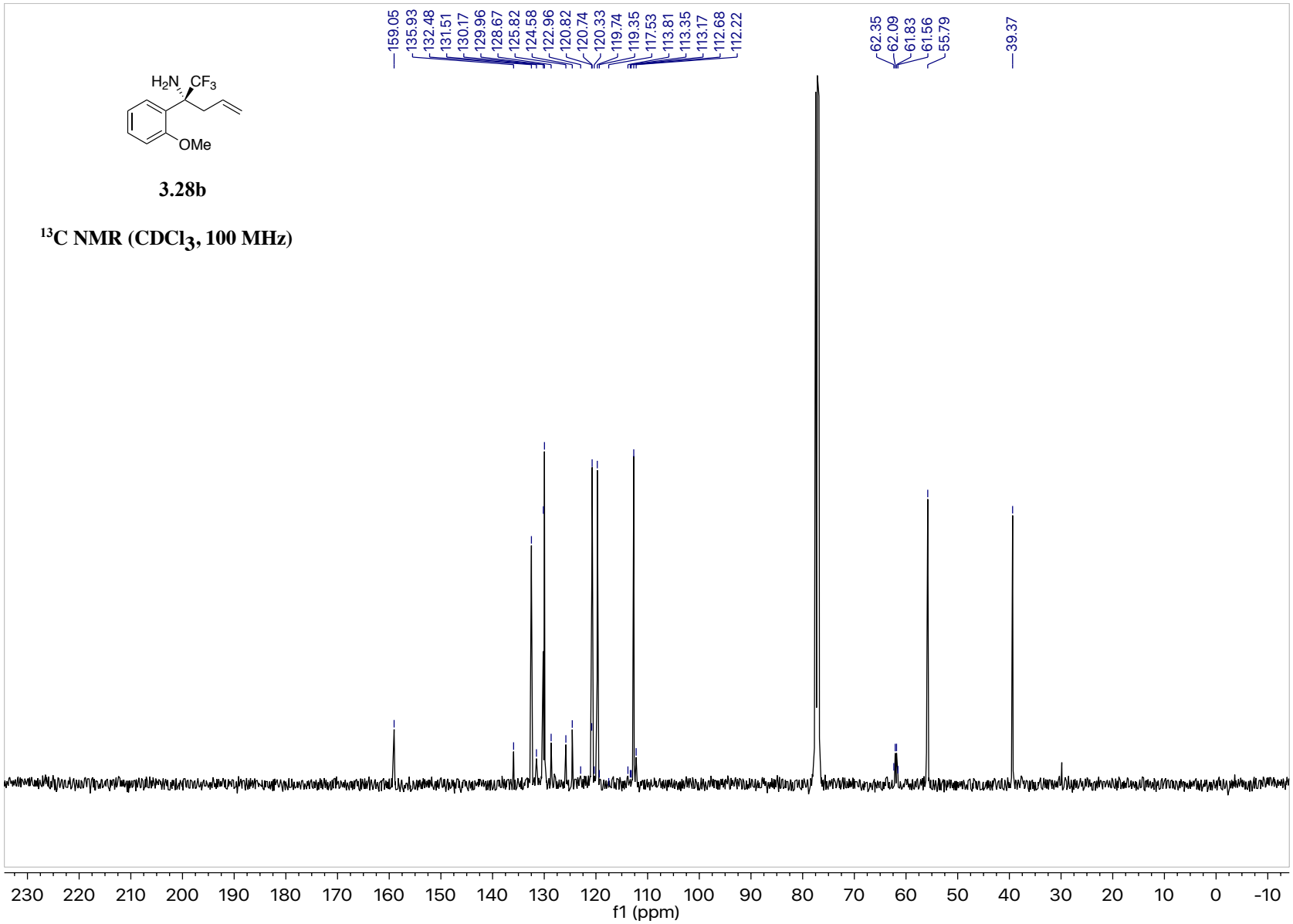
159.05
135.93
132.48
131.51
130.17
129.96
128.67
125.82
124.58
122.96
120.82
120.74
120.33
119.74
119.35
117.53
113.81
113.35
113.17
112.68
112.22
62.35
62.09
61.83
61.56
55.79
39.37
H2N
CF3
OMe
3.28b
13C NMR (CDCl3, 100 MHz)
230 220 210 200 190 180 170 160 150 140 130 120 110 100 90 80 70 60 50 40 30 20 10 0 -10
f1 (ppm)

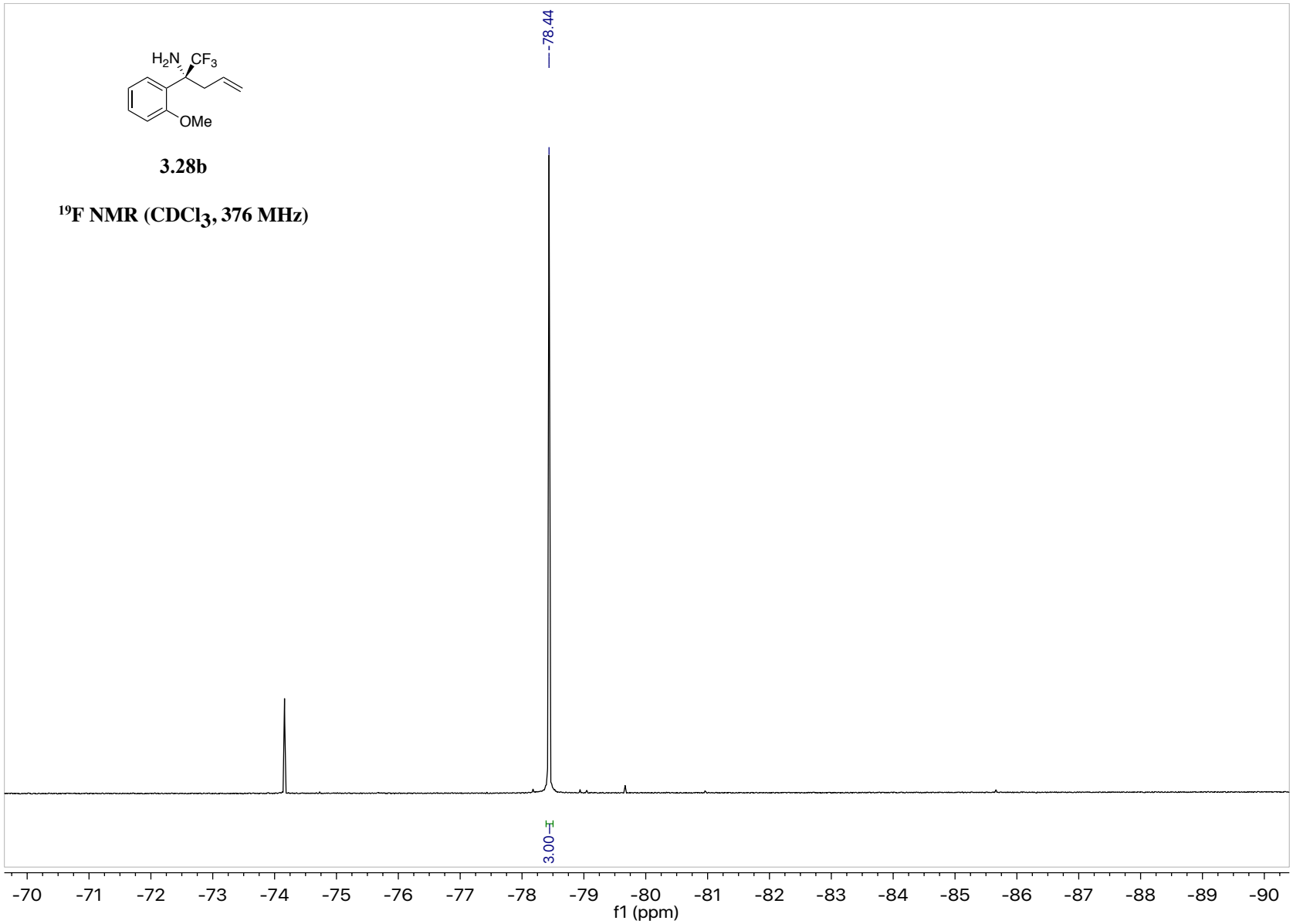

3.28b

^{19}F NMR ($CDCl_3$, 376 MHz)

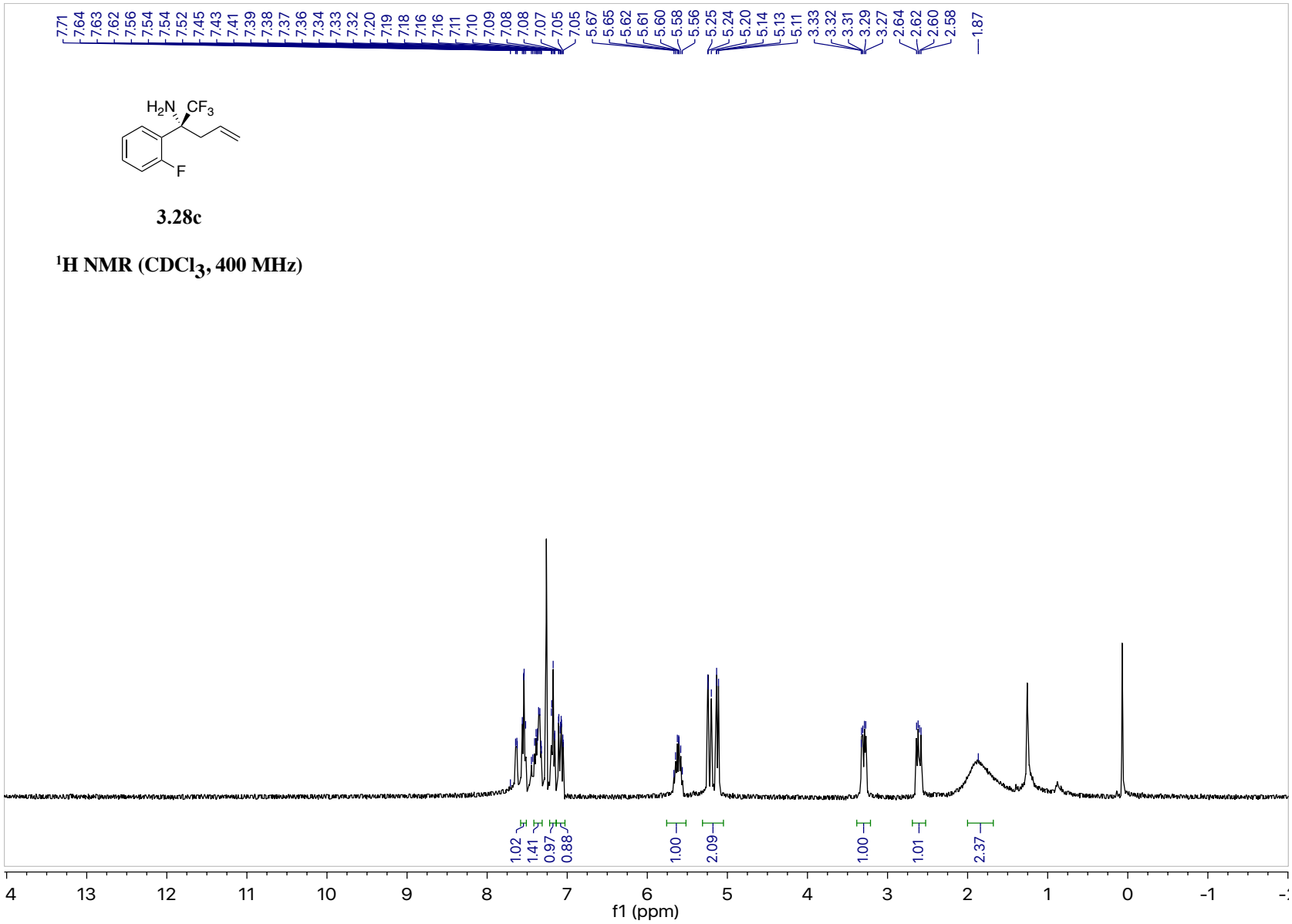

3.28c

^{1}H NMR ($CDCl_3$, 400 MHz)

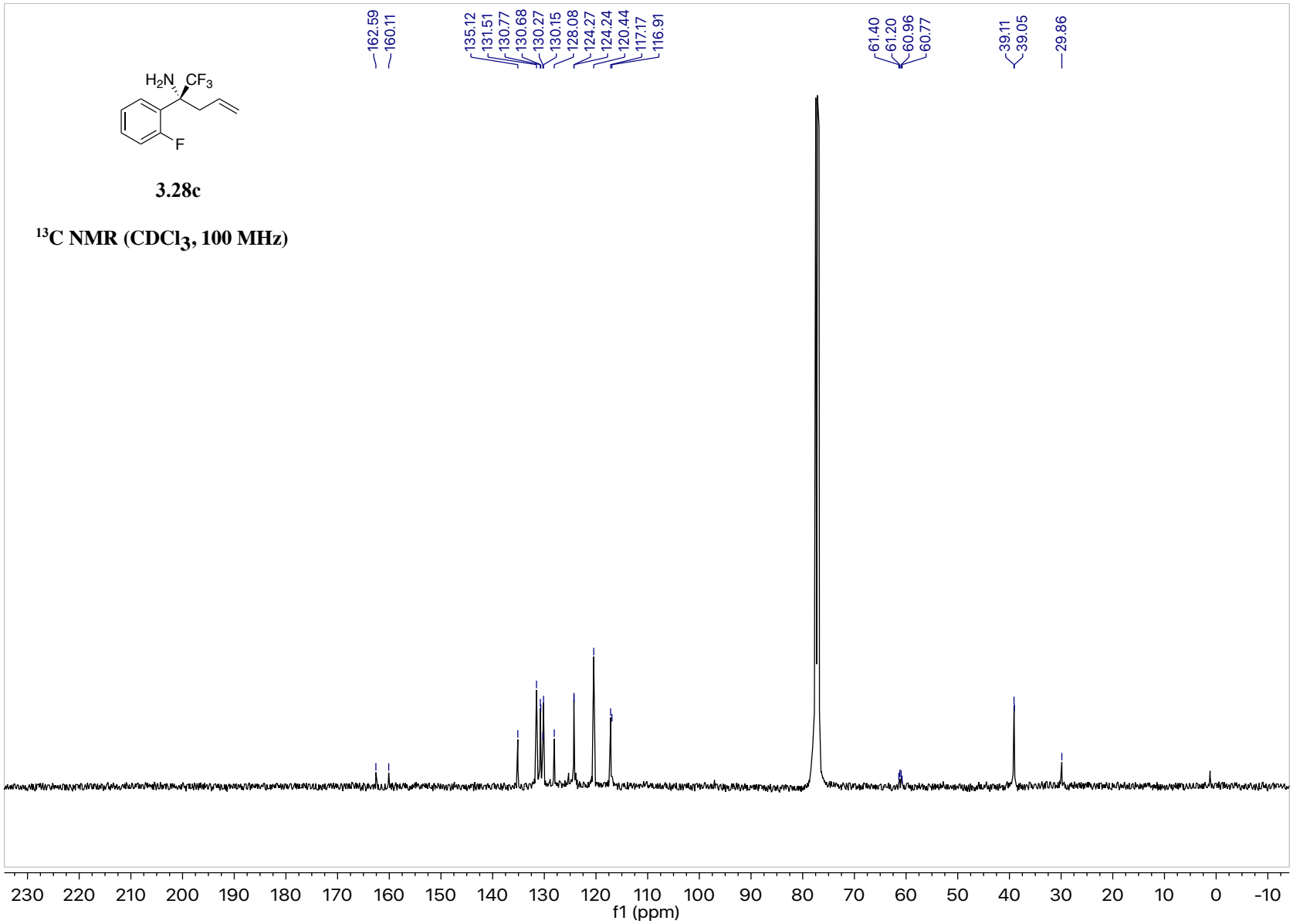

3.28c

^{13}C NMR ($CDCl_3$, 100 MHz)

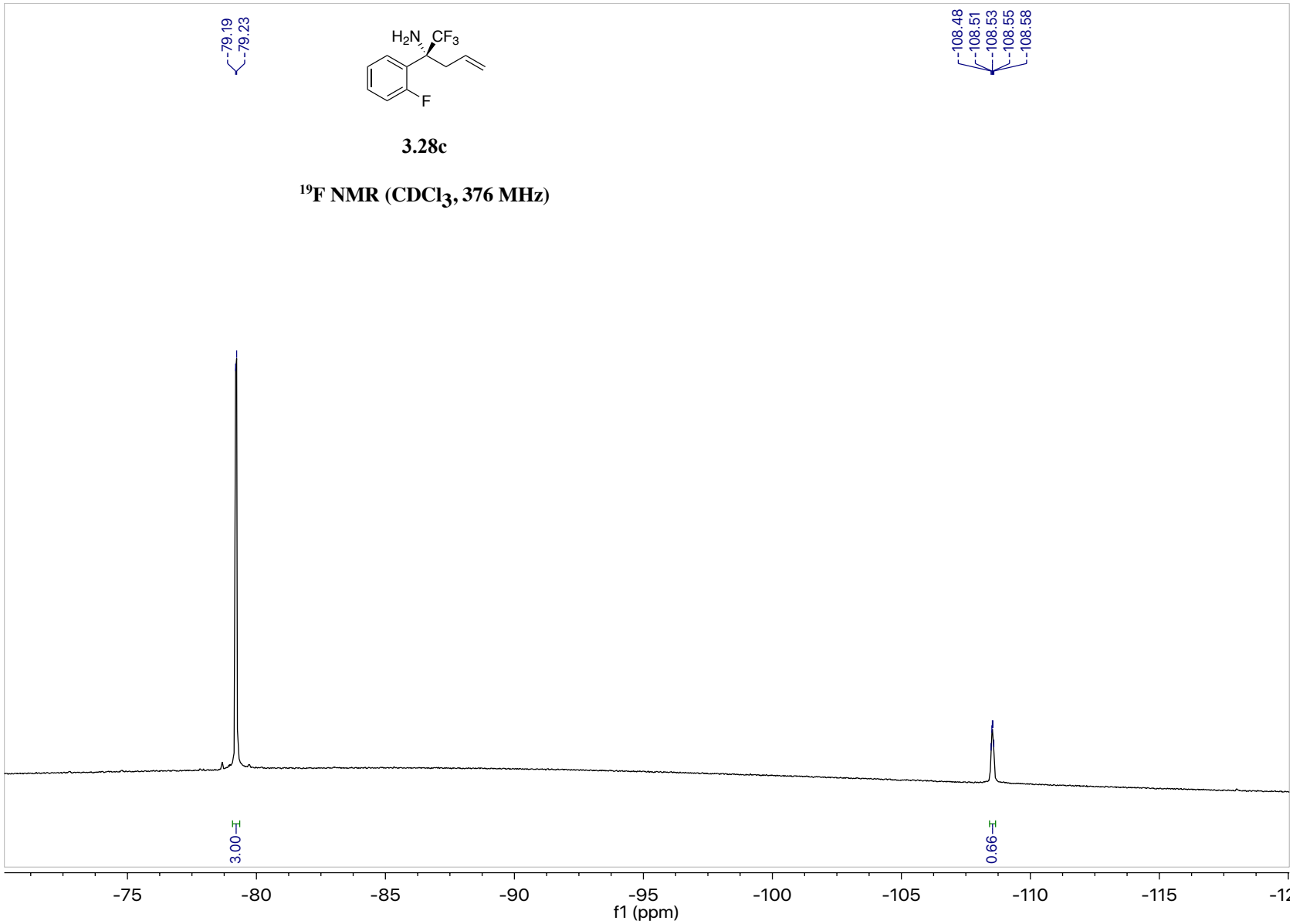

3.28c

^{19}F NMR ($CDCl_3$, 376 MHz)

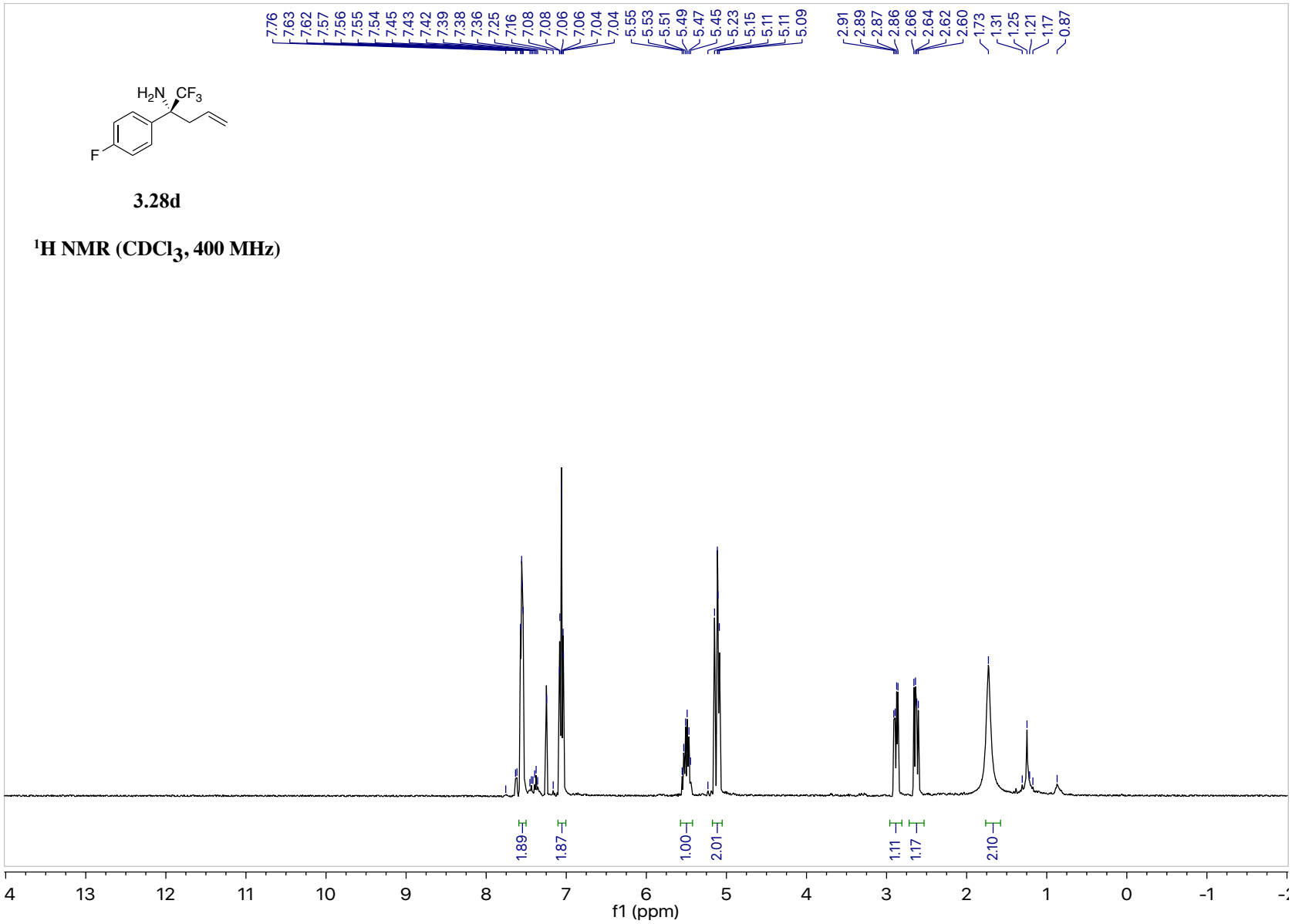

3.28d

^{1}H NMR ($CDCl_3$, 400 MHz)

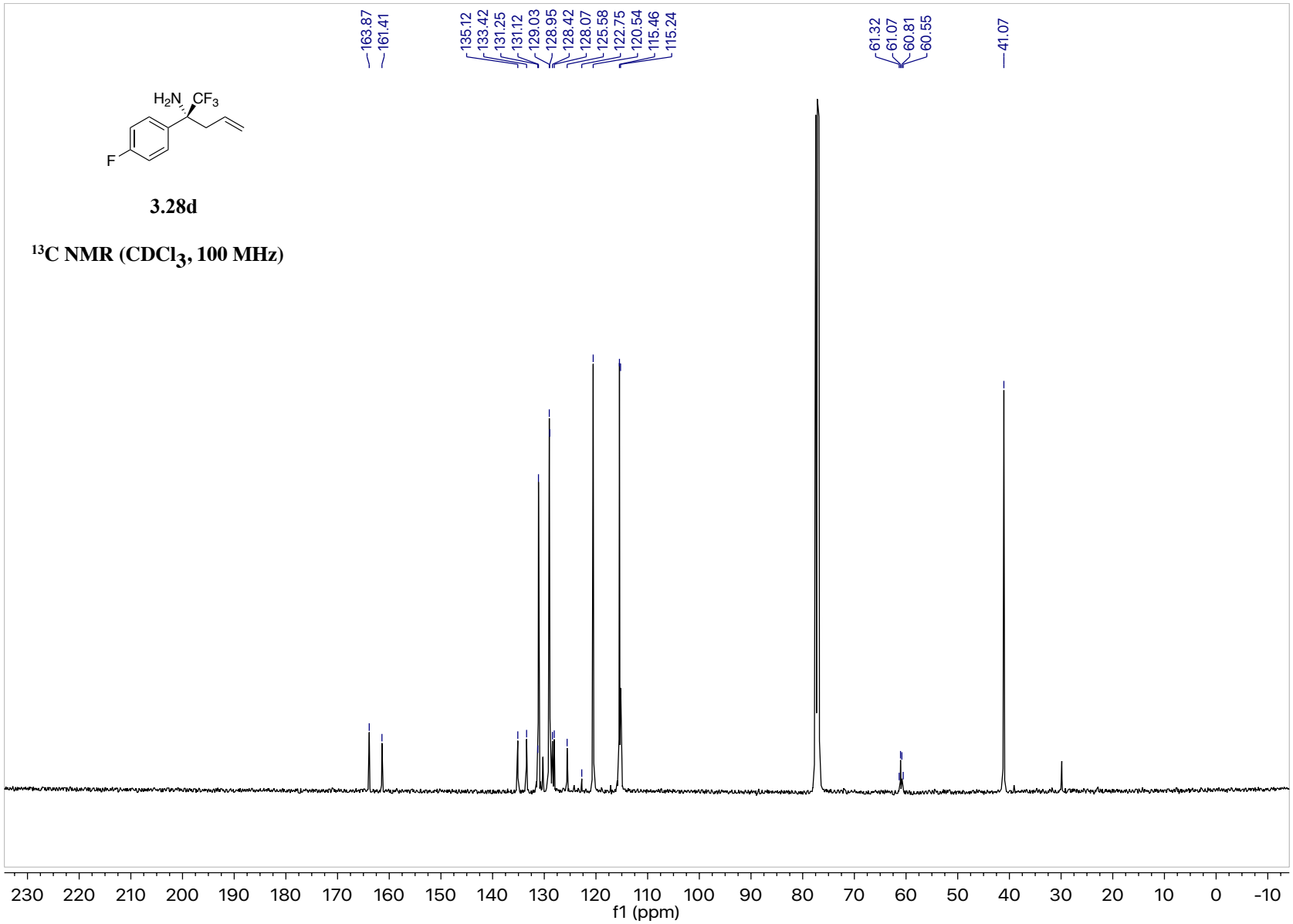

3.28d

^{13}C NMR ($CDCl_3$, 100 MHz)

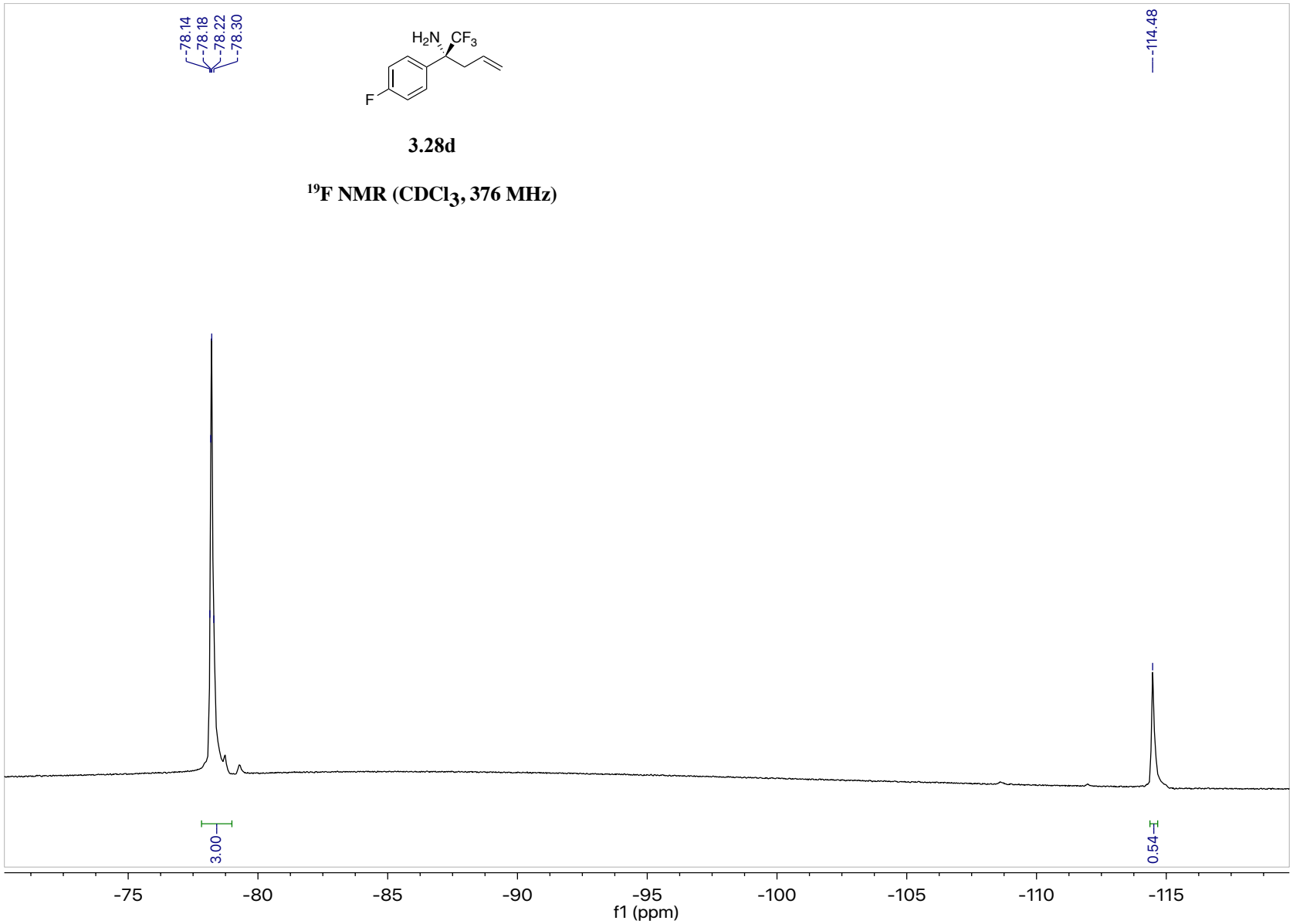

3.28d

^{19}F NMR ($CDCl_3$, 376 MHz)

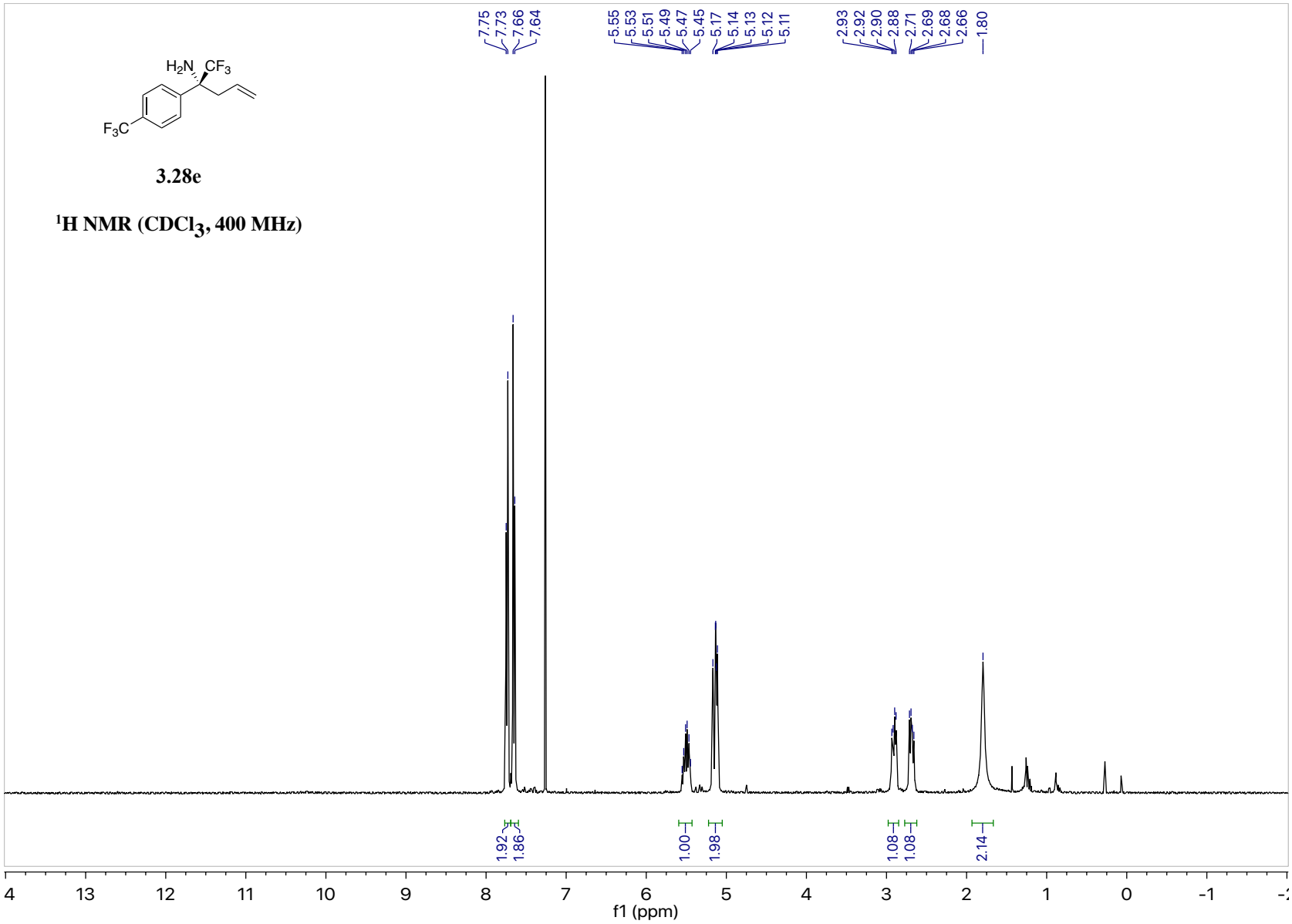

3.28e

^{1}H NMR ($CDCl_3$, 400 MHz)

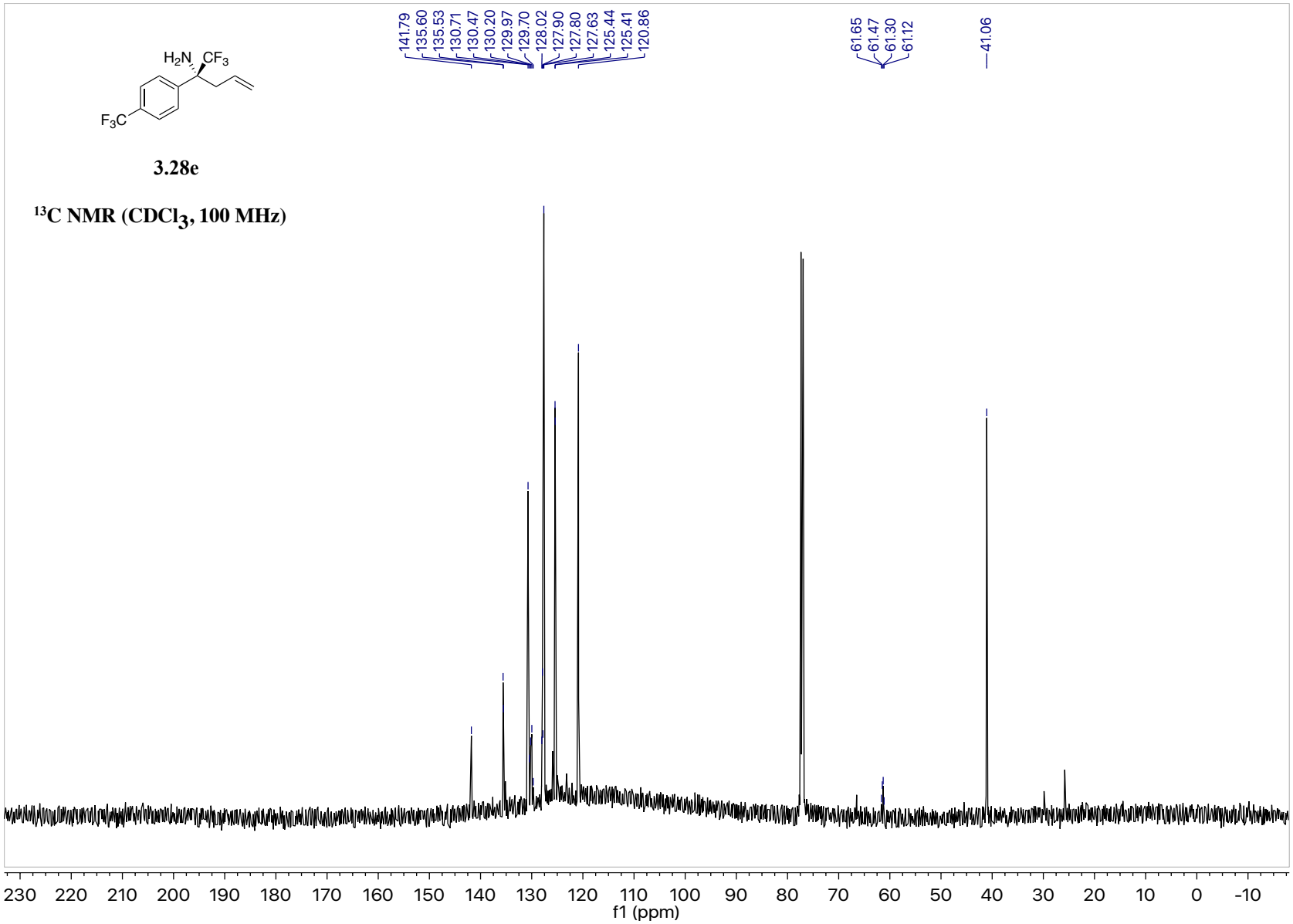

3.28e

^{13}C NMR ($CDCl_3$, 100 MHz)

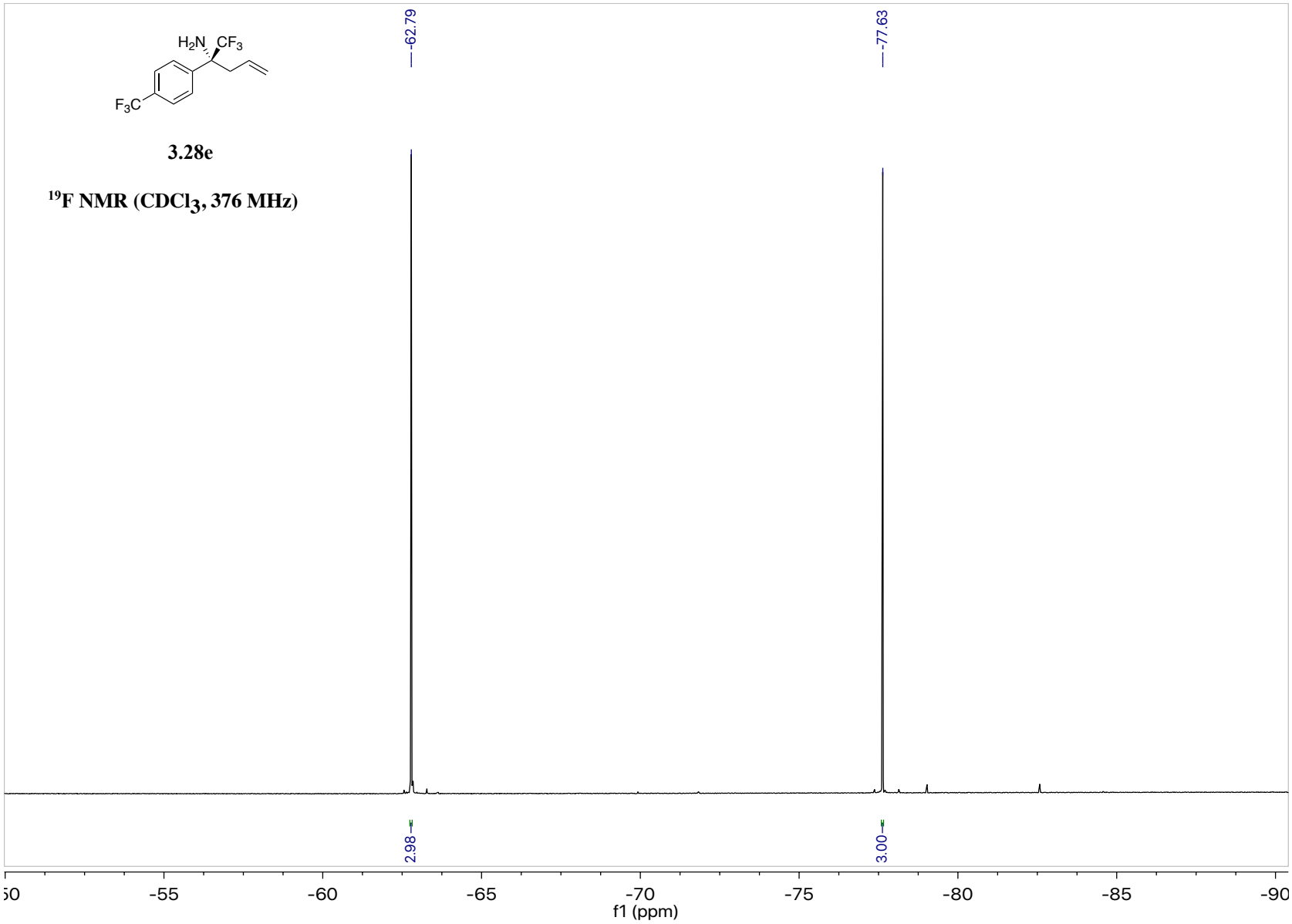

3.28e

^{19}F NMR ($CDCl_3$, 376 MHz)

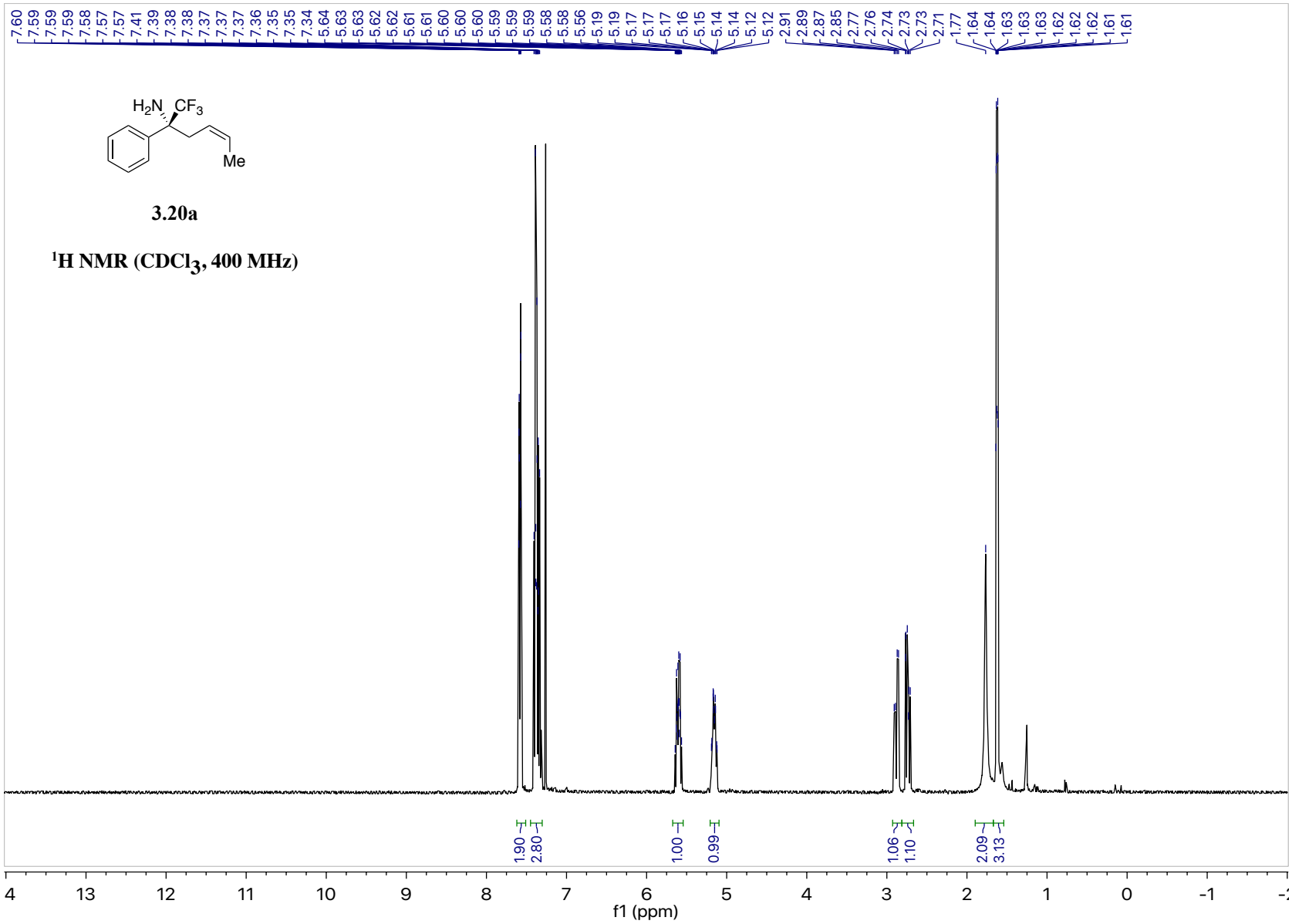
7.60 7.59 7.59 7.59 7.58 7.57 7.57 7.41 7.39 7.38 7.38 7.37 7.37 7.37 7.36 7.35 7.35 7.34 5.64 5.63 5.63 5.62 5.62 5.61 5.61 5.60 5.60 5.60 5.59 5.59 5.59 5.58 5.58 5.56 5.19 5.19 5.17 5.17 5.17 5.16 5.15 5.14 5.14 5.12 5.12 2.91 2.89 2.87 2.85 2.77 2.76 2.74 2.73 2.73 2.71 1.77 1.64 1.64 1.63 1.63 1.62 1.62 1.62 1.61 1.61
H2N CF3
Me
3.20a
1H NMR (CDCl3, 400 MHz)
1.90 2.80 1.00 0.99 1.06 1.10 2.09 3.13
4 13 12 11 10 9 8 7 6 5 4 3 2 1 0 -1
f1 (ppm)

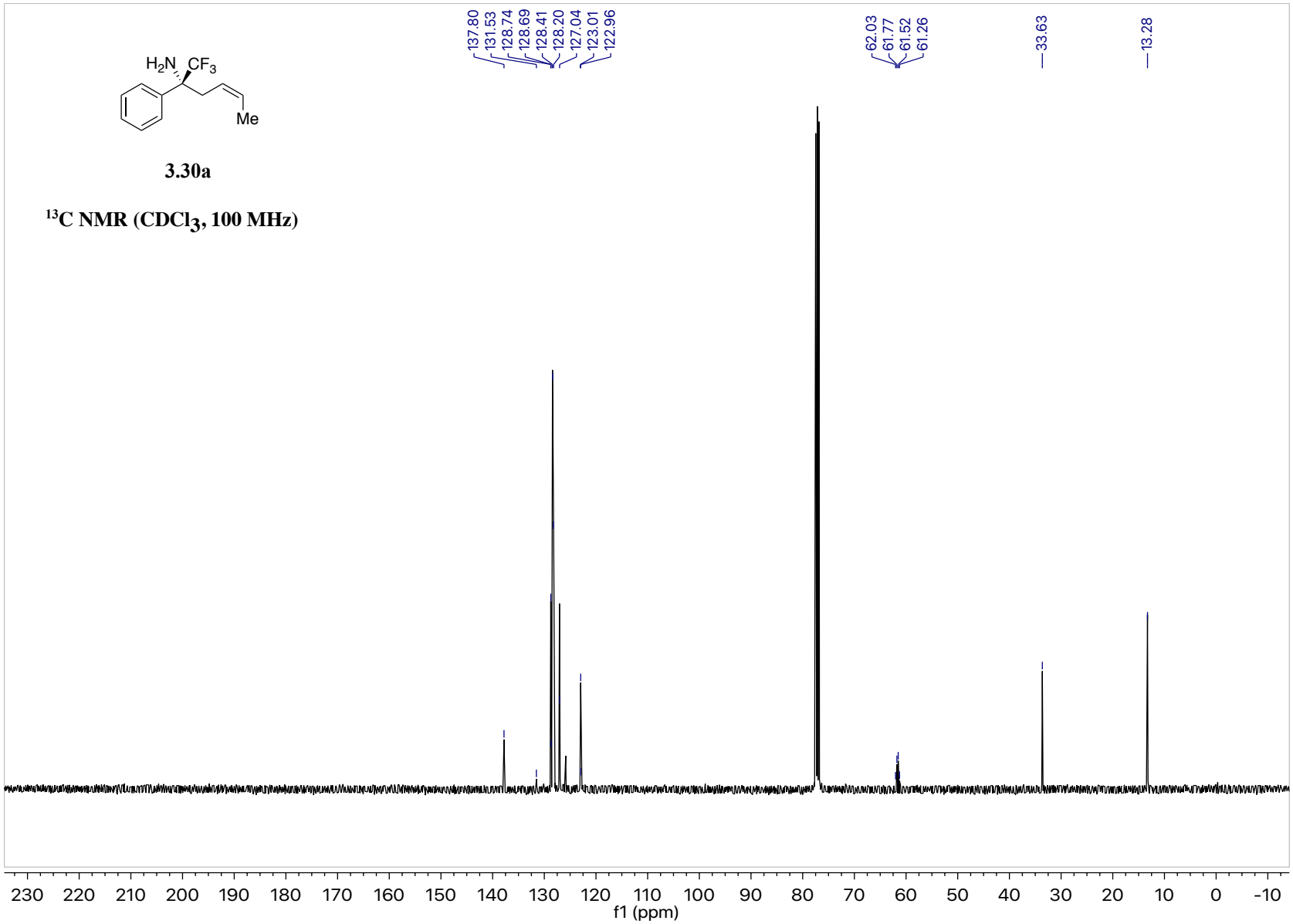
137.80
131.53
128.74
128.69
128.41
128.20
127.04
123.01
122.96
62.03
61.77
61.52
61.26
33.63
13.28
H2N
CF3
Me
3.30a
13C NMR (CDCl3, 100 MHz)
230 220 210 200 190 180 170 160 150 140 130 120 110 100 90 80 70 60 50 40 30 20 10 0 -10
f1 (ppm)

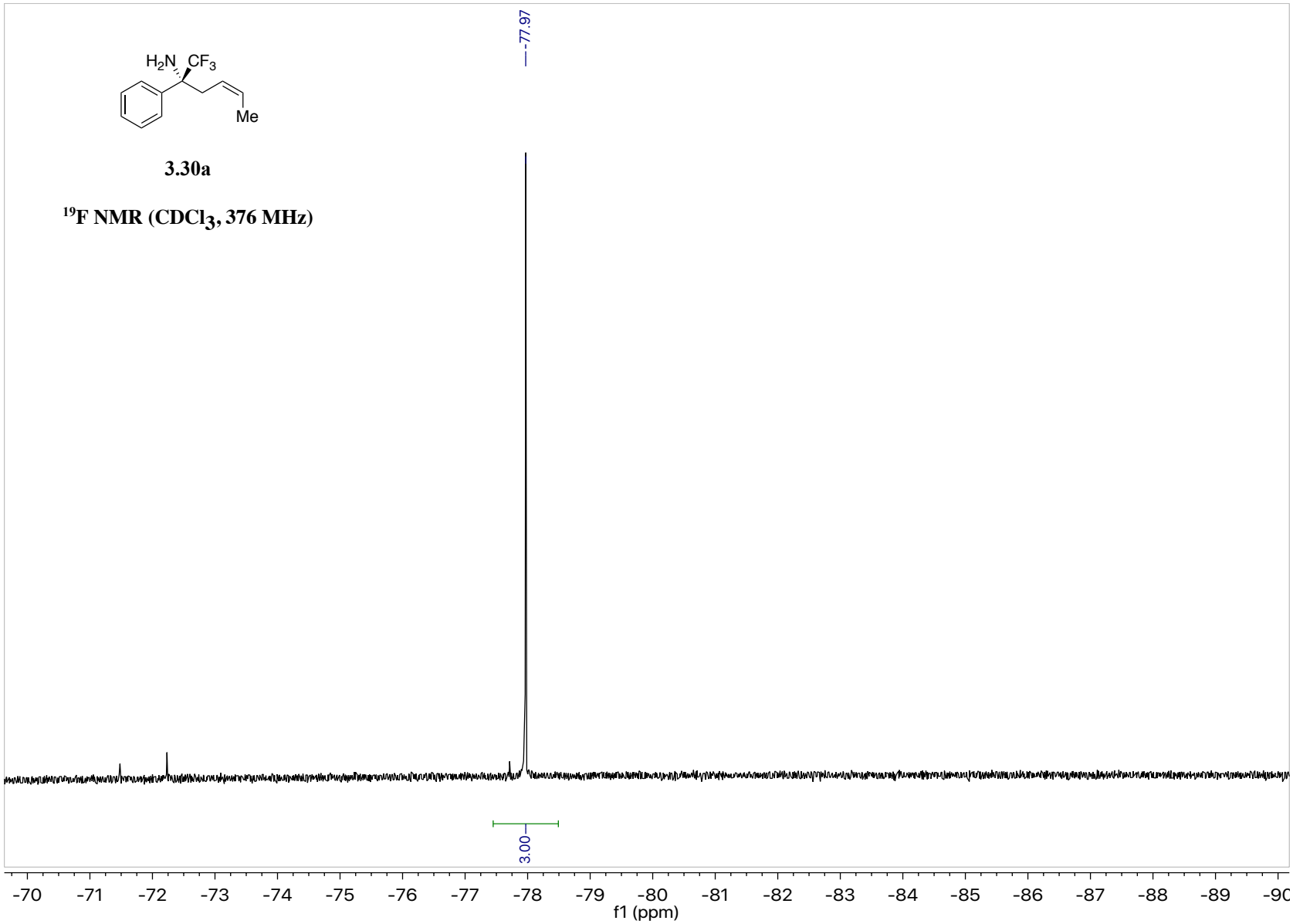

3.30a

^{19}F NMR ($CDCl_3$, 376 MHz)

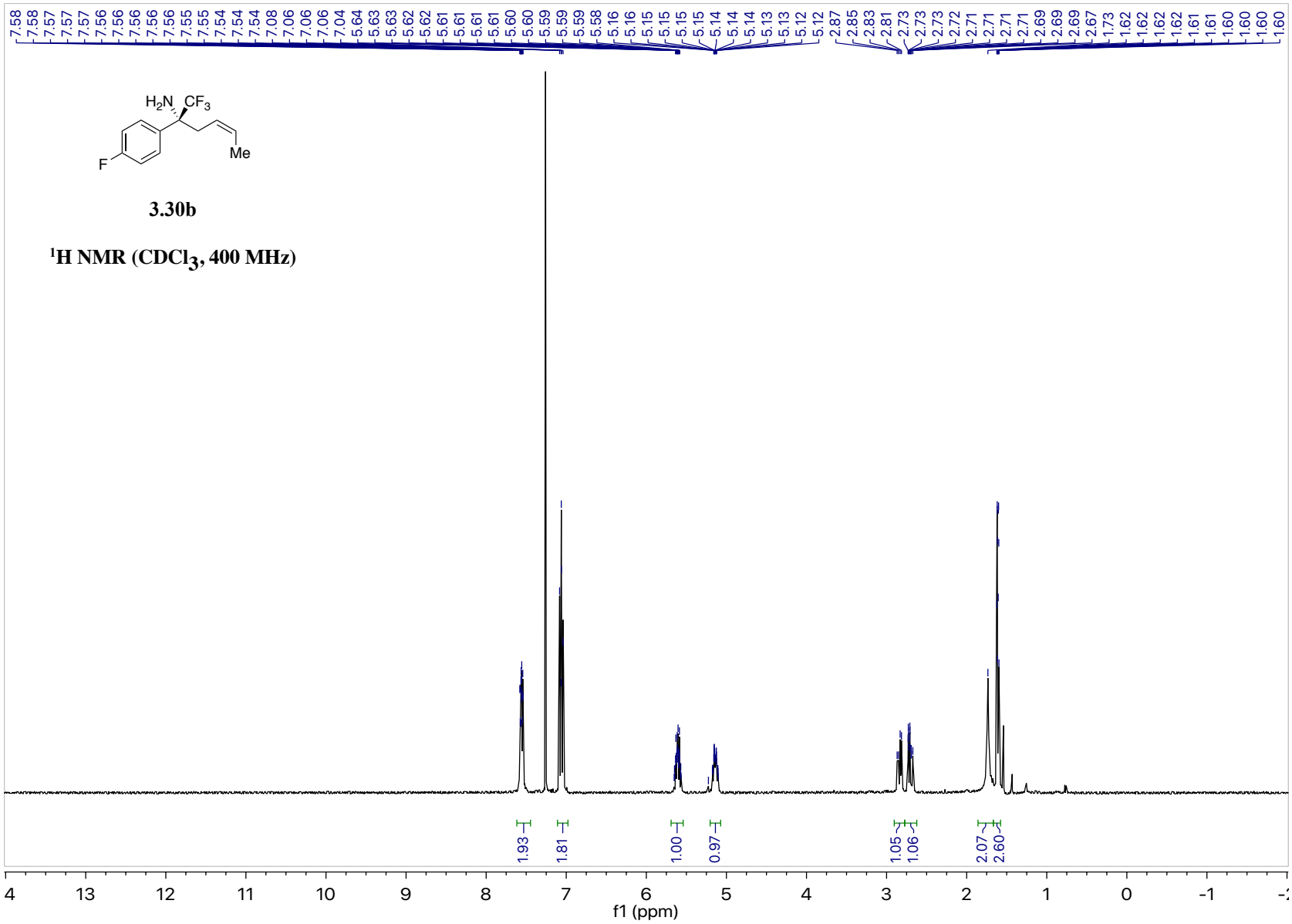

3.30b

^{1}H NMR ($CDCl_3$, 400 MHz)

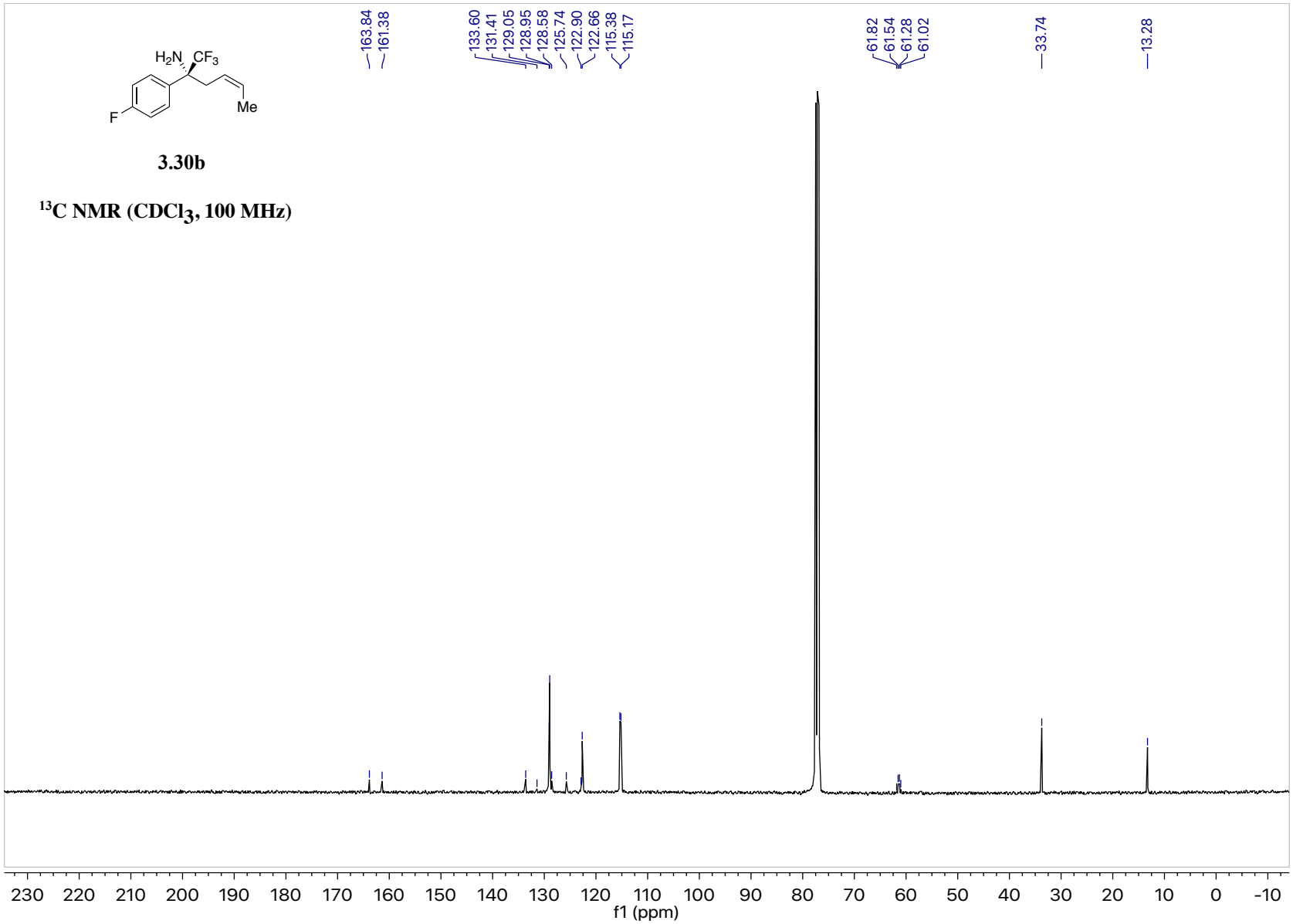

3.30b

^{13}C NMR ($CDCl_3$, 100 MHz)

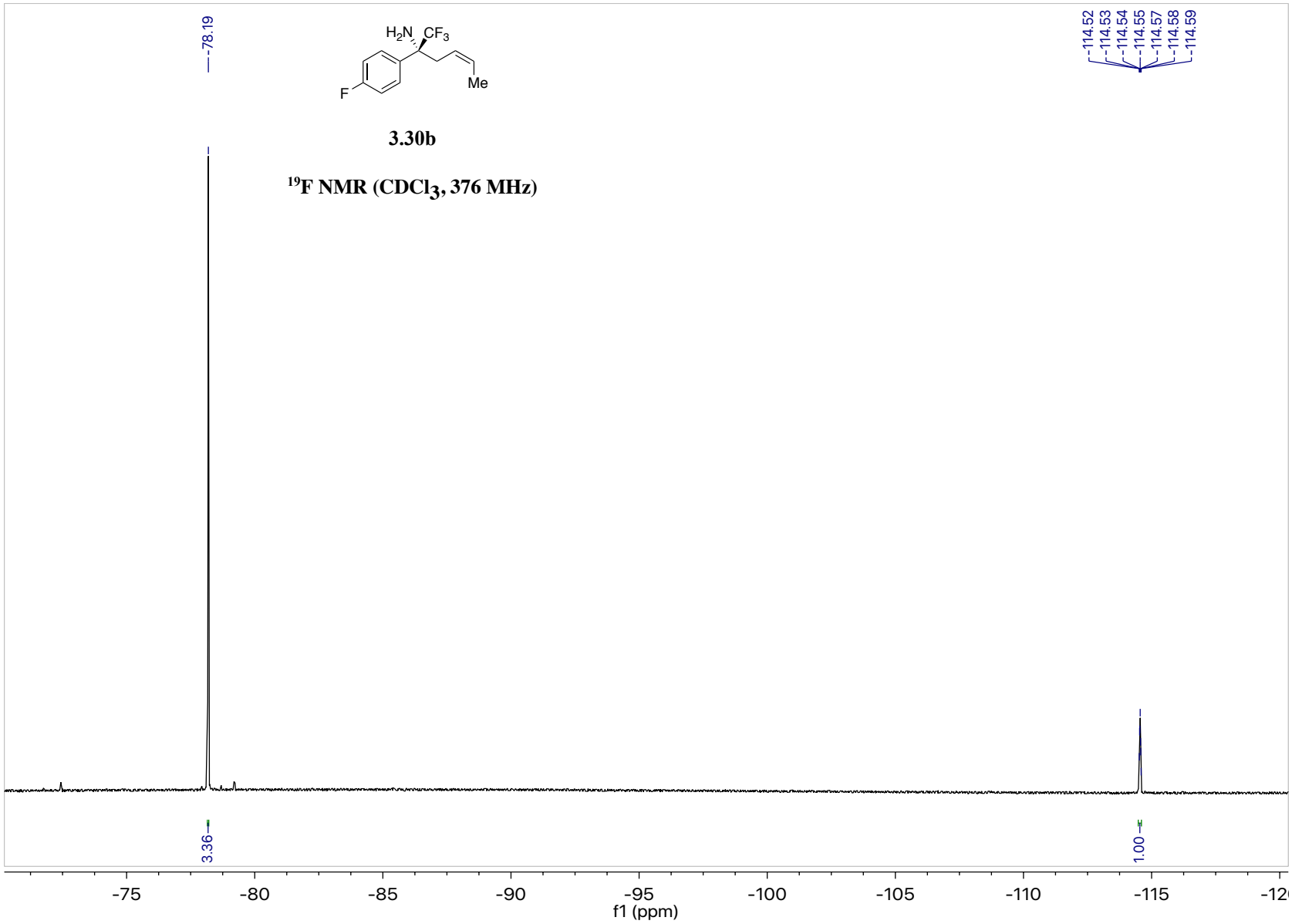

3.30b

^{19}F NMR ($CDCl_3$, 376 MHz)

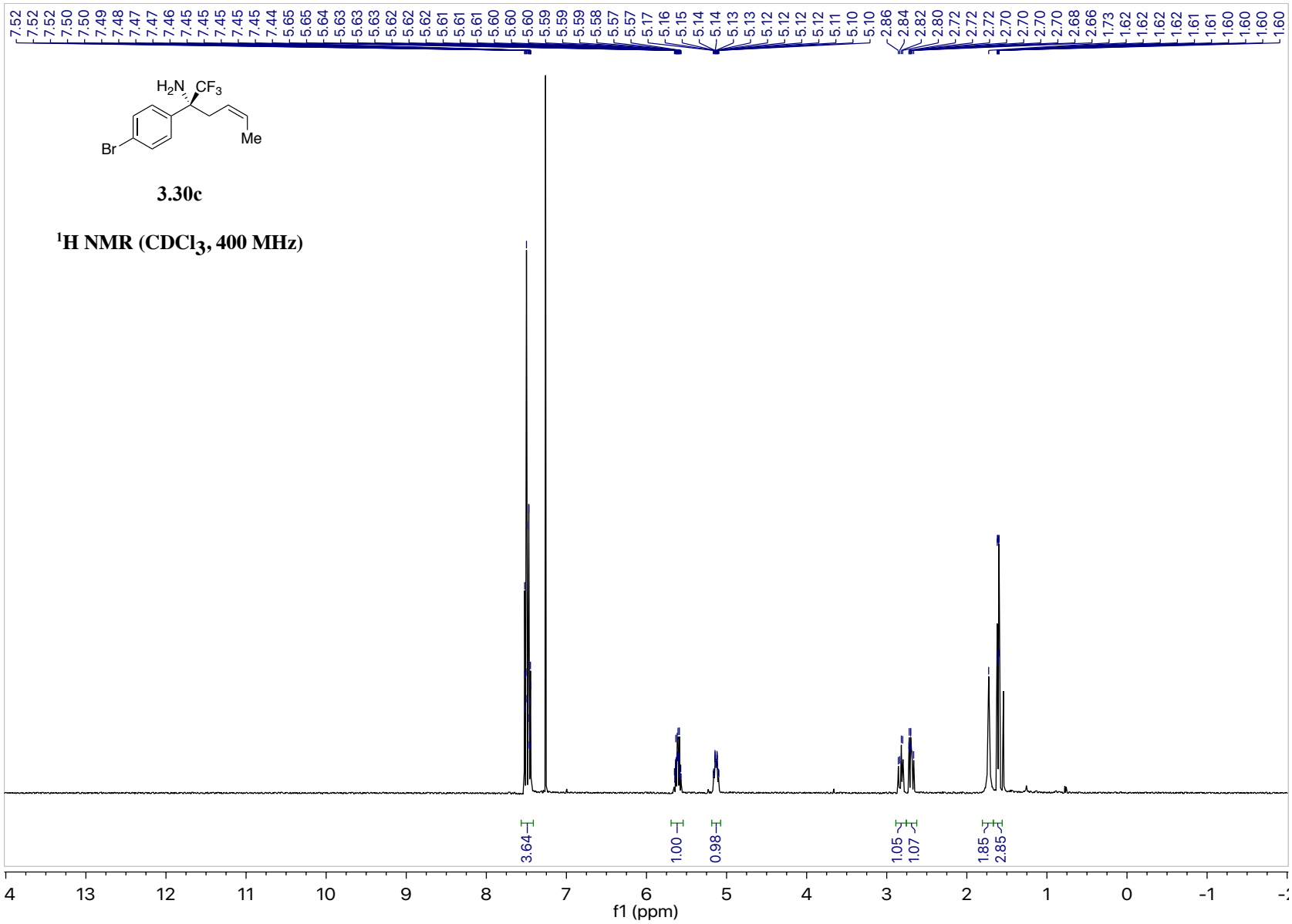

3.30c

^{1}H NMR ($CDCl_3$, 400 MHz)

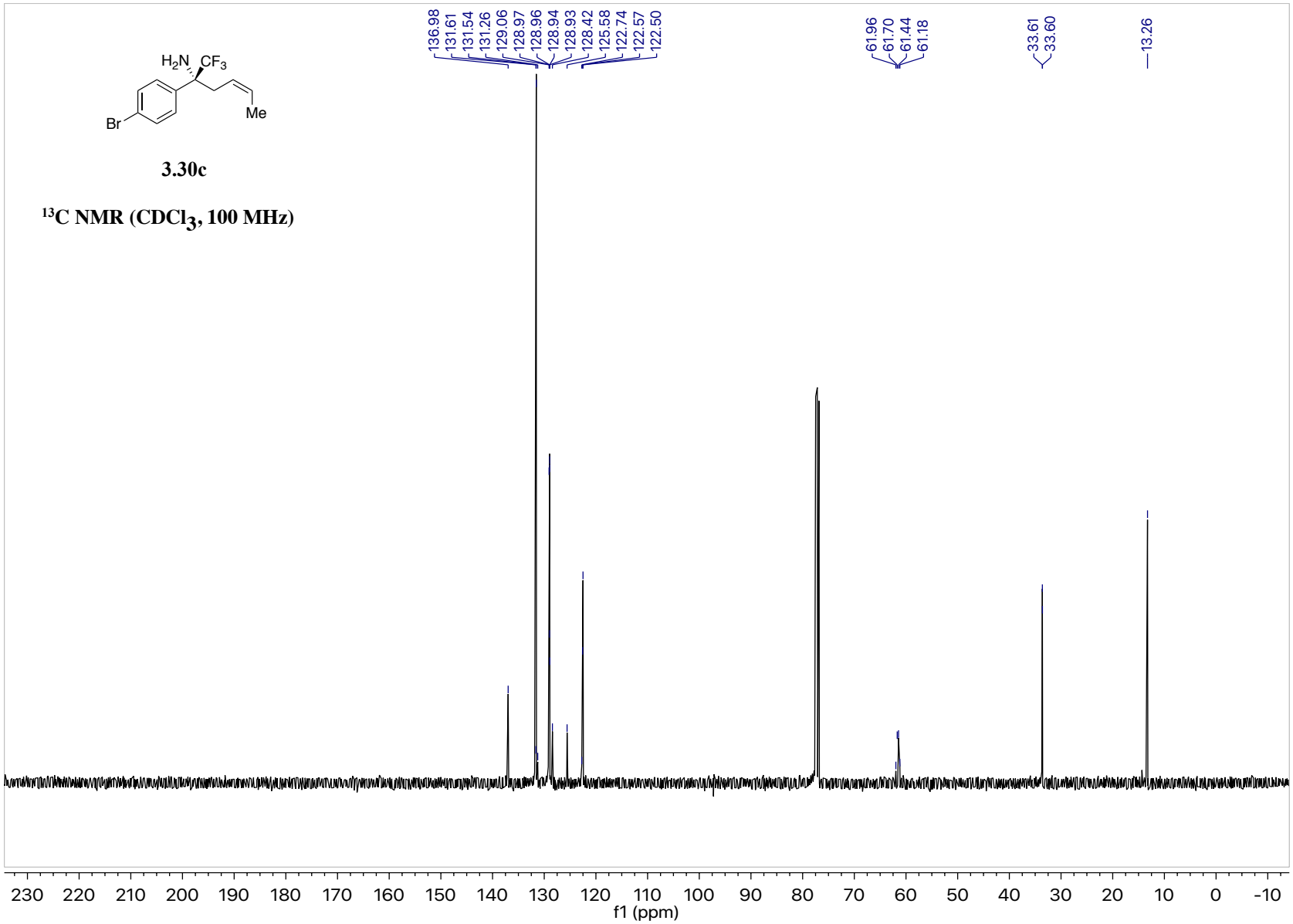

3.30c

^{13}C NMR ($CDCl_3$, 100 MHz)

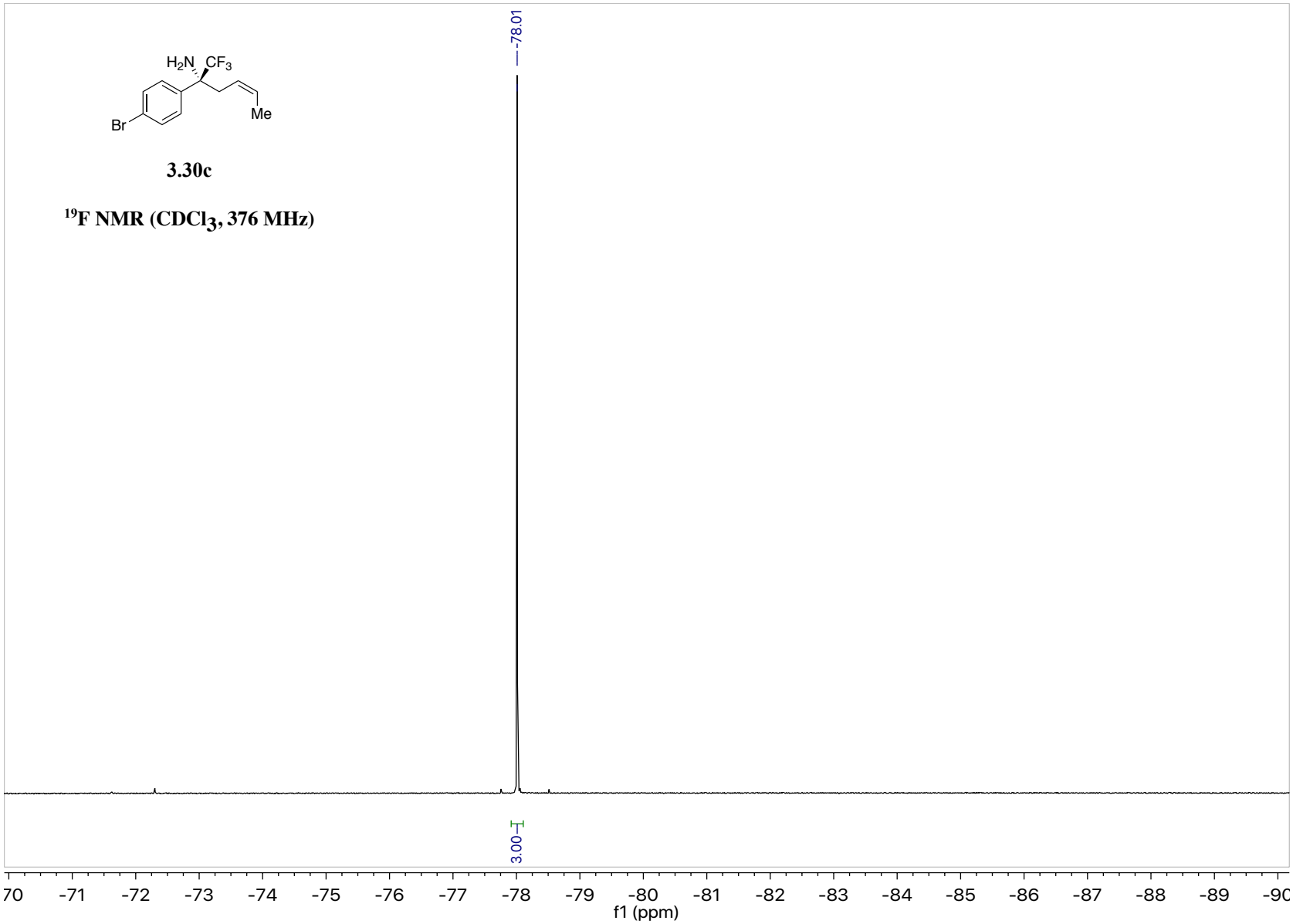

3.30c

^{19}F NMR ($CDCl_3$, 376 MHz)

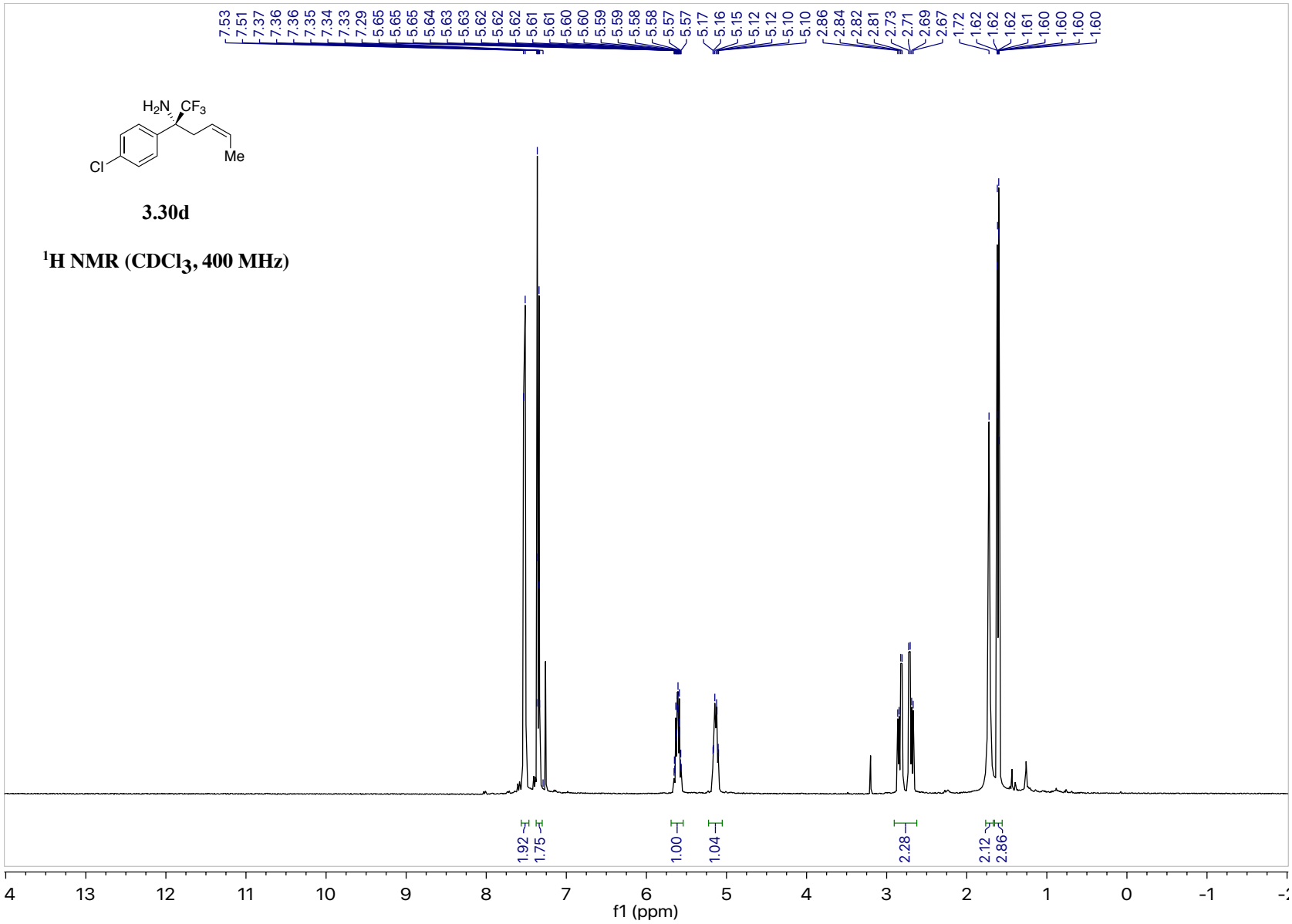
7.53
7.51
7.37
7.36
7.36
7.35
7.34
7.33
7.29
5.65
5.65
5.64
5.63
5.63
5.62
5.62
5.62
5.61
5.61
5.60
5.60
5.59
5.59
5.58
5.58
5.57
5.57
5.17
5.16
5.15
5.12
5.12
5.10
5.10
2.86
2.84
2.82
2.81
2.73
2.71
2.69
2.67
1.72
1.62
1.62
1.62
1.61
1.60
1.60
1.60
1.60
H2N
CF3
Cl
Me
3.30d
1H NMR (CDCl3, 400 MHz)
1.92
1.75
1.00
1.04
2.28
2.12
2.86
4
13
12
11
10
9
8
7
6
5
4
3
2
1
0
-1
f1 (ppm)

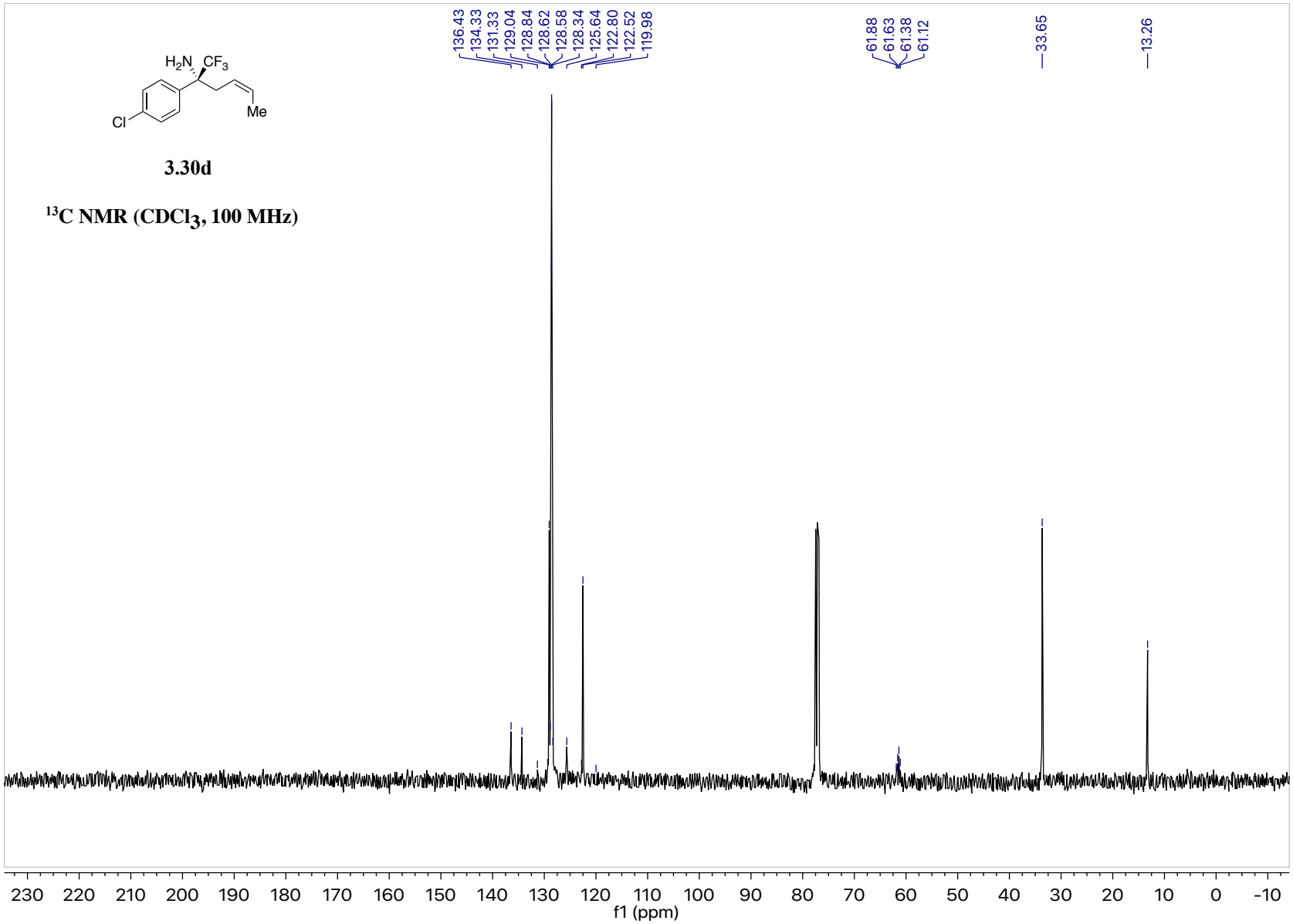

3.30d

^{13}C NMR ($CDCl_3$, 100 MHz)

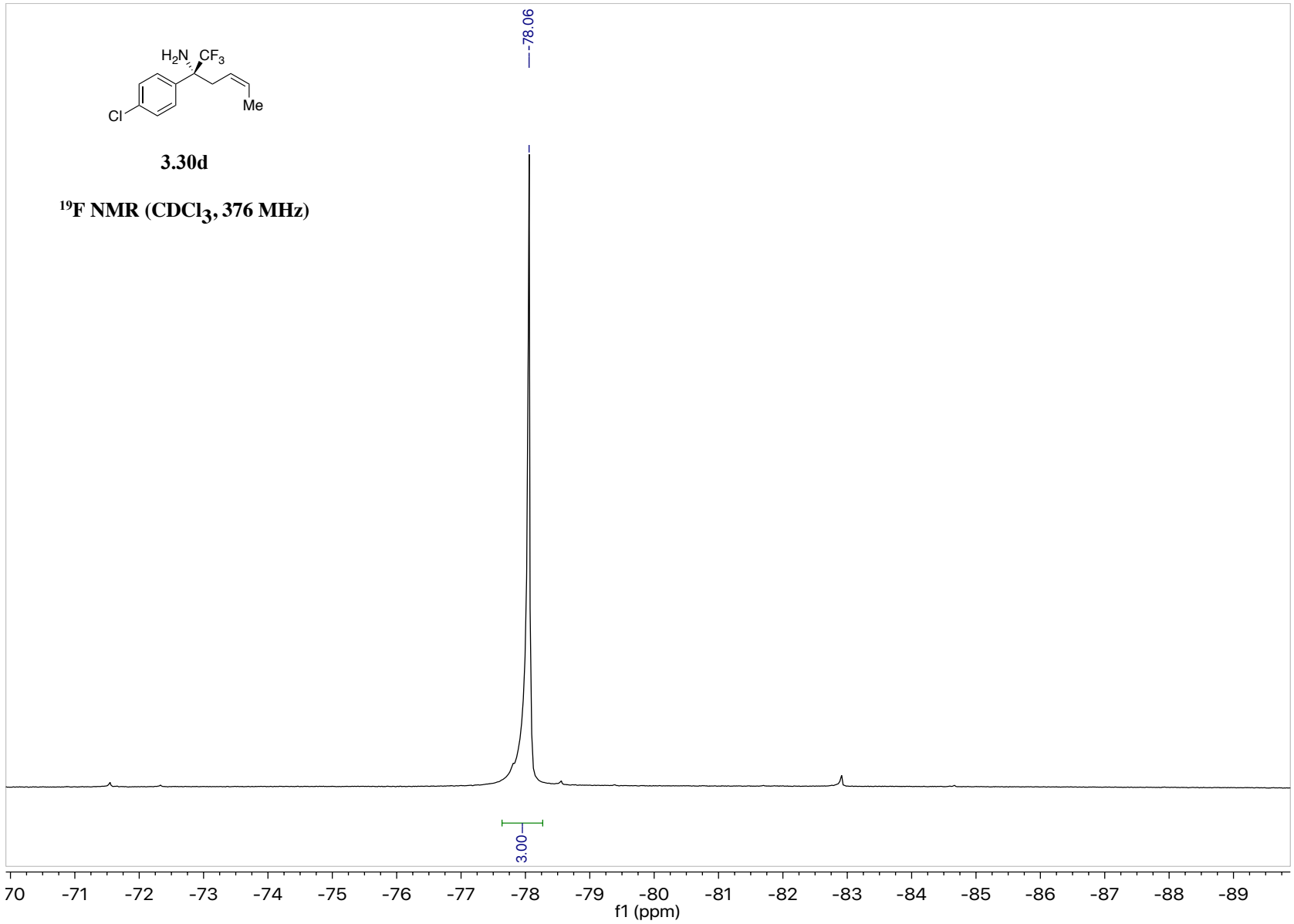
H2N
CF3
Cl
Me
3.30d
19F NMR (CDCl3, 376 MHz)
-78.06
3.00
70
-71
-72
-73
-74
-75
-76
-77
-78
-79
-80
-81
-82
-83
-84
-85
-86
-87
-88
-89
f1 (ppm)

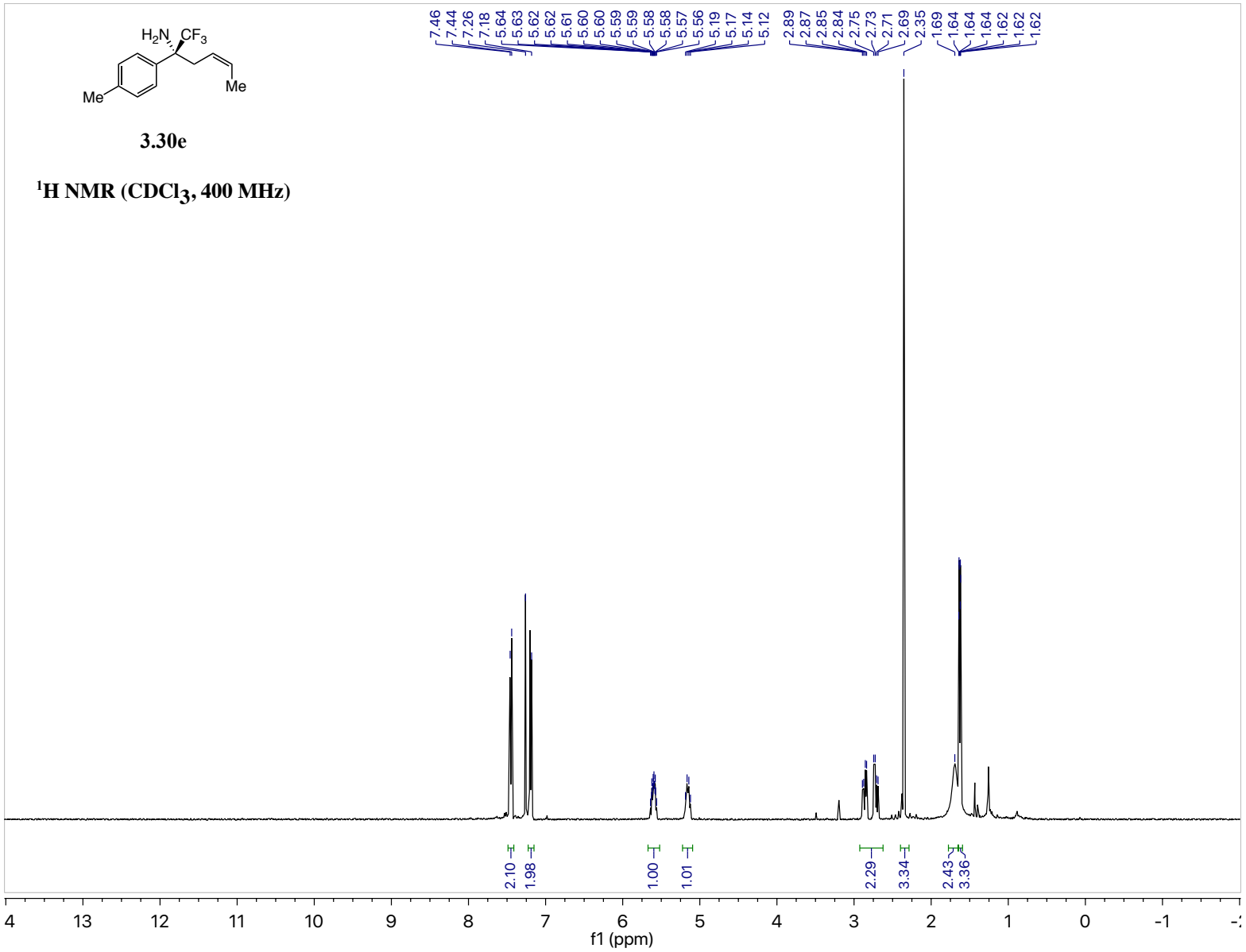

3.30e

^{1}H NMR ($CDCl_3$, 400 MHz)

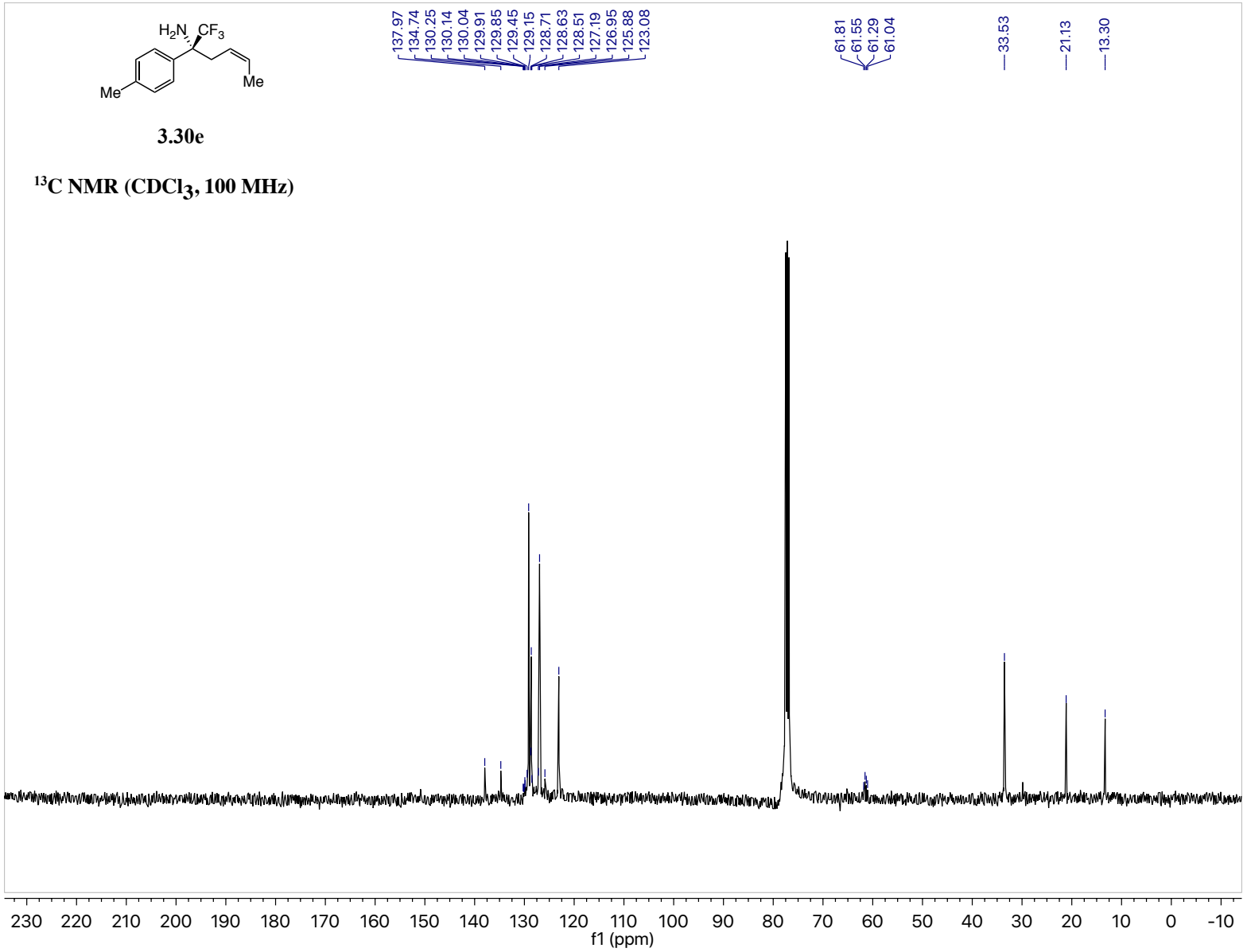

3.30e

^{13}C NMR ($CDCl_3$, 100 MHz)

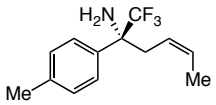

3.30e

^{19}F NMR ($CDCl_3$, 376 MHz)

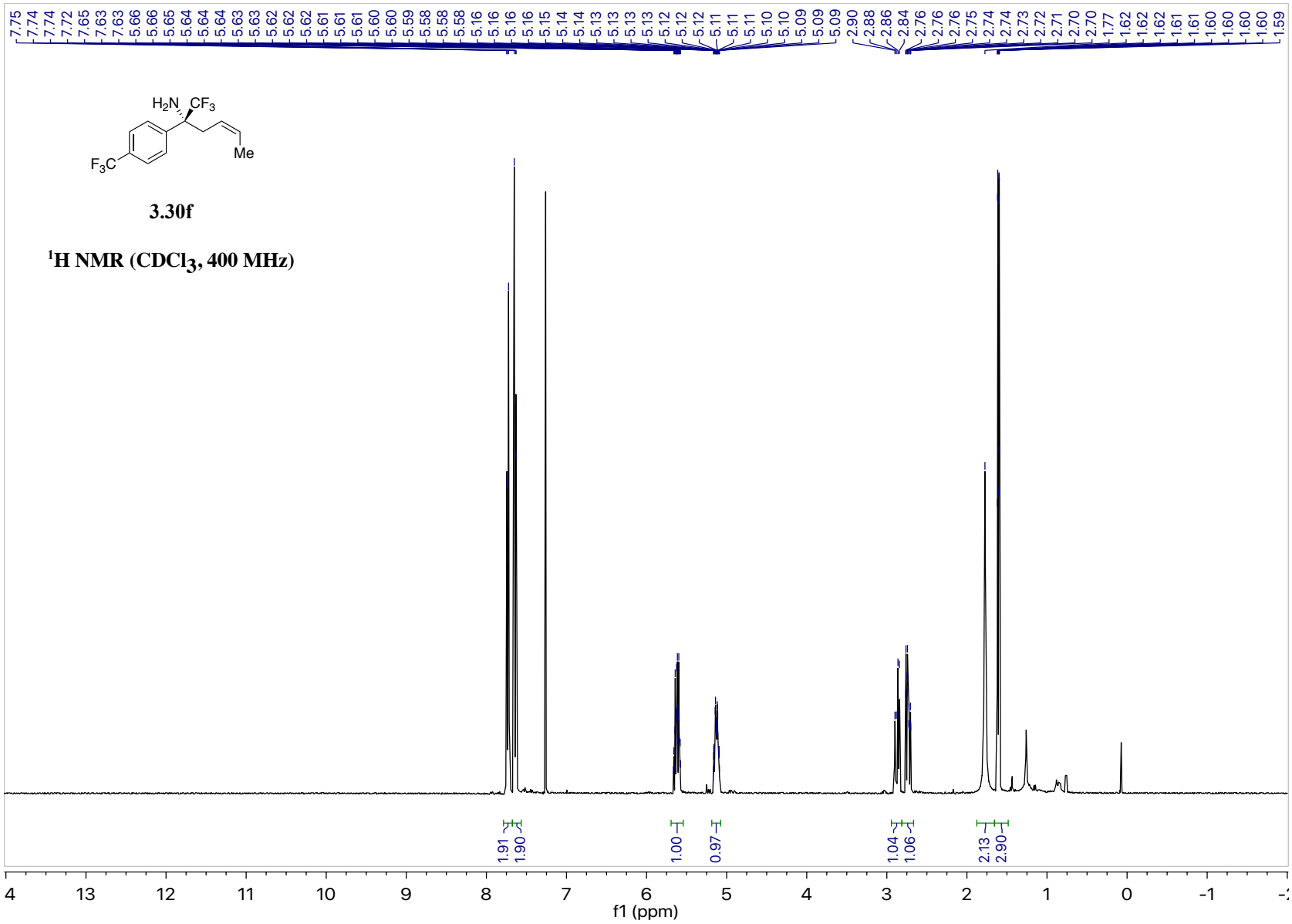
7.75 7.74 7.74 7.72 7.65 7.63 7.63 5.66 5.65 5.64 5.64 5.64 5.63 5.63 5.62 5.62 5.62 5.61 5.61 5.61 5.60 5.60 5.59 5.58 5.58 5.58 5.16 5.16 5.16 5.15 5.14 5.14 5.13 5.13 5.13 5.12 5.12 5.12 5.11 5.11 5.11 5.10 5.10 5.09 5.09 5.09 2.90 2.88 2.86 2.84 2.76 2.76 2.76 2.75 2.74 2.74 2.73 2.72 2.71 2.70 2.70 1.77 1.62 1.62 1.62 1.61 1.61 1.60 1.60 1.60 1.60 1.59
H2N CF3
F3C
Me
3.30f
1H NMR (CDCl3, 400 MHz)
1.91
1.90
1.00
0.97
1.04
1.06
2.13
2.90
4 13 12 11 10 9 8 7 6 5 4 3 2 1 0 -1
f1 (ppm)

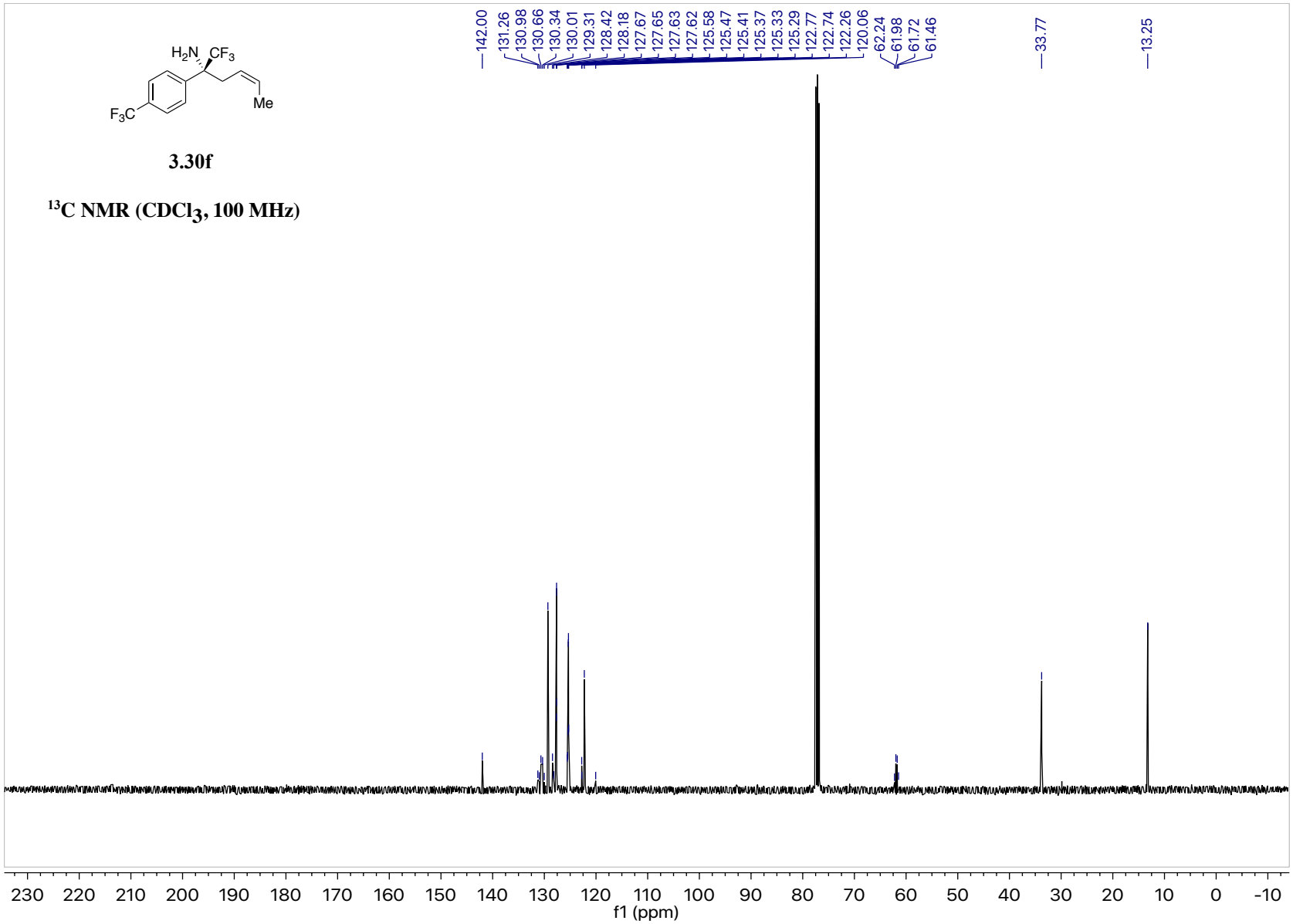

3.30f

^{13}C NMR ($CDCl_3$, 100 MHz)

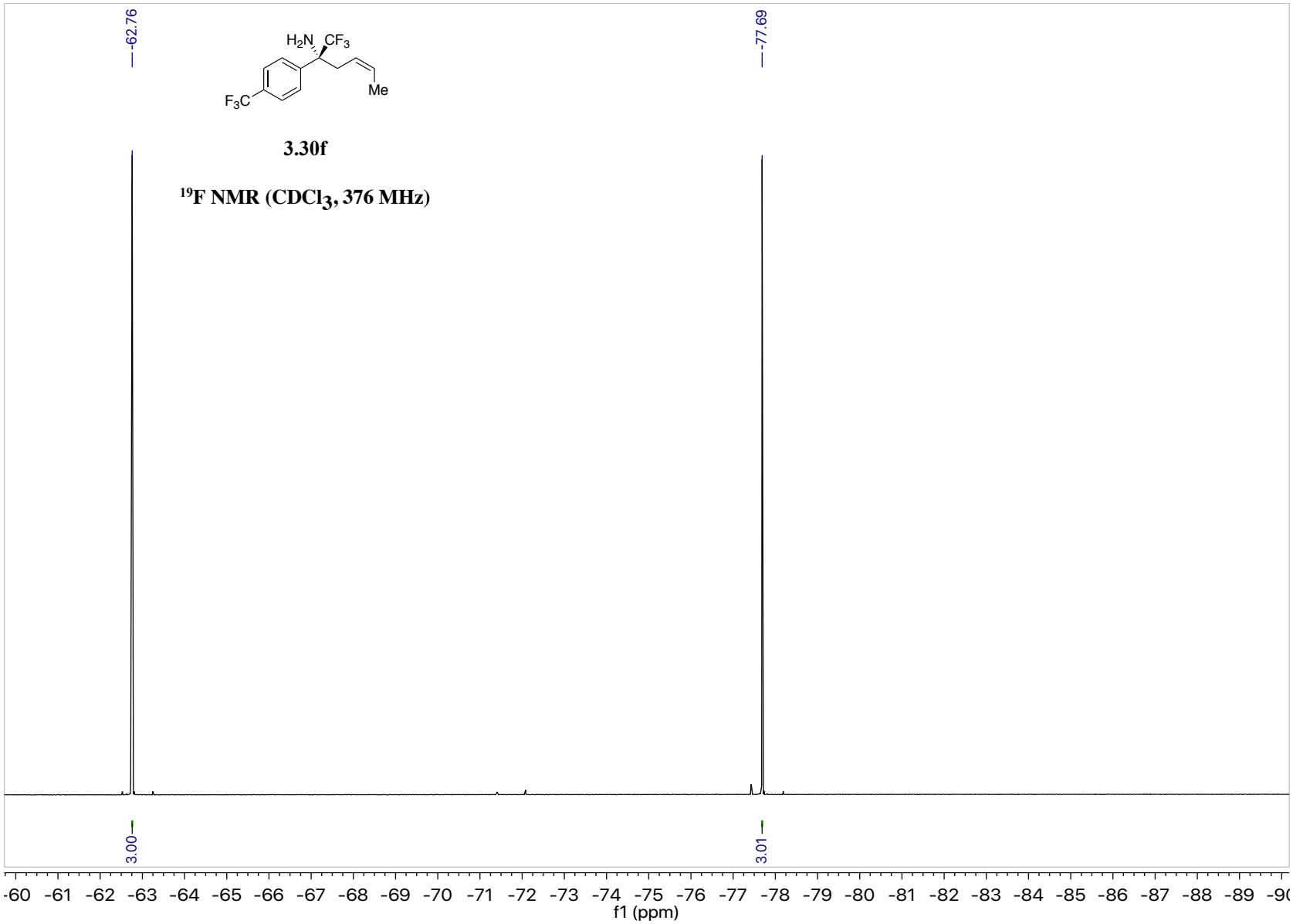
-62.76
-77.69
H2N
CF3
F3C
Me
3.30f
19F NMR (CDCl3, 376 MHz)
3.00
3.01
-60 -61 -62 -63 -64 -65 -66 -67 -68 -69 -70 -71 -72 -73 -74 -75 -76 -77 -78 -79 -80 -81 -82 -83 -84 -85 -86 -87 -88 -89
f1 (ppm)

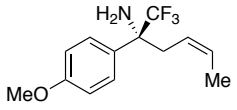

3.30g

^{1}H NMR ($CDCl_3$, 400 MHz)

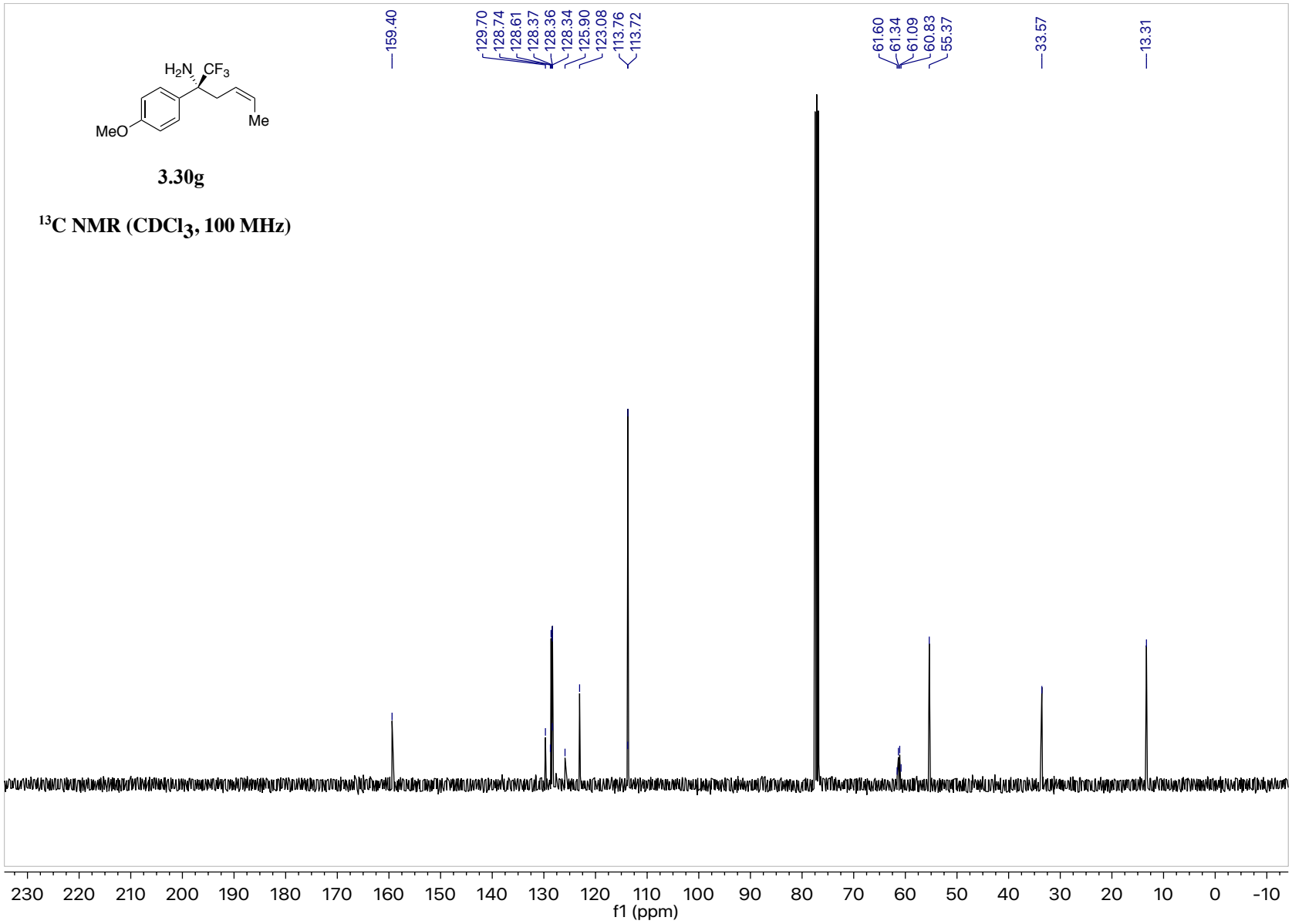
159.40
129.70
128.74
128.61
128.37
128.36
128.34
125.90
123.08
113.76
113.72
61.60
61.34
61.09
60.83
55.37
33.57
13.31
H2N
CF3
MeO
Me
3.30g
13C NMR (CDCl3, 100 MHz)
230 220 210 200 190 180 170 160 150 140 130 120 110 100 90 80 70 60 50 40 30 20 10 0 -10
f1 (ppm)

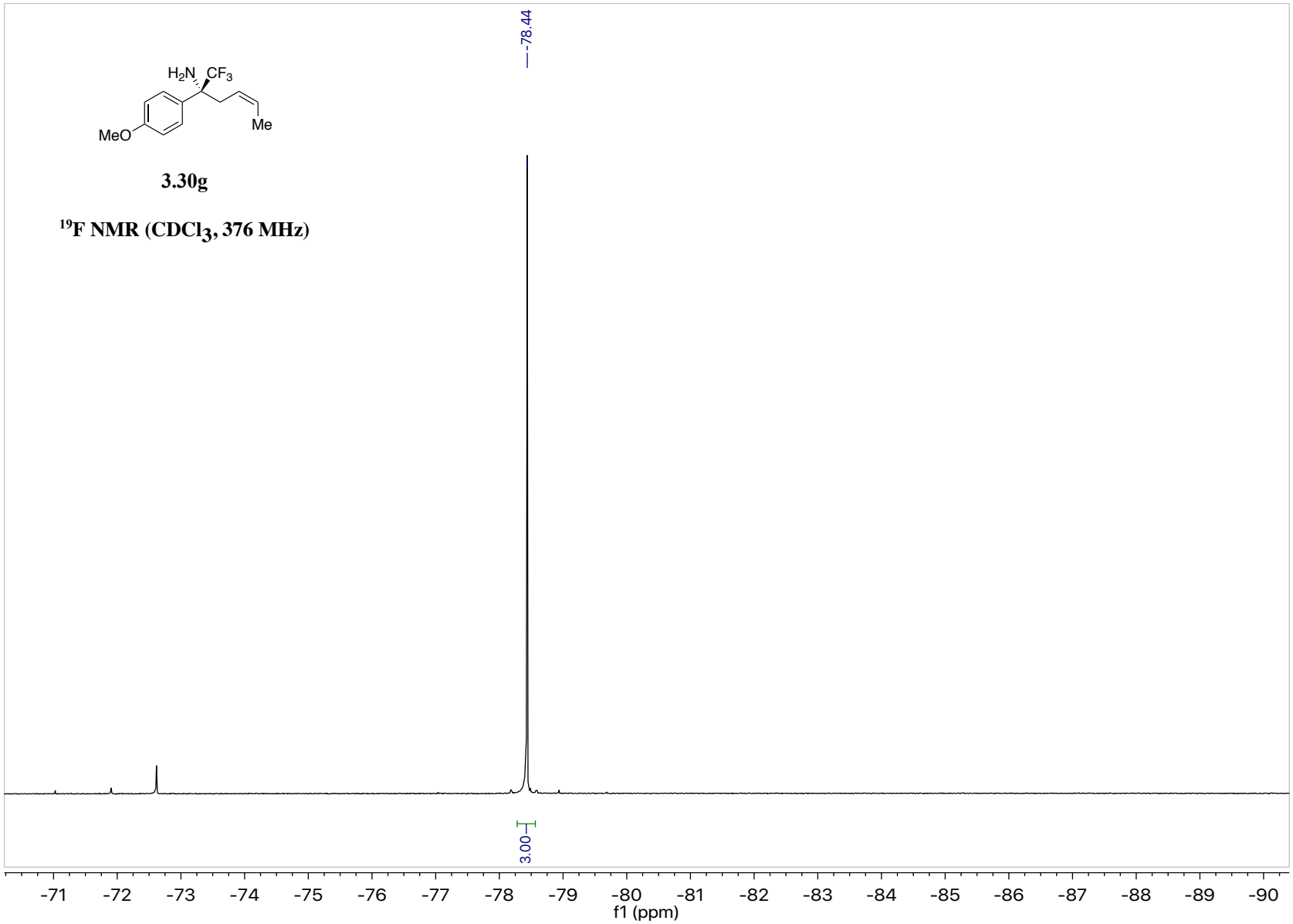
-78.44
H2N
CF3
MeO
Me
3.30g
19F NMR (CDCl3, 376 MHz)
3.00
-71
-72
-73
-74
-75
-76
-77
-78
-79
-80
-81
-82
-83
-84
-85
-86
-87
-88
-89
-90
f1 (ppm)

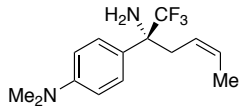

3.30h

^{1}H NMR ($CDCl_3$, 400 MHz)

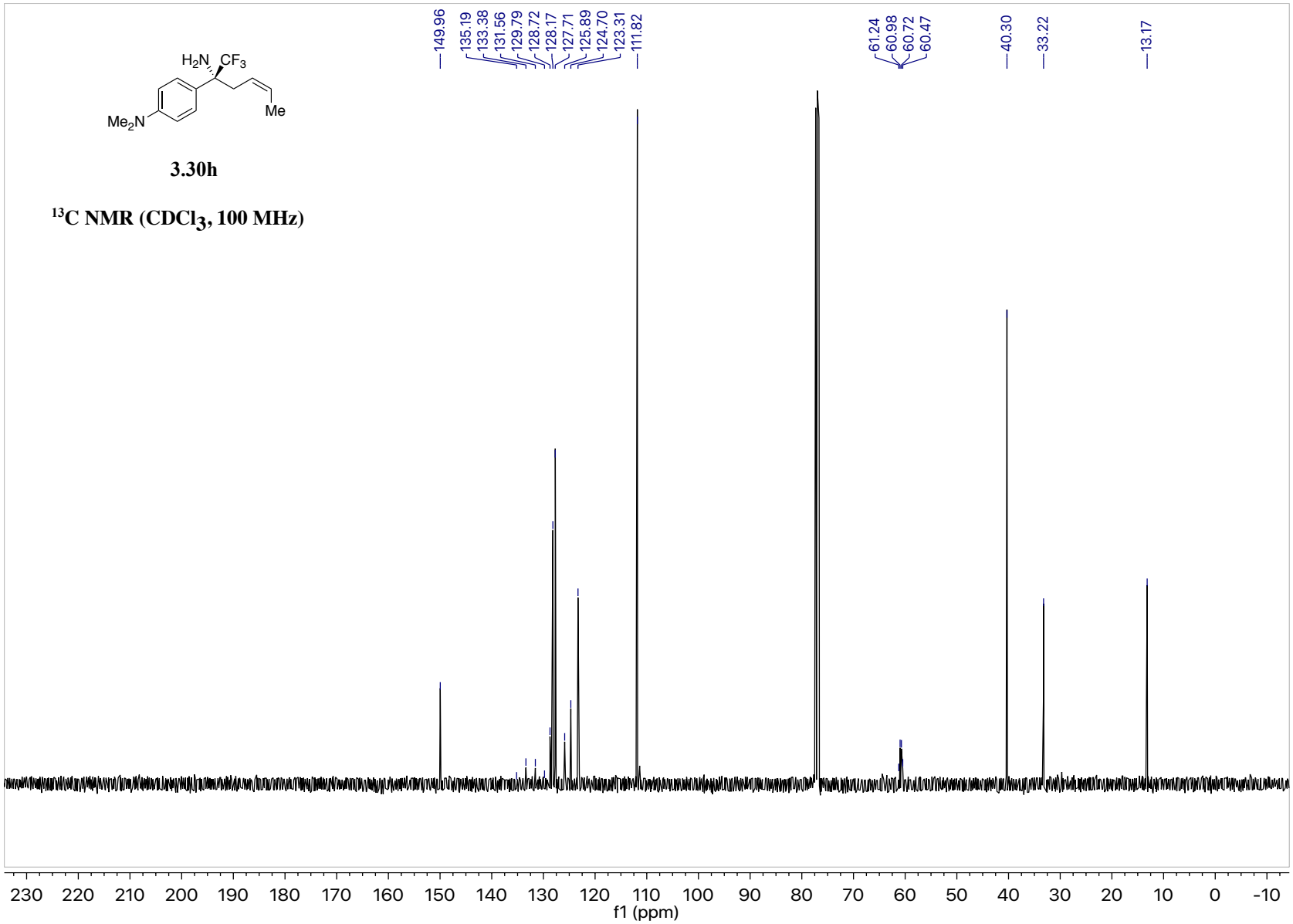

3.30h

^{13}C NMR ($CDCl_3$, 100 MHz)

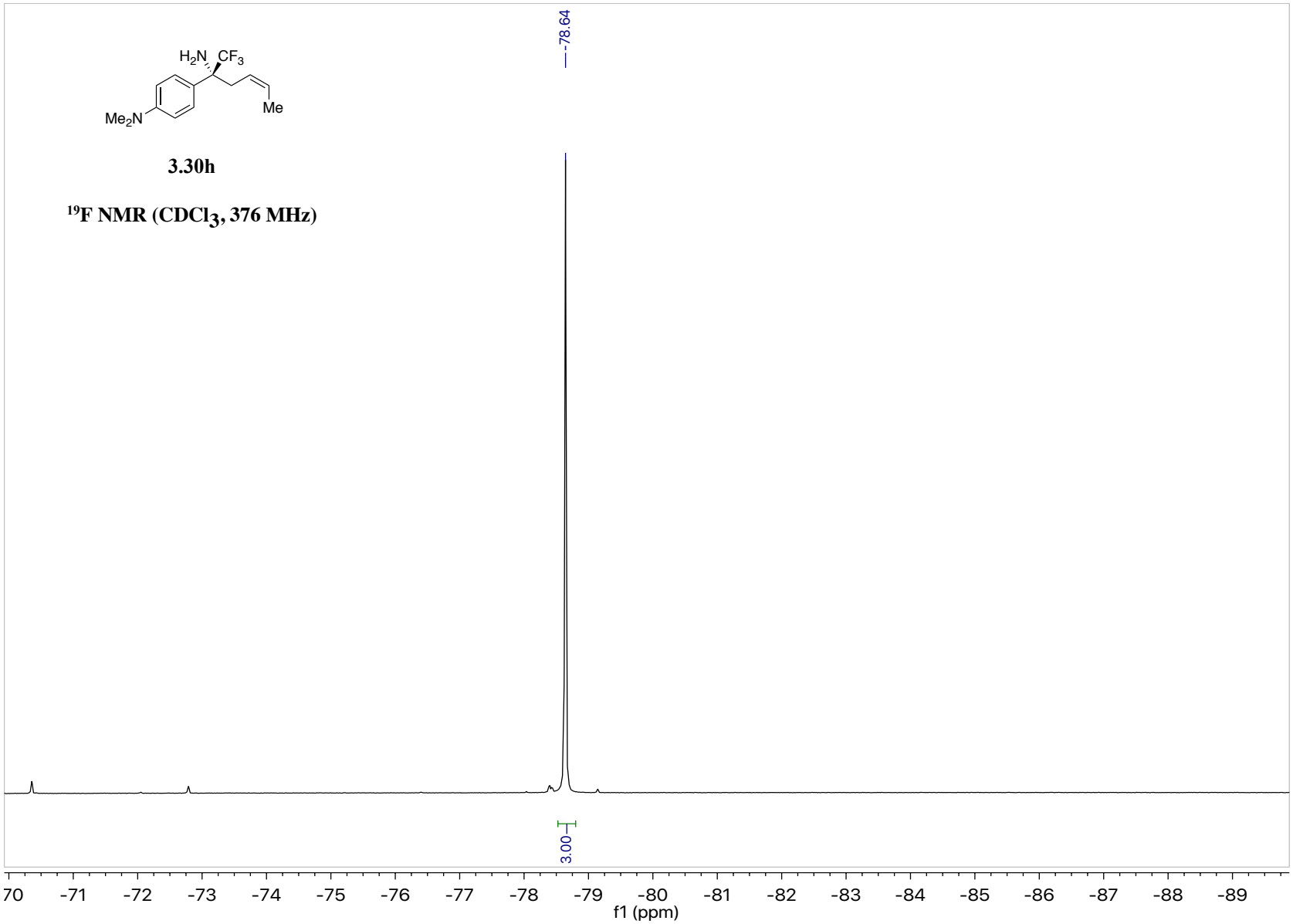

3.30h

^{19}F NMR ($CDCl_3$, 376 MHz)

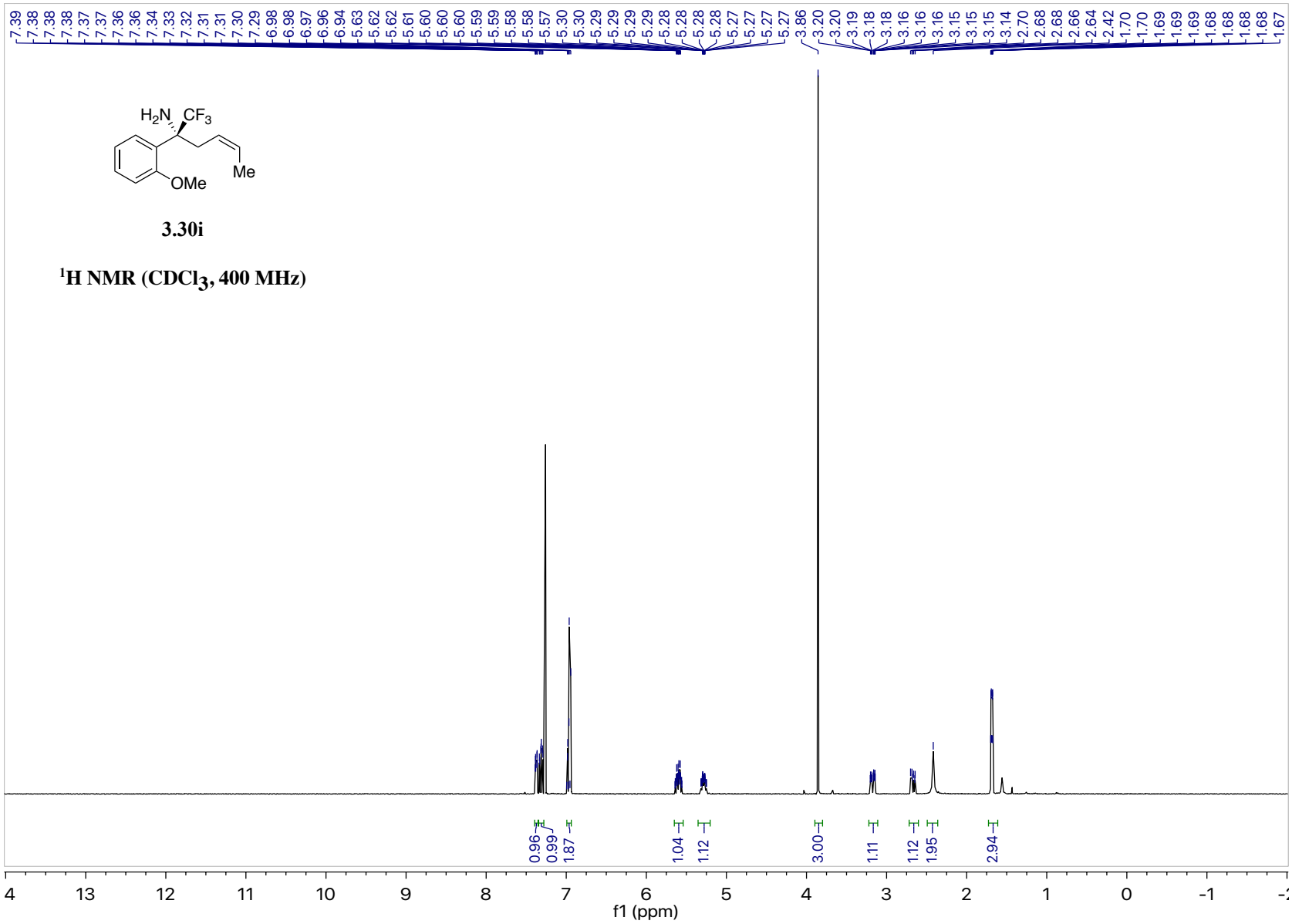

3.30i

^{1}H NMR ($CDCl_3$, 400 MHz)

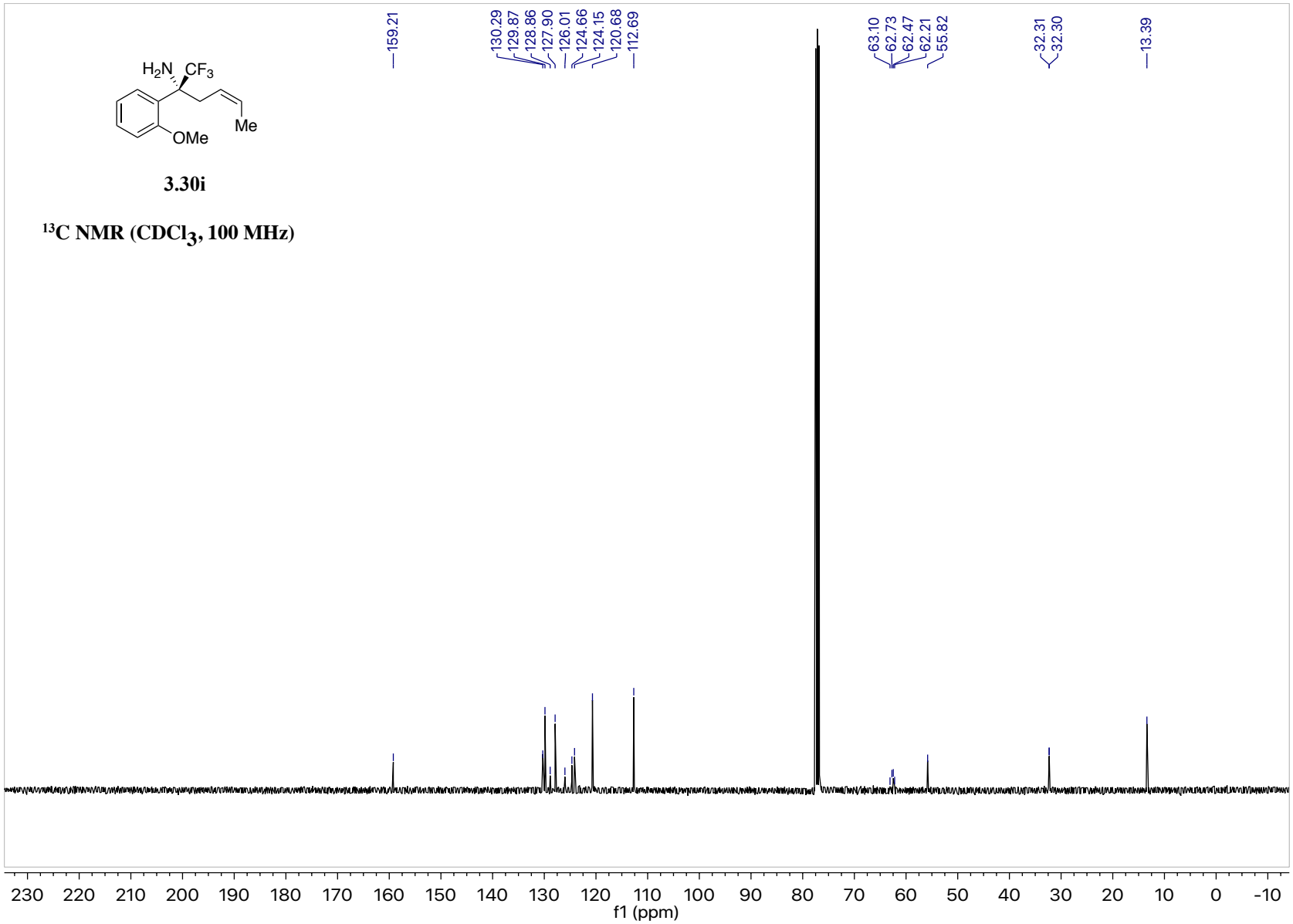

3.30i

^{13}C NMR ($CDCl_3$, 100 MHz)

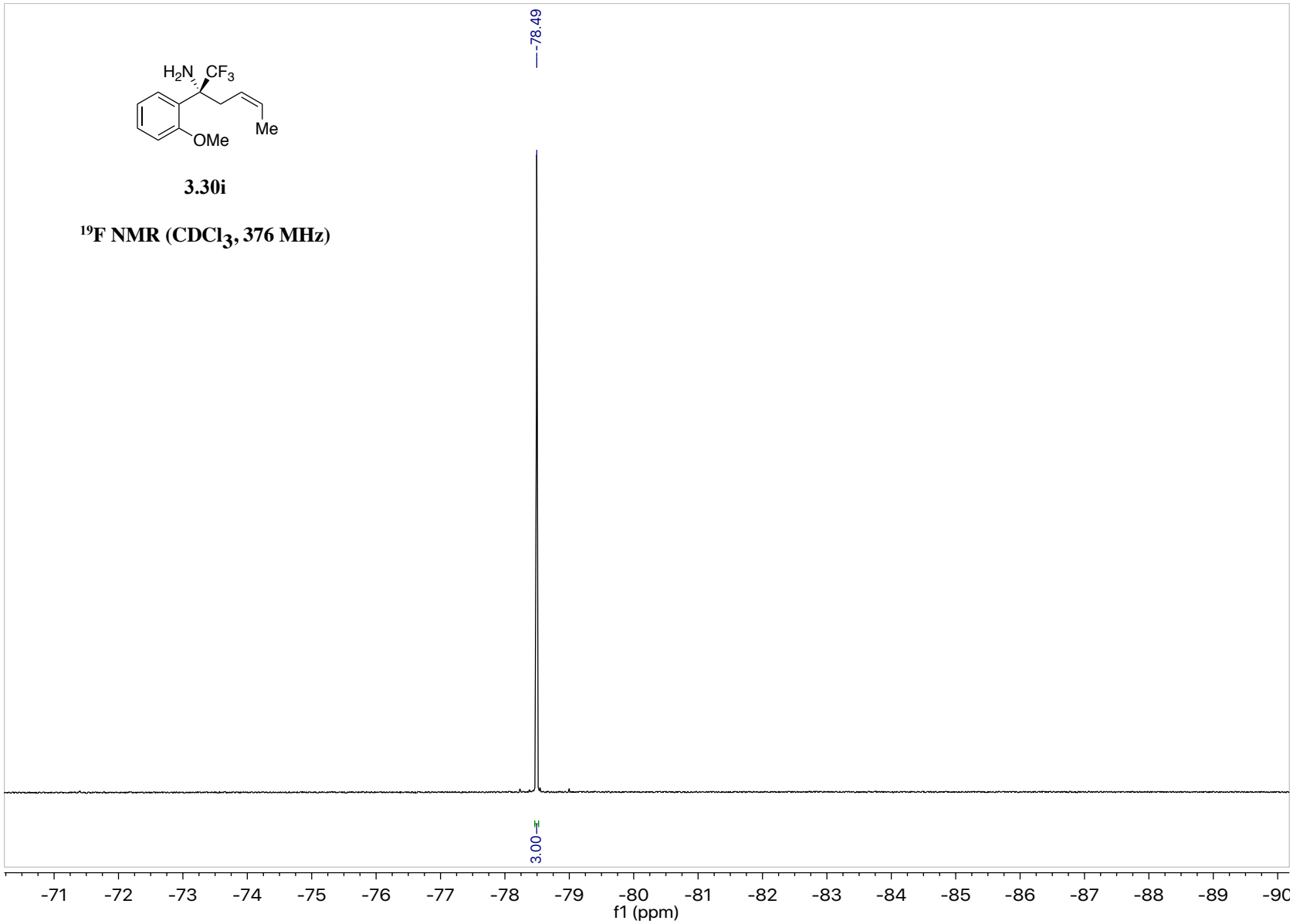

3.30i

^{19}F NMR ($CDCl_3$, 376 MHz)

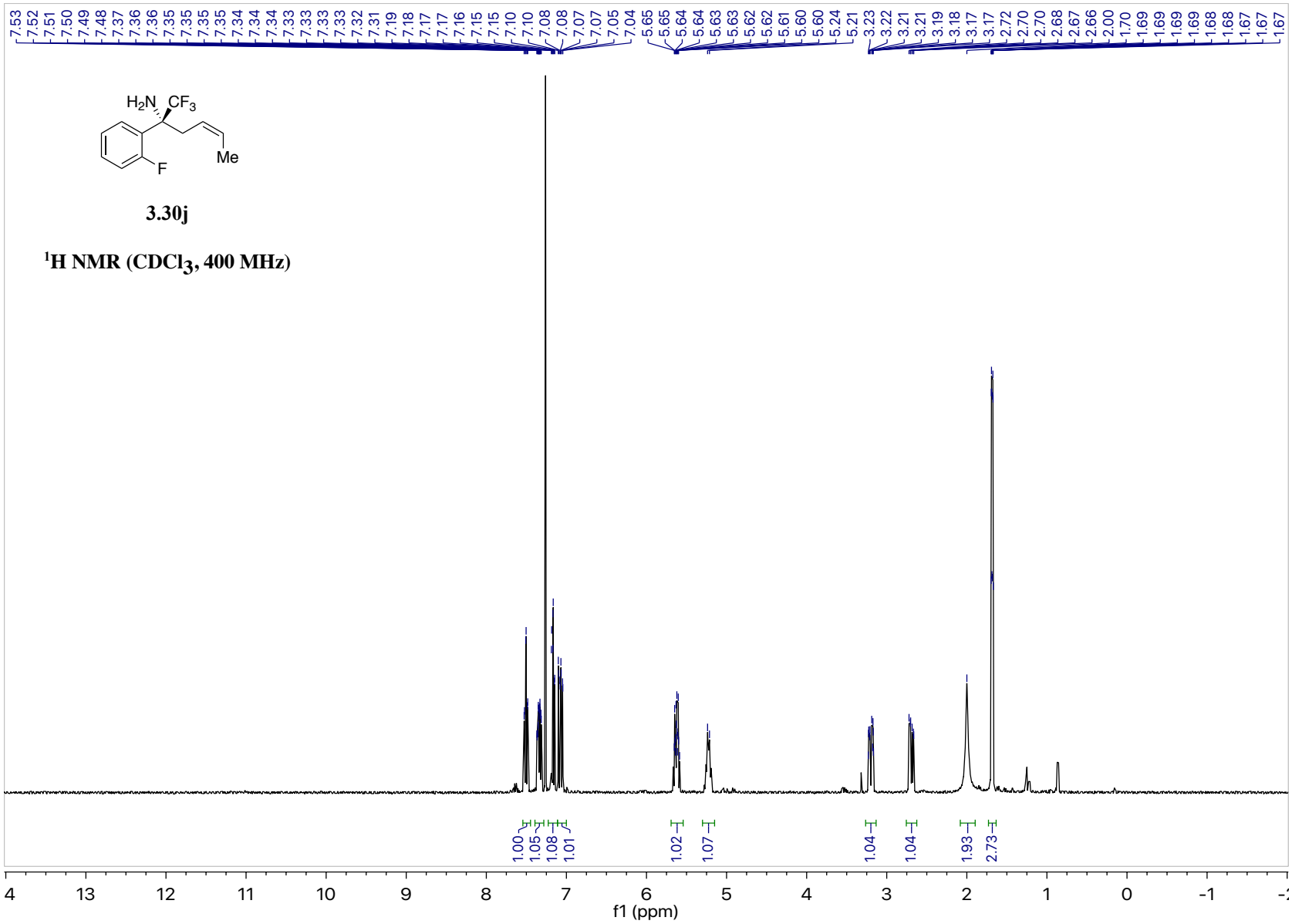
7.53 7.52 7.51 7.50 7.49 7.48 7.37 7.36 7.36 7.35 7.35 7.35 7.35 7.34 7.34 7.34 7.33 7.33 7.33 7.33 7.32 7.31 7.19 7.18 7.17 7.17 7.16 7.15 7.15 7.10 7.10 7.08 7.08 7.07 7.07 7.05 7.04 5.65 5.65 5.64 5.64 5.63 5.63 5.62 5.62 5.61 5.60 5.60 5.24 5.21 3.23 3.22 3.21 3.21 3.19 3.18 3.17 3.17 2.72 2.70 2.70 2.68 2.67 2.66 2.00 1.70 1.69 1.69 1.69 1.69 1.68 1.68 1.67 1.67 1.67
H2N CF3
F
Me
3.30j
1H NMR (CDCl3, 400 MHz)
1.00 1.05 1.08 1.01 1.02 1.07 1.04 1.04 1.93 2.73
4 13 12 11 10 9 8 7 6 5 4 3 2 1 0 -1
f1 (ppm)

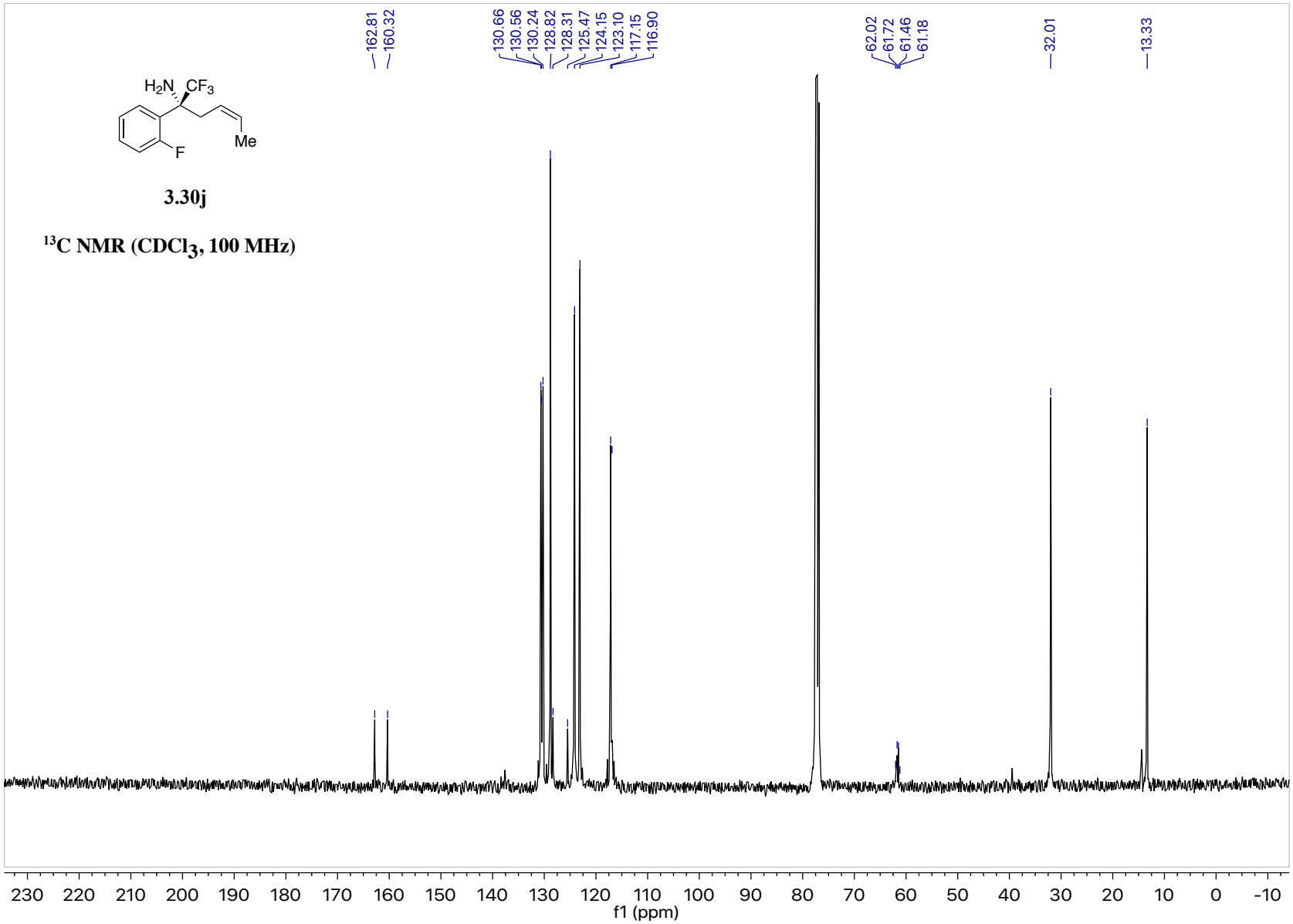
162.81
160.32
130.66
130.56
130.24
128.82
128.31
125.47
124.15
123.10
117.15
116.90
62.02
61.72
61.46
61.18
32.01
13.33
H2N
CF3
F
Me
3.30j
13C NMR (CDCl3, 100 MHz)
230 220 210 200 190 180 170 160 150 140 130 120 110 100 90 80 70 60 50 40 30 20 10 0 -10
f1 (ppm)

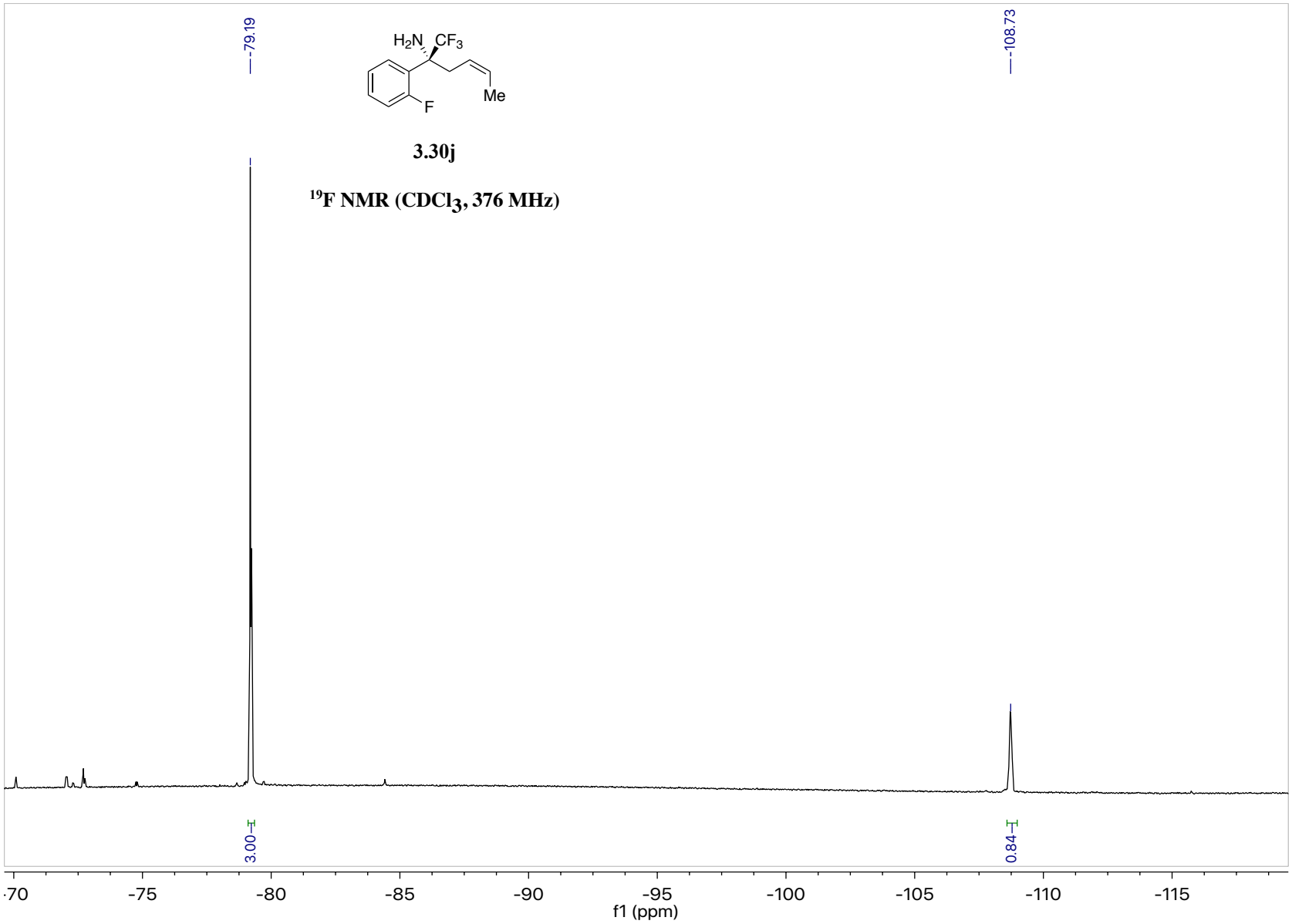
-79.19
-108.73
H2N
CF3
Me
F
3.30j
19F NMR (CDCl3, 376 MHz)
3.00
0.84
-70
-75
-80
-85
-90
-95
-100
-105
-110
-115
f1 (ppm)

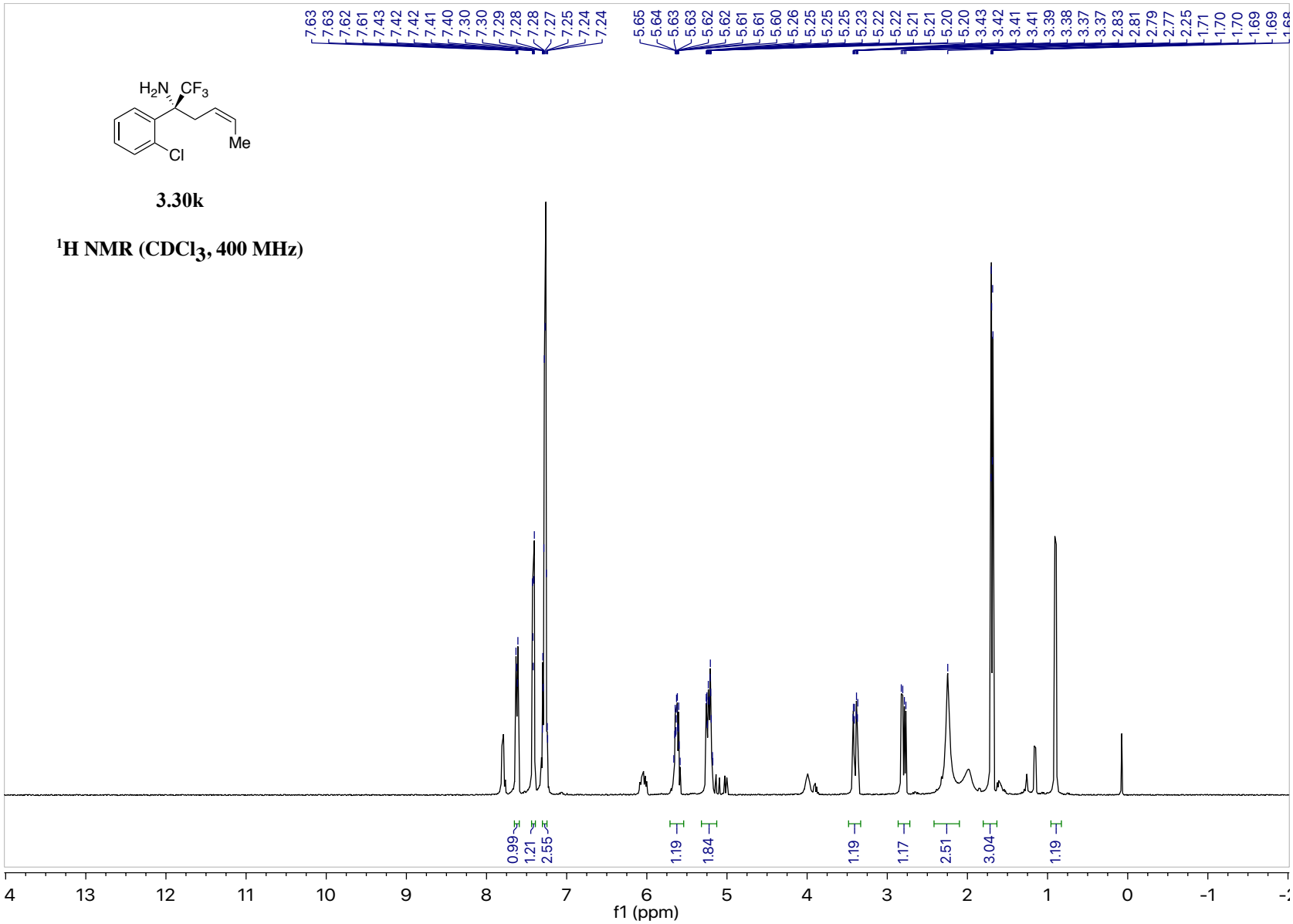

3.30k

^{1}H NMR ($CDCl_3$, 400 MHz)

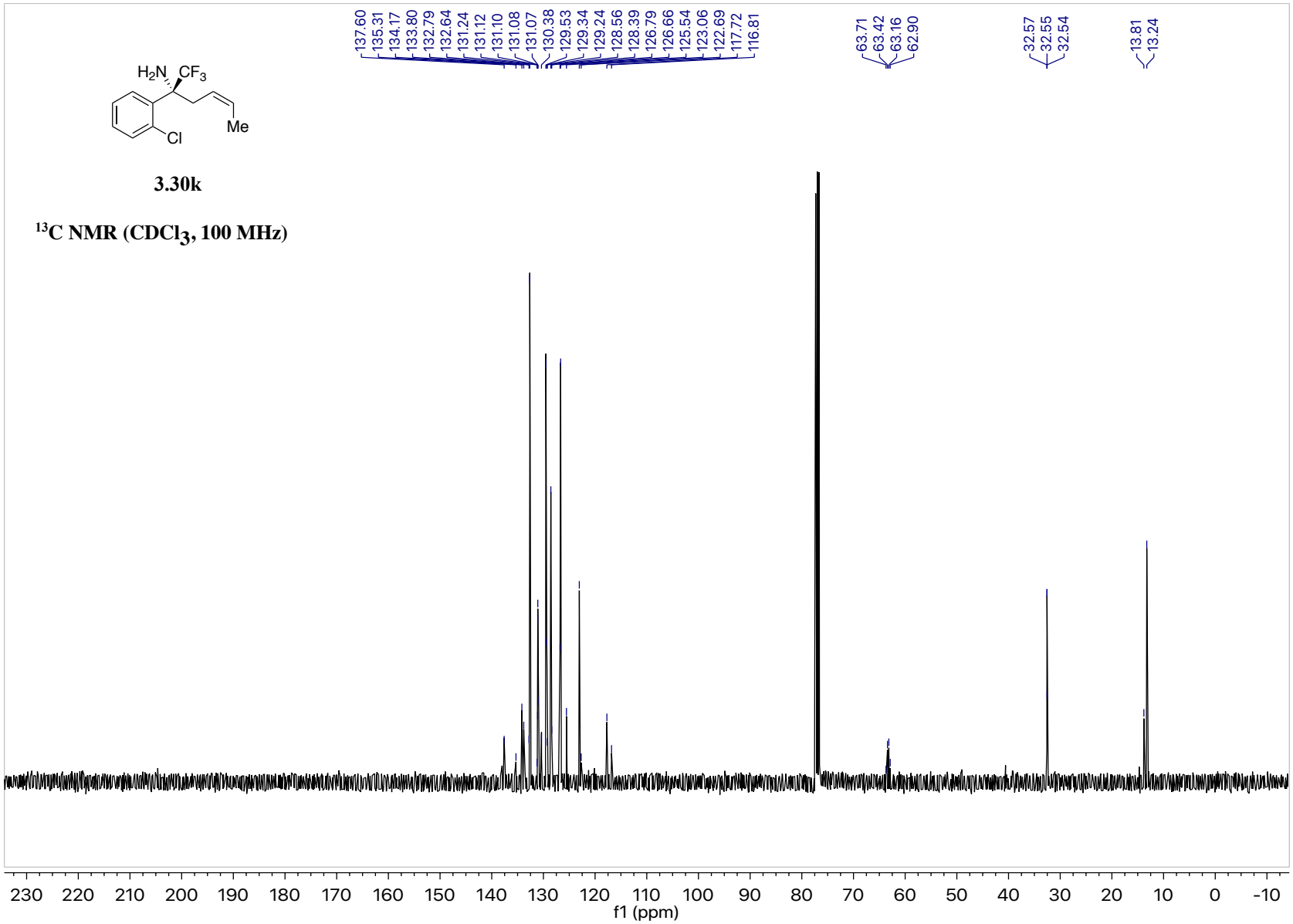

3.30k

^{13}C NMR ($CDCl_3$, 100 MHz)

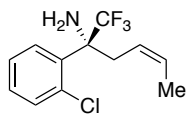

3.30k

^{19}F NMR ($CDCl_3$, 376 MHz)

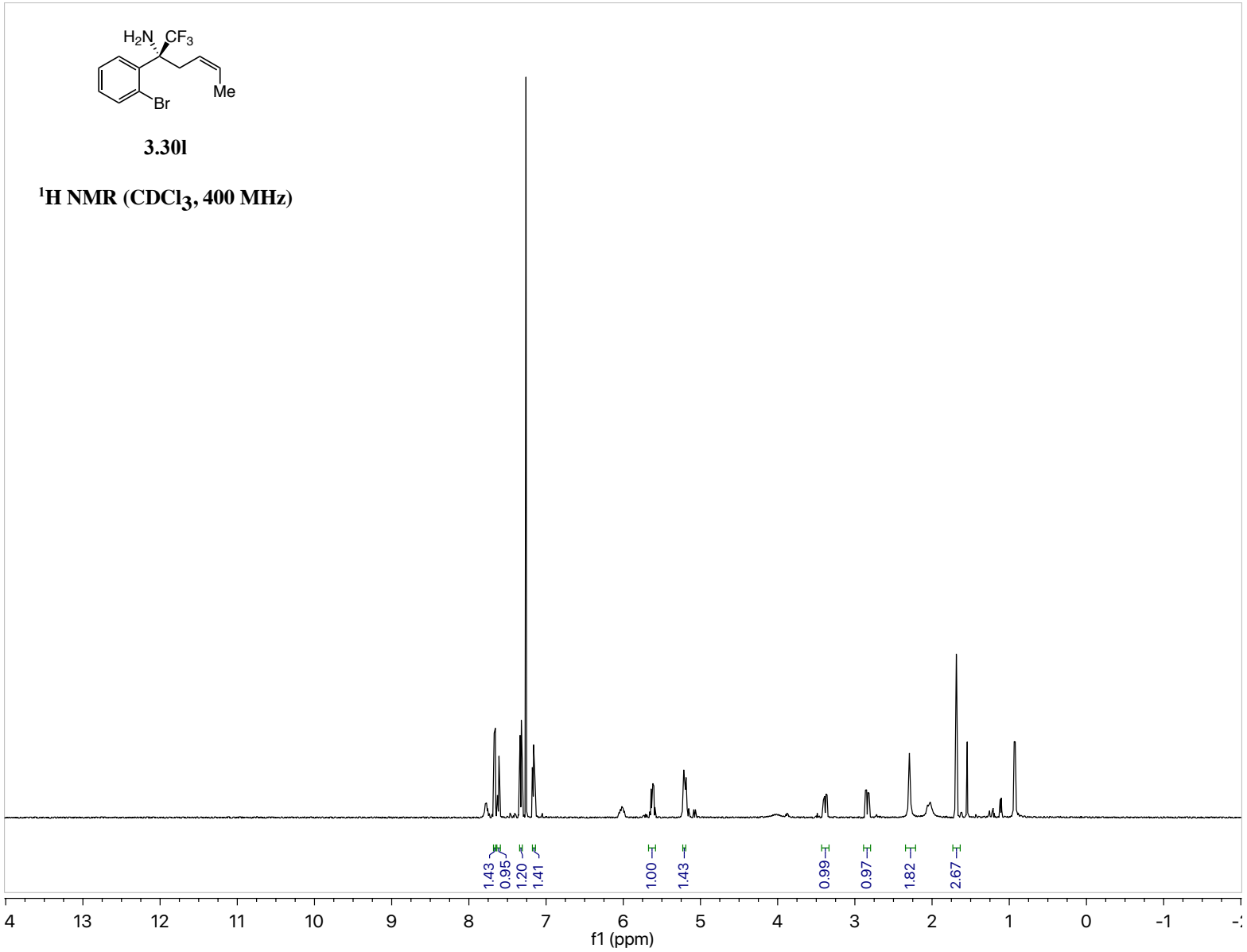
H2N
CF3
Me
Br
3.30l
1H NMR (CDCl3, 400 MHz)
1.43
0.95
1.20
1.41
1.00
1.43
0.99
0.97
1.82
2.67
f1 (ppm)

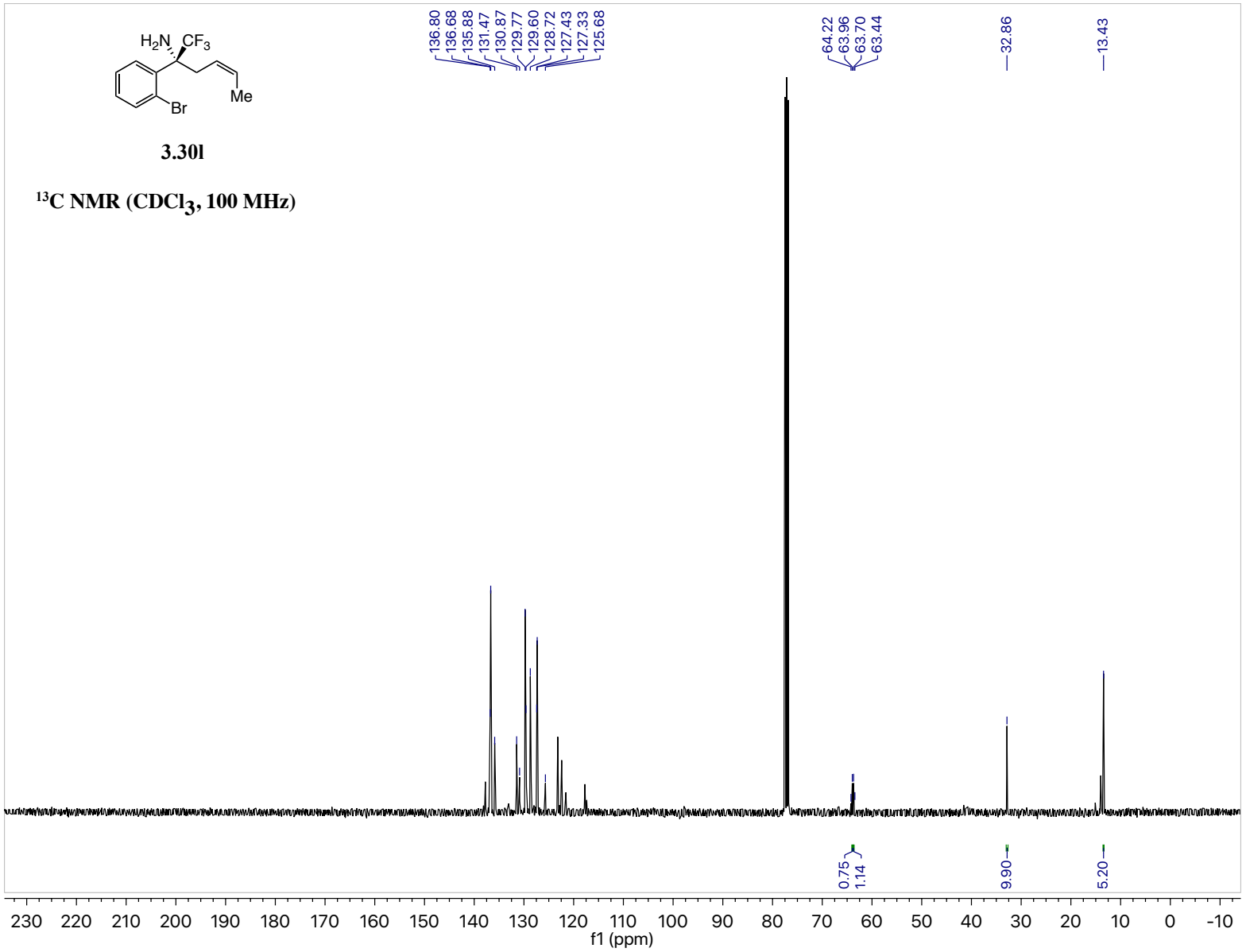

3.30l

^{13}C NMR ($CDCl_3$, 100 MHz)

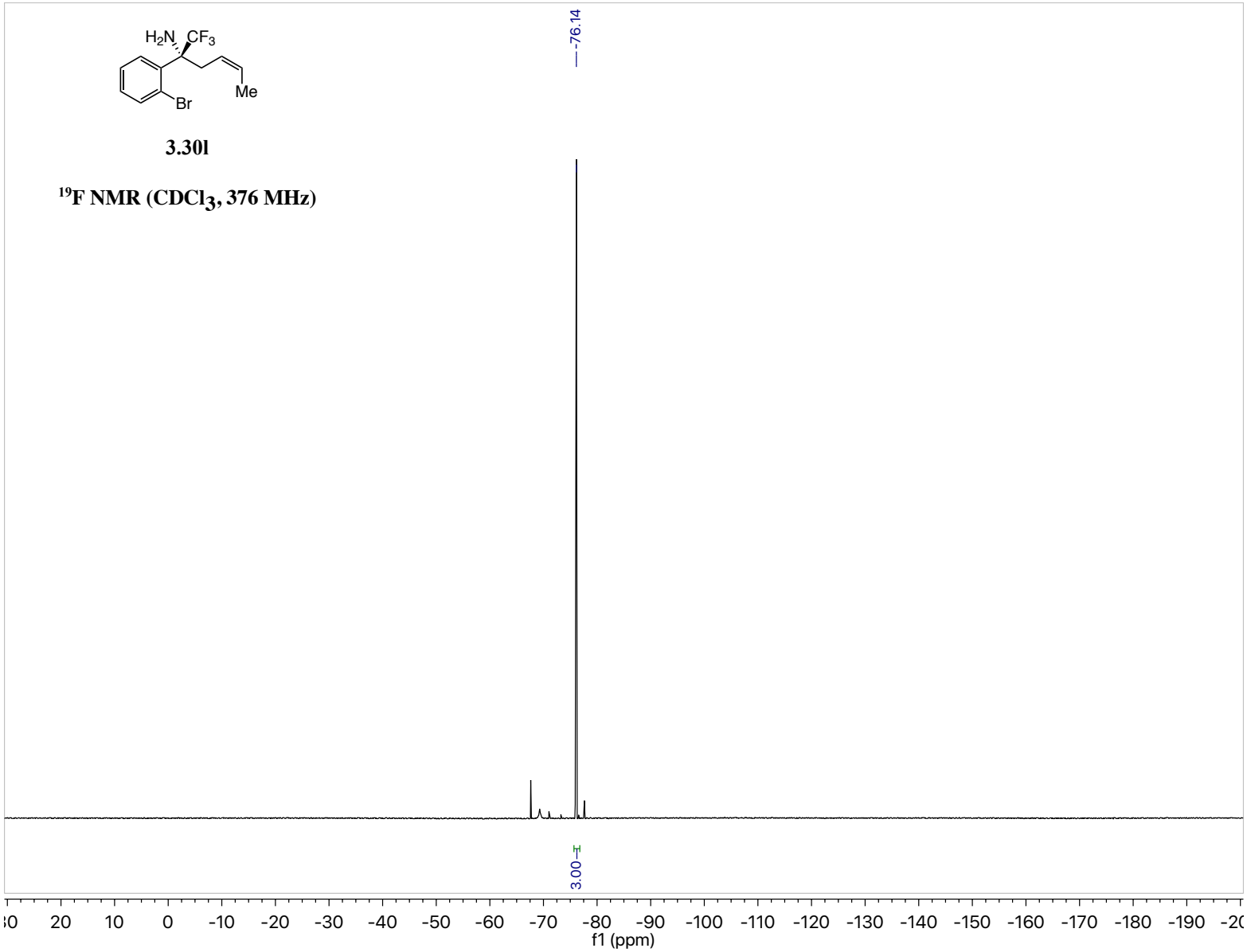

3.30l

^{19}F NMR ($CDCl_3$, 376 MHz)

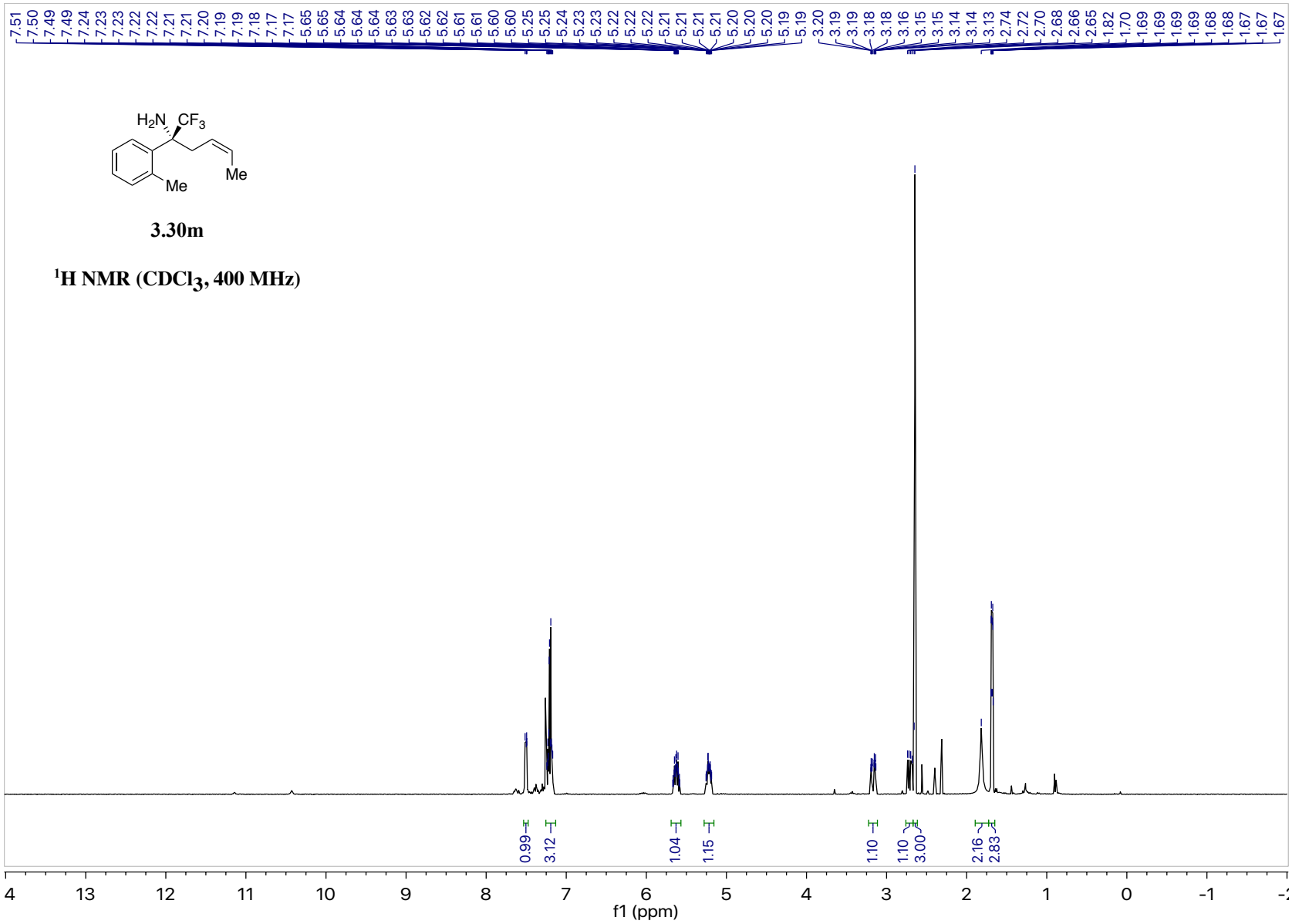

3.30m

^{1}H NMR ($CDCl_3$, 400 MHz)

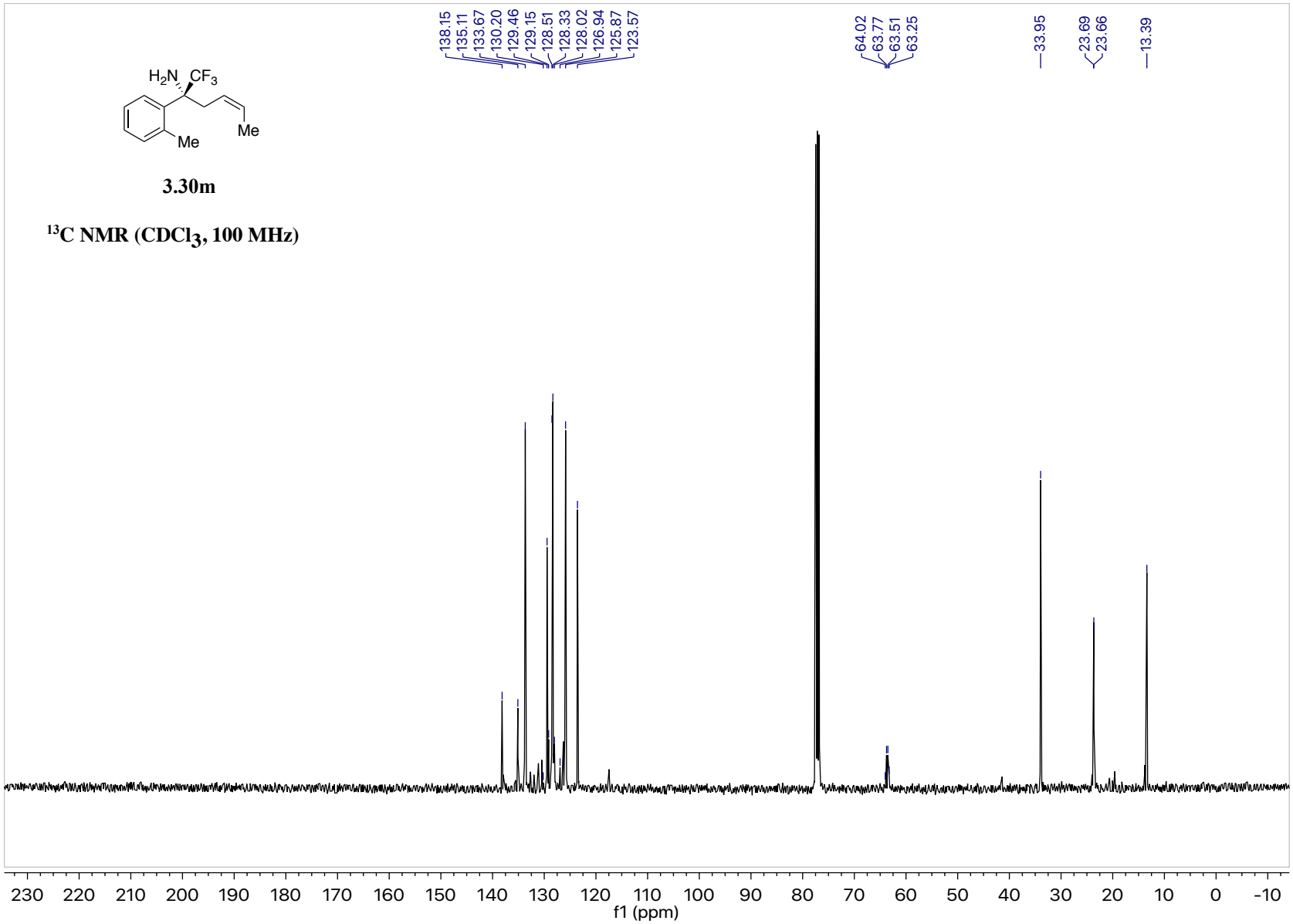

3.30m

^{13}C NMR ($CDCl_3$, 100 MHz)

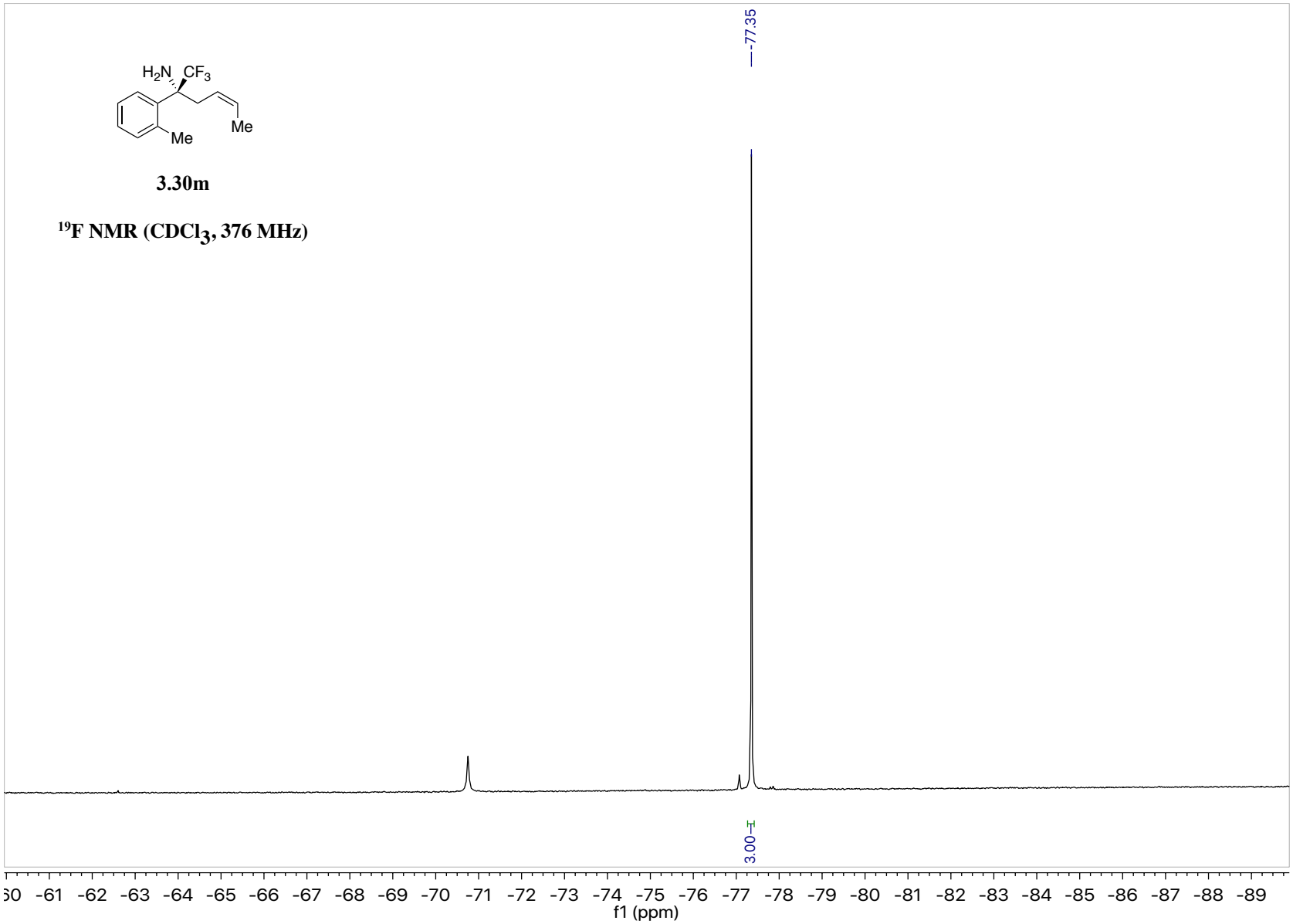

3.30m

^{19}F NMR ($CDCl_3$, 376 MHz)

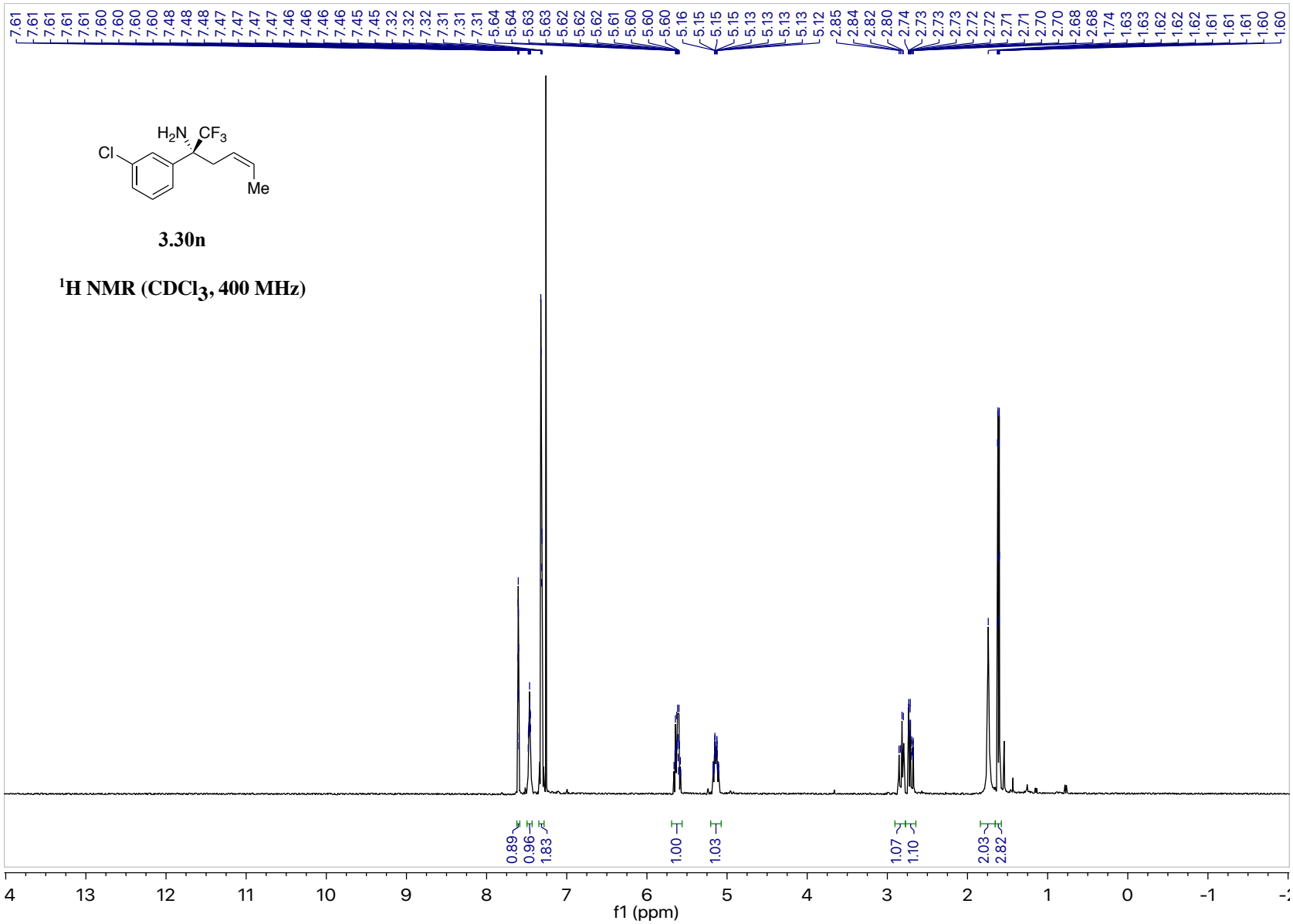

3.30n

^{1}H NMR ($CDCl_3$, 400 MHz)

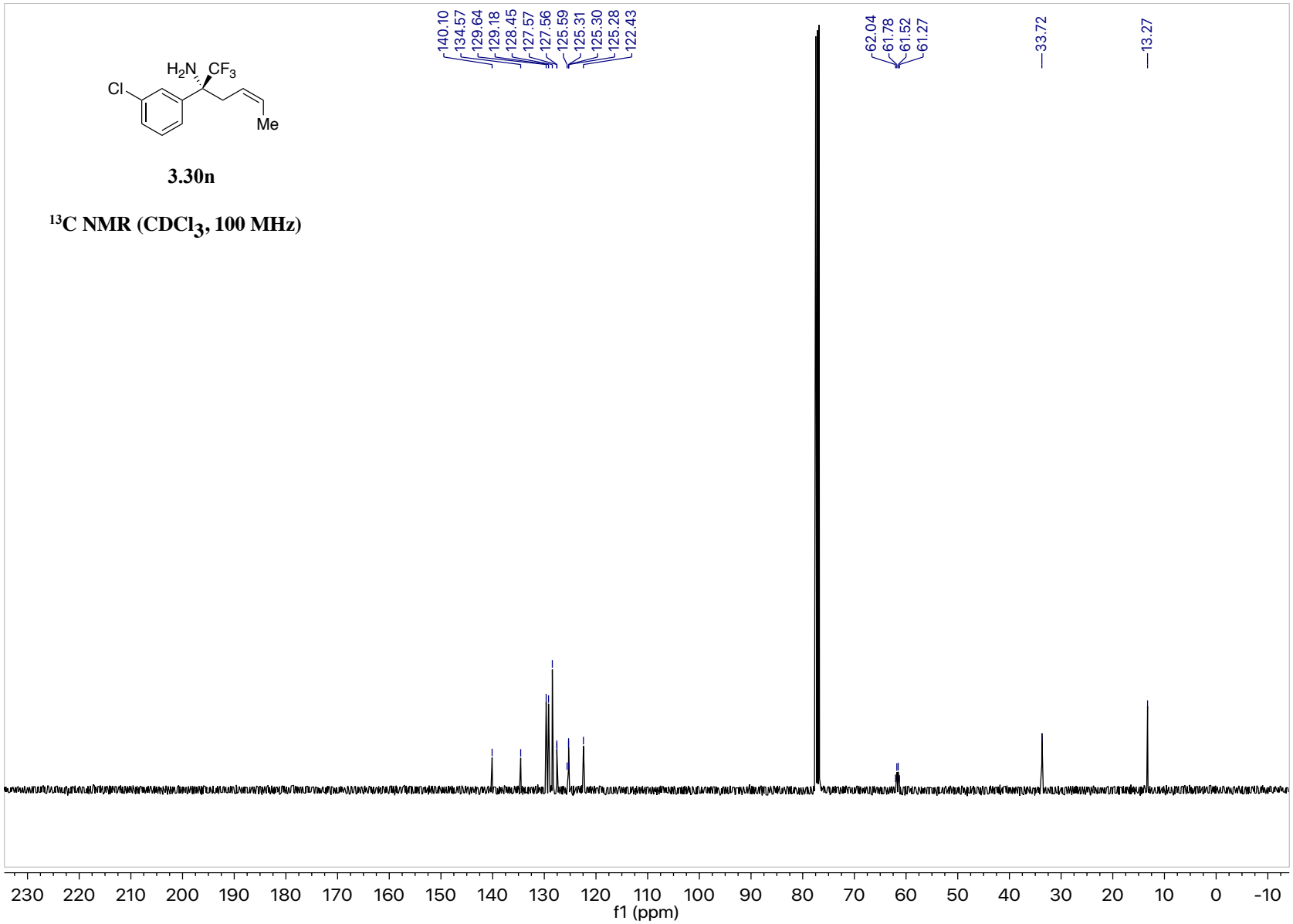

3.30n

^{13}C NMR ($CDCl_3$, 100 MHz)

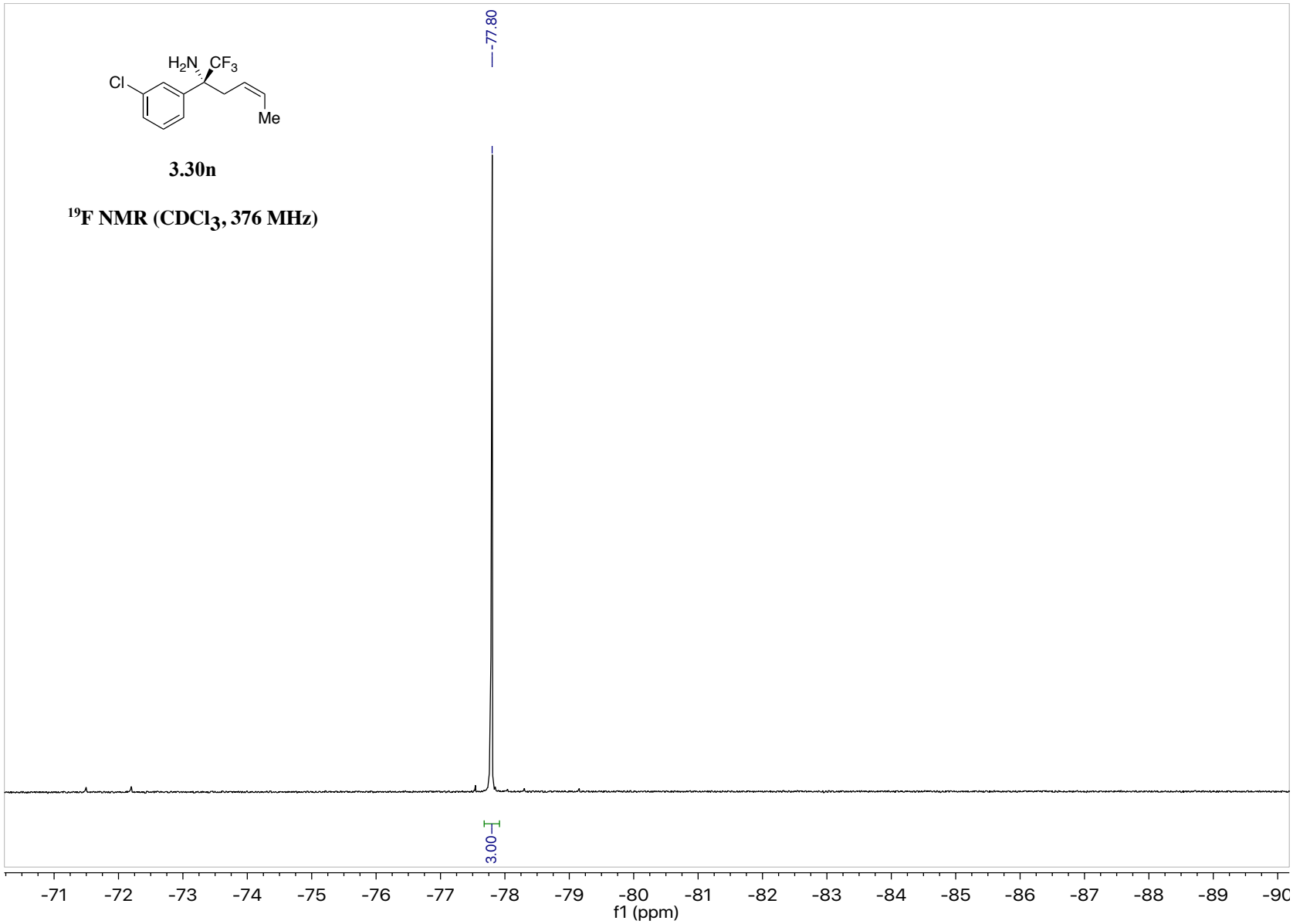

3.30n

^{19}F NMR ($CDCl_3$, 376 MHz)

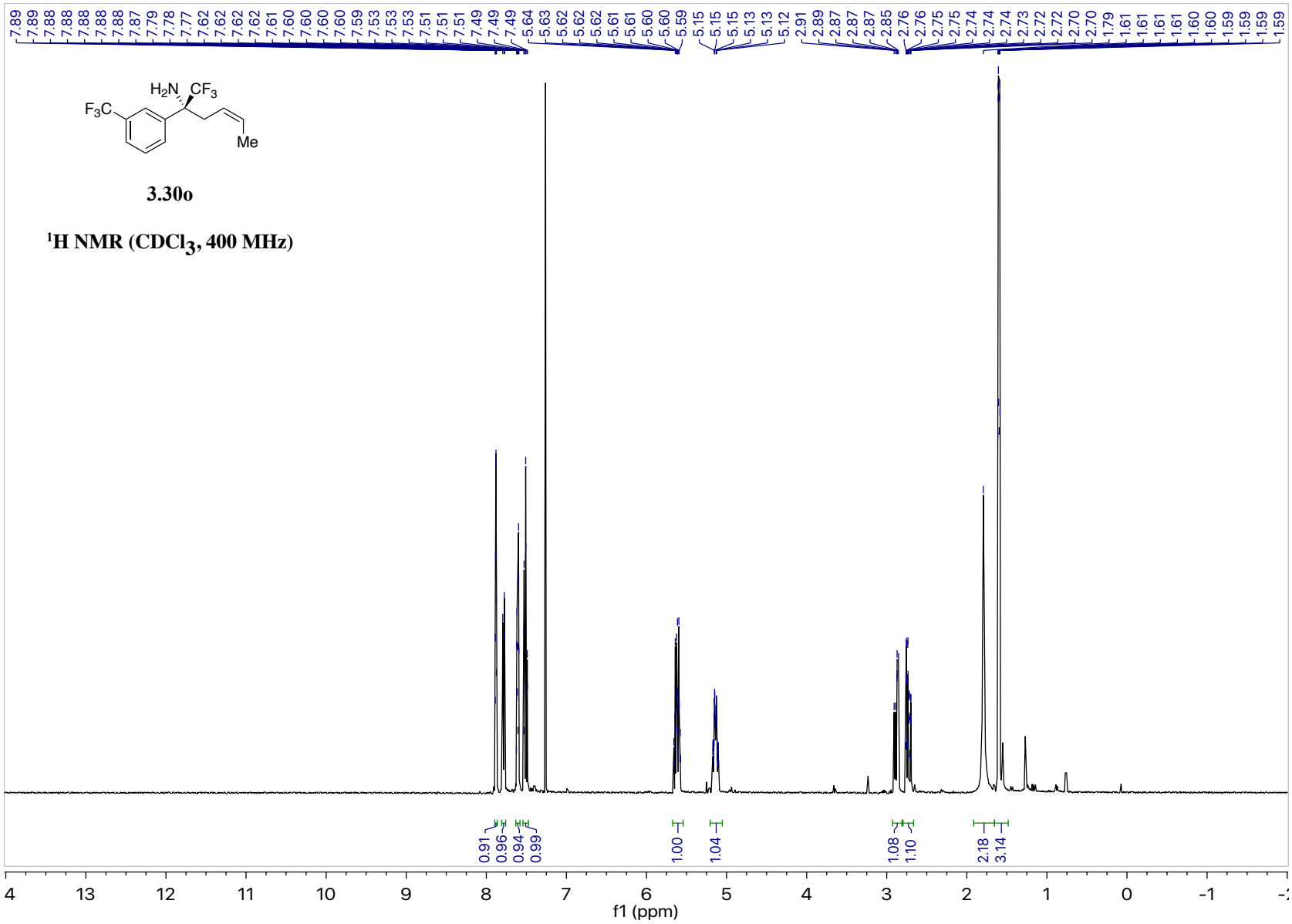
7.89 7.89 7.88 7.88 7.88 7.88 7.87 7.79 7.78 7.77 7.62 7.62 7.62 7.61 7.60 7.60 7.60 7.60 7.59 7.53 7.53 7.51 7.51 7.49 7.49 7.49 7.64 5.63 5.62 5.62 5.62 5.61 5.61 5.60 5.60 5.59 5.15 5.15 5.13 5.13 5.12 2.91 2.89 2.87 2.87 2.87 2.85 2.76 2.76 2.75 2.75 2.74 2.74 2.74 2.73 2.72 2.72 2.70 2.70 1.79 1.61 1.61 1.61 1.61 1.60 1.60 1.59 1.59 1.59 1.59
H2N CF3
F3C
Me
3.30o
1H NMR (CDCl3, 400 MHz)
0.91 0.96 0.94 0.99 1.00 1.04 1.08 1.10 2.18 3.14
4 13 12 11 10 9 8 7 6 5 4 3 2 1 0 -1
f1 (ppm)

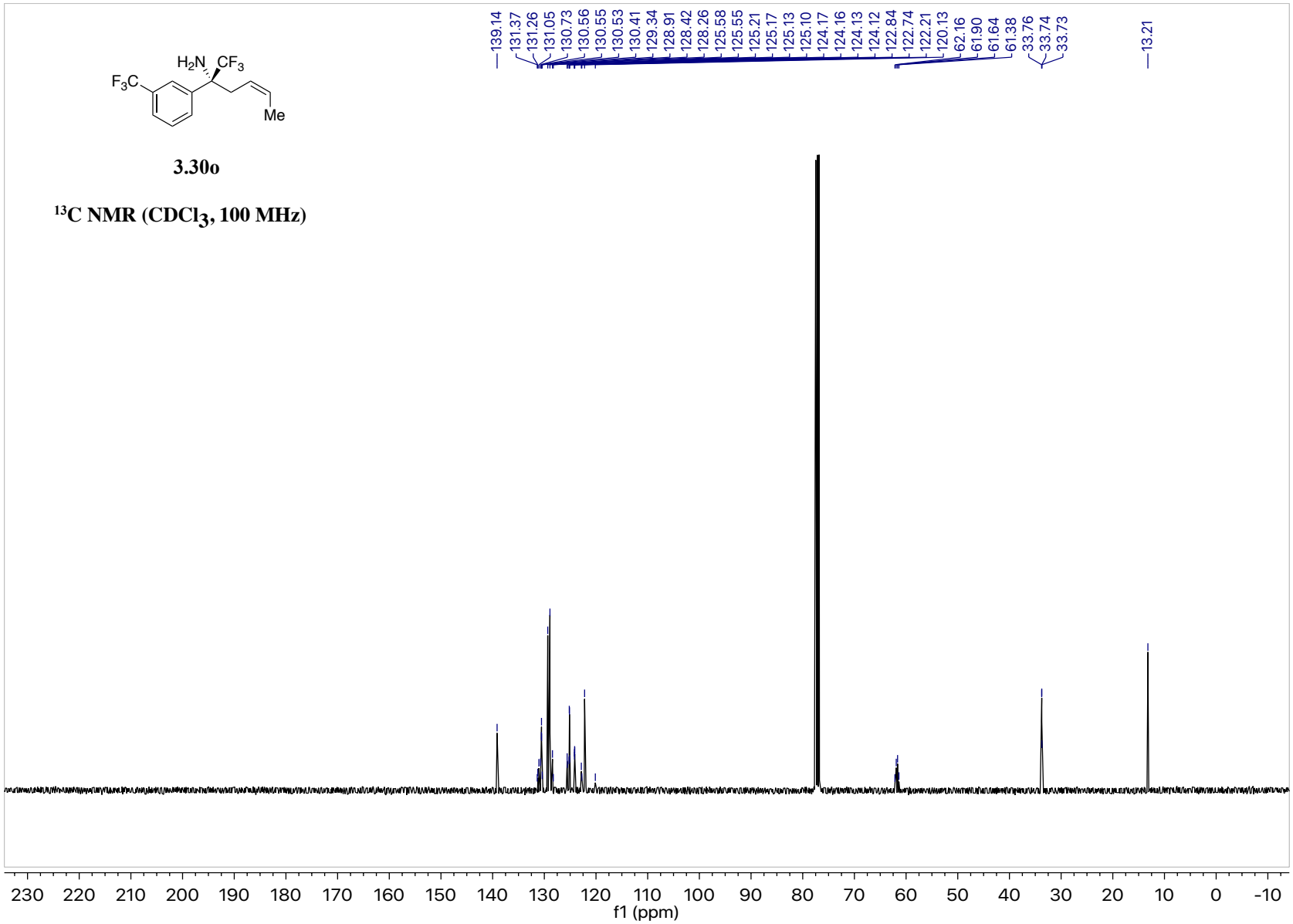

3.30o

^{13}C NMR ($CDCl_3$, 100 MHz)

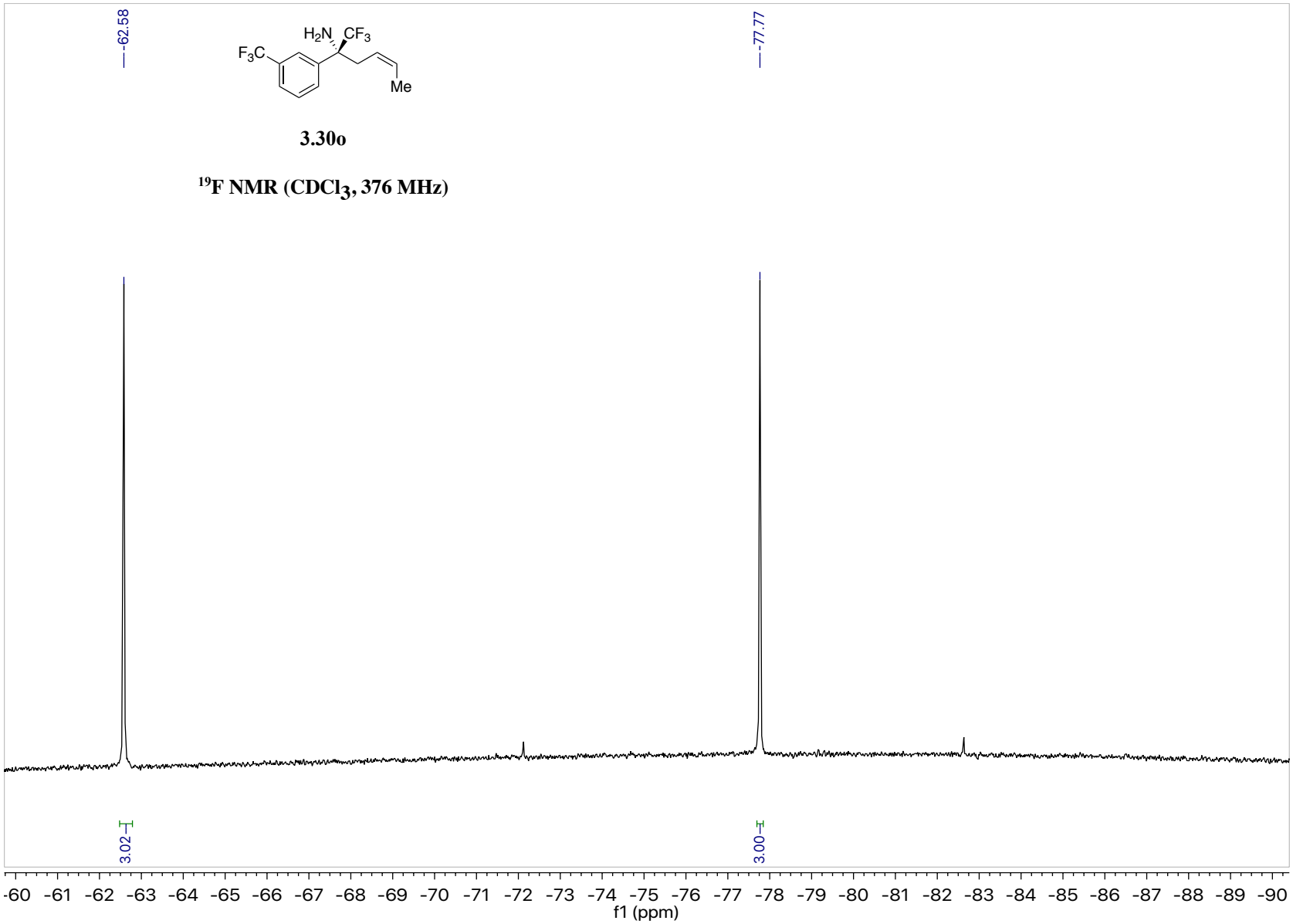

3.30o

^{19}F NMR ($CDCl_3$, 376 MHz)

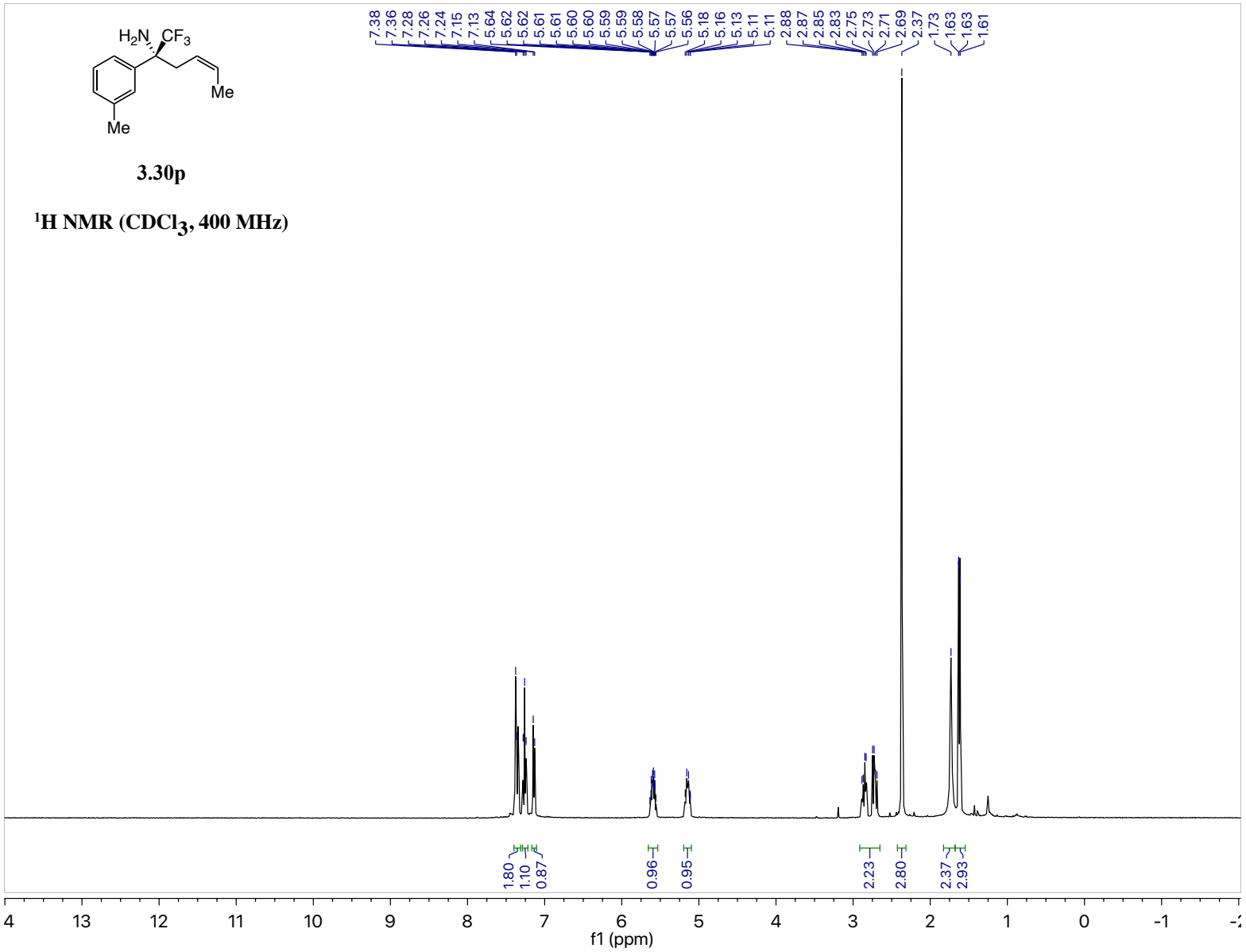

3.30p

^{1}H NMR ($CDCl_3$, 400 MHz)

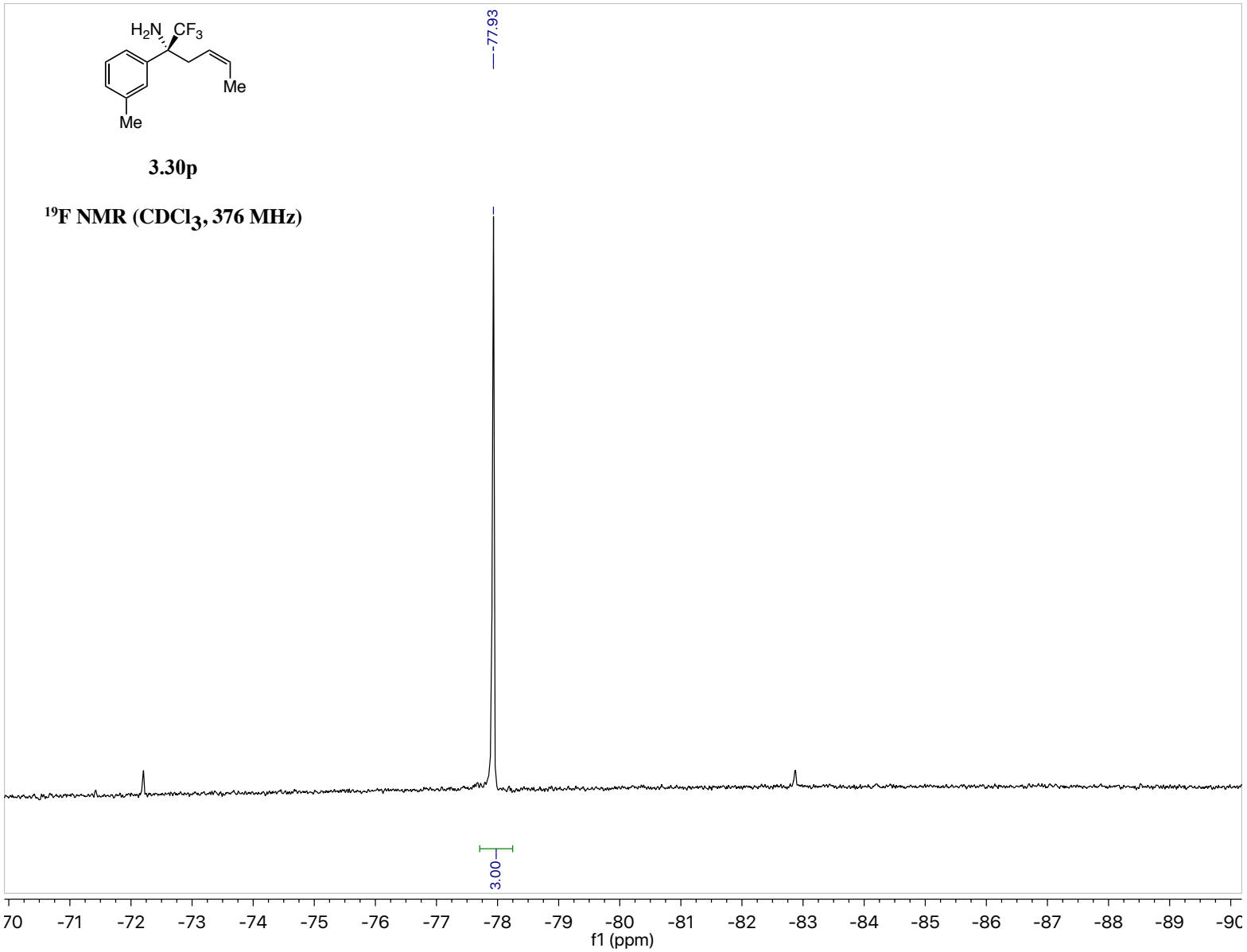

3.30p

^{19}F NMR ($CDCl_3$, 376 MHz)

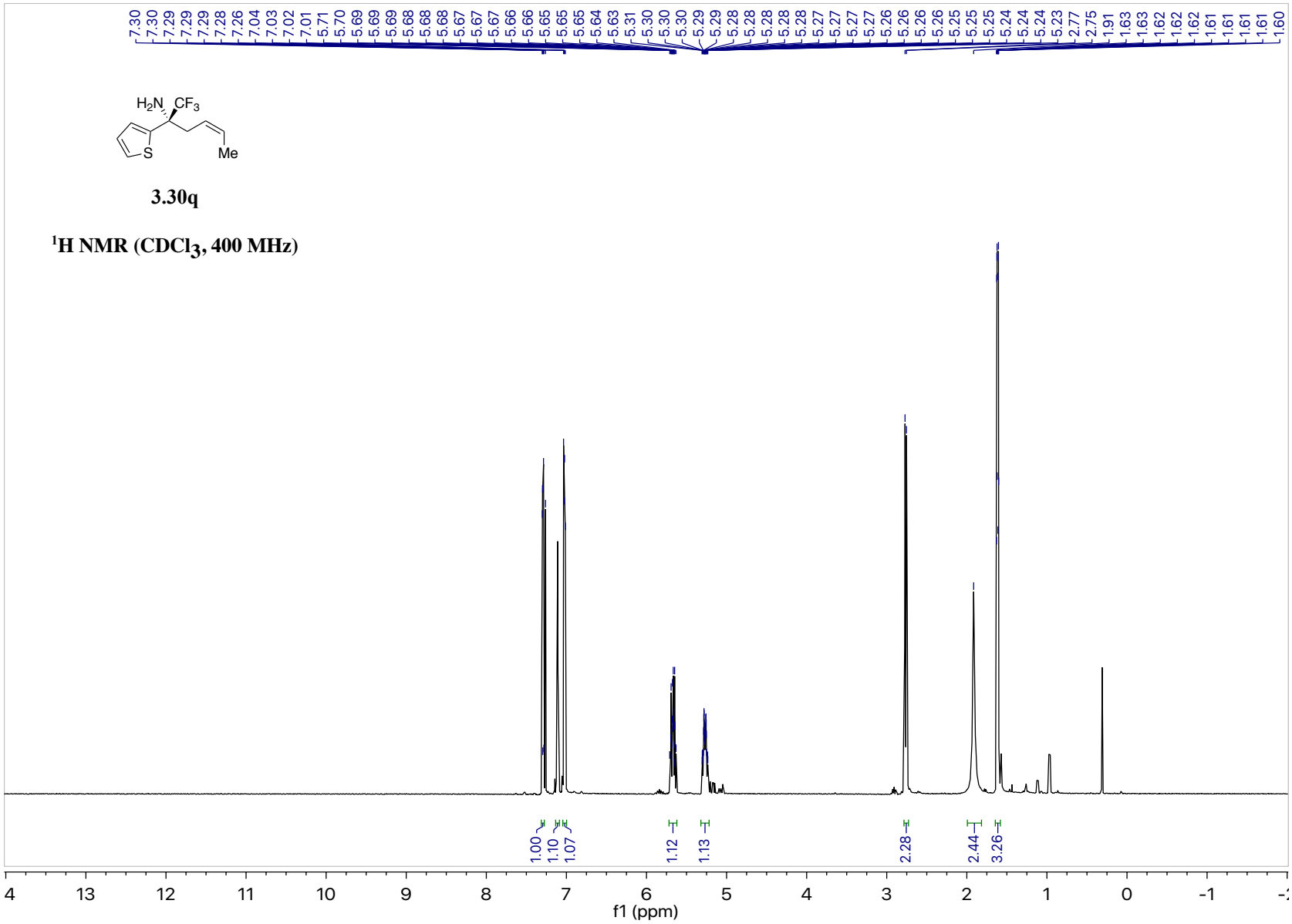

3.30q

^{1}H NMR ($CDCl_3$, 400 MHz)

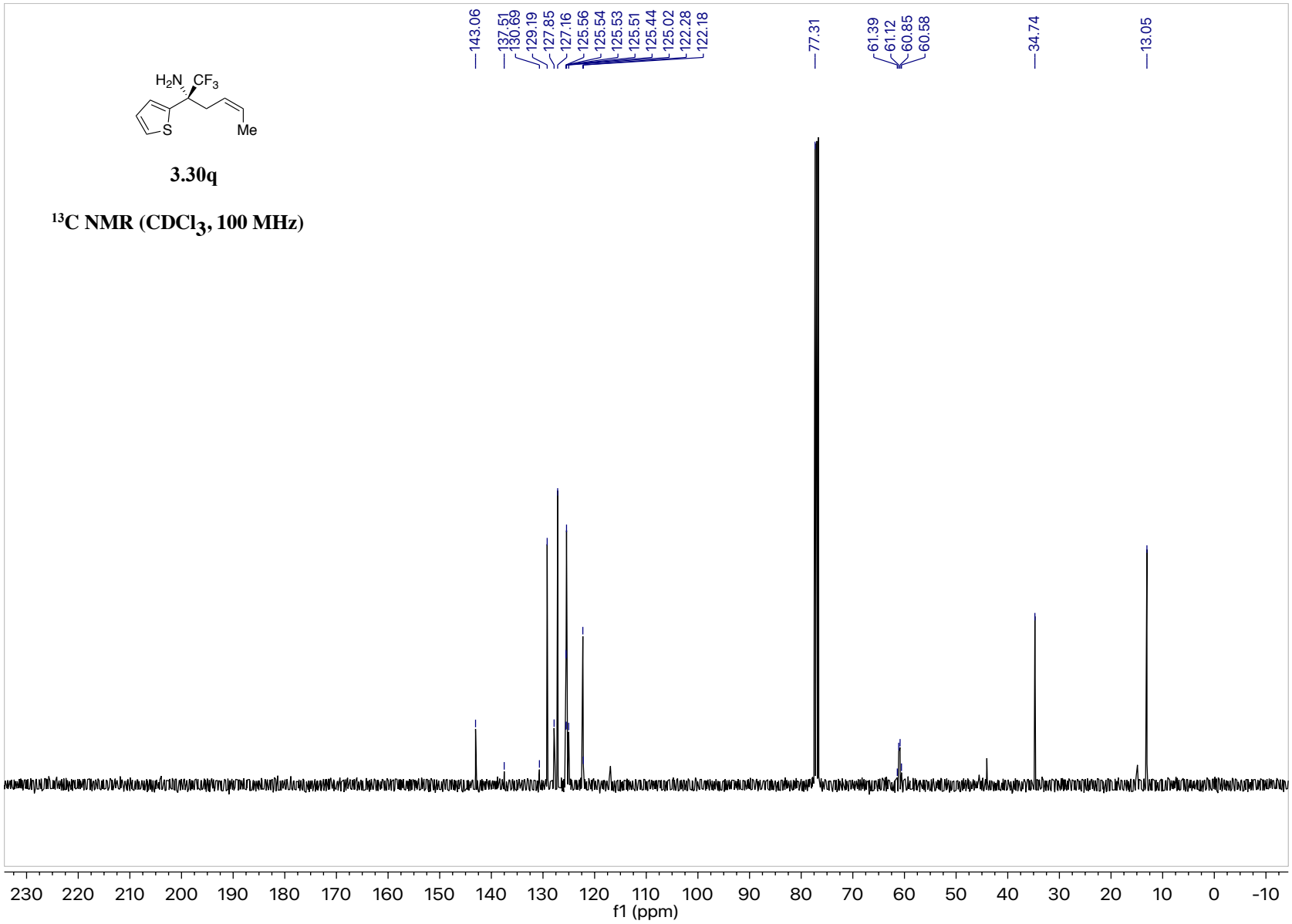

3.30q

^{13}C NMR ($CDCl_3$, 100 MHz)

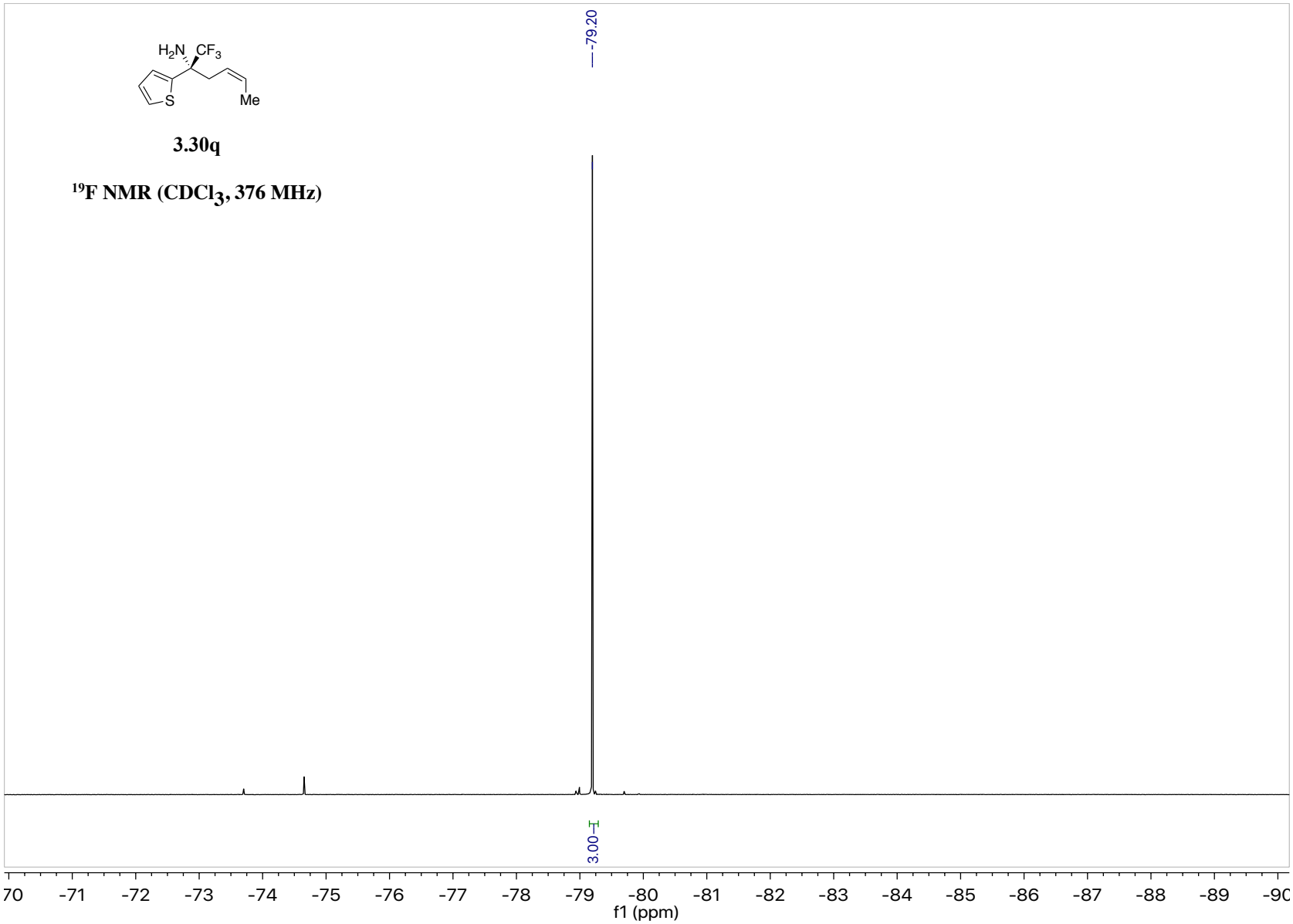

3.30q

^{19}F NMR ($CDCl_3$, 376 MHz)

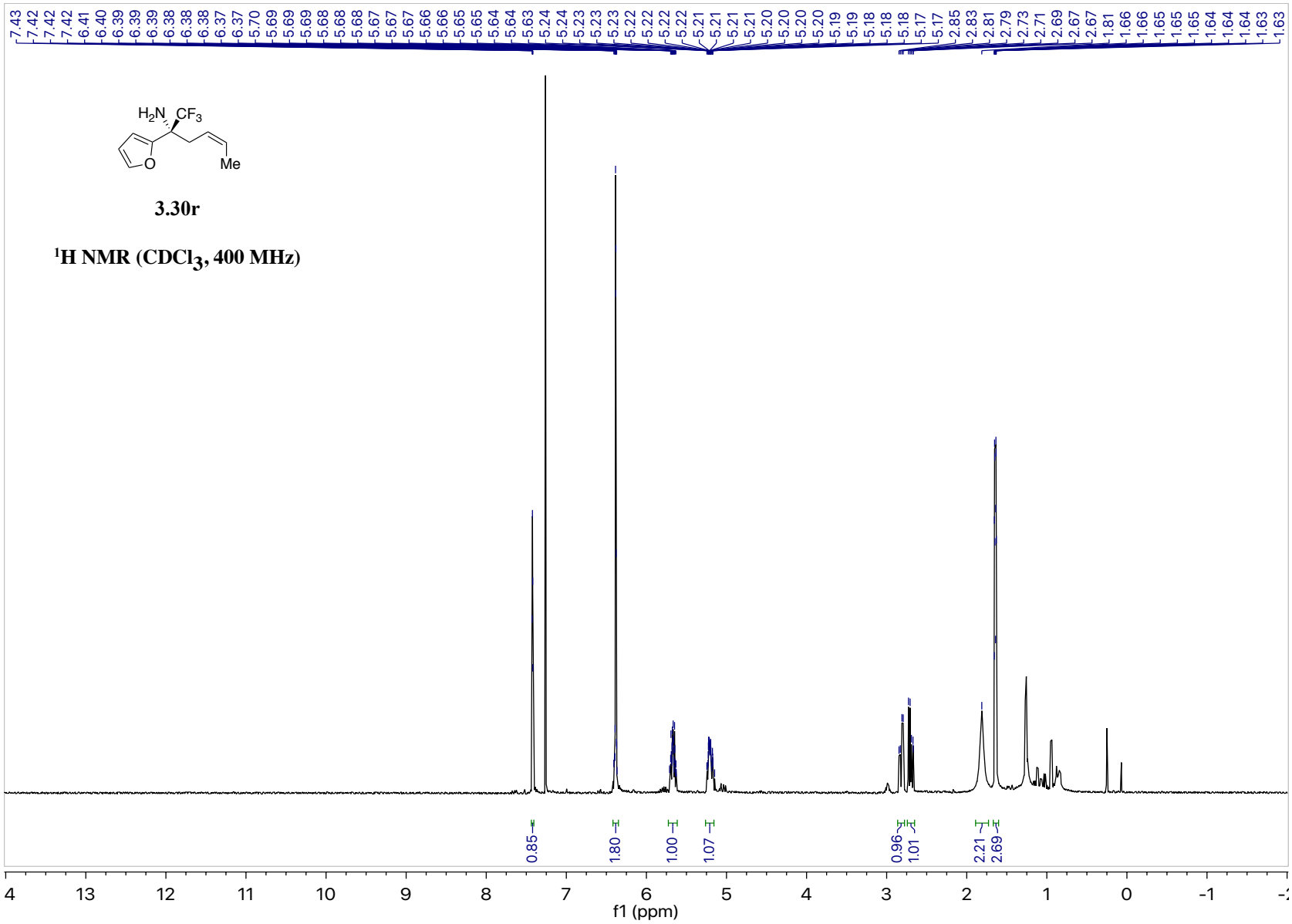
7.43 7.42 7.42 7.42 6.41 6.40 6.39 6.39 6.39 6.38 6.38 6.38 6.37 6.37 5.70 5.69 5.69 5.69 5.68 5.68 5.68 5.67 5.67 5.67 5.66 5.66 5.65 5.65 5.64 5.64 5.63 5.24 5.24 5.23 5.23 5.23 5.22 5.22 5.22 5.22 5.21 5.21 5.21 5.20 5.20 5.20 5.19 5.19 5.18 5.18 5.18 5.17 5.17 2.85 2.83 2.81 2.79 2.73 2.71 2.69 2.67 2.67 1.81 1.66 1.66 1.65 1.65 1.65 1.64 1.64 1.64 1.63 1.63
H2N CF3
O
Me
3.30r
1H NMR (CDCl3, 400 MHz)
0.85
1.80
1.00
1.07
0.96
1.01
2.21
2.69
4 13 12 11 10 9 8 7 6 5 4 3 2 1 0 -1
f1 (ppm)

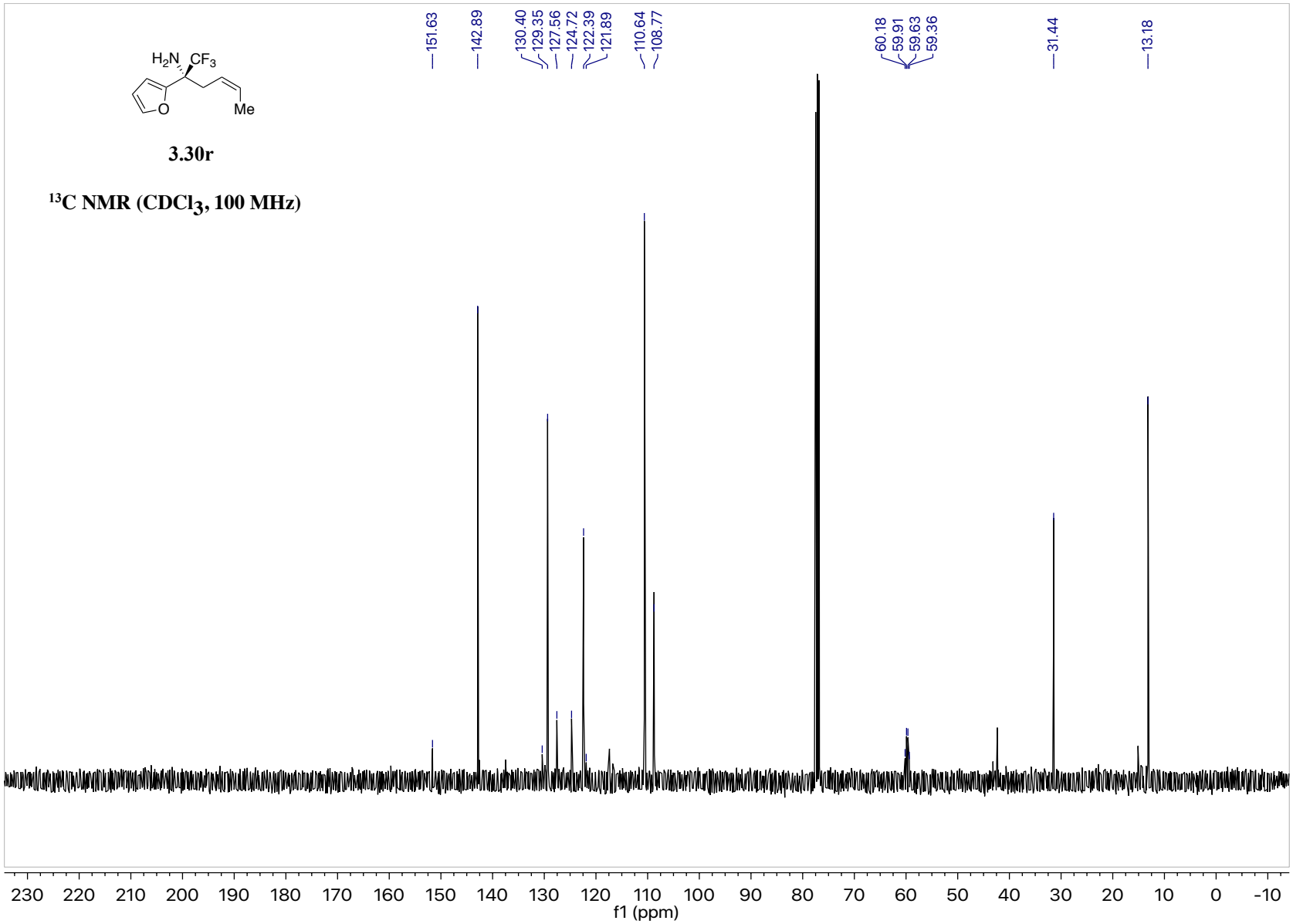
H2N CF3
O
Me
3.30r
13C NMR (CDCl3, 100 MHz)
151.63
142.89
130.40
129.35
127.56
124.72
122.39
121.89
110.64
108.77
60.18
59.91
59.63
59.36
31.44
13.18
230 220 210 200 190 180 170 160 150 140 130 120 110 100 90 80 70 60 50 40 30 20 10 0 -10
f1 (ppm)

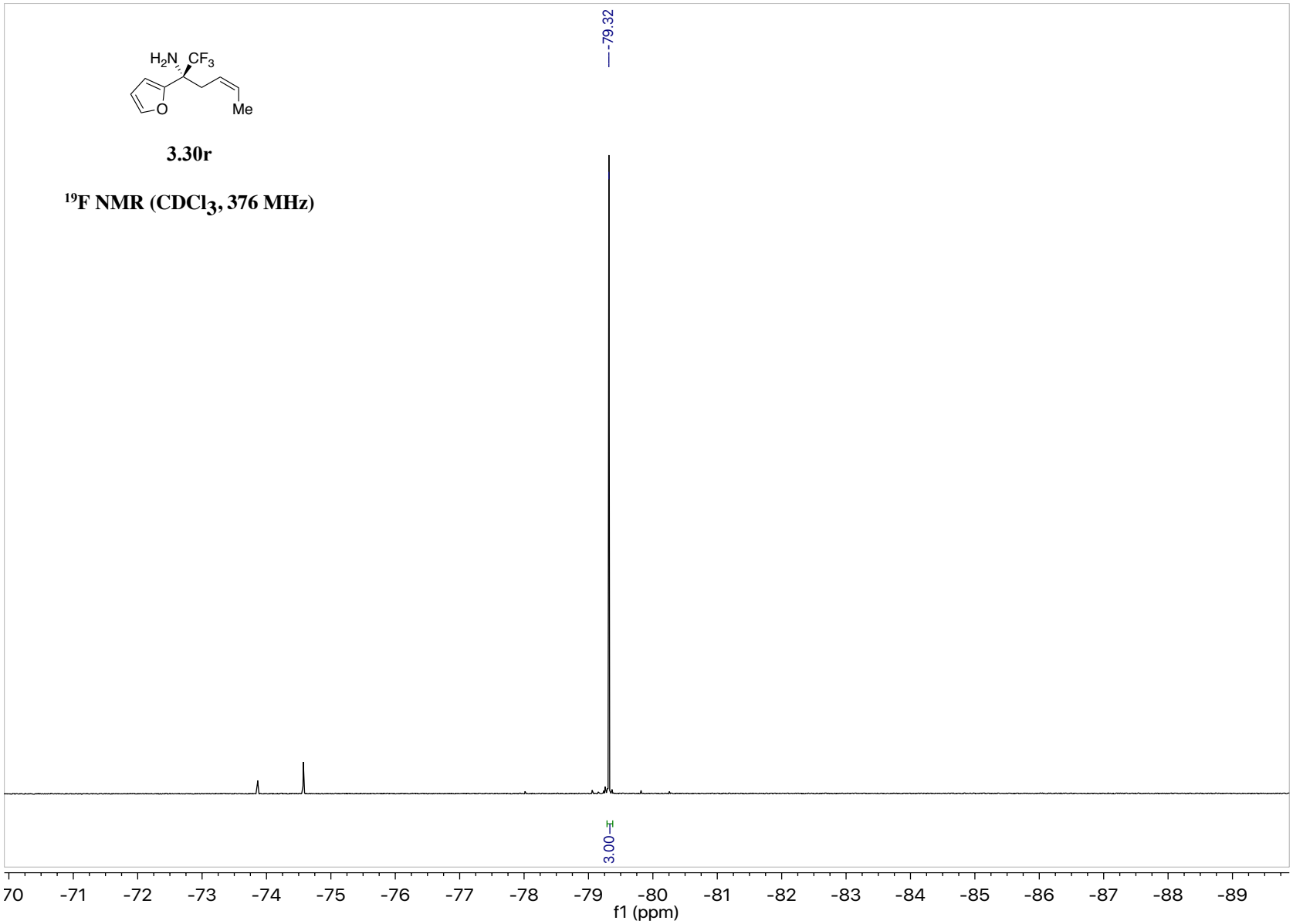

3.30r

^{19}F NMR ($CDCl_3$, 376 MHz)

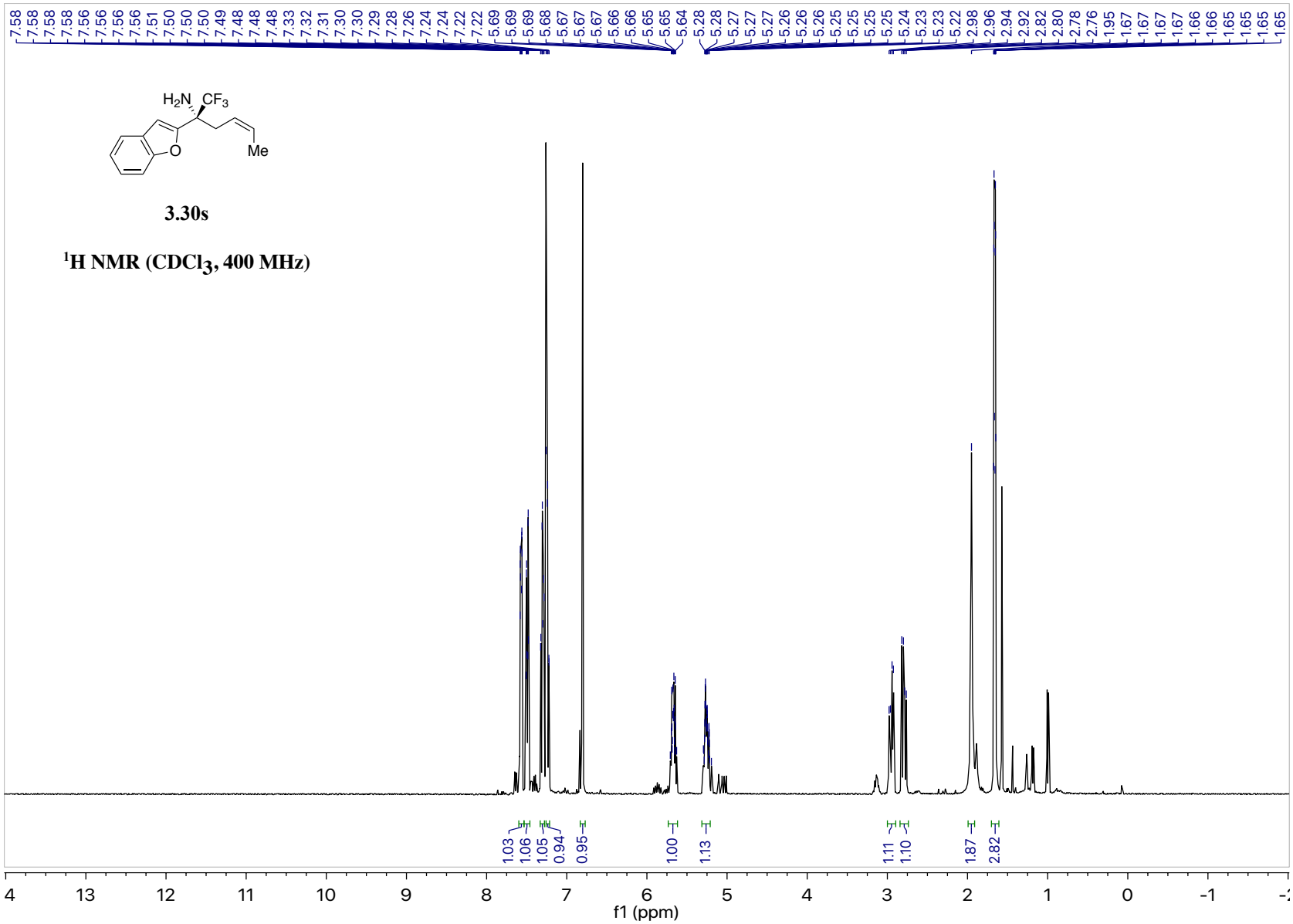
H2N CF3
O
Me
3.30s
1H NMR (CDCl3, 400 MHz)
f1 (ppm)

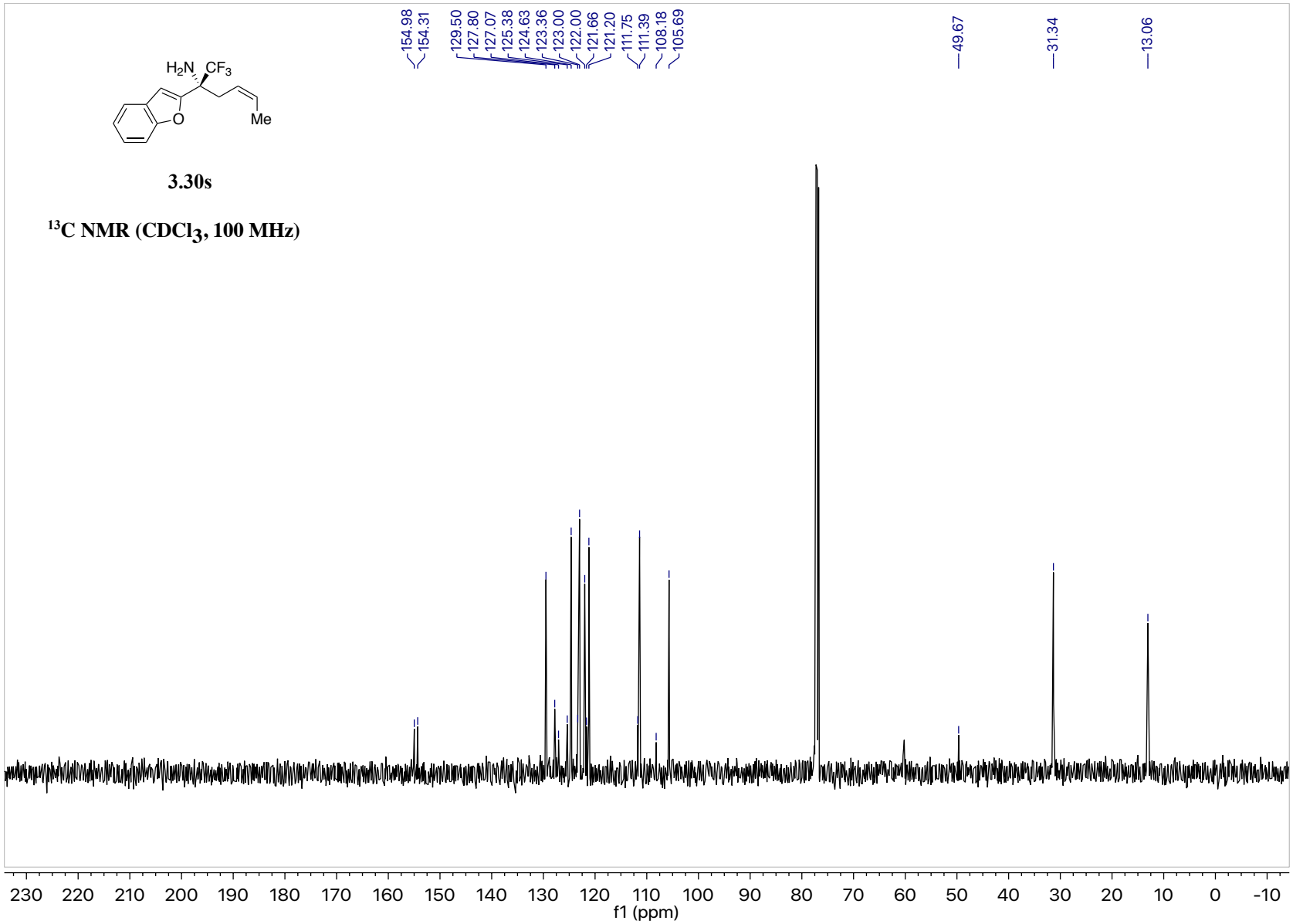
154.98
154.31
129.50
127.80
127.07
125.38
124.63
123.36
123.00
122.00
121.66
121.20
111.75
111.39
108.18
105.69
49.67
31.34
13.06
H2N
CF3
O
Me
3.30s
13C NMR (CDCl3, 100 MHz)
230 220 210 200 190 180 170 160 150 140 130 120 110 100 90 80 70 60 50 40 30 20 10 0 -10
f1 (ppm)

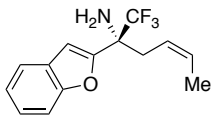

3.30s

^{19}F NMR ($CDCl_3$, 376 MHz)

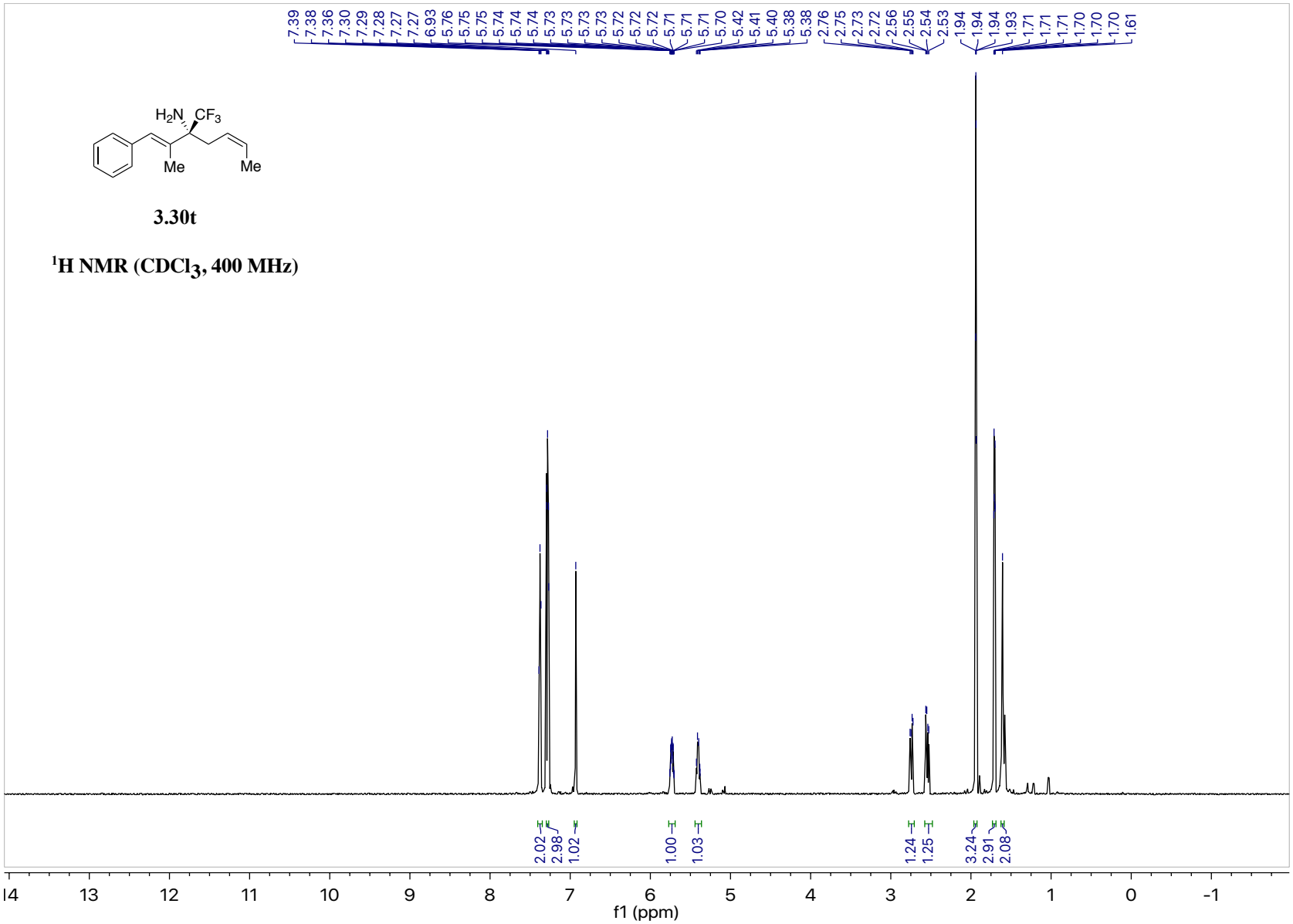

3.30t

^{1}H NMR ($CDCl_3$, 400 MHz)

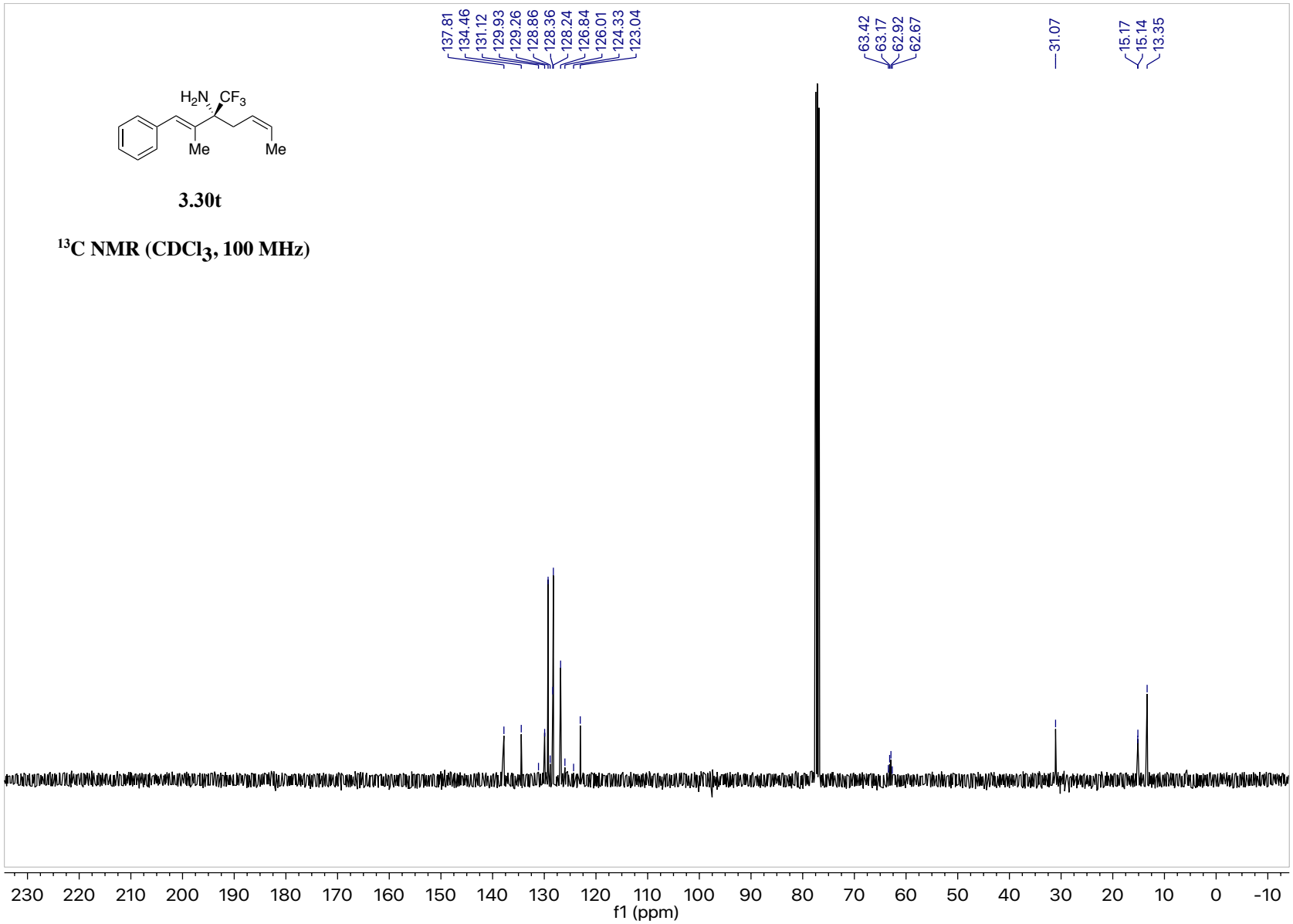

3.30t

^{13}C NMR ($CDCl_3$, 100 MHz)

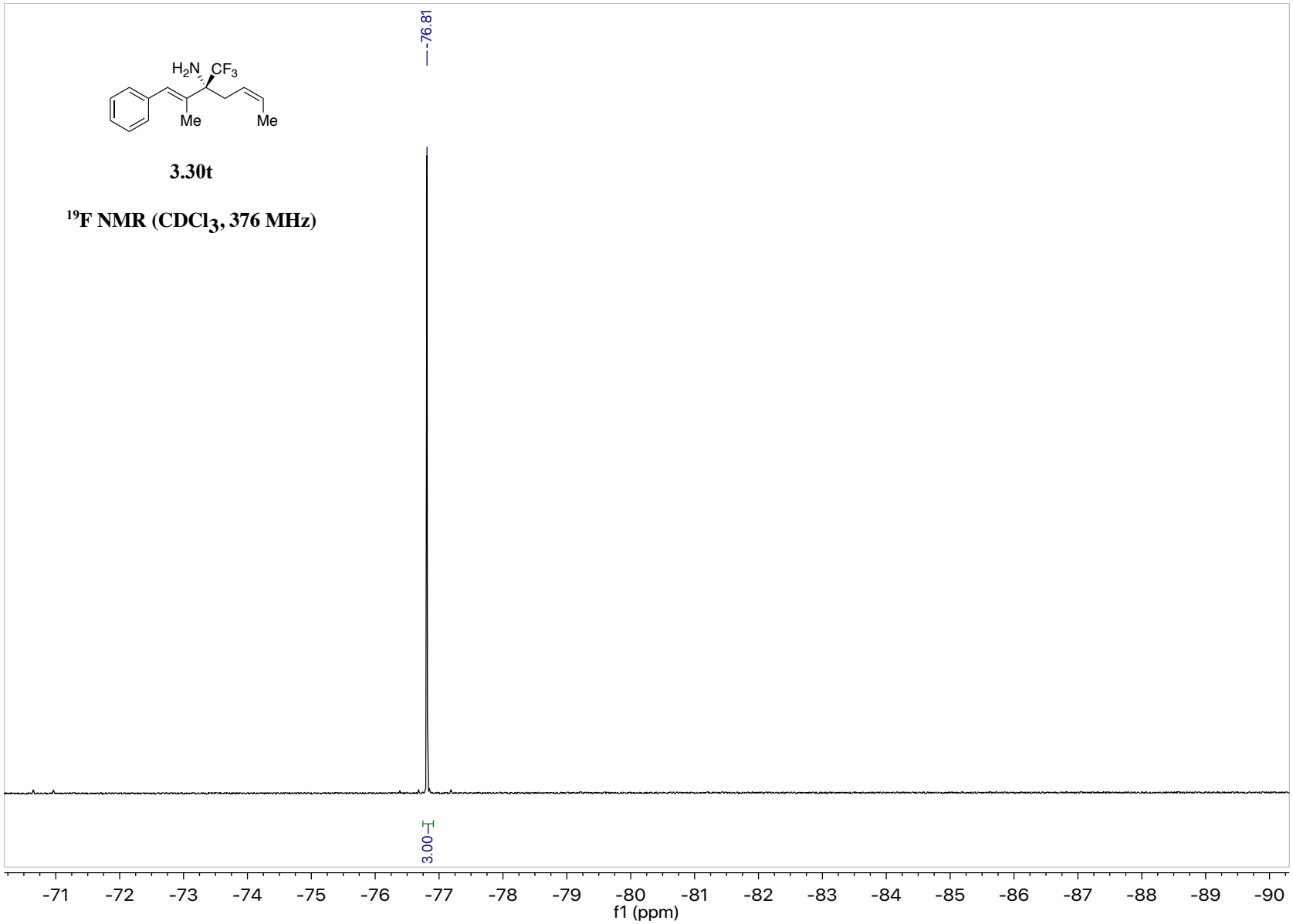

3.30t

^{19}F NMR ($CDCl_3$, 376 MHz)

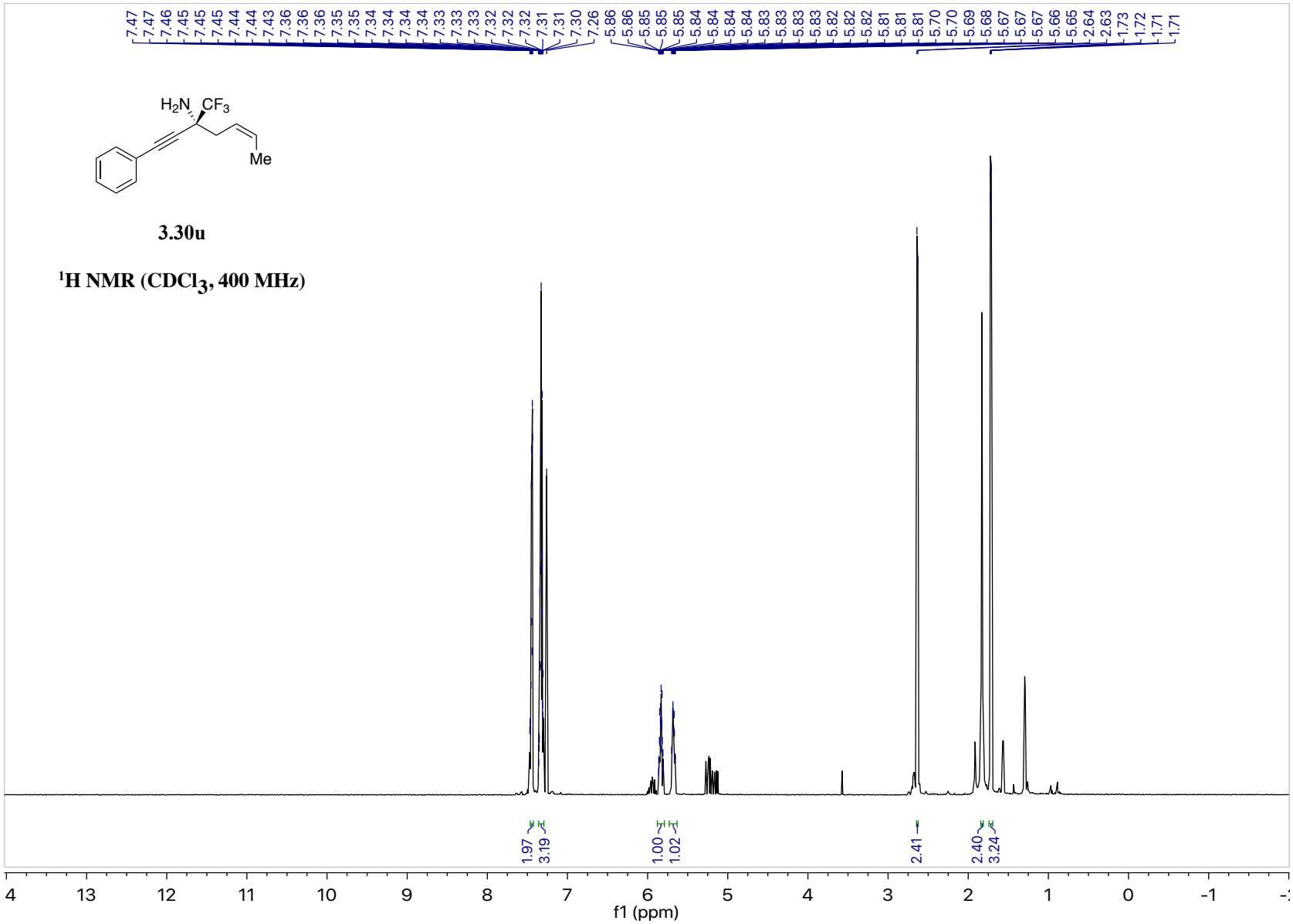
7.47 7.47 7.46 7.45 7.45 7.45 7.44 7.44 7.43 7.36 7.36 7.36 7.35 7.35 7.34 7.34 7.34 7.34 7.33 7.33 7.33 7.32 7.32 7.32 7.31 7.31 7.30 7.26
5.86 5.86 5.85 5.85 5.85 5.84 5.84 5.84 5.84 5.83 5.83 5.83 5.83 5.82 5.82 5.82 5.81 5.81 5.81 5.70 5.70 5.69 5.68 5.67 5.67 5.67 5.66 5.65 2.64 2.63 1.73 1.72 1.71 1.71
H2N CF3
Me
3.30u
1H NMR (CDCl3, 400 MHz)
1.97
3.19
1.00
1.02
2.41
2.40
3.24
4 13 12 11 10 9 8 7 6 5 4 3 2 1 0 -1
f1 (ppm)

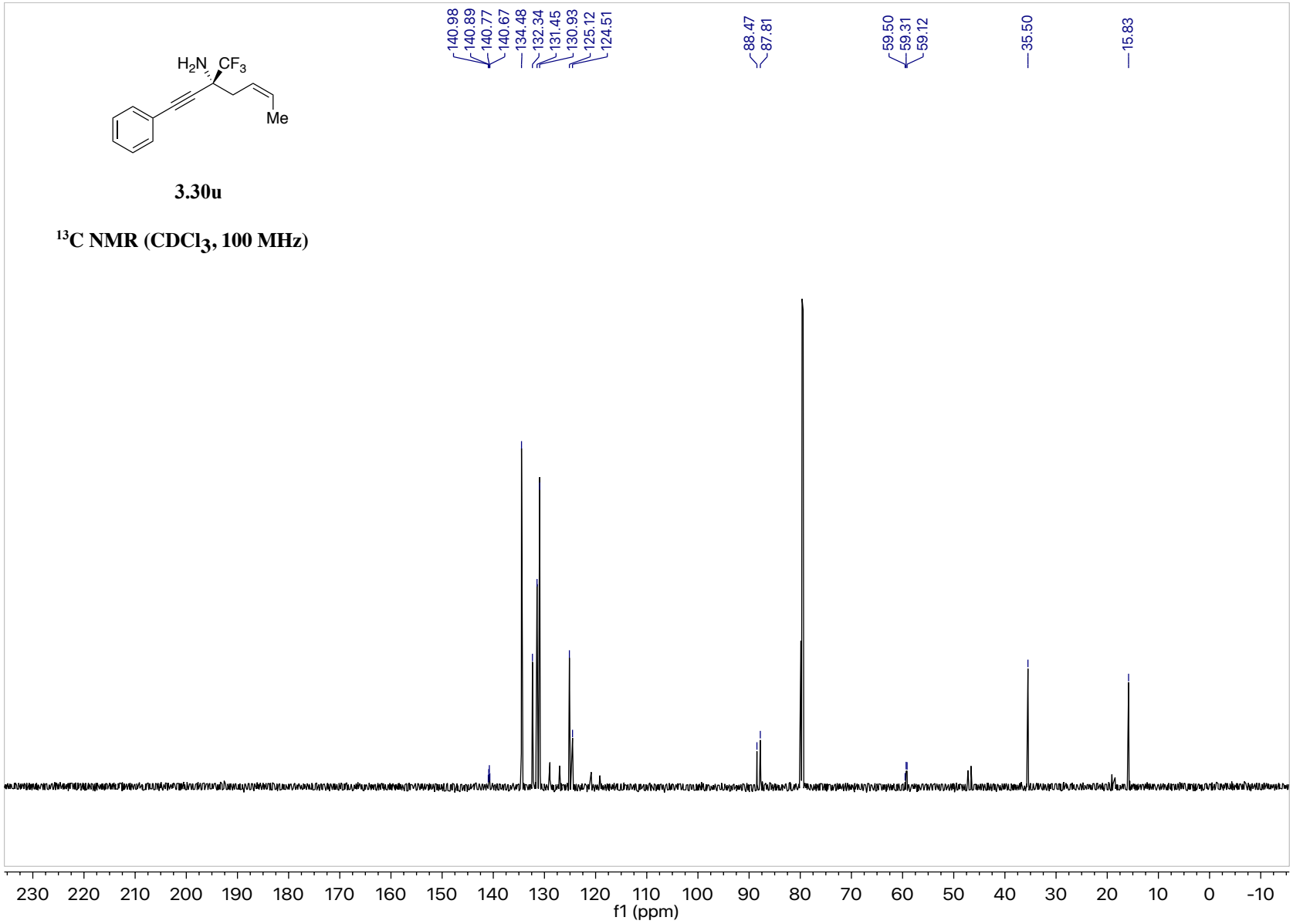

3.30u

^{13}C NMR ($CDCl_3$, 100 MHz)

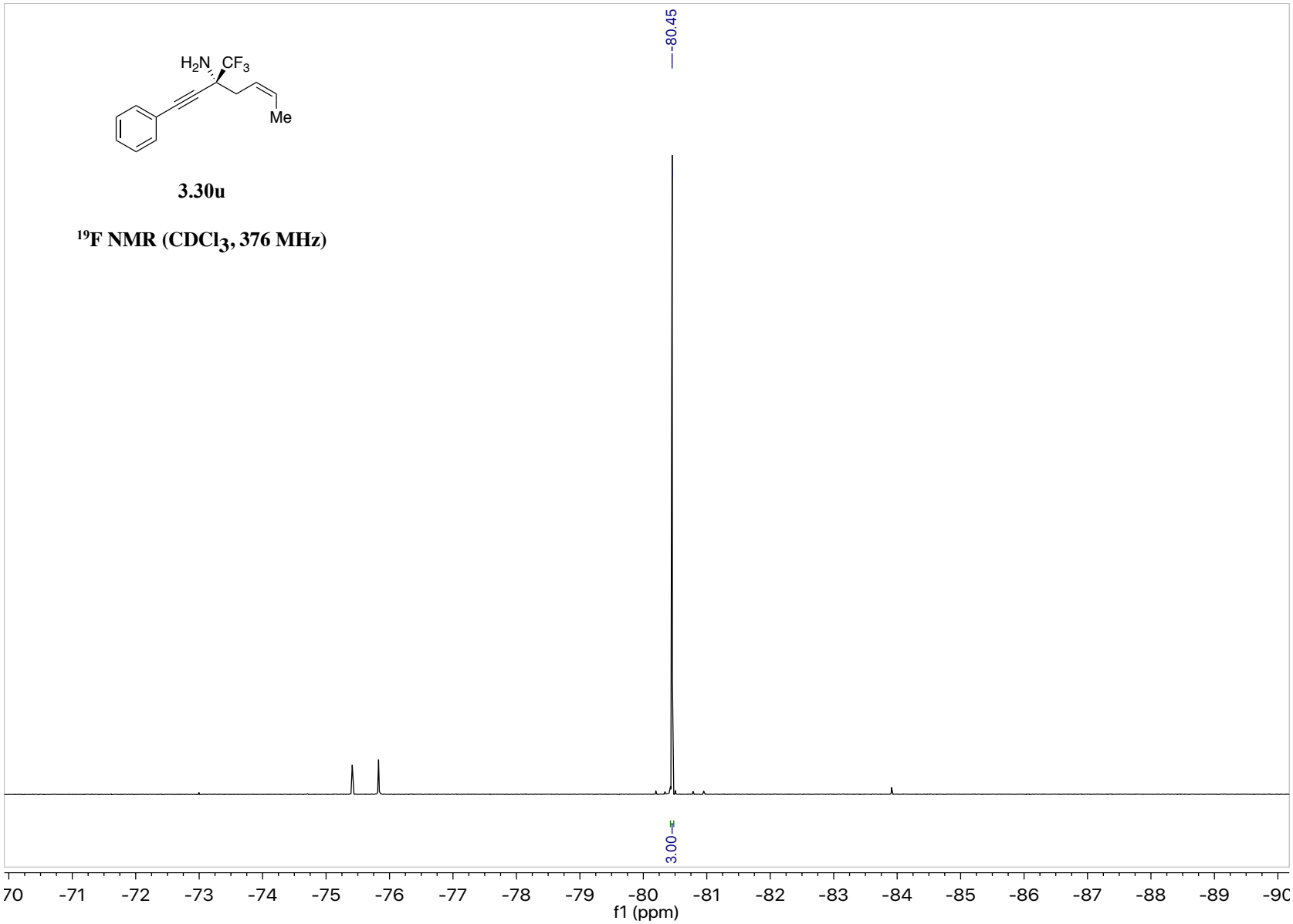

3.30u

^{19}F NMR ($CDCl_3$, 376 MHz)

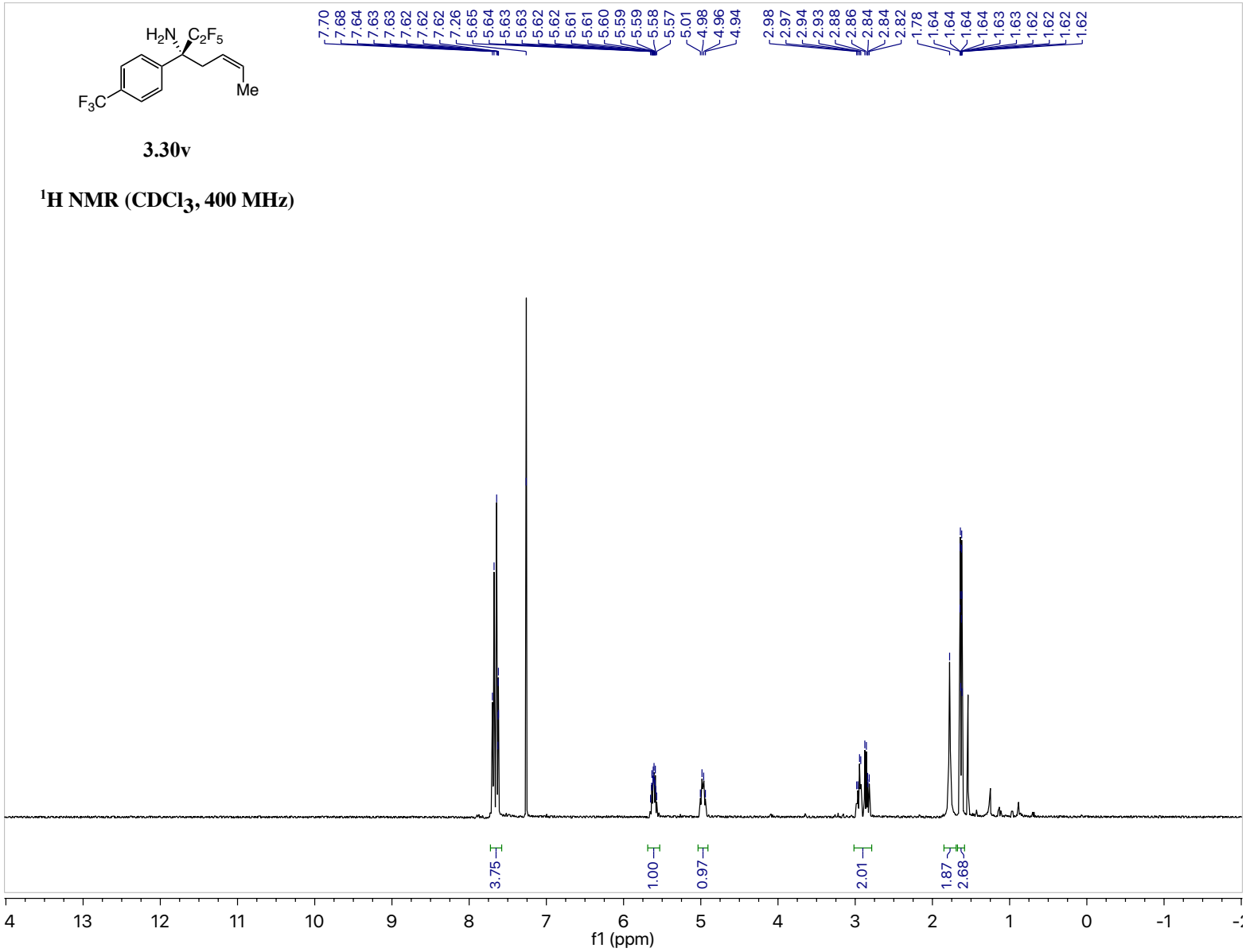

3.30v

^{1}H NMR ($CDCl_3$, 400 MHz)

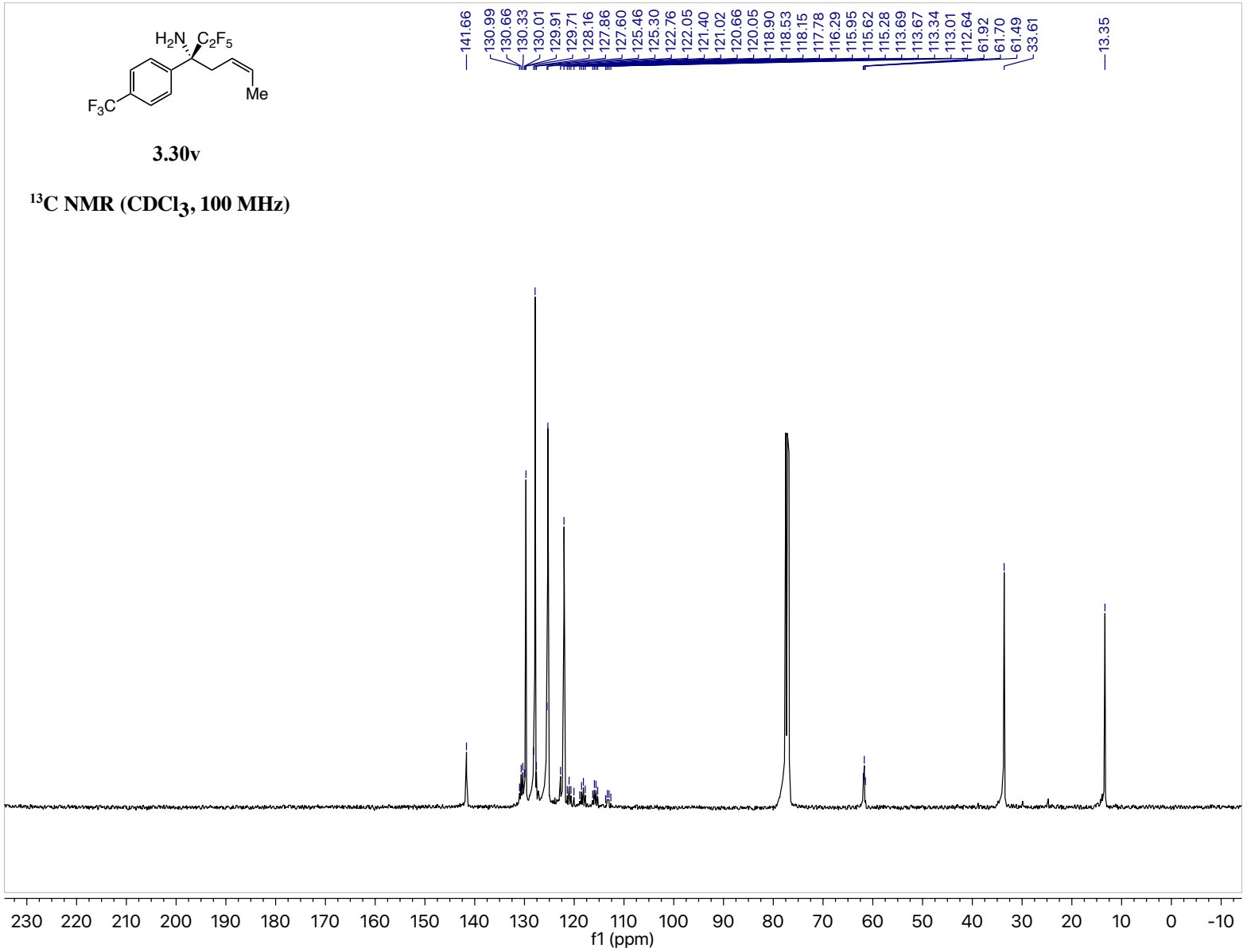

3.30v

^{13}C NMR ($CDCl_3$, 100 MHz)

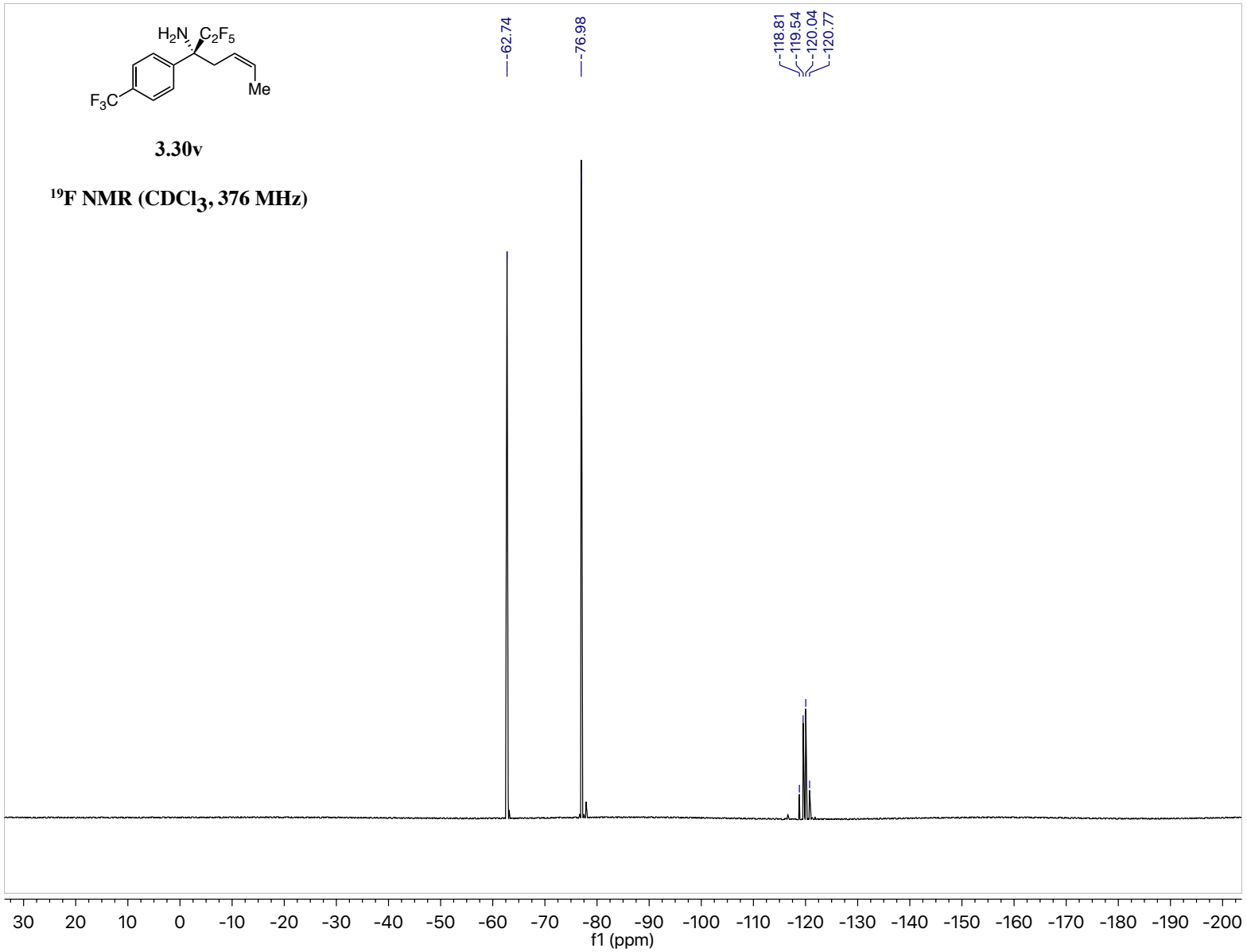

3.30v

^{19}F NMR ($CDCl_3$, 376 MHz)

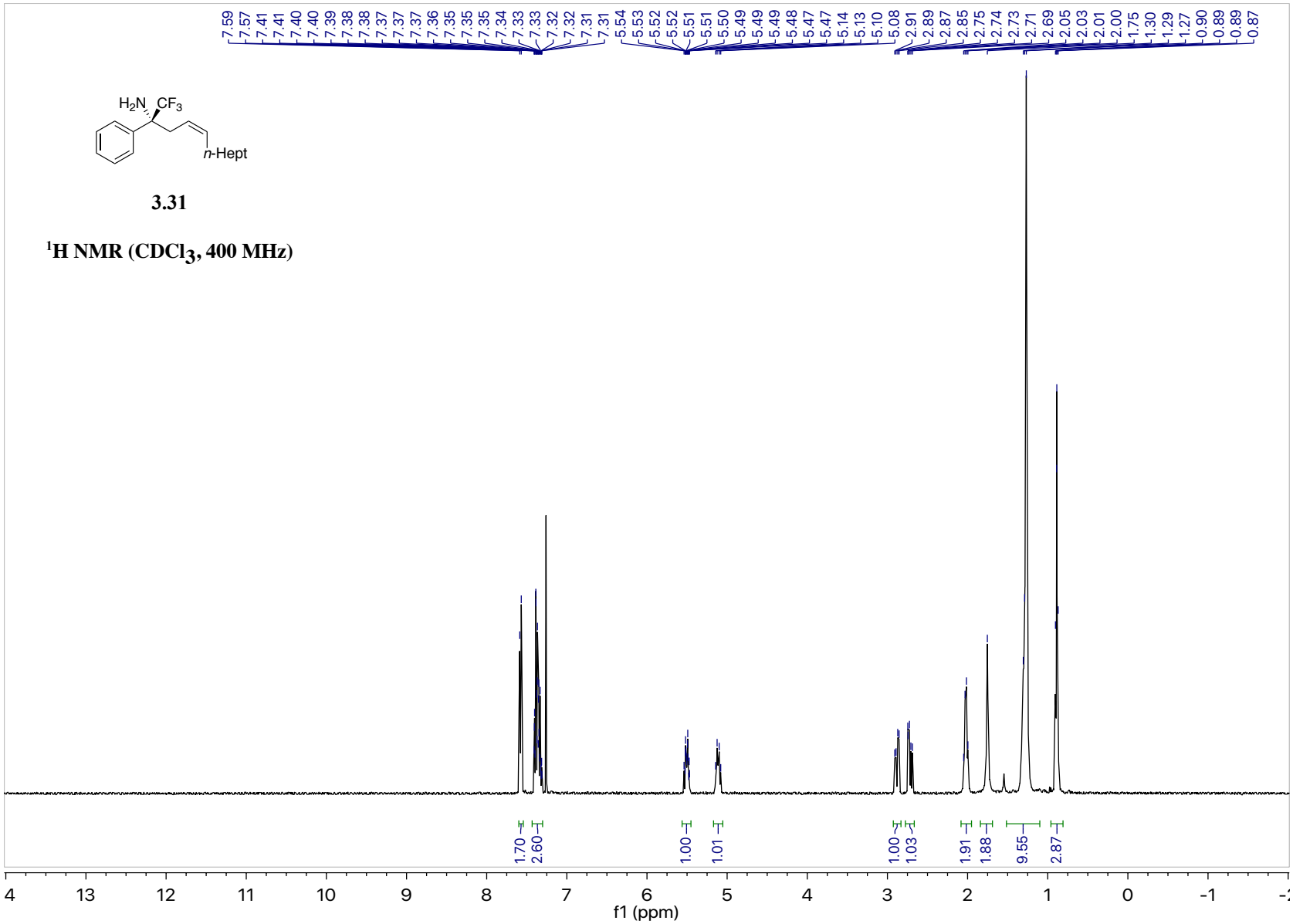

3.31

^{1}H NMR ($CDCl_3$, 400 MHz)

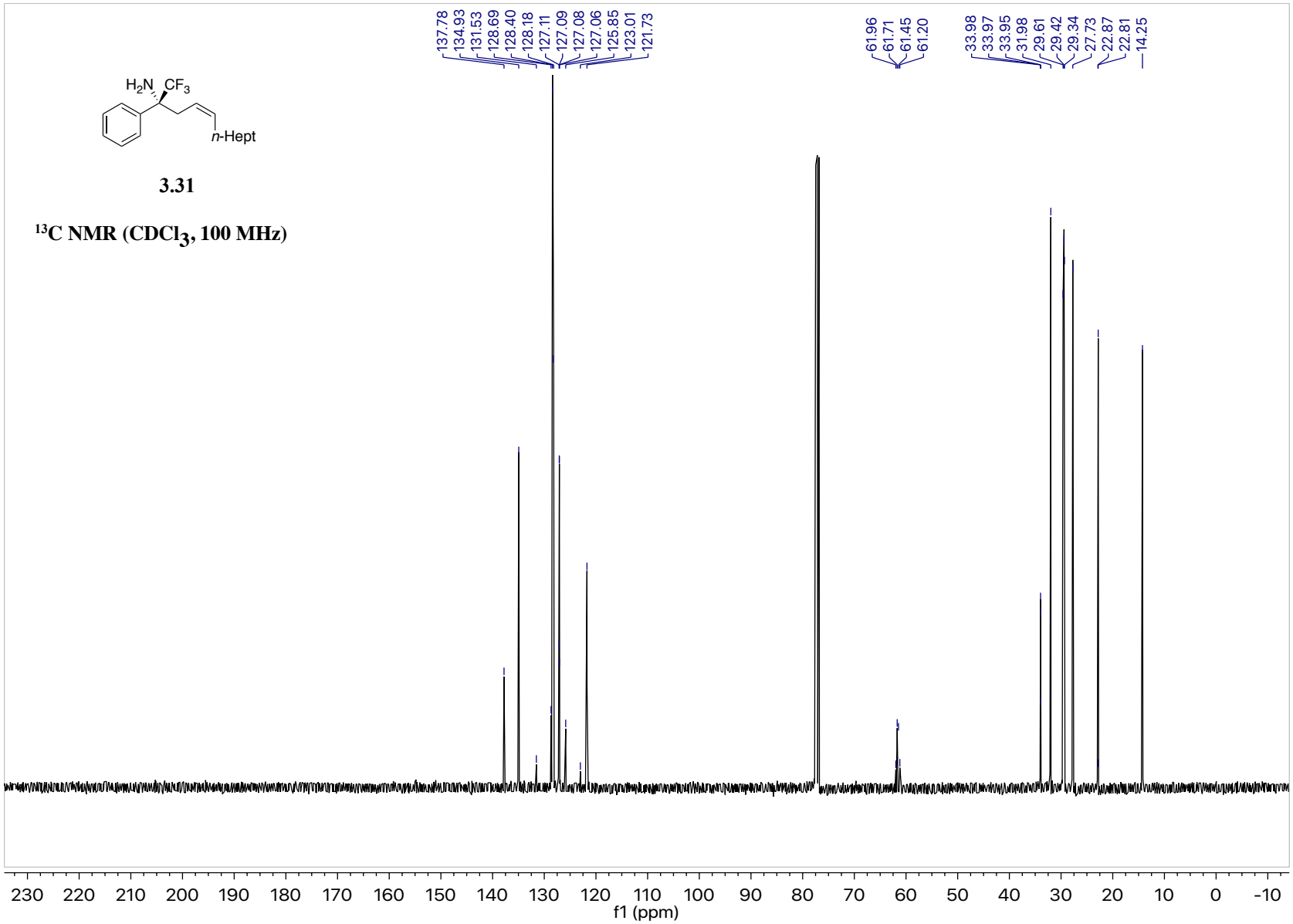

3.31

^{13}C NMR ($CDCl_3$, 100 MHz)

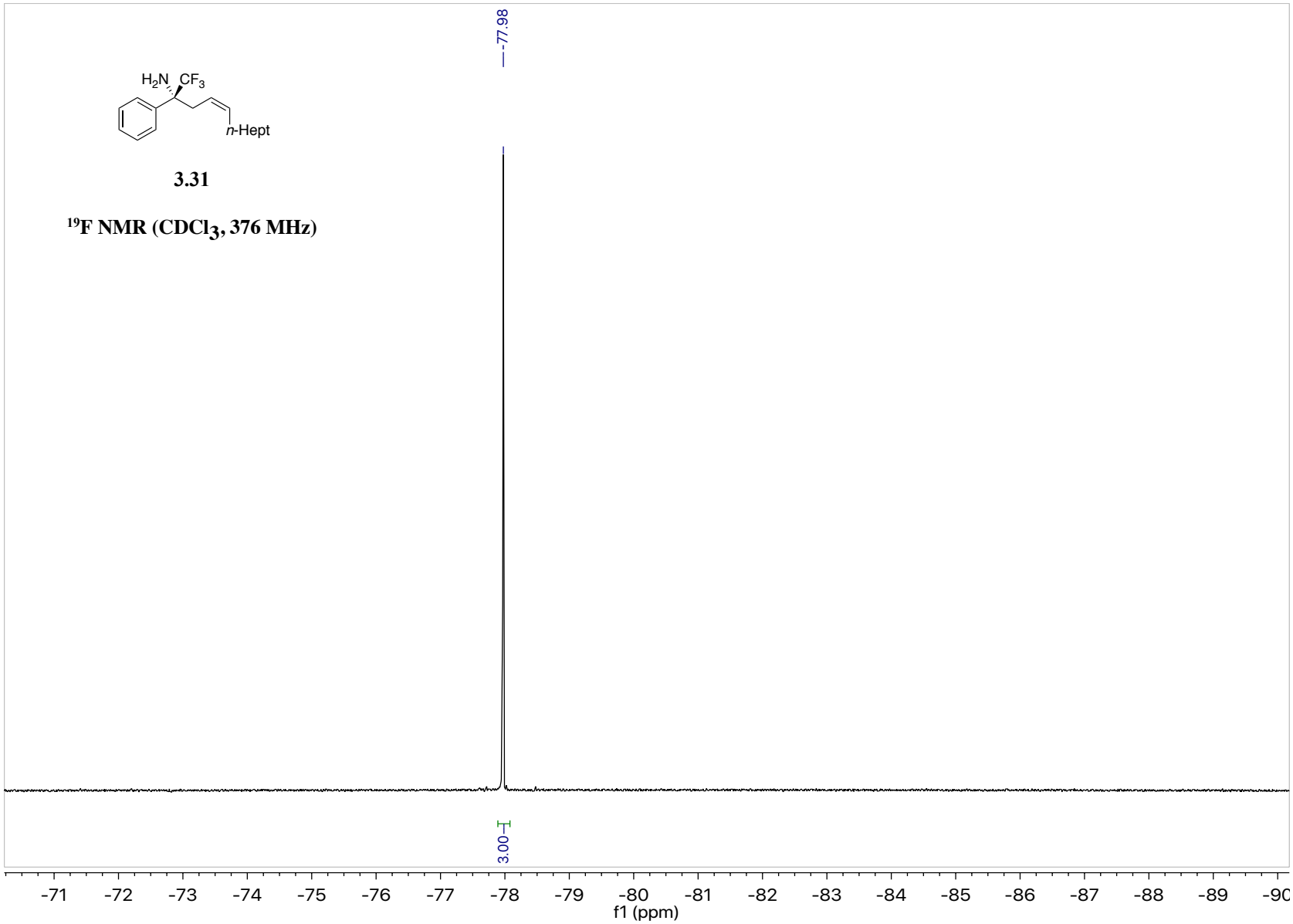

3.31

^{19}F NMR ($CDCl_3$, 376 MHz)

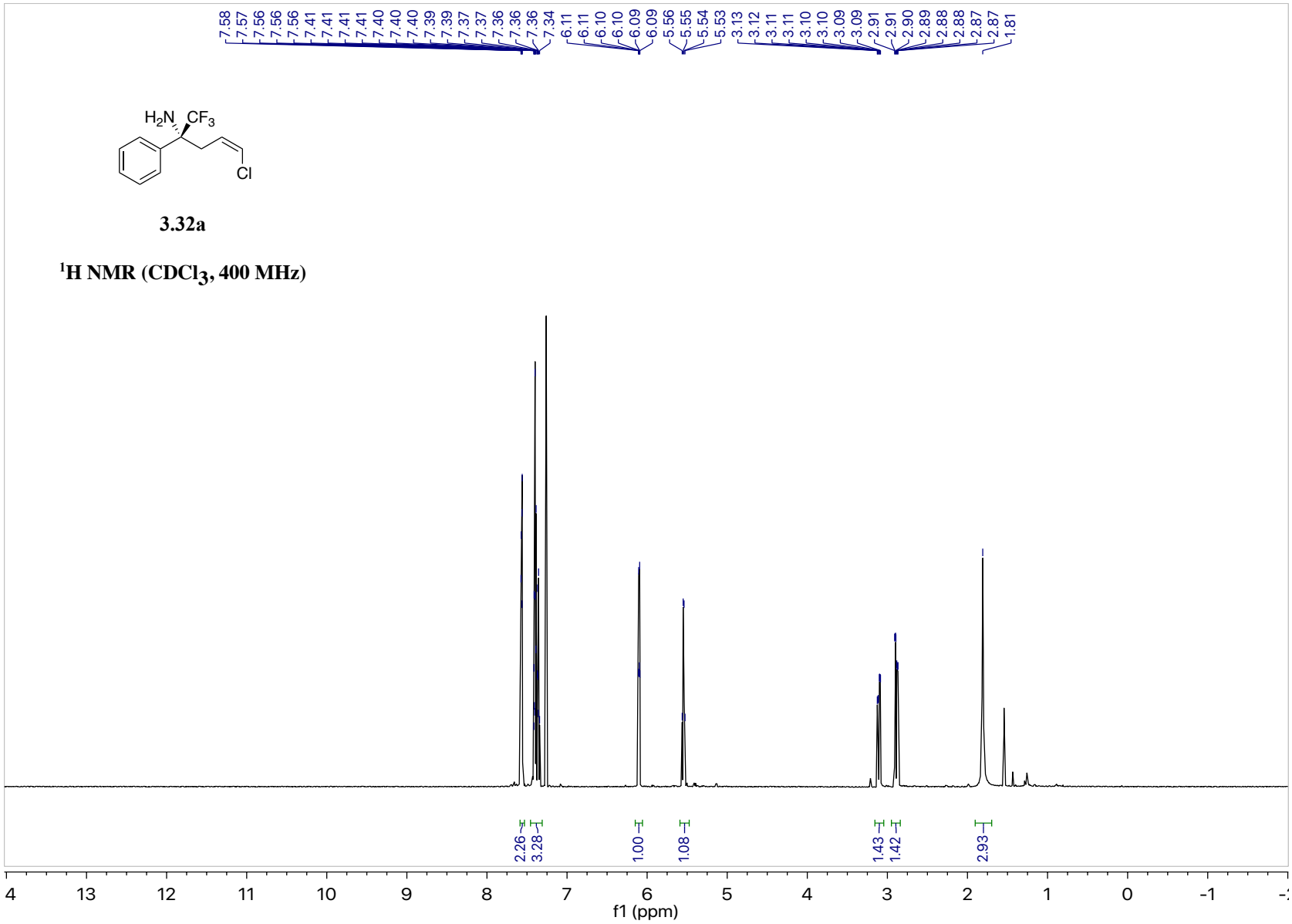

3.32a

^{1}H NMR ($CDCl_3$, 400 MHz)

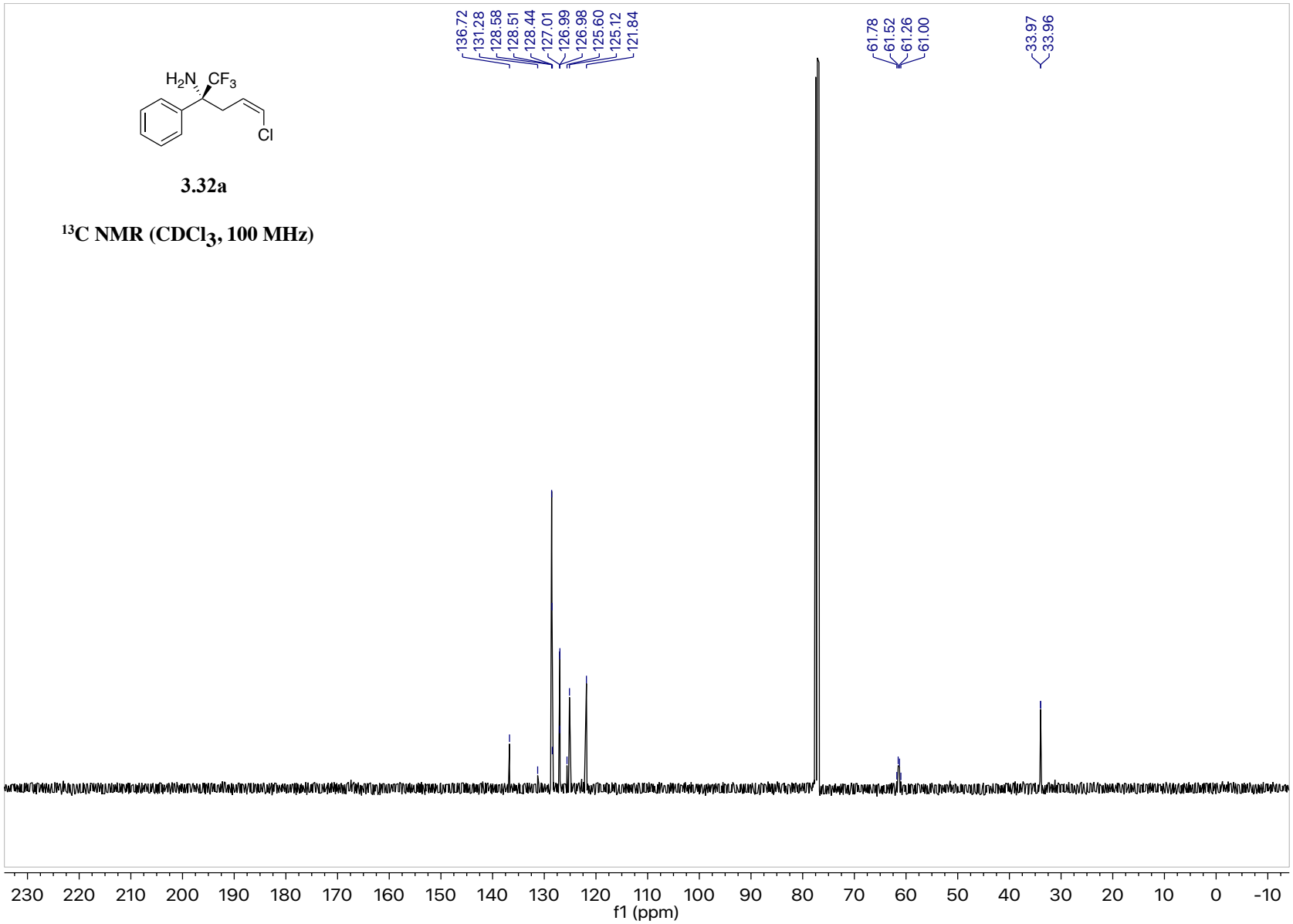

3.32a

^{13}C NMR ($CDCl_3$, 100 MHz)

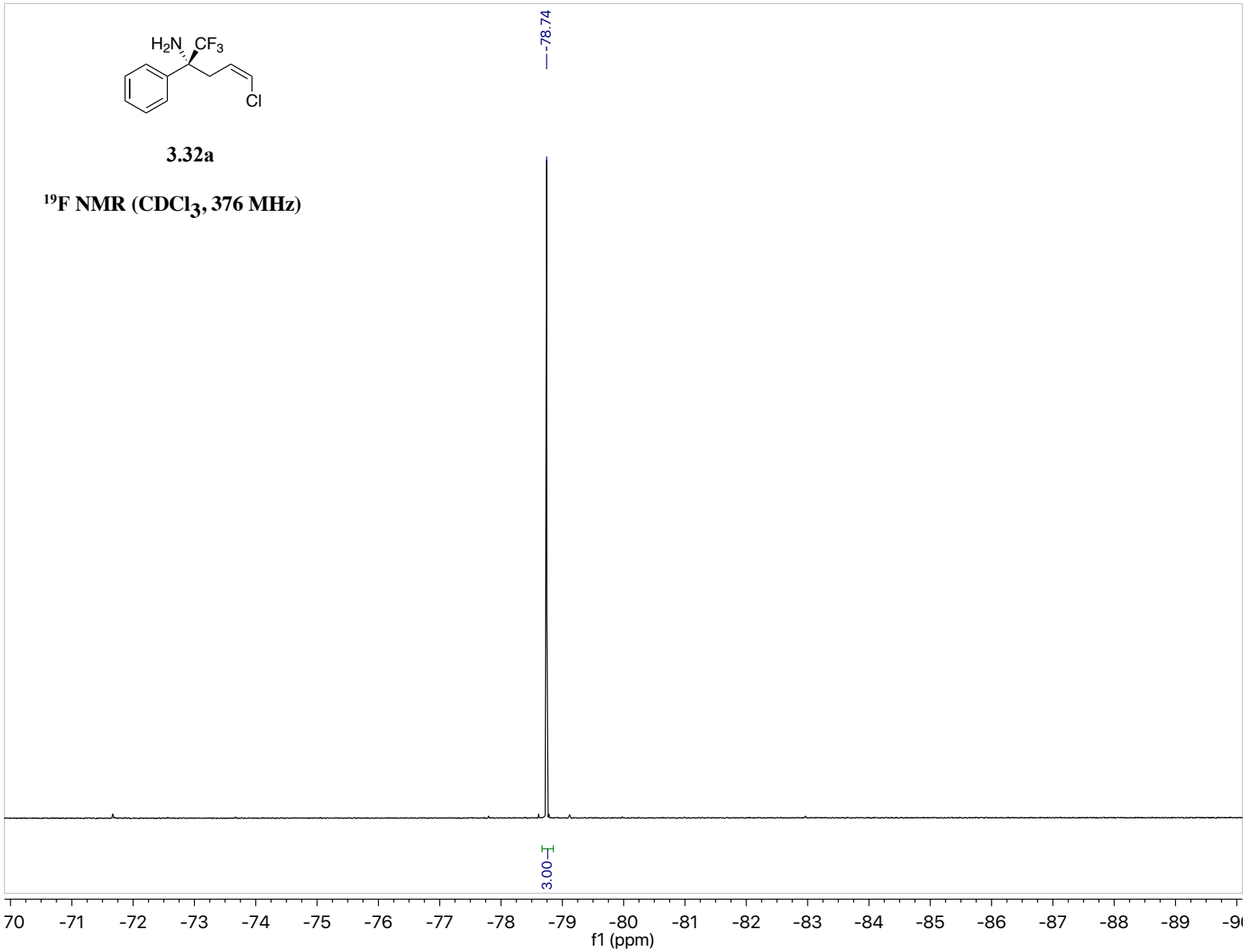
H2N
CF3
Cl
3.32a
19F NMR (CDCl3, 376 MHz)
-78.74
3.00
70
-71
-72
-73
-74
-75
-76
-77
-78
-79
-80
-81
-82
-83
-84
-85
-86
-87
-88
-89
f1 (ppm)

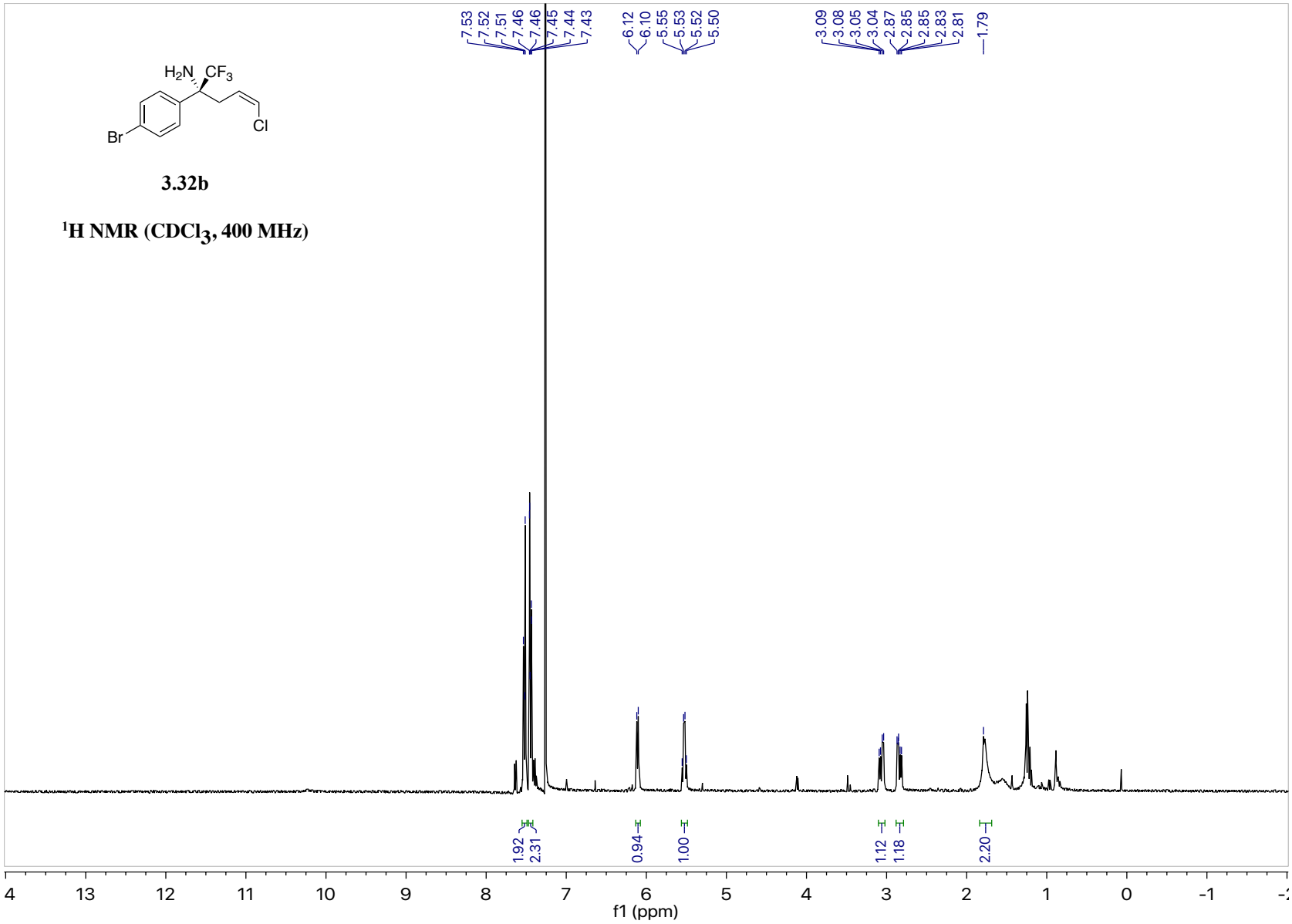

3.32b

^{1}H NMR ($CDCl_3$, 400 MHz)

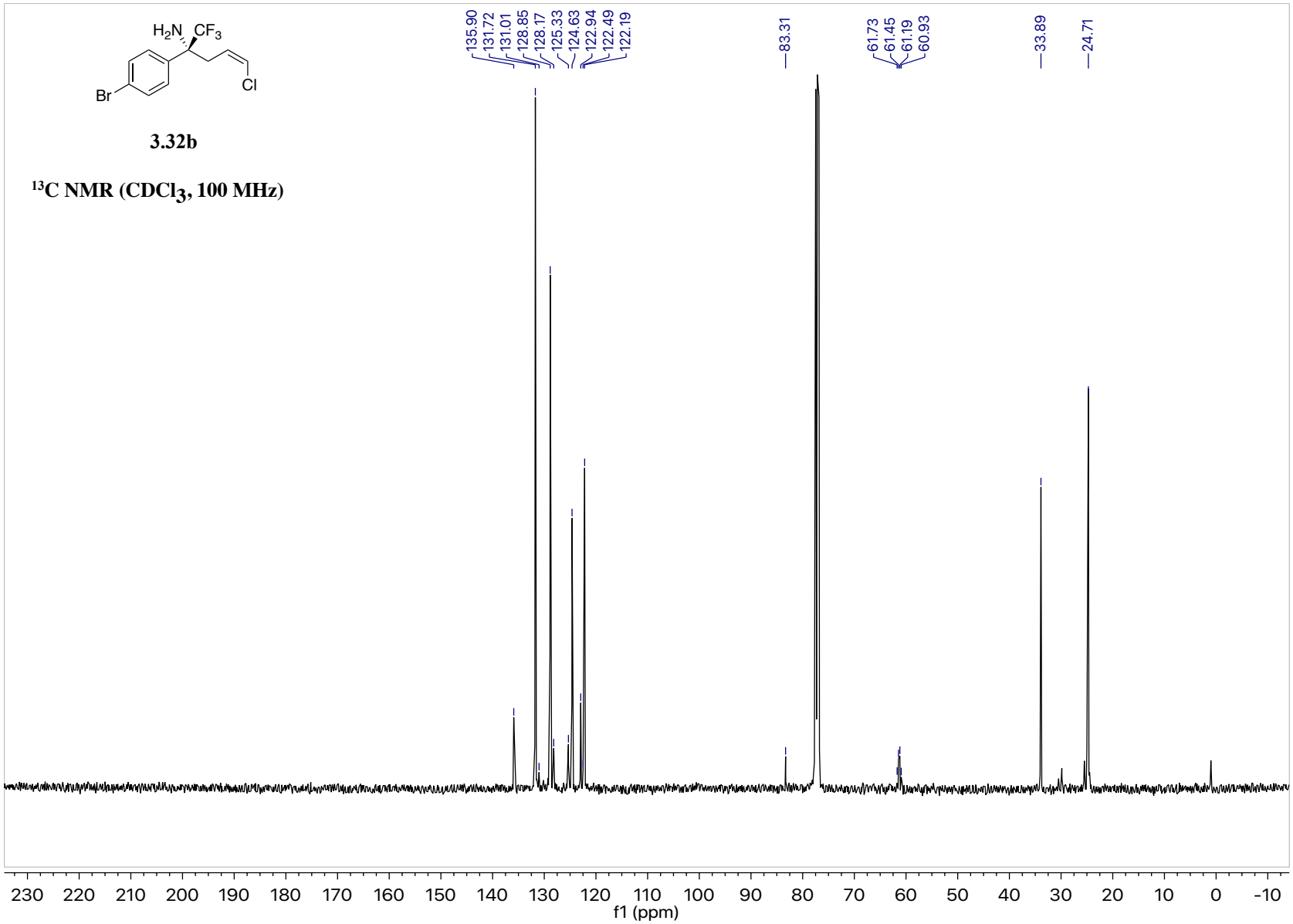

3.32b

^{13}C NMR ($CDCl_3$, 100 MHz)

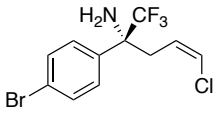

3.32b

^{19}F NMR ($CDCl_3$, 376 MHz)

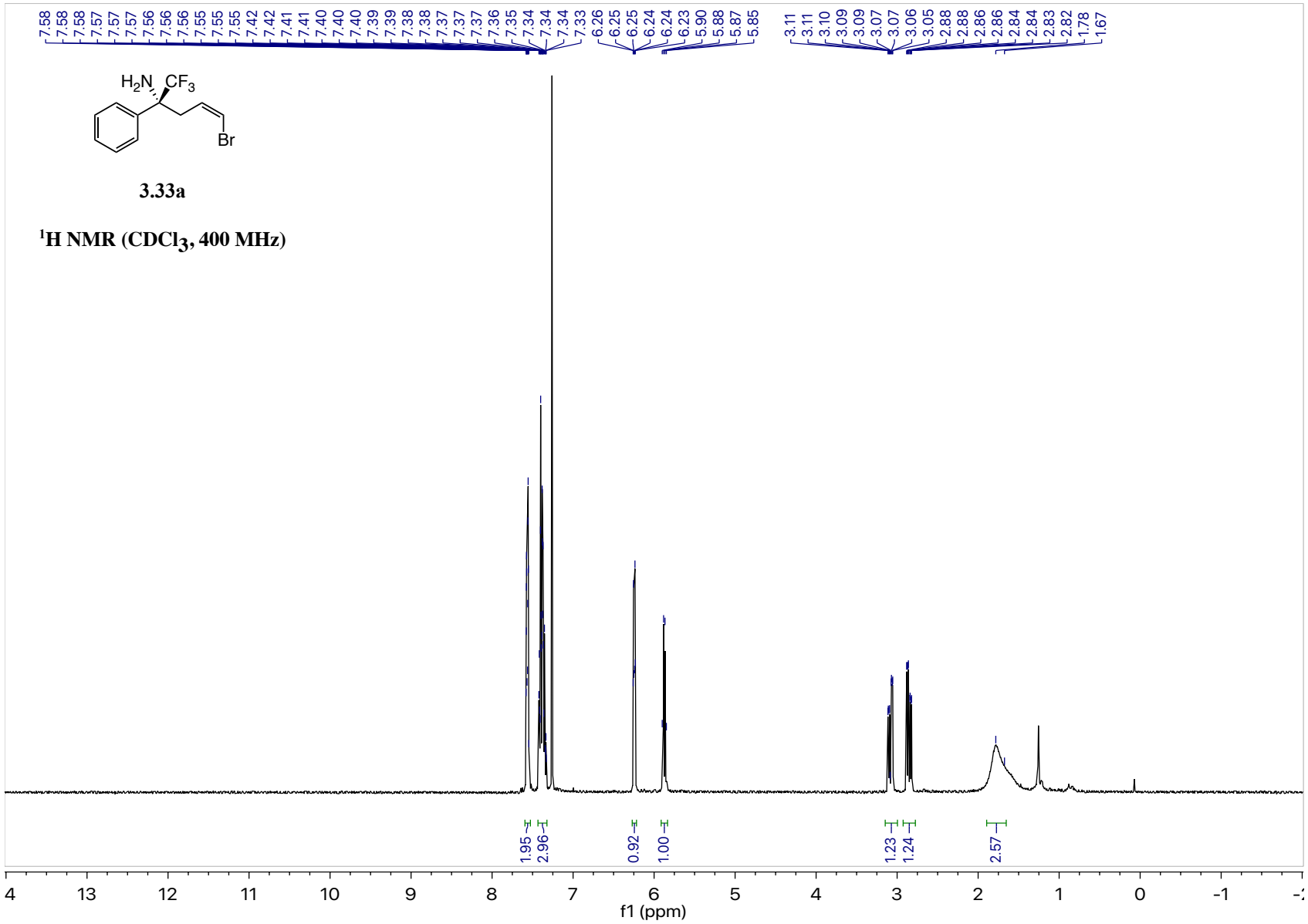

3.33a

^{1}H NMR ($CDCl_3$, 400 MHz)

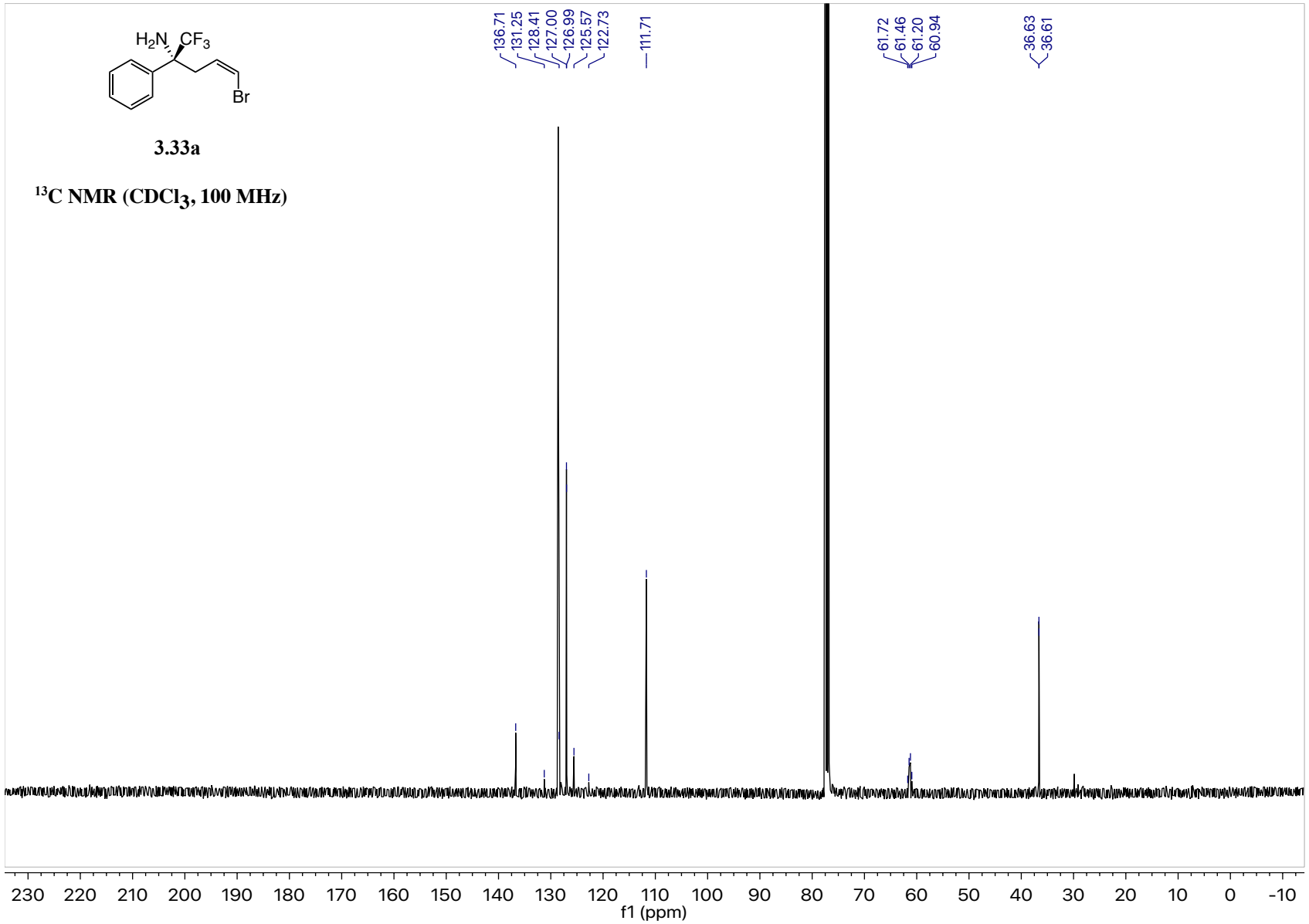
H2N
CF3
Br
3.33a
13C NMR (CDCl3, 100 MHz)
136.71
131.25
128.41
127.00
126.99
125.57
122.73
111.71
61.72
61.46
61.20
60.94
36.63
36.61
230 220 210 200 190 180 170 160 150 140 130 120 110 100 90 80 70 60 50 40 30 20 10 0 -10
f1 (ppm)

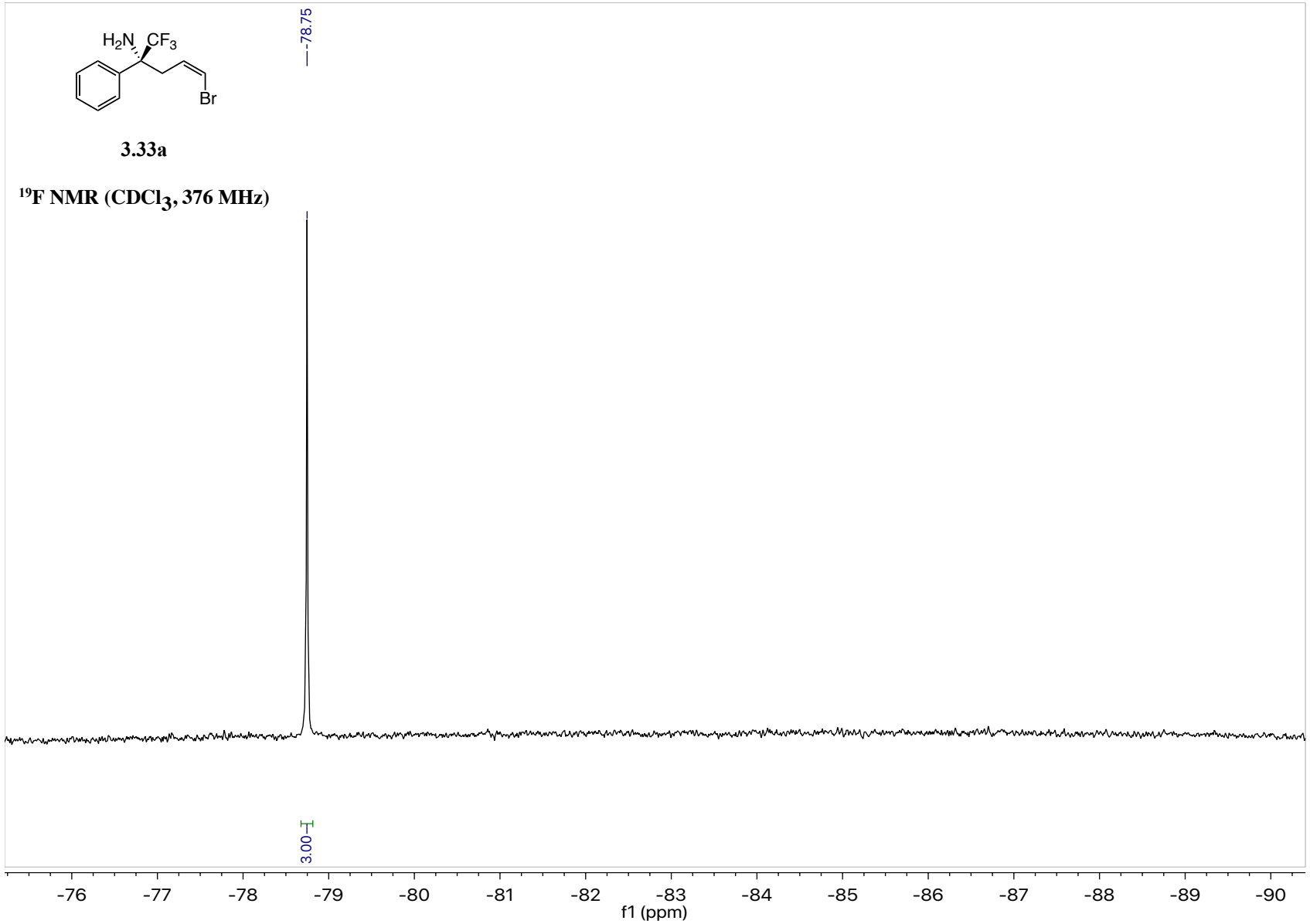

3.33a

^{19}F NMR ($CDCl_3$, 376 MHz)

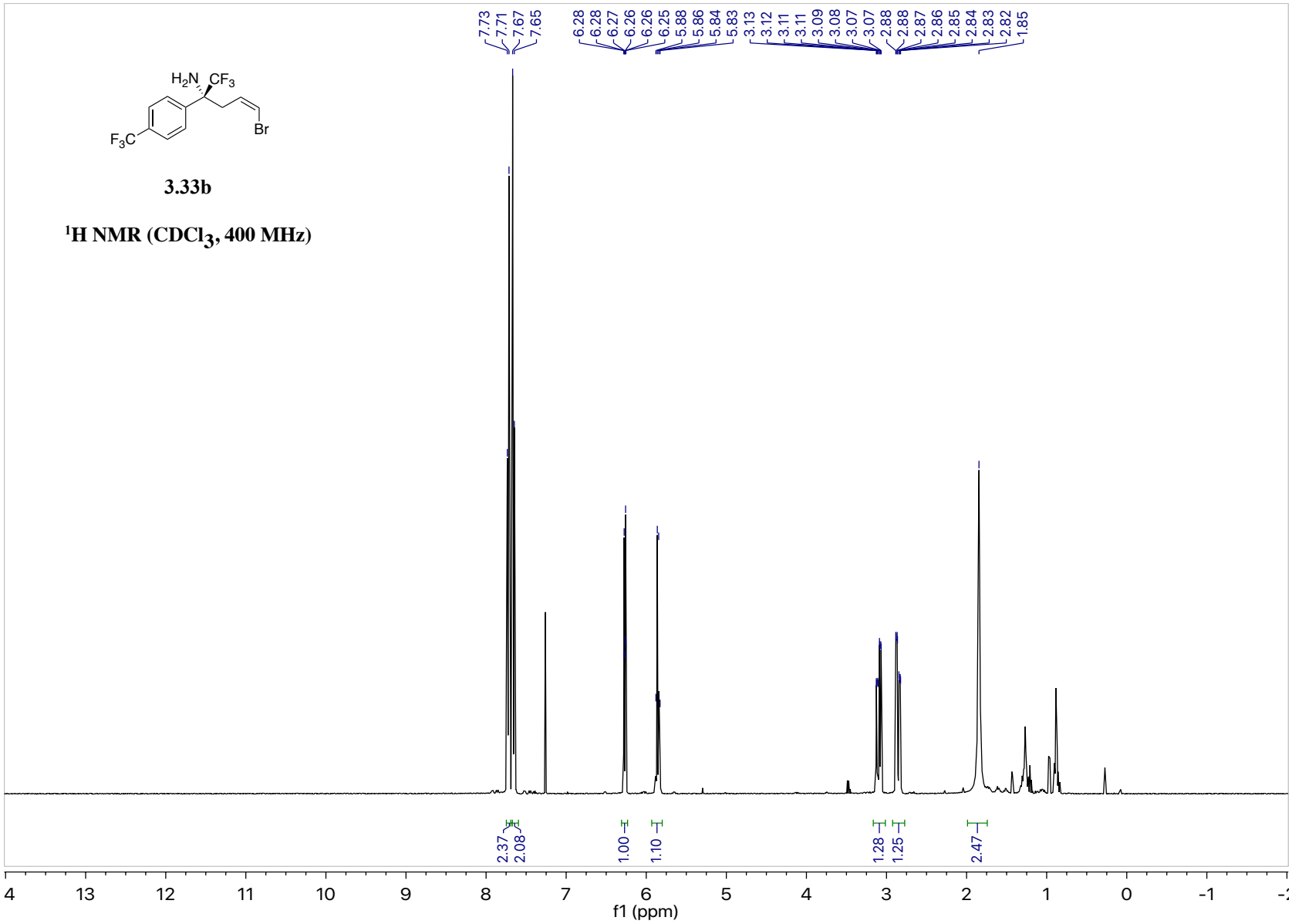
H2N CF3
F3C
Br
3.33b
1H NMR (CDCl3, 400 MHz)
7.73
7.71
7.67
7.65
6.28
6.28
6.27
6.26
6.26
6.25
5.88
5.86
5.84
5.83
3.13
3.12
3.11
3.11
3.09
3.08
3.07
3.07
2.88
2.88
2.87
2.86
2.85
2.84
2.83
2.82
1.85
2.37
2.08
1.00
1.10
1.28
1.25
2.47
f1 (ppm)

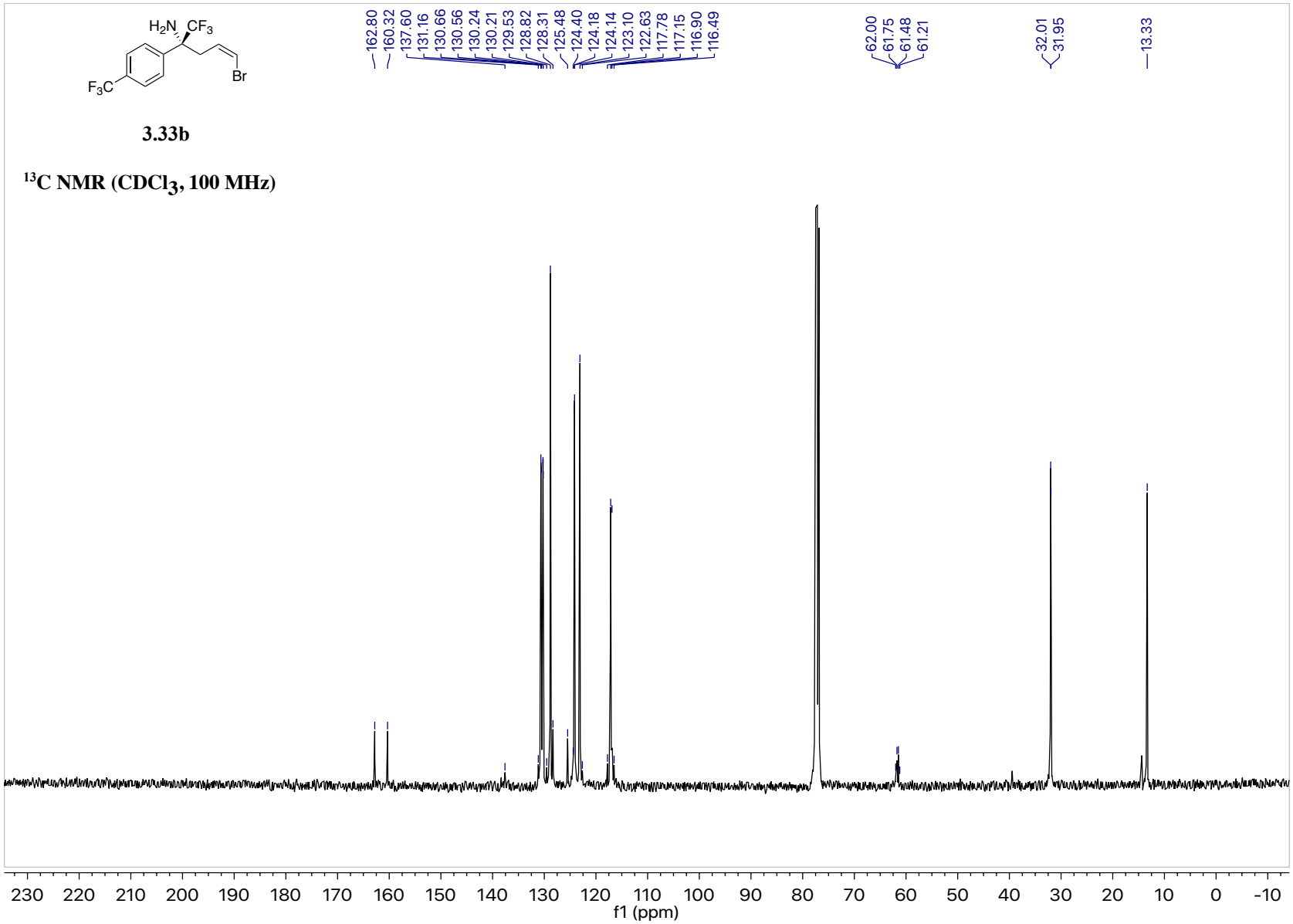

3.33b

^{13}C NMR ($CDCl_3$, 100 MHz)

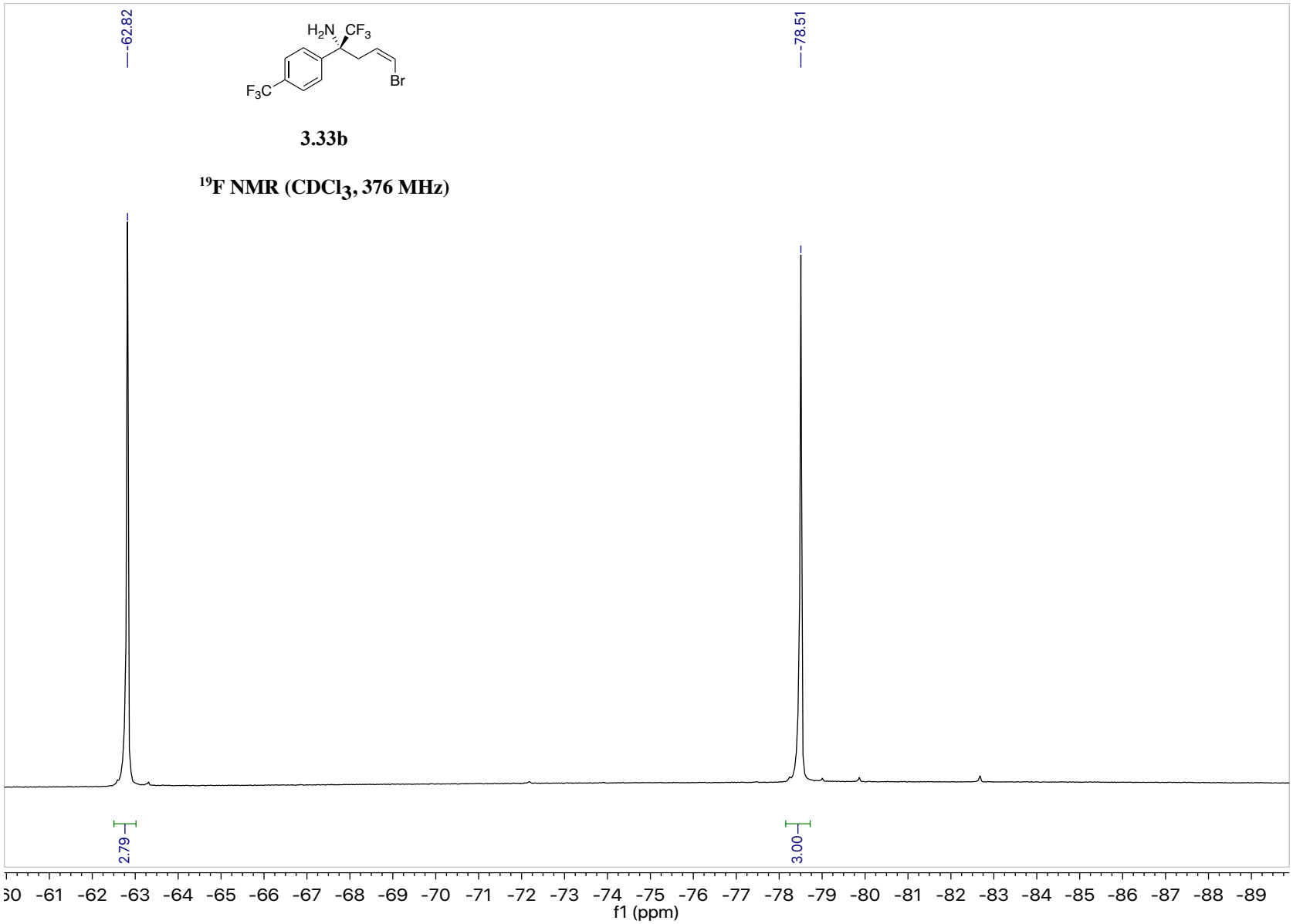

3.33b

^{19}F NMR ($CDCl_3$, 376 MHz)

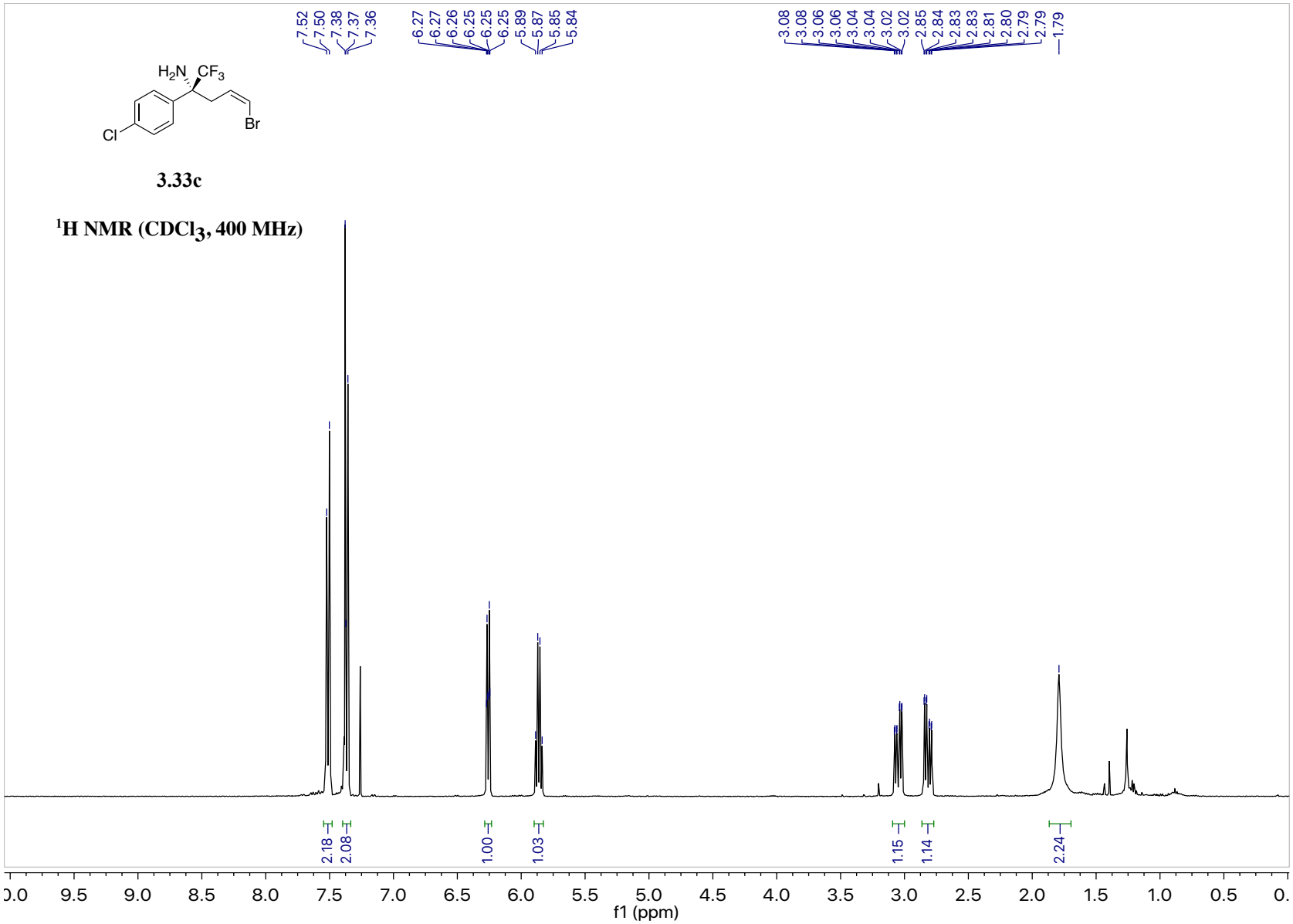

3.33c

^{1}H NMR ($CDCl_3$, 400 MHz)

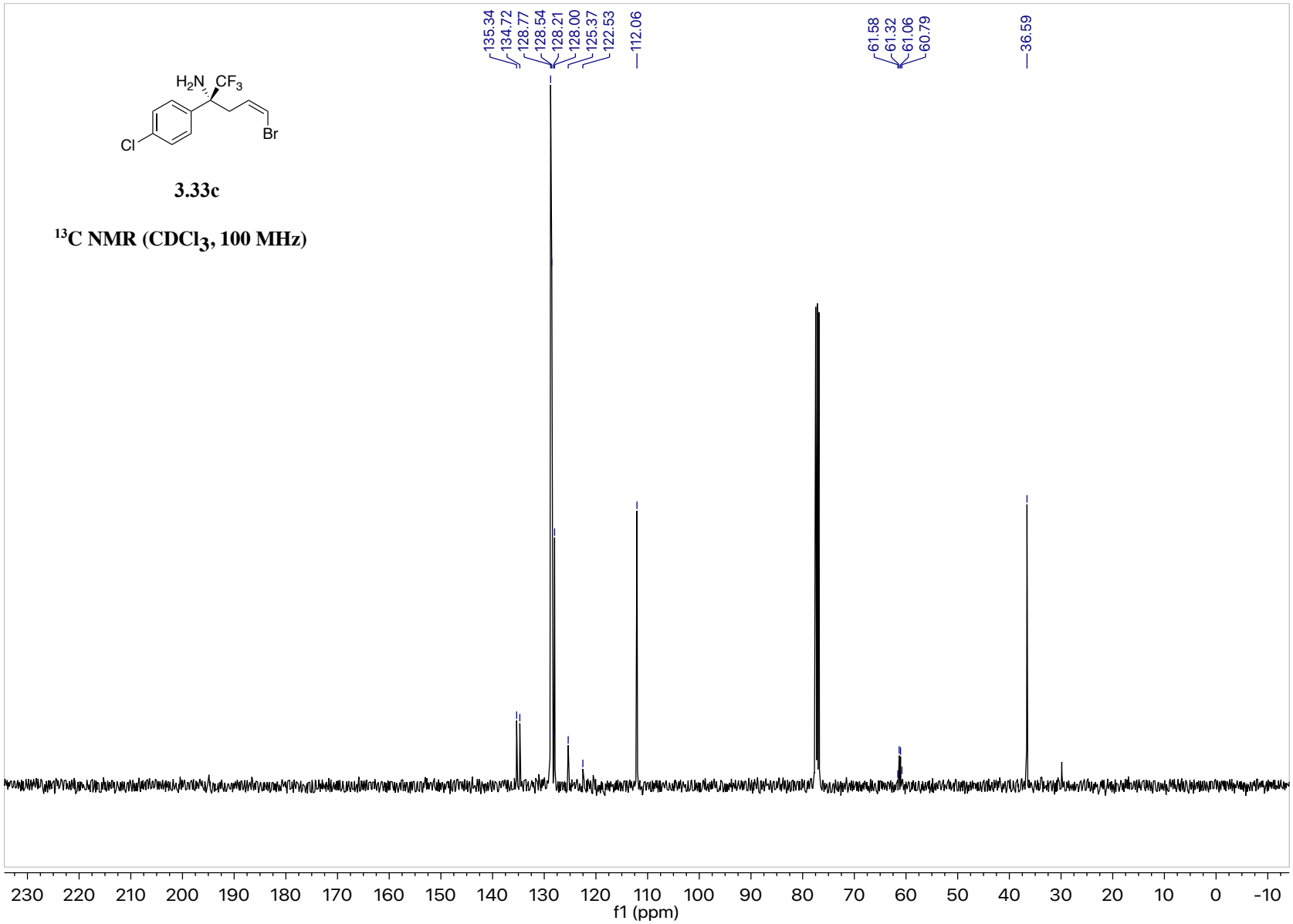
135.34
134.72
128.77
128.54
128.21
128.00
125.37
122.53
112.06
61.58
61.32
61.06
60.79
36.59
H2N CF3
Cl
Br
3.33c
13C NMR (CDCl3, 100 MHz)
230 220 210 200 190 180 170 160 150 140 130 120 110 100 90 80 70 60 50 40 30 20 10 0 -10
f1 (ppm)

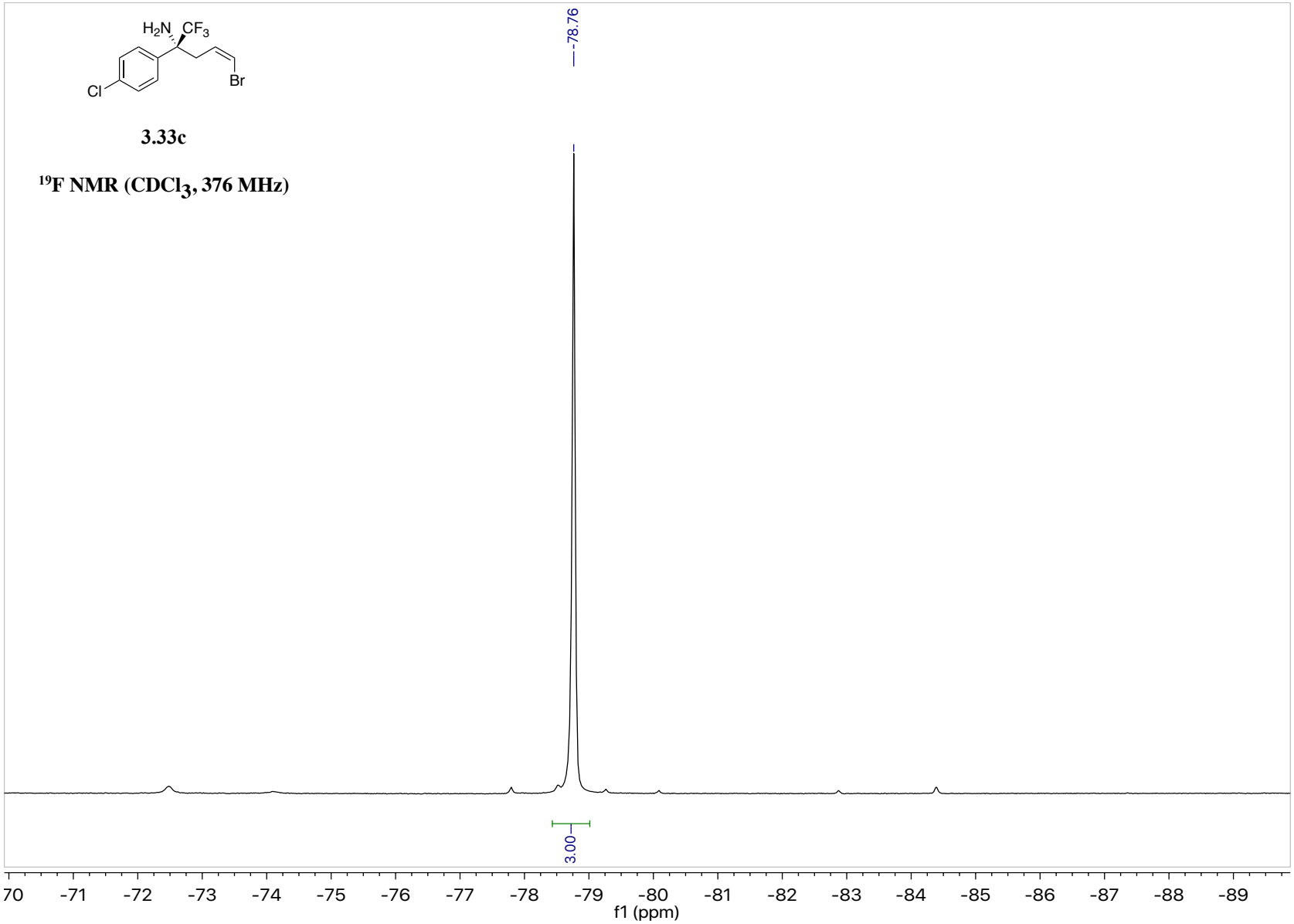
H2N
CF3
Cl
Br
3.33c
19F NMR (CDCl3, 376 MHz)
-78.76
3.00
70
-71
-72
-73
-74
-75
-76
-77
-78
-79
-80
-81
-82
-83
-84
-85
-86
-87
-88
-89
f1 (ppm)

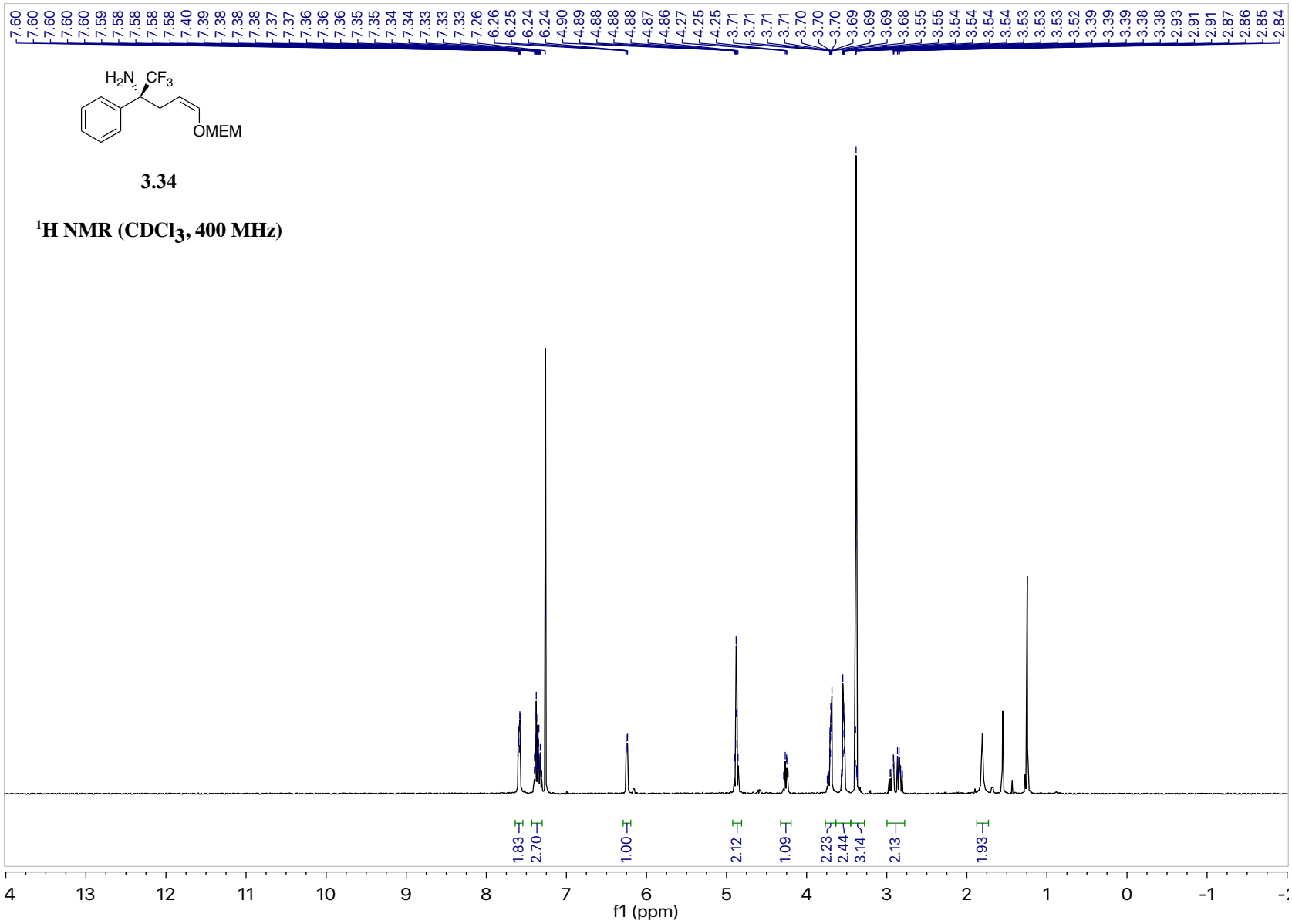

3.34

^{1}H NMR ($CDCl_3$, 400 MHz)

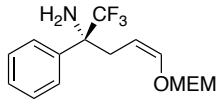

3.34

^{13}C NMR ($CDCl_3$, 100 MHz)

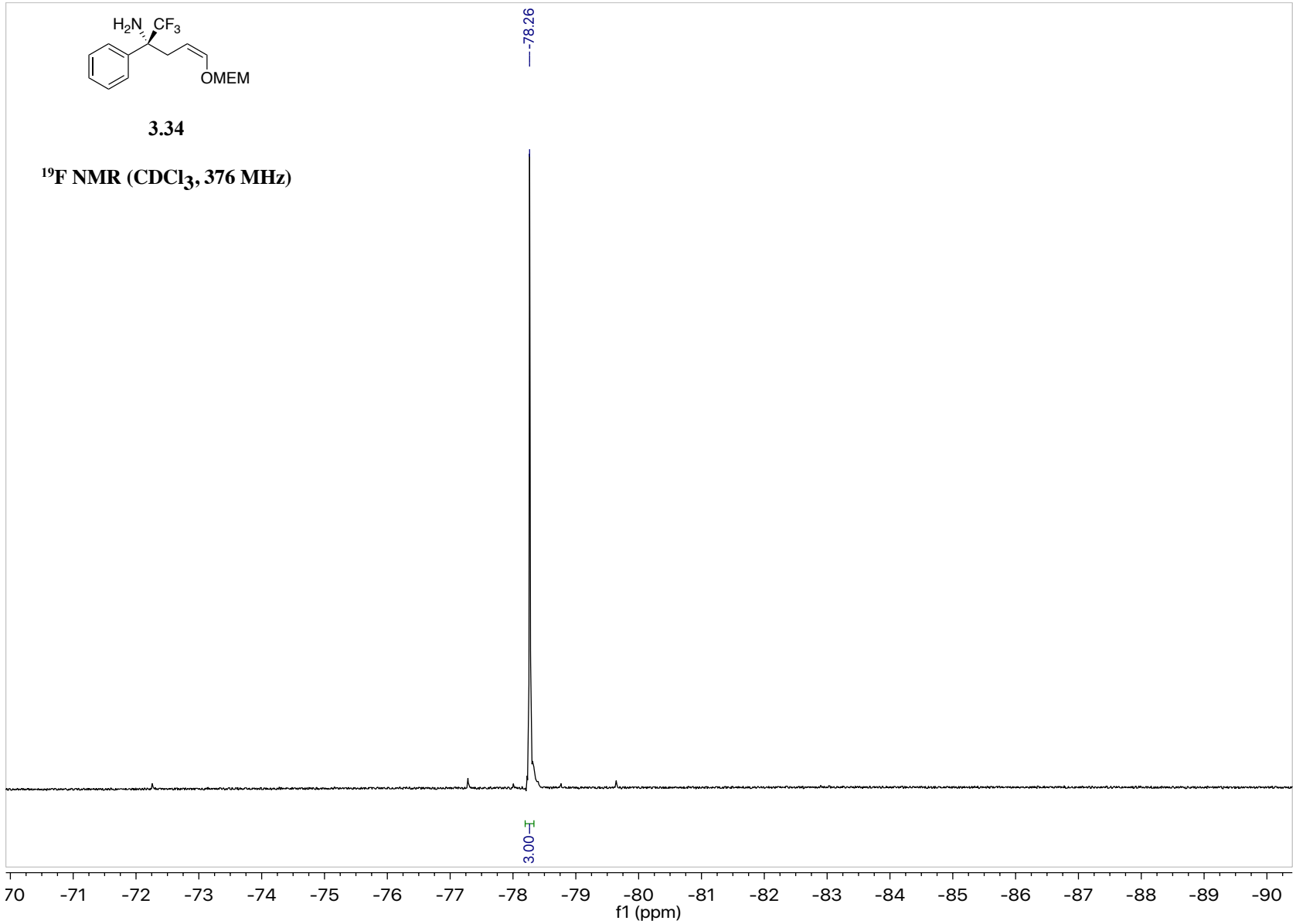

3.34

^{19}F NMR ($CDCl_3$, 376 MHz)

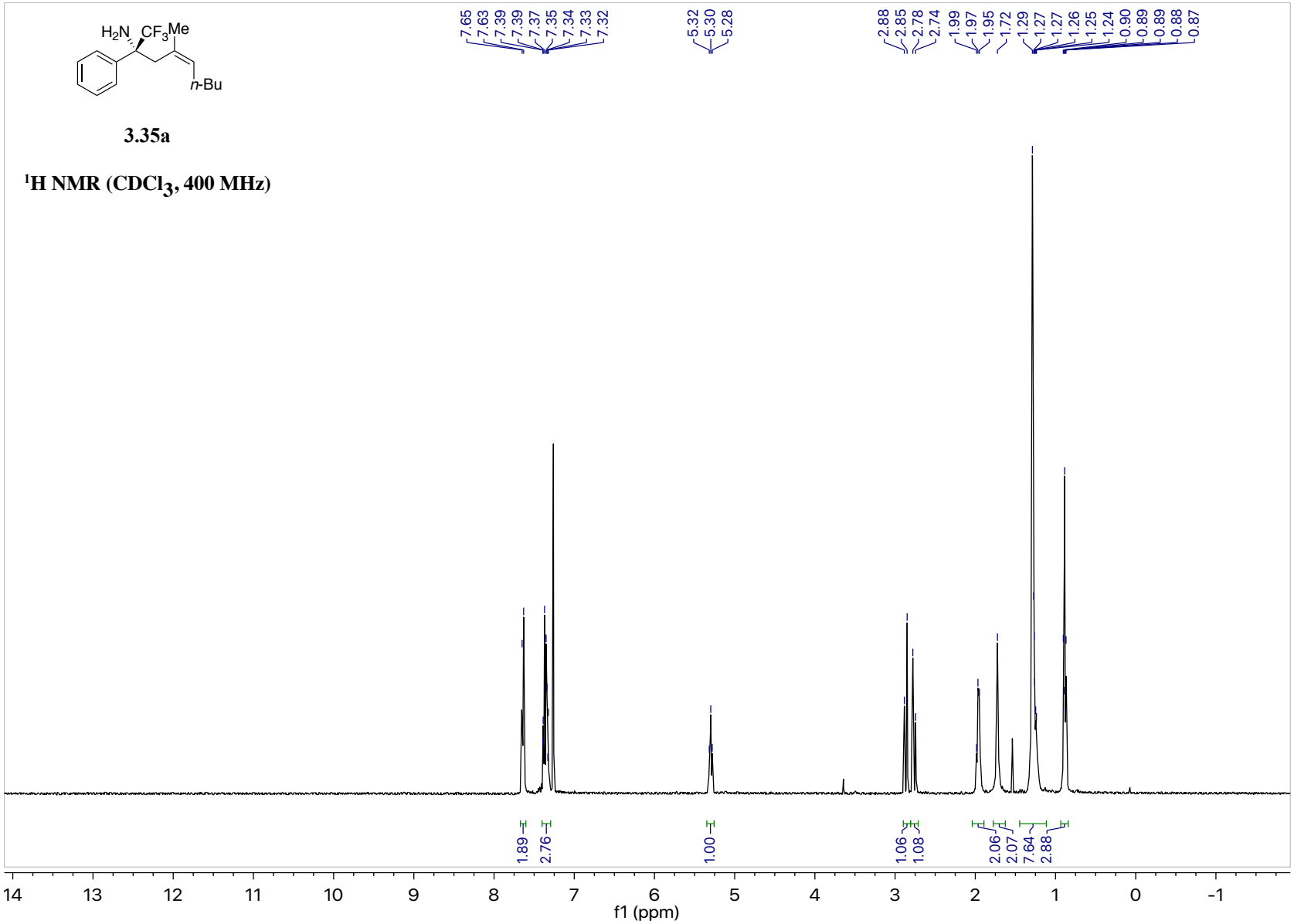

3.35a

^{1}H NMR ($CDCl_3$, 400 MHz)

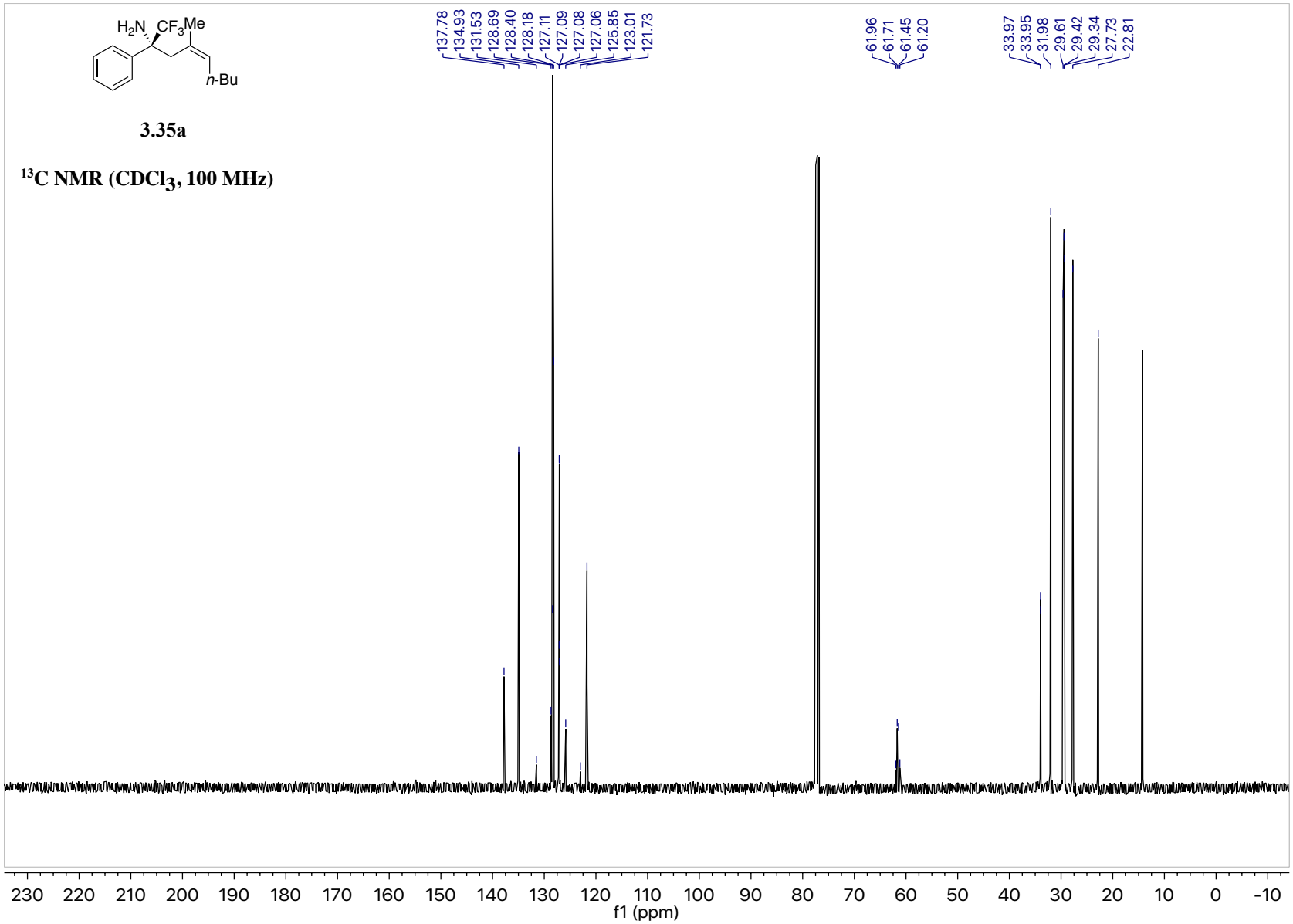

3.35a

^{13}C NMR ($CDCl_3$, 100 MHz)

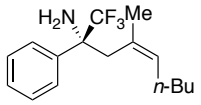

3.35a

^{19}F NMR ($CDCl_3$, 376 MHz)

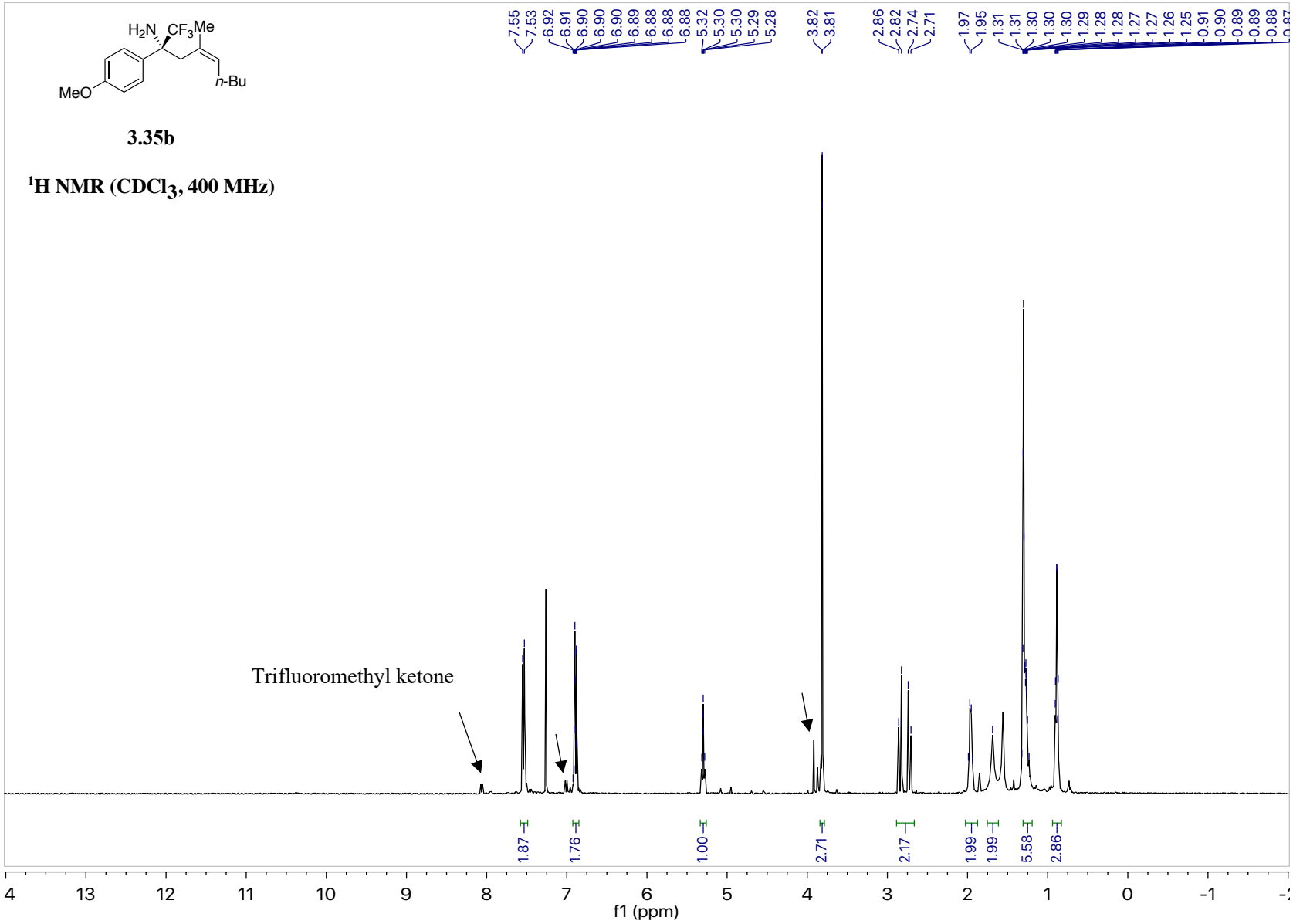
H2N
CF3Me
MeO
n-Bu
3.35b
1H NMR (CDCl3, 400 MHz)
7.55
7.53
6.92
6.91
6.90
6.90
6.90
6.89
6.88
6.88
6.88
5.32
5.30
5.30
5.29
5.28
3.82
3.81
2.86
2.82
2.74
2.71
1.97
1.95
1.31
1.31
1.30
1.30
1.30
1.29
1.28
1.28
1.27
1.27
1.26
1.25
0.91
0.90
0.89
0.89
0.88
Trifluoromethyl ketone
1.87
1.76
1.00
2.71
2.17
1.99
1.99
5.58
2.86
4
13
12
11
10
9
8
7
6
5
4
3
2
1
0
-1
f1 (ppm)

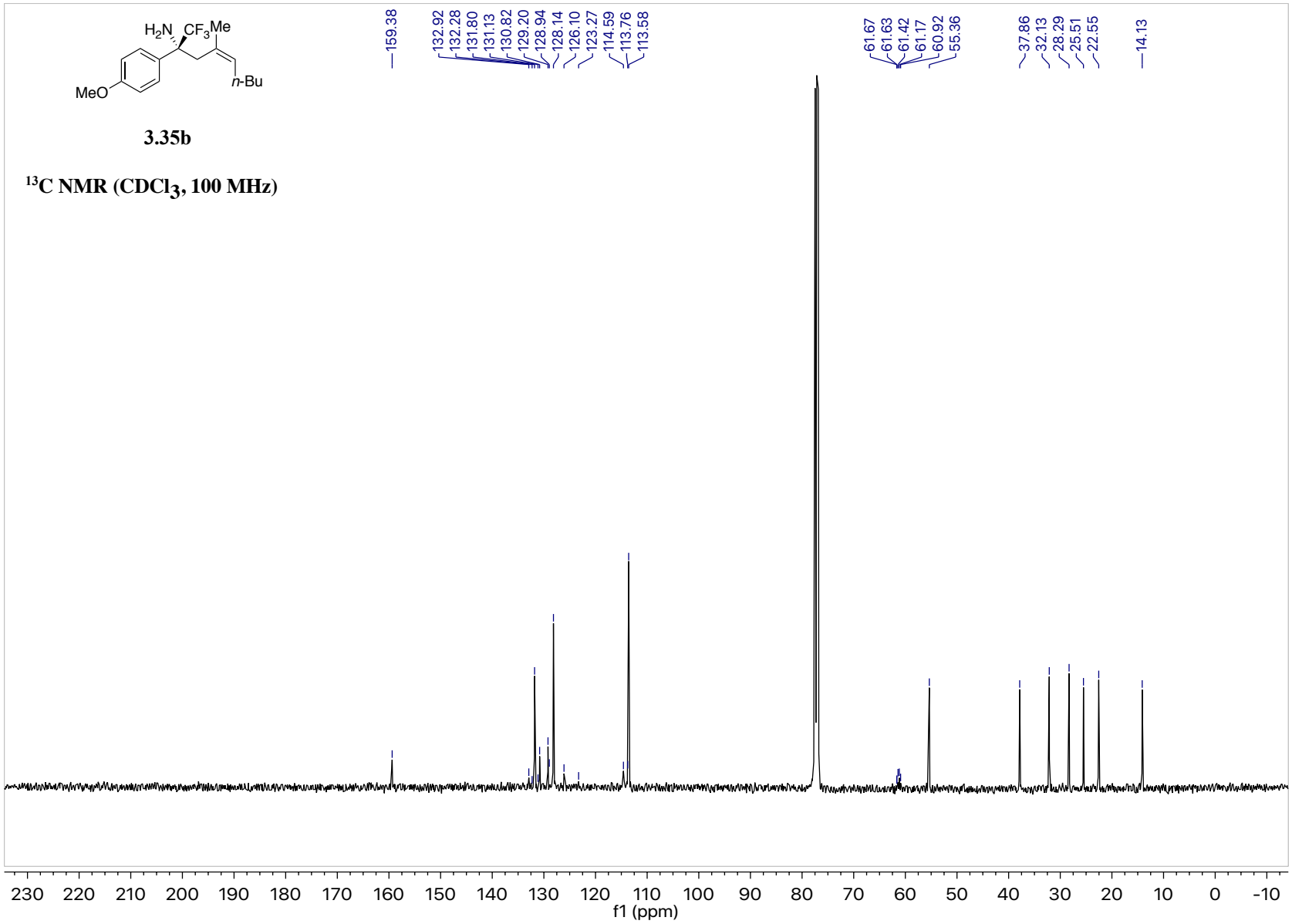

3.35b

^{13}C NMR ($CDCl_3$, 100 MHz)

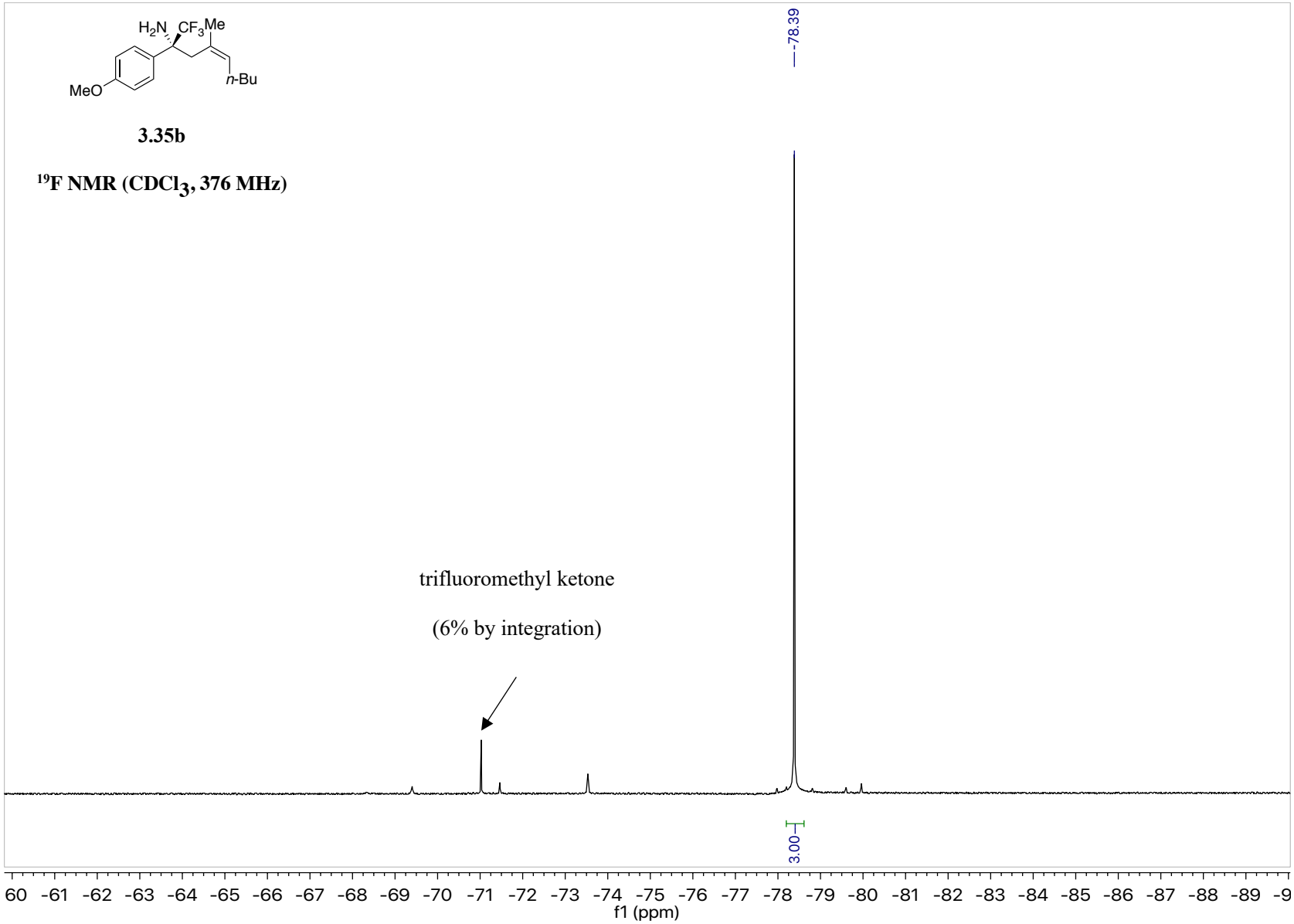
H2N
CF3
Me
MeO
n-Bu
3.35b
19F NMR (CDCl3, 376 MHz)
-78.39
trifluoromethyl ketone
(6% by integration)
3.00
60 -61 -62 -63 -64 -65 -66 -67 -68 -69 -70 -71 -72 -73 -74 -75 -76 -77 -78 -79 -80 -81 -82 -83 -84 -85 -86 -87 -88 -89 -9
f1 (ppm)

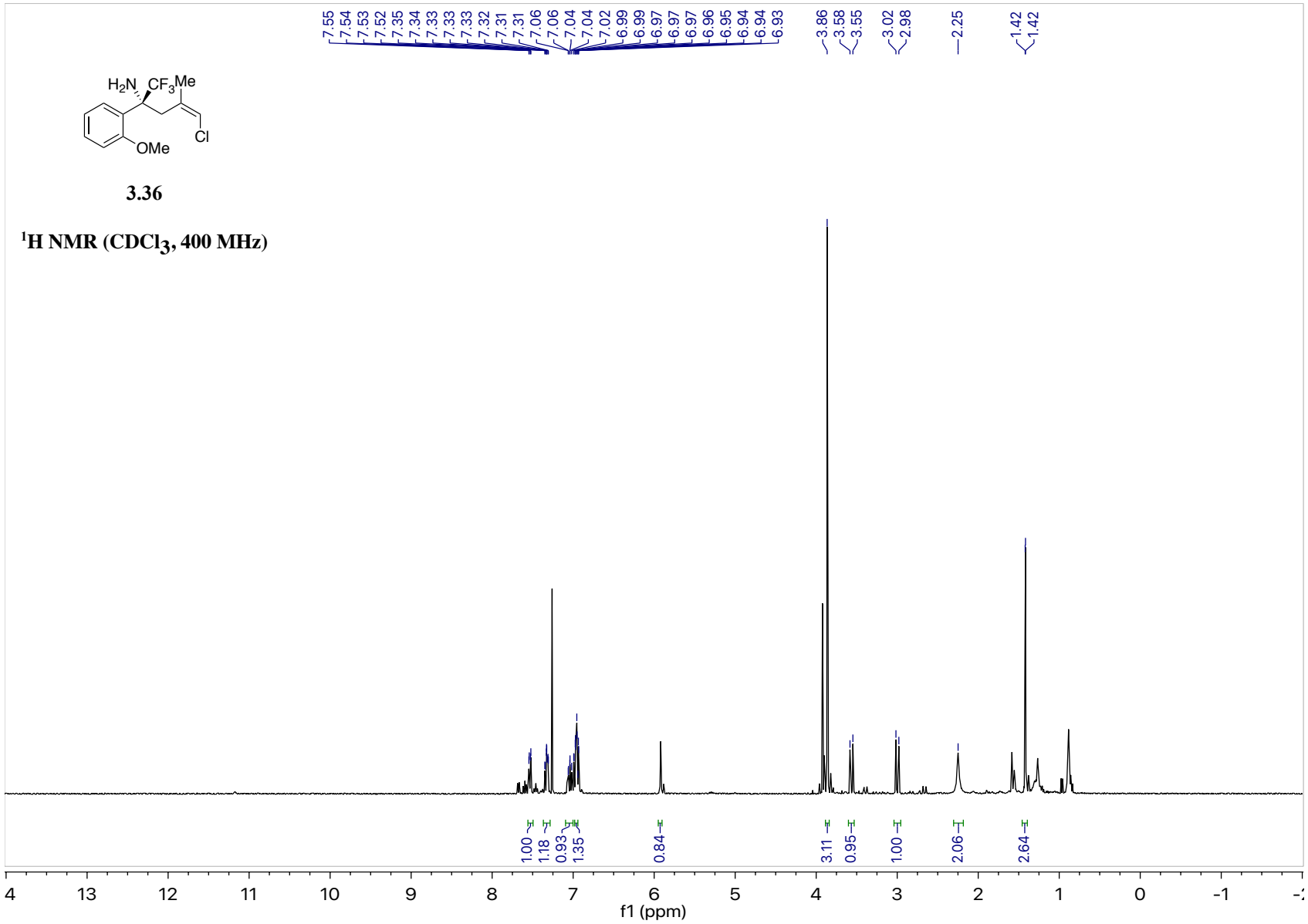

3.36

^{1}H NMR ($CDCl_3$, 400 MHz)

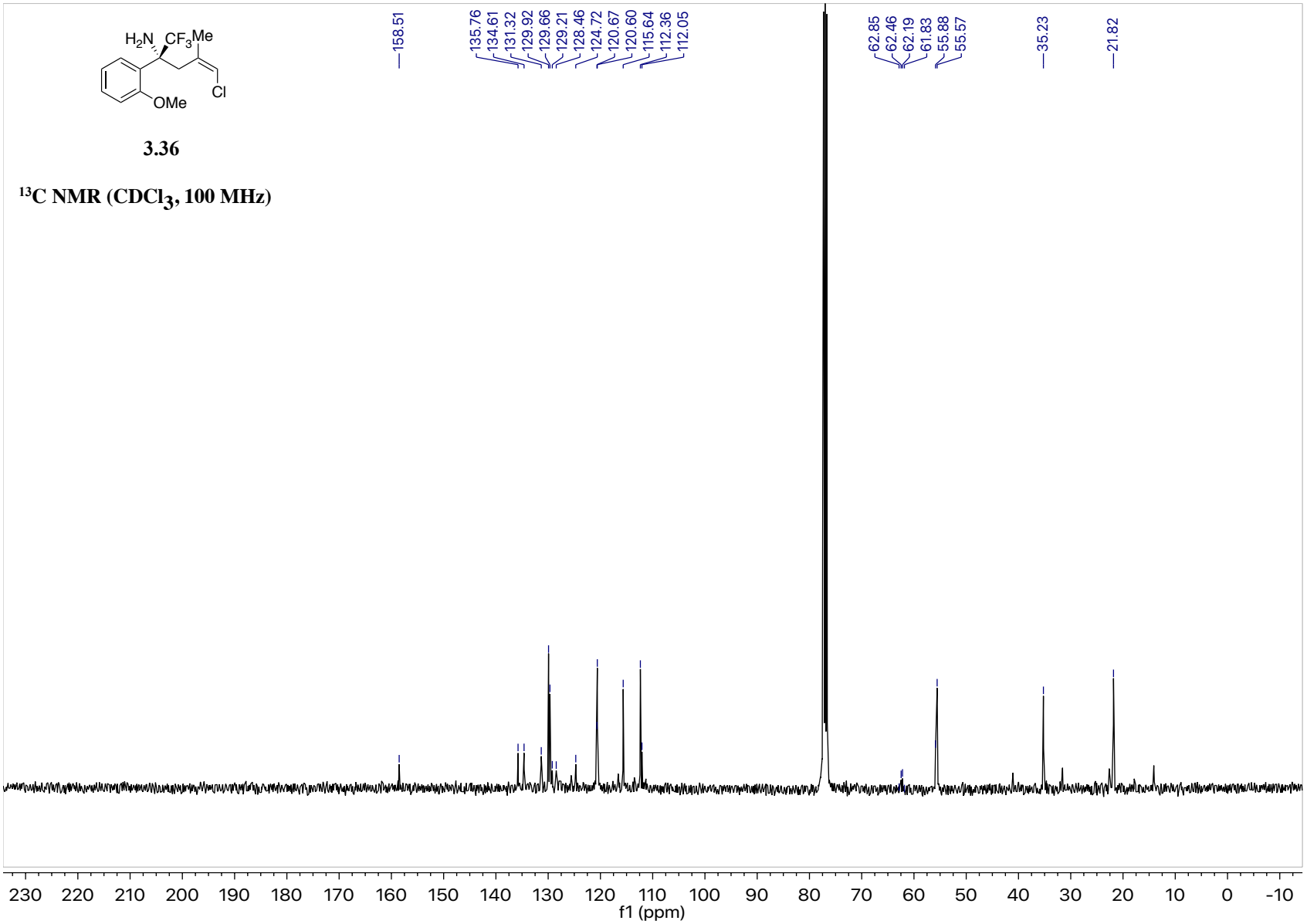

3.36

^{13}C NMR ($CDCl_3$, 100 MHz)

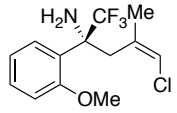

3.36

^{19}F NMR ($CDCl_3$, 376 MHz)

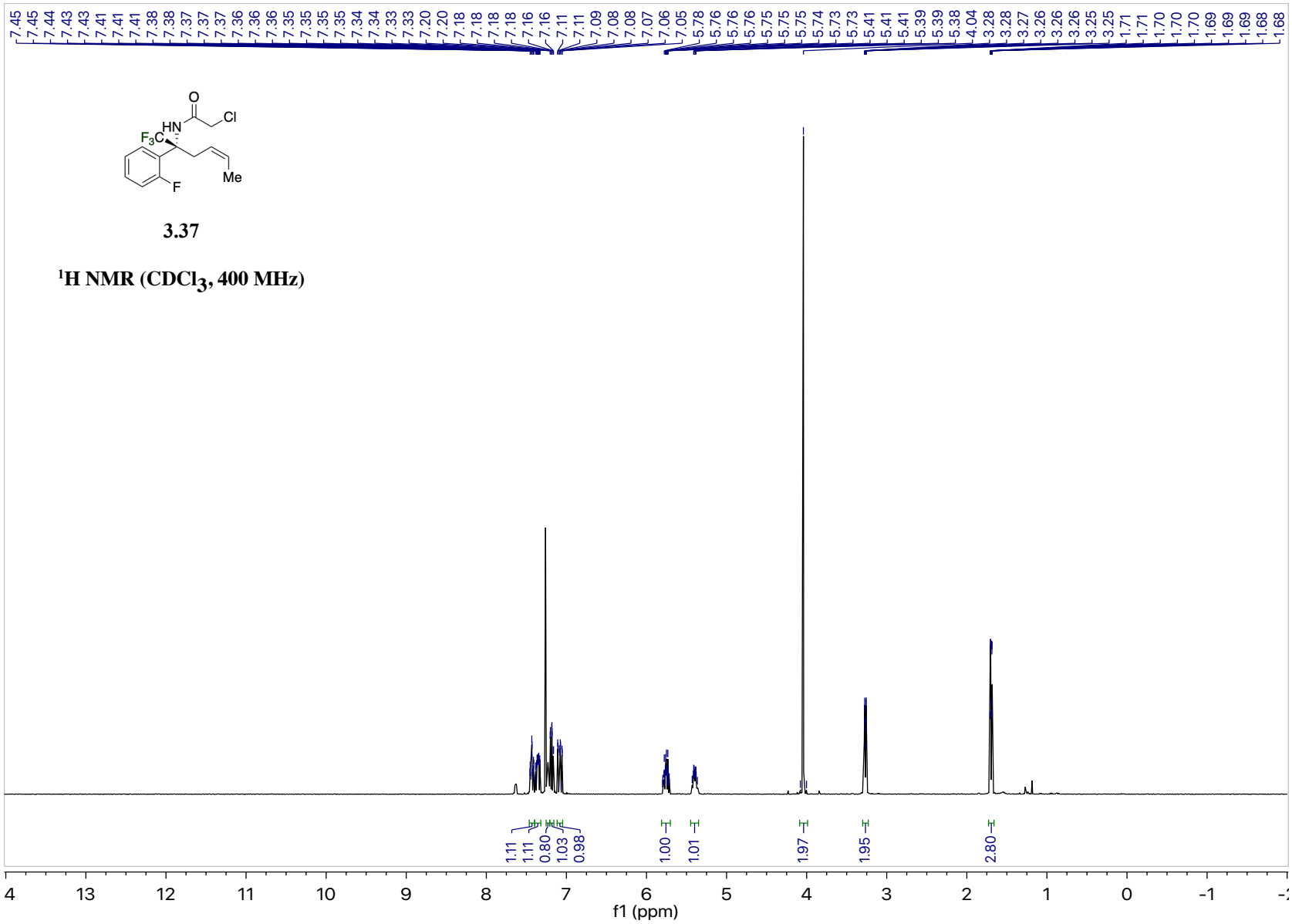

3.37

^{1}H NMR ($CDCl_3$, 400 MHz)

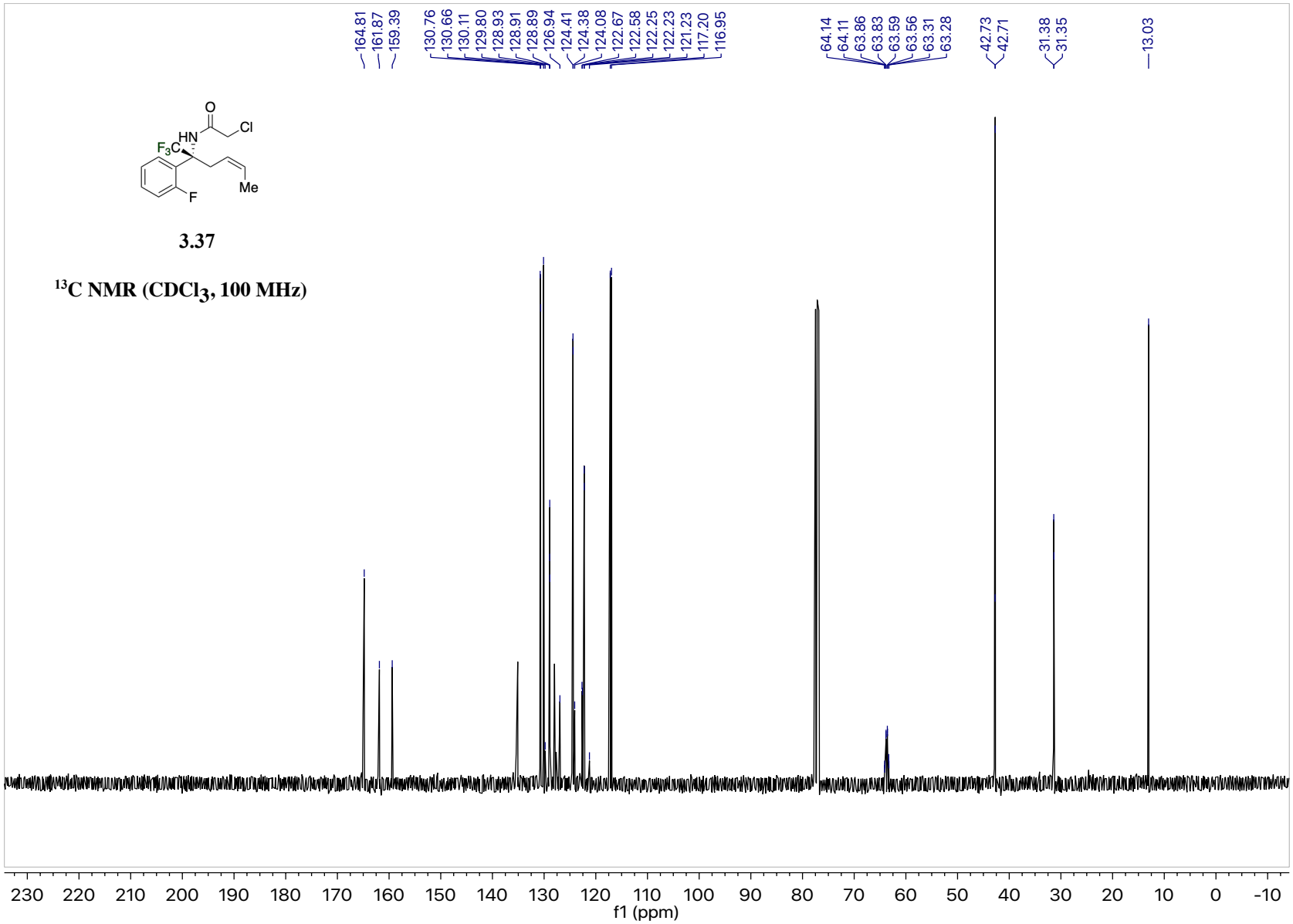

3.37

^{13}C NMR ($CDCl_3$, 100 MHz)

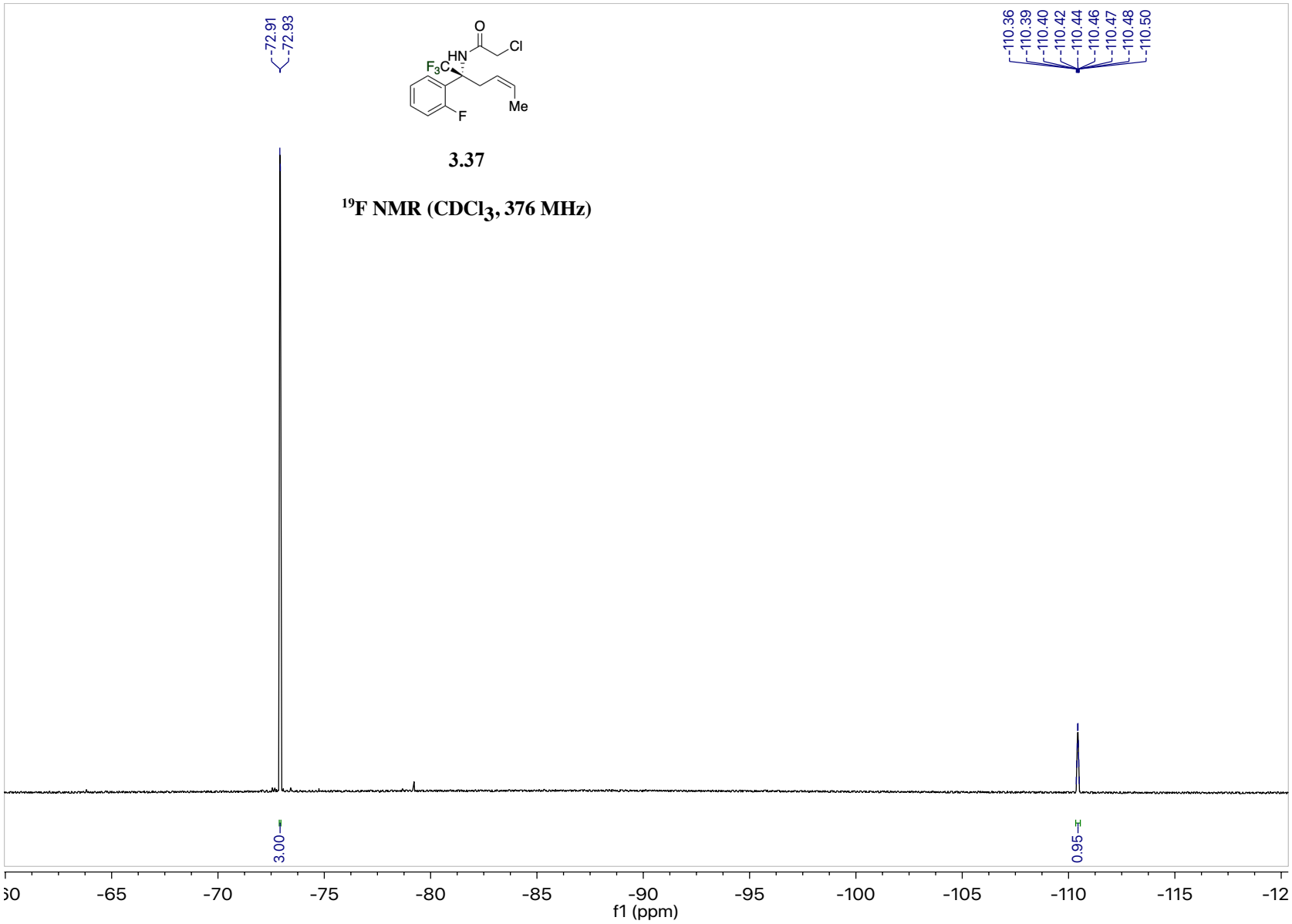

3.37

^{19}F NMR ($CDCl_3$, 376 MHz)

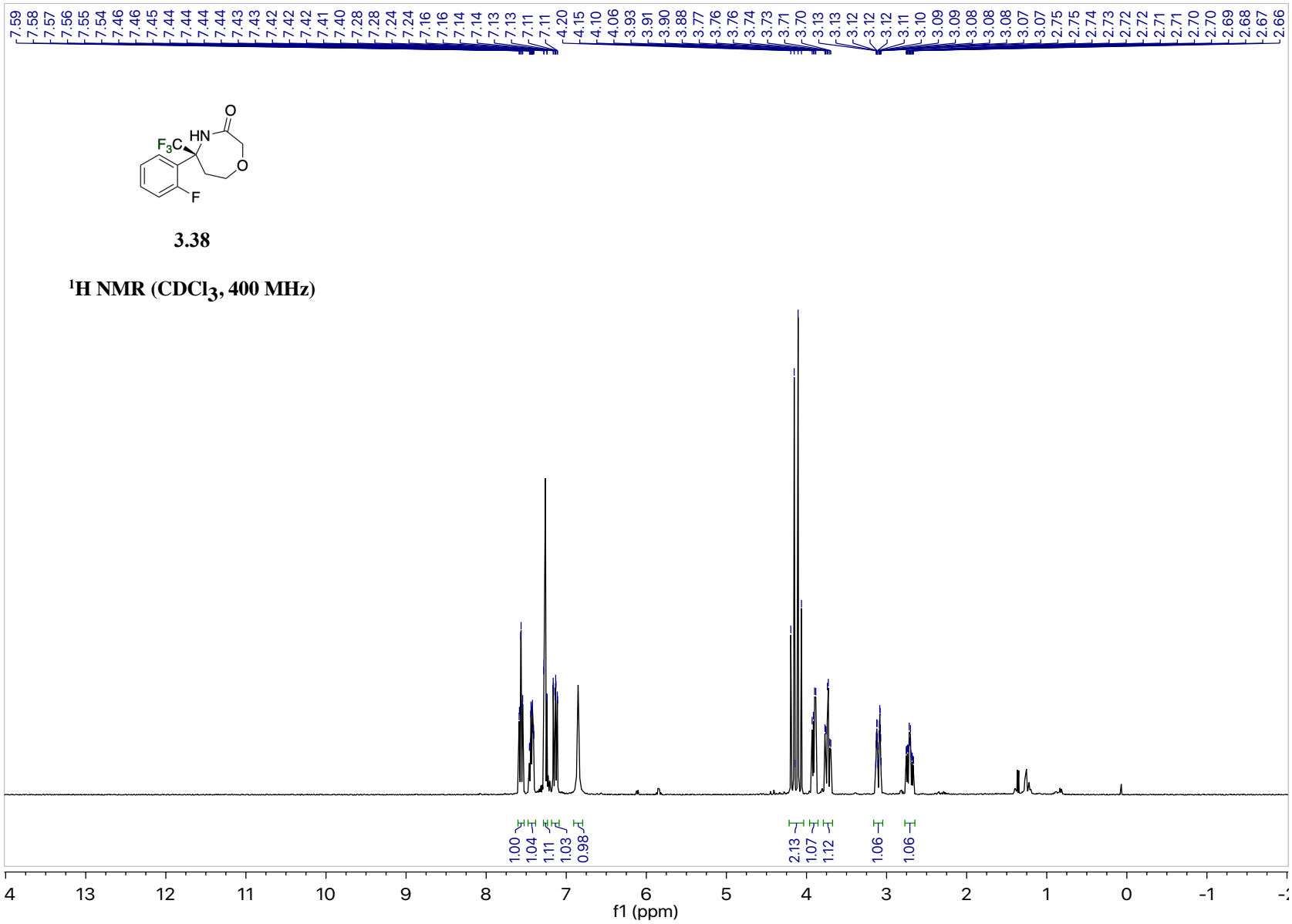

3.38

^{1}H NMR ($CDCl_3$, 400 MHz)

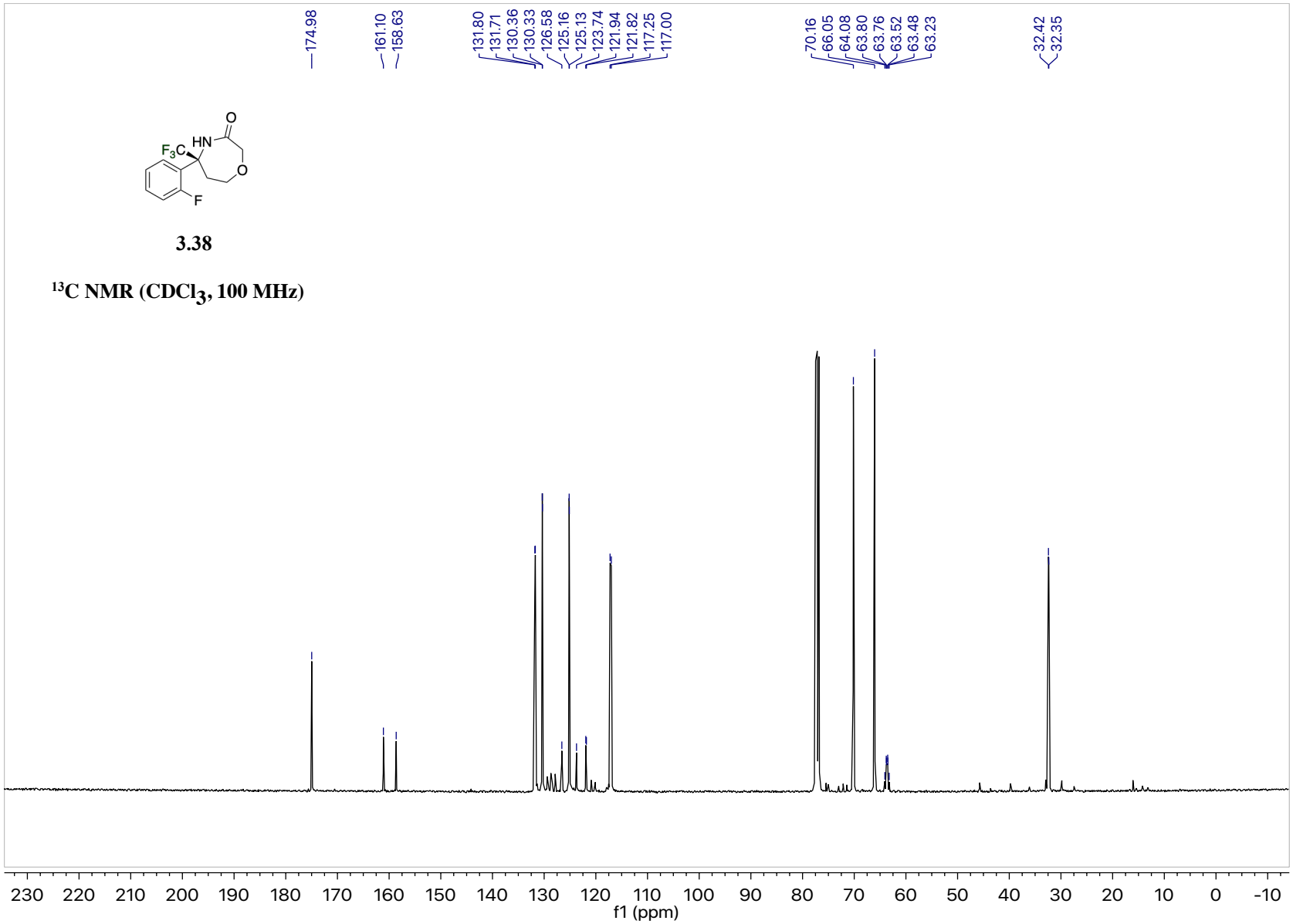

3.38

^{13}C NMR ($CDCl_3$, 100 MHz)

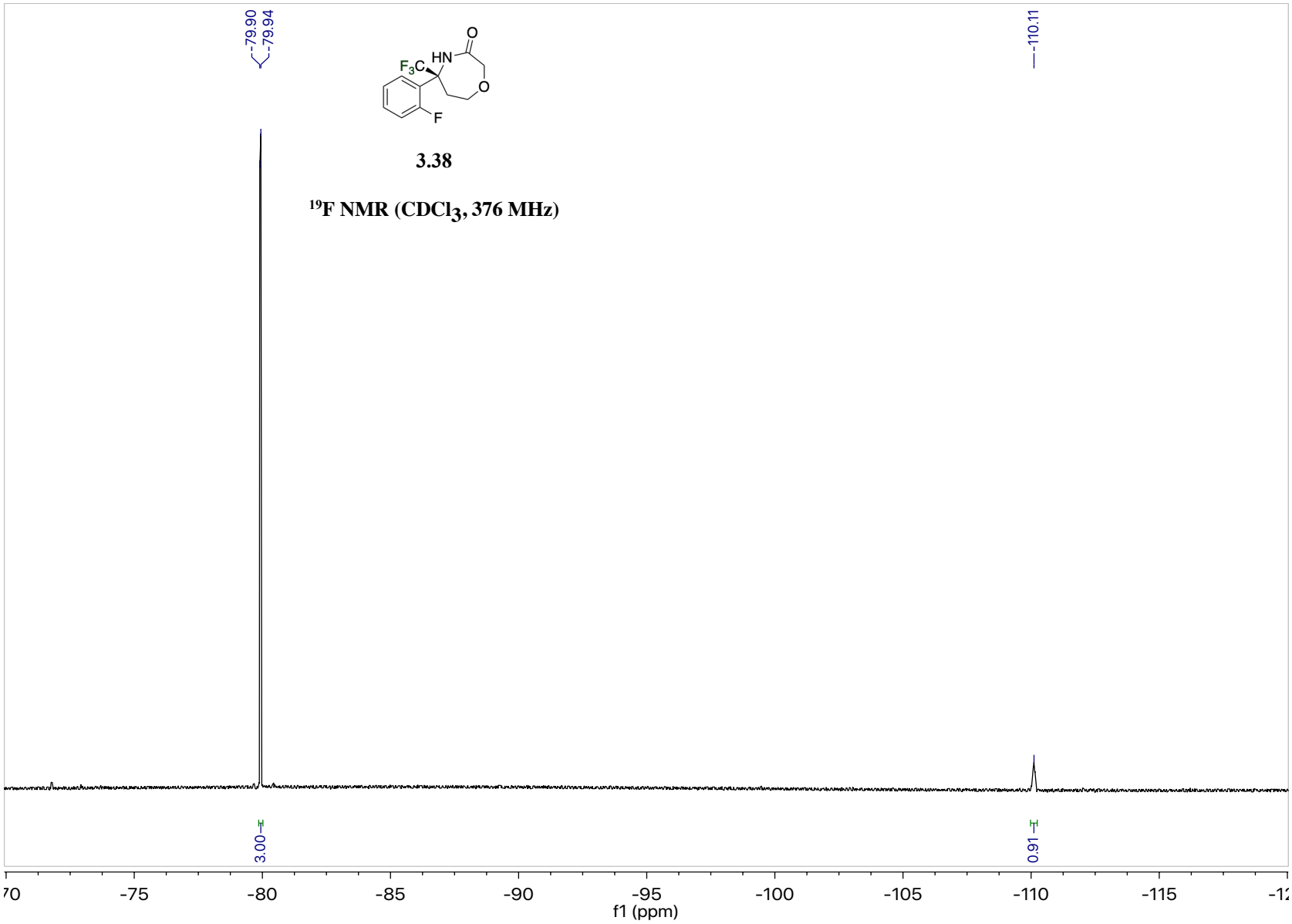

3.38

^{19}F NMR ($CDCl_3$, 376 MHz)

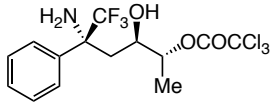

3.39

^{1}H NMR ($CDCl_3$ & CD_2Cl_2, 400 MHz)

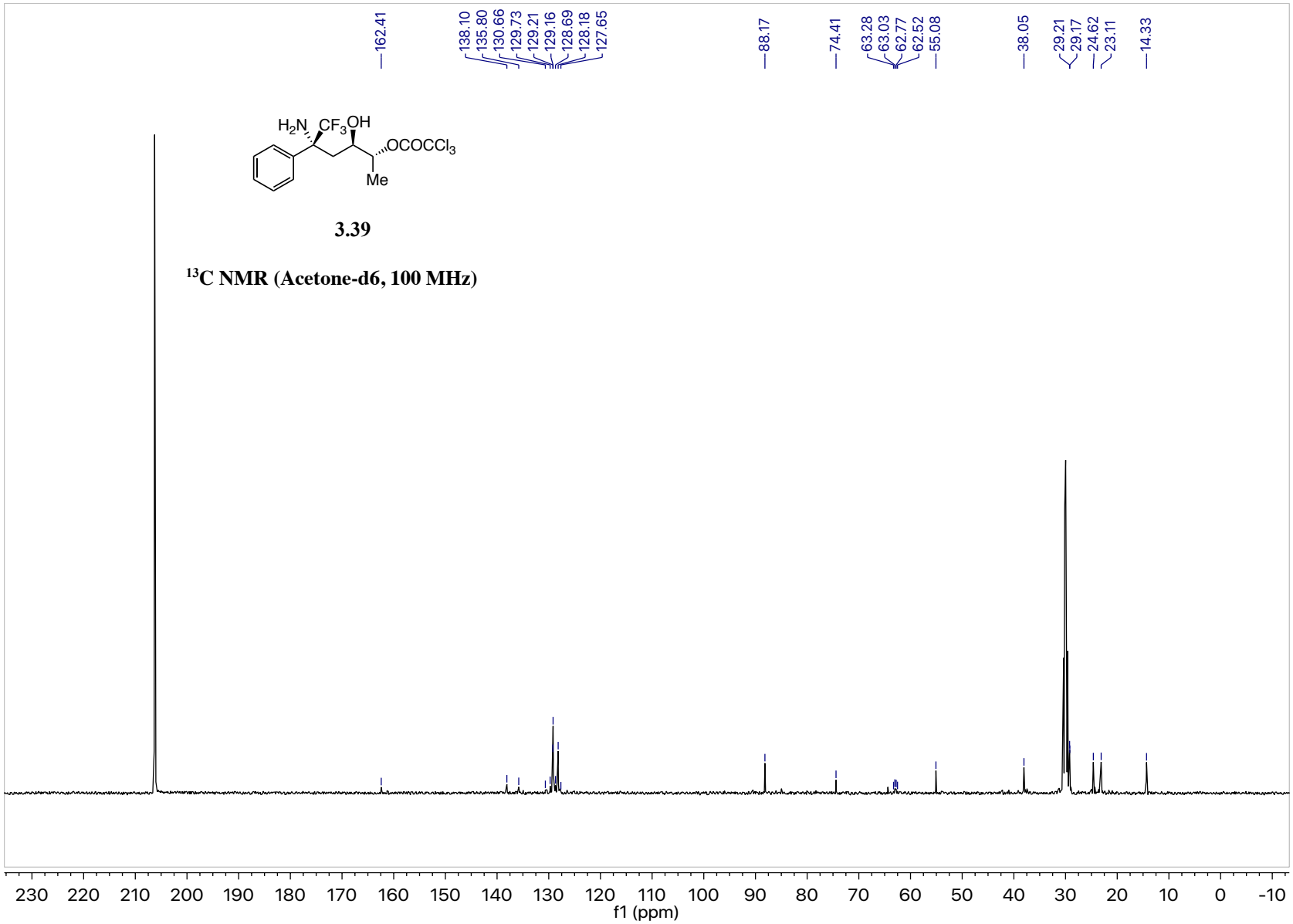

3.39

^{13}C NMR (Acetone-d6, 100 MHz)

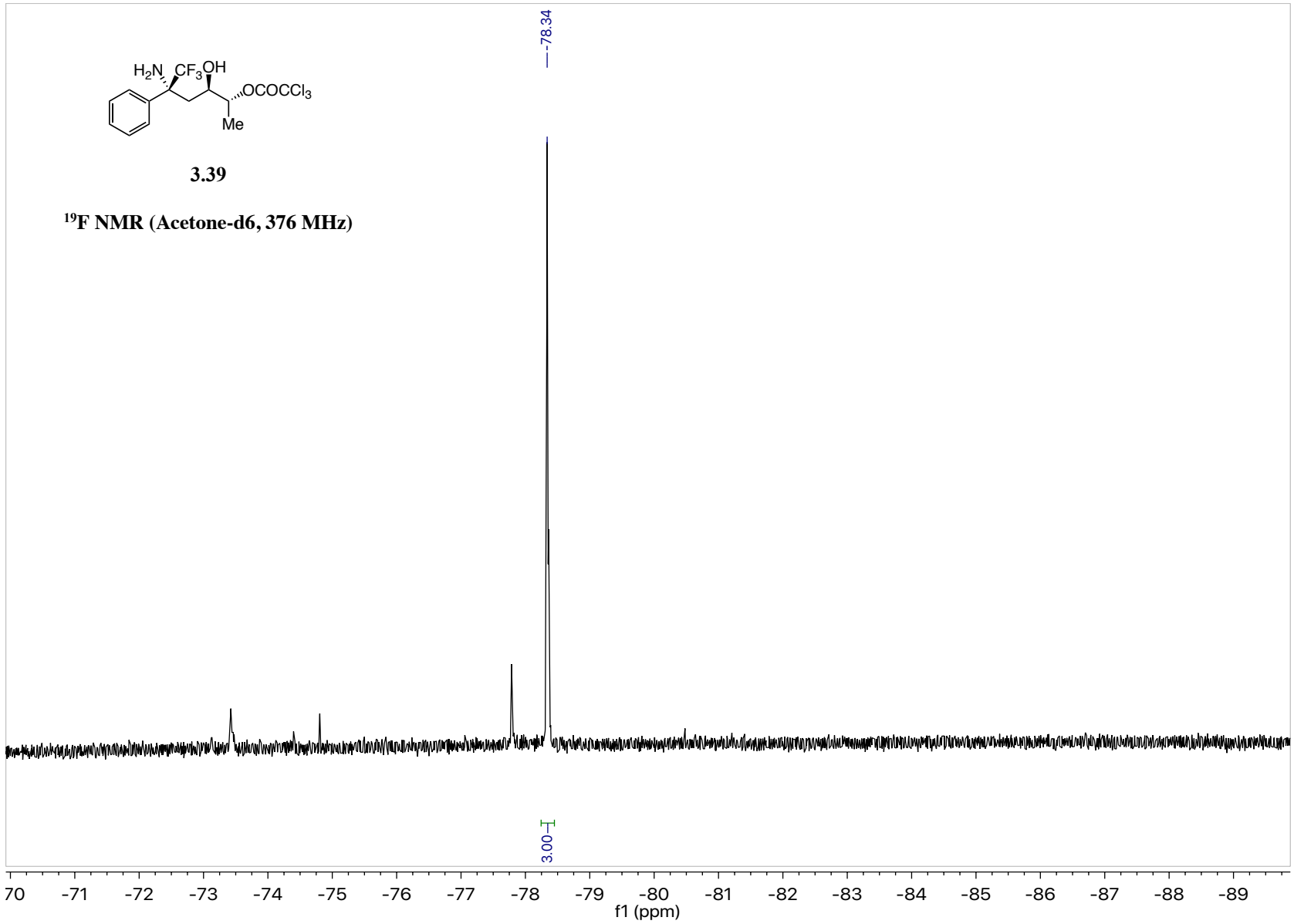
H2N
CF3
OH
OCOCCl3
Me
3.39
19F NMR (Acetone-d6, 376 MHz)
-78.34
3.00
70 -71 -72 -73 -74 -75 -76 -77 -78 -79 -80 -81 -82 -83 -84 -85 -86 -87 -88 -89
f1 (ppm)

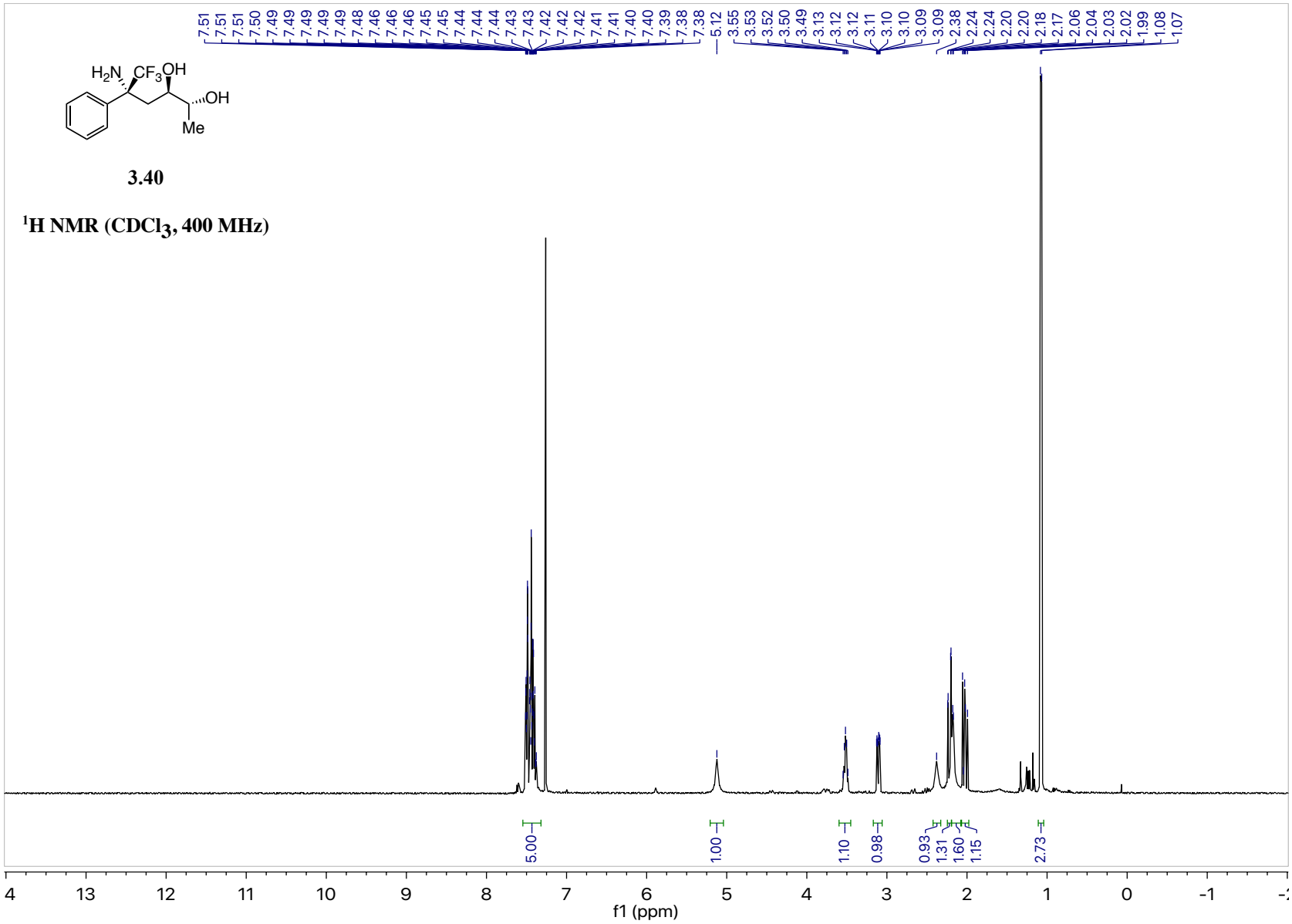

3.40

^{1}H NMR ($CDCl_3$, 400 MHz)

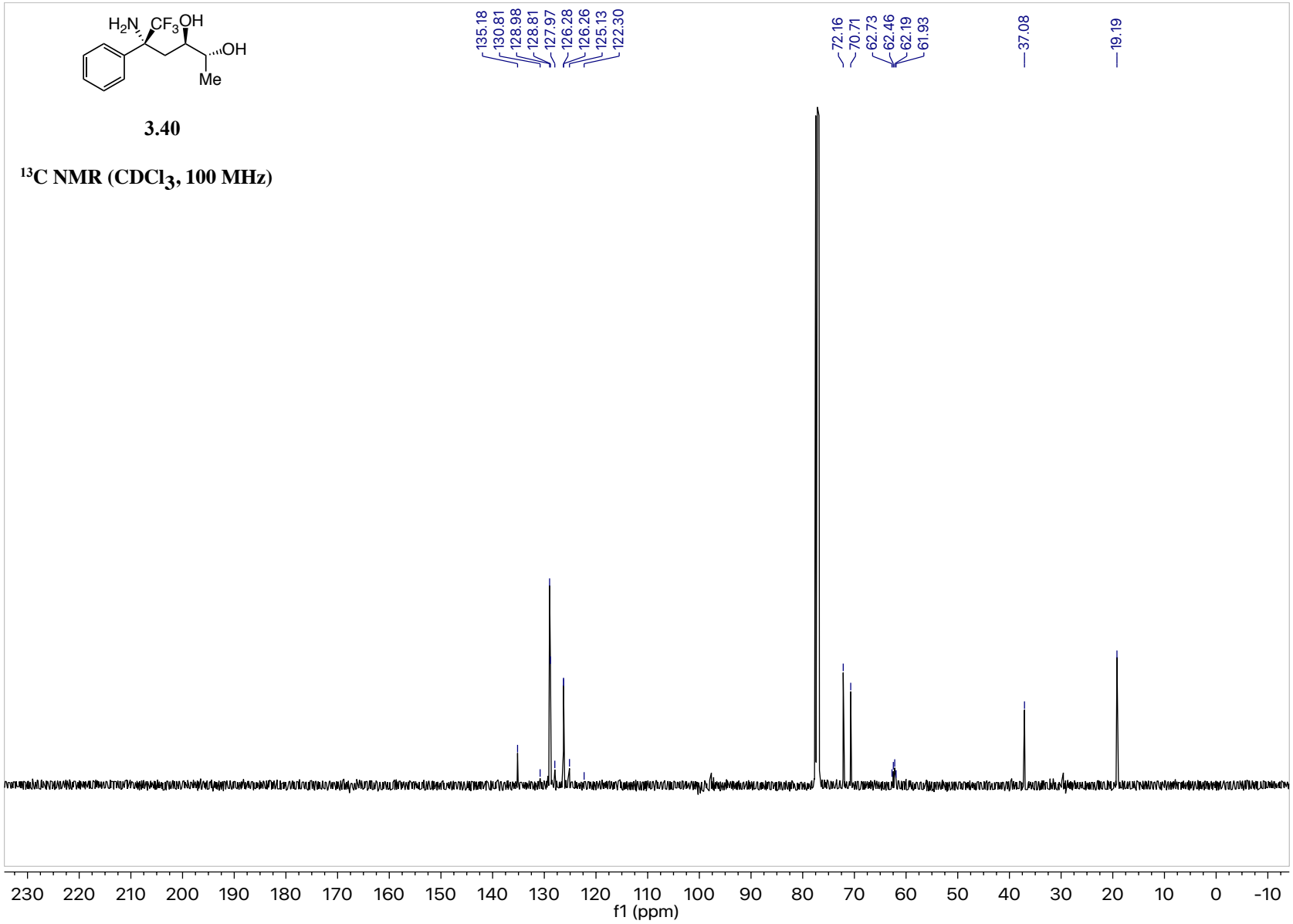

3.40

^{13}C NMR ($CDCl_3$, 100 MHz)

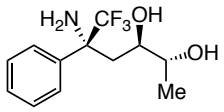

3.40

^{19}F NMR ($CDCl_3$, 376 MHz)

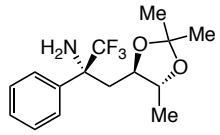

S-1

^{1}H NMR ($CDCl_3$, 400 MHz)

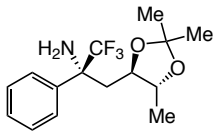

S-1

^{13}C NMR ($CDCl_3$, 100 MHz)

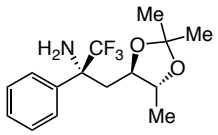

S-1

^{19}F NMR ($CDCl_3$, 376 MHz)

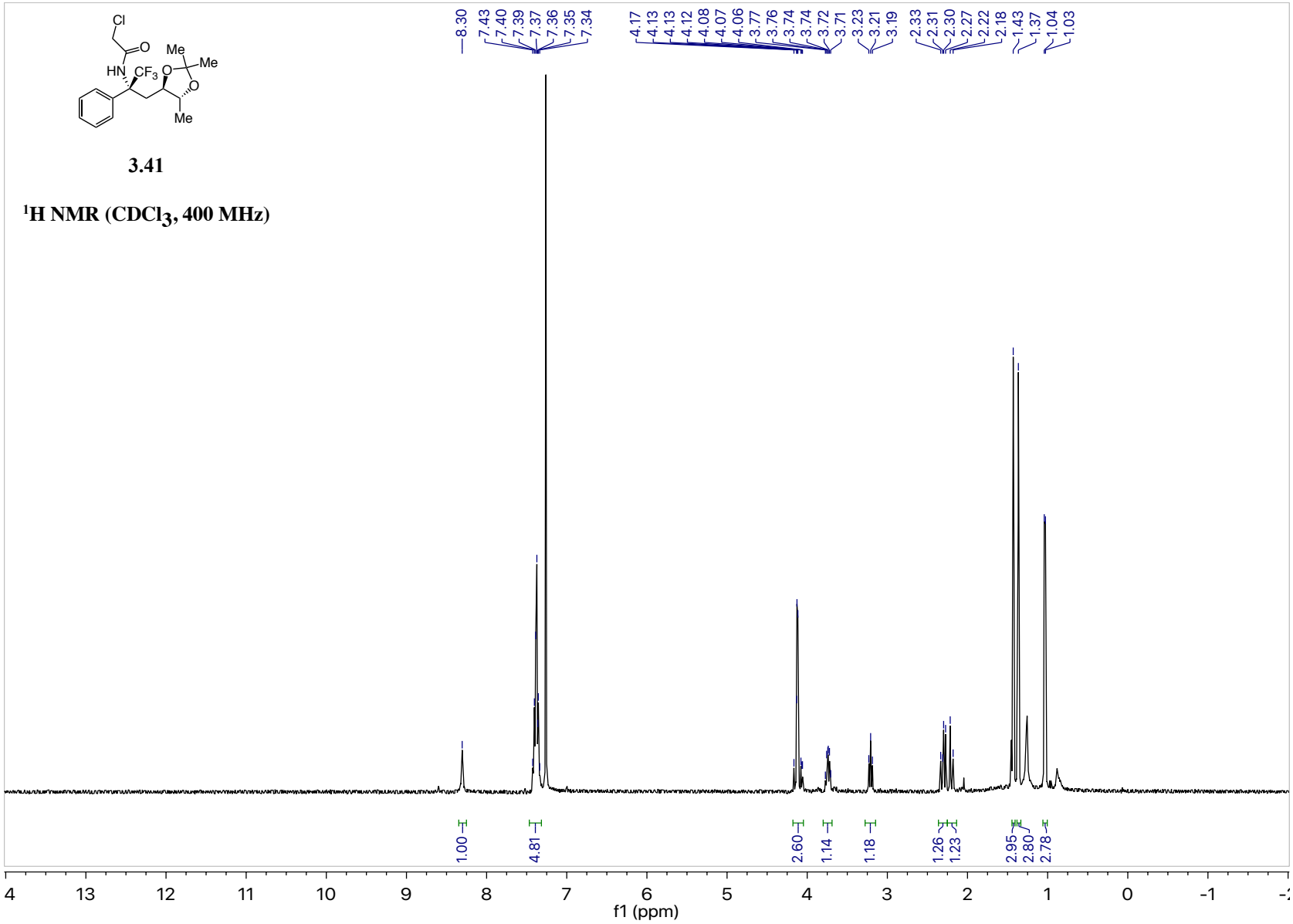

3.41

^{1}H NMR ($CDCl_3$, 400 MHz)

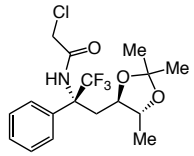

3.41

^{13}C NMR ($CDCl_3$, 100 MHz)

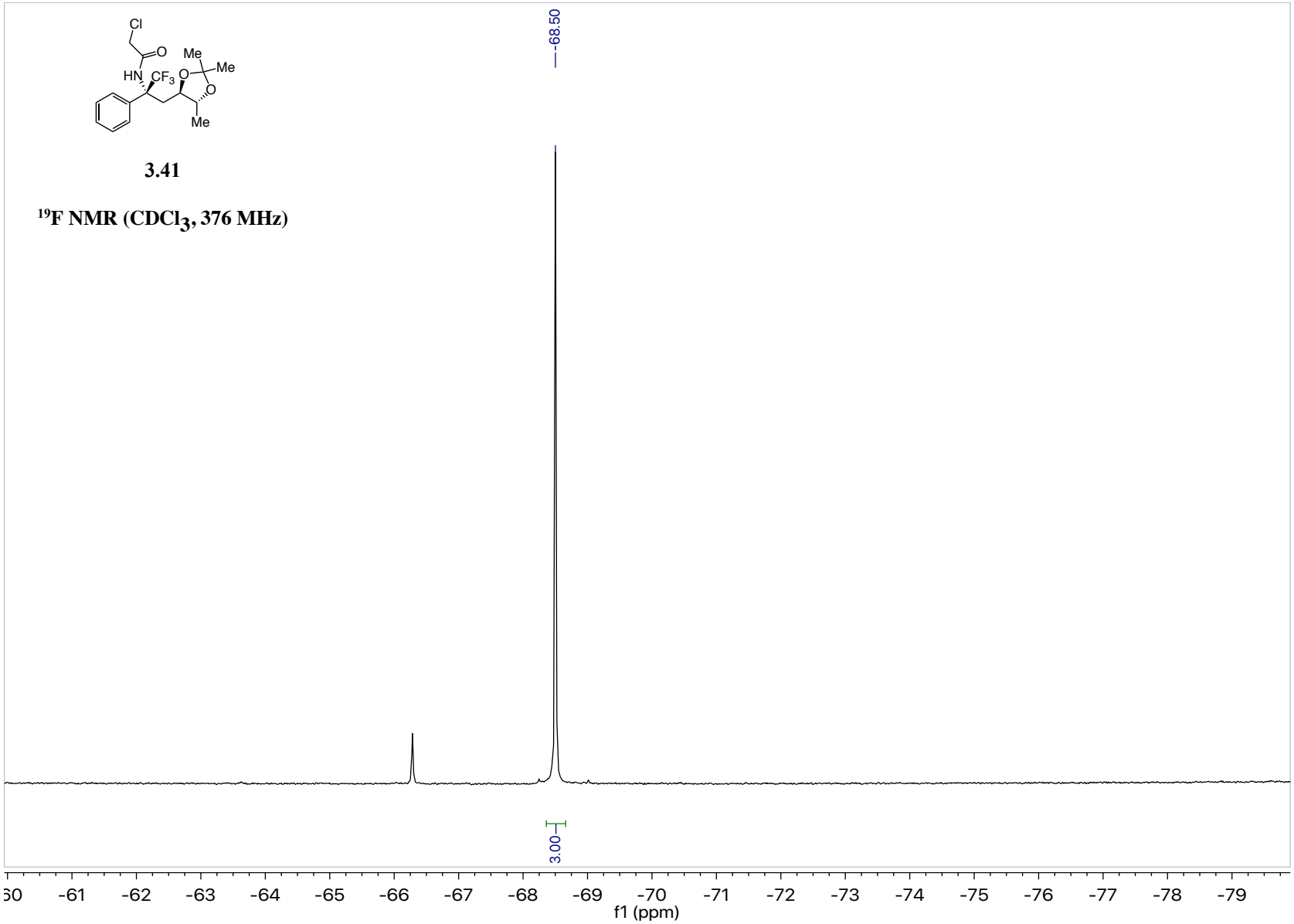

3.41

^{19}F NMR ($CDCl_3$, 376 MHz)

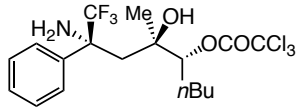

3.42

^{1}H NMR ($CDCl_3$ & CD_2Cl_2, 400 MHz)

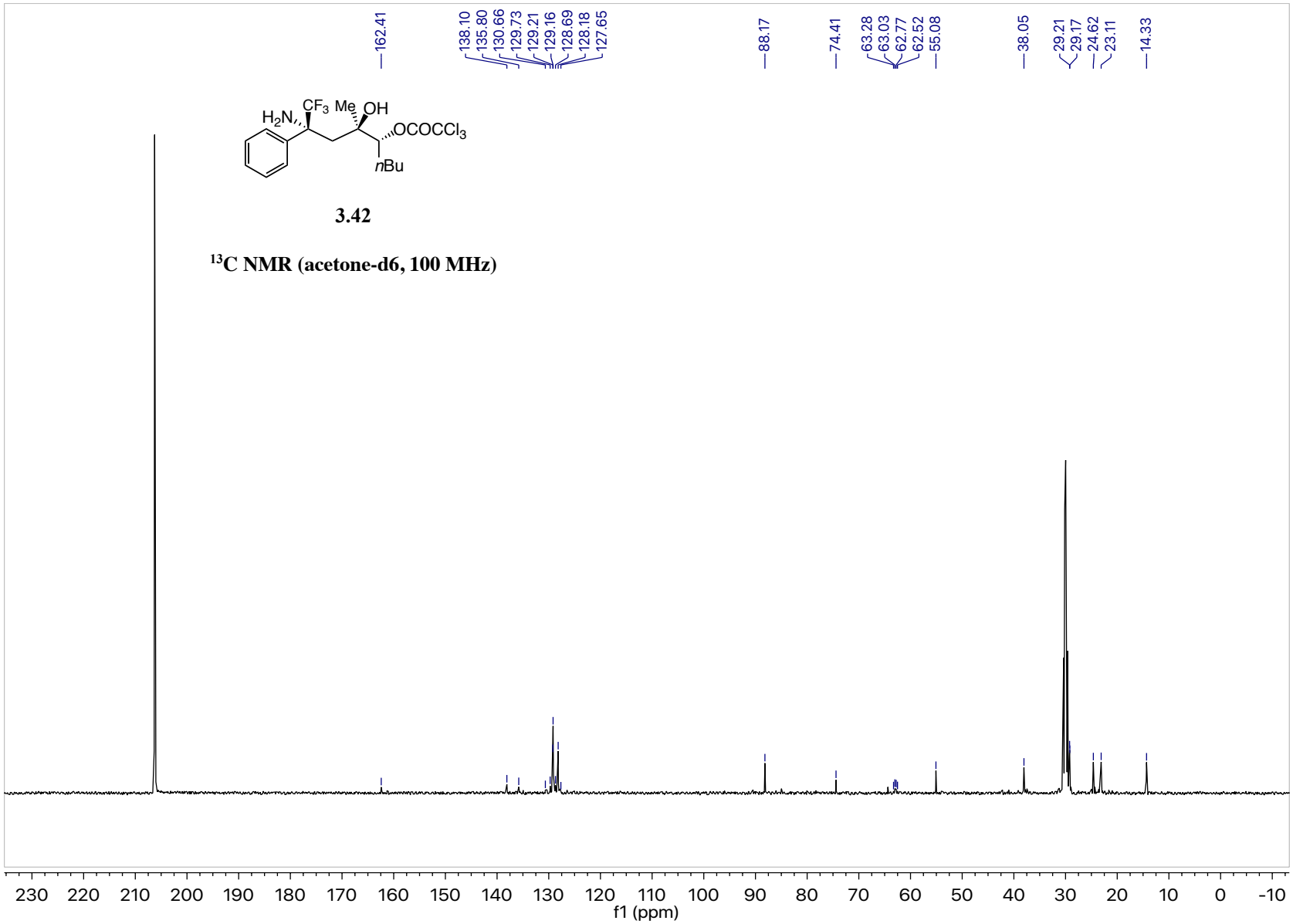

3.42

^{13}C NMR (acetone-d6, 100 MHz)

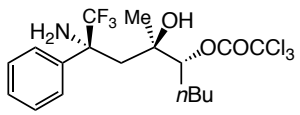

3.42

^{19}F NMR (acetone-d6, 376 MHz)

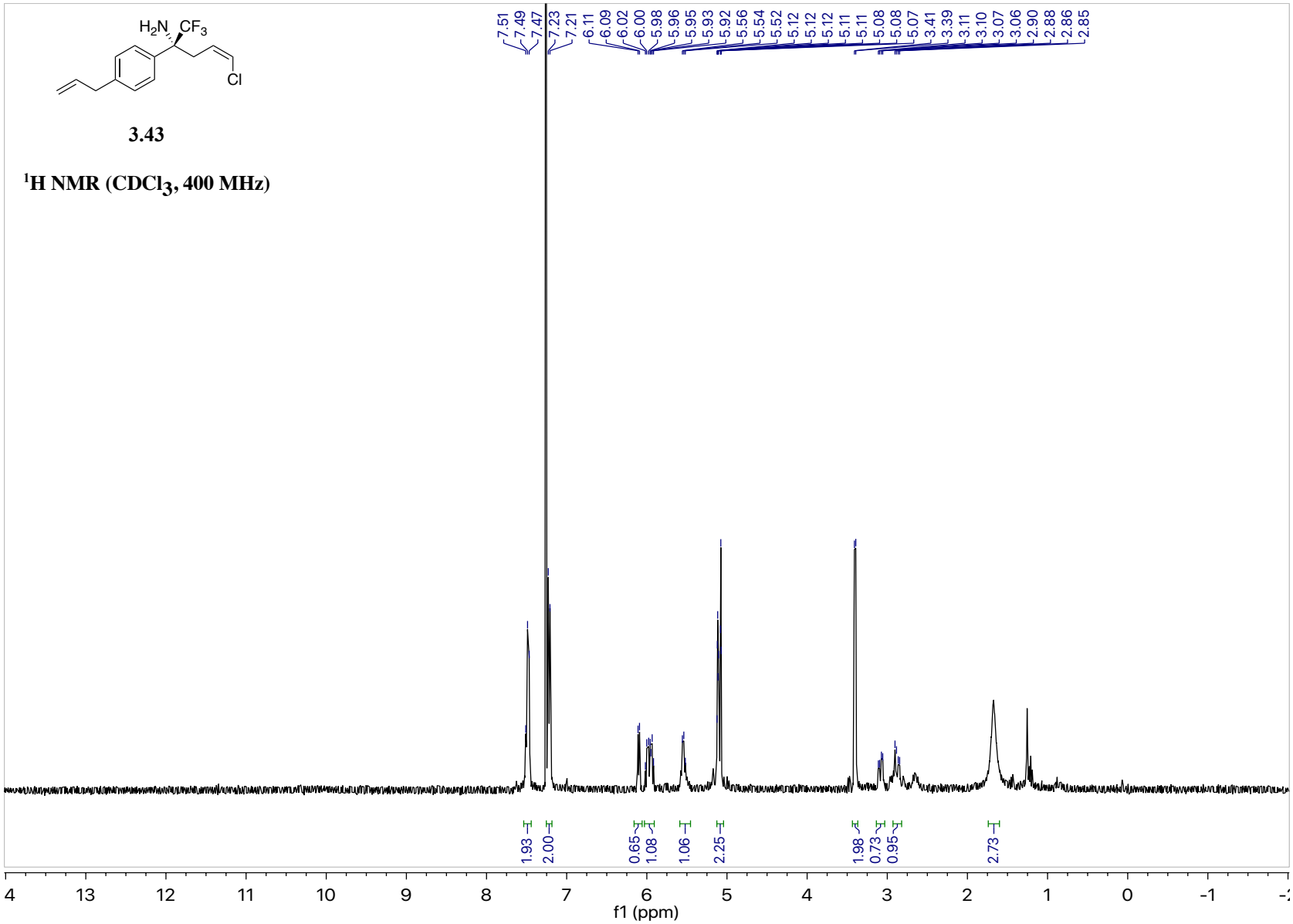

3.43

^{1}H NMR ($CDCl_3$, 400 MHz)

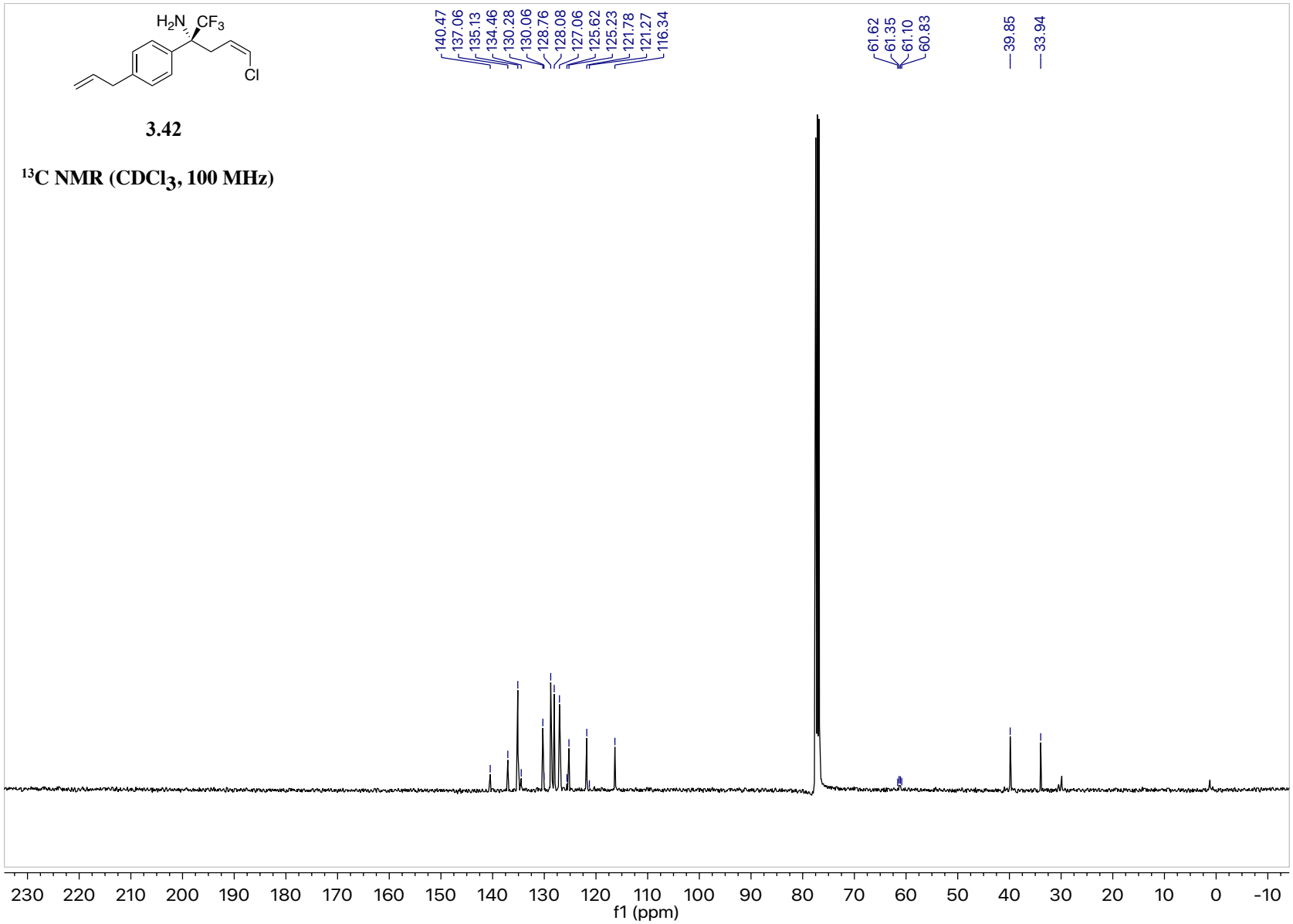

3.42

^{13}C NMR ($CDCl_3$, 100 MHz)

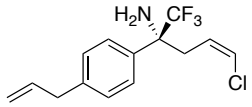

3.43

^{19}F NMR ($CDCl_3$, 376 MHz)

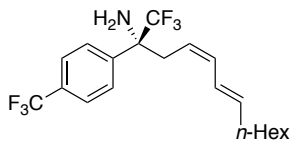

3.44

^{1}H NMR ($CDCl_3$, 400 MHz)

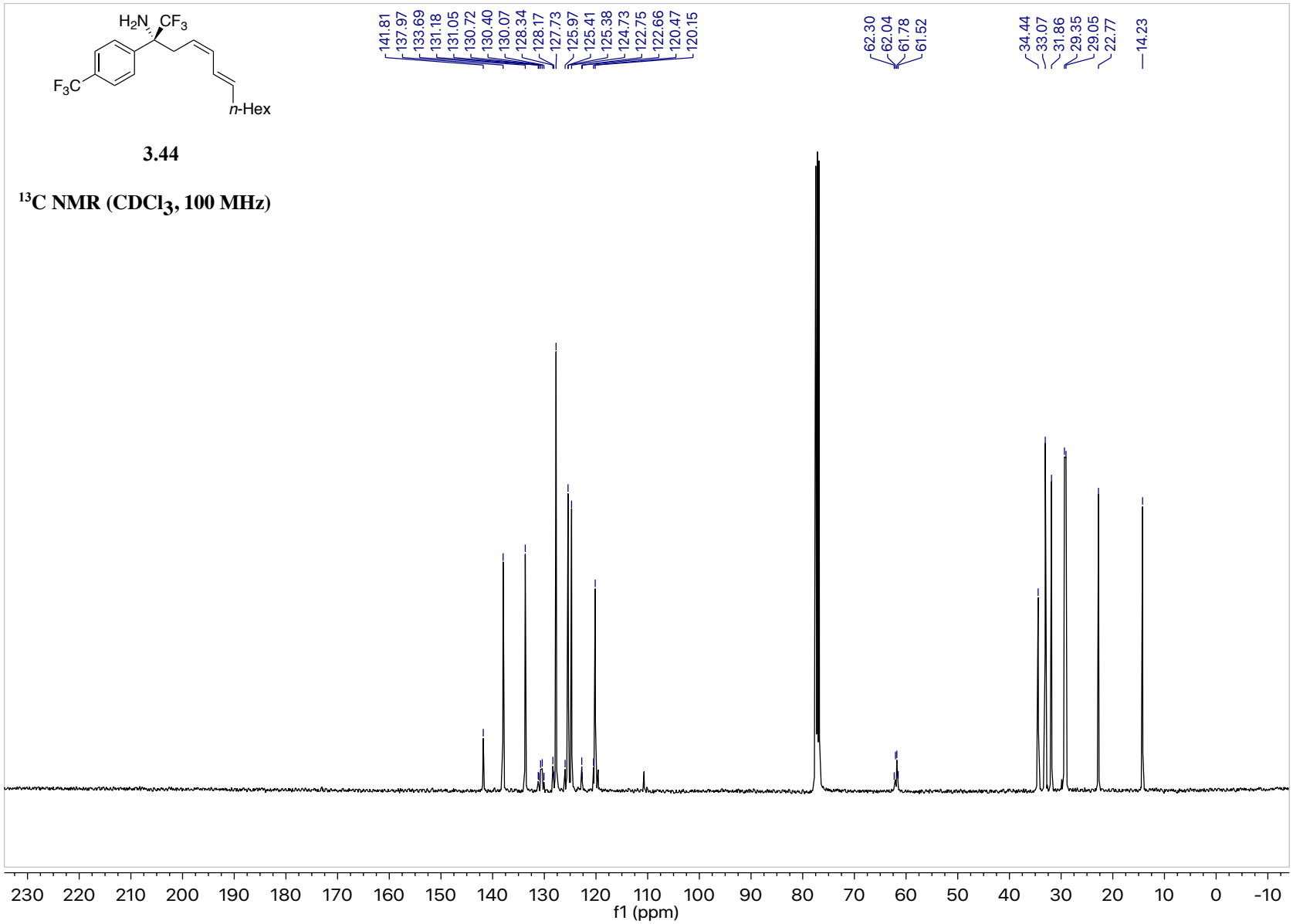

3.44

^{13}C NMR ($CDCl_3$, 100 MHz)

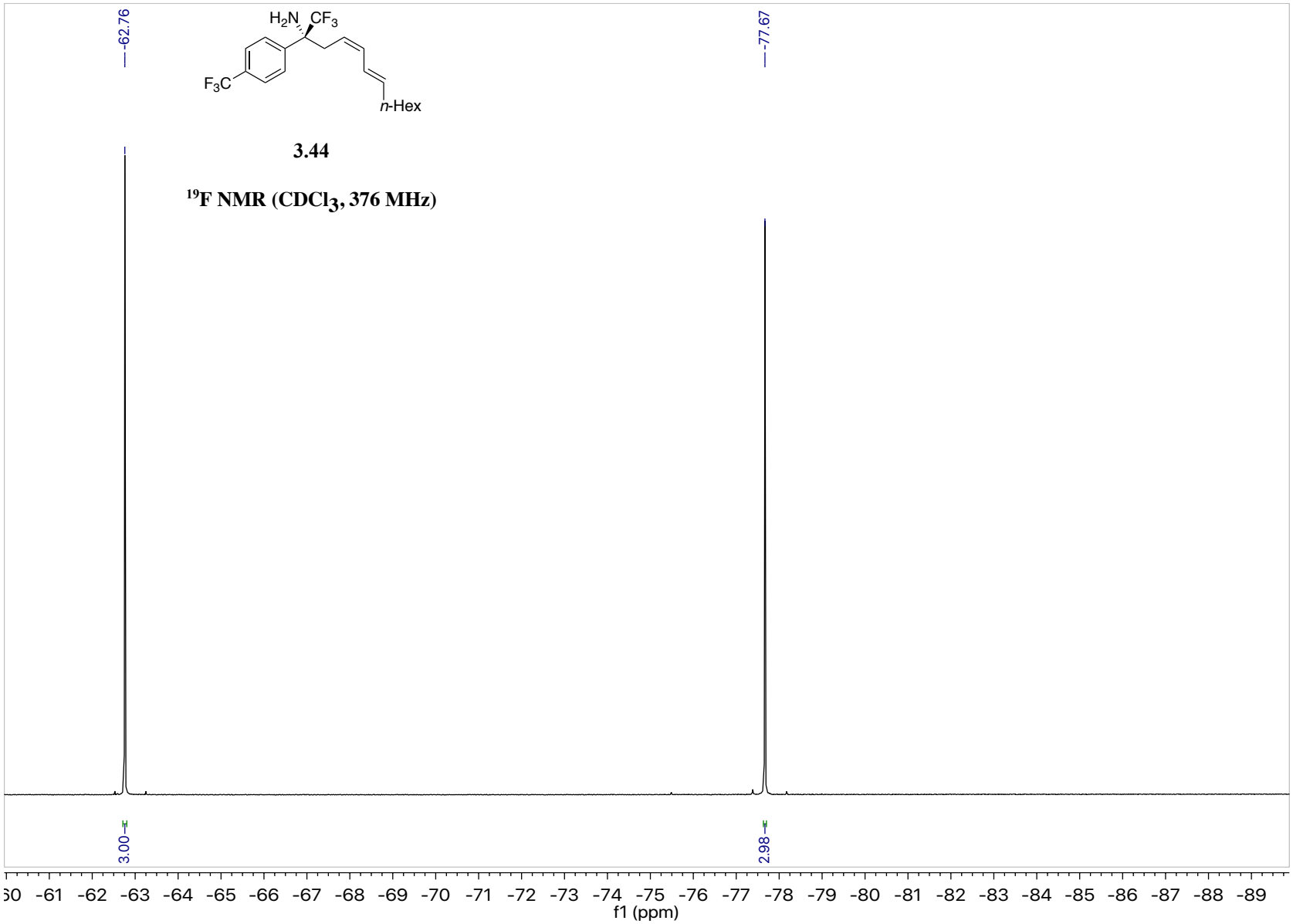

3.44

^{19}F NMR ($CDCl_3$, 376 MHz)

3.7.10. Crystallographic Data

3.7.10.1. (*R*,*Z*)-2-Chloro-*N*-(1,1,1-trifluoro-2-(2-fluorophenyl)hex-4-en-2-yl)acetamide (3.37) [CCDC #: 1977677]

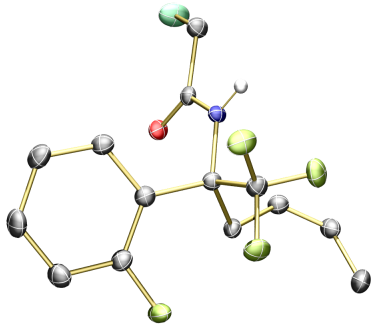

Table S1. Crystal data and structure refinement for C14 H14 Cl F4 N O

Identification code	C14 H14 Cl F4 N O	
Empirical formula	C14 H14 Cl F4 N O	
Formula weight	323.71	
Temperature	100(2) K	
Wavelength	1.54178 Å	
Crystal system	Tetragonal	
Space group	$P4_3$	
Unit cell dimensions	a = 9.6746(3) Å	a= 90°.
	b = 9.6746(3) Å	b= 90°.
	c = 15.2638(5) Å	c = 90°.
Volume	1428.66(10) $Å^3$	
Z	4	
Density (calculated)	1.505 Mg/m^3	
Absorption coefficient	2.793 mm^{-1}	
F(000)	664	
Crystal size	0.250 x 0.100 x 0.100 mm^3	
Theta range for data collection	7.093 to 66.613°.	
Index ranges	-11<=h<=11, -10<=k<=8, -17<=l<=15	
Reflections collected	6738	
Independent reflections	2293 [R(int) = 0.0268]	
Completeness to theta = 67.679°	97.5 %	

Refinement method	Full-matrix least-squares on F^2
Data / restraints / parameters	2293 / 1 / 191
Goodness-of-fit on F^2	1.658
Final R indices [I>2sigma(I)]	R1 = 0.0245, wR2 = 0.0605
R indices (all data)	R1 = 0.0246, wR2 = 0.0607
Absolute structure parameter	0.086(7)
Extinction coefficient	n/a
Largest diff. peak and hole	0.195 and -0.255 e.$Å^{-3}$

Table S2. Atomic coordinates ($x10^4$) and equivalent isotropic displacement parameters ($Å^2x10^3$) for C14 H14 Cl F4 N O. U(eq) is defined as one third of the trace of the orthogonalized U^{ij} tensor

	x	y	z	U(eq)
Cl(01)	7488(1)	3176(1)	3774(1)	38(1)
F(002)	5562(1)	10537(1)	4621(1)	26(1)
F(003)	4660(1)	9303(1)	3600(1)	27(1)
F(004)	6834(1)	9762(1)	3573(1)	28(1)
F(005)	5428(1)	9492(1)	6307(1)	27(1)
O(001)	6791(2)	5391(1)	4992(1)	21(1)
N(001)	6275(2)	7035(2)	3994(1)	15(1)
C(001)	6601(2)	5744(2)	4232(1)	17(1)
C(002)	7403(2)	8363(2)	5206(1)	18(1)
C(003)	4788(2)	7847(2)	5218(1)	18(1)
C(004)	5780(2)	9442(2)	4105(1)	20(1)
C(005)	6075(2)	8134(2)	4644(1)	17(1)
C(006)	3785(2)	6893(2)	4953(1)	21(1)
C(014)	4541(2)	8508(2)	6008(1)	21(1)
C(007)	3413(2)	8235(2)	6535(1)	26(1)
C(008)	9753(2)	8990(2)	4605(1)	23(1)
C(009)	6704(2)	4743(2)	3463(1)	23(1)
C(010)	9730(2)	10515(2)	4771(2)	29(1)
C(011)	8758(2)	8073(2)	4758(1)	21(1)
C(012)	2453(2)	7264(2)	6264(2)	27(1)
C(013)	2634(2)	6600(2)	5464(2)	26(1)

Table S3. Bond lengths [Å] and angles [°] for C14 H14 Cl F4 N O

Cl(01)-C(009)	1.760(2)
F(002)-C(004)	1.338(2)
F(003)-C(004)	1.337(2)
F(004)-C(004)	1.340(3)
F(005)-C(014)	1.361(2)
O(001)-C(001)	1.224(3)
N(001)-C(001)	1.339(3)
N(001)-C(005)	1.467(2)
N(001)-H(007)	0.8800
C(001)-C(009)	1.525(3)
C(002)-C(011)	1.505(3)
C(002)-C(005)	1.561(3)
C(002)-H(00A)	0.9900
C(002)-H(00B)	0.9900
C(003)-C(014)	1.385(3)
C(003)-C(006)	1.400(3)
C(003)-C(005)	1.548(3)
C(004)-C(005)	1.536(3)
C(006)-C(013)	1.389(3)
C(006)-H(00D)	0.9500
C(014)-C(007)	1.382(3)
C(007)-C(012)	1.384(3)
C(007)-H(00F)	0.9500
C(008)-C(011)	1.330(3)
C(008)-C(010)	1.497(3)
C(008)-H(00G)	0.9500
C(009)-H(00C)	0.9900
C(009)-H(00E)	0.9900
C(010)-H(00H)	0.9800
C(010)-H(00I)	0.9800
C(010)-H(00J)	0.9800
C(011)-H(00K)	0.9500
C(012)-C(013)	1.391(4)

C(012)-H(00L)	0.9500
C(013)-H(00M)	0.9500

C(001)-N(001)-C(005)	121.58(16)
C(001)-N(001)-H(007)	119.2
C(005)-N(001)-H(007)	119.2
O(001)-C(001)-N(001)	123.59(18)
O(001)-C(001)-C(009)	122.89(19)
N(001)-C(001)-C(009)	113.52(17)
C(011)-C(002)-C(005)	116.17(16)
C(011)-C(002)-H(00A)	108.2
C(005)-C(002)-H(00A)	108.2
C(011)-C(002)-H(00B)	108.2
C(005)-C(002)-H(00B)	108.2
H(00A)-C(002)-H(00B)	107.4
C(014)-C(003)-C(006)	115.89(19)
C(014)-C(003)-C(005)	123.28(17)
C(006)-C(003)-C(005)	120.82(18)
F(003)-C(004)-F(002)	106.92(16)
F(003)-C(004)-F(004)	106.97(17)
F(002)-C(004)-F(004)	107.12(16)
F(003)-C(004)-C(005)	112.12(16)
F(002)-C(004)-C(005)	111.47(16)
F(004)-C(004)-C(005)	111.93(16)
N(001)-C(005)-C(004)	105.01(15)
N(001)-C(005)-C(003)	111.05(15)
C(004)-C(005)-C(003)	107.54(16)
N(001)-C(005)-C(002)	111.50(15)
C(004)-C(005)-C(002)	109.28(16)
C(003)-C(005)-C(002)	112.12(15)
C(013)-C(006)-C(003)	121.9(2)
C(013)-C(006)-H(00D)	119.1
C(003)-C(006)-H(00D)	119.1
F(005)-C(014)-C(007)	115.85(18)
F(005)-C(014)-C(003)	120.44(18)
C(007)-C(014)-C(003)	123.71(19)

C(014)-C(007)-C(012)	119.02(19)
C(014)-C(007)-H(00F)	120.5
C(012)-C(007)-H(00F)	120.5
C(011)-C(008)-C(010)	128.1(2)
C(011)-C(008)-H(00G)	115.9
C(010)-C(008)-H(00G)	115.9
C(001)-C(009)-Cl(01)	111.58(15)
C(001)-C(009)-H(00C)	109.3
Cl(01)-C(009)-H(00C)	109.3
C(001)-C(009)-H(00E)	109.3
Cl(01)-C(009)-H(00E)	109.3
H(00C)-C(009)-H(00E)	108.0
C(008)-C(010)-H(00H)	109.5
C(008)-C(010)-H(00I)	109.5
H(00H)-C(010)-H(00I)	109.5
C(008)-C(010)-H(00J)	109.5
H(00H)-C(010)-H(00J)	109.5
H(00I)-C(010)-H(00J)	109.5
C(008)-C(011)-C(002)	125.83(19)
C(008)-C(011)-H(00K)	117.1
C(002)-C(011)-H(00K)	117.1
C(007)-C(012)-C(013)	119.48(19)
C(007)-C(012)-H(00L)	120.3
C(013)-C(012)-H(00L)	120.3
C(006)-C(013)-C(012)	119.99(19)
C(006)-C(013)-H(00M)	120.0
C(012)-C(013)-H(00M)	120.0

Symmetry transformations used to generate equivalent atoms:

Table S4. Anisotropic displacement parameters ($Å^2x10^3$) for C14 H14 Cl F4 N O. The anisotropic displacement factor exponent takes the form: $-2\pi^2[h^2 a^{*2}U^{11} + ... + 2 h k a^* b^* U^{12}]$

	U^{11}	U^{22}	U^{33}	U^{23}	U^{13}	U^{12}
Cl(01)	59(1)	18(1)	37(1)	-2(1)	-8(1)	14(1)

F(002)	36(1)	15(1)	29(1)	-4(1)	-2(1)	4(1)
F(003)	32(1)	21(1)	29(1)	2(1)	-12(1)	5(1)
F(004)	33(1)	24(1)	27(1)	8(1)	6(1)	2(1)
F(005)	23(1)	32(1)	27(1)	-13(1)	2(1)	-7(1)
O(001)	25(1)	19(1)	18(1)	3(1)	-3(1)	-1(1)
N(001)	20(1)	14(1)	13(1)	1(1)	-1(1)	1(1)
C(001)	14(1)	18(1)	19(1)	1(1)	0(1)	-2(1)
C(002)	17(1)	20(1)	18(1)	1(1)	-1(1)	-2(1)
C(003)	17(1)	17(1)	20(1)	1(1)	-2(1)	3(1)
C(004)	21(1)	17(1)	22(1)	-1(1)	0(1)	1(1)
C(005)	18(1)	15(1)	17(1)	-1(1)	-1(1)	1(1)
C(006)	20(1)	22(1)	22(1)	-3(1)	-3(1)	1(1)
C(014)	18(1)	22(1)	23(1)	-1(1)	-3(1)	-1(1)
C(007)	22(1)	31(1)	25(1)	-5(1)	3(1)	3(1)
C(008)	18(1)	28(1)	22(1)	-4(1)	1(1)	-1(1)
C(009)	28(1)	18(1)	22(1)	-1(1)	0(1)	2(1)
C(010)	30(1)	27(1)	30(1)	-1(1)	4(1)	-9(1)
C(011)	20(1)	20(1)	23(1)	-3(1)	-1(1)	2(1)
C(012)	18(1)	32(1)	32(1)	1(1)	7(1)	0(1)
C(013)	19(1)	24(1)	34(1)	-3(1)	-2(1)	-2(1)

Table S5. Hydrogen coordinates ($x10^4$) and isotropic displacement parameters ($Å^2x10^3$) for C14 H14 Cl F4 N O

	x	y	z	U(eq)
H(007)	6178	7230	3434	18
H(00A)	7411	9335	5409	22
H(00B)	7341	7769	5732	22
H(00D)	3894	6432	4408	25
H(00F)	3297	8707	7076	31
H(00G)	10582	8633	4360	27
H(00C)	7251	5175	2988	27
H(00E)	5766	4554	3233	27

H(00H)	8866	10764	5067	43
H(00I)	9792	11009	4212	43
H(00J)	10516	10769	5142	43
H(00K)	8917	7151	4568	25
H(00L)	1678	7052	6622	33
H(00M)	1969	5947	5267	31

Table S6. Torsion angles [°] for C14 H14 Cl F4 N O

C(005)-N(001)-C(001)-O(001)	-2.0(3)
C(005)-N(001)-C(001)-C(009)	177.59(16)
C(001)-N(001)-C(005)-C(004)	177.74(16)
C(001)-N(001)-C(005)-C(003)	-66.3(2)
C(001)-N(001)-C(005)-C(002)	59.5(2)
F(003)-C(004)-C(005)-N(001)	59.6(2)
F(002)-C(004)-C(005)-N(001)	179.39(15)
F(004)-C(004)-C(005)-N(001)	-60.7(2)
F(003)-C(004)-C(005)-C(003)	-58.8(2)
F(002)-C(004)-C(005)-C(003)	61.0(2)
F(004)-C(004)-C(005)-C(003)	-179.00(16)
F(003)-C(004)-C(005)-C(002)	179.28(16)
F(002)-C(004)-C(005)-C(002)	-60.9(2)
F(004)-C(004)-C(005)-C(002)	59.1(2)
C(014)-C(003)-C(005)-N(001)	163.62(17)
C(006)-C(003)-C(005)-N(001)	-17.0(3)
C(014)-C(003)-C(005)-C(004)	-82.0(2)
C(006)-C(003)-C(005)-C(004)	97.4(2)
C(014)-C(003)-C(005)-C(002)	38.1(2)
C(006)-C(003)-C(005)-C(002)	-142.46(18)
C(011)-C(002)-C(005)-N(001)	30.6(2)
C(011)-C(002)-C(005)-C(004)	-85.0(2)
C(011)-C(002)-C(005)-C(003)	155.82(17)
C(014)-C(003)-C(006)-C(013)	-1.7(3)
C(005)-C(003)-C(006)-C(013)	178.84(18)
C(006)-C(003)-C(014)-F(005)	-177.48(17)

C(005)-C(003)-C(014)-F(005)	1.9(3)
C(006)-C(003)-C(014)-C(007)	2.2(3)
C(005)-C(003)-C(014)-C(007)	-178.37(19)
F(005)-C(014)-C(007)-C(012)	178.8(2)
C(003)-C(014)-C(007)-C(012)	-0.9(3)
O(001)-C(001)-C(009)-Cl(01)	-13.2(2)
N(001)-C(001)-C(009)-Cl(01)	167.24(14)
C(010)-C(008)-C(011)-C(002)	-5.2(3)
C(005)-C(002)-C(011)-C(008)	117.5(2)
C(014)-C(007)-C(012)-C(013)	-1.0(3)
C(003)-C(006)-C(013)-C(012)	0.0(3)
C(007)-C(012)-C(013)-C(006)	1.4(3)

Symmetry transformations used to generate equivalent atoms:

3.7.10.2. 2-Chloro-*N*-((*R*)-1,1,1-trifluoro-2-phenyl-3-((4*R*,5*R*)-2,2,5-trimethyl-1,3-dioxolan-4-yl)propan-2-yl)acetamide (3.41) [CCDC #: 1977676]

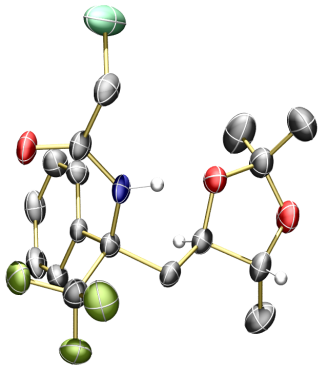

Table S7. Crystal data and structure refinement for C17H21ClF3NO3

Identification code	C17H21ClF3NO3
Empirical formula	C17 H21 Cl F3 N O3
Formula weight	379.80
Temperature	173(2) K
Wavelength	1.54178 ≈
Crystal system	Tetragonal

Space group	$P4_32_12$	
Unit cell dimensions	a = 9.6003(2) ≈	a= 90∞.
	b = 9.6003(2) ≈	b= 90∞.
	c = 41.0420(14) ≈	c = 90∞.
Volume	3782.7(2) ≈^{3}	
Z	8	
Density (calculated)	1.334 Mg/m^3	
Absorption coefficient	2.191 mm^{-1}	
F(000)	1584	
Crystal size	0.460 x 0.370 x 0.220 mm^3	
Theta range for data collection	4.730 to 66.407∞.	
Index ranges	-11<=h<=11, -10<=k<=11, -48<=l<=48	
Reflections collected	40047	
Independent reflections	3300 [R(int) = 0.0240]	
Completeness to theta = 66.407∞	99.2 %	
Absorption correction	Semi-empirical from equivalents	
Max. and min. transmission	0.7528 and 0.6464	
Refinement method	Full-matrix least-squares on F^2	
Data / restraints / parameters	3300 / 1 / 230	
Goodness-of-fit on F^2	1.072	
Final R indices [I>2sigma(I)]	R1 = 0.0298, wR2 = 0.0800	
R indices (all data)	R1 = 0.0304, wR2 = 0.0806	
Absolute structure parameter	0.03(2)	
Extinction coefficient	n/a	
Largest diff. peak and hole	0.224 and -0.342 e.≈$^{-3}$	

Table S8. Atomic coordinates (x10^4) and equivalent isotropic displacement parameters (≈^{2}x10^3) for C17H21ClF3NO3. U(eq) is defined as one third of the trace of the orthogonalized U^{ij} tensor

	x	y	z	U(eq)
Cl(1)	8272(1)	-232(1)	6572(1)	75(1)
F(1)	7089(2)	4861(2)	5913(1)	53(1)
F(2)	8189(2)	6719(2)	6042(1)	53(1)
F(3)	9301(2)	4970(2)	5852(1)	60(1)
N(1)	8919(2)	3293(2)	6364(1)	30(1)

O(1)	6881(2)	2306(2)	6199(1)	41(1)
O(2)	10243(2)	3902(2)	6978(1)	39(1)
O(3)	11605(2)	5220(2)	7316(1)	47(1)
C(1)	8879(2)	843(2)	6254(1)	41(1)
C(2)	8117(2)	2222(2)	6267(1)	32(1)
C(3)	8503(2)	4743(2)	6398(1)	29(1)
C(4)	9769(2)	5538(2)	6542(1)	32(1)
C(5)	9993(2)	5331(2)	6904(1)	32(1)
C(6)	10973(3)	3876(3)	7282(1)	45(1)
C(7)	11304(2)	6026(3)	7032(1)	38(1)
C(8)	11144(3)	7537(3)	7121(1)	54(1)
C(9)	7234(2)	4944(2)	6620(1)	27(1)
C(10)	6834(2)	3907(2)	6835(1)	33(1)
C(11)	5765(2)	4126(3)	7055(1)	41(1)
C(12)	5086(2)	5388(3)	7067(1)	42(1)
C(13)	5489(2)	6434(3)	6862(1)	42(1)
C(14)	6553(2)	6222(2)	6637(1)	35(1)
C(15)	8253(2)	5321(3)	6051(1)	40(1)
C(16)	12072(4)	2763(4)	7257(1)	69(1)
C(17)	9963(3)	3676(4)	7561(1)	76(1)

Table S9. Bond lengths [≈] and angles [∞] for C17H21ClF3NO3

Cl(1)-C(1)	1.762(3)
F(1)-C(15)	1.328(3)
F(2)-C(15)	1.344(3)
F(3)-C(15)	1.338(3)
N(1)-C(2)	1.344(3)
N(1)-C(3)	1.455(3)
N(1)-H(1N)	0.847(19)
O(1)-C(2)	1.222(3)
O(2)-C(5)	1.426(3)
O(2)-C(6)	1.433(3)
O(3)-C(7)	1.428(3)
O(3)-C(6)	1.433(3)

C(1)-C(2)	1.513(3)
C(1)-H(1A)	0.9900
C(1)-H(1B)	0.9900
C(3)-C(9)	1.534(3)
C(3)-C(15)	1.549(3)
C(3)-C(4)	1.551(3)
C(4)-C(5)	1.515(3)
C(4)-H(4A)	0.9900
C(4)-H(4B)	0.9900
C(5)-C(7)	1.519(3)
C(5)-H(5A)	1.0000
C(6)-C(16)	1.505(4)
C(6)-C(17)	1.511(4)
C(7)-C(8)	1.503(4)
C(7)-H(7)	1.0000
C(8)-H(8A)	0.9800
C(8)-H(8B)	0.9800
C(8)-H(8C)	0.9800
C(9)-C(10)	1.384(3)
C(9)-C(14)	1.392(3)
C(10)-C(11)	1.384(3)
C(10)-H(10)	0.9500
C(11)-C(12)	1.376(3)
C(11)-H(11)	0.9500
C(12)-C(13)	1.369(4)
C(12)-H(12)	0.9500
C(13)-C(14)	1.390(3)
C(13)-H(13)	0.9500
C(14)-H(14)	0.9500
C(16)-H(16A)	0.9800
C(16)-H(16B)	0.9800
C(16)-H(16C)	0.9800
C(17)-H(17A)	0.9800
C(17)-H(17B)	0.9800
C(17)-H(17C)	0.9800

C(2)-N(1)-C(3)	127.11(17)
C(2)-N(1)-H(1N)	117.4(17)
C(3)-N(1)-H(1N)	115.3(17)
C(5)-O(2)-C(6)	106.56(17)
C(7)-O(3)-C(6)	108.82(16)
C(2)-C(1)-Cl(1)	109.07(15)
C(2)-C(1)-H(1A)	109.9
Cl(1)-C(1)-H(1A)	109.9
C(2)-C(1)-H(1B)	109.9
Cl(1)-C(1)-H(1B)	109.9
H(1A)-C(1)-H(1B)	108.3
O(1)-C(2)-N(1)	125.0(2)
O(1)-C(2)-C(1)	121.2(2)
N(1)-C(2)-C(1)	113.77(18)
N(1)-C(3)-C(9)	113.35(16)
N(1)-C(3)-C(15)	107.26(16)
C(9)-C(3)-C(15)	112.28(16)
N(1)-C(3)-C(4)	106.99(15)
C(9)-C(3)-C(4)	109.52(15)
C(15)-C(3)-C(4)	107.13(16)
C(5)-C(4)-C(3)	114.81(16)
C(5)-C(4)-H(4A)	108.6
C(3)-C(4)-H(4A)	108.6
C(5)-C(4)-H(4B)	108.6
C(3)-C(4)-H(4B)	108.6
H(4A)-C(4)-H(4B)	107.5
O(2)-C(5)-C(4)	111.05(16)
O(2)-C(5)-C(7)	102.06(16)
C(4)-C(5)-C(7)	113.67(17)
O(2)-C(5)-H(5A)	109.9
C(4)-C(5)-H(5A)	109.9
C(7)-C(5)-H(5A)	109.9
O(2)-C(6)-O(3)	106.05(18)
O(2)-C(6)-C(16)	107.2(2)
O(3)-C(6)-C(16)	110.4(2)
O(2)-C(6)-C(17)	110.4(2)

O(3)-C(6)-C(17)	108.2(2)
C(16)-C(6)-C(17)	114.2(3)
O(3)-C(7)-C(8)	110.26(19)
O(3)-C(7)-C(5)	102.31(17)
C(8)-C(7)-C(5)	115.0(2)
O(3)-C(7)-H(7)	109.7
C(8)-C(7)-H(7)	109.7
C(5)-C(7)-H(7)	109.7
C(7)-C(8)-H(8A)	109.5
C(7)-C(8)-H(8B)	109.5
H(8A)-C(8)-H(8B)	109.5
C(7)-C(8)-H(8C)	109.5
H(8A)-C(8)-H(8C)	109.5
H(8B)-C(8)-H(8C)	109.5
C(10)-C(9)-C(14)	118.11(18)
C(10)-C(9)-C(3)	120.56(17)
C(14)-C(9)-C(3)	120.95(17)
C(11)-C(10)-C(9)	120.8(2)
C(11)-C(10)-H(10)	119.6
C(9)-C(10)-H(10)	119.6
C(12)-C(11)-C(10)	120.6(2)
C(12)-C(11)-H(11)	119.7
C(10)-C(11)-H(11)	119.7
C(13)-C(12)-C(11)	119.3(2)
C(13)-C(12)-H(12)	120.3
C(11)-C(12)-H(12)	120.3
C(12)-C(13)-C(14)	120.6(2)
C(12)-C(13)-H(13)	119.7
C(14)-C(13)-H(13)	119.7
C(13)-C(14)-C(9)	120.5(2)
C(13)-C(14)-H(14)	119.7
C(9)-C(14)-H(14)	119.7
F(1)-C(15)-F(3)	106.86(18)
F(1)-C(15)-F(2)	106.48(19)
F(3)-C(15)-F(2)	105.70(18)
F(1)-C(15)-C(3)	113.74(17)

F(3)-C(15)-C(3)	110.69(19)
F(2)-C(15)-C(3)	112.87(18)
C(6)-C(16)-H(16A)	109.5
C(6)-C(16)-H(16B)	109.5
H(16A)-C(16)-H(16B)	109.5
C(6)-C(16)-H(16C)	109.5
H(16A)-C(16)-H(16C)	109.5
H(16B)-C(16)-H(16C)	109.5
C(6)-C(17)-H(17A)	109.5
C(6)-C(17)-H(17B)	109.5
H(17A)-C(17)-H(17B)	109.5
C(6)-C(17)-H(17C)	109.5
H(17A)-C(17)-H(17C)	109.5
H(17B)-C(17)-H(17C)	109.5

Symmetry transformations used to generate equivalent atoms:

Table S10. Anisotropic displacement parameters ($\approx^2$x 10^3) for C17H21ClF3NO3. The anisotropic displacement factor exponent takes the form: $-2\pi^2[h^2 a^{*2}U^{11} + ... + 2 h k a^* b^* U^{12}]$

	U^{11}	U^{22}	U^{33}	U^{23}	U^{13}	U^{12}
Cl(1)	65(1)	53(1)	108(1)	26(1)	25(1)	11(1)
F(1)	48(1)	68(1)	43(1)	14(1)	-18(1)	-14(1)
F(2)	61(1)	50(1)	49(1)	20(1)	-4(1)	-9(1)
F(3)	55(1)	90(1)	36(1)	8(1)	12(1)	3(1)
N(1)	15(1)	37(1)	37(1)	-5(1)	0(1)	1(1)
O(1)	21(1)	47(1)	55(1)	-6(1)	-6(1)	-2(1)
O(2)	38(1)	41(1)	38(1)	3(1)	-9(1)	-6(1)
O(3)	40(1)	59(1)	42(1)	-1(1)	-12(1)	-9(1)
C(1)	30(1)	39(1)	54(1)	-12(1)	4(1)	-1(1)
C(2)	22(1)	39(1)	34(1)	-6(1)	3(1)	-3(1)
C(3)	21(1)	33(1)	32(1)	2(1)	0(1)	-2(1)
C(4)	22(1)	36(1)	38(1)	1(1)	1(1)	-6(1)
C(5)	24(1)	36(1)	36(1)	-3(1)	2(1)	-4(1)
C(6)	41(1)	56(2)	39(1)	6(1)	-8(1)	-9(1)

C(7)	28(1)	52(1)	36(1)	-4(1)	-1(1)	-10(1)
C(8)	61(2)	52(2)	51(1)	-11(1)	-2(1)	-18(1)
C(9)	18(1)	32(1)	31(1)	0(1)	-3(1)	-1(1)
C(10)	29(1)	34(1)	36(1)	3(1)	1(1)	3(1)
C(11)	36(1)	53(1)	36(1)	5(1)	6(1)	1(1)
C(12)	27(1)	66(2)	34(1)	-8(1)	1(1)	9(1)
C(13)	32(1)	45(1)	47(1)	-12(1)	-9(1)	13(1)
C(14)	29(1)	33(1)	44(1)	4(1)	-6(1)	2(1)
C(15)	34(1)	50(1)	36(1)	6(1)	0(1)	-5(1)
C(16)	66(2)	66(2)	75(2)	14(2)	-25(2)	4(2)
C(17)	70(2)	115(3)	42(1)	11(2)	1(1)	-34(2)

Table S11. Hydrogen coordinates ($x10^4$) and isotropic displacement parameters ($\approx^2x10^3$) for C17H21ClF3NO3

	x	y	z	U(eq)
H(1N)	9780(20)	3130(30)	6393(6)	36
H(1A)	9893	999	6278	49
H(1B)	8712	387	6042	49
H(4A)	10619	5235	6425	39
H(4B)	9644	6545	6499	39
H(5A)	9162	5671	7027	38
H(7)	12075	5917	6870	46
H(8A)	10939	8078	6924	82
H(8B)	10379	7641	7277	82
H(8C)	12010	7876	7219	82
H(10)	7300	3034	6832	39
H(11)	5497	3400	7199	50
H(12)	4344	5530	7217	51
H(13)	5038	7314	6872	50
H(14)	6818	6955	6495	42
H(16A)	12594	2716	7462	103
H(16B)	11628	1862	7215	103

H(16C)	12710	2987	7078	103
H(17A)	10477	3660	7767	114
H(17B)	9293	4445	7563	114
H(17C)	9466	2792	7533	114

Table S12. Torsion angles [∞] for C17H21ClF3NO3

C(3)-N(1)-C(2)-O(1)	-1.6(3)
C(3)-N(1)-C(2)-C(1)	179.40(18)
Cl(1)-C(1)-C(2)-O(1)	-69.5(2)
Cl(1)-C(1)-C(2)-N(1)	109.50(18)
C(2)-N(1)-C(3)-C(9)	54.8(3)
C(2)-N(1)-C(3)-C(15)	-69.8(2)
C(2)-N(1)-C(3)-C(4)	175.58(18)
N(1)-C(3)-C(4)-C(5)	-77.2(2)
C(9)-C(3)-C(4)-C(5)	46.0(2)
C(15)-C(3)-C(4)-C(5)	168.02(18)
C(6)-O(2)-C(5)-C(4)	157.29(17)
C(6)-O(2)-C(5)-C(7)	35.8(2)
C(3)-C(4)-C(5)-O(2)	61.0(2)
C(3)-C(4)-C(5)-C(7)	175.36(18)
C(5)-O(2)-C(6)-O(3)	-22.1(2)
C(5)-O(2)-C(6)-C(16)	-140.1(2)
C(5)-O(2)-C(6)-C(17)	94.9(3)
C(7)-O(3)-C(6)-O(2)	-2.0(2)
C(7)-O(3)-C(6)-C(16)	113.8(2)
C(7)-O(3)-C(6)-C(17)	-120.5(2)
C(6)-O(3)-C(7)-C(8)	146.2(2)
C(6)-O(3)-C(7)-C(5)	23.4(2)
O(2)-C(5)-C(7)-O(3)	-35.9(2)
C(4)-C(5)-C(7)-O(3)	-155.57(18)
O(2)-C(5)-C(7)-C(8)	-155.46(19)
C(4)-C(5)-C(7)-C(8)	84.9(2)
N(1)-C(3)-C(9)-C(10)	18.1(2)
C(15)-C(3)-C(9)-C(10)	139.82(19)

C(4)-C(3)-C(9)-C(10)	-101.3(2)
N(1)-C(3)-C(9)-C(14)	-169.13(17)
C(15)-C(3)-C(9)-C(14)	-47.4(2)
C(4)-C(3)-C(9)-C(14)	71.5(2)
C(14)-C(9)-C(10)-C(11)	1.6(3)
C(3)-C(9)-C(10)-C(11)	174.56(19)
C(9)-C(10)-C(11)-C(12)	-0.7(3)
C(10)-C(11)-C(12)-C(13)	-0.7(3)
C(11)-C(12)-C(13)-C(14)	1.4(3)
C(12)-C(13)-C(14)-C(9)	-0.5(3)
C(10)-C(9)-C(14)-C(13)	-0.9(3)
C(3)-C(9)-C(14)-C(13)	-173.91(18)
N(1)-C(3)-C(15)-F(1)	73.5(2)
C(9)-C(3)-C(15)-F(1)	-51.6(3)
C(4)-C(3)-C(15)-F(1)	-171.89(18)
N(1)-C(3)-C(15)-F(3)	-46.8(2)
C(9)-C(3)-C(15)-F(3)	-171.93(17)
C(4)-C(3)-C(15)-F(3)	67.8(2)
N(1)-C(3)-C(15)-F(2)	-165.02(17)
C(9)-C(3)-C(15)-F(2)	69.8(2)
C(4)-C(3)-C(15)-F(2)	-50.4(2)

Symmetry transformations used to generate equivalent atoms:

Table S13. Hydrogen bonds for C17H21ClF3NO3 [≈ and ∞]

D-H...A	d(D-H)	d(H...A)	d(D...A)	<(DHA)
N(1)-H(1N)...O(1)#1	0.847(19)	2.10(2)	2.913(2)	161(2)

Symmetry transformations used to generate equivalent atoms:

#1 x+1/2,-y+1/2,-z+5/4

3.7.10.3. (*R*,*Z*)-2-chloro-*N*-(1,1,1-trifluoro-2-phenylhex-4-en-2-yl)acetamide (S-2) [CCDC #: 1977675]

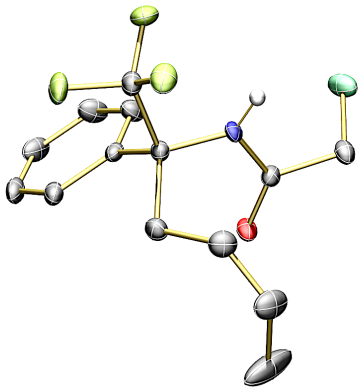

Table S14. Crystal data and structure refinement for C14H15ClF3NO

Identification code	C14H15ClF3NO	
Empirical formula	C14 H15 Cl F3 N O	
Formula weight	305.72	
Temperature	100(2) K	
Wavelength	1.54178 ≈	
Crystal system	Orthorhombic	
Space group	$P2_12_12_1$	
Unit cell dimensions	a = 9.1349(4) ≈	α= 90∞.
	b = 9.3369(4) ≈	β= 90∞.
	c = 17.2799(7) ≈	γ = 90∞.
Volume	1473.83(11) ≈^{3}	
Z	4	
Density (calculated)	1.378 Mg/m^3	
Absorption coefficient	2.573 mm^{-1}	
F(000)	632	
Crystal size	0.600 x 0.380 x 0.260 mm^3	
Theta range for data collection	5.385 to 69.524∞.	
Index ranges	-11<=h<=11, -11<=k<=11, -21<=l<=20	
Reflections collected	18445	
Independent reflections	2753 [R(int) = 0.0258]	
Completeness to theta = 67.679∞	99.5 %	
Absorption correction	Semi-empirical from equivalents	

Max. and min. transmission	0.7532 and 0.6007
Refinement method	Full-matrix least-squares on F^2
Data / restraints / parameters	2753 / 1 / 186
Goodness-of-fit on F^2	1.088
Final R indices [I>2sigma(I)]	R1 = 0.0238, wR2 = 0.0626
R indices (all data)	R1 = 0.0238, wR2 = 0.0626
Absolute structure parameter	0.011(4)
Extinction coefficient	n/a
Largest diff. peak and hole	0.226 and -0.262 e.$\approx^{-3}$

Table S15. Atomic coordinates ($x10^4$) and equivalent isotropic displacement parameters ($\approx^2x10^3$) for C14H15ClF3NO. U(eq) is defined as one third of the trace of the orthogonalized U^{ij} tensor

	x	y	z	U(eq)
Cl(1)	2344(1)	5556(1)	7013(1)	30(1)
F(1)	7180(1)	3967(1)	5982(1)	26(1)
F(2)	8341(1)	3366(1)	7011(1)	24(1)
F(3)	9340(1)	4806(1)	6199(1)	26(1)
O(1)	5285(1)	7473(1)	7680(1)	19(1)
N(1)	5922(2)	5311(2)	7188(1)	14(1)
C(1)	7261(5)	7188(3)	9303(1)	60(1)
C(2)	7551(3)	5679(2)	9063(1)	31(1)
C(3)	8000(2)	5223(2)	8379(1)	21(1)
C(4)	8336(2)	6141(2)	7684(1)	18(1)
C(5)	7395(2)	5764(2)	6957(1)	14(1)
C(6)	5015(2)	6204(2)	7559(1)	15(1)
C(7)	3585(2)	5538(2)	7814(1)	19(1)
C(8)	8066(2)	4474(2)	6537(1)	18(1)
C(9)	7335(2)	6991(2)	6364(1)	16(1)
C(10)	8519(2)	7922(2)	6283(1)	20(1)
C(11)	8491(2)	8990(2)	5719(1)	24(1)
C(12)	7297(3)	9138(2)	5242(1)	28(1)
C(13)	6111(3)	8217(2)	5322(1)	30(1)
C(14)	6131(2)	7142(2)	5879(1)	23(1)

Table S16. Bond lengths [≈] and angles [∞] for C14H15ClF3NO

Cl(1)-C(7)	1.789(2)
F(1)-C(8)	1.341(2)
F(2)-C(8)	1.344(2)
F(3)-C(8)	1.339(2)
O(1)-C(6)	1.228(2)
N(1)-C(6)	1.339(2)
N(1)-C(5)	1.465(2)
N(1)-H(1N)	0.864(19)
C(1)-C(2)	1.492(3)
C(1)-H(1A)	0.9800
C(1)-H(1B)	0.9800
C(1)-H(1C)	0.9800
C(2)-C(3)	1.322(3)
C(2)-H(2)	0.9500
C(3)-C(4)	1.507(3)
C(3)-H(3)	0.9500
C(4)-C(5)	1.562(2)
C(4)-H(4A)	0.9900
C(4)-H(4B)	0.9900
C(5)-C(8)	1.534(2)
C(5)-C(9)	1.538(2)
C(6)-C(7)	1.513(3)
C(7)-H(7A)	0.9900
C(7)-H(7B)	0.9900
C(9)-C(14)	1.390(3)
C(9)-C(10)	1.395(3)
C(10)-C(11)	1.394(3)
C(10)-H(10)	0.9500
C(11)-C(12)	1.375(3)
C(11)-H(11)	0.9500
C(12)-C(13)	1.390(3)
C(12)-H(12)	0.9500
C(13)-C(14)	1.391(3)
C(13)-H(13)	0.9500

C(14)-H(14)	0.9500

C(6)-N(1)-C(5)	121.24(15)
C(6)-N(1)-H(1N)	116.7(16)
C(5)-N(1)-H(1N)	120.1(16)
C(2)-C(1)-H(1A)	109.5
C(2)-C(1)-H(1B)	109.5
H(1A)-C(1)-H(1B)	109.5
C(2)-C(1)-H(1C)	109.5
H(1A)-C(1)-H(1C)	109.5
H(1B)-C(1)-H(1C)	109.5
C(3)-C(2)-C(1)	127.4(2)
C(3)-C(2)-H(2)	116.3
C(1)-C(2)-H(2)	116.3
C(2)-C(3)-C(4)	126.37(19)
C(2)-C(3)-H(3)	116.8
C(4)-C(3)-H(3)	116.8
C(3)-C(4)-C(5)	113.61(15)
C(3)-C(4)-H(4A)	108.8
C(5)-C(4)-H(4A)	108.8
C(3)-C(4)-H(4B)	108.8
C(5)-C(4)-H(4B)	108.8
H(4A)-C(4)-H(4B)	107.7
N(1)-C(5)-C(8)	105.62(14)
N(1)-C(5)-C(9)	111.31(14)
C(8)-C(5)-C(9)	106.44(14)
N(1)-C(5)-C(4)	110.59(14)
C(8)-C(5)-C(4)	109.75(15)
C(9)-C(5)-C(4)	112.79(14)
O(1)-C(6)-N(1)	123.94(17)
O(1)-C(6)-C(7)	121.37(17)
N(1)-C(6)-C(7)	114.69(15)
C(6)-C(7)-Cl(1)	108.58(13)
C(6)-C(7)-H(7A)	110.0
Cl(1)-C(7)-H(7A)	110.0
C(6)-C(7)-H(7B)	110.0

Cl(1)-C(7)-H(7B)	110.0
H(7A)-C(7)-H(7B)	108.4
F(3)-C(8)-F(1)	107.11(14)
F(3)-C(8)-F(2)	106.39(15)
F(1)-C(8)-F(2)	106.06(15)
F(3)-C(8)-C(5)	111.86(15)
F(1)-C(8)-C(5)	112.01(15)
F(2)-C(8)-C(5)	112.98(15)
C(14)-C(9)-C(10)	119.35(17)
C(14)-C(9)-C(5)	120.38(17)
C(10)-C(9)-C(5)	120.20(17)
C(11)-C(10)-C(9)	120.11(19)
C(11)-C(10)-H(10)	119.9
C(9)-C(10)-H(10)	119.9
C(12)-C(11)-C(10)	120.36(19)
C(12)-C(11)-H(11)	119.8
C(10)-C(11)-H(11)	119.8
C(11)-C(12)-C(13)	119.78(18)
C(11)-C(12)-H(12)	120.1
C(13)-C(12)-H(12)	120.1
C(12)-C(13)-C(14)	120.3(2)
C(12)-C(13)-H(13)	119.8
C(14)-C(13)-H(13)	119.8
C(9)-C(14)-C(13)	120.06(19)
C(9)-C(14)-H(14)	120.0
C(13)-C(14)-H(14)	120.0

Symmetry transformations used to generate equivalent atoms:

Table S17. Anisotropic displacement parameters ($\approx^2$x10^3) for C14H15ClF3NO. The anisotropic displacement factor exponent takes the form: $-2\pi^2[h^2 a^{*2}U^{11} + ... + 2 h k a^* b^* U^{12}]$

	U^{11}	U^{22}	U^{33}	U^{23}	U^{13}	U^{12}
Cl(1)	18(1)	32(1)	41(1)	-14(1)	-3(1)	0(1)
F(1)	32(1)	23(1)	22(1)	-10(1)	2(1)	-1(1)

F(2)	28(1)	13(1)	29(1)	2(1)	6(1)	5(1)
F(3)	22(1)	21(1)	35(1)	-1(1)	15(1)	1(1)
O(1)	20(1)	11(1)	25(1)	-1(1)	5(1)	0(1)
N(1)	14(1)	9(1)	17(1)	2(1)	2(1)	-2(1)
C(1)	136(3)	26(1)	19(1)	2(1)	8(2)	11(2)
C(2)	51(1)	21(1)	19(1)	5(1)	-3(1)	1(1)
C(3)	25(1)	18(1)	21(1)	2(1)	-5(1)	4(1)
C(4)	16(1)	19(1)	19(1)	-1(1)	-2(1)	-1(1)
C(5)	14(1)	14(1)	16(1)	-1(1)	2(1)	-1(1)
C(6)	17(1)	12(1)	15(1)	2(1)	1(1)	2(1)
C(7)	18(1)	13(1)	26(1)	0(1)	4(1)	0(1)
C(8)	19(1)	16(1)	21(1)	-1(1)	5(1)	-1(1)
C(9)	21(1)	13(1)	14(1)	-2(1)	4(1)	-1(1)
C(10)	21(1)	17(1)	21(1)	-2(1)	6(1)	-1(1)
C(11)	30(1)	18(1)	26(1)	1(1)	12(1)	-5(1)
C(12)	50(1)	18(1)	17(1)	4(1)	3(1)	-4(1)
C(13)	43(1)	25(1)	21(1)	4(1)	-11(1)	-4(1)
C(14)	28(1)	19(1)	20(1)	2(1)	-4(1)	-6(1)

Table S18. Hydrogen coordinates ($x10^4$) and isotropic displacement parameters ($\approx^2 x\ 10^3$) for C14H15ClF3NO

	x	y	z	U(eq)
H(1N)	5700(30)	4410(20)	7198(13)	18(6)
H(1A)	7336	7819	8852	90
H(1B)	7982	7478	9693	90
H(1C)	6274	7257	9523	90
H(2)	7395	4964	9445	37
H(3)	8124	4219	8319	26
H(4A)	9384	6032	7551	21
H(4B)	8167	7158	7821	21
H(7A)	3167	6087	8251	23
H(7B)	3752	4541	7988	23

H(10)	9345	7828	6613	24
H(11)	9303	9618	5665	29
H(12)	7282	9867	4859	34
H(13)	5283	8323	4994	36
H(14)	5320	6512	5929	27

Table S19. Torsion angles [∞] for C14H15ClF3NO

C(1)-C(2)-C(3)-C(4)	0.6(5)
C(2)-C(3)-C(4)-C(5)	-121.3(2)
C(6)-N(1)-C(5)-C(8)	-178.66(15)
C(6)-N(1)-C(5)-C(9)	-63.5(2)
C(6)-N(1)-C(5)-C(4)	62.7(2)
C(3)-C(4)-C(5)-N(1)	34.3(2)
C(3)-C(4)-C(5)-C(8)	-81.80(19)
C(3)-C(4)-C(5)-C(9)	159.70(16)
C(5)-N(1)-C(6)-O(1)	5.9(3)
C(5)-N(1)-C(6)-C(7)	-175.28(15)
O(1)-C(6)-C(7)-Cl(1)	95.92(19)
N(1)-C(6)-C(7)-Cl(1)	-82.94(17)
N(1)-C(5)-C(8)-F(3)	171.25(14)
C(9)-C(5)-C(8)-F(3)	52.83(19)
C(4)-C(5)-C(8)-F(3)	-69.52(18)
N(1)-C(5)-C(8)-F(1)	50.98(18)
C(9)-C(5)-C(8)-F(1)	-67.44(18)
C(4)-C(5)-C(8)-F(1)	170.21(14)
N(1)-C(5)-C(8)-F(2)	-68.72(18)
C(9)-C(5)-C(8)-F(2)	172.86(15)
C(4)-C(5)-C(8)-F(2)	50.5(2)
N(1)-C(5)-C(9)-C(14)	-26.8(2)
C(8)-C(5)-C(9)-C(14)	87.8(2)
C(4)-C(5)-C(9)-C(14)	-151.82(17)
N(1)-C(5)-C(9)-C(10)	156.11(16)
C(8)-C(5)-C(9)-C(10)	-89.28(19)
C(4)-C(5)-C(9)-C(10)	31.1(2)

C(14)-C(9)-C(10)-C(11)	-0.2(3)
C(5)-C(9)-C(10)-C(11)	176.87(16)
C(9)-C(10)-C(11)-C(12)	0.3(3)
C(10)-C(11)-C(12)-C(13)	-0.1(3)
C(11)-C(12)-C(13)-C(14)	-0.3(3)
C(10)-C(9)-C(14)-C(13)	-0.2(3)
C(5)-C(9)-C(14)-C(13)	-177.27(18)
C(12)-C(13)-C(14)-C(9)	0.5(3)

Symmetry transformations used to generate equivalent atoms:

Table S20. Hydrogen bonds for C14H15ClF3NO [≈ and ∞].

D-H...A	d(D-H)	d(H...A)	d(D...A)	<(DHA)
N(1)-H(1N)...O(1)#1	0.864(19)	2.03(2)	2.879(2)	166(2)

Symmetry transformations used to generate equivalent atoms:

#1 -x+1, y-1/2, -z+3/2

Chapter Four

Multicomponent Additions to Nitriles for Synthesis of Nitrogen-Containing Heterocycles

4.1. Introduction

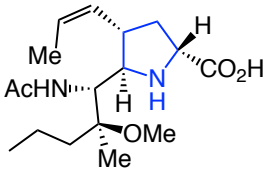

A-315675
antiviral

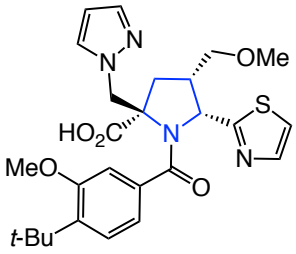

GSK 625433
anti-hepatitis C

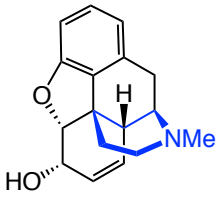

morphine
narcotic, pain relief

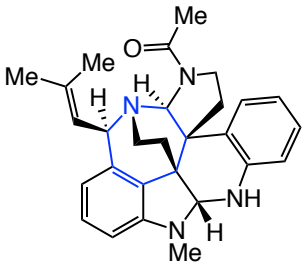

(–)-communesin F
anti-leukemia

Amines are prevalent in nature, from amino acids, nucleic acids, and neurotransmitters, to natural products, medicines, dyes, and insecticides.[236] In particular, enantioenriched nitrogen-containing heterocycles can be found in many natural products and biologically active molecules and as a result, strategies that allow for their synthesis are desirable. Methods to access cyclic amines either require lengthy syntheses or require the use of a cyclic amine precursor, often from the chiral pool. Approaches designed to offer access to nitrogen-containing heterocycles from readily available, inexpensive or, ideally, feedstock starting materials would be particularly valuable, enhancing the efficiency with which these sought-after fragments are synthesized.

[236] (a) Hager, A.; Vrielink, N.; Hager, D.; Lefranc, J.; Trauner, D. *Nat. Prod. Rep.* **2016**, *33*, 491–522. (b) Zha, G.-F.; Rakesh, K. P.; Manukumar, H. M.; Shantharam, C. S.; Long, S. *Eur. J. Med. Chem.* **2019**, *162*, 465–494.

4.2. Background

4.2.1. Synthesis of Cyclic Amines

A common way to synthesize cyclic amines is by a Pictet-Spengler reaction. The first catalytic enantioselective variant was reported by Jacobsen in 2004 utilizing activated acylated imine substrates and a thiourea-based catalyst.[237] In 2006, List *et al.* reported a method for the synthesis of tryptamines from unprotected H_2N-amine starting materials (**4.1**) using a chiral phosphoric acid catalyst (Scheme 4.1).[238] Shortly thereafter, Hiemstra *et al.* applied the method to the synthesis of several natural products and developed a complementary method using a TRIP ligand.[239] In 2009 and 2010, Dixon *et al.* disclosed the results of mechanistic investigations, which arose from their application of cascade reactions to natural product synthesis.[240] In 2011, Bernardi, Bencivenni, and Franz outlined a series of related spirocyclizations. That same year, Tian *et al.* utilized the approach for synthesis of benzazapines.[241] The abovementioned Pictet-Spengler

---

[237] (a) Taylor, M. S.; Jacobsen, E. N. *J. Am. Chem. Soc.* **2004**, *126*, 10558–10559. (b) Doyle, A. G.; Jacobsen, E. N. *Chem. Rev.* **2007**, *107*, 5713–5743. (c) Raheem, I. T.; Thiara, P. S.; Peterson, E. A.; Jacobsen, E. N. *J. Am. Chem. Soc.* **2007**, *129*, 13404–13405. (d) Mergott, D. J.; Zuend, S. J.; Jacobsen, E. N. *Org. Lett.* **2008**, *10*, 745–748. (e) Raheem, I. T.; Thiara, P. S.; Jacobsen, E. N. *Org. Lett.* **2008**, *10*, 1577–1580. (f) Peterson, E.A.; Jacobsen, E. N. *Angew. Chem., Int. Ed.* **2009**, *48*, 6328–633. (g) Klausen, R. S.; Jacobsen, E. N. *Org. Lett.* **2009**, *11*, 887–890. (h) Knowles, R.R.; Lin, S.; Jacobsen, E. N. *J. Am. Chem. Soc.* **2010**, *132*, 5030–5032. (i) Lee, Y.; Klausen, R. S.; Jacobsen, E. N. *Org. Lett.* **2011**, *13*, 5564–5567.

[238] Seayad, J.; Seayad A. M.; List, B. *J. Am. Chem. Soc.* **2006**, *128*, 1086–1087.

[239] (a) Wanner, M. J.; van der Haas, R. N. S.; de Cuba, K. R.; van Maarseveen J. H.; Hiemstra, H. *Angew. Chem., Int. Ed.* **2007**, *46*, 7485–7487. (b) Sewgobind, N. V.; Wanner, M. J.; Ingemann, S.; de Gelder, R.; van Maarseveen J. H.; Hiemstra, H. *J. Org. Chem.* **2008**, *73*, 6405–6408. (c) Wanner, M. J.; Boots, R. N. A.; Eradus, B.; de Gelder, R.; van Maarseveen J. H.; Hiemstra, H. *Org. Lett.* **2009**, *11*, 2579–2581. (d) Herle, B.; Wanner, M. J.; van Maarseveen, J. H.; Hiemstra, H. *J. Org. Chem.* **2011**, *76*, 8907–8912. (e) Wanner, M. J.; Claveau, E.; van Maarseveen, J. H.; Hiemstra, H. *Chem. Eur. J.* **2011**, *17*, 13680–13683. (f) Mons, E.; Wanner, M. J.; Ingemann, S.; van Maarseveen, J. H.; Hiemstra, H. *J. Org. Chem.* **2014**, *79*, 7380–7390. (g) Ruiz-Olalla, A.; Würdemann, M. A.; Wanner, M. J.; Ingemann, S.; van Maarseveen, J. H.; Hiemstra, H. *J. Org. Chem.* **2015**, *80*, 5125–5132.

[240] (a) Muratore, M. E.; Holloway, C. A.; Pilling, A. W.; Storer, R. I.; Trevitt G.; Dixon, D. J. *J. Am. Chem. Soc.* **2009**, *131*, 10796–10797. (b) Holloway, C. A.; Muratore, M. E.; Storer, R. I.; Dixon, D. J. *Org. Lett.* **2010**, *12*, 4720–4723.

[241] Cheng, D.-J.; Wu, H.-B.; Tian, S.-K. *Org. Lett.* **2011**, *13*, 5636–5639.

methods have major limitations, however. The substrates must be indole-based, the newly formed ring is restricted to a six- or seven-membered ring, and the reactions can take up to five days.

Scheme 4.1. Pictet-Spengler Approach to Synthesis of Cyclic Amines

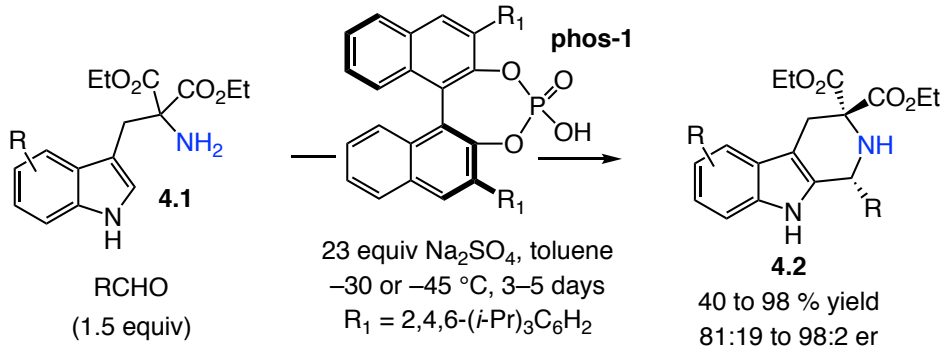

Limitations:
- Restricted to indole-containing molecules
- New ring can only be 6-membered
- Long reaction times

Cyclic amines can also be synthesized by way of hydroamination, often in an intramolecular fashion. In 2007, Toste *et al.* reported the first catalytic enantioselective variant using bisphosphine–Au(I) complexes to generate both pyrrolidines (**4.4**, Scheme 4.2a) and piperidines (**4.4**, Scheme 4.2b).[242] Soon after, many reports of similar transformations[243] involving the use of different catalysts, including copper-[244], palladium-[245], titanium-[246], zirconium-[247], and

[242] LaLonde, R. L.; Sherry, B. D.; Kang, E. J.; Toste, F. D. *J. Am. Chem. Soc.* **2007**, *129*, 2452–2453.

[243] (a) Chiarucci, M.; Bandini, M. *Beilstein J. Org. Chem.* **2013**, *9*, 2586–2614. (b) Michon, C.; Medina, F.; Abadie, M.-A.; Agbossou-Niedercorn, F. *Organometallics* **2013**, *32*, 5589–5600. (c) Li, H.; Lee, S. D.; Widenhoefer, R. A. *J. Organomet. Chem.* **2011**, *696*, 316–320.

[244] Turnpenny, B. W.; Hyman, K. L.; Chemler, S. R. *Organometallics* **2012**, *31*, 7819–7822.

[245] Adamson, N. J.; Hull, E.; Malcolmson, S. J. *J. Am. Chem. Soc.* **2017**, *139*, 7180–7183.

[246] Sha, F.; Mitchell, B. S.; Ye, C. Z.; Abelson, C. S.; Reinheimer, E. W.; LeMagueres, P.; Ferrara, J. D.; Takase, M. K.; Johnson, A. R. *Dalton Trans.* **2019**, *48*, 9603–9616.

[247] Manna, K.; Xu, S.; Sadow, A. D. *Angew. Chem., Int. Ed.* **2011**, *50*, 1865–1868.

lanthanide-based[248] complexes, as well as non-organometallic[249] promoters were introduced. Two major drawbacks of these hydroamination methods are the use of precious metal salts and the requirement for *N*-protected amine substrates, the synthesis of which can require up to five steps and seven days.

Scheme 4.2. Catalytic Enantioselective Intramolecular Hydroamination

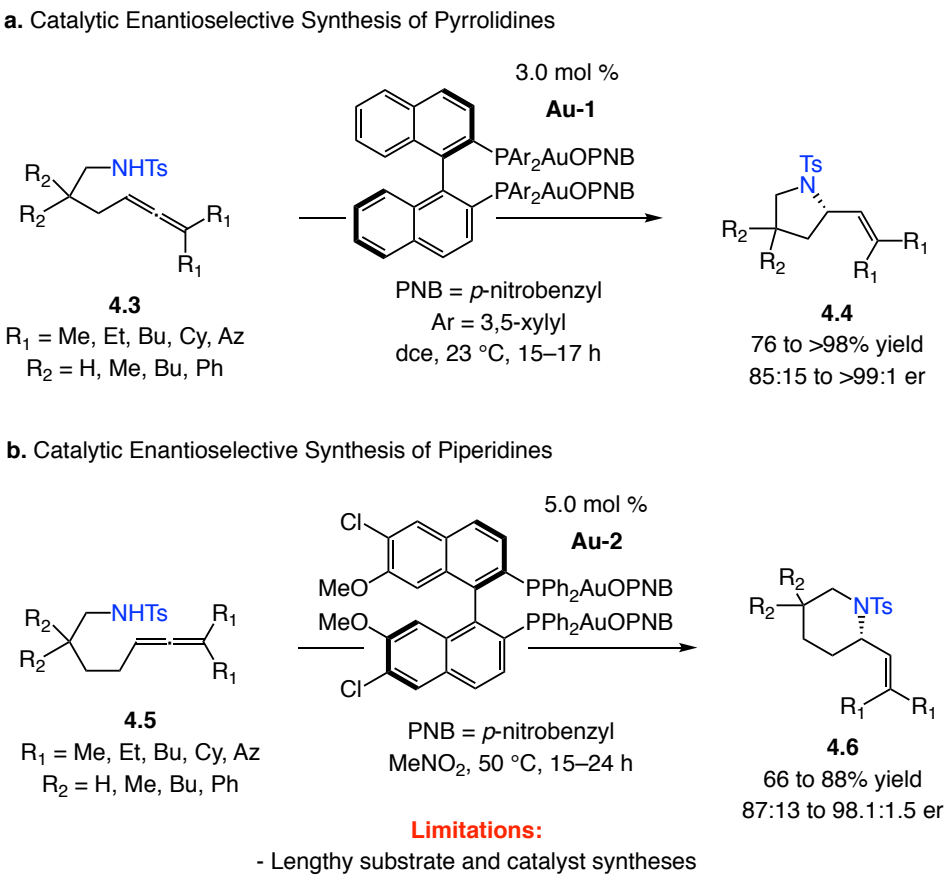

In 2017, Bower *et al.* disclosed the first catalytic enantioselective aza-Heck cyclization catalyzed by a SPINOL–Pd complex to afford cyclic imine (**4.8**), which upon reduction, was

[248] (a) Queffelec, C.; Boeda, F.; Pouilhès, A.; Meddour, A.; Kouklovsky, C.; Hannedouche, J.; Collin, J.; Schulz, E. *ChemCatChem* **2011**, *3*, 122–126. (b) Chapurina, J.; Ibrahim, H.; Guillot, R.; Kolodziej, E.; Collin, J.; Trifonov, A.; Schulz, E.; Hannedouche, J. *J. Org. Chem.* **2011**, *76*, 10163–10172.

[249] (a) Ogata, T.; Ujihara, A.; Tsuchida, S.; Shimizu, T.; Kaneshige, A.; Tomioka, K. *Tetrahedron Lett.* **2007**, *48*, 6648–6650. (b) Ogata, T.; Kimachi, T.; Yamada, K.; Yamamoto, Y.; Tomioka, K. *Heterocycles* **2012**, *86*, 469–485.

converted to a pyrrolidine (**4.10**) enantioselectively (Scheme 4.3).[250] High reaction temperature (80–120 °C) was required, however, and the ensuing reduction proceeded with low diastereoselectivity.

Scheme 4.3. Aza-Heck Cyclization for Enantioselective Preparation of Pyrrolidines

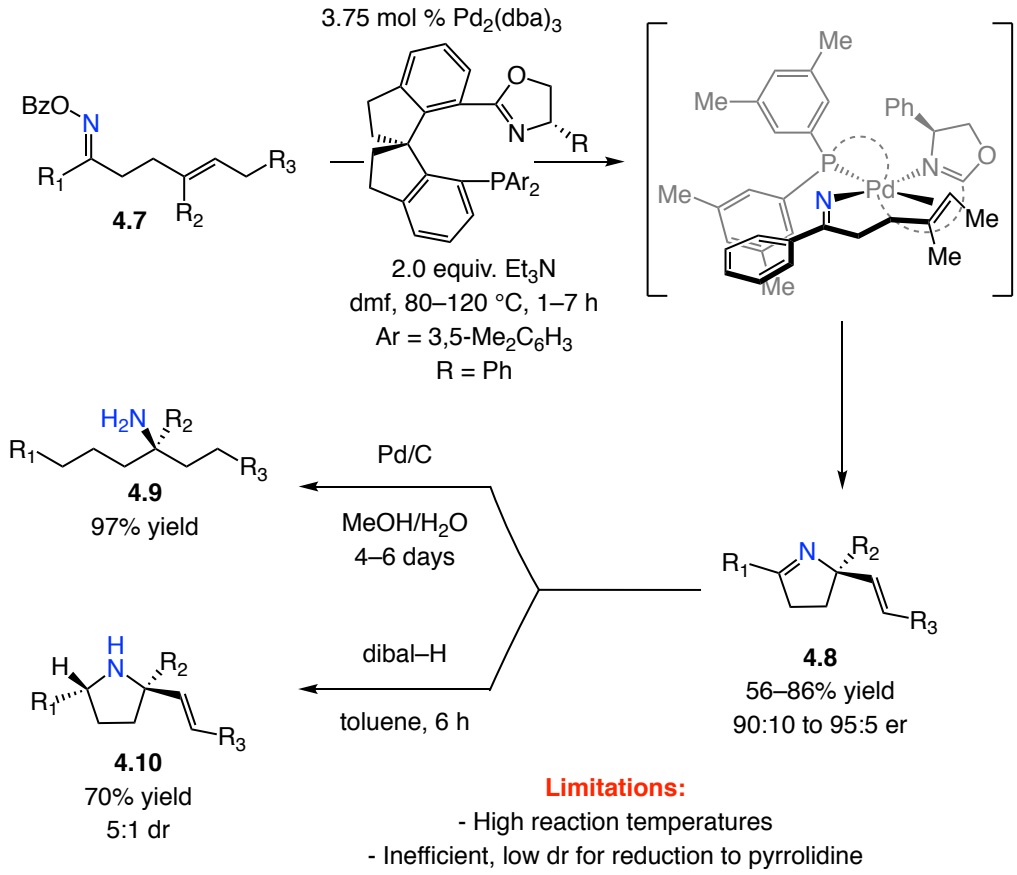

A four-reaction/single-vessel proline-catalyzed Mannich-type cyclization that delivers cyclic amines was outlined by Kumar *et al.,* who used the strategy to prepare a piperidine-based

[250] (a) Race, N. J.; Faulkner, A.; Fumagalli, G.; Yamaguchi, T.; Scott, J. S.; Rydén-Landergren, M.; Sparkes, H. A.; Bower, J. F. *Chem. Sci.* **2017**, 8, 1981–1985. (b) Race, N. J.; Hazelden, I. R.; Faulkner, A.; Bower, J. F. *Chem. Sci.* **2017**, *8*, 5248–5260. (c) Ma, X.; Hazelden, I. R.; Langer, T.; Munday, R. H.; Bower, J. F. *J. Am. Chem. Soc.* **2019**, *141*, 3356–3360.

GABA reuptake inhibitor (**4.12**, Scheme 4.4a).[251] Mannich-type cyclizations have also been used to synthesize [5,5]-, [5,6]-, [6,6]-, and [6,7]-fused ring systems.

Scheme 4.4. Catalytic Enantioselective Mannich-Type Cyclizations

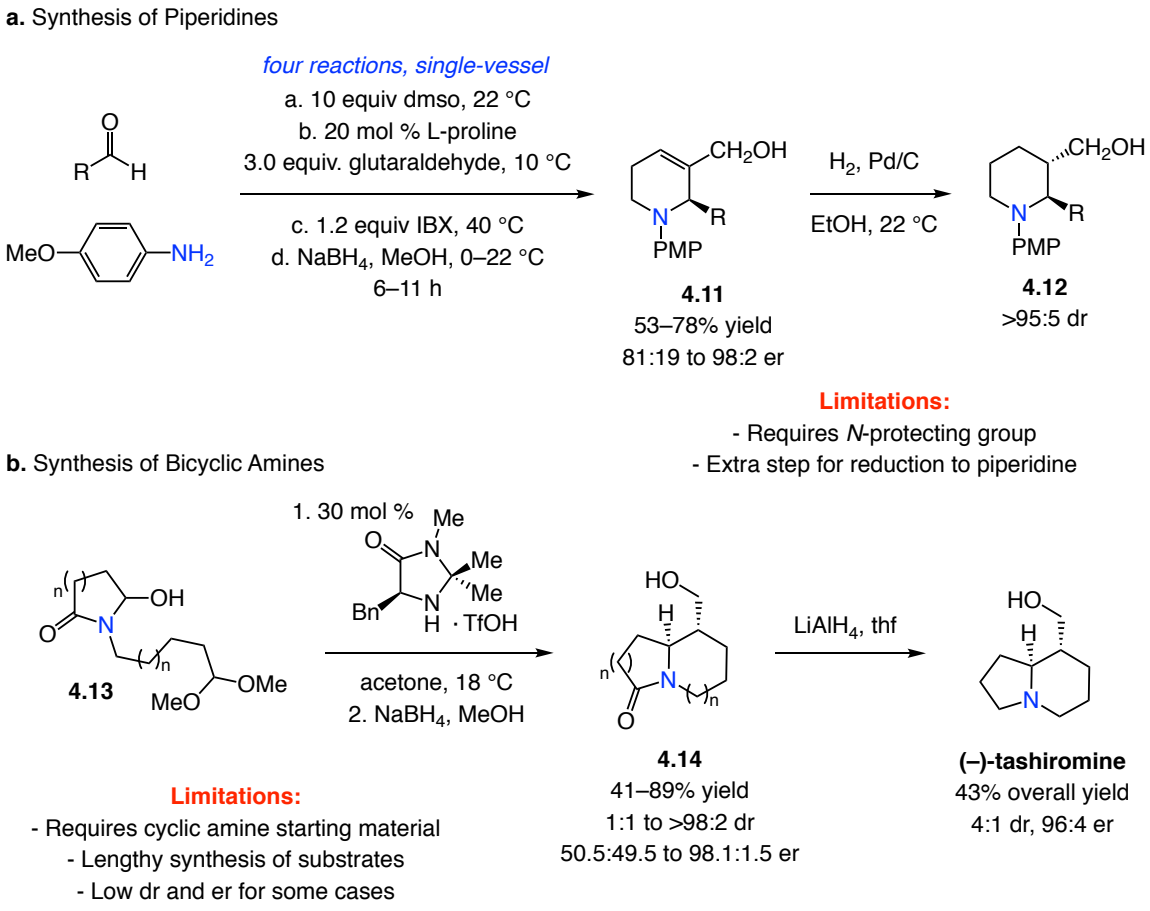

A report from Koley *et al.* (2014) involved the use of an imidazolidinone-based enamine catalyst, which was subsequently applied to the synthesis of three natural products (Scheme 4.4b).[252] The requisite cyclic amine starting materials require up to five steps to prepare, and only bicyclic products can be synthesized.

[251] Ramaraju, P.; Mir, N. A.; Singh, D.; Kumar, I. *RSC Adv.* **2016**, *6*, 60422–60432.

[252] Koley, D.; Krishna, Y.; Srinivas, K.; Khan, A. A.; Kant, R. *Angew. Chem., Int. Ed.* **2014**, *53*, 13196–13200.

It is worth noting that the Dixon group at the University of Oxford has published several catalytic enantioselective cascade processes that generate cyclic amines; these reactions were later applied to complex molecule synthesis.[253] There are a number of recently developed catalytic enantioselective cycloaddition[254], annulation[255], and cyclization[256] processes that are limited in scope. Other strategies include cyclization[257], cycloaddition[258], ring expansion[259], and reduction of the corresponding aromatic heterocycles, however, these methods are not enantioselective.[260]

Despite the abovementioned advances, several key issues in the current state-of-the-art remain unaddressed. Strategies are needed that obviate the use protection/deprotection sequences, precious metals and/or difficult-to-access ligands, are complete within a few hours, and can be performed at ambient temperature. Substrates should be easily accessible and the desired products should be obtained directly, without an additional reduction step. Equally importation, a catalytic enantioselective approach must be reasonably broad in scope (i.e., offer access to pyrrolidines, piperidines, and azepanes).

---

[253] (a) Gabriel, P.; Gregory, A. W.; Dixon D. J. *Org. Lett.* **2019**, *21*, 6658–6662. (b) Leitch, J. A.; Fuentes de Arriba, A. L.; Tan, J.; Hoff, O.; Martinez, C. M.; Dixon D. J. *Chem. Sci.* **2018**, *9*, 6653–6658. (c) Manzano, R.; Datta, S.; Paton, R. S.; Dixon, D. J. *Angew. Chem., Int. Ed.* **2017**, *56*, 5834–5838. (d) Gammack Yamagata, A. D.; Datta, S.; Jackson, K. E.; Stegbauer, L.; Paton, R. S.; Dixon, D. J. *Angew. Chem., Int. Ed.* **2015**, *54*, 4899–4903. (e) Gregory, A. W.; Chambers, A.; Hawkins, A.; Jakubec, P.; Dixon, D. J. *Chem. Eur. J.* **2015**, *21*, 111–114. (f) Barber, D. M.; Duriš, A; Thompson, A. L.; Sanganee, H. J.; Dixon, D. J. *ACS Catal.* **2014**, *4*, 634–638. (g) Gregory, A. W.; Jakubec, P.; Turner, P.; Dixon, D. J. *Org. Lett.* **2013**, *15*, 4330–4333. (h) Duriš, A.; Barber, D. M.; Sanganee H. J.; Dixon, D. J. *Chem. Commun.* **2013**, *49*, 2777–2779.

[254] Arai, T.; Yokoyama, N.; Mishiro, A.; Sato, H. *Angew. Chem., Int. Ed.* **2010**, *49*, 7895–7898.

[255] Kramer, S.; Fu, G. C. *J. Am. Chem. Soc.* **2015**, *137*, 3803–3806.

[256] Struble, T. J.; Lankswert, H. M.; Pink, M.; Johnston, J. N. *ACS Catal.* **2018**, *8*, 11926–11931.

[257] (a) Ebule, R.; Mudshinge, S.; Nantz, M. H.; Mashuta, M. S.; Hammond, G. B.; Xu, B. *J. Org. Chem.* **2019**, *84*, 3249–3259. (b) Marcotullio, M. C.; Campagna, V.; Sternativo, S.; Costantino, F.; Curini, M. *Synthesis* **2006**, 2760–2766. (c) Minakata, S; Morino, Y.; Oderaotoshi, Y.; Komatsu, M. *Org. Lett.* **2006**, *8*, 3335–3337. (d) Gandon, L. A.; Russel, A. G.; Güveli, T.; Brodwolf, A. E.; Kariuki, B. M.; Spencer, N.; Snaith, J. S. *J. Org. Chem.* **2006**, *71*, 5198–5207.

[258] Han, M.-Y.; Jia, J.-Y.; wang, W. *Tetrahedron Lett.* **2014**, *55*, 784–794.

[259] Métro, T.-X.; Pardo, D. G.; Cossy, J. *J. Org. Chem.* **2007**, *72*, 6556–6561.

[260] (a) Maegawa, T.; Akashi, A. Sajiki, H. *Synlett* **2006**, 1440-1442. (b) Zhou, Q.; Zhang, L.; Meng, W.; Feng, X.; Yang, J.; Du, H. *Org. Lett.* **2016**, *18*, 5189–5191.

4.2.2. Multicatalytic Additions to Imines or Nitriles for Synthesis of α-Secondary and α-Tertiary Amines

In 2017, our group reported a multicomponent, catalytic, diastereo- and enantioselective addition to ketimines to afford homoallylic α-tertiary amines (**4.16**, Scheme 4.5).[261] The ketimine salts (**4.15**) were generated by the addition of an organolithium reagent to a nitrile. Although the multicomponent method is efficient and affords α-tertiary amines in high enantiomeric purity, we wondered whether there was a way to use the nitrile directly and generate the ketimine in situ.

Scheme 4.5. Multicomponent Additions to NH-Ketimines

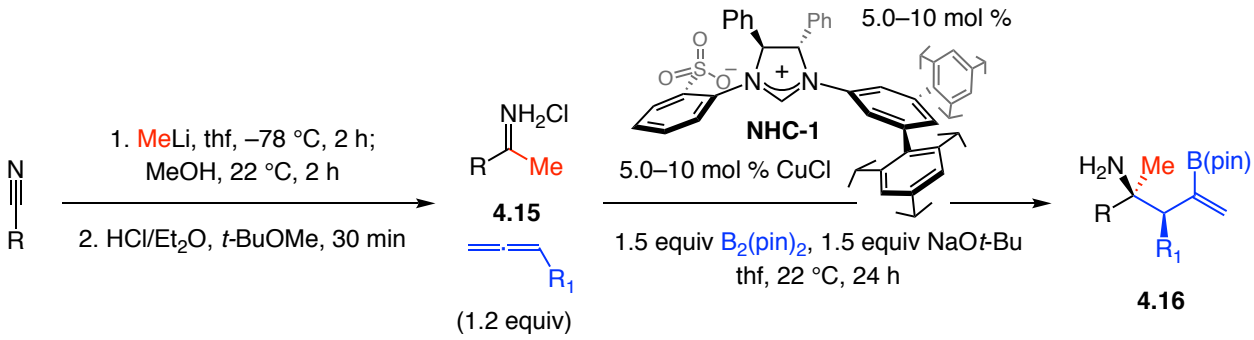

In 2019, we reported just that. Using readily available nitrile feedstock starting materials, we performed a multicomponent, catalytic, diastereo-, and enantioselective addition to give ketimine **4.17**, followed by an in situ reduction to afford the corresponding α-secondary amines (**4.18**, Scheme 4.6).[262] The NH-ketimine intermediate may be modified in other ways (vs in situ reduction).[263] For instance, hydrolysis of the ketimine by aqueous workup affords the

[261] Jang, H.; Romiti, F.; Torker, S.; Hoveyda, A. H. *Nat. Chem.* **2017**, 9, 1269–1275.

[262] Zhang, S.; del Pozo, J.; Romiti, F.; Mu, Y.; Torker, S.; Hoveyda, A. H. *Science* **2019**, *364*, 45–51.

[263] Zhang, S. C.; del Pozo, J.; Xu, S.; Conger, R.; Hoveyda, A. H., manuscript in preparation.

corresponding ketone, which can undergo subsequent reduction or addition of carbon-based nucleophiles to afford different homoallylic alcohols.[264]

Scheme 4.6. Diastereo- and Enantioselective Catalytic Multicomponent Additions to Nitriles

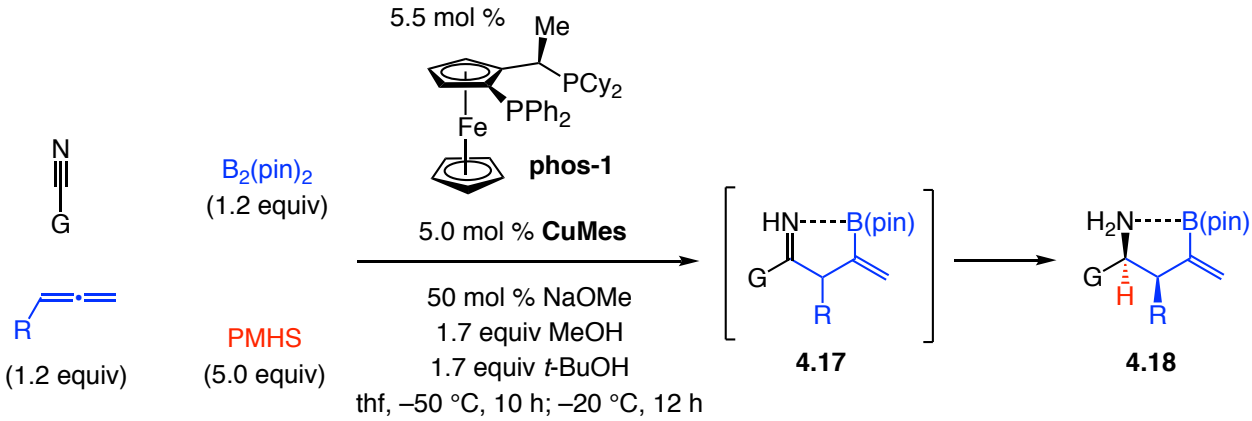

After detailed mechanistic studies, it was proposed that reaction proceeds through a dual catalytic cycle with Cu–B(pin) and Cu–H complexes present simultaneously (Scheme 4.7). The reactivities of the two catalysts are competitive, with the Cu–H complex forming and reacting faster. However, to form the desired products efficiently, the Cu–B(pin) complex must react first. A non-productive side cycle was therefore incorporated to obtain the desired order of events. Thus, under optimal conditions, the Cu–O*t*-Bu precursor (**i**) is first converted to the Cu–B(pin) complex (**ii**), which adds to the allene to afford allyl–Cu intermediate (**iii**), which in turn reacts with the nitrile to furnish Cu–ketimine (**iv**). The Cu–O*t*-Bu complex (**i**) is subsequently regenerated by protonolysis of Cu–ketimine (**iv**) to form NH-ketimine (**v**). Concurrently, the Cu–H complex (**vi**) is occupied within the delay loop by *t*-BuOH. When NH-ketimine (**v**) becomes available, the Cu–H complex (**vi**) readily reduces the NH-ketimine to deliver the H_2N-amine (**viii**), after

[264] Zhang, S. C.; del Pozo, J.; Xu, S.; Conger, R.; Hoveyda, A. H., manuscript in preparation.

protonolysis. The efficiency and diastereoselectivity for the reduction are likely due to the internal N=C→B coordination, as evidenced by ^{11}B NMR: δ 9.7 ppm (i.e., tetra-coordinate boron).

Scheme 4.7. Delayed Catalyst Function in Multicomponent Additions to Nitriles

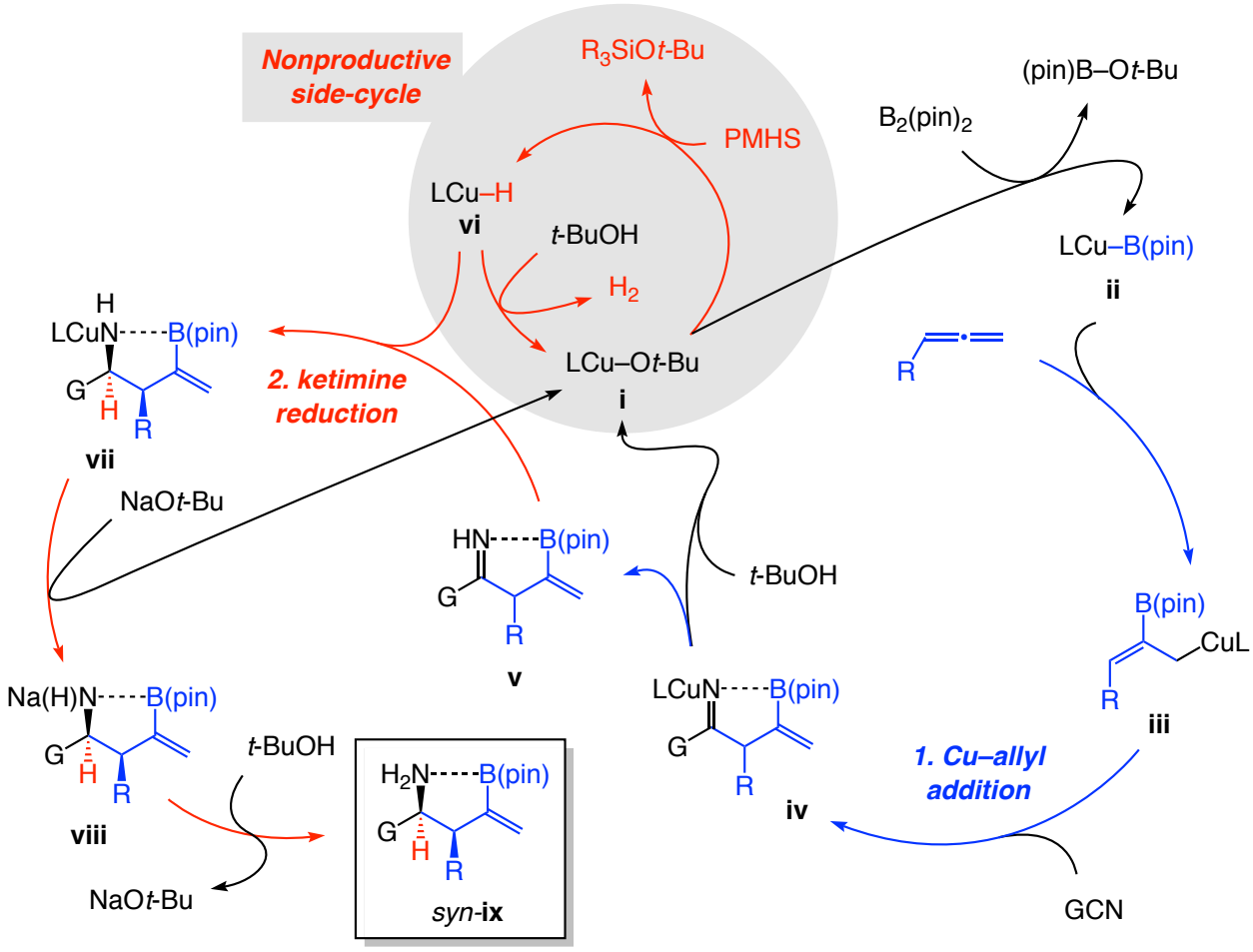

A variety of nitriles (aryl, allyl, alkenyl, alkyl, heterocyclic, and hindered) and allenes (alkoxy-, alkyl-, ester-, aryl-, alkenyl-substituted) proved to be suitable substrates, providing access to a considerable array of H_2N-amine products. The catalytic strategy was applied to a

nine-step enantioselective total synthesis of the naturally occurring anticancer agent, (+)-tangutorine (28% overall yield versus 26 steps and 10% overall yield, previously[265]).

4.2.3. Alternative Disconnections and Their Limitations

We reasoned that by using the two-catalyst multicomponent strategy, we could convert nitriles to cyclic amines by a single operation. For instance, Cu–allyl addition to commercially available haloalkyl nitrile substrate (**4.19**, Scheme 4.8a) might afford NH-ketimine **4.20**, which would undergo intramolecular cyclization to the cyclic NH-ketimine (**4.21**). Ensuing reduction would deliver cyclic amine (**4.22**).

Scheme 4.8. Multicatalytic/Multicomponent Enantioselective Synthesis of Cyclic NH-Amines

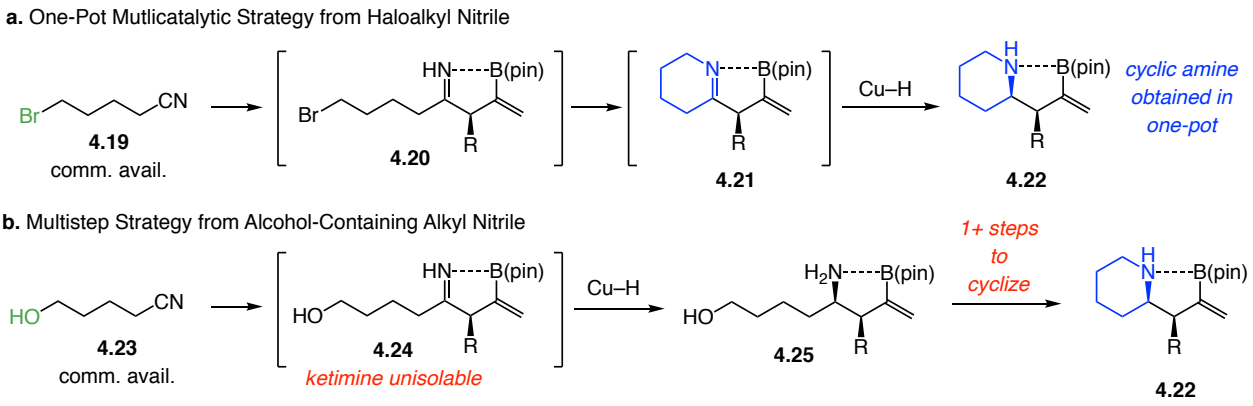

Another starting point would involve an alcohol-containing alkyl nitrile (e.g., **4.23**), which could undergo addition/reduction en route to the desired cyclic NH-amine (**4.25**). However, this would require additional steps in order to afford the cyclic amine at a later stage (Scheme 4.8b). In fact, this approach has been utilized by Christmann *et al.*[266] Starting from the appropriate

[265] Nemoto, T.; Yamamoto, E.; Franzén, R.; Fukuyama, T.; Wu, R.; Fukumachi, T.; Kobayashi, H.; Hamada, Y. *Org. Lett.* **2010**, *12*, 872–875.

[266] de Figueiredo, R. M.; Fröhlich, R.; Christmann, M. *J. Org. Chem.* **2006**, *71*, 4147–4154.

aldehyde, enantioselective Mannich dimerization was used to generate a *N*-PMB α-secondary amine bearing a β-stereogenic center. Subsequent removal of the silyl protecting group, azetidines, pyrrolidines, and piperidines were generated. However, cyclization conditions were strongly oxidizing and may not be applicable to comparatively sensitive complex molecules. Another possible approach would involve alcohol-to-bromide conversion followed by cyclization, but acidic conditions would be required, limiting applicability.

A related approach has been reported by Nagib *et al.* regarding catalytic enantioselective δ C–H-to-C–N transformations (**4.26**, Scheme 4.9). Subsequent cyclization afforded a piperidine with high enantiospecificity (es) (**4.28**).[267] Although the approach is enantioselective, involves readily available materials, and is performed at ambient temperatures, it is limited to preparation of piperidines that are substituted solely at C3.

Scheme 4.9. Enantioselective Conversion of Nitriles to Piperidines

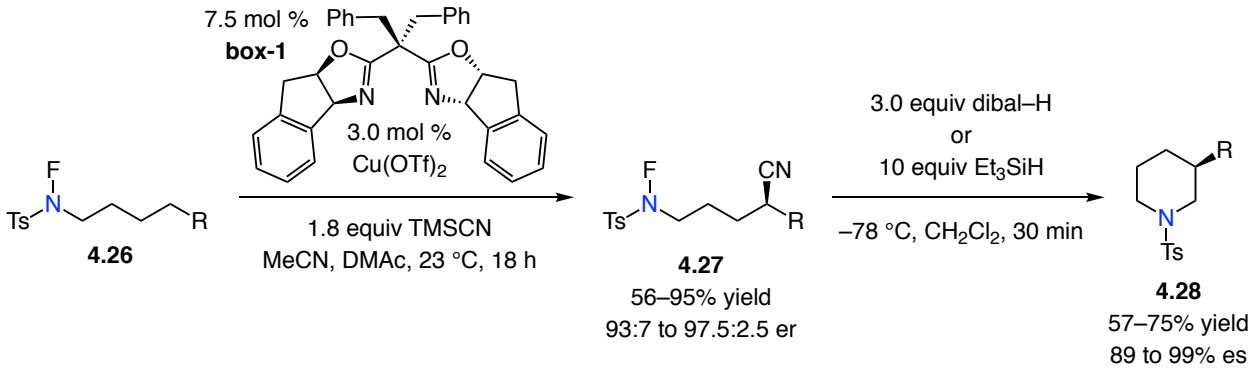

To summarize, we envisioned an approach entailing the use of a commercially available nitrile to deliver readily modifiable cyclic NH-amines after a single operation. What is more, we would be able to access α-tertiary amines by excluding PMHS and using a carbon-based nucleophile.

---

[267] Zhang, Z.; Zhang, X.; Nagib, D. A. *Chem* **2019**, *5*, 3127–3134.

4.3. Identification of Optimal Conditions and Substrate Scope

4.3.1. Condition Optimization

Screening of the conditions formerly used for the multicomponent addition to nitriles afforded cyclic amine product **4.29a** in >98% conversion and >98:2 diastereomeric ratio (dr) (Scheme 4.10). Examination of the ^{11}B NMR spectrum of **4.29a** revealed that there was indeed N→B chelation (δ 23.2 ppm, ^{11}B NMR) consistent with a cyclic amine.[268]

Scheme 4.10. Initial Data. Enantioselective Conversion of a Nitrile to a Cyclic NH-Amine[a]

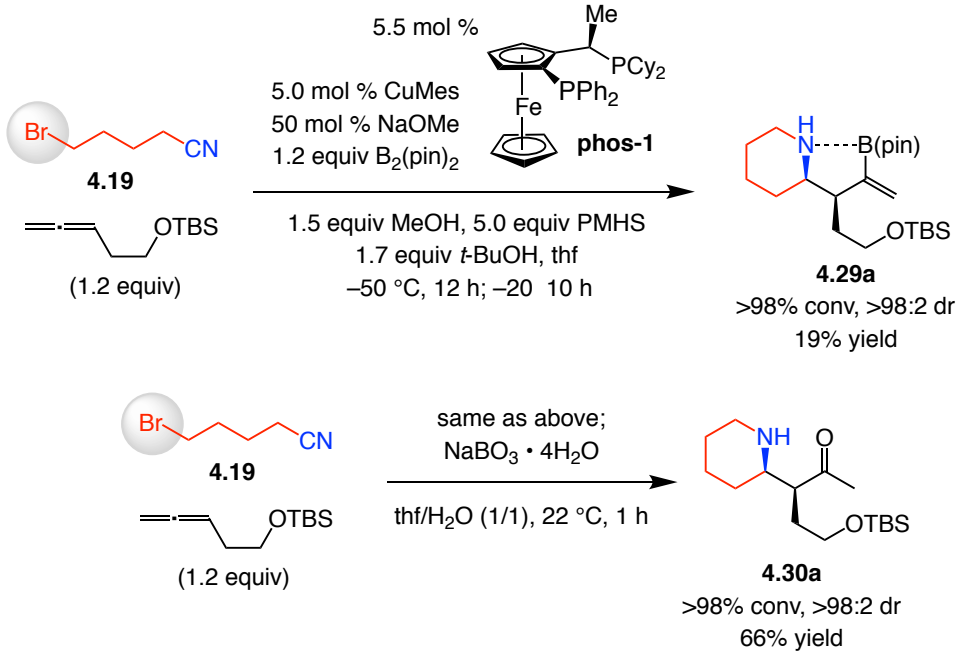

[a] All reactions performed under N_2 atmosphere. Conversion and diastereomeric ratio determined by analysis of ^{1}H NMR spectra of unpurified mixtures; conv (±2%). Yield of isolated and purified material (±5%). Enantioselectivity determined by HPLC analysis (±1%). See Experimental Section for details.

Early attempts at purification resulted in low yields (<30%) owing to the increased polarity of alkyl amines. The initial alkenyl–B(pin) compound was obtained after silica gel

[268] (a) Wrackmeyer, B. in Nuclear Magnetic Resonance Spectroscopy of Boron Compounds Containing Two-, Three-, and Four-Coordinate Boron, Academic Press Limited, 1988, pp 93. (b) Kliegel, W. *J. Organomet. Chem.* **1983**, *253*, 9–16.

chromatography (100:1.5:0.4→100:6.0:0.2). Oxidation of the alkenyl–B(pin) afforded ketone **4.30a**, which is more robust and its purification more straightforward.

4.3.2. Future Plans Regarding Substrate Scope

Several different alkyl nitriles, varying by alkyl chain length, are commercially available allowing access to pyrrolidines (**4.31**), piperidines (**4.29**), and azepanes (**4.32**) (Scheme 4.11). A variety of allenes will be prepared and used to synthesize products containing β-tertiary and β-quaternary stereogenic centers (i.e., a disubstituted allene may be converted to **4.29c**).

Scheme 4.11. Proposed Scope of Pyrrolidine, Piperidine, and Azepane Products

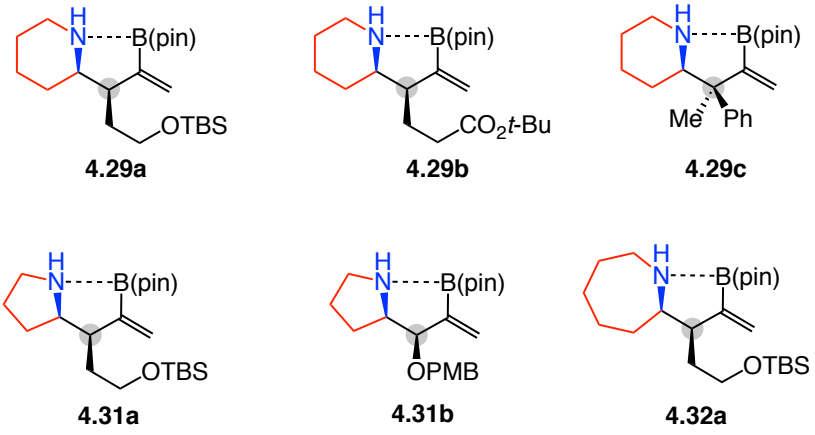

Ester-containing nitriles are expected to allow access to enantiomerically enriched lactams (after reduction; **4.34a**, Scheme 4.12). Catalytic enantioselective transformations that lead to other ring sizes, found in bioactive natural products, will be developed as well.[269]

[269] (a) Saldívar-González, F. I.; Lenci, E.; Trabocchi, A.; Medina-Franco, J. L. *RSC Adv.* **2019**, *9*, 27105–27116. (b) Caruano, J.; Muccioli, G. G.; Robiette, R. *Org. Biomol. Chem.* **2016**, *14*, 10134–10156. (c) Pitts, C. R.; Leckta, T. *Chem. Rev.* **2014**, *114*, 7930–7953.

Scheme 4.12. Proposed Synthesis of Lactams

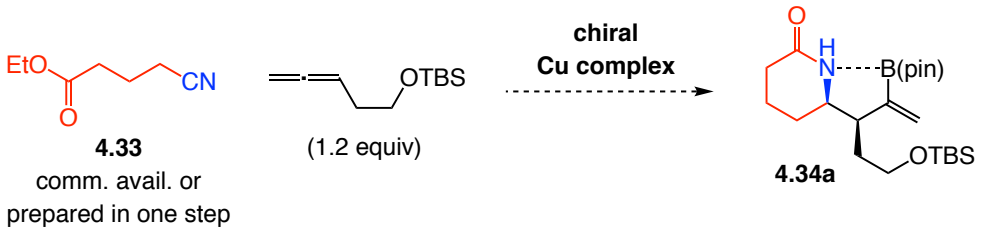

4.3.3. *Syn*- or *Anti*-Selective Reductions

Catalytic enantioselective approaches that are diastereodivergent are highly valuable, but relatively uncommon.[270] For example, in drug discovery research, the ability to access various possible stereoisomers of a candidate is important. Our group has recently developed diastereodivergent reductions of NH-ketimines using either chelation-controlled or Felkin–Anh additions (Scheme 4.13).[262]

Scheme 4.13. Diastereodivergent Reduction of an In Situ Generated Cyclic NH-Ketimine[a]

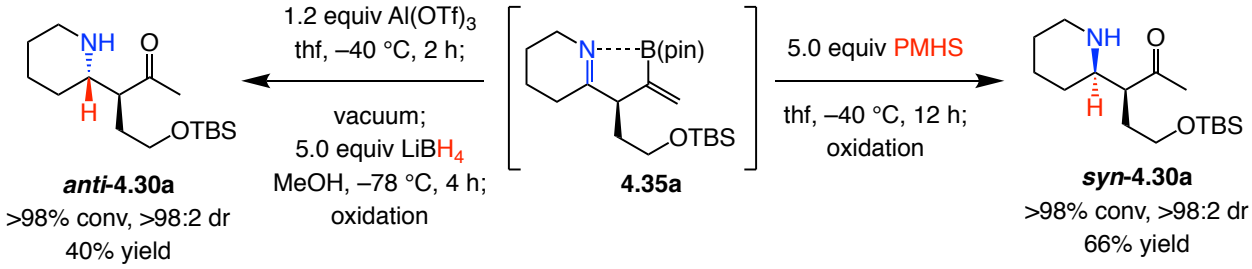

[a] All reactions performed under N_2 atmosphere. Conversion and diastereomeric ratio determined by analysis of ^1H NMR spectra of unpurified mixtures; conv (±2%). Yield of isolated and purified material (±5%). Enantioselectivity determined by HPLC analysis (±1%). See Experimental Section for details.

Catalytic reduction of **4.35a**, in which the imine is coordinated to the neighboring B(pin) unit, affords ***syn*-4.30a** as a single diastereomer. Alternatively, addition of $Al(OTf)_3$ disrupts

[270] (a) Krautwalk, S.; Sarlah, D.; Schafroth, M. A. Carreira, E. M. *Science* **2013**, *340*, 1065–1068. (b) Krautwalk, S.; Carreira, E. M. *J. Am. Chem. Soc.* **2017**, *139*, 5627–5639. (c) Zhang, S.; del Pozo, J.; Romiti, F.; Mu, Y.; Torker, S.; Hoveyda, A. H. *Science* **2019**, *364*, 45–51.

C=N→B coordination, allowing ketimine reduction to occur through a Felkin-Anh-type transition state to afford ***anti*-4.30a** as a single diastereomer.

4.4. Summary and Outlook

In summary, we have taken the first steps towards the development of a broadly applicable method for catalytic enantioselective synthesis of cyclic NH-amines that contain tertiary and quaternary β-stereogenic carbon centers. Reactions are promoted by readily available catalysts and ligands and use commercially available or readily accessible alkyl nitriles and allenes as substrates. Once the full range of suitable nitriles and allenes is established, the utility of the approach will be tested in the context of application to a concise enantioselective synthesis of a bioactive alkaloid.

4.5. Experimental Section

4.5.1. Experimental

4.5.1.1. General

Infrared (IR) spectra were recorded on a Bruker alpha spectrophotometer, λ_{max} in cm^{-1}. Bands are characterized as broad (br), strong (s), medium (m), and weak (w). ^{1}H NMR spectra were recorded on a Varian Unity INOVA 400 (400 MHz) spectrometer. Chemical shifts are reported in ppm from tetramethylsilane with the solvent resonance as the internal standard ($CDCl_3$: δ 7.26 ppm). Data are reported as follows: chemical shift, integration, multiplicity (s = singlet, d = doublet, t = triplet, q = quartet, sept = septet, br = broad, m = multiplet), and coupling constants (Hz). ^{13}C NMR spectra were recorded on a Varian Unity INOVA 400 (100 MHz) with complete proton decoupling. Chemical shifts are reported in ppm from tetramethylsilane with the solvent resonance as the internal standard ($CDCl_3$: δ 77.16 ppm). Data are reported as follows: chemical shift, multiplicity (singlet unless otherwise noted), and coupling constants (Hz). High-resolution mass spectrometry was performed on a JEOL AccuTOF-DART (positive mode) at the Mass Spectrometry Facility, Boston College.

4.5.1.2. Solvents

Unless otherwise noted, reactions were carried out with distilled and degassed solvents under an atmosphere of dry N_2 in oven- (135 °C) or flame-dried glassware with standard dry box or vacuum-line techniques. Solvents were purified under a positive pressure of dry argon by a modified Innovative Technologies purification system. Tetrahydrofuran (thf; Aldrich Chemical Co.) was purified by distillation from sodium benzophenone ketyl immediately prior to use unless otherwise specified. $CDCl_3$ was purchased from Cambridge Isotope Laboratories and stored over activated 4Å molecular sieves prior to use. All work-up and purification procedures were carried out with reagent grade solvents (purchased from Fisher Scientific, Inc.) in air.

4.5.1.3. Reagents

Aluminum trifluoromethanesulfonate was purchased from Aldrich and used as received.

Bis(pinacolato)diboron (B_2pin_2) was purchased from Frontier, recrystallized from hexanes and dried under vacuum prior to use.

5-Bromovaleronitrile was purchased from Combi Blocks and used as received.

Copper(I) chloride was purchased from Strem and used as received.

(*R*)-1-[(S_P)-2-(Diphenylphosphino)ferrocenyl]ethyldicyclohexylphosphine (phos-1) was purchased from Strem and used as received.

Imidazole was purchased from Oakwood and used as received.

Lithium borohydride (2.0 M in thf) was purchased from Sigma-Aldrich and used as received.

Mesitylcopper(I) was prepared according to previously reported procedures.[271]

Methanol was purchased from Fisher Scientific, dried over Mg turnings and distilled prior to use.

Paraformaldehyde was purchased from Aldrich and used as received.

Polymethylhydrosiloxane (**PMHS**) was purchased from Alfa Aesar and used as received.

Propargyl alcohol was purchased from Aldrich and used as received.

---

[271] (a) Tsuda, T.; Yazawa, T.; Watanabe, K.; Fujii, T.; Saegusa, T. *J. Org. Chem.* **1981**, *46*, 192–194. (b) Stollenz, M.; Meyer, F. *Organometallics* **2012**, *31*, 7708–7727.

Sodium methoxide was purchased from Strem and used as received.

Sodium perborate tetrahydrate was purchased from Oakwood and used as received.

***tert*-Butanol** was purchased from Aldrich, dried over Mg turnings and distilled prior to use.

***tert*-Butyldimethylsilyl chloride** was purchased from Oakwood and used as received.

4.5.2. Procedures for Multicomponent Additions to Nitriles for Synthesis of Cyclic Amines

4.5.2.1. For synthesis of *syn*-4.29a

In a N_2-filled glove box, an oven-dried one-dram vial containing a magnetic stir bar was charged with **phos-1** (3.1 mg, 0.0055 mmol), CuMes (0.9 mg, 0.0050 mmol) and thf (0.5 mL). The vial was sealed with a Teflon cap and the solution was allowed to stir at 22 °C for 10 min. Methanol (5.5 mg, 0.17 mmol) was added and the mixture was allowed to stir for an additional 10 min at 22 °C. At this point, NaOMe (2.7 mg, 0.050 mmol) was added and the vial was resealed and allowed to cool to –50 °C, followed by drop-wise addition of a solution containing $B_2(pin)_2$ (30.5 mg, 0.120 mmol), nitrile **4.19** (16.2 mg, 0.100 mmol), allene (23.8 mg, 0.120 mmol), *t*-BuOH (12.3 mg, 0.166 mmol), PMHS (30.0 mg, 0.500 mmol), and thf (0.4 mL). The mixture was allowed to stir at –50 °C for 12 h, at which time the vial placed in a –20 °C freezer and allowed to stand for 10 h. The reaction was quenched by passing the mixture through a short plug of celite and silica gel, followed by elution with 10:1 Et_2O:MeOH (2x10 mL). The filtrate was concentrated in vacuo to afford yellow oil, which was purified by silica gel chromatography [CH_2Cl_2:MeOH:HCO_2H 100:1.5:0.4 until all the pinacol was removed as judged by thin layer chromatography (tlc), followed by 100:6.0:0.2].

NOTE: The silica gel used must be flushed with 2% v/v solution of formic acid in CH_2Cl_2 (3x3 mL). To remove the formic acid, the samples containing the desired product (as judged by tlc analysis) were collected and allowed to stir over solid K_2CO_3 (500 mg) for 15 min. The suspension was filtered through a short plug of sand and the volatiles were removed in vacuo to afford yellow oil and white solid. Diethyl ether (5 mL) was added and the suspension was filtered through a pad of celite. Removal of the volatiles in vacuo afforded ***syn*-4.29a** as yellow oil.

(*R*)-2-((*R*)-5-((*tert*-Butyldimethylsilyl)oxy)-2-(4,4,5,5-tetramethyl-1,3,2-dioxaborolan-2-yl)pent-1-en-3-yl)piperidine (4.29a): Yellow oil, 7.7 mg, 19% yield, 0.019 mmol; **IR (neat):** 3276 (w), 2930 (s), 1711 (s), 1669 (m), 1454 (m), 1370 (m), 1252 (m), 1095 (m), 837 (w) cm^{-1}; **^{11}B NMR (192 MHz, $CDCl_3$):** δ 23.19; **HRMS (DART):** Calcd for $C_{22}H_{45}BNO_3Si$ $[M+H]^+$: 410.3256; Found: 410.3257.

4.5.2.2. For synthesis of *syn*-4.30a

In a N_2-filled glove box, an oven-dried one-dram vial containing a magnetic stir bar was charged with **phos-1** (3.1 mg, 0.0055 mmol, 5.5 mol %), CuMes (0.9 mg, 0.0050 mmol, 5.0 mol %) and thf (0.5 mL). The vial was sealed with a Teflon cap and the solution was allowed to stir at 22 °C for 10 min. Methanol (5.5 mg, 0.17 mmol, 1.7 equiv) was added and the mixture was allowed to stir for an additional 10 min at 22 °C. At this point, NaOMe (2.7 mg, 0.050 mmol, 50 mol %) was added and the vial was resealed and allowed to cool to –50 °C, followed by drop-wise addition of a solution containing $B_2(pin)_2$ (30.5 mg, 0.120 mmol, 1.2 equiv), nitrile **4.19** (16.2 mg, 0.100 mmol, 1.0 equiv), allene (23.8 mg, 0.120 mmol, 1.2 equiv), *t*-BuOH (12.3 mg, 0.166 mmol, 1.7 equiv), PMHS (30.0 mg, 0.500 mmol, 5.0 equiv), and thf (0.4 mL). The mixture was allowed to stir at –50 °C for 12 h, at which time the vial placed in a –20 °C freezer and allowed to stand for 10 h. The reaction was quenched by passing the mixture through a short plug of celite and silica gel, followed by elution with 10:1 Et_2O:MeOH (2x10 mL). The filtrate was concentrated in vacuo to afford ***syn*-4.29a** as yellow oil. Unpurified ***syn*-4.29a** was dissolved in 1:1 thf:H_2O (1 mL) and then $NaBO_3 \cdot 4H_2O$ (77 mg, 5.0 equiv) was added and the mixture allowed to stir at 22 °C for 1 h. The reaction was quenched by the addition of water (1 mL) and extracted with Et_2O (2x2 mL). The organic layers were combined, dried over $MgSO_4$, and concentrated in vacuo to afford orange oil. The residue was purified by silica gel chromatography with 10:1 Et_2O:MeOH (2x10 mL) followed by 10:1 CH_2Cl_2:MeOH (2x10 mL). Removal of the volatiles in vacuo afforded ***syn*-4.30a** as orange oil.

(*S*)-5-((*tert*-Butyldimethylsilyl)oxy)-3-((*R*)-piperidin-2-yl)pentan-2-one (*syn*-4.30a): Orange oil, 19.8 mg, 66% yield, 0.066 mmol; **IR (neat):** 3267 (w), 2951 (m), 2854 (m), 1708 (w), 1470 (m), 1253 (m), 1096 (s), 833 (s), 772 (s), 660 (m) cm^{-1}; **^{1}H NMR (400 MHz, $CDCl_3$):** δ 3.68–3.59 (m, 1H), 3.57–3.49 (m, 1H), 2.20 (s, 1H), 1.66–1.55 (m, 3H), 1.46 (d, J = 13.8 Hz, 2H), 1.43 (s, 1H), 1.39–1.32 (m, 1H), 1.27–1.25 (m, 2H), 1.25 (s, 3H), 1.25–1.18 (m, 2H), 0.88 (d, J = 4.5 Hz, 9H), 0.12 to –0.03 (m, 6H); **HRMS (DART):** Calcd for $C_{16}H_{34}NO_2Si$ $[M+H]^+$: 300.2348; Found: 300.2353.

4.5.2.3. For synthesis of *anti*-4.30a

In a N_2-filled glove box, an oven-dried one-dram vial containing a magnetic stir bar was charged with **phos-1** (3.1 mg, 0.0055 mmol, 5.5 mol %), CuMes (0.9 mg, 0.0050 mmol, 5.0 mol %) and Et_2O (0.5 mL). The vial was sealed with a Teflon cap and the solution was allowed to stir at 22 °C for 10 min. Methanol (5.5 mg, 0.17 mmol, 1.7 equiv) was added and the mixture was allowed to stir for an additional 10 min at 22 °C. At this point, a solution containing $B_2(pin)_2$ (30.5 mg, 0.120 mmol, 1.2 equiv), nitrile **4.19** (16.2 mg, 0.100 mmol, 1.0 equiv), allene (23.8 mg, 0.120 mmol, 1.2 equiv), and Et_2O (0.4 mL) was added in a drop-wise manner. The mixture was allowed

to stir at –40 °C for 10 h, at which time $Al(OTf)_3$ (56.9 mg, 0.120 mmol, 1.2 equiv) was added and the mixture allowed to stir at –40 °C for 2 h. The volatiles were then removed in vacuo and the resulting residue was dissolved in MeOH (0.8 mL) and cooled to –78 °C in a dry ice/acetone bath. $LiBH_4$ (0.25 mL, X mmol, 5.0 equiv) was added dropwise at –78 °C and the mixture was allowed to stir at –78 °C for 4 h. The reaction was quenched by addition of saturated aqueous ammonium chloride (1.0 mL) and potassium sodium tartrate (1.0 mL) and allowed to stir at 22 °C for 30 minutes. The organic layer was separated and the aqueous layer was subsequently extracted with CH_2Cl_2 (2x5 mL). The organic layers were combined and dried over $MgSO_4$, and concentrated in vacuo to afford ***anti*-4.29a** as yellow oil. Unpurified ***anti*-4.29a** was dissolved in 1:1 thf:H_2O (1 mL) and then $NaBO_3 \cdot 4H_2O$ (77 mg, 5.0 equiv) was added and the mixture allowed to stir at 22 °C for 1 h. The reaction was quenched by the addition of water (1 mL) and extracted with Et_2O (2x2 mL). The organic layers were combined, dried over $MgSO_4$, and concentrated in vacuo to afford orange oil. The residue was purified by silica gel chromatography with 10:1 Et_2O:MeOH (2x10 mL) followed by 10:1 CH_2Cl_2:MeOH (2x10 mL). Removal of the volatiles in vacuo afforded ***anti*-4.30a** as orange oil.

(*S*)-5-((*tert*-Butyldimethylsilyl)oxy)-3-((*S*)-piperidin-2-yl)pentan-2-one (*anti*-4.30a): Orange oil, 12.1 mg, 40% yield, 0.040 mmol; **IR (neat):** 3308 (w), 2926 (m), 1709 (w), 1446 (m), 1251 (m), 1047 (m), 832 (s), 775 (s), 619 (w) cm^{-1}; **^{1}H NMR (400 MHz, $CDCl_3$):** δ 4.28 (s, 1H), 3.65–3.48 (m, 5H), 2.41 (t, *J* = 6.8 Hz, 3H), 1.99–1.90 (m, 2H), 1.90–1.80 (m, 2H), 1.62 (br s, 1H), 1.43–1.31 (m, 2H), 0.90 (s, 9H), 0.09 (s, 6H); **HRMS (DART):** Calcd for $C_{16}H_{34}NO_2Si$ $[M+H]^+$: 300.2354; Found: 300.2353.

4.5.3. NMR Spectra

NMR spectra appear on the following pages:

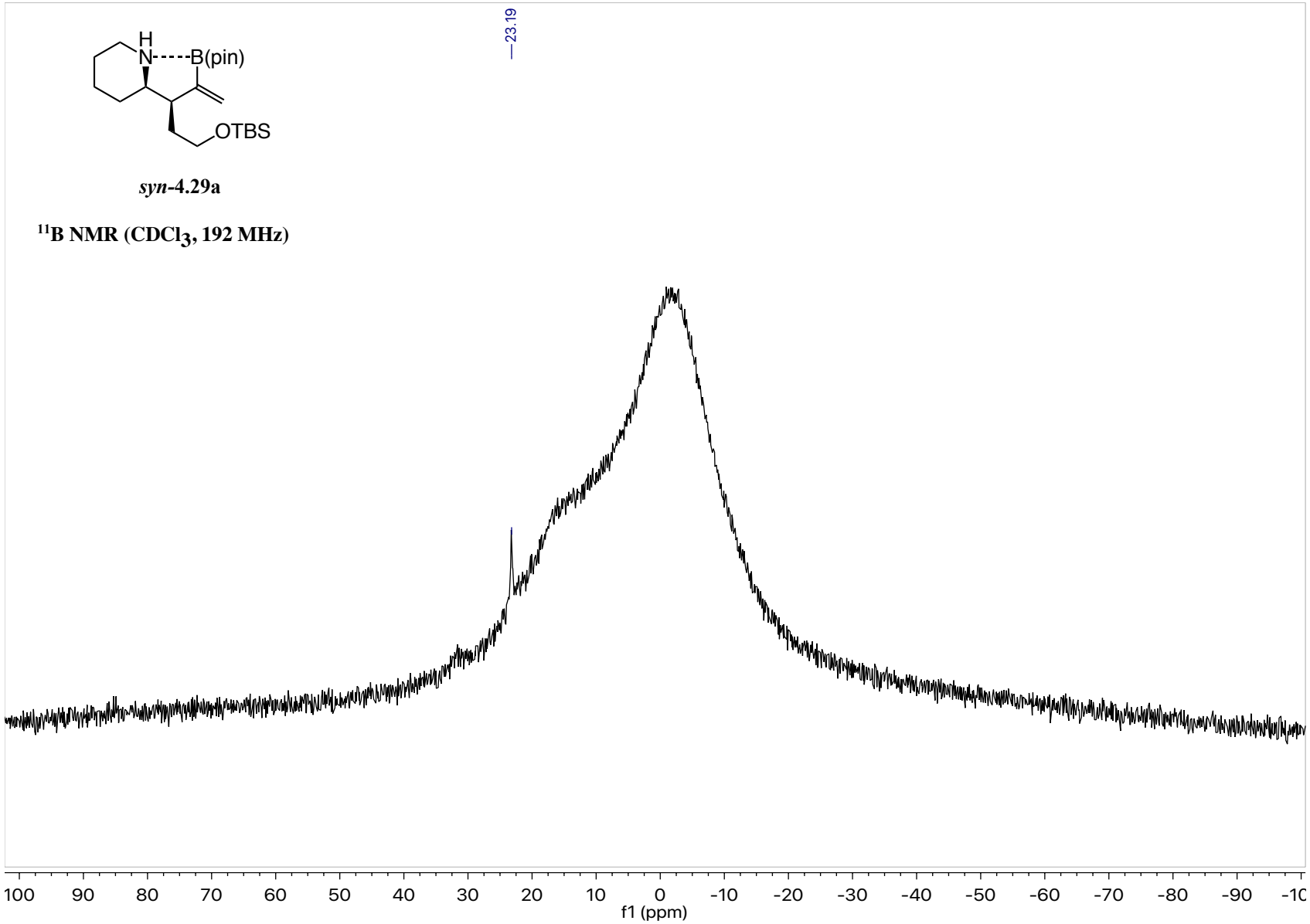

***syn*-4.29a**

^{11}B NMR ($CDCl_3$, 192 MHz)

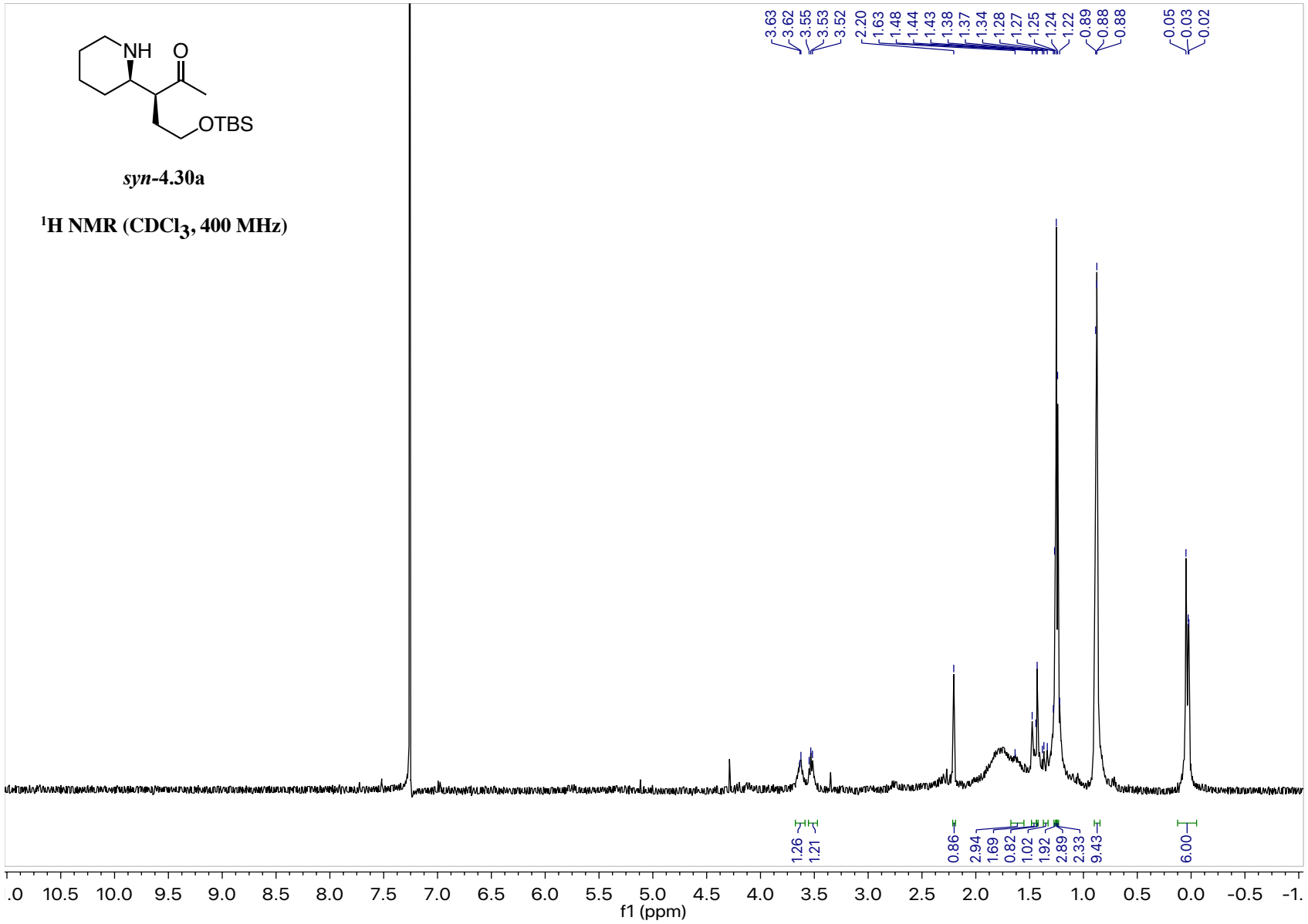

syn-4.30a

^{1}H NMR ($CDCl_3$, 400 MHz)

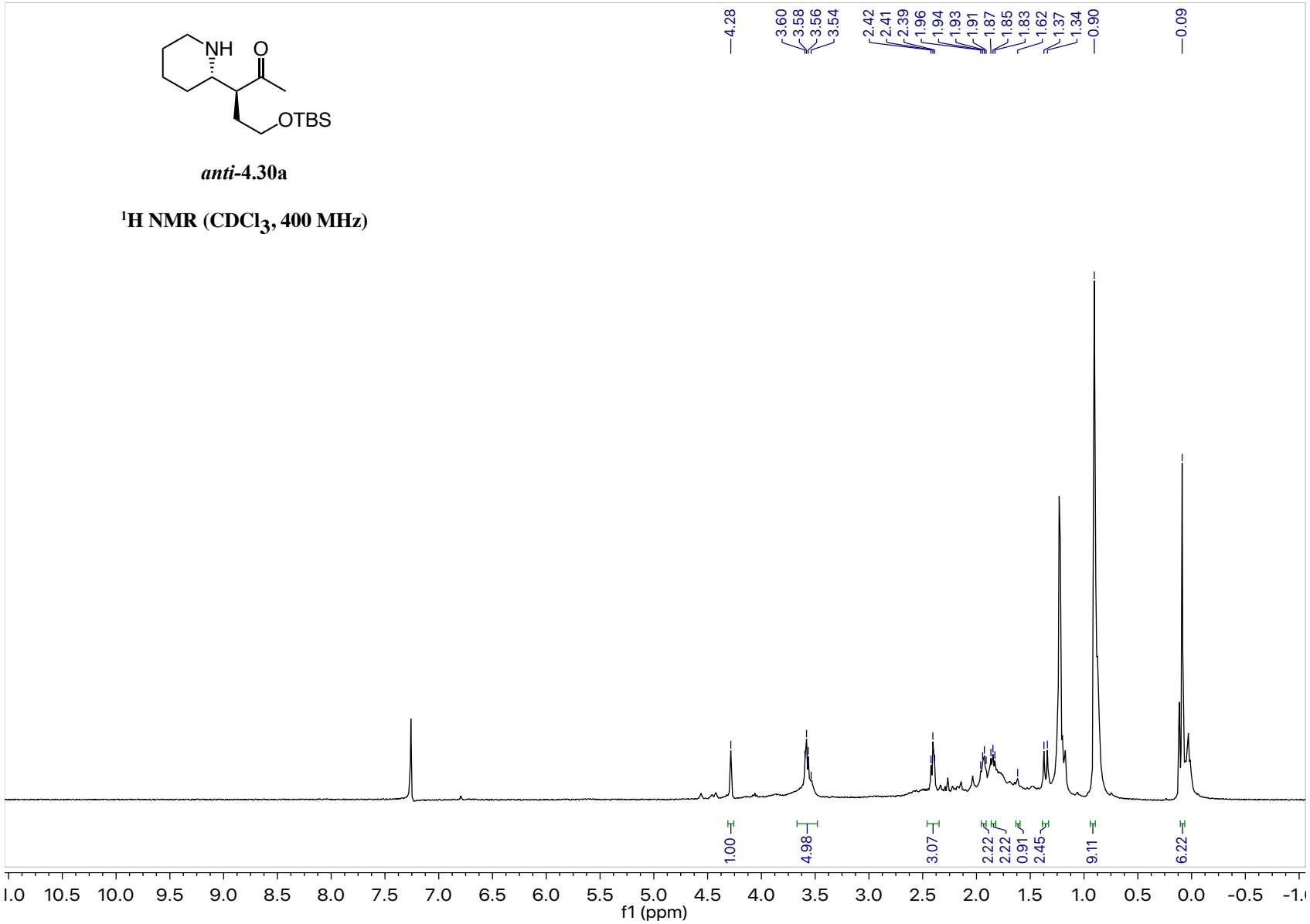

***anti*-4.30a**

^{1}H NMR ($CDCl_3$, 400 MHz)